PROGRESS IN THE CHEMISTRY OF ORGANIC NATURAL PRODUCTS

100

Editors
A.D. Kinghorn · H. Falk · J. Kobayashi

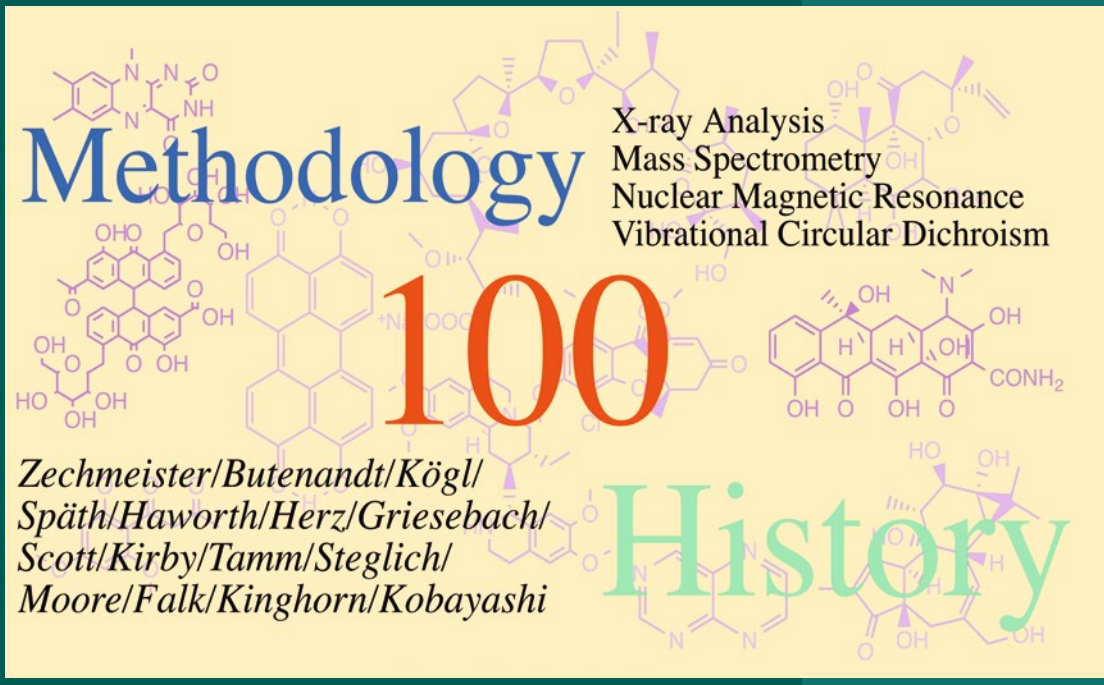

Springer

Progress in the Chemistry
of Organic Natural Products

Founded by L. Zechmeister

100

Progress in the Chemistry of Organic Natural Products

Authors:
U. Wagner, Ch. Kratky

H. Budzikiewicz

W.F. Reynolds, E.P. Mazzola

P. Joseph-Nathan, B. Gordillo-Román

R.W. Soukup, K. Soukup

Springer

Prof. A. Douglas Kinghorn, College of Pharmacy,
Ohio State University, Columbus, OH, USA

em. Univ.-Prof. Dr. H. Falk, Institut für Organische Chemie,
Johannes-Kepler-Universität, Linz, Austria

Prof. Dr. J. Kobayashi, Graduate School of Pharmaceutical Sciences,
Hokkaido University, Sapporo, Japan

ISSN 2191-7043 ISSN 2192-4309 (electronic)
ISBN 978-3-319-05274-8 ISBN 978-3-319-05275-5 (eBook)
DOI 10.1007/978-3-319-05275-5
Springer Cham Heidelberg New York Dordrecht London

Library of Congress Control Number: 2014954988

Printed on acid-free paper

Springer is part of Springer Science+Business Media (www.springer.com)

Foreword

To reach Volume 100 of a scientific book series is certainly an occasion to celebrate. We thought that this might be best achieved in two ways: on the one hand to assemble timely overviews of present-day methodology for the structural analysis of organic natural products, and on the other hand to discuss the historical aspects of the over 400 past contributions to the series founded in 1938 by *László Zechmeister*.

The first aspect is covered by contributions from pioneers and experts of the various analytical methods used widely in natural products characterization. Thus, the field is introduced by "Structure Elucidation of Natural Compounds by X-ray Crystallography" written by *Ulrike Wagner* and *Christoph Kratky* of the University of Graz (Austria)—interestingly enough, the father of the latter author was an author in Volume 1 of our book series. This contribution is followed by "Mass Spectrometry in Natural Product Structure Elucidation" by *Herbert Budzikiewicz* of the University of Cologne (Germany), "Nuclear Magnetic Resonance in the Structural Elucidation of Natural Products" by *William F. Reynolds* of the University of Toronto (Canada) and *Eugene P. Mazzola* of the University of Maryland (USA), and finally by "Vibrational Circular Dichroism Absolute Configuration Determination of Natural Products" by *Pedro Joseph-Nathan* and the late *Bárbara Gordillo-Roman* from the Instituto Politécnico Nacional, Mexico City (Mexico).

The second aspect is covered by the contribution "The Series "Progress in the Chemistry of Organic Natural Products": 75 Years of Service in the Development of Natural Product Chemistry" by *Rudolf Werner Soukup* and *Klara Soukup* of the Vienna University of Technology and St. Anna Kinderspital (Austria), and short descriptions of each of the past contributions of Volumes 1–99 are provided.

Past hallmarks of this book series have been the broad range of the subject matter covered and the internationally acclaimed chapter authors who have represented all six continents. Many thousands of natural products are presently known from

marine and terrestrial organisms, and their number and potential uses grow annually. In future years, the present Series Editors of "Progress in the Chemistry of Organic Natural Products" intend to build on the considerable momentum that has already been established by our illustrious editorial predecessors.

Columbus, OH — A.D. Kinghorn
Linz, Austria — H. Falk
Sapporo, Japan — J. Kobayashi

Contents

Listed in PubMed

Contributors

Christoph Kratky Institut für molekulare Biowissenschaften, Karl Franzens Universität Graz, Graz, Austria
christoph.kratky@uni-graz.at

Ulrike Wagner Institut für molekulare Biowissenschaften, Karl Franzens Universität Graz, Graz, Austria
Ulrike.wagner@uni-graz.at

Herbert Budzikiewicz Institut für Organische Chemie, Universität zu Köln, Köln, Germany
aco88@uni-koeln.de

Eugene P. Mazzola University of Maryland-FDA Joint Institute, College Park, MD, USA
emazzola@umd.edu

William F. Reynolds Department of Chemistry, University of Toronto, Toronto, ON, Canada
wreynold@chem.utoronto.ca

Pedro Joseph-Nathan Departamento de Química, Centro de Investigación y de Estudios Avanzados del Instituto Politécnico Nacional, México, DF, Mexico
pjoseph@cinvestav.mx

Bárbara Gordillo-Román Departamento de Química, Centro de Investigación y de Estudios Avanzados del Instituto Politécnico Nacional, México, DF, Mexico

Klara Soukup St. Anna Children's Cancer Research Institute, Vienna, Austria

Rudolf Werner Soukup Institute of Chemical Technologies and Analytics, Vienna University of Technology, Vienna, Austria
rudolf.werner@kabelnet.at

About the Authors

Christoph Kratky was born in Graz (Austria), where he attended elementary and high school. After one year of military service, he studied chemistry at ETH (Swiss Federal Institute of Technology) in Zürich, followed by a Ph.D. thesis at ETH Zürich under the supervision of Prof. J. D. Dunitz. In 1976, he obtained a Max-Kade Fellowship for a postdoctoral in the laboratory of Martin Karplus at the Department of Chemistry, Harvard University. In 1977 he accepted the position of a University Assistant at the Institute of Physical Chemistry, University of Graz. There, he obtained his habilitation in physical chemistry in 1978. Following an eight-month sabbatical in Ada Yonath's research group in Structural Molecular Biology of the Max-Planck Institute in Hamburg, he became a full professor of physical chemistry at University of Graz in 1995. From 2005 to 2013, Kratky has been the President of the Austrian Science Foundation FWF, and in 2001 he became a member of the Austrian Academy of Sciences. His research interests include the structure and function of enzymes with a B_{12} cofactor and enzymes for industrial biocatalysis, structural genomics of lipid metabolism, and the methodology of protein crystallography.

Ulrike Wagner was born in Mödling, Austria in 1960. After studying chemistry at the Karl Franzens University in Graz, Austria, she completed her Ph.D. thesis in 1997 in the group of Prof. Dr. Christoph Kratky and in collaboration with Prof. Dr. Heinz Falk of the University of Linz, Austria, on structural characterization of pyrrole systems. After two years postdoctoral study at the Weizmann Institute of Science in Rehovot, Israel in the group of Prof. Joel Sussman, working on the structure of superoxide dismutases, and another 16 months at the Sandoz Research Institute in Vienna, Austria in the group of Dr. Manfred Auer, she returned to Graz and performed her habilitation work on the structure determination of enzymes. In 1999, she spent five months at the European Synchrotron Facility (ESRF) in Grenoble, France in the group of Dr. Michael Wulff working on time-resolved crystallography. Her research interests are focused on the structure and function of enzymes for biocatalysis, time-resolved crystallography, and the methodology of protein crystallography.

Herbert Budzikiewicz was born Feb 20, 1933, in Vienna (Austria). He received his Dr. Phil. degree in chemistry in 1959 from the University of Vienna. In 1961–1965 he was head of the mass spectrometry facilities of the Department of Chemistry at Stanford University (CA, USA). In collaboration with the research group of Prof. C. Djerassi he investigated the fragmentation processes mainly of natural products (alkaloids, steroids, terpenoids) using the results for structure elucidation. In the years 1965–1969 he spent at the University of Braunschweig (Germany) where he received the *venia legendi* for organic chemistry. In 1970 he became *professor ordinarius* at the Institute of Organic Chemistry of the University at Köln (Germany). He was several times dean of the Faculty of Sciences. Since 1998 he has been *emeritus.*

The fields of research of Herbert Budzikiewicz are mass spectrometry and natural products chemistry where he specialized in bacterial metabolites. He is the author of over 500 research publications and he authored and coauthored several books on mass spectrometry. In 2008 he received the Honor Medal of the German Mass Spectrometry Society.

Eugene P. Mazzola was born on Feb 2, 1942 in Montclair, New Jersey. He obtained an A.B. degree in 1964 from Franklin and Marshall College in Lancaster, PA and a Ph.D. degree in 1971 in Organic Chemistry from the University of Pittsburgh. From 1970 to 1972, he was a post-doctoral fellow with Professor Harold Goldwhite at the California State University, Los Angeles, applying NMR spectroscopy to dynamic systems in organophosphorus compounds. He joined the Bureau of Foods of the U.S. Food and Drug Administration in Washington, DC in 1972 and took charge of the Bureau's NMR Facility in 1974, a position that he currently holds.

His research has focused primarily on the structural elucidation of natural product food contaminants and food colorant manufacturing impurities. He has taught NMR short courses at the Iowa State University, the Ohio State University, the University of Pittsburgh, and the Virginia Polytechnic Institute and State University, at the 1986 U.S./Brazil NMR Workshop, and at the 2007 American Society of Pharmacognosy Annual Meeting. He has served on the Editorial Advisory Board of *Magnetic Resonance in Chemistry* since 1996 and the Organizing Committee of the Small Molecule NMR Conference since 1999. He is Adjunct Professor of Chemistry at the University of Maryland and the Virginia Polytechnic Institute and State University and coauthor of the NMR text, "Nuclear Magnetic Resonance Spectroscopy: An Introduction to Theory, Applications, and Experimental Methods."

William F. Reynolds was born Oct 30, 1937 in Bissett, a small mining town in northern Manitoba, Canada. In 1959, he obtained a B.Sc. (Honors Chemistry) degree from the University of Manitoba. In 1963, he obtained a Ph.D. degree in Physical Chemistry from the same institution, specializing in NMR spectroscopy under the supervision of the late Professor Ted Schaefer. From 1963 to 1965, he was the Sir William Ramsey Fellow for Canada at University College London with Sir Ronald Nyholm, applying NMR spectroscopy to problems in Inorganic Chemistry. In 1965, he joined the Department of Chemistry at the University of Toronto, initially as an Assistant Professor, but subsequently as Associate Professor and later Full Professor. In 1997, he became a Lifetime Emeritus Professor, remaining active in research.

His initial research at Toronto mainly focused on investigations of transmission of electronic effects in aromatic molecules by measurements of substituent-induced chemical shifts and long-range coupling constants. However, since 1983, his major interest has been investigations of natural products, particularly using 2D NMR spectroscopy. Of his over 300 scientific publications, more than 200 have been in the natural product field, carried out in collaboration with scientists and students from Mexico, Jamaica, Trinidad, Barbados, and Guyana. He has also taught two short courses in NMR at American Society of Pharmacognosy meetings and eight others at various locations in Mexico and the West Indies. From 1993 to 2005 he was an Editor of *Magnetic Resonance in Chemistry* with particular responsibility for organic structure elucidation manuscripts. In 1998, he received the Gerhard Herzberg Award from the Spectroscopy Society of Canada and, in the same year, was made the first Canadian member of La Academia Mexicana de Ciancias, the latter award in recognition of his contributions to Mexican Chemistry.

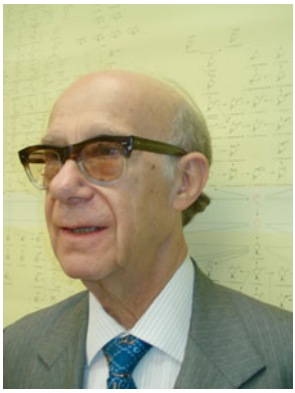

Pedro Joseph-Nathan was born in Mexico City, Mexico on Sept 17, 1941. He undertook Chemistry and Chemical Engineering undergraduate studies simultaneously, obtaining degrees in 1963 and 1964, respectively, from UNAM in Mexico City where he continued graduate work to obtain his Doctor in Chemical Sciences degree in 1966. He became a faculty member at the Department of Chemistry, CINVESTAV-IPN in Mexico City in 1966, was promoted to Professor of Chemistry in 1972, and has been *Emeritus* since 1996. He has traveled extensively through Latin America, for meetings, scientific collaboration, and related activities, where he is corresponding or honorary member of scientific societies and academies in Argentina, Bolivia, Chile, Colombia, Peru, Puerto Rico, and Venezuela. He also holds *Honorary Professor* titles from the Universidad Nacional Mayor de San Marcos in Peru and from the Universidad Nacional de Jujuy in Argentina and has doctorates *Honoris causa* from the Universidad Nacional de Tucuman in Argentina, the Universidad Michoacana de San Nicolas de Hidalgo in Mexico, and the Universidad de Magallanes in Chile.

His preferred amusement is the natural products field of Ibero-American species including structural elucidation, chemical transformations, and some physical methods for chemical analysis like nuclear magnetic resonance, single crystal X-ray diffraction, and more recently vibrational circular dichroism. He has coauthored over 450 research publications and has received many scientific awards, including the 1991 National Award of Sciences and Arts from the Government of Mexico.

Bárbara Gordillo-Román was born in Mexico City, Mexico on Dec 4, 1958. She undertook Chemistry undergraduate studies obtaining her degree from Universidad Autonoma de Puebla, Mexico in 1983, and continued graduate work at CINVESTAV-IPN in Mexico City to obtain a Master's degree in 1985 and a Doctor in Sciences degree in 1988. After postdoctoral training at the Department of Chemistry, University of North Carolina in Chapel Hill, NC, USA from 1988 to 1990, she became a faculty member at the Department of Chemistry, CINVESTAV-IPN in Mexico City in 1990 and was promoted to Professor of Chemistry in 1995 from where she was on sabbatical leave at the Department of Chemistry, Northwestern University, Evanston, IL, USA in 2001–2002. During her scientific career she accumulated some 50 research articles until she delivered her final statement to the Creator in the city of Puebla, Mexico on August 7, 2013.

Klara Soukup earned a Bachelor's degree in Food and Biotechnology in 2010 and received her Master's degree from the University of Natural Resources and Life Sciences Vienna in Biotechnology in 2013. She conducted her Master's Thesis at St. Anna Children's Cancer Research Institute Vienna, where she is currently working on her Ph.D. thesis in the Tumor Immunology Department. Her research is focused on preclinical development of dendritic cell-based tumor immunotherapies. During her studies, she spent five months at University College Cork, Ireland and completed several internships at pharmaceutical companies.

Rudolf Werner Soukup is Privatdozent of Chemical History at the Vienna University of Technology. His current fields of research include alchemy and early chemistry, especially the chemical technology of the sixteenth century, chemical research in the Hapsburg monarchy since the beginning of the eighteenth century, and on Robert Bunsen's library in Althofen (Carinthia). He studied chemistry at the Technische Hochschule in Vienna and philosophy at the University of Vienna. During his academic career, he has published papers on chemical kinetics, solvent properties, didactics, and chemical history. R. Werner Soukup is the author or editor of the following books: *Alchemistisches Gold—Paracelsistische Pharmaca* (Vienna 1997, together with Helmut Meyer); *Die wissenschaftliche Welt von gestern* (Vienna 2004), *Chemie in Österreich* (Vienna 2007); and *Pioniere der Sexualhormonforschung* (Vienna 2010, together with Christian Noe).

Structure Elucidation of Natural Compounds by X-Ray Crystallography

Ulrike Wagner and Christoph Kratky

1 Contents

U. Wagner • Ch. Kratky (✉)
Institut für molekulare Biowissenschaften, Karl Franzens Universität Graz,
Humboldtstrasse 50, 8010 Graz, Austria
e-mail: ulrike.wagner@uni-graz.at; christoph.kratky@uni-graz.at

A.D. Kinghorn, H. Falk, J. Kobayashi (eds.), *Progress in the Chemistry of Organic Natural Products, Vol. 100*, DOI 10.1007/978-3-319-05275-5_1,

1 Introduction

This contribution deals with the methodology of X-ray crystallography, which offers the most powerful techniques for the elucidation of the three-dimensional structure of molecules or molecular assemblies at atomic resolution, in particular of natural products. The topic was previously reviewed in this series in 1968 (*1*). Modern crystallography can roughly be divided into two sub-disciplines, the crystallography of "small molecules" (*i.e.* of molecules with molecular masses up to few thousand Daltons) and "macromolecular" crystallography (dealing with molecules or molecular assemblies above, say, 5 kDa). While the two sub-disciplines are based on the same physical phenomenon—the diffraction of X-rays by crystals—they differ distinctly with respect to the technology for each step of structure analysis, and they very distinctly differ with respect to the time and effort required to carry out a structure analysis. Thus, the structure analysis of a crystal of a natural product of low molecular mass is nowadays a routine enterprise, requiring (at least in favorable cases) a few hours of manpower and involving in-house equipment. In contrast, structure analysis of a (natural, biological) macromolecule—in spite of continuous improvements in automation—is still a major undertaking, involving the collection of diffraction data at synchrotron sources and requiring typically months of manpower. The present contribution will attempt to describe the methodology of both crystallographic sub-disciplines, but a bias towards macromolecular crystallography will be unavoidable. This is due to a variety of reasons, among them the much larger complexity and diversity of techniques, the more dramatic developments during the last few decades and not least the personal research interests of the authors.

Besides X-ray crystallography, nuclear magnetic resonance (NMR) spectroscopy is the second major method for atomic-level structure determination. While, for many years, the two techniques competed for being the "most relevant technique for structure analysis", it is now recognized that NMR and crystallography are largely complementary, with each of them having specific strengths and weaknesses. Thus, the application of NMR techniques is still subject to limits in the size of molecules to be investigated. Such limits are much less severe for crystallography: the largest molecular assembly for which the three-dimensional structure has been deposited in the Protein Data Bank is the yeast 80S ribosome (*2*), consisting of 45 peptide chains with a total structural weight of more than 1.8 MDa. On the other hand, crystallographers depend on the availability of crystals in contrast to NMR spectroscopists, who only need a sufficiently concentrated solution for their experiments. It becomes more and more apparent that—at least in biological crystallography—the crystallization step is the crucial bottle neck for a crystallographic structure elucidation.

2 History

The physical foundations of crystallography have been known slightly more than a century. It started in 1895 with the discovery of X-rays by *Conrad Wilhelm Röntgen* (*3*), followed—in 1912—by the ground-breaking observation by *Walter Friedrich*,

Paul Knipping, and *Max von Laue* that the interaction of these—at the time quite mysterious—X-rays with a crystal of zincblende produces interference patterns, which were interpreted as being the result of a regular three-dimensional arrangement of zinc and sulfur atoms (*4*). In fact, *René-Just Haüy* had already predicted in the eighteenth century that a crystal consists of a three-dimensional repetition of smaller units. After *von Laue*'s landmark experiment, the theoretical background for structure determination with X-rays was developed by *William Henry Bragg* and *William Lawrence Bragg* (*5*–*7*). Although the early crystal structure analyses performed with this new technique were from very simple substances, such as rock salt (*8*), diamond (*9*), or copper (*10*), they had immediate implications on the discovery and understanding of chemical phenomena, eventually culminating in *Linus Pauling*'s seminal book on "The Nature of the Chemical Bond" (*11*). In those early days, structure determination even for small molecules was very time-consuming, requiring virtually years of hard manual labor.

A landmark for the development of the crystallography of natural compounds was the work of *Dorothy Hodgkin*, who contributed to the advancement of the field with several seminal structure analyses. Most importantly, she confirmed the chemical structure of penicillin (*12*, *13*) that *Ernst Boris Chain* had previously surmised (*14*), and subsequently elucidated the crystal structures of vitamin B_{12} (*15*–*17*), of coenzyme B_{12} (*18*) and of other B_{12} derivatives (*19*) (Fig. 1). *Hodgkin*'s

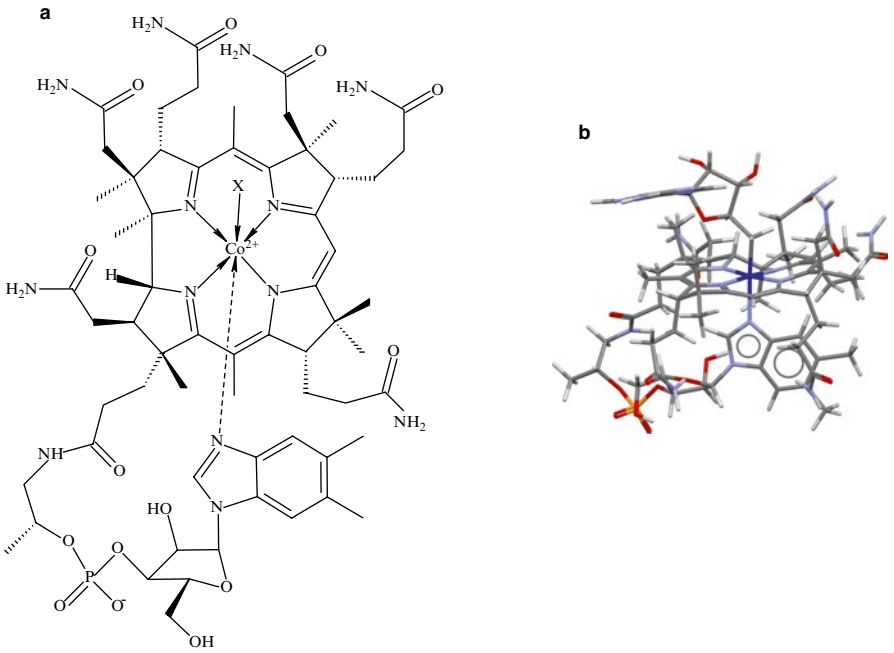

Fig. 1 (**a**) Chemical constitution and configuration of the B_{12} derivatives coenzyme B_{12} (5′-deoxyadenosyl cobalamin, X = 5′-deoxyadenosyl), vitamin B_{12} (cyanocobalamin, X = CN) and B_{12r} (cob(II)alamin, X = e). (**b**) The B_{12} moiety in the crystal structure of coenzyme B_{12} (*18*)

crystallographic work on B_{12} was specifically significant for a number of reasons: coenzyme B_{12} is the most complex non-polymeric natural product, and the first one for which the chemical structure was elucidated by X-ray crystallography. In fact, the X-ray analysis revealed a feature of coenzyme B_{12}—a cobalt-carbon bond—which was completely unexpected and which would never have been discovered with any other technique available at the time. In 1964, *Dorothy Hodgkin* was awarded the *Nobel* Prize in chemistry "for her determinations by X-ray techniques of the structures of important biochemical substances". In subsequent years, *Hodgkin* continued with substantial contributions to the analysis of the three-dimensional structure of important natural products, including that of insulin (*20*).

Herbert Aaron Hauptman and *Jerome Karle* developed a statistical method to solve the phase problem of small molecules (*21*)—the direct methods—for which they received the *Nobel* Prize in 1985. It is largely due to the direct methods—combined with the availability of computers—that small-molecule crystallography, in particular of most natural products, is a routine technique today.

The situation is quite different for the crystallography of natural macromolecules. Although *Joseph Burton Sumner* showed as early as 1926 that a protein (urease) can be crystallized (*22*), it took more than three decades until the first crystal structure (myoglobin at 6 Å resolution) was reported, and an additional three years for the (almost) completed structure (*23*) to be published. The second protein crystal structure—hemoglobin—was reported several years later (*24*, *25*). For their pioneering work, *John Kendrew* and *Max Perutz* were awarded the *Nobel* Prize in 1962. Subsequent breakthroughs in macromolecular crystallography include the elucidation of the structure of the photosynthesis reaction center, the first membrane-protein complex for which the structure was determined at atomic resolution, by *Johann Deisenhofer*, *Hartmut Michl*, and *Robert Huber* in 1984 (*26*) (*Nobel* Prize 1988). In 2009, the *Nobel* Prize in chemistry was awarded to *Venkatraman Ramakrishnan*, *Thomas Arthur Steitz,* and *Ada Yonath* "for studies of the structure and function of the ribosome". Besides the enormous biological relevance of ribosomes, for which the function can now be rationalized at atomic resolution, it is the breathtaking complexity of ribosomal particles—with molecular masses far exceeding one million Daltons—which make the achievements of *Ramakrishnan*, *Steitz*, and *Yonath* so outstanding (*27*–*30*).

3 Theoretical Background

3.1 Heuristic Introduction

By its very nature, X-ray crystallography is a microscopic technique, for which the specifics can be rationalized with reference to a microscope (Fig. 2a): a microscopic object interacts with electromagnetic radiation, resulting in elastic scattering of a

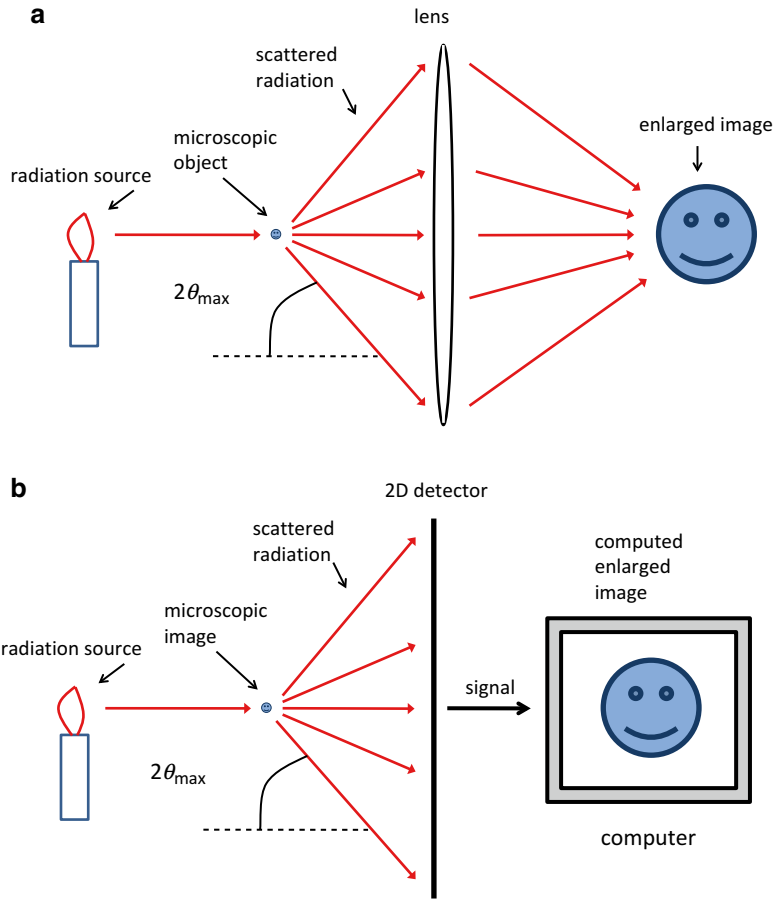

Fig. 2 (**a**) Concept of a microscope and (**b**) of a diffraction experiment

small fraction of the incoming light. The scattered radiation passes through an optical system of lenses, that recombines the scattered light to an enlarged image of the original object. The resolution—defined as the minimum distance of two points which can still be distinguished—of such an optical imaging process is

$$d_{min} = \frac{\lambda}{2\sin\vartheta_{max}} \tag{1}$$

Here, λ is the wavelength of the electromagnetic radiation, and ϑ_{max} is half the maximum angle between incoming radiation and scattered radiation. Thus, in order to image objects of molecular dimensions, radiation with a wavelength in the

order of minimum distances between atoms has to be employed. Hence, X-rays with wavelengths between 0.7 and 1.5 Å are used for crystallographic experiments. Since optical systems for radiation of such a wavelength do not exist,[1] the experiment has to be modified as shown in Fig. 2b, *i.e.* the system of lenses is replaced by a detector, which records the intensity of scattered radiation. The job of recombining scattered radiation to an image is "left to the computer". Since a detector can only record the intensity of scattered radiation and not its phase, information is lost when the experiment is performed as shown in Fig. 2b. The process of numerically recombining scattered radiation to form an image therefore has to cope with a non-trivial problem frequently referred to as the "phase problem" of crystallography.

The simplified representation of Fig. 2 overlooks yet another much more serious problem: in order to form an image of an object of molecular dimensions, a linear magnification by about eight orders of magnitude (!) is required, which has to be compared to the maximum linear magnification of optical microscopes by three to four orders of magnitude. A linear magnification by a factor of 10^8 corresponds to projecting a slide onto a screen with the size of Germany. A light source of tremendous brilliance would be required for such an undertaking, for which the unbelievably high energy would destroy the molecular object within picoseconds.[2]

The trick of crystallographers to overcome the problem of radiation intensity and radiation damage is to investigate crystals instead of individual molecules. Crystals consist of regular three-dimensional arrangements of identical objects (atoms or molecules). The fact that different components are related by translation symmetry has the consequence that the scattering of each of the components interferes constructively in a few directions (defined by simultaneously satisfying the three *Laue* equations (8) or the *Bragg* equation, see below), where the scattered intensity is then at least proportional to the number of components in the crystal, while the scattered radiation interferes essentially destructively in all other directions. This leads to diffraction images characterized by sharp spots of high intensity (often referred to as reflections) surrounded by a comparably weak background, as shown in Fig. 3.

3.2 Scattering Theory

In the following, we give a brief summary of the theoretical basis of X-ray diffraction. More detailed descriptions of the theory of X-ray scattering from crystal scan be found elsewhere (*31*–*33*).

[1] The refractive index for X-rays is very close to 1 for all known materials, and all materials absorb X-rays to some extent. However, X-ray lenses based on multilayer-systems and *Fresnel* zone plates are in the process of being developed for X-ray microscopy.

[2] Such brilliant radiation sources will in fact become available in the future with the advent of free electron lasers, and imaging experiments on single molecules are indeed forseeable.

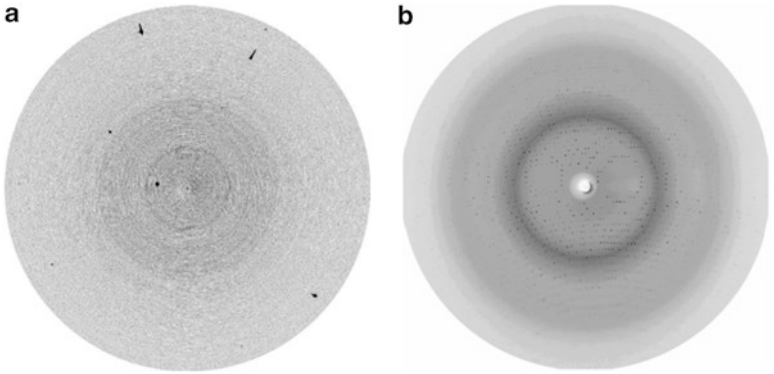

Fig. 3 (**a**) Diffraction pattern of an organic crystal, and (**b**) of a protein crystal. Both patterns were recorded under identical experimental conditions ($\lambda = 1.54$ Å, distance crystal-detector = 120 mm, radius of detector = 90 mm, 1° oscillation)

The mathematical concept describing the translation symmetry of a crystal is called a lattice. A lattice is an infinitely large three-dimensional arrangement of points for which the location in space can be described by three non-coplanar translation vectors $\vec{a}$, $\vec{b}$, and $\vec{c}$. These vectors are defined in such a way that—starting from any point within the lattice—an integer multiple of the three vectors will always end up on another lattice point, and that any lattice point can be reached by an integer linear combination of the three lattice vectors. The parallelepiped defined by the three vectors $\vec{a}$, $\vec{b}$, and $\vec{c}$ is called the unit cell, which can contain anything between one atom and a complicated arrangement of many macromolecules. If $\rho(\vec{r})$ is the electron density at any location $\vec{r}$ within the crystal, then the translational symmetry of the crystal can also be specified as

$$\rho(\vec{r}) = \rho(\vec{r} + m\vec{a} + n\vec{b} + p\vec{c}) \tag{2}$$

With m, n, and p being integer numbers. The scalar quantities

$$\begin{aligned} a &= |\vec{a}|, \quad b = |\vec{b}|, \quad c = |\vec{c}|, \\ \alpha &= \cos^{-1}\frac{\vec{b}\vec{c}}{|\vec{b}||\vec{c}|}, \quad \beta = \cos^{-1}\frac{\vec{a}\vec{c}}{|\vec{a}||\vec{c}|}, \quad \gamma = \cos^{-1}\frac{\vec{a}\vec{b}}{|\vec{a}||\vec{b}|} \end{aligned} \tag{3}$$

are called the cell constants. The vector $\vec{r}$ pointing to a location within the crystal is usually expressed in terms of the lattice translation vectors $\vec{a}$, $\vec{b}$, and $\vec{c}$:

$$\vec{r} = X\vec{a} + Y\vec{b} + Z\vec{c} \tag{4}$$

X, Y, and Z are called fractional coordinates.

A diffraction experiment can be described by two vectors $\vec{s}_0$ and $\vec{s}_1$, where $\vec{s}_0$ is a vector along the incoming X-ray beam, and $\vec{s}_1$ is a vector pointing in the direction of a diffracted beam. Both vectors have length $1/\lambda$, where λ is the X-ray wavelength. The diffraction vector $\vec{R}$ is defined as

$$\vec{R} = \vec{s}_1 - \vec{s}_0 \tag{5}$$

It can be shown that the diffraction of an object described by the electron density $\rho(\vec{r})$ only depends on $\vec{R}$ (and not on the individual vectors $\vec{s}_0$ and $\vec{s}_1$), and it can be described by the complex function $F(\vec{R})$, which is the *Fourier* transform of $\rho(\vec{r})$:

$$F(\vec{R}) = \left|F(\vec{R})\right| e^{2\pi i \Phi(\vec{R})} = \iiint_{-\infty}^{\infty} \rho(\vec{r}) e^{2\pi i \vec{r}\vec{R}} d^3\vec{r} \tag{6}$$

$F(\vec{R})$ is called the scattering function, which is not directly experimentally observable. The observable scattered intensity can be computed from $F(\vec{R})$ by

$$I(\vec{R}) = F(\vec{R}) \times F^*(\vec{R}) \tag{7}$$

Laue was the first to define the geometric condition for constructive interference of scattering functions resulting from translation-equivalent objects (Fig. 4).

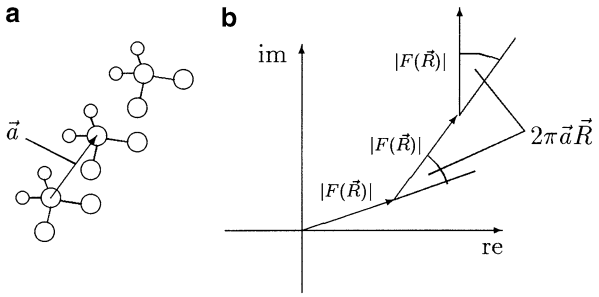

Fig. 4 (**a**) The phase shift of two translation-equivalent objects related by the vector $\vec{a}$ for diffraction in the direction $\vec{R}$ is $2\pi\vec{a}\vec{R}$. (**b**) The diffraction of an infinite number of translationally equivalent objects will only constructively interfere if the phase shift for successive objects is zero, hence $\vec{a}\vec{R} = integer$

As illustrated in this figure, a one-dimensional array of translation-equivalent objects related by the translation vector $\vec{a}$ will yield maximum constructive interference if $\vec{a}\vec{R}$ is zero or an integer number. For three-dimensional crystals, this condition has to be fulfilled simultaneously for all three translation directions, leading to the *Laue* equations:

$$\begin{aligned} \vec{a}\vec{R} &= h \\ \vec{b}\vec{R} &= k \\ \vec{c}\vec{R} &= l \end{aligned} \tag{8}$$

h, k, and l are integer numbers called the *Miller*-indices.

The reciprocal lattice is a useful concept to visualize the conditions for observability of a reflection. It can be shown that the three *Laue* equations are fulfilled when

$$\vec{R} = h\vec{a}^* + k\vec{b}^* + l\vec{c}^* \tag{9}$$

h, k, and l are the *Miller* indices and $\vec{a}^*$, $\vec{b}^*$, and $\vec{c}^*$ the reciprocal lattice vectors defined as follows:

$$\vec{a}^* = \frac{\vec{b}\times\vec{c}}{\vec{a}\cdot\left(\vec{b}\times\vec{c}\right)}, \quad \vec{b}^* = \frac{\vec{a}\times\vec{c}}{\vec{a}\cdot\left(\vec{b}\times\vec{c}\right)}, \quad \vec{c}^* = \frac{\vec{a}\times\vec{b}}{\vec{a}\cdot\left(\vec{b}\times\vec{c}\right)} \tag{10}$$

Thus, all possible integer linear combinations of $h\vec{a}^* + k\vec{b}^* + l\vec{c}^*$ define a lattice, for which the grid points have to coincide with the diffraction vector in order for a reflection to be observable.[3] This is illustrated in Fig. 5.

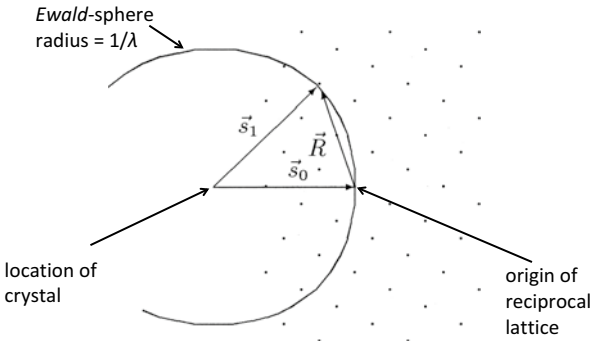

Fig. 5 In order to observe the intensity associated with a reciprocal lattice point, the crystal has to be rotated in such a way that the lattice point coincides with the surface of the *Ewald* sphere (*301*)

Thus, the translational symmetry within crystals leads to a "sampling" of the scattering function, which is zero everywhere except at the reciprocal lattice points, where

$$F_{crystal} = NF_{unit\,cell} \tag{11}$$

With N being the number of unit cells in the crystal. Hence

$$I_{crystal} = \left|F_{crystal}\right|^2 = N^2 I_{unit\,cell} \tag{12}$$

[3] This is equivalent to the well-known *Bragg* equation $n\lambda = 2d\sin\vartheta$, where λ is the wavelength and ϑ is the angle between incoming wave and the plane of lattice points with spacing d.

Since the structure factor $F\left(\vec{R}\right)$ is the *Fourier* transform of the electron density $\rho\left(\vec{r}\right)$, inverse *Fourier* transform will allow the computation of $\rho\left(\vec{r}\right)$ from $F\left(\vec{R}\right)$. Moreover, since $F\left(\vec{R}\right)$ is only non-zero on reciprocal lattice points, the *Fourier*-integral can be simplified to a summation:

$$\rho(r)=\rho(X,Y,Z)=\iiint_{-\infty}^{\infty} F\left(\vec{R}\right)e^{-2\pi i\vec{r}\vec{R}}d^3\vec{R}=\sum_h\sum_k\sum_l F(h,k,l)e^{-2\pi i(hX+kY+lZ)} \tag{13}$$

Thus, computation of the electron density would be a straightforward summation if the structure factors $F(h,k,l)$ were known, However, $F(h,k,l)$ is a complex quantity, of which only the modulus $|F(h,k,l)|=\sqrt{I(h,k,l)}$ is experimentally accessible. This constitutes the crystallographic phase problem.

While computation of the electron density from observed intensities is thus non-trivial, the reverse—computation of structure factors for a known structure—is straightforward. Crystallographic structures are not described in terms of a continuous electron density but rather in terms of atomic positions within the unit cell.

$$\rho\left(\vec{r}\right)=\sum_{i=1}^{n}\rho_i\left(\vec{r}-\vec{r}_i\right) \tag{14}$$

Where $\vec{r}_i$ is the location of atom i, and the summation runs over all atoms in the unit cell. The structure factor calculation simplifies then to a summation:

$$F(h,k,l)=\sum_{i=1}^{n}f_i(h,k,l)e^{2\pi i(hX_i+kY_i+lZ_i)} \tag{15}$$

f_i are the atomic scattering factors for spherically symmetric atoms, which are assumed to be only dependent on the scattering angle 2ϑ (see below).

3.3 Symmetry in Crystals

The most relevant type of symmetry—translational symmetry—has been dealt with above. Additional point-group symmetry also occurs in crystals. It can be demonstrated that infinite periodic three-dimensional objects can have only specific point group symmetry elements, such as inversion centers, mirror planes and 2-, 3-, 4-, and 6-fold rotation axes. In addition, combinations of these point group symmetry elements with a translation component by a fraction of a lattice translation—leading to screw axes and glide planes—are possible in crystals.

Analysis of all possible combinations of the point group symmetry elements leads to 32 different crystallographic point groups. If one combines these 32 point groups with the screw axes and glide planes and includes the 14 possible lattice types—the so-called *Bravais* lattices—one ends up with a total of 230 space groups (*34*), which describe the possible combinations of symmetry elements in a crystal. Each crystal can be assigned to exactly one space group.

The symmetry properties of the crystal structure $\rho(X,Y,Z)$ has an effect on the symmetry of the diffraction pattern $F(h,k,l)$. It can be shown that the point group symmetry of the crystal structure is reflected in the point group symmetry of the diffraction pattern. However, since the diffraction pattern is always centrosymmetric (*Friedel*'s law (*35*)),[4] the 32 crystallographic point groups map on 11 possible point groups of the diffraction pattern, the so-called 11 *Laue* Classes. Occurrence of symmetry elements with a translation component—screw axes, glide planes, and lattice centering—leads to what is called systematic extinctions in the diffraction pattern. These systematic extinctions are sufficiently characteristic to allow unambiguous identification of each symmetry element with a translation component. Finally, the existence or non-existence of centro-symmetry in the crystal structure—which cannot be deduced from the symmetry of the diffraction pattern because of *Friedel*'s law—can usually be derived from a statistical analysis of the distribution of observed reflection intensities (*32*). However, the latter question may be academic whenever one knows from the chemical configuration that the crystal structure cannot be centrosymmetric, as it is the case in macromolecular crystallography.

In summary: the deduction of the space group symmetry of a crystal from properties (symmetry, systematic extinctions, intensity statistics) of the diffraction pattern is usually straightforward. Occasionally, these observables are compatible with two or three different space groups, in which case structure solution has to be attempted for each of the possible space groups.

An important concept related to the crystal symmetry is the *asymmetric unit*. The unit cell always contains an integer number of asymmetric units related by the crystallographic symmetry elements. In terms of the molecular constituents of the crystal, the asymmetric unit may consist of one molecule, but it may also consist of a fraction of a molecule (in which case a symmetry operation transforms a molecule into itself) or of several molecules. The latter case is quite frequent in macromolecular crystallography, and is referred to as *non-crystallographic symmetry*.

3.4 Crystallographic Resolution

Equation (1), describing the resolution of an optical system, implies that better resolution (*i.e.* lower d_{min}) can be attained by either lowering the wavelength λ or by increasing the maximum angle of observation $2\vartheta_{max}$. These are both parameters under the control of the experimenter. However, in the vast majority of cases it is not the experimental setup that limits the resolution but rather the sample, limiting in turn the maximum angle of observation by not showing any significant diffraction beyond a certain scattering angle. This is readily seen from Fig. 3, which shows that the diffraction of an organic crystal extends well to the edge of the detector (Fig. 3a), while the diffraction of a biological macromolecule (recorded under identical experimental conditions) rapidly fades away at relatively small scattering angles (Fig. 3b).

[4] *Friedel*'s law only holds when anomalous dispersion effects are negligible. Significant anomalous effects allow to determine the absolute configuration of molecules (*36*) and form the basis for a powerful set of techniques to determine the phases of macromolecular crystals (see Sect. 4).

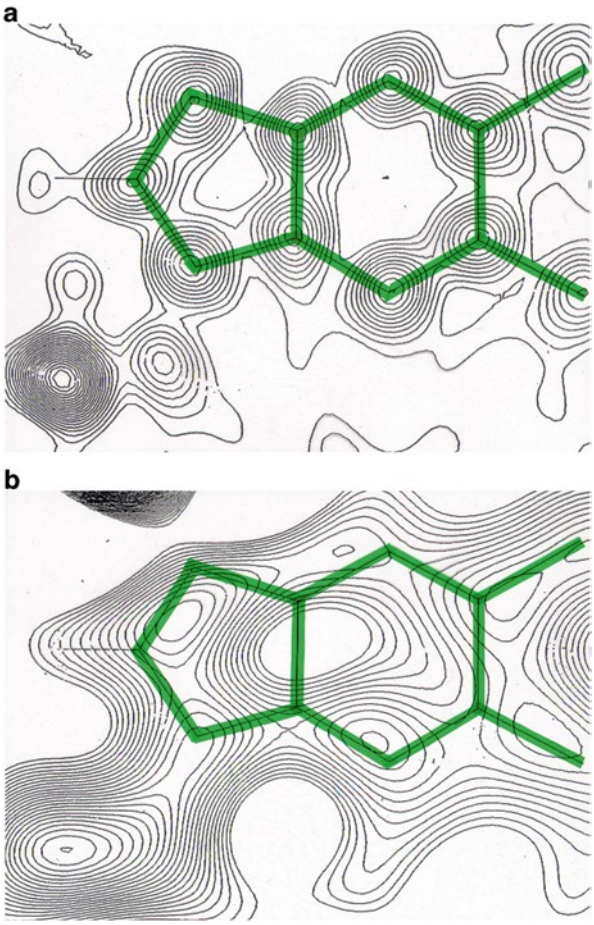

Fig. 6 Two-dimensional section through the electron density map for a vitamin B_{12} derivative (*302*). The section passes through the dimethylbenzimidazole moiety (indicated in *green*). (**a**) Map calculated with data extending to 0.91 Å resolution; (**b**) map calculated with data to 2.0 Å resolution

Figure 3 reveals a number of significant and characteristic differences between the diffraction patterns of protein crystals and crystals of small molecules:

1. Small-molecule crystals typically diffract to atomic resolution ($d_{min} < 1.3$Å), which occurs only in exceptional cases with protein crystals. The resolution has dramatic effects on the interpretability of density maps (as shown in Fig. 6), and it has implications on structure solution and structure refinement.
2. Diffracted intensities are much higher for small-molecule crystals compared to protein crystals. This is evident from the fact that the diffracted intensity is proportional to N^2, with N being the number of unit cells. For macromolecular crystals, the cell constants are orders-of-magnitude larger than for small-molecule crystals, with a concomitantly smaller N for protein crystals.

3. Diffraction spots are much closer in protein crystals. This is due to the larger cell constants, which lead to smaller reciprocal cell constants und therefore many more reciprocal lattice points simultaneously coinciding with the *Ewald* sphere.

The difference in attainable resolution between small-molecule crystals and macromolecular crystals becomes immediately obvious when one analyzes the packing of individual molecules into the crystal environment. While—as shown in Fig. 7—small molecules pack very tightly, with many contacts between neighboring molecules and few voids, the packing of protein crystals is extremely loose—adjacent molecules form few contacts, and there are huge spaces filled with (usually disordered) solvent. Up to 85% of the space of macromolecular crystals is occupied by solvent. Thus, macromolecular crystals are very soft and brittle—frequently referred to as ordered solutions.

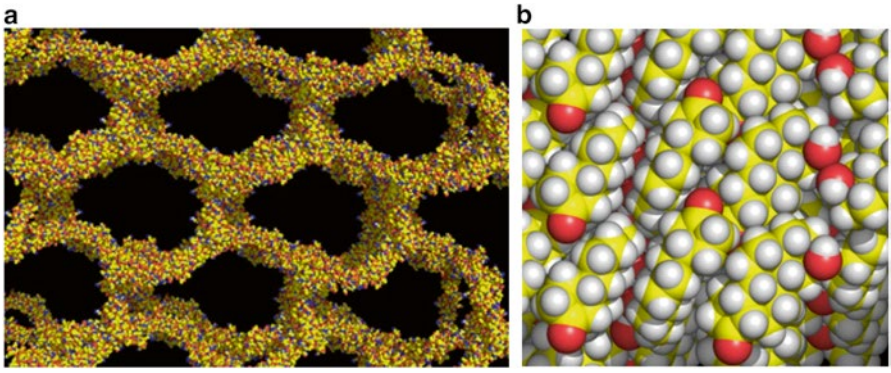

Fig. 7 (**a**) The packing in a protein crystal (β2-glycoprotein I, pdb-code 1c1z, (*303*)) with a solvent content of 85%. (**b**) Packing of 2β-hydroxygonane (CSD code AFAAWOU (*304*)). Atoms are displayed as *spheres* with the following color scheme: carbon-*yellow*, nitrogen-*blue*, oxygen-*red*, hydrogen-*white*. Pictures were generated with the program pymol (*305*)

3.5 *Anomalous Dispersion*

In the structure factor calculation (equation 15), f_i are the atomic scattering factors, which are assumed to be real quantities only dependent on the scattering angle. Under these conditions, *Friedel*'s law, *i.e.* the centrosymmetry of the diffraction pattern $I(h,k,l) = I(\bar{h},\bar{k},\bar{l})$, readily emerges even for non-centrosymmetric structures, since

$$I(h,k,l) = F(h,k,l) \times F^{*}(h,k,l) \tag{16}$$

The assumption that the f_i are real quantities only holds as long as all atoms behave as elastic scatterers, *i.e.* as long as the absorption edges of all atoms in the

unit cell are far removed from the energy of the X-rays. For a typical diffraction experiment ($\lambda \sim 1$Å), this is generally a good approximation for atoms in the first row of the periodic system. The assumption breaks down when atoms have absorption edges close to the X-ray wavelength, in which case the atomic scattering factors become complex quantities of the form

$$f_{(\vartheta,\lambda)} = f_{\vartheta}^{0} + f_{\lambda}^{'} + if_{\lambda}^{''} \tag{17}$$

Atoms with significant f'' are referred to as anomalous scatterers. It is obvious that their presence will lead to a breakdown of *Friedel*'s law for non-centrosymmetric structures (*i.e.* for all biomolecular structures). Anomalous differences, *i.e.* the difference between *Bijvoet* pairs $I(h,k,l) - I(\bar{h},\bar{k},\bar{l})$ carry information about the location of such anomalous scatterers, which can be utilized for structure solution as described later.

3.6 The Patterson Function

The calculation of the electron density within a crystal

$$\rho(X,Y,Z) = \sum_{h}\sum_{k}\sum_{l} \left|F(h,k,l)\right| e^{2\pi i\varphi(h,k,l)} e^{-2\pi i(hX+kY+lZ)} \tag{18}$$

is impeded by a lack of knowledge of the phases $\varphi(h,k,l)$. However, the related function

$$P(X,Y,Z) = \sum_{h}\sum_{k}\sum_{l} \left|F(h,k,l)\right|^{2} e^{-2\pi i(hX+kY+lZ)} \tag{19}$$

can readily be computed from observed diffraction data. This is called the *Patterson* function, and it can be shown that $P(X,Y,Z)$ is the autocorrelation function of the electron density $\rho(X,Y,Z)$, *i.e.*

$$P(\vec{u}) = \iiint \rho(\vec{r})\,\rho(\vec{u}-\vec{r})\,d^{3}\vec{r} \tag{20}$$

In simple cases, it is possible to deconvolute $P(X,Y,Z)$, *i.e.* to deduce the electron density from the *Patterson* function. However, as a tool for *ab initio* structure solution, the *Patterson* function has little significance because it becomes exceedingly complex for any non-trivial structure. Thus, for an electron density with N peaks, the *Patterson* function will show $N\times(N-1)$ peaks. Nevertheless, $P(X,Y,Z)$ is still highly relevant for a number of special applications in macromolecular crystallography: in cases where appropriate subtraction leads to intensity contributions from one or few atoms (such as anomalous differences or differences between a native structure and an isomorphous derivative), a *Patterson* map will readily reveal the

position(s) of the contributing heavy atoms. A second application of *Patterson* maps is the computation of rotation functions.

The rotation function is used to find the correct orientation of a model in the crystal lattice. It is defined as follows:

$$R(C) = \int P_1(\vec{r}) P_2(\vec{r}') dV \tag{21}$$

P_1 and P_2 are the *Patterson* functions computed from the diffraction data and from the model, respectively. The matrix C defines a rotation of $\vec{r}$ with respect to $\vec{r}'$. Calculating the rotation function is one step in a structure solution technique called molecular replacement (see below). A special case of rotation function is the self rotation function, *i.e.* both P_1 and P_2 are computed from the diffraction data. The self rotation function is used to identify non-crystallographic symmetry (see below).

4 Crystal Structure Analysis

Although myriads of techniques and technologies exist for the structure elucidation with crystallographic methods, the process necessarily has to involve the following steps 1. to 5.

1. *Crystallization,*
2. *Collection of Diffraction Data,*
3. *Structure Solution,*
4. *Refinement,*
5. *Interpretation and Publication.*

4.1 Crystallization

Crystallization of small-molecule organic or inorganic compounds is mostly straightforward and has been carried out by chemists for a long time. In fact, recrystallization has always been a routine purification operation in synthesis chemistry. To obtain crystals useful for crystallographic purposes (*i.e.* with a diameter >0.1 mm), it is usually enough to decrease the solubility of the substance by *e.g.* slow cooling, evaporation of solvent or slow addition of a less-good solvent. Crystals will typically appear as a matter of a few days, at most.

In macromolecular crystallography, crystallization is much less straightforward (*37*). Many efforts have been invested to understand the process of crystallization, and to find ways to systematically control it (*38*). Cunning techniques were devised (*39*); protein solutions were even flown into space with the hope to improve the chance for crystal growth and the diffraction quality of crystals (*40*, *41*). In spite of all these efforts, we have to admit that the growth of macromolecular crystals is still

Table 1 Some factors affecting crystallizability of biological macromolecules (left column) and some frequently used precipitants (right column)

Concentration of Biomolecule	Ammonium Sulfate
Purity of Biolomecule	Polyethylene Glycol
pH and Buffer	2-Methyl-2,4-pentanediol
Ionic Strength of Solution	Na- or K-Phosphate
Temperature	Ethanol
Nature and Concentration of Precipitant	NaCl
Biological Origin	Other Salts
Additives (Ligands, Ions, etc.)	Other Organic Solvents
Detergents	

a very empirical exercise, primarily requiring patience, perseverance and luck. In fact, crystallization is today by far the most severe bottleneck of macromolecular crystallography.

Recently (*42*), a technique was described that does away with the necessity to crystallize a substance prior to its structure analysis. The method involves specific metal complexes that form crystals with large pores. Such crystals are soaked in a solution of the substance to be analyzed. When done properly, target molecules bind specifically within the pores, and the complex can then be subjected to crystal structure analysis. The authors demonstrated that as little as 80 ng of a sample are enough for structure analysis. Using this method, they successfully determined the 3D structure of a marine natural product from only 5 μg of the compound. The general applicability of this technique will undoubtedly be the subject of future research.

Macromolecular crystals are grown by adding precipitants to a solution of the substance to be crystallized. Many factors were identified that affect—or might affect—crystallogenesis, and a large number of precipitants were used to crystallize biological macromolecules (see Table 1). The problem is that conditions optimized for the crystallization of one system cannot be transferred to another system, even if the two systems are closely related. The search for crystallization conditions amounts to a search through a very high-dimensional phase diagram, and experience has shown that areas in this phase diagram where crystals occur tend to be narrow. Searching for crystallization conditions amounts to looking for the notorious needle in a haystack—hundreds or even thousands of different conditions are often searched, without any guarantee that any set of conditions exist at all where the system under scrutiny will crystallize.

The general procedure adopted for any set of conditions can be illustrated with reference to Fig. 8, which shows a two-dimensional section through a schematic phase diagram of a prototypical biological macromolecule. The two dimensions are protein concentration and concentration of a precipitant, and we assume that the conditions are such that crystallogenesis is possible. Conceptually, we distinguish three regions in this section through a phase diagram: a “blue” region where a clear monodisperse solution of bio-molecule exists and a “pink” region consisting of two phases, solution and crystalline bio-molecule. In between, there exists a metastable region belonging thermodynamically to the “pink” region, however no spontaneous

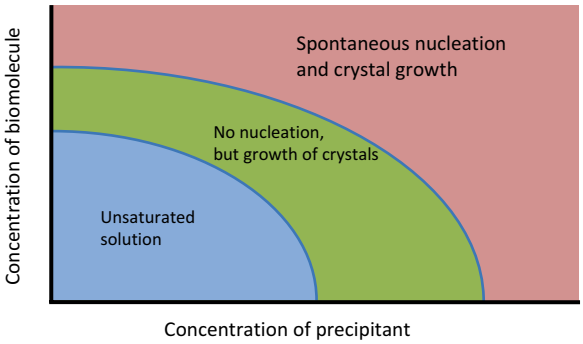

Fig. 8 Schematic phase diagram of a system consisting of a solution of biomolecule plus dissolved precipitant

phase separation occurs in this region, although crystals will be stable in this part of the phase diagram and will even grow.

A crystallization experiment starts at some point in the first (blue) region where the protein is completely dissolved, as are the precipitants. The experiment typically consists in slowly removing water from the solution, thus increasing the concentration of biomolecule and of precipitant(s). At some point, the border between the metastable region and the biphasic region will be crossed, whereupon heterogeneous nucleation starts. Precipitation of the first crystals will decrease the concentration of the biomolecules within the solution, thus moving the system back into the metastable region, where these first small crystals will hopefully increase in size. Since crystal formation and crystal growth is diffusion controlled, they are slow processes. If the transition from the metastable into the biphasic region is too rapid, a non-crystalline precipitant will appear instead of crystals.

4.1.1 Crystallization Methodology

Thus, the problem of macromolecular crystallization is to increase the concentration of the macromolecule and precipitant in a slow and very controlled way, hoping that this change will guide the system through the relevant regions of the phase diagram, as described above. This experiment has to be conducted for a large number of initial conditions, *i.e.* each experiment should require only minute amounts of precious macromolecule. Typical modern crystallization set-ups use 1 mm^3 of macromolecular solution each. Another important condition for a crystallization setup is good view on the protein solution through a microscope, since identification of macromolecular microcrystals can be non-trivial. Countless gadgets and devices were designed for this purpose, with the most common ones based on one of the following principles:

Vapor diffusion. Here, controlled evaporation of solvent from a crystallization setup will lead to the required increase in the concentration of biomolecule and precipitant. Typical setups comprise the classical methods of hanging and sitting drops. Drops are prepared by mixing the sample solution with the reservoir solution, which contains

the precipitants, buffers, and salts. They sit or hang above a reservoir solution with higher precipitant concentration. Water will evaporate from the less concentrated drops to the reservoir und thereby increase the concentration of macromolecules and precipitant inside the drop. The process can be slowed down—which often leads to better results—by overlaying oil above the reservoir solution (Fig. 9).

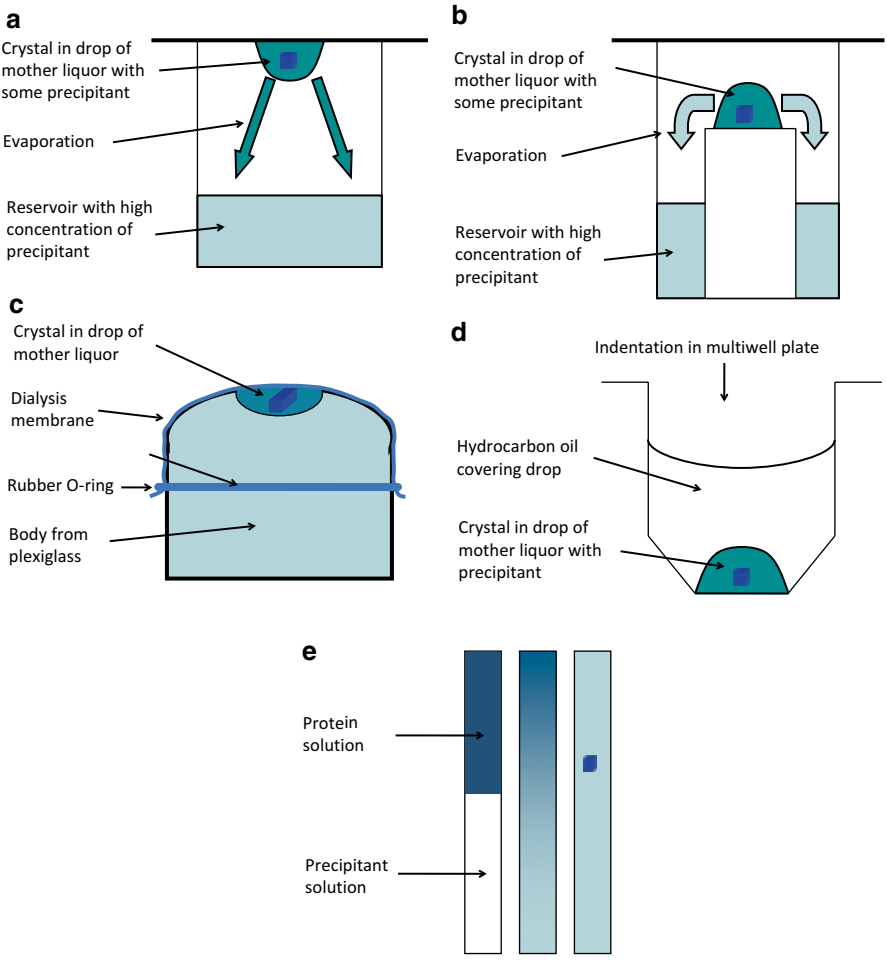

Fig. 9 Several ways to set up crystallization trials. (**a**) hanging drop vapor diffusion; (**b**) sitting drop vapor-diffusion; (**c**) dialysis button for liquid-liquid diffusion; (**d**) microbatch setup under oil; (**e**) three stages of free-interface diffusion in a capillary

In the *liquid-liquid diffusion* method a semi-permeable membrane separates sample solution from precipitant solution, which allows small reagent molecules to pass but prevents biological macromolecules from crossing the membrane. Dialysis will then slowly increase precipitant concentration inside the droplet. Dialysis buttons are typically used as shown in Fig. 9. Buttons are made from transparent material.

Batch crystallization was among the very early methods to crystallize proteins. Today this technique is very popular for initial screening setups in a micro-batch format. Very small sample droplets are covered with oil, which allows for slow evaporation of water. Contrary to many other techniques, no equilibrium will be reached, *i.e.* the drops will simply "dry out".

In the *free-interface diffusion* technique, the protein solution and the precipitant are placed into contact along a microfluidic free interface and allowed to mix by diffusion without convective flow across the interface (*43*).

Although—as stated above—success in crystallization can never be guaranteed, there are a few parameters, which should always be carefully controlled. A first and very crucial parameter is sample purity. It is almost obvious that sample purity will enhance the rate of success. Besides the chemical purity, macromolecular samples should be conformationally pure, *i.e.* they should be homogenously folded. While chemical purity can be checked with the usual biochemical techniques, conformational uniformity can be characterized with dynamic light scattering and the occurrence of a distinct three-dimensional fold can be validated by circular dichroism.

Another very crucial factor is the concentration of biomolecules. Protein samples are almost always produced recombinantly, and it can be a substantial challenge to obtain a sufficiently concentrated solution of folded recombinant protein. For initial crystallization trials, one usually aims at a concentration of about 10 mg/cm^3. Although higher concentrations—if attainable—will typically increase the chance of crystal formation, Fig. 10 shows that there are cases described in the crystallization databank where substantially lower concentrations also led to success.

Temperature is another factor, which is believed to play an important role in crystallization. Most crystals are grown at room temperature but—as shown in Fig. 10—a substantial number of crystals were also grown in the cold-room, where biomolecular samples are less prone to degradation. Other important parameters are listed in Table 1.

According to entries in the Biological Macromolecule Crystallization Database (BMCD) (*44*), 2-methylpentane-2,4-diol has so far been the most successful agent in the crystallization of biological macromolecules (*45*). However, a normalized frequency analysis of 55 reagents in random screening showed that poly(ethylene glycol) methyl ethers and poly(ethylene glycols) exhibit significantly higher crystallization propensity (*46*). This information was incorporated into commercially available crystallization screens, which are available for different kinds of biomolecular systems, such as soluble proteins, DNAs, and membrane proteins. Such commercially available screens have been optimized to cover a wide range of different conditions (*47*). They are widely used, at least for initial crystallization trials. Once such initial trials led to the identification of promising conditions, a tedious optimization process attempts to obtain parameters for well-diffracting crystals.

It frequently happens that small crystals are obtained, but it turns out to be difficult to improve their size and quality. In such cases, specialized techniques have to be applied, such as seeding methods. Three different techniques are commonly applied to improve the quality of crystals: streak-seeding (*48*), micro-seeding (*49*, *50*), and macro-seeding (*51*). The micro-seed screening opens a way to pick up

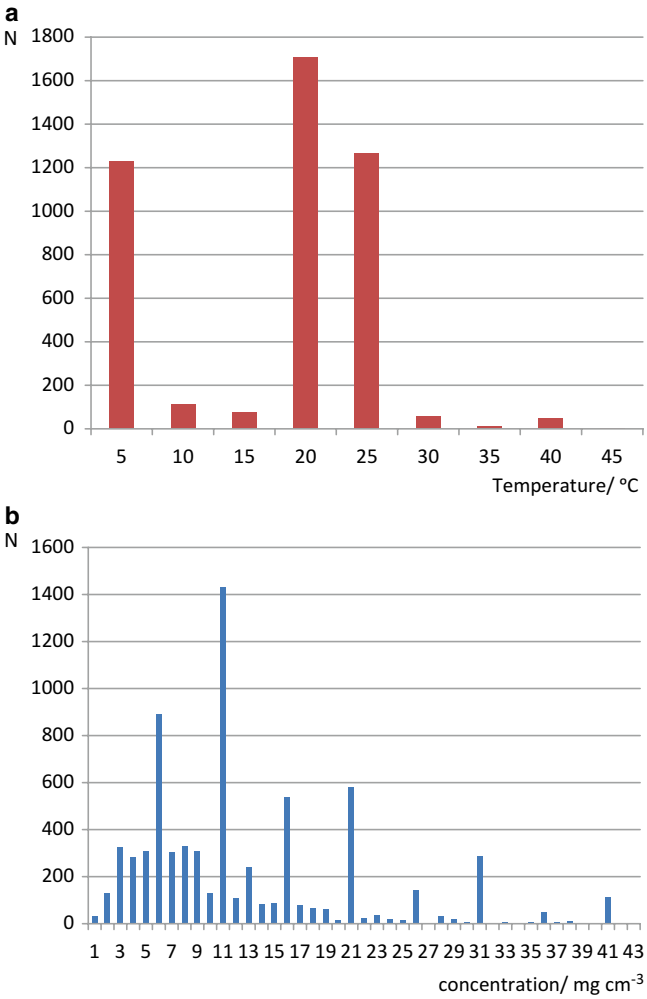

Fig. 10 (**a**) Histogram of temperatures and (**b**) of macromolecular concentrations (mg/cm^3) for crystallizations described in the crystallization databank BMCD (*44*)

entirely new crystallization conditions (*49*, *50*). Cross-seeding is a special form of micro-seeding utilizing crystals of a closely related protein (*51*). Another method with the capability to improve crystal quality is gel crystallization using either agarose gel (*52*) or silica gel (*51*).

Today, protein crystallization setups are rarely done by hand. In most cases robots and commercially available screens are used (*47*, *53*). This has the advantage of better reproducibility and shorter setup times. In many countries high-throughput crystallization centers were established, often in connection with structural genomics centers (*54*).

4.1.2 Crystallization of Membrane Proteins

Proteins integrated into or closely associated with lipid membranes pose very specific problems for crystallographers. In fact, up to 30% of all naturally occurring proteins are membrane proteins (MP), and they are of concomitantly large biological significance. Thus, approximately 50% of all approved therapeutic drugs target membrane proteins (*55*). Membrane proteins perform a wide range of biological functions including respiration, signal transduction and molecular transport. In spite of their importance, structural knowledge of membrane proteins is only a partially conquered area, which is due to difficulties in producing, solubilizing and crystallizing MP's.

The obvious difficulty is the hydrophobicity of the membrane-embedded parts, which necessitates the use of detergents during all steps of protein purification (*56*) and crystallization (*57*). Since detergents not only solubilize biomolecules but also denature them, the choice of detergents is absolutely critical, and their properties have a significant influence on the stability of MP's (*58*). Protocols for the crystallization of membrane proteins can be divided into two major groups. The surfactant based method is the traditional way of MP crystallization: mixed micelles are produced by surfactants that incorporate the protein as well as a detergent and possibly residual lipids (Fig. 11). Such water-soluble dispersions are then used for crystallization trials in the same way as soluble proteins (*59*). Naturally, the nature and concentration of detergents adds additional degrees of freedom in the search for crystallization conditions, which makes the whole enterprise much more challenging than for water-soluble proteins. Additional problems might arise as a result of inherent protein flexibility and lack of conformational homogeneity.

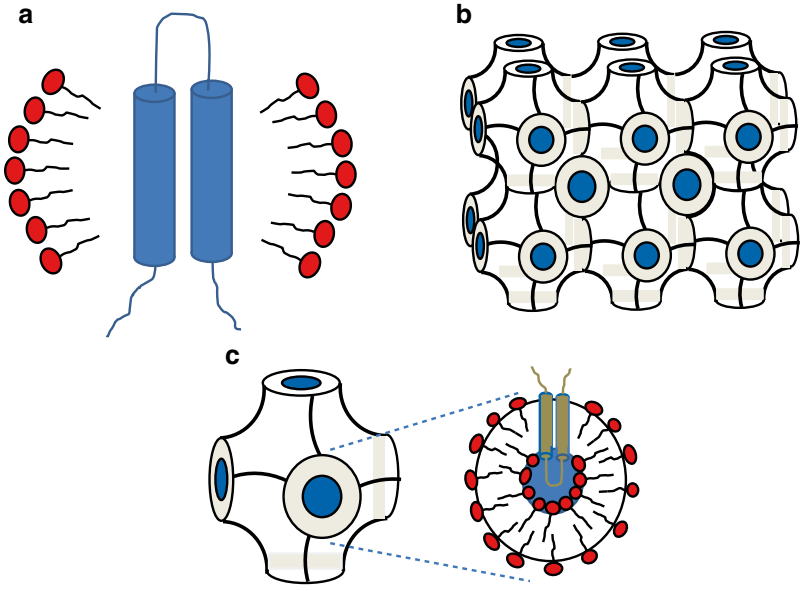

Fig. 11 (**a**) Schematic view of a solubilized membrane protein, for which the membrane-spanning regions are covered with detergent molecules; (**b**) topology of the lipid cubic phase; (**c**) mode of insertion of the membrane protein into the lipid cubic phase

The second group of techniques comprises methods using extended bilayers consisting of target protein, detergent and lipids. These are the lipid cubic phase method, the meso-phase method and the lipid sponge-phase method.

The *lipid cubic phase* method (LCP) was first described in 1996 by *Landau* and *Rosenbusch* (*60*). Lipid cubic phases are three-dimensional self-assemblies of semisolid lipid bilayers with extended water channels, where the protein is stabilized in a membrane-like environment and can be crystallized. The dimensions of these phases lie in the 6–25 nm range. Several crystal structures have been reported making use of the LCP method. A recent article describes the pros and cons and gives a survey of databases that may help for ready referral while using this method (*61*).

The *lipid mesophase* technique involves the production of an artificial lipid bilayer incorporating the protein of interest. The bilayer is formed initially in a highly ordered cubic mesophase and is shifted by addition of "precipitants" to a second mesophase from which the protein can crystallize. The difficulty lies in obtaining the initial cubic phase, which is difficult to work with, as it is extremely viscous and sticky, making it difficult to handle and to dispense accurately and reproducibly in nanoliter volumes. The advantage of the approach is that the target protein is taken out of the potentially harmful environment of a detergent micelle (in which the protein was solubilized), and is instead placed in a more natural environment. The method was first described in 2000 by *Ai* and *Caffrey* (*62*).

The *lipid sponge phase* (LSP) method (*63*) attempts to overcome the limits of the LCP methods concerning the size of proteins. Cubic phases are relatively rigid and have small pores that may cause undesired interferences between the hydrophilic parts of the protein and the LCP matrix. LSP is the liquid analogue of the LCP, which allows considerably larger sizes of the aqueous domains in membrane proteins.

To summarize, any of the methods used in MP crystallization are hampered by the immense complexity of the physical chemistry of lipid-detergent-water systems, which is well illustrated in Ref. (*64*).

4.1.3 Crystallization of Protein-DNA Complexes

In addition to the critical parameters encountered in "normal" protein crystallography, crystallization of protein-DNA complexes adds additional complications (*65*).

Proteins binding DNA are often composed of several domains with different functions. This may make them flexible and thus difficult to crystallize. It is common to restrict the structure analysis to the functional part, for which the definition is often unpredictable. A typical example is the lambda repressor, where the usual helix turn helix motif binds in the major groove (*66*) and a flexible arm wraps around the minor groove (*67*).

Length and sequence of the DNA-oligomer are obviously relevant for the success in crystallization (*68*). While the sequence should be specific for the protein partner

to enhance complex formation, it is worthwhile to try blunt ends as well as sticky ends for the DNA. The latter can polymerize to form a repetitive linear array, which potentially facilitates crystal growth (*69*, *70*). Like for proteins, DNA-oligomers should always be purified to enhance the crystallization probability. The protein/DNA ratio is crucial for the stability of the complex. Very often, a slight excess of DNA is necessary (typical is a 20% excess of DNA) because the efficiency of single stranded oligomers annealing to DNA duplex is often less than 100%.

Once the protein-DNA complex is formed, crystallization experiments follow the same scheme as "normal" protein crystallization (*51*, *71*).

4.2 Data Collection

Collection of crystallographic diffraction data is in principle a straightforward enterprise, but in fact it usually constitutes a measurement rather than an experiment. The principle of the setup is shown in Fig. 12.

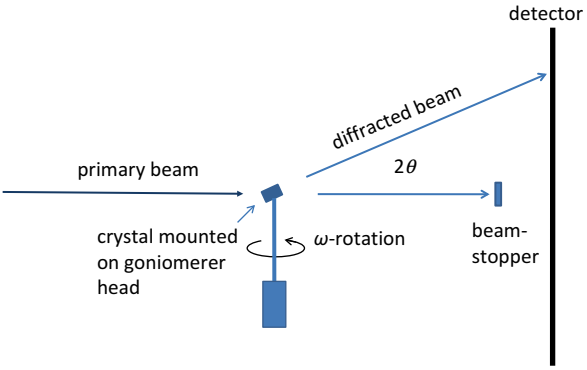

Fig. 12 Setup of a crystallographic diffraction experiment

A collimated and monochromatic X-ray beam (dimension between 0.1 mm and 0.5 mm) impinges upon the sample crystal. The diffraction produced by the crystal is recorded on a two-dimensional detector. During exposure to the X-rays, the crystal performs an oscillatory rotation in order to move reciprocal lattice points through the *Ewald* sphere. The angle of oscillation depends on the cell constants of the crystal, and it is typically between less than 1° for macromolecular crystals and a few degrees for small-molecule crystals. Exposure times vary between a few seconds and several minutes for each frame. Detector readouts are stored electronically for further processing (see above).

4.2.1 X-ray Source

4.2.1.1 Laboratory Source

Traditional X-ray sources based on the emission of X-rays from metal surfaces upon impact of high-energy electrons have been the workhorse of crystallographers for many decades. These sources offer a limited choice of wavelength, which have depended on the anode material (copper ($\lambda_{K\alpha}$=1.54Å), molybdenum ($\lambda_{K\alpha}$=0.71Å) and chromium ($\lambda_{K\alpha}$=2.29Å). Laboratory sources use either sealed tubes, which are reliable, but limited in brilliance, or rotating anodes, which have roughly one order of magnitude higher brilliance, but at the price of reduced reliability. Today, most of small-molecule crystallography is still based on sealed-tube sources, whereas macromolecular crystallographers collect their data mostly on synchrotrons. However, most laboratories still run rotating anode generators to characterize and screen crystals prior to data collection at the synchrotron.

4.2.1.2 Synchrotrons

Synchrotrons were originally constructed to accelerate charged particles for high-energy physics experiments. Some of the energy required to keep these particles—which fly with a speed close to the speed of light—in a circular path is emitted as electromagnetic radiation. While this radiation was originally considered a nuisance ("parasitic radiation"), crystallographers started during the 1980s to realize that some of its properties make synchrotron radiation an ideal source for macromolecular crystallography. Among these properties are extremely high brilliance (many orders of magnitude higher than from conventional sources) and tuneability across a large range of wavelengths. By the beginning of the 1990s, the potential of synchrotron radiation for protein crystallography had been demonstrated convincingly (*72*). In fact, synchrotron radiation was one of the main drivers of the explosive growth of macromolecular crystallography during the last two decades.

Synchrotron radiation has revolutionized macromolecular crystallography in two ways: on the one hand, its stronger and much more brilliant beam has enabled the collection of better data sets in less time, thus allowing to tackle much more complicated structures. The structure determination of the ribosome—one of the most complicated structures determined until now—would have been impossible without the availability of synchrotron sources. On the other hand, tuneability of the wavelength has enabled new ways for structure solution using anomalous diffraction data. Today, an increasing number of macromolecular structures are solved exploiting the effect of anomalous dispersion of selenomethionine, selenocysteine, metals, and even sulfur (*73*).

While in the early days of synchrotron crystallography, crystallographers were at the behest of those physicists using the synchrotron for high-energy physics experiments, the situation has changed during the last two decades. Synchrotrons dedicated and optimized for the production of X-rays were constructed worldwide (*74*), and today outnumber the instruments available for particle sciences. More than 30 synchrotrons hosting macromolecular beam-lines are currently in operation

(eight in North America, thirteen in Europe, eight in Asia), with several more under construction. Crystallographers are by no means the only users of synchrotron radiation, modern synchrotrons have dozens of dedicated beam-lines for applications ranging from spectroscopy to microscopy.

Modern synchrotrons have different kinds of crystallographic beam-lines, optimized for different crystallographic applications: beam-lines for micro crystals, beam-lines for multiple anomalous dispersion experiments, beam-lines with a "white" beam for time resolved *Laue* experiments and beam lines for the automatic collection of native data sets, *etc.* For example, the European Synchrotron Radiation Facility (ESRF) in Grenoble, France, hosts seven classic protein crystallographic beam-lines, three additional beam-lines optimized for highly automated, high-throughput sample evaluation and a *Laue* beam-line for time-resolved studies (*75*).

Automation can clearly be seen as the current trend in macromolecular data collection. Previously, a scientist was assigned one or several days of beam time, whereupon he (or she) travelled with a team of collaborators and a number of crystals to the synchrotron to collect data. Today, beam-lines are increasingly equipped with automatic sample changers. Thus, it is often sufficient to send frozen crystals by mail and control and watch the diffraction experiment over the Internet. This development dramatically increases in the number of samples that can be tested for diffraction quality before carrying out any full data collections, and it thereby helps to raise the productivity of beam-lines. For example, during the past seven years the number of structures elucidated using data collected at the ESRF has increased more than threefold (*76*).

4.2.1.3 Compton Source

This type of source is still under development. High repetition-rate lasers are used to excite oscillation in electron beams and thus generate highly directed, highly polarized and tuneable X-ray beams (*77–80*).

4.2.2 Crystal Mounting

For a small-molecule crystal, mounting is relatively straightforward: crystals—of 0.1–0.3 mm size—are typically glued to the tip of a glass fiber and mounted on a goniometer head, which allows for centering. Crystals that are unstable under ambient conditions—*e.g.* because they react with oxygen or because solvent of crystallization evaporates, which leads to crystal disintegration—are often investigated at cryo-temperature, typically at 100 K. Instrumentation allowing for cryo-cooling of a crystal during data collection by blowing a cold stream of nitrogen gas at the sample is standard on modern diffractometers (*81*).

Crystals of biological macromolecules pose special problems since they normally contain between 30 and 70% of unordered water. While this is frequently quoted as an argument that the crystalline state is very close to the state of the corresponding molecule in solution, and while it permits various soaking experiments

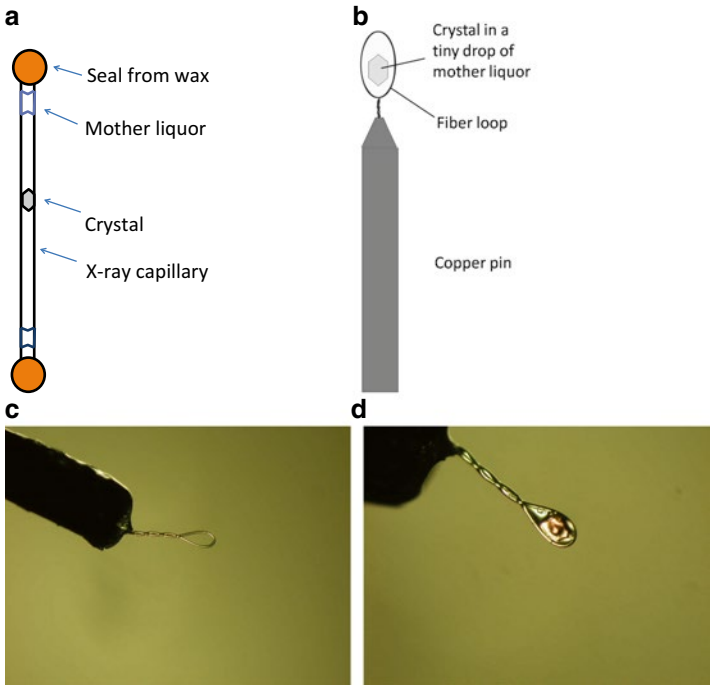

Fig. 13 Several ways to mount macromolecular crystals. (**a**) Mounting inside a thin-walled capillary to prevent their drying-out during data collection at ambient temperature; (**b**)–(**d**) mounting of macromolecular crystals for cryotemperature data collection; (**b**) principle of cryoloop; (**c**) photograph of an empty cryoloop; (**d**) photograph of a lysozyme crystal in a cryoloop

to diffuse substrates, inhibitors or heavy metals into crystals, the high water content makes macromolecular crystals unstable under ambient conditions. Water rapidly evaporates as soon as the crystal is exposed to air and the crystal will decay. The traditional way to overcome this problem has been to put the crystal inside a thin-walled capillary, next to a drop of mother liquor and hermetically sealed on both ends. Such an assembly is shown in Fig. 13a.

While mounting of the crystal in a capillary allows the collection of diffraction data under physiological conditions, it turned out that such crystals are very sensitive to radiation damage, particularly when exposed to an intense synchrotron beam. In some cases dozens of crystals were required to collect a full data set. To overcome this problem, techniques were developed to cool crystals of biological macromolecules to 100 K for data collection, which dramatically reduced the problem of radiation damage (*82*, *83*). An early success of macromolecular crystallography at cryogenic temperatures was the possibility of obtaining a full diffraction data set from one single crystal of the physically fragile and radiation-sensitive 50S ribosome particle (*84*).

The main problem that has to be overcome when cooling macromolecular crystals to cryogenic temperatures is destruction of the crystalline order through the formation of ice crystals within solvent regions. To prevent this, dipping them into

liquid nitrogen following a short soaking period in a cryoprotectant solution cools crystals very rapidly. If this is done properly, the solvent water will not crystallize but rather remains in a glass-like state. It turned out that frozen crystals not only survive longer in the X-ray beam but also frequently diffract to higher resolution through reduced thermal vibrations and reduced conformational disorder. Radiation damage still occurs even on frozen crystals, but it is reduced by orders of magnitude, since free radicals formed upon interaction with X-ray photons are prevented from diffusing through the crystal. Thus, radiation damage is reduced to the direct impact of X-rays, except for very special circumstances (*85*).

The technique of freezing crystals and collecting data at 100 K has become the standard methodology. Today, crystals are usually mounted in commercially available cryo-loops (Fig. 13), of which several variants exist, *e.g.* special loops for very small crystals and thin plates. A cryo-loop consists of a twisted nylon fiber, which is mounted to the top of a metal pin. With such a loop, a crystal is extracted from its mother liquor, transferred into a drop of cryo-protectant and—after a few seconds of soaking time—picked up again and quickly dipped into liquid nitrogen.

The conditions of flash-cooling typically have to be optimized with respect to the composition of cryoprotectant and the duration of soaking. Occasionally, flash cooling decreases the data quality (compared to data from a room temperature data collection) due to an increase in the mosaicity of the crystal. Special techniques were developed to deal with such situations.

One such technique is called *hyperquenching*, which amounts to increasing the rate of flash cooling. When a crystal is dipped into liquid nitrogen it has to pass through a zone of cold gas overlaying the liquid. The cooling process in the gas phase is much slower because of its lower heat transfer rate and thus prevents fast quenching rates. Removing the cold nitrogen gas with a stream of dry nitrogen it is possible to achieve super-fast quenching rates (*86*).

A second technique—*annealing*—does exactly the opposite. It consists in taking an already frozen crystal and subjecting it to several warming up and cooling down cycles. Occasionally, this procedure decreases the mosaicity and increases resolution. This effect is believed to be due to the relief of strain accumulated during crystal growth or during flash cooling, which improves the alignment of domains (*87*). Such a strain might also be due to a mismatch in the thermal expansion coefficients of protein and solvent (*88*). A combination of mounting crystals with cryo-loops and protection with capillaries for screening and data collection at room temperature was described by *Li et al.* (*89*).

4.2.3 Goniometer

In order to collect the complete diffraction pattern the crystal has to be turned about at least one axis during data collection. This rotation is performed by a goniometer. In the majority of cases, it is sufficient to rotate about the axis on which the pin with the crystal is mounted. This means that the rotation axis will have an accidental relationship with the reciprocal lattice, since the orientation of the crystal within the

cryo-loop is arbitrary. Nevertheless, the orientation of the crystal with respect to the goniometer rotation axis will be irrelevant in the majority of cases, and will not compromise the quality or the completeness of the data set. Thus, the majority of beam-lines are equipped with what is called a one-circle goniometer. In very special cases, *i.e.* with very large unit cell dimensions or special macroscopic crystal shapes, it can be necessary to be able to define the rotation axis relative to the reciprocal lattice vectors of the crystal. In such cases, it can be advantageous to have a three- or four-circle goniometer with κ—or *Euler* geometry, which allows for full control of the rotation axis relative to the crystal lattice vectors, thus minimizing reflection overlap in cases of very large cell constants or high crystal mosaicity.

4.2.4 Detectors

Detectors used in crystallography are almost exclusively two-dimensional area detectors, which will collect on one frame all reflections passing the *Ewald*-sphere over a small rotation range. An ideal crystallographic X-ray detector would combine several properties, such as high count rates, high detective quantum efficiency, high dynamic range, high framing rate, small pixel size, high signal to noise ratio and a small point spread function. Different types of detectors are currently used, each of them having specific pros and cons.

4.2.4.1 Imaging Plate Detector

Imaging plate (IP) detectors (*90*) are based on the principle of photo-stimulated luminescence. They consist of a flat metal plate covered with a phosphorescent layer consisting of BaFBr doped with Eu^{2+} ions. Incoming X-rays excite electrons, which are trapped in the crystal lattice of the phosphor material until stimulated by a second illumination. Thus, IP detectors "store" the incoming X-ray photons until the detector is scanned with a readout-laser, which generates stimulated emission events. The emitted photons are amplified with a photomultiplier and stored as a digital image. Before reusing the detector the plate has to be erased with white light. Although this type of detector has a high spatial resolution and an acceptable linear range, the long readout time makes them less suitable for application on synchrotrons: with exposure times in the range of seconds a readout time in the range of minutes is unacceptable. However, at the much weaker laboratory sources, the ratio between exposure time and readout time reverses, and thus IP detectors are still commonly used on laboratory sources.

4.2.4.2 CCD Detector

Charged coupled device (CCD) detectors (*91*) consist of a thin phosphor screen that converts the incident X-rays into photons. A tapered optical fiber system transmits

these photons to a CCD chip, which records them. Charged coupled device detectors have been the ultimate detector type in macromolecular crystallography for many years. The pixel size is about 10–50 μm and will be reduced further with the availability of bigger CCD chips. Compared to imaging plates, their big advantage is the short readout times in the range of one second. Today, they are still the most used detector type.

4.2.4.3 Solid State Detector

This type of detector (*92*) consists of silicon or germanium crystals that convert the incident photons (ionizing radiation) directly into electric pulses. The sensitivity of solid state detectors increases when the random formation of charge carriers by thermal vibration is suppressed, which requires their operation at the temperature of liquid nitrogen. Solid state detectors feature many advantages such as no readout noise, good signal-to-noise ratio, readout times of 5 ms, and a high dynamic range.

4.3 Data Reduction

Data reduction refers to the process of converting the raw pixel intensities of the collected detector frames to a list of scaled intensities for all $I(h,k,l)$ values inside the collected data range. This is by no means a trivial process, and has to include several iterations. In a first pass, the positions of a sufficiently large number of strong reflections are located in reciprocal space. These reflections have to be "indexed", *i.e.* reciprocal lattice vectors a^*, b^*, and c^* have to be identified, such that the position of each of the observed reflection positions are integer multiples of these reciprocal lattice vectors, *i.e.* $ha^* + kb^* + lc^*$, with h, k, and l integers. In a next step, the intensities of all reflections within the scanned section of reciprocal space are integrated and the corresponding backgrounds are subtracted. Various profile-fitting algorithms are available for this crucial step of data reduction. Following the application of various corrections, the *Laue* class of the diffraction pattern is determined, and the observed intensities of symmetry-equivalent and multiply recorded reflections are averaged.

While a program for data-reduction is typically part of the data collection software in small-molecule crystallography (where the whole process is relatively straightforward due to the relatively small cell constants), dedicated software packages exist for the reduction of macromolecular diffraction data. These include mosflm (*93*, *94*), XDS (*95*, *96*), XENGEN (*97*), d*TREK (*98*), and HKL2000/denzo-scalepack (*99*). Since each package has is specific strengths and weaknesses, most crystallographic laboratories have access to several of these program packages in order to pick the most-suited for any given problem. Major differences exist in profile fitting (two versus three dimensions) and in the capability of handling data from different goniometers and detectors.

Irrespective of the software used for data reduction, the result is a list (in the form of a computer file) of intensities and their standard deviation for each unique reflection, together with statistics about the data quality. To that end, the most frequently quoted indicator is the linear residual factor R_{merge}

$$R_{merge} = \frac{\sum_h \sum_{i=1}^{N_h} \left| I_{h_i} - \bar{I}_h \right|}{\sum_h \sum_{i=1}^{N_h} I_{h_i}} \tag{22}$$

Here, the summation over h denotes summation over all observed combinations of unique h, k, l, and the summation over i includes all symmetry equivalent or independently measured reflections h_i. N_h is thus the redundancy of reflection h. One significant drawback of R_{merge} is that it does not properly take care of redundancy. Lower redundancy will always result in lower R_{merge}, although of course higher redundancy will improve the accuracy of the intensities. The precision-indicating R-value R_{pim} is defined as

$$R_{pim} = \frac{\sum_h \left(\frac{1}{N_h - 1} \right)^{1/2} \sum_{i=1}^{N_h} \left| I_{h_i} - \bar{I}_h \right|}{\sum_h \sum_{i=1}^{N_h} I_{h_i}} \tag{23}$$

and has the property that it decreases with the average redundancy. The indicator R_{pim} is particularly useful in conjunction with anomalous diffraction data.

The anomalous R-value R_{anom} is used to estimate anomalous differences.

$$R_{anom} = 2 \frac{\sum_h \left| I_{-h} - I_{+h} \right|}{\sum_h \left(I_{-h} + I_{+h} \right)} \tag{24}$$

Naturally, the quality of a data set will increase with decreasing R_{merge} or R_{pim}. High-quality data sets have R_{merge} values in the order of a few percent. In order for anomalous data to be sufficiently significant for structure solution, the quotient R_{anom}/R_{pim} should exceed a value of 1.5 (*100*).

The completeness of a data set (expressed as a percentage of observed unique reflections to the total number of unique reflections for a given resolution) is another important quality indicator, since missing data may introduce noise in calculated density maps. The average signal/noise ratio $\langle I/\sigma(I) \rangle$ is an obvious indicator for the usefulness of data; often, the outermost shells of reflections near the resolution limit are discarded based on this indicator.

Another useful check for data quality is the so-called *Wilson* plot. For a random distribution of atoms, it can be shown (*101*) that

$$\ln\left(\frac{\langle I_h\rangle}{\sum_j \left(f_j\right)^2}\right) = -2\left(\ln(\mathrm{k}) + \mathrm{B}\sin^2\vartheta/\lambda^2\right) \tag{25}$$

Here, $\langle I_h\rangle$ is the average reflection intensity for a small $\sin\vartheta/\lambda$ range, and f_j in $\sum_j \left(f_j\right)^2$ is the atomic scattering factor of atom j for that scattering angle, with the summation running over all atoms in the unit cell. Thus, a plot of the left side of the above equation against $\sin^2\vartheta/\lambda^2$ for small resolution ranges should give a straight line with a slope of $-2B$, where B is called the overall temperature factor. Deviations from linearity in the *Wilson* plot are not uncommon—there is typically a depression at 5 Å, and low-resolution data generally do not show a linear descent—but nevertheless non-linearity outside these areas as well as a very high B-value does indicate inaccurate primary data.

Twinning is a frequently occurring and often very inconvenient phenomenon. The simplest form—macroscopic twins, *i.e.* two independent crystals mounted on the pin—is often relatively trivial to handle. It is typically detected when difficulties are encountered with indexing reflections, since the two lattices are rotationally unrelated. The most obvious solution is to repeat the data collection with a new crystal specimen, where one carefully tries to isolate a single-crystal specimen under the microscope. In favorable cases, *e.g.* if one crystal is much smaller than the other, it may be possible to index both lattices separately, and use the diffraction data of the bigger crystal. This is possible when the cell constants are not too large so that overlap of reflections from the two crystals is infrequent.

Much more difficult to deal with are forms of twinning where different domains have superimposable lattices. When the lattices of the different domains overlap in three dimensions, one speaks of merohedral twinning (*102*). This typically manifests itself by a number of "unusual" phenomena, *e.g.* the rotational symmetry of the lattice exceeds the rotational symmetry of the crystal space group, the metric symmetry of the cell parameters is higher than the *Laue* symmetry, implausible or unusual systematic absences, inconsistent reflection statistics, *etc.*

In the special case of hemihedral twinning (*102*), when there are two domains, each observed diffraction intensity is a weighted sum of two crystallographically distinct, twin-related, reflections. Once the problem has been recognized, it may be possible to "detwin" the data. To that end, one has to determine the twin factor, *i.e.* the volume ratio of the two domains, and the "twinning law", *i.e.* the transformation between the twin-related reflections. If the twin-factor equals one-half—a situation called "perfect twinning"—the observed diffraction pattern acquires the additional symmetry imposed by the twinning operation, and the true crystallographic intensities cannot be recovered from the observed measurements.

Unless the statistics from data reduction are inspected carefully, twinning can easily be overlooked, and will manifest itself by difficulties with structure solution. Data reduction programs often include a test for crystal twinning and offer the option to de-twin data (*103*).

Another question, typically emerging at the data reduction stage, is the number of molecules per asymmetric unit. Very often more than one molecule connected by non-crystallographic symmetry (NCS) is present in the asymmetric unit. A first indication is obtained typically by a calculation of the *Matthews* coefficient (*104*, *105*), which predicts the number of molecules per asymmetric unit based on the average density of proteins. To calculate this quantity, only the cell constants, the molecular mass and the space group have to be known. More conclusive evidence is provided by calculation of a self rotation function (*106*), which will show a maximum at the rotation angle of the non-crystallographic symmetry element, *e.g.* at 180° for a twofold NCS like that shown in Fig. 14.

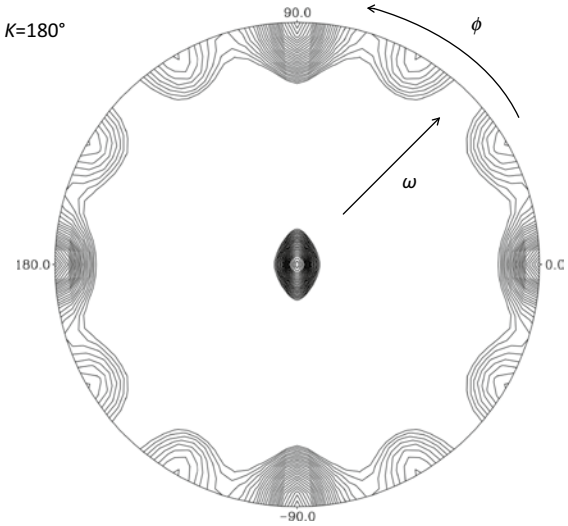

Fig. 14 Self rotation function of the *sec*-alkylsulfatase Pisa1 (pdb 2yhe), indicating the presence of a non-crystallographic two-fold rotation axis. The self rotation function denotes the overlap between the *Patterson* function and the same *Patterson* function rotated by an angle κ. The diagram shows the value of the self-rotation function for a rotation angle of 180° ($\kappa = 180°$) about an axis for which the orientation is described by the inclination angle ω (corresponding to the radial distance from the origin in the above diagram) and the azimuth angle φ (defined by an anticlockwise rotation about an axis normal to the plane of the paper)

The occurrence of non-crystallographic symmetry is generally considered an advantage in macromolecular crystallography, since it can help in the structure solution and refinement steps. Problems in structure solution and refinement might arise, however, as a consequence of special NCS, which results in pseudo symmetry (*107*, *108*). Translational pseudo symmetry is observed in crystals where the NCS axis is

nearly parallel to a crystallographic symmetry axis. Careful inspection of a native *Patterson* map can reveal pseudo symmetries. Rotational pseudo-symmetry originates from the point-group symmetry of the lattice being higher than the point group symmetry of the crystal. This may be caused by a NCS operator parallel to the symmetry operator of a lattice, which is not also a symmetry operator of the crystal (*108*).

4.3.1 Challenges in Data Reduction

Crystals with large unit cell dimensions (>500 Å) are still a challenge for data collection and data reduction. Spots tend to overlap even with small oscillation angles, and indexing errors are common. Programs for overlap correction exist, mainly implemented in data collected using "white" beams in the *Laue* technique (see below). A common and straightforward approach in such cases is to collect data with very small oscillation angles (fine slicing) and use data reduction programs applying three dimensional profile fitting (*93–96*).

4.4 Solving the Structure: The Phase Problem

Structure solution refers to the process of finding an initial set of approximate phases $\varphi_1(h,k,l)$ that are close enough to the "true" phases to show most of the relevant features of the crystal structure. These features should emerge from an electron density calculation of the form

$$\rho_1(X,Y,Z) = \sum_h \sum_k \sum_l \left|F(h,k,l)\right| e^{2\pi i \varphi_1(h,k,l)} e^{-2\pi i(hX+kY+lZ)} \tag{26}$$

A subsequent structure factor calculation with the features observed in ρ_1 will yield new phases $\varphi_2(h,k,l)$, leading to electron density ρ_2 hopefully showing features missing in ρ_1. In principle, this cyclic process is repeated until all features (*i.e.* atomic positions) of the crystal structure have been identified, although in reality the process may be more elaborate.

The phase problem—the fact that for each observed structure factor $|F(h,k,l)|$ a phase $\varphi_2(h,k,l)$ is unknown—seems to be unsolvable *prima vista*, although in a paradox way: the more structure factors are observed, the more phases are lacking. This paradox seems to be aggravated by the observation that the phases are much more relevant to show the correct structural features than are the structure factors. It is easy to demonstrate (Fig. 15) that a density calculation with random structure factors and correct phases will display the more or less correct structure, while the inverse—a summation with correct structure amplitudes and random phases—will invariably show nothing but noise.

This pessimistic view can be brightened up by the following consideration: for an average small-molecule crystal structure with say 30 non-hydrogen atoms in the

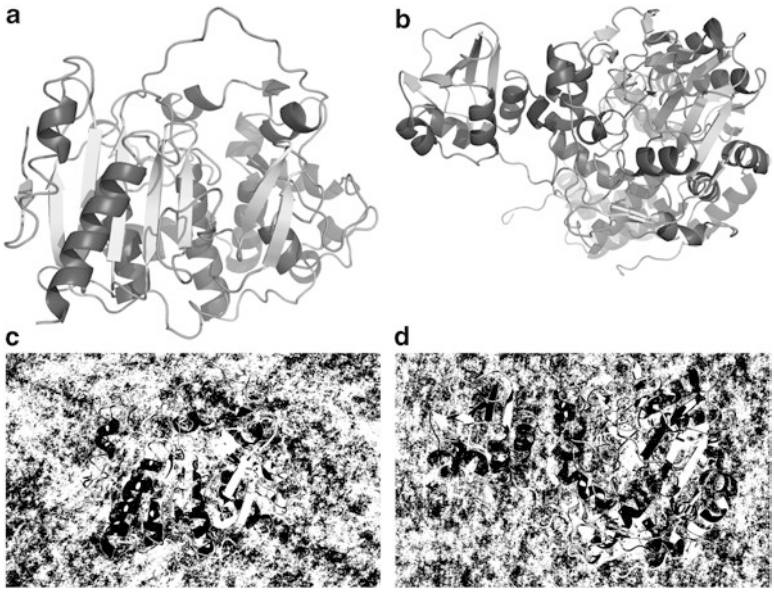

Fig. 15 Illustration of the fact that phases are more important than amplitudes. (**a**) image of the esterase 3zyt; (**b**) image of the sulfatase 2yhe; (**c**) image generated with phases from the esterase and amplitudes from the sulfatase; (**d**) image generated with phases from the sulfatase and amplitudes from the esterase

asymmetric unit, the electron density can be described to a first approximation by the atomic positions of these 30 atoms, *i.e.* by 90 parameters. The number of independent intensity observations is, however, at least ten times larger when data have been collected to atomic resolution. Thus, the problem is—at least in small-molecule crystallography—heavily over-determined.

4.4.1 Direct Methods

An electron density map computed with observed structure factors and random phases will yield a physically unrealistic density: it will almost invariably show regions of negative density, and it will show peaks that are unrealistically close together. In other words, physically plausible densities pose restrictions on the phases, which can in fact be exploited to calculate phases. The methodology derived from such considerations—the mathematics of which is rather involved—is called direct methods, and it has indeed revolutionized small-molecule crystallography (see (*109*) and references therein).

For simplicity, the following brief theoretical sketch will be limited to centrosymmetric structures, where the phase problem reduces to a problem of sign. Analogous equations also exist for non-centrosymmetric structures. As early as 1952, *Sayre* could show that

$$F(h,k,l) = \Omega(h,k,l) \sum_{h'} \sum_{k'} \sum_{l'} F(h',k',l') F(h-h',k-k',l-l') \tag{27}$$

In this equation, $\Omega(h,k,l)$ is a readily computable scale factor. To compute the amplitude and phase of one reflection, amplitudes and phases of all reflections for which indices add up to (h,k,l) have to be known. However, this *Sayre* equation is useful as a check for consistency of a set of phases, and there are computer programs that generate a large number of random phase sets and check their consistency using the *Sayre* equation (*110*).

While the *Sayre* equation is an exact equation, it is possible to derive from it a number of approximate equations of the form

$$s(h,k,l) \cdot s(h',k',l') \cdot s(h-h',k-k',l-l') \approx +1 \tag{28}$$

Where $s(h,k,l)$ is the sign of $F(h,k,l)$. The probability that this equation is correct is proportional to the magnitude of the three structure factors

$$p(+) \propto \left| F(h,k,l) \cdot F(h',k',l') \cdot F(h-h',k-k',l-l') \right| \tag{29}$$

Computer programs for direct methods generate a large number of triples of reflections with the property that the indices of one reflection equal the sum of the indices of the other two reflections. The program then tries to find a consistent set of phases satisfying as many of the above equations with high probability as possible. Solutions of direct methods programs are by its very nature potential solutions of the phase problem, which have to be validated by electron density calculations showing a refineable structure.

The theoretical foundations for the direct methods were pioneered by *Gerhard Hauptman*, *Jerome Karle*, and his wife *Isabella*, for which *Hauptmann* and *Karle* received the *Nobel* Prize in Chemistry in 1984. The implementation of this methodology into appropriate computer software (*111*) has rendered the phase problem almost a triviality for small molecules, up to a size of 1,000 atoms in the asymmetric unit (*112*–*114*), diffracting to atomic resolution (1.2 Å or better).[5]

In contrast to small-molecule crystallography, direct methods have so far played a minor role in structural biology, due to the high complexity of structures, which typically diffract to lower resolution. Exceptional cases include the recent structure solution making use of 1.95 Å data (*115*). Here, a combination of localizing fragments with Phaser (*116*) and density modification with SHELXE (*117*) were employed. Nevertheless, structural biology usually has to employ different means to solve the phase problem. The most relevant ones involve the use of a model (molecular replacement) or additional diffraction experiments to obtain experimental phases.

[5] A frequently cited criterion for atomic resolution requests that 50% of the reflections between 1.2 and 1.1 Å have to be observed above 3σ.

4.4.2 Molecular Replacement

If the three-dimensional structure of a molecule is known, the problem of structure solution reduces to finding its orientation and its location within the unit cell (*118*). This is the conceptual basis of molecular replacement, which was found to be a powerful tool to solve the phase problem even for search molecules, which are not identical but only similar to the one present in the crystal. Molecular replacement is a very powerful and robust technique as long as a good search model is available (see below). The obvious problem with this technique is to find such a model for an as yet "unknown" structure.

4.4.2.1 The Search Model

In many cases, the choice of the search model is easy: if the structure is already known and should be solved for a new crystal form, or if the structure of a homolog from another organism is known, the search model is obvious. A more difficult situation exists if one deals with a "new" structure, although the structure is unlikely to display an entirely unknown fold: Fig. 16 shows the number of new folds deposited in the Protein Data Bank (PDB) each year, plus the total number of different folds present in the data bank. It is obvious that in spite of several thousand new structures deposited each year, the number of distinctly different folds appears to have stagnated around 1,400. Thus, for any new peptide under scrutiny, it is very likely that it is comprised of already known folds contained in the PDB.

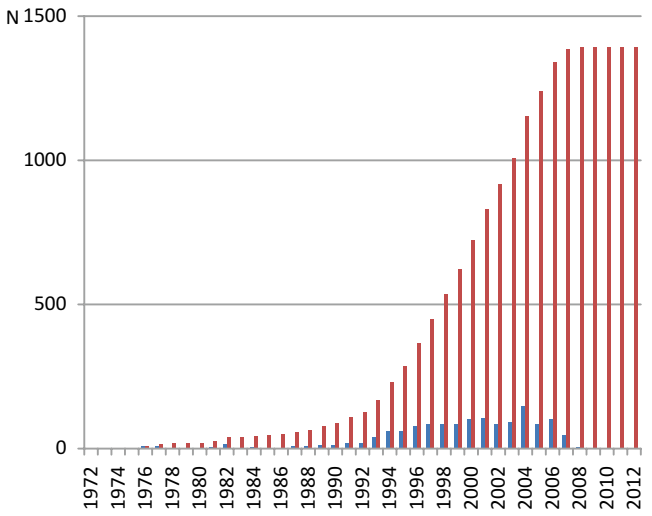

Fig. 16 Number of new folds in the annually deposited structures (*blue*) and total number of distinct folds in the data base (*red*). Data from RCSB Protein Data Bank

The easiest way is to perform a BLAST (*119*) search for structures with high sequence identity to the target molecule, since high identity invariably implies a close structural relationship. As a rule of thumb, models with sequence identity to the target exceeding 35% are very likely to enable structure solution. When provided with a sequence alignment obtained from BLAST or FASTA (*120*), the program MODELLER (*121*) is frequently used to build a model for the target molecule, applying special restraints and loop modeling. However, it is a common experience that molecules with low sequence identity might as well exhibit a highly homologous three-dimensional structure. Thus, in cases where no models with high sequence identity are available, one has to resort to fold-recognition algorithms implemented in several programs (*122*–*125*) to predict models with structural similarity. Other programs prepare different variants of search models (*126*, *127*) or perturb the models in the direction of one or two normal modes (*128*, *129*). The JCSGMR pipeline (*130*) comprises model building, integrated phasing and automated refinement.

In cases where no substantial sequence identity to a known structure exists, chances critically depend on the state of affairs in model prediction. Available software has continuously improved during the past decades. The Protein Structure Prediction Center (*131*) regularly organizes Critical Assessment of Protein Structure Prediction (CASP) experiments "to provide the means of objective testing of these methods *via* the process of blind prediction". The sequences of unpublished protein structures are used as targets for structure prediction. The outcomes are compared with the actual structures and thus establish the current state of the art in protein structure prediction. CASP-1 was held in 1994 and the most recent one, CASP-10, in 2012 (*132*).

4.4.2.2 The Technicalities of Molecular Replacement

Prerequisites for structure solution using MR are a good search model and data as complete as possible. Particularly important are low-order reflections, whose absence may compromise the success of structure solution.

Placing the search model into the unit cell in the right orientation and at the right location is in principle a six-dimensional problem (searching three rotation angles and three translation vectors), which would require substantial computational resources. Therefore, most programs use the so-called "divide-and-conquer" strategy, where the six-dimensional search is broken up into a three-dimensional rotation search followed by a three-dimensional translation search.

Molecular replacement programs traditionally compute rotation and translation functions in *Patterson* space. Different cutoffs are applied in order to reduce the noise: thus, the rotation function involves intramolecular vectors, whereas the translation search involves intermolecular vectors. Most programs apply the fast rotation function, based on an algorithm originally developed by *Crowther* (*133*) and later improved by *Navaza* (*134*). Although this approach usually works well, problems arise if more than one copy of the molecule is in the asymmetric unit. In such cases the relative contribution of each monomer decreases, and the signal might become undetectable. This situation can be improved if one succeeds in

finding non-crystallographic symmetry (NCS) in a self rotation function. A predefined NCS axis decreases the search space and thus increases the signal to noise ratio. The programs MOLREP (*135*) and AMORE (*134*) use this strategy.

If the search model has internal degrees of flexibility a *Patterson*-correlation (PC) refinement may improve the initial rotation solution and hence improve the chances of succeeding in the subsequent step. Variable domains are considered as rigid bodies, which can move relative to one another. *Patterson*-correlation refinement is implemented in the programs BRUTE (*136*) and CNS (*137*) and yielded admirable results (*138*).

Likelihood-based target functions instead of *Patterson* functions have become more popular recently. Each likelihood-based function tests whether an orientation for the search model is consistent with the data and tends to give better results. Programs like PHASER (*116*) and BEAST (*139*) are based on this method. Given a target sequence and experimental structure factors, the molecular replacement pipeline MrBUMP (*140*) will search for homologous structures, create a set of suitable search models from the template structures, do molecular replacement, and test the solutions with several rounds of restrained refinement. Recently, a new method using a combination of the molecular replacement tools of Phenix and integrated Rosetta structure modeling with autobuild chain tracing was presented (*141*), and shown to succeed in an example with only 18% sequence identity to the model.

Six-dimensional searches are an ultimate resort if the traditional methods fail. CNS (*137*) and BEAST (*139*) provide facilities for doing six-dimensional searches with the obvious drawback of long computing times. The program EPMR (*142*) employs a "Genetic Algorithm" that speeds up the six-dimensional search to an acceptable level.

The main challenge in molecular replacement continues to be the search for appropriate models, as well as methodological aspects, such as minimization steps during refinement (*141*, *143*). The ultimate ambition would be to input a sequence and obtain the solved structure even in cases of low sequence similarity. This aim is still far away.

4.4.3 Experimental Structure Solution

In cases where molecular replacement fails, one has to resort to experimental methods to determine phases, which are necessarily more involved.

4.4.3.1 Multiple Isomorphous Replacement

For many years, multiple isomorphous replacement (MIR) has been the standard method to solve the crystal structure of biological macromolecules. No previous knowledge about the three-dimensional structure is necessary. The concept of the method is to insert one or several atoms into well-defined locations in the crystal structure of a biomolecule, without changing the remainder of the structure

(isomorphous replacement). If the introduced atom(s) have a detectable effect on the diffraction of the crystal, *i.e.* if the intensities observed in the "derivative" data set differ detectably from the ones of the "native" data set, the observed differences can be used to extract phase information, as described below.

Biomolecules and natural products in general consist primarily of atoms from the first and—to a much lesser extent (sulfur and phosphorus)—from the second row of the periodic system. Since the contribution of an atom to the structure factor is proportional to the number of electrons (hence the contribution to the scattered intensity is roughly proportional to the square of the number of electrons), a heavy metal atom (such as mercury or gold) can make a substantial difference to the scattered intensities, if the atom is well ordered and the site has high occupancy. The rule of *Crick* and *Magdoff* (*144*) helps to estimate the height of the isomorphous signal considering the number of electrons and the occupancy of the heavy atom in relation to the size of the protein.

To a first approximation, the diffraction of the macromolecule with an ordered heavy atom equals the sum of the native structure contribution plus the heavy atom contribution, *i.e.* $F_{PA} = F_P + F_A$.

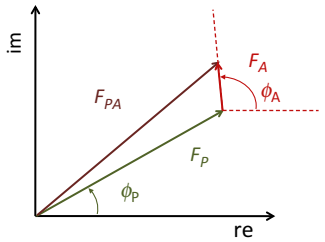

Fig. 17 Contribution of the heavy atom (F_A) to the native structure factor (F_P) to yield the structure factor of the derivative structure (F_{PA})

It is obvious from Fig. 17 that this relationship is true for the complex structure factors, but not for their amplitudes, *i.e.* $|F_A| \neq |F_{PA}| - |F_P|$, keeping in mind that $|F_P|$ and $|F_{PA}|$ are values obtained through data collection of the native protein and the isomorphous heavy atom derivative, respectively (note that $|F_P|$ and $|F_{PA}|$ denote the full datasets, encompassing all values of h, k, l). Nevertheless, the absolute differences in structure amplitudes from derivative and native datasets seem to be a sufficiently good approximation to the amplitudes of the heavy-atom contribution that a *Patterson* map using $|F_{PA}| - |F_P|$ will reveal the position of the heavy atom(s), which then allows computation of the complex structure factor F_H. Alternatively, the heavy atom position(s) may also be obtained by direct methods.

Knowledge of F_A, $|F_P|$, and $|F_{PA}|$ opens the way to obtain phase information, as shown in Fig. 18. The first circle with its center at the origin has a radius with the length $|F_P|$. The phase is unknown at this point, and therefore may take any value. The second circle with radius $|F_{PA}|$ has its center shifted from the origin by $-F_A$. Thus, each of the intersections of the two circles fulfills the condition, $F_{PA} = F_P + F_A$, *i.e.* the phase of F_P cannot be determined unambiguously from one heavy atom

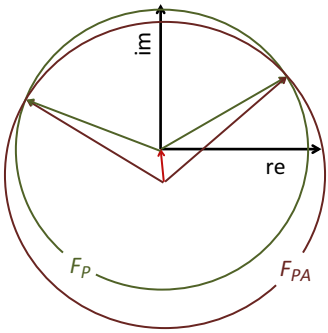

Fig. 18 Geometric construction showing that a heavy atom derivative reduces the phase ambiguity to two possible values

derivative, but it can be narrowed down to two possibilities. Therefore, at least a second independent heavy atom derivative is required in order to solve the phase problem unambiguously.

In practice, a probability mass function (*145*, *146*) is used to calculate the highest probability for each phase angle. The position of the heavy atom has to be refined further in order to get an interpretable electron density map. General problems are lack of isomorphism between native and derivative crystal and low occupancy of the heavy atom.

4.4.3.2 Single Isomorphous Replacement

The starting position is the same as with MIR, but only one derivative is used. As shown above, each structure factor has a phase ambiguity of 2. Figure 19 shows that the two solutions are symmetrically ordered around the single isomorphous replacement (SIR) centroid phase F_{SIR}, with F_{SIR} collinear to F_A. A map reconstructed using SIR centroid phases will have contribution from 50% wrong phases and 50% right phases, with the latter ones smeared by experimental error. It is not possible to build a model based on this map, but density modification techniques (see below) may substantially improve such maps to allow correct model building.

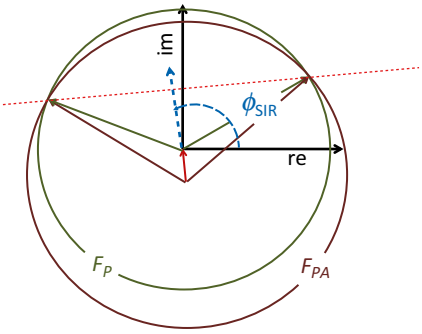

Fig. 19 Phase determination with the Single Isomorphous Derivative method

4.4.3.3 Anomalous Dispersion

Atoms having absorption edges close to the X-ray wavelength are called anomalous scatterers. As shown in equation (17), their atomic scattering factors are complex quantities. Figure 20 shows that the presence of such atoms in a crystal structure leads to a breakdown of *Friedel*'s law. It is easy to demonstrate—similar to the case of an isomorphous heavy atom—that this can be used to extract phase information, as shown in Fig. 21. Assuming that the position of the heavy atom is known [which is typically the case when the anomalous scattering stems from an isomorphous heavy atom (SIRAS—single isomorphous replacement with anomalous scattering)], the two structure factors $F_A(+)$ and $F_A(-)$ are known, together with the amplitudes $|F_P|$, $|F_{PA}(+)|$ and $|F_{PA}(-)|$. The intersection of circles with radii $|F_{PA}(+)|$ and $|F_{PA}(-)|$ with the one with radius $|F_P|$ yields four possible values for phases, two for $|F_{PA}(+)|$ and two for $|F_{PA}(-)|$. It has to be stressed at that point that the anomalous "signal" is much weaker than a typical signal from an isomorphous derivative,

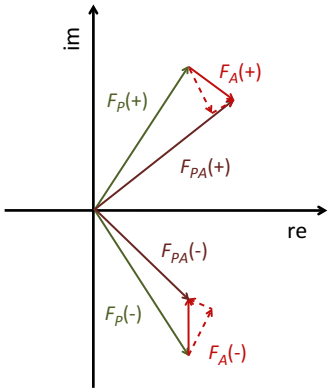

Fig. 20 Anomalous scattering leads to a breakdown of *Friedel*'s law. Note that the anomalous contribution of the heavy atom is exaggerated

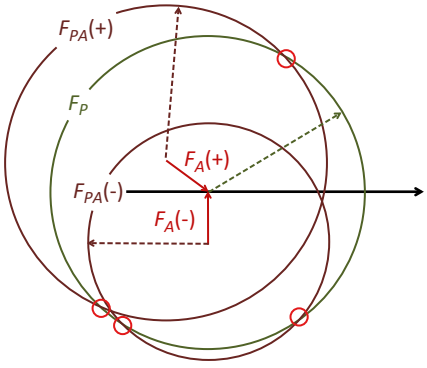

Fig. 21 Phasing in a SIRAS experiment

hence the differences between the intensity of the *Bijvoet* pairs have to be collected with high accuracy and redundancy. A modified rule by *Hedrickson* and *Teeter* (*147*) helps to estimate the strength of the anomalous signal.

Atoms used for anomalous diffraction include the usual heavy atoms (Ag, Hg, *etc.*). A particularly interesting element is selenium, which can be introduced covalently into proteins by expression with selenomethionine instead of methionine (*148*). Selenium has a reasonably strong anomalous signal, and incorporation into proteins as selenomethionine usually does not affect the protein fold. Among the elements present in native proteins, sulfur is the only one suitable for anomalous phasing (*147*, *149*), although its anomalous signal is very weak and long wavelengths have to be employed.

A particularly elegant way to solve the phase problem is the MAD (multi-wavelength anomalous diffraction) technique. This technique requires only a crystal of the heavy-atom labeled biomolecule, *e.g.* of a protein expressed with selenomethionine. The concept of the technique is based on collecting data at different wavelengths, so that the wavelength-dependent contributions to the heavy-atom atomic form factor have different magnitudes, *i.e.* the anomalous diffraction can be "switched on" and "switched off" by changing the wavelength. A "full" MAD experiment starts with a "fluorescence scan", *i.e.* the recording of the fluorescence spectrum of the heavy atom within the crystal. Data are then collected at wavelengths corresponding to the peak of the spectrum, to the point of inflection and at a "remote" wavelength. In reality, one is usually satisfied with collecting peak and remote data.

When using only *Bijvoet* pairs collected at one wavelength (SAD—single anomalous diffraction) the same problem will arise as in the case of SIR, *i.e.* there are two possible phase values for each structure factor. Again, a map calculated with the centroid SAD phase will be uninterpretable, but density modification often yields interpretable maps. SAD phasing works best when the solvent content is high and good data to 2.5 Å resolution or better are available. Recently, the structure of a lysosomal 66.3 kDa protein from mouse was solved through sulfur *de novo* SAD phasing (*149*).

4.4.4 Density Modification and NCS Averaging

Once a very approximate structural model has been obtained, there are rather powerful techniques available to improve phases. Thus, if the density is still largely uninterpretable but it is possible to see a clear distinction between solvent and the protein region, useful phase information can be extracted from the fact that the density is essentially flat within the solvent region. A number of techniques have been developed along such considerations, known as solvent flattening, histogram matching, and solvent flipping (*150*). Application of these algorithms can indeed improve the phases dramatically leading to an interpretable map. Similarly, if there are several molecules in the asymmetric unit related by non-crystallographic symmetry,

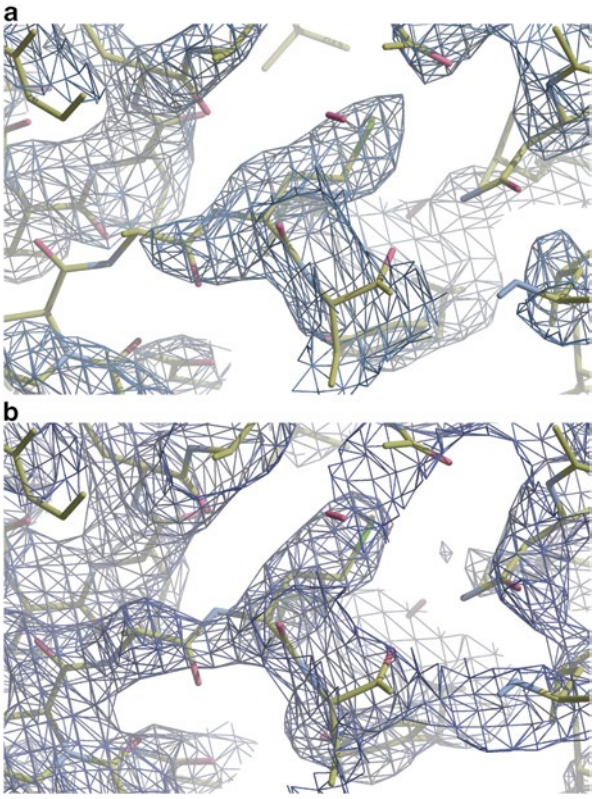

Fig. 22 The effect of solvent flattening and/or NCS averaging on the map interpretability. (**a**) COOT (*155*) electron density map after MAD solution with solve (*146*) and (**b**) after density modification with resolve (*306*). The chain corresponds to the final model

phases can be improved by NCS averaging. The effect of solvent flattening and/or NCS averaging on the map interpretability is shown in Fig. 22.

Although solving the phase problem has become a nearly automated process in "simple" cases, it can still be very challenging in less trivial ones, where crystallographic experience is required to prevent wasting time with false solutions. It is one of the puzzling features of crystallography that it is easy to recognize the correct structure solution once obtained, but it may be very hard to recognize a partially correct solution and to decide whether structure solution is progressing in the right direction.

4.5 Model Building and Refinement

In small-molecule crystallography, "model building" is mostly a trivial process: from the density computed with phases obtained by direct methods, atomic

positions are deduced and assembled to chemically reasonable molecules. Since from atomic-resolution data such atomic positions are readily identifiable, this process is largely automatic. The researcher typically has to decide whether the structure is "complete", or whether there are missing atoms, which have to be identified in a map computed with phases calculated from the incomplete molecular fragment, as described above. Once the structure is "complete", it will be subjected to least-squares refinement, as described below.

For macromolecular crystallography, life is not so easy. Due to the inherently much poorer resolution—atomic resolution is exceptional, particularly at the early stages of structure solution—the process of fitting a molecular model into the density obtained from (still erroneous) experimental phases can be a very demanding undertaking. In addition to poor resolution, experimental phases suffer from errors as a consequence of inaccurate heavy atom position and incomplete occupancy. For many years, models had to be built by hand—on a graphics terminal—into a map obtained from experimental phases, requiring much experience to recognize secondary structure elements and find a continuous main chain. Today, sophisticated software exists (ARP/WARP (*151*), resolve (*152*) or buccaneer (*153*, *154*)) to build initial models, reducing the need for manual intervention to problem regions. If the structure was solved initially by molecular replacement, a model—though probably wrong in places—already exists. In any case, these incomplete and/or inaccurate initial models are subjected to further improvement and refinement.

Structure refinement is an iterative process in macromolecular crystallography, where model building into the electron density (in an automatic way or "by hand") alternate with restrained least-squares refinement of the model parameters. Model building involves the use of interactive graphics programs that allow fitting residues into three-dimensional calculated electron density maps. Commonly used interactive graphics programs are COOT (*155*), O (*156*) and xfit (*157*). Two types of maps are used for graphical fitting: $F_o - F_c$ and $nF_o - mF_c$ where n and m comprise integers and $n > m$. The implication is shown in Fig. 23. A variety of methods exists to improve phases by minimizing bias, such as sigma A weighting (*158*), shake and bake (*159*), *etc.*

4.5.1 Least-Squares Refinement

Refinement refers to the process of fitting model parameters to experimental observations, usually by applying a least-squares condition. In crystallography, the complexity of the model to be adopted depends on the crystallographic resolution, *i.e.* on the number of significant observations. In small-molecule crystallography, where data almost invariably extend to atomic resolution (<1.2 Å), the crystallographic model involves three positional coordinates for each atom in the asymmetric unit ($X_i, Y_i, Z_i, i = 1 \ldots N$), and at least one parameter ("temperature factor") per atom accounting for deviations of the atom from its mean position. This "smearing out" is described by convoluting the density with a *Gaussian* function, which can have

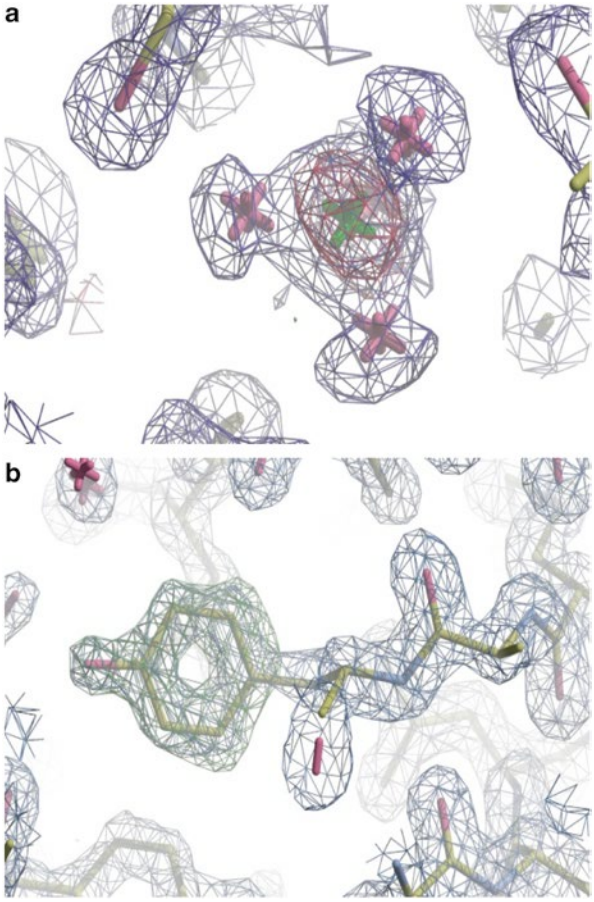

Fig. 23 $F_o - F_c$ versus $2F_o - F_c$ maps. Parts of the electron density from a molybdenum binding protein (pdb code: 1FR3, (*307*)) drawn in the program COOT (*155*). The *2Fo–Fc* map is colored in *blue*, the *red* map comprises the negative and the *green* map the positive *Fo–Fc* map. (**a**) The molybdenum binding site calculated with full occupancy of the metal, while the actual occupancy is only 50%. (**b**) A tyrosine that was refined as an alanine

spherical symmetry ("isotropic temperature factor", one parameter per atom) or ellipsoidal symmetry ("anisotropic temperature factor", six parameters per atom). For such a model, a structure factor calculation has the following form

$$F_{calc}\left(h,k,l\right) = \sum_{i=0}^{n} f_i e^{2\pi i\left(hX_i + kY_i + lZ_i\right)} T_i\left(h,k,l\right) \tag{30}$$

Here, $T_i(h,k,l)$ is the temperature factor of atom i, which has different mathematical expressions for the isotropic (one parameter) or the anisotropic (six parameters) case.

Least-squares refinement then involves finding "optimum" values for each parameter subject to the condition that

$$D = \sum_{hkl} \Delta_i^2 = \sum_{hkl} (|F_{obs}(h,k,l) - F_{calc}(h,k,l|)^2 = \min \tag{31}$$

Least-squares refinement is a straightforward enterprise for linear problems. However, the structure factor calculation is a highly non-linear equation. Therefore, it has to be linearized by *Taylor* expansion, which is only valid near the minimum. Accordingly, least-squares is unsuitable to find a structure solution, since it can only improve an already "correct" structure. Due to the approximate nature of the *Taylor* expansion, refinement has to be performed in cycles, which will converge if the starting point was reasonable. The result of the least-squares refinement affords least-squares estimators $<p_i>$ for each parameter p_i, together with a standard deviation $\sigma(p_i)$.

It is common in crystallography to quote a quality index for the result of a refinement. The best-known index is the crystallographic *R*-value defined as follows

$$R = \frac{\sum_{hkl} \left| |F_{obs}(hkl)| - \kappa |F_{calc}(hkl)| \right|}{\sum_{hkl} |F_{obs}(hkl)|} \tag{32}$$

Here κ is a scale factor. The correlation factor, which has the advantage of being independent of the scale factor, is defined as follows:

$$CC_F = \frac{\sum_{hkl} |F_{obs}(hkl) - \bar{F}_{obs}| \cdot |F_{calc}(hkl) - \bar{F}_{calc}|}{\left(\sum_{hkl} |F_{obs}(hkl) - \bar{F}_{obs}|^2 \cdot |F_{calc}(hkl) - \bar{F}_{calc}|^2 \right)^{1/2}} \tag{33}$$

In small-molecule crystallography, *R* values below 5% are quite common, with observables-to-parameter ratios of ten or higher.

4.5.2 Restrained Refinement

Refinement of small molecules is usually straightforward on the basis of the of observed reflection intensities alone, due to the large observations/parameter ratio. This is radically different in macromolecular crystallography, where this ratio often does not substantially exceed unity. Unrestrained least-squares refinement is not possible under such conditions. Remedies have been devised, the simplest one being to restrain the refinement by adding an appropriate term to equation (31), which punishes deviations from ideal geometry. This is then referred to as "restrained refinement". The relative weights of the part of the target function based on experimental data and the one based on deviations from ideal geometry is of course a non-trivial question, which depends very much on the quality and completeness of

experimental observations. An alternative—though much less popular—way to prevent the structure from assuming an unreasonable geometry during least-squares refinement is to introduce constraints, which amounts to enforcing geometric parameters to exactly maintain ideal values during refinement. Evidently, the complexity of the crystallographic model has to be adapted to the available data, which means in reality that atomic displacement parameters are limited to isotropic librational parameters, at best.

One problem in the refinement of macromolecular structures against "insufficient" data is "overfitting", meaning that the residual R in fact decreases although the model gets worse. This led to the introduction of the free R value R_{free} and the free correlation coefficient: After data reduction, about 5% of randomly chosen reflections are "set aside", *i.e.* they are not included in refinement, but are just used as a cross validation tool. The residual calculated for these reflections is called R_{free}. Compared to the residual computed from reflections included in the refinement, R_{free} is always higher, but the difference between R and R_{free} should not exceed five percent at the end of refinement.

An alternative and complementary refinement algorithm is called real space refinement (*160*, *161*). Here, the target function is the deviation between experimental electron density and electron density computed for a molecular model, for which the geometry is heavily constrained. Thus, the function minimized is of the form

$$f = \int_V \left(\varrho_o(XYZ) - \rho_c(XYZ) \right)^2 d^3V \tag{34}$$

Here, $\varrho_o(XYZ)$ is the "observed" density, *i.e.* the density calculated with the available phases, and $\rho_c(XYZ)$ is the model density. More sophisticated refinement tools, such as maximum likelihood refinement algorithms (*162*, *163*) have been used increasingly in recent years.

4.6 Structure Validation

Technically, the final step in the elucidation of a macromolecular structure consists in checking the plausibility of the structural results. On the one hand, this consists in assessing various crystallographic figures of merit, such as the fit between observed and calculated data reflected through the R-factor and the correlation factor, as well as visually checking the optimal fit of the structural model to the experimental electron density. On the other hand and more significantly, structure validation consists in extensive tests of the conformation of the peptide chain (*e.g.* through a *Ramachandran* plot (*164*)) and of specific sidechains (His, Asn, Gln, Thr, *etc.*). A variety of computer programs is available for this task, such as molprobity (*165*), procheck (*166*) and checkif (*167*) (Fig. 24).

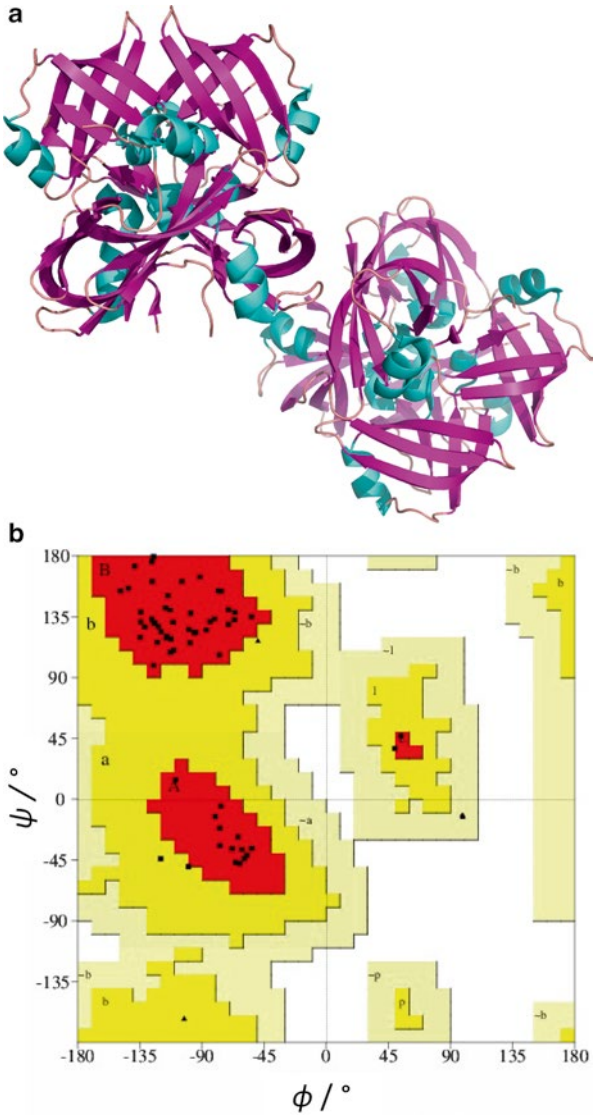

Fig. 24 Final result of a protein crystal structure analysis. (**a**) Overall structure drawn with pymol (*305*) and (**b**) *Ramachandran* output of Procheck (*166*) for a molybdenum binding protein (pdb-code: 1FR3, (*307*))

5 Results

It is far beyond the scope of this contribution to give an overview of the results of crystallographic structure analyses—in fact they constitute a large fraction of the modern stereochemical knowhow. Since the rise of crystallography went in parallel with the advent of modern computers, and since the crystallographic model is well suited

for standardization, crystallographers were among the first scientists who stored their experimental results in databases, which can be searched and from which structural data can readily be retrieved. Several such databases with excellent coverage exist for different groups of natural compounds. The most established ones are described below.

5.1 Cambridge Structural Database

The Cambridge structural database (CSD) (*168*) is a licensed database that hosts structural data of "organic" compounds, defined by the presence of a C-H bond.

For academic users, subscription to the database is based on a country-wide membership, the costs of which are calculated on the basis of the country's wealth. The database is distributed together with a comprehensive package of software for database access, structure visualization, and data analysis. The CSD System also includes a knowledge base of intermolecular interactions, containing data derived from both the CSD and the protein data bank.

The CSD records bibliographic, chemical, and crystallographic information for organic molecules and metal-organic compounds (*i.e.* compounds containing at least one carbon-hydrogen bond) for which three-dimensional structures have been determined with X-ray or neutron diffraction. The CSD does not store biopolymers (polypeptides, polysaccharides, oligonucleotides), which have their own archives (see below). For several decades, the number of entries of the CSD database has been growing exponentially (see Fig. 25).

As of January 2012, the Cambridge Structural Database contained a total of 596,810 structures of 544,565 different compounds. Of these, 254,475 are purely organic structures (containing only C, N, O, and H atoms), 319,188 contain an additional transition metal. All in all, the CSD contains more than 45 million three-dimensional atomic coordinates.

5.2 Crystallographic Open Database

The crystallographic open database (COD) database (*169*, *170*) started in 2003 with the intention of providing open access to crystal data of small molecules, *i.e.* organic, inorganic, metal-organic compounds and minerals but excluding biopolymers. The maintenance of the database and the evaluation of uploaded structures are fully automated. Thus, uploaded structures are accessible almost immediately.

5.3 Protein Data Bank

In 2003, the worldwide Protein Data Bank (wwPDB) (*171*) was founded with the mission "to maintain a single Protein Data Bank Archive of macromolecular structural data from all structure determination methods that is freely and publicly available to the global community". The founding members were RCSBPDB (*172*–*175*) (USA),

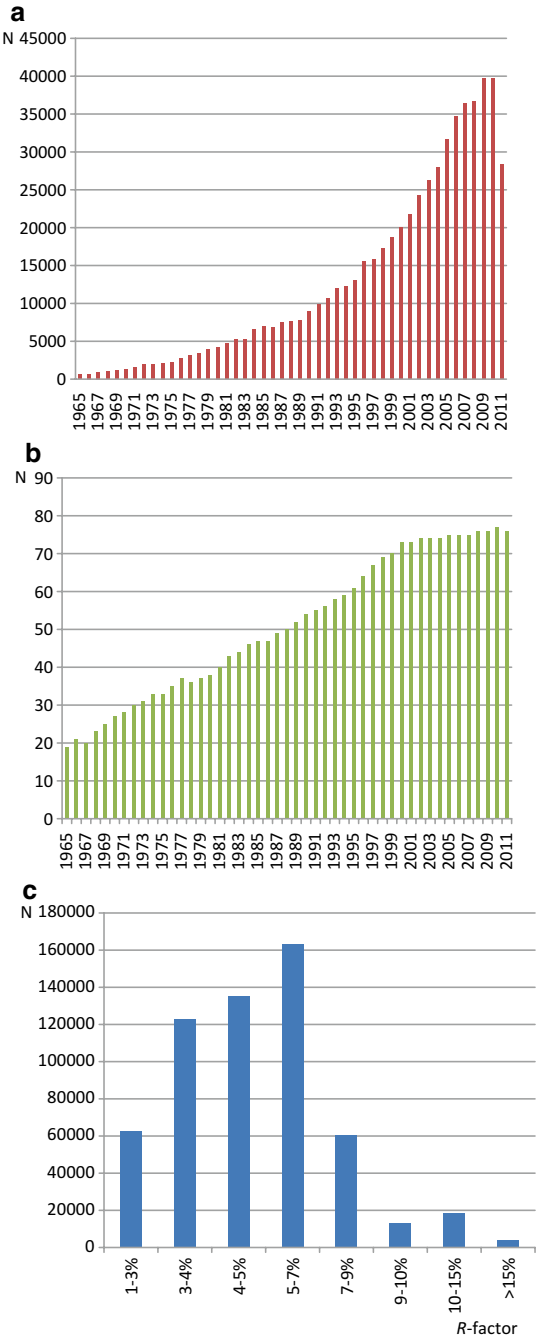

Fig. 25 (**a**) Number of crystal structures deposited in the CSD in each of the years 1965–2011. Data for 2011 are incomplete on January 1st 2012. (**b**) Average number of atoms per structure for each of the years 1965–2011, showing an increase in complexity of published structures. (**c**) *R*-factor statistics of the CSD. Data from (*230*)

PDBe (*176*) (Europe) and PDBj (*177*) (Japan). The BMRB (Biological Magnetic Resonance Data Bank) joined the wwPDB in 2006. The wwPDB partners also collaborate on issues of policy, formats, standards, curation procedures, and validation. Each of the four members of wwPDB can act as deposition, data processing and distribution centers for PDB data.

The wwPDB is a repository for the three-dimensional structural data of large biological molecules, such as proteins, carbohydrates, and nucleic acids. The data, obtained by X-ray crystallography, NMR spectroscopy and cryo-electron microscopy are submitted by biologists and biochemists from around the world and are then checked automatically for plausibility. Most scientific journals require scientists to submit their structural data to the wwPDB and include the pdb-code in the publication. The number of depositions has been growing rapidly during the last decades, as shown in Fig. 26.

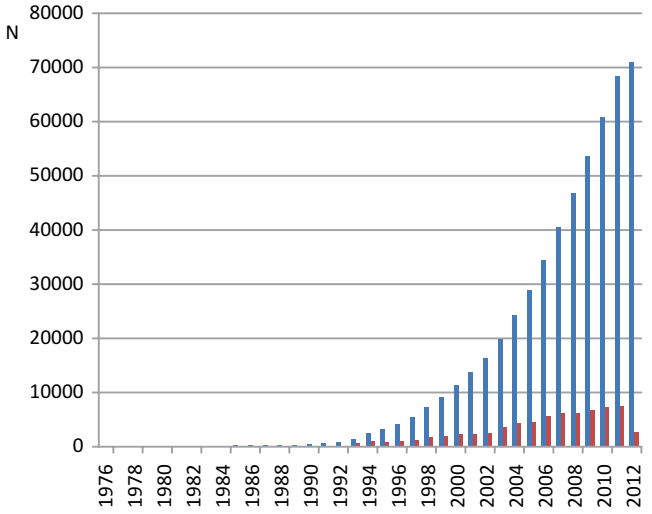

Fig. 26 Deposition to the PDB data bank, new data in *red*, accumulated data in *blue*. Data from (*308*)

In recent years, the size of the proteins that were crystallized and whose structures were determined by crystallography has increased dramatically. Figure 27 shows a histogram of the number of structures deposited at the PDB against their size.

The increase in complexity of structures is particularly evident from Fig. 28, which compares the three-dimensional structure of lysozyme (which was the first enzyme structure reported) with that of the recently determined eukaryotic ribosome.

5.3.1 Nucleic Acid Data Bank

The Nucleic Acid Data Bank (NDB) (*178*) started in 1992 (*179*) and is a open access repository of three-dimensional crystal structures of nucleic acids. As of January 2012 it hosted more than 5,600 structures. Since nucleic acid

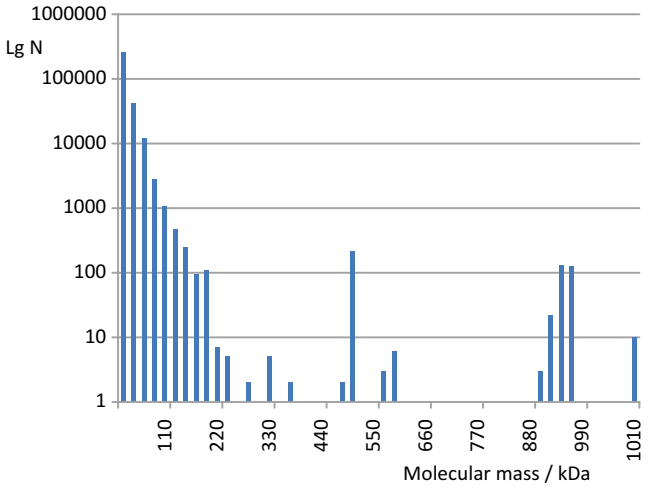

Fig. 27 Histogram of the sizes of structures below one million Daltons deposited at the PDB. Note the logarithmic scale on the ordinate. Data from (*308*)

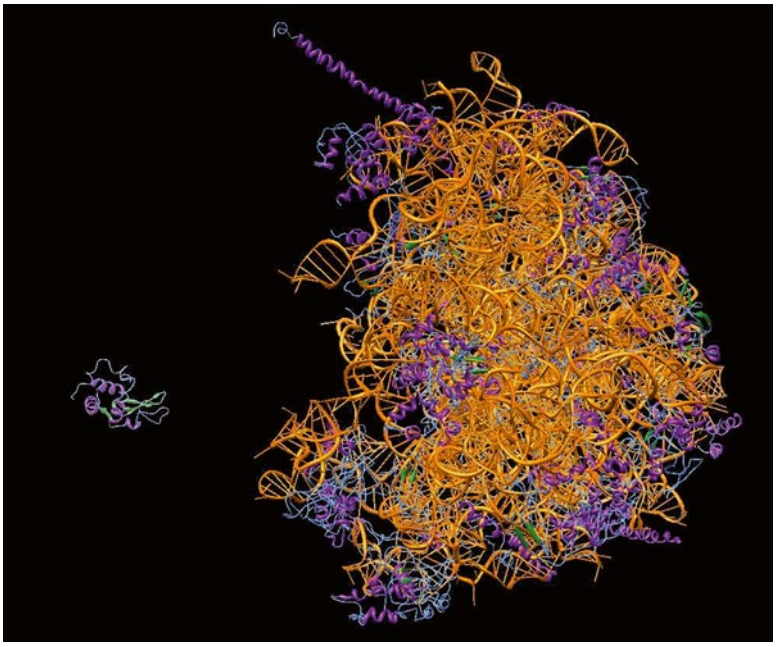

Fig. 28 Relation in size between the first enzyme solved—lysozyme (*309*) (pdb entry 1lyz, 14.3 kDa)—and the largest molecule stored in the PDB database the eukaryotic ribosome (*2*) (pdb entry 3o58, 1.8 MDa)

structures are also contained in the PDB, structures can be deposited to the NDB and PDB simultaneously.

5.3.2 Membrane Proteins of Known Three-Dimensional Structure

The website of *Steven White*'s Laboratory at the University of California at Irvine (*180*) contains what is called a "Membrane and Protein Biophysics Resource", which includes a continuously updated list of membrane protein structures determined by X-ray and electron diffraction with links to the Protein Data Bank. Currently (January 2012) it comprises coordinates of 919 membrane proteins, of which 310 are unique. Although absolute numbers are comparatively small, the number of membrane protein structures shows an impressive growth (Fig. 29).

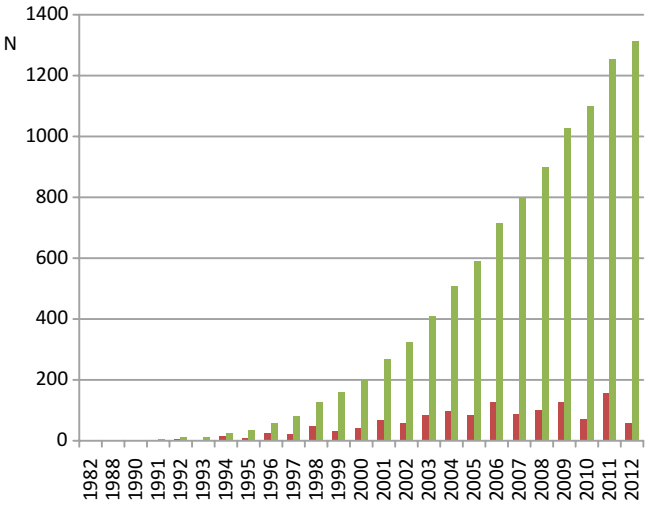

Fig. 29 Number of membrane protein structures deposited each year at the PDB (*red*) and the accumulated number of structures (*green*). Data from (*308*)

5.3.3 Protein-DNA Complexes

Like membrane proteins, protein-DNA complexes constitute special challenges (*181*). In view of their biological relevance they are intensely investigated, which resulted in a substantial number of crystal structures, as shown in Fig. 30.

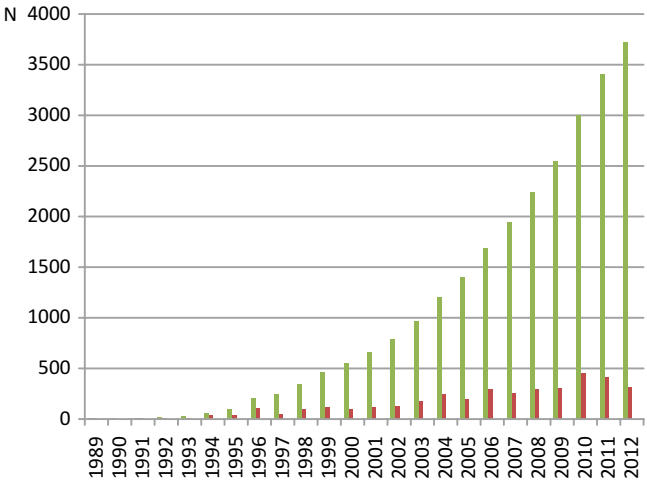

Fig. 30 **N**umber of protein-DNA complex structures deposited each year at the PDB (*red*) and the accumulated number of structures (*green*). Data from (*308*)

5.4 Other Databases

There exists a variety of other databases containing results of crystal structure analyses, however, these are beyond the scope of the present contribution. They concern inorganic structures stored in the Inorganic Crystal Structure Database (*182*) as well as metals and alloys, which are stored in CRYSTMET® (*183*).

6 Special Techniques

6.1 Time-Resolved Crystallography

Crystallography has traditionally been a "slow" technique, since a large number of reflection intensities have to be measured. In the "old" days of data collection on home sources, collection of a comprehensive data set took days or even weeks. With the advent of synchrotron sources together with fast detectors, this process was speeded up substantially, making it possible to collect a fairly comprehensive data set within less than a second. These developments paved the way to "four-dimensional" crystallography (*184–186*), *i.e.* the time-dependence of structural change can be monitored, which allows following chemical kinetics by X-ray crystallography (*187–189*). In extreme cases, synchrotron radiation in combination with the *Laue* technique allows experiments with nanosecond or even picosecond time

resolution. Myoglobin (*190*–*200*), hemoglobin (*201*, *202*), the photoactive yellow protein PYP (*195*, *203*–*209*), the Ha-Ras p21 protein (*210*), the heme-bound domain of the FixL protein (*211*), the photosynthesis reaction center complex of *Blastochlorisviridis* (*212*), the hammerhead ribozyme (*213*, *214*), and bovine trypsin (*215*) were, among others, the subjects of investigations of the time-dependence of their biological function.

Since a protein crystal consists of a large number of molecules, the major problem for time-dependent experiments consists in "synchronizing" constituent molecules (*216*, *217*). Kinetic experiments, which involve reactions on substrates, are invariably limited by substrate diffusion into protein crystals, a process that takes just seconds. Processes that are substantially faster are typically initiated by a short laser pulse, which is then synchronized with rapid data collection after a predefined time. With such a setup, it was possible to monitor changes in structure in the nanosecond range. Systems with a "cyclic" reaction pathway are advantageous for time-resolved studies since they allow reapplying stimulation and data collection on the same crystal specimen. To monitor a one-way reaction requires a concomitantly larger number of crystals.

The *Laue* technique (*218*–*221*) uses a "white" X-ray beam, *i.e.* a beam with a broad spectrum of energies. This brings a correspondingly larger part of the reciprocal lattice simultaneously into diffraction position, as shown in Fig. 31a. A single "shot" of X-rays can then yield diffracted intensities of a substantial fraction of the reciprocal lattice, as shown in Fig. 31b. The technical requirements for a *Laue*-experiment are enormous, which are only met by dedicated beam-lines. Such beamlines for time-resolved studies exist in only a few synchrotron sources in the world, such as the ESRF Grenoble (ID09B (*222*)) and APS, Argonne National Laboratory (BioCARS, ID-14 (*184*)).

Recently a method using "five-dimensional crystallography" (the temperature as the fifth dimension) with the potential to comprehensively map kinetic mechanisms by macromolecular crystallography was reported (*223*). Time series of crystallographic data from photoactive yellow protein crystals were collected at 293 as well as 303 K. Measurable differences for the relaxation times at both temperatures confirmed the feasibility of five-dimensional crystallography.

While the principal potential of time-resolved crystallography is enormous (*220*, *224*–*227*), it must be admitted that this technology still has to struggle with severe limitations. This is why most of the work reported so far concerned questions of general feasibility—using a limited number of model proteins, such as myoglobin or PYP—rather than pressing biological questions. While the crystallographic possibilities are indeed impressive (*198*) and by no means limiting, there are a number of practical restrictions often not met by "real life" proteins. The *Laue*-technique requires crystals with relatively small unit cell constants and low mosaicity, diffracting to high resolution. Other problems concern crystal degradation (*228*) (many kinetic experiments have to be performed at ambient temperatures) and, above all, the "synchronization problem" (see above). All in all, time-resolved crystallography has so far not conformed to the high expectations of one or two decades ago.

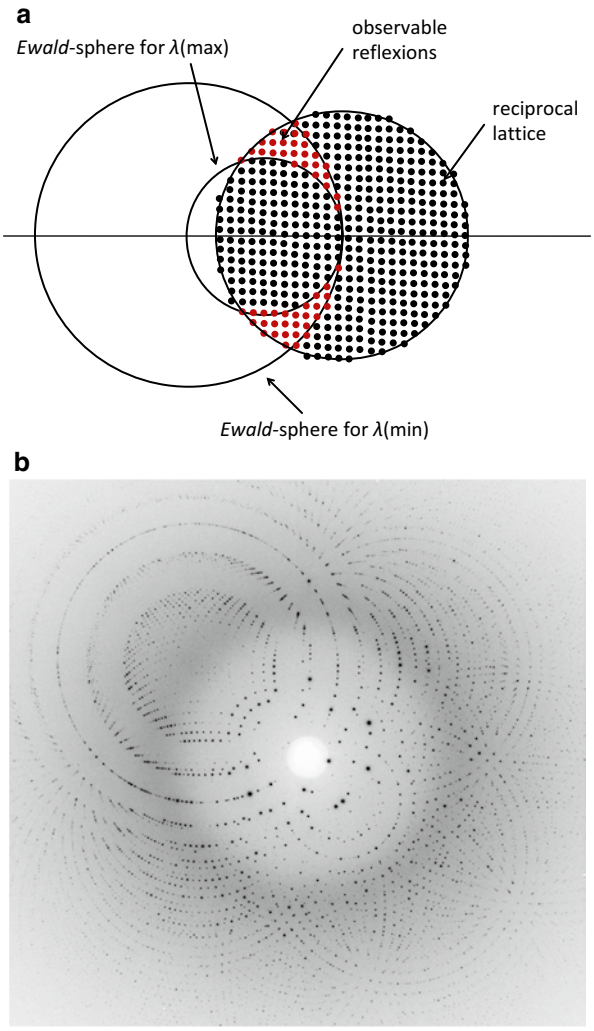

Fig. 31 (**a**) Principle of the *Laue* technique; (**b**) *Laue* image of a crystal of photoactive yellow protein (PYP) taken with a single pulse (5×10^9 photons in a 100 ps pulse, 18 keV). Courtesy of *Michael Wulff*, ESRF Grenoble

6.2 Neutron Crystallography

Diffraction effects cannot only be observed with electromagnetic radiation, but also with particle beams. According to the *de Broglie* equation, a particle behaves like a wave, with the wavelength depending on the mass of the particle and on its speed. Thermal neutrons, *i.e.* neutrons with a speed of approximately 2.2 km/s, have the proper wavelength (~1.8 Å) for crystallographic diffraction experiments, for which they have a number of interesting properties (*229*).

Neutrons have no charge, and they consequently interact only weakly with matter (in contrast to electrons and protons). Therefore, they can be used in combination with equipment (high-pressure cells, low temperature cryostats), which is typically incompatible with diffraction experiments with X-rays. Similarly, they are very suitable to investigate crystals that strongly absorb X-rays. In addition, due to their non-ionizing nature, radiation damage is much less of a problem with neutrons than with X-rays.

While X-rays are diffracted by the electrons surrounding atomic nuclei, neutrons interact only with the atomic nuclei. The spatial extension of the electron density leads to a fall-off of atomic structure factors with increasing scattering angle for X-rays, which is not the case for neutrons due to the small size of the atomic nuclei. Thus, very accurate nuclear positions can be obtained by neutron diffraction in principle, while X-ray experiments only yield the centre of gravity of the electron density surrounding the nuclei. The size of atomic scattering factors for X-rays increases with increased atomic number. This is not the case for neutrons, which all lie within a relatively narrow range, and can show marked variation for isotopes of the same element. For natural compounds, the difference between hydrogen and deuterium is particularly relevant: the scattering length of deuterium is about twice as large as that of hydrogen. Moreover, hydrogen is the only nucleus with a negative scattering length, permitting a variety of very interesting isotope-exchange experiments.

These very interesting properties are contrasted by several very serious shortcomings. First and foremost, neutron beams from available neutron sources (neutron reactors and neutron spallation sources) suffer from low brilliance, many orders of magnitude lower than for synchrotron X-ray beams. This necessitates very long data collection times and very large crystal specimens, typically millimeters as opposed to tens of micrometers for X-ray experiments. Overall, neutrons are many orders of magnitude more expensive than X-rays, so neutron diffraction experiments can only be performed at a small number of facilities worldwide. Therefore, neutron experiments have to be limited to problems that cannot be tackled by X-rays. For natural compounds, these are not many.

A second shortcoming of neutron crystallography as applied to the investigation of natural compounds is the fact that neutrons are not only scattered by elastic, but also by inelastic events. This inelastic and hence incoherent scattering carries no structural information, but increases the background and thus decreases the signal-to-noise ratio. Unfortunately, hydrogen has a particularly large incoherent scattering cross section, more than ten times larger than deuterium or carbon. Thus, exchange of hydrogen by deuterium is highly advisable wherever possible when investigating proteins or other natural compounds.

For small molecules, neutron crystallography has nevertheless been used quite extensively to accurately determine nuclear positions. Thus, the CSD (*168*) contains more than 1,500 entries describing organic compounds for which the three-dimensional structure was determined by single-crystal neutron diffraction analysis (*230*).

In spite of the fact that the low flux of neutron sources is a particular problem when dealing with macromolecular crystals, neutron protein crystallography has a relatively long history (*231*, *232*). Here, the growth of crystals with dimensions of

several millimeters in each direction is very challenging indeed (*233*–*237*), and so is the production of per-deuterated protein (*238*–*240*). While early data collections from protein crystals involving small and easily crystallizing proteins (*e.g.* myoglobin (*241*)) were performed with monochromatic radiation and classical diffractometers, macromolecular neutron crystallography was considerably advanced when equipment involving cylinder-shaped area detectors in combination with polychromatic neutron beams (*242*) became available. This has led to a renaissance of neutron protein crystallography in recent years (*243*–*247*). There are now several neutron centers with beam-lines that allow the collection of high-resolution (typically 2 Å) diffraction data from protein crystals in the course of hours or days rather than weeks or months (Los Alamos Neutron Science Center (*248*, *249*); Institut *Laue-Langevin* (*250*); Japan Proton Accelerator Research Complex (*251*)). Nevertheless, the number of high-resolution structure determinations with neutrons is still in the order of a few dozen.

Coenzyme B_{12} provides a good example for the power and limitations of neutron crystallography for a natural compound. Both from its molecular mass (about 1,500 Da) and from the architecture of its crystals (they contain channels of partly disordered solvent molecules), B_{12} is intermediate between a small molecule and a macromolecular natural compound. The crystallography of a large variety of B_{12} derivatives is well characterized (*252*). A neutron diffraction analysis (*253*) on a crystal of coenzyme B_{12r} was carried out on a crystal with dimensions $4.5 \times 1.4 \times 1.3$ mm grown from a mixture of D_2O and perdeuterated acetone. Thus, the crystal had all exchangeable protons exchanged by deuterons. Two experiments were performed on the same crystal specimen: collection of a comprehensive data set using a classical diffractometer in front of a monochromatic beam-line (data collected to about 1 Å, more than four weeks data collection time), and collection of a second (incomplete) data set using the neutron single-crystal diffractometer LADI utilizing a narrow-band *Laue* concept and a cylindrical imaging plate (*242*) (data collected to 1.43 Å, 36 h data collection time). A third data set extending to 0.9 Å was collected (from a much smaller crystal specimen) on the synchrotron. Density maps computed with these three data sets are shown in Fig. 32.

In spite of the superior definition of H or D positions in the high-resolution neutron maps, the 1.43 Å LADI maps show considerable power for the determination of the location of hydrogen and deuterium atoms, quite comparable to maps obtained from X-ray data extending beyond 1 Å. Only very few protein crystals diffract to such high resolutions.

In view of the various shortcomings, high-resolution neutron protein crystallography always follows a structure determination with X-rays, in order to answer questions of states of protonation or hydration in the interior or at the surface of the protein (*254*). Such studies were performed on crambin (*255*), myoglobin (*256*), lysozyme (*257*), human transthyretin (*258*), gamma-chymotrypsin (*259*), type-III antifreeze protein (*260*), the trypsin-BPTI complex (*261*), hemoglobin (*262*–*265*), carbonic anhydrase II (*266*), insulin (*267*), ribonuclease A (*268*), elastase (*269*), HIV protease (*270*, *271*), diisopropyl fluorophosphatase (*272*), photoactive yellow protein (PYP) (*273*), dihydrofolate reductase (*274*), D-xylose isomerase (*275*), human

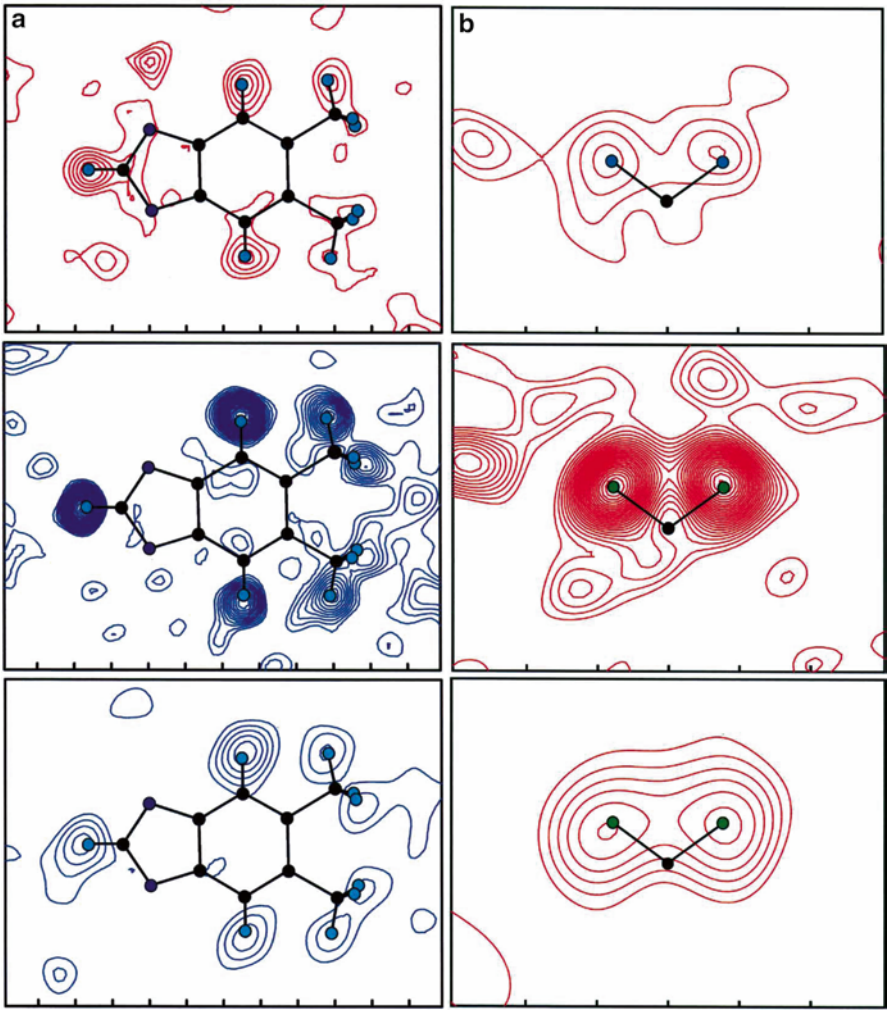

Fig. 32 Difference-density omit maps for the crystal structure of cob(II)alamin (see Fig. 1a) computed from synchrotron X-ray data (0.9 Å resolution, *top*), monochromatic neutron-diffraction data (1.0 Å resolution, *center*) and incomplete neutron *Laue*-diffraction data (1.43 Å resolution, *bottom*). (**a**) Map computed for a plane passing through the non-H atoms of the dimethylbenzimidazole base, after omitting its three H atoms. Contouring started at a signifcance level of $\pm 1\sigma$, with 1σ difference between subsequent contour lines. Negative contours are represented in *blue* and positive contours in *red*. (**b**) Omit maps through the atoms of water molecule W1. The two H or D atoms have been omitted for the phase calculation (*253*)

aldose reductase (*276*), concanavalin A (*277*, *278*), rubredoxin (*279*), and endothiapepsin (*280*). Preliminary reports describing the collection of neutron diffraction data concern endoxylanase II from *Trichoderma longibrachiatum* (*281*), human ABO(H) blood group A glycosyltransferase (*282*), porcine pancreatic elastase (*270*),

Pyrococcus furiosus rubredoxin (*283*), urate oxidase (*284*), gamma-chymotrypsin (*285*), thaumatin (*286*), and sulfite reductase D (*287*).

The possibility of influencing the diffraction of neutrons by the exchange of one isotope by another allows a number of interesting experiments. Thus, low-resolution neutron studies combined with H_2O/D_2O contrast variation were used successfully to trace detergent regions surrounding membrane protein molecules in single crystals (*288*) for OmpF porin from *Escherichia coli* (*289*, *290*), and the *Rhodobacter sphaeroides* photochemical reaction center (*291*) as well as to locate detergents in a lipase-colipase complex (*292*).

Neutrons are polarized, permitting experiments that probe into magnetic properties of crystals, which is highly relevant for material sciences, but less so for natural compounds. In addition, neutrons permit the location of hydrogen atoms next to very heavy metal atoms, which is exceedingly difficult to do with X-rays. While this is a very appealing property for inorganic crystallographers, its relevance for the investigation of natural compounds is limited.

6.3 Electron Crystallography

Electron crystallography uses the electron microscope to generate diffraction patterns which can be used to solve crystal structures from nano-sized crystallites (*293*). For inorganic materials, the technique is well developed and can be applied when other diffraction methods fail due to insufficient crystal size (*294*). For the study of biological macromolecules, electron crystallography is almost routinely used to analyze membrane proteins with resolutions approaching atomic resolution (up to 3 Å) (*295*–*297*).

7 Outlook

Crystallography of natural compounds—be they of low molecular weight or macromolecular—offers today a wealth of techniques and technologies. Thus, the determination of a crystal structure of a low-molecular natural compound is a routine operation with a guarantee of success provided crystals of the substance are available. Macromolecular crystallography is much less of a routine, although even here the wealth of techniques makes it very likely that a three-dimensional structure will sooner or later be obtained, provided well-diffracting crystals are at hand. The time required to perform a structure analysis has dropped dramatically in the course of the last few decades, thanks to excellent hardware (crystallization robots, synchrotrons with automatic beam lines, *etc*.) and software.

Virtually all structural data from single-crystal crystallographic experiments have been deposited and are worldwide available from appropriate data bases (*e.g.* CSD, pdb). The amount of structural information contained in these data bases is indeed breathtaking—it constitutes a major part of the foundations of modern

structural chemistry and of the molecular biosciences. What are open challenges, what can we expect from the future and how will the discipline evolve?

The main open challenge is still the serendipitous nature of the crystallization process. This is less of a problem for low-molecular weight compounds, but very much so for macromolecular natural compounds. Particularly challenging are membrane proteins and molecular assemblies, such as macromolecular machines like ATP synthase or bacterial ribosomes. The difficulty with such systems starts long before crystallography sets in, *i.e.* many of the difficulties are not related to crystallography. For many such systems it is already very difficult to produce the substance in sufficient quantity, and to obtain a mono-disperse solution of sufficient concentration. Nevertheless, the crystallization problem is being alleviated by the increased availability of high-brilliance micro-focus beam-lines, which permit the collection of diffraction data sets from crystals in the micrometer-range. It is likely that the problem of radiation damage—which is currently a limiting factor for such experiments—will be dramatically reduced with the next generation of X-ray sources (see below).

Time-resolved crystallography constitutes yet another challenge. At present, time-resolved diffraction experiments have been limited to a relatively small number of systems, which mostly have been used to demonstrate feasibility rather than to solve pressing biological questions. Again, it is possible that the advent of the next generation of X-ray sources might bring radically new opportunities for time-resolved crystallography, although optimism is somewhat reduced by past experience. So, what can we expect for the future?

It is clear that automation—both on the side of hardware and of software—will be developed further. Already today, there are robots available for high-throughput crystallization, beam-lines with automatic mounting, centering and data collection capabilities, and crystallographic programs solving and refining structures with almost no user input. Automation of all steps of the pipeline—from the gene to the crystal structure—will undoubtedly progress.

A second forseeable development is the increased integration of X-ray crystallography with other biochemical or biophysical techniques, such as electron and light microscopy, small angle X-ray diffraction, NMR spectroscopy, *etc.* The combination of different techniques will and on the one hand allow extending the range of accessible macromolecular systems, on the other hand allows it functional studies. Recently, a European consortium was formed to facilitate this process (*298*).

To date, there are several centers in the world (*54*) that determine crystal structures on a different scale and with a different concept than traditional protein-crystallographic laboratories. These so-called structural genomics centers systematically attempt to express all genes of an organism or even of a class of organisms, or genes selected by other criteria, such as potential structural novelty or medical or biotechnological usefulness. Proteins that are successfully expressed are then subjected to structure analysis, either by X-ray crystallography or by NMR spectroscopy. This “production line” crystallography has a number of advantages and simultaneously a number of shortcomings. Advantages are undoubtedly high efficiency, since specialized and very experienced personnel are available for each step in the pipeline from protein expression to structure refinement. On the other

hand, this approach has been criticized as unscientific, as "a fishing expedition" with no underlying scientific hypothesis. Irrespective of this discourse, this type of large-scale crystallography is likely to grow, and to produce a growing mass of structural data. Many of these structural genomics centers are likely to be associated with large-scale facilities, typically with synchrotron sources, and have the most advanced instrumentation and technology at their disposal. In view of the fierce competition in the molecular biosciences, it is quite likely that professional and "full time" macromolecular crystallographers will cease to exist outside a few such specialized centers a few decades from now.

Finally, very exciting opportunities can be expected to arise from the next generation of X-ray sources, the so-called free electron lasers (FEL) (*299*). The brilliance of these sources will exceed present synchrotrons by several orders of magnitude. Essentially, a short pulse of less than a nanosecond will deliver enough photons to the target crystal to collect a full data set, which will expand present possibilities in at least two different ways. On the one hand, FELs are expected to be a more powerful tool than existing synchrotrons for time-resolved crystallography. However, since present-day time-resolved studies do not yet fully exploit the power of existing synchrotron sources, it may well be that the effect of FELs on time-resolved macromolecular crystallography will be limited. On the other hand, it is quite likely that FELs will induce a quantum jump in the use of nano-crystals for crystallographic data collections (*300*). Radiation damage is a limiting factor when using nano-crystals for data collection, even at cryo-temperature. It is anticipated that with next-generation sources it will be possible to collect a comprehensive data set from a crystal in such a short time that crystal decay only sets in after enough photons have been scattered.

Acknowledgments *UGW* wants to thank Prof. *Randy Read* for providing his program fftimg and assisting with its implementation, and *Judith Kerstner* for help with the manuscript. We thank *Michael Wulff* for providing Fig. 31b.

References

1. Corey RB, Marsh RE (1968) X-Ray Diffraction Studies of Crystalline Amino Acids, Peptides and Proteins. Fortschr Chem Org Naturst 26:1
2. Ben-Shem A, Jenner L, Yusupova G, Yusupov M (2010) Crystal Structure of the Eukaryotic Ribosome. Science 330:1203
3. Röntgen WC (1895) Über Eine Neue Art Von Strahlen. Sitzungsber Würzb PhyMed Ges:137
4. Friedrich W, Knipping P, Laue Mv (1913) Interferenzerscheinungen Bei Röntgenstrahlen. Ann Phys 41:971
5. Bragg WH, Bragg WL (1913) The Reflection of X-Rays by Crystals. Proc Royal Soc A 88:428
6. Bragg WH, Bragg WL (1913) The Reflection of X-Rays by Crystals. Phys Z 14:472
7. Bragg WL (1912) The Specular Reflexion of X-Rays. Nature 90:410
8. Bragg WL (1913) The Structure of Some Crystals as Indicated by Their Diffraction of X-Rays. Proc Royal Soc A 89:248
9. Bragg WH, Bragg WL (1914) The Structure of the Diamond. Proc Royal Soc A 89:277

10. Bragg WL (1914) The Crystalline Structure of Copper. Phil Mag 28:355
11. Pauling L (1939) The Nature of the Chemical Bond. Cornell University Press, Ithaca, NY
12. Hodgkin DC (1949) The X-Ray Analysis of the Structure of Penicillin. Adv Sci 6:85
13. Crowfoot D, Bunn CW, Roger-Low BM, Turner-Jones A (1949) The Chemistry of Penicillins. Princeton University Press, Princeton, NJ, p 310
14. Chain E (1980) Penicillin - the Crucial Experiment. CHEMTECH 10:474
15. Hodgkin DC (1955) The Crystal Structure of the Hexacarboxylic Acid Derived from Vitamin B_{12} and the Molecular Structure of the Vitamin. Nature 176:325
16. Hodgkin DC (1957) The Structure of Vitamin B_{12}: (I) an Outline of the Crystallographic Investigation of Vitamin B_{12}. Proc Royal Soc Lond A242:228
17. Hodgkin DC (1959) The Structure of Vitamin B_{12}: (II) the Crystal Structure of Hexacarboxylic Acid Obtained by the Degradation of Vitamin B_{12}. Proc R Soc Lond A251:306
18. Lenhert PG, Hodgkin DC (1961) Structure of the 5,6-Dimethylbenzimidazolylcobamide Coenzyme. Nature 192:937
19. Hodgkin DC (1958) X-Ray Analysis and the Structure of Vitamin B_{12}. Fortschr Chem Org Naturst 15:167
20. Adams MJ, Blundell TL, Dodson EJ, Dodson GG, Vijayan M, Baker EN, Harding MM, Hodgkin DC, Rimmer B, Sheats S (1969) Structure of Rhombohedral 2 Zinc Insulin Crystals. Nature 224:491
21. Hauptman HA, Karle J (1953) Solution of the Phase Problem. I. The Centrosymmetric Crystal. American Crystallographic Association, Pittsburgh
22. Sumner JB (1926) The Isolation and Crystallization of the Enzyme Urease. J Biol Chem 69:435
23. Kendrew JC, Bodo G, Dintzis HM, Parrish RG, Wyckoff H, Phillips DC (1958) A Three-Dimensional Model of the Myoglobin Molecule Obtained by X-Ray Analysis. Nature 181:662
24. Muirhead H, Perutz MF (1963) Structure of Haemoglobin - a 3-Dimensional Fourier Synthesis of Reduced Human Haemoglobin at 5.5 Ångstrom Resolution. Nature 199:633
25. Perutz MF, M.G. Rossmann, Cullis AF, Muirhead H, Will G, North AC (1960) Structure of Haemoglobin: A Three-Dimensional Fourier Synthesis at 5.5-A. Resolution, Obtained by X-Ray Analysis. Nature 185:416
26. Deisenhofer J, Epp O, Miki K, Huber R, Michel H (1984) X-Ray Structure-Analysis of a Membrane-Protein Complex - Electron-Density Map at 3 Ångstrom Resolution and a Model of the Chromophores of the Photosynthetic Reaction Center from *Rhodopseudomonas viridis*. J Mol Biol 180:385
27. Ban N, Nissen P, Hansen J, Moore PB, Steitz TA (2000) The Complete Atomic Structure of the Large Ribosomal Subunit at 2.4 Ångstrom Resolution. Science 289:905
28. Harms J, Schluenzen F, Zarivach R, Bashan A, Gat S, Agmon I, Bartels H, Franceschi F, Yonath A (2001) High Resolution Structure of the Large Ribosomal Subunit from a Mesophilic Eubacterium. Cell 107:679
29. Schluenzen F, Tocilj A, Zarivach R, Harms J, Gluehmann M, Janell D, Bashan A, Bartels H, Agmon I, Franceschi F, Yonath A (2000) Structure of Functionally Activated Small Ribosomal Subunit at 3.3 Ångstroms Resolution. Cell 102:615
30. Wimberly BT, Brodersen DE, Clemons WM, Jr., Morgan-Warren RJ, Carter AP, Vonrhein C, Hartsch T, Ramakrishnan V (2000) Structure of the 30S Ribosomal Subunit. Nature 407:327
31. Shmueli U (ed) (1993) International Tables for Crystallography: Kluwer Academic Publishers, Dordrecht, The Netherlands, Boston, London
32. Dunitz JD (1979) X-Ray Analysis and the Structure of Organic Molecules. Cornell University Press, Ithaca, NY
33. Rupp B (2009) Biomolecular Crystallography: Principles, Practice, and Application to Structural Biology. Garland Science, New York
34. Hahn T (ed) (2011) International Tables for Crystallography. Volume A, Space-Group Symmetry: International Union of Crystallography, John Wiley & Sons, New York

35. Friedel G (1913) Crystalline Symmetry as Revealed by the Diffraction of *Röntgen* Rays. Compt Rend 157:1533
36. Bijovoet JM, Peerdeman AF, Bommel AJv (1951) Determination of the Absolute Configuration of Optically Active Compounds by Means of X-Rays. Nature 168:271
37. Friedmann D, Messick T, Marmorstein R (2011) Crystallization of Macromolecules. Curr Protoc Protein Sci 66:17.4.1
38. Saridakis E, Chayen NE (2003) Systematic Improvement of Protein Crystals by Determining the Supersolubility Curves of Phase Diagrams. Biophys J 84:1218
39. Saridakis E, Khurshid S, Govada L, Phan Q, Hawkins D, Crichlow GV, Lolis E, Reddy SM, Chayen NE (2011) Protein Crystallization Facilitated by Molecularly Imprinted Polymers. Proc Nat Acad Sci USA 108:11081
40. http://www.nasa.gov/centers/marshall/news/background/facts/apcf.html
41. McPherson A, Malkin AJ, Kuznetsov YG, Koszelak S, Wells M, Jenkins G, Howard J, Lawson G (1999) The Effects of Microgravity on Protein Crystallization: Evidence for Concentration Gradients around Growing Crystals. J Cryst Growth 196:572
42. Inokuma Y, Yoshioka S, Ariyoshi J, Arai T, Hitora Y, Takada K, Matsunaga S, Rissanen K, Fujita M (2013) X-Ray Analysis on the Nanogram to Microgram Scale Using Porous Complexes. Nature 495:461
43. Salemme FR (1985) Protein Crystallization by Free Interface Diffusion. Meth Enzymol 114:140
44. Tung M, Gallagher DT (2009) The Biomolecular Crystallization Database Version 4: Expanded Content and New Features. Acta Cryst D 65:18
45. Anand K, Pal D, Hilgenfeld R (2002) An Overview on 2-Methyl-2,4-Pentanediol in Crystallization and in Crystals of Biological Macromolecules. Acta Cryst D 58:1722
46. Rupp B, Wang J (2004) Predictive Models for Protein Crystallization. Methods 34:390
47. http://www.jenabioscience.com/cms/en/1/browse/1399_macromolecular_crystallography.html; http://hamptonresearch.com/menus.aspx?id=2&cid=1; http://www.moleculardimensions.com/shopdisplaycategories.asp?id=1&cat=Crystallization+Screens; http://www.sigmaaldrich.com/life-science/proteomics/protein-structural-analysis/xray-crystallography/basic-crystallography-kit.html
48. Stura EA, Wilson IA (1991) Applications of the Streak Seeding Technique in Protein Crystallization. J Cryst Growth 110:270
49. Ireton GC, Stoddard BL (2004) Microseed Matrix Screening to Improve Crystals of Yeast Cytosine Deaminase. Acta Cryst D 60:601
50. D'Arcy A, Villard F, Marsh M (2007) An Automated Microseed Matrix-Screening Method for Protein Crystallization. Acta Cryst D 63:550
51. Ducruix A, Giegé R (eds) (1999) Crystallization of Nucleic Acids and Proteins: Oxford University Press, New York
52. Biertümpfel C, Basquin J, Suck D, Sauter C (2002) Crystallization of Biological Macromolecules Using Agarose Gel. Acta Cryst D 58:1657
53. http://www.douglas.co.uk/; http://www.dunnlab.de/lab_ARI_deutsch.htm; http://zinsser-analytic.net/Catalogue/exeDefault/?id=22
54. http://www.thesgc.org/; http://www.jcsg.org/; http://www.nigms.nih.gov/Research/FeaturedPrograms/PSI/; http://www.proteinstrukturfabrik.de/; http://www.ec-fesp.org/
55. Baker M (2010) Making Membrane Proteins for Structures: A Trillion Tiny Tweaks. Nature Methods 7:429
56. Arnold T, Linke D (2008) The Use of Detergents to Purify Membrane Proteins. Curr Protoc Protein Sci 4:4.8.1
57. Privé GG (2007) Detergents for the Stabilization and Crystallization of Membrane Proteins. Methods 41:388
58. Clarke S (1975) The Size and Detergent Binding of Membrane Proteins. J Biol Chem 250:5459
59. Newby ZER, O'Connell JD, Gruswitz F, Hays FA, Harries WEC, Harwood IM, Ho JD, Lee JK, Savage DF, Miercke LJW, Stroud RM (2009) A General Protocol for the Crystallization of Membrane Proteins for X-Ray Structural Investigation. Nature Protoc 4:619

60. Landau EM, Rosenbusch JP (1996) Lipidic Cubic Phases: A Novel Concept for the Crystallization of Membrane Proteins. Proc Nat Acad Sci USA 93:14532
61. Kulkarni CV, Ales I (2010) In Cubo Crystallization of Membrane Proteins. Advances in Planar Lipid Bilayers and Liposomes: Academic Press, San Diego, p 237
62. Ai X, Caffrey M (2000) Membrane Protein Crystallization in Lipidic Mesophases: Detergent Effects. Biophys J 79:394
63. Wadsten P, Wöhri AB, Snijder A, Katona G, Gardiner AT, Cogdell RJ, Neutze R, Engström S (2006) Lipidic Sponge Phase Crystallization of Membrane Proteins. J Mol Biol 364:44
64. http://www.sbkb.org/update/2010/02/images/th_psisgkb.2010.04-i1_full.jpg
65. http://bric.postech.ac.kr/myboard/read.php?Board=protocol&id=1688
66. Jordan SR, Pabo CO (1988) Structure of the Lambda Complex at 2.5 Ångstrom Resolution: Details of the Repressor-Operator Interactions. Science 242:893
67. Clarke ND, Beamer LJ, Goldberg HR, Berkower C, Pabo CO (1991) The DNA Binding Arm of Lambda Repressor: Critical Contacts from a Flexible Region. Science 254:267
68. Jordan SR, Whitcombe TV, Berg JM, Pabo CO (1985) Systematic Variation in DNA Length Yields Highly Ordered Repressor-Operator Cocrystals. Science 230:1383
69. Rice PA, Yang S, Mizuuchi K, Nash HA (1996) Crystal Structure of an Ihf-DNA Complex: A Protein-Induced DNA U-Turn. Cell 87:1295
70. Schultz SC, Shields GC, Steitz TA (1990) Crystallization of *Escherichia coli* Catabolite Gene Activator Protein with Its DNA Binding Site. The Use of Modular DNA. J Mol Biol 213:159
71. Tan S, Hunziker Y, Pellegrini L, Richmond TJ (2000) Crystallization of the Yeast Matalpha2/Mcm1/DNA Ternary Complex: General Methods and Principles for Protein/DNA Cocrystallization. J Mol Biol 297:947
72. Hendrickson WA (1991) Determination of Macromolecular Structures from Anomalous Diffraction of Synchrotron Radiation. Science 254:51
73. Lartigue A, Gruez A, Briand L, Blon F, Bezirard V, Walsh M, Pernollet JC, Tegoni M, Cambillau C (2004) Sulfur Single-Wavelength Anomalous Diffraction Crystal Structure of a Pheromone-Binding Protein from the Honeybee *Apis mellifera* L. J Biol Chem 279:4459
74. http://biosync.sbkb.org/
75. http://www.esrf.eu
76. http://www.esrf.eu/news/general/sb-productivity/
77. Leemans WP, Schoenlein RW, Volfbeyn P, Chin AH, Glover TE, Balling P, Zolotorev M, Kim KJ, Chattopadhyay S, Shank CV (1996) X-Ray Based Subpicosecond Electron Bunch Characterization Using 90 Degrees Thomson Scattering. Phys Rev Lett 77:4182
78. Hartemann FV, Gibson DJ, Brown WJ, Rousse A, Phuoc KT, Mallka V, Faure J, Pukhov A (2007) Compton Scattering X-Ray Sources Driven by Laser Wakefield Acceleration. Phys Rev Special Topics-Accelerators and Beams 10:1
79. Luo W, Xu W, Pan QY, Cai XZ, Chen JG, Chen YZ, Fan GT, Fan GW, Guo W, Li YJ, Liu WH, Lin GQ, Ma YG, Shen WQ, Shi XC, Xu BJ, Xu JQ, Xu Y, Zhang HO, Yan Z, Yang LF, Zhao MH (2010) A Laser-Compton Scattering Prototype Experiment at 100 Mev Linac of Shanghai Institute of Applied Physics. Rev Sci Instr 81:13304
80. Luo W, Xu W, Pan QY, Cai XZ, Chen YZ, Fan GT, Fan GW, Li YJ, Liu WH, Lin GQ, Ma YG, Shen WQ, Shi XC, Xu BJ, Xu JQ, Xu Y, Zhang HO, Yan Z, Yang LF, Zhao MH (2010) X-Ray Generation from Slanting Laser-Compton Scattering for Future Energy-Tunable Shanghai Laser Electron Gamma Source. Appl Phys B-Lasers and Optics 101:761
81. http://www.oxcryo.com/coolers-for-diffraction/cryostream/
82. Hope H (1988) Cryocrystallography of Biological Macromolecules: A Generally Applicable Method. Acta Cryst B 44:22
83. Hope H (1990) Crystallography of Biological Macromolecules at Ultra-Low Temperature. Ann Rev Biophys Biophys Chem 19:107
84. Hope H, Frolow F, von Bohlen K, Makowski I, Kratky C, Halfon Y, Danz H, Webster P, Bartels KS, Wittmann HG, Yonath A (1989) Cryocrystallography of Ribosomal Particles. Acta Cryst B 45:190
85. Holton JM (2007) Xanes Measurements of the Rate of Radiation Damage to Selenomethionine Side Chains. J Synchrotron Radiat 14:51

86. Warkentin M, Berejnov V, Husseini NS, Thorne RE (2006) Hyperquenching for Protein Cryocrystallography. J Appl Crystallogr 39:805
87. Kriminski S, Caylor CL, Nonato MC, Finkelstein KD, Thorne RE (2002) Flash-Cooling and Annealing of Protein Crystals. Acta Cryst D 58:459
88. Juers DH, Matthews BW (2004) The Role of Solvent Transport in Cryo-Annealing of Macromolecular Crystals. Acta Cryst D 60:412
89. Li SJ, Suzuki M, Nakagawa A (2005) Using Cryoloops for X-Ray Data Collection from Protein Crystals at Room Temperature: A Simple Applicable Method. J Cryst Growth 281:592
90. Miyahara J, Takahashi K, Amemiya Y, Kamiya N, Satow Y (1986) A New Type of X-Ray Area Detector Utilizing Laser Stimulated Luminescence. Nucl Instr Meth Phys Res A246:572
91. http://www.proteincrystallography.org/detectors/
92. https://www.kvi.nl/~wortche/detectors2003/detectors2003_files/solid_state.pdf
93. Leslie AG (2006) The Integration of Macromolecular Diffraction Data. Acta Cryst D 62:48
94. Leslie AGW, Powell HR, Read RJ, Sussman JL (2007) Processing Diffraction Data with Mosflm. Evolving Methods for Macromolecular Crystallography: Springer, Dordrecht, The Netherlands, p 41
95. Kabsch W (2010) Xds. Acta Cryst D 66:125
96. Kabsch W (2010) Integration, Scaling, Space-Group Assignment and Post-Refinement. Acta Cryst D 66:133
97. Howard AJ, Gilliland GL, Finzel BC, Poulos TL, Ohlendorf DH, Salemme FR (1987) The Use of an Imaging Proportional Counter in Macromolecular Crystallography. J Appl Crystallogr 20:383
98. Pflugrath JW (1999) The Finer Things in X-Ray Diffraction Data Collection. Acta Cryst D 55:1718
99. Otwinowski Z, Minor W (1997) Processing of X-Ray Diffraction Data Collected in Oscillation Mode. Meth Enzymol 276:307
100. Weiss MS (2001) Global Indicators of X-Ray Data Quality. J Appl Crystallogr 34:130
101. Wilson AJC (1942) Determination of Absolute from Relative X-Ray Intensity Data. Nature 150:151
102. Parsons S (2003) Introduction to Twinning. Acta Cryst D 59:1995
103. http://ccp4wiki.org/~ccp4wiki/wiki/images/a/a3/Murshudov-Oulu08-twinning.pdf
104. Matthews BW (1968) Solvent Content of Protein Crystals. J Mol Biol 33:491
105. Kantardjieff KA, Rupp B (2003) Matthews Coefficient Probabilities: Improved Estimates for Unit Cell Contents of Proteins, DNA, and Protein-Nucleic Acid Complex Crystals. Protein Sci 12:1865
106. Rossmann MG, Blow DM (1962) The Detection of Subunits within the Crystallographic Asymmetric Unit. Acta Cryst 15:24
107. Chook YM, Lipscomb WN, Ke HM (1998) Detection and Use of Pseudo-Translation in Determination of Protein Structures. Acta Cryst D 54:822
108. Zwart PH, Grosse-Kunstleve RW, Lebedev AA, Murshudov GN, Adams PD (2008) Surprises and Pitfalls Arising from (Pseudo) Symmetry. Acta Cryst D 64:99
109. Woolfson MM (1987) Direct Methods - from Birth to Maturity. Acta Cryst A 43:593
110. Sayre D (1952) The Squaring Method - a New Method for Phase Determination. Acta Cryst 5:60
111. Sheldrick GM (2008) A Short History of SHELX. Acta Cryst A 64:112
112. Usón I, Sheldrick GM (1999) Advances in Direct Methods for Protein Crystallography. Curr Opin Struct Biol 9:643
113. Hauptman H (1997) Phasing Methods for Protein Crystallography. Curr Opin Struct Biol 7:672
114. Hauptman HA (1997) Shake-and-Bake: An Algorithm for Automatic Solution *ab Initio* of Crystal Structures. Meth Enzymol 277:3
115. Rodríguez DD, Grosse C, Himmel S, González C, de Ilarduya IM, Becker S, Sheldrick GM, Usón I (2009) Crystallographic *ab Initio* Protein Structure Solution below Atomic Resolution. Nature Methods 6:651

116. McCoy AJ, Grosse-Kunstleve RW, Adams PD, Winn MD, Storoni LC, Read RJ (2007) Phaser Crystallographic Software. J Appl Crystallogr 40:658
117. Sheldrick GM (2002) Macromolecular Phasing with Shelxe. Z Kristallogr 217:644
118. http://www-structmed.cimr.cam.ac.uk/Course/MolRep/molrep.html
119. Altschul SF, Gish W, Miller W, Myers EW, Lipman DJ (1990) Basic Local Alignment Search Tool. J Mol Biol 215:403
120. Lipman DJ, Pearson WR (1985) Rapid and Sensitive Protein Similarity Searches. Science 227:1435
121. Eswar N, Webb B, Marti-Renom MA, Madhusudhan MS, Eramian D, Shen MY, Pieper U, Sali A (2006) Comparative Protein Structure Modeling Using Modeller. Curr Protoc Bioinformatics 5:6
122. Söding J, Biegert A, Lupas AN (2005) The Hhpred Interactive Server for Protein Homology Detection and Structure Prediction. Nucleic Acids Res 33:W244
123. Söding J (2005) Protein Homology Detection by Hmm-Hmm Comparison. Bioinformatics 21:951
124. Jaroszewski L, Rychlewski L, Li Z, Li W, Godzik A (2005) Ffas03: A Server for Profile–Profile Sequence Alignments. Nucleic Acids Res 33:W284
125. Shi J, Blundell TL, Mizuguchi K (2001) Fugue: Sequence-Structure Homology Recognition Using Environment-Specific Substitution Tables and Structure-Dependent Gap Penalties. J Mol Biol 310:243
126. Lebedev AA, Vagin AA, Murshudov GN (2008) Model Preparation in Molrep and Examples of Model Improvement Using X-Ray Data. Acta Cryst D 64:33
127. Stein N (2008) Chainsaw: A Program for Mutating Pdb Files Used as Templates in Molecular Replacement. J Appl Crystallogr 41:641
128. Suhre K, Sanejouand YH (2004) Elnemo: A Normal Mode Web Server for Protein Movement Analysis and the Generation of Templates for Molecular Replacement. Nucleic Acids Res 32:W610
129. Suhre K, Sanejouand YH (2004) On the Potential of Normal-Mode Analysis for Solving Difficult Molecular-Replacement Problems. Acta Cryst D 60:796
130. Schwarzenbacher R, Godzik A, Jaroszewski L (2008) The Jcsg Mr Pipeline: Optimized Alignments, Multiple Models and Parallel Searches. Acta Cryst D 64:133
131. http://predictioncenter.org/
132. http://www.predictioncenter.org
133. Crowther RA (1972) The Fast Rotation Function in the Molecular Replacement Method. Int Sci Rev 13:173
134. Navaza J (2001) Implementation of Molecular Replacement in Amore. Acta Cryst D 57:1367
135. Vagin A, Teplyakov A (1997) Molecular Replacement with Molrep. Acta Cryst D 66:22
136. Fujinaga M, Read RJ (1987) Experiences with a New Translation-Function Program. J Appl Crystallogr 20:517
137. Brünger AT, Adams PD, Clore GM, DeLano WL, Gros P, Grosse-Kunstleve RW, Jiang JS, Kuszewski J, Nilges M, Pannu NS, Read RJ, Rice LM, Simonson T, Warren GL (1998) Crystallography & NMR System: A New Software Suite for Macromolecular Structure Determination. Acta Cryst D 54:905
138. Ban N, Escobar C, Garcia R, Hasel K, Day J, Greenwood A, McPherson A (1994) Crystal-Structure of an Idiotype Antiidiotype Fab Complex. Proc Natl Acad Sci USA 91:1604
139. Read RJ (2001) Pushing the Boundaries of Molecular Replacement with Maximum Likelihood. Acta Cryst D 57:1373
140. Keegan RM, Winn MD (2008) Mrbump: An Automated Pipeline for Molecular Replacement. Acta Cryst D 64:119
141. DiMaio F, Terwilliger TC, Read RJ, Wlodawer A, Oberdorfer G, Wagner U, Valkov E, Alon A, Fass D, Axelrod HL, Das D, Vorobiev SM, Iwai H, Pokkuluri PR, Baker D (2011) Improved Molecular Replacement by Density- and Energy-Guided Protein Structure Optimization. Nature 473:540
142. Kissinger CR, Gehlhaar DK, Fogel DB (1999) Rapid Automated Molecular Replacement by Evolutionary Search. Acta Cryst D 55:484

143. DiMaio F, Tyka MD, Baker ML, Chiu W, Baker D (2009) Refinement of Protein Structures into Low-Resolution Density Maps Using Rosetta. J Mol Biol 392:181
144. Crick FHC, Magdoff BS (1956) The Theory of the Method of Isomorphous Replacement for Protein Crystals. Acta Cryst 9:901
145. Bricogne G, Vonrhein C, Flensburg C, Schiltz M, Paciorek W (2003) Generation, Representation and Flow of Phase Information in Structure Determination: Recent Developments in and around Sharp 2.0. Acta Cryst D 59:2023
146. Terwilliger TC, Berendzen J (1999) Automated Mad and Mir Structure Solution. Acta Cryst D D55:849
147. Hendrickson WA, Teeter MM (1981) Structure of the Hydrophobic Protein Crambin Determined Directly from the Anomalous Scattering of Sulfur. Nature 290:107
148. Doublie S (1997) Preparation of Selenomethionyl Proteins for Phase Determination. Meth Enzymol 276:523
149. Lakomek K, Dickmanns A, Mueller U, Kollmann K, Deuschl F, Berndt A, Lubke T, Ficner R (2009) *De Novo* Sulfur Sad Phasing of the Lysosomal 66.3 Kda Protein from Mouse. Acta Cryst D 65:220
150. Wang BC (1985) Resolution of Phase Ambiguity in Macromolecular Crystallography. Meth Enzymol 115:90
151. Langer G, Cohen SX, Lamzin VS, Perrakis A (2008) Automated Macromolecular Model Building for X-Ray Crystallography Using Arp/Warp Version 7. Nature Protoc 3:1171
152. Terwilliger TC (2003) Automated Main-Chain Model Building by Template Matching and Iterative Fragment Extension. Acta Cryst D 59:38
153. Cowtan K (2006) The Buccaneer Software for Automated Model Building. 1. Tracing Protein Chains. Acta Cryst D 62:1002
154. Cowtan K (2008) Fitting Molecular Fragments into Electron Density. Acta Cryst D 64:83
155. Emsley P, Lohkamp B, Scott WG, Cowtan K (2010) Features and Development of COOT. Acta Cryst D 66:486
156. Jones TA, Zou JY, Cowan SW, Kjeldgaard M (1991) Improved Methods for Building Protein Models in Electron-Density Maps and the Location of Errors in These Models. Acta Cryst A 47:110
157. McRee DE (1999) Xtalview Xfit - a Versatile Program for Manipulating Atomic Coordinates and Electron Density. J Struct Biol 125:156
158. Read RJ (1986) Improved Fourier Coefficients for Maps Using Phases from Partial Structures with Errors. Acta Cryst A 42:140
159. Miller R, DeTitta GT, Jones R, Langs DA, Weeks CM, Hauptman HA (1993) On the Application of the Minimal Principle to Solve Unknown Structures. Science 259:1430
160. Diamond R (1971) Real Space Refinement Procedure for Proteins. Acta Cryst A 27:436
161. Diamond R (1985) Real Space Refinement. Meth Enzymol 115:237
162. Bricogne G (1993) Direct Phase Determination by Entropy Maximization and Likelihood Ranking: Status Report and Perspectives. Acta Cryst D 49:37
163. Blanc E, Roversi P, Vonrhein C, Flensburg C, Lea SM, Bricogne G (2004) Refinement of Severely Incomplete Structures with Maximum Likelihood in Buster-Tnt. Acta Cryst D 60:2210
164. Ramachandran GN, Ramakrishnan C, Sasisekharan V (1963) Stereochemistry of Polypeptide Chain Configurations. J Mol Biol 7:95
165. Davis IW, Murray LW, Richardson JS, Richardson DC (2004) Molprobity: Structure Validation and All-Atom Contact Analysis for Nucleic Acids and Their Complexes. Nucleic Acids Res 32:W615
166. Laskowski RA, MacArthur MW, Moss DS, Thornton JM (1993) Procheck: A Program to Check the Stereochemical Quality of Protein Structures. J Appl Crystallogr 26:283
167. http://checkcif.iucr.org/
168. http://www.ccdc.cam.ac.uk/products/csd/
169. http://cod.ibt.lt/

170. Grazulis S, Chateigner D, Downs RT, Yokochi AFT, Quiros M, Lutterotti L, Manakova E, Butkus J, Moeck P, Bail AL (2009) Crystallography Open Database – an Open-Access Collection of Crystal Structures. J Appl Cryst 42:726

171. http://www.wwpdb.org/

172. http://www.rcsb.org/pdb/

173. Berman HM (2008) Harnessing Knowledge from Structural Genomics. Structure 16:16

174. Berman HM (2008) The Protein Data Bank: A Historical Perspective. Acta Cryst A 64:88

175. Rose PW, Beran B, Bi C, Bluhm WF, Dimitropoulos D, Goodsell DS, Prlić A, Quesada M, Quinn GB, Westbrook JD, Young J, Yukich B, Zardecki C, Berman HM, Bourne PE (2010) The Rcsb Protein Data Bank: Redesigned Web Site and Web Services. Nucleic Acids Res 39:D392

176. Velankar S, Alhroub Y, Alili Al, Best C, Boutselakis HC, Caboche Sgn, Conroy MJ, Dana JM, van Ginkel G, Golovin A, Gore SP, Gutmanas A, Haslam P, Hirshberg M, John M, Lagerstedt I, Mir S, Newman LE, Oldfield TJ, Penkett CJ, Pineda-Castillo J, Rinaldi L, Sahni G, Sawka Gg, Sen S, Slowley R, Sousa da Silva AW, Suarez-Uruena A, Swaminathan GJ, Symmons MF, Vranken WF, Wainwright M, Kleywegt GJ (2010) Pdbe: Protein Data Bank in Europe. Nucleic Acids Res 39:D402

177. Kinjo AR, Yamashita R, Nakamura H (2010) Pdbj Mine: Design and Implementation of Relational Database Interface for Protein Data Bank Japan. Database (Oxford) 2010:baq021

178. http://ndbserver.rutgers.edu/

179. Berman HM, Olson WK, Beveridge DL, Westbrook J, Gelbin A, Demeny T, Hsieh SH, Srinivasan AR, Schneider B (1992) The Nucleic Acid Database. A Comprehensive Relational Database of Three-Dimensional Structures of Nucleic Acids. Biophys J 63:751

180. http://blanco.biomol.uci.edu/Membrane_Proteins_xtal.html

181. http://mcl1.ncifcrf.gov/nihxray/Tips-and-Tricks_Crystallization_Protein-DNA.html

182. http://www.fiz-karlsruhe.de/icsd_content.html

183. http://www.tothcanada.com/

184. http://cars9.uchicago.edu/biocars/pages/timeresolved.shtml

185. Moffat K, Ren Z (1997) Synchrotron Radiation Applications to Macromolecular Crystallography. Curr Opin Struct Biol 7:689

186. Hajdu J, Neutze R, Sjogren T, Edman K, Szoke A, Wilmouth RC, Wilmot CM (2000) Analyzing Protein Functions in Four Dimensions. Nat Struct Biol 7:1006

187. Moffat K (1998) Ultrafast Time-Resolved Crystallography. Nat Struct Biol 5: 641

188. Moffat K (2001) Time-Resolved Biochemical Crystallography: A Mechanistic Perspective. Chem Rev 101:1569

189. Rajagopal S, Kostov KS, Moffat K (2004) Analytical Trapping: Extraction of Time-Independent Structures from Time-Dependent Crystallographic Data. J Struct Biol 147:211

190. Srajer V, Teng T, Ursby T, Pradervand C, Ren Z, Adachi S, Schildkamp W, Bourgeois D, Wulff M, Moffat K (1996) Photolysis of the Carbon Monoxide Complex of Myoglobin: Nanosecond Time-Resolved Crystallography. Science 274:1726

191. Ostermann A, Waschipky R, Parak FG, Nienhaus GU (2000) Ligand Binding and Conformational Motions in Myoglobin. Nature 404:205

192. Srajer V, Ren Z, Teng TY, Schmidt M, Ursby T, Bourgeois D, Pradervand C, Schildkamp W, Wulff M, Moffat K (2001) Protein Conformational Relaxation and Ligand Migration in Myoglobin: A Nanosecond to Millisecond Molecular Movie from Time-Resolved *Laue* X-Ray Diffraction. Biochemistry 40:13802

193. Bourgeois D, Vallone B, Arcovito A, Sciara G, Schotte F, Anfinrud PA, Brunori M (2006) Extended Subnanosecond Structural Dynamics of Myoglobin Revealed by *Laue* Crystallography. Proc Natl Acad Sci USA 103:4924

194. Schmidt M, Nienhaus K, Pahl R, Krasselt A, Anderson S, Parak F, Nienhaus GU, Srajer V (2005) Ligand Migration Pathway and Protein Dynamics in Myoglobin: A Time-Resolved Crystallographic Study on L29w Mbco. Proc Natl Acad Sci USA 102:11704

195. Ihee H, Rajagopal S, Srajer V, Pahl R, Anderson S, Schmidt M, Schotte F, Anfinrud PA, Wulff M, Moffat K (2005) Visualizing Reaction Pathways in Photoactive Yellow Protein from Nanoseconds to Seconds. Proc Natl Acad Sci USA 102:7145

196. Schotte F, Soman J, Olson JS, Wulff M, Anfinrud PA (2004) Picosecond Time-Resolved X-Ray Crystallography: Probing Protein Function in Real Time. J Struct Biol 147:235
197. Schotte F, Lim M, Jackson TA, Smirnov AV, Soman J, Olson JS, Phillips GN, Jr., Wulff M, Anfinrud PA (2003) Watching a Protein as It Functions with 150-Ps Time-Resolved X-Ray Crystallography. Science 300:1944
198. Brunori M, Bourgeois D, Vallone B (2008) Structural Dynamics of Myoglobin. Meth Enzymol 437:397
199. Aranda Rt, Levin EJ, Schotte F, Anfinrud PA, Phillips GN, Jr. (2006) Time-Dependent Atomic Coordinates for the Dissociation of Carbon Monoxide from Myoglobin. Acta Cryst D 62:776
200. Bourgeois D, Vallone B, Schotte F, Arcovito A, Miele AE, Sciara G, Wulff M, Anfinrud P, Brunori M (2003) Complex Landscape of Protein Structural Dynamics Unveiled by Nanosecond *Laue* Crystallography. Proc Natl Acad Sci USA 100:8704
201. Knapp JE, Pahl R, Srajer V, Royer WE (2006) Allosteric Action in Real Time: Time-Resolved Crystallographic Studies of a Cooperative Dimeric Hemoglobin. Proc Natl Acad Sci USA 103:7649
202. Knapp JE, Pahl R, Cohen J, Nichols JC, Schulten K, Gibson QH, Srajer V, Royer WE, Jr. (2009) Ligand Migration and Cavities within Scapharca Dimeric Hbi: Studies by Time-Resolved Crystallography, Xe Binding, and Computational Analysis. Structure 17:1494
203. Perman B, Srajer V, Ren Z, Teng T, Pradervand C, Ursby T, Bourgeois D, Schotte F, Wulff M, Kort R, Hellingwerf K, Moffat K (1998) Energy Transduction on the Nanosecond Time Scale: Early Structural Events in a Xanthopsin Photocycle. Science 279:1946
204. Rajagopal S, Anderson S, Srajer V, Schmidt M, Pahl R, Moffat K (2005) A Structural Pathway for Signaling in the E46q Mutant of Photoactive Yellow Protein. Structure 13:55
205. Tripathi S, Srajer V, Purwar N, Henning R, Schmidt M (2012) pH Dependence of the Photoactive Yellow Protein Photocycle Investigated by Time-Resolved Crystallography. Biophys J 102:325
206. Genick UK, Borgstahl GE, Ng K, Ren Z, Pradervand C, Burke PM, Srajer V, Teng TY, Schildkamp W, McRee DE, Moffat K, Getzoff ED (1997) Structure of a Protein Photocycle Intermediate by Millisecond Time-Resolved Crystallography. Science 275:1471
207. Anderson S, Srajer V, Pahl R, Rajagopal S, Schotte F, Anfinrud P, Wulff M, Moffat K (2004) Chromophore Conformation and the Evolution of Tertiary Structural Changes in Photoactive Yellow Protein. Structure 12:1039
208. Baxter RH, Ponomarenko N, Srajer V, Pahl R, Moffat K, Norris JR (2004) Time-Resolved Crystallographic Studies of Light-Induced Structural Changes in the Photosynthetic Reaction Center. Proc Natl Acad Sci USA 101:5982
209. Ren Z, Perman B, Srajer V, Teng TY, Pradervand C, Bourgeois D, Schotte F, Ursby T, Kort R, Wulff M, Moffat K (2001) A Molecular Movie at 1.8 Å Resolution Displays the Photocycle of Photoactive Yellow Protein, a Eubacterial Blue-Light Receptor, from Nanoseconds to Seconds. Biochemistry 40:13788
210. Schlichting I, Almo SC, Rapp G, Wilson K, Petratos K, Lentfer A, Wittinghofer A, Kabsch W, Pai EF, Petsko GA, Goody RS (1990) Time-Resolved X-Ray Crystallographic Study of the Conformational Change in Ha-Ras P21 Protein on Gtp Hydrolysis. Nature 345:309
211. Key J, Srajer V, Pahl R, Moffat K (2007) Time-Resolved Crystallographic Studies of the Heme Domain of the Oxygen Sensor Fixl: Structural Dynamics of Ligand Rebinding and Their Relation to Signal Transduction. Biochemistry 46:4706
212. Wohri AB, Katona G, Johansson LC, Fritz E, Malmerberg E, Andersson M, Vincent J, Eklund M, Cammarata M, Wulff M, Davidsson J, Groenhof G, Neutze R (2010) Light-Induced Structural Changes in a Photosynthetic Reaction Center Caught by Laue Diffraction. Science 328:630
213. Scott WG (1998) RNA Catalysis. Curr Opin Struct Biol 8:720
214. Scott WG (2002) Visualizing the Structure and Mechanism of a Small Nucleolytic Ribozyme. Methods 28:302

215. Singer PT, Smalas A, Carty RP, Mangel WF, Sweet RM (1993) The Hydrolytic Water Molecule in Trypsin, Revealed by Time-Resolved *Laue* Crystallography. Science 259:669
216. Hadfield A, Hajdu J (1994) On the Photochemical Release of Phosphate from 3,5-Dinitrophenyl Phosphate in a Protein Crystal. J Mol Biol 236:995
217. Stoddard BL (2001) Trapping Reaction Intermediates in Macromolecular Crystals for Structural Analyses. Methods 24:125
218. Moffat K, Szebenyi D, Bilderback D (1984) X-Ray *Laue* Diffraction from Protein Crystals. Science 223:1423
219. Bourgeois D, Wagner U, Wulff M (2000) Towards Automated *Laue* Data Processing: Application to the Choice of Optimal X-Ray Spectrum. Acta Cryst D 56:973
220. Bourgeois D, Schotte F, Brunori M, Vallone B (2007) Time-Resolved Methods in Biophysics. 6. Time-Resolved *Laue* Crystallography as a Tool to Investigate Photo-Activated Protein Dynamics. Photochem Photobiol Sci 6:1047
221. Schmidt M, Krasselt A, Reuter W (2006) Local Protein Flexibility as a Prerequisite for Reversible Chromophore Isomerization in Alpha-Phycoerythrocyanin. Biochim Biophys Acta 1764:55
222. http://www.esrf.eu/UsersAndScience/Experiments/SoftMatter/ID09B
223. Schmidt M, Graber T, Henning R, Šrajer V (2010) Five-Dimensional Crystallography. Acta Cryst A 66:198
224. Schmidt M, Ihee H, Pahl R, Srajer V (2005) Protein-Ligand Interaction Probed by Time-Resolved Crystallography. Methods Mol Biol 305:115
225. Fromme P, Spence JC (2011) Femtosecond Nanocrystallography Using X-Ray Lasers for Membrane Protein Structure Determination. Curr Opin Struct Biol 21:509
226. Westenhoff S, Nazarenko E, Malmerberg E, Davidsson J, Katona G, Neutze R (2010) Time-Resolved Structural Studies of Protein Reaction Dynamics: A Smorgasbord of X-Ray Approaches. Acta Cryst A 66:207
227. Moffat K (2003) The Frontiers of Time-Resolved Macromolecular Crystallography: Movies and Chirped X-Ray Pulses. Faraday Discuss 122:65
228. Schmidt M, Srajer V, Purwar N, Tripathi S (2012) The Kinetic Dose Limit in Room-Temperature Time-Resolved Macromolecular Crystallography. J Synchrotron Radiat 19:264
229. Wilson CC (2000) Single Crystal Neutron Diffraction from Molecular Materials. Scientific Publishing Co., Singapore
230. http://www.ccdc.cam.ac.uk/products/csd/statistics/
231. Schoenborn BP (2010) A History of Neutrons in Biology: The Development of Neutron Protein Crystallography at Bnl and Lanl. Acta Cryst D 66:1262
232. Schoenborn BP (1976) Advantages of Neutron Scattering for Biological Structure Analysis. Brookhaven Symp Biol 27:110
233. Meher AK, Blaber SI, Lee J, Honjo E, Kuroki R, Blaber M (2009) Engineering an Improved Crystal Contact across a Solvent-Mediated Interface of Human Fibroblast Growth Factor 1. Acta Cryst F 65:1136
234. Honjo E, Tamada T, Adachi M, Kuroki R, Meher A, Blaber M (2008) Mutagenesis of the Crystal Contact of Acidic Fibroblast Growth Factor. J Synchrotron Radiat 15:285
235. Yamaguchi S, Kamikubo H, Shimizu N, Yamazaki Y, Imamoto Y, Kataoka M (2007) Preparation of Large Crystals of Photoactive Yellow Protein for Neutron Diffraction and High Resolution Crystal Structure Analysis. Photochem Photobiol 83:336
236. Maeda M, Chatake T, Tanaka I, Ostermann A, Niimura N (2004) Crystallization of a Large Single Crystal of Cubic Insulin for Neutron Protein Crystallography. J Synchrotron Radiat 11:41
237. Terzyan SS, Bourne CR, Ramsland PA, Bourne PC, Edmundson AB (2003) Comparison of the Three-Dimensional Structures of a Human Bence-Jones Dimer Crystallized on Earth and Aboard Us Space Shuttle Mission Sts-95. J Mol Recognit 16:83
238. Blum MM, Tomanicek SJ, John H, Hanson BL, Ruterjans H, Schoenborn BP, Langan P, Chen JC (2010) X-Ray Structure of Perdeuterated Diisopropyl Fluorophosphatase (Dfpase): Perdeuteration of Proteins for Neutron Diffraction. Acta Cryst F 66:379

239. Meilleur F, Weiss KL, Myles DA (2009) Deuterium Labeling for Neutron Structure-Function-Dynamics Analysis. Methods Mol Biol 544:281
240. Samuel-Landtiser M, Zachariah C, Williams CR, Edison AS, Long JR (2007) Incorporation of Isotopically Enriched Amino Acids. Curr Protoc Protein Sci 26:26.3
241. Phillips SE, Schoenborn BP (1981) Neutron Diffraction Reveals Oxygen-Histidine Hydrogen Bond in Oxymyoglobin. Nature 292:81
242. Cipriani F, Castagna JC, Wilkinson C, Lehmann MS, Buldt G (1996) A Neutron Image Plate Quasi-*Laue* Diffractometer for Protein Crystallography. Basic Life Sci 64:423
243. Glusker JP, Carrell HL, Kovalevsky AY, Hanson L, Fisher SZ, Mustyakimov M, Mason S, Forsyth T, Langan P (2010) Using Neutron Protein Crystallography to Understand Enzyme Mechanisms. Acta Cryst D 66:1257
244. Adams PD, Mustyakimov M, Afonine PV, Langan P (2009) Generalized X-Ray and Neutron Crystallographic Analysis: More Accurate and Complete Structures for Biological Macromolecules. Acta Cryst D 65:567
245. Blakeley MP, Langan P, Niimura N, Podjarny A (2008) Neutron Crystallography: Opportunities, Challenges, and Limitations. Curr Opin Struct Biol 18:593
246. Myles DA (2006) Neutron Protein Crystallography: Current Status and a Brighter Future. Curr Opin Struct Biol 16:630
247. Meilleur F, Myles DA, Blakeley MP (2006) Neutron Laue Macromolecular Crystallography. Eur Biophys J 35:611
248. Kovalevsky A, Fisher Z, Johnson H, Mustyakimov M, Waltman MJ, Langan P (2010) Macromolecular Neutron Crystallography at the Protein Crystallography Station (Pcs). Acta Cryst D 66:1206
249. Langan P, Fisher Z, Kovalevsky A, Mustyakimov M, Sutcliffe Valone A, Unkefer C, Waltman MJ, Coates L, Adams PD, Afonine PV, Bennett B, Dealwis C, Schoenborn BP (2008) Protein Structures by Spallation Neutron Crystallography. J Synchrotron Radiat 15:215
250. Blakeley MP, Teixeira SC, Petit-Haertlein I, Hazemann I, Mitschler A, Haertlein M, Howard E, Podjarny AD (2010) Neutron Macromolecular Crystallography with Ladi-III. Acta Cryst D 66:1198
251. Tanaka I, Kusaka K, Hosoya T, Niimura N, Ohhara T, Kurihara K, Yamada T, Ohnishi Y, Tomoyori K, Yokoyama T (2010) Neutron Structure Analysis Using the Ibaraki Biological Crystal Diffractometer (Ibix) at J-Parc. Acta Cryst D 66:1194
252. Kratky C, Kräutler B (1999) X-Ray Crystallography of B_{12}. In: Banerjee R (ed) Chemistry and Biochemistry of B_{12}. John Wiley & Sons, New York, p 9
253. Langan P, Lehmann M, Wilkinson C, Jogl G, Kratky C (1999) Neutron *Laue* Diffraction Studies of Coenzyme Cob(II)Alamin. Acta Cryst D 55:51
254. Munshi P, Chung SL, Blakeley MP, Weiss KL, Myles DA, Meilleur F (2012) Rapid Visualization of Hydrogen Positions in Protein Neutron Crystallographic Structures. Acta Cryst D 68:35
255. Chen JC, Fisher Z, Kovalevsky AY, Mustyakimov M, Hanson BL, Zhurov VV, Langan P (2012) Room-Temperature Ultrahigh-Resolution Time-of-Flight Neutron and X-Ray Diffraction Studies of H/D-Exchanged Crambin. Acta Cryst F 68:119
256. Shu F, Ramakrishnan V, Schoenborn BP (2000) Enhanced Visibility of Hydrogen Atoms by Neutron Crystallography on Fully Deuterated Myoglobin. Proc Natl Acad Sci USA 97:3872
257. Bon C, Lehmann MS, Wilkinson C (1999) Quasi-*Laue* Neutron-Diffraction Study of the Water Arrangement in Crystals of Triclinic Hen Egg-White Lysozyme. Acta Cryst D 55:978
258. Yokoyama T, Mizuguchi M, Nabeshima Y, Kusaka K, Yamada T, Hosoya T, Ohhara T, Kurihara K, Tomoyori K, Tanaka I, Niimura N (2012) Hydrogen-Bond Network and pH Sensitivity in Transthyretin: Neutron Crystal Structure of Human Transthyretin. J Struct Biol 177:283
259. Lazar LM, Fisher SZ, Moulin AG, Kovalevsky A, Novak WR, Langan P, Petsko GA, Ringe D (2011) Time-of-Flight Neutron Diffraction Study of Bovine Gamma-Chymotrypsin at the Protein Crystallography Station. Acta Cryst F 67:587
260. Howard EI, Blakeley MP, Haertlein M, Petit-Haertlein I, Mitschler A, Fisher SJ, Cousido-Siah A, Salvay AG, Popov A, Muller-Dieckmann C, Petrova T, Podjarny A (2011) Neutron

Structure of Type-Iii Antifreeze Protein Allows the Reconstruction of Afp-Ice Interface. J Mol Recognit 24:724

261. Kawamura K, Yamada T, Kurihara K, Tamada T, Kuroki R, Tanaka I, Takahashi H, Niimura N (2011) X-Ray and Neutron Protein Crystallographic Analysis of the Trypsin-Bpti Complex. Acta Cryst D 67:140

262. Mueser TC, Griffith WP, Kovalevsky AY, Guo J, Seaver S, Langan P, Hanson BL (2010) Hemoglobin Redux: Combining Neutron and X-Ray Diffraction with Mass Spectrometry to Analyse the Quaternary State of Oxidized Hemoglobins. Acta Cryst D 66:1249

263. Kovalevsky A, Chatake T, Shibayama N, Park SY, Ishikawa T, Mustyakimov M, Fisher SZ, Langan P, Morimoto Y (2010) Protonation States of Histidine and Other Key Residues in Deoxy Normal Human Adult Hemoglobin by Neutron Protein Crystallography. Acta Cryst D 66:1144

264. Kovalevsky AY, Chatake T, Shibayama N, Park SY, Ishikawa T, Mustyakimov M, Fisher Z, Langan P, Morimoto Y (2010) Direct Determination of Protonation States of Histidine Residues in a 2 Å Neutron Structure of Deoxy-Human Normal Adult Hemoglobin and Implications for the *Bohr* Effect. J Mol Biol 398:276

265. Chatake T, Shibayama N, Park SY, Kurihara K, Tamada T, Tanaka I, Niimura N, Kuroki R, Morimoto Y (2007) Protonation States of Buried Histidine Residues in Human Deoxyhemoglobin Revealed by Neutron Crystallography. J Amer Chem Soc 129:14840

266. Fisher SZ, Kovalevsky AY, Domsic JF, Mustyakimov M, McKenna R, Silverman DN, Langan PA (2010) Neutron Structure of Human Carbonic Anhydrase II: Implications for Proton Transfer. Biochemistry 49:415

267. Iwai W, Yamada T, Kurihara K, Ohnishi Y, Kobayashi Y, Tanaka I, Takahashi H, Kuroki R, Tamada T, Niimura N (2009) A Neutron Crystallographic Analysis of T6 Porcine Insulin at 2.1 Å Resolution. Acta Cryst D 65:1042

268. Yagi D, Yamada T, Kurihara K, Ohnishi Y, Yamashita M, Tamada T, Tanaka I, Kuroki R, Niimura N (2009) A Neutron Crystallographic Analysis of Phosphate-Free Ribonuclease a at 1.7 Å Resolution. Acta Cryst D 65:892

269. Tamada T, Kinoshita T, Kurihara K, Adachi M, Ohhara T, Imai K, Kuroki R, Tada T (2009) Combined High-Resolution Neutron and X-Ray Analysis of Inhibited Elastase Confirms the Active-Site Oxyanion Hole but Rules against a Low-Barrier Hydrogen Bond. J Amer Chem Soc 131:11033

270. Kuroki R, Okazaki N, Adachi M, Ohhara T, Kurihara K, Tamada T (2010) Towards Investigation of the Inhibitor-Recognition Mechanisms of Drug-Target Proteins by Neutron Crystallography. Acta Cryst D 66:1126

271. Adachi M, Ohhara T, Kurihara K, Tamada T, Honjo E, Okazaki N, Arai S, Shoyama Y, Kimura K, Matsumura H, Sugiyama S, Adachi H, Takano K, Mori Y, Hidaka K, Kimura T, Hayashi Y, Kiso Y, Kuroki R (2009) Structure of HIV-1 Protease in Complex with Potent Inhibitor Kni-272 Determined by High-Resolution X-Ray and Neutron Crystallography. Proc Natl Acad Sci USA 106:4641

272. Blum MM, Mustyakimov M, Ruterjans H, Kehe K, Schoenborn BP, Langan P, Chen JC (2009) Rapid Determination of Hydrogen Positions and Protonation States of Diisopropyl Fluorophosphatase by Joint Neutron and X-Ray Diffraction Refinement. Proc Natl Acad Sci USA 106:713

273. Fisher SZ, Anderson S, Henning R, Moffat K, Langan P, Thiyagarajan P, Schultz AJ (2007) Neutron and X-Ray Structural Studies of Short Hydrogen Bonds in Photoactive Yellow Protein (Pyp). Acta Cryst D 63:1178

274. Bennett B, Langan P, Coates L, Mustyakimov M, Schoenborn B, Howell EE, Dealwis C (2006) Neutron Diffraction Studies of *Escherichia coli* Dihydrofolate Reductase Complexed with Methotrexate. Proc Natl Acad Sci USA 103:18493

275. Meilleur F, Snell EH, van der Woerd MJ, Judge RA, Myles DA (2006) A Quasi-*Laue* Neutron Crystallographic Study of D-Xylose Isomerase. Eur Biophys J 35:601

276. Blakeley MP, Mitschler A, Hazemann I, Meilleur F, Myles DA, Podjarny A (2006) Comparison of Hydrogen Determination with X-Ray and Neutron Crystallography in a Human Aldose Reductase-Inhibitor Complex. Eur Biophys J 35:577

277. Blakeley MP, Kalb AJ, Helliwell JR, Myles DA (2004) The 15-K Neutron Structure of Saccharide-Free Concanavalin A. Proc Natl Acad Sci USA 101:16405
278. Habash J, Raftery J, Nuttall R, Price HJ, Wilkinson C, Kalb AJ, Helliwell JR (2000) Direct Determination of the Positions of the Deuterium Atoms of the Bound Water in Concanavalin A by Neutron *Laue* Crystallography. Acta Cryst D 56:541
279. Chatake T, Kurihara K, Tanaka I, Tsyba I, Bau R, Jenney FE, Jr., Adams MW, Niimura N (2004) A Neutron Crystallographic Analysis of a Rubredoxin Mutant at 1.6 Å Resolution. Acta Cryst D 60:1364
280. Coates L, Erskine PT, Wood SP, Myles DA, Cooper JB (2001) A Neutron *Laue* Diffraction Study of Endothiapepsin: Implications for the Aspartic Proteinase Mechanism. Biochemistry 40:13149
281. Kovalevsky AY, Hanson BL, Seaver S, Fisher SZ, Mustyakimov M, Langan P (2011) Preliminary Joint X-Ray and Neutron Protein Crystallographic Studies of Endoxylanase II from the Fungus *Trichoderma longibrachiatum*. Acta Cryst F 67:283
282. Schuman B, Fisher SZ, Kovalevsky A, Borisova SN, Palcic MM, Coates L, Langan P, Evans SV (2011) Preliminary Joint Neutron Time-of-Flight and X-Ray Crystallographic Study of Human Abo(H) Blood Group a Glycosyltransferase. Acta Cryst F 67:258
283. Gardberg AS, Del Castillo AR, Weiss KL, Meilleur F, Blakeley MP, Myles DA (2010) Unambiguous Determination of H-Atom Positions: Comparing Results from Neutron and High-Resolution X-Ray Crystallography. Acta Cryst D 66:558
284. Oksanen E, Blakeley MP, Bonnete F, Dauvergne MT, Dauvergne F, Budayova-Spano M (2009) Large Crystal Growth by Thermal Control Allows Combined X-Ray and Neutron Crystallographic Studies to Elucidate the Protonation States in *Aspergillus flavus* Urate Oxidase. J Royal Soc Interface 6:S599
285. Novak WR, Moulin AG, Blakeley MP, Schlichting I, Petsko GA, Ringe D (2009) A Preliminary Neutron Diffraction Study of Gamma-Chymotrypsin. Acta Cryst F 65:317
286. Teixeira SC, Blakeley MP, Leal RM, Mitchell EP, Forsyth VT (2008) A Preliminary Neutron Crystallographic Study of Thaumatin. Acta Cryst F 64:378
287. Chatake T, Mizuno N, Voordouw G, Higuchi Y, Arai S, Tanaka I, Niimura N (2003) Crystallization and Preliminary Neutron Analysis of the Dissimilatory Sulfite Reductase D (Dsrd) Protein from the Sulfate-Reducing Bacterium *Desulfovibrio vulgaris*. Acta Cryst D 59:2306
288. Timmins PA, Pebay-Peyroula E (1996) Protein-Detergent Interactions in Single Crystals of Membrane Proteins Studied by Neutron Crystallography. Basic Life Sci 64:267
289. Penel S, Pebay-Peyroula E, Rosenbusch J, Rummel G, Schirmer T, Timmins PA (1998) Detergent Binding in Trigonal Crystals of Ompf Porin from *Escherichia coli*. Biochimie 80:543
290. Pebay-Peyroula E, Garavito RM, Rosenbusch JP, Zulauf M, Timmins PA (1995) Detergent Structure in Tetragonal Crystals of Ompf Porin. Structure 3:1051
291. Roth M, Arnoux B, Ducruix A, Reiss-Husson F (1991) Structure of the Detergent Phase and Protein-Detergent Interactions in Crystals of the Wild-Type (Strain Y) *Rhodobacter sphaeroides* Photochemical Reaction Center. Biochemistry 30:9403
292. Hermoso J, Pignol D, Penel S, Roth M, Chapus C, Fontecilla-Camps JC (1997) Neutron Crystallographic Evidence of Lipase-Colipase Complex Activation by a Micelle. EMBO J 16:5531
293. Gilmore CJ (2003) Nanocrystals: Solving Crystal Structures Using Electron Crystallography. Crystallogr Rev 9:17
294. Martinez-Franco R, Moliner M, Yun Y, Sun J, Wan W, Zou X, Corma A (2013) Synthesis of an Extra-Large Molecular Sieve Using Proton Sponges as Organic Structure-Directing Agents. Proc Nat Acad Sci USA 110:3749
295. Raunser S, Walz T (2009) Electron Crystallography as a Technique to Study the Structure on Membrane Proteins in a Lipidic Environment. Annu Rev Biophys 38:89
296. Hite RK, Raunser S, Walz T (2007) Revival of Electron Crystallography. Curr Opin Struct Biol 17:389

297. Fujiyoshi Y (2011) Electron Crystallography for Structural and Functional Studies of Membrane Proteins. J Electron Microsc (Tokyo) 60 Suppl 1:149
298. http://www.instruct-fp7.eu/
299. Aquila A, Hunter MS, Doak RB, Kirian RA, Fromme P, White TA, Andreasson J, Arnlund D, Bajt S, Barends TR, Barthelmess M, Bogan MJ, Bostedt C, Bottin H, Bozek JD, Caleman C, Coppola N, Davidsson J, DePonte DP, Elser V, Epp SW, Erk B, Fleckenstein H, Foucar L, Frank M, Fromme R, Graafsma H, Grotjohann I, Gumprecht L, Hajdu J, Hampton CY, Hartmann A, Hartmann R, Hau-Riege S, Hauser G, Hirsemann H, Holl P, Holton JM, Homke A, Johansson L, Kimmel N, Kassemeyer S, Krasniqi F, Kuhnel KU, Liang M, Lomb L, Malmerberg E, Marchesini S, Martin AV, Maia FR, Messerschmidt M, Nass K, Reich C, Neutze R, Rolles D, Rudek B, Rudenko A, Schlichting I, Schmidt C, Schmidt KE, Schulz J, Seibert MM, Shoeman RL, Sierra R, Soltau H, Starodub D, Stellato F, Stern S, Struder L, Timneanu N, Ullrich J, Wang X, Williams GJ, Weidenspointner G, Weierstall U, Wunderer C, Barty A, Spence JC, Chapman HN (2012) Time-Resolved Protein Nanocrystallography Using an X-Ray Free-Electron Laser. Opt Express 20:2706
300. Kirian RA, White TA, Holton JM, Chapman HN, Fromme P, Barty A, Lomb L, Aquila A, Maia FR, Martin AV, Fromme R, Wang X, Hunter MS, Schmidt KE, Spence JC (2011) Structure-Factor Analysis of Femtosecond Microdiffraction Patterns from Protein Nanocrystals. Acta Cryst A 67:131
301. Ewald PP (1969) Introduction to the Dynamical Theory of X-Ray Diffraction. Acta Cryst A 25:103
302. Kräutler B, Keller W, Kratky C (1989) Coenzyme B_{12} Chemistry: The Molecular Structure of Cob(II)alamin. J Amer Chem Soc 111:8936
303. Schwarzenbacher R, Zeth K, Diederichs K, Gries A, Kostner GM, Laggner P, Prassl R (1999) Crystal Structure of Human Beta-2-Glycoprotein I: Implications for Phospholipid Binding and the Antiphospholipid Syndrome. EMBO J 18:6228
304. Wang C, Rath NP, Covey DF (2007) Neurosteroid Analogues. 13. Synthetic Methods for the Preparation of 2β-Hydroxygonane Derivatives as Structural Mimics of *ent*-3α-Hydroxysteroid Modulators of $GABA_{(A)}$ Receptors. Tetrahedron 63:7977
305. Schrodinger LLC (2010) The Pymol Molecular Graphics System. 1.3r1 ed
306. Terwilliger TC (2000) Maximum-Likelihood Density Modification. Acta Cryst D D56:965
307. Wagner UG, Stupperich E, Kratky C (2000) Structure of the Molybdate/Tungstate Binding Protein Mop from *Sporomusa ovata*. Structure 8:1127
308. http://www.rcsb.org/pdb/static.do?p=general_information/pdb_statistics/index.html
309. Diamond R (1974) Real-Space Refinement of Structure of Hen Egg-White Lysozyme. J Mol Biol 82:371

Mass Spectrometry in Natural Product Structure Elucidation

Herbert Budzikiewicz

Contents

H. Budzikiewicz (✉)
Institut für Organische Chemie, Universität zu Köln,
Greinstr. 4, 50939 Köln, Germany
e-mail: aco88@uni-koeln.de

A.D. Kinghorn, H. Falk, J. Kobayashi (eds.), *Progress in the Chemistry of Organic Natural Products, Vol. 100*, DOI 10.1007/978-3-319-05275-5_2,

1 Introduction

The mass spectrometric investigation of natural products started around 1960 in several laboratories. *E. Stenhagen* and *R. Ryhage* (Karolinska Institutet, Stockholm) investigated fatty acid esters and related compounds with a home-made instrument (*1*); *R. I. Reed* (Glasgow University) obtained mass spectra of carbohydrates (*2*), followed in this field closely by *N. K. Kotchetkov* and *O. S. Chizhov* (*3*) (Soviet Academy of Sciences) and by *K. Heyns* (*4*) (University of Hamburg); *K. Biemann* and his group (MIT, Cambridge, MA) opened the field for alkaloids (*5*) and amino acids (*6*); *H. Budzikiewicz* and *C. Djerassi* concentrated on steroids (*7*), triterpenoids (*8*), and alkaloids (*9*), strongly relying on the confirmation of proposed fragmentation mechanisms by deuterium labeling. However, the real origin of natural products mass spectrometry lay somewhere else. Petroleum companies needed in the pre-gas chromatography days a means for the analysis of crude oils and their fractions. For this purpose the electron mass spectra of hydrocarbons and other constituents were determined under strictly standardized conditions with an accuracy never reached since, and with sets of simultaneous equations the qualitative and quantitative compositions of mixtures were determined. The API (American Institute of Petroleum) Catalog (*10*) comprising hundreds of spectra became the core of later spectra collections (see also (*11*)). Thus, commercial mass spectrometers were available suitable for the analysis of other more or less volatile organic compounds.

The topic "Mass Spectrometry—Natural Products" has been treated twice in the *Progress in the Chemistry of Organic Natural Products* series. In 1966 *Biemann* covered primarily alkaloids (*12*) and in 1985 *Howe* and *Jarman* introduced the then new ionization techniques and their applications to various classes of natural products (*13*). Encyclopedic reviews appeared in 1964 (*14*) and in 1972 (*15*) with a supplement in 1980 (*16*), constituting together over 2,000 U.S. letter-sized pages. After this, only specific classes of natural products were treated; the amount of material to be

covered had become too large. Thus, as a continuation of the "*Biochemical Applications of Mass Spectrometry*" books (*15*, *16*) the journal "*Mass Spectrometry Reviews*" (Wiley, New York, N.Y.) was founded in 1982. This, in addition to original contributions contains the series "Collected Reviews on Mass Spectrometric Topics" reporting the titles of review articles appearing in other publications.

In this contribution, several specific classes of natural products will be presented where structural information can be obtained from the fragmentation patterns beyond the molecular mass and elemental composition, and where enough experimental material is available to allow some generalization of the conclusions. It should be remembered, however, that for structure elucidation in most cases, it would be necessary to have more information regarding the type of compound one is dealing with. The dictum from the early days of mass spectrometry, in that this technique is not able to sort out the debris of a blown-up pharmacist's shop, is still true. Another criterion for the selection will be the demonstration of specific problems and ways by which they may circumvented. Historical developments will also be considered.

The manuscript was delivered to the Editors in December 2012. Not to let the time gap unused until the manuscript reaches the printer, literature references starting with (*594*) are added to the References and an Addendum is provided. In this way the chapter is kept as up to date as possible, while renumberings are avoided.

Using the example of pentacyclic triterpenoids, it is shown how structural studies using electron ionization have been developed over the years. Vertebrate alkaloids cover a field where the structural studies mainly stem from the last twenty years relying also on electron ionization but in part introducing more recent techniques. The sections on lipids and on carbohydrates demonstrate specifically how the ionization techniques have allowed the handling of involatile compounds and have extended the area of structural research step by step. The sections covering peptides and nucleotides show the extension to very high masses and to three-dimensional information of molecules. Fast computers with almost unlimited data storage capacities have made possible automated structural studies and the analysis of complex mixtures.

The last section contains a list of mass spectra collections (mainly electron ionization) from the natural products field. All these collections should be used with due caution, especially when they are based on compilations of literature data. Possible sources of error may lie in the recording (thermal degradation, purity of the sample, calibration of the mass spectrometer), the data processing (especially older data digitalized from analog recordings by hand, mistakes in data transfer), and after all—the published structure may be wrong. Whenever possible the original literature should be consulted.

Most of the earlier reviews could rely on thorough investigations of the fragmentation behavior of specific substance classes, usually accompanied by extensive deuterium labeling studies. Problems in updating arise because in many of the more recent publications only a selection of masses is reported according to the judgment of the authors as to what might be relevant (for an example see Sect. 3.2.7), so proposals for fragment geneses are often based only on one example. Also systematic investigations have concentrated on very specific areas, which may be *en vogue,* such as proteomics.

2 Mass Spectrometric Techniques

In this section a short introduction will be given into the various mass spectrometric techniques (*17*) that have gained importance in the investigation of natural products.

2.1 Ionization Techniques

Electron ionization (*EI*) is effected by interaction of the substrate molecules with an electron beam resulting in the formation of molecular ions lacking one electron (radical ions, $M^{+\cdot}$) with surplus vibrational energy, which causes their decomposition. The fragmentation processes are well understood and in many cases offer structural information. EI is, however, restricted to compounds available in pure form (at least after chromatographic separation), which can be evaporated in a non-decomposed form under high vacuum.

Chemical ionization (*CI*) (*18*). The substrate is introduced into an EI source together with a large excess of a reagent gas, which is ionized preferentially. Ionization of the substrate molecules occurs either by charge transfer yielding $M^{+\cdot}$ or by ion-molecule reactions resulting *e.g.* in $[M+H]^+$. Chemical ionization with isobutane in connection with GC is commonly used to form only $[M+H]^+$ (and no fragment) ions from the GC fractions. CI with NO has gained some importance for the localization of double or triple bonds in unsaturated aliphatic compounds.

Surface ionization methods. The substance to be investigated is applied to a solid surface in pure form or dissolved in a matrix and is subjected to a beam of high energy particles (FAB and related techniques as secondary ion mass spectrometry, SIMS), to a laser beam (MALDI), or to a strong non-homogeneous electric field (FD). The habit of the mass spectra depends on the ionization method used and on the sample preparation (matrix, additives, *etc.*). Field desorption (FD) (*19*) and fast atom bombardment (FAB) (*20*) were used starting from about 1970, *in praxi* covering mass ranges up to ~1,000 Da. Today they have been superseded by spray techniques. In matrix assisted laser desorption/ionization (MALDI) (*21*) the sample together with a matrix absorbing at the appropriate wave length is irradiated with a pulsed laser (UV or IR), which causes the desorption of mainly singly charged sample ions with masses up to the 10^6 Da mass range. Fragmentation can be induced by collision with gas molecules (collision activation, CA, or collision induced decomposition, CID).

Spray techniques (*22*). A cloud of charged droplets is accelerated towards a counter electrode. On their way the droplets lose solvent molecules by various mechanisms until *e.g.* $[M+H]^+$ or $[M-H]^-$ or at higher mass ranges (up to and beyond 1 MDa) multiply charged species (*e.g.* $[M+nH]^{n+}$) remain. Fragmentation of singly or doubly charged ions can be induced by collision with gas molecules (CA). Here, as well as for the surface ionization techniques mentioned above the most convincing results with CA are obtained from structured substrates such as polypeptides and polysaccharides.

2.2 Ion Separation Techniques

Magnetic fields. Ions are accelerated in an electric field and the ion beam is deflected in a magnetic field. Ion separation, according to the mass-to-charge ratios of the ions is effected by scanning either field. The speed of the (mainly used) magnetic scan is low compared with other ion separation methods. Deflection in the magnetic field can be combined with that in an electric field (double focusing instruments). This allows exact mass measurements.

Time of flight (TOF) (*23*). The accelerated ions flying in a drift tube reach the detector after time intervals corresponding to their mass. With modern instruments the ions are reflected by an electric field into a second drift tube. This increases resolution and allows specific detection techniques. TOF instruments operate in a pulsed manner (ions are formed, accelerated and separated repeatedly) and are therefore ideally suited for combination with ionization by pulsed lasers.

Quadrupoles (*24*). The accelerated ion beam is subjected to AC electric fields, which allow the transmission of ions with specific masses at a time. Since electric fields can be altered quickly, "jumping" from one mass to another is achieved easily. This allows the registration of specific masses only in mixture analyses (see below). In *quadrupole ion traps* (*quistors*) ions are stored in complicated closed paths and those with specific masses are released and recorded (*25*).

Ion cyclotron resonance (*ICR*) (*26*). Ions circulate in the field of a supraconducting magnet with angular frequencies inversly proportional to their mass. The ions are brought into phase by a radiofrequency signal. They induce in a condenser plate a complex electromagnetic wave from which by *Fourier*-transformation the mass spectrum can be calculated. The most important feature of ICR instruments is the ultra-high resolution obtainable (for an example see Sect. 4.3). *Orbitraps* (*27*) working on a similar principle do not need superconducting magnets.

Ion mobility spectrometers (*IM*). The technique is a gas phase electrophoresis at atmospheric pressure. The ionized substrate is accelerated in a pulsed manner into a short drift tube to which an electric field gradient is applied. The drift speed depends on the mass of the substrate and on the number of collisions with air molecules and hence on the molecular shape. Different conformers of *e.g.* proteins can thus be separated. The ions leaving the drift tube are introduced into a TOF mass spectrometer for further analysis (*28*, *29*).

Tandem instruments use the sequential arrangement of two or more analyzers. Ions of a specific mass-to-charge ratio can be selected in the first analyzer and be caused in the following one to fragment by collision with gas molecules (CA) in order to get structural information (see mixture analysis below). Various systems are in use such as an electrostatic and a magnetic analyzer, several quadrupole units, quadrupole and TOF, *etc.* (*17*).

2.3 Analysis of Mixtures

With the exception of special cases such as the petroleum analysis mentioned above mass spectrometric investigation requires pure compounds. Combinations with separation systems such as gas or liquid chromatography (GC, LC) were hampered in the early days by instrumental shortcomings, such as low scanning and registration speed, low sensitivity, and calibration problems. The first attempts with packed GC columns necessitated clumsy separators to remove excess carrier gases. When fast-scanning quadrupole instruments and computer-assisted operation became available, GC with capillary columns became standard. The gas chromatogram is usually reconstructed from the total ion current (TIC) (*i.e.* the sum of all ions reaching the detector in a given time interval).

For LC coupling the techniques used vary with the ionization method. In flow-FAB (*30*), matrix material is added to the LC eluate. The mixture is introduced into the ion source and spreads on the target. Flow-FAB is superseded by the spray techniques where the LC eluate is introduced into the spray capillary. There are restrictions regarding solvents and additives. Other separation techniques such as electrophoresis are used also.

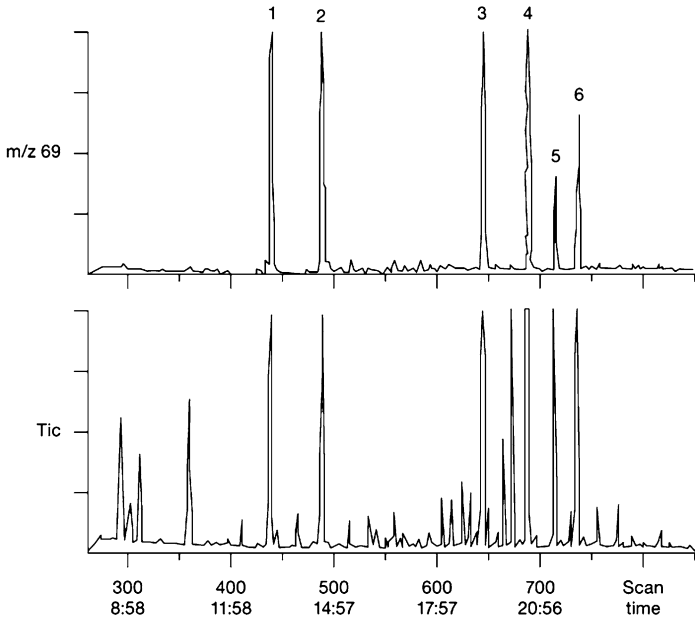

Fig. 1 GC of an extract containing trifluoroacetylated amino acid isopropyl esters reconstructed from the TIC. Only the Gly (1), Ser (2), Dab (3), Phe (4) Orn (5), and Lys (6) containing fractions show a signal at *m/z* 69 (CF_3^+). Reproduced from (*17*) with kind permission of Wiley-VCH Verlag GmbH & Co. KGaA (© 2012)

In cases of complex mixtures in which only the presence or absence of one or few specific components is of interest, separation techniques can be combined with special recognition strategies such as the registration of the interesting molecular species only, using characteristic fragment ions (possibly after group specific derivatization, such as CF_3^+ (*m/z* 69) after trifluoroacetylation of amino acids) (Fig. 1). A less frequently applied possibility is the use of specific reagent gases in CI (*e.g.* NH_3 for nitrogen-containing substances) (Fig. 2).

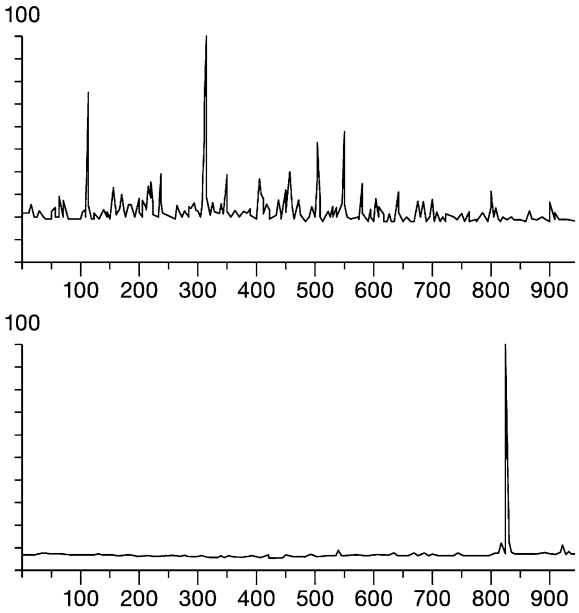

Fig. 2 GC of an extract from sausage for detection of nitrosamines. Upper trace CI with CH_4 ionizing all organic compounds, lower trace CI with NH_3 ionizing only N-containing compounds. With kind permission of Thermo Fisher Scientific, Bremen, Germany

Tandem-mass spectrometry. Where a chromatographic separation is not possible one may try to produce molecular ion species only (*e.g.* $[M+H]^+$ by CI with CH_4 or with isobutane) from the various components of the mixture, by selecting them one after the other by the first analyzer system and inducing fragmentation by CA for further characterization in a following sector of the instrument (Fig. 3). Obviously isomeric compounds having identical molecular masses cannot be separated in this way.

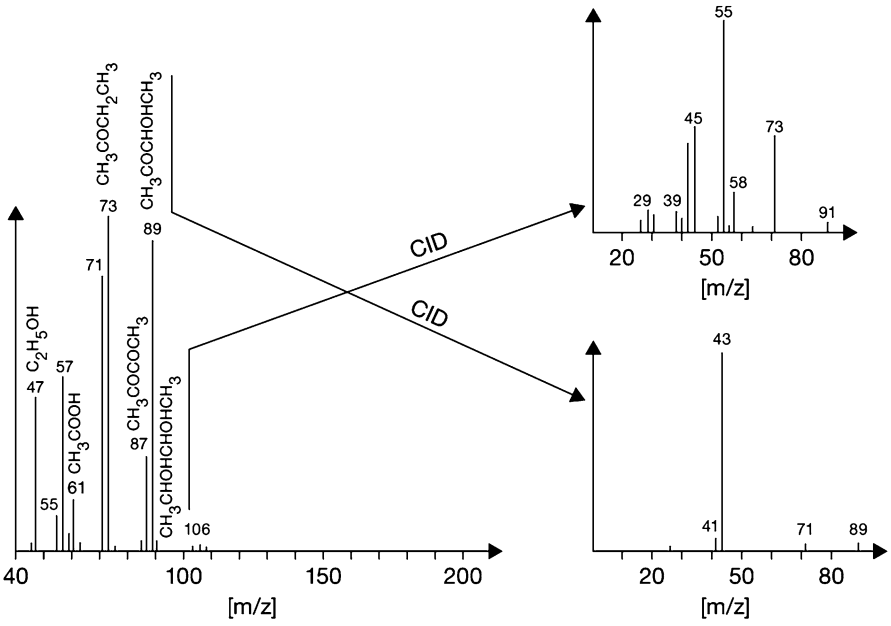

Fig. 3 CI(CH_4) spectrum of a fermentation broth. The left spectrum shows essentially only $[M+H]^+$ ions that subsequently are fragmented by CA (examples are *m/z* 89, 3-hydroxybutan-2-one and *m/z* 91, 2,3-butanediol: right spectra). Adapted from (*31*) with kind permission of the American Chemical Society (© 1987)

2.4 High and Extremely High Masses

When going into a region of very high masses two peculiarities have to be considered. First, carbon consists to 98.93% of ^{12}C and to 1.07% of ^{13}C. Therefore, starting from C_{91} the first isotope peak ($^{12}C_{90}{}^{13}C$) is more abundant than $^{12}C_{91}$, which represents the so-called nominal mass. The other common elements contribute also. For bovine proinsulin, as an example with the elemental composition $C_{381}H_{586}N_{107}O_{114}S_6$, the most abundant ion occurs 9 Da above the nominal mass based on C 12 Da, H 1 Da *etc.* The maximum of the envelope curve is still half a Da higher. In the case that the resolution of the instrument is not high enough, the envelope curve squeezed to a line at the mass of the maximum will be recorded. As a rule of thumb the "molecular weight" calculated from tables based on the elemental isotopic mixtures in the high mass regions will be rather close to that of the maximum of the envelope curve (Fig. 4).

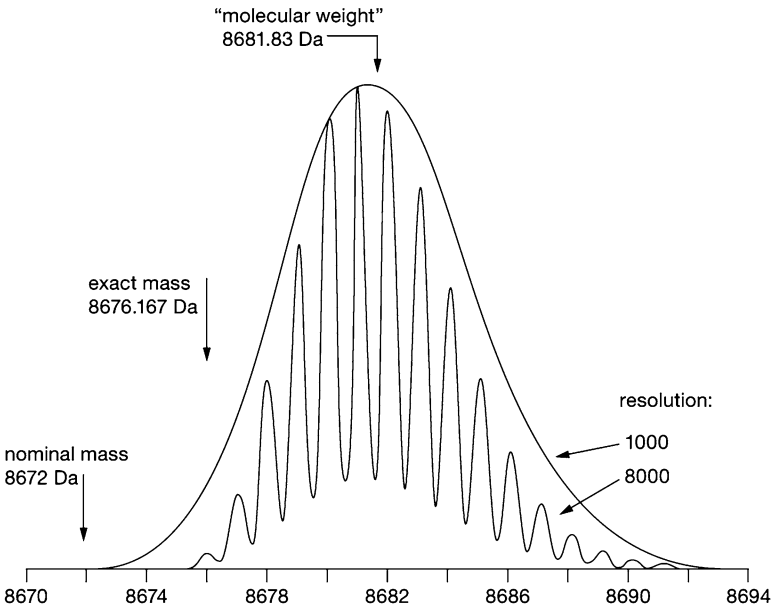

Fig. 4 Molecular ion region of bovine proinsulin (see text). With kind permission of Thermo Fisher Scientific, Bremen, Germany

Second, the exact mass of ^{12}C is by definition 12.00000, and that of ^{1}H 1.00783. 128 H atoms amount to a difference of 1 Da between nominal mass and exact mass. N has also a positive, and O and S have negative mass increments. This should be kept in mind by setting mass windows *e.g.* for quadrupole instruments.

3 Pentacyclic Triterpenes

The major structural types with five six-membered rings are the oleanane (β-amyrin type, **1**, $R^2 = CH_3$) and ursane (α-amyrin type, **2**, $R^1 = CH_3$) groups differing in the location of one methyl group in ring E; those with a five-membered ring E are derived from lupane (**3**) and hopane (**4**). In addition, several rearranged types such as the friedelane (**5**) derivatives have been encountered (*728*) (Fig. 5).

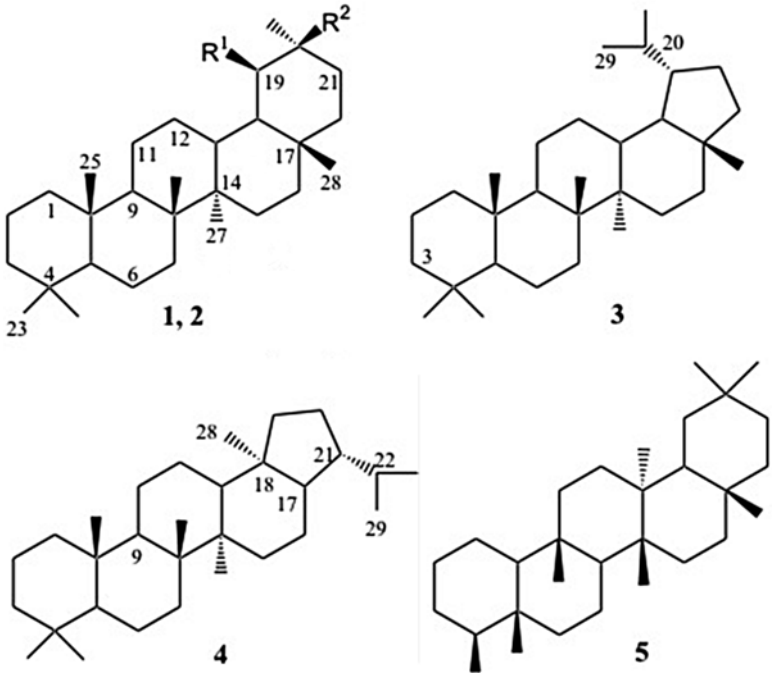

Fig. 5 Triterpene structural types

Common fragmentation reactions are the losses of functional groups such as H_2O from hydroxy compounds both from $M^{+\cdot}$ and from fragment ions, the elimination of $\cdot CH_3$ especially from quaternary or allylic positions, and of $\cdot C_3H_7$ for lupane derivatives and related structures. These processes will be mentioned only in special cases. Typical skeletal fragmentations are started by bond cleavages next to a quaternary center. Specific processes are the *retro-Diels-Alder* (*RDA*) opening of cyclohexene systems (*cf.* Fig. 11), or the *McLafferty* rearrangement (transfer of a γ-H atom to a carbonyl oxygen with concomitant cleavage of the α,β-C–C-bond; *cf.* Fig. 15) when the structural prerequisites are present in a molecule. These two reactions are well-established processes. However, in the literature the geneses of many other fragment ions are depicted involving multi-step bond cleavages and H-transfers. Most of them stem from the 1960s when it was attempted to rationalize the formation of almost any fragment ion. Only in rare cases did labeling studies substantiate the proposed fragmentation mechanisms. These will not be repeated in this chapter.

3.1 Saturated Triterpenes

Compounds of the oleanane or ursane type that are substituted in rings A, B, or E only show, besides the obvious losses of functional groups, cleavage in ring C accompanied by the loss of an additional H atom giving an ion tentatively

formulated as **a** (*m/z* 191 for the hydrocarbon skeleton) (Fig. 6). Substitution results in appropriate mass shifts and in secondary eliminations (as *e.g.* of H_2O for 3-hydroxy derivatives). An analogous cleavage product comprising rings D/E, which would coincide in mass with **a** (*m/z* 191) for the parent hydrocarbon as *e.g.* **a′** from oleanane (*32*), is usually missing (*33*); see also Fig. 7 where the **a′** analog *m/z* 219 is essentially absent.

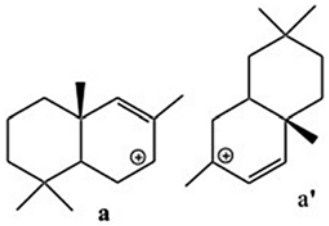

Fig. 6 Skeletal fragments of saturated triterpenes

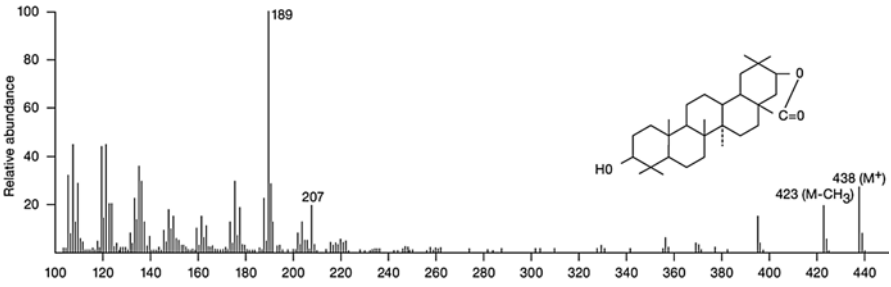

Fig. 7 EI mass spectrum of dihydromachaerinic acid lactone

Introduction of an oxo group at C-12 results in the loss of rings A/B without H-transfer (*m/z* 234 for unsubstituted D/E rings, further loss of $^{\cdot}CH_3$ gives *m/z* 219) for in rings D/E unsubstituted representatives. Different modes of ion formation have been discussed (*59*, *64*).

Gammacerane (the 17,20,20-trisnor-18α,22,22-trimethyl analog of **1**) is also dominated by *m/z* 191 (**a**) coinciding with the analogous ring D/E fragment, which is shifted to *m/z* 207 for the 21-OH derivative tetrahymanol (*34*, *35*).

Structural changes as in the case of friedelane (**5**) and its ursane analog cymbopogone (*36*) result in a completely different fragmentation behavior (Fig. 8). Cleavages at various places of the five rings result in ions of medium to large abundance influenced also by additional substituents—even oxo groups in rings A or E can alter the fragmentation pattern drastically. The published data for friedelan-3-one (friedelin) differ substantially in their ion abundances (*36–41*). Experimental

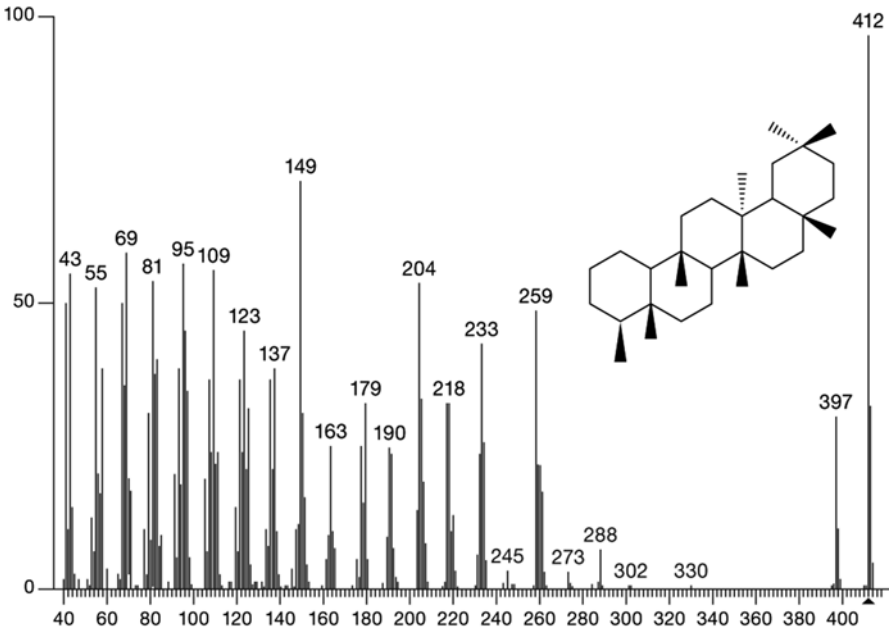

Fig. 8 EI mass spectrum of friedelane (**5**). Spectrum from the NIST library with kind permission from MasCom, Bremen, Germany

conditions such as excess energy and reaction time seem to have appreciable influence since the energy requirements for competing processes are not very different.

The mass spectra of lupane (**3**) and hopane (**4**), except for minor differences in ion abundances, are identical and differ from that of oleanane (**1**) by the presence of small fragment ions due to $[M–C_3H_7]^+$ (*m/z* 369) (*32*, *34*); incidentally the fragments [M–41/42/43 Da]$^+$ cannot be used for distinguishing between isopropyl and isopropenyl groups, see *e.g.* (*43*). All three spectra are dominated by *m/z* 191 (**a** and **a′** analogs). In contrast to oleanane and its derivatives both fragments are formed with comparable likeliness. For hop-22(29)-ene (with an isopropenyl group), *m/z* 189 and 191 are of almost equal abundance (91:100) (*44*), but a survey of geological samples differing in the C-21 substituent and the C-17/C-21 stereochemistry shows differences in the abundance ratios (*45*, *46*) (see also Fig. 9). The masses of the two fragments can be used for additional characterization of the substitution pattern of fossil hopane derivatives, *e.g.* (*47*). A computer compatible program for the classification of triterpene hydrocarbons in geological extracts from mass spectral data has been developed (*48*). For a collection of mass spectral data, see (*50*).

The introduction of oxygenated functionalities (hydroxy, acetoxy, or oxo groups, acid functions) in rings A and/or E results in appropriate mass shifts of **a**- and **a′**-type fragments (additional losses of H_2O or CH_3COOH are possible) (*43*, *49*, *51*–*53*). While a 7-hydroxy group yields the expected *m/z* 207 and 189 (–H_2O) ions, *m/z* 207 is obtained also from the 7-oxo analog probably due to H-transfer to the

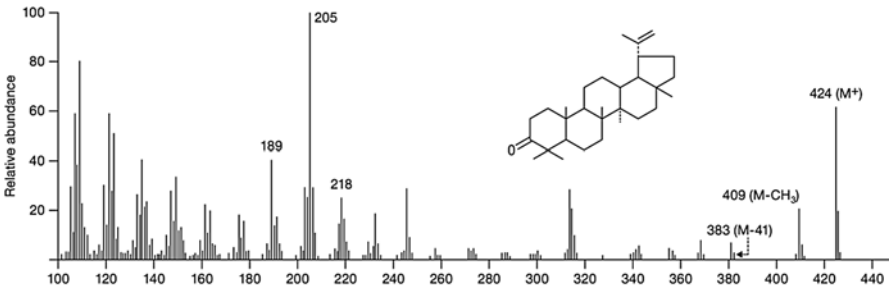

Fig. 9 EI mass spectrum of lup-20(29)-en-3-one

keto group (*54*). The fragments induced by the presence of a 12-oxo group (see above) are of low to medium abundance depending on the remaining substitution pattern, while **a**-type ions prevail (*42*, *53*). Anomalies have been reported for 27-hydroxylupane derivatives (*55*, *56*). For 4α-hydroxyfilican-3-one (**6**) (Fig. 10), the ring D/E fragment (*m/z* 205 due to the additional methyl group) with medium abundance and an unexpected ion with *m/z* 191 of unknown genesis were reported (*57*). Hopane derivatives with modified C-21 side chains, mainly from bacterial origin were discussed in detail (*58*).

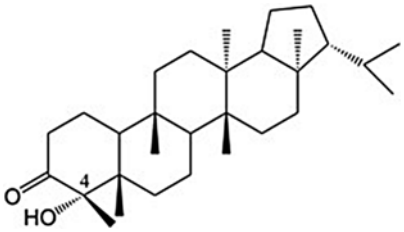

Fig. 10 4α-Hydroxyfilican-3-one (**6**)

There are other fragments that have been considered to be characteristic for lupane and hopane derivatives, but, in summarizing, it can be said that one should be careful in relying on these in the process of structure elucidation of a new compound. The ions *m/z* 189/191 or their substituted congeners may be missing or may be present when not expected (*e.g.* *52*, *57*).

3.2 Triterpenes with Double Bonds

One of the major possibilities of triterpene mass spectrometry is the localization of double bonds.

3.2.1 Δ^{12}-Oleanenes and -Ursenes

Δ^{12}-Double bonds can be recognized readily in EI mass spectra. They induce a *retro-Diels-Alder* (*RDA*) decomposition of ring C. The positive charge is retained preferentially with the diene fragment (*8*, *59*, *60*). Deuterium-labeling studies revealed that no hydrogen rearrangements occur during this process (*59*, *60*). Substituents can be coordinated with the two parts of the molecule by calculating the mass difference with respect to that of **b** (Fig. 11, *m/z* 218 for the unsubstituted hydrocarbon

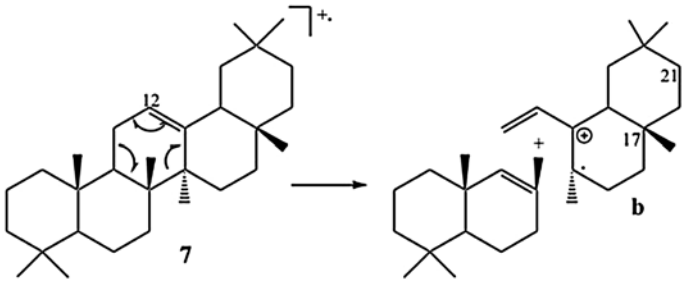

Fig. 11 Fragmentation of Δ^{12}-oleanene (**7**)

species (**7**)). This characteristic fragmentation mode has been reported for a large variety of compounds (*e.g.* (*8*, *55*, *60*)), even for complex molecules (*e.g.* (*61*, *62*)). The diene fragment may however lose substituents and be exceeded in abundance by its decomposition products, depending on the location of the substituents (Fig. 12,

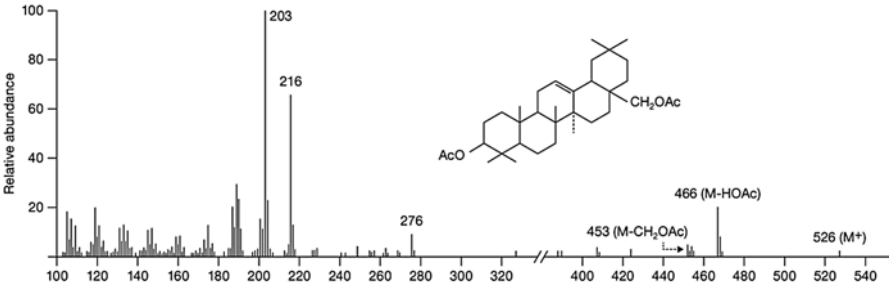

Fig. 12 EI mass spectrum of erythrodiol diacetate

m/z 216: loss of CH_3COOH, *m/z* 203: loss of $-CH_2OCOCH_3$); *cf.* Fig. 13). The importance of this fragmentation reaction could be demonstrated during the structure elucidation of macherinic acid lactone (a 17-carboxylic acid 21-hydroxy lactone)—against chemical evidence (*63*).

Oxo groups in the vicinity of the 12,13-double bond change the fragmentation behavior. Thus, a 11-oxo group (**8**) induces a *McLafferty*-rearrangement followed by

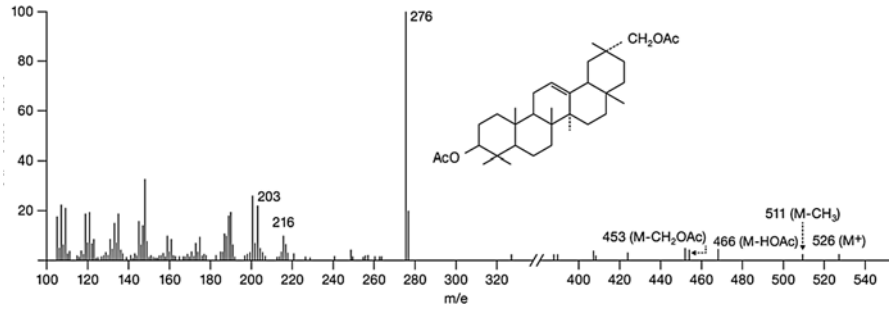

Fig. 13 EI mass spectrum of 30-hydroxy-β-amyrin diacetate

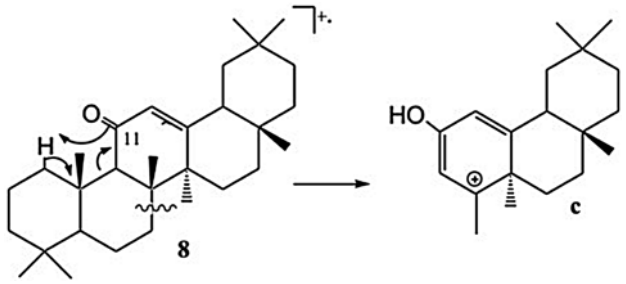

Fig. 14 Fragmentation of **8**

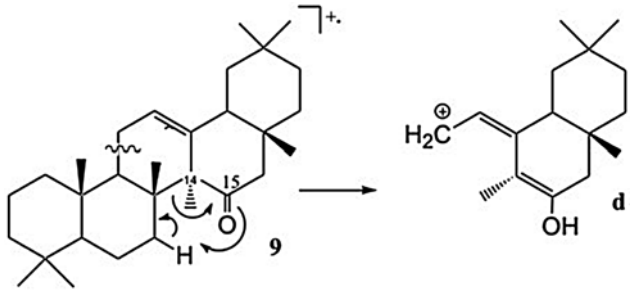

Fig. 15 Fragmentation of **9**

cleavage of the 7,8-bond resulting in ion **c** (Fig. 14) in addition to the *RDA* product (*m/z* 273 and 232, respectively, for ring D/E unsubstituted compounds). The relative abundance of the two species depends on the stereochemistry at C-18: for the $\beta-$H series the ion of the *RDA*-fragment is much reduced in intensity (*60*, *64–66*).

A 15-oxo group (**9**) induces an analogous reaction sequence leading to ion **d** (Fig. 15) (*m/z* 233 for ring D/E unsubstituted compounds). For the reported example a *RDA*-fragment is missing (*64*). This may be due to the 18β-H stereochemistry. A 16-oxo group has no influence (*64*).

3.2.2 Δ^{12}-Lupenes and -Hopenes

In (*64*) it is stated that lup-12-ene derivatives show *RDA* fragments only to a negligible extent, but later (*67*) it was mentioned that the reported examples did actually not contain the C-12 double bond. In more recent publications (*50*, *53*, *68*–*70*, *744*) ions of appreciable abundance are reported, for which their genesis could well be due to this process.

The $\Delta^{12,18}$-dienes yield the *RDA* fragment combined with the loss of a 21-isopropyl group as the most abundant ion (*68*). For 28-acetoxylup-12-en-11-one the analog of ion **c** (*m/z* 131, 100%) and a *RDA* ion (*m/z* 290, 11%) were observed (*53*).

3.2.3 Δ^{5}-Triterpenes

Representatives containing this structural element decompose also by *RDA* with preferred charge retention at the ene-fragment as is typical for 4a-methyl-octalene-2 systems for energetic reasons (*67*). In the spectrum (Fig. 16) of glutinone (**10**) ion **e** (*m/z* 274) (Fig. 17) yields the base peak, which to some extent loses ·CH_3 (*m/z* 259). References to further examples, which also give *RDA* fragments with high abundance, may be found in (*55*); see also (*71*). Lupane derivatives and related systems with an isopropyl side chain show loss of 43 Da (·C_3H_7) from the ene-fragment.

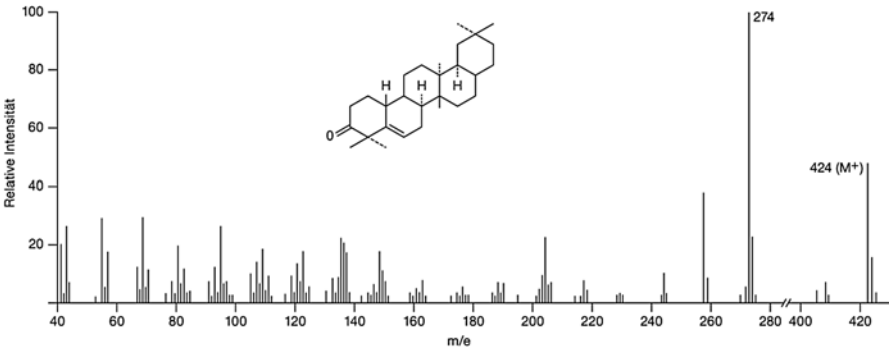

Fig. 16 EI mass spectrum of glutinone (**10**). Reproduced from (*67*) with kind permission from Elsevier (© 1965)

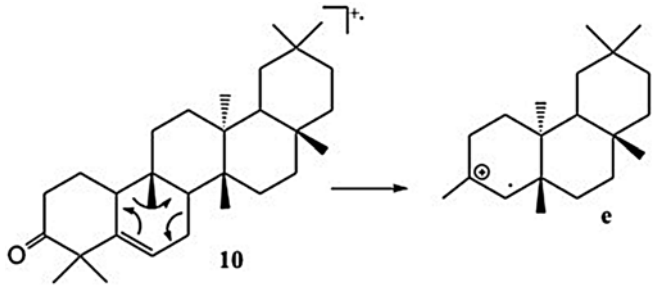

Fig. 17 Fragmentation of **10**

3.2.4 $\Delta^{9(11)}$-Triterpenes

For $\Delta^{9(11)}$ unsaturated compounds one would expect *RDA* fragments (**11**, Fig. 18) with *m/z* 218 (diene-) and 192 (ene-fragment) for the hydrocarbon, but the scarce literature data are contradictory in this respect. In (*72*) partial mass spectral data of

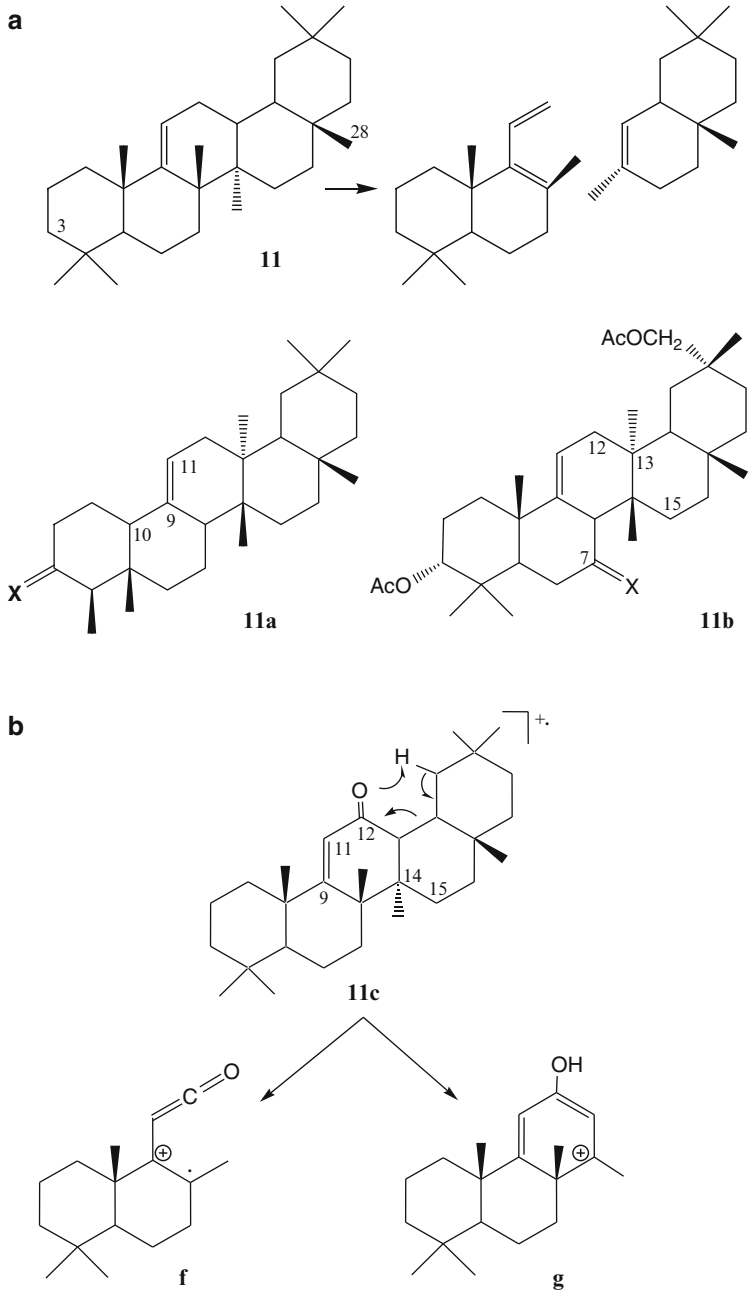

Fig. 18 (**a**) $\Delta^{9(11)}$-Terpenoids. (**b**) Fragmentation of oxygenated $\Delta^{9(11)}$-terpenoids

3β-hydroxyolean-9(11)-en-28-oic acid and of its 3-oxo analog are reported. Both of them yield an abundant fragment *m/z* 248 and not the expected ones, *m/z* 234/232 (diene-) and/or 222 (ene-part). The ion *m/z* 248 could be interpreted as the C-28-carboxyl analog of **b**. This would suggest that rather the 12-ene isomer had been obtained. For 3β-acetoxy-11ξ,12ξ-epoxyolean-9(11)-ene *m/z* 234 (100%) is reported, but since *m/z* 234 (100%) is also given for the 9(11) saturated compound, the formation of this ion cannot be induced by the double bond (*655*).

For the 25-*nor*-D:A-*friedo*-olean-9(11)-ene derivatives putrone (**11a**; X = O) and acetylated putrol (**11a**; X = H, OAc), abundant ene-fragments at *m/z* 206 (87 and 77% rel. int., respectively) with subsequent loss of $\cdot CH_3$ (*m/z* 191, 100%) are reported (*73*). However, for the hydrocarbon (**11a**, X = H, H), ions *m/z* 205 and 191 are mentioned (*74*). In the spectrum (Fig. 29) of arborene (**20** with a 9(11) double bond) neither *m/z* 206 nor *m/z* 191 is of any importance, as it is for several structurally related compounds (*84*, *92*, *93*). The abundant even mass ions in the spectra (*75*) of D:C-*friedo*-olean-9(11)-ene-3α,29-diol diacetate (**11b**, X = H,H) (*m/z* 276, 31% rel. int.) and of its 7-oxo derivative (**11b**, X = O) (*m/z* 278, 100% rel. int.[1]) cannot be correlated with either *RDA* fragment.

Mass spectra of the 12-oxo derivatives (*e.g.* olean-9(11)-en-12-one, **11c**) show two characteristic fragmentation processes (Fig. 18), *RDA* (**f**, *m/z* 232) and *McLafferty*-rearrangement with subsequent cleavage of the 14,15-bond (**g**, *m/z* 271), in both cases with charge retention in the ring A/B/C part (*64*, *72*). The data reported for $\Delta^{9(11),12}$-dienes are contradictory. Two different fragmentation characteristics have been reported. In (*76*, *77*, *741*) a very abundant ion comprising rings D/E plus part of ring C is documented amounting to 218 Da for the unsubstituted hydrocarbon skeleton. References (*78–80*, *740*) mention two fragments of low to medium abundance comprising rings A/B/C and C/D/E, respectively, with equal masses of 255 Da for the hydrocarbon, shifted accordingly upon substitution. For glyyunnansapogenins G and H (the 3β,21α,29-triol and the 29-acid), ions of low to medium abundance are listed attributable to both types of fragmentation, but in the same set of compounds the pattern is not consistent (*80*). The $\Delta^{11,13(18)}$ double bond isomers do not exhibit a characteristic fragmentation pattern (*44*, *740*, *742*); see also the Addendum.

3.2.5 Δ^{14}-Taraxerenes

This group of compounds is characterized by two types of fragments (Figs. 19 and 20). *RDA* fragmentation leads to ion **h** (*m/z* 286 for the hydrocarbon **12**), which readily loses a methyl group, also in combination with the typical eliminations of ring-A substituents (*e.g.* CH_3OH for **13**). The genesis of the second species (*m/z* 204 for the hydrocarbon) is not clear; it is usually formulated as the rearranged ion **i**, which readily loses the C-17 substituent (*m/z* 189 for CH_3) (*50*, *56*, *81–83*). For pteron-14-ene (**14**, Fig. 21), *RDA* fragmentation is of no importance in contrast to its 17β-methyl-19-isopropyl isomer lactuc-14-ene; *m/z* 204 yields for both the base peak. A 7-hydroxy group does not influence the fragmentation pattern for all three structural types (*50*).

[1] *McLafferty* rearrangement (transfer of the C-15 H) of the 7-oxo compound with subsequent cleavage of the 12,13-bond (*cf.* **11c → g**) would lead to an ion *m/z* 277).

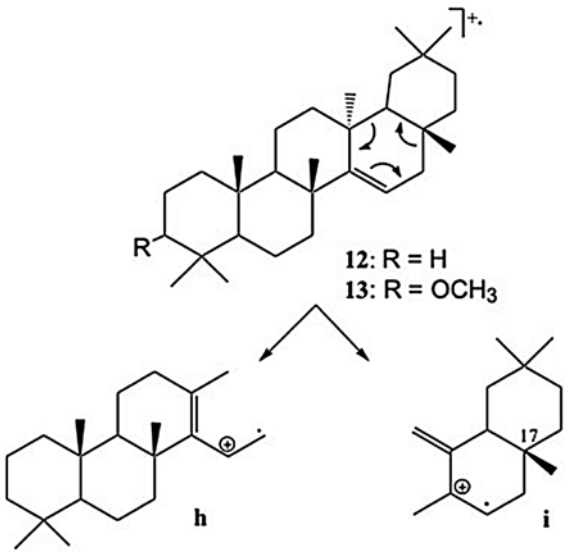

Fig. 19 Fragmentation of **12**

Fig. 20 EI mass spectrum of 3-methoxy-Δ^{14}-taraxerene (**13**). Reproduced from (*81*) with kind permission from Elsevier (© 1969)

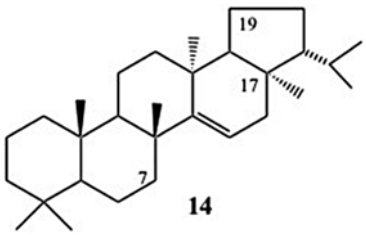

Fig. 21 Pteron-14-ene

3.2.6 $\Delta^{13(18)}$-Oleanene

Several fragments stemming from the C/D/E-rings part of $\Delta^{13(18)}$-oleanane (**15**) (Fig. 22) molecules are reported (*50*, *84*), *viz. m/z* 218, 203–205, and a cluster around *m/z* 191 (Fig. 23). Neohop-13(18)-ene (18-*nor*-17-α-methyl-**4**) (*50*) and its 3-oxo derivative hopanone II (*43*) show an analogous fragmentation behavior.

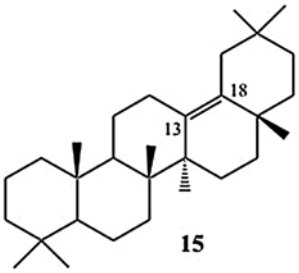

Fig. 22 $\Delta^{13(18)}$-Oleanene (**15**)

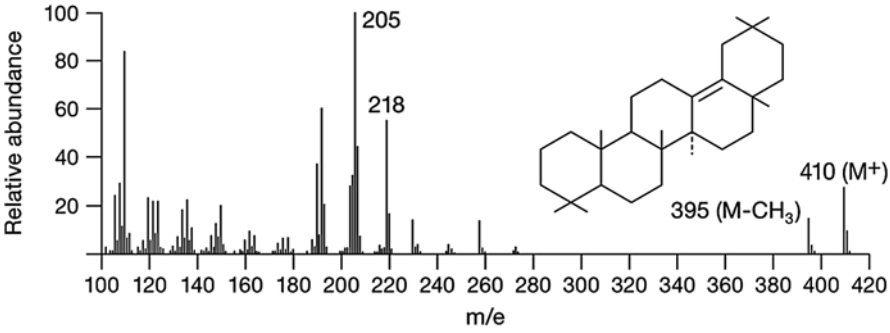

Fig. 23 EI mass spectrum of $\Delta^{13(18)}$-oleanene (**15**)

3.2.7 Δ^{11}-Ursenes and -Oleanenes

For this group no complete EI mass spectra are available in the literature, only listings of selected fragments. For 3β-hydroxy-urs-11-ene (nudicauline A, **15a**) (Fig. 24), *m/z* 364 is reported as the main fragment, but the 3β-acetoxy derivative (nudicauline B) shows no analogous ions. Mentioned for both compounds are **a**-type ions (*m/z* 207 and 189) (*85*).

The main fragmentation processes of 11,12-dehydroursolic acid lactone (**15b**, in the literature occasionally named incorrectly ursolic acid lactone) and its derivatives are the loss of CO_2 and to a lesser extent of CO from $M^{+\cdot}$. The fragment *m/z* 169 (15%), assumed to be formed by cleavage of the 7,8- and the 9,10-bonds under

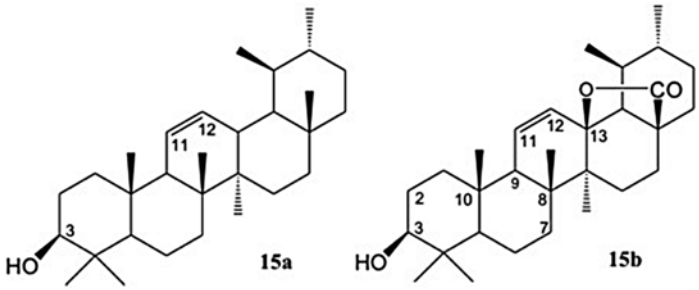

Fig. 24 3β-Hydroxy-urs-11-ene (nudicauline A, **15a**), and 11,12-dehydroursolic acid lactone (**15b**)

transfer of one H atom (besides the complement *m/z* 241 (3%) no other fragment ions are mentioned), was considered as characteristic (*86*). It is shifted in mass to *m/z* 201 ($C_{11}H_{21}O_3$, 30%), mentioned among the fragments listed for the 2α,3β,7β-trihydroxy analog (*87*), but corresponding ions are not reported under the scarce data published for the 3-formoxy derivative of **15b**, camaldulin (*88*) and for its oleanolic acid isomer of **15b** (*89*, *90*). Ions of type **a** are mentioned in some cases. Complete EI spectra of 11,12-dehydroursolic acid lactone (**15b**) and of camaldulin[2] gave a different picture. They showed a large number of ions of similar abundance. The skeletal fragments discussed above are not especially prominent and are imbedded in clusters of ions. The mass spectra are dominated by $[M–CO_2]^{+\cdot}$ (base peak) and $[M–CO]^{+\cdot}$.

3.2.8 Δ^{18}-Oleanenes and -Friedelenes

All representatives (*e.g.* **15c**, Fig. 25)) exhibit a rather pronounced loss of the C-17 substituent due to allylic activation. Major fragments comprise rings D and E or parts of them with or without the C-17 substituent. Mechanisms of their formation have been proposed. Their relative abundance depends on the substitution pattern of the compound. Among these an even mass species can reach high abundance for the Δ^{18}-oleanenes. Its mass is *m/z* 204 for D/E unsubstituted compounds and it is shifted accordingly upon substitution, but its abundance can be reduced drastically when elimination processes prevail[3] (*8*, *50*, *64*, *620*–*622*). Regarding the fragment *m/z* 204, see also Sect. 3.2.5.

[2] Kindly provided by Prof. Dr. *Sabira Begum*, University of Karachi, Pakistan.

[3] As an example for the danger possibly arising from relying on an isolated literature reference: for olean-18-ene-3-one (*50*) quotes the expected *m/z* 204 with 64% rel. int. and *m/z* 218 with 24%, while (*91*) quotes *m/z* 218 with 100% and not *m/z* 204.

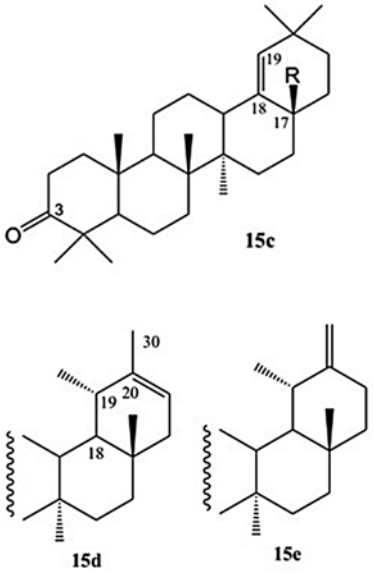

Fig. 25 Δ^{18}-Terpenoids (**15c**): olean-18-en-3-one (R = CH_3), methyl moronate (R = $COOCH_3$) and the Δ^{20}, $\Delta^{20(30)}$-compounds, ψ-taraxasterol (**15d**), and taraxasterol (**15e**)

3.2.9 Δ^{20}- and $\Delta^{18(30)}$-Ursenes

The fragmentation pattern of ψ-taraxasterol (**15d**, Fig. 25) resembles that of saturated compounds, with the **a**-type ions *m/z* 207 and 189 being the main fragments. Of interest is an ion of low intensity at $[M–82]^{+\cdot}$. It was ascribed to a *retro-Diels-Alder* reaction in ring E resulting in the loss of 3-methyl-pentadiene (*64*). Whether the complementary ion *m/z* 82 is formed also cannot be said; the reported mass spectra do not go down that far in mass. The mass spectra of ψ-taraxasterol (**15d**) and of taraxasterol (**15e**) are similar differing only in the relative intensities (*713*). The fragmentation processes occurring in ring E have been studied in detail (*714*). During the formation of $[M–82]^{+\cdot}$ a deuterium label at C-18 is retained and the labels at C-22 and C-30 are lost. Rearrangement to ψ-taraxasterol with subsequent *retro-Diels-Alder* reaction was suggested, but allylic cleavage of the 18,19-bond and subsequently of the 17,22-bond may also be considered. Another ion of low abundance is $[M–69]^{+}$, the genesis of which comprises the loss of the C-19–C-21 part of ring E as shown by D-labeling. Again, cleavage of the 18,19-bond could be the first step.

3.3 Baueranes, Multifloranes, and Swertanes

The members bauerane, multiflorane, and swertane (**16–18**) of this group (Fig. 26) possess methyl groups at C-13 and C-14 for which the location influences the

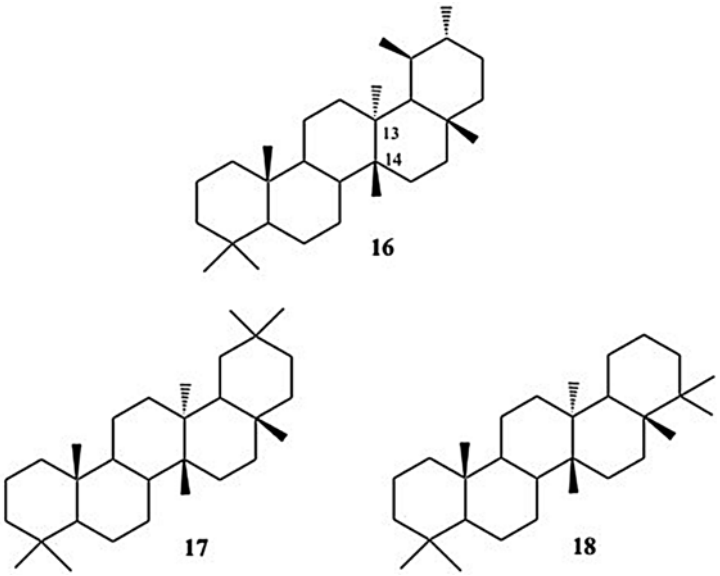

Fig. 26 Bauerane (**16**), multiflorane (**17**), and swertane (**18**)

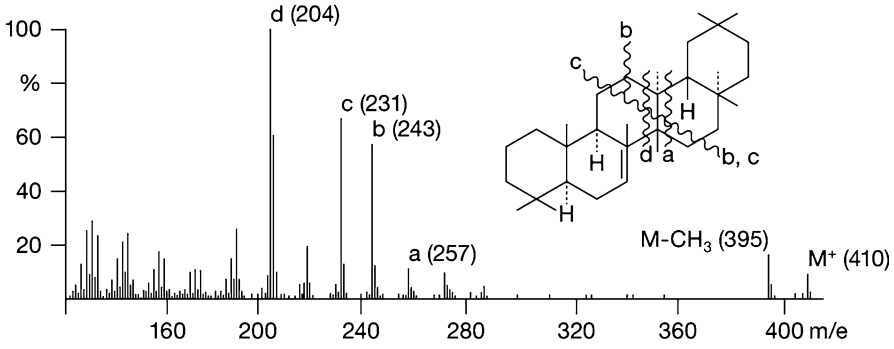

Fig. 27 EI mass spectrum of multiflor-7-ene. Reproduced from (*94*) with kind permission of Wiley-VCH Verlag GmbH & Co. KGaA (© 1963)

fragmentation pattern in a characteristic manner while the position of the double bond (Δ^7, Δ^8, $\Delta^{9(11)}$ for the isomeric multiflorenes) changes only the relative abundance of certain fragments (Fig. 27, Table 1), with the exception of *m/z* 204. This ion yields the base peak for Δ^7 (*m/z* 218 for the 3-oxo compound) comprising rings A, B, and part of C (*64*, *92*). It is of minor importance for the other isomers (*12*, *64*, *82*, *92*, *712*). Surprisingly, *m/z* 204 is of secondary importance for bauer-7-ene (20%), which differs from the isomeric multiflor-7-ene only in the position of one methyl

Table 1 EI mass spectra of the double bond isomers of multiflorene (values from (*44*, *93*))

m/z	410	395	271	257	243	231	218	206	205	204	203	191	189
Δ^7	9	14	7	9	47	46	19	26	55	100	8	24	12
Δ^8	16	20	4	9	100	72	20	36	53	12	5	35	8
$\Delta^{9(11)}$	18	20	5	12	50	40	100	40	38	17	28	75	17

group in ring E (*92*). This behavior is confirmed in the bauer-7-ene derivatives (3-one, 3-methoxy) (*82*, *92*). Data for this group are compiled in (*50*, *92*, *93*). For suggested fragmentation pathways, see the original literature. Arborane, which was tentatively included in this group (*64*, *94*, *95*), was later shown to have structure **20**.

3.4 Fernane and Arborane Derivatives

The derivatives of fernane (**19**) and arborane (**20**) are characterized by C-13/C-14 methyl groups (Fig. 28), but their fragmentation pattern differs from that of the bauerene group. Also for this group of triterpenoids the position of a Δ^7, Δ^8, or $\Delta^{9(11)}$ double bond is of no importance. Thus, the EI mass spectra of the three isomeric fernenes are reported to be indistinguishable (*50*), *cf.* also (*44*, *99*). In addition, the orientation of the isopropyl group has no influence (*84*). The characteristic fragment for ring D/E unsubstituted compounds is due to the loss of 167 Da ($C_{12}H_{23}$) from $M^{+\cdot}$ formulated as arising from the cleavage of the 12,13-, the 13,14-, and the 15,16-bond accompanied by H rearrangements (*cf.* wavy line b in Fig. 27). The $[M–167]^+$ ion is accompanied by ions formed by the loss of a C-3-substituent (*82*, *84*, *94*, *594*) (Fig. 29). An ion $[M–153]^+$ (loss of rings D/E+H) is of secondary abundance but becomes the most important one for $\Delta^{7,9(11)}$-dienes (*50*, *93*, *739*). Pertinent literature has been compiled and reviewed in (*55*) and (*50*, *93*).

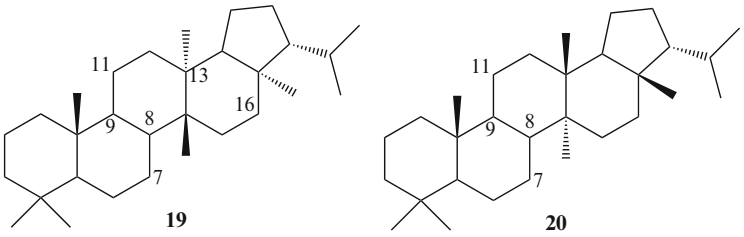

Fig. 28 Fernane (**19**) and arborane (**20**)

Δ^5-Compounds show *RDA* fragments as described above. Thus, the spectrum of simiarenol (3-oxofern-5-ene) differs from that of glutinone (**10**, Fig. 17) only by some loss of $\cdot C_3H_7$ from *m/z* 274 (*96*, *97*). The reported fragmentation patterns of $\Delta^{9(11)}$ compounds oxygenated at the 12 position (oxo, hydroxy, acetoxy) give no clear picture (*98*, *99*).

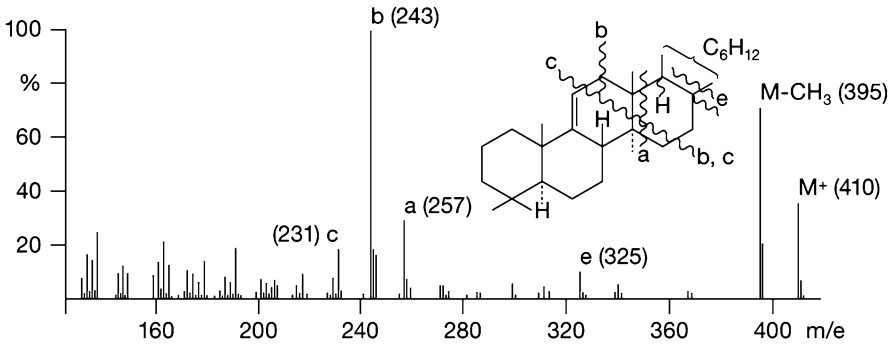

Fig. 29 EI mass spectrum of arbor-9(11)-ene (**20** with a 9(11) double bond). Reproduced from (*94*) with kind permission of Wiley-VCH Verlag GmbH & Co. KGaA (© 1963)

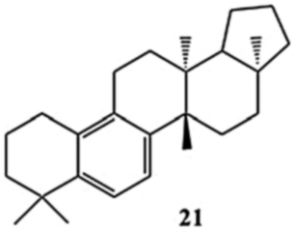

Fig. 30 22,25,29,30-Tetra-*nor*-18β-ferna-5,7,9-triene (**21**)

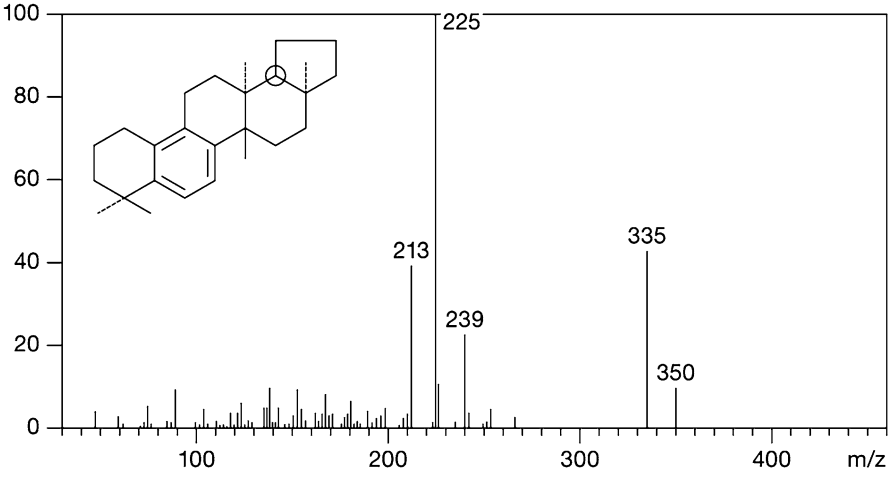

Fig. 31 EI mass spectrum of 22,25,29,30-tetra-*nor*-18β-ferna-5,7,9-triene (**21**). Reproduced from (*100*) with kind permission from Elsevier (© 1992)

From geological material, fernane/hopane derivatives were isolated that possess an aromatic ring B. The type representative of 22,25,29,30-tetra-*nor*-18β-ferna-5,7,9-triene (**21**) (Fig. 30) yields ions at *m/z* 213, 225, and 239 from the left-hand part of the molecule (Fig. 31) (*100*).

4 Alkaloids from Vertebrates

What actually are alkaloids? In 1819 *Carl Wilhelm Friedrich Meissner*, pharmacist at Halle (Germany) (*101*), introduced the term alkaloid for basic ("alkali-like") plant constituents.[4] Several restrictive definitions to be found in the literature[5] (plant origin, heterocyclic nitrogen compounds) had to be given up over the years when animal alkaloids became known or when peptidic compounds (*105*, *106*) and polyamines (*107*) were added to the list of alkaloids. What remains as a *criterium sine quo non* is besides a natural origin is the presence of nitrogen, as reflected in a recent definition by *Hesse*: "Alkaloids are nitrogen-containing organic substances of natural origin with greater or lesser degree of basic characters." (*108*). Certainly proteins, nucleotides, amino carbohydrates, and their constituents have to be excluded, but with respect to other groups of natural products such as antibiotics (*109*, *110*) or siderophores (*111*) the boundaries are shifting (*cf.* Sect. 4.2).

The mass spectra of plant alkaloids have been reviewed in detail (*112*–*114*); for polyamine alkaloids, see (*107*), for peptide alkaloids (*105*), and for steroidal alkaloids (*115*). A newer wide field is constituted by the alkaloids extracted from the skins of amphibia, especially those from poisonous frogs, which the late *John W. Daly* pioneered (*116*, *117*). In his review from 1987 (*118*) over 200 compounds are mentioned, and by 2005 the number had grown to over 800 (*119*), with such research still going on (*120*). Mass spectrometry plays an important role, including electron ionization (EI) and chemical ionization (CI) (*121*) for the determination of molecular masses, for structural work, and especially for correlating closely related structures. The following section will try to cover the major aspects.

An area where mass spectrometry could play a role in future in addition to structural work is the question of the origin of the isolated alkaloids. The β-arylethylamines clearly stem from amino acid metabolism, and salamander alkaloids are synthesized by the animal from cholesterol. Originally it was assumed that the frog alkaloids were synthesized by the animals and thus could be used for chemotaxonomy, but it

[4] "Ueberhaupt scheint es mir auch angemessen, die bis jetzt bekannten alkalischen Pflanzenstoffe nicht mit dem Namen Alkalien, sondern Alkaloide zu belegen, da sie doch in manchen Eigenschaften von den Alkalien sehr abweichen." (Actually, it seems to me as adequate to designate the alkaline plant constituents known till now not as alkalis but rather as alkaloids as they differ much in several aspects from the alkalis) (*102*).

[5] "Unter Alkaloiden im engeren Sinn verstehen wir dagegen Verbindungen mit heterocyklisch gebundenen Stickstoffatomen, mehr oder weniger stark ausgeprägtem basischem Charakter, ausgesprochener physiologischer Wirkung, kompliziertem molekularem Bau, die in Pflanzen gefunden werden, …" (Under alkaloids in a more restrictive sense we understand however compounds with heterocyclic bound nitrogen atoms, more or less pronounced basic character, explicit physiological activity, complicated molecular structure, which are found in plants, …) (*103*). This classical definition by *Winterstein* and *Trier* from 1910 was criticized by *Pelletier* in the introductory chapter of the first volume of the series *Alkaloids: Chemical and Biological Perspectives* (*104*). He offered a rather vague new definition—"An alkaloid is a cyclic organic compound containing nitrogen in a negative oxidation state which is of limited distribution among living organisms."—and justified the wording as excluding compounds that should not be considered as alkaloids.

later turned out that many of the frogs' toxins have been acquired in the food (*116*, *737*), with some involved in a multi-step chain from plants *via* arthropods, and some of them with structural modifications by the animals (*123*); and it has been suggested that bacteria may be involved as the ultimate source (*122*). GC/MS in comparison with published data has been used to establish the origin of frog alkaloids in ants (*125*–*127*), millipedes, and beetles (*128*), or in mites (*124*, *130*, *131*, *133*), although many of the taxa of mites found in the stomachs of frogs do not produce alkaloids (*132*, *134*). A classical field of mass spectrometry would be to follow the fate of isotopically labeled putative precursors, and since every metabolic step results in changing of the isotope composition, $^{12}C/^{13}C$ and other isotope ratio analyses might provide clues for metabolic changes of sequestered alkaloids (*cf.* (*135*)).

4.1 Amphibia

The skin secretions of amphibia constitute a defense system containing besides antimicrobial peptides (*136*) a variety of alkaloids.[6] The largest number of amphibial alkaloids stems from dendrobatid poisonous frogs primarily from the Central and South American rain forests. The frogs use them as defense agents[7] against predators (*139*), warning at the same time by their bright colors (*138*, *595*). Variations in the alkaloid contents have been reported in terms of the locality and time of the year (*129*, *141*), sex (*130*), and age (*142*) of the animals. The broad variability of alkaloid profiles has been demonstrated for the Argentinian toad *Melanophryniscus rubriventris* (*602*). The subsequent discussion follows the three review articles, Refs. (*117*–*119*), which should be consulted for quotations of additional original literature. For most alkaloids a listing of the major ions from EI mass spectra is available, which can be found in (*118*, *119*) and in the original publications.[8]

In the early days of research, trivial names were given to the alkaloids of poisonous frogs, but to cope with their increasing number, a simplified system was introduced, in which the molecular mass in bold characters is followed by a capital letter

[6] In a detailed GC/MS study it could be shown that alkaloids present in the skin of the Brazilian toad *Melanophryniscus simplex* were also to be found in the same relative portions in muscles, liver *etc.* (*137*).

[7] Feeding on poisonous prey with the purpose to sequester toxic compounds for their own defense is spread over the entire animal kingdom (for examples, see Sect. 4.2). It is an ongoing field of interdisciplinary research (*140*) where mass spectrometry plays an important role (screening and identification, structural transformations, labeling studies, *etc.*).

[8] In (*119*) under Supporting Information, with the exception of the steroidal alkaloids, all known amphibian alkaloids are listed, including samples for which the structures have not been established yet or are considered as tentative. The listing follows the shorthand designation (see above) and hence the molecular masses. The data comprise elemental formulas (for unknown structures based on high resolution MS measurements), diagnostic EI-MS fragments, GC and other characteristic data, and where known, assignment to a structural class, natural origin *etc.* It should be mentioned that 127 complete EI mass spectra of frog alkaloids can be found in (*602*).

when several alkaloids have the same nominal mass. In numbering ring systems, the mode used in (*119*) is followed here for easier cross-reference, even if it is not consistent with current IUPAC rules.

4.1.1 Toads and Frogs (*Anura*)

As will be shown, today the idea prevails that most *Anura* alkaloids are not produced by the animals, but are rather acquired *via* the food and at best chemically modified (*120*, *737*, *747*). This is certainly not true for the first group.

4.1.1.1 Biogenic Amines

Serotonin (5-hydroxytryptamine) and its *N*-methyl derivatives (*603*) (as *e.g.* bufotenine, **22**) are secreted by toads together with a number of other biogenic amines (β-phenylethylamine derivatives as epinephrine and dopamine, *etc.*; tryptamine derivatives as bufotenidine, *i.e.* the *N,N,N*-trimethyl betaine of **22**, bufoviridine, *i.e.* the *O*-sulfate of bufotenidine, the cyclization product dehydrobufotenine (**23**, (*143*), for a recent synthesis see (*144*)) and its *O*-sulfate bufothionine (*604*) *etc.* (see *e.g.* (*145*)); see also histamine and derivatives by various toads (*146*) (Fig. 32).

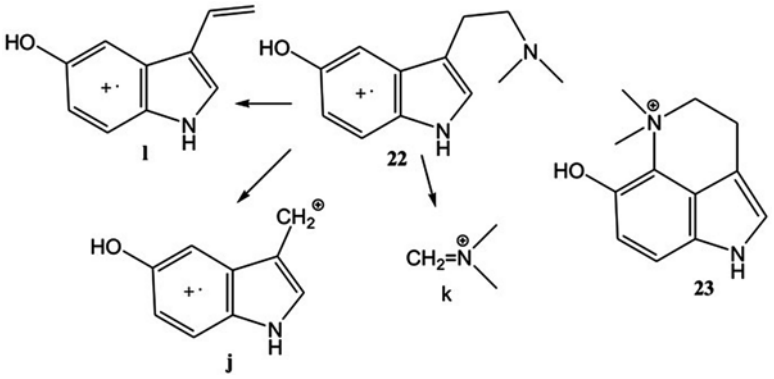

Fig. 32 Bufotenine (**22**), dehydrobufotenine (**23**), and the main fragments of **22**

Bufotenine[9] (**22**) was first isolated from the skin of the common toad (*Bufo bufo*) and subsequently from other species such as the aga toad (Australian cane toad; *Bufo marinus,* new name *Rhinella marina*), and the Australian golden bell frog (*Litoria aurea*). A comparative study of the indole alkylamine patterns of various Brazilian toad species based on chromatography combined with ESI-MS/MS has been reported (*615*). The main fragments are $[\mathbf{l}+H]^+$ ions.

[9] A poisonous substance from toad skin glands was apparently first isolated by *Phisalix* and *Betrand* in 1893 (*148*) and named *bufoténine* (*149*). *Jensen* and *Chen* (*150*) described in 1932 several bufotenines, which they characterized as indole derivatives. The constitution of **22** was finally established 1934 by *Wieland et al.* (*151*).

In the EI spectrum (Figs. 32 and 33) (*147*) the characteristic fragmentation process of $M^{+\cdot}$ (*m/z* 204) is the cleavage of the benzylic bond yielding the fragment ions **j** (*m/z* 146) and (preferentially) **k** (*m/z* 58) (*cf.* Sect. 7). The elimination of $HN(CH_3)_2$ resulting in **l** (*m/z* 159) is of minor importance but becomes the main process in the ESI-CA spectrum (Fig. 34, *m/z* 160 is protonated **l**) (*145*, *152*). By either method

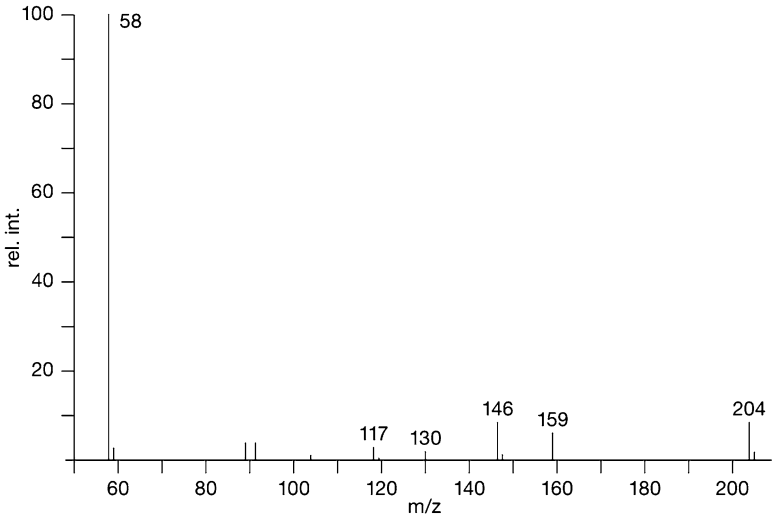

Fig. 33 EI mass spectrum of bufotenine (**22**): *m/z* 146 (**j**), 58 (**k**), 159 (**l**), 204 ($M^{+\cdot}$)

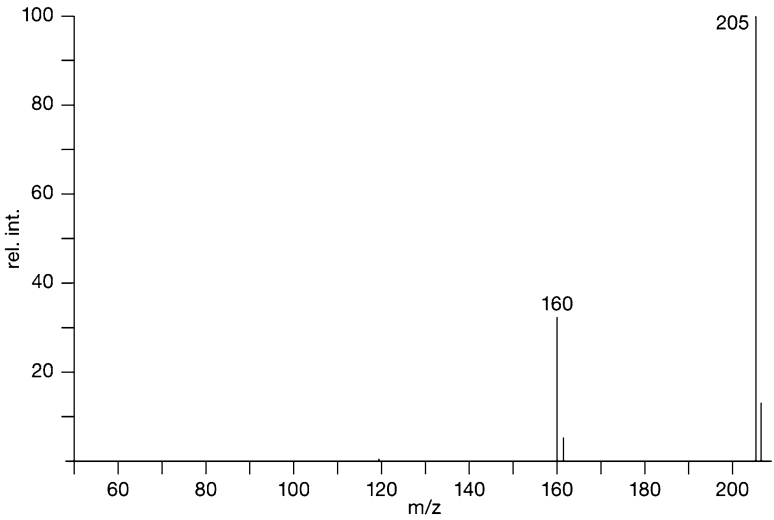

Fig. 34 ESI-CA spectrum of bufotenine (**22**): *m/z* 160 ($[\mathbf{l}+H]^+$, 205 ($[M+H]^+$)

related compounds can be characterized showing varying substitutions in the indole part and of the NH_2 group of tryptamine. Other β-arylethylamine derivatives show analogous fragmentation (see also the Addendum).

The aquatic toads of the genus *Bombina* ("Unken" in German) produce secretions containing *inter alia* serotonin, amino acids, and small to medium-sized peptides (*663*), several of them N-terminally blocked by a pyroglutamic acid unit (*664*). Structurally related characteristic members are named "bombinins" after the first representative "bombinin" for which the primary sequence of 24 amino acids had been revealed (*667*). Some of the peptides show antimicrobial (*665*, *668*) and/or insulinotropic (*666*) activities. The structure elucidation followed the methods outlined in Sect. 7.2 including sequencing by tandem MS (*668*).

4.1.1.2 Steroidal Alkaloids: Batrachotoxin and Tauromantellic Acid

From a large number of the arrow poison frogs, like *Phyllobates aurotaenia* (*153*), the highly toxic batrachotoxins (BTX) **24**–**26** were obtained in sufficient amounts for structural analysis by spectroscopic methods (*154*). The structure of batrachotoxinin A (**24**), a complex steroid alkaloid, was confirmed by X-ray analysis (*153*) and synthesis (*155*).

From a mass spectral analysis, high-resolution EI data are available (*154*). The $M^{+\cdot}$ ions of low abundance (*m/z* 538 for **25**) lose the pyrrole-3-carboxylic acid substituents (or H_2O for **24**; yielding *m/z* 399 for **24**–**26**) responsible for the ions *m/z* 139 for **25** and *m/z* 153 for **26**. The ion *m/z* 399 eliminates the C-13/C-14 bridge (C_4H_9NO) giving *m/z* 312. Several losses of H_2O follow. An important ion is the *retro-Diels-Alder* fragment *m/z* 184 (**m**), the observation of which in the mass spectra of 4*β*-hydroxy derivatives of **25** and **26** (two minor alkaloids) aided the localization of the additional hydroxy group (*156*). For the possible genesis of the alkaloids, see Sect. 4.4 below.

The Madagascar poison frogs *Mantella baroni* and *M. betsileo* could be shown by GC/MS analysis to sequester a series of alkaloids from food (*129*), but they also produce by themselves an alkaloid derived from a bile acid, a partially degraded 7*α*-hydroxycholestan-3-one substituted with 2-aminoethanesulfonic acid. This was named tauromantelic acid (**26a**, Fig. 35). Its structure was elucidated by NMR and mass spectral analysis. The molecular formula could be established by positive and negative ESI. CA of $[M+H]^+$ resulted in partial degradation of the C-17 side chain, but the main fragments were found to be *m/z* 126 (H_3N^+-CH_2-CH_2-SO_3H) and *m/z* 208 (the ionized side chain) (*157*).

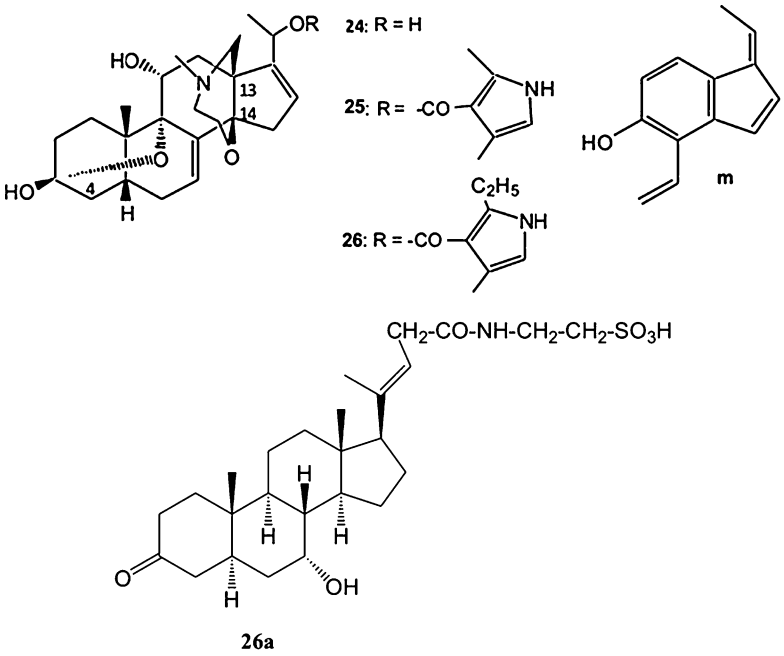

Fig. 35 Batrachotoxinin A (**24**), batrachotoxin (**25**), homobatrachotoxin (**26**), and tauromantelic acid (**26a**)

4.1.1.3 Pyrrolidines and Piperidines

2,5-Dialkylpyrrolidines and 2,6-dialkylpiperidines (the latter category may have a C-4-hydroxy group) on EI show the loss of either alkyl substituent, preferentially the larger one (*158*). Unexpected results supplementing the EI data were obtained with CI(NH_3) after CA (Fig. 36). Ring opening of the protonated molecules results in the two fragments *m/z* 128 and 114, as depicted in Fig. 37 for 2-*n*-heptyl-5-*n*-hexylpyrrolidine (alkaloid **253I** (**27**)). Higher homologues of the two fragments are observed with low abundance (Fig. 36). A competing fragmentation sequence starting from $[M+H–NH_3]^+$ resulting in the series of ions *m/z* 81, 95, 109, … occurs with varying preponderance in all CI(NH_3) spectra discussed here and below (*121*).

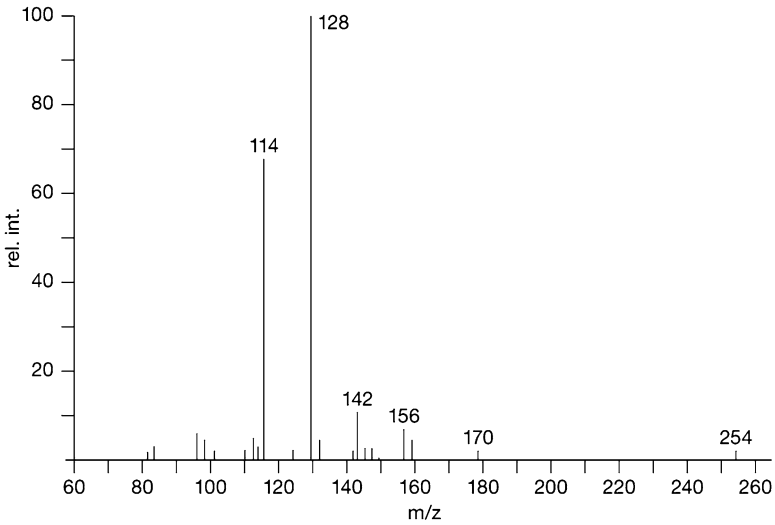

Fig. 36 CI (NH_3) CA mass spectrum of 2-*n*-heptyl-5-*n*-hexylpyrrolidine (**27**). Adapted from (*121*) with kind permission of John Wiley and Sons (© 1999)

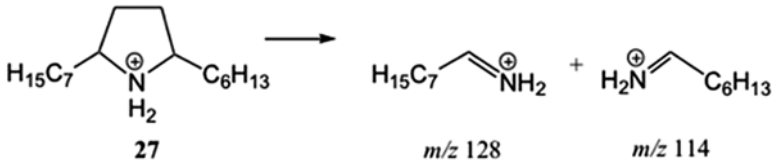

Fig. 37 CI (NH_3) CA induced fragmentation of 2-*n*-heptyl-5-*n*-hexylpyrrolidine (**27**)

4.1.1.4 Histrionicotoxins

The spiro-piperidines are the main alkaloids of the South American *Dendrobates histrionicus* (*159*). They differ by the nature of R^1 and R^2, in terms of whether there are saturated or (preferentially) unsaturated short alkyl groups. The main EI fragments are the loss of R^1 by α-cleavage induced by the nitrogen function, and an abundant ion at *m/z* 96, most likely **n** (Fig. 38) (*118*). CI (isobutane) yields mainly $[M+H]^+$ and $[M+H–H_2O]^+$. An ant is probably the dietary source of the histrionicotoxins (**28**). For a total synthesis, see (*160*).

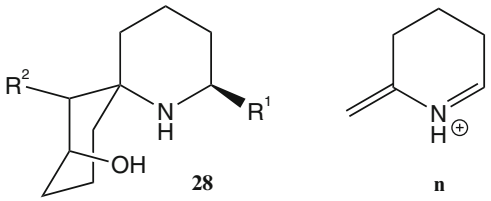

Fig. 38 EI induced fragmentation of histrionicotoxins (**28**)

4.1.1.5 Decahydroquinolines

Many frog species were found to provide decahydroquinoline derivatives (**29**) as additional alkaloids. Residues R^1 and R^2 are short saturated or unsaturated alkyl chains. Various stereochemical arrangements (substituents, ring juncture[10]) have been encountered. Occasionally, a ring-OH group is observed. The main EI fragment arises from the loss of R^2. For a significant loss of R^1, a mechanism was suggested comprising the opening of the 4a,8a-bond to yield **o** (Fig. 39) (*162*). Recently, *N*-methyl derivatives were described also (*125*). In CI(NH_3) allyl substituents are lost as propene by the *McLafferty* rearrangement (*761*).

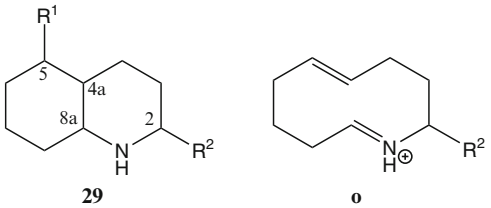

Fig. 39 Loss of R^1 from **29**

4.1.1.6 3,5-Disubstituted Pyrrolizidines and Indolizidines, 4,6-Disubstituted Quinolizidines, and Lehmizidines

3,5-Disubstituted pyrrolizidines (**30**) and indolizidines (**31**) with varying stereochemistry of the ring juncture relative to the substituents, 4,6-disubstituted quinolizidines (**32**) and lehmizidines (**33**) (Fig. 40) are minor secondary alkaloids of various frogs and toads. The lehmizidines can be hydroxylated in the seven-membered ring. Ants are the dietary source (*163*). The precursors of the "izidines" are probably dialkylated pyrrolodines and piperidines (*164*). For syntheses, see (*163*, *165*).

The substituents for all structural types are small, saturated or unsaturated, partially oxygenated alkyl groups. Loss of either substituent by α-cleavage is observed

[10] For an enantioselective synthesis of the alkaloids *cis*-**195A**, (pumiliotoxin C) and *trans*-**195A**, see (*161*).

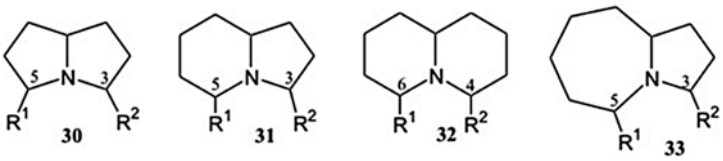

Fig. 40 "Izidine" alkaloids

in their EI mass spectra, the larger one being lost preferentially. The α-cleavage products can lose the second substituent by *McLafferty* rearrangement, as in the formation of $[M-{}^{\cdot}CH_3-C_3H_6]^+$ from alkaloid **195C** (**32**, $R^1=CH_3$, $R^2=n\text{-}C_3H_7$) (*163*, *164*, *754*). In CI(NH_3), all α,α′-disubstituted "izidines" upon CA yield two characteristic fragments as shown for 3-methyl-5-*n*-nonylpyrrolizidine (**34**, Figs. 41 and 42). The ring with the larger substituent is lost preferentially. When the two rings are of different size and/or differentially substituted location of the substituents is possible. Thus, for 3-*n*-butyl-5-*n*-propylindolizidine the masses of the two fragments coincide at *m/z* 126. For the 5-*n*-butyl-3-*n*-propyl isomer an ion pair at *m/z*

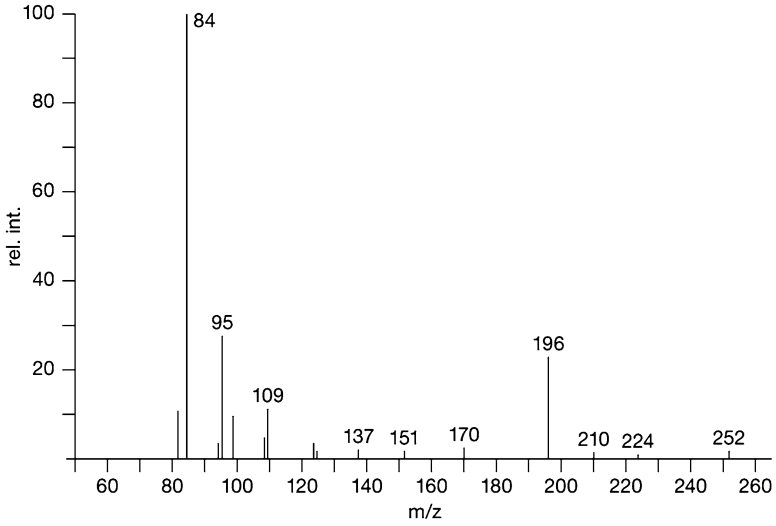

Fig. 41 CI (NH_3) CA spectrum of 3-methyl-5-*n*-nonylpyrrolizidine (**34**). Adapted from (*121*) with kind permission of John Wiley and Sons (© 1999)

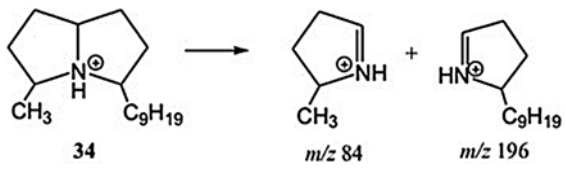

Fig. 42 CI (NH_3) CA induced fragmentation of 3-methyl-5-*n*-nonylpyrrolizidine (**34**)

112 and 140 would have been expected (*cf.* 3-*n*-butyl-5-methylindolizidine,[11] which yields fragments at *m/z* 126 and 98) (*121*).

4.1.1.7 Spiropyrrolizidines

The alkaloids **222** and **236** are compounds substituted at C-1 with an oxime or an *O*-methyloxime group (**35**) and at C-7 with a spirocyclopentane structure. They have been obtained from Panamanian dendrobatid frogs. The dominant fragment **p** in the EI mass spectra arises from the loss of C-6 and C-7 (*m/z* 126 for **35**) as shown from the appropriate shifts upon substitution (Fig. 43). They apparently originate from millipedes (*166*). The precursor is nitropolyzonamine (**35** with a *β*-oriented nitro group at C-1) for which the main fragment is the nitro analog of **p** after the loss of NO_2 (**p′**, *m/z* 82) (*167*).

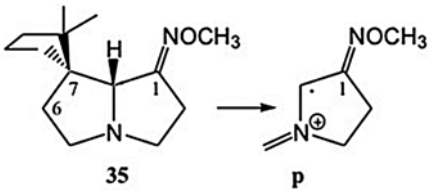

Fig. 43 Fragmentation of spiropyrrolizidines upon EI

4.1.1.8 5,8-Disubstituted Indolizidines and 1,4-Disubstituted Quinolizidines

This group of alkaloids with varying stereochemistry stems mainly from dendrobatid frogs.[12] The EI mass spectra of **36**-type alkaloids (*120*) show two characteristic fragments, loss of the C-5 substituent (**q**) and subsequent *retro-Diels-Alder* (*RDA*) decomposition yielding a fragment with *m/z* 96 (**r**). An additional substituent at C-6 shifts the RDA fragment accordingly in mass. If a 6,7-double bond is present, the $[M–R^1]^+$ ion loses subsequently H_2, probably due to complete aromatization of the six-membered ring (**s**) (Fig. 44). An alternative path leading to aromatization consists in the loss of R^1, R^2 and H yielding an significant ion with mass *m/z* 120.

[11] Dr. *H.M. Garraffo*, Bethesda, MD, private communication.

[12] For syntheses of 5,8-disubstituted indolizidines, see (*168, 169*).

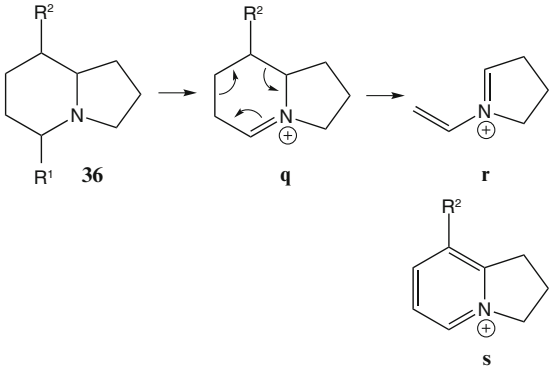

Fig. 44 Fragmentation of 5,8-disubstituted indolizidines (**36**) upon EI

1,4-Disubstituted quinolizidines (**37**) show an analogous fragmentation behavior, with loss of R^1 and subsequent *RDA* yielding ion **t** at *m/z* 110 (Fig. 45) (*120*).

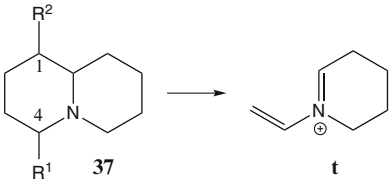

Fig. 45 Fragmentation of 1,4-disubstituted quinolizidines upon EI

4.1.1.9 Pumiliotoxins (*170*) and Related Compounds

Alkaloids from this indolizidine-derived group have been encountered in a variety of frogs from South America, Madagascar, and Australia, and recently also in Cuban dwarf frogs (*171*). The major types contain the partial structure **38**, some with hydroxy groups at C-8 or at C-7 and C-8. The R substituents can be saturated or unsaturated alkyl groups, with some carrying hydroxy groups. The EI spectra vary with the substitution pattern, but an abundant ion at *m/z* 70 (probably from the pyrrolidine ring) seems to be a common feature (*120*). 7,8-Dehydro-8-desmethylpumiliotoxins show an abundant $[M–H]^+$ ion, loss of methyl, and the loss of R (*m/z* 162) as the main fragment. The accompanying ion *m/z* 160 is due to complete aromatization of the six-membered ring to a pyridinium system (*172*). Homopumiliotoxins (**39**) are decahydroquinoline analogs yielding accordingly an ion at *m/z* 84 (Fig. 46). A dietary chain from mites (*131*, *133*) through ants has been suggested; final modifications by the frog are possible (*135*), but an origin from bacteria symbiontic with ants also has been discussed (*122*).

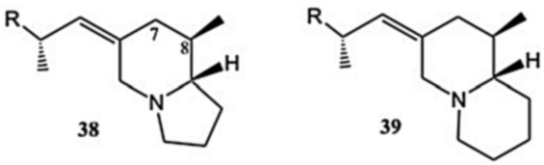

Fig. 46 Pumiliotoxins and homopumiliotoxins

4.1.1.10 Tricyclic Compounds

Gephyrotoxins (**40**) (*170*) with unsaturated alkyl groups as R were found in the skin of a Colombian frog *Dendrobates histrionicus*, originating from ants. Typically loss of the $-(CH_2)_2OH$ group by α-cleavage represents the main fragment.

Precoccinelline (**41**) was isolated originally from ladybugs (*173*, *174*). It and related compounds (ring systems with one or two five-membered rings, with double bonds, variously substituted, *e.g.* alkaloid (–)-**205B** (*175*, *176*)) were discovered in various frogs. The only common mass spectral feature is an abundant $[M–H]^+$ peak, and otherwise the fragmentation patterns are rather complex and vary with the particular structures being considered (Fig. 47).

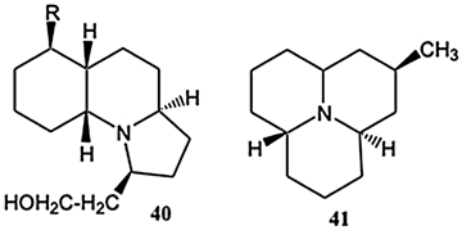

Fig. 47 Tricyclic poison frog alkaloids: gephyrotoxins (**40**), precoccillenine (**41**)

Cyclopentaquinolizidines (**42**) were obtained from a Colombian frog. R^1 can be CH_3, CH_2OH or CHO, R^2 can be H or OH, and R^3, in turn, H or alkyl. The alkaloid **251F** ($R^2=CH_2OH$, $R^1=R^3=H$) was investigated by high-resolution EI and MS/MS. It shows an abundant $[M–H]^+$ ion, a pronounced loss of $^{\cdot}CH_2OH$ (78%), and a base peak at *m/z* 111 (**u**) (Fig. 48). The reasons for the fairly pronounced losses of $^{\cdot}CH_3$ (27%) and of CH_2O (30%) are not obvious (*177*).

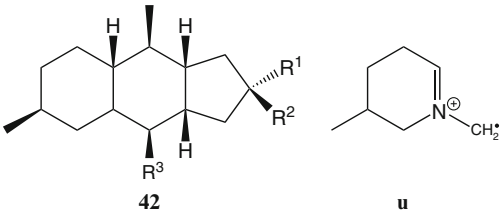

42 u

Fig. 48 Fragment formation upon EI of alkaloid **251F** (**42**)

4.1.1.11 Pseudophrynamines

These alkaloids got their name from the Australian frog *Pseudophryne coriacea* from which they are found together with pumiliotoxins (see above). In structure **43**, R^1 is H or CH_3 and R^2 can be CH_3 and any of its oxidation products (CH_2OH, CHO, $COOCH_3$) (Fig. 49). Two molecules can be connected *via* an ester bridge between their R^2 residues. The benzene ring may be substituted by methoxy groups. While pumiliotoxins came from a dietary source (arthropods), pseudophrynamines are biosynthesized by the frogs (or possibly stem from symbiotic bacteria) (*123*).

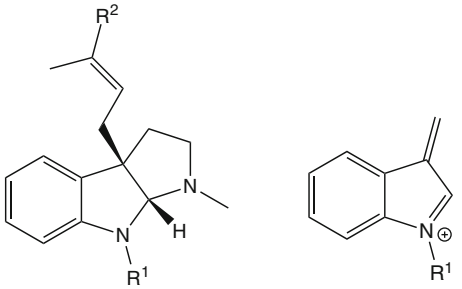

43 v

Fig. 49 Fragment formation upon EI of pseudophrynamines (**43**)

In the EI mass spectra two characteristic fragments are observed, for which the genesis was corroborated by appropriate mass shifts in the substituted analogs and upon deuterium exchange. For R^1 = H and an unsubstituted benzene ring loss of the isoprenoid chain yields *m/z* 173, while skeletal degradation results in *m/z* 130 (**v**) (*178*).

4.1.1.12 Epibatidine

From the skins of *ca.* 750 Ecuadoran tree frogs, *Epipedobates tricolor* (*179*), in addition to pumiliotoxin (see above) the trace alkaloid (–)-epibatidine (**44**), somewhat structurally related to (–)-nicotine (**45**, R = H), was isolated (Fig. 50). Its structure was elucidated by a combination of physical methods including high-resolution EI mass

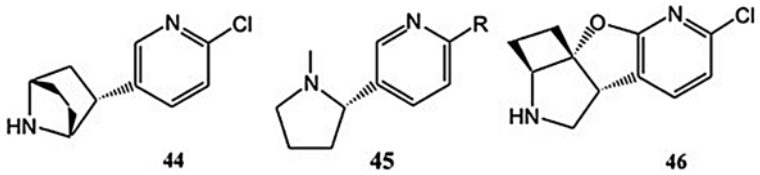

Fig. 50 Epibatidine (**44**), nicotine (**45**, R = H), and the derivative, phantasmidine (**46**)

spectrometry (*180*). The main fragments are formed by cleavages of the azabicycloheptane system setting free C_2-units: $[M–C_2H_5]^+$ (**x**, *m/z* 179/181), protonated 2-chloro-5-vinylpyridine (**y**, *m/z* 140/142), C_4H_7N (**z**, *m/z* 69) (Fig. 51). The structure of **44** was confirmed by synthesis and its physiological effects were investigated in detail (*179*).

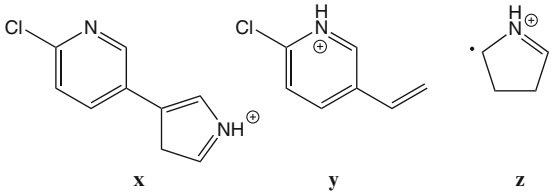

Fig. 51 The main fragments of epibatidine (**44**)

From *Epipedobates anthonyi* a related alkaloid **46** was obtained (*181*) to which the name phantasmidine was given. The EI pattern shows the main fragments $[M–C_3H_5N]^{+\cdot}$, the complementary $C_3H_6N^+$ (probably $CH_2=N^+H\text{-}CH=CH_2$ initiated by the typical 2 + 2 cleavage of cyclobutane derivatives and α-cleavage induced by the N-function), and *m/z* 80 (*m/z* 94 for the *N*-methyl derivative) .

Three other pyridine alkaloids were obtained from dendrobatid frogs, nicotine (**45**, R = H), pyridylnicotine (**45**, R = 3-pyridyl), and noranabasamine (**45**, R = 3-pyridyl, piperidine instead of methylpyrrolidine ring). An ultimate plant source has been considered. The base peak in the EI mass spectrum is in each case *m/z* 84 due to the loss of the pyridine part by α-cleavage (*119*).

4.1.1.13 Zetekitoxin AB (Atelopidtoxin)

From the skin of the Panamanian golden frog *Atelopus zeteki* an alkaloid (*182*) was obtained that in earlier reviews was treated together with the tetrodotoxin group. Its original name atelopidtoxin was later changed to zetekitoxin. It was considered a mixture of related compounds, with the major component obtained by electrophoresis possibly still comprising two components, termed AB, and the minor one C. A Cf-plasma desorption mass spectrum (precursor technique of fast atom bombardment, FAB) proved inconclusive regarding the molecular mass (*183*). It took

another 35 years before its structure elucidation was reported (*184*, *649*) based on extensive mass spectrometric and NMR studies (**47**). It was found to be structurally related to saxitoxin (**48**) (*185*, *186*) (see below) (Fig. 52). The minor component C is probably the desulfated compound.

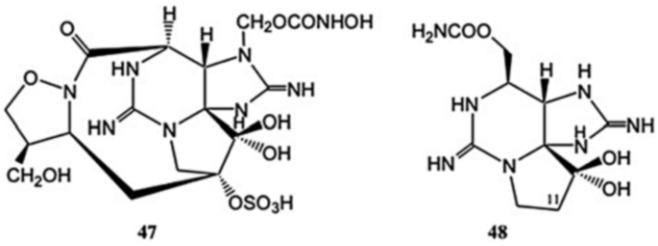

Fig. 52 Zetekitoxin AB (**47**) and saxitoxin (**48**)

ESI-MS gave according to the mode (positive or negative) a $[M+H]^+$ ion at *m/z* 553 and a $[M–H]^+$ at *m/z* 551, with the exact mass agreeing with the elemental composition. H/D exchange showed the presence of 11 exchangeable protons in $[M+H]^+$. CA experiments resulted in the loss of SO_3 (*m/z* 473) and, in addition, of OH(CO)NHOH (*m/z* 396) from *m/z* 553.

Regarding the additional structural units of zetekitoxin (**47**) compared with saxitoxin (**48**), it is worth mentioning that natural saxitoxin analogs have been found containing some of its constituent functionalities, such as a carbamoyl-*N*-hydroxy group (*187*), a -CH_2COOH group at C-11 (*188*), and an -OSO_3H group at C-11 (*189*).

Saxitoxin (**48**) is reported to be produced by dinoflagellates (*e.g. Alexandrium* spp.). In being taken up during the algal bloom by various mussels, it may be responsible for incidences of shellfish poisoning. However, the ultimate source of saxitoxin may be from bacteria (*190*, *191*) (*cf.* tetrodotoxin **49**, below Sect. 4.3), and possibly also in the case of zetekitoxin (**47**).

4.1.1.14 Chiriquitoxin

From the Costa Rican frog *Atelopus chiriquiensis*, in addition to tetrodotoxin (**49**) (*cf.* below Sect. 4.3), a second compound **50** was isolated and given the name chiriquitoxin (Fig. 53). Its molecular mass and elemental composition was verified by FAB mass spectrometry and its structure was established by NMR spectroscopy (*192*). For literature regarding the occurrence of tetrodotoxin and analogs in other frogs, see (*183*, *193*, *689*, *690*) and Sect. 4.3.

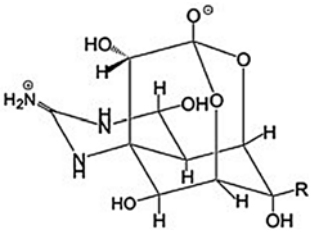

Fig. 53 Tetrodotoxin (**49**) R = CH_2OH and chiriquitoxin (**50**) (R = (*R*)-CHOH-(*S*)-$CHNH_2$-COOH)

4.1.1.15 Alkaloids of Plant Origin Found in Amphibians

From the skin of *Phyllobates terribilis* two indole alkaloids were isolated and identified as (–)-calycanthine (**51**) and (+)-chimonanthine (**52**). These compounds—as concluded from the optical rotation data—are the antipodes of the same alkaloids when isolated from plants (*156*). The EI spectrum of **51** shows $M^{+\cdot}$ at *m/z* 346, loss of CH_3-NH-$CH_2^{\cdot}$ (*m/z* 302) and of one of the two bridges, $^{\cdot}CH_2$-CH_2-$NHCH_3$ (*m/z* 288) and subsequently of CH_2-CH_2-NCH_3 (*m/z* 231), giving the fully aromatic system protonated 6,12-diazachrysene (*194*); the ESI-MS/MS of $[M+H]^+$ results in partial (CH_3NH_2) and complete losses of the bridges (*195*). The EI mass spectrum of **52** is dominated by an ion at *m/z* 173 (cleavage in two halves) and shows *m/z* 172 and 130 peaks (*cf.* **j** above) (*196*). A food chain from plant to arthropod to frog has to be considered (*119*). Morphine (**53**) (see below Sect. 4.4) was found in the skin of the aga toad (*Bufo marinus*) (*197*) (Fig. 54).

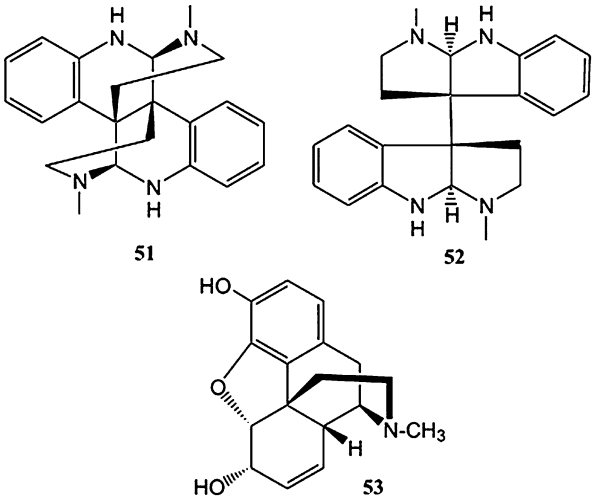

Fig. 54 (–)-Calycanthine (**51**), (+)-chimonanthine (**52**), and (–)-morphine (**53**)

4.1.1.16 Toad Venoms

Toads (*Bufo* spp.) produce (for a LC-MS analysis see (*670*)) in their skin glands, in addition to biogenic amines and various peptides (Sect. 4.1.1.1) steroidal toxins (for mass spectrometric analysis see (*724*, *725*)), as a protection against predators. Some of them are linked to amino acids and considered as alkaloids. The prototype is bufotoxin (**53a**) (Fig. 55) (*198*), derived from the bufodienolide bufotalin with a

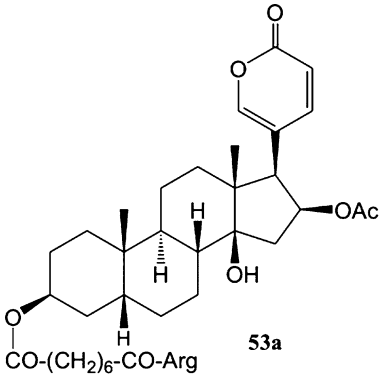

Fig. 55 Bufotoxin (**53a**)

3*β*-*O*-subaroyl-arginine substituent (*199*). Later on, several related compounds were identified. Variations of the steroid part include cardenolide structures with a γ- instead of a δ-lactone C-17 substituent, smaller linking dicarboxylic acids down to succinic acid (*200*, *605*, *608*, *653*) and glutamine (*201*), histidine or 3-methyl-histidine (*202*, *605*, *608*) instead of arginine as the amino acid part. The free constituents pimeloyl and suberoyl arginine were also found in the secretion (*721*). Mass spectral data are available for screening procedures (LC-ESI) (*721*, *722*), degradation products (EI) (*200*) and for metabolites (LC-ESI) (*203*). ESI-MS/MS data show the formation of protonated suberoyl arginine (*m/z* 331) from $[M+H]^+$ (*723*). For the linkers adipinic acid and succinic acid accordingly fragments with *m/z* 303 and 275, respectively, are mentioned (*725*), but in this study *m/z* 331 is also reported for adipic (in one case), sebacic, and pelargonic (?) acid. No explanation is offered and only the one fragment ion is given for quantification by the multiple reaction monitoring (*17*) method (MRM).

4.1.2 Salamanders and Newts (Caudata)

From the eggs of the Californian newt *Taricha torosa* tarichatoxin was isolated, which was shown to be identical with tetrodotoxin (Fig. 53, **49**) (*204*); see below Sect. 4.3. For literature regarding the occurrence of tetrodotoxin and analogs in other salamanders and newts, see (*183*, *193*) and Sect. 4.3. Doubts of its bacterial origin (see below Sect. 4.3) have been voiced (*205*).

From the skin of the European species *Salamandra maculosa* and *S. atra* a series of steroidal alkaloids was obtained; for reviews, see (*146*, *183*, *764*). They are synthesized by the animals from cholesterol (*206*). For all of them, ring A is enlarged to an azacycloheptane structure. EI mass spectral analyses are available (*207*, *208*). Samanine (**54a**) (Fig. 56) (*753*) shows *m/z* 44 CH_3-$^+$NH=CH_2 (shifted to *m/z* 58 for *N*-methyl compounds) as main fragment. 1-Hydroxy compounds such as samandiol (**54b**) shows in addition $[M-{\cdot}CHO]^+$ by loss from C-1 (M−29 Da). Minor ions comprise ring A/B fragments (Fig. 57). The isomeric neosamandiol (**54a** with a C-19

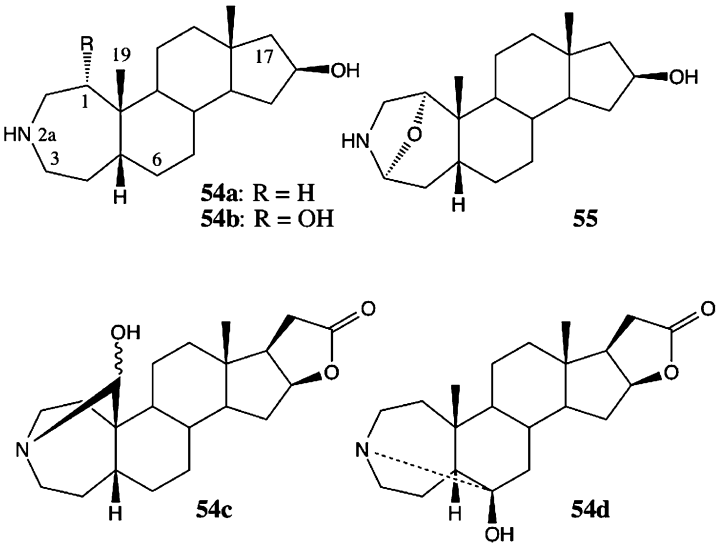

Fig. 56 Salamander alkaloids **54a** - **54d**

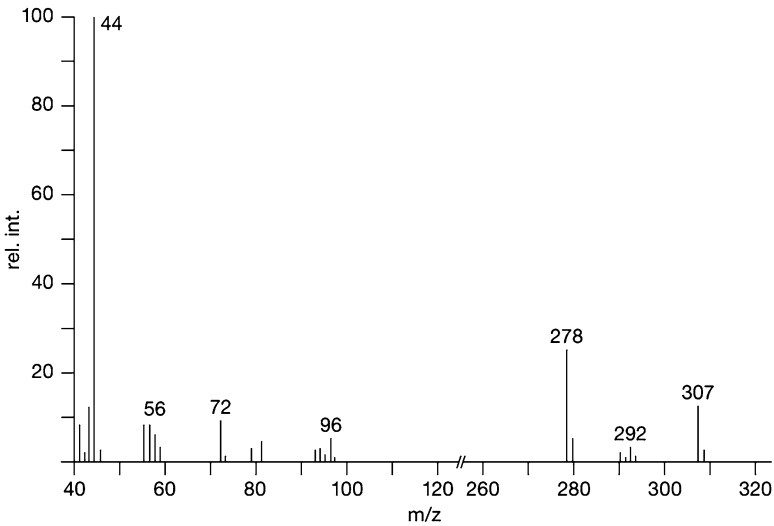

Fig. 57 EI mass spectrum of samandiol (**54b**). Reproduced from (*207*) with kind permission of Wiley-VCH Verlag GmbH & Co. KGaA (© 1967)

hydroxy group) yields besides *m/z* 44 the loss of the angular CH_2OH group (M–31 Da) as base peak. A C-19 aldehyde (cycloneosamandione) forms an equilibrium with a carbinolamine structure by reaction with the NH function. The only fragment of importance is $[M-\cdot CHO]^+$ (*208*, *209*, *750*).

In (*752*), *Habermehl* proposed structure **54c** (Fig. 56) for cycloneosamandaridine. A compound of this structure was synthesized subsequently (*750*). However its EI mass spectrum (*m/z* 345, 15%, $M^{+\cdot}$; 330, 32%, $-CH_3^{\cdot}$; 316, 100%, $-CHO^{\cdot}$) differed from the one reproduced in (*752*) ($[M-H]^+$ instead of $M^{+\cdot}$, also the characteristic $[M-\cdot CHO]^+$ ion is missing). *Oka* and *Hara* suggested structure **54d** (Fig. 56) the compound isolated by *Habermehl* (*cf. 208*), but this suggestion has not been verified by synthesis. Fragments characteristic for the C-16/C-17 lactone ring have not been observed (*207*).

Compounds with a 1,3-ether bridge such as samandarin (**55**)[13] fragment (*207*, *656*) to $[M-CO]^{+\cdot}$ by the loss of C-1 (M–28 Da) and show major fragments at *m/z* 56/57 and *m/z* 85/86. For the lower masses the structures **aa** and **ab** were suggested (Fig. 58). For a GC/MS analysis, see (*211*).

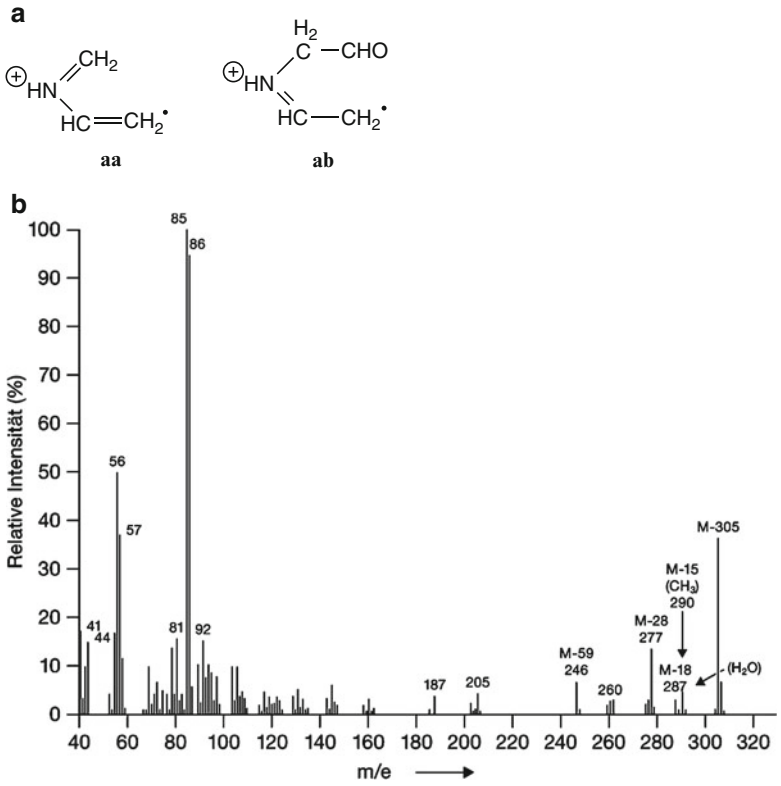

Fig. 58 (**a**) EI fragments of samandarin (**55**), (**b**) EI mass spectrum of **55**. Reproduced from (*207*) with kind permission of Wiley-VCH Verlag GmbH & Co. KGaA (© 1967)

[13] The 17*β*-hydroxy isomer of **55** allegedly (*212*) obtained (*cf.* (*183*)) from the Asian salamander *Cryptobranchus maximus* exists only as a synthesis product (*209*). For a total synthesis of samandarone (16-oxo analog of **55**) see (*210*). For additional literature, see (*671*).

4.2 Reptiles

The venoms of toxic snakes[14] and of the Gila monster (*Heloderma suspectum*) and its relative, the Mexican Beaded Lizard (*H. horridum*) are peptidic compounds.[15] Borderline alkaloids of some reptiles are the nucleic acid degradation products uric acid (**56**, $R^1 = R^2 = OH$) (*218*) and its mono- and dihydroxy precursors, hypoxanthine (**57**, $R^1 = R^2 = H$) and xanthine (**58**, $R^1 = OH$, $R^2 = H$) (*219*) (Fig. 59). EI mass spectra can be found in (*220*). Fragmentation occurs preferentially by degradation of the six-membered ring (*e.g.* $[M–CONH]^{+\cdot}$ for **58**; *cf.* *221*, *222*). Purine alkaloids are also found in birds and mammals (*cf.* Sect. 8.1) (Fig. 59).

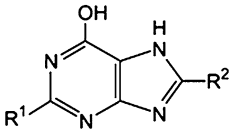

Fig. 59 Purine alkaloids **56**–**58** (see text)

[14] Californian garter snakes (*Thamnophis* sp.) can accumulate tetrodotoxin (**49**) especially in the liver and store it for prolonged periods of time. In this way the non-venomous snake becomes poisonous for its mainly avian predators. Tetrodotoxin is sequestered by eating newts (*Taricha sirtalis*) (see Sect. 4.1.2) (*140*, *223*), whose skin contains the toxin. The snake has become resistant by changing the amino acid pattern of the muscular Na^+ channels (*224*) in the area critical for the binding of tetrodotoxin.

A second example constitutes the Asian snake *Rhabdophis tigrinus*, which collects in its nuchal glands dietary toad venoms (see Sect. 4.1.1.16) (*225*, *226*).

Another defense system of snakes consists of the ejection of an evil-smelling fluid from anal glands. GC/EI-MS analysis of the volatile components of the secretions of garter snakes (*Thamnophis* spp.) resulted in the identification of small (C_2 to C_5) carboxylic acids, $(CH_3)_3N$, and 2-piperidone. The same compounds were also found in the secretions of species from other snake families (*672*). Analysis of the secretion of *Dumaril's* ground boa (*Acrantophis dumerili*) (*673*, *674*) yielded cholesterol, fatty acids, and their amides. Among the volatile compounds small carboxylic acids (C_3 to C_5) were identified by GC/EI-MS. Three compounds were tentatively classified as amines. The ion *m/z* 30 of high abundance accompanied by *m/z* 44 (20% rel. int.) suggests the presence of a $-CH_2-CH_2-NH_2$ end group. The low abundance of all other ions would be in agreement with aliphatic amines (*17*), but the ions *m/z* 172, 186, and 200 considered as molecular ions would have to be $[M+H]^+$ species. In the secretion of the western diamondback rattlesnake (*Crotalus atrox)* 1-*O*-monoalkylglycerols were found (*676*) and identified by the EI spectra of their trimethylsilyl and isopropylidene derivatives; *cf.* Sect. 5.2.1.

[15] For example, exendin-3 and -4 with 39 amino acids (*213*, *214*), helodermin with 35 amino acids (*215*), helospectin I and II with 38 and 37 amino acids, respectively (*216*), or helothermine containing approximately 220 amino acids (*217*). For mass spectrometric techniques used for the structure elucidation, see Sect. 7.2.1.

4.3 *Fishes*

4.3.1 Tetrodotoxin

Tetrodotoxin (**49**) (usually abbreviated as TTX) has become known as being responsible for casualties after eating Japanese puffer fish ("fugu") meals (*227*). In addition it has turned out that tetrodotoxin and related compounds (for a listing see Table 2) can be found in a variety of animals, included amphibians ((*690*) and literature cited therein), an octopus, crabs, and starfish (*183*, *229*). For a detailed listing, see (*647*, *648*). It seems that the ultimate sources of this compound are bacteria, especially *Pseudomonas* sp. (*230*, *231*), *Bacillus* sp. (*232*), and *Vibrio* sp. (*228*, *233*), although such results have been subjected to later doubt (*205*, *234*, *235*)

Table 2 Tetrodotoxin-type compounds (left ketal form, right lactone form). For literature references to the single compounds see (*183*, *228*, *689*, *690*), for a more detailed list see (*647*)

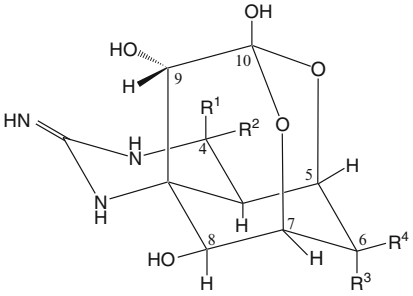

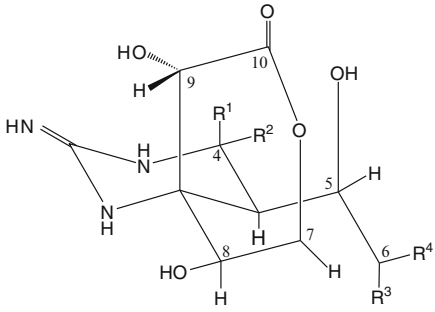

Name	R^1	R^2	R^3	R^4	Remarks
Tetrodotoxin (**49**)	H	OH	OH	CH_2OH	
4-*epi*	OH	H	OH	CH_2OH	
6-*epi*	H	OH	CH_2OH	OH	
11-deoxy	H	OH	OH	CH_3	R^4 … C-11
6,11-dideoxy	H	OH	H	CH_3	R^4 … C-11
11-*nor*-(6*S*)-ol	H	OH	OH	H	R^4 … C-11
11-*nor*-(6*R*)-ol	H	OH	H	OH	R^4 … C-11
4,9-anhydro		H	OH	CH_2OH	4,9-ether bridge
6-*epi*-4,9-anhydro		H	CH_2OH	OH	4,9-ether bridge
5-deoxy	H	OH	OH	CH_2OH	5,10-ether bridge missíng,
5,11-dideoxy	H	OH	OH	CH_3	C-10 = O (7,10-lactone) R^4 … C-11 5,10-ether bridge missíng, C-10 = O (7,10-lactone) also with 1-*N*-OH
5,6,11-trideoxy	H	OH	H	CH_3	R^4 … C-11 5,10-ether bridge missíng, C-10 = O (7,10-lactone) also with 1-*N*-OH

(a reason for negative results could be that symbiotic bacteria need an elicitor from the host organism to start the synthesis of tetrodotoxin (*689*)). For a comprehensive listing of bacterial sources, see (*648*). The pathways by which tetrodotoxin might be ending up in marine animals and in amphibians have been summarized in (*229*). Attempts to establish the biogenesis of tetrodotoxin have been reviewed in (*648*, *758*); see also (*689*) where a biosynthetic intermediacy of 5,6,11-tridesoxy TTX with subsequent hydroxylation is suggested). For a review, see (*758*).

A gas chromatography-mass spectrometry (GC/MS) method was developed to detect and quantify traces of tetrodotoxin in organic material (*236*, *641*). Treatment with OH^- results in the formation of 2-amino-8-hydroxy-6-hydroxymethylquinazoline (**59**, Fig. 60), which is trimethylsilylated. The EI mass spectrum of the *N,O,O*-tris-TMS derivative shows a $M^{+\cdot}$ peak at *m/z* 407, loss of $^{\cdot}CH_3$ (*m/z* 392, base peak), and a *m/z* 376 ion of unknown structure (in (*230*) of low abundance). The mass spectrum of the alleged *O,O*-bis-TMS derivative is difficult to understand: $M^{+\cdot}$ (*m/z* 335) is missing and $[M-{\cdot}CH_3]^+$ (*m/z* 320) is of low abundance. The base peak at *m/z* 270, to judge from the reported isotope pattern, should contain Si atoms. It is followed by abundant peaks at *m/z* 221, 165, 147, 97, and 73, with the exception of the last one ($(CH_3)_3Si^+$) hard to explain and highly atypical for this compound. However, the same spectrum has been reported again (*228*).[16] To make the confusion more complete, *Matsumura* (*234*) reported that polypeptone and yeast extracts used for bacterial cultures, which definitely contained no tetrodotoxin, gave the HPLC and GC/MS peaks and EI fragments *m/z* 407, 392, and 376, considered characteristic for the toxin. It should be kept in mind that not tetrodotoxin but a derivative obtained by drastic degradation (**59**) (Fig. 60) is being detected, which can be formed also from congeners (*e.g.* (*237*, *238*)). Therefore, reports of the presence of tetrodotoxin based on the mass spectrum of the bis-TMS derivative of **59** should be considered with

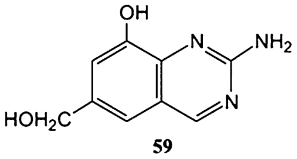

59

Fig. 60 Degradation product **59** of tetrodotoxin

care. For a general critique on earlier analysis methods for TTX, see (*688*).

Modern instrumentation allows the mass spectrometric analysis of genuine material. Positive FAB yields $[M+H]^+$ followed by twice loss of H_2O (*240*), negative FAB $[M-H]^-$.

Liquid chromatography can be combined with spray techniques and MS/MS (*748*, *749*). The CA spectra of the $[M+H]^+$ ions of tetrodotoxin and of its congeners

[16] Ions *m/z* 73, 147, and 221 have been observed in GC column bleeding (*239*).

were recorded (*193*, *241–243*, *689*, *690*). The main fragments besides the loss of one and two molecules of H_2O comprise the 2-aminoquinazoline nucleus, as confirmed by exact mass measurements (*689*). However, the mass shifts observed for the various compounds are difficult to reconcile with the structures. Tetrodotoxin yields an ion at *m/z* 162 (protonated hydroxy-2-aminoquinazoline) accompanied by one at *m/z* 178 (the dihydroxy analog) (Fig. 61), which is shifted to *m/z* 146/162 for 5-deoxy compounds (see Table 2). The presence or absence of a C-11 substituent seems to play no role in the resultant mass spectra. CA spectra help to identify known congeners of TTX and occasionally they reveal the existence of new representatives. Thus, from the South American frogs *Brachycephalus* spp. two compounds occurred with molecular masses 28 and 10 Da, respectively, higher than TTX but very similar fragmentation patterns. Since the ion *m/z* 256 present in the CA spectra of TTX and of both new compounds comprises the complete TTX structure without C-10 and some H atoms (*689*), some peripheral modification as in the case of chiriquitoxin (**50**) (Sect. 4.1.1.14) seems likely.

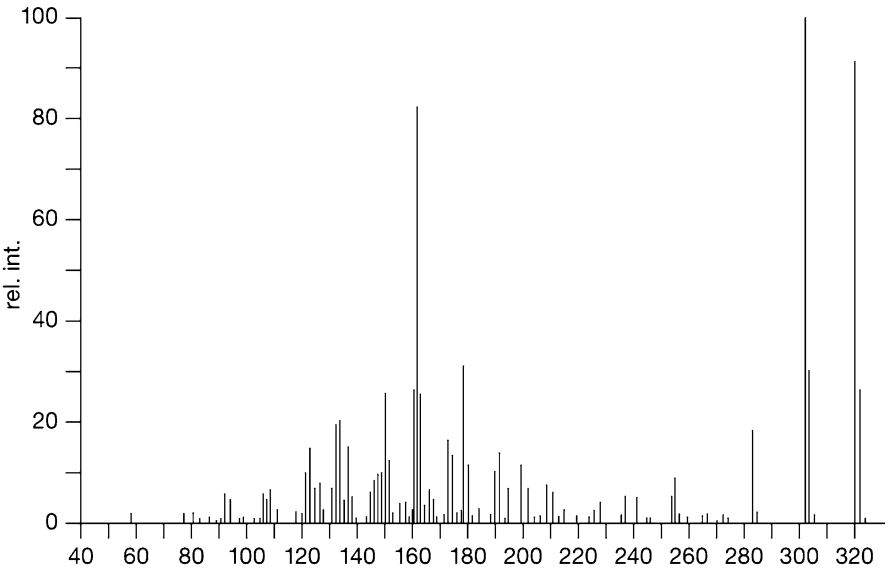

Fig. 61 CA spectrum of $[M+H]^+$ (*m/z* 320) obtained by ESI-CA from tetrodotoxin. Reproduced from (*193*) with kind permission from Elsevier (© 2001)

Chromatographic and spectroscopic methods applied to the analysis of TTX and of related compounds are summarized in (*647*).

4.3.2 Steroids

The search for antibiotic substances led to the isolation of the aminosteroid squalamine (**60-1**) from the stomach tissue of the dogfish shark *Squalus acanthias* (*244–246*) (Fig. 62). It is contained also in other organs, especially in the liver. Later, a series of congeners (**60-2**–**60-8**) was identified (*247*). Squalamine comprises a spermidine residue β-linked to C-3 of a cholestane skeleton. Its molecular mass was determined by positive and negative FAB-MS. The $[M+H]^+$ ion shows loss of SO_3 and of H_2SO_4, $[M–H]^-$ instead cleavages of the spermidine chain next to the nitrogen atoms. The alkaloid **60-8** contains instead of a spermidine the larger spermine residue. Biosynthetic precursors of the alkaloids are probably the bile alcohols of the shark, but the observation of the C_{28}-skeleton in **60-6** with a C-24-substituent

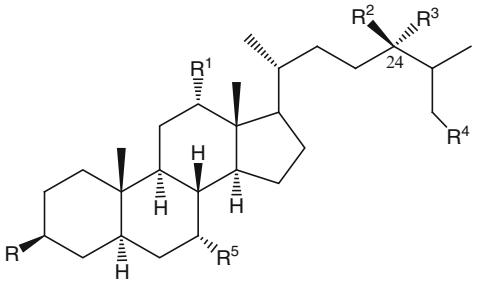

Cpd.	R	R^1	R^2	R^3	R^4	R^5
60-1	a	H	OSO_3H	H	H	OH
60-2	a	H		=O	d	OH
60-3	a	H	OH	H	OSO_3H	OH
60-4	a	H		=O	OSO_3H	OH
60-5	a	OH	OSO_3H	H	H	OH
60-6	a	H	OSO_3H	CH_2OH	H	OH
60-7	a	H		=O	$=CH_2$	OH
60-8	b	H	OSO_3H	H	H	OH
60-9	a	H	OSO_3H	H	H	OH
60-10	c	H	OSO_3H	H	H	OSO_3H

a: H_2N-$(CH_2)_4$-NH-$(CH_2)_3$-NH-

b: H_2N-$(CH_2)_3$-NH-$(CH_2)_4$-NH-$(CH_2)_3$-NH-

c:

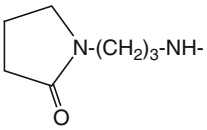

d: SCH_2-$CHNH_2$-COOH

Fig. 62 Squalamine (**60-1**) and related compounds

suggests an ultimate plant origin of the steroid part (*cf.* campesterol). In the context of clinical studies with squalamine lactate possible degradation by heat, acid, base *etc.* were investigated by LC/MS techniques (ESI, MS/MS, EI). Products formed by the loss of SO_3, H_2SO_4, H_2O from various *loci*, and lactamide formation with the terminal NH_2 group could thus be identified (*650*).

A further member of this aminosteroid group, petromyzonamine disulfate (PADS, **60**-**9**) with a degraded spermidine residue is a constituent of the pheromone cocktail guiding adult sea lampreys (*Petromyzon marinus*) to spawning grounds (*248*). For its structure elucidation special mass spectrometric techniques were applied in addition to the determination of the molecular mass by negative ESI- and positive MALDI-MS. Loss of H_2SO_4 plus SO_3 suggested the presence of at least two sulfate groups. H/D exchange of the molecular ion of the di-Na salt evidenced the presence of only one exchangeable hydrogen atom. Exact mass measurements under ultra-high resolution (180,000 FWHM[17]) performed with a ICR instrument allowed investigators to establish[18] the presence of exactly two sulfur atoms (*249*) and $C_{34}H_{60}N_2O_9S_2$ as the elemental composition of $[M–H]^-$. A LC/MS/MS method was developed to quantify PADS and its congener pheromones in river water (*599*).

4.3.3 Ichthyotoxins

For this compound group, see the Addendum.

4.4 Birds

From the New Guinea passerine bird genus, *Pitohui*, homobatrachotoxin (**26**) (Sect. 4.1.1) was found, especially in the feathers and the skin, and to a lesser extent in the muscles and even less in the organs. Supposedly, this alkaloid is a protective means against predators. The structure was confirmed by color tests, chromatographic R_f values, and the EI mass spectrum (*250*). Later on, in a second New Guinea bird, *Ifrita kowaldi*, a whole series of batrachotoxin-type compounds was detected (*251*), with some not encountered previously in frogs. Among these are batrachotoxinin-A-(20*R*)-*cis*-crotonate and -3′-hydroxypentanoate, and a C-20 → C-16

[17] FWHM: full width half maximum (*17*), a term used to define mass spectral resolution.

[18] $[M–H]^-$ comprises the main ion (nominal mass 703, exact mass 703.3667 Da) consisting of ^{12}C, ^{1}H, ^{14}N, ^{16}O and ^{32}S isotopes, and it is accompanied by a series of satellites containing heavier isotopes. The ions 2 mass units higher (705 Da) comprise a species containing ^{34}S and several other species made up of combinations of ^{13}C, ^{2}H, ^{15}N, ^{17}O, ^{18}O, ^{33}S, all of them differing somewhat in their exact masses. With sufficiently high resolution obtainable with an ICR instrument they can be separated. The signal representing the ^{34}S-containing ion can be recognized by the exact mass difference between ^{32}S and ^{34}S (1.9958 Da) and its high intensity (4.4% of the intensity of the *m/z* 703 signal for each S atom present in the molecule; all the other *m/z* 705 signals amounting to about 1% or less). The observed intensity of 8.6% establishes the presence of two S atoms.

rearranged acetate. These structures were confirmed by chemical and mass spectrometric evidence (*251*).

A burning question had been how could these complex steroidal alkaloids be found in such genetically and geographically widely distant animals? An original suggestion of an independent evolution (*250*) seems highly unlikely. Also acquisition with the food appears at the first glance as to be neglected. Sparrow-sized birds do not eat frogs and appropriately toxic frogs are not reported from New Guinea to date. However, a possible solution came from the discovery that certain beetles of the genus *Choresine* found in New Guinea contain appreciable amounts of batrachotoxins inclusive of some new structural varieties. Residues of these beetles have been found in the stomachs of these birds. Relatives of these beetles occur also in South American rain forests (*252*), but they have not been tested yet for batrachotoxins. Beetles are not known to synthesize steroids. So, phytosterols acquired and modified (by themselves or by symbionts) may be the ultimate source of the alkaloids. Thus, an active field of research is still very much open (*cf.* also the problems with tetrodotoxin above in Sect. 4.3).

4.5 Mammals and Mankind

For earlier reviews, see (*253*, *254*). β-Arylethylamines (genuine or administered as drugs) can react with aldehydes giving tetrahydroisoquinolines. Thus, β-3,4-dihydroxyphenyl ethylamine (dopamine) with acetaldehyde (*e.g.* from ethanol) yields salsolinol (**61**, $R^1 = CH_3$, $R^2 = H$), or dopamine oxidized by monoamine oxidase (MAO) to the corresponding aldehyde yields, with a second molecule of dopamine, the benzylisoquinoline tetrahydropapaveroline **61**, $R^1 = (OH)_2C_6H_3\text{-}CH_2$, $R^2 = OH$) (Fig. 63). Under EI the main fragment is the loss of a C-1 substituent (*255*). In the same way from tryptamine, tetrahydro-β-carboline derivatives (**62**, Fig. 63) can be obtained; dehydrogenation yields *e.g.* harmane (**63**, Fig. 63). β-Arylethylamines may also be the precursors of endogenous morphine (**53**) (Fig. 54) (*256*); for its EI spectrum see (*255*). These metabolites generated in living tissue are referred to as leucomaines, while those formed by bacterial and other biochemical transformations as autolysis *post mortem* are termed ptomaines ("cadaveric toxins or alkaloids", *Leichengifte*). Many of them are simple degradation products of amino

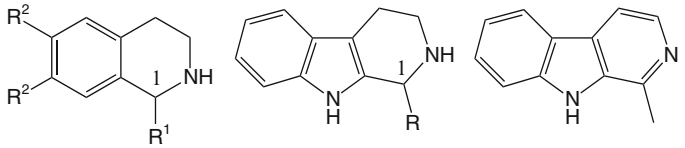

61 **62** **63**

Fig. 63 C-1 Substituted tetrahydroisoquinolines (**61**), tetrahydro-β-carbolines (**62**), and harmane (**63**)

acids (*e.g.* primary amines) and can be easily identified and quantified by GC/EI-MS with reference to data collections (*257*) or by interpretation of the fragmentation pattern (*258*). They play an important role in thanatochemistry. See also the Addendum.

Several animals secrete strongly smelling substances (*684*) for defense, marking territories or alluring sexual partners. Skatole (3-methylindole, EI *m/z* 131, $M^{+\cdot}$; 130, $[M–H]^+$, base peak), responsible for the fecal smell of the civet (*259*), is a borderline example. It is formed by microbial degradation of tryptophan in the rumen of animals (*260*, *261*) together with indole (EI *m/z* 117, $M^{+\cdot}$; base peak; losses of HCN and H_2CN (*262*)).

Other compounds can be classified as true alkaloids. Thus, *R*-(+)-muscopyridine (**64**) is a low percentage constituent of musk from the musk deer *Moschus moschiferus*, derived from muscone ((3*R*)-methylcyclopentadecanone) (*263*). Its EI spectrum shows a series of ions of comparable abundance arising from the degradation of the hydrocarbon part of the molecule (*264*). Muscopyridine is accompanied by two hydroxy derivatives carrying the OH substituent on the methylene groups neighboring the pyridine ring. Their EI spectra show an $[M–OH]^+$ ion in addition to fragments formed by losses of hydrocarbon units (*265*) (Fig. 64).

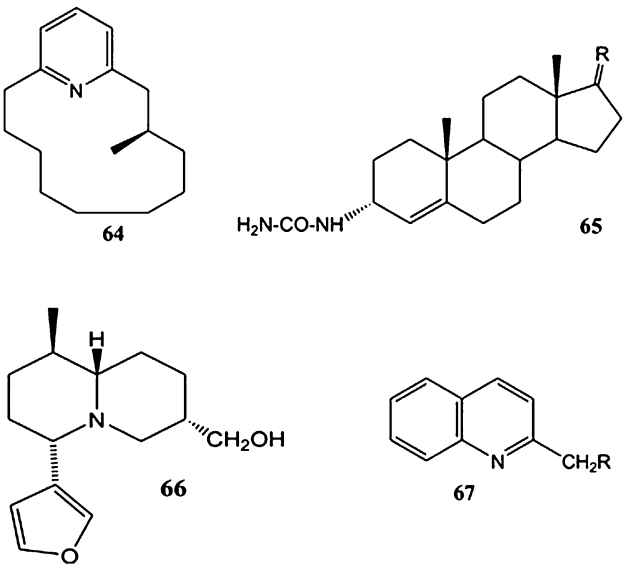

Fig. 64 Muscopyridine (**64**), musk steroids (R = H,OH or =O) (**65**), castoramine (**66**), and quinoline compounds (**67**) from the skunk

3α-Ureido-androst-4-en-17β-ol and the corresponding 17-one (**65**) are derivatives of male steroids also present in musk. EI degradation of the ureido group is observed ($[M–NHCO]^{+\cdot}$, *m/z* 287, and $[M–NH_2CONH]^+$, *m/z* 271), fragmentation of the steroid skeleton has not been mentioned (*266*). For CA of $[M+H]^+$ obtained by ESI, the product ions *m/z* 271, *m/z* 253 ($–H_2O$), and *m/z* 81($C_6H_9^+$, base peak) are reported (*600*).

Widely used in the cosmetic industry are synthetic nitro compounds with a musk smell such as musk xylene (5-*tert*-butyl-2,4,6-trinitroxylene). These compounds have been found accumulated and partially degraded ($-NO_2 \rightarrow NH_2$) in fresh water fish (*e.g.*, *644*, *645*). Negative and positive CI can be used for detection, and by positive EI the typical fragmentation of the substituents (*17*) is observed. EI and EI-MS/MS spectra of amino metabolites have been reported in (*646*).

Castoramine (**66**) (*267*) is a constituent of the odoriferous secretion (*castoreum*, *Bibergeil*) of the beaver (*Castor fiber*, *C. canadensis*) and obviously derived from yellow water-lily (*Nuphar* sp.) alkaloids taken up with the food. It is accompanied by small amounts of related compounds varying in the substitution pattern of the quinolizidine part (CH_3, OH), an indolizidine analog, and several pyrazine, quinoxaline and phenazine derivatives (*268*).

Fragmentation of the EI mass spectrum of **66** and its congeners occurs by cleavage processes in the quinolizidine part of the molecules. The main fragments are found at *m/z* 94, 114 and 136 shifted in mass accordingly with changes in the substitution pattern (Fig. 64) (*269*, *270*).

The defensive secretion of skunks (*Mephitis mephitis* and related species) besides an array of aliphatic sulfur compounds contains 2-methylquinoline (**67**, R = H) and its thiol and thioacetate derivatives (R = SH and $SCOCH_3$, respectively), as shown by GC/MS. EI mass spectra contain ions formed by degradation of the substituents (loss of $^{\cdot}H$, $^{\cdot}SH$, and of CH_2CO from the acetate (*271*).

From urine, feces, anal and preputial glands of the African wild dog *Lycaon pictus* over one hundred volatile compounds were identified by GC/MS and comparison with authentic material and/or data from the NIST library. Among these were also a number of heterocyclic compounds (pyrrole, pyridine, pyrazine derivatives). Especially mentioned are 1-methyl-2,4-imidazolidinedione (1-methylhydantoin), its 5-methyl isomer, and 1-methylimidazole-5-carboxyaldehyde (*596*), which in the same way as purines (Sect. 4.2) can be considered as borderline alkaloids. After EI ionization $M^{+\cdot}$ of 1-methylhydantoin (Fig. 65, **67a**: $R^1 = CH_3$, $R^2 = H$) eliminates CO (*m/z* 86, mainly from C-4 as shown by labeling) or NHCO (*m/z* 71); *m/z* 42/43 ($CH_2CO^{+\cdot}$ (?), $HNCO^{+\cdot}$) are the main fragments (*597*). From $M^{+\cdot}$ of 1-methylimidazole-5-carboxyaldehyde (**67a**: $R^1 = CH_3$, $R^2 = CHO$) losses $H^{\cdot}$ (*m/z* 109) and of $^{\cdot}CHO$ followed by HCN (*m/z* 81/54) (*598*) are observed. A similar set of aromatic N-heterocyclics (simple pyrrole, pyridine, pyrazine derivatives, 5-methylhydantoin, *etc.*) were also found in the scent marks of marmoset monkeys (*Callithrix jacchus*) (*685*).

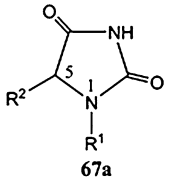

67a

Fig. 65 Hydantoin derivatives **67a** from wild dogs

The short-beaked echidna (*Tachyglossus aculeatus setosus*) uses the scent produced in a cloacal gland to attract mates. By GC/MS analysis of the secretion partially after derivatization and comparison of the EI spectra with library data structures of the major part of *ca*. 200 components could be suggested. Among these are a variety of aliphatic compounds, terpenes, steroids, *etc.*, but only a few nitrogen-containing ones ($(CH_3)_3N$, 1-methyl-2-pyrrolidinone, methyl-2, 4-imidazolidinedione), which are probably degradation products of amino acids (*683*).

Venomous mammals are rare (*657*) and besides the monotremata species[19] and the slow loris (*Nycticebus* sp.)[20] so far only shrews have been encountered[21], which produce in their submaxillar glands protein toxins (*658*). Only the lethal venom of the American short-tailed shrew *Blarina brevicauda*, blarina toxin (BLTX), was investigated in detail by enzymatic degradation, MALDI-MS, and cloning studies (see Sects. 7.2 and 7.3). The active mature protein is composed of 253 amino acids with two glycosylated Asn residues (*659*). The structural prerequisites for the toxicity have been investigated (*660*).

5 Fatty Acids and Lipids

In this section it can be seen how the advent of new mass spectrometric techniques added further possibilities for structural work step by step. For earlier reviews, see (*272*–*275*) and for a recent summary, see (*276*).

[19] *Platypus* and *Echidna* (in German Schnabeltier and Ameisenigel) produce in crural glands connected to a spur on each hind limb toxic proteins of 4–6 kDa size (*679*–*681*), which in part resemble those of reptiles (*682*).

[20] The lorises when threatened raise their arms and eject the content of brachial glands together with saliva. GC/MS analysis of the secretion has revealed the presence of a host of compounds, and LC/MS a single 17.6 kDa protein component consisting of two chains (7.8 and 9.8 kDa) linked by two disulfide bridges (*720*).

[21] "*It is a ravening beast, …, being touched it biteth deepe, and poisoneth deadly.*" *M.J. Dufton* (*657*) in a historical review quotes from an English natural history text from 1607 enlarging then on the evil fame the shrew had in Britain and—probably introduced from there—in the USA. In the "Thierbuch" by Swiss Naturalist *C. Gesner* (1606) a similar statement can be found ("Ein klein fräsig/räubig Thier ist die Spitzmaus/eines unbarmhertzigen/trüglichen sins:.. und dañ so sie mag/ so ertödtet sie mit ihrem giftigen biß" (A voraceous, rapaceous animal is the shrew, of a pitiless, deceptive mind: …and then if she wants she kills with her venomous bite) (*662*). In continental Europe, however, the fear seems to have been less pronounced: in a Swiss Natural History from 1809 there is nothing anymore from the deadly bite: "*Es ist ein Irrthum, daß man sie für giftig hält, weil Hunde und Katzen sie nicht fressen, …*" (It is an error to consider her as poisonous because dogs and cats don't eat her) (*661*).

5.1 *Fatty Acids*

5.1.1 Saturated and Unsaturated Fatty Acids

Fatty acid esters were among the first natural products to be investigated by mass spectrometry (*1*, *277*, *278*). The characteristic fragmentation reactions are (mass numbers for hexacosanoic acid methyl ester, Fig. 66):

- Formation of R-CO^+ (*m/z* 379),
- *McLafferty* rearrangement in the alkyl (*m/z* 74) and in the alkoxyl chain (loss of an alkene molecule), provided the chains are long enough (Fig. 67),

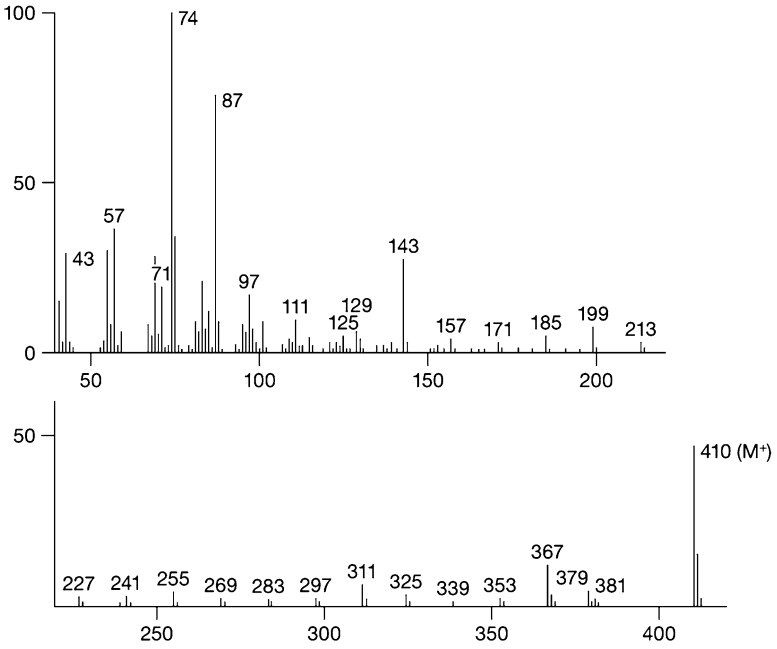

Fig. 66 EI mass spectrum of hexacosanoic acid methyl ester

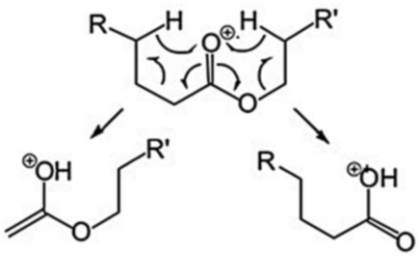

Fig. 67 *McLafferty*-rearrangement in the alkyl and in the alkoxyl chain, respectively, of alkanoic acid esters

- With increasing length of the alkoxyl chain gaining in importance compared to the *McLafferty* rearrangement a double H-transfer resulting in R-$COOH_2^+$,
- In particular, from long-chain acids and esters a series of ions $((CH_2)_nCOOR)^+$ where the species with n = 2, 6, 10 … (*m/z* 87, 143, 199, …) are more pronounced than their neighbors.

Of the mono-unsaturated methyl esters (*279*), only the Δ^2-representatives show a characteristic fragment ion, *m/z* 113, of medium to high abundance (much more abundant than for the double-bond isomers with the same chain length) (*280*, *281*). For its formation, cleavage of the 5,6-bond and concomitant cyclization to a dihydropyrylium ion (Fig. 68) is suggested. As to be expected, *m/z* 113 is more abundant for the (*Z*)-isomers (*282*). The $\Delta^{2,4}$-compound sorbic acid methyl ester yields the pyrylium ion *m/z* 111.

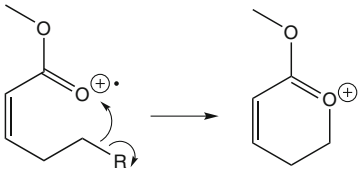

Fig. 68 Formation of the ion *m/z* 113 from Δ^2-alkenoic acid methyl esters

The EI mass spectra of the double bond isomeric hexenoic acid methyl esters (*280*), notwithstanding the characteristic ion *m/z* 113 for the Δ^2-isomer, differ in relative abundances of their ions, but with increasing chain length the mass spectra of double-bond isomers assimilate more and more until they become practically indistinguishable (*283*).

Publications reporting characteristic fragments for specific double bond positions are rare. An example is the localization of R-CH = CH-CH_2-CH = CH- units. Their EI mass spectra show enhanced abundances of R-$C_6H_7^{+\cdot}$ ions (*m/z* 108 for R = C_2H_5, *m/z* 150 for R = C_5H_{11}, and *m/z* 192 for R = C_8H_{17}) (*643*).

From the foregoing it is obvious that rearrangement reactions of the molecular ions of alkenoic acid esters occur. This is also manifested by the observation of *m/z* 74 and *m/z* 87 (see above), ions obtained also from Δ^2-methyl esters. It is well established that hydrogen migrations do take place in alkene systems (*284*). For a double bond location other approaches than the evaluation of EI spectra of esters needed to be found. These will be treated in some detail because they may be used for other unsaturated compounds as well.

One possibility is the derivatization of the double bond(s) by introduction of functional groups that initiate fragmentation in a specific way. Incidentally, derivatization is the oldest ancillary technique of mass spectrometry, both with the intention to increase volatility and to induce characteristic fragmentation reactions, especially in EI mass spectrometry (*285*). Both aspects have proved to be of importance for unsaturated fatty acids. The disadvantages of this approach are the requirements

in time and material, the non-quantitative yields especially from polyene compounds, as well as side reactions. The methods have been reviewed in detail (*279*, *286*) and will only be summarized here (see also (*287*, *288*)):

- -*O*-derivatives based on peracid oxidation (epoxides), reaction with OsO_4 or $KMnO_4$ (diols), or methoxy mercuriation ($Hg(OCOCH_3)_2/CH_3OH$). Epoxides can be transformed into mixtures of two hydroxy ($LiAlH_4$), hydroxy methoxy (CH_3OH/BF_3) or hydroxy dimethylamino derivatives ($(CH_3)_2NH$), and into ketones (NaI), while diols can be transformed into dimethoxy (CH_3I), di-trimethylsilyl ($(CH_3)_3SiCl$) and isopropylidene derivatives (CH_3COCH_3) or alkylboronates ($RB(OH)_2$), methoxy mercuriation products into mixtures of two methoxy ($NaBH_4$) derivatives. Free hydroxy groups can be trimethylsilylated to increase the volatility.
- –*N*-derivatives from epoxides, see above.
- –*S*-derivatives. By reaction with $(CH_3)_2S/I_2$ *vicinal* di-CH_3S-compounds are obtained.

Subsequent fragmentation under EI occurs by cleavage of the C,C-bonds neighboring the functionalized atoms. Low ion abundances and secondary processes such as eliminations may obscure the picture. In addition, pairs of compounds obtained by the derivatization complicate GC separations.

Another approach consists in a cross-metathesis with small unsaturated compounds catalyzed by Ru complexes, as *e.g.*

$$\begin{aligned} &R\text{-}CH{=}CH\text{-}R' + CH_2{=}CH\text{-}COOCH_3 \rightarrow \\ &R\text{-}CH{=}CH\text{-}COOCH_3 + CH_3OOC\text{-}CH{=}CH\text{-}R' \end{aligned}$$

in addition to side products. The reaction mixture is subjected to LC-MS or GC-MS analysis for identification of the pertinent fractions. Di- and poly-unsaturated fatty acids yielded only the reaction products of the double bond closest to the carboxyl group (*289*). For a corresponding CI-MS method, see below (Fig. 69).

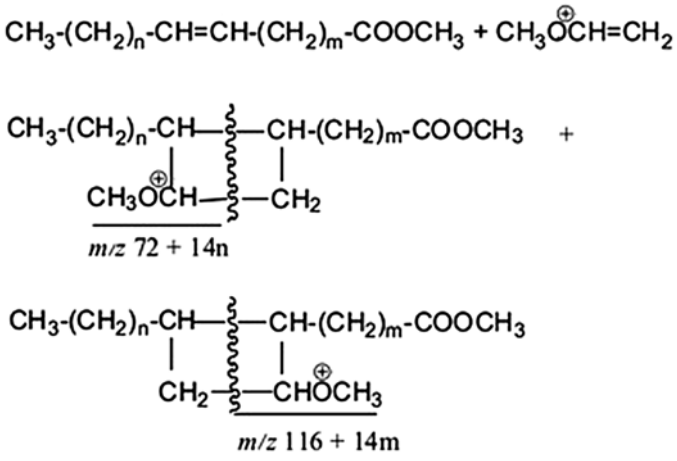

Fig. 69 Addition of MVE to alkenoic acid methyl esters and subsequent fragmentation

EI mass spectra of long-chain polyunsaturated fatty acid esters do not allow the localization of double bonds (*290*, *291*). Methoxy and trimethylsilyloxy derivatives may give useful results with EI or with CI using NH_3 or isobutane as reagent gases (*292–295*).

It was a logical step in trying to transfer the derivatization process into the mass spectrometer. This should be possible by CI (*296*, *297*). Best results with monounsaturated fatty acid methyl esters were obtained with an ionizing gas mixture consisting of 75% N_2, 20% CS_2, and 5% methyl vinyl ether (MVE) (*287*). The large percentage of N_2 minimizes polymerization of MVE and the low ionization energy of CS_2 (10.1 eV) prevents the formation of excited $M^{+\cdot}$ ions of the ester by charge transfer resulting in extensive fragmentation. Thus, the characteristic processes become clearly recognizable: reaction of the ester double bond in a 2+2 cycloaddition with ionized MVE results in two cyclobutane species, which in a *retro*-process give two fragments from the masses of which the position of the ester double bond can be calculated (Fig. 69).

Polyunsaturated fatty acids give no useful results with MEV (*292*). Disadvantages of the procedure are a severe contamination of the ion source and probable difficulties in attempting a GC coupling.

NO^+ as a CI reagent gas was investigated extensively in view of its reactions with double and triple bonds (*296*, *297*). Regarding alkenoic acids, two processes have been described for Δ^5 to Δ^{11} long-chain esters (*298*)

$$\begin{gathered}\mathrm{R\text{-}CH_2\text{-}CH_2\text{-}CH=CH\text{-}(CH_2)_nCOOCH_3 + NO^+ – CH_3OH – R\text{-}CH=CH_2 \rightarrow}\\ \mathrm{HON=CH\text{-}CH^+\text{-}(CH_2)_{n-1}\text{-}CH=C=O \rightarrow N\equiv C\text{-}CH^+\text{-}(CH_2)_{n-1}\text{-}CH=C=O + H_2O}\end{gathered}$$

and (*301–303*).

$$\begin{gathered}\mathrm{R\text{-}CH_2\text{-}CH_2\text{-}CH=CH\text{-}(CH_2)_nCOOCH_3 + NO^+ \rightarrow}\\ \mathrm{R\text{-}CH_2\text{-}CH_2\text{-}CHO^{+\cdot} + {}^{\cdot+}OCH\text{-}(CH_2)_nCOOCH_3}\end{gathered}$$

It could be shown that the prevalence of either process is governed drastically by experimental conditions (*299*). Within limitations, CI with NO^+ can also be used for the analysis of homoconjugated tri- and tetraenes (*300*). It may be added that NO^+ is detrimental to the electron emitting filaments of the ion source (*304*).

The location of one or more double bonds or of other irregularities (triple bonds, methyl branching, hydroxy groups, *etc.*) can be determined by resorting to "charge remote controlled fragmentation" induced by collision activation (*305*). In case the charge of the molecular ion is strictly localized (*e.g.* $-COO^-$, $-COOLi_2^+$, protonated acid amide structures) fragmentation of an alkyl chain will occur as depicted in Fig. 70a (one of the suggested mechanisms to be found in the literature (*305*)), resulting in a series of ions such as $CH_2=CH\text{-}(CH_2)_n\text{-}COO^-$ (Fig. 70b, top). Any "anomaly" in the chain will be reflected in an interruption of the series (Fig. 70b, bottom; the series ends with $CH_2=CH\text{-}(CH_2)_6COO^-$, *m/z* 155 and starts again with $CH_2=CH\text{-}CH=CH\text{-}(CH_2)_8COO^-$, *m/z* 209) (*306–308*). For a recent study of electrospray/CA spectra of primary fatty acid amides (saturated and unsaturated $R\text{-}CONH_3^+$), see (*309*).

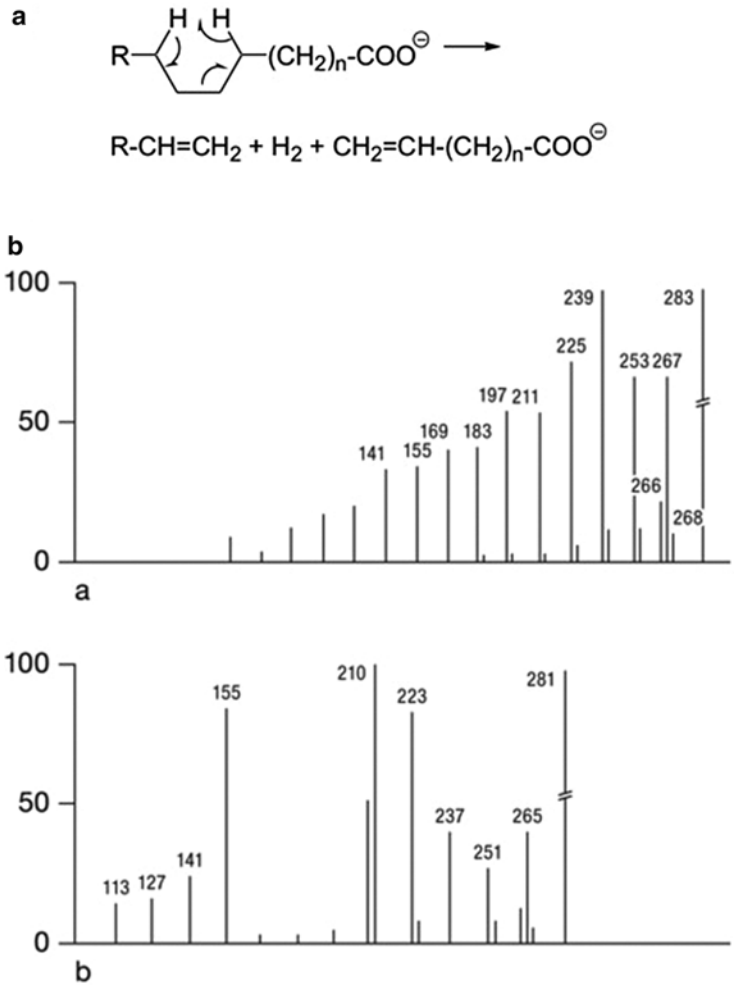

Fig. 70 (**a**) Fragmentation pattern. (**b**) Charge remote controlled fragmentation collision activation spectra of eicosanoate (**a**) and of the eicos-11-enoate anion (**b**). Reproduced from (*306*) with kind permission of John Wiley & Sons Ltd. (© 1986)

5.1.2 Furan Fatty Acids

In 1974 a new class of fatty acids was discovered in piscine lipids containing a furan ring (*701*); for a review see (*691*). These furan fatty acids ("F acids") are enzymatic oxidation products of homoconjugated fatty acids (such as linoleic acid) in lower and higher plants (*693*, *694*, *698*, *700*), taken up by food and found incorporated in the lipids of fishes (*691*, *692*) and other aquatic animals (*699*, *704*), mammals (*697*), and bacteria (*775*). The major types are R = H or CH_3, m = 1 or 3 (propyl or pentyl), and n = 8, 10 or 12, but other homologs have also been encountered (*698*, *704*). The ring methyl groups are incorporated in a subsequent step. The EI spectra of their methyl

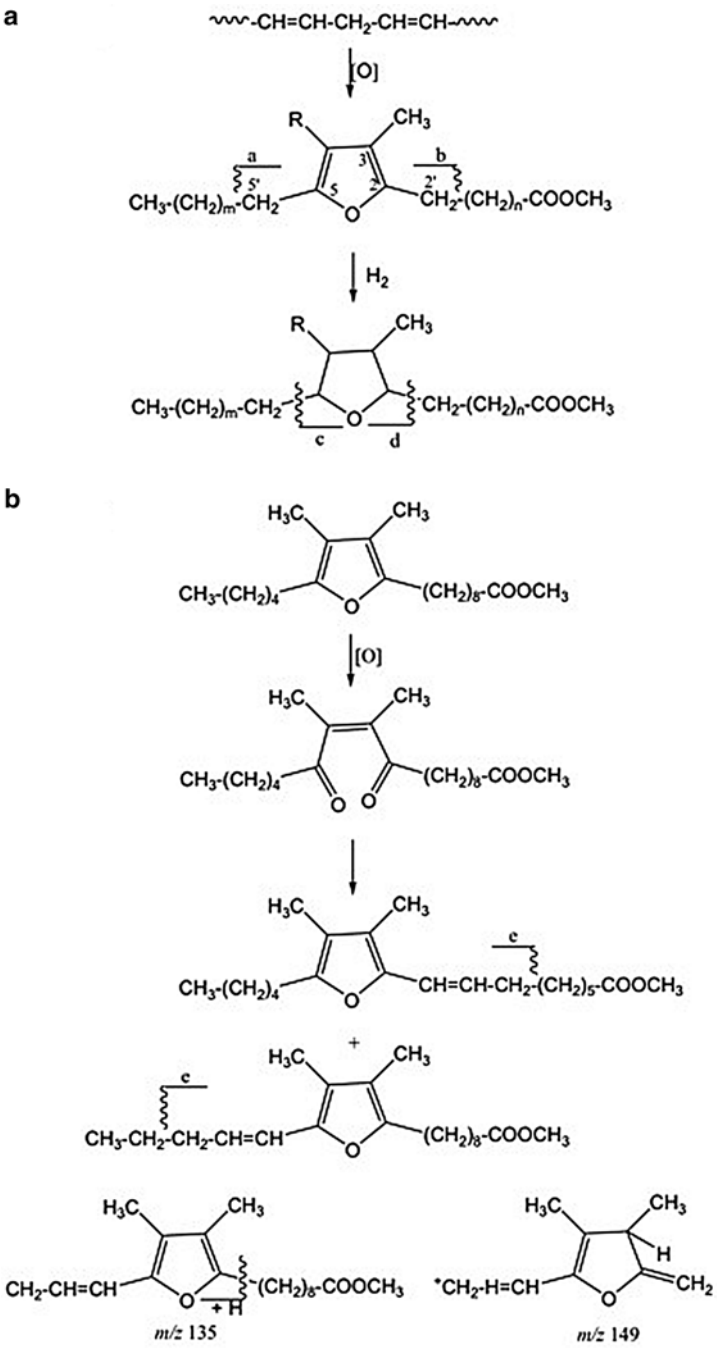

Fig. 71 Formation and EI fragmentation of furan fatty acids

esters show a straight-forward fragmentation pattern (Fig. 71a), benzylic cleavage of the two side chains (**a** and **b**, the ion **b** being responsible for the base peak). The fragments **a** and **b** can further lose an alkene residue by a *McLafferty*- type rearrangement with retention of the benzylic CH_2-group (*cf.* below) (*17*) yielding *m/z* 109 for the mono-methyl and *m/z* 123 for the di-methyl representatives. Deuterium labeling in the 2′,2″-positions results in the appropriate mass shifts (*694*). When n = 1 (propionic ester side chain) the fragment **a** loses $HCOOCH_3$ instead (*m/z* 135) (*704*). Additional structural confirmation can be obtained by hydrogenation. The tetrahydrofuran derivatives lose the entire side chains, **c** and **d** (*692*). Irregularities in the fatty acid side chain such as unsaturation could be detected by fragmentation induced by a suitably modified carboxyl group. First attempts were made with pyrrolidine amides, but the pyrrolidine ring cannot compete with the furan ring in charge localization, hence the characteristic fragments are rather weak or even absent (*709*). Further research also in view of charge remote controlled fragmentation (see above) would be worthwhile. The numbering of the various representatives (F_1–F_8) to be found in Table 1 of (*692*) has been used in various later publications to designate the common F-acids.

F-acids are potent radical scavengers (*775*) and thus valuable food ingredients (*707*). Isolation from food samples, identification by GC/EI-MS and quantification has been described (*708*). For a synthetic analog lacking the furan methyl groups, see (*706*). The EI mass spectrum of its methyl ester follows the paths outlined above.

Furan fatty acids with unsaturated substituents in the C-2 or C-5 position (*699*, *700*) are considered to be artifacts formed during the work-up and separation. The furan ring is opened by oxidation to a diketo compound, which in turn is recyclized to two compounds with a double bond conjugated to the furan ring in either side chain (Fig. 71b) (*699*, *700*, *717*). The fragmentation pattern shows allylic cleavage of the unsaturated substituent (**e**). Not obvious is the formation of an abundant ion *m/z* 135 occurring independent from which substituent contains the double bond and from the size of the methyl ester substituent. Alkene elimination from the allylic cleavage products as mentioned above would lead to ion *m/z* 149.[22]

Enzymatic oxidation of furan fatty acids in humans leads to urofuran acids, which can be found in urine and other body liquids. The C-3 methyl group is oxidized to a carboxyl group, and CH_2-groups of the C-5 alkyl chain can be transformed into CHOH- or CO-groups while the acid substituent is degraded. EI-mass spectra of the methyl esters of various oxidation products have been reported (*695*, *696*, *711*, *715*, *716*).

In cattle and in rats oxidative catabolism leads primarily to a transformation of the terminal methyl group of the C-5 alkyl chain into a carboxyl group. EI mass spectral data of the methyl esters are given in (*702*, *703*, *705*, *717*).

A further group of furan fatty acids are compounds with antifungal activity, with (*Z*)-14-(furan-2yl)-tetradeca-9-en-11,13-diynoic acid (EV-086) obtained from cell

[22] A few hints regarding the genesis of *m/z* 135 are: a compound lacking 3,4-methyl groups yields *m/z* 107, hence these methyl groups are not involved (*710*); compounds where both side chains contain double bonds conjugated with the furan ring yield the two ions arising from allylic cleavage (*711, 717*); small model compounds give no information (*718*); neither do analogous pyrrole compounds (*718*).

cultures of *Anarrhinum bellidifolium* (Scrophulariaceae) being the prototype (*718*). The ESI mass spectra[23] show $[M+H]^+$ and $[M–H]^-$ ions, respectively, upon collision activation, losses of H_2O and of CO in both modes, and abundant loss of CO_2 followed by H_2O and CO from $[M–H]^-$. The formation of other ions must be preceded by rearrangement processes as is to be expected for unsaturated aliphatic compounds and the prolonged time of residence of low energy ions subjected to collision experiments. Fragments formed by charge remote processes (see above) from $[M–H]^-$ are not observed.

5.2 Glycerol Derivatives

For an earlier review, see (*310*) and literature compiled in (*311*), and for the analysis of archeological samples (*312*).

5.2.1 Glycerol Ethers from Archaebacteria and Sediments

A short survey of these unusual compounds will be presented to show how combined structure elucidation approaches including mass spectral techniques may be applied. From Archaebacteria, glycerol 1,2-diethers with phytol and long-chain alcohols have been obtained. Glycerol mono- and diethers allow the localization of substituents, as shown in Fig. 72 (*313*, *316*).

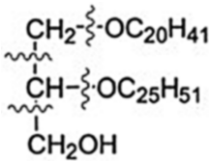

Fig. 72 Characteristic fragments of a glycerol 1,2-diether

Limited EI data are available for derivatives. The characteristic fragment for bis-trimethylsilyl ethers of 1-*O*-alkyl compounds is *m/z* 205 ($[M–CH_2OR]^+$), and for the 2-*O*-alkyl isomers, *m/z* 218 ($[M–ROH]^{+\cdot}$. Molecular ions can be seen (*676*, *677*). The 2,3-iopropylidene derivatives of 1-*O*-alkyl compounds yield $[M–CH_3]^+$ and *m/z* 101 ($[M–OR]^+$) as characteristic fragments of varying abundance; fragmentation of R may prevail (*676*, *678*).

Typical constituents of the core lipids are tetra-ethers (with symmetrical or unsymmetrical diols) such as *e.g.* compound **68**, Fig. 73. One glycerol unit can be replaced by a branched nonitol (calditol) (*314*). These compounds can also be found in geological specimens (*315*).

[23] Kindly provided by Dr. *P. Knechtle*, Evolva SA, Reinach, Switzerland.

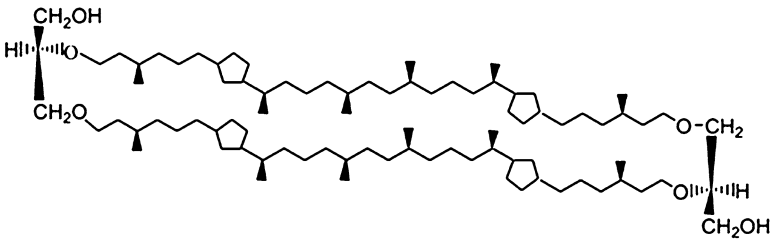

Fig. 73 Glycerol-dialkyl-glycerol-tetraether (**68**) from *Sulfolobus solfataricus* (*313*)

The molecular masses of the genuine or of the acetylated more complex compounds (as for **68**) can be determined by various mass spectrometric techniques. Structure elucidation of the diol part(s) requires *e.g.* cleavage of the ether bonds with HI and reduction of the di-iodides with $LiAlH_4$ to hydrocarbons, which can be subjected to EI analysis. However, structure elucidation needed subsidiary NMR support; the mass spectra by themselves did not offer sufficient information (see Fig. 74), although comparison with derivatives obtained by introduction of terminal D-atoms by reduction with $LiAlD_4$ or of SCH_3 or TMSO groups may be of assistance (*313*–*315*). For related compounds, see (*756*).

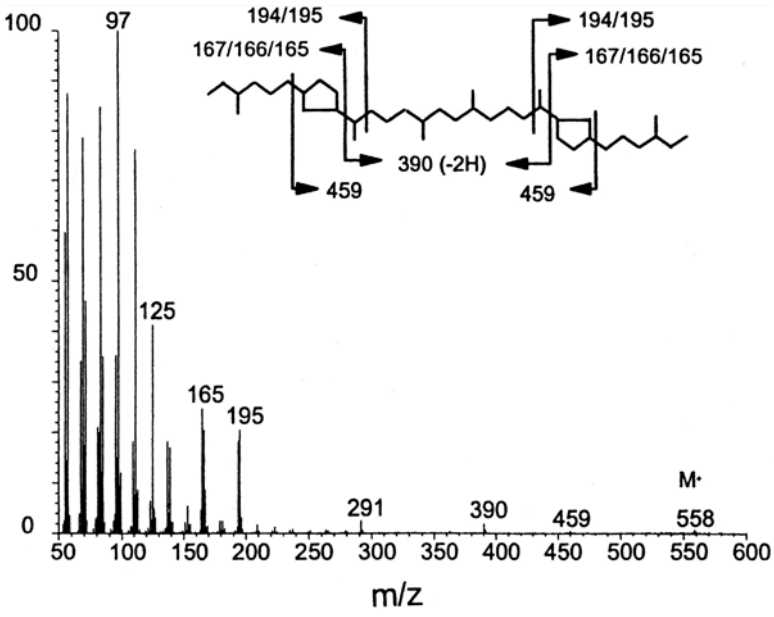

Fig. 74 EI-mass spectrum of the hydrocarbon obtained by degradation of the compound depicted in Fig. 73. Reproduced from (*315*) with kind permission from Elsevier (© 1998)

5.2.2 Triglycerides

The EI mass spectra of triglycerides were investigated in detail and proposed fragmentation mechanisms were confirmed by deuterium labeling (*317*, *318*). The molecular mass peaks $M^{+\cdot}$ and $[M–H_2O]^{+\cdot}$ are of low abundance. For triglycerides with three identical acid residues the main fragment is $[M–R\text{-}COO]^+$, accompanied by $[M–R\text{-}COOH]^{+\cdot}$ of lower abundance, RCO^+, $[RCO+74]^+$ (**ac**), and $[RCO+128]^+$ (**ad**) (Fig. 75). Triglycerides with differing acid residues show this pattern for each substituent. Those at the terminal positions can be recognized by $[M–R\text{-}COOCH_2]^+$ ions of relatively low abundance.

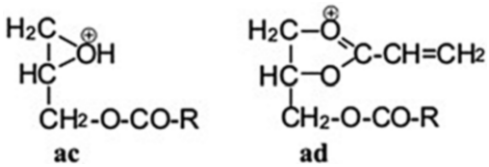

Fig. 75 Triglyceride ions **ac** and **ad** after loss of the acid units from C-1 and C-2 of glycerol

Abundant quasi-molecular ions can be obtained by FAB ionization and information regarding the mass of the acid units can be gained by CA (*320*), but Fig. 76 shows the extreme dependence from sample preparation (*319*). To tris myristyl glycerol dissolved in a mixture of CH_2Cl_2, CH_3OH, and NaI the matrices glycerol (G), thioglycerol (T) or *m*-nitrobenzylalcohol (N) were added. In the first case (spectrum a) only clusters of G and NaI were obtained; in the second (spectrum b) mainly NaI clusters and $[M+Na]^+$ can be seen. Only with *m*-nitrobenzylalcohol (spectrum c), in addition to a very abundant $[M+Na]^+$ ion, some characteristic fragments are obtained such as $[M+Na–RCOOH]^+$ (*m/z* 517), $[M+H–RCOOH]^+$ (*m/z* 495), or RCO^+ (*m/z* 211). For a discussion of the matrix glycerol, see (*669*).

Electrospray ionization (ESI) with subsequently induced decomposition of fragment ions (tandem mass spectrometry) allows a detailed analysis of triglycerides (*311*). Addition of LiOH to the analyte solution results in the formation of $[M+Li]^+$ ions, which when subjected to CA yield abundant $[M+Li–RCOOH]^+$ fragments. For compounds with three different acid units the middle one is lost at a lower rate than the terminal ones (at least for similar chain lengths). Further decomposition of the $[M+Li–RCOOH]^+$ ions allows the location of double bonds in unsaturated acyl groups by charge remote fragmentation (see above).

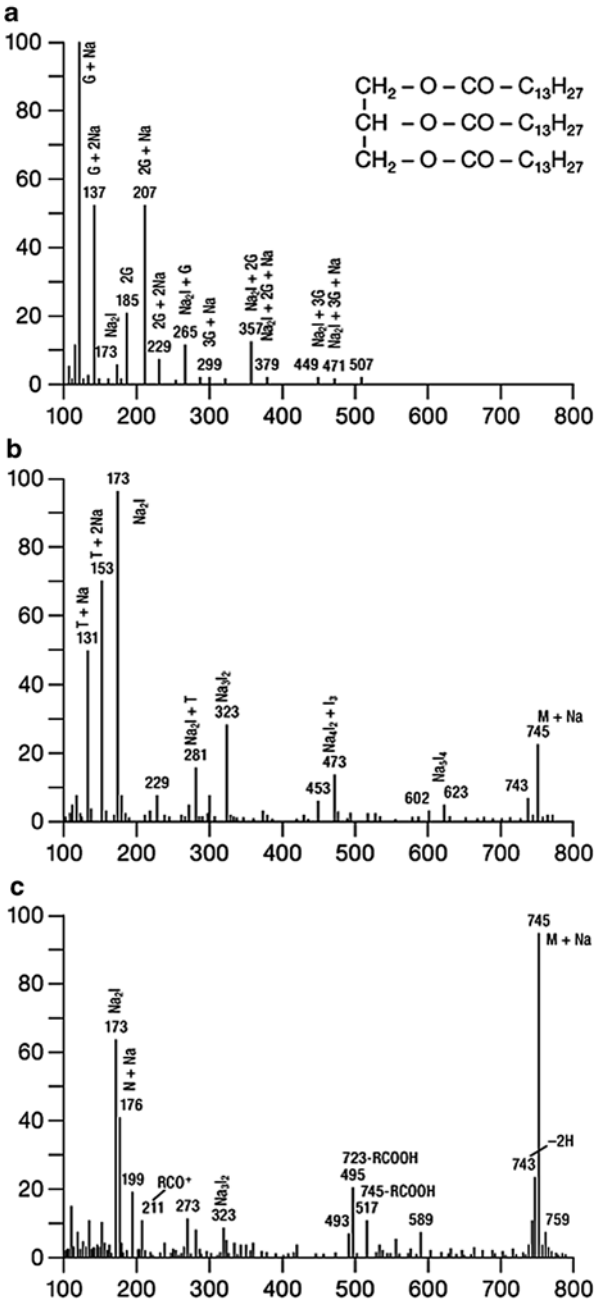

Fig. 76 FAB spectra of trismyristyl glycerol (see text). Reproduced from (*319*) with kind permission of Wiley-VCH Verlag GmbH & Co. KGaA (© 2005)

5.2.3 Glycerophospholipids

From the glycerophospholipids, the 1,2-diacyl-glycerophosphocholines were selected for a more detailed discussion, since they allow one to demonstrate how the advent of new mass spectrometric techniques provided increasingly more information (for an earlier review, see (*321*)) (Fig. 77).

Fig. 77 General structure of glycerophospholipids

Direct inlet EI spectra (*322*) of 1,2-diacyl-glycerophosphocholines (Fig. 78) show a hardly recognizable $M^{+\cdot}$ ion. By analogy to the elimination of $RCOO^{\cdot}$ from triglycerides, a loss of a phosphocholine radical plus some degradation in the acyl part is observed. CI with NH_3 (*323*) results in rather weak $[M+H]^+$ ions and loss of the phosphocholine residue, RCO^+ and $[RCO+74]^+$ (**ac**, Fig. 75). Field desorption (*324*) at low anode temperatures gives mainly $[M+H]^+$ and at higher temperatures some decomposition yielding choline, choline phosphate and loss of the latter, but also (pre-ionization?) rearrangements such as intermolecular methyl migration or the formation of dicholine phosphate.

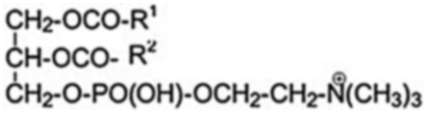

Fig. 78 1,2-Diacyl-phosphatidylcholines

A real breakthrough came with FAB ionization (*325*–*329*). The positive ion spectrum of 1-palmitoyl-2-stearyl-glycero-3-phosphocholine and of its 1-stearoyl-2-palmitoyl isomer (Fig. 79) shows $[M+H]^+$ (protonation of the phosphate anion, *m/z* 762), and both partial (*m/z* 550 and 578) and complete loss (*m/z* 478 and 506) of either a RCOOH molecule or of both $RCOO^{\cdot}$ radicals (*m/z* 224). The dominating ion is *m/z* 184 (choline phosphate), the formation of which involves H transfer from the α-position of the glycerol-C-2 acyl unit to the phosphate group (*330*, *331*). Intensity differences for isomeric pairs (*m/z* 524/496 and 506/478 in Fig. 79) have been invoked for positional assignments (*332*), but a decision is easier in the negative mode where abundant $RCOO^-$ ions are formed (*m/z* 255 and 283 in Fig. 80), with the ion coming from cleavage at C-2 being more abundant (*327*, *329*). Difficulties may arise with highly unsaturated acids or in case the two acyl groups differ much in size, but CA of $[M–CH_3]^-$ gives an unambiguous result

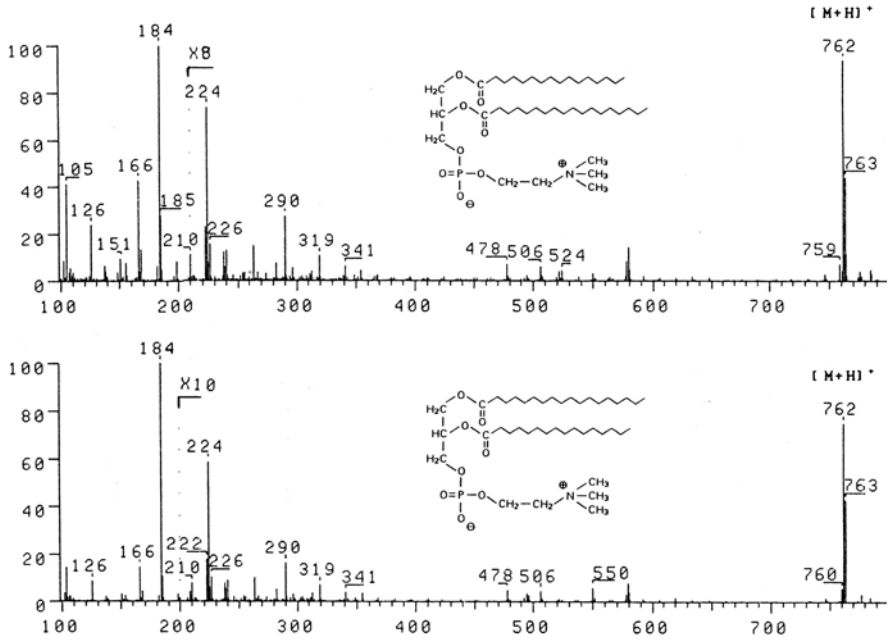

Fig. 79 Positive FAB spectra of 1-palmitoyl-2-stearyl-glycero-3-phosphocholine and of 1-stearyl-2-palmitoyl-glycero-3-phosphocholine. Reproduced from (*329*) with kind permission of Dr. *H. Münster*, Bremen

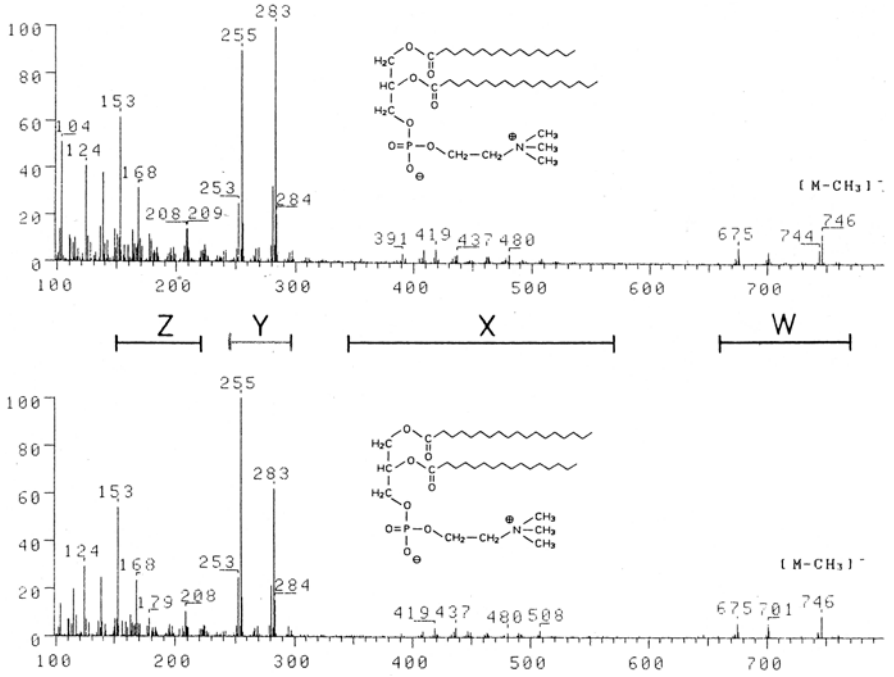

Fig. 80 Negative FAB spectra of 1-palmitoyl-2-stearyl-glycero-3-phosphocholine and of 1-stearyl-2-palmitoyl-glycero-3-phosphocholine (W … molecular ion region, Y… fatty acid residue region). Reproduced from (*329*) with kind permission of Dr. *H. Münster*, Bremen

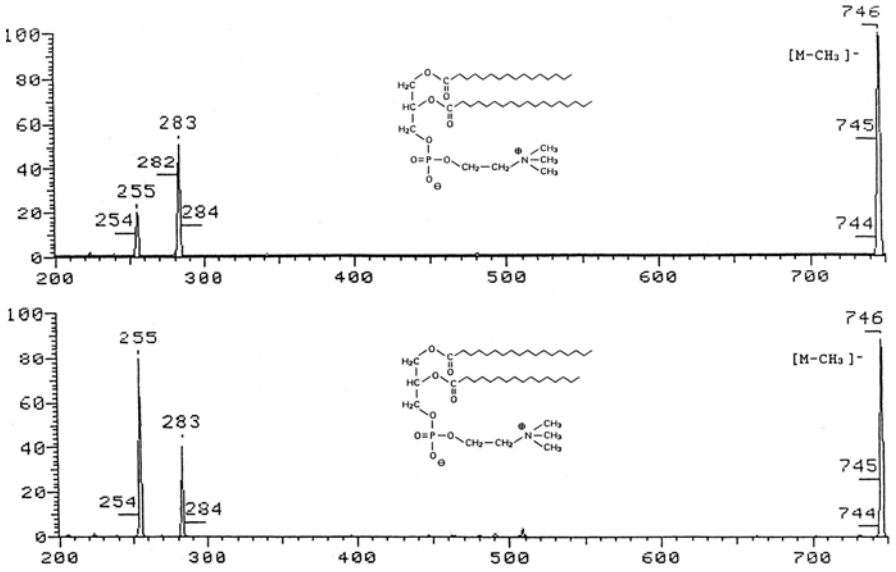

Fig. 81 CA spectra of $[M–CH_3]^-$ from 1-palmitoyl-2-stearyl-glycero-3-phosphocholine and of 1-stearyl-2-palmitoyl-glycero-3-phosphocholine. Reproduced from (*329*) with kind permission of Dr. *H. Münster*, Bremen

(Fig. 81). It must be pointed out that negative FAB spectra of choline derivatives show an $[M–CH_3]^-$ ion and can thus not be distinguished from analogous dimethylaminoethanol derivatives giving $[M–H]^-$, but switching to the positive mode solves this problem.

Electrospray ionization (*341*) gives essentially the same results as FAB but with a higher sensitivity (*333*) and avoids some of the matrix problems. In particular, the choline phosphate ion *m/z* 184 has been used for mixture analysis by precursor ion scanning with a tandem mass spectrometer yielding the molecular species (*334*). For MALDI tandem MS, see (*335*).

For the determination of double bond positions charge remote fragmentation (see above) may be applied. An alternative method is the use of an oxygen/ozone mixture as ESI gas. The ozonide formed in the first place decomposes in the presence of CH_3OH yielding two fragments that are 48 Da apart (see Fig. 82).

$$R\text{-}CH_2\text{-}CH=CH\text{-}CH_2 \sim\!\!\rightarrow R\text{-}CH_2\text{-}CHO + R\text{-}CH_2\text{-}C(OOH)OCH_3$$

Ozone can be produced in a standard generator or by using high ESI voltages in an oxygen-rich environment (*336*, *337*, *769*). See also the Addendum.

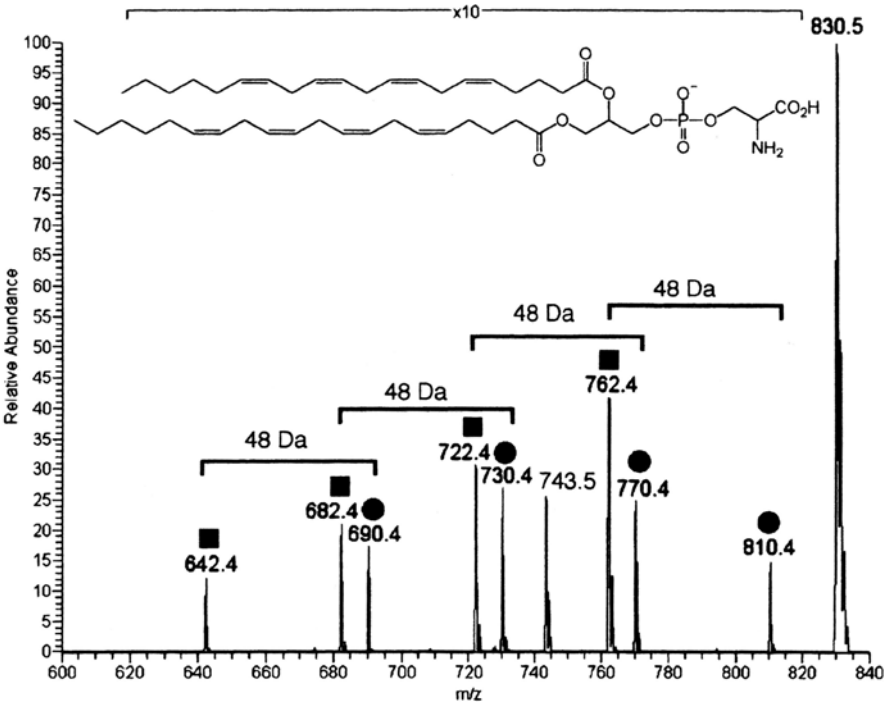

Fig. 82 ESI-MS (negative) of a methanolic solution of 1,2-di-arachidonyl-*sn*-glycero-3-phosphoserine (nebulizing gas O_2, ESI voltage—5 kV). *Filled squares* aldehydes, *bullets* methoxyhydroperoxides. Reproduced from (*336*) with kind permission of the American Chemical Society (© 2006)

5.3 Lipidomics

Fatty acids can be found attached to almost any class of natural products. Accordingly, the analysis of complex lipids ("lipidomics") covers a wide field applying mainly ionization techniques like ESI and MALDI. A detailed coverage would go beyond the limits of this chapter. Therefore, only some references will be given: references (*338*, *339*) discuss the MALDI-TOF analyses of lipids (glycerol derivatives, cholesterol derivatives, phospholipids, sphingo- and glycolipids), also in view of complex mixture analysis. References (*340*, *341*) discuss the application of ESI to the analysis of cellular phospholipids. Reference (*342*) reports the analysis of oxidized phospholipids. Reference (*343*) provides algorithms for automatic processing of data from mass spectrometric analyses of lipids. For a recent review, see (*344*).

6 Carbohydrates

6.1 Monosaccharides

Carbohydrate mass spectrometry started in 1959 when *Reed* and coworkers (*2*) reported appearance energy data of the $C_6H_{11}O_5^+$ ion from methyl glucosides and disaccharides and interpreting them in view of the weaker α- as compared with the β-glycosidic bond. However, it took another few years before more detailed studies were presented by the Glasgow group (*345*) and by three other ones, *viz.* from the Soviet Academy of Sciences (*3*, *346*), from MIT (*347*), and from the University of Hamburg (*4*). For earlier reviews, see (*348*–*353*).

Investigations of carbohydrates with EI mass spectrometry are hampered by their low volatility and thermal lability. Therefore, the early investigations were concentrated on various derivatives, but even those suffer from thermal degradations, resulting in differences in the data reported from different laboratories especially in the abundances of certain fragments (*352*), although qualitatively there is a substantial agreement between most of the published data. Another problem with most derivatives is an absence of molecular ion signals and the low abundances of upper mass ions. However, CI mass spectra using NH_3 as reagent gas give abundant $[M+NH_4]^+$ ions (*354*, *355*).

Acetyl derivatives of monosaccharides have been investigated in detail (*4*, *356*, *357*). The mass spectra are dominated by elimination of CH_3COOH and/or of $CH_2{=}CO$ from fragment ions (combinations of 60 and 42 Da). Of structural interest are the losses of the substituents neighboring the ether oxygen ($^{\cdot}OCOCH_3$ and $^{\cdot}CH_2OCOCH_3$, 59 and 73 Da, *m/z* 331 and 317 for peracetylated hexoaldopyranoses (*e.g.* **69**), and $^{\cdot}OCOCH_3$ and $^{\cdot}CH(OCOCH_3)CH_2OCOCH_3$, 59 and 145 Da, for hexoaldofuranoses). It should be remembered, however, that 3-hydroxytetrahydropyran compounds can rearrange in a way to yield fragments characteristic for the isomeric 2-hydroxymethyl tetrahydrofuran isomers (*358*). From the various ring fragments a sequence will be mentioned that leads to abundant fragments for *e.g.* β-D-glucopyranose penta-acetate (**69**). It starts (Fig. 83) with the loss of CH_3COOH (**ae**) and *retro-Diels-Alder* (*RDA*) ring opening (**af**, *m/z* 242) followed by losses of $CH_2{=}CO$ (*m/z* 200),

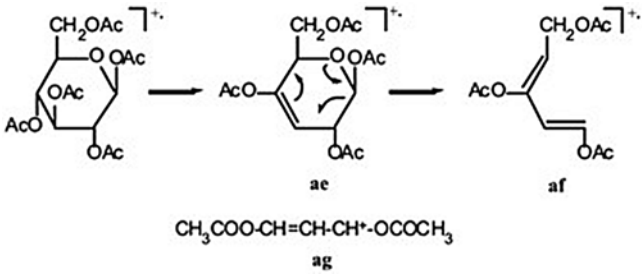

Fig. 83 Ring fragmentation of **69**

CH_3COOH (*m/z* 140), and of $CH_2{=}CO$ (*m/z* 98). Another ring fragment comprising C-2 to C-4 is $CH_3COOCH{=}CH\text{-}CH^+\text{-}OCOCH_3$ (**ag**) (*m/z* 157), which loses $CH_2{=}CO$ twice (*m/z* 115 and 73) (Fig. 84). Analogous fragments are also observed for other carbohydrate derivatives.

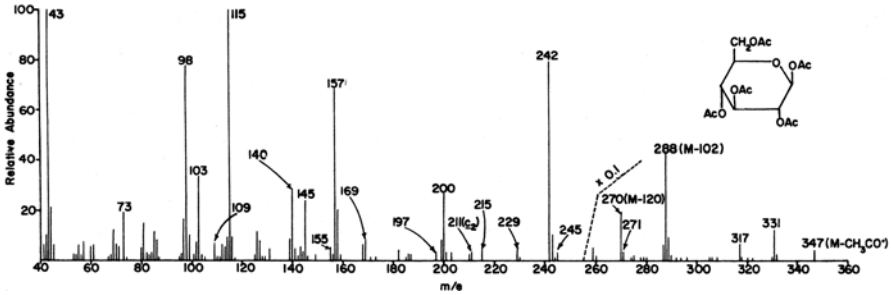

Fig. 84 EI mass spectrum of *β*-D-glucopyranose penta-acetate (**69**). The ions *m/z* 43 (CH_3CO^+), 103 ($(CH_3CO)_2O^+H$) and 145 ($(CH_3CO)_3O^+$) are found in all mass spectra of acetylated carbohydrates

EI mass spectra of peracetylated di- and oligosaccharides have been reported (*359*, *360*); but they offer no advantages over permethyl ethers (see below).

The EI mass spectra of permethylated monosaccharides suffer from the same problems as those of the peracetylated ones, in that molecular ions cannot be recognized and ions in the upper mass range are of low abundance. Yet they are still of great importance for structural studies. The fragmentation patterns of various types of this group have been studied by extensive deuterium labeling (*346*, *350*, *361*–*365*). Methyl tetra-2,3,4,6-*O*-methyl-*α*,D-glucopyranoside (**70**, Fig. 85) will be

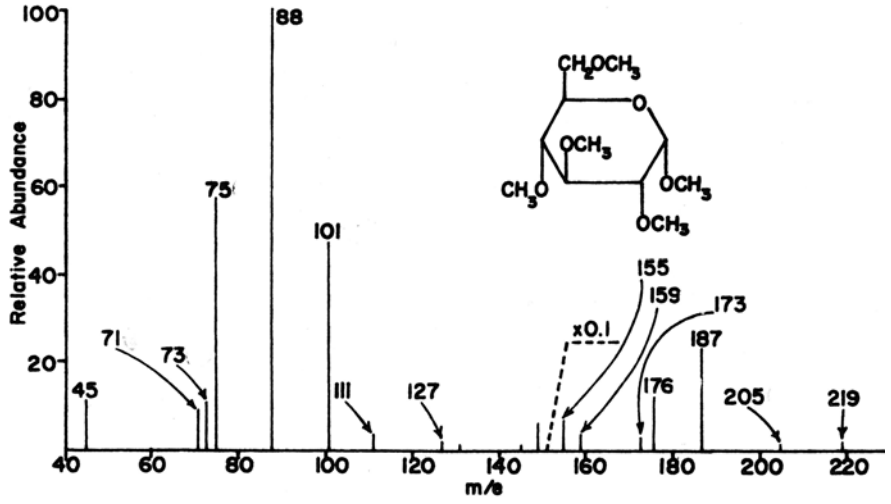

Fig. 85 EI mass spectrum of methyl tetra-2,3,4,6-*O*-methyl-*α*,D-glucopyranoside (**70**)

discussed in more detail. It shows losses of the two substituents neighboring the ring oxygen atom (–·OCH_3 and –CH_2OCH_3). Subsequent elimination of CH_3OH (–32 Da) is less pronounced than that of CH_3COOH from the acetates above. A protonated *RDA* fragment (*cf*. **af**) occurs at *m/z* 159 (1:1 $\mathbf{ah}_1$ and $\mathbf{ah}_2$) (Fig. 86). Other ring fragments are observed at *m/z* 176, 101, 88, and 75.

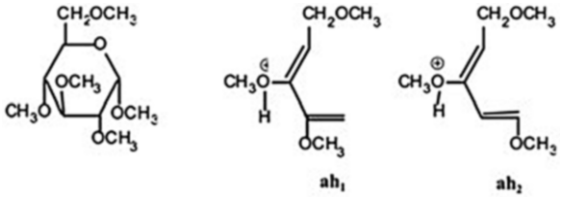

Fig. 86 *RDA* fragments of **70**

Schemes like those of Table 3 are available for various methylated monosaccharides or can be constructed from labeling data (*346*, *361–365*). They can readily be used for connection studies of di- and oligosaccharides. The saccharide is permethylated and hydrolyzed. The hydrolysis products are separated and their resulting free hydroxyl groups transformed with CD_3I into OCD_3 derivatives. In their mass spectra only those fragments that according to the appropriate table contain the label, will be

Table 3 Fragmentation and labeling data of methyl tetra-2,3,4,6-*O*-methyl-α,D-glucopyranoside (**70**)

m/z	Fragment	OCH_3 Loss from Carbon Atom	Contribution/%
219	– ·OCH_3	1	100
187	219—CH_3OH	2	9
		3	75
		4	16
155	219—2 CH_3OH	3+4, 3+6	66
		2+4, 2+6	34
205	– ·CH_2OCH_3	5	100
173	205—CH_3OH	3	100
176	$CH_3O\dot{C}H$-$CHOCH_3$-$CHOCH_3$-$CH=O^+CH_3$	6	100
159	$\mathbf{ah_1}$	1+2	50
	$\mathbf{ah_2}$	1+3	50
101	$(CH)_3(OCH_3)_2$	1+2+3	9
		1+3+6	60
		2+4+6	2
		1+4+6	26
		3+4+6	3
88	$CH_3O\dot{C}H$-$CH=O^+CH_3$	3+4+6	5
		1+4+6	79
		1+2+6	16
75	$CH_3OCH=CH_2O^+H_2$	1+3+4+6	15
		1+2+4+6	72
		1+2+3+6	13

shifted in their mass by 3 Da. Thus, from permethylated maltose (**71**) the labeled constituents **72** and **73** are obtained. Loss of $^{\cdot}OCD_3$ from $M^{+\cdot}$ indicates for both compounds the original substitution at C-1. The second OCH_3 group of **73** at C-4 can be localized from the shifts of $[M–CH_2OCH_3]^+$ (not at C-6) and of $\mathbf{ah}_1$ and $\mathbf{ah}_2$ (common substituent at C-4). Alternative methods to label the free positions of partially methylated monosaccharides are acetylation (*366*) or trimethylsilylation (*367*, *368*) (Fig. 87).

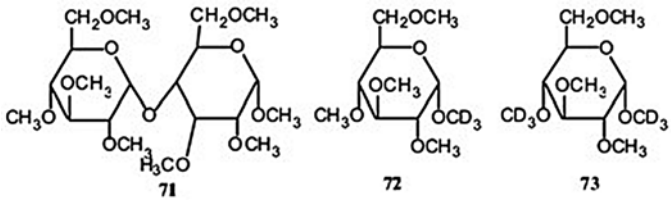

Fig. 87 Permethylated maltose (**71**) and its degradation products **72** and **73**

Other derivatives investigated more or less intensively are *inter alia* trifluoroacetates (*369*), trimethylsilyl ethers (*370–372*), boronates (*373*, *374*), *O*-isopropylidene derivatives (*375*), or dithioacetals (*376*).

6.2 Di-, Oligo-, and Polysaccharides

Overviews are given in (*377*, *378*). The EI and CI mass spectra of derivatized oligosaccharides have been discussed such as peracetates (*355*, *360*), permethyl ethers (*379*), or per-trimethylsilyl ethers (*360*, *380*, *381*). Structurally, most important are the product ions obtained by cleavage at the glycosidic linkage. Ring fragmentations as described for monosaccharides give further information. For denoting fragment ions of saccharides a nomenclature has been developed as depicted in Fig. 88. Branched chains are distinguished by Greek letters. For further details, see the original publication (*382*).

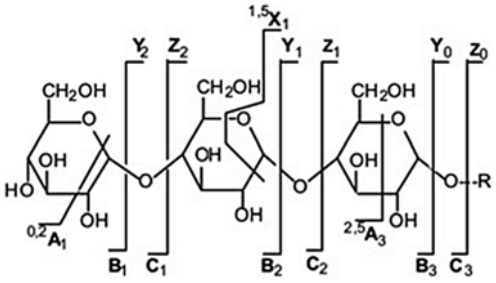

Fig. 88 Nomenclature for glycoconjugate fragment ions after (*382*). R designates an aglycone

The advent of field desorption (FD) has allowed one to obtain abundant molecular ions of oligosaccharides and at higher anode temperatures structural information

due to interglycosidic cleavages (probably due to thermolytic and/or proteolytic processes) (*383*).

Fast atom bombardment (FAB) both in the positive and negative modes of free and of derivatized oligosaccharides yields quasi-molecular ions ($[M+H]^+$, $[M+\text{metal ion}]^+$; ($[M-H]^-$) and bond cleavages at the glycosidic linkages (*384*, *385*). Fragmentation can also be induced by collision activation (CA) using tandem techniques (Fig. 89) (*386*).

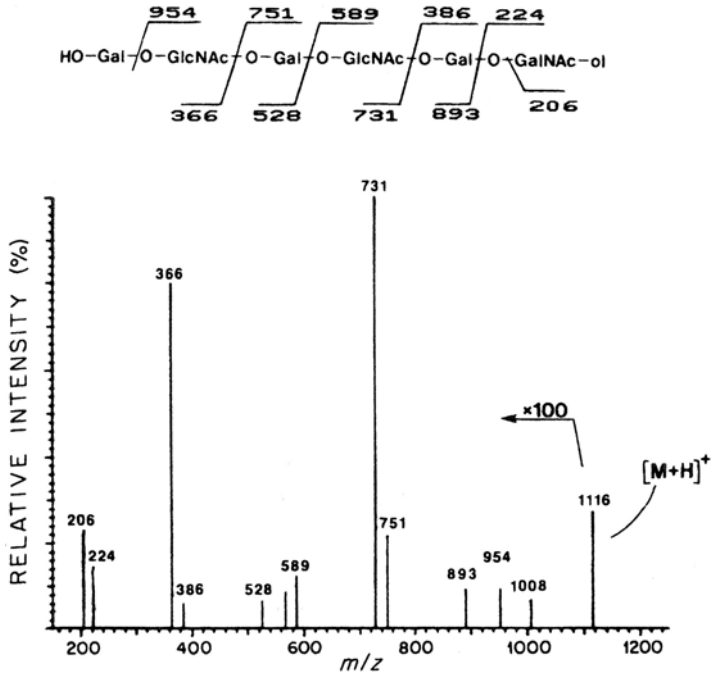

Fig. 89 Fragments obtained by CA of $[M+H]^+$ formed by positive FAB of a hexasaccharide. Reproduced from (*386*) with kind permission of John Wiley & Sons Ltd. (© 1999)

The standard ionization techniques used today for carbohydrate analysis using CA are electrospray (ESI) (*387*) and MALDI (*388*, *389*). Using ESI, the correct selection of solvents and additives is critical. For abundant molecular ions it is essential that the sample molecules are concentrated at the surface of the droplets, and MALDI matrices for the respective compound class have to be chosen. The resulting mass spectra can be highly complex especially for branched molecules. Fragmentation starts from all the termini and fragments may coincide in mass (Fig. 90). The apparent chaos can be sorted by tandem mass spectrometry selecting specific fragment ions and cause them to further decompose by CA as demonstrated for isomaltotetraose, *i.e.* (glucosyl($\alpha 1 \rightarrow 6$))$_3$ glucose. Spectrum (a) presents the ions obtained upon CA of $[M+Li]^+$, (b) and (c) those obtained by CA of the selected product ions $\mathbf{C}_3$ (*m/z* 511) and C_2 (*m/z* 349) (MS^3), and (d) finally those from the $\mathbf{C}_2$ fragment obtained from $\mathbf{C}_3$ (MS^4) (Fig. 91). Multi-step analyses either need a multi-quadrupole system, an ion trap (*391*), or an ICR analyzer (*390*).

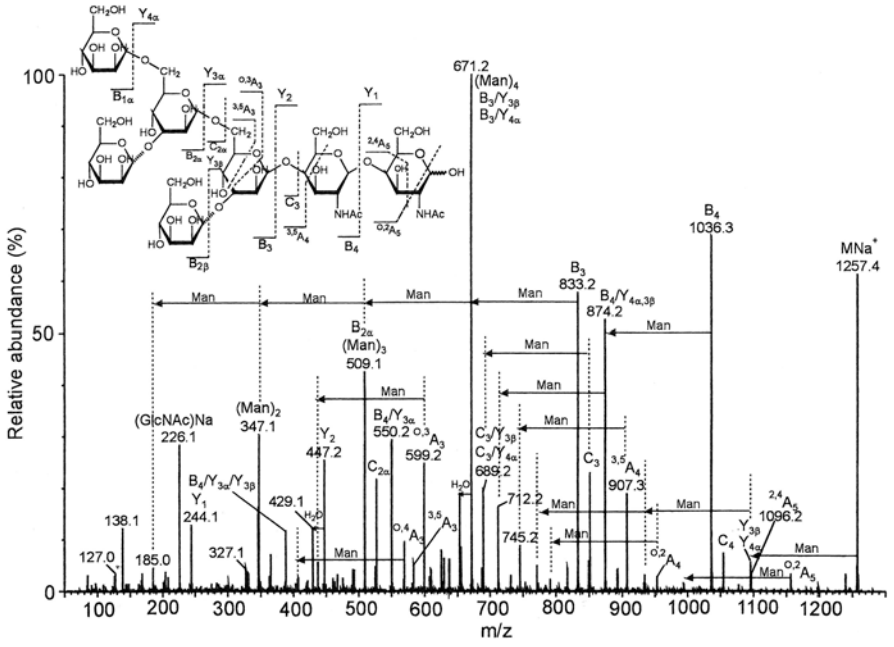

Fig. 90 MALDI-TOF MS/MS spectrum of $(Man)_5(GlcNAc)_2$. Reproduced from (*388*) with kind permission of John Wiley & Sons Ltd. (© 2006)

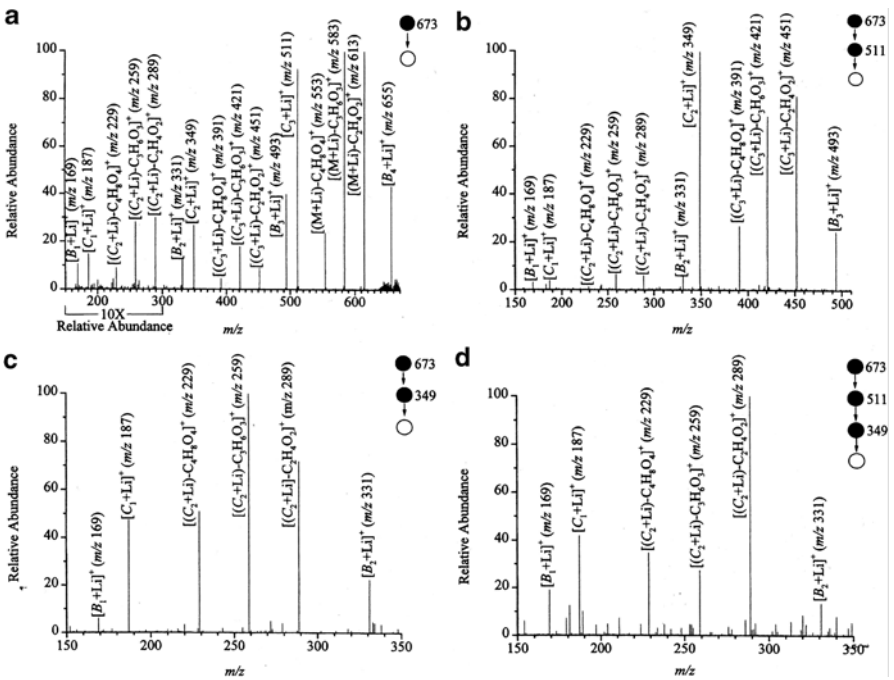

Fig. 91 Sequential fragmentation steps of lithiated isomaltotreose obtained by ESI (see text). Solid circles indicate the precursor ions, empty circles the product ions obtained in the respective step. Reproduced from (*391*), Fig. 6, with kind permission from Springer Science+Business Media (© 1997)

Additional structural information can be obtained from derivatized (permethylated or peracetylated) saccharides. They allow *e.g.* the differentiation between linear and branched isomers (*392*, *393*). Reaction with hydrazine derivatives can be used to label the reducing terminus of a saccharide by hydrazone formation (*687*).

A different approach to linkage position determination is tandem MS after cationization with metal ions other than the usually used Na^+ and Li^+. Thus, **C**-type ions obtained from $[M + Co^{2+} – H^+]^+$ yielded upon CA cross-ring fragments characteristic for $1 \rightarrow 2$, $1 \rightarrow 3$, $1 \rightarrow 4$, and $1 \rightarrow 6$ linkages (*394*). Ion mobility mass spectrometry has been suggested for the separation of cationized isomeric disaccharides (*601*).

Also, computer programs have been developed to cope with the mass of data obtained. STAT (*395*), after input of all available data, such as precursor ion masses, possible monosaccharide moieties, and product ion masses the program creates all possible structures that may fit the precursor mass and the product ion pattern giving a rating on the likelihood.

From polysaccharides, molecular mass distributions can be obtained as shown for the MALDI spectrum of an algal laminarin (Fig. 92). The number of free hydroxy groups can be determined by permethylation (*396*). Even cyclic structures like cycloglucans that are not amenable to enzymatic degradation such as cyclodextrins yield structural information. Thus, from $[M + Na]^+$ of γ-cyclodextrin losses of one up to five glucose units were observed (*397*). Degradation studies were necessary for the analysis of pectins (*398*).

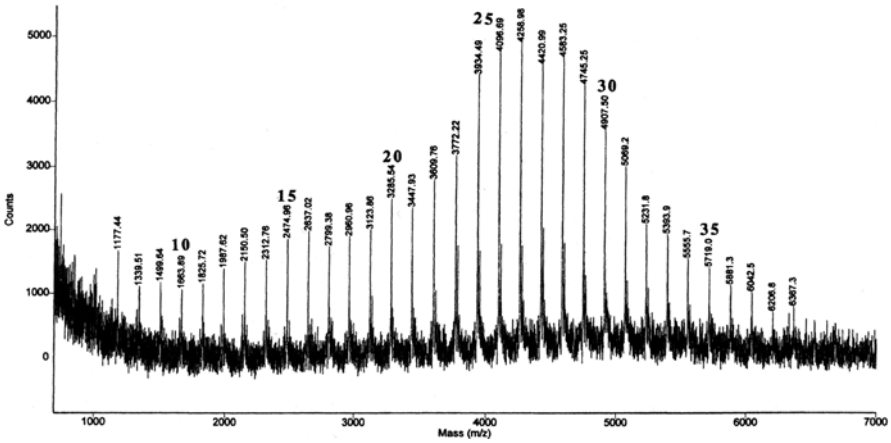

Fig. 92 MALDI-TOF mass spectrum of the laminarin from *Laminaria cichorioides*. The main signals stem from $[M + Na]^+$ ions accompanied by $[M + K]^+$ The mass differences correspond to $C_6H_{10}O_5$ units. Reproduced from (*396*) with kind permission from Elsevier (© 1998)

6.3 Glycosides

In Nature, many structural types have been found to be linked to sugar moieties for various reasons: increased hydrophilicity for transport in aquatic media, recognition of specific compounds at cell surfaces (*399*), membrane structures (*400*), *etc.* MALDI usually allows one to determine within limits molecular masses, and possibilities exist for structural analyses by tandem mass spectrometry, depending on the type of compound investigated. For example, flavonoid (*401*), steroid, or terpenoid glycosides yield information regarding the mass of the aglycone and to some extent regarding the composition of the sugar part (*377*). From highly complex compounds, peptide and protein glycosides will be selected to demonstrate how different approaches have been chosen to obtain maximal results: LC/MS (*402*), FAB, MALDI, ESI (*403*), PSD-MALDI[24] (*404*), multi-stage MS/MS (*405*), and electron capture MS (*406*). Questions to be answered are the molecular mass, the sequence of the sugar components, and the connections between them, the type of linkage to the peptide part (*O* or *N*), and if there is more than one possibility for the linkage site determination. There are limits to what mass spectrometry can do and other techniques such chemical and enzymatic degradation studies or NMR spectroscopy may be needed for assistance.

For simple compounds the carbohydrate sequence can be established readily from the CA data (Fig. 93). The sequence can be confirmed by tandem experiments

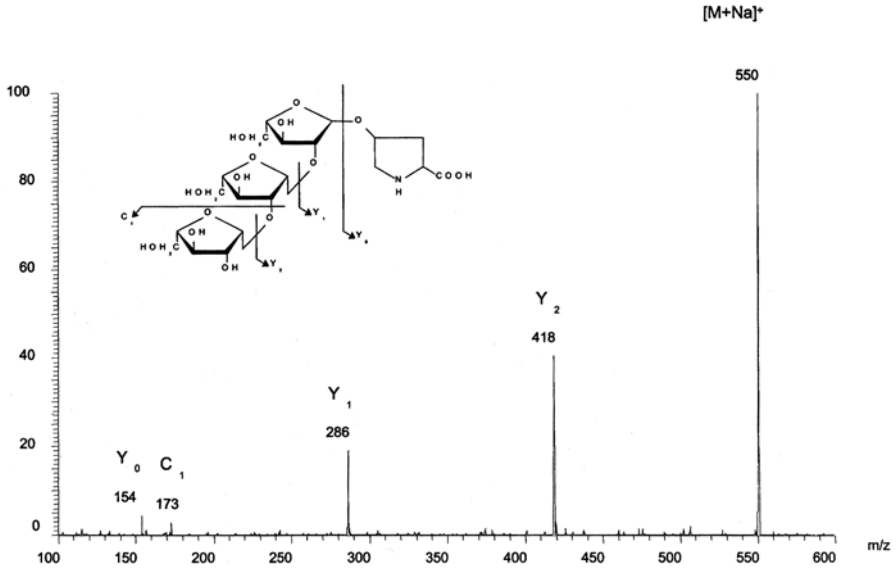

Fig. 93 ESI-CA spectrum of $[M+Na]^+$ of Hyp-Ara_3). Reproduced from (*410*) with kind permission of Wiley-VCH Verlag GmbH & Co. KGaA (© 2005)

[24] Post-source decay, this constitutes an ion fragmentation technique used with reflector-TOF instruments (*17*).

(especially for branched sugar parts), and the connection sites between the sugar molecules by the methylation (*407*) and deuteromethylation technique described above (*408*, *409*).

Regarding complex structures two short descriptions will be given to illustrate the topic. The first describes the determination of glycosylation sites and the characterization of sugar parts of mouse cylooxygenase-2 (mCOX-2) (*399*). The enzyme mCOX-2 contains five potential glycosylation sites, Asn 53, 130, 396, 580, and 592. To determine the number of actually occupied sites the intact protein was subjected to nano-ESI-MS, which showed the presence of three glycoforms with average masses of (1) 71.4, (2) 72.7, and (3) 73.9 kDa with mass differences of 162 Da between the peaks of each group (hexoses, probably mannoses from earlier studies). For (1), an average sugar residue of $Man_8GlcNAc_2$ at two sites and GlcNHAc at two sites, for (2), $Man_7Glc\mathit{N}Ac_2$ at three sites and Glc*NH*Ac at one site, and for (3), $Man_7Glc\mathit{N}Ac_2$ at four sites, were calculated (see below). There is a second set of peaks ca. 80 Da higher, possibly due to sulfate or phosphate derivatives. Further analyses were performed using ESI and MALDI on components obtained after tryptic digests, both before and after deglycosylation. The various Asn-containing fragments were analyzed for their glycosylation. The results are shown in Table 4. The sites of linkage between the sugar molecules could not be determined.

Table 4 Glycosylation sites of COX-2 and the extent of glycosylation. Adapted from Ref (*399*) with kind permission of the American Chemical Society (© 2001)

Glyco-form	MW (kDa)	Asn 53	Asn 130	Asn 396	Asn 580	Asn 592
1	71.4	$Man_{7\text{-}9}GlcNAc_2$	$Man_{6\text{-}10}GlcNAc_2$	GlcNAc	GlcNac	None
2	72.7	$Man_{7\text{-}9}GlcNAc_2$	$Man_{6\text{-}10}GlcNAc_2$	GlcNAc	$Man_7GlcNAc_2$	None
2	72.7	$Man_{7\text{-}9}GlcNAc_2$	$Man_{6\text{-}10}GlcNAc_2$	$Man_{5\text{-}7}GlcNAc_2$	GlcNAc	None
3	73.8	$Man_{7\text{-}9}GlcNAc_2$	$Man_{6\text{-}10}GlcNAc_2$	$Man_{5\text{-}7}GlcNAc_2$	$Man_7GlcNAc_2$	None

An alternative method has been developed to determine glycosylated Asn sites in a protein (*411*). Enzymatic hydrolysis in the presence of 50% $H_2{}^{18}O$ yields a product with an Asp in the peptide sequence displaying a peak doublet in its mass spectrum two Da apart. The product can be used for peptide sequencing by nano-ESI. For a comparison with databases, the spectra have to be recalculated for the mass of Asn.

Recent reviews (*412*) discuss the isolation methods for glycoproteins laying special emphasis on microarray techniques and factors influencing the peak intensities of molecular ions in mixture analyses (structural differences, work-up procedures, ionization techniques (*675*)).

7 Amino Acids, Peptides, and Proteins

7.1 Amino Acids

Amino acids were among the first groups of natural products to be investigated by EI mass spectrometry (*6*, *413*). Amino acids in being zwitterionic compounds are involatile and hence the main emphasis centered on the search for suitable derivatives. Methyl and ethyl esters were scrutinized by *Stenhagen* and by *Biemann* (*6*, *414*, *415*). They show the typical fragmentation behavior of primary aliphatic amines (*416*) as can be seen for leucine ethyl ester (Fig. 94). α-Cleavage of aliphatic representatives (*414–417*) results in the loss of the ester group (**ai**, *m/z* 86) and to a lesser extent of the alkyl residue (**aj**, *m/z* 102) (Fig. 95).

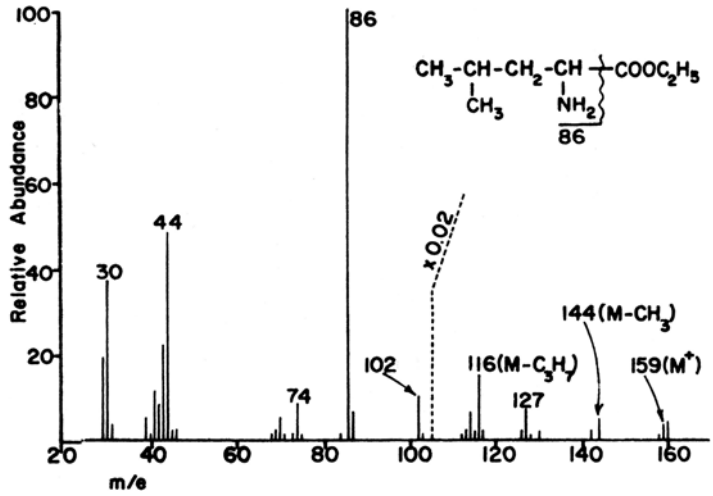

Fig. 94 EI mass spectrum of leucine ethyl ester

$H_2N^+{=}CH\text{-}COOC_2H_5$ ← $(CH_3)_2CH\text{-}CH_2\text{-}CHN^+H_2\text{-}COOC_2H_5$ → $(CH_3)_2CH\text{-}CH_2\text{-}CH{=}N^+H_2$

aj **ai**

↓ ↓

$CH_2{=}N^+H_2$ $CH_2{=}CH\text{-}N^+H_3$

ak **al**

Fig. 95 Main fragments of α-amino acid ethyl esters

The ion **ai** can decompose further giving **ak** (*m/z* 30) and **al** (*m/z* 44). They have the same masses as the α-cleavage products of glycine and alanine, respectively, and should not wrongly be taken as an indication of an admixture of these two amino acids. Secondary fragmentation sequences can be used to differentiate *e.g.* between isomeric amino acids.

In methionine, the sulfur atom can compete in charge stabilization with the nitrogen yielding $CH_3S^+=CH_2$ as the main fragment. Similarly for aromatic amino acid esters Ar-CH_2-$CHNH_2$-$COOC_2H_5$ (phenylalanine, tyrosine, tryptophan) the ions Ar-CH_2^+ are of importance. N-Acylated esters (*418–421*) bring no advantages. The fragmentations induced by the acyl group complicate the picture.

The fragmentation rules developed for peptidic amino acids have been used for the structure elucidation of new natural products as exemplified for lysopine diethyl ester (**69**) (*422*). The molecular ion (*m/z* 274) loses one carbethoxyl group (*m/z* 201) and subsequently NH_3 (*m/z* 184) typical for lysine ethyl ester (*6*). This structural moiety is confirmed by the base peak at *m/z* 84 due to the analogous loss of the substituted Nα, *i.e.* $CH_3CH(NH_2)COOC_2H_5$ from the ion *m/z* 201. The absence of ion **aj** excludes a ~$CH(NH_2)COOC_2H_5$ terminus. The proposed structure **74** (Fig. 96) was confirmed by synthesis.

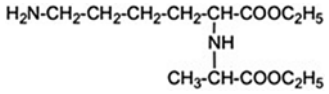

Fig. 96 Lysopine (**74**)

Chemical ionization (CI) ((*423*) and below) complements the armamentarium: CI with methane or isobutane produces abundant $[M+H]^+$ ions while EI suffers from low intensities in the molecular ion region. However, EI offers more structural information than CI especially for the distinction of isomers or when unexpected compounds are encountered.

New approaches regarding derivatization began with the GC (*424*) and especially with the GC/MS era. Trimethylsilyl derivatives are obtained by reaction with trimethylsilyl chloride (*425*). By treatment with *N*-methyl-*N*-*tert*-butyldimethylsilyltrifluoroacetamide all active H-atoms on N, O, and S are replaced and the corresponding *tert*-butyldimethylsilyl derivatives are obtained (*426*). $[M–CH_3]^+$ or $[M–C_4H_9]^+$ ions allow the determination of the molecular masses. Treatment of amino acids with $ClCOOC_2H_5$ in ethanol/water/pyridine yields *N*-ethoxycarbonyl amino acid ethyl esters (*427*), which show typical α-cleavages. The advantage of these methods is that the derivatives can be obtained in a one-step synthesis. The preparation of the *N*-perfluoroacyl amino acid alkyl esters requires two steps. Both EI and CI spectra of trifluoroacetyl and pentafluoropropionyl derivatives of methyl, *n*- and *i*-propyl and *n*-butyl esters were recorded (*428–432*) and allow the identification also of unusual amino acids and of decomposition products. Characteristic common ions can be used for single ion detection techniques (Fig. 1, Sect. 2). When the GC analysis is performed with a enantioselective column D- and L-amino acids can be identified. With a L-Chirasil Val capillary the D-enantiomers are eluted before the L-enantiomers. Calibration is possible with a racemic mixture of amino acids (*430*, *433*).

7.2 Peptides

Amino acid sequence analysis has become the basis of proteomics.

7.2.1 Linear Peptides

For designating fragments of a peptide chain a common nomenclature is in use (*434*). When a specific bond is cleaved before, in or after an amide group N-terminal fragments are designated by **a**, **b**, and **c**, and the C-terminal ones by **x**, **y**, and **z** (see Fig. 97). A subscript indicates the number of amino acids retained in a given fragment. Hyphens indicate the number of additional hydrogen atoms present in a fragment (*e.g.* $\mathbf{y}_1''$ would be $^{+}NH_3$-CHR_4-COOH). In older publications, individual systems may be found (as the capital letters in Figs. 103, 104, 105, and 106, or the system used in (*454*).

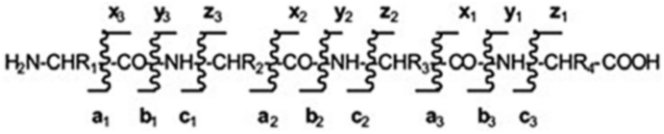

Fig. 97 Designation of peptide fragments

Biemann (*435*, *436*) proposed to reduce the peptides with $LiAlH_4$ to polyaminoalcohols that give sequence-characteristic α-cleavage products. This approach is of no importance anymore for peptide analysis but the results are the basis for the structure elucidation of polyamines as found in spider venoms (*e.g.*, **75**, Fig. 98) (*437*, *438*, *639*).

p-HO-C_6H_4-CO-NH-$(CH_2)_3$-NH-$(CH_2)_3$-NH-$(CH_2)_3$-NH-$(CH_2)_3$-NH-$(CH_2)_3$-NH_2

Fig. 98 Spider venom polyamine **75**

The EI mass spectra of trifluoroacetyl peptide methyl esters show a large number of fragments for which the genesis can be explained by cleavages along the chain and by side chain losses, but the sequence specific ones are not very prominent (*439*). Nevertheless, an interpretation scheme was developed starting with the identification of the $[M–NH\text{-}CHR\text{-}COOCH_3]^+$ ion by trying all possible R residues and continuing by the search for the next ion with a mass difference of NH-CHR′-CO, *etc.* (*440*).

Subsequent techniques started with the identification of the acylated N-terminal fragment and going then on as above (*441*). The starting point was the structure elucidation of a nonapeptide from *Mycobacterium fortuitum* named fortuitine (*442*). The N-terminal valine is substituted by equal amounts of C_{20}- and C_{22}-fatty acids

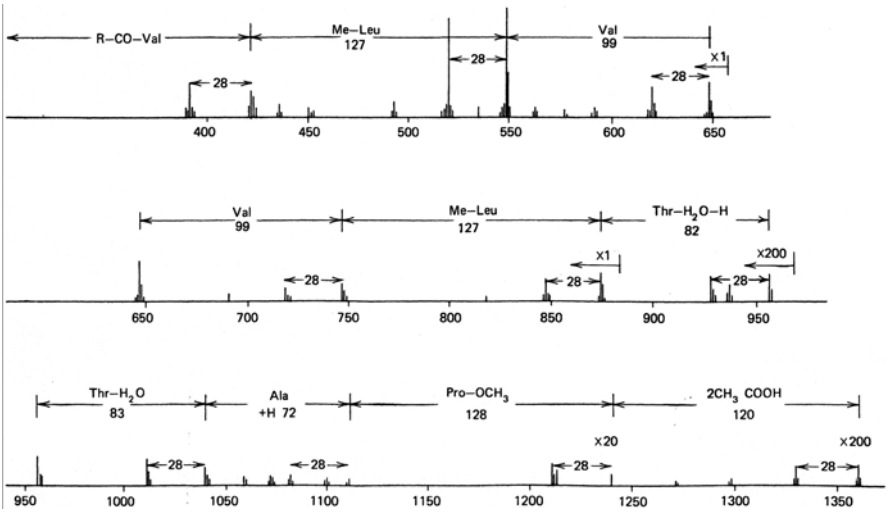

Fig. 99 EI mass spectrum of fortuitine methyl ester $CH_3(CH_2)_{18/20}CO$-Val-MeLeu-Val-MeLeu-Thr(Ac)-Thr(Ac)-Ala-Pro-$COOCH_3$. Reproduced from (*442*) with kind permission from Elsevier (© 1965)

resulting in pairs of fragment ions differing in mass by 28 Da (Fig. 99) and moving the N-terminal fragment out of the low mass range, which is confusing because of the large number of uncharacteristic secondary fragments. As a result, synthetic derivatives of amino acids with equimolar mixtures of homologous (*443*) or deuterated and nondeuterated fatty acids (*444*) were investigated. The next step was the N-methylation of the peptide linkages, which not only increased the volatility, but also simplified the mass spectra that are dominated now by cleavages of the peptide bonds with charge retention on the carbonyl groups (Fig. 100) (*445*, *446*). Computer programs were developed for determining the amino acid sequences of derivatized oligopeptides (*447*, *448*).

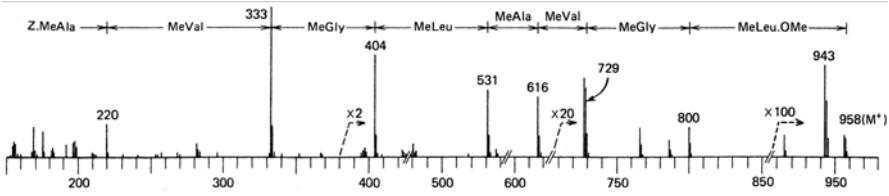

Fig. 100 EI mass spectrum of Z-MeAla-MeVal-MeGly-MeLeu-MeAla-MeVal-MeGly-MeLeu-OMe (Z = C_6H_5-CH_2-OCO). Reproduced from (*446*) with kind permission from Elsevier (© 1968)

A further step forward was the introduction of the field desorption (FD) technique. It allowed the recognition also of $[M+H]^+$ ions for amino acids as arginine or cystine that could not be detected by EI or CI (*449*), as well as those of peptides (*450*, *451*). At increased anode currents, fragment ions are obtained that can be

correlated with the amino acid sequences allowing for mass deviations of ± 2 Da from the calculated mass for direct cleavage. This is due to the occurrence of competing thermal processes (Fig. 101).

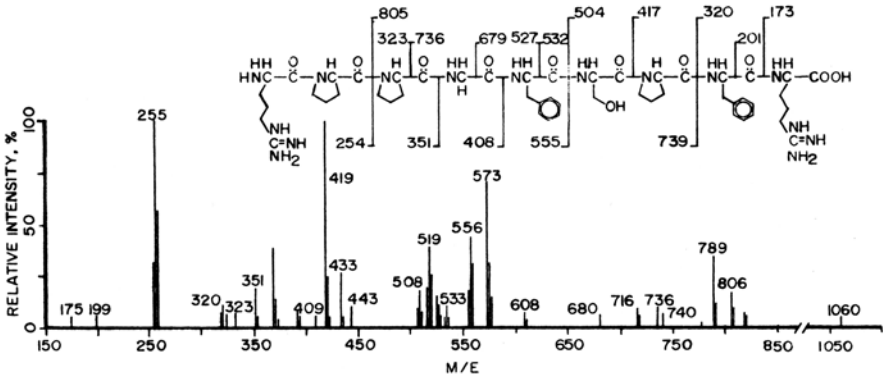

Fig. 101 FD mass spectrum of Arg-Pro-Pro-Gly-Phe-Ser-Pro-Phe-Arg. Reproduced from (*451*) with kind permission of John Wiley & Sons Ltd. (© 1975)

Fast atom bombardment (FAB) mass spectrometry has been used for many years for sequence analyses. Figure 102 gives an example. **b**-Ions can be recognized in the positive mode with the exception of tyrosine (*m/z* 164) where the ion **a** (*m/z* 136) prevails, probably due to the better charge stabilization. In the negative mode, $\mathbf{y}^-$ ions can be seen. A problem is caused by the many ions formed by further

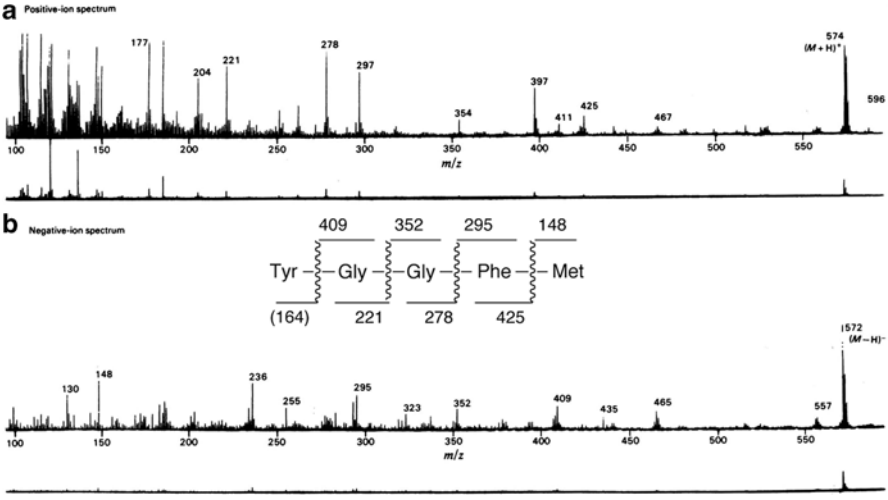

Fig. 102 FAB mass spectrum of methionine encephalin. Upper spectrum positive mode (**b** ions), lower spectrum negative mode ($\mathbf{y}^-$ ions). Reproduced from (*452*) with kind permission of Portland Press Ltd. (© 1981) by the Biochemical Society

decomposition of the primary cleavage products or by side chain fragmentation (*452*). Clearer results can be obtained by a combination of FAB with collision activation (CA) (*453*), which allows the recognition of unusual amino acids, such as >CH-OCH_3 groups containing species found in dolastatin 10, a peptide obtained from the sea hare (*Dolabella aurecularia*) (*454*). $[M+H]^+$ ions can be obtained up to a mass region of several thousands (*455*). Therefore, information stated in Sect. 2.4 should be kept in mind concerning high masses with respect to mass shifts and isotope patterns.

The primarily used techniques today are ESI and MALDI in conjunction with CA. The ESI results depend on the techniques used and the type of molecular species activated. $[M+H]^+$ or $[M+2\ H]^{2+}$ give more information than *e.g.* $[M+Na]^+$ because the localization of a proton in an amide bond facilitates its cleavage (*456*, *457*). Residence of a proton in the N-terminal part will result in **b** ions, and residence in the C-terminal part in **y**″ ions. The binding of metal ions on amide bonds was investigated by infrared multiple-photon dissociation spectroscopy. K^+ is associated with the carbonyl oxygen, while *e.g.* Ni^{2+} is bound to N after deprotonation (*458*).

The information that can be obtained depends on various factors. Thus, the residence time of ions in an octopole unit is much shorter than in an ion trap where hydrogen migrations and rearrangement processes are more likely. The octopole CA spectrum both from $[M+H]^+$ and from $[M+2\ H]^{2+}$ of the chromopeptide **76** (Fig. 103) shows mainly fragments from the vicinity of the chromophore where

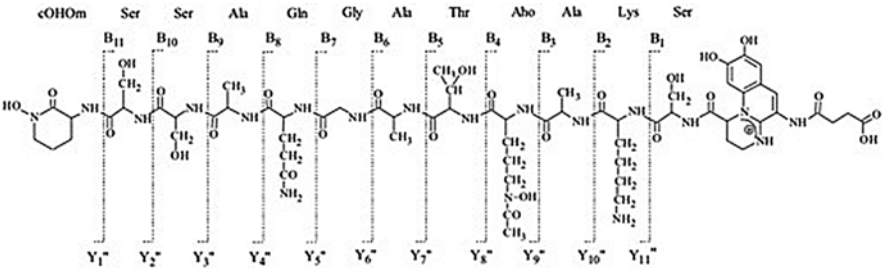

Fig. 103 Sequence-specific fragments of a pyoverdin from *Pseudomonas fluorescens* (**76**)

one proton is strictly localized in the aromatic system (Fig. 104). The ion trap CA spectrum of $[M+H]^+$ (Fig. 105) shows predominantly fragments in the molecular ion region for the same reason, but sequence specific (mainly **b**) fragments of low abundance can be seen. These (and also the **y**″ ions) are much more abundant in the $[M+2\ H]^{2+}$ CA spectrum (Fig. 106) where one proton can move freely (*460*). Repetitive CA induced fragmentation (MS^n spectra) may provide additional information.

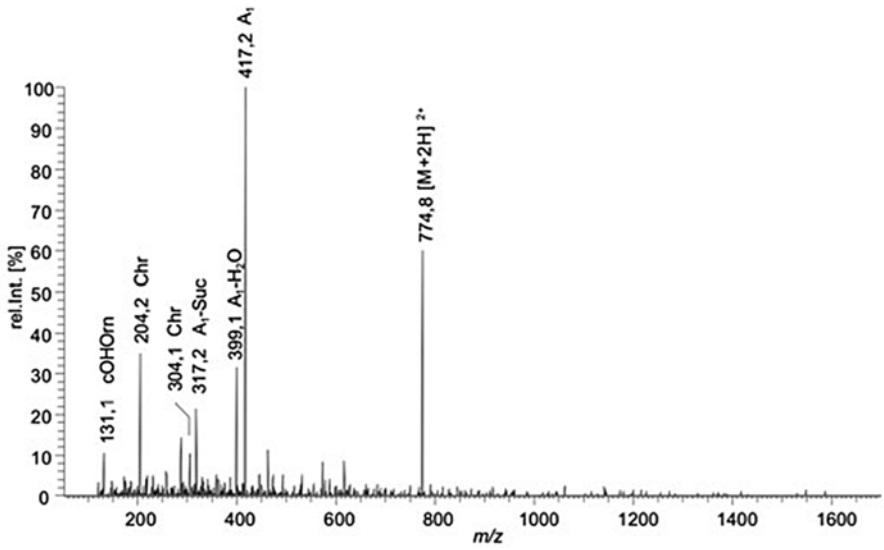

Fig. 104 ESI octopole CA spectrum of $[M+2\,H]^{2+}$ of **76**

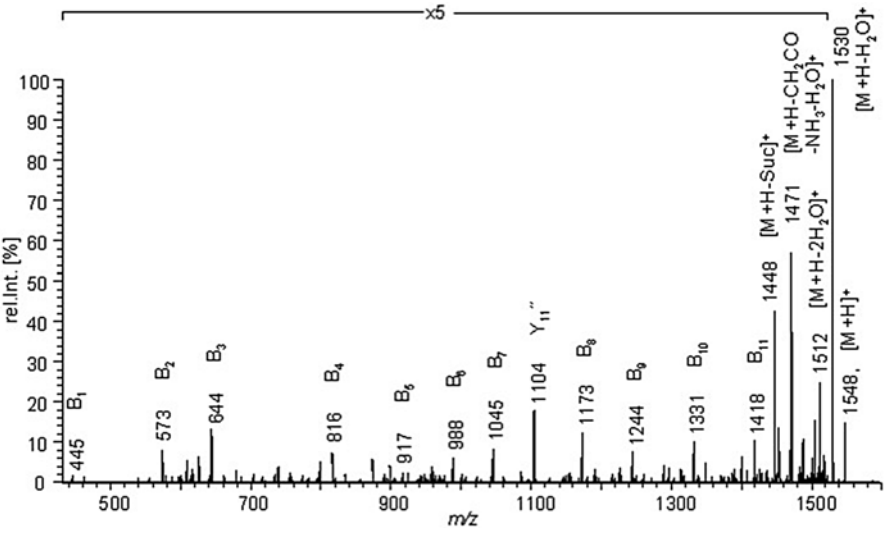

Fig. 105 ESI ion trap CA spectrum of $[M+H]^{+}$ of **76**

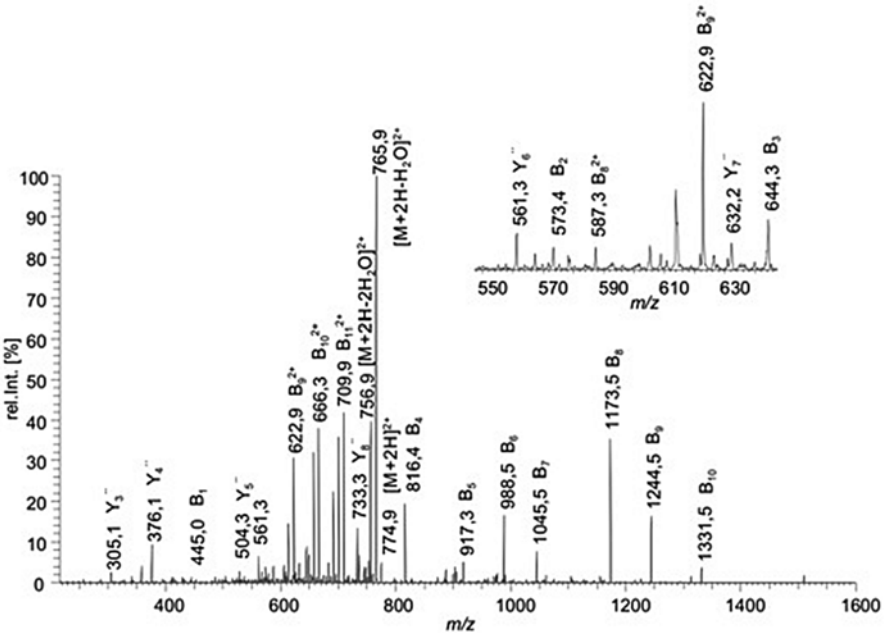

Fig. 106 ESI ion trap CA spectrum of $[M+2\,H]^{2+}$ of **76**

Fragmentation mechanisms explaining the preferred formation of **b** ions have been proposed (*462*) and more complex fragmentation sequences including rearrangement steps have been discussed (*460–462*). Thus, a collision induced degradation of the peptide chain that can outweigh the formation of **b** ions involves the loss of NH=CHR+CO units starting from the C-terminus and resulting in a chain shortened by one amino acid. This process can occur repeatedly several times. A side reaction is the loss of $CO+H_2O$ (*463*) (Scheme 1).

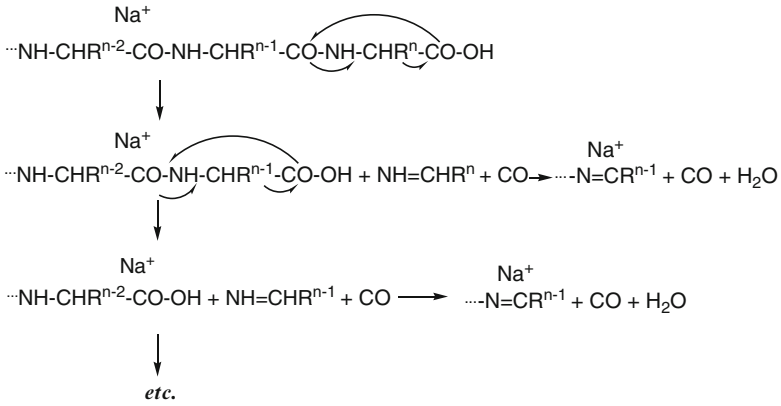

Scheme 1 CA induced degradation of a peptide chain with OH-rearrangement

As a side aspect, pyoverdins varying in their peptide part have been used for the classification of the bacterial genus *Pseudomonas* (*459*, *464*) and for characterizing new species (*e.g.* (*465*)).

As an example of fairly large peptides analyzed by MALDI-CA, the results allowing a differentiation between archeological sheep and goat bones are summarized (Fig. 107), in which sequential differences in collagen peptide samples were established (*466*); see also (*766*).

For a review on spectrometric methods to distinguish between isomeric amino acid residues in peptides and proteins, see (*467*).

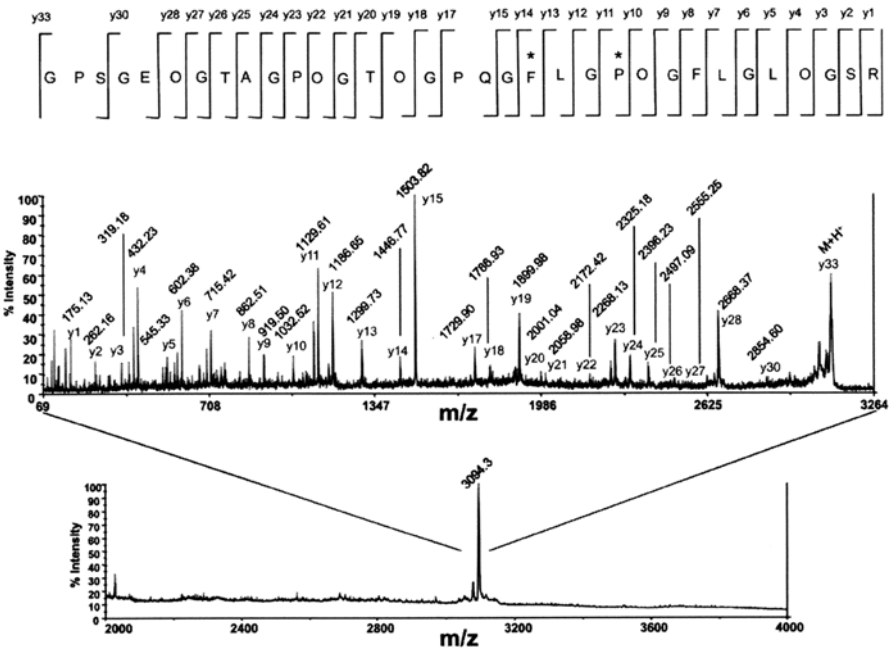

Fig. 107 MALDI-CA spectrum of a goat collagen peptide. Reproduced from (*466*) with kind permission from Elsevier (© 2010)

7.2.2 Cyclopeptides and Cyclodepsipeptides

Cyclodipeptides (2,5-dioxopiperazines, *e.g.* cyclo-leucine-proline, **77** (Fig. 108) show upon EI a rather low abundant $M^{+\cdot}$ (*m/z* 210) and preferred ring fragmentation (*468*–*471*), *i.e.* loss of CO (*m/z* 182 and (more abundant) of HNCO (*m/z* 167). Accompanied by a hydrogen migration, ions *m/z* 70 and 84 are formed. Longer alkyl chains are lost by a *McLafferty* rearrangement ($[M–C_4H_8]^{+\cdot}$ for leucine, *m/z* 154) (*469*) (Fig. 109).

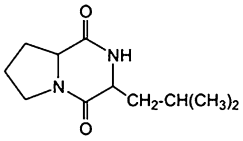

Fig. 108 Cyclo-leucine-proline (**77**)

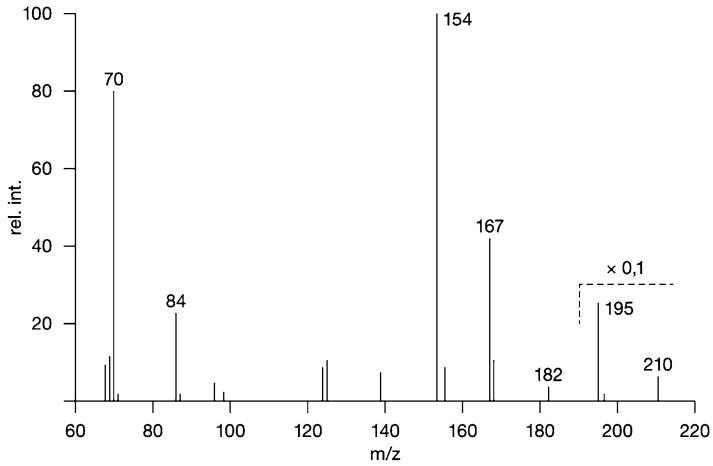

Fig. 109 EI mass spectrum of cyclo-leucine-proline (**77**)

The amino acid sequence analysis of cyclopeptides by CA by fragmentation of their (abundant) $[M+H]^+$ ions poses problems for several reasons. Unless one of the amide nitrogen atoms is protonated preferentially (such as secondary amines like proline or N-methylated amino acids) (*472–474*), ring opening by cleavage of all amide bonds occurs with comparable likelihood. Thus, a series of isomeric structures is formed that can fragment further by losses from their N- or C-terminal sites (Fig. 110), resulting in a complex fragmentation pattern. Isomeric amino acids may be distinguished by secondary cleavage processes (*475*). Finally, sequence and *retro*-sequence (-A-B-C-···-X- and -X-···-C-B-A-) have to be distinguished (*476*). The situation is easier for depsipeptides. Here, the ester bond is cleaved preferentially (*473*, *474*, *477*). Two schemes have been developed for coping with these problems (*476*, *478*) and a sequencing software tool is available (*686*), which allows also for nonribosomal building blocks so far encountered in fungal and bacterial metabolites.

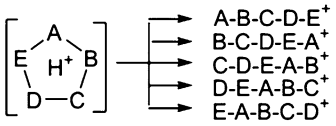

Fig. 110 Fragmentation paths of cylopeptides

A special variety of cyclic peptides are alkaloids of type **78** (Fig. 111) and related structures (*479*, *480*). In their EI mass spectra (*e.g.* Fig. 112) the main fragments are due to the loss of R and the formation of R-CH=$N^+(CH_3)_2$. Several ring fragments may allow the structure elucidation of new members of this group (*479*).

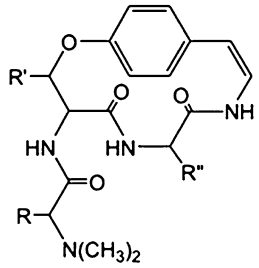

Fig. 111 Peptide alkaloids of type **78**

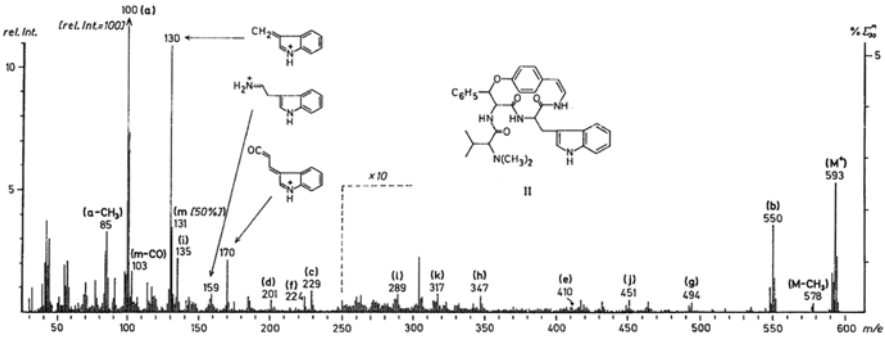

Fig. 112 EI mass spectrum of integerine (**78**, R = *i*-C_3H_7, R′ = C_6H_5, R″ = methylindolyl): $[M–R]^+$ *m/z* 550, R-CH=$N^+(CH_3)_2$ *m/z* 100. Reproduced from (*479*), Fig. 1b, with kind permission from Springer Science + Business Media (© 1968)

7.3 Proteomics

Proteomics is an umbrella term for structural investigations of proteins, their post-translational transformations, their interactions with other substances, and their structures including spatial arrangements, *etc.* This topic is discussed below wherein mass spectrometry is in some way involved.

Three approaches have been described for protein analysis, and are referred to as Bottom Up, Top Down, and Middle Down (*481*). Bottom Up implies enzymatic or chemical digestion of the protein into small peptides, their separation (*482*) and sequencing by standard methods, and subsequently putting together the structural puzzle. Top-Down (*483*) requires a strict purification of the protein, ESI or MALDI and tandem experiments with high-resolution instruments (FT-ICR). Modifications in the amino acid sequence can be recognized as demonstrated for swine cardiac troponin I,

for which some deviations from the published amino acid backbone, N-terminal acetylation and phosphorylation at Ser22/Ser23 were detected (*484*). Middle-Down analysis resorts to the protein cleavage by proteases targeting less frequent amino acids and yielding fragments with ~3,000 Da. Algorithms have been developed to combine tandem mass spectral data with database searches coping as far as possible with unusual amino acids and with post-translational modifications (*485–487*, *738*).

An alternative method to determine the amino acid sequence in proteins is the deduction from the base sequence of the corresponding gene. However, a cross check by mass spectrometry *e.g.* of peptides obtained by a tryptic digest can reveal mistakes due to the misidentification of single bases (*488*).

Sequence analysis of peptides can be assisted by comparing the original spectrum with those of compounds chemically modified as *e.g.* by esterification (indicates free carboxyl groups), H/D-exchange (identifies mobile protons (*489*)), ^{18}O-labeling (*767*), or modifications of SH-groups (*490*, *491*).

Analysis of phosphorylated proteins (*492*) is hampered by the presence of large quantities of unphosphorylated precursor proteins and by the lability of the phosphate group (*745*). When high-resolution is available phosphorus-containing ions can be recognized by the large mass defect of ^{31}P (30.9738) that separates them from the P-free ions.[25] Another possibility is the identification of phosphorylated peptides and determination of their degree of phosphorylation by coupling capillary liquid chromatography with the element specific detection by inductively coupled plasma mass spectrometry (*493*, *494*). A characteristic fragmentation reaction is the loss of H_3PO_4 (98 Da) from phosphorylated serine or threonine and of HPO_3 (80 Da) from tyrosine. Tandem mass spectrometry techniques were reviewed (*495*) discussing also the problem of phosphate migrations (see also (*496*)).

An intriguing topic is the analysis of protein complexes (*497*) as it has been shown that the structures characteristic for the condensed phases are retained essentially when going to ionized clusters in the gas phase. The first point is stoichiometry. For homo-oligomers upon CA one subunit will be eliminated, so from its mass and that of the complex the number of subunits can be calculated. Interestingly, the charge distribution between monomer and "stripped complex" does not occur according to the stoichiometry of the fragments; the monomer carries an overproportional number of charges. From hetero-complexes usually only the peripheral subunits are lost. Core-subunits can be identified from a denaturated sample. Computer programs exist to calculate the number of each subunit in the complex. An idea of the macromolecular shape of the complex may be gained from ion mobility (IM) mass spectrometry (see Sect. 2.2). The drift time is proportional to the collision cross section of an ion and its dimensions are derived from a scale calibrated with proteins with defined cross sections (*498*). Distinct conformational states can be recognized in this way as demonstrated for hepatitis B virus capsids (*499*) and in the analysis of the structural basis of protein misfolding diseases (*638*).

Mass spectrometric investigation by electrospray and ion mobility mass spectrometry (*500*) of the proteasome complex 20S of the archeon *Methanosarcina*

[25] One must keep in mind that phosphate and sulfate residues have the same nominal mass and similar negative mass increments (-PO_3H_2 … 80.974, -SO_3H … 80.965); see also (*775*).

thermophila may serve as an example demonstrating possibilities and limits of the approach and dealing also with the question as to what extent the tertiary and quaternary structure of the isolated complex in the gas phase can be correlated with those in the condensed phase.

According to an X-ray analysis, the quaternary structure of the complex resembles a staple of four tires (Fig. 113). Both the two external (α) and the two internal (β) tires consist of seven peptide chains ($\alpha_7\beta_7\beta_7\alpha_7$). An ESI spectrum (Fig. 114)

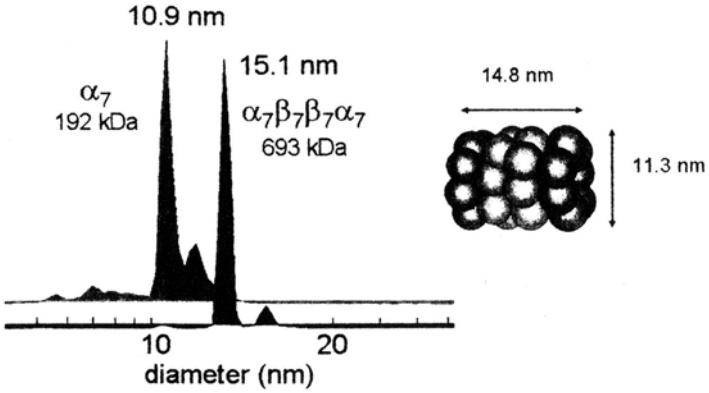

Fig. 113 ESI-IM-MS data for α_7 and for the $\alpha_7\beta_7\beta_7\alpha_7$ 20S proteasome complex of *Methanosarcina thermophila*. The right inlay gives the dimensions obtained by X-ray crystallography. Reproduced from (*500*), Fig. 7, with kind permission from Springer Science + Business Media (© 2005)

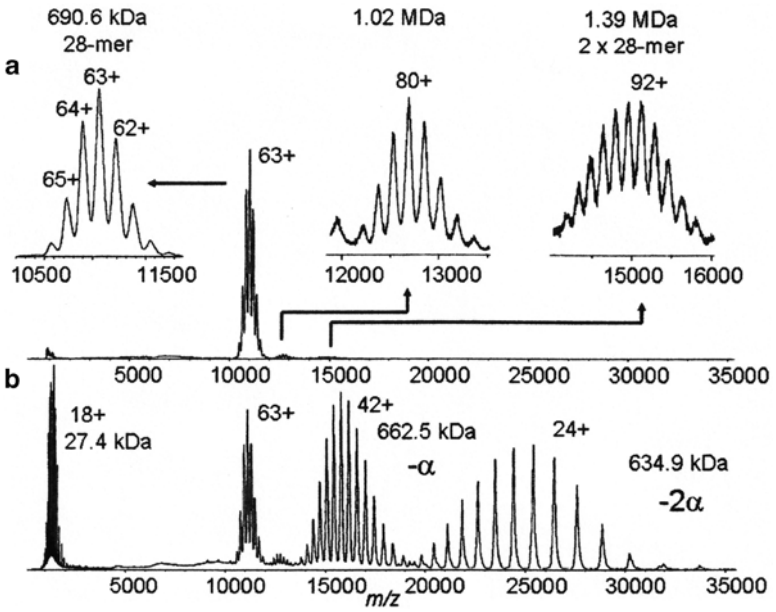

Fig. 114 (**a**) ESI-MS of the $\alpha_7\beta_7\beta_7\alpha_7$ 20S proteasome complex of *Methanosarcina thermophila*. (**b**) ESI-CA-MS. Reproduced from (*500*), Fig. 2, with kind permission from Springer Science + Business Media (© 2005)

acquired with a quadrupole TOF tandem instrument (see Sect. 2.2) shows a signal cluster at ~11,000 Da around $[M+63\ H]^{63+}$, according to a molecular mass of 690.6 kDa (theoretical value 689.3 kDa) as well as small clusters at ~15,000 and at ~12,700 Da corresponding to a dimer (1.39 MDa) and a not identified aggregate (1.02 MDa). CA of $[M+63\ H]^{63+}$ yielded one α-unit (27.4 kDa) as well as ions corresponding to the loss of one (662.5 kDa) and two α-units (634.9 kDa). Apparently, only the outer rings are degraded (the setting free of β-units is only observed from denatured material). It should be remembered that each peak in Fig. 114 is again a cluster of isotopomers, as explained in Fig. 4, Sect. 2).

Ion mobility (IM) mass spectrometric analysis (*500*) (Fig. 113) resulted in molecular masses of 192 kDa for the ring α_7 (theoretically 191.9 kDa) and 693 kDa for $\alpha_7\beta_7\beta_7\alpha_7$ as well as cross section values for α_7 and for the complex. They agree well with the X-ray data in the condensed phase. The smaller signals at higher values in Fig. 113 stem from singly charged dimers.

The results show that ESI data can be obtained from multiply protonated ions of molecular aggregates in the MDa region. There are obviously limitations in the accuracy of mass determinations. A mass deviation of ±0.1 kDa between measured and calculated mass values corresponds to about one amino acid increment (-NH-CHR-CO-). The observation that upon CA only elements from the outer rings are lost and the calculated dimensions suggest that the quaternary structures were not disturbed drastically during ionization and the transition to the gas phase. However, amino acid sequence analyses are not possible any more in this mass region.

Besides the IM-MS analysis there are other mass spectrometric techniques (*501*) giving information on conformations and conformational changes:

- It is well known that the accumulation of multiple charges in ESI depends on the structure of the substrate. Tightly folded protein molecules can accommodate fewer charges than the less structured ones, but there are exceptions (*502*). Thus, cytochrome c in its compact native state in an aqueous solution at *p*H 6.4 forms mainly $[M+8\ H]^{8+}$, while at *p*H 2.3 it is completely unfolded giving a cluster of ions centered at $[M+17\ H]^{17+}$. At intermediate *p*H values the transition can be followed (*503*). Increasing the number of charges and thus causing partial unfolding can be achieved by adding a small amount of *m*-nitrobenzyl alcohol ("supercharging reagent") to the solution. The effect can be followed by IM (*504*, *768*).
- There are differences in H/D exchange rates between freely accessible amide groups, with those shielded by hydrogen bonds or hidden in the center of a rigid structure requiring a (partial) unfolding for exchange (*505*). Kinetic studies can be performed by quenching at 0 °C or by dropping the p*H* to ~2.5 (*506*) after different periods of time. A localization of the labels is possible by degradation, *e.g.* with pepsin, and analysis of the fragments (*507*, *508*). Problems of the exchange technique (sample preparation, factors influencing

the reproducibility of the results, identification of single amino acids, *etc.*) were discussed (*509*).

- Radical reactions ($OH^{\cdot}$) (*510*), also with subsequent deuterium incorporation (*511*) allow the identification of solvent-accessible parts of the molecule.
- From the interaction of a reagent with specific sites of a protein structural conclusions are possible. Thus, 18-crown-6 binds noncovalently to lysine residues. A lack of binding can come from inaccessibility for steric reasons or from nonavailability due to hydrogen bonding or due to salt bridges (*512*).
- Intra- and intermolecular distances in tertiary and quaternary structures of proteins can be determined by cross-linking reactions between active sites ($-NH_2$, -SH, -COOH) with reagents of varying length. Localization of the linked sites can then be determined by the Bottom-Up or the Top-Down approach (*513*, *514*). A recent approach consists of using linkers that can be degraded by CA. In this way, the originally linked amino acids are obtained in a derivatized form and can thus be identified (*515*, *516*, *636*, *637*). Degradation mechanisms have been studied in detail (*517*, *637*). An example is depicted in Fig. 115. Upon CA, the linker loses N_2 and the derivatized amino groups retain the cyanopentanoyl radical residues. Further CA allows the standard sequence determination.
- For more complex approaches, see (*518*, *519*).

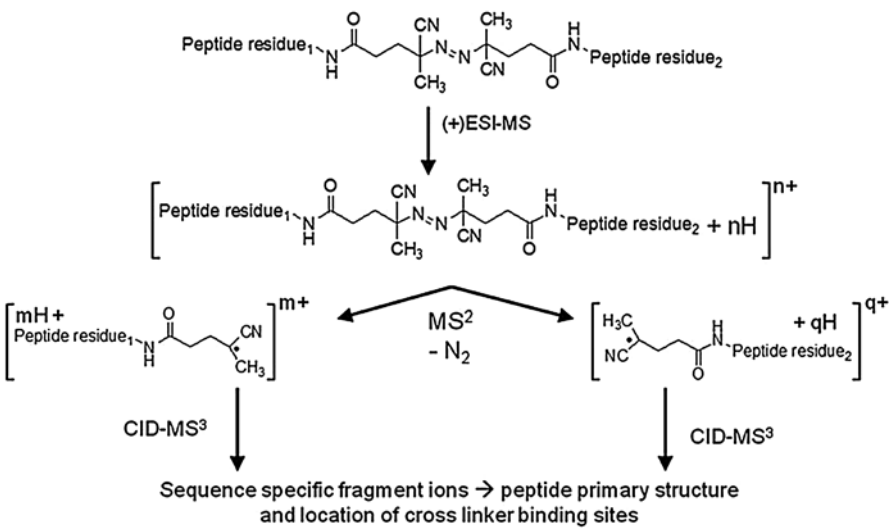

Fig. 115 Ionization and CA degradation of cross-linked peptides (depicted is *inter* molecular linking; in the case of *intra* molecular linking the two peptide residues are connected). The number of charges, n, is distributed between the two fragments (n = m + q). With kind permission of Dr. M. Schäfer, Köln

A developing technique is the ESI-MS analysis of *in vitro* non-covalent associations of proteins with other molecules (carbohydrates, lipids, DNA, *etc.*). Within limits it allows the determination of the stoichiometry of the associate, its dependence on various parameters, the analysis of competitive interactions, and the calculation of the association constants K_a. However, there are sources of error mainly based on changes in concentration, p*H*, and temperature caused by the transition from the solution to the droplet and finally to the ion in the gas phase (*520*). A recent example is the analysis of the interaction of an antitoxin, a 291 amino acid glycoprotein from an immune animal (opossum) with a snake venom metalloproteinase (*521*) dealing *inter alia* with problems of stoichiometry and transition from the liquid to the gas phase.

Another step forward offers MALDI imaging mass spectrometry (*522*), which allows an analysis of thin tissue sections by determining in single measurements the distribution of a large number of compounds present in specific areas of the object. The tissue sample is sprayed with matrix material and the pulsed laser beam is applied locally, migrating along an x- and/or y-axis. The pixel size is determined by the diameter of the laser beam. Series of molecular ions are obtained with each shot. Thus *e.g.* protein profiles may be gained in cancer diagnosis (*523*). Instead of laser impact particle bombardment ionization may be used. Advantages and disadvantages of the methods (resolution, mass range, possible decompositions) have been discussed (*524*).

Limitations and pitfalls in protein identification in view of sample preparation, mass spectrometric techniques, data processing, databases, and problems inherent in the protein structure have been considered (*485*). *Esther van Duijn* (*525*) slipped into the role of an *advocata diaboli* pointing out some cases where question marks are appropriate (and stating a reluctance of authors to report negative experiences). To these belong:

- Disagreements of results: ultracentrifugation of chlorite dismutase of *Azospira oryzae* suggested a tetrameric assembly, X-ray crystallography a hexameric and mass spectrometry a pentameric one;
- Inhomogeneity of sample material with components that differ only slightly in mass resulting in overlapping signals such as human hepatitis B virus capsids, which incorporate varying RNA pieces;
- Carrying off of a major portion of charges in CA dissociation of a protein complex by the first departing subunit, leaving the stripped complex with too few charges for further dissociation;
- Problems in the calibration of the scale of protein complex cross sections for IM-MS due to the lack of standard material.

The corollary is that mass spectrometry has become an indispensable tool in proteomics, but—to use a term from business life—*caveat emptor.*

8 Nucleosides, Nucleotides, and Nucleic Acids

As for proteins and their elements (see the preceding Sect. 7), mass spectrometry plays an important role for structural work in the nucleic acid field. The techniques for sample preparation and for the various ionization modes have been reviewed in detail (*526*–*532*, *757*).

8.1 Nucleobases, Mono-Nucleosides, and Mono-Nucleotides

The nucleobases fragment under electron ionization (EI) by elimination of parts of the rings (CO, NHCO, NH_3, *etc.*). Such investigations started with the publications by *Rice* and by *Dudek* (*533*, *534*), and many others (*e.g., 221*, *222* above) including related compounds followed. Detailed discussions of the fragmentation sequences and literature lists can be found in (*235*, *236*). *Biemann* and *McCloskey* (*537*) pioneered the investigation of ribonucleosides. The main fragments are the free and the protonated nucleobase ($[\mathbf{B}+H]^{+\cdot}$ and $[\mathbf{B}+2H]^{+}$), as well as **B** with parts of the ribose (+30, + 44 Da) (Fig. 116). The sugar part **S** is observed occasionally. Again, detailed discussions and lists of compounds investigated as well as investigations on more volatile derivatives (TMS, acetyl, trifluoroacetyl, isopropylidene) have been composed, and references of pertinent literature are available (*535*, *536*). For structural work, permethyl derivatives (preferentially CD_3 to distinguish between native and introduced methyl groups) are preferable; base and sugar fragments can easily be identified (*538*) (Fig. 116).

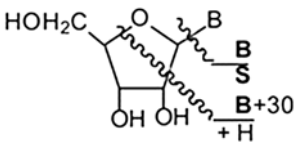

Fig. 116 Fragmentation of ribonucleosides under EI

Chemical ionization (CI) with CH_4 as reagent gas yields abundant $[M+H]^+$ ions and as above $[\mathbf{B}+H]^{+\cdot}$, $[\mathbf{B}+2H]^+$, $[\mathbf{B}+30]^+$, and $\mathbf{S}^+$ fragments (*539*), field desorption (FD) produces $[\mathbf{B}+H]^{+\cdot}$, $[\mathbf{B}+2H]^+$, and $\mathbf{S}^+$ ions (*540*). Analogous results were obtained with positive fast atom bombardment (FAB), while negative FAB yields $[M-H]^-$ and $\mathbf{B}^-$ (*541*). FD and FAB spectra of nucleoside antibiotics have been reported (*542*). A review on structure elucidation of modified nucleosides can be found in (*543*) (Fig. 116).

Free mono-nucleotides are too involatile for EI or CI investigations (*544*). Trimethylsilylated (*545*) and methylated (*546*) derivatives have proved to be

amenable to EI analysis. $[\mathbf{B}+2H]^+$ ions can be seen, but the spectra are dominated by ions derived from the sugar part and from phosphoric acid. 3′- and 5′-Monophospates can be distinguished by abundance differences of the $[M–base]^+$ ions of their TMS derivatives (*547*). FD spectra of free nucleotides were recorded (*540*, *548*). At low emitter temperatures $[M+H]^+$ is observed. With increasing emitter heating, $[\mathbf{B}+H]^{+\cdot}$ and its decomposition products, **S** fragments, and $H_4PO_4^+$ prevail. Metastable fragmentation of deprotonated nucleotides yields mainly ions stemming from the sugar part and from phosphoric acid (*549*).

8.2 Di- and Oligo-Nucleotides

The EI mass spectra of trimetylsilylated di-nucleotides allow one to determine the nature of the nucleobases present, but isomers such as ApU and UpA differ only in the relative abundances of pairs of ions (*550*). Field desorption spectra of di-ribonucleoside phosphates show $[M+H]^+$ and abundant $[\mathbf{B}+2H]^+$ ions (*551*). CA spectra exhibit intensity differences of several fragments obtained from isomeric pairs such as ApC and CpA (*552*. Methylation products of ApU and UpA were studied by FD (*553*).

Negative FAB mass spectrometry allows the sequencing of oligodesoxyribonucleotides up to ten base units. The ion of highest mass is $[M–H]^-$. Two series of fragment ions are observed: cleavages of the phosphate-5′-desoxyribose bonds (ions **z** in Fig. 117) establish the sequence starting from the 3′-end, while cleavages of the phosphate-3′-desoxyribose bonds (ions **w**) give the reversed sequence of ions starting from the 5′-end of the molecule, see Fig. 118 (*554*, *555*). Negative FAB combined with CA eliminates interferences with matrix ions, but pronounced competing fragmentation reactions such as the loss of bases interfere with the recognition of sequence specific ions (*556*).

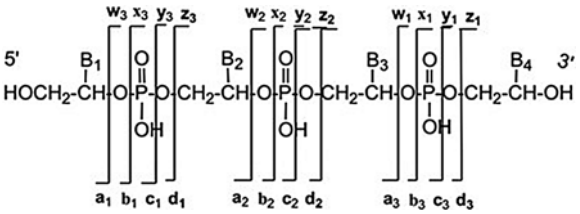

Fig. 117 Nomenclature proposal for fragment ions of oligonucleotides (after (*557*))

The current ionization method for structural studies is electrospray (ESI) combined either with a quadrupole or an ICR analyzer (*557*). The advantage of the latter is the possibility of exact mass measurements, which for the molecular ions

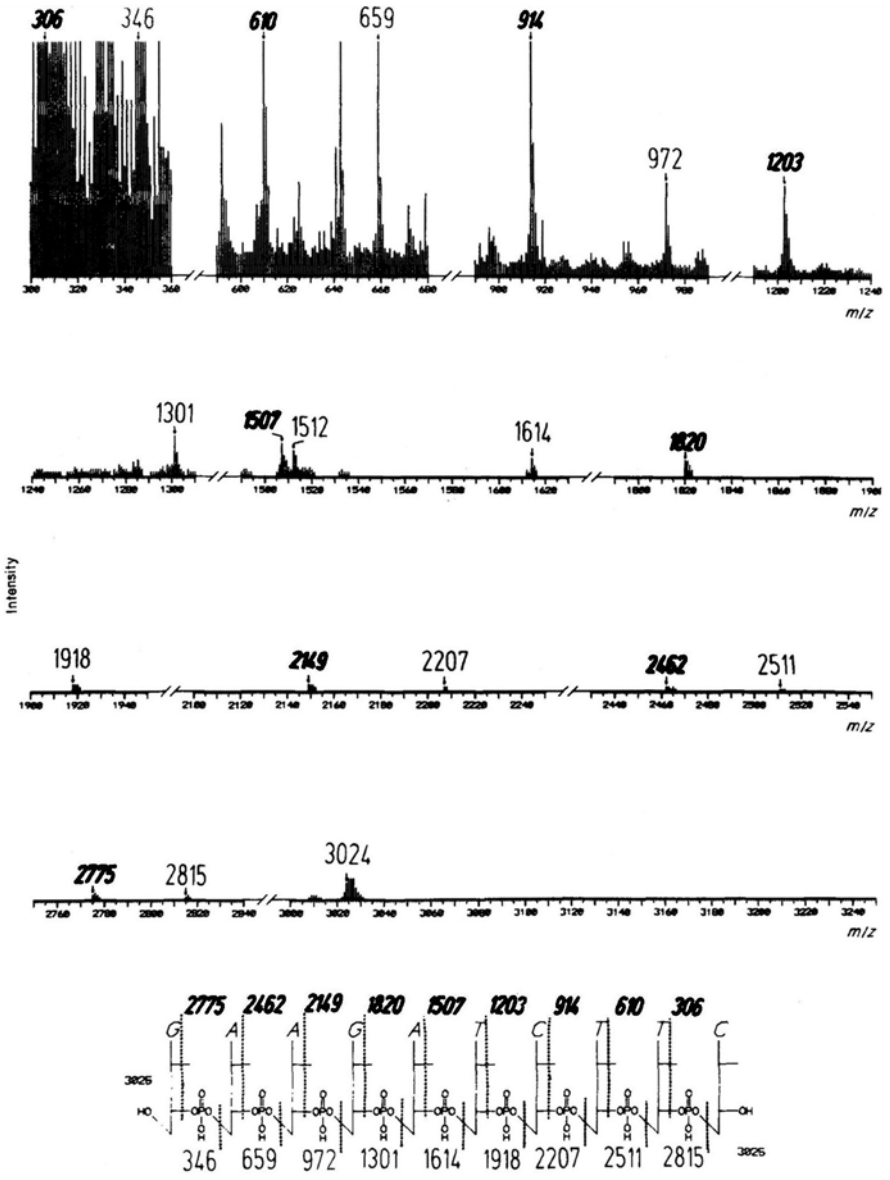

Fig. 118 Negative FAB mass spectrum (sequence relevant regions) of d(GAAGATCTTC). Reproduced from (*555*) with kind permission of John Wiley & Sons Ltd. (© 1985)

allow the determination of a unique combination of base units present or at least of a limited number of combinations. It also allows the unambiguous identification of fragment ions, especially to differentiate between U and C + H containing species (U and C differ in mass only by 1 Da). The main sequence-determining fragments are **w** and (**a**–base) ions (Fig. 119) (*558*); see the Addendum.

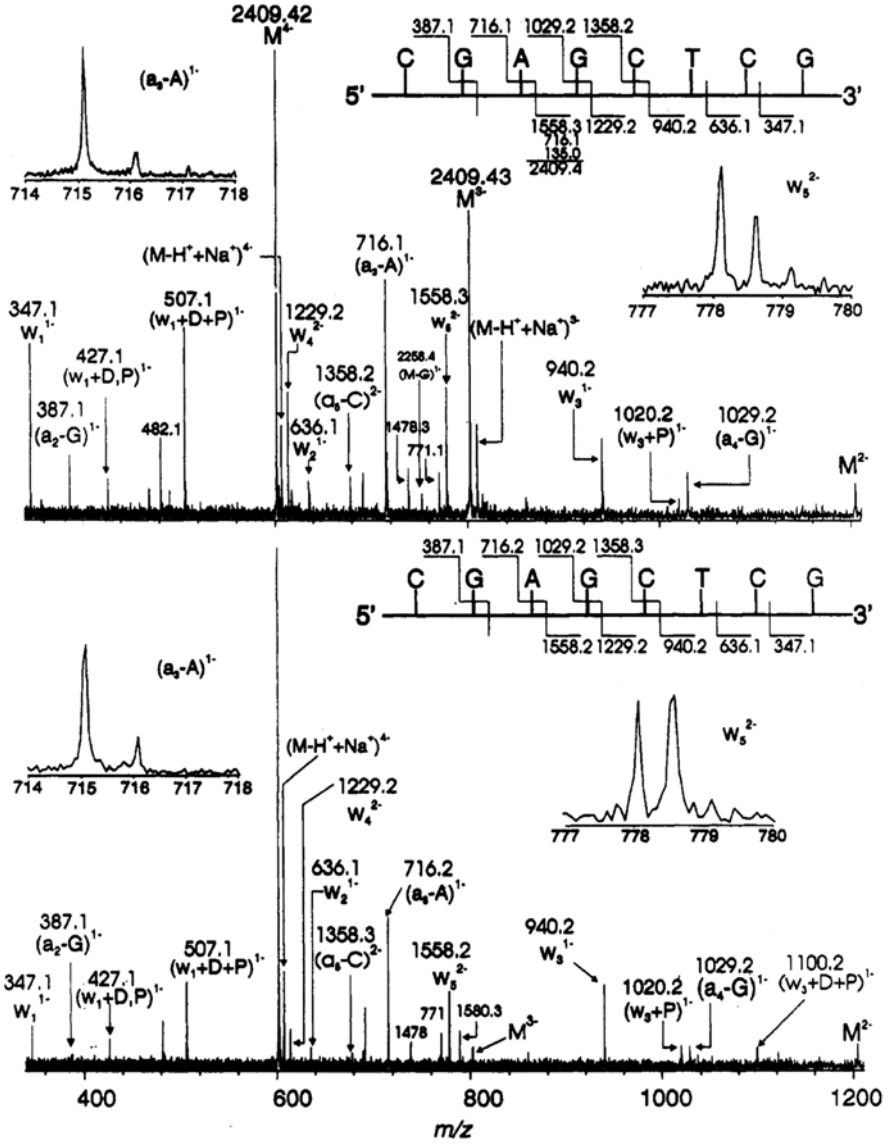

Fig. 119 ESI-ICR spectrum from 5′-(CGAGCTCG)-3′. Adapted from (*558*) with kind permission of the American Chemical Society (© 1994)

8.3 Polynucleotides, DNA, and RNA

For a review on the role of mass spectrometry in the post-genomics age, see (*559*).

The ionization methods mainly used today in nucleomics are ESI and MALDI. In a detailed review (*560*), the main aspects and problems are discussed. Typically, $[M-nH]^{n-}$ or $[M+nH]^{n+}$ as well as $[M+nNa/K]^{n+}$ ions are formed, for ESI preferably with higher charge states (for supercharging see (*729*) cf. Sect. 7.3) and for MALDI typically singly charged ions. The appearance of the mass spectra is improved when the ubiquitous alkali ions are replaced by NH_4^+. Additives to the ESI spray solutions and proper selection of the MALDI matrix and laser wavelength have been surveyed. The fragmentation mechanisms are reported and the two methods are compared and their respective limitations are described (ESI allows the access to higher mass ranges, but there are difficulties in handling complex mixtures; the sensitivity towards salt admixtures is lower for MALDI, which in turn has problems with the stability of large ions). A mass error of <0.01% is stated for the analysis of oligonucleotides and larger nucleic acids if ESI is coupled with a quadrupole analyzer, and ~0.001% for coupling with ICR (*560*). Occasionally, better results are reported (1 ppm) (*561*). In the latter publication also the problem is addressed of correctly identifying the isotopic composition of the most abundant peak in the observed cluster.

Mass spectrometry seems not to play the same role in nucleomics as it does in proteomics. The first attempts to gain information using mass spectrometry were made with pyrolysis EI of RNA and DNA samples that allowed at least recognition of the bases present (*562*, *563*). The next step was the determination of exact molecular masses (error less than 0.01%) obtained by averaging calculations from the experimental values of a series of multiply charged ions (*564*).

Much effort has been put into indirect methods of sequencing that imply degradation of DNA or RNA, separation and mass spectrometric analysis of the fragments—techniques that are comparable with the Bottom Up approaches used for the analysis of proteins (*528*, *530*). Among the degradation methods besides acid or base cleavages, are the use of base-specific endonucleases (*565*), and of non-specific endonucleases generating di- to octa-deoxynucleotides (*566*), and of exonucleases (*567*). Also a combination of mass spectrometric base sequencing in combination with *Sanger* (*568*) degradation (*569*) or reversed *Sanger* degradation (*570*) has been attempted. There are advantages compared with the standard gel electrophoresis approach (speed, avoiding hazardous chemicals), but there is also a number of problems in an automatized routine application (*560*). In relation to genome projects mass spectrometry seems to play no major role (*571*, *572*).

Attempts were made to use mass spectral techniques to obtain information on 3D structures (*573*). One recent example is the reaction with spacers to establish distances between specific domains of the HIV-1 ψ-RNA (*574*).

A field of lively research is the investigation of the molecular details of genetic aberrations subsumed under the term “epigenetics” (*578*). So far 144 modifications of nucleobases in RNA have been recorded (*618*). Mass spectrometry can be applied both on the protein (*579*) and on the DNA/RNA side, so as to demonstrate and quantify variations in the methylation of CpG units (*580*), especially in cancer

research. The combination of a quadrupole with an ICR analyzer allows the Top-Down analysis of modified RNA, taking advantage of the need for minimal amounts of material, fragmentation by CA, and ultra-high resolution, possibly in combination with ancillary techniques like obtaining ^{13}C or ^{15}N labeled RNA from cultures grown with respective substrates. In this way modified nucleobases can be identified and located in the base sequence (*619*).

8.4 Interaction with Other Compounds

Nucleotides can interact with many compounds and in many different ways. One group comprises the covalent binding to O- or N-functions (*654*), especially N-7 of guanine, such as *e.g.* with aflatoxin B_1 (*575*). One of the major analytical problems is the low concentration of modified material together with large quantities of native material. Refined separation techniques are necessary (*576*). To cope with the enormous amount of mass spectral data, computer programs have been developed (*577*).

Degradation to the level of the modified base or nucleoside allows recognition of the nature of the modification, but does not give any structural information. Enzymatic degradation leads to oligonucleotide fragments where the modified base can be located (*566*). Under favorable circumstances, very simple mass spectra may be obtained, see Fig. 120 (*581*).

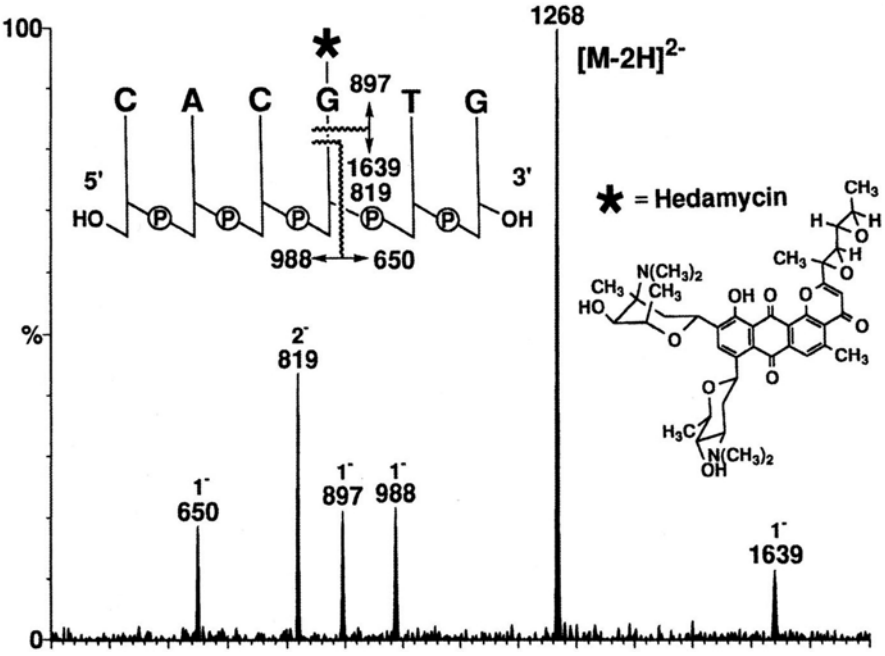

Fig. 120 ESI-MS/MS spectrum of a hexanucleotide containing hedamycin bound to G; the charge state of the ions (1^- or 2^-) is indicated. Adapted from (*581*) with kind permission of the American Chemical Society (© 1997)

More complicated is the analysis of non-covalently bound compounds. This type of binding can occur by electrostatic interaction (cationic ligands with the polyanionic backbone), intercalation of planar ring systems, and hydrogen bonds to nucleobases, or a combination of modes. Model studies with oligonucleotidic assemblies have been reviewed (*582*).

A special structural type are the DNA G-quadruplexes. Nucleic acids containing series of adjacent guanine residues can form square G-quartets, which can be stacked to tower-like structures. Small cations as well as organic ligands can be bound. Mass spectrometry plays an important role in structural studies, stoichiometry, stability, and ligand exchange kinetics (*616*). However, as for protein complexes (see above), it may be asked whether the solution-phase structure is retained during the transition into the mass spectrometer (*617*).

For analysis of metal complexes high-resolution mass spectrometry is advantageous in coping with the complicated isotope patterns of many metals, especially if several metal atoms are present. Metal ions can interact electrostatically with the phosphate residues, but they can also be bound covalently to the N-7 atoms of the purine bases as, *e.g.,* platinum. Thus, cisplatin (**79**, Fig. 121) reacts with the two guanines of 5′-CACGTG-3′ (**80**). The positive CA spectrum of $[^{195}Pt(NH_3)_2 + \mathbf{80} - H]^+$ (*m/z* 2019) allows one to recognize $[\mathbf{w}_3 - NH_3]^+$ (*m/z* 1191) containing the two guanines and Pt, $[\mathbf{w}_2 - NH_3]^+$ (*m/z* 1191) and $[Pt + 2G + NH_3]^+$ (*m/z* 513) (Fig. 122). Further information may be obtained from CA of the ion *m/z* 1191 (*583*). A comparative study of various activation/dissociation techniques (collision activation, CA; UV photodissociation, UVPD; IR multiphoton dissociation, IRMPD; electron transfer dissociation, ETD) performed with oligonucleotide cisplatin adducts showed that the best structural results were obtained with photodissociation (UV or IR) (*635*).

Binding experiments of the anticancer drug BBR3464 (**81**, Fig. 121) containing three *trans*-configured Pt centers, with single and double stranded DNA and RNA pieces containing 20 bases, showed that the drug could react with one or with both Cl atoms, as evidenced by ESI-FTIR mass spectrometry. CA gave no further structural

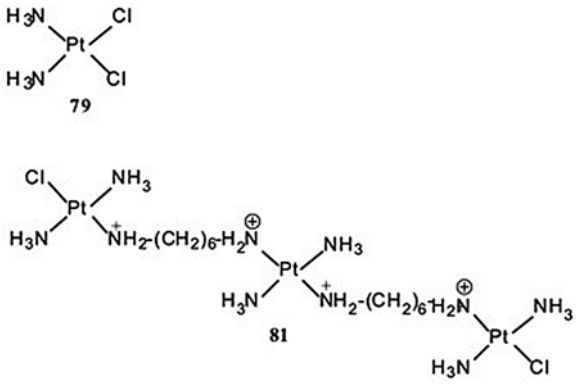

Fig. 121 Cisplatin (**79**) and BBR3464 (**81**)

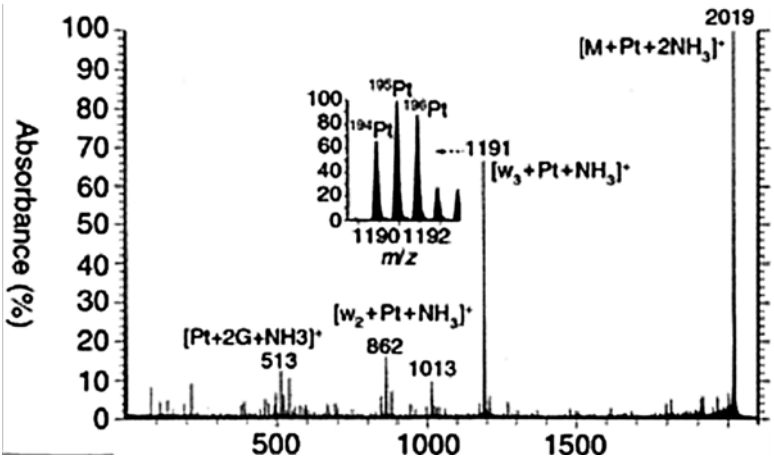

Fig. 122 Positive ESI-CA spectrum of the cisplatin complex of **80**. Reproduced from (*583*) with kind permission of the Royal Society of Chemistry (© 2000)

information (*584*). A detailed study deals with the ESI tandem MS analysis of the interaction of the duplex hexamer d(5′GCATGC) with metal dications bound to several antibiotics. The intention was to provide "a basis for the assessment of the possible binding modes between duplex oligonucleotides and metallocomplexes" (*585*).

Non-covalent protein/DNA or RNA conjugates play an important role in many cellular processes. Some of these are only fleeting intermediates. Mass spectrometric analysis especially with ESI has been employed to answer some questions. A major problem is the sample preparation because stabilization of the complex and requirements of ESI are not easy to be reconciled, as there are buffers, salt concentration, *p*H, temperature, *etc.* Experiments with essential fragments of either component, investigations with native material and subsequent degradation, studies with spacers linking the two components have been performed. To determine for the latter the connection *loci* sequencing is possible, taking into account that for the nucleotide and for the peptide part different techniques are necessary (*586*). On the whole, the matter is too complex for a detailed coverage here; two review articles should be consulted for further information (*582*, *587*).

9 Mass Spectra Collections

A systematic collecting of EI mass spectra started with the API catalog (*10*). The contributors had realized that the appearance of an EI mass spectrum depended to some extent on experimental parameters, and API spectra were determined under strictly standardized conditions with an accuracy never reached since. Recent collections such as the Wiley Registry™ draw their material from many sources and the quality of the spectra varies drastically. The main sources of the shortcomings are impure samples and incompletely separated mixtures, wrong structures, and mistakes in the evaluation of analog-recorded spectra.

The majority of collections comprise EI spectra, sometimes together with chromatographic data such as *Kovats* indices, or with other spectral data as in the NIST collection (*220*). Those for other ionization techniques are mainly dedicated to limited substance classes. Search algorithms have been developed, for EI spectra *e.g.* (*592*, *593*); some for special areas are mentioned in the preceding sections.

9.1 General

Golm Metabolome Data Base provides GC-MS data of plant metabolites (*589*).

Human Metabolome Data Base contains LC- and GC-MS data of endogenous metabolites (*591*).

MassBank collects mass spectra (EI, FAB, ESI-MS^2 *etc.* of compounds with masses <3,000 Da from life sciences. A detailed description can be found in (*588*).

NIST/EPA/NIH Mass Spectral Library (NIST11) contains EI spectra of over 200,000 compounds measured specifically for the library.

Wiley Registry™ 10th Edition/NIST 2012 Mass Spectral Library (2011). Wiley: Hoboken, NJ, USA. Offers spectra of over 700,000 compounds.

Yarkov A (2004) Mass Spectra of Organic Compounds (SpecData). Wiley: Hoboken, NJ, USA. Offers spectra of almost 40,000 compounds.

9.2 Alkaloids

Hesse M (1974) Indolalkaloide, Teil 2: Spektren. In: Budzikiewicz H (ed) Progress in Mass Spectrometry, vol 1. Verlag Chemie: Weinheim, Germany. This volume contains spectra of 241 indole alkaloids. See also (*113*, *114*).

9.3 Drugs, Poisons, Pesticides, and Pollutants

Kühnle R (2006) Mass Spectra of Pharmaceuticals and Agrochemicals, Wiley-VCH: Weinheim, Germany. The collection includes 4,563 mass spectra.

Kühnle R (2009) Mass Spectra of Pesticides, Wiley-VCH: Weinheim, Germany. The collection includes 1,238 mass spectra.

Maurer HH, Pfleger K, Weber AA (2011) Mass Spectral and GC Data of Drugs, Poisons, Pesticides, Pollutants and Their Metabolites, 4th Ed, 1,624 pages, Wiley-VCH: Weinheim, Germany. The collection comprises almost 9,000 data sets from potentially harmful substances.

Oberacher H (2012) Wiley Registry of Tandem Mass Spectral Data, MS for ID. This high mass-accuracy LC-MSMS library contains 10,000 positive and negative mode spectra of over 1,200 compounds of interest for forensics, toxicology, and pathology (illicit drugs, pharmaceutical compounds, pesticides, and small bioorganic molecules) (*642*).

Parr MK, Opfermann G, Schänzer W, Makin HLJ (2011) Mass Spectra of Physiologically Active Substances: Including Drugs, Steroid Hormones, and Endocrine Disruptors. Wiley-VCH: Weinheim, Germany. This contains over 4,000 mass spectra and chemical structures.

Rösner P (2013) Mass Spectra of Designer Drugs, Wiley-VCH: Weinheim, Germany. This contains over 19,000 mass spectra of over 19,000 substances, mainly EI but also other types of spectra. Data on warfare agents were added in the 2010 edition.

9.4 Flavors and Fragrances

Mondello L (2011) FFNSC 2.0 Flavors and Fragrances of Natural and Synthetic Compounds—Mass Spectral Data Base. Wiley: Hoboken, NJ, USA. The collection contains 3000 mass specra.

9.5 Geo- and Petrochemicals

De Leew JW (2003) Mass Spectra of Geochemicals, Petrochemicals and Biomarkers. Wiley-VCH: Weinheim, Germany. Contains 1100 mass spectra.

9.6 Lipids

For prostaglandins and related compounds, see (*590*).

9.7 Steroids

Makin HLJ, Nolan J, Trafford DJH (1998) Mass Spectra and GC Data of Steroids: Androgens and Estrogens. Wiley-VCH, Weinheim, Germany.

Makin HLJ (2008) Mass Spectra of Androgens, Estrogens and other Steroids. Wiley-VCH: Weinheim, Germany. This contains 3722 mass spectra.

9.8 Terpenes

Adams RP (2007) Identification of Essential Oil Components by Gas Chromatography/Mass Spectrometry, 4th edn. Allured Publishing Corporation, Carol Stream, IL, USA.

Gaskin P, MacMillan J (1991) GC/MS of Gibberellins and Related Compounds: Methodology and a Library of Spectra. Cantock's Enterprises, Bristol, UK.

10 Addendum

To Sect. 3.2.4 D9(11)-Triterpenes

The ion $[M-167]^+$ of high abundance (*cf. m/z* 243, ion **b** in Figs. 23 and 25) claimed to be characteristic for $\Delta^{9(11)}$-*friedo* systems (*728*) unsubstituted in rings C/D/E (*726*) are also observed for $\Delta^{7,8}$- (*94, 712*) and $\Delta^{8,9}$-compounds (*727*). Analogous loss ($[M-225]^+$) from 29-acetoxy compounds ($\Delta^{8,9}$ and $\Delta^{9(11)}$) is of low abundance (*75*).

To Sect. 4.1.1.1 Biogenic Amines

The toxic constituents of the skin of the Chinese giant toad *Bufo bufo gargarizans*, used in Chinese traditional medicine, have been investigated in detail (for a review of the compounds isolated from the skin of the toad, see (*609*)). In addition to serotonin and its known derivatives (*603*, *610*) an *N*,*N*-dimethyl-*N*-*oxide*[26] (**22**- *N*-oxide) was found (*610*). Further previously unincountered derivatives of serotonin are bufobutanoic acid,[27] *i.e.* the *N*-succinamide of **22**, bufopyramide **85** (*613*), and the bufoserotonins A-C (*640*), serotonin with a terminal urea unit, the *N*-suberamide and a compound where the amino group is incorporated in a 2-acetyl-4-acetamido pyrrole ring. In addition, a compound derived from tyrosamine (**82**) is reported (*608*), as well as derivatives of a strange amino acid, the latter suggesting a combination of serine or alanine with 4-hydroxyornithine (Fig. 123). These compounds were named bufogargarizanine B (**83**, R=CH_2OH), C (**84**) (*606*) and D (**83**, R=CH_3) (*607*).[28,29] From these compounds only FAB and/or ESI mass spectral data are given. In addition, imidazole, purine, and pyrazolopyridazine derivatives were found (*777*). From the skin secretion of the African frog *Phrynomantis microps*, which protects against aggressive ants, two peptides comprising nine and eleven amino acids, respectively could be isolated as the main components. Their structures were established by LC-ESI-CID tandem mass spectrometry and confirmed by synthesis (*743*).

To Sect. 4.3.3 Ichthyotoxins

The term "ichthyotoxin" is ambiguous. It comprises compounds toxic to fish as well as those obtained from venomous fishes, the latter acquired either by food as *e.g.* from dinoflagellates or genuine, peptidic poisons such as the pardaxins (*623*),

[26] Reference is given to (*611*). There are among other data major ions of an EI mass spectrum reported. The ion referred to as $M^{+\cdot}$ (*m/z* 204) is 16 Da too low and the fragment ions correspond to those obtained from **22** (see Fig. 33). This would mean that the true $M^{+\cdot}$ (*m/z* 220) is missing completely and only $[M-O]^{+\cdot}$ is obtained, an unlikely proposition (generally not observed for *N*-oxides; even the EI mass spectrum of $(CH_3)_3NO$ yields $M^{+\cdot}$ (*m/z* 75) with 100% and $[M-O]^{+\cdot}$ with 50% relative intensity. It seems more likely that the mass spectrum of **22** had been obtained.

[27] For total syntheses, see (*614*).

[28] In the Master's thesis of *Li-Ping Dai* (*612*) bufogargarizanine D is designated as bufogargarizanine A. In addition to NMR data the ESI mass spectra of all three bufogargarizanines are reproduced, but they show besides $[M+H]^+$ or $[M-H]^-$ signals of low to medium abundance a large number of peaks not belonging to the compounds in question.

[29] Bufogargarizanines should not be confused with bufogargarizins, which are 19-*nor*-bufadienolides from the same animal (*652*).

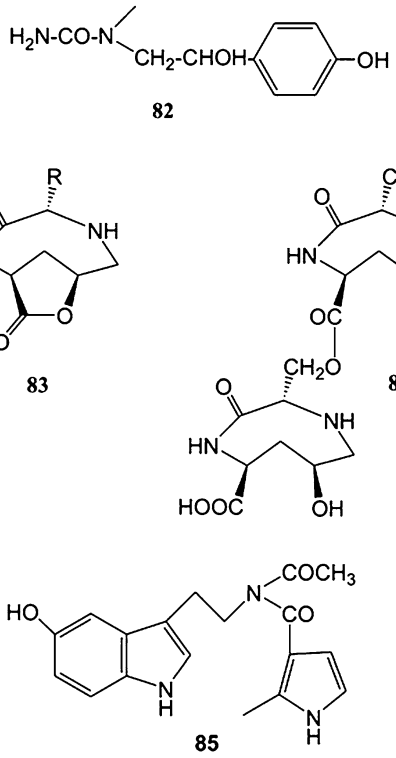

Fig. 123 Compounds obtained from the skin of *Bufo bufo gargarizans*

steroids such as the mosesins (*624*), and a few others that due to having a nitrogen atom can be mentioned in this contribution.

To these belong the *pavoninins* related to the *mosesins* above from the sole *Pardachirus pavoninus* (*625*, *626*), cholesterol derivatives with an *O*-acetyl group at C-26 and an *N*-acetylglucosamine residue at C-7 or C-15. SIMS- and FD mass spectrometry was used to determine the molecular masses and show losses of the sugar residue and of ketene from the acetate unit. EI data document analogous losses.

From the smooth trunkfish *Lactophrys triqueter* the palmitic acid ester of choline (**86**) was obtained accompanied by a small amount of the margarinic (C_{17}) acid ester. The structure of **86** was established by identification of the hydrolysis products and by synthesis. CI mass spectrometry with NH_3 yielded $[M–Cl]^+$, CI with CH_4 the characteristic fragments of palmitic acid (see Sect. 5.1) (*627*). From the Hawaiian boxfish *Ostracion lentiginosus* stems was obtained a related compound named pahutoxin, the choline ester of (*S*)-3-acetoxy-hexadecanoic (palmitic) acid (**87**) (*628*, *629*).

$$(S)\text{-}C_{13}H_{27}\text{-}CHR\text{-}CH_2\text{-}COO\text{-}CH_2\text{-}CH_2\text{-}N^+(CH_3)_3\ Cl^-$$
86: R = H, **87**: R = CH_3COO

From the mucus of the soapfish *Diploprion bifsciatum* the 18-membered polyamine lactam (**88**), lipogrammistin-A, could be isolated. Its absolute stereochemistry was established by total synthesis (*630*, *631*) (configurations (*S*) at each of the three chiral centers). The EI mass spectrum of **88** shows $M^{+\cdot}$ (*m/z* 590), loss of $C_4H_9^{\cdot}$

and of $C_4H_9CO^{\cdot}$ (*m/z* 533 and 505), and as the main fragment the ion *m/z* 437 (α-cleavage of the $C_{11}H_{21}$ chain). EI mass spectral data of the synthetic intermediates are also reported (*631*).

From the roe of the northern blenny *Stichaeus grigorjewi* a mixed adenosine-containing phospholipid named *dinogunnelin* was obtained. Based on degradation (adenine, ribose, aspartic acid, NH_3, saturated and unsaturated fatty acids, glycerophosphoric acid) studies and rather crude IR and NMR spectra in 1976 the structure **89** was suggested (*632*, *633*). It took another 33 years until a modified structure **90** based on FAB mass spectrometry and modern NMR techniques could be presented (*634*). The data having led to **89** can be reconciled with **90** with the exception of the fatty acid composition (mainly $C_{16,}$ C_{18}, C_{20} saturated and mono-unsaturated *vs.* C_{18} and C_{20} highly unsaturated) and especially of glycerophosphoric acid. The crude extract of the eggs should be investigated in more detail (Fig. 124).

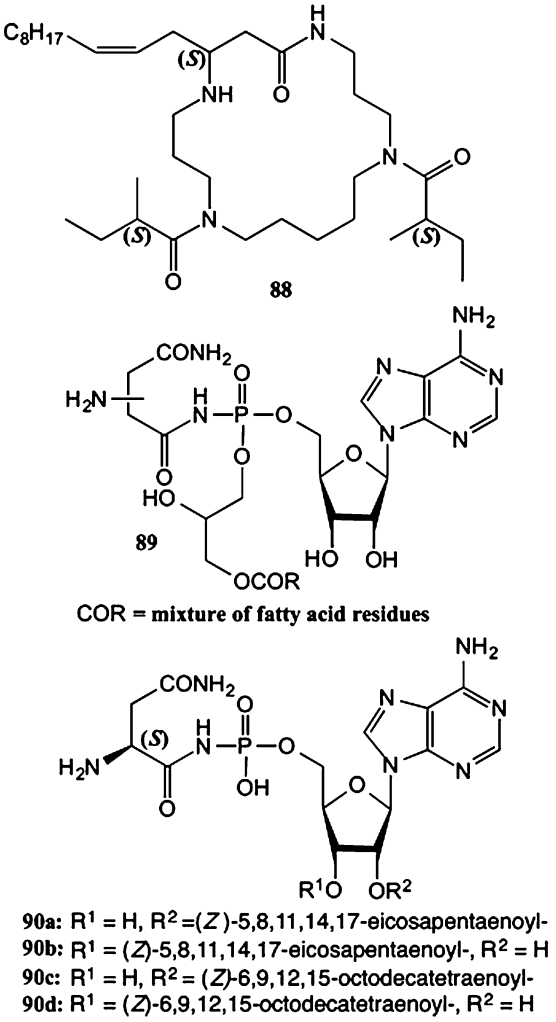

Fig. 124 Ichthyotoxins **90a** - **90d**

Painful encounters (*770*) with the toxic spines of the weever fish (*Trachinus*, "Petermännchen" in German) are reported each summer especially from the European coasts. Active substances in the poison of *Trachinus vipera* are serotonin and a histamine-releasing protein (*771*, *772*), in that of *Trachinus draco* histamine, epinephrine, norepinephrine (*773*), and a protein (dracotoxin, molecular mass about 105 kDa) with hemolytic activity (*774*). The identification of the biogenic amines (*cf.* Section 4.1.1.1) had been effected by chromatography and color reactions; their re-investigation and that of dracotoxin with modern techniques would be advisable.

Food poisoning by spoiled fish may be caused by large amounts of histamine resulting from bacterial degradation of peptides and enhanced by urocanic acid (imidazolyl-4-acrylic acid) formed by elimination of NH_3 from histidine (*730*); for an EI mass spectrum, see (*731*).

To Sect. 4.5 Mammals and Mankind

5α,6α-Cholesterol epoxide reacts *in vitro* under enzyme catalysis with histamine to give dendrogenin A (**91**, Fig. 125), which was also detected in mammalian cells showing antitumor activity (*cf.* squalamine, Sect. 4.3.2). ESI mass spectrometry yields $[M+H]^+$ (*m/z* 514), MS^2 and MS^3 result in consecutive losses of H_2O, MS^4 in the degradation of the histamine chain by partially not obvious reactions. A mass shift of 7 Da of all these ions in the spectrum of the 25,26,26,26,27,27,27-D_7-analog of **91** indicates that fragmentation cannot have occurred in the hydrocarbon side chain. For the mass spectra, see Supplementary Material of the manuscript (*651*). For the early history of leucomaine and ptomaine investigation, see (*755*).

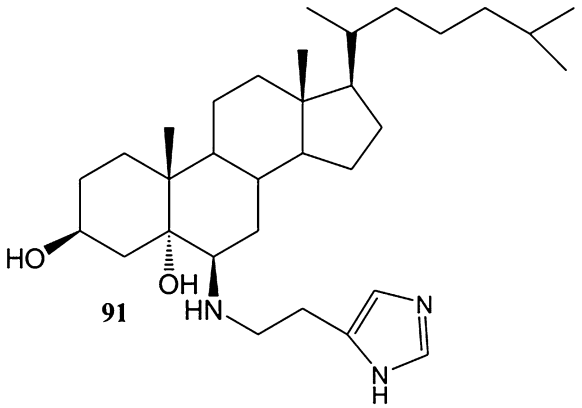

91

Fig. 125 Dendrogenin A (**91**)

From tissue samples modified amino acids have been obtained. Among these are urocanic acid (see above) (*731*), urocanic acid substituted at *N*-1 with $-C(CH_3)_2-CH_2-COCH_3$ (partial EI-MS of the methyl ester) (*732*), cyclodipeptides (Hyp-Pro and Hyp-Leu; *cf.* Sect. 7.2.2) (*733*), and hydantoins (*734*), for EI-MS data, see (*597, 735, 736*).

To Sect. 5.2.3. Glycerophospholipids

Isolates of glycerophospholipids from natural sources are mixtures of subclasses with an *O*-acyl group, an *O*-alkyl group or an *O*-alk-1-enyl group at C-1 of glycerol (Fig. 77). A differentiation especially of the latter two groups is possible by multistage ESI-MS in the negative mode starting from $[M–H]^-$ as demonstrated for ethanol amine representatives (*762*). $[M–H]^-$ upon CID yields abundant fragment ions corresponding to $R\text{-}COO^-$ from the C-2 substituent and to ions due to the loss of the acid (R-COOH) and of the corresponding ketene. Further CID of the $[M–H–ketene]^-$ ion results for *O*-alc-1-enyl compounds in the loss of the alcohol unit, the formation of the alcoholate anion, and in the loss of ethanol amine; additional CID of the latter ion yields again the alcoholate anion (Fig. 126)

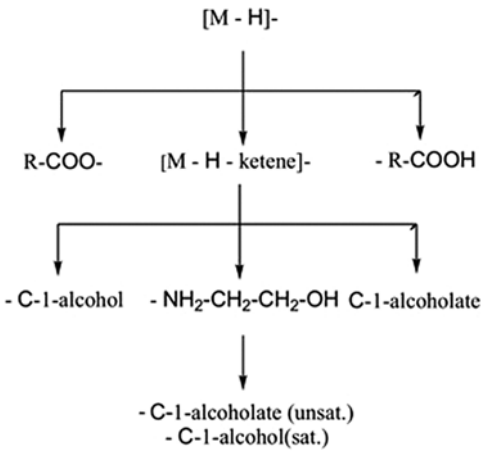

Fig. 126 Glycerophospholipid fragmentation scheme under ESI-MS-CID

For C-1 saturated alkyl ethers CID of the $[M–H–ketene]^-$ ion produces only low abundance ions due to the loss of the alcohol, but CID of the [M–ketene–ethanol–amine]$^-$ ion results in an abundant loss of the alcohol. Thus, an unambiguous distinction between the groups of saturated and unsaturated C-1 ethers is possible.

This technique can also be applied to other classes of glycerophospholipids (Fig. 77) except for choline compounds, which do not form $[M–H]^-$ ions. For these, an analogous scheme starting from $[M–CH_3]^-$ has been developed (*763*).

For the analysis of oxidation products of glycerophospholipids by ESI-MS/MS, see (*746*, *765*).

To Sect. 8.2. Di- and Oligonocleotides

The collision induced fragmentation of $[M+H]^+$, $[M+2H]^{2+}$, and of $[M-H]^-$ obtained by electrospray ionization of cyclic dinucleotides (bacterial messenger substances (*760*)) were compared (*759*). Splitting off of base units and degradations initiated by cleavage of phosphate bonds are the main processes.

Acknowledgments I wish to thank Mag. *W. Dollhäubl* and his team at Springer Verlag Wien for their competent help in preparing the figures in this contribution, as well as Prof. Dr. *Sabira Begum*, Karachi, Pakistan, Dr. *H.M. Garaffo*, Bethesda, MD, USA, Dr. *P. Knechtle*, Reinach, Switzerland, Dr. *H. Münster*, Bremen, Germany, and Dr. *M. Schäfer*, Köln Germany for spectral material.

References

1. Ryhage R, Stenhagen E (1959) Mass Spectrometric Studies. I. Methyl Esters of Saturated Normal Chain Carboxylic Acids. Arkiv Kemi 13:523
2. Finan PA, Reed RI, Snedden W (1958) The Application of Mass Spectrometry to Carbohydrate Chemistry. Chem Ind:1172
3. Kotchetkov NK, Wulfson NS, Chizhov OS, Zolotarev BM (1962) Investigation of Carbohydrates by Mass Spectrometry. Methyl Ethers of Monosaccharides. Докл Акад Наук CCCP 147:1369
4. Heyns K, Scharmann H (1963) Massenspektroskopische Untersuchungen, II. Die Massenspektren von Derivaten der Monosaccharide und Aminozucker. Liebigs Ann Chem 667:183
5. Biemann K (1960) The Determination of Carbon Skeleton of Sarpagine by Mass Spectrometry. Tetrahedron Lett 1(36):9
6. Biemann K, Seibl J, Gapp F (1959) Mass Spectrometric Identification of Amino Acids. Biochem Biophys Res Commun 1:307
7. Budzikiewicz H, Djerassi C (1962) Mass Spectrometry in Structural and Stereochemical Problems. I. Steroid Ketones. J Am Chem Soc 84:1430
8. Djerassi C, Budzikiewicz H, Wilson JM (1962) Mass Spectrometry in Structural and Stereochemical Problems. VIII. Unsaturated Pentacyclic Triterpenoids. Tetrahedron Lett 3:263
9. Gilbert B, Ferreira JM, Owellen RJ, Swanholm CE, Budzikiewicz H, Durham LJ, Djerassi C (1962) Mass Spectrometry in Structural and Stereochemical Problems. II. Pyrifoline and Refractidine. Tetrahedron Lett 3:59
10. Selected Mass Spectral Data (Matrix) and (Standard) (1972) American Petroleum Institute Research Project 44, Texas A&M University, College Station, TX, USA
11. Hood A (1963) The Molecular Structure of Petroleum. In: McLafferty FW (ed) Mass Spectrometry of Organic Ions. Academic Press, New York, p 597
12. Biemann K (1966) Mass Spectrometry of Selected Natural Products. In: Zechmeister L (ed) Progress in the Chemistry of Organic Natural Products. Springer-Verlag, Wien, Austria, vol 24, p 1
13. Howe I, Jarman M (1985) New Techniques for the Mass Spectrometry of Natural Products. In: Herz W, Grisebach H, Kirby GW, Tamm Ch (eds) Progress in the Chemistry of Organic Natural Products. Springer-Verlag, Wien, Austria, vol 47, p 107

14. Budzikiewicz H, Djerassi C, Williams DH (1964) Structure Elucidation of Natural Products by Mass Spectrometry, Vol I: Alkaloids, Vol II: Steroids, Terpenoids, Sugars, and Miscellaneous Classes. Holden-Day, San Francisco
15. Waller GR, Ed. (1972) Biochemical Applications of Mass Spectrometry. Wiley, New York
16. Waller GR, Dermer OC, Eds. (1980) Biochemical Applications of Mass Spectrometry. First Supplementary Volume. Wiley, New York
17. Budzikiewicz H, Schäfer M (2012) Massenspektrometrie. Eine Einführung. 6. Aufl. Wiley-VCH, Weinheim, Germany
18. Harrison AG (1992) Chemical Ionization Mass Spectrometry; 2nd Edn. CRC Press, Boca Raton, FL, USA
19. Beckey HD (1977) Principles of Field Ionization and Field Desorption Mass Spectrometry. Pergamon, Oxford, UK
20. Fenselau C, Cotter RJ (1987) Chemical Aspects of Fast Atom Bombardment. Chem Rev 87:501
21. Zenobi R, Knochenmuss R (1998) Ion Formation in MALDI Mass Spectrometry. Mass Spectrom Rev 17:337
22. Gaskell SJ (1997) Electrospray. Principles and Practice. J Mass Spectrom 32:677
23. Mamyrin BA (2001) Time of Flight Mass Spectrometry (Concepts, Achievements, and Prospects). Int J Mass Spectrom 206:251
24. Miller PE, Denton MB (1986) The Quadrupole Mass Filter: Basic Operating Concepts. J Chem Educ 63:617
25. March RE (1997) An Introduction to Quadrupole Ion Trap Mass Spectrometry. J Mass Spectrom 32:351
26. Marshall AG, Hendrickson CL (2002) Fourier Transform Ion Cyclotron Resonance Detection: Principles and Experimental Configurations. Int J Mass Spectrom 215:59
27. Perry RH, Cooks RG, Noll RJ (2008) Orbitrap Mass Spectrometry: Instrumentation, Ion Motion and Applications. Mass Spectrom Rev 27:661
28. Kanu AB, Dwivedi P, Tam M, Matz L, Hill HH Jr (2008) Ion Mobility-Mass Spectrometry. J Mass Spectrom 43:1
29. Uetrecht C, Rose RJ, van Duijn E, Lorenzen K, Heck AJR (2010) Ion Mobility Mass Spectrometry of Proteins and Protein Assemblies. Chem Soc Rev 39:1633
30. Caprioli RM (1990) Continuous-Flow Fast Atom Bombardment Mass Spectrometry. Anal Chem 62:477A
31. Bier ME, Cooks RG (1987) Membrane Interface for Selective Introduction of Volatile Compounds Directly into the Ionization Chamber of a Mass Spectrometer. Anal Chem 59:597
32. Nytoft HP, Bojesen-Koefoed JA, Christiansen FG, Fowler MG (2002) Oleanane or Lupane? Reappraisal of the Presence of Oleanane in Cretaceous-Tertiary Oils and Sediments. Org Geochem 33:1225
33. Panosyan AG, Mnatsakanyan VA (1977) Structure of a Pentacyclic Triterpene Alcohol from *Centaurea aquarrosa*. Chem Nat Comp 13:50
34. Henderson W, Wollrab V, Eglinton G (1969) Identification of Steranes and Triterpanes from a Geological Source by Capillary Gas Liquid Chromatography and Mass Spectrometry. Earth Sciences (Adv Org Geochem 1968) 31:181
35. Caspi E, Greig JB, Zander JM, Mandelbaum A (1969) Incorporation of Deuterium from Deuterium Oxide into Tetrahymanol Biosynthesised from Squalene. Chem Commun:28
36. Crawford M, Hanson SW, Koker MES (1975) The Structure of Cymbopogone, a Novel Triterpenoid from Lemongrass. Tetrahedron Lett 16:3099
37. Courtney JL, Shannon JS (1963) Studies in Mass Spectrometry. Triterpenoids: Structure Assignment to Some Friedelane Derivatives. Tetrahedron Lett 4:13
38. Shannon JS, MacDonald CG, Courtney JL (1963) Studies in Mass Spectrometry. Triterpenoids: Structure Assignment to Friedelane-y-one (y-al) and Derivatives. Tetrahedron Lett 4:173

39. Igoli OJ, Gray IA (2008) Friedelanone and other Triterpenoids from *Hymenocardia acida.* Int J Phys Sci 3:156

40. Hirota H, Moriyama Y, Tsuyuki T, Tanahashi Y, Takahashi T, Katoh Y, Satoh H (1975) The High Resolution Mass Spectra of Shionane and Fridelane Derivatives. Bull Chem Soc Japan 48:1884

41. Sengupta P, Chakraborty AK, Duffield AM, Durham LJ, Djerassi C (1968) Chemical Investigation on *Putranjiva roxburghii.* The Structure of a New Triterpene, Putranjivadione. Tetrahedron 24:1205

42. Protiva J, Pouzar V, Vystrčil A (1976) Mass Spectra of 12-Oxolupane Derivatives. Coll Czech Chem Commun 41:2225

43. Galbraith MN, Miller CJ, Rawson JWL, Ritchie E, Shannon JS, Taylor WC (1965) Moretenol and Other Triterpenes from *Ficus macrophylla* Desf. Aust J Chem 18:226

44. Ageta H, Arai Y (1983) Fern Constituents: Pentacyclic Triterpenoids Isolated from *Polypodium niponicum* and *P. formosanum.* Phytochemistry 22:1801

45. Van Dorsselaer A, Albrecht P, Ourisson G (1977) Identification of Novel (17αH)-Hopanes in Shales, Coals, Lignites, Sediments and Petroleum. Bull Soc Chim Fr:165

46. Hills IR, Whitehead EV (1970) Pentacyclic Triterpanes from Petroleum and Their Significance. Earth Sciences (Adv Org Geochem, 1966) 32:89

47. Ekweozor CM, Okogun JI, Ekong DEU, Maxwell JR (1979) Preliminary Organic Geochemical Studies of Samples from the Niger Delta (Nigeria). I. Analyses of Crude Oils for Triterpanes. Chem Geol 27:11

48. Wardroper AMK, Brooks PW, Humberston MJ, Maxwell JR (1977) Analysis of Steranes and Triterpanes in Geolipid Extracts by Automatic Classification of Mass Spectra. Geochim Cosmochim Acta 41:499

49. Kumar N, Seshadri TR (1976) A New Triterpene from *Pterocarpus santalinus* Bark. Phytochemistry 15:1417

50. Shiojima K, Arai Y, Masuda K, Takase Y, Ageta T, Ageta H (1992) Mass Spectra of Pentacyclic Triterpenoids. Chem Pharm Bull 40:1683

51. Herz W, Santhanam PS, Wahlberg I (1972) 3-*epi*-Betulinic Acid, a New Triterpenoid from *Picramnia pentandra.* Phytochemistry 11:3061

52. Roitman JN, Jurd L (1978) Triterpenoid and Phenolic Constituents of *Colubrina granulosa.* Phytochemistry 17:491

53. Protiva J, Tureček F, Vystrčil A (1977) Revised Structure of Thurberine. Synthesis of 3,12-Lupanedione. Coll Czech Chem Commun 42:140

54. Corbett RE, Young H (1966) Lichens and Fungi. Part II. Isolation and Structural Elucidation of 7β-Acetoxy-22-hydroxyhopane from *Stricta billardierii* Del. J Chem Soc (C):1556

55. Ogunkoya L (1981) Application of Mass Spectrometry in Structural Problems in Triterpenes. Phytochemistry 20:121

56. Hui WH, Li MM (1976) Structures of Eight New Triterpenoids and Isolation of Other Triterpenoids and Epi-ikshusterol from Stems of *Lithocarpus cornea.* J Chem Soc Perkin Trans I:23

57. Nakane T, Maeda Y, Ebihara H, Arai Y, Masuda K, Takano A, Ageta H, Shiojima K, Cai SQ, Abdel-Halim OB (2002) Fern Constituents: Triterpenoids fom *Adiantum capillus-veneris.* Chem Pharm Bull 50:1273

58. Řezanka T, Siristova L, Melzoch K, Sigler K (2010) Hopanoids from Bacteria and Cyanobacteria - Their Role in Cellular Biochemistry and Physiology, Analysis and Occurrence. Mini-Rev Org Chem 7:300

59. Karliner J, Djerassi C (1966) Terpenoids. LXVII. Mass Spectral and Nuclear Magnetic Resonance Studies of Pentacyclic Triterpene Hydrocarbons. J Org Chem 31:1945

60. Shannon JS (1963) Studies in Mass Spectrometry. VII. Triterpenoids: Ifflaionic Acid. Aust J Chem 16:683

61. Tschesche R, Axen U, Snatzke G (1963) Über Triterpene, XI. Die Konstitution des Äscins. Liebigs Ann Chem 669:171

62. Wünsche C, Löw I (1966) Zur retro-*Diels-Alder*-Reaktion pentacyclischer Triterpene unter Elektronenbeschuß. Protoäscigenin und verwandte Verbindungen. Tetrahedron 22:1893
63. Tursch B, Tursch E, Harrison IT, da Silva GBCT de CB, Monteiro HJ, Gilbert B, Mors WB, Djerassi C (1963) Terpenoids. LIII. Demonstration of Ring Conformational Changes in Triterpenes of the β-Amyrin Class Isolated from *Stryphnodendron coriaceum*. J Org Chem 28:2390
64. Budzikiewicz H, Wilson JM, Djerassi C (1963) Mass Spectrometry in Structural and Stereochemical Problems. XXXII. Pentacyclic Triterpenes. J Am Chem Soc 85:3688
65. Wyrzykiewicz E, Wrzeciono U, Zaprutko L (1989) Triterpenoids. Part IV. Mass Spectrometry of Pentacyclic Triterpenoids: 18β- and 18α-11-Oxooleanic Acid Derivatives. Org Mass Spectrom 24:105
66. Elgamal MHA, Fayez MBE, Snatzke G (1965) Constituents of Local Plants - VI. Liquoric Acid, a New Triterpenoid from the Roots of *Glycyrrhiza glabra* L. Tetrahedron 21:2109
67. Budzikiewicz H, Brauman JI, Djerassi C (1965) Massenspektrometrie und ihre Anwendung auf strukturelle und stereochemische Probleme - LXVII. Zum retro-Diels-Alder-Zerfall organischer Moleküle unter Elektronenbeschuß. Tetrahedron 21:1855
68. Berti G, Bottari F, Marsili A, Morelli I, Mandelbaum A (1968) Rearrangements of the Oxides of Hopene-I and Hopene-II under the Action of Boron Trifluoride. Tetrahedron Lett 9:529
69. Protiva J, Vystrčil A (1976) Reaction of Amides of 28-Lupanoic Acid with Lead Tetraacetate and Iodine. Mass Spectra of 12-Lupene Derivatives. Coll Czech Chem Commun 41:1200
70. Ageta H, Shiojima K, Masuda K, Lin T (1981) Composite Constituents: Four New Triterpenoids, Neolupenol, Tarolupenol and their Acetates Isolated from the Roots of a Japanese Dandelion, *Taraxacum japonicum.* Tetrahedron Lett 22:2289
71. Sultana N, Khalid A (2010) Phytochemical and Enzyme Inhibitory Studies on Indigenous Medicinal Plant *Rhazia stricta.* Nat Prod Res 24:305
72. Honda T, Round BAV, Bore L, Finley HJ, Favaloro FG Jr, Suh N, Wang Y, Sporn MB, Gribble GW (2000) Synthetic Oleanane and Ursane Triterpenoids with Modified Rings A and C: A Series of Highly Active Inhibitors of Nitric Oxide Production in Mouse Macrophages. J Med Chem 43:4233
73. Aiyar VN, Chopra GR, Jain AC, Seshadri TR (1973) Constitution of Putrone & Putrol. Indian J Chem 11:525
74. Sengupta P, Sen M, Rao SN, Das KG (1979) Terpenoids and Related Compounds. Part 25. Structures of the 25-Nortriterpenoids Putrol and Putrone. J Chem Soc Perkin Trans I:60
75. Akihisa T, Kokke WCMC, Tamura T, Nambara T (1992) 7-Oxodihydrokarounidiol [7-Oxo-D:C-friedo-olean-8-ene-3α,29-diol], a Novel Triterpene from *Trichosanthes kirilowii.* Chem Pharm Bull 40:1199
76. Rozen S, Shahak I, Bergmann ED (1975) Reactions of Ring C in Glycyrrhetic Acid Derivatives. Isr J Chem 13:234
77. Amirova GS (1982) The Structure of Isomeristotropic Acid. Хим Природ Соед 262 (Chem Nat Comp 18:246)
78. Diaz, JG, Fraga BM, Gonzales AG, Gonzáles P, Hernandez MG, Miranda JM (1984) Triterpenes from *Ferula linkii.* Phytochemistry 23:1471
79. Gonzáles AG, Ferro EA, Ravelo AG (1987) Triterpenes from *Maytenus horrida*. Phytochemistry 26:2785
80. Zeng L, Zhang RY, Wang D, Lou ZC (1990) Two Triterpenoids from Roots of G*lycyrrhiza yunnanensis.* Phytochemistry 29:3605
81. Kutney JP, Eigendorf G, Rogers IH (1969) Mass Spectral Fragmentation Studies of Triterpenes Related to Serratenediol. Tetrahedron 25:3753
82. Bryce TA, Martin-Smith M, Osske G, Schreiber K, Subramanian G (1967) Sterols and Triterpenoids - XI. Isolation of Arundoin and Sawamilletin from Cuban Sugar Cane Wax. Tetrahedron 23:1283
83. Salmykova IA, Zorina AD, Lushchizkaya IM, Matyukhina LG, Martynov VF (1983) Miricolon - New Triterpenoid from the Bark of *Alnaster fructicosus* Ledeb. Ж Общей Хим 53:2412

84. Heupel RC (1985) Varietal Similarities and Differences in the Polycyclic Isopentenoid Composition of *Sorghum.* Phytochemistry 24:2929
85. Ahmed Z, Ali D, Malik A (2006) Structure Determination of Ursene-type Triterpenes by NMR Techniques. Magn Reson Chem 44:717
86. Savina AA, Sokolskaya TA, Zakharov VF (1988) 11,12-Dehydroursolic Acid Lactone from Leaves of *Eucalyptus viminalis.* Chem Nat Comp 24:253 (Original: Хим Прир Соед 1988:295)
87. Siddiqui BS, Sultana I, Begum S (2000) Triterpenoidal Constituents from *Eucalyptus camaldulensis* var. *obtusa* Leaves. Phytochemistry 54:861
88. Begum S, Farhat, Sultana I, Siddiqui BS, Shaheen F, Gilani AH (2000) Spasmolytic Constituents from *Eucalyptus camaldulensis* var. *obtusa* Leaves. J Nat Prod 63:1265
89. Pereda-Miranda R, Delgado G (1990) Triterpenoids and Flavonoids from *Hyptis albida.* J Nat Prod 53:182
90. Misra L, Laatsch H (2000) Triterpenoids, Essential Oil and Photo-Oxidative 28 → 13-Lactonization of Oleanolic Acid from *Lantana camera.* Phytochemistry 54:969
91. Arai Y, Kusumoto Y, Nagao M, Shiojima K, Ageta H (1983) Composite Substituents: Aliphatics and Triterpenoids Isolated from the Whole Plants of *Ixeris debilis* and *I. dentata.* Yakugaku Zasshi 103:356
92. Nishimoto K, Ito M, Natori S, Ohmoto T (1968) The Structures of Arundoin, Cylindrin and Fernenol. Triterpenoids of Fernane and Arborane Groups of *Imperata cylindica* var. *koenigii.* Tetrahedron 24:735
93. Ageta H, Shiojima K, Arai Y (1987) Acid-Induced Rearrangement of Triterpenoid Hydrocarbons Belonging to the Hopane and Migrated Hopane Series. Chem Pharm Bull 35:2705
94. Vorbrüggen H, Pakrashi SC, Djerassi C (1963) Terpenoide LIV. Arborinol, ein neuer Triterpen-Typus. Liebigs Ann Chem 668:57
95. Kennard O, Riva di Sanseverino L, Vorbrüggen H, Djerassi C (1965) The Complete Structure of the Triterpene Arborinol. Tetrahedron Lett 6:3433
96. Arthur HR, Hui WH, Aplin RT (1965) The Structure of Simiarenol from the Hong Kong Species of *Rhododendron simiarum.* Tetrahedron Lett 6:937
97. Aplin RT, Arthur HR, Hui WH (1966) The Structure of the Triterpene Simiarenol (an E:B *friedo*-Hop-5-ene) from the Hong Kong Species of *Rhododendron simiarum.* J Chem Soc (C):1251
98. Gonzáles AG, Martín JD, Pérez C (1974) Three New Triterpenes from the Lichen *Xanthoria resendei.* Phytochemistry 13:1547
99. Singh H, Kapoor VK, Piozzi F, Passannanti S, Paternostro M (1978), Isomotiol, a New Triterpene from *Strychnos potatorum*. Phytochemistry 17:154
100. Hauke V, Graff R, Wehrung P, Trendel JM, Albrecht P, Riva A, Hopfgartner G, Gülaçar FO, Buchs A, Eakin PA (1992) Novel Triterpene-Derived Hydrocarbons of the Arborane/Fernane Series in Sediments: Part II. Geochim Cosmochim Acta 56:3595
101. Friedrich C, von Domarus C (1998) *Carl Friedrich Wilhelm Meissner* (1792-1853) - Apotheker und Alkaloidforscher. Pharmazie 53:67
102. Meissner W (1819) II. Ueber ein neues Pflanzenalkali *(Alkaloid).* J Chem Phys 25:377 (*recte* 379)
103. Winterstein E, Trier G (1910) Die Alkaloide. Eine Monographie der natürlichen Basen. Gebrüder Borntraeger, Berlin
104. Pelletier SW (1983) The Nature and Definition of an Alkaloid. In: Pelletier SW (ed) Alkaloids: Chemical and Biological Perspectives. Wiley-Interscience, New York, Vol 1, p 1.
105. Fehlhaber HW (1968) Massenspektrometrische Strukturermittlung von Peptid-Alkaloiden. Fresenius Z Anal Chem 235:91
106. Giacomelli SR, Maldaner G, Gonzaga WA, Garcia CM, da Silva UF, Dalcol II, Morel AF (2004) Cyclic Peptide Alkaloids from the Bark of *Discaria americana.* Phytochemistry 65:933
107. Bienz S, Bisegger P, Guggisberg A, Hesse M (2005) Polyamine Alkaloids. Nat Prod Rep 22:647

108. Hesse M (2005) Alkaloids. In: Gross ML, Caprioli RM, Nibbering NMM (eds) The Encyclopedia of Mass Spectrometry, vol 4. Elsevier, Amsterdam, p 748
109. Rinehart KL Jr, Van Lear GE (1970) Antibiotics. In: Waller GR (ed) Biochemical Applications of Mass Spectrometry. Wiley-Interscience, New York, p 449
110. Borders DB, Hargreaves RT (1980) Antibiotics. In: Waller GR, Dermer OC (eds) Biochemical Applications of Mass Spectrometry. First Supplementary Volume. Wiley-Interscience, New York, p 567
111. Budzikiewicz H (2010) Microbial Siderophores. In: Kinghorn AD, Falk H, Kobayashi J (eds) Progress in the Chemistry of Organic Natural Products. Springer-Verlag, Wien, Austria, vol 92, p 1
112. Budzikiewicz H, Djerassi C, Williams DH (1964) Structure Elucidation of Natural Products by Mass Spectrometry, vol 1: Alkaloids. Holden-Day, San Francisco
113. Hesse M (1974) Indolalkaloide. In: Budzikiewicz H (ed) Progress in Mass Spectrometry, vol 1. Verlag Chemie, Weinheim, Germany
114. Hesse M, Bernhard HO (1975) Alkaloide außer Indol-, Triterpen- und Steroidalkaloide. In: Budzikiewicz H (ed) Progress in Mass Spectrometry, vol 3. Verlag Chemie, Weinheim, Germany
115. Budzikiewicz H (1970) Steroids. In: Waller GR (ed) Biochemical Applications of Mass Spectrometry. Wiley-Interscience, New York, p 283
116. Saporito RA, Spande TF, Garraffo HM, Donnelly MA (2009) Arthropod Alkaloids in Poison Frogs: A Review of the 'Dietary Hypothesis'. Heterocycles 79:277
117. Daly JW, Brown GB, Mensah-Dwumah M, Myers CW (1978) Classification of Skin Alkaloids from Neotropical Poison-Dart Frogs (Dendrobatidae). Toxicon 16:163
118. Daly JW, Myers CW, Whittaker N (1987) Further Classification of Skin Alkaloids from Neotropical Poison Frogs (Dendrobatidae), with a General Survey of Toxic/Noxious Substances in the Amphibia. Toxicon 25:1023
119. Daly JW, Spande TF, Garraffo HM (2005) Alkaloids from Amphibian Skin: A Tabulation of Over Eight-Hundred Compounds. J Nat Prod. 68:1556
120. Saporito RA, Donnelly MA, Spande TF, Garraffo HM (2012) A Review of Chemical Ecology in Poison Frogs. Chemoecology 22:159
121. Garraffo HM, Spande TF, Jones TH, Daly JW (1999) Ammonia Chemical Ionization Tandem Mass Spectrometry in Structure Determination of Alkaloids. I. Pyrrolidines, Piperidines, Decahydroquinolines, Pyrrolizidines, Indolizidines, Quinolizidines, and an Azabicyclo[5.3.0] decane. Rapid Commun Mass Spectrom 13:1553
122. Smith SQ, Jones TH (2004) Tracking the Cryptic Pumiliotoxins. Proc Natl Acad Sci USA 101:7841
123. Smith BP, Tyler MJ, Kaneko T, Garraffo HM, Spande TF, Daly JW (2002) Evidence for the Biosynthesis of Pseudophrynamine Alkaloids by an Australian Myobatrachid Frog (*Pseudophryne*) and for Sequestration of Dietary Pumiliotoxins. J Nat Prod 65:439
124. Saporito RA, Donnelly MA, Norton RA, Garraffo HM, Spande TF, Daly JW (2007) Oribatid Mites as a Major Dietary Source for Alkaloids in Poison Frogs. Proc Natl Acad Sci USA 104:8885
125. Daly JW, Ware N, Saporito RA, Spande TF, Garraffo HM (2009) *N*-Methyldecahydroquinolines: An Unexpected Class of Alkaloids from Amazonian Poison Frogs (Dendrobatidae) J Nat Prod 72:1110
126. Saporito RA, Garraffo HM, Donnelly MA, Edwards AL, Longino JT, Daly JW (2004) Formicine Ants: An Arthropod Source for the Pumiliotoxin Alkaloids of Dendrobatid Poison Frogs. Proc Natl Acad Sci USA 101:8045
127. Mebs D, Jansen M, Köhler G, Pogoda W, Kauert G (2010) Myrmacophagy and Alkaloid Sequestration in Amphibians: a Study on *Ameerega picta* (Dendrobatidae) and *Elachistocleis* sp. (Microhylidae) Frogs. Salamandra 46:11
128. Clark VC, Raxworthy CJ, Rakotomalala V, Sierwald P, Fisher BL (2005) Convergent Evolution of Chemical Defense in Poison Frogs and Arthropod Prey between Madagascar and the Neotropics. Proc Natl Acad Sci USA 102:11617

129. Clark VC, Rakotomalala V, Ramilijaona O, Abrell L, Fisher BL (2006) Individual Variation in the Alkaloid Content of Poison Frogs of Madagascar (*Mantella*; Mantellidae). J Chem Ecol 32:2219
130. Saporito RA, Donnelly MA, Madden AA, Garraffo HM, Spande TF (2010) Sex-Related Differences in Alkaloid Chemical Defenses of the Dendrobatid Frog *Oophaga pumilio* from Cayo Nancy, Bocas del Toro, Panama. J Nat Prod 73:317
131. Takada W, Sakata T, Shimano S, Enami Y, Mori N, Nishida R, Kuwahara Y (2005) Scheloribatid Mites as the Source of Pumiliotoxins in Dendrobatid Frogs. J. Chem. Ecol 31:2403
132. Raspotnig G, Norton RA, Heethoff M (2011) Oribatid Mites and Skin Alkaloids in Poison Frogs. Biol Lett 7:555
133. Saporito RA, Norton RA, Andriamaharavo NR, Garraffo HM, Spande TF (2011) Alkaloids in the Mite *Scheloribates laevigatus*: Further Alkaloids Common to Oribatid Mites and Poison Frogs. J Chem Ecol 37:213
134. Vences M, Schulz S, Poth D, Rodriguez A (2011) Defining Frontiers in Mite and Frog Alkaloid Research. Biol Lett 7:557
135. Daly JW, Garraffo HM, Spande TF, Clark VC, Ma J, Ziffer H, Cover JF Jr (2003) Evidence for an Enantioselective Pumiliotoxin 7-Hydroxylase in Dendrobatid Poison Frogs of the *Dendrobates*. Proc Natl Acad Sci USA 100:11092
136. Simmaco M, Mignogna G, Barra D (1998) Antimicrobial Peptides from Amphibian Skin: What Do They Tell Us? Pept Sci 47:435
137. Grant T, Colombo P, Verrastro L, Saporito RA (2012) The Occurrence of Defensive Alkaloids in Non-Integumentary Tissues of the Brazilian Red-Belly Toad *Melanophryniscus simplex* (Bufonidae). Chemoecology 22:169
138. Maan ME, Cummings ME (2012) Poison Frog Colors are Honest Signals of Toxicity, Particularly for Bird Predators. Am Nat 179:E1
139. Gray HM, Kaiser H, Green DM (2010) Does Alkaloid Sequestration Protect the Green Poison Frog, *Dendrobates auratus,* from Predator Attacks? Salamandra 46:235
140. Savitzky AH, Mori A, Hutchinson DA, Saporito RA, Burghardt GM, Lillywhite HB, Meinwald J (2012) Sequestered Defensive Toxins in Tetrapod Vertebrates: Principles, Patterns, and Prospects for Further Studies. Chemoecology 22:141
141. Daly JW, Wilham JM, Spande TF, Garraffo HM, Gil RR, Silva GL, Vaira M (2007) Alkaloids in Bufonid Toads (*Melanophryniscus*): Temporal and Geographic Determinants for Two Argentinian Species. J Chem Ecol 33:871
142. Saporito RA, Isola M, Maccachero VC, Condon K, Donnelly MA (2010) Ontogenetic Scaling of Poison Glands in a Dendrobatid Poison Frog. J Zool 282:238
143. Robinson B, Smith GF, Jackson AH, Shaw D, Frydman B, Deulofeu V (1961) Dehydrobufotenin. Proc Chem Soc:310
144. Stoffman EJL, Clive DLJ (2010) Synthesis of 4-Haloserotonin Derivatives and Synthesis of the Toad Alkaloid Dehydrobufotenine. Tetrahedron 66:4452
145. Maciel NM, Schwartz CA, Pires OR Jr, Sebben A, Castro MS, Sousa MV, Fontes W, Schwartz ENF (2003) Composition of Indolealkylamines of *Bufo rubescens* Cutaneous Secretions Compared to Six Other Brazilian Bufonids with Phylogenetic Implications. Comp Biochem Physiol B 134:641
146. Habermehl G (1969) Chemie und Biochemie von Amphibiengiften. Naturwissenschaften 56:615
147. Becker H (1984) Inhaltsstoffe der Erdkröte (*Bufo bufo*). Pharm Z 13:129
148. Phisalix, Bertrand (1893) Toxicité comparée du sang et du venin de chapaud commun considerée au point de vue de la *sécrétion interne* des glandes cutanées de cet animal. Compt Rend Hebd Séances Mém Soc Biol 45:477
149. Phisalix C, Bertrand G (1902) Sur les principes de venin de chapaud commun (*Bufo vulgaris* L.). Compt Rend Hebd Séances Mém Soc Biol 54:932
150. Jensen H, Chen KK (1932) Chemische Studien über Krötengifte, V. Mitteil.: Die basischen Bestandteile des Kröten-Sekrets. Ber Dtsch Chem Ges 65:1310

151. Wieland H, Konz W, Mittasch H (1934) Die Konstitution von Bufotenin und Bufotenidin. Über Kröten-Giftstoffe. VII. Liebigs Ann Chem 513:1
152. McClean S, Robinson RC, Shaw C, Smyth WF (2002) Characterisation and Determination of Indole Alkaloids in Frog-Skin Secretions by Electrospray Ionisation Ion Trap Mass Spectrometry. Rapid Commun Mass Spectrom 16:346
153. Karle IL, Karle J (1969) The Structural Formula and Crystal Structure of *O*-*p*-Bromobenzoate Derivative of Batrachotoxinine A, $C_{31}H_{38}NO_6Br$, a Frog Venom and Steroidal Alkaloid. Acta Cryst B 25:428
154. Tokuyama T, Daly J, Witkop B (1969) The Structure of Batrachotoxin, a Steroidal Alkaloid from the Colombian Arrow Poison Frog, *Phyllobates aurotaenia*, and Partial Synthesis of Batrachotoxin and its Analogs and Homologs. J Am Chem Soc 91:3931
155. Kurosu M, Marcin LR, Grinsteiner TJ, Kishi Y (1998) Total Synthesis of (±)-Batrachotoxinin A. J Am Chem Soc 120:6627
156. Tokuyama T, Daly JW (1983) Steroidal Alkaloids (Batrachotoxins and 4*β*-Hydroxybatrachotoxins), "Indole Alkaloids" (Calycanthine and Chimonanthine) and a Piperidinyldipyridine Alkaloid (Noranabasamine) in Skin Extracts from the Colombian Poison-Dart Frog *Phyllobates terribilis* (Dendrobatidae). Tetrahedron 39:41
157. Clark VC, Harinantenaina L, Zeller M, Ronto W, Rocca J, Dossey AT, Rakotondravony D, Kingston DGI, Shaw C (2012) An Endogenous Bile Acid and Dietary Sucrose from Skin Secretions of Alkaloid-Sequestring Poison Frogs. J Nat Prod 75:473
158. Spiteller-Friedmann M, Spiteller G (1965) Schlüsselbruchstücke in den Massenspektren von Alkaloiden. 4. Mitt.: Piperidin-Alkaloide. Monatsh Chem 96:104
159. Daly JW, Karle I, Myers CW, Tokuyama T, Waters JA, Witkop B (1971) Histrionicotoxins: Roentgen-Ray Analysis of the Novel Allenic and Acetylenic Spiroalkaloids Isolated from a Colombian Frog, *Dendrobates histrionicus.* Proc Nat Acad Sci USA 68:1870
160. Adachi Y, Kamei N, Yokoshima S, Fukuyama T (2011) Total Synthesis of (–)-Histrionicotoxin. Org Lett 13:4446
161. Gärtner M, Qu J, Helmchen G (2012) Enantioselective Syntheses of the Alkaloids *cis*-195A (Pumiliotoxin C) and *trans*-195A Based on Multiple Application of Asymmetric Catalysis. J Org Chem 77:1186
162. Spande TF, Jain P, Garraffo HM, Pannell LK, Yeh HJC, Daly JW, Fukumoto S, Imamura K, Tokuyama T, Torres JA, Snelling RR, Jones TH (1999) Occurrence and Significance of Decahydroquinolines from Dendrobatid Poison Frogs and a Myrmicine Ant: Use of ^{1}H and ^{13}C NMR in Their Conformational Analysis. J Nat Prod 62:5
163. Jones TH, Gorman JST, Snelling RR, Delabie JHC, Blum MS, Garraffo HM, Jain P, Daly JW, Spande TF (1999) Further Alkaloids Common to Ants and Frogs: Decahydroquinolines and a Quinolizidine. J Chem Ecol 25:1999
164. Garraffo HM, Jain P, Spande TF, Daly JW, Jones TH, Smith LJ, Zottig VE (2001) Structure of Alkaloid 275A, a Novel 1-Azabicylo[5.3.0]decane from a Dendrobatid Frog, *Dendrobates lehmanni:* Synthesis of the Tetrahydrodiastereomers. J Nat Prod 64:421
165. Lesma G, Sacchetti A, Silvani A (2010) Total Synthesis of 275A Lehmizidine Frog Skin Alkaloid (or its Enantiomer). Tetrahedron: Asymmetry 21:2329
166. Saporito RA, Donnelly MA, Hoffman RL, Garraffo HM, Daly JW (2003) A Siphonotid Millipede (*Rhinotus*) as the Source of Spiropyrrolizidine Oximes of Dendrobatid Frogs. J Chem Ecol 29:2781
167. Meinwald J, Smolanoff J, McPhail AT, Miller RW, Eisner T, Hicks K (1975) Nitropolyzonamine: A Spirocyclic Nitro Compound from the Defensive Glands of a Millipede (*Polyzonium rosalbum*). Tetrahedron Lett 28:2367
168. Kobayashi S, Toyooka N, Zhou D, Tsuneki H, Wada T, Sasaoka T, Sakai H, Nemoto H, Garraffo HM, Spande TF, Daly JW (2007) Flexible Synthesis of Poison-Frog Alkaloids of the 5,8-Disubstituted Indolizidine-Class. II: Synthesis of (–)-209B, (–)-231C, (–)-233D, (–)-235B″, (–)-221I, and an Epimer of 193E and Pharmacological Effects at Neuronal Nicotinic Acetylcholine Receptors. Beilstein J Org Chem 3, No. 30

169. Zhou DJ, Toyooka N (2012) Synthesis of 5,8-Disubstituted Indolizidine Poison-Frog Alkaloids. Chem J Chin Univ 33:511
170. Daly JW, Witkop B, Tokuyama T, Nishikawa T, Karle IL (1977) Gephyrotoxins, Histrionicotoxins and Pumiliotoxins from the Neotropical Frog *Dendrobates histrionicus.* Helv Chim Acta 60:1128
171. Rodrígues A, Poth D, Schulz S, Vences M (2011) Discovery of Skin Alkaloids in Miniaturized Eleutherodactylid Frog from Cuba. Biol Lett 7:414
172. Adriamaharavo NR, Adriantsiferana M, Stevenson PA, O'Mahony G, Yeh HJC, Kaneko T, Garraffo HM, Spande TF, Daly JW (2005) A Revised Structure for Alkaloid 235C Isolated from Skin Extracts of Mantellid (*Mantella*) Frogs of Madagascar. J Nat Prod 68:1743
173. Tursch B, Daloze D, Dupont M, Pasteels JM, Tricot MC (1971) A Defense Alkaloid in a Carnivorous Beetle. Experientia 27:1380
174. Sloggett JJ, Obrycki JJ, Hayness KF (2009) Identification and Quantification of Predation: Novel Use of Gas Chromatography - Mass Spectrometric Analysis of Prey Alkaloid Markers. Funct Ecol 23:416
175. Tokuyama T, Nishimori N, Shimada A, Edwards MW, Daly JW (1987) New Classes of Amidine, Indolizidine and Qinolizidine Alkaloids from a Poison-Frog, *Dendrobates pumilio* (Dendrobatidae). Tetrahedron 43:643
176. Tsukanov SV, Comins DL (2011) Concise Total Synthesis of the Frog Alkaloid (–)-205B. Angew Chem 123:8785 (Int Ed 50:8626)
177. Spande TF, Garraffo HM, Yeh HJC, Pu QL, Pannell LK, Daly JW (1992) A New Class of Alkaloids from Dendrobatid Poison Frog: A Structure for Alkaloid **251F**. J Nat Prod 55:707
178. Daly JW, Garraffo HM, Pannell LK, Spande TF, Severini C, Erspamer V (1990) Alkaloids from Australian Frogs (Myobatrachidae): Pseudophrynamines and Pumiliotoxins. J Nat Prod 53:407
179. Müller CE (1996) Epibatidin - ein nicotinartiges, analgetisch wirksames Alkaloid aus Pfeilgiftfröschen. Pharm Z 25:85
180. Spande TF, Garaffo HM, Edwards MW, Yeh HJC, Pannell L, Daly JW (1992) Epibatidine: A Novel (Chloropyridyl)azabicycloheptane with Potent Analgesic Activity from an Ecuadoran Poison Frog. J Am Chem Soc 114:3475
181. Fitch RW, Spande TF, Garraffo HM, Yeh HCJ, Daly JW (2010) Phantsmidine: An Epibatidine Congener from the Ecuadorian Poison Frog *Epipedobates anthonyi*. J Nat Prod 73:331
182. Fuhrman FA, Fuhrman GJ, Mosher HS (1969) Toxin from Skin of Frogs of the Genus *Atelopus*. Differentiation from Dendrobatid Toxins. Science 165:1376
183. Daly JW, Garraffo HM, Spande TF (1993) Amphibian Alkaloids. In: Cordell GA (ed) The Alkaloids. Chemistry and Pharmacology. Academic Press, San Diego, CA, USA, vol 43, p 185
184. Yotsu-Yamashita M, Kim YH, Dudley SC Jr, Choudhary G, Pfahnl A, Oshima Y, Daly JW (2004) The Structure of Zetekitoxin AB, a Saxitoxin Analog from the Panamanian Golden Frog *Atelopus zeteki*: A Potent Sodium-Channel Blocker. Proc Natl Acad Sci USA 101:4346
185. Tanino H, Nakata T, Kaneko T, Kishi Y (1977) A Stereospecific Total Synthesis of *d,l*-Saxotoxin. J Am Chem Soc 99:2818
186. Schantz EJ, Ghazarossian VE, Schnoes HK, Strong FM, Springer JP, Pezzanite JO, Clardy J (1975) The Structure of Saxitoxin. J Am Chem Soc 97:1238
187. Arakawa O, Noguchi T, Shida Y, Onoue Y (1994) Occurrence of Carbamoyl-*N*-hydroxy Derivatives of Saxitoxin and Neosaxitoxin in a Xanthid Crab *Zosimus aeneus.* Toxicon 32:175
188. Arakawa O, Nishio S, Noguchi T, Shida Y, Onoue Y (1995) A New Saxitoxin Analogue from Xanthid Crab *Atergatis floridus.* Toxicon 33:1577
189. Llewellyn LE (2006) Saxitoxin, a Toxic Marine Natural Product that Targets a Multitude of Receptors. Nat Prod Rep 23:200
190. Kodama M, Ogata T, Sakamoto S, Sato S, Honda T, Miwatani T (1990) Production of Paralytic Shellfish Toxins by a Bacterium *Moraxella* sp. Isolated from *Protogonyaulax tamarensis.* Toxicon 28:707

191. Sevcik C, Noriega J, D'Suze G (2003) Identification of *Enterobacter* Bacteria as Saxitoxin Producers in Cattle's Rumen and Surface Water from Venzuelan Savannahs. Toxicon 42:359
192. Yotsu M, Yasumoto T, Kim YH, Naoki H, Kao CY (1990) The Structure of Chiriquitoxin from the Costa Rican Frog *Atelopus chiriquiensis.* Tetrahedron Lett 31:3187
193. Shoji Y, Yotsu-Yamashita M, Miyazawa T, Yasumoto T (2001) Electrospray Ionization Mass Spectrometry of Tetrodotoxin and its Analogs: Liquid Chromatography/Mass Spectrometry, Tandem Mass Spectrometry, and Liquid Chromatography/Tandem Mass Spectrometry. Anal Biochem 290:10
194. Hesse M, Bernhard HO (1975) Alkaloide außer Indol-,Triterpen- und Steroidalkaloide. In: Budzikiewicz H (ed) Progress in Mass Spectrometry. Verlag Chemie, Weinheim, Germany, vol 3, p 217
195. Zhang JW, Gao JM, Xu T, Zhang XC, Ma YT, Jarussophon S, Konishi Y (2009) Antifungal Activity of Alkaloids from the Seeds of *Chimonanthus praecox.* Chem Biodivers 6:838
196. Hesse M (1974) Indolalkaloide. In: Budzikiewicz H (ed) Progress in Mass Spectrometry. Verlag Chemie, Weinheim, Germany, vol 1 p 238
197. Oka K, Kantrowitz JD, Spector S (1985) Isolation of Morphine from Toad Skin. Proc Natl Acad Sci USA 82:1852
198. Wieland H, Alles R (1922) Über den Giftstoff der Kröte. Ber Deutsche Chem Ges 55: 1789
199. Urscheler HR, Tamm C, Reichstein T (1955) Die Giftstoffe der Europäischen Erdkröte. Über Krötengifte, 8. Mitt. Helv Chim Acta 4:883
200. Shimada K, Fujii Y, Yamashita E (née Mitsuishi), Niizaki Y, Sato Y, Nambara T(1977) Studies on Cardiotonic Steroids from the Skin of Japanese Toad. Chem Pharm Bull 25:714
201. Shimada K, Nambara T (1980) Isolation and Characterization of a New Type of Bufotoxin from the Skin of *Bufo americanus.* Chem Pharm Bull 28:1559
202. Shimada K, Ohishi K, Nambara T (1984) Isolation of Bufotalin 3-Suberoyl-histidine and -3-Methylhistidine esters from the Skin of *Bufo melanostictus* Schneider. Tetrahedron Lett 25:551
203. Shimada K, Miyashiro Y, Nishio T (2006) Characterization of *in vitro* Metabolites of Toad Venom Using High-Perfomance Liquid Chromatography and Liquid Chromatography-Mass Spectrometry. Biomed Chromatogr 20:1321
204. Buchwald HD, Durham L, Fischer HG, Harada R, Mosher HS, Kao CY, Fuhrman FA (1964) Identity of Tarichatoxin and Tetrodotoxin. Science 143:474
205. Lehman EM, Brodie ED Jr, Brodie ED III (2004) No Evidence for an Endosymbiotic Bacterial Origin of Tetrodotoxin in the Newt *Taricha granulosa*. Toxicon 44:243
206. Habermehl G, Haaf A (1968) Cholesterin als Vorstufe in der Biosynthese der Salamanderalkaloide. Chem Ber 101:198
207. Habermehl G, Spiteller G (1967) Massenspektren der Salamander-Alkaloide. Liebigs Ann Chem 706:213
208. Habermehl G, Göttlicher S (1965) Die Konstitution und Konfiguration des Cycloneosamandions. Chem Ber 98:1
209. Benn M, Shaw R (1974) A Salamander Alkaloid Synthesis. Can J Chem 52:2936
210. Hara S, Oka K (1967) A Total Synthesis of Samandarone. J Am Chem Soc 89:1041
211. Mebs D, Pogoda W (2005) Variability of Alkaloids in the Skin Secretion of the European Fire Salamander (*Salamandra salamandra terrestris*). Toxicon 45:603
212. Hara S, Oka M (1970) 3-Aza-A-homo-5β-androstan-17-β-ol-1α,4α-oxide. Japan Pat 7018, 663 (Chem Abstr 73:56316)
213. Eng J, Kleinman WA, Singh L, Singh G, Raufman JP (1992). Isolation and Chatacterization of Exendin-4, an Exendin-3 Analogue, from *Heloderma suspectum* Venom. Further Evidence for an Exendin Receptor on Dispersed Acini from Guinea Pig Pancreas. J Biol Chem 267:7402
214. Eng J, Andrews PC, Kleinman WA, Singh L, Raufman JP (1990). Purification and Structure of Exendin-3, a New Pancreatic Secretagogue Isolated from *Helioderma horridum* Venom. J Biol Chem 265:20259

215. Hoshino M, Yanaihara C, Hong YM, Kishida S, Katsumaru Y, Vandermeers A, Vandermeers-Piret MC, Robberecht P, Christophe J, Yanaihara N (1984) Primary Structure of Helodermin, a VIP-Secretin-Like Peptide Isolated from Gila Monster Venom. FEBS Lett 178:233
216. Parker DS, Raufman JP, O'Donohue TL, Bledsoe M, Yoshida H, Pisano JJ (1984) Amino Acid Sequences of Helospectins, New Members of the Glucagon Superfamily, Found in Gila Monster Venom. J Biol Chem 259:11751
217. Mochea-Morales J, Martin BM, Possani LD (1990) Isolation and Characterization of Helothermine, a Novel Toxin from *Heloderma horridum horridum* (Mexican Beaded Lizard) Venom. Toxicon 28:299
218. Hesse M (2000) Alkaloide. Fluch oder Segen der Natur? Verlag Helvetica Chimica Acta, Zürich, p 73
219. Lyman JF (1908) A Note on the Chemistry of the Muscle and Liver of Reptiles. J Biol Chem 5:125
220. Standard Reference Data Program, National Institute of Standards and Technology (NIST), Gaithersburg, MD, USA
221. Spiteller G, Spiteller-Friedmann M (1962) Vergleichende massenspektrometrische Untersuchung einiger Purinderivate. Monatsh Chem 93:632
222. Pochelov II, Kluev MO, Petrenko VV (2002) Mass Spectrometry of the Purine Bases and their Derivatives. Фарм Ж (Київ) 45
223. Williams BL, Brodie ED Jr, Brodie ED III (2004) A Resistant Predator and its Toxic Prey: Persistence of Newt Toxin Leads to Poisonous (not Venomous) Snakes. J Chem Ecol 30:1901
224. Feldmann CR, Brodie ED Jr, Brodie ED III, Pfrender ME (2009) The Evolutionary Origins of Beneficial Alleles during the Repeated Adaptation of Garter Snakes to Deadly Prey. Proc Natl Acad Sci USA 106:13415
225. Hutchinson DA, Mori A, Savitzky AH, Burghardt GM, Meinwald J, Schroeder FC (2007) Dietary Sequestration of Defensive Steroids in Nuchal Glands of the Asian Snake *Rhabdophis tigrinus.* Proc Natl Acad Sci USA 104:2265
226. Hutchinson DA Savitzky AH, Mori A, Burghardt GM, Wu X, Meinwald J, Schroeder FC (20012) Chemical Investigations of the Defensive Steroid Sequestration by the Asian Snake *Rhabdophis tigrinus.* Chemoecology 22:199
227. Tsuda K (1966) Über Tetrodotoxin, Giftstoff der Bowlfische. Naturwissenschaften 53:171
228. Lee MJ, Jeong DY, Kim WS, Kim HD, Kim CH, Park WW, Park YH, Kim KS, Kim HM, Kim DS (2000) A Tetrodotoxin-Producing *Vibrio* Strain, LM-1, from the Puffer Fish *Fugu vermicularis radiatus.* Appl Environ Microbiol 66:1698
229. Noguchi T, Arakawa O (2008) Tetrodotoxin - Distribution and Accumulation in Aquatic Organisms, and Cases of Human Intoxication. Mar Drugs 6:220
230. Yotsu M, Yamazaki T, Meguro Y, Endo A, Murata M, Naoki H, Yasumoto T (1987) Production of Tetrodotoxin and its Derivatives by *Pseudomonas* sp. Isolated from the Skin of a Pufferfish. Toxicon 25:225
231. Yasumoto T, Yasumura D, Yotsu M, Michishita T, Endo A, Kotaki Y (1986) Bacterial Production of Tetrodotoxin and Anhydrotetrodotoxin. Agric Biol Chem 50:793
232. Wang J, Fan Y (2010) Isolation and Characterization of a *Bacillus* Species Capable of Producing Tetrodotoxin from the Puffer Fish *Fugu obscurus*. World J Microbiol Biotechnol 26:1755
233. Simidu U, Noguchi T, Hwang DF, Shida Y, Hashimoto K (1987) Marine Bacteria which Produce Tetrodotoxin. Appl Environ Microbiol 53:1714
234. Matsumura K (1995) Reexamination of Tetrodotoxin Production by Bacteria. Appl Environ Microbiol 61:3468
235. Matsumura K, Kim DS, Kim CH (2001) No Ability to Produce Tetrodotoxin in Bacteria. Appl Environ Microbiol 67:2393
236. Suenaga K, Kotoku S (1980) Detection of Tetrodotoxin in Autopsy Material by Gas Chromatography. Arch Toxicol 44:291
237. Narita H, Noguchi T, Maruyama J, Nara M, Hashimoto K (1984) Occurrence of a Tetrodotoxin-Associated Substance in a Gastropod, "Hanamushirogai" *Zeuxis siquijorensis.* Bull Japan Soc Sci Fish 50:85

238. Inaoka H, Shiomi K, Yamanaka H, Kikuchi T, Noguchi T, Hashimoto K, Shida Y (1985) Occurrence of a Tetrodotoxin-like Compound as a Minor Toxin in the Puffer Fish, *Fugu flavidus.* Agric Biol Chem 49:2287
239. Spiteller M, Spiteller G (1973) Massenspektrensammlung von Lösungsmitteln, Verunreinigungen, Säulenbelegmaterialien und einfachen aliphatischen Verbindungen. Springer-Verlag, Wien, Austria
240. Maruyama J, Noguchi T, Matsunaga S, Hashimoto K (1984) Fast Atom Bombardment- and Secondary Ion-Mass Spectrometry of Paralytic Shellfish Poisons and Tetrodotoxin. Agric Biol Chem 48:2783
241. Quilliam MA, Thomson BA, Scott GJ, Siu KWM (1989) Ion-Spray Mass Spectrometry of Marine Neurotoxins. Rapid Commun Mass Spectrom 3:145
242. Jang JH, Lee JS, Yotsu-Yamashita M (2010) LC/MS Analysis of Tetrodotoxin and its Deoxy Analogs in the Marine Puffer Fish *Fugu niphobles* from the Southern Coast of Korea, and in the Brackishwater Puffer Fishes *Tetraodon nigroviridis* and *Tetraodon biocellatus* from Southeast Asia. Mar Drugs 8:1049
243. Leung KSY, Fong BMW, Tsoi YK (2011) Analytical Challenges: Determination of Tetrodotoxin in Human Urine and Plasma by LC-MS/MS. Mar Drugs 9:2291
244. Moore KS, Wehrli S, Roder H, Rogers M, Forrest JN JR, McCrimmon D, Zasloff M (1993) Squalamine: An Aminosterol Antibiotic from the Shark. Proc Natl Acad Sci USA 90:1354
245. Wehrli SL, Moore KS, Roder H, Durell S, Zasloff M (1993) Structure of the Novel Steroidal Antibiotic Squalamine Determined by Two-Dimensional NMR Spectroscopy. Steroids 58:370
246. Zhang DH, Cai F, Zhou XD, Zhou WS (2003) A Concise and Stereolselective Synthesis of Squalamine. Org Lett 5:3257
247. Rao MN, Shinnar AE, Noecker LA, Chao TL, Feibush B, Snyder B, Sharkansky I, Sarkahian A, Zhang X, Jones SR, Kinney WA, Zasloff M (2000) Aminosterols from the Dogfish Shark *Squalus acanthias.* J Nat Prod 63:631
248. Hoye TR, Dvornikovs V, Fine JM, Anderson KR, Jeffrey CS, Muddiman DC, Shao F, Sorensen PW, Wang J (2007) Details of the Structure Determination of the Sulfated Steroids PSDS and PADS: New Components of the Sea Lamprey (*Petromyzon marinus*) Migratory Pheromone. J Org Chem 72:7544
249. Shi SDH, Hendrickson CL, Marshall AG (1998) Counting Individual Sulfur Atoms in a Protein by Ultrahigh-Resolution Fourier Transform Ion Cyclotron Resonance Mass Spectrometry: Experimental Resolution of Isotopic Fine Structure in Proteins. Proc Natl Acad Sci USA 95:11532
250. Dumbacher JP, Beehler BM, Spande TF, Garraffo HM, Daly JW (1992) Homobatrachotoxin in the Genus *Pitohui*: Chemical Defense in Birds? Science 258:799
251. Dumbacher JP, Spande TF, Daly JW (2000) Batrachotoxin Alkaloids from Passerine Birds: A Second Toxic Bird Genus (*Ifrita kowaldi*) from New Guinea. Proc Natl Acad Sci USA 97:12970
252. Dumbacher JP, Wako A, Derrickson SR, Samuelson A, Spande TF, Daly JW (2004) Melyrid Beetles (*Choresine*): A Putative Source for the Batrachotoxin Alkaloids Found in Poison-Dart Frogs and Toxic Passerine Birds. Proc Natl Acad Sci USA 101:15857
253. Stammel W, Thomas H (2007) Endogene Alkaloide in Säugetieren. Naturw Rundsch 60:117
254. Brossi A (1993) Mammalian Alkaloids II. In: Cordell GA (ed) The Alkaloids. Chemistry and Pharmacology. Academic Press, San Diego, vol 43, p 119
255. Hesse M, Bernhard HO (1975) Alkaloide außer Indol-,Triterpen- und Steroidalkaloide. In: Budzikiewicz H (ed) Progress in Mass Spectrometry. Verlag Chemie, Weinheim, Germany, vol 3, pp 59 and 149
256. Weitz CJ, Lowney LI, Faull KF. Feistner G (1986) Morphine and Codeine from Mammalian Brain. Proc Nat Acad Sci USA 83:9784
257. Wachowiak R (2003) The Chemical Structure of Endogenous Compounds of the Biological Background and their Significance in Identification Analysis of Xenobiotics. Problems Forensic Sci 54:60

258. Bonte W, Theusner J (1979) Nachweis und thanatologische Bedeutung von δ-Aminovaleriansäure. Z Rechtsmed. 83:139
259. Walbaum H (1900) Ueber Zibeth, Jasmin und Rosen. Ber Dtsch Chem Ges 33:1903
260. Mohammed N, Onodera N, Or-Raschid MM (2003) Degradation of Tryptophane and Related Indolic Compounds by Ruminal Bacteria, Protozoa and their Mixture *in vitro*. Amino Acids 24:73
261. Schreurs NM, Tavendale MH, Lane GA, Barry TN, Marotti DM, McNabb WC (2003) Postprandial Indole and Skatole Formation in the Rumen when Feeding White Clover, Perennial Ryegrass and *Lotus corniculatus.* Proc NZ Soc Anim Prod 63:14
262. Powers JC (1968) The Mass Spectrometry of Simple Indoles. J Org Chem 33:2044
263. Biemann K, Büchi G, Walker BH (1957) The Structure and Synthesis of Muscopyridine. J Am Chem Soc 79:5558
264. Hadj-Abo F, Hesse M (1992) Synthese von (±)-Muscopyridin über eine C-ZIP-Ringerweiterungsreaktion. Helv Chim Acta 75:1834
265. Yu D-Q, Das BC (1983) Structure of Hydroxymuscopyridine A and Hydroxymuscopyridine B, Two New Constituents of Musk. Planta Med 49:183
266. Oh SR, Lee JP, Chang SY, Shin DH, Ahn KS, Min BS, Lee HK (2002) Androstane Alkaloids from Musk of *Moschus moschiferus*. Chem Pharm Bull 50:663
267. Valenta Z, Khaleque A (1959) The Structure of Castoramine. Tetrahedron Lett 1(12):1
268. Maurer B, Ohloff G (1976) Zur Kenntnis der Stickstoffhaltigen Inhaltsstoffe von Castoreum. Helv Chim Acta 59:1169
269. LaLonde RT, Wong CF, Woolever JT, Auer E, Das KC, Tsai AIM (1974) Electron-Impact Mass Spectrometry of *Nuphar* Alkaloids. Org Mass Spectrom 9:714
270. Wrobel JT, Iwanow A, Braekman-Danheux C, Martin TI, MacLean DB (1972) the Structure of Nupharolutine, an Alkaloid of *Nuphar luteum.* Can J Chem 50:1831
271. Wood WF (1990) New Components in Defensive Secretion of the Striped Skunk, *Mephitis mephitis*. J Chem Ecol 16:2057
272. Odham G, Stenhagen E (1972) Fatty Acids. In: Waller GR (ed) Biochemical Applications of Mass Spectrometry. Wiley-Interscience, New York, p 211
273. Odham G, Stenhagen E (1972) Complex Lipids. In: Waller GR (ed) Biochemical Applications of Mass Spectrometry. Wiley-Interscience, New York, p 229
274. Odham G (1980) Fatty Acids. In: Waller GR, Dermer OC (eds) Biochemical Applications of Mass Spectrometry. First Supplementary Volume. Wiley-Interscience, New York, p 153
275. Wood GW (1980) Complex Lipids. In: Waller GR, Dermer OC (eds) Biochemical Applications of Mass Spectrometry. First Supplementary Volume. Wiley-Interscience, New York, p 173
276. Murphy RC, Axelsen PH (2011) Mass Spectrometric Analysis of Long-Chain Lipids. Mass Spectrom Rev 30:579
277. Ryhage R, Stenhagen E (1959) Mass Spectrometric Studies. II. Saturated Normal Long-Chain Esters of Ethanol and Higher Alcohols. Arkiv Kemi 14:483
278. Ryhage R, Stenhagen E (1963) Mass Spectrometry of Long-Chain Esters. In: McLafferty FW (ed) Mass Spectrometry of Organic Ions. Academic Press, New York, p 399
279. Budzikiewicz H (1985) Massenspektrometrische Analyse ungesättigter Fettsäuren. In: Fresenius W, Günzler H, Huber W, Lüderwald I, Tölg G, Wisser H (eds) Analytiker-Taschenbuch. Springer, Berlin, vol 5, p 135
280. Rohwedder WK, Mabrouk AF, Selke E (1965) Mass Spectrometric Studies of Unsaturated Methyl Esters. J Phys Chem 69:1711
281. Lauwers W, Serum JW, Vandewalle M (1973) Studies in Organic Mass Spectrometry XIII: Investigation of Electron-Impact-Induced Isomerisation of α,β- and β,γ-Unsaturated Esters. Org Mass Spectrom 7:1027
282. Ryhage R, Ställberg-Stenhagen S, Stenhagen E (1961) Mass Spectrometric Studies. VII. Methyl Esters of α,β-Unsaturated Long-Chain Acids. On the Structure of C_{27}-Phthienoic Acid. Arkiv Kemi 18:179
283. Andersson BÅ, Holan RT (1974) Pyrrolidides for Mass Spectrometric Determination of the Position of the Double Bond in Monounsaturated Fatty Acids. Lipids 9:185

284. Borchers F, Levsen K, Schwarz H, Wesdemiotis C, Winkler HU (1977) Isomerization of Linear Octene Cations in the Gas Phase. J Am Chem Soc 99:6359
285. Zaikin V, Halket J (2009) A Handbook of Derivatives for Mass Spectrometry. IM Publications, Chichester, UK
286. Minnikin DE (1978) Location of Double Bonds and Cyclopropane Rings in Fatty Acids by Mass Spectrometry. Chem Phys Lipids 21:313
287. Chai R, Harrison AG (1981) Location of Double Bonds by Chemical Ionization Mass Spectrometry. Anal Chem 53:34
288. Schmitz B, Klein RA (1986) Mass Spectrometric Localization of Carbon-Carbon Double Bonds: a Critical Review of Recent Methods. Chem Phys Lipids 39:285
289. Kwon Y, Lee S, Oh DC, Kim S (2011) Simple Determination of Double-Bond Positions in Long-Chain Olefins by Cross-Metathesis. Angew Chem 123: 8425; Int Ed 50:8275
290. Hussain MG, Gunstone FD (1979) Polyunsaturated Acids. Part IV. Mass Spectral Fragmentation Pattern of Long-Chain Polyunsaturated Fatty Acid Methyl Esters and Thiol Esters. Bangladesh J Sci Ind Res 14:105
291. Araki E, Ariga T, Murata T (1976) Chemical Ionization Mass Spectrometry of Polyunsaturated Fatty Acids of Human Serum. Biomed Mass Spectrom 3:261
292. Lankelma J, Ayanoglu E, Djerassi C (1983) Double-bond Location in Long-Chain Polyunsaturated FattyAcids by Chemical Ionization-Mass Spectrometry. Lipids 18:853
293. Schmitz B, Egge H (1979) Determination of Double Bond Position in Tri- to Hexaenoic Fatty Acids by Mass Spectrometry. Chem Phys Lipids 25:287
294. Suzuki M, Ariga T, Sekine M, Araki E, Miyatake T (1981) Identification of Double Bond Positions in Polyunsaturated Fatty Acids by Chemical Ionization Mass Spectrometry. Anal Chem 53:985
295. Dommes V, Wirtz-Peitz F, Kunau WH (1976) Structure Determination of Polyunsaturated Fatty Acids by Gas Chromatography-Mass Spectrometry - a Comparison of Fragmentation Patterns of Various Derivatives. J Chromatogr Sci 14:360
296. Budzikiewicz H (1984) Chemoionisationsmassenspektrometrie - Eine neue Methode zur Fettsäureanalytik? GIT Fachz Lab 28:406
297. Budzikiewicz H (1985) Structure Elucidation by Ion-Molecule Reactions in the Gas Phase: The Location of C,C-Double and Triple Bonds. Fresenius Z Anal Chem 321:150
298. Brauner A, Budzikiewicz H, Francke W (1985) Chemical Ionization (NO) Spectra of *n*-Alkenoic Acids and their Esters. Org Mass Spectrom 20:578
299. Budzikiewicz H, Schneider B, Busker E, Boland W, Francke W (1987) Studies in Chemical Ionization Mass Spectrometry Part XVI: Are the Reactions of Aliphatic C=C Double Bonds with NO^+ Governed by Remote Functional Groups? Org Mass Spectrom 22:458
300. Brauner A, Budzikiewicz H, Boland W (1982) Studies in Chemical Ionization Mass Spectrometry V – Localization of Homoconjugated Triene and Tetraene Units in Alphatic Compounds. Org Mass Spectrom 17:161
301. Schneider B, Budzikiewicz H (1991) Experiments on the Formation of Acylium Ions from Alkenic Compounds Following Chemical Ionization with NO^+. Org Mass Spectrom 26:498
302. Einhorn J, Malosse C (1990) Optimized Production of the Acylium Diagnostic Ions in Chemical Ionization NO^+ Mass Spectra of Long-Chain Monoolefins. Org Mass Spectrom 25:49
303. Malosse C, Einhorn J (1990) Nitric Oxide Chemical Ionization Mass Spectrometry of Long-Chain Unsaturated Alcohols, Acetates, and Aldehydes. Anal Chem 62:287
304. Schneider B, Breuer M, Hartmann H, Budzikiewicz H (1989) Chemical Ionization with Aggressive Gases - a Simple Glow Discharge Source for Sector Field Instruments. Org Mass Spectrom 24:216
305. Cheng C, Gross ML (2000) Applications and Mechanisms of Charge-Remote Fragmentation. Mass Spectrom Rev 19:398
306. Bambagiotti A M, Coran SA, Vincieri FF, Petrucciani, Traldi P (1986) High Energy Collisional Spectroscopy of $[RCOO]^-$ Anions from Negative Ion Chemical Ionization of Fatty Acid Methyl Esters. Org Mass Spectrom 21:485

307. Deterding LJ, Gross ML (1988) Tandem Mass Spectrometry for Identifying Fatty Acid Derivatives that Undergo Charge-Remote Fragmentations. Org Mass Spectrom 23:169
308. Adams J, Gros ML (1988) Structural Determination of Modified Fatty Acids by Collision Activation of Cationized Molecules. Org Mass Spectrom 23:307
309. Divito EB, Davic AP, Johnson ME, Cascio M (2012) Electrospray Ionization and Collision Induced Dissociation Mass Spectrometry of Primary Fatty Acid Amides. Anal Chem 84:2388
310. Zehethofer N, Pinto DM (2008) Recent Developments in Tandem Mass Spectrometry for Lipidomic Analysis. Anal Chim Acta 627:62
311. Hsu FF, Turk J (2010) Electrospray Ionization Multiple-Stage Linear Ion-Trap Mass Spectrometry for Structural Elucidation of Triacylglycerols: Assignment of Fatty Acyl Groups on the Glycerol Backbone and Location of Double Bonds. J Am Soc Mass Spectrom 21:657
312. Regert M (2011) Analytical Strategies for Discriminating Archeological Fatty Substances from Animal Origin. Mass Spectrom Rev 30:177
313. De Rosa M, Gambacorta A (1988) The Lipids of Archaebacteria. Prog Lipid Res 27:153
314. De Rosa M, Gambacorta A, Nicolaus B, Chappe B, Albrecht P (1983) Isoprenoid Ethers; Backbone of Complex Lipids of the Archaebacterium *Sulfolobus solfataricus.* Biochim Biophys Acta 753:249
315. Schouten S, Hoefs MJL, Koopmans MP, Bosch HJ, Sinninghe Damsté JS (1998) Structural Characterization, Occurrence and Fate of Archaeal Ether-Bound Acyclic and Cyclic Biphytanes and Corresponding Diols in Sediments. Org Geochem 29:1305
316. Hallgren B, Larsson S (1962) The Glyceryl Ethers in the Liver Oils of Elasmobranch Fish. J Lipid Res 3:31
317. Lauer WM, Aasen AJ, Graff G, Holman RT (1970) Mass Spectrometry of Triglycerides: I. Structural Effects. Lipids 5:861
318. Aasen AJ, Lauer WM, Holman RT (1970) Mass Spectrometry of Triglycerides: II. Specifically Deuterated Triglycerides and Elucidation of Fragmentation Mechanisms. Lipids 5:869
319. Budzikiewicz H, Schäfer M (2005) Massenspektrometrie. Eine Einführung. 5. Aufl. Wiley-VCH, Weinheim, Germany, p 27
320. Cheng C, Gross ML, Pittenauer E (1998) Complete Structural Elucidation of Triacylglycerols by Tandem Sector Mass Spectrometry. Anal Chem 70:4417
321. Jensen NJ, Gross ML (1988) A Comparison of Mass Spectrometry Methods for Structural Determination and Analysis of Phospholipids. Mass Spectrom Rev 7:41
322. Klein RA (1971) Mass Spectrometry of the Phosphatidylchinolines: Fragmentation Processes for Dioleoyl and Stearoyl-Oleoyl Glycerylphosphorylcholine. J Lipid Res 12:628
323. Crawford CG, Plattner RD (1983) Ammonia Chemical Ionization Mass Spectrometry of Intact Diacyl Phosphatitylcholine. J Lipid Res 24:456
324. Wood GW, Lau PY, Rao GNS (1976) Field Desorption Mass Spectrometry of Phospholipids. II - Fragmentation of Dipalmitoylphosphatidyl Choline from Comparison of d_0, d_4 and d_9 Species. Biomed Mass Spectrom 3:172
325. Fenwick GR, Eagles J, Self R (1983) Fast Atom Bombardment Mass Spectrometry of Intact Phospholipids and Related Compounds. Biomed Mass Spectrom 10:382
326. Murphy RC, Harrison KA (1994) Fast Atom Bombardment Mass Spectrometry of Phospholipids. Mass Spectrom Rev 13:57
327. Münster H, Stein J, Budzikiewicz H (1986) Structure Analysis of Underivatized Phospholipids by Negative Fast Atom Bombardment Mass Spectrometry. Biomed Environ Mass Spectrometry 13:423
328. Münster H, Budzikiewicz H (1987) Structural Analysis of Phospholipids by Fast Atom Bombardment/Collisional Activation with a Tandem Mass Spectrometer. Rapid Commun Mass Spectrom 1:126
329. Münster H (1988) Anwendung der Fast Atom Bombardment- und Tandem-Massenspektrometrie für die Strukuraufklärung von Phospholipiden und Triglyceriden. Dissertation, Universität zu Köln, Germany

330. Hsu FF, Turk J (2003) Electrospray Ionization/Tandem Quadrupole Mass Spectrometric Studies on Phosphatidylcholines: The Fragmentation Processes. J Am Soc Mass Spectrom 14:352
331. Haroldsen PE, Gaskell SJ (1989) Quantitative Analysis of Paletelet-Activating Factor Using Fast Atom Bombardment/Tandem Mass Spectrometry. Biomed Environ Mass Spectrom 18:439
332. Ohashi Y (1984) Structure Determination of Phospholipids by Secondary Ion Mass Spectrometric Techniques: Differentiation of Isomeric Esters. Biomed Mass Spectrom 11:383
333. Han X, Gross RW (1994) Electrospray Ionization Mass Spectroscopic Analysis of Human Erythrocyte Plasma Membrane Phospholipids. Proc Natl Acad Sci USA 91:10635
334. Lehmann WD, Koester M, Erben G, Keppler D (1997) Characterization and Quantification of Rat Bile Phosphatidylcholine by Electrospray-Tandem Mass Spectrometry. Anal Biochem 246:102
335. Zehethofer N, Pinto DM (2008) Recent Developments in Tandem Mass Spectrometry for Lipodimic Analysis. Anal Chim Acta 627:62
336. Thomas MC, Mitchell TW, Blanksby SJ (2006) Ozonolysis of Phospholipid Double Bonds during Electrospray Ionization: a New Tool for Structure Determination. J Am Chem Soc 128:58
337. Thomas MC, Mitchell TW, Harman DG, Deeley JM, Murphy RC, Blanksby SJ (2007) Elucidation of Double Bond Position in Unsaturated Lipids by Ozone Electrospray Ionization Mass Spectrometry. Anal Chem 79:5013
338. Schiller J, Süß R, Fuchs B, Müller M, Zschörnik O, Arnold K (2007) MALDI-TOF MS in Lipidomics. Front Biosci 12:2568
339. Schiller J, Süß R, Arnhold J, Fuchs B, Leßig J, Müller M, Petković M, Spalteholz H, Zschörnik O, Arnold K (2004) Marix-Assisted Laser Desorption and Ionization Time-of-Flight (MALDI-TOF) Mass Spectrometry in Lipid and Phospholipid Research. Progr Lipid Res 43:449
340. Milne S, Ivanova P, Forrester J, Brown HA (2006) Lipidomics: An Analysis of Cellular Lipids by ESI-MS. Methods 39:92
341. Pulfer M, Murphy RC (2003) Electrospray Mass Spectrometry of Phospholipids. Mass Spectrom Rev 22:332
342. Domingues MRM, Reis A, Domingues P (2008) Mass Spectrometry Analysis of Oxidized Phospholipids. Chem Phys Lipids 156:1
343. Song H, Ladenson J, Turk J (2009) Algorithms for Automatic Processing of Data from Mass Spectrometric Analyses of Lipids. J Chromatogr B 877:2847
344. Khalil MB, Hou W, Zhou H, Elisma F, Swayne LA, Blanchard AP, Yao Z, Bennett SAL, Figeys D (2010) Lipidomics Era: Accomplishments and Challenges. Mass Spectrom Rev 29:877
345. Finan PA, Reed RI, Snedden W, Wilson JM (1963) Electron Impact and Molecular Dissociation. Part X. Some Studies of Glycosides. J Chem Soc:5945
346. Kochetkov NK, Wulfson NS, Chizhov OS, Zolotarev BM (1963) Mass Spectrometry of Carbohydrate Derivatives. Tetrahedron 19:2209
347. Biemann K, Schnoes HK, McCloskey JA (1963) Application of Mass Spectrometry to Structure Problems. Carbohydrates and their Derivatives. Chem Ind:448
348. Radford T, DeJongh DC (1972) Carbohydrates. In: Waller GR (ed) Biochemical Applications of Mass Spectrometry. Wiley-Interscience, New York, p 313
349. Radford T, DeJongh DC (1980) Carbohydrates. In: Waller GR, Dermer OC (eds) Biochemical Applications of Mass Spectrometry. First Supplementary Volume. Wiley-Interscience, New York, p 255
350. Heyns K, Grützmacher HF, Scharmann H, Müller D (1966) Massenspektrometrische Strukturanalysen von Kohlenhydraten. Fortschr Chem Forsch 5:448
351. Kochetkov NK, Chizhov OS (1972) Mass Spectrometry of Carbohydrates. In: Whistler RL, Bemiller JN (eds) Methods in Carbohydrate Chemistry, Academic Press, New York, vol 6, p 540

352. Budzikiewicz H, Djerasssi C, Williams DH (1964) Carbohydrates. In: Structure Eleucidation of Natural Products by Mass Spectrometry, Holden-Day, San Francisco, vol 2, p 203
353. Rodrigues JA, Taylor AM, Sumpton DP, Reynolds JC, Pickford R, Thomas-Oates J (2008) Mass Spectrometry of Carbohydrates: Newer Aspects. In: Horton D (ed) Advances in Carbohydrate Chemistry and Biochemistry, Elsevier, Amsterdam, vol 61, p 59
354. Hogg AM, Nagabhushan TL (1972) Chemical Ionization Mass Spectra of Sugars. Tetrahedron Lett 13:4827
355. Dougherty RC, Roberts JD, Binkley WW, Chizhov OS, Kadentsev VI, Solov'yov AA (1974) Ammonia-Isobutane Chemical Ionization Mass Spectra of Oligosaccharide Peracetates. J Org Chem 39:451
356. Biemann K, DeJongh DC, Schnoes HK (1963) Application of Mass Spectrometry to Structure Problems. XIII. Acetates of Pentoses and Hexoses. J Am Chem Soc 85:1763
357. Heyns K, Müller D (1966) Massenspektroskopische Untersuchungen XV. Umlagerungsreaktionen bei der durch Elektronenstoss induzierten Fragmentierung peracetylierter Pento- und Hexo-Pyranosen. Tetrahedron Lett 7:6061
358. Budzikiewicz H, Grotjahn L (1972) Massenspektroskopische Fragmentierungsreaktionen - III. Das scheinbar anomale Verhalten von 3-Hydroxytetrahydroypyransystemen. Tetrahedron 28:1881
359. Das KG, Thayumanavan B (1975) EI amd IKE Spectra of Some Aldosyl Disaccharide Peracetates. Org Mass Spectrom 10:455
360. Binkley WW, Dougherty RC, Horton D, Wander JD (1971) Physical Studies on Oligosaccharides Related to Sucrose. Part II. Mass-Spectral Identification of D-Fructofuranosyl Residues. Carbohydrate Res 17:127
361. Kochetkov NK, Chizhov OS (1965) Mass Spectrometry of Methylated Methyl Glycosides. Principles and Analytical Application. Tetrahedron 21:2029
362. Kochetkov NK, Chizhov OS (1964) Application of Mass Spectrometry to Methylated Monosaccharides Identification. Biochim Biophys Acta 83:134
363. Heyns K, Müller D (1965) Massenspektrometrische Untersuchungen - VI. Massenspektrometrische Untersuchung deuteriummarkierter Methyl-2,3,4-*O*-methyl-*β*-arabopyranoside. Tetrahedron 21:55
364. Ott AYa, Zolotarev BM, Chizhov OS (1978) New Results on the Fragmentation of Methylhexopyranosides Methyl Ethers upon Electron Impact. Изв Акад Наук, Сер Хим 377 (Russian Chem Bull 27:325)
365. Ott AYa, Zolotarev BM, Chizhov OS (1979) Synthesis and Mass Spectra of Selectively Deuterated *β*-Methyl-2,3,4-tri-*O*-methyl-L-arabinopyoranosides. Изв Акад Наук, Сер Хим 1915 (Russian Chem Bull 28:178)
366. De Jongh DC, Biemann K (1963) Application of Mass Spectrometry to Structure Problems. XIV. Acetates of Partially Methylated Pentoses and Hexoses. J Am Chem Soc 85:2289
367. Petersson G, Samuelson O (1968) Determination of the Number and Position of Methoxyl Groups in Methylated Aldopentoses by Mass Spectrometry of their Trimethylsilyl Derivatives. Svensk Papperstidning 71:77
368. Petersson G, Samuelson O (1968) Determination of the Number and Position of Methoxyl Groups in Methylated Aldohexoses by Mass Spectrometry of their Trimethylsilyl Derivatives. Svensk Papperstidning 71:731
369. König WA, Bauer H, Voelter W, Bayer E (1973) Gaschromatographie und Massenspektrometrie trifluoracetylierter Kohlenhydrate. Chem Ber 106:1905
370. Chizhov OS, Molodtsov NV, Kochetkov NK (1967) Mass Spectrometry of Trimethylsilyl Ethers of Carbohydrates. Carbohyd Res 4:273
371. DeJongh DC, Radford T, Hribar JD, Hanessian S, Bieber M, Dawson G, Sweeley CC (1969) Analysis of Trimethylsilyl Derivatives of Carbohydrates by Gas Chromatography and Mass Spectrometry: J Am Chem Soc 91:1728
372. Karady S, Pines SH (1970) Mass Spectrometry of the Trimethylsilyl Ethers of 2-Ketohexoses. Tetrahedron 26:4527

373. Reinhold VN, Wirtz-Peiz F, Biemann K (1974) Synthesis, Gas-liquid Chromatography, and Mass Spectrometry of Per-*O*-trimethylsilyl Carbohydrate Boronates. Carbohyd Res 37:203
374. Robinson DS, Eagles J, Self R (1973) The Mass Spectra of Benzeneboronate Derivatives of some Hexopyranosides. Carbohyd Res 26:204
375. De Jongh DC, Biemann K (1964) Mass Spectra of *O*-Isopropylidene Derivatives of Pentoses and Hexoses. J Am Chem Soc 86:67
376. DeJongh DC (1965) Mass Spectrometry in Carbohydrate Chemistry. Dithioacetals of Common Monosaccharides. J Org Chem 30:1563
377. Zaia J (2004) Mass Spectrometry of Oligosaccharides. Mass Spectrom Rev 23:161
378. An HJ, Lebrilla CB (2011) Structure Elucidation of Native N- and O-linked Glycans by Tandem Mass Spectrometry (Tutorial). Mass Spectrom Rev 30:560
379. Moor J, Waight ES (1975) The Mass Spectra of Permethylated Oligosaccharides. Biomed Mass Spectrom 2:36
380. Kamerling JP, Vliegenthart JFG, Vink J, de Ridder JJ (1972) Mass Spectrometry of Pertrimethylsilyl Oligosaccharides Containing Fructose Units. Tetrahedron 28:4375
381. Kotchetkov NK, Chizhov OS, Molodtsov NV (1968) Mass Spectrometry of Oligosaccharides. Tetrahedron 24:5587
382. Domon B, Costello CE (1988) A Systematic Nomenclature for Carbohydrate Fragmentations in FAB-MS/MS Spectra of Glycoconjugates. Glycoconjugate J 5:397
383. Moor J, Waight ES (1974) The Field Desorption Mass Spectra of Some Oligosaccharides and Their Permethylates and Peracetylates. J Mass Spectrom 9:903
384. Dell A, Morris HR, Egge H, von Nicolai H, Strecker G (1983) Fast-Atom-Bombardment Mass-Spectrometry for Carbohydrate-Structure Determination. Carbohydr Res 115:41
385. Egge H, Peter-Katalinć J (1987) Fast Atom Bombardment Mass Spectrometry for Structural Elucidation of Glycoconjugates. Mass Spectrom Rev 6:331
386. Carr SA, Reinhold VN, Green BN, Hass JR (1985) Enhancement of Structural Information in FAB Ionized Carbohydrate Samples by Neutral Gas Collision. Biomed Mass Spectrom 12:288
387. Reinhold VN, Reinhold BB, Costello CE (1995) Carbohydrate Molecular Weight Profiling, Sequence, Linkage, and Branching Data: ES-MS and CID. Anal Chem 67:1772
388. Harvey DJ (2006) Analysis of Carbohydrates and Glycoconjugates by Matrix-Assisted Laser Desorption/Ionization Mass Spectrometry: an Update Covering the Period 1999-2000. Mass Spectrom Rev 25:595
389. Harvey DJ (1999) Matrix-assisted Laser Desorption/Ionization Mass Spectrometry of Carbohydrates. Mass Spectrom Rev 18:349
390. Park Y, Lebrilla CB (2005) Application of *Fourier* Transform Ion Cyclotron Resonance Mass Spectrometry to Oligosaccharides. Mass Spectrom Rev 24:232
391. Asam MR, Glish GR (1997) Tandem Mass Spectrometry of Alkali Cationized Polysaccharides in a Quadrupole Ion Trap. J Am Soc Mass Spectrom 8:987
392. Domon B, Müller DR, Richter WJ (1990) High Performance TandemMass Spectrometry for Sequence, Branching and Interglycosidic Linkage Analysis of Peracetylated Oligosaccharides. Biomed Mass Spectrom 19:390
393. Viseux N, de Hoffmann E, Domon B (1997) Structural Analysis of Permethylated Oligosaccharides by Electrospray Tandem Mass Spectrometry. Anal Chem 69:3193
394. König S, Leary JA (1998) Evidence for Linkage Position Determination in Cobalt Coordinated Pentasaccharides Using Ion Trap Mass Spectrometry. J Am Soc Mass Spectrom 9:1125
395. Gaucher SP, Morrow J, Leary JA (2000) STAT: A Saccharide Topology Analysis Tool Used in Combination with Tandem Mass Spectrometry. Anal Chem 72:2331
396. Chizhov AO, Dell A, Morris HR, Reason AJ, Haslam SM, McDowell RA, Chizhov OS, Usov AI (1998) Structural Analysis of Laminarans by MALDI and FAB Mass Spectrometry. Carbohydr Res 310:203
397. Yamagaki T, Ishizuka Y, Kawabata SI, Nakanishi H (1996) Post-Source Decay Fragment Spectra of Cyclomalto-Octaose and Branched Cyclomalto-Hexaose by Matrix-Assisted

Laser Desorption/Ionization Time-of-Flight Mass Spectrometry. Rapid Commun Mass Spectrom 10:1887
398. Ralet MC, Lerouge P, Quéméner B (2009) Mass Spectrometry for Pectin Structure Analysis. Carbohydr Res 344:1798
399. Nemeth JF, Hochensang GP Jr, Marnett LJ, Caprioli RM (2001) Characterization of the Glycosylation Sites in Cyclooxygenase-2 Using Mass Spectrometry. Biochemistry 40:3109
400. Banoub JH, El Aneed A, Cohen AM, Joly N (2010) Structural Investigation of Bacterial Lipopolysaccharides by Mass Spectrometry and Tandem Mass Spectrometry. Mass Spectrom Rev 29:606
401. Vukics V, Guttman A (2010) Structural Characterization of Flavonoid Glycosides by Multi-Stage Mass Spectrometry. Mass Spectrom Rev 29:1
402. Wuhrer M, Deelder AM, Hokke CH (2005) Protein Glycosylation Analysis by Liquid Chromatography-Mass Spectrometry. J Chromatogr B 825:124
403. Morelle W, Michalski JC (2005) The Mass Spectrometric Analysis of Glycoproteins and Their Glycan Structures. Curr Anal Chem 1:29
404. Goletz S, Thiede B, Hanisch FG, Schultz M, Peter-Katalinic J, Müller S, Seitz O, Karsten U (1997) A Sequencing Strategy for the Localization of O-Glycosylation Sites of MUC1 Tandem Repeats by PSD-MALDI Mass Spectrometry. Glycobiology 7:881
405. Sheeley DM, Reinhold VN (1998) Structural Characterization of the Carbohydrate Sequence, Linkage, and Branching in a Quadrupole Ion Trap Mass Spectrometer: Neutral Oligosaccharides and N-Linked Glycans. Anal Chem 70:3053
406. Mirgorodskaya E, Roepstorff P, Zubarev RA (1999) Localization of O-Glycosylation Sites in Peptides by Electron Capture Dissociation in a *Fourier* Transform Mass Spectrometer. Anal Chem 71:4431
407. O'Neill MA, Roberts K (1981) Methylation Analysis of the Cell Wall Glycoproteins and Glycopeptides from *Chlamydomonas reinhardii.* Phytochemistry 20:25
408. Kilz S, Waffenschmidt S, Budzikiewicz H (2000) Mass Spectrometric Analysis of Hydroxyproline Glycans. J Mass Spectrom 35:689
409. Bollig K, Lamshöft M, Schweimer K, Marner FJ, Budzikiewicz H, Waffensschmidt S (2007) Structural Analysis of Linear Hydroxyproline-Bound *O*-Glycans of *Chlamydomonas reinhardtii* - Conservation of the Inner Core in *Chlamydomonas* and Land Plants. Carbohydr Res 342:2557
410. Budzikiewicz H, Schäfer M (2005) Massenspektrometrie. Eine Einführung. 5. Aufl. Wiley-VCH, Weinheim, Germany, p 151
411. Küster B, Mann M (1999) ^{18}O-Labeling of N-Glycosylation Sites to Improve the Identification of Gel-Separated Glycoproteins Using Peptide Mass Mapping and Database Searching. Anal Chem 71:1431
412. Patwa T, Li C, Simeone DM, Lubman DM (2010) Glycoprotein Analysis Using Protein Microarrays and Mass Spectrometry. Mass Spectrom Rev 29:830
413. Andersson CO (1958) Mass Spectrometric Studies on Amino Acids and Peptide Derivatives. Acta Chem Scand 12:1353
414. Biemann K, Seibl J, Gapp F (1961) Mass Spectra of Organic Molecules. I. Ethyl Esters of Amino Acids. J Am Chem Soc 83:3795
415. Andersson CO, Ryhage R, Ställberg-Stenhagen S, Stenhagen E (1962) Mass Spectrometric Studies IX. Methyl and Ethyl Esters of some Aliphatic α-Amino Acids. Arkiv Kemi 19:405
416. Budzikiewicz H, Djerassi C, Williams DH (1967) Mass Spectrometry of Organic Compounds. Holden-Day, San Francisco, p 297
417. Barbier M, Bogdanovsky D, Vetter W, Lederer E (1963) Synthese und Eigenschaften des Lycomarasmins und der Aspergillomarasmine. Liebigs Ann Chem 668:132
418. Heyns K, Grützmacher HF (1961) Die Massenspektren der *N*-Formyl-α-aminosäure-methylester. Z Naturforsch 16b:293
419. Manusadzhyan VG, Varshavskii YaM (1964) Application of the Mass-Spectrometric Method to the Study of Derivatives of Amino Acids and Short Peptides. I. Study of Possibilities of

Identifying of Amino Acids from the Characteristic Peaks in the Mass Spectra of the Esters of their *N*-Acyl Derivatives. Извест Акад Наук Армян ССР 17:137

420. Heyns K, Grützmacher HF (1963) Massenspektrometrische Untersuchungen, III. Massenspektren von freien und *N*-acetylierten Aminosäuren. Liebigs Ann Chem 667:194

421. Andersson CO, Ryhage R, Stenhagen E (1962) Mass Spectrometric Studies X. Methyl and Ethyl Esters of N-Acetylamino Acids. Arkiv Kemi 19:417

422. Biemann K, Lioret C, Asselineau J, Lederer E, Polonsky J (1960) On the Structure of Lysopine, a New Amino Acid Isolated from Crown Gall Tissue. Biochim Biophys Acta 40:369

423. Milne GWA, Axenrod T, Fales HM (1970) Chemical Ionization Mass Spectrometry of Complex Molecules. IV. Amino Acids. J Am Chem Soc 92:5170

424. Hušek P, Macek K (1975) Gas Chromatography of Amino Acids. J Chromatogr 113:139

425. Baker KM, Shaw MA, Williams DH (1969) Mass Spectra of Trimethylsilyl Derivatives of Some Amino-Acids and Peptides. Chem Commun:1108

426. Biermann CJ, Kinoshita CM, Marlett JA, Steele RD (1986) Analysis of Amino Acids as *tert*.-Butyldimethylsilyl Derivatives by Gas Chromatography. J Chromatogr A 357:330

427. Huang ZH, Wang J, Gage DA, Watson JT, Sweeley CC, Hušek P (1993) Characterization of N-Ethoxycarbonyl Ethyl Esters of Amino Acids by Mass Spectrometry. J Chromatogr 635:271

428. Dallakian P, Budzikiewicz H (1997) Gas Chromatography-Chemical Ionization Mass Spectrometry in Amino Acid Analysis of Pyoverdins. J Chromatogr 787:195

429. Leimer KR, Rice RH, Gehrke CW (1977) Complete Mass Spectra of *N*-Trifluoroacetyl-*n*-butyl Esters of Amino Acids. J Chromatogr 141:121

430. Demange P, Abdallah MA, Frank H (1988) Assignment of the Configurations of the Amino Acids in Peptidic Siderophores. J Chromatogr 438:291

431. Metges CC, Petzke KJ, Henning U (1996) Gas Chromatography/Combustion/Isotope Ratio Mass Spectrometric Comparison of *N*-Acetyl- and *N*-Pivaloyl Amino Acid Esters to Measure ^{15}N Isotopic Abundances in Physiological Samples: A Pilot Study of Amino Acid Synthesis in the Upper Gastro-intestinal Tract of Minipigs. J Mass Spectrom 31:367

432. Low GKC, Duffield AM (1984) Positive and Negative Ion Chemical Ionization Mass Spectra of Amino Acid Carboxy-*n*-butyl Ester *N*-Pentafluoropropionate Derivatives. Biomed Mass Spectrom 11:223

433. Dallakian P, Voss J, Budzikiewicz H (1999) Assignment of the Absolute Configuration of the Amino Acids of Pyoverdins by GC/MS. Chirality 11:381

434. Roepstorff P, Fohlman J (1984) Proposal for a Common Nomenclature for Sequence Ions in Mass Spectra of Peptides. Biomed Mass Spectrom 11:601

435. Biemann K, Vetter W (1960) Separation of Peptide Derivatives by Gas Chromatography Combined with the Mass Spectrometric Determination of the Amino Acid Sequence. Biochem Biophys Res Commun 3:578

436. Biemann K, Gapp F, Seibl J (1959) Application of Mass Spectrometry to Structure Problems. I. Amino Acid Sequence in Peptides. J Am Chem Soc 81:2274

437. Chesnov S, Bigler L, Hesse M (2000) The Spider *Paracoelotes birulai*: Detection and Structure Elucidation of New Acylpolyamines by On-line Coupled HPLC-APCI-MS and HPLC-APCI-MS/MS. Helv Chim Acta 83:3295

438. Chesnov S, Bigler L, Hesse M (2001) The Acylpolyamines from the Venom of the Spider *Aglenopsis aperta.* Helv Chim Acta 84:2178

439. Stenhagen E (1961) Massenspektrometrie als Hilfsmittel bei der Strukturbestimmung organischer Verbindungen, besonders bei Lipiden und Peptiden. Fresenius Z Anal Chem 181:462

440. Weygand F, Prox A, Fessel HH, Sun KK (1965) Massenspektrometrische Sequenzanalyse von Peptiden als *N*-Trifluoracetyl-peptid-ester. Z Naturforsch B 20:1169

441. Shemyakin MM (1968) Primary Structure Determination of Peptides and Proteins by Mass Spectrometry. Pure Appl Chem 17:313

442. Barber M, Jollès P, Vilkas E, Lederer E (1965) Determination of Amino Acid Sequences in Oligopeptides by Mass Spectrometry. I. The Structure of Fortuitine, an Acylnonapeptide Methyl Ester. Biochem Biophys Res Commun 18:469

443. Bricas E, van Heijenoort J, Barber M, Wolstenholme WA, Das BC, Lederer E (1965) Determination of Amino Acid Sequences in Oligopeptides by Mass Spectrometry. IV. Synthetic *N*-Acyl Oligopeptide Methyl Esters. Biochemistry 4:2254
444. van Heijenoort J, Bricas E, Das BC, Lederer E, Wolstenholme WA (1967) Détermination de sequences d'acides aminés dans des oligopeptides par la spectrometrie de masse - IX. (A) Acylation avec de nouveaux radicaux mixtes; (B) peptides contenant des acides aminés trifonctionels. Tetrahedron 23:3403
445. Das BP, Gero SD, Lederer E (1967) N-Methylation of *N*-Acyl Amino Acids. Biochem Biophys Res Commun 29:211
446. Thomas DW, Das BC, Géro SD, Lederer E (1968) Advantages and Limitations of the Mass Spectrometric Sequence Determination of Permethylated Oligopeptide Derivatives. Biochem Biophys Res Commun 32:199
447. Biemann K, Cone C, Webster BR (1966) Computer-Aided Interpretation of High-Resolution Mass Spectra. II. Amino Acid Sequence of Peptides. J Am Chem Soc 88:2597
448. Senn M, Venkataraghavan R, McLafferty FW (1966) Mass Spectrometric Studies of Peptides. III. Automated Determination of Amino Acid Sequences. J Am Chem Soc 88:5593
449. Winkler HU, Beckey HD (1972) Field Desorption Mass Spectrometry of Amino Acids. Org Mass Spectrom 6:655
450. Winkler HU, Beckey HD (1972) Field Desorption Mass Spectrometry of Peptides. Biochem Biophys Res Commun 46:391
451. Asante-Poku S, Wood GW, Schmidt DE Jr (1975) Field Desorption Mass Spectra of the Peptides Pro-Leu-Gly-NH_2, Cbz-Gly-Pro-Leu-Gly-Pro and Bradykinin. Biol Mass Spectrom 2:121
452. Barber M, Bordoli RS, Garner GV, Gordon DB, Sedgwick RD, Tetler LW, Tyler AN (1981) Fast-Atom Bombardment Mass Spectra of Enkephalins. Biochem J 197:401
453. Ziegler R, Eckart K, Schwarz H, Keller R (1985) Amino Acid Sequence of *Manduca sexta* Adipokinetic Hormone Elucidated by Combined Fast Atom Bombardment (FAB)/Tandem Mass Spectrometry. Biochem Biophys Res Commun 133:337
454. Pettit GR, Kamano Y, Herald CL, Tuinman AA, Boettner FE, Kizu H, Schmidt JM, Baczynskyj L, Tomer KB, Bontems RJ (1987) The Isolation and Structure of a Remarkable Marine Animal Antineoplastic Constituent: Dolastatin 10. J Am Chem Soc 109:6883
455. Barber M, Bordoli RS, Sedgwick RD, Tyler AN, Garner GV, Gordon DB, Tetler LW, Hider RC (1982) Fast Atom Bombardment Mass Spectrometry of the Large Oligopeptides Melittin, Glucagon and the B-Chain of Bovine Insulin. Biol Mass Spectrom 9:265
456. Harrison AG, Yalcin T (1997) Proton Mobility in Protonated Amino Acids and Peptides. Int J Mass Spectrom Ion Proc 165:339
457. Boyd R, Somogyi Á (2010) The Mobile Proton Hypothesis in Fragmentation of Protonated Peptides: a Perspective. J Am Soc Mass Spectrom 21:1275 and Contributions Following in the "Focus: Mobile Proton Model" Series
458. Dunbar RC, Polfer NC, Berden G, Oomens J (2012) Metal Ion Binding to Peptides: Oxygen or Nitrogen Sites? Int J Mass Spectrom 330-332:71
459. Buzikiewicz H (2004) Siderophores of the Pseudomonadaceae *sensu stricto* (Fluoresccent and Non-fluorescent *Pseudomonas* spp.). In: Herz W, Falk H, Kirby GW (eds) Progress in the Chemistry of Organic Natural Products. Springer-Verlag, Wien, Austria, vol 87, p 81
460. Fuchs R, Budzikiewicz H (2001) Structural Studies of Pyoverdins by Mass Spectrometry. Curr Org Chem 5:265
461. Fuchs R, Budzikiewicz H (2001) Rerrangement Reactions in the Electrospray Ionization Mass Spectra of Pyoverdins. Int J Mass Spectrom 210/211:603
462. Harrison AG (2009) To b or not to b: the Ongoing Saga of Peptide b Ions. Mass Spectrom Rev 28:640
463. Pauwelyn E, Huang CJ, Ongena M, Leclère V, Jacques P, Bleyaert P, Budzikiewicz H, Schäfer M, Höfte M. 2013. New Linear Lipopeptides Produced by *Pseudomonas cichorii* SF1-54 are Involved in Virulence, Swarming Motility, and Biofilm Formation. Mol Plant-Microbe Interact 26:585

464. Meyer JM, Gruffaz C, Raharinosy V, Bezverbnaya I, Schäfer M, Budzikiewicz H (2008) Siderotyping of Fluorescent *Pseudomonas*: Molecular Mass Determination by Mass Spectrometry as a Powerful Pyoverdine Siderotyping Method. Biometals 21:259
465. Behrendt U, Ulrich A, Schumann P, Meyer JM, Spröer C (2007) *Pseudomonas lurida* sp. nov., a Fluorescent Species Associated with the Phyllosphere of Grasses. Int J Syst Evol Microbiol 57:979
466. Buckley M, Kansa SW, Howard S, Campbell S, Thomas-Oates J, Collins M (2010) Distinguishing between Archeological Sheep and Goat Bones Using a Single Collagen Peptide. J Archaeolog Sci 37:13
467. Hurtado PP, O'Connor PB (2012) Differentiation of Isomeric Amino Acid Residues in Proteins and Peptides using Mass Spectrometry. Mass Spectrom Rev 31:609
468. Svec H, Junk GA (1964) The Mass Spectra of Dipeptides. J Am Chem Soc 86:2278
469. Belič I, Cimerman A, Sočič H (1972) Cyclo (Proline-Leucine) - a Metabolite of *Nocardia restricta.* Mikrobiologija 9:251
470. Ginz M, Engelhardt UH (2000) Identification of Proline-Based Diketopiperazines in Roasted Coffee. J Agric Food Chem 48:3528
471. Ginz M, Engelhardt UH (2001) Identification of New Diketopiperazines in Roasted Coffee. Eur Food Res Technol 213:8
472. Tomer KB, Crow FW, Gross ML, Kopple KD (1984) Fast Atom Bombardment Combined with Tandem Mass Spectrometry for the Determination of Cyclic Peptides. Anal Chem 56:880
473. Havliček V, Jegorov A, Sedmera P, Ryska M (1993) Sequencing of Cyclosporins by Fast Atom Bombardment and Linked-scan Mass Spectrometry. Org Mass Spectrom 28:1440
474. Kuzma M, Jegorov A, Hesso A, Tornaeus J, Sedmera P, Havliček V (2002) Role of Amino Acid *N*-Methylation in Cyclosporins on Ring Opening and Fragmentation Mechanisms During Collisionally Induced Dissociation in an Ion Trap. J Mass Spectrom 37:292
475. Havliček V, Jegorov A, Sedmera P, Wagner-Redeker W, Ryska M (1995) Distinguishing Isobaric Amino Acids in Sequence Analysis of Cyclosporins by Fast Atom Bombardment and Linked-Scan Mass Spectrometry. J Mass Spectrom 30:940
476. Eckart K, Schwarz H, Tomer KB, Gross ML (1985) Tandem Mass Spectrometry Methodology for the Sequence Determination of Cyclic Peptides J Am Chem Soc 107:6765
477. Voßen W, Fuchs R, Taraz K, Budzikiewicz H (2000) Can a Peptide Chain of a Pyoverdin Be Bound by an Ester Bond to the Chromophore? - The Old Problem of Pseudobactin 7SR1. Z Naturforsch 55c:153
478. Nakamura T, Nagaki H, Kinoshita T (1986) Amino Acid Sequence Determination of Cyclic Peptides by Tandem Mass Spectrometry Coupled with Fast Atom Bombardment Ionization. Mass Spectrosc 34:307
479. Fehlhaber HW (1968) Massenspektrometrische Strukturermittlung von Peptid-Alkaloiden. Fresenius Z Anal Chem 235:91
480. Giacomelli SR, Maldaner G, Gonzaga WA, Garcia CM, da Silva UF, Dalcol II, Morel AF (2004) Cyclic Peptide Alkaloids from the Bark of *Discaria americana.* Phytochemistry 65:933
481. Garcia BA (2010) What Does the Future Hold for Top Down Mass Spectrometry? J Am Soc Mass Spectrom 21:193
482. Wiśniewski JR, Zougman A, Nagaraj N, Mann M (2009) Universal Sample Preparation Method for Proteome Analysis. Nat Methods 6:359
483. Kelleher NL (2004) Top-Down Proteomics. Anal Chem 76:196A
484. Zhang J, Dong X, Hacker TA, Ge Y (2010) Deciphering Modifications in Swine Cardiac Troponin I by Top-Down High-Resolution Tandem Mass Spectrometry. J Am Soc Mass Spectrom 21:940
485. Lubec G, Afjehi-Sadat L (2007) Limitations and Pitfalls in Protein Identification by Mass Spectrometry. Chem Rev 107:3568
486. Hernandez P, Gras R, Frey J, Appel RD (2003) Popitam: Towards New Heuristic Strategies to Improve Protein Identification from Tandem Mass Spectrometry Data. Proteomics 3:870

487. Bradshaw RA, Medzihradszky KF; Chalkley RJ (2010) Protein PTMs: Post-Translational Modifications or Pesky Trouble Makers? J Mass Spectrom 45:1095
488. Gibson BW, Biemann K (1984) Strategy for the Mass Spectrometric Verification and Correction of the Primary Structures of Proteins Deduced from their DNA Sequences. Proc Natl Acad Sci USA 81:1956
489. Bienvenut WV, Müller M, Palagi PM, Gasteiger E, Heller M, Jung E, Giron M, Gras R, Gay S, Binz PA, Hughes GJ, Sanchez JC, Appel RD, Hochstrasser DF (2001) Proteomics and Mass Spectrometry: Some Aspects and Recent Developments. In: Housby JN (ed) Mass Spectrometry and Genomic Analysis, Kluwer Academic Publishers, Dordrecht, The Netherlands, p 93
490. Giron P, Dayon L, Sanchez JC (2011) Cysteine Tagging of MS-Based Proteomics. Mass Spectrom Rev 30:366
491. Wang Z, Zhang Y, Zhang H, Harrington PB, Chen H (2012) Fast and Selective Modification of Thiol Proteins/Peptides by *N*-(Phenylseleno)phtalimide. J Am Soc Mass Spectrom 23:520
492. Boersema PJ, Mohammed S, Heck AJR (2009) Phosphopeptide Fragmentation and Analysis by Mass Spectrometry. J Mass Spectrom 44:861
493. Wind M, Edler M, Jakubowski N, Linscheid M, Wesch H, Lehmann WD (2001) Analysis of Protein Phosphorylation by Capillary Liquid Chromatography Coupled to Element Mass Spectrometry with ^{31}P Detection and to Electrospray Mass Spectrometry. Anal Chem 73:29
494. Wind M, Wesch H, Lehmann WD (2001) Protein Phosphorylation Degree: Determination by Capillary Liquid Chromatography and Inductively Coupled Plasma Mass Spectrometry. Anal Chem 73:3006
495. Palumbo AM, Smith SA, Kalcic CL, Dantus M, Stemmer PM, Reid GE (2011) Tandem Mass Spectrometry Strategies for Phosphoproteome Analysis. Mass Spectrom Rev 30:600
496. Rožman M (2011) Modelling of the Gas-Phase Phosphate Group Loss and Rearrangement in Phosphorylated Peptides. J Mass Spectrom 46:949
497. Sharon M (2010) How Far Can We Go with Structural Mass Spectrometry of Protein Complexes? J Am Soc Mass Spectrom 21:487
498. Ruotolo BT, Benesch JLP, Sandercock AM, Hyung SJ, Robinson CV (2008) Ion Mobility-Mass Spectrometry Analysis of Large Protein Complexes. Nat Prot 3:1139
499. Uetrecht C, Versluis C, Watts NR, Wingfield PT, Steven AC, Heck AJR (2008) Stability and Shape of Hepatitis B Virus Capsids *in Vacuo*. Angew Chem 120:6343
500. Loo JA, Berhane B, Kaddis CS, Wooding KM, Xie Y, Kaufman SL, Chernushevich IV (2005) Electrospray Ionization Mass Spectrometry and Ion Mobility Analysis of the 20S Proteasome Complex. J Am Soc Mass Spectrom 16:998
501. Serpa JJ, Parker CE, Petrochenko EV, Han J, Pan J, Borchers CA (2012) Mass Spectrometry-Based Structural Proteomics. Eur J Mass Spectrom 18:251
502. Hall Z, Robinson CV (2012) Do Charge State Signatures Guarantee Protein Conformations? J Am Soc Mass Spectrom 23:1161
503. Konermann L, Douglas DJ (1998) Unfolding of Proteins Monitored by Electrospray Ionization Mass Spectrometry: A Comparison of Positive and Negative Ion Modes. J Am Soc Mass Spectrom 9:1248
504. Sterling HJ, Daly MP, Feld GK, Thoren KL, Kintzer AF, Krantz BA, Williams ER (2010) Effects of Supercharging Reagents on Noncovalent Complex Structure in Electrospray Ionization from Aqueous Solutions. J Am Soc Mass Spectrom 21:1762
505. Englander SW (2000) Protein Folding Intermediates and Pathways Studied by Hydrogen Exchange. Annu Rev Biophys Biomol Struct 29:213
506. Rob T, Wilson DJ (2012) Time-Resolved Mass Spectrometry for Monitoring Milisecond Time-Scale Solution-Phase Processes. Eur J Mass Spectrom 18:205
507. Wales TE, Engen JR (2006) Hydrogen Exchange Mass Spectrometry for the Analysis of Protein Dynamics. Mass Spectrom Rev 25:158
508. Marcisin SR, Engen JR (2010) Hydrogen Exchange Mass Spectrometry: What It Is and What It Can Tell Us. Anal Bioanal Chem 397:967

509. Iacob RE, Engen JR (2012) Hydrogen Exchange Mass Spectrometry: Are We Out of the Quicksand? J Am Soc Mass Spectrom 23:1003
510. Kiselar JG, Chance MR (2010) Future Directions of Structural Mass Spectrometry Using Hydroxyl Radical Footprinting. J Mass Spectrom 45:1373
511. Goshe MB, Chen YH, Anderson VE (2000) Identification of Sites of Hydroxyl Radical Reaction with Peptides by Hydrogen/Deuterium Exchange: Prevalence of Reactions with Side Chains. Biochemistry 39:1761
512. Liu Z, Cheng S, Gallie DR, Julian RR (2008) Exploring the Mechanism of Selective Noncovalent Adduct Protein Probing Mass Spectrometry Utilizing Site-Directed Mutagenesis to Examine Ubiquitin. Anal Chem 80:3846
513. Sinz A (2006) Chemical Cross-Linking and Mass Spectrometry to Map Three-Dimensional Protein Structures and Protein-Protein Interactions. Mass Spectrom Rev 25:663
514. Petrotchenko EV, Borchers CH (2010) Crosslinking Combined with Mass Spectrometry for Structural Proteomics. Mass Spectrom Rev 29:862
515. Müller MQ, Dreiocker F, Ihling CH, Schäfer M, Sinz A (2010) Cleavable Cross-Linker for Protein Structure Analysis: Reliable Identification of Cross-linking Products by Tandem MS. Anal Chem 82:6958
516. Clifford-Nunn B, Showalter HDH, Andrews PC (2012) Quaternary Diamines as Mass Spectrometry Cleavable Crosslinkers for Protein Interactions. J Am Soc Mass Spectrom 23:201
517. Falvo F, Fiebig L, Dreiocker F, Wang R, Armentrout PB, Schäfer M (2012) Fragmentation Reactions of Thiourea- and Urea-Compounds Examined by Tandem MS-, Energy-Resolved CID Experiments, and Theory. Int J Mass Spectrom 330-332:124
518. Kaltashov IA, Eyles SJ (2002) Studies of Biomolecular Conformations and Conformational Dynamics by Mass Spectrometry. Mass Spectrom Rev 21:37
519. Fabris D, Yu ET (2010) Elucidating the Higher-Order Structure of Biopolymers by Structural Probing and Mass Spectrometry: MS3D. J Mass Spectrom 45:841
520. Kitova EN, El-Haviet A, Schnier PD, Klassen JS (2012) Reliable Determinations od Protein-Ligands Interactions by Direct ESI-MS Measurements. Are We There Yet? J Am Soc Mass Spectrom 23:431
521. Brand GD, Salbo R, Jørgensen TJD, Bloch C Jr, Erba BE, Robinson CV, Tanjoni I, Mourada-Silva AM, Roepstorff P, Domont GB, Perales J, Valente RH, Neves-Ferreira AGC (2012). The Interaction of the Antitoxin DM43 with a Snake Venom Metalloproteinase Analyzed by Mass Spectrometry and Surface Plasmon Resonance. J Mass Spectrom 47:567
522. Cornett DS, Reyzer ML, Chaurand P, Caprioli RM (2007) MALDI Imaging Mass Spectrometry: Molecular Snapshots of Biochemical Systems. Nat Methods 4:828
523. Rauser S, Marquardt C, Balluff B, Deininger SO, Albers C, Belau E, Hartmer R, Suckau D, Specht K, Ebert MP, Schmitt M, Aubele M, Höfler H, Walch A (2010) Classsification of HER2 Receptor Status in Breast Cancer Tissues by MALDI Imaging Mass Spectrometry. J Proteome Res 9:1854
524. McDonnell LA, Heeren RMA (2007) Imaging Mass Spectrometry. Mass Spectrom Rev 26:606
525. van Duijn E (2010) Current Limitations in Native Mass Spectrometry Based Structural Biology. J Am Soc Mass Spectrom 21:971
526. Crain PF (1990) Mass Spectrometric Techniques in Nucleic Acid Research. Mass Spectrom Rev 9:505
527. Koomen JM, Russell WK, Tichy SE, Russell DH (2002) Accurate Mass Measurement of DNA Oligonucleotide Ions Using High-Resolution Time-of-Flight Mass Spectrometry. J Mass Spectrom 37:357
528. Huber CG, Oberacher H (2001) Analysis of Nucleic Acids by On-line Liquid Chromatography-Mass Spectrometry. Mass Spectrom Rev 20:310
529. Nordhoff E, Kirpekar F, Roepstorff P (1996) Mass Spectrometry of Nucleic Acids. Mass Spectrom Rev 15:67

530. Limbach PA (1996) Indirect Mass Spectrometric Methods for Characterizing and Sequencing Oligonucleotides. Mass Spectrom Rev 15:297
531. Hofstadler SA, Sannes-Lowery KA, Hannis JC (2005) Analysis of Nucleic Acids by FTICR MS. Mass Spectrom Rev 24:265
532. Slowikowski DL, Schram KH (1985) Fast Atom Bombardment Mass Spectrometry of Nucleosides, Nucleotides and Oligonucleotides. Nucleosides Nucleotides 4:309
533. Rice JM, Dudek GO, Barber M (1965) Mass Spectra of Nucleic Acid Derivatives. Pyrimidines. J Am Chem Soc 87:4569
534. Rice JM, Dudek GO (1967) Mass Spectra of Nucleic Acid Derivatives. II. Guanine, Adenine, and Related Compounds. J Am Chem Soc 89:2719
535. McCloskey JA (1974) Mass Spectrometry. In: Ts'o POP (ed) Basic Principles in Nucleic Acid Chemistry, vol 1. Academic Press, New York, p 209
536. Hignite C (1970) Nucleic Acids and Derivatives. In: Waller GR (ed) Biochemical Applications of Mass Spectrometry. Wiley-Interscience, New York, p 429
537. Biemann K, McCloskey JA (1962) Application of Mass Spectrometry to Structure Problems. VI. Nucleosides. J Am Chem Soc 84:2005
538. von Minden DL, McCloskey JA (1973) Mass Spectrometry of Nucleic Acid Components. *N*,*O*-Permethyl Derivatives of Nucleosides. J Am Chem Soc 95:7480
539. Hunt DF, Shabanowitz J, Botz FK (1977) Chemical Ionization Mass Spectrometry of Salts and Thermally Labile Organics with Field Desorption Emitters as Solids Probes. Anal Chem 49:1160
540. Schulten RH, Beckey HD (1973) High Resolution Field Desorption Mass Spectrometry - I: Nucleosides and Nucleotides. Org Mass Spectrom 7:861
541. Crow FW, Tomer KB, Gross ML, McCloskey JA, Bergstrom DE (1984) Fast Atom Bombardment Combined with Tandem Mass Spectrometry for the Determination of Nucleosides. Anal Biochem 139:243
542. Fukushima K, Arai T (1978) Field Desorption Mass Spectrometry of Nucleoside Antibiotics. J Antibiot 31:377
543. Hignite C (1980) Nucleic Acids and Derivatives. In: Waller GR, Dermer OC (eds) Biochemical Applications of Mass Spectrometry. First Supplementary Volume. Wiley-Interscience, New York, p 527
544. Budzikiewicz H (1974) Biochemical Applications of Mass Spectrometry. Adv Mass Spectrom 6:163
545. Lawson AM, Stillwell RN, Tacker MM, Tsuboyama K, McCloskey JA (1971) Mass Spectrometry of Nucleic Acid Components. Trimethylsilyl Derivatives of Nucleotides. J Am Chem Soc 93:1014
546. Pettit GR, Einck JJ, Brown P (1978) Structural Biochemistry. 15 - Mass Spectrometry of Permethylated Nucleotides. Biomed Mass Spectrom 5:153
547. Budzikieiwicz H, Feistner G (1978) Mass Spectrosocopic Differentiation between 3′- and 5′-Nucleoside Monophosphoric Acids. Biomed Mass Spectrom 5:512
548. Budzikiewicz H, Linscheid M (1977) Field Ionization Mass Spectrometry I - Field Desorption Spectra of Nucleotides - Experimental Problems. Biomed Mass Spectrom 4:103
549. Bald I, Flosadóttir HD, Ómarsson B, Ingólfsson O (2012) Metastable Fragmentation of a Thymidine-Nucleotide and its Components. Int J Mass Spectrom 313:15
550. Hunt DF, Hignite CE, Biemann K (1968) Structure Elucidation of Dinucleotides by Mass Spectrometry. Biochem Biophys Res Commun 33:378
551. Schulten HR, Schiebel HM (1976) Sequence Specific Fragments in the Field Desorption Mass Spectra of Dinucleoside Phosphates. Nucleic Acids Res 3:2027
552. Linscheid M, Burlingame AL (1983) Collisionally Activated Dissociation of Field Desorbed Protonated Dinucleoside Phosphates. Org Mass Spectrom 18:245
553. Linscheid M, Feistner G, Budzikiewicz H (1978) Field Ionization Mass Spectrometry. II. FD Spectra of Nucleotides - Analysis of Methylation Products of Dinucleoside Phosphates. Isr J Chem 17:163

554. Grotjahn L, Frank R, Blöcker H (1982) Ultrafast Sequencing of Oligodesoxyribonucleotides by FAB-Mass Spectrometry. Nucleic Acids Res 10:4671
555. Grotjahn L, Blöcker H, Frank R (1985) Mass Spectroscopic Sequence Analysis of Oligonucleotides. Biomed Mass Spectrom 12:514
556. Cerny RL, Tomer KB, Gross ML, Grotjahn L (1987) Fast Atom Bombardment Combined with Tandem Mass Spectrometry for Determining Structures of Small Oligonucleotides. Anal Biochem 165:175
557. McLuckey SA, Van Berkel GJ, Glish GL (1992) Tandem Mass Spectrometry of Small, Multiply Charged Oligonucleotides. J Am Soc Mass Spectrom 3:60
558. Little DP, Chorush RA, Speir JP, Senko MW, Kelleher NL, McLafferty FW (1994) Rapid Sequencing of Oligonucleotides by High-Resolution Mass Spectrometry. J Am Chem Soc 116:4893
559. Fabris D (2010) A Role of the MS Analysis of Nucleic Acids in the Post-Genomics Age. J Am Soc Mass Spectrom 21:1
560. Nordhoff E, Kirpekar F, Roepstorff P (1996) Mass Spectrometry of Nucleic Acids. Mass Spectrom Rev 15:67
561. Senko MW, Beu SC, McLafferty FW (1995) Determination of Monoisotopic Masses and Ion Populations for Large Biomolecules from Resolved Isotopic Distributions. J Am Soc Mass Spectrom 6:229
562. Charnock GA, Loo JL (1970) Mass Spectral Studies of Deoxyribonucleic Acid. Anal Biochem 37:81
563. Gross ML, Lyon PA, Dasgupta A, Gupta NK (1978) Mass Spectral Studies of Probe Pyrolysis Products of Intact Oligoribonucleotides. Nucleic Acids Res 5:2695
564. Limbach PA, Crain PF, McCloskey JA (1995) Molecular Mass Measurement of Intact Ribonucleic Acids *via* Electrospray Ionization Quadrupole Mass Spectrometry. J Am Soc Mass Spectrom 6:27
565. Kowalak JA, Pomerantz SC, Crain PF, McCloskey JA (1993) A Novel Method for the Determination of Posttranscriptional Modification of RNA by Mass Spectrometry. Nucleic Acids Res 21:4577
566. Janning P, Schrader W, Linscheid M (1994) A New Mass Spectrometric Approach to Detect Modifications in DNA. Rapid Commun Mass Spectrom 8:1035
567. Pieles U, Zürcher W, Schär M, Moser HE (1993) Matrix Assisted Laser Desorption Ionization Time-of-Flight Mass Spectrometry: A Powerful Tool for the Mass and Sequence Analysis of Natural and Modified Oligonucleotides. Nucleic Acids Res 21:3191
568. Sanger F, Nicklen S, Coulson AR (1977) DNA Sequencing with Chain-Terminating Inhibitors. Proc Natl Acad Sci USA 74:5463
569. Kwon YS, Tang K, Cantor CR, Köster H, Kang C (2001) DNA Sequencing and Genotyping by Transcriptional Synthesis of Chain-Terminated RNA Ladders and MALDI-TOF Mass Spectrometry. Nucleic Acids Res 29:e11
570. Spottke B, Gross J, Galla HJ, Hillenkamp F (2004) Reverse Sanger Sequencing of RNA by MALDI-TOF Mass Spectrometry after Solid Phase Purification. Nucleic Acids Res 32(12):e97
571. Mardis ER (2008) Next-Generation DNA Sequencing Methods. Ann Rev Genomics Hum Genet 9:387
572. Schuster SC (2008) Next-Generation Sequencing Transforms Today's Biology. Nature Methods 5:16
573. Fabris D, Yu ET (2010) Elucidating the Higher-Order Structure of Biopolymers by Structural Probing and Mass Spectrometry: MS3D. J Mass Spectrom 45:841
574. Yu ET, Hawkins A, Eaton J, Fabris D (2008) MS3D Structural Elucidation of the HIV-1 Packaging Signal. Proc Natl Acad Sci USA 105:12248
575. Croy RG, Essigmann JM, Reinhold VN, Wogan GN (1978) Identification of the Principal Aflatoxin B1-DNA Adduct Formed *in vivo* in Rat Liver. Proc Natl Acad Sci USA 75:1745
576. McCloskey JA, Crain PF (1992) Progress in Mass Spectrometry of Nucleic Acid Constituents: Analysis of Xenobiotic Modifications and Measurements at High Mass. Int J Mass Spectrom Ion Proc 118/119:593

577. Sharma VK, Glick J, Liao Q, Shen C, Vouros P (2012) GenoMass Software: a Tool Based on Electrospray Ionization Tandem Mass Spectrometry for Characterization and Sequencing of Oligonucleotide Adducts. J Mass Spectrom 47:490
578. Ragoussis J, Elvidge GP, Kaur K, Colella S (2006) Matrix-Assisted Laser Desorption/ Ionisation, Time-of-Flight Mass Spectrometry in Genomics Research. PLoS Genet 2:e100
579. Kessler BM (2010) Challenges Ahead for Mass Spectrometry and Proteomics Applications in Epigenetics. Epigenomics 2:163
580. Tost J, Schatz P, Schuster M, Berlin K, Gut IG (2003) Analysis and Accurate Quantification of CpG Methylation by MALDI Mass Spectrometry. Nucleic Acids Res 31(9):e50
581. Iannitti P, Sheil MM, Wickham G (1997) High Sensitivity and Fragmentation Specificity in the Analysis of Drug-DNA Adducts by Electrospray Tandem Mass Spectrometry. J Am Chem Soc 119:1490
582. Beck J, Colgrave ML, Ralph SF, Sheil MM (2001) Electrospray Ionization Mass Spectrometry of Oligonucleotide Complexes with Drugs, Metals, and Proteins. Mass Spectrom Rev 20:61
583. Iannitti-Tito P, Weimann A, Wickham G, Sheil MM (2000) Structural Analysis of Drug-DNA Adducts by Tandem Mass Spectrometry. Analyst 125:627
584. Kloster MBG, Hannis JC, Muddiman DC, Farrell N (1999) Consequences of Nucleic Acid Conformation on the Binding of a Trinuclear Platinum Drug. Biochemistry 38:14731
585. Anichina J, Bohme DK (2009) Mass-Spectrometric Studies of the Interaction of Selected Metalloantibiotics and Drugs with Deprotonated Hexadeoxynucleotide GCATGC. J Phys Chem 113:328
586. Krivos KL, Limbach PA (2010) Sequence Analysis of Peptide:Oligonucleotide Heteroconjugates by Electron Capture Dissociation and Electron Transfer Dissociation. J Am Soc Mass Spectrom 21:1387
587. Rusconi F, Guilloneau FPF, Praseuth D (2002) Contribution of Mass Spectrometry in the Study of Nucleic Acid-Binding Proteins and of Nucleic Acid-Protein Interactions. Mass Spectrom Rev 21:305
588. Horai H, Arita M, Kanaya S, Nihei Y, Ikeda T, Suwa K, Ojima Y, Tanaka K, Tanaka S, Aoshima K, Oda Y, Kakazu Y, Kusano M, Tohge T, Matsuda F, Sawada Y, Hirai MY, Nakanishi H, Ikeda K, Akimoto N, Maoka T, Takahashi K, Ara T, Sakurai N, Suzuki H, Shibata T, Neumann S, Iida T, Tanaka K, Funatsu K, Matsuura F, Soga T, Taguchi R, Saito K, Nishioka T (2010) MassBank: a Public Repository for Sharing Mass Spectral Data for Life Sciences. J Mass Spectrom 45:703
589. Kopka J, Schauer N, Krueger S, Birkermeyer C, Usadel B, Bergmüller E, Dörmann P, Weckwerth W, Gibon Y, Stitt M, Willmitzer L, Fernie AR, Steinhauser D (2005) GMD@ CSB.DB: the Golm Metabolome Database. Bioinformatics 21:1635
590. Pace-Asciak CR (1989) Mass Spectra of Prostaglandins and Related Products. Adv Prostaglandin Thromboxane Leucotriene Res 18:1
591. Wishart DS, Knox C, Guo AC, Eisner R, Young N, Gautam B, Hau DD, Psychogios N, Dong E, Bouatra S, Mandal R, Sinelnikov I, Xia J, Jia L, Cruz JA, Lim E, Sobsey CA, Shrivastava S, Huang P, Liu P, Fang L, Peng J, Fradette R, Cheng D, Tzur D, Clements M, Lewis A, De Souza A, Zuniga A, Dawe M, Xiong Y, Clive D, Greiner R, Nazyrova A, Shaykhutdinov R, Li L, Vogel HJ, Forsythe I (2009) HMDB: a Knowledgebase for the Human Metabolome. Nucleic Acid Res 37 (Suppl 1):D603
592. Damen H, Henneberg D, Weimann B (1978) Siscom - a New Library Search System for Mass Spectra. Anal Chim Acta 103:289
593. Stein SE, Scott DR (1994) Optimization and Testing of Mass Spectral Library Search Algorithms for Compound Identification. J Am Soc Mass Spectrom 5:859
594. Jacob J, Disnar JR, Boussafir M, Spadano Albuquerque AL, Sifeddine A, Turcq B (2005) Pentacyclic Triterpene Methyl Ethers in Recent Lacustrine Sediments (Lagoa do Caçó, Brazil). Org Geochem 36:449
595. Hegna RH, Saporito RA, Donnelly MA (2013) Not All Colors Are Equal: Predation and Color Polytypism in the Aposematic Poison Frog *Oophaga pumilio.* Evol Ecol 27:831

596. Apps P, Mmualefe L, McNutt JW (2012) Identification of Volatiles from the Secretions and Excretions of African Wild Dogs (*Lycaon pictus*). J Chem Ecol 38:1450

597. Corral RA, Orazi OO, Duffield AM, Djerassi C (1971) Mass Spectrometry in Structural and Stereochemical Problems - CCIV. Spectra of Hydantoins II. Electron Impact Induced Fragmentation of Some Substituted Hydantoins. Org Mass Spectrom 5:551

598. Cert A, Delgado-Cobos P, Trujillo Pérez-Lanzac M (1986) Mass Spectrometry of Imidazole-4(5)-carboxaldehyde and Some 1-Methyl and Nitro Derivatives. Org Mass Spectrom 21:499

599. Stewart M, Baker CF, Cooney T (2011) A Rapid, Sensitive, and Selective Method for Quantitation of Lamprey Migratory Pheromones in River Water. J Chem Ecol 37:1203

600. Thevis M, Schänzer W, Geyer H, Thieme D, Grosse J, Rautenberg C, Flenker U, Beuck S, Thomas A, Holland R, Dvorak J (2013) Traditional Chinese Medicine and Sport Drug Testing: Identification of Natural Steroid Administration in Doping Control Urine Samples Resulting from Musk (Pod) Extracts. Br J Sports Med 47:109

601. Fasciotti M, Sanvido GB, Santos VG, Lalli PM, McCullagh M, de Sá GF, Daroda RJ, Peter MG, Eberlin MN (2012) Separation of Isomeric Disaccharides by Travelling Wave Ion Mobility Mass Spectrometry using CO_2 as Drift Gas. J Mass Spectrom 47:1643

602. Garraffo HM, Andriamaharavo NR, Varia M, Quiroga MF, Heit C, Spande TF (2012) Alkaloids from Single Skins of the Argentinian Toad *Melanophryniscus rubriventris* (ANURA, BUFONIDAE): an Unexpected Variability in Alkoid Profiles and a Profusion of New Structures. SpringerPlus 1:51

603. Qu T, Gao HM, Chen LM, Wang ZM, Zhang QW, Cheng YY (2012) Content of Indole Alkaloids and Bufadienolides Contained in Toad Medicines. Zhongguo Zhong Yao Za Zhi (China J Chinese Materia Medica) 37:3086

604. Honda K, Goto M, Kurahashi M, Akizawa T, Yoshioka M, Butler VP Jr (1991) Structure of Bufothionin. Acta Cryst C 47:1506

605. Yang LH, Zhang HZ, Zhang B, Chen F, Lai ZH, Xu LF, Jin XQ (1992) Studies on the Chemical Constituents from the Skin of *Bufo bufo gargarizans* Cantor. Yao Xue Xue Bao (Acta Pharm Sinica) 27:679

606. Dai LP, Gao HM, Wang ZM, Wang WH (2007) Isolation and Structure Identification of Chemical Constituents from the Skin of *Bufo bufo gargarizans.* Yao Xue Xue Bao (Acta Pharm Sinica) 42:858

607. Cao XT, Wang D, Wang N, Cui Zheng (2009) Water-Soluble Constituents from the Skin of *Bufo bufo gargarizans* Cantor. Chin J Nat Med 7:181

608. Wu FK, Qiu YK, Zhao HY, Wu Z, Li FM, Jiang YT, Chen JY (2011) Cytotoxic Constituents from the Skin of the Toad *Bufo bufo gargarizans*. J Asian Nat Prod Res 13:111

609. Wang DL, Qi FH, Tang W, Wang FS (2011) Chemical Constituents and Bioactivities of the Skin of *Bufo bufo gargarizans* Cantor. Chem Biodiversity 8:559

610. Zhang P, Cui Z, Liu Y, Wang D, Liu N, Yoshikawa M (2005) Qualitative Evaluation of Traditional Chinese Drug Toad Venom from Different Origins Through a Simultaneous Determination of Bufogenins and Indole Alkaloids by HPLC. Chem Pharm Bull 53:1582

611. Ueno A, Ikeya Y, Fukushima S, Tadataka N, Morinaga K, Kuwano H (1978) Studies on the Constituents of *Desmodium caudatum* DC. Chem Pharm Bull 26:2411

612. Dai LP (2004) Chemical Studies on the Water-Soluble Fraction Extracted from Skin of *Bufo bufo gargarizans.* Master's Thesis, Henan College of Traditional Chinese Medicine (to be obtained under http://www.doc88.com/p-979163575236.html)

613. Kamano Y, Morita H, Takano R, Kotake A, Nogawa T, Hashima H, Takeya K, Itokawa H, Pettit GR (1999) Bufobutanoic Acid and Bufopyramide, Two New Indole Alkaloids from the Chinese Traditional Drug *Ch'An Su*. Heterocycles 50:499

614. Kurauchi T, Nagahama Y, Hasegawa M, Yamada K, Somei M (2000) The First Total Synthesis of Bufobutanoic Acid byTwo Routes Based on Nucleophilic Substitution Reaction on Indole Nucleus. Heterocycles 53:1017

615. Maciel NM, Schwartz CA, Pires OR Jr, Sebben A, Castro MS, Sousa MV, Fontes W, Ferroni Schwartz EN (2003) Composition of Indolealkylamines of *Bufo rubescens* Cutaneous Secretions Compared to Six other Brazilian Bufonids with Phylogenetic Implications. Comp Biochem Physiol B 134:641

616. Yuan G, Zhang Q, Zhou J, Li H (2011) Mass Spectrometry of G-Quadruplex DNA: Formation, Recognition, Property, Conversion, and Conformation. Mass Spectrom Rev 30:1121
617. Balthasart F, Plavec J, Gabelica V (2013) Ammonium Ion Binding to DNA Q-Quadruplexes: Do Electrospray Mass Spectra Faithfully Reflect the Solution-Phase Species? J Am Soc Mass Spectrom 24:1
618. Machnicka MA, Milanowska K, Oglou OO, Purta E, Kurkowska M, Olchowik A, Januszewski W, Kalinowski S, Dunin-Horkawitz S, Rother KM, Helm M, Bujnicki JM, Grosjean H (2013) MODOMICS: a Database of RNA Modification Pathsways - 2013 Update. Nucleic Acids Res 41:D262
619. Helm M, Kellner S. (2013) Massenspektrometrie von Modifizierten Nukleinsäuren. Nachr Chem 61:307
620. Gonzales AG, Mendoza JJ, Ravelo AG, Luis JG (1989) Δ^{18} Oleane Triterpenes from *Schaefferia cuneifolia.* J Nat Prod 52:567
621. Osorio AA, Muñóz A, Torres-Romero D, Bedoya LM, Perestelo NR, Jiménez IA, Alcamí J, Bazzocchi IL (2012) Olean-18-ene Triterpenoids from Celastraceae Species Inhibit HIV Replication Targeting NF-κB and Sp1 Dependent Transcription. Eur J Med Chem 52:295
622. Oyo-Ita OE, Ekpo BO, Oros DR, Simoneit BRT (2010) Occurrence and Sources of Triterpenoid Methyl Ethers and Acetates in Sediments of the Cross-River System, Southeast Nigeria. Int J Anal Chem, Article ID 502076
623. Thompson SA, Tachibana K, Nakanishi K, Kubota I (1986) Melittin-Like Peptides from the Shark-Repelling Defense Secretion of the Sole *Pardachirus pavoninus.* Science 233:341
624. Tachibana K, Gruber SH (1988) Shark Repellent Lipophilic Constituents in the Defense Secretion of the Moses Sole (*Pardachirus marmoratus*). Toxicon 26:839
625. Tachibana K, Sakaitanai M, Nakanishi K (1984) Pavoninins: Shark-Repelling Ichthyotoxins from the Defense Secretion of the Pacific Sole. Science 226:703
626. Tachibana K, Sakaitani M, Nakanishi K (1985) Pavoninins, Shark-Repelling and Ichthyotoxic Steroid *N*-Acetylglucosaminides from the Defense Secretion of the Sole *Pardachirus pavoninus* (Soleidae). Tetrahedron 41:1027
627. Goldberg AS, Wasylyk J, Renna S, Reisman J, Nair MSR (1982) Isolation and Structural Elucidation of an Ichthyocrinotoxin from the Smooth Trunkfish (*Lactophrys triqueter* Linnaeus). Toxicon 20:1069
628. Boylan DB, Scheurer PJ (1967) Pahutoxin: a Fish Poison. Science 155:52
629. Yoshikawa M, Sugimura T, Tai A (1989) Pahutoxin: Synthesis and Determination of its Absolute Configuration. Agric Biol Chem 53:37
630. Onuki H, Tachibana T, Fusetani N (1993) Structure of Lipogrammistin-A, a Lipophilic Ichthyotoxin Secreted by the Soapfish *Diploprion bifsciatum.* Tetrahedron Lett 34:5609
631. Onuki H, Ito K, Kobayashi Y, Matsumori N, Tachibana K (1998) Absolute Structure and Total Synthesis of Lipogrammistin-A, a Lipophilic Ichthyotoxin of the Soapfish. J Org Chem 63:3925
632. Hatano M, Hashimoto Y (1974) Properties of a Toxic Phospholipid in the Northern Blenny Roe. Toxicon 12:231
633. Hatano M, Marumoto R, Hashimoto Y (1976) Structure of a Toxic Phospholipid in Northern Blenny Roe. In: Ohsaka A, Hayashi K, Sawai Y, Murata R, Funatsu M (eds) Animal, Plant, and Microbial Toxins. Plenum, New York, vol 2, p 145
634. Matsunaga S, Takahashi N, Fusetani N (2009) Dinogunnellins A-D: Putative Ichthyotoxic Phospholipids of Northern Blenny *Stichaeus grigorjewi* Eggs. Pure Appl Chem 81:1001
635. Xu Z, Shaw JB, Brodbelt JS (2013) Comparison of MS/MS Methods for Characterization of DNA/Cisplatin Adducts. J Am Soc Mass Spectrom 24:265
636. Hodyss R, Cox HA, Beauchamp JL (2005) Bioconjugates for Tunable Peptide Fragmentation: Free Radical Initiated Peptide Sequencing (FRIPS). J Am Chem Soc 127:12436
637. Falvo F, Fiebig L, Schäfer M (2013) Presentation of a Homobifunctional Azo-reagent for Protein Structure Analysis by Collision-Induced Dissociative Chemical Cross-Linking: Proof-of-Principle. Int J Mass Spectrom 354-355:26

638. Williams DM, Pukala DL (2013) Novel Insights into Protein Misfolding Diseases Revealed by Ion Mobility-Mass Spectrometry. Mass Spectrom Rev 32:169
639. Tzouros M, Chesnov S, Bigler L, Bienz S (2013) A Template Approach for the Characterization of Linear Polyamines and Derivatives in Spider Venom. Eur J Mass Spectrom 19:57
640. Liu RH, Lao H, Li YL, Yang M, Li HL, Shen YH, Zhang C, Su J, Zhang WD (2007) Three New Alkaloids from the Chinese Medicine *Chan-Su*. Helv Chim Acta 90:2427
641. Kurono S, Hattori H, Suzuki O, Yamada T, Seno H (2001) Sensitive Analysis of Tetrodotoxin in Human Plasma by Solid-Phase Extractions and Gas Chromatography/Mass Spectrometry. Anal Lett 34:2439
642. Oberacher H, Whitley G, Berger B, Weinmann W (2013) Testing an Alternative Search Algorithm for Compound Identification with the 'Wiley Registry of Tandem Mass Spectral Data, MSforID'. J Mass Spectrom 48:497
643. Fellenberg AJ, Johnson DW, Poulos A; Sharp P (1987) Simple Mass Spectrometric Differentiation of the *n*-3, *n*-6 and *n*-9 Series of Methylene Interrupted Polyenoic Acids. Biomed Environm Mass Spectrom 14:127
644. Yamagishi T, Miyazaki T, Horii S, Kaneko S (1981) Identification of Musk Xylene and Musk Ketone in Freshwater Fish Collected from the Tama River, Tokyo. Bull Environm Contam Toxicol 26:656
645. Mottaleb MA, Osemwengie LI, Islam MR, Sovocool GW (2012) Identification of Bound Nitro Musk-Protein Adducts in Fish Liver by Gas Chromatography-Mass Spectrometry: Biotransformation, Dose-Response and Toxicokinetics of Nitro Musk Metabolites Protein Adducts in Trout Liver as Biomarkers of Exposure. Aquat Toxicol 106-107:164
646. Herren D, Berst JD (2000) Nitro Musk, Nitro Musk Amino Metabolites and Polycyclic Musks in Sewage Sludges. Quantitative Determination by HRGC-Ion Trap-MS/MS and Mass Spectral Characterization of the Amino Metabolites. Chemosphere 40:565
647. Asakawa M, Shida Y, Miyazawa K, Noguchi T (2012) Instrumental Analysis of Tetrodotoxin. In: Chromatography - The Most Versatile Method Of Chemical Analysis (de Azevedo Calderon L, ed) InTech: Rijeka, Croatia, Chapter 10
648. Chau R, Kalaitzis JA, Neilan BA (2011) On the Origin and Biosynthesis of Tetrodotoxin. Aquat Toxicol 104:61
649. Yotsu-Yamashita, M (2006) Spectroscopic Study of Zetekitoxin AB. In: Kiyota H, Gupta RR (eds) Marine Natural Products, Springer, Berlin, Heidelberg, New York. Top Heterocycl Chem, 5:53
650. Li CJ, Kari UP, Noecker LA, Jones SR, Sabo AM, McCormick TJ, Johnston SM (2003) Determination of Degradation Products of Squalamine Lactate Using LC/MS. J Pharm Biomed Anal 32:85
651. de Medina P, Paillasse MR, Segala G, Voisin M, Mhamdi L, Dalenc F, Lacroix-Triki M, Filleron T, Pont F, Saati TA, Morisseau C, Hammock BD, Silvente-Poirot S, Poirot M (2013) Dendrogenin A Arises from Cholesterol and Histamine Metabolism and Shows Cell Differentiation and Anti-Tumor Properties. Nature Commun 4:1840
652. Tian HY, Wang L, Zhang XQ, Wang Y, Zhang DM, Jiang RW, Liu Z, Liu JS, Li YL, Ye WC (2010) Bufogargarizins A and B: Novel 19-Norbufadienolides with Unprecedented Skeletons from the Venom of *Bufo bufo gargarizans.* Chem Eur J 16:10989
653. Zhao HY, Wu FK, Qiu YK, Wu Z, Jiang YT, Chen JY (2010) Studies on Cytotoxic Constituents from the Skin of the Toad *Bufo bufo gargarizans.* J Asian Nat Prod Res 12:793
654. Silvestri C, Brodbelt JS (2013) Tandem Mass Spectrometry for Characterization of Covalent Adducts of DNA with Anticancer Therapeutics. Mass Spectrom Rev 32:247
655. Fingolo CE, de S. Santos T, Vianna Filho MDM, Kaplan MAC (2013) Triterpene Esters: Natural Products from *Dorstenia arifolia* (Moraceae). Molecules 18:4247
656. Habermehl G, Vogel G (1969) Samandinine, a Minor Alkaloid from *Salamandra maculosa* Laur. Toxicon 7:163
657. Dufton MJ (1992) Venomous Mammals. Pharmacol Ther 53:199
658. Folinsbee KE (2013) Evolution of Venom Across Extant and Extinct Eulipotyphlans. C R Palevol 12:531

659. Kita M, Nakamura Y, Okumura Y, Ohdachi SD, Oba Y, Yoshikuni M, Kido H, Uemura D (2004) Blarina Toxin, a Mammalian Lethal Venom from the Short-Tailed Shrew *Blarina brevicauda*: Isolation and Characterization. Proc Natl Acad Sci USA 101:7542
660. Aminetzach YT, Srouji JR, Kong CY, Hoekstra HE (2009) Convergent Evolution of Novel Protein Function in Shrew and Lizard Venom. Curr Biol 19:1925
661. Römer JJ, Schinz HR (1809) Naturgeschichte der in der Schweiz einheimischen Säugethiere. Ein Handbuch für Kenner und Liebhaber. H. Geßner, Zürich, p 139
662. Gesner (1606) Thierbuch. A. Cambler, Heidelberg, p 113
663. Kiss G, Michl H (1962) Über das Giftsekret der Gelbbauchunke, *Bombina variegata* L. Toxicon 1:33
664. Anastasi A, Erspamer V, Bucci M (1972) Isolation and Amino Acid Sequences of Alytesin and Bombesin, Two Analogous Active Tetradecapeptides from the Skin of European Discoclossid Frogs. Arch Biochem Biophys 148:443
665. Lai R, Zheng YT, Shen JH, Liu GJ, Liu H, Lee WH, Tang SZ, Zhang Y (2002) Antimicrobial Peptides from Skin Secretions of Chinese Red Belly Toad *Bombina maxima*. Peptides 23:427
666. Marenah L, Flatt PR, Orr DF, McLean S, Shaw C, Abdel-Wahab YHA (2004) Skin Secretion of the Toad *Bombina variegata* Contains Multiple Insulin-Releasing Peptides Including Bombesin and Entirely Novel Insulinotropic Structures. Biol Chem 385:315
667. Csordás A, Michl H (1970) Isolierung und Strukturaufklärung eines hämolytisch wirkenden Poypeptides aus dem Abwehrsekret europäischer Unken. Monatsh Chem 101:182
668. Gibson BW, Tangt D, Mandrell R, Kelly M, Spindel ER (1991) Bombinin-like Peptides with Antimicrobial Activity from Skin Secretions of the Asian Toad, *Bombina orientalis.* J Biol Chem 266:23103
669. Ligon WV Jr, Dorn SB (1986) Understanding the Glycerol Surface as it Relates to the Secondary Ion Mass Spectrometry Experiment. A Review. Int J Mass Spectrom Ion Proc 78:99
670. Sciani JM, Angeli CB, Antoniazzi MM, Jared C, Pimenta DC (2013) Differences and Similarities among Parotoid Macrogland Secretions in South American Toads: A Preliminary Biochemical Delineation. Sci World J Article ID 937407
671. Weldon PJ, Flachsbarth B, Schulz S (2008) Natural Products from the Integument of Nonavian Reptiles. Nat Prod Rep 25:738
672. Wood WF, Parker JM, Weldon PF (1995) Volatile Compounds in the Scent Gland Secretions of Garter Snakes (*Thamnophis* spp.). J Chem Ecol 21:213
673. Simpson JT, Weldon PJ, Sharp TR (1988) Identification of Major Lipids from the Scent Gland Secretions of Dumaril's Ground Boa (*Acrantophis dumerili* Jan) by Gas Chromatography-Mass Spectrometry. Z Naturforsch 43c:914
674. Simpson JT, Sharp TR, Wood WF, Weldon PJ (1993) Further Analysis of Lipids from the Scent Gland Secretions of Dumaril's Ground Boa (*Acrantophis dumerili* Jan). Z Naturforsch 48c:953
675. Stavenhagen K, Hinneburg H, Thaysen-Andersen M, Hartmann L, Silva DV, Fuchser J, Kaspar S, Rapp E, Seeberger PH, Kolarich (2013) Quantitative Mapping of Glycoprotein Micro-heterogeneity and Macro-heterogeneity: an Evaluation of Mass Spectrometry Signal Strengths Using Synthetic Peptides and Glycopeptides. J Mass Spectrom 48:627
676. Weldon PJ, Lloyd HA, Blum MS (1990) Glycerol Monoethers in the Scent Gland Secretions of the Western Diamond Back Rattlesnake (*Crotalus atrox*; Serpentes Crotalinae). Experientia 46:774
677. Myher JJ, Marai L, Kuksis A (1974) Identification of Monoacyl- and Monoalkylglycerols by Gas-liquid Chromatography-Mass Spectrometry Using Polar Siloxane Liquid Phases. J Lipid Res 15:586
678. Hallgren B, Ställberg G (1967) Methoxy-substituted Glycerol Ethers Isolated from Greenland Shark Liver Oil. Acta Chem Scand 21:1519
679. Torres AM, Wang X, Fletcher JI, Alewood D, Alewood PF, Smith R, Simpsons RJ, Nicholson GM, Sutherland SK, Gallagher CH, King GF, Kuchel PW (1999) Solution Structure of a Defensin-like Peptide from Platypus Venom. Biochem J 341:785
680. Torres AM, de Plater GM, Doverskog M, Birinyi-Strachans LC, Nicholson GM, Gallagher CH, Kuchel PW (2000) Defensin-like Peptide-2 from Platypus Venom: Member of a Class of Peptides with a Distinct Structural Fold. Biochem J 348:649

681. Koh JMS, Haynes L, Belov K, Kuchel PW (2100) L-to-D-Peptide Isomerase in Male *Echidna* Venom. Aust J Zool 58:284
682. Whittington CM, Papenfuss AT, Bansal P, Torres AM, Wong ESW, Deakin JE, Graves T, Alsop A, Schatzkamer K, Kremitzki C, Ponting CP, Temple-Smith P, Warren WC, Kuchel PW, Belov K (2008) Defensins and the Convergent Evolution of Platypus and Reptile Venom Genes. Genome Res 18:986
683. Harris RL, Davies NW, Nicol SC (2012) Chemical Composition of the Odorous Secretions in the Tasmanian Short-Beaked Echidna (*Tachyglossus aculeatus setosus*). Chem Senses 37:819
684. Burger BV (2005) Mammalian Semiochemicals. Topics Curr Chem 240:231
685. Smith TE, Tomlinson AJ, Mlotkiewicz JA, Abbott DH (2001) Female Marmoset Monkeys (*Callithrix jacchus*) Can Be Identified from the Chemical Composition of Their Scent Marks. Chem Senses 26:449
686. Kavan D, Kuzma M, Lemr K, Schug KA, Havlicek V (2013) CYCLONE - a Utility for *de Novo* Sequencing of Microbial Cyclic Peptides. J Am Soc Mass Spectrom 24:1177
687. Lattová E, Perreault H (2013) The Usefulness of Hydrazine Derivatives for Mass Spectrometric Analysis of Carbohydrates. Mass Spectrom Rev 32:366
688. Matsumura K (2001) No Ability to Produce Tetrodotoxin in Bacteria. Appl. Environ Microbiol 67:2393
689. Yotsu-Yamashita M, Abe Y, Kudo Y, Ritson-Williams R, Paul VJ, Konoki K, Cho Y, Adachi M, Imazu T, Nishikawa T, Isobe M (2013) First Identification of 5,11-Dideoxytetrodotoxin in Marine Animals, and Characterization of Major Fragment Ions of Tetrodotoxin and its Analogs by High Resolution ESI-MS/MS. Mar Drugs 11:2799
690. Pires OR Jr, Sebben A, Schwartz EF, Morales RAV, Bloch C Jr, Schwartz CA (2005) Further Report of the Occurrence of Tetrodotoxin and New Analogs in the Anuran Family Brachycephalidae. Toxicon 45:73
691. Spiteller G (2005) Furan Fatty Acids: Occurrence, Synthesis, and Reactions. Are Furan Fatty Acids Responsible for the Cardioprotective Effects of a Fish Diet? Lipids 40:755
692. Glass RL, Krick TP, Sand DM, Rahn CH, Schlenk H (1975) Furanoid Fatty Acids from Fish Lipids. Lipids 10:695
693. Hasma H, Subramaniam A (1978) The Occurrence of a Furanoid Fatty Acid in *Hevea brasiliensis* Latex. Lipids 13:905
694. Guth H, Grosch W (1991) Detection of Furanoid Fatty Acids in Soya-Bean Oil - Cause for the Light-Induced Off-Flavor. Fat Sci Technol 93:249
695. Spiteller M, Spiteller G, Hoyer GA (1980) Urofuransäuren - eine bisher unbekannte Klasse von Stoffwechselprodukten. Chem Ber 113:699
696. Pfordt J, Thoma H, Spiteller G (1981) Identifizierung, Strukturableitung und Synthese bisher unbekannter Uroforansäuren im menschlichen Blut. Liebigs Ann Chem:2298
697. Guth H, Grosch W (1992) Furan Fatty Acids in Butter and Butter Oil. Z Lebensm Unters Forsch 194:360
698. Wahl HG, Chrzanowski A, Liebich HM, Hoffmann A (1994) Identification of Furan Fatty Acids in Nutritional Oils and Fats by Multidimensional GC-MSD. Gerstl ApplNote 6/1994, Gerstl GmbH & CoKG, Mülheim/R, Germany
699. Ishii K, Okajima H, Koyamatsu T, Okada Y, Watanabe H (1988) The Composition of Furan Fatty Acids in the Crayfish. Lipids 23:694
700. Roselli E, Grob K, Lercker G (2000) Determination of Furan Fatty Acids in Extra Virgin Olive Oil. J Agric Food Chem 48:2868
701. Glass RL, Krick TP, Eckhardt AE (1974) New Series of Fatty Acids in Northern Pike (*Esox lucius*). Lipids 9:1004
702. Sand DM, Schlenk H, Thoma H, Spiteller G (1983) Catabolism of Fish Furan Fatty Acids to Urofuran Acids in the Rat. Biochim Biophys Acta 751:455
703. Bauer S, Spiteller G (1985) Furancarbonsäuren aus Rinderharn. Helv Chim Acta 68:1635
704. Groweiss A, Kashman Y (1978) A New Furanoid Fatty Acid from the Soft Corals *Sarcophyton glaucum* and *gemmatum*. Experientia 34:299
705. Schödel R, Dietel P, Spiteller G (1986) F-Säuren als Vorstufen der Urofuransäuren. Liebigs Ann Chem:127

706. Ellamar JB, Song KS, Kim HR (2011) One-Step Production of a Biologically Active Novel Furan Fatty Acid from 7,10-Dihydroxy-8(*E*)-octadecenoic Acid. J Agric Food Chem 59:8175
707. Vetter W, Wendlinger C (2013) Furan Fatty Acids - Valuable Minor Fatty Acids in Food. Lipid Technol 25:7
708. Vetter W, Laure S, Wendlinger C, Mattes A, Smith AWT, Knight DW (2012) Determination of Furan Fatty Acids in Food Samples. J Am Oil Chem Soc 89:1501
709. Wynne P, Jenkinson L, Marrow G, Lahoutifard N, Hodges L, Macrides T. GCMS Based Structure Assignment for Furan Fatty Acids Isolated from European Carp (*Cyprinus carpio*). SGE Analytical Science TP-0181-C
710. Göckler S (2009) Metabolismus und genetische Toxizität von Furanfettsäuren, sowie deren Einfluss auf Zellmembranen *in vitro*. Dissertation, University of Karlsruhe
711. Pompizzi R (1999) Furanfettsäuren als Vorläufer von Aromastoffen. Dissertation, ETH Zürich
712. Shiojima K, Masuda K, Suzuki H, Lin T, Ooishi Y, Ageta H (1995) Composite Constituents: Forty-Two Triterpenoids Including Eight Novel Compounds Isolated from *Picris hieracioides* subsp. *japonica.* Chem Pharm Bull 43:1634
713. Hooper SN, Chandler RF, Lewis E, Jamieson WD (1982) Simultaneous Determination of *Sonchus arvensis* L. Triterpenes by Gas Chromatography-Mass Spectrometry. Lipids 17:60
714. Lee HD, Eichmeier LS, Piatak DM (1985) Mass Spectral Study of Ring *E* of Taraxasterol and Compounds with Similar Ring Substitution. Org Mass Spectrom 20:247
715. Pfordt J, Thoma H, Spiteller G (1981) Identifizierung, Strukturableitung und Synthese Bisher Unbekannter Urofuransäuren im Menschlichen Blut. Liebigs Ann Chem:2298
716. Bauer S, Spiteller G (1985) Strukturaufklärung und Synthese bisher unbekannter Furancarbonsäuren im Humanurin. Liebigs Ann Chem:813
717. Dietel P, Spiteller G (1988) Inkubation von 2,5-disubstituierten F-Säuren mit Rinderleberhomogenisat. Liebigs Ann Chem:397
718. Baltes W, Bochmann G (1987) Model Reactions on Roast Aroma Formation. II. Mass Spectrometric Identification of Furans and Furanones from the Reaction of Serine and Threonine with Sucrose under the Conditions of Coffee Roasting. Z Lebensm Unters Forsch 184:179
719. Knechtle P, Diefenbacher M, Greve KBV, Brianza F, Folly C, Heider H, Lone MA, Long L, Meyer JP, Roussel P, Ghannoum MA, Schneiter R, Sorensen AS (2013) The Natural Diyne-Furan Fatty Acid EV-086 is an Inhibitor of Fungal Delta-9 Fatty Acid Desaturation with Efficacy in a Model of Skin Dermatophytosis. Antimicrob Agents Chemother 58:455
720. Nekaris KAI, Moore RS, Rode EJ, Fry BG (2013) Mad, Bad and Dangerous to Know: the Biochemistry, Ecology and Evolution of Slow Loris Venom. J Venom Anim Toxins Incl Trop Dis 19:21
721. Jing J, Ren WC, Li C, Bose U, Parekh HS, Wei MQ (2013) Rapid Identification of Primary Constituents in Parotoid Gland Secretions of the Australian Cane Toad Using HPLC/MS-Q-TOF. Biomed Chromatogr 27:685
722. Gao H, Zehl M, Leitner A, Wu X, Wang Z, Kopp B (2010) Comparison of Toad Venoms from Different *Bufo* species by HPLC and LC-DAD-MS/MS. J Ethnopharmacol 131:368
723. Yoshika M, Komiyama Y, Konishi M, Akizawa T, Kobayashi T, Date M, Kobatake S, Masuda M, Masaki H, Takahashi H (2007) Novel Digitalis-like Factor, Marinobufotoxin, Isolated from Cultured Y-1 Cells, and its Hypertensive Effect in Rats. Hypertension 49:209
724. Ye M, Guo DA (2005) Analysis of Bufadienolides in the Chinese Drug *ChanSu* by High-Performance Liquid Chromatography with Atmospheric Pressure Chemical Ionization Tandem Mass Spectrometry. Rapid Commun Mass Spectrom 19:1881
725. Hu Y, Yu Z, Yang ZJ, Zhu G, Fong W (2011) Comprehensive Chemical Analysis of *Venenum Bufonis* by Using Liquid Chromatography/Eletrospray Ionization Tandem Mass Spectrometry. J Pharm Biomed Anal 56:210
726. Eglinton G, Hamilton RJ, Martin-Smith M, Smith SJ, Subramanian G (1964) Arundoin - a Naturally Occurring D:C-*friedo*-Oleana-9(11)-ene. Tetrahedron Lett 5:2323
727. Nakanishi K, Lin YY, Kakisawa H, Hsü HY, Hsiu HC (1963) Davallic Acid, a Triterpene with a Novel Skeleton. Tetrahedron Lett 4:1451

728. Allard S, Ourisson G (1957) Remarques sur la nomenclature des triterpènes. Tetrahedron 1:277
729. Brahim B, Alves S, Cole RB, Tabet JC (2013) Charge Enhancement of Single-Stranded DNA in Negative Electrospray Ionization Using the Supercharging Reagent *meta*-Nitrobenzyl Alcohol. J Am Soc Mass Spectrom 24:1988
730. Lehane L, Olley J (2000) Histamine Fish Poisoning Revisited. Int J Food Microbiol 58:1
731. Safer D, Brenes M, Dunipace S, Schad G (2007) Urocanic Acid is a Major Chemoattractant for the Skin-Penetrating Parasitic Nematode *Strongyloides stercoralis*. Proc Natl Acad Sci USA 104:1627
732. Ienaga K, Yamamoto A, Yamada T, Joh Y (1988) A Novel Urocanic Acid Derivative from Skin Tissue Extracts: (*E*)-3-[1-(1,1-Dimethyl-3-oxobutyl)imidazo-4-yl]-4-propenoic Acid. J Heterocycl Chem 25:1037
733. Ienaga K, Nakamura K, Goto T (1987) Bioactive Compounds Produced in Animal Tissues (I); Two Diketopiperadine Plant Growth Regulators Containing Hydroxyproline Isolated from Rabbit Skin Tissue Extract. Tetrahedron Lett 28:1285
734. Ienaga K, Nakamura K, Goto T, Konishi J (1987) Ienaga K, Nakamura K, Goto T (1987) Bioactive Compounds Produced in Animal Tissues (II); Two Hydantoin Plant Growth Regulators Isolated from Inflamed Rabbit Skin Tissue. Tetrahedron Lett 28:4587
735. Locock RA, Coutts RT (1970) The Mass Spectra of Succinimides, Hydantoins, Oxazolidinediones and other Medicinal Anti-Epileptic Agents. Org Mass Spectrom 3:735
736. Ishikawa Y, Suzuki O, Hattori H, Kumazawa T, Takahashi T (1988) Positive and Negative Ion Mass Spectrometry of Antiepileptik Hydantoins and their Analogs. Z Rechtsmed 99:253
737. Hantak MM, Grant T, Reinsch S, Meginnity D, Loring M, Toyooka N, Saporito RA (2013) Dietary Alkaloid Sequestration in a Poison Frog: An Experimental Test of Alkaloid Uptake in *Melanophryniscus stelzneri* (Bufonidae). J Chem Ecol 39:1400
738. Naldi M, Giannone FA, Baldassarre M, Domenicali M, Caraceni P, Bernardi M, Bertucci C (2013) A Fast and Validated Mass Spectrometry Method for the Evaluation of Human Serum Albumin Structural Modifications in the Clinical Field. Eur J Mass Spectrom 19:491
739. Ibraheim ZZ (2002)Triterpenes from *Rubia cordifolia* L. Bull Pharm Sci, Assiut Univ 25:155
740. Tanaka R, Msatsunaga S (1988) Triterpene Dienols and other Constituents from the Bark of *Phyllanthus flexuosus.* Phytochemistry 27:2273
741. Zeng L, Zhang RY, Wang D, Zhang ZL, Lou ZC (1991) Glyyunnansapogenins G and H: Two New Pentacyclic Triterpenoids of the 18*αH*-Oleano-9(11),12-diene Type from *Glycyrrhiza yunnanensis* Roots. Planta Med 57:165
742. Ikuta A, Kamiya K, Satake T, Saiki Y (1995) Triterpenoids from Callus Tissue Cultures of *Paeonia* Species. Phytochemistry 38:1203
743. Rödel MO, Brede C, Hirschfeld M, Schmitt T, Favreau P*,* Stöcklin R, Wunder C, Mebs D (2013) Chemical Camouflage - A Frogs Strategy to Co-Exist with Aggressive Ants. PLoS ONE 8(12) e81950.
744. Guttérrez RMP (2005) Pentacyclic Triterpenes from *Cirsium pascuarense*. J Chil Chem Soc 50:587
745. Cui L, Yapici I, Borthan B, Reid GE (2014) Quantification of Competing H_3PO_4 versus HPO_3 + H_2O Neutral Losses from Regioselective ^{18}O-Labeled Phosphopeptides. J Am Soc Mass Spectrom 25:141
746. Reis A, Domingues P, Domingues RM (2013) Structural Motifs in Primary Oxidation Products of Palmitoyl-arachidonoyl-phosphatidylcholines by LC-MS/MS. J Mass Spectrom 48:1207
747. Mebs D, Alvarez JV, Pogoda W, Toennes SW, Köhler G (2014) Poor Alkaloid Sequestration by Arrow Poison Frogs of the Genus *Phyllobates* from Costa Rica. Toxicon 80:73
748. McNabb P, Selwood AI, Mundy R, Wood SA, Taylor DI, MacKenzie LA, van Ginkel R, Rhodes LL, Cornelisen C, Heasman K, Holland PT, King C (2010) Detection of Tetrodotoxin from the Grey Side-gilled Sea Slug - *Pleurobranchea maculata*, and Associated Dog Neurodoxicosis on Beaches Adjacent to the Hauraki Gulf, New Zealand. Toxicon 56:466

749. Khor S, Wood SA, Salvitti L, Taylor DI, Adamson J, McNabb P, Cary C (2014) Investigating Diet as the Source of Tetrodotoxin in *Pleurobranchea maculata.* Mar Drugs 12:1
750. Oka K, Hara S (1977) Denial of the Proposed Structure of Salamander Alkaloid, Cycloneosamandaridine. Total Synthesis of Cycloneosamandione and Supposed Cycloneosamandaridine. J Am Chem Soc 99:3859
751. Oka K, Hara S (1978) Synthesis of γ-Lactone Ring Fused to Steroidal Ring D of Salamander Alkaloids. J Org Chem 43:4408
752. Habermehl G, Haaf G (1965) Cycloneosamandaridin, ein neues Nebenalkaloid aus *Salamandra maculosa.* Chem Ber 98:3001
753. Cristofoli WA, Benn M (1991) Synthesis of Samanine. J Chem Soc Perkin Trans 1:1825
754. Wang X, Tsuneki H, Urata N, Tezuka Y, Wada T, Sasaoka T, Sakai H, Saporito RA, Toyooka N (2012) Synthesis and Biological Activities of the 3,5-Disubstituted Indolizidine Poison Frog Alkaloid 239Q and its Congeners. Eur J Org Chem:7082
755. Brown AM (1887) A Treatase on the Animal Alkaloids, Cadaveric and Vital; or, The Ptomaïnes and Leukomaïnes: Chemically, Physiologically, and Pathologically Considered in Relation to Scientific Medicine. Baillière, Tindall, and Cox: London. Brown AM (1889) The Animal Alkaloids, Cadaveric and Vital; or, The Ptomaines and Leukomaines. Chemically, Physiologically, and Pathologically Considered in Relation to Scientific Medicine. Second Edn. Hirschfeld Brothers: London
756. Zhu C, Meador TB, Dummann W, Hinrichs KU (2014) Identification of Unusual Butanetriol Dialkyl Glycerol Tetraether and Pentanetriol Dialkyl Glycerol Tetraether Lipids in Marine Sediments. Rapid Commun Mass Spectrom 28:332
757. Dudley E, Bond L (2013) Mass Spectrometry Analysis of Nucleosides and Nucleotides. Mass Spectrom Rev. Published online in Wiley Online Library 27. 11. 2013, 33:302
758. Bane V, Lehane M, Dikshit M, O'Riordan, Furey A (2014) Tetrodotoxin: Chemistry, Toxicity, Source, Distribution and Detection. Toxins 6:693
759. Sabareesh V, Manikandan K, Sinha KM (2014) Understanding Dissociation of Cyclic Dinucleotide Ions by Electrospray Mass Spectrometry. Int J Mass Spectrom 364:9
760. Schirmer T, Jenal U (2009) Structural and Mechanistic Determinants of c-di-GMP Signalling. Nature Rev Microbiol 7:724
761. Chai YF, Pan YJ (2014) The Effect of Cation Size (H^+, Li^+, Na^+, and K^+) on *McLafferty*-Type Rearrangement of Even-Electron Ions in Mass Spectrometry. Science China, Chemistry 57:662
762. Hsu FF, Turk J (2007) Differentiation of 1-*O*-Alk-1′-enyl-2-acyl and 1-*O*-2-Acylalkyl Glycerophospholipids by Multiple-Stage Linear Ion-Trap Mass Spectrometry with Electrospray Ionization. J Am Soc Mass Spectrom 18:2065
763. Hsu FF, Lodhi IJ, Turk J, Semenkovich CF (2014) Structural Distinction of Diacyl-, Alkylacyl, and Alk-1-enylacyl Glycerophosphocholins as $[M - 15]^-$ Ions by Multiple-Stage Linear Ion-Trap Mass Spectrometry with Electrospray Ionization. J Am Soc Mass Spectrom. Published online 30.4.2014. DOI : 10.1007/s13361-014-0908-x
764. Vences M, Sanchez E, Hauswaldt JS, Eikelmann D, Rodríguez A, Carranza S, Donaire D, Gehara M, Helfer V, Lötters S, Werner P, Schulz S, Steinfart S (2014) Nuclear and Mitochondrial Multilocus Phylogeny and Survey of Alkaloid Content in True Salamanders of the Genus *Salmandra* (Salmandridae). Mol Phylogen Evol 73:208
765. Melo T, Santos N, Lopes D, Alves E, Maciel E, Faustino MAF, Tomé JPC, Neves MGPMS, Almeida A, Domingues P, Segundo MA, Domingues MRM (2013) Photosensitized Oxidation of Phosphatidylethanolamines Monitored by Electrospray Tandem Mass Spectrometry. J Mass Spectrom 48:1357
766. Cappellini E, Collins MJ, Gilbert MTP (2014) Unlocking Ancient Protein Palimpsests. Science 343:1320
767. Voráč A, Šedo O, Havliš J, Zdráhal Z (2014) A Simplified Method for Peptide *de novo* Sequencing Using ^{18}O Labeling. Eur J Mass Spectrom 20:255
768. Chingin K, Xu N, Chen H (2014) Soft Supercharging of Biomolecular Ions in Electrospray Ionization Mass Spectrometry. J Am Soc Mass Spectrom 25:928

769. Poad BLJ, Pham HT, Thomas MC, Nealon JR, Campbell JL, Mitchell TW, Blsanksby SJ (2010) Ozone-Induced Dissociation on a Modified Tandem Linear Ion-Trap: Observation of Different Reactivity for Isomeric Lipids. J Am Soc Mass Spectrom 21:1989
770. Duran FY, Duran Ö (2014) Weever Fish Sting: an Unusual Problem. J Acad Emerg Med 13:42
771. Carlisle DB (1962) The Venom of the Lesser Weeverfish, *Trachinus vipera.* J Mar Biol Assoc UK 42:155
772. Dehaan A, Ben-Meir P, Sagi A (1991) A "Scorpion Fish" (*Trachinus vipera*) Sting: Fishermen's Hazard. Br J Ind Med 48:718
773. Haavaldsen R, Fonnum F(1963) Weever Venom. Nature 199:286
774. Chhatwal I, Dreyer F (1992) Isolation and Characterization of Dracotoxin from the Venom of the Greater Weeverfish *Trachinus draco.* Toxicon 30:87
775. Lemke RAS, Peterson AC, Ziegelhoffer EC, Westphall MS, Tjellström H, Coon JJ, Donohue TJ (2014) Synthesis and Scavenging Role of Furan Fatty Acids. Proc Natl Acad Sci USA 111:E3457
776. Robinson MR, Moore KL, Brodbelt S (2014) Direct Identification of Tyrosin Sulfation by Using Ultraviolet Photodissociation Mass Spectrometry. J Am Soc Mass Spectrom 25:1461
777. Li X, Huang R, Liu Y, Jin H, Wan H, Zhao J, Zhao W, Liang X (2014) Efficient Purification of Low Molecular Weight Nitrogen Polar Compounds from the Skin of *Bufo bufo gargarizans* Cantor by Reversed Phase High Performance Liquid Chromatography with a Polar-Copolymerized C18 Stationary Phase. Anal Methods 6:5183

Nuclear Magnetic Resonance in the Structural Elucidation of Natural Products

William F. Reynolds and Eugene P. Mazzola

Contents

W.F. Reynolds (✉)
Department of Chemistry, University of Toronto, Toronto, ON, Canada M5S 3H6
e-mail: wreynold@chem.utoronto.ca

E.P. Mazzola
University of Maryland-FDA Joint Institute, College Park, MD, 20742 USA
e-mail: emazzola@umd.edu

A.D. Kinghorn, H. Falk, J. Kobayashi (eds.), *Progress in the Chemistry of Organic Natural Products, Vol. 100*, DOI 10.1007/978-3-319-05275-5_3,

1 Introduction

For at least the first 60 years of the twentieth century, natural product structure elucidation was a lengthy and extremely difficult task, usually involving numerous synthetic and degradative reactions. As such, it attracted the attention of many of the world's leading synthetic organic chemists. However, since then, dramatic improvements in nuclear magnetic resonance (NMR) spectroscopy, along with similar advances in mass spectrometry, X-ray crystallography, and chromatography, have totally revolutionized natural product structure elucidation. For example, although strychnine (**1**) had been purified from its plant source over a century earlier, it took more than 40 years of effort by several research groups, before its structure was finally determined by Sir *Robert Robinson* in 1946 (*1*) and later confirmed by a total synthesis of strychnine by *R.B. Woodward* and co-workers (*2*). Now with modern NMR methods and a state-of-the-art NMR spectrometer, the total structure of strychnine could be determined in 24 h using less than 1 mg of sample.

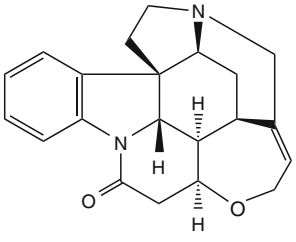

1

This is partly due to dramatic improvements in spectrometers. For example, one of the authors (*WFR*) got his start in NMR in 1960, using a 60-MHz spectrometer with a guaranteed proton signal/noise (*S/N*) of 10:1 for 1.0% ethylbenzene. Now spectrometers are available up to 1,000 MHz, and *S/N* specifications on

cryogenically cooled probes are approaching 10,000:1 for 0.1% ethylbenzene! However, developments in methodology have been equally critical. Of these, the development of *Fourier* transform (FT) NMR by *Wes Anderson* and *Richard Ernst* in 1966 (*3*) and two-dimensional (2D) NMR by *Richard Ernst* in 1976 (*4*) were particularly important, with *Ernst* receiving the 1991 *Nobel* Prize in Chemistry for his contributions (*5*).

This chapter is written with the goal of helping natural product chemists use modern NMR methods as effectively as possible for natural product structure elucidation. It is assumed that the reader will have at least a basic knowledge of the use of NMR in organic chemistry, at the level covered in senior undergraduate or graduate courses in spectroscopic methods for organic structure determination and as provided by texts such as *Silverstein et al.* (*6*) or *Lambert et al.* (*7*). Therefore, topics such as typical values of chemical shifts and coupling constants and factors affecting these parameters will not be discussed. Instead, emphasis will be placed on the rapid determination as to whether an isolated compound is known or new, the information content of different 2D and selective 1D experiments, their use in combination for structure elucidation, possible pitfalls in structure determination by NMR and how these can be avoided or overcome, and the use of computer-assisted structure elucidation (CASE). Considerable space will also be devoted as to how to make the correct choices of acquisition parameters and data processing methods and parameters. While this topic has been discussed in two books (*8, 9*) and at least two review articles (*10, 11*), the importance of this topic seems to be underappreciated by most users of NMR. In this regard, it is important to recognize that the default parameters provided in the manufacturers' software packages or a widely used book, which provides default parameters for many NMR experiments (*8*), may not be ideal and that sometimes dramatic improvements in results can be obtained by different choices (*12*).

The references given in the various sections are intended to be representative rather than comprehensive and are often chosen from our own published work. Finally, in places the authors refer to specific NMR spectrometer manufacturers and their products. This is done so that the reader is aware of various options available and the different procedures that sometimes have to be followed in processing or interpreting the data obtained on different spectrometers due to hardware and/or software differences. It should not be taken as indicating a preference of one spectrometer over another.

2 Dereplication: Distinguishing Between New and Known Natural Products

Much of current natural product research involves bioassay screening of crude chromatographic fractions, followed by separation of fractions with promising activity into pure compounds for further detailed testing. Both in terms of time and cost, it is important to be able to quickly identify any known compounds to avoid wasting valuable analytical instrument time on detailed characterization of known

compounds. However, it is also important that this identification process be sufficiently reliable so that there is minimal risk of mistaking an unknown compound for a known compound. Unfortunately, these two requirements conflict, forcing one to compromise either speed or reliability to a certain extent. The advantages and disadvantages of the various approaches that can be used are discussed below.

In view of its intrinsic high sensitivity, mass spectrometry (MS) is a logical initial choice for dereplication, most commonly in conjunction with liquid chromatography (see this volume, *Budzikiewicz H* (2014) Mass Spectrometry in Natural Product Structure Elucidation. Progr Chem Org Nat Prod 100:77). Only a small fraction of the crude extract will often be sufficient for an LC-MS investigation, using either low (LR) or high (HR) resolution MS. While LR-MS is quicker, it is not sufficiently accurate to determine exact molecular formulae, and there are often a large number of structures consistent with the parent ion. HR-MS will give the empirical formulae for a much smaller number of possible structures. Even in the ideal situation where only one empirical formula is consistent with the exact mass within acceptable error limits (usually 5 ppm), there can still be a number of isomeric structures consistent with this mass. However, MS databases (see this volume, *Budzikiewicz H* (2014) will usually list all known structures consistent with an empirical formula. In principle, one may be able to use MS fragmentation patterns to favor one structure over the others. However, the fragmentation pattern and/or the relative intensities of fragment ions can be different, depending on the ionization source and/or ionization energy. In addition, there can be ambiguities in the interpretation of fragmentation patterns. For example, a number of years ago, we determined the structure of a triterpene, 3-acetylaleuritolic acid (**2**), by 2D NMR and discovered that three different structures (one of which was correct) had been proposed for the same compound, mainly based on different interpretations of the MS fragmentation pattern (*13*).

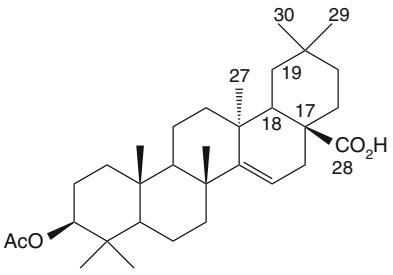

2

An alternative, intermediate sensitivity, approach is to use ^{1}H NMR spectroscopy for dereplication. While in principle this can be done by LC-NMR in flow mode, it is better to collect the samples in solid phase extraction cartridges and then transfer them to NMR tubes (see Sect. 11). Ideally, spectra should be obtained using either a cryogenically cooled probe or microprobe for maximum sensitivity (see Sect. 12),

but unfortunately these probes are not available to many natural product groups. However, even using 5-mm tubes in an ambient temperature probe, one can get adequate ^{1}H spectra in no more than one minute with 1 mg of sample. The main problem with ^{1}H NMR for dereplication purposes is that the appearance of these spectra can change significantly with spectrometer frequency and solvent. Thus, it may be difficult to determine with certainty whether a particular spectrum is identical to one from a database, which was obtained under different experimental conditions. However, several open access and commercial databases also include programs, that will predict the appearance of a ^{1}H spectrum for a given structure at a given frequency (NMRWiki provides a list of NMR databases (*14*)). Thus, if one has a list of candidate structures from HR-MS, one can compare the calculated spectra for these compounds with an experimental spectrum, hopefully leading to the most probable structure.

Clearly, the most reliable identification of a known compound would be provided by a combination of a ^{13}C NMR spectrum and a HR-MS spectrum. For that reason, journals increasingly require both a good quality ^{13}C spectrum and a HR-MS spectrum when reporting a new organic compound. Unfortunately, however, the intrinsic low sensitivity of ^{13}C NMR often makes it impractical to use a full ^{13}C spectrum for dereplication purposes unless one is fortunate enough to have access to a cryogenically cooled probe optimized for ^{13}C detection. However, a good compromise is to obtain a DEPT-135 spectrum (Sect. 14) or an edited HSQC spectrum (Sect. 10). Both spectra give ^{13}C data for all protonated compounds with CH and CH_3 peaks of opposite phase to CH_2 peaks and can be obtained in similar time and significantly more quickly than for a full ^{13}C spectrum (*10*). However, the HSQC spectrum has the additional major advantage of providing the chemical shifts of the proton(s) attached to each specific carbon. In addition, the use of non-uniform sampling along the evolution axis (*15*) has the potential to further increase the sensitivity of HSQC spectra (*16*).

Even greater time saving can be achieved by using either the SOFAST-HMQC sequence of *Brutscher* (*17*) or the ASAP-HMQC sequence of *Kupce* and *Freeman* (*18*). Both of these sequences allow the use of far shorter than usual relaxation delays, dramatically reducing the time to acquire a 2D $^{1}H–^{13}C$ correlation spectrum. For example, it has recently been shown that one can obtain a high quality HMQC spectrum on a 400-MHz spectrometer in under one minute for a 5 mg sample of a compound of over 400 molecular weight, using the ASAP-HMQC sequence (*19*). The only disadvantages of these sequences are that they do not provide spectral editing and have poorer ^{13}C resolution than provided by HSQC spectra. Nevertheless, they have tremendous potential, particularly for rapid screening and dereplication.

It is unfortunate that, so far as we are aware, none of the existing $^{1}H/^{13}C$ databases are integrated to take advantage of the additional information provided by HSQC or HMQC, *i.e.* they do not correlate ^{1}H chemical shifts with the ^{13}C chemical shifts of the carbons to which the protons are bonded. However, we understand that this integration is in progress and, when integrated $^{1}H/^{13}C$ databases are available, this in conjunction with HR-MS will provide a highly reliable approach for dereplication.

One problem with the use of NMR databases for dereplication is that full spectral assignments are not available for many older known compounds. Unfortunately, natural product journals usually will not allow publication of assignments for known compounds unless one has data for a significant number of related compounds. However, several open access databases will accept these data (*14*). Thus, we would strongly encourage natural product chemists to carry out full assignments for known compounds, where these are not available, and deposit the information in at least one of these databases, for the benefit of all in the field. Procedures for making these assignments, using combinations of 2D NMR spectra, are discussed in Sect. 4. The same procedures can be used to identify the structures and fully assign the spectra of new compounds.

3 Quantitative NMR

One very important advantage of ^{1}H NMR over all of the other types of spectroscopy used in natural product chemistry is that it is intrinsically quantitative. To realize this advantage, it is necessary to take reasonable care in the choice of acquisition parameters, but this is not difficult (see Sect. 14 for a discussion of parameter choices). There has been a recent significant increase in interest in the use of quantitative NMR in the natural product field (*20, 21*), and there is now a website devoted to this topic, which is an excellent source of information (*22*).

There are two ways in which quantitative ^{1}H NMR measurements can be carried out. The first approach, which is particularly suitable for natural product investigations, is to use these measurements to determine the relative amounts of different compounds in a complex mixture (*20*). There are two basic requirements. First, there must be at least one well-resolved peak (corresponding to a known number of protons) for each compound so that the relative amounts can be estimated from the integrated areas of the resolved peaks. It may be difficult to meet this requirement for complex mixtures so the use of the highest field available spectrometer is strongly recommended. Second, ideally one should know the identities of the different compounds in the mixture. Unfortunately, this often is not known and may be difficult to determine for minor components. However, if the goal is to determine the relative purity of a single major component, then the knowledge of the exact structures of minor components may not be essential (*23*).

Alternatively, quantitative ^{1}H NMR can be used to determine the absolute concentration of a compound. This requires the use of a reference standard of known concentration. In the past, some form of internal reference has been commonly used. The reference compound needs to be non-volatile (so that the amount added to the sample can be accurately weighed), not react with the compound of interest, and have a peak (preferably a singlet) in a region of the spectrum otherwise free of peaks. It is also desirable that reference compounds not have other peaks that overlap with the spectrum of the compound for which the concentration is to be

determined. The internal reference should also be a compound that can be easily separated from the natural product to facilitate recycling of rare samples after NMR spectroscopy!

An alternative approach, which is increasingly being adopted, is to use an external reference. The two major NMR spectrometer manufacturers favor different methods of referencing. The first approach, which goes by the name, ERETIC, is most commonly used with Bruker spectrometers (*24*). This involves electronically adding a reference signal of known intensity. The signal is injected into an unused coil on the spectrometer (*e.g*. the heteronuclear coil when acquiring proton spectra) at a clear region of the spectrum. The reference signal can be calibrated by comparing its integral with that of a standard solution of known concentration. The main problem with this approach is that the relative areas of the reference signal and the sample signals (which are detected on different coils of the probe) are slightly dependent on the nature of the sample solution, with the biggest problems occurring with "lossy" samples, particularly those with high salt concentrations. Various procedures to correct this type of error have been suggested, *e.g*. PULCON (*25*) and QUANTAS (*26*), which can reduce the uncertainties in this type of measurement to under 1%. This requires accurate recalibration of the 90° pulse width for each sample to ensure maximum precision.

The second approach, favored by Agilent (*27*), takes advantage of the high linearity and reproducibility of modern NMR spectrometers. In this case, the reference standard is first measured in one tube then the sample is run in the second tube. Ideally, the same solvent should be used for both tubes. If the reference sample is measured periodically, the reported precision is similar to that reported using PULCON or QUANTAS. However, if the reference measurement is repeated before each new sample, even higher precision (well under 1%) is claimed. It appears that environmental conditions (particularly variations in the laboratory temperature) provide the largest source of error with either method and this is minimized if the calibration is repeated for each new sample (*27*).

^{13}C NMR spectroscopy can, in principle, also be used for quantitative measurements, with the increased resolution of ^{13}C spectra an attractive feature for complex mixtures. However, this is very difficult in practice. The major stumbling block is the far lower sensitivity of ^{13}C NMR relative to ^{1}H NMR, making it very difficult to obtain accurate integrals of peak areas. In addition, there are large differences in T_1 relaxation times between protonated and non-protonated carbons in organic compounds, requiring extremely long relaxation delays in order to get comparable signal intensities for the two types of carbons. A related problem is that the nuclear *Overhauser* enhancements (N*O*Es) are often significantly smaller for non-protonated than protonated carbons. In order to make the entire spectrum quantitative, one must combine a long relaxation delay (ideally $5T_1$ of the slowest relaxing carbons) with N*O*E suppression. The latter is accomplished by gating the decoupler off during the relaxation delay, turning it on only during the acquisition period. Unfortunately, this aggravates the problem of low ^{13}C sensitivity by further reducing the signal/noise (*S*/*N*) through N*O*E suppression.

However, if the goal is specifically to determine the relative amounts of two or more compounds in a mixture or the absolute amount of a single component relative to a reference compound, these problems can be minimized by solely measuring peak areas for one or more protonated carbons. Particularly, T_1 values for methine or methylene carbons of natural products are typically less than 1 s, allowing the use of a relatively short relaxation delay. However, if precise quantitative data are required, N*O*E suppression should still be used because the N*O*E values for different carbons may not be exactly the same. Finally, the possibility of carrying out quantitative ^{13}C NMR measurements is significantly improved if one has access to a cryogenically cooled probe, particularly when optimized for ^{13}C detection.

4 Using 2D NMR to Determine Skeletal Structures of Natural Products

By 1984, it was apparent that 2D NMR was a potentially powerful technique for investigating structures of natural products (*28*). However, the investigations up to that time had involved the use of ^{1}H–^{1}H homonuclear correlation spectroscopy (COSY) and one-bond ^{1}H–^{13}C heteronuclear correlation spectroscopy. These two types of spectra together could determine protonated carbon fragments of molecules but could not provide total structures. However, three publications in 1984 demonstrated the use of long-range (*i.e*. separated by two or three bonds) ^{1}H–^{13}C heteronuclear correlation spectroscopy to determine complete structures by combining different protonated carbon fragments together into complete structures *via* correlations to quaternary carbons and/or through heteroatoms from one protonated carbon fragment to another (*29–31*). The first two of these publications mainly focused on correlations to carbonyl groups in polypeptides, but the third applied the technique more broadly to assign the structure and spectra of a diterpene, kauradienoic acid (**3**).

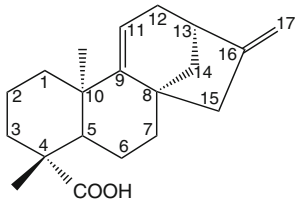

3

This provided the basic combination of techniques, which is still used for natural product structure elucidation, and a large number of publications using long-range correlation soon appeared. We believe that the earliest example, which most clearly indicated of the power of this technique, was provided by the determination of the structure of guyanin (**4**), a tetranortriterpene of unprecedented structure, solely by this combination of 2D experiments (*32*). Guyanin (**4**) has 36 heavy atoms (28 carbons and 8 oxygens) but only 17 protonated carbons and no sequences of protonated

carbons greater than two. Thus, it would have been impossible to determine the full skeletal structure without long-range $^{1}H–^{13}C$ correlation data.

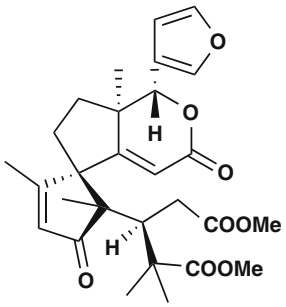

4

The basic COSY sequence (*33*) is still in wide use to date, usually with the use of z-axis gradients for coherence pathway selection. This is sometimes supplemented by TOCSY ("total correlation") spectra, which can provide correlations in a whole sequence of coupled protons (*34*). Early $^{1}H–^{13}C$ correlation experiments involved ^{13}C ("direct") detection. One-bond correlation spectra were mainly obtained with the HETCOR sequence (*35*) while long-range experiments were either obtained with the basic HETCOR sequence optimized for long-range coupling constants (*29, 31*) or with one of three sequences specifically designed for this purpose (*30*, *36*). However, the $^{1}H–^{13}C$ correlation experiments are now almost exclusively obtained using ^{1}H ("indirect") sequences to take advantage of their higher sensitivity. One-bond spectra were originally mainly obtained with the HMQC sequence (*37*) but now often with the HSQC sequence (*38*). Long-range $^{1}H–^{13}C$ correlation spectra are almost exclusively obtained with one of the variants of the basic HMBC sequence (*39*). The relative advantages and disadvantages of some of the alternative versions of the various 2D sequences are discussed in the following section.

The basic approach to assembling a structure from the correlation data from different 2D experiments is similar to putting together the pieces of a jigsaw puzzle. This has been illustrated in detail for T-2 toxin (**5**) (*40*). We will illustrate the same approach using spectra for kauradienoic acid (**3**) in Sect. 7.

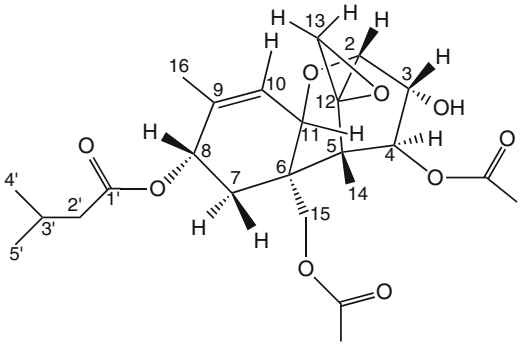

5

The largest obstacle until now in using this approach to determine skeletal structures of natural products and other organic compounds is the lack of any sequence that could clearly distinguish between 2-bond and 3-bond $^{1}H–^{13}C$ correlations to non-protonated carbons. This can lead to ambiguities and possible alternative structures. However, it has recently been shown that the 1,1-ADEQUATE sequence (*41*) can be used to specifically identify all two-bond H-C correlations (*42, 43*). In turn, this can dramatically decrease the amount of time needed and the number of alternative structures generated when using computer-assisted structure elucidation (CASE, see Sect. 8) (*43*). The problem is that this experiment requires one-bond $^{13}C–^{13}C$ coupling, a 0.01% probability. Consequently, this is really only feasible if one has access to a ^{1}H-optimized cryogenically cooled probe. For example, it has recently been shown that one can obtain an acceptable quality 1,1-ADEQUATE spectrum overnight with less than 1 mg of strychnine, using a 1.7-mm cryogenically cooled 600-MHz probe (*44*). These authors used covariance processing of the 1,1-ADEQUATE spectrum and an edited HSQC spectrum to generate an improved quality spectrum (*44*). However, it should be noted that this approach still requires sufficient *S*/*N* of the original 1,1-ADEQUATE correlations for them to appear in the covariance spectrum. Covariance processing mathematically combines the results of two different 2D spectra to produce a new spectrum, which, although it does not actually contain new information, may display key correlation data in a manner that is more obvious and easier to interpret (*45*). It is particularly valuable when it can use two high-sensitivity spectra to generate a spectrum with good *S*/*N* that corresponds to one of much lower intrinsic sensitivity and which otherwise would take far longer to acquire.

While ^{14}N is a reasonably high sensitivity NMR nucleus (with almost 100% abundance), it is a quadrupolar nucleus, and its resultant extremely broad lines make it of extremely limited value for natural product investigations. However, ^{15}N NMR spectra can provide very useful structural information for nitrogen-containing natural products (*46, 47*). The low natural abundance of ^{15}N (0.37%) combined with its low frequency (~50 MHz on a 500-MHz spectrometer make it unsuitable for direct detection. However, indirect (proton) detection provides a tenfold enhancement, and all recent applications in the natural product field have used indirect detection methods, mainly involving HSQC, HMQC, and HMBC spectra or variants of these experiments. There are two further problems with ^{15}N for natural product research in addition to sensitivity limitations (*46*). First, while one-bond $^{1}H–^{15}N$ coupling constants fall in a narrow (90–100 Hz) range, two-bond and longer range couplings tend to show much greater variability than the corresponding $^{1}H–^{13}C$ couplings (*46*). This makes it difficult to detect all expected long-range $^{1}H–^{15}N$ correlations in an HMBC experiment with a fixed $^{1}H–^{15}N$ delay. Second, ^{15}N has an extremely large chemical shift range (*ca*. 600 ppm) while most H/X and H/C/N probes have relatively long ^{15}N 90° pulse widths (*ca*. 40 μs), which cannot uniformly excite the entire ^{15}N spectral window, risking failure to detect peaks near either end of the window.

Fortunately, advances in instrumentation and pulse sequence design have minimized these problems. First, cryogenically cooled probes have significantly reduced

the sample requirements. For example, *Martin et al*. have shown that a recently developed 1.7-mm cryo-microprobe can provide useable ^{15}N HMBC spectra overnight with well under 1 mg of sample (*48*). The same probe had a 90° pulse width of 25 μs, allowing 90% or more excitation over about a 500-ppm shift range for ^{15}N (*48*). Various solutions have been proposed to minimize the problem of the variation in long-range ^{1}H–^{15}N coupling constants (*47*). As an example, *Cheatham et al*. have developed the ^{15}N CIGAR sequence, which uses an "accordion" delay that is optimized for ^{1}H–^{15}N couplings in the 3–10 Hz range (*49*). There are at least two other time-saving approaches. First, since there are typically only a very small number of ^{15}N peaks in a nitrogen-containing natural product (often only one), one can usually utilize a lower *F*1 resolution by decreasing the number of time increments used (and correspondingly increasing the number of scans per time increment to improve sensitivity).

Second, if the natural product contains both protonated and non-protonated nitrogens, one does not need to acquire separate one-bond (HSQC or HMQC) spectra along with an HMBC-type spectrum. Instead, one can eliminate the "*J* filter" present in HMBC sequences and simultaneously observe both one-bond and n-bond correlations, with the former distinguished from the latter by the observation of a large (90–100 Hz) doublet splitting due to the direct ^{1}H–^{15}N coupling (*49*).

5 Avoiding Getting the Wrong Skeletal Structure

One might assume that, with all of the modern techniques available, it would be unlikely that incorrect structures are reported in the chemical literature. However, there have been a surprisingly large number of incorrect structures reported (*50*). Many of these involve errors in stereochemistry, which often can be quite tricky to determine, particularly in acyclic compounds or those with conformationally mobile rings (see Sect. 6 for a discussion of the determination of stereochemistry). However, some involve incorrect skeletal structures where errors should be easier to avoid. One example of the latter kind of error, which attracted a lot of attention and controversy, is hexacyclinol (**6**) (*51*). Fortunately, there are several precautions that one can take to minimize the risk of mistakes. These are discussed below.

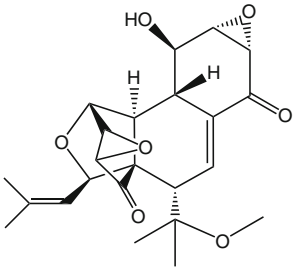

6

1. Do not try to fit the data to a preconceived notion of structure but rather allow the data to determine possible structure(s). This problem is most likely to occur if there is severe overlap in at least part of the spectrum and/or marginal signal/noise, which may cause ambiguities in assigning correlations. In this situation, trying to save time by collecting too few scans and/or too few data points (particularly *F*1 increments) is actually counterproductive by maximizing the risks of ambiguity. An old trick of aromatic solvent-induced shifts (*52*) can often be used to minimize overlap by repeating the spectrum with added increments of C_6D_6. The present authors have found this to often be valuable for natural product structure elucidation (*13*).
2. Tabulate all 2D data and check carefully for unexpected peaks and missing expected peaks. A peak of significant intensity in an HMBC spectrum, which is not consistent with a proposed structure, should be taken as a strong warning sign that the structure is probably incorrect. On the other hand, the absence of an expected peak may not always be as significant since this may just be due to a relatively small 2-bond or 3-bond $^{1}H–^{13}C$ coupling constant. A common case where a peak is either not observed or very weak is for 2-bond correlations in aromatic or olefinic groups. Another case where weak peaks often occur is for 3-bond correlations involving *axial* protons in cyclohexane-like rings. A general knowledge of expected n-bond $^{1}H–^{13}C$ coupling constants for different types of structural units is helpful (*53*). Some representative values for aliphatic, olefinic, and aromatic derivatives are: 0–3 Hz for 2-bond olefinic and aromatic couplings, 8 Hz for 3-bond aromatic and *cis*-olefinic couplings, 12 Hz for *trans*-olefinic couplings, 3–5 Hz for 2-bond aliphatic couplings, 2–4 Hz for 3-bond *gauche*-aliphatic couplings and 6–9 Hz for *anti*-aliphatic couplings. Longer range (4-bond and 5-bond) couplings are generally less than 2 Hz but may occasionally show up as weak HMBC correlations, particularly in conjugated derivatives or from methyl protons.
3. Beware of deceptively appearing spectra. In our experience this may take one of two forms. First, due to a combination of effects, a ^{13}C peak may occur at a chemical shift, which seems more consistent with an entirely different type of functional group. For example, a conjugated lactone (**7**) had a ^{13}C peak at δ 182.6 ppm that was initially assumed, based on the chemical shift, to be either a carboxylic acid group or a highly conjugated ketone. However, it was eventually assigned as the non-protonated olefinic carbon, based on HMBC cross-peaks to all three methyl proton signals and the two pseudo-equatorial methylene protons (*54*). A second situation is when there is accidental equivalence between two coupled proton signals. While one learns very early in NMR that no coupling will be observed between equivalent protons, it is still easy to forget this in the case of accidental equivalence. One example of this was provided by the marine sterol gorgost-5-ene-3β,9α,11α-triol (**8**) (*55*). In this case, the expected H-21 methyl doublet appeared as a slightly broadened singlet, initially leading to the assumption of some type of rearrangement of the steroid side chain. However, examination of the HSQC spectrum showed that H-20 and H-21 had the same chemical shift while the HMBC spectrum showed a strong cross-peak between H-21 and C-20, confirming that the methyl singlet was due to accidental equivalence of H-20 and H-21.
4. Just because a structure appears to fit the correlation data, do not assume that this is the only structure consistent with the data. This error, which is extremely easy

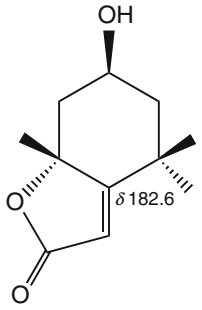

7

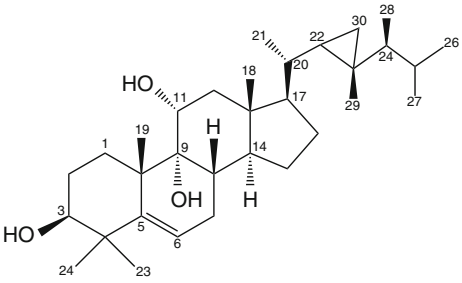

8

to make, can be best avoided by the use of computer-assisted structure elucidation (CASE) (see Sect. 8). The program Structure Elucidator (*56*), provided by ACD, is the one with we have the most experience. This will not only determine all possible structures consistent with the correlation data but will rank them in order of probability based on a comparison of observed ^{1}H and ^{13}C chemical shifts with those calculated by the program for the different structures. In cases where there is no clear distinction between two or more possible skeletal structures, examination of the structure may suggest additional experiments, which may allow this distinction (*57*). The program also alerts the user to ambiguous assignments due to severe spectral overlap so that these problems can be considered individually (*57*).

6 Determination of Configuration and/or Conformation of Natural Products

The degree of difficulty of this task is mainly determined by whether the molecule exists in a single, relatively rigid, conformation or is undergoing rapid interconversion between two or more conformations. The latter situation is particularly difficult to deal with, but even determining the configuration and conformation of a rigid molecule can still pose problems. Also note that NMR alone will rarely provide absolute configurations. We will begin by considering the investigation of rigid molecules.

The two main tools to address these problems are *vicinal* $^{1}H–^{1}H$ coupling constants (*58*) and nuclear *Overhauser* enhancements (N*O*Es) (*59*). *Vicinal* coupling constants can be used to estimate $^{1}H–C–C–^{1}H$ dihedral angles, usually with the aid of some type of *Karplus* relationship such as the *Altona* equation (*60*). However, one must recognize that splittings in a proton multiplet are not always identical to coupling constants, particularly in the case of strong coupling. For example, if a pair of methylene protons has a near-zero chemical shift difference, they will appear to be equally coupled to an adjacent methine proton, regardless of the actual *vicinal* coupling constants, a phenomenon known as "virtual coupling" (*61*). However, provided that the methylene protons are, in principle, diastereotopic, it may be possible to separate them by using solvent effects such as aromatic solvent-induced shifts and thus determine the *vicinal* couplings. Another problem occurs if the two *vicinal* protons are equivalent by symmetry or by accident since one then will not observe a coupling between them. In either case, a coupled HSQC spectrum will allow one to measure the coupling since the large one-bond CH coupling within the $^{1}H–^{13}C–^{12}C–^{1}H$ fragment effectively makes the protons non-equivalent (*62*, *63*). This is a modification of the old idea of using ^{13}C satellites in a proton spectrum for this purpose (*64*). Alternatively, in the case of accidental equivalence, one could again try to use solvent effects to separate the two proton signals.

Nuclear *Overhauser* enhancements can be measured either from 2D N*O*ESY (*65*) or R*O*ESY (*66*) spectra or by selective 1D equivalents. These have usually been used in a qualitative "yes–no" sense to determine whether pairs of protons are relatively close or relatively far apart. However, driven by improvements in selective 1D pulse sequences (*67*) and spectrometer hardware, there has been a recent revival of interest in using selective 1D N*O*ESY or R*O*ESY measurements to make quantitative distant measurements in organic molecules (*68*). Unlike, the earlier N*O*E-difference measurements which measure steady-state N*O*Es, the selective 1D experiments (and their 2D analogues) measure transient N*O*Es by selectively inverting a chosen proton multiplet and then following the buildup of N*O*Es for other cross-relaxed protons as the inverted proton relaxes back towards its initial value (*59*). The usual approach has been to plot N*O*E intensity *versus* mixing time and determine the slope from the initial linear region of the plot, the initial rate approximation (IRA) (*59*). However, this can be time consuming. Recently, *Butts et al.* have championed the alternative of using a single mixing time, which is short enough to fall in the regime where the IRA holds (*68*). By using the known distance between methylene protons as a calibration point, this group has not only measured the distances between other pairs of protons in strychnine with surprising accuracy (~3%) but also detected the presence of a previously unknown minor conformation of strychnine (*68*). The main limitation of this approach is that for higher molecular weight compounds and/or viscous solutions, the IRA may only be valid for short mixing times (<0.2 s) where the N*O*E peaks will be quite weak. However, the range of acceptable mixing times can be significantly extended by applying the PANIC correction developed by *Macura* for 2D N*O*ESY measurements (*69*) and extended by *Hu* for 1D N*O*ESY and R*O*ESY measurements (*70*). This requires a second measurement for each proton with zero mixing time with a correction for the N*O*E

peaks obtained from the ratio of the areas of the inverted peak with zero and the chosen mixing time.

An alternative approach, which is being increasingly applied, is to measure residual dipolar $^{1}H–^{13}C$ and/or $^{1}H–^{1}H$ couplings for a molecule in a weakly aligning medium (*71*, *72*). The relative magnitudes of different residual dipolar couplings are determined by the relative orientations of C–H or H–H bond vectors relative to the alignment tensor of the molecule. Unfortunately, this has a $(3\cos^2\theta - 1)$ relationship, and thus one cannot determine directly whether an individual bond has an angle θ, or $180° - \theta$, with respect to the alignment tensor. Nevertheless, provided one can measure at least five residual dipolar couplings, one can determine the alignment tensor (*71*). Obviously, the more values that can be determined, the better the molecular configuration and conformation will be defined. A series of alignment media suitable for polar and non-polar organic solvents are available, and measurements of 1-bond $^{1}H–^{13}C$ and *geminal* $^{1}H–^{1}H$ dipolar couplings are usually carried out with one or more modified versions of the coupled HSQC sequence (*71*). This is performed by determining the differences of these couplings in isotropic and partially aligning media. A number of relative configurations and conformations of rigid organic molecules have been determined in this way (*71*, *72*). One recent intriguing example of the power of this technique was the determination of the structure of a reaction impurity, which could not be determined by 2D NMR techniques (*73*). Nevertheless, this is a laborious technique, which, in our opinion, should be regarded as a last-resort method.

Any of the three approaches discussed above can be carried out in conjunction with calculations of molecular conformation of rigid molecules, either with classical molecular mechanics calculations or more increasingly with *ab initio* quantum mechanical calculations. However, calculations to determine the relative free energies and consequently the relative populations of different conformations are absolutely essential if one is dealing with a flexible molecule with two or more significantly populated conformations. Unfortunately, even small differences in calculated free energies correspond to significant differences in populations. Thus, while there has been some progress in interpreting both N*O*E measurements (*74*) and residual dipolar couplings (*71*) for flexible molecules, the conversion of the weight-averaged data from these measurements into accurately determined conformations of these molecules will require increasingly accurate energy calculations to make this at least semi-routine. Fortunately, the increasing speed of computers may make this feasible in the near future.

Normally, one can only determine the relative configuration of a natural product from NMR data. However, the conversion of secondary CH(OH) groups into chiral esters by *Mosher*'s method can often determine the absolute stereochemistry of that carbon in a natural product (*75*). While this is an empirical approach based on induced chemical shifts by the chiral ester, it seems surprisingly reliable. One example where we found this to be valuable was in determining the absolute stereochemistries of the two CH(OH) centers of the cembrane, cleospinol-A (**9**), which contained a flexible 14-membered macrocyclic ring (*76*). With the knowledge of the absolute stereochemistry at these two centers and the configurations of other chiral

centers relative to these two, it was possible to determine the absolute stereochemistry of the entire molecule. Another approach is to combine NMR measurements of relative stereochemistries within a molecule with a chiral spectroscopic method such as vibrational circular dichroism (see this volume: *Joseph-Nathan P* and *Gordillo-Román B* (2014) Vibrational Circular Dichroism Absolute Configuration Determination of Natural Products. Progr Chem Org Nat Prod 100:311), which gives the absolute stereochemistry (*77*).

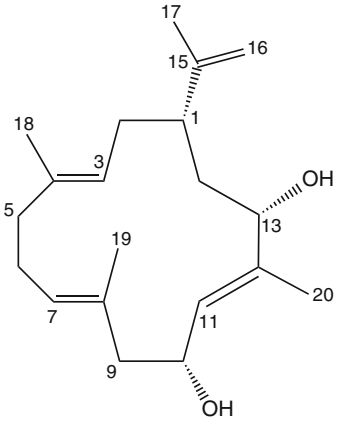

9

7 An Example of a Solved Structure: Kauradienoic Acid

A considerable number of NMR experiments have been introduced and discussed in the previous section. In order to illustrate how a series of such experiments is used in practice, the authors will take readers through a complete structural elucidation exercise for the compound kauradienoic acid (**3**). The structure of this compound was originally proposed in 1971 (*78*), and its ^{1}H and ^{13}C NMR spectra were assigned completely in 1984 (*31*). If one had no knowledge of the compound's structure, such a study would begin with the determination of its infrared, ^{1}H, and ^{13}C NMR spectra, and high-resolution mass spectrum. This compound is a white solid that is soluble in chloroform.

The mass spectrum indicated a molecular weight of *ca.* 300 and provided several pieces of information about the compound. The even molecular weight establishes that the unknown contains an *even* number of nitrogen atoms and probably none (zero, as in spectral-edited experiments, is considered to be an even number). If we make the preliminary, and usually justified, assumption that the unknown compound contains only carbon, hydrogen, and oxygen, the high-resolution, mass spectrometric-determined molecular weight supports a molecular formula of $C_{20}H_{28}O_2$. This formula, in turn, dictates the presence of seven units of unsaturation.

A strong infrared absorption centered at 1,760 cm^{-1} suggests the presence of a carbonyl group. Moreover, the occurrence of two oxygens in the molecular formula supports the inference that the carbonyl absorption could be due to an acid or ester group.

7.1 HSQC Data

After initial ^{1}H and ^{13}C NMR spectra have been determined for an unknown compound, it is useful to establish which hydrogens are directly attached to specific carbons by an HMQC or HSQC experiment. The latter is the experiment of choice because of its better resolution in the *F*1 domain (see Sect. 10). An edited-HSQC spectrum of a small sample of the unknown compound is shown in Fig. 1. Coupling constants, which have been measured in the ^{1}H NMR spectrum for those multiplets that are not severely overlapped, correspond to proton cross peaks in the COSY spectrum (see Sect. 7.2) and are included in parentheses in Table 1.

A cursory examination of the HSQC data in Table 1 indicates that the unknown compound is essentially aliphatic in nature. The highest frequency signal (182.74 ppm) is in the acid carbonyl range, while those carbons with chemical shifts from 158.56 to 105.48 ppm appear to be alkenic and require the presence of one methylene (105.48 ppm), one methine (114.90 ppm), and two quaternary sp^2

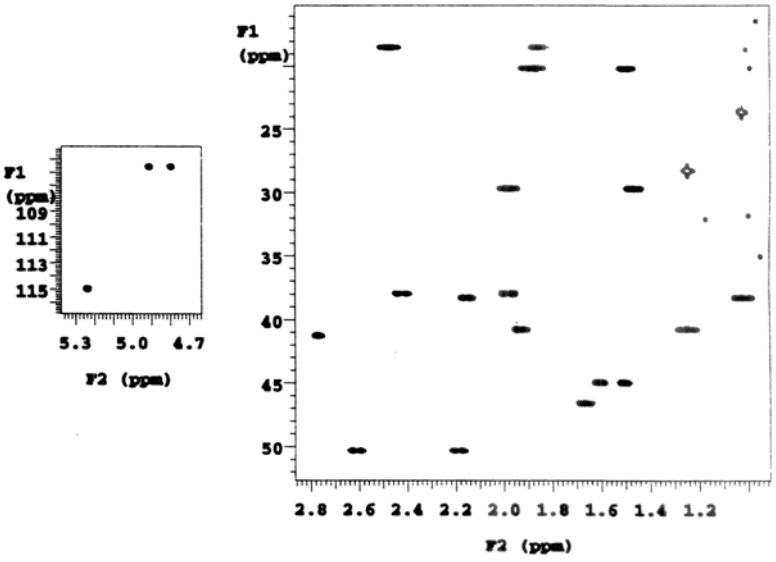

Fig. 1 Gradient-selected HSQC spectrum for kauradienoic acid (**3**) with aliphatic region on the *right* and olefinic region on the *left*

Table 1 HSQC data for kauradienoic acid (**3**)

δ_C/ppm	Attached hydrogens (with selected couplings)	
182.74	–	
158.56	–	
155.92	–	
114.90	5.24 ddd (4, 2.7, <1)	
105.48	4.91 brs	4.80 brs
50.32	2.62	2.20
46.56	1.67 d (11)	
44.94	1.60 d (5.2)	1.50 d (2.7)
44.69	–	
42.27	–	
41.24	2.77 dddd (5.2, 4.6, 2.7, 2, <1)	
40.75	1.93	1.24
38.79	–	
38.31	2.16	1.02
37.93	2.43 dd (4.6, 2.7)	1.99 dd (4, 2)
29.66	1.97 dd (10.8, 9)	1.46 dd (9, 1)
28.23	1.24 s (CH_3)	
23.62	1.02 s (CH_3)	
20.16	1.88	1.50
18.48	2.47 dddd (11, 9, 8.7, 1)	1.68 ddd (11, 8.9, 8.7)

carbons. Resonances of the remaining carbons are generally in the chemical shift range for aliphatic carbons that are not attached to oxygen.

The HSQC spectrum reveals the presence of two methyl, nine methylene, and three methine carbons. Subtracting these 14 protonated carbons from the 20-carbon total identifies the remaining six quaternary carbons. In addition, summing the six methyl, 18 methylene, and three methine protons accounts for 27 hydrogens. Since the molecular formula requires 28 hydrogens, the final proton must be attached to oxygen.

7.2 COSY and TOCSY Data

The construction of proton spin-coupling networks is achieved by COSY and TOCSY experiments. ^{1}H spin systems are observed in the COSY (Fig. 2) and TOCSY (Fig. 3) contour plots. Two are relatively simple and comprise (i) a 6-spin system of three contiguous methylene groups: a terminal pair of protons (1.93 and 1.24 ppm), an interior pair (1.88 and 1.50 ppm), and another terminal pair (2.16 and 1.02 ppm) (**10**) and (ii) a 5-spin system containing an isolated proton (1.67 ppm), an adjacent (middle) methylene pair of protons (2.47 and 1.68 ppm) and another methylene pair (1.97 and 1.46 ppm) (**11**).

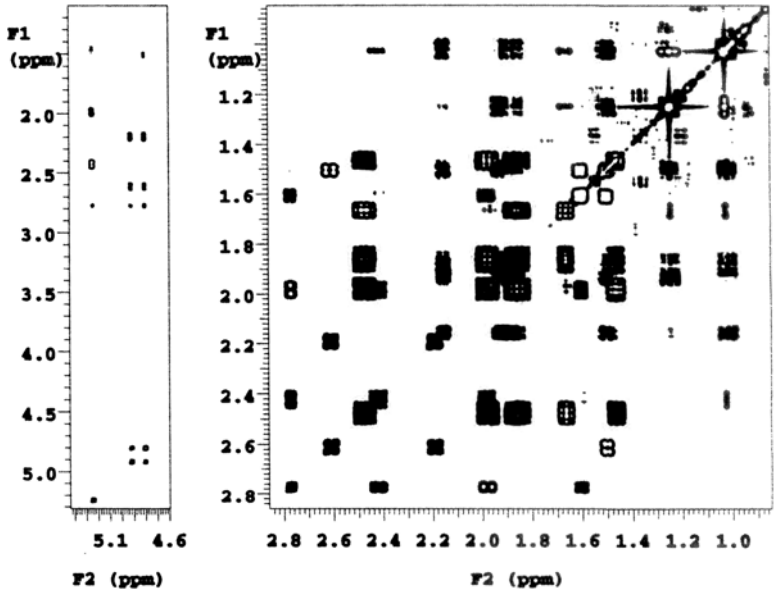

Fig. 2 Gradient-selected absolute-value COSY spectrum of kauradienoic acid (**3**). The *spectrum on the right* shows correlations between aliphatic protons while that on the *left* shows correlations between olefinic and aliphatic protons

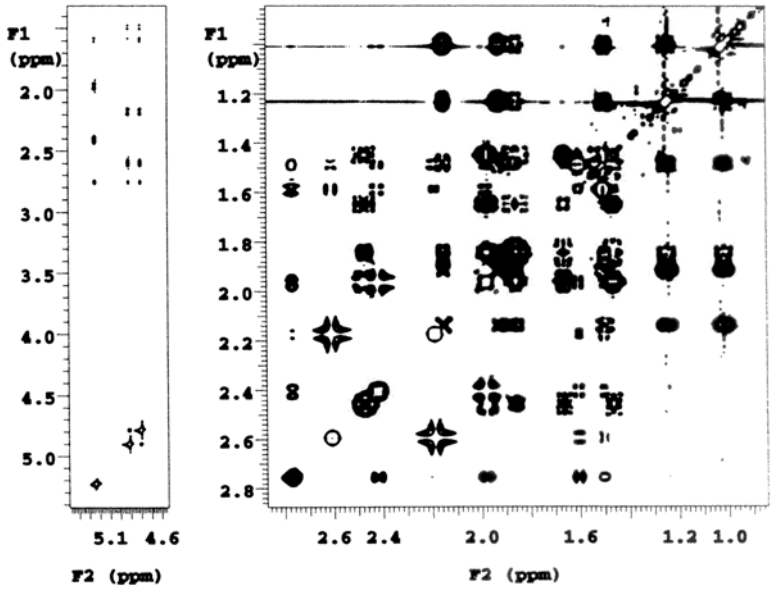

Fig. 3 Gradient-selected TOCSY spectrum of kauradienoic acid (**3**). The expansions are similar to those in Fig. 2. The spectrum was obtained with the original TOCSY sequence, without a zero-quantum filter, and shows some distortions of multiplet structures

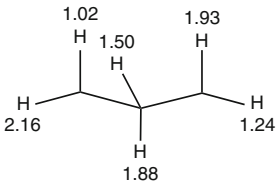

10

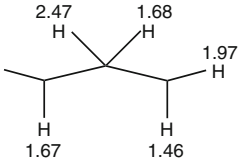

11

The third spin system is extensive and encompasses ten protons: two methines (5.24 and 2.77 ppm) and four methylenes (4.91 and 4.80, 2.62 and 2.20, 2.43 and 1.99, and 1.60 and 1.50 ppm). A 1D-Z-TOCSY trace, through the alkenic proton (Fig. 4), elegantly illustrates how it is coupled to the methylene protons at 2.43 and

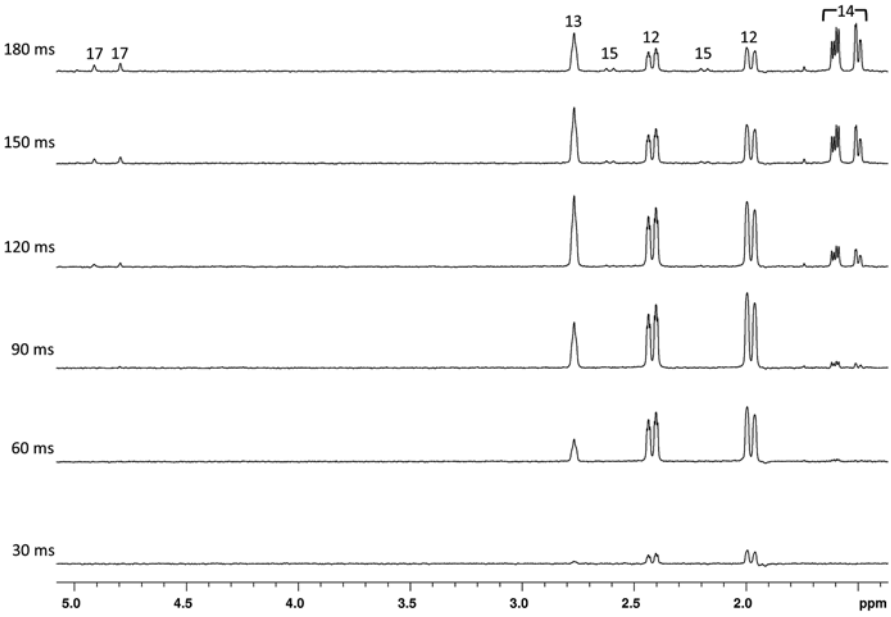

Fig. 4 1D Z-TOCSY spectra with different mixing times, obtained by selective irradiation of H-11 (5.24 ppm) of kauradienoic acid (**3**). Mixing times are listed at the *left* of each spectrum and proton assignments are listed at the *top*. The spectra illustrate nicely how a sequence of coupled protons can be fully assigned by a series of 1D TOCSY spectra with incremented mixing times. Also note that the zero-quantum filter allows observation of undistorted proton multiplets

1.99 ppm, the methine proton at 2.77 ppm, the methylene protons at 1.60 and 1.50 ppm, and finally to the alkenic protons at 4.91 and 4.80 ppm and the methylene protons at 2.62 and 2.20 ppm (**12**). The data for these spin systems are summarized in Tables 2 and 3.

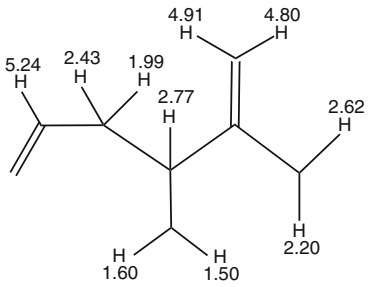

12

Table 2 COSY data for kauradienoic acid (**3**)

δ_H/ppm	Spin-coupled partners
5.24	2.77, 2.43, 1.99
4.91	4.80, 2.77, 2.62, 2.20
4.80	4.91, 2.77, 2.62, 2.20
2.77	5.24, 4.91, 4.80, 2.62, 2.43, 1.99, 1.60, 1.50
2.62	4.91, 4.80, 2.77, 2.20, 1.50
2.47	1.97, 1.68, 1.67, 1.46
2.43	5.24, 2.77, 1.99
2.20	4.91, 4.80, 2.62
2.16	1.88, 1.50, 1.02
1.99	5.24, 2.77, 2.43, 1.60
1.97	2.47, 1.68, 1.46
1.93	1.88, 1.50, 1.24
1.88	2.16, 1.93, 1.50, 1.24, 1.02
1.68	2.47, 1.97, 1.46
1.67	2.47
1.60	2.77, 1.99, 1.50
1.50[a]	2.77, 2.62, 2.16, 1.93, 1.88, 1.60, 1.24, 1.02
1.50[a]	
1.46	2.47, 1.97, 1.68
1.24	1.93, 1.88, 1.50
1.24 (CH_3)	(none)[b]
1.02	2.16, 1.88, 1.50
1.02 (CH_3)	(none)[c]

[a] Correlations cannot be differentiated for the pair of hydrogens at 1.50 ppm because of their identical chemical shift

[b,c] Since the methyl signals are singlets, COSY correlations must be to the individual hydrogens at 1.24 and 1.02 ppm, respectively

Table 3 TOCSY data for kauradienoic acid (**3**)

δ_H/ppm	Spin-system members
5.24	2.77, 2.43, 1.99, 1.60, 1.50
4.91	4.80, 2.77, 2.62, 2.43, 2.20, 1.99, 1.60, 1.50
4.80	4.91, 2.77, 2.62, 2.43, 2.20, 1.99, 1.60, 1.50
2.77	5.24, 4.91, 4.80, 2.62, 2.43, 2.20, 1.99, 1.60, 1.50
2.62	4.91, 4.80, 2.77, 2.20, 1.99, 1.60, 1.50
2.47	1.97, 1.68, 1.67, 1.46
2.43	5.24, 2.77, 1.99, 1.60, 1.50
2.20	4.91, 4.80, 2.77, 2.62, 1.60, 1.50
2.16	1.93, 1.88, 1.50, 1.24, 1.02
1.99	5.24, 2.77, 2.62, 2.43, 1.60, 1.50
1.97	2.47, 1.68, 1.67, 1.46
1.93	2.16, 1.88, 1.50, 1.24, 1.02
1.88	2.16, 1.93, 1.50, 1.24, 1.02
1.68	2.47, 1.97, 1.46
1.67	2.47, 1.97, 1.46
1.60	5.24, 4.91, 4.80, 2.77, 2.62, 2.43, 2.20, 1.99, 1.50
1.50[a]	5.24, 4.91, 4.80, 2.77, 2.62, 2.43, 2.20, 2.16, 1.99
1.50[a]	1.93, 1.88, 1.60, 1.24, 1.02
1.46	2.47, 1.97, 1.68, 1.67
1.24[b]	2.16, 1.93, 1.88, 1.50, 1.02
1.24 (CH_3)	(none)
1.02[c]	2.16, 1.93, 1.88, 1.50, 1.24
1.02 (CH_3)	(none)

[a]TOCSY correlations cannot be differentiated for the pairs of hydrogens at 1.50, 1.24, and 1.02 ppm because of their identical chemical shifts

[b,c]Since the methyl signals are singlets, TOCSY correlations must be to the individual hydrogens at 1.24 and 1.02 ppm, respectively

7.3 HMBC Data

Since the ^{13}C NMR spectrum of the unknown compound is far less congested than its ^{1}H spectrum, HMBC is the experiment of choice to establish the longer range, C-H correlation networks. HMBC and CIGAR-HMBC spectra of the unknown compound were recorded, and the HMBC spectrum is shown in Fig. 5. The HMBC data from these contour plots are summarized in Table 4 and will be extensively discussed below in Sect. 7.5.

Two points that can now be made are that, first, methyl signals are particularly helpful in the interpretation of HMBC spectra. Just as their signals are almost

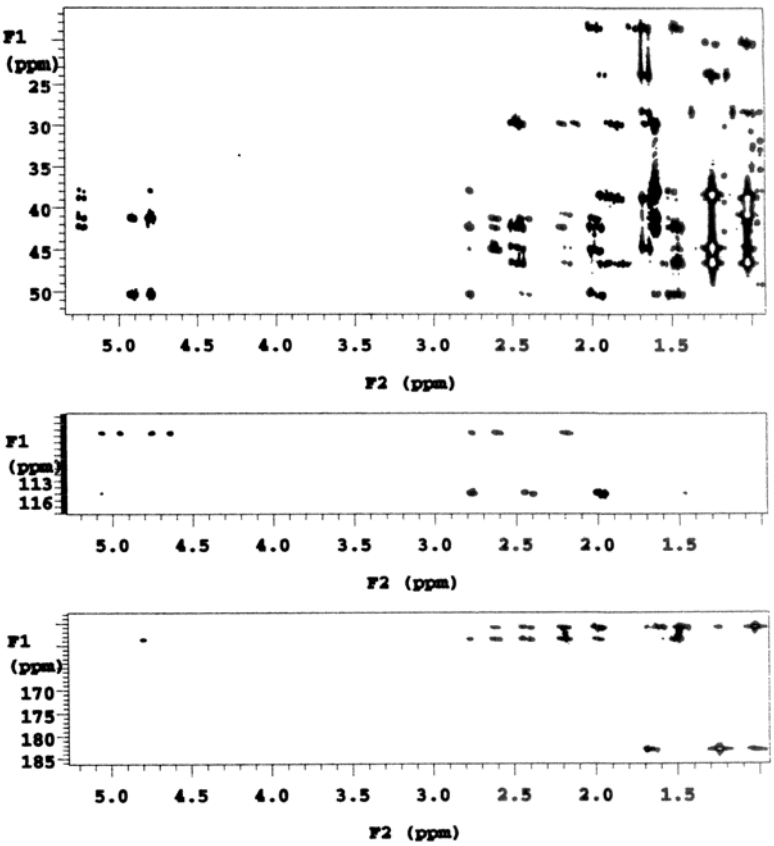

Fig. 5 Expansions of a gradient-selected absolute-value HMBC spectrum for kauradienoic acid (**3**), illustrating the 2-bond and 3-bond C–H correlations for different ^{13}C regions

always the largest resonances in ^{1}H NMR spectra, so their cross-peaks are generally the strongest in HMBC spectra where they exhibit prominent 2-bond and 3-bond connectivities. Second, in cyclohexane chair conformers, *vicinal* C–H couplings due to *equatorial* protons are generally larger to ring carbons three bonds removed than those due to *axial* protons because of the *ca*. 180° dihedral angles of the former compared to the *ca*. 60° dihedral angles of the latter. As a result, *equatorial* protons generally give rise to stronger three-bond HMBC cross-peaks to ring carbons than their *axial* counterparts.

Table 4 HMBC data[a] for kauradienoic acid (**3**)

δ_C/ppm	Correlated hydrogen chemical shifts
182.74	2.16, 1.67(s), 1.24, 1.02(s)
158.56	5.24, 2.62, 2.43, 2.20(s), 1.99, 1.60(s), 1.50, 1.02
155.92	2.62, 2.43, 2.20, 1.99, 1.60, 1.50
114.90	2.77, 2.43, 1.99
105.48	2.77, 2.62, 2.20
50.32	5.24, 4.91, 4.80, 2.77, 1.97, 1.60, 1.50
46.56	2.47, 2.16, 1.93, 1.46, 1.24, 1.02
44.94	2.62, 2.43, 1.99, 1.97, 1.46
44.69	2.47, 2.16, 1.68, 1.67, 1.50(s), 1.24 1.02
42.27	5.24, 2.77, 2.62, 2.47, 2.20, 1.97, 1.60, 1.50, 1.46
41.24	5.24, 4.91, 4.80, 2.62, 2.43, 1.99, 1.60, 1.50
40.75	2.16(s), 1.88, 1.67, 1.50, 1.02
38.79	5.24, 1.93, 1.88, 1.68, 1.67, 1.50(s), 1.24, 1.02
38.31	1.93(s), 1.88, 1.50, 1.24
37.93	5.24, 4.80, 2.77, 1.60, 1.50
29.66	2.47, 2.20, 1.68, 1.67, 1.60
28.23	1.67, 1.02
23.62	1.93, 1.67(s), 1.24(s)
20.16	2.16, 1.93, 1.24, 1.02
18.48	1.97, 1.67, 1.46

[a]From HMBC and CIGAR-HMBC experiments

7.4 General Molecular Assembly Strategy

Of the many techniques available to the NMR spectroscopist in structural elucidations, none are so valuable as the indirect, chemical shift correlation experiments like HMBC, TOCSY (both homo- and heteronuclear varieties), and FLOCK (*36b*). FLOCK is an X-nucleus detected experiment analogous to HMBC. While it is significantly less sensitive than HMBC, it is useful in those instances where very high ^{13}C resolution is essential. Once molecular fragments have been identified by the COSY and HSQC experiments, combination of these fragments is attempted by means of the above techniques. As indispensable as these methods have become to NMR spectroscopists, they suffer a common limitation in that two-bond, C–H couplings cannot generally be directly distinguished from three-bond, C–H coupling constants. However, these two classes of C–H couplings can be differentiated, for adjacent protonated carbons, by examination of HSQC and COSY spectra (*vide infra*).

The process of molecular assembly can be approached in the following manner. If possible, a carbon atom is selected from which the remainder of the molecular skeleton can be built in just *one* direction. Methyl groups are, of course, excellent starting points. As mentioned above, adjacent protons, if any, can be identified from a COSY contour plot and longer-range coupled protons from a TOCSY spectrum. Conversely, the carbons to which the just-identified protons are directly attached can be determined from an HSQC or HMQC plot. The HMBC or FLOCK spectra can

then be scanned using either the contour plot, for uncongested spectra, or methyl-proton or methyl-carbon traces (more commonly the latter, but the choice depends on which spectral axis is less congested) if spectral congestion or weak cross peaks are a problem. Cross-peaks may be found for (i) the adjacent carbon (if methyl-proton traces are viewed) or protons (if methyl-carbon traces are observed, again, more likely), which represent two-bond couplings in either case, and (ii) any other carbons or protons, indicative of three-bond couplings (but always being mindful that one, or more, members of the latter group could possibly be due to ${}^{n}J_{CH}$ >3). The fortunate redundancy of these 2D experiments is seen, whereby an adjacent carbon may be identified by a combination of COSY (${}^{3}J_{HH}$) and HSQC/HMQC (${}^{1}J_{CH}$) connectivities and also by HMBC/FLOCK (${}^{2}J_{CH}$) correlations.

The third carbon atom in the fragment (two carbons removed from the original methyl group) will likely show two-bond, C–H couplings with adjacent proton(s), if present, both backward to the second carbon and forward to the fourth carbon in the series. Carbon-atom connectivities can thus be built up using (i) two- and three-bond, C–H couplings to generally confirm previously determined C–C correlations and then (ii) three-bond, H–H and C–H couplings to extend the developing molecular structure.

Even when a methyl ^{1}H signal is nothing more than a broadened singlet, the COSY spectrum (either the contour plot or the methyl trace) can be scanned for cross-peaks due to long-range coupling. Turning then to HMBC or FLOCK spectra, either the contour plot or the methyl ^{13}C trace (HMBC spectrum) or ^{1}H trace (FLOCK spectrum) can be examined for cross-peaks due to (i) two-bond coupling to adjacent (quaternary) carbons and (ii) three-bond coupling to farther-removed carbons (with the usual ${}^{n}J_{CH}$ >3 *caveat*). Finally, a note of caution should be mentioned. Like N*O*Es, the intensities of three-bond, C–H correlations are not necessarily symmetrical, *e.g*. in the four-carbon fragment pictured in Fig. 6, a strong cross-peak may, in fact, be observed between H_A and C_3 while a weak one, or none at all, is seen between H_C and C_1. The main reason for these weak or missing correlations is the dependence of vicinal couplings on the H-A–C-1–C-2–C-3 and H-C—C-3—C-2—C-1 dihedral angles, which are seldom identical. Since similar considerations are largely absent for two-bond couplings, cross-peaks should be detected between H-A and C-2 and also between H-B and C-1. Extensive redundancy of the type described above, however, is in fact observed routinely for *vicinal* C–H correlations and is invaluable in the construction of molecular structures.

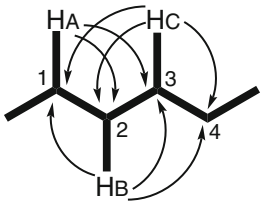

Fig. 6 Examples of 2-bond and 3-bond C–H connectivities in a typical organic chemical fragment in which ${}^{3}J(H_AC_3)$ can be quite different from ${}^{3}J(H_CC_1)$ and results in HMBC cross-peaks of differing intensities

The same factors that influence H–H couplings, *e.g*. dihedral angle dependence, substituent electronegativity, bond length, and bond order, apply to C–H couplings. As a general rule, C–H coupling constants are approximately 2/3 the value of the corresponding H–H couplings. In alkenes, for example, average *cis* and *trans* H–H couplings are *ca*. 11 and 18 Hz, while the corresponding C–H coupling constants are *ca*. 7 and 12 Hz.

7.5 *A Specific Molecular Assembly Procedure*

Examination of the attached-proton data in Table 1 demonstrates the presence of two methyl groups, which are both singlets at 1.24 and 1.02 ppm. Inspection of the HMBC and CIGAR-HMBC data shows that the methyl signal at 1.24 ppm exhibits strong connectivities to the carbons at 182.74, 46.56, 44.69, and 38.31 ppm. Further observation reveals that the methyl signal at 1.02 ppm displays strong connectivities to the carbons at 158.56, 46.56, 40.75, and 38.79 ppm. In addition, both methyl groups have an HMBC correlation to the carbon at 46.56 ppm. Obtaining the chemical shifts of the protons attached to these carbons from Table 1 yields the molecular fragment **13**.

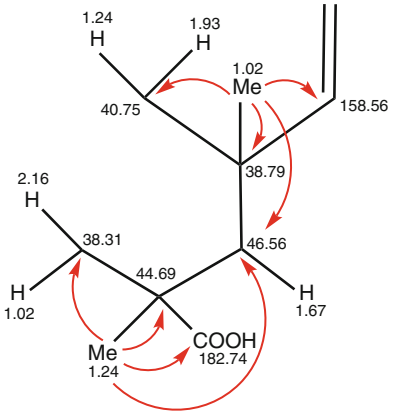

13

At this point, an ambiguity arises because there also happen to be two methine protons with the same chemical shifts as the two methyl groups, *viz*. 1.24 and 1.02 ppm, and in sufficiently close proximity to these two methyl groups that there is a possibility that the assignments of both the methyl groups and their adjacent methylene groups could be interchanged (**14**), a consideration that will be further examined in Sect. 8.3. The HMBC data in Table 4 show that the methyl group at 1.02 ppm in **14** could exhibit an HMBC connectivity to the carboxyl-carbon (182.74 ppm). However, a problem arises with the potential reversed assignments because the methyl group at 1.24 ppm in **14** should, likewise, display a strong HMBC connectivity to the alkenic-carbon at 158.56 ppm, but none is observed. The absence of such an important HMBC correlation, subsequent N*O*ESY correlations, and critical HMBC traces (Sect. 7.6)

dictate that the reversed assignments given in **14** are incorrect. We will discuss this reversed-assignment situation later, at greater length, in this section.

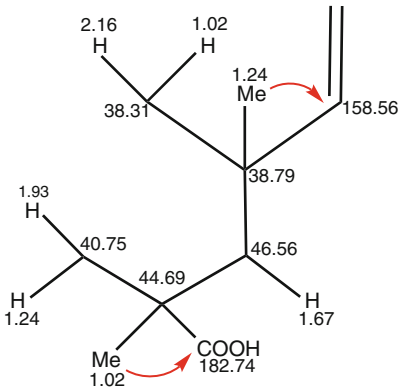

14

Note too that the chemical shift of the carbon at 182.74 ppm is appropriate for a carboxylic acid, and this carbon has been assigned as such. The two oxygens required by the molecular formula are thus accounted for.

Fragment **13** contains the terminal methylene groups shown in **10**, and insertion of the central methylene group of **10** to close the A-ring produces **15** (note that additions to an existing fragment are shown in red).

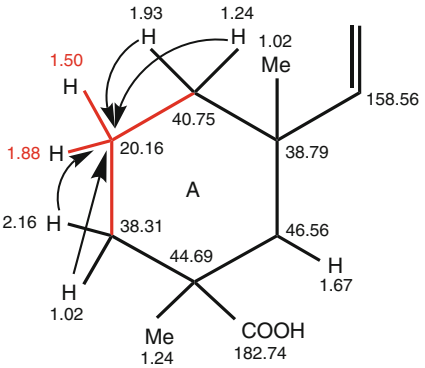

15

Both carbons at 40.75 and 38.31 ppm in **15** display HMBC connectivities to protons at 1.88 and 1.50 ppm. In addition, the protons at 1.93 and 1.24 ppm (on the carbon at 40.75 ppm) and the protons at 2.16 and 1.02 ppm (on the carbon at 38.31 ppm) exhibit HMBC correlations to the carbon at 20.16 ppm, to which the protons at 1.88 and 1.50 are attached. At this point, three of the seven units of unsaturation have been accounted for.

Continuing elucidation of the unknown compound, fragment **11** contains the same proton (1.67 ppm) for which the attached methine carbon (46.56 ppm) exhibited HMBC connectivities to both methyl groups. This fragment can then be added to the developing structure by means of HMBC correlations to produce **16**. HMBC data reveal that the proton at 1.68 ppm shows correlations to the carbons at 44.69 and 38.79 ppm and that at 2.47 ppm displays connectivities to the carbons at 46.56 and 44.69 ppm.

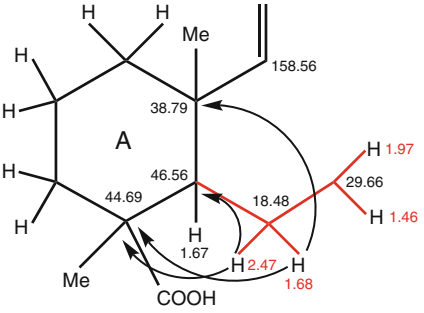

16

The next step in this structural determination is closure of an apparent ring. Protons in **16** at 2.47, 1.97, and 1.46 ppm exhibit HMBC correlations to a carbon at 42.27 ppm and suggest that it be placed between the carbons at 158.56 and 29.66 ppm to complete the B-ring (**17**). Supporting evidence comes from the alkenic, methine proton at 5.24 ppm, which is attached to the carbon at 114.90 ppm and shows HMBC connectivities to the previously identified carbons at 158.56 ppm (two-bond) and 38.79 ppm (three-bond). It also exhibits a strong HMBC correlation to the above carbon at 42.27 ppm, which is consistent with this quaternary carbon being located in an (*E*)-alkenic position between the carbons at 158.56 and 29.66 ppm, thus supporting structure **17**.

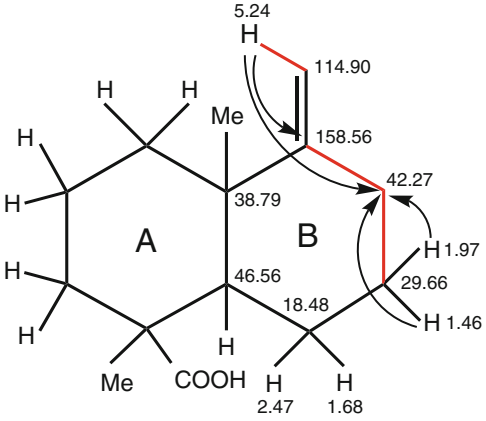

17

The alkenic methine proton at 5.24 ppm and its attached carbon at 114.90 ppm are also part of the fragment shown in **12**. Adding this large piece to structure **17** produces **18**, which contains five of the seven units of unsaturation.

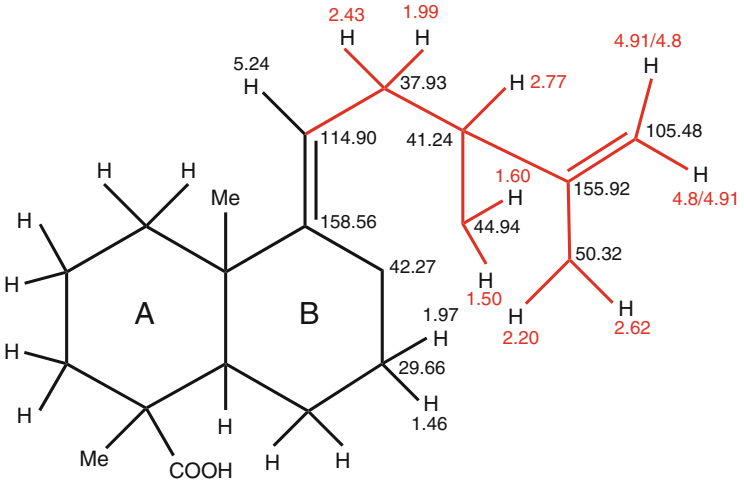

18

Closure of an apparent ring again requires additional HMBC connectivities. In particular, (i) the B-ring methylene group (protons at 1.97 and 1.46 ppm, carbon at 29.66 ppm) and (ii) the two newly added methylene groups (1.60 and 1.50 ppm/44.94 ppm and 2.62 and 2.20 ppm/50.32 ppm) appear well positioned to complete the unknown molecular structure. First, the protons at 2.62, 2.20, 1.60, and 1.50 ppm show HMBC connectivities to the quaternary carbon at 42.27 ppm, thus closing the C- and D-rings (**19**).

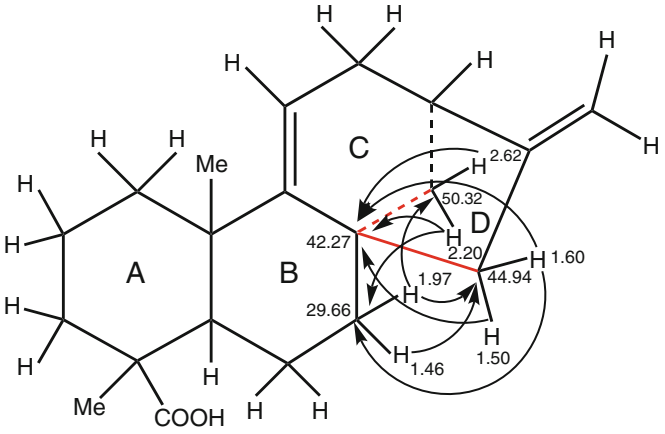

19

Second, the proton at 1.97 ppm displays HMBC correlations to both methylene carbons at 44.94 and 50.32 ppm, and the proton at 1.46 ppm exhibits an HMBC

connectivity to the carbon at 44.94 ppm. In addition, the protons at 2.20 and 1.60 ppm display complementary HMBC correlations to the carbon at 29.66 ppm.

At this point all of the carbons, hydrogens, and oxygens are accounted for. The complete, numbered, structure **20** of the unknown compound satisfies the required seven units of unsaturation.

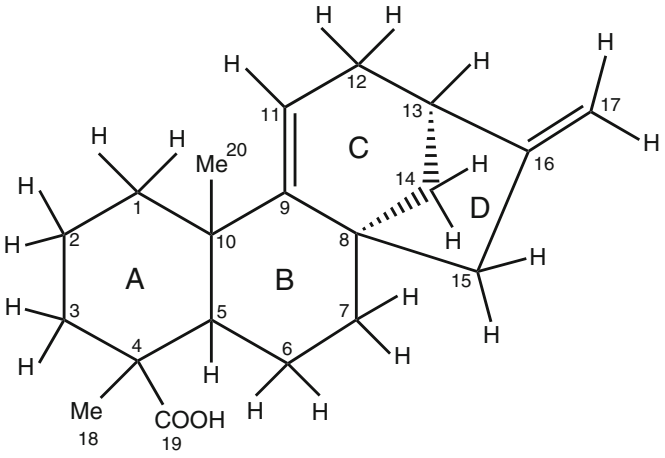

20

7.6 Determination of Overall Stereochemistry and Proton Chemical Shift Assignments

With completion of the two-dimensional structural elucidation of the unknown compound, questions arise concerning its three-dimensional shape, *i.e.* the relative orientations of substituents (*e.g.* whether methyl-18 at C-4 is *axial* or *equatorial*) at various carbons. For a molecule of MW = 300, a N*O*ESY experiment can provide a wealth of such stereochemical information. The N*O*ESY spectrum of the "unknown," kauradienoic acid (**3**), is shown in Fig. 7. The data from these and R*O*ESY contour plots are summarized in Table 5 and illustrated, in part, in a numbered, stereochemical drawing (**21**).

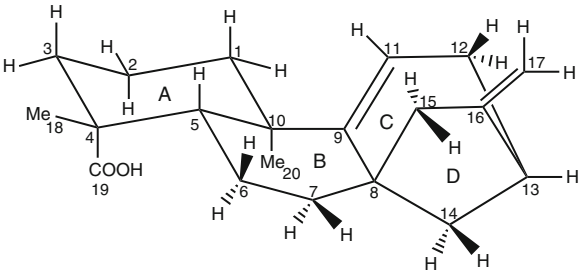

21

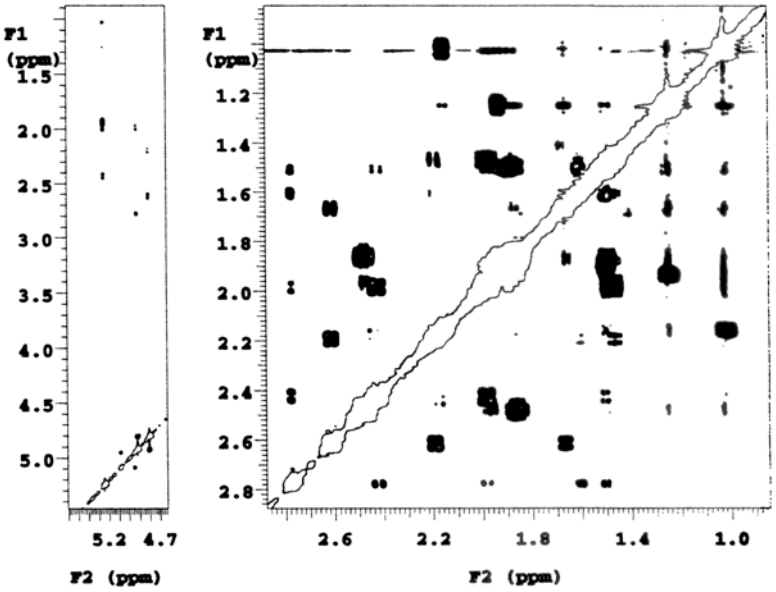

Fig. 7 N*O*ESY spectrum for kauradienoic acid (**3**) with a 0.5-s mixing time. The expansions are similar to those in Fig. 2

Table 5 N*O*E and R*O*E data for kauradienoic acid (**3**)

δ_H/ppm	Dipolar-coupled partners
5.24	2.43, 1.99, 1.93, 1.24, 1.02
4.91[a]	4.80, 2.77, 1.99
4.80[b]	4.91, 2.62, 2.20
2.77	4.91, 2.43, 1.99, 1.60, 1.50
2.62	4.80, 2.20, 1.68, 1.67
2.47	1.97, 1.68, 1.46, 1.24, 1.02
2.43	5.24, 2.77, 1.99, 1.50
2.20	4.80, 2.62, 1.60, 1.46
2.16	1.88, 1.50, 1.24, 1.02
1.99	5.24, 4.91, 2.77, 2.43
1.97	2.47, 1.50, 1.46, 1.02
1.93	5.24, 1.50, 1.24, 1.02
1.88	2.16, 1.50, 1.02
1.68	2.62, 2.47, 1.46
1.67	2.62, 1.24, 1.02
1.60	2.77, 2.20, 1.50
1.50[c]	2.77, 2.43, 2.16, 1.97, 1.93, 1.88, 1.60,
1.50[c]	1.24, 1.02
1.46	2.47, 2.20, 1.97, 1.68
1.24[d]	5.24, 2.47, 2.16, 1.93, 1.67, 1.50, 1.02
1.24[d] (CH_3)	
1.02[e]	5.24, 2.47, 2.16, 1.97, 1.93, 1.88,
1.02[e] (CH_3)	1.67, 1.50, 1.24

[a]*cis* to C-13
[b]*cis* to C-15
[c,d,e]Correlations cannot be differentiated for the pairs of hydrogens at 1.50, 1.24, and 1.02 ppm because of their identical chemical shifts

Since the 300 molecular weight of kauradienoic acid (**3**) is well outside of the zero-crossing limit, the N*O*ESY and R*O*ESY spectra were expected to be virtually identical, an expectation that was borne out, and subsequent references will be to "N*O*ESY" data only. A combination of N*O*ESY and HMBC spectra can permit the determination of substituent stereochemistry, especially for 6-membered ring systems that exist in chair conformations, in the following way: actual or quasi-*equatorial* protons exhibit strong HMBC correlations by virtue of their ~180° dihedral angles while actual or quasi-*axial* protons display strong N*O*Es with other *axial* protons and methyl groups because of their proximity (note that N*O*Es vary with the sixth power of the internuclear distance).

The following overall structural relationships were thus deduced for kauradienoic acid. Strong N*O*Es among (i) H-1*β,ax.*; H-3*β,ax.*; and H-5*β,ax.* and (ii) between H-2*α,ax.* and methyl-20*ax.* and strong HMBC correlations between (i) H-1*α,eq.* and C-3 and C-5; H-2*β,eq.* and C-4 and C-10; H-3*α,eq.* and C-1 and C-5, (ii) H-1*β,ax.* and C-20, and (iii) H-3*β,ax.* and C-19 demonstrate that the A-ring exists in a chair conformation in which H-1*β*, H-3*β*, and H-5*β* are on the "top face" of the molecule while H-2*α* and methyl-20 are on the "bottom face."

X-ray data show that the B-ring occurs as a slightly distorted boat conformer, in which methyl-20 and H-7*α* are at the "flagpole" positions. However, this conformation could have been reasonably inferred from the strong N*O*Es that are observed between these flagpole groups and the strong HMBC connectivities (due to ~180° dihedral angles) that are seen between H-6*α* and C-8 and between H-7*β* and C-5. *Dreiding* models suggest that the B-ring might also exist partially as a quasi-half chair conformer, in which C-6 would be well below the C-5–C-10–C-9–C-8 plane and C-7 slightly below this plane. However, this conformation places methyl-20 relatively distant from H-7*α* (1.97 ppm) and much closer to H-6*α* (2.47 ppm). The relatively weak N*O*E observed between methyl-20 and H-6*α* and strong N*O*E seen for methyl-20 and H-7*α* indicate that the distorted half-chair conformer is unimportant in solution.

Strong HMBC correlations between H-11 and C-8 and C-13, and H-13 and C-11 are consistent with the C-ring occurring in a rigid conformation in which carbons 8, 9, 11, 12, and 13 are approximately coplanar and C-14 well below the plane. Additional strong HMBC connectivities between H-14*β* and C-9 and C-12 and between H-12*β* and C-14 support this inference.

The remaining 5-membered D-ring is situated approximately orthogonally to the A,B,C-ring system, and descriptions of the 15-protons as being "*α*" or "*β*" must, therefore, be clarified (in Table 6, *vide infra*, they are described as pointing "toward" or "away from" the viewer, respectively). Strong HMBC correlations between H-14*α* and C-15 and C-16; H-15*α* and C-9; H-15*β* and C-14; and H-12*α* and C-16 support this conclusion. One sees then that H-14*β* is quasi-*equatorial* with respect to the C-ring while H-14*α* is quasi-*equatorial* with respect to the D-ring.

Proton assignments were either made or confirmed on the basis of N*O*E data. Strong N*O*ESY correlations between the protons at 1.97 ppm (at C-7) and 1.50 ppm

(at C-14) indicate that both are similarly oriented. Since the 7-*geminal* partner at 1.46 ppm has been shown, *via* the HMBC experiments, to be β, the H-7 at 1.97 ppm must, therefore, be α. Thus, H-14 at 1.50 ppm is confirmed to be α by virtue of its strong N*O*E interaction with H-7α. N*O*ESY connectivities were also used to assign the alkenic methylene protons at C-17. H-17A (4.91 ppm) shows a strong N*O*E with H-13 (2.77 ppm) and is thus *cis* to it while H-17B (4.80 ppm) displays equally strong N*O*Es to the *cis* 15-protons at 2.62 and 2.20 ppm.

Finally, two additional pieces of evidence support the previous assignment of methyl-20 at 1.02, not 1.24 ppm, and protons 1β and 3β at 1.24 and 1.02 ppm, respectively, both of which can be seen in **22**: (i) strong N*O*Es (shown as arrows) that can exist only between methyl-20 and H-2*ax*. (1.88 ppm) and H-7α (1.97 ppm) and (ii) HMBC traces through carbons 9 (158.56 ppm) and 19 (COOH, 182.74 ppm) show particular emphasis on the fine structure of H-1*ax*. (1.24 ppm) and H-3*ax*. (1.02 ppm) (Fig. 8).

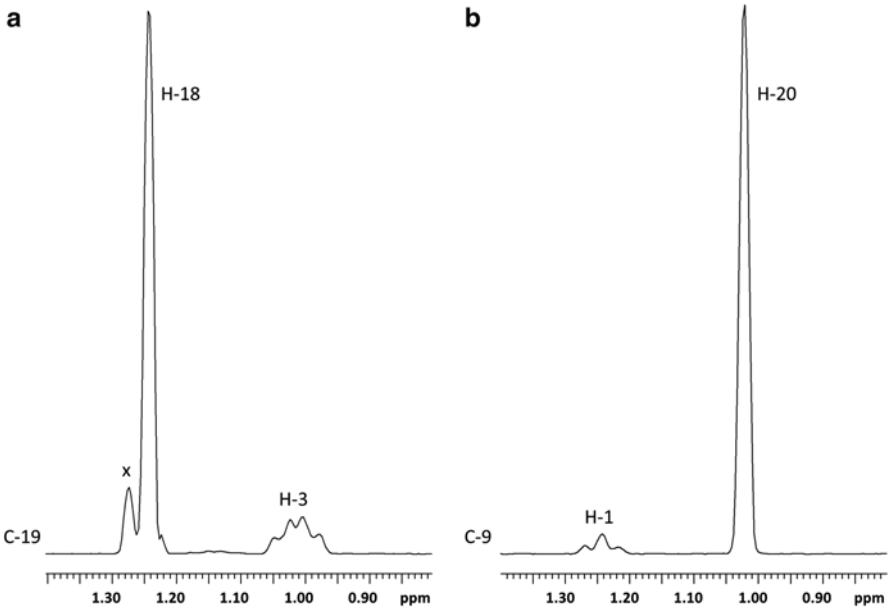

Fig. 8 Cross-sections through C-9 and C-19 from an HMBC spectrum of kauradienoic acid (**3**). The observation of multiplet structures for H-1 and H-3 *axial* protons allows one to clearly distinguish these two protons from the H-18 and H-20 methyl singlets, which overlap with these protons in the ^{1}H spectrum. The *peak* marked "x" is a minor methyl impurity peak. H-3 appears as an apparent quartet due to a *geminal* H–H coupling to H-3 *eq*., an *anti* H–H coupling to H-2 *ax.*, and an *anti* C–H coupling to C-19. H-1 appears as an apparent triplet due to a *geminal*-coupling to H-1 *eq*. and an *anti*-coupling to H-2 *ax*. In both cases, the resolution is insufficient to observe *gauche* H–H couplings and the *gauche* C–H coupling of H-1 to C-9

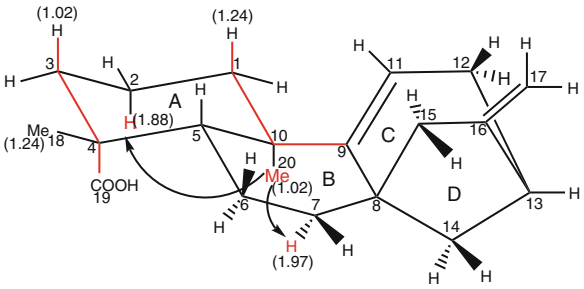

22

H-3*ax.* appears as a triple doublet (an apparent 1:3:3:1 "quartet") by virtue of the magnitude of its similar *geminal*-coupling to H-3 *eq.*, *axial*-coupling to H-2*ax.*, and *axial* C-H coupling to 19-COOH, the third pathway shown in red in **22**. However, H-1*ax.* is seen as a doublet of doublets (an apparent 1:2:1 "triplet") due to its similar *geminal*-coupling to H-1 *eq.* and *axial*-coupling to H-2*ax*. Its third coupling is *equatorial* to C-9 (also shown in red) and too small to cause observable splitting. With the interpretation of these final HMBC and N*O*ESY correlations, the two- and three-dimensional structural elucidation of kauradienoic acid (**3**) is complete, and final descriptions of the skeletal protons are given in Table 6.

Table 6 ^{1}H and ^{13}C NMR data for kauradienoic acid (**3**)

Position	δ_C/ppm	Attached hydrogens	
1	40.75	1.93 *α,eq.*	1.24 *β,ax.*
2	20.16	1.50 *β,eq.*	1.88 *α,ax.*
3	38.31	2.16 *α,eq.*	1.02 *β,ax.*
4	44.69	–	
5	46.56	1.67 β, *ax.*	
6	18.48	1.68 *β*	2.47 *α*
7	29.66	1.46 *β*	1.97 *α*
8	42.27	–	
9	158.56	–	
10	38.79	–	
11	114.90	5.24	
12	37.93	1.99 *β*	2.43 *α*
13	41.24	2.77	
14	44.94	1.60 *β*	1.50 *α*
15	50.32	2.62[a]	2.20[b]
16	155.92	–	
17	105.48	4.91[c]	4.80[d]
18	28.23	1.24 *β,eq.* (CH_3)	
19	182.74	–	
20	23.62	1.02 *α,ax.* (CH_3)	

[a]Pointing away from the viewer
[b]Pointing toward the viewer
[c]*cis* to C-13
[d]*cis* to C-15

8 Computer-Assisted Structure Elucidation

By the late 1950s, chemists realized that NMR spectroscopy was a powerful tool for identifying the structure of organic compounds. The first computer-assisted structure elucidation (CASE) programs, for small organic compounds, were developed in the late 1960s: DENDRAL (*79*), CHEMICS (*80*), CASE (*81*), and StRec (*82*). However, early elucidation attempts were severely limited by a number of factors, not the least of which was the relatively primitive nature of computers at that time. In addition, chemists were essentially limited to ^{1}H NMR spectroscopy, as practical one-dimensional ^{13}C and two-dimensional NMR experiments were years away.

The situation changed dramatically with the advent of powerful personal computers, ^{13}C NMR spectroscopy, and a variety of 2D NMR experiments to establish direct and long-range homo- and heteronuclear connectivities. A second generation of considerably more powerful structural elucidation programs appeared several decades later and included Structure Elucidator (*56*), SESAMI (*83*), LSD (*84*), CISOC-SES (*85*), LUCY (*86*), and COCON (*87*).

One of the greatest difficulties in elucidating the structure of an unknown compound arises when spectroscopic data are consistent and *appear* to lead to one structure. This problem is especially acute if a chemist has isolated, or been given, similar compounds in the past, and the current unknown seems to be another analog in this series. The obvious advantage of CASE programs is that they do not suffer a similar bias. Some of their proposed structures may be highly implausible, but they can also suggest classes of structures that the chemist has not even considered.

Section 7 has illustrated a typical workflow for the elucidation of an unknown structure in the absence of a computer-assisted elucidation. Advanced Chemistry Development, Ltd. (ACD/Labs) markets a program, "ACD/Structure Elucidator" (*56*); by comparison, their automated determination of structures occurs in the following general manner.

(1) Spectral data requirements:

   (a) ^{1}H NMR data: useful for peak integral information.
   (b) ^{1}H/^{13}C HSQC, ^{1}H/^{1}H COSY, and ^{1}H/^{13}C HMBC.
   (c) ^{1}H/^{1}H TOCSY: useful when COSY spectra indicate the presence of complex spin systems.
   (d) ^{13}C NMR data: very helpful for identifying quaternary carbons, if sample quantities permit its acquisition in a reasonable amount of time and can be critical for quaternary carbons that do not exhibit HMBC connectivities.
   (e) High-resolution MS to provide a molecular formula.
   (f) IR and UV/vis spectral data to furnish information on functional groups.

(2) NMR data are submitted in one of the following two formats:

   (a) As raw one- and two-dimensional spectral data (FIDs together with their processing parameters) in which 1D and 2D NMR cross-peaks are selected by the software. This is preferable because data entry is both rapid and direct.
   (b) As text (TXT) files in which the chemist/spectroscopist has analyzed the NMR spectra to establish various homo- and heteronuclear connectivities.

The latter approach is less favored because it can involve laborious data entry and introduces the serious possibility of transcription errors.

(3) Numerous conditions can be applied to NMR data processing, but as a general rule, the following are applied:

(a) HMBC correlations are assigned as follows:

(i) Strong: ^{2}J(CH) – ^{3}J(CH)
(ii) Weak: ^{2}J(CH) – ^{4}J(CH)

(b) Direct heteroatom-to-heteroatom connectivities are disallowed
(c) Triple bonds within 3-, 4-, and 5-membered rings are disallowed

(4) A molecular-connectivity map is then generated, which shows all of the NMR data in one place and is correlated to the molecular formula. The NMR data include heteronuclear (HMBC) and homonuclear (COSY and, possibly, TOCSY) connectivities. While interesting, these maps are generally too complicated to be used alone to produce possible structures.

(5) Potential structures, numbering in the tens or hundreds, are generated and ^{13}C chemical shifts calculated for each candidate structure. Differences between predicted and experimental data are reported as a "fast-deviation" statistic, $d_F(^{13}C)$, and possible structures initially ranked in order of increasing $d_F(^{13}C)$.

(6) More accurate ^{13}C chemical shifts calculations are next performed on the smaller of either (i) all structures with $d_F(^{13}C) \leq 4$ ppm/carbon or (ii) the first 50 ranked structures. Differences between the more accurately predicted and experimental data are reported as an "accurate-deviation" statistic, using "neural net" [$d_N(^{13}C)$] values and/or "HOSE" (Hierarchically Ordered Spherical Description of Environment) [$d_A(^{13}C)$]. The two methods give somewhat similar results, but the HOSE method yields better results when compounds, which are similar to the unknown, are contained in the ACD spectral library. Potential structures are re-ranked in order of increasing $d_{A/N}(^{13}C)$ numbers. Structures having $d_{A/N}(^{13}C)$ values > 4 ppm/carbon are generally discarded. ACD/Labs' experience is that the correct structure is usually identified at this point (*88*).

(7) In situations where the smallest calculated $d_{A/N}(^{13}C)$ values are very close, a best structure may be arrived at by calculating $d_{A/N}(^{1}H)$, and, if good MS data are available, d(MS) can be calculated as well. In the following sections, three test compounds were submitted to ACD/Labs to determine how the performance of their ACD/Structure Elucidator program would compare to that of an experienced NMR spectroscopist.

8.1 Guyanin

The structure of guyanin (**4**) was determined in 1986 (*32, 89*) and represents one of the first and most unusual structures determined solely by NMR methods. The structure was so unprecedented that one of the senior co-authors felt that confirming

X-ray data should be obtained. The results of X-ray analysis finally arrived, just prior to submission of the manuscript, and completely supported the NMR-determined structure.

Critical 2- and 3-bond H-C connectivities were established by the XCORFE experiment, which preceded development of the HMBC experiment. Since the original NMR data for guyanin (**4**) are no longer available, the following data tables were reconstructed from data in the original manuscripts and submitted to ACD/Labs as TXT files: HETCOR (direct H-C chemical-shift correlation (Table 7), COSY (Table 8), and XCORFE (longer-range H-C chemical-shift correlation, Table 9).

Table 7 HETCOR[a] data for guyanin (**4**)

δ_C/ppm	Attached hydrogens (with coupling constants)	
208.41	–	
176.95	–	
175.28	–	
173.67	–	
173.24	–	
164.25	–	
142.86	7.44 t (1.7)	
140.25	7.56 t (1.7)	
128.89	5.87 q (1.3)	
120.85	–	
117.45	5.90 s	
108.51	6.38 dd (1.7, 0.8)	
79.95	5.94 dd (1.7, 0.8)	
68.95	–	
61.45	–	
51.98	3.68 s	
51.25	3.60 s	
46.57	–	
46.30	–	
40.91	3.26 d (10)	
34.39	1.71 td (13, 13, 6)	1.56 dd (13, 6)
34.33	2.55 dd (17, 10)	2.19 d (17)
28.31	2.29 ddd (15, 13, 6)	2.16 dd (15, 6)
27.80	0.98 s	
23.65	1.27 s	
20.67	1.43 s	
18.99	1.16 s	
16.37	2.04 d (1.3)	

[a]A carbon-detected, direct heteronuclear chemical shift correlation experiment

Table 8 COSY data for guyanin (**4**)

δ_H/ppm	Spin-coupled partners
7.56	7.44, 5.94
7.44	7.56, 6.38
6.38	7.44, 5.94
5.94	7.56, 6.38
5.90	(none)
5.87	2.04
3.68 (CH_3)	(none)
3.60 (CH_3)	(none)
3.26	2.55
2.55	3.26, 2.19
2.29	2.16, 1.71, 1.56
2.19	2.55
2.16	2.29, 1.71
2.04 (CH_3)	5.87
1.71	2.29, 2.16, 1.56
1.56	2.29, 1.71
1.43 (CH_3)	(none)
1.27 (CH_3)	(none)
1.16 (CH_3)	(none)
0.98 (CH_3)	(none)

The Structure Elucidator program generated a molecular connectivity diagram (Fig. 9) and a single structure (**23**). As it turned out, the COSY data were not needed. Only one structure, the correct one, was produced with a generation time of 1 s. Table 10 contains ^{13}C and ^{1}H chemical shift data that are sorted by position number.

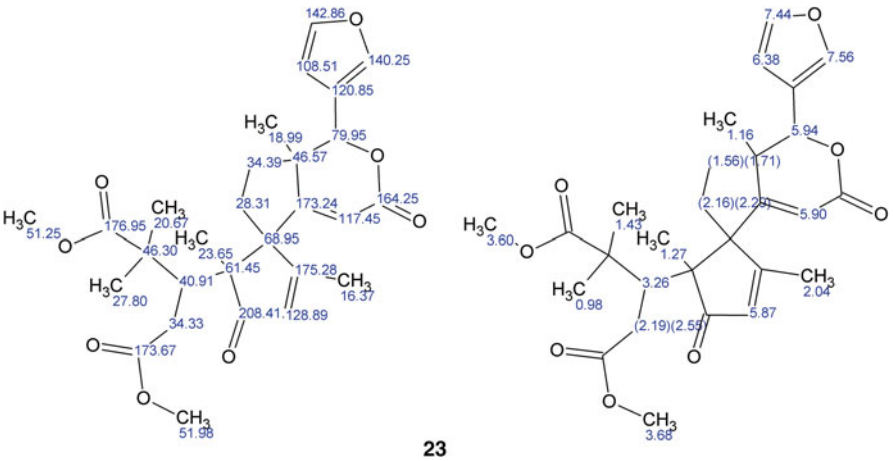

23

Table 9 XCORFE[a] data for guyanin (**4**)

δ_C/ppm	Long-range correlated hydrogens
208.41	5.87, 3.26, 2.04, 1.27
176.95	3.60, 3.26, 1.43, 0.98
175.28	5.87, 2.29, 2.04
173.67	3.68, 3.26, 2.55, 2.19
173.24	5.94, 5.90, 2.16, 1.56, 1.16
164.25	5.94, 5.90
142.86	7.56, 6.38
140.25	7.44, 6.38, 5.94
128.89	2.04
120.85	7.56, 7.44, 6.38, 5.94
117.45	(none)
108.51	7.56, 7.44, 5.94
79.95	1.71, 1.16
68.95	5.90, 5.87, 3.26, 2.29, 2.16, 2.04, 1.56, 1.27
61.45	5.87, 3.26, 2.29, 2.19, 2.16, 1.27
51.98	(none)
51.25	(none)
46.57	5.94, 5.90, 2.16, 1.71, 1.56, 1.16
46.30	3.26, 2.55, 2.19, 1.43, 0.98
40.91	2.55, 2.19, 1.43, 1.27, 0.98
34.39	2.29, 2.16, 1.16
34.33	3.26
28.31	1.71, 1.56
27.80	3.26, 1.43
23.65	3.26
20.67	3.26, 0.98
18.99	5.94, 1.71, 1.56
16.37	5.87

[a]A carbon-detected, indirect heteronuclear chemical shift correlation experiment

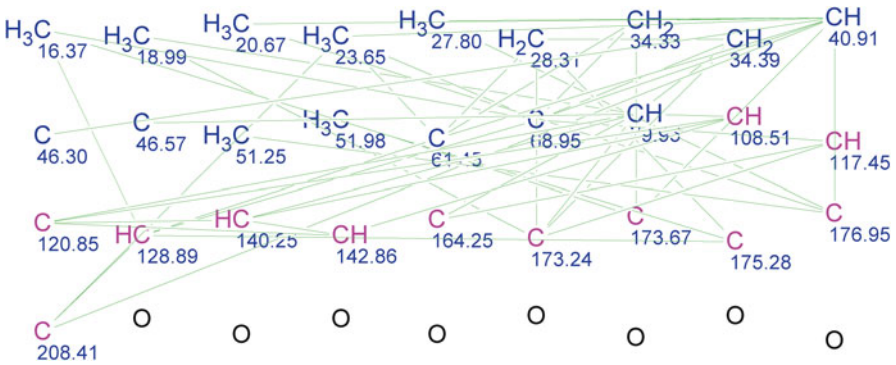

Fig. 9 An ACD molecular connectivity diagram for guyanin (**4**) showing the various carbon–carbon connections

Table 10 ^{1}H and ^{13}C NMR data for guyanin (**4**)

Position	δ_C/ppm	Attached hydrogens	
1	176.95	–	
2	46.30	–	
3	40.91	3.26 d (10)	
4	34.33	2.55 dd (17, 10)	2.19 d (17)
5	173.67	–	
6	61.45	–	
7	208.41	–	
8	128.89	5.87 q (1.3)	
9	175.28	–	
10	68.95	–	
11	28.31	2.29 ddd (15,13,6)	2.16 dd (15, 6)
12	34.39	1.71 td (13,13,6)	1.56 dd (13, 6)
13	46.57	–	
14	173.24	–	
15	117.45	5.90 s	
16	164.25	–	
17	79.95	5.94 dd (1.7, 0.8)	
18	120.85	–	
19	108.51	6.38 dd (1.7, 0.8)	
20	142.86	7.44 t (1.7)	
21	140.25	7.56 t (1.7)	
22	18.99	1.16 s	
23	16.37	2.04 d (1.3)	
24	23.65	1.27 s	
25	27.80	0.98 s	
26	20.67	1.43 s	
27	51.25	3.60 s	
28	51.98	3.68 s	

8.2 T-2 Toxin

The sesquiterpene T-2 toxin is a member of the trichothecene family of mycotoxins. Its structure (**5**) was determined in 1968 (*90*). Proton and ^{13}C NMR data were collected at 400 and 100 MHz, as a teaching aid, to illustrate the structural elucidation of medium-sized organic molecules and to check the assignments, with regard to relative orientations, of various protons within the molecule (*40*).

In this case, raw one- and two-dimensional spectral data (FIDs and their processing parameters) were submitted to ACD/Labs for analysis. Summaries of these data are given in the following tables: HSQC (Table 11), COSY (Table 12), and HMBC (Table 13).

The Structure Elucidator program generated a molecular connectivity diagram (Fig. 10) and four possible structures (**24**). Of these four, only the two structures with epoxy groups (**25** and **26**) passed filtering, *viz*. their $d_A(^{13}C)$ values, used here because they are more discriminating than the corresponding $d_N(^{13}C)$ values, are less

Table 11 HSQC data for T-2 toxin (**5**)

δ_C/ppm	Attached hydrogens (with coupling constants)	
173.00	–	
172.80	–	
170.39	–	
136.59	–	
123.77	5.81 d (5.0)	
84.68	5.31 d (2.4)	
78.81	3.70 d (5.0)	
78.48	4.16 ddd (5.0, 2.4, 2.4[a])	
68.13	5.29 d (5.5)	
67.43	4.35 d (5.0)	
64.69	4.29 d (12.6)	4.06 d (12.6)
64.60	–	
48.68	–	
47.30	3.07 d (4.0)	2.80 d (4.0)
43.67	2.16 d (6.3) [2H]	
43.25	–	
27.87	2.41 dd (14.0, 5.5)	1.91 d (14.0)
25.88	2.10 m [1H]	
22.55	0.97 d (6.4) [CH_3]	
22.48	0.96 d (6.4) [CH_3]	
21.15	2.04 s [CH_3]	
21.10	2.15 s [CH_3]	
20.45	1.75 s [CH_3]	
6.95	0.81 s [CH_3]	
–	3.19 d (2.4[a]) [OH]	

[a]Spin coupling observed between these signals in a fresh sample

Table 12 COSY data for T-2 toxin (**5**)

δ_H/ppm	Spin-coupled partners
5.81	5.29, 4.35, 1.75
5.31	4.16
5.29	5.81, 2.41, 1.75
4.35	5.81, 4.06, 1.91, 1.75
4.29	4.06, 2.41
4.16	5.31, 3.70, 3.19[a]
4.06	4.35, 4.29
3.70	4.16
3.19 [OH]	4.16[a]
3.07	2.80
2.80	3.07
2.41	5.29, 4.29, 1.91
2.16 [2H]	2.10
2.15 [CH_3]	(none)
2.10	2.16, 0.97, 0.96
2.04 [CH_3]	(none)
1.91	4.35, 2.41
1.75 [CH_3]	5.81, 5.29, 4.35
0.97 [CH_3]	2.10
0.96 [CH_3]	2.10
0.81 [CH_3]	(none)

[a]Spin coupling is observed between these protons in a fresh sample

Table 13 HMBC data for T-2 toxin (**5**)

δ_C/ppm	Longer-range correlated hydrogens
173.00	5.31, 2.04
172.80	5.29, 2.16
170.39	4.29, 4.06, 2.15
136.59	5.29, 4.35, 1.91, 1.75
123.77	5.29, 4.35, 1.75
84.68	4.16, 3.70, 0.81
78.81[a]	5.31, 3.07, 2.80
78.48[a]	5.31, 3.70
68.13	5.81, 4.35, 2.41, 1.91, 1.75
67.43	5.81, 4.29, 4.06, 3.70, 1.91, 1.75
64.69	5.31, 4.35, 2.41, 1.91
64.60	5.31, 4.29, 4.06, 3.70, 3.07, 2.80, 0.81
48.68	5.31, 4.35, 4.29, 4.06, 3.70, 3.07, 2.80, 2.41, 1.91, 0.81
47.30	3.70
43.67	2.10, 0.97, 0.96
43.25	5.81, 5.31, 5.29, 4.35, 4.29, 4.06, 2.41, 1.91, 0.81
27.87	5.29, 4.35, 4.29, 4.06
25.88	2.16, 0.97, 0.96
22.55	2.16, 2.10, 0.96
22.48	2.16, 2.10, 0.97
21.15	(none)
21.10	(none)
20.45	5.81, 5.29, 4.35
6.95	3.70

[a]HMBC connectivity is observed to the OH signal (δ3.19) in a fresh sample

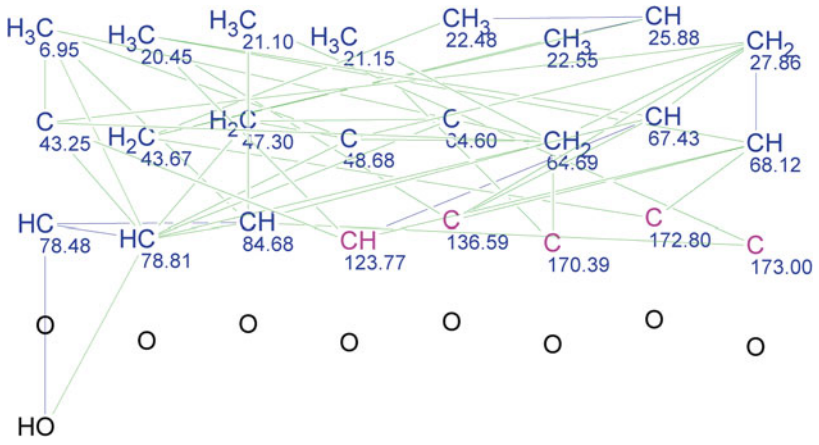

Fig. 10 An ACD molecular connectivity diagram for T-2 toxin (**5**) showing the various carbon–carbon connections

than 4 ppm. These structures differ in the placement of the methylene carbon at 27.86 ppm. However, **25** had a considerably better $d_A(^{13}C)$ value than **26** (0.816 *vs.* 2.187 ppm) and proved to be correct.

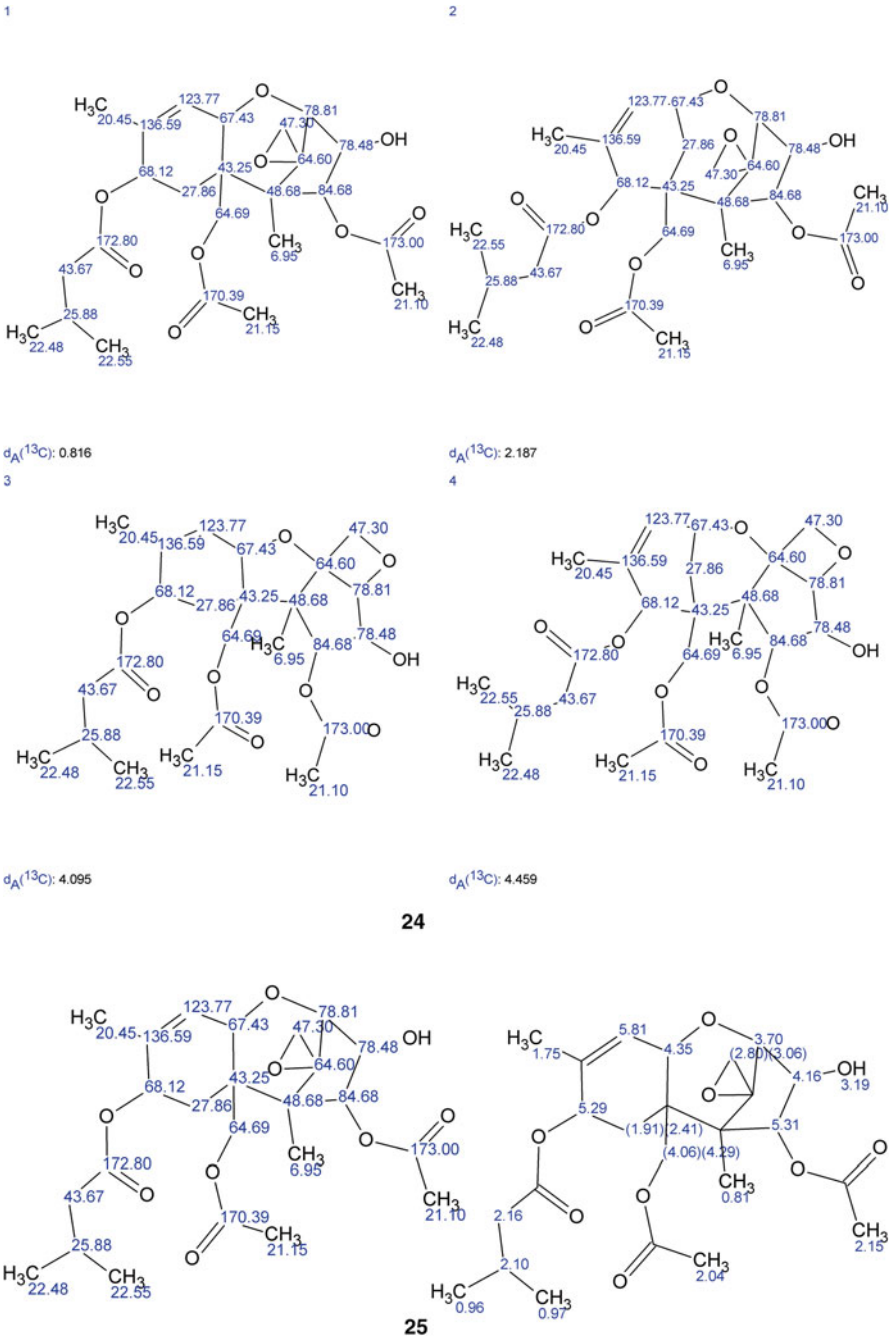

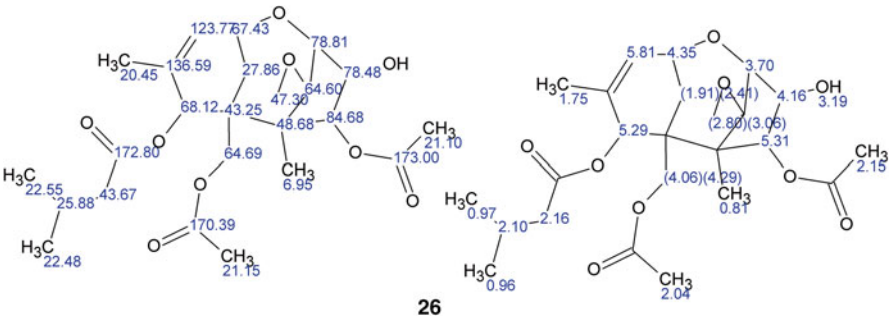

26

It might be surprising that the incorrect structure, which involves the shift of a methylene carbon, would score as well as it did. Part of the reason is that critical HMBC correlations are observed in both structures, being two-bond in one and three-bond in the other, which cannot be distinguished. The presence of a key COSY correlation between the protons at 2.41 and 5.29 ppm permits identification of the correct structure. Table 14 contains ^{13}C and ^{1}H chemical shift data that are sorted by position number.

Table 14 ^{1}H and ^{13}C data for T-2 toxin (**5**)

Position	δ_C/ppm	Attached hydrogens	
2[a]	78.81	3.70 d (5.0)	
3	78.48	4.16 ddd (5.0, 2.4, 2.4[b])	
4	84.68	5.31 d (2.4)	
5	48.68	–	
6	43.25	–	
7	27.87	2.41 dd (14.0, 5.5)	1.91 d (14.0)
8	68.13	5.29 d (5.5)	
9	136.59	–	
10	123.77	5.81 d (5.0)	
11	67.43	4.35 d (5.0)	
12	64.60	–	
13	47.30	3.07 d (4.0)	2.80 d (4.0)
14	6.95	0.81 s	
15	64.69	4.29 d (12.6)	4.06 d (12.6)
16	20.45	1.75 s	
1'	172.80	–	
2'	43.67	2.16 d (6.3) [2H]	
3'	25.88	2.10 m	
4'	22.55	0.97 d (6.4)	
5'	22.48	0.96 d (6.4)	
4-OAcCH_3	21.15	2.04	
15-OAcCH_3	21.10	2.15	
4-OAc	173.00	–	
15-OAc	170.39	–	
		3.19 d (2.4[b]) [OH]	

[a]Position 1 is assigned to the ether oxygen between carbons 2 and 11
[b]Spin coupling is observed between these protons in a fresh sample

8.3 Kauradienoic Acid

As mentioned in Sect. 7, kauradienoic acid is a diterpene, for which the structure **3** was determined in 1971 (*78*) and its ^{1}H and ^{13}C NMR spectra completely assigned in 1984 (*31*). This compound was used earlier in the section to illustrate how a general structural elucidation could be achieved through the systematic analysis of ^{1}H, ^{13}C, HSQC, COSY, TOCSY, and HMBC spectra. The process is somewhat laborious, even for a relatively small-molecular weight compound, due to the occurrence of many close-lying proton NMR signals.

Raw one- and two-dimensional spectral data (FIDs and their processing parameters) were again submitted to ACD/Labs for analysis. Summaries of these data are included in the following tables: HSQC (Table 1), COSY (Table 2), TOCSY (Table 3), and HMBC (Table 4), which are given in Sect. 7.

The ACD/Structure Elucidator program generated a molecular connectivity diagram (Fig. 11) and two structures, **27** and **28**. Inspection of the two structures reveals the same problem that was encountered in Sect. 7, *viz*. that ^{1}H and ^{13}C assignments for two methyl groups and their two adjacent methylene groups are interchanged. In this case, use of $d_N(^{13}C)$ values gave slightly better discrimination. However, it was not surprising that very similar numbers, 1.17 and 1.26 ppm, were calculated for identical structures with three differing assignments. Again, the correct structure was the lower one. Assignment of the proton chemical shifts was made especially difficult due to accidental chemical shift equivalence of three sets of protons: H-3β and methyl-20 (1.02 ppm), H-1β and methyl-18 (1.24 ppm), and H-2β and H-14α (1.50 ppm) (Table 6). As a result, structures **27** and **28** both exhibit composite assignments in which the assignments of ^{1}H chemical shifts for methyl (1.02 and 1.24 ppm) and certain methylene protons (1.50, 1.60, 1.88, 1.93, and 2.16 ppm) can be interchanged.

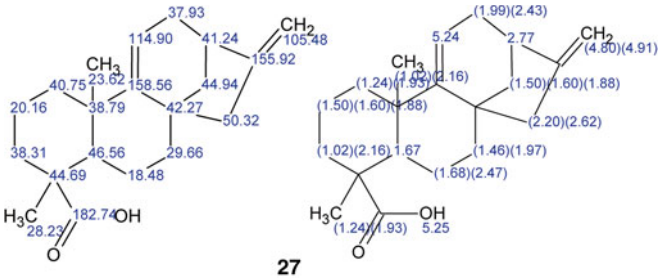

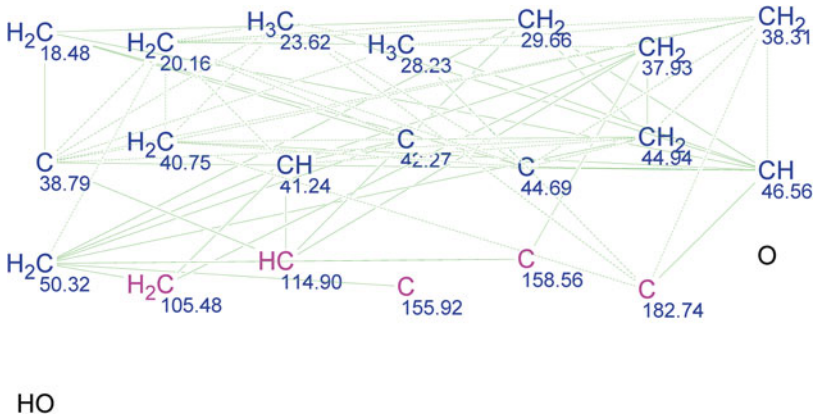

Fig. 11 An ACD molecular connectivity diagram for kauradienoic acid (**3**) showing the various carbon–carbon connections

However, as was seen at the conclusion of Sect. 7.6, several lines of reasoning based on the analysis N*O*ESY connectivities and HMBC traces demonstrated unequivocally that only the ^{1}H and ^{13}C assignments shown in **13** (in Sect. 7.5) and **27** (in this section) could be correct. ^{13}C and ^{1}H chemical shift data for kauradienoic acid (**3**), which are sorted by position number, are presented in Table 6 in Sect. 7.6.

The examples, illustrated in Sects. 8.1–8.3, demonstrate that the ACD/Structure Elucidator program is an important addition to the arsenal of chemists engaged in the determination of structures of organic compounds. Moreover, it is best when used in conjunction with a knowledgeable NMR spectrometer operator, who can distinguish between different structural possibilities by closer examination of the NMR spectra.

9 The Effect of Dynamic Processes on the Appearance of NMR Spectra of Natural Products and Other Organic Compounds

There are a number of exchange processes (conformational interchange, tautomerism, epimerization, *etc*.), which can affect the appearance of an NMR spectrum. In considering how these processes can alter the appearance of an NMR spectrum, it is important to recognize that what matters is the frequency difference between a pair of peaks interchanged by the exchange process, compared to the frequency of exchange. For this reason, the present authors dislike the commonly used term "NMR time scale" since this implies a single time scale for a spectrum measured on a particular spectrometer. While the peak separations for individual pairs of peaks are directly proportional to the spectrometer operating frequency, different pairs of exchanging peaks for the same compound will generally have different peak

separations, *i.e*. there are several different "time scales" for a single compound at a single acquisition frequency. A further objection to this term is seen when considering ^{13}C and ^{1}H spectra run on the same spectrometer. While the acquisition frequency for the ^{13}C spectrum is almost exactly ¼ of that for ^{1}H, the ^{13}C chemical shift range (in ppm) is typically *ca*. 20 times that for ^{1}H. Consequently, peak separations (in frequency units) for pairs of exchanging ^{13}C peaks are typically significantly larger than the peak separations for corresponding ^{1}H pairs. Thus, rather than having a longer "NMR time scale" (as would be implied by the lower frequency), ^{13}C spectra actually usually have shorter "time scales," *i.e*. faster exchange rates are needed to cause full spectral averaging.

A number of years ago, one of the authors took advantage of this difference in ^{1}H and ^{13}C "time scales" to resolve a dispute in the literature concerning the site of protonation of amides in strong ($\ll$pH 1) acid solutions. While it had previously been generally accepted that the carbonyl oxygen was the site of amide protonation in strong acids, *Liler* argued that, in very strong sulfuric acid solutions, there was switch-over to N-protonation (*91*). This was based on the 60-MHz ^{1}H spectrum of *N,N*-dimethylformamide in these solutions. This showed two methyl ^{1}H peaks in both neutral and weakly acidic solutions, due to hindered rotation about the central C–N bond. However, the two methyl signals collapsed to a singlet as acidity increased. *Liler* believed that this indicated predominant N-protonation at high acidity since this would lower the barrier to C–N rotation by minimizing C–N double bond character (*91*). Since this conclusion was doubted, the ^{13}C spectrum of *N,N*-dimethylformamide was recorded under the same conditions (*92*). These spectra showed two methyl ^{13}C signals at all acidities, although the signals did broaden to a limited extent at intermediate acidity values. This indicated predominant O-protonation at all acidities, but with a small proportion of N-protonation at intermediate acidities and with fast exchange between the two tautomeric forms. This small fraction of N-protonation allowed slightly faster rotation about the C–N bond that was sufficient to coalesce the slightly separated (*ca*. 6 Hz at 60 MHz) ^{1}H methyl signals but not the more widely separated ^{13}C signals, which instead were only slightly broadened (*92*).

When considering exchange processes, one can define three exchange regimes: the slow exchange regime where the frequency of exchange is significantly lower than the peak separation, the intermediate exchange region where the two values are comparable in magnitude, and the fast exchange regime where the exchange rate is much larger than the frequency difference. In the slow exchange region, one will observe separate, relatively sharp, spectra for the two (or more) different forms. In the fast exchange regime, one will observe a single, relatively sharp, spectrum corresponding to the weight average of the spectra for the different exchanging forms. Finally, the appearance of the spectrum of a compound in the intermediate exchange regime will depend strongly on the relationship between the frequency separations between individual pairs of exchanging peaks and the exchange rate. Thus, pairs of peaks with a small frequency separation may appear as a broadened single peak while a pair with a larger chemical shift difference may appear as two broadened peaks. A further complication occurs when the relative populations of the

exchanging forms are significantly different. Consider the exchange between two forms, A and B, in relative proportions of 10:1. The back exchange rate B→A will be 10 times as great as A→B, and peaks for form B will broaden 10 times as fast as the corresponding A peaks with the onset of exchange. Under these circumstances, the minor form may not be observed, particularly if signal/noise is marginal.

Dynamic effects on NMR spectra can create different kinds of problems for a natural product chemist, depending upon which exchange regime is involved. One common problem is very fast interconversion of two or more conformations of a molecule. Provided that the exchange rate is sufficiently fast, the researcher may not be aware that conformational averaging is occurring since the spectrum will not be different in overall appearance from that of a molecule with a fixed conformation. However, both chemical shifts and ^{1}H–^{1}H coupling constants will be the weight averages of the values for the different conformers. Since one often relies heavily on vicinal ^{1}H–^{1}H coupling constants in determining stereochemistry, this could result in misleading conclusions. Furthermore, interproton distances also vary with conformation, so the observed N*O*E between a pair of protons will also be an average of the N*O*Es for the different conformations. However, since N*O*Es vary as r^{-6} (*59*), the observed N*O*E will not be a simple weight average but will be strongly biased towards the N*O*E of the conformer with the shortest interproton distance, even if this is a minor conformer (*68b*). Thus, N*O*E data in conformationally mobile systems can be highly misleading if not interpreted with care.

Situations where low barriers are probable to interconversion between conformations of similar energy include molecules with five-membered rings, six-membered rings with fused *cis*-ring junctions, and larger macrocyclic molecules. Unfortunately, there is no easy solution to this problem. If a molecule is in the fast exchange regime at room temperature, the interconversion barrier must be low. Consequently, it may not always be possible to slow the exchange by cooling the solution to the point where well-resolved spectra for individual conformers can be obtained and coupling constants determined, even on a high-field spectrometer. An alternative is to use either molecular mechanics or quantum mechanics calculations to estimate the 3-dimensional structures and relative energies of different significantly populated conformers. A relationship such as the *Altona* equation (*60*) can then be used to predict the vicinal ^{1}H–^{1}H couplings in the different conformers and determine whether their calculated weight average values are consistent with the observed values.

Systems in the intermediate exchange region present entirely different problems. The biggest risk is that some signals may be so broad that they are not clearly observed. This is most likely to be a problem for ^{13}C spectra because the typically much larger ^{13}C chemical shift differences make extreme broadening more probable. Oddly, this is a situation where the use of a higher field spectrometer can actually be a disadvantage because the larger frequency difference between exchanging signals makes extreme broadening more likely. A second factor is that the lower sensitivity of ^{13}C spectra makes it more likely that a broadened peak cannot be clearly distinguished from noise. One approach that we find effective in cases where this problem is suspected is to reprocess the ^{13}C spectrum with extreme line broadening (*e.g.* 25 Hz). As illustrated in Fig. 12, this aids in distinguishing broad peaks

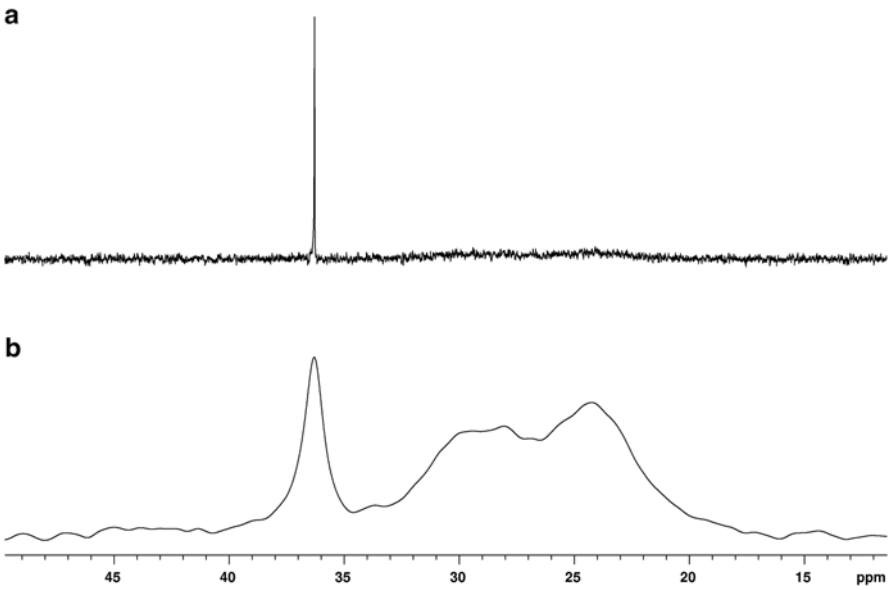

Fig. 12 125-MHz ^{13}C spectrum of *cis*-decalin at 25 °C: (**a**) with 1-Hz line broadening (**b**) with 100-Hz line broadening. This illustrates how severe line broadening allows one to detect peaks that are severely broadened by an intermediate exchange rate

from noise. In addition, due to a smaller frequency separation, the proton bonded to the broadened ^{13}C peak may be much sharper. In this case, it is sometimes possible to detect a correlation between a directly bonded $^{1}H/^{13}C$ pair in an HSQC spectrum, which will allow one to determine the ^{13}C chemical shift with adequate precision (*93*). Similar correlations between indirectly bonded $^{1}H/^{13}C$ pairs may be observed in an HMBC spectrum, although the lower sensitivity of the latter spectrum may make this less likely. Finally, one can repeat the measurements at higher or lower temperatures to attempt, respectively, to move the system to the fast or slow exchange regime. Heating the sample will sharpen the broadened peaks and make them easier to detect. Cooling the sample will potentially allow one to detect and identify the two (or more) exchanging conformations or tautomers. However, this will generally require a significant lowering of temperature to slow the exchange sufficiently to allow sharp peaks to be observed. The choice of which approach to use will also be determined by the liquid range of the solvent used, relative to room temperature. For example, C_6D_6 and, particularly, DMSO-d_6 are suitable for high temperature measurements but freeze not far below room temperature. On the other hand, $CDCl_3$ and CD_3OD are good for low temperature measurements but of limited value for high temperature measurements due to relatively low boiling points.

One compound, which nicely illustrates many of these problems (and solutions), is lupane-3β-ol-30-al (**29**) (93). The original ^{13}C spectrum appeared to show only 25 peaks, which suggested a sesterterpene or possibly a degraded steroid. However, the

^{1}H spectrum, which showed several methyl singlets, seemed more consistent with a triterpene or possibly a tetranortriterpene. Repeating the ^{13}C spectrum at –40 °C revealed four additional peaks, which were between 20 and 40 Hz wide at half-height. Finally, the HSQC and HMBC spectra revealed correlations to another carbon for which the line was still too broad to be clearly observed even in the low temperature ^{13}C spectrum. The NMR data, in combination with molecular modeling calculations, revealed that the observed dynamic effects were due to slow interconversion of two conformations of the side chain aldehyde group (*93*).

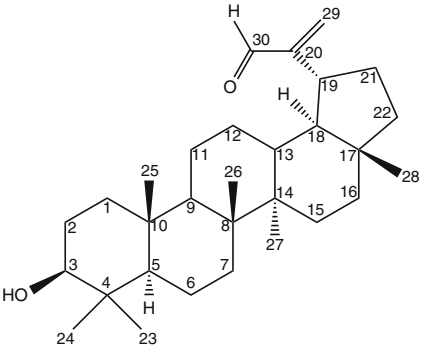

29

In the slow exchange limit, it may not be clear initially whether one is dealing with two interconverting forms or a mixture of two compounds of relatively similar structure. Here, the best approach is to rely on an EXSY spectrum to distinguish between these possibilities (*65*). This spectrum will show symmetric off-diagonal peaks between the corresponding protons in two exchanging forms. An EXSY spectrum can be obtained with the same pulse sequence that is used for obtaining either a N*O*ESY or R*O*ESY spectrum (*65*). However, the difference is that EXSY peaks have the same phase as the diagonal peaks while N*O*ESY peaks (for small molecules) and R*O*ESY peaks (always) are of opposite phase to the diagonal peaks. For this reason, N*O*ESY and R*O*ESY spectra should always be obtained in the phase-sensitive mode so that exchange peaks can be distinguished from N*O*E peaks. Another application of EXSY correlations in the natural product area is the detection of OH peaks hidden beneath other proton peaks. The OH peaks often show EXSY peaks with residual water in the solvent and can be detected by taking a cross-section through the water peak in the N*O*ESY or R*O*ESY spectrum. With the aid of EXSY spectra in combination with other 2D spectra, we find that it is possible to totally assign the structures and spectra of two interconverting forms of even complex natural products. An example is a prenylated benzophenone **30**, where the two tautomeric forms were fully assigned in this way (*94*). The main problem with this approach occurs when one of the forms is present in only a minor amount since, as noted at the beginning of this section, the minor component peaks may be severely broadened.

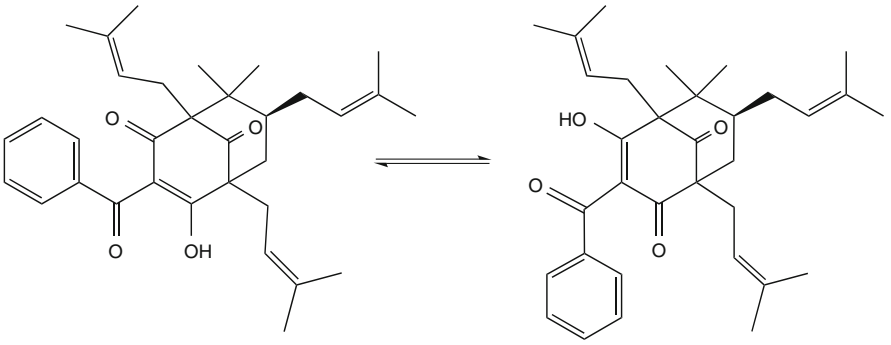

30

10 The Relative Advantages and Disadvantages of Different Pulse Sequences

This topic was extensively discussed in a 2002 review article (*10*), and the conclusions from that article will be only briefly summarized here. Rather, we will focus mainly on developments since that time. Two key choices, which were previously discussed in the earlier review, were between HMQC and HSQC for one-bond ^{1}H–^{13}C correlations and between N*O*ESY and R*O*ESY for investigating N*O*Es. Our recommendations were to use HSQC in preference to HMQC and R*O*ESY in preference to N*O*ESY. More recent improvements in pulse sequences and hardware support these recommendations, as discussed below.

The original argument for favoring HMQC over HSQC is that the latter requires more pulses and particularly 180° ^{13}C pulses. Therefore, the latter sequences would be prone to poor performance due to incorrect probe tuning, inhomogeneous RF pulses, and incomplete inversion by ^{13}C 180-pulses over the entire spectral window on high-field spectrometers. However, HMQC has the disadvantage that ^{1}H–^{1}H coupling appears along both *F*1 and *F*2 axes while only along *F*2 in HSQC. This yields a sensitivity and ^{13}C resolution advantage for HSQC (*95*). In addition, HSQC can be run in a phase-sensitive, edited mode (see below) while HMQC is usually run in an absolute-value (magnitude) mode and cannot provide edited spectra. Furthermore, the availability of automatic probe tuning eliminates the first concern about HSQC while modern probe designs now give better pulse homogeneity. Another important advance has been the replacement of "hard" ^{13}C 180-pulses by frequency-swept adiabatic pulses with much greater inversion efficiency (*96*). Adiabatic pulses also provide more efficient ^{13}C decoupling (*96*), allowing one to increase the acquisition time and the ^{1}H resolution without concerns about decoupler heating. This does not require an increased total experiment time since the relaxation delay can be correspondingly decreased to keep the acquisition time constant (*10*).

A particularly useful version of HSQC is the edited version, which gives peaks of opposite phase for CH_2 carbons relative to CH and CH_3 carbons (*97*). This provides

the same information as an edited ^{13}C DEPT experiment (*10*) in comparable time, with the important added advantage of providing the chemical shifts of attached protons (*10*). However, it has the disadvantage that peaks near the outer edges of the spectral window may be severely attenuated due to a mismatch between the average value of the $^{1}H–^{13}C$ coupling used to calculate delays and the actual coupling for that CH_n pair. A clever approach to this problem was the design of an adiabatic pulse (CRISIS), which took advantage of the approximate linear relationship between ^{13}C chemical shifts and $^{1}H–^{13}C$ coupling constants to minimize this problem (*98*). A more recent improvement includes a modified CRISIS refocusing pulse during the evolution period with broadband ^{1}H and ^{13}C inversion pulses during the INEPT and reverse-INEPT stages. The same sequence also provides further sensitivity enhancement by simultaneous acquisition of the two coherence pathways (*99*). These improvements provide a much more robust version of HSQC, as can be seen in Fig. 13, which shows spectra obtained with the basic gradient HSQC sequence and

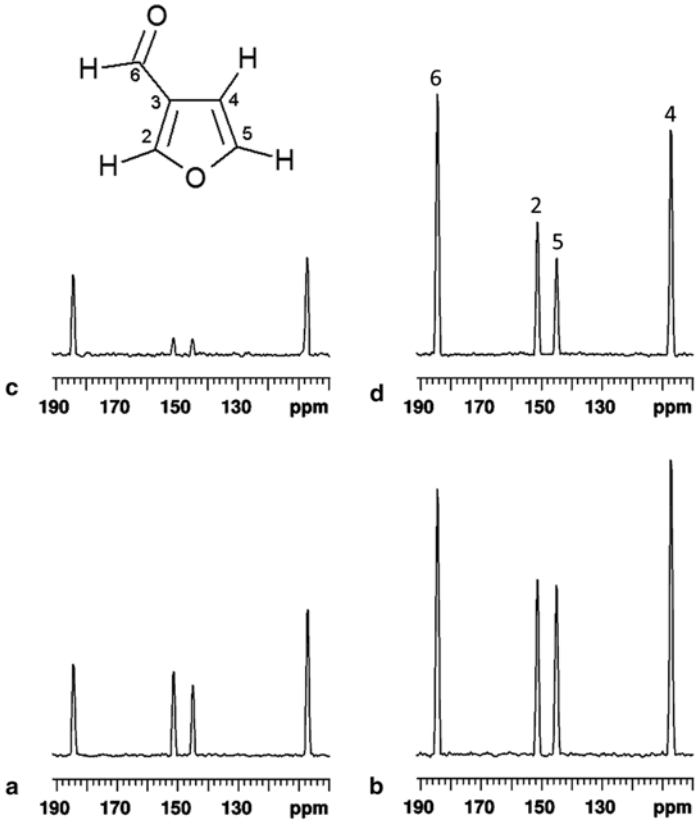

Fig. 13 "Skyline" projection spectra for 3-furanaldehyde, using different versions of gradient-selected HSQC pulse sequences: (**a**) unedited spectrum with the basic gHSQC sequence, (**b**) unedited spectrum with an improved gHSQC (Agilent gc2hsqcse) sequence, (**c**) edited spectrum with the basic sequence, (**d**) edited spectrum with the improved sequence. Carbon numbers are shown at the *top of spectrum* (**d**)

one with all of the recent improvements. There are still some sensitivity losses with editing, but these are not nearly as great as with the original sequence.

Recent developments of very fast HMQC sequences (*17–19*) make them an attractive alternative to HSQC, particularly for rapid screening and dereplication (see Sect. 2). However, these give poorer ^{13}C resolution and cannot provide edited spectra.

Since the wide ^{13}C spectral window is the time-incremented axis, ^{13}C resolution may still be a problem with HSQC (and even more so HMQC), even with the aid of linear prediction. If one is not sample-limited (or if one is fortunate to have access to a ^{13}C-optimized cryogenically cooled probe), it is worth considering acquiring a HETCOR spectrum (*35*) in cases of severe ^{13}C spectral crowding. As we have shown (*100*), this can give resolution of close-spaced peaks, which is not possible with HSQC.

There have been numerous proposed modifications of the basic HMBC spectrum, and these have recently been extensively reviewed (*101*, *102*). Unfortunately, in an attempt to improve information content, most of these involve some loss of sensitivity from what is already a low-sensitivity experiment. In contrast, we have shown that one can potentially obtain significant sensitivity enhancements of HMBC spectra by correct choices of acquisition and processing parameters (*12*). This is illustrated in Fig. 14, which shows a comparison of HMBC spectra of strychnine (**1**) obtained using our recommended parameters (*12*) and those from a

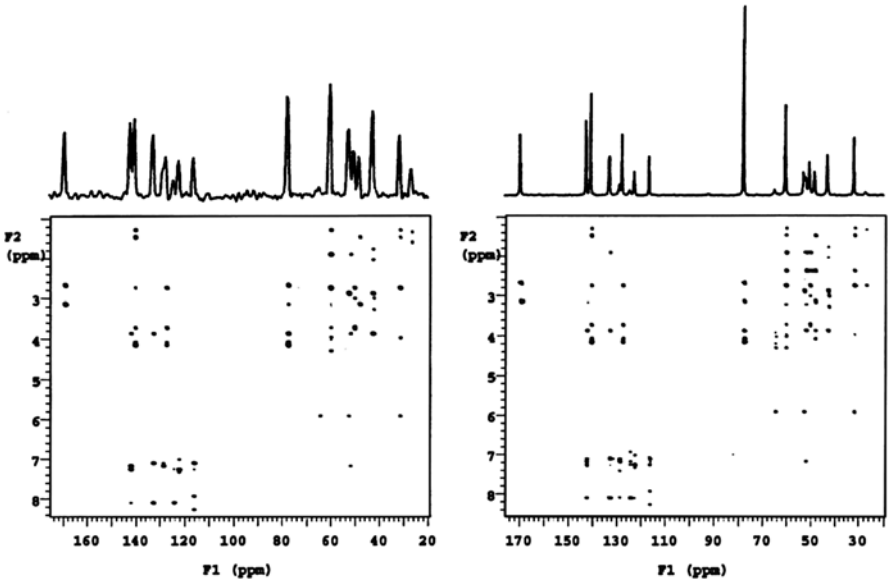

Fig. 14 Absolute-value mode gHMBC spectra of kauradienoic acid (**3**) with summed projection spectra along the *top*. The *left-hand spectrum* was obtained using suggested acquisition and processing parameters from (*8*). The *right-hand spectrum* was obtained using recommended parameters from (*12*). The summed spectrum on the *left* is plotted at 10 times the vertical scale of the summed spectrum on the *right*, and the two summed spectra have respective signal/noise of 22:1 and 150:1. This clearly illustrates the importance of parameter choices in obtaining 2D spectra. This figure was taken from (*12*) with permission of the publishers

widely used book, which suggests acquisition and processing parameters for numerous 1D and 2D experiments (*8*). The improvement in *S*/*N*, shown in Fig. 14, is actually greater than one would obtain by switching from an ambient temperature probe to a cryogenically cooled probe. In addition, the basic HMBC sequence can be further improved to a limited degree by the incorporation of adiabatic pulses (*103*).

The types of HMBC modifications that have potential advantages fall into three main categories. The first is a group of sequences, which can separate 2-bond and 3-bond C–H correlations. Of these, the most widely used is the H2BC sequence (*104*). This relies on the presence of vicinal ^{1}H–^{1}H couplings to generate only ^{1}H–^{12}C–^{13}C correlations. The 2D display produced is similar to that for an HMBC spectrum. Thus, from a side-by-side comparison of the two spectra, one can directly distinguish between 2-bond and 3-bond correlations since only the latter will appear in the HMBC spectrum. However, there are three disadvantages. First, since the correlation information is relayed *via* the vicinal couplings, it does not generate any correlations involving non-protonated carbons, and thus 2-bond and 3-bond correlations to these carbons cannot be distinguished. Second, it requires acquisition of an additional, relatively low-sensitivity, spectrum. Finally, it does not contain any information that could not be deduced from a COSY spectrum or, in case of spectral crowding, from the combination of COSY and HSQC spectra. This suggests an alternative to H2BC. Instead, since one normally would have acquired both COSY and HSQC spectra, covariance processing (*45*) could be used to generate an HSQC-COSY spectrum from these spectra. Alternatively, one could directly generate an HSQC-COSY spectrum, but this again would require acquiring an additional spectrum. This illustrates what we regard as the biggest advantage of covariance processing, *i.e*. the ability to use two existing high-sensitivity spectra to generate a new spectrum, which would otherwise require significant additional spectrometer time.

One problem with the HMBC sequence is that it uses a fixed delay to generate correlations. This typically is chosen to be optimum for 8-Hz ^{1}H–^{13}C couplings. However, this may give very weak correlation peaks in cases where the actual coupling is significantly different from 8 Hz. The second group of modifications are those designed to sample a wider range of long-range ^{1}H–^{13}C couplings to minimize this problem. One example is the ACCORD sequence (*105*), which uses the "accordion" approach to sample couplings over a range as large as 2–25 Hz. This clearly generates a wider range of correlations with good sensitivity (*105*) but at the cost of introducing a new problem. HMBC spectra, like HMQC, have ^{1}H–^{1}H coupling appearing along both *F*1 and *F*2, generating skewed cross-peaks. The accordion section in ACCORD significantly increases the width of this skew pattern along *F*1, with resultant loss of resolution along that axis. In an attempt to maintain the advantages of ACCORD, while minimizing the skewing problem, *Krishnamurthy* and *Martin* developed the CIGAR sequence (*106*). This uses a modified accordion section, which can be adjusted to totally eliminate the cross-peak skew, producing an HMBC spectrum with no ^{1}H–^{1}H coupling along *F*1 (similar to HSQC). This can produce significantly improved resolution in regions of spectral crowding (*10*). However, it also introduces extra delays, which can significantly decrease *S*/*N*, particularly for larger (>400 molecular weight) molecules with shorter relaxation

times. Fortunately, *F*1 spectral crowding in natural product HMBC spectra is often restricted to a relatively narrow region of the spectrum. While one could run a band-selective HMBC spectrum for this region, an alternative would be to obtain a band-selective CIGAR spectrum. Other approaches to sampling a wide range of couplings include converting HMBC to a 3D experiment with J_{CH} forming the third axis or by combining the data from three or four experiments with delays corresponding to different values of J_{CH}. The advantages and problems of these approaches are discussed elsewhere (*101*, *102*).

The third, and in our view most promising, HMBC modification is the IMPACT-HMBC sequence, which was recently developed by *Furrer* (*107*). This is similar in design to the ASAP-HMQC sequence of *Kupce* and *Freeman* (*18*) in that it uses cross-polarization of protons to allow a far shorter (*ca*. 0.2 s) relaxation delay. This either permits one to acquire spectra more quickly or to collect more scans per time increment in a given time, increasing the signal/noise.

We have previously argued for the use of R*O*ESY in place of N*O*ESY for N*O*E investigations (*10*). The main advantage of R*O*ESY is that cross-peak intensities are nearly independent of molecular weight while N*O*ESY cross-peaks change sign as molecular weight increases. Depending on solvent viscosity, the crossover point typically occurs somewhere in the 500–1,500 molecular-weight region. Consequently, particularly for larger natural products, N*O*ESY cross peaks may be very small. However, one problem with R*O*ESY has been that the spin-lock generates heat if it is too long. Recent improvements replace the original spin-lock, which used hard pulses with a lower power adiabatic pulse spin-lock that allows the use of longer mixing times (*108*).

Finally, one disadvantage of the original TOCSY sequence (*34*) was phase distortions, which altered the appearance of cross-peaks. This has been minimized by the more recent Z-TOCSY experiment, which incorporates a zero-quantum filter, yielding cleaner spectra and well-phased peaks (*67*). These can also be incorporated in the selective 1D TOCSY sequence. An example of this was given in Sect. 7.

11 Liquid-Chromatography–NMR

Since high-pressure liquid chromatography (HPLC) is so widely used for isolating pure natural products from chromatographic fractions or other complex mixtures, the combination of LC with NMR would seem to be a logical approach to use in natural product research. This approach has been investigated widely over a number of years (*109*). However, the relatively low sensitivity of NMR has been a persistent problem when trying to use continuous flow LC in combination with NMR. The conditions for optimum resolution of LC peaks usually leave too little sample in the flow cell of the NMR probe during acquisition to allow one to obtain anything more than a routine ^{1}H spectrum. While this problem can be partially overcome if one is fortunate enough to have access to a cryogenically cooled flow probe (see Sect. 12), the consensus seems to be that it is better to use the two techniques separately.

One intermediate approach would be to use stop flow LC for sample collection. However, most workers in the field seem to agree that the best approach is to use solid phase extraction (SPE) cartridges to collect the LC fractions (*109*). The samples can then be dissolved off the cartridges using deuterated solvents and either injected into a flow NMR probe or placed in NMR tubes to be used in conjunction with a sample changer and a regular NMR probe. There are two major advantages to this approach. First, the LC separation can be carried out with protonated solvents, minimizing costs. Second, one can use repeat injections to increase the amounts of samples collected, if necessary.

A further modification of this approach is to combine LC, mass spectrometry (MS), and NMR (*110*). Liquid chromatography is used to separate a complex mixture into individual components, using protonated solvents. As each component is detected, usually by a UV-visible detector, the fraction concerned is split, with a small amount sent for MS analysis, with the remainder sent to an SPE cartridge for collection. If the MS does not allow identification of the fraction as a known compound, the solvent can be removed from the SPE cartridge and the sample reconstituted in the appropriate deuterated solvent for NMR investigation. Although neither of the authors has extensive experience of combining LC with mass and NMR spectroscopic analysis, we believe that this is a promising approach since it combines dereplication (*i.e*. distinguishing known from unknown compounds) with full structure determination, when the latter is required.

12 Probe Choices

In most cases, a natural product chemist may have limited probe choices available, as determined by the available probes in the NMR facility. However, it is still useful to have a general knowledge of the relative advantages and disadvantages of different probe types. These are discussed below.

12.1 Essential Probe Features for Natural Product Research

Any probe should have H/X capabilities, *i.e*. observation of both proton and heteroatoms (most commonly ^{13}C but preferably also at least ^{15}N). This can involve either an H-channel and a tunable X-channel or a three-channel (H/C/N) probe with separate channels tuned to the three nuclei. It should also have a z-axis gradient coil for gradient shimming and performing gradient-selected 2D NMR sequences. Finally, it is highly desirable to have auto-tuning capabilities for both H and X channels. This is particularly important if the spectrometer is being operated with an autosampler but also for multi-pulse experiments (*e.g*. 2D NMR) where having one or both channels out of tune can significantly degrade performance and introduce artifact peaks.

12.2 Ambient-Temperature Probes

The main advantages of ambient-temperature probes are their low capital and operating costs, but they are significantly less sensitive than the alternative cryogenically cooled probes (see below). They most commonly have inserts for either 5-mm or 3-mm sample tubes. A key feature, particularly in the past, has been the geometry of the two coils in an H/X probe since the inner coil was relatively more sensitive than the outer coil (often by a significant extent). If the H-coil is inside, this is commonly called an indirect-detection probe while, if the X-coil is inside, it is called a direct-detection probe. This odd terminology is a historical one, dating to the time when 2D H/X experiments almost always involved X-detection. The difference in coil sensitivities has been a problem for natural product chemists since one usually wished to obtain both a 1D ^{13}C spectrum and a series of ^{1}H-detected 2D spectra on the same sample, preferably without having to change probes. Fortunately, some of the latest generation of probes from both Bruker and Agilent have minimized this problem by providing good sensitivity on both coils. For example, a probe of this type, to which both authors of this chapter have access, is the Agilent "OneNMR" probe that gives ^{1}H and ^{13}C *S*/*N* specifications, which are, respectively, almost identical with the corresponding specifications for ^{1}H on an indirect-detection probe and ^{13}C on a direct-detection probe from the same manufacturer.

12.3 Cryogenically Cooled Probes

With these probes, the coils and the preamplifiers are cryogenically cooled, usually with liquid He, but with the sample at ambient temperature. The actual coil temperature is usually about 20 K. This very significantly reduces random thermal noise, leading to a dramatic increase in *S*/*N* compared to ambient-temperature probes. The enhancement factor is usually quoted as about 4:1, but the actual *S*/*N* enhancement appears to be strongly solvent-dependent with larger than 4:1 enhancements for some common organic solvents (*e.g.* $CDCl_3$ and C_6D_6, in particular) and less than 4:1 for aqueous solutions, particularly "salty" solutions. While the sensitivity of these probes is obviously a major advantage, the disadvantage is that they are not only far more costly than regular probes but also require expensive routine maintenance every 1–2 years. They also appear to be more prone to other damage and are costly and time-consuming to repair. In times of shrinking budgets, one must carefully balance the sensitivity advantages against the significant maintenance costs in deciding whether to acquire this type of probe. If one does have sufficient funds to include a cryogenically cooled probe in a spectrometer purchase, one should also consider the alternative of extra ambient-temperature probes plus a significantly extended warranty on the entire spectrometer package. The most common cryogenically cooled probes are indirect-detection H/C/N probes. While these were designed mainly for protein NMR studies, they

are also quite suitable for natural product investigations. Alternatively, both major manufacturers offer high sensitivity ^{13}C-optimized probes, which still give ^{1}H *S/N* specifications well in excess of ambient-temperature indirect-detection probes. Arguably, these would be a better choice for natural product research since they can quickly provide the good quality ^{13}C spectra, which are required by journal editors for publication, while still providing excellent sensitivity for ^{1}H-detected 2D experiments.

Cryogenically cooled probes are most commonly designed for 5-mm or 3-mm tubes although Bruker also offers an H/C/N 1.7-mm probe. One point to remember is that, with a 5-mm probe, there are often *S/N* advantages in using 3-mm tubes (*111*). The reason is that, with the cryogenic cooling of coils and preamplifier, the main source of thermal noise is the sample. Thus, providing that solubility is not an issue, there is an advantage in reducing the sample volume with a 3-mm tube.

Bruker has recently offered indirect-detection liquid N_2-cooled H/X probes for 400–600 MHz instruments. While the *S/N* is only about half of that of the LHe-cooled probes, capital costs are lower. However, they require continuous cooling with liquid N_2, so operating costs will be higher than for ambient probes.

Finally, the ultimate cryogenically cooled probe for natural product research is one built specially for the National High Field Magnet Laboratory in Florida (*112*). This not only has cooling of the coils and preamplifiers but also has coils fabricated from superconducting materials. It has been used to elucidate structures of marine natural products at the nanomole level (*113*). While there are rumors of a possible commercial version of this probe in the future, it would undoubtedly be considerably more expensive than current cryogenically cooled probes.

12.4 Microprobes

Microprobes represent a different approach to probe design, which is particularly suitable for sample-limited cases, namely, to have a very small sample volume. A commercial version of a probe of this type is the Protasis CapNMR probe, which is compatible with spectrometers from all major manufacturers. The probe requires about 15 mμ^3 of solution with an active volume (in the form of a flow cell within the probe) of 5 mμ^3. This is available as an H/C probe, either with a single-flow cell plus gradient coils or with dual-flow cells without gradients. The latter arrangement allows for parallel acquisition of spectra from two samples. Samples can be loaded with a robot auto-sampler, allowing for high throughput operation. The main limitation would appear to be sample solubility. Nevertheless, CapNMR does provide an intermediate cost alternative to cryogenically cooled probes and has proved useful in natural product research, particularly when used in combination with HPLC-SPE separation techniques (*114*).

13 A Fully Automated Setup of 2D NMR Experiments for Organic Structure Determination

There have been a number of advances in spectrometer operation, which minimize the extent of operator interaction with the spectrometer. These include robots for sample changing, automated locking and probe tuning, gradient shimming and improved software for experiment setup. However, with the increasing speed and power of computers, we believe there is still room for further significant improvement, particularly in automated setup of acquisition and processing parameters for 2D experiments. This would allow replacing the default parameters currently included with the spectrometer software for different pulse sequences with parameters optimized for the actual sample, without requiring expert knowledge on the part of the operator. A possible future program to fully achieve these goals is outlined below. However, in the interim, some of the ideas could be quickly implemented, *e.g.* using a quick ^{1}H T_1 measurement to choose optimum recycle times for different experiments.

The program could provide a menu of standard 2D experiments (probably at least COSY-45 or COSY-90, N*O*ESY/R*O*ESY, TOCSY, HSQC, and HMBC), along with a Help file indicating the information content and the relative sensitivity of different experiments. It could also provide the option of inputting an estimated ^{13}C spectrum (calculated with existing 3rd party software), provided that the probable structure was known with reasonable certainty. The first step would be to specify the 2D experiments to be run and also whether the operator wished to obtain a DEPT-135 or DEPT-Q ^{13}C spectrum. The spectrometer would then be instructed to acquire a proton spectrum with a default number of scans (probably 16) and with a wide spectral window to ensure that no peaks are missed. The spectrometer could then reacquire the spectrum with the spectral width narrowed to include only regions where peaks appeared and the number of scans adjusted to the minimum number needed to give good signal/noise. The next step would be to have the spectrometer measure proton T_1 values by finding nulls in a quick inversion-recovery experiment. It could be programmed to ignore the most intense peaks (solvent peaks and methyl signals) so that T_1 values were determined only from the weaker CH and CH_2 multiplets (CH_3 signals usually have longer relaxation times but are also much more intense. Thus, one can afford to have a shorter than optimum recycle time for these protons).

Based on the measured signal/noise and number of scans for the ^{1}H spectrum and the known relative ^{1}H and ^{13}C sensitivity of the probe in use, the program could then calculate the time needed to run a 1D ^{13}C spectrum or else either a DEPT-135 or a DEPT-Q spectrum (the former giving only peaks for protonated carbons while the latter includes all types of carbons but with significantly reduced sensitivity for quaternary carbons). Next, it could optimize the acquisition parameters for the chosen 2D experiments. The minimum number of data points required for the acquisition axis depends on the extent of ^{1}H spectral crowding. One way to estimate this would be to use a binning technique for the proton spectrum similar to that used in metabonomics investigations by NMR, *i.e.* the spectrum could be divided into a

series of "bins" of equal frequency width (maybe 20 Hz) and integrated. The density of peaks could be estimated from the fraction of bins with significant integrated area and/or the number of consecutive bins with significant area. This would allow the computer to choose the minimum number of *F*2 data points and acquisition times for all 2D experiments. The recycle time (acquisition time plus relaxation delay) would be set at 1.3 times the average T_1 determined above for most experiments except for N*O*ESY or R*O*ESY where 2.5 times T_1 would be more appropriate. The minimum number of required data points determined by binning could then also be used as the number of *F*1 time increments for homonuclear 2D experiments (the number of time increments should include both acquired and linearly predicted increments to minimize total time).

If the operator wished to include heteronuclear experiments (*e.g*. HSQC and HMBC), the program could again use the number of scans and the signal/noise for the initial proton spectrum plus the known relative ^{1}H and ^{13}C sensitivities for the installed probe to calculate the number of scans needed to acquire these experiments. If a calculated ^{13}C spectrum were available, then the HSQC and HMBC ^{13}C spectral windows could initially be chosen based on this spectrum. Alternatively, it could initially choose a default value of 225 ppm for HMBC and a default value for HSQC of 170 ppm or it could scan the initial ^{1}H spectrum and choose the latter spectral window based on the presence or absence of peaks in regions characteristic of aromatic/olefinic and aldehyde protons. If a calculated ^{13}C spectrum were available, then the program could use average peak separations to determine the minimum number of measured and linearly predicted time increment spectra needed to get adequately resolved HSQC and HMBC spectra. Otherwise, it could use the extent of proton spectral crowding to estimate the number of required time increments.

In addition, the program would then list the time for each experiment (including the alternative 1D ^{13}C options) and the total time. The operator could then choose to instruct the spectrometer to proceed with the full set of experiments or, if the calculated time exceeded the available time on the spectrometer, eliminate one or more experiments from the queue. Assuming that either a DEPT-135 spectrum and a full ^{13}C spectrum or else only a DEPT-Q spectrum were run first, the ideal arrangement would be for the spectrometer to have on-line access to a large 1D ^{13}C data library of known compounds. If a close match to a known compound were found, then 2D acquisition could be automatically aborted unless the operator had indicated that it should proceed even if a match were found. Finally, if HSQC and HMBC spectra were to be acquired, the program could first re-optimize the ^{13}C windows for these experiments, based on the ^{13}C spectra if these had been obtained. The same approach could be used for multiple samples in an overnight or weekend run. There could be a "multiple sample" option. In this case, the spectrometer would be programmed to sequentially run the ^{1}H setup experiments on each sample and then list the times for each sample. The operator could then choose to delete individual experiments, or entire samples from the queue, if the total time were too long.

After completion of data acquisition, the spectrometer could be programmed to process the spectra, based on the pre-determined best weighting function for each axis for each experiment, with the value of the weighting function based on the number of points/number of increments and the chemical shift window. While the

whole procedure may seem cumbersome, it actually closely mirrors the thought processes that a highly experienced operator would use in setting up a series of 2D experiments for organic structure elucidation, while avoiding the risk of operator error. It is also easily within the capabilities of current high-speed computers and would require a minimum of calculation time. Finally, the availability of an artificial intelligence software program of this type would, in combination with automated probe tuning and gradient shimming, allow even an inexperienced operator to acquire a high quality set of ^{1}H, ^{13}C, and 2D NMR spectra necessary for organic structure elucidation in the minimum possible time.

While a fully automated program of this kind would be ideal, there are also partial steps that could easily be incorporated into current spectrometer software, which would improve the ability of an inexperienced operator to obtain good quality spectra in minimum acquisition times. Software already exists that allows one to estimate the times needed to obtain different 2D spectra, based on the *S/N* for a 1D proton spectrum. An automated program for ^{1}H T_1 measurements could be added, with the results used to calculate optimum recycle times for 2D experiments, thus avoiding the common problem of wasted time due to unnecessarily long relaxation delays (*10*).

14 Parameter Choices for Acquisition and Processing of 1D and 2D NMR Spectra

We include in this section some of the basic background, which explains the reasons for various parameter choices. Sections 14.1 and 14.3 are recommended reading for anyone who likes to understand why some parameter choices are better than others. For those who just want to have simple "menus" for acquiring spectra, Sects. 14.2 and 14.4 partially satisfy this need. However, even then, it is still essential to make some parameter choices, depending on sample amount, molecular weight and the extent of spectral crowding, in order to get the best quality spectra in the shortest possible time. Therefore, we will give ranges of values for key parameters for each type of spectrum, briefly indicating how to choose the most appropriate values. Simply relying on one standard data set for each type of experiment, regardless of the nature of the compound being, will often yield inadequate results.

14.1 Basics of NMR Data Acquisition

14.1.1 Sampling Rate

The *Nyquist* theorem tells us that to define a spectral window that is N Hz wide, we must sample the data at a rate of 2 N data points per second. The actual number of data points collected will depend on the acquisition time, which is typically of the order of 1–5 s in 1D NMR but shorter in 2D NMR.

14.1.2 Analog to Digital Conversion

The signal detected in the NMR receiver is in continuous (analog) form and must be converted to a digital format for data storage and processing. This is done with an Analog-to-Digital Converter (ADC). The ADC has two key characteristics. The first is the maximum speed of the ADC in Hz, which in turn determines the maximum spectral window that can be determined (1/2 of the maximum sampling speed). The second is the binary bit length, which determines the dynamic range of the ADC, *i.e*. the ability to detect weak signals in the presence of strong signals. Until recently, maximum sampling rates of ADCs were typically in the range of 100–500 KHz while a typical ADC had 16 bits. With one bit used to determine the sign, the remaining 15 bits provided a theoretical dynamic range of 32,768:1. However, since it takes 2–3 bits to define a weak peak with reasonable precision, the effective dynamic range was less. In addition, it was critical to adjust the receiver gain so that the detected signal almost filled the ADC in order to achieve this dynamic range. However, the latest model NMR spectrometers have much faster ADCs (up to 80 MHz). This has allowed a new approach to data acquisition, called digital oversampling, which dramatically increases the effective dynamic range of the ADC.

14.1.3 Digital Oversampling

With digital oversampling, instead of sampling at a rate of two times the desired spectral width in Hz (as stipulated by the *Nyquist* theorem), one instead samples at the maximum rate of the ADC. For example, consider a situation where the desired spectral window is 5,000 Hz, but instead of sampling at 10 KHz, one sampled at 80 MHz, *i.e*. 8,000 times faster than the nominal rate. Then, each successive block of 8,000 points is summed to produce a single point. The final result would be a collected FID with the appropriate number of data points for the desired spectral window. With modern high-speed computers, this can be done "on the fly" (in 32-bit arithmetic), *i.e.* during the actual data acquisition. In this case, information theory tells us that the dynamic range is increased by the square root of the extent of oversampling, *i.e*. by about 90:1 for oversampling by 8,000. The 80-MHz ADC on the authors' latest spectrometers actually has a 14-bit ADC, but oversampling effectively converts it to about a 20-bit ADC, *i.e*. a dynamic range of ~500,000:1. However, there is one caveat to this. Since the data are processed in the ADC prior to the averaging process, it will still be necessary in cases of extremely strong solvent signals (*e.g*. H_2O) to use some form of solvent suppression to avoid overload. On the other hand, in the absence of one or more very strong peaks, it is no longer critical to set the gain as carefully at the start of the experiment.

There is one additional advantage to oversampling. The ADC does not distinguish between a signal, which only partially fills a bit, from one that almost completely fills it. This introduces randomness, called digitization noise. The act of summing a large number of points almost totally eliminates this source of noise. This may have a minimal effect when using an ambient-temperature probe, where thermal noise will usually be the predominant noise source. However, it can make a

significant difference for cryogenically cooled probes where cooling the coils and preamplifier to *ca*. 20 K minimizes thermal noise.

14.1.4 Quadrature Detection

The receiver in an NMR spectrometer is actually a phase-sensitive detector, *i.e*. it measures frequencies relative to the transmitter frequency rather than absolute frequencies. A single phase-sensitive detector cannot distinguish between frequencies that are positive or negative with respect to the carrier frequency. In the early days of FT NMR, this problem was avoided by having the transmitter frequency at one end of the spectral window so that all peaks would have the same sign. However, this introduced two other problems. First, this required a more intense transmitter pulse in order to uniformly excite the entire spectral window. Second, noise would be detected at both positive and negative frequencies, and the noise from the other side of the pulse would "fold in" to the spectral window, reducing signal/noise by $\sqrt{2}$. Both of these problems were solved by the technique of quadrature detection. This involves detecting two signals at right angles to each other. When performed, this permits distinction of positive and negative frequencies, allowing one to put the carrier frequency at the mid-point of the spectral window. In the past, this was normally done by splitting the signal and routing it to two phase-sensitive detectors with a phase shift of 90° between them (accomplished by a very slight delay in sending the signal to the second detector). The signals are sent to different ADCs for digitization and then to two separate memory blocks in the computer for storage. The signals are then *Fourier* transformed and added to provide the final spectrum. Older Varian spectrometers used this approach. Newer Varian/Agilent spectrometers differ in that the signal is first digitized with a high speed ADC and then split into two signals phase-shifted by 90° for storage. This allows the use of a single ADC in place of two of these. A different approach is used on older Bruker spectrometers, which also allowed the use of a single ADC. In these cases, data were actually sampled at a frequency of 4 N Hz, with a 90° phase shift for each successive data point. However, newer model Bruker spectrometers use an approach, which we believe is similar to that used on Agilent spectrometers.

14.1.5 Fold-in Peaks

The collection of digitized data introduces another problem. The RF pulse also excites peaks outside the chosen spectral window. Since one is sampling at finite intervals, it is impossible to distinguish between peaks, which are just outside the spectral window and those just inside it. Thus, the former peaks will also appear within the spectral window. However, their exact positions depend on the form of quadrature detection used. With the older Varian method, peaks which are outside the right hand (low frequency) side of the window by x Hz will appear x Hz inside the left hand end of the spectral window and *vice versa*. On the other hand, with the older Bruker method, peaks outside of either end of the spectral window will appear at an equal

distance inside the same end of the spectral window. It is often possible to distinguish fold-in peaks because they have different phases than other peaks in the spectrum. Fortunately, newer spectrometers from both manufacturers use filters, which are extremely effective at suppressing fold-in peaks so this is no longer a concern.

14.1.6 Analog *Versus* Digital Filters

In addition to peaks folding in, noise will also fold in from outside the spectral window, degrading signal/noise. To minimize this problem, spectrometers are equipped with audio-frequency filters. Older model spectrometers applied filtration to the analog signal and are thus called analog filters. While they were set to cut off frequencies just outside either end of the spectral window, this cut-off was not very sharp, with the result that intensities of peaks near either end of the spectral window were somewhat attenuated while some fold-in of peaks could also still be observed. Newer model spectrometers all employ digital filters, which have much sharper cut-offs and thus avoid the problems of analog filters. However, because they are so efficient, one must use caution to ensure that the spectral window is wide enough to include all possible peaks. Otherwise, the user will not be aware that these peaks are actually present in the true spectrum.

14.2 Recommended Acquisition and Processing Parameters for 1D Spectra

14.2.1 Spectral Widths

Since one can usually acquire ^{1}H spectra very quickly, the authors recommend acquiring an initial "scan" spectrum with a very wide spectral window (*ca.* −1.0 to +15 ppm) to ensure there are no unexpected peaks with unusual chemical shifts. Then, a second spectrum can be obtained using a spectral window, which is narrowed to include only observed peaks in order to get better resolution. However, if using an older spectrometer with analog filters, one should leave regions (of *ca.* 1 ppm) with no peaks on both sides of the spectral window, particularly if one wants quantitative peak intensities. Since the lower signal/noise of ^{13}C spectra and longer acquisitions will usually make it undesirable to obtain two spectra, it is recommended using a spectral window wide enough (*ca.* −5 to 225 ppm) to include all possible peaks when acquiring ^{13}C spectra.

14.2.2 Number of Data Points and Acquisition Times

The number of data points, NP, will be given by NP = 2(SW)(*AT*) where SW is the spectral width and *AT* is the acquisition time. One typically chooses the number of points to be some power of 2, *e.g.* 32,768 or 65,536 (often abbreviated as 32 K or

64 K), although this is not essential. For a ^{1}H spectral width of 5,000 Hz, these two values of NP would, respectively, correspond to acquisition times of *ca.* 3 and 6 s. while for a 30,000-Hz ^{13}C spectral width, *AT* would respectively be *ca*. 0.5 and 1 s. *AT* values of 3–6 s will give reasonable data point resolution for ^{1}H spectra (see Sect. 14.2.4) so either 32 K or 64 K would be an acceptable choice. However, the use of 64 K points is recommended for ^{13}C. Alternatively, if one is setting *AT*, 4–5 s for ^{1}H and 1 s for ^{13}C are suggested as acceptable values.

14.2.3 Number of Scans (Transients)

With earlier model spectrometers, it was recommended that the number of scans (NS) should be some multiple of four. This was to allow for a four-step phase cycle, which cancelled "quadrature image" peaks. These arose from imperfections in spectrometer hardware and appeared as weak mirror images of very strong peaks in the spectrum. However, now that quadrature detection is carried out on digitized data, quadrature images are non-existent on later generation spectrometers. Thus, ^{1}H spectra can be obtained with as little as one scan. The exact number of scans will depend on sample concentration and probe sensitivity. ^{13}C spectra will generally require many more scans. If this option is available, use of the "block size" command is strongly recommended. This is set at a value such as 1 or 40, and the data are stored at the end of each block. This allows one to monitor the *S*/*N* during acquisition and terminate it when *S*/*N* is satisfactory.

14.2.4 Zero Filling and Data Point Resolution

Fourier transformation of a FID yields both real and imaginary spectra, with half of the data points used to define each spectrum. Thus, the data point resolution (in Hz/point) is given by 2SW/NP (or 1/*AT*). However, the data point resolution can be improved by a factor of two, simply by adding an equal number of zeros to the end of the digitized FID. This method, called zero filling, effectively allows the use of all of the experimental data points to define the real spectrum. In this case, the data point resolution becomes SW/NP (or 1/2*AT*) Hz/point. This will provide improved spectral resolution, particularly if the natural line widths of spectral peaks are less than the data point resolution. Zero filling by more than a factor of two will not further narrow spectral peaks. However, it will provide better definition of peak frequencies and a cosmetic improvement in the appearance of complex multiplets. For that reason, we strongly recommend using extra zero filling up to at least 4NP or even higher. On Varian/Agilent spectrometers, this is set by the parameter "fn" while on Bruker spectrometers, the corresponding parameter is "si."

14.2.5 Pulse Widths and Delay Times

For most ^{1}H spectra obtained using a 4–5 s acquisition time, one can obtain at least semi-quantitative peak areas using 90° pulses and no relaxation delays, although the areas of methyl groups, which typically will have the longest relaxation times, may be partially suppressed. However, if quantitative peak areas are important, then one has the choice of either using a shorter pulse or including a relaxation delay between scans. *Richard Ernst* investigated this problem in the early days of FT NMR and demonstrated that it was better to use a reduced pulse angle rather than a relaxation delay (*3*). This can be understood by a simple trigonometric argument. If, for example, one chooses a pulse width corresponding to a 45° rotation of the magnetization vector (a 45° pulse), the component of magnetization along the y-axis is ~71%. However, the residual component along the z-axis is also ~71% ($\sin\theta = \cos\theta = 0.71$). Thus, it takes significantly less time for magnetization to return to equilibrium along the z-axis. The optimum *Ernst* angle is given by $\cos\theta = \exp(-AT/T_1)$ where T_1 is the relaxation time, which decreases with molecular size. In practice, we find that a 45° pulse plus a 4–5 s acquisition time will yield quantitative results for most typical natural products, other than those of very low molecular weight (<250 Da). In the latter case, a 30° pulse is suggested, possibly along with a relaxation delay.

The choices for ^{13}C spectra are more difficult, because the acquisition times are shorter, and there are typically much wider ranges of relaxation times, with quaternary carbons having the longest values of T_1. However, due to differences in N*O*Es for different carbons, ^{13}C spectra are rarely quantitative. Thus, the authors believe a pulse width of 45°, combined with a 1-s relaxation delay, will generally give satisfactory results.

14.2.6 Apodization (Weighting) Functions

With ^{1}H spectra, it should not usually be necessary to use any form of apodization function, provided that the FID has decayed below the noise level at the end of the acquisition time. However, for spectra with poor *S*/*N*, a small amount (*ca*. 0.1–0.3 Hz) of exponential line broadening can be used. This will improve signal/noise at the cost of a small loss of resolution. On the other hand, if one wants to improve the resolution of a spectrum, a resolution enhancement function can be used, which combines a positive *Gaussian* function with a negative line broadening function. The right combination of these two parameters can be set by the spectrometer software (for Varian/Agilent spectrometers the command is "resolv"). These parameters should be chosen based on twofold zero filling, *e.g.* 32 K to 64 K points. However, after the parameters are chosen, one can further increase the amount of zero filling. This will aid in accurately determining splittings in multiplet patterns. Note, however, that resolution enhancement will degrade signal/noise and that relative peak areas may no longer be quantitative. In particular, if a spectrum has both well-resolved multiplets and broad peaks, the latter will be suppressed.

In the case of ^{13}C spectra, some extent of line broadening is usually needed to improve signal/noise. If there is an interactive weighting program available on a given spectrometer ("wti" on Varian/Agilent spectrometers), the ideal approach is to choose a weighting function having the same decay time as the FID (a "matched filter"). Otherwise, the authors suggest 1–3 Hz line broadening, depending on the signal/noise.

14.2.7 ^{13}C Spectral Editing

When assigning ^{13}C spectra, it is helpful to assign the type of carbon, *i.e.* quaternary, methine, methylene or methyl, to each signal. There are two basic ways of achieving this, with neither entirely satisfactory. The first is to use the APT sequence, which produces peaks for quaternary and methylene carbons, and are of opposite phase to those for methine and methyl carbons (*115*). This sequence has two disadvantages: it is less sensitive than a regular ^{13}C spectrum and is sensitive to variations in the one-bond $^{13}C–^{1}H$ coupling constants, potentially giving misleading results (*10*). The second is the DEPT spectrum (*116*). This involves polarization transfer from directly bonded protons to carbons and can be either used to generate a spectrum (DEPT-135) with methylene carbons of opposite phase to methine and methyl carbons) or, by combining DEPT-45, DEPT-90, and DEPT-135 spectra, to produce separate spectra for the three types of carbons (*10*). The main advantages of DEPT are that it has better signal/noise than a regular ^{13}C spectrum and is significantly less sensitive than APT to variations in $^{1}J_{CH}$. The main disadvantage is that it only gives peaks for protonated carbons and thus it will still be necessary to also record a standard ^{13}C spectrum to observe all carbons. An alternative version of DEPT, called DEPT-Q, has been developed that also shows quaternary carbons (*117*). However, the quaternary carbon signals are generally weaker than those observed in a standard ^{13}C spectrum obtained in the same time. Nevertheless, it may still be faster to obtain a DEPT-Q spectrum than separate DEPT and standard ^{13}C spectra. Finally, an alternative approach, which the authors favor, is to instead acquire an edited HSQC spectrum. This provides the same information as DEPT in comparable or less time, with the additional major advantage of providing assignments for the directly bonded hydrogen(s) associated with each carbon (*10*). However, it does not provide as accurate ^{13}C chemical shifts as DEPT and, again, provides no information about quaternary carbons.

The parameter choices for APT spectra will generally be the same as would be used for standard ^{13}C spectra. The suggested value of $^{1}J_{CH}$ used to calculate editing delays is 145 Hz. However, an unusual feature of APT is that one should not replace the initial ^{13}C 90° pulse by a 45° pulse. Since there is a later ^{13}C 180° pulse, this will convert the residual z-magnetization remaining after the original pulse to −z-magnetization, requiring an even longer relaxation delay. Instead, the initial pulse should be a 135° pulse since, in this case, the initial residual z-magnetization will be along the −z-axis but converted to + z-magnetization, decreasing the needed relaxation delay. With this modification, a 1-s relaxation delay should be sufficient.

With DEPT, one is transferring magnetization from ^{1}H to ^{13}C, so it is the ^{1}H relaxation time that matters. Since ^{1}H decoupling is applied during acquisition, the relaxation delay must allow recovery of this magnetization. The recommended delay is $1.3T_1$, so a relaxation delay of 1–1.5 s should be sufficient for typical natural products. Again, a value of $^{1}J_{CH}$ of 145 Hz is suggested. Finally, since residual ^{13}C magnetization is cancelled by phase cycling, it is essential to include a series of steady-state (dummy) scans before acquiring data in order to establish steady-state ^{13}C magnetization. Otherwise a residual solvent peak will be observed which may obscure desired peaks. Generally, 16 dummy scans should be sufficient.

14.3 Basics of 2D NMR

14.3.1 General Features of 2D NMR Sequences

2D NMR sequences are generally composed of three components: an initial relaxation delay, a variable evolution period designated as *t*1 and usually initiated by a 90° pulse, and finally an acquisition period, usually labeled *t*2. A series of spectra are generated by incrementing the evolution time, usually in a regular fashion. The *F*1 spectral window is determined by the number of increments and the time between increments. The latter is automatically calculated by the pulse sequence program based on the specified number of increments and *F*1 spectral width. The key differences between different sequences almost all occur during *t*1, in the form of additional fixed delays and/or additional pulses. The FIDs acquired during *t*2 for different values of *t*1 are *Fourier* transformed to yield a series of *F*2 spectra. Then, the phase and intensity of each point in *t*2 for the different time-incremented spectra is used to generate a series of *t*1 interferograms, which resemble FIDs. These are then *Fourier* transformed to produce the second frequency axis, labeled *F*1. Conventionally, spectra are plotted with *F*2 as the horizontal axis and *F*1 as the vertical axis.

14.3.2 Homonuclear and Heteronuclear 2D NMR Spectra

Homonuclear spectra have spectral information for the same nucleus (usually ^{1}H) along both axes. The spectrum has a 1D spectrum along a diagonal from bottom-left to top-right and symmetric off-diagonal peaks between interacting nuclei. COSY or TOCSY spectra are generated when the interaction between different nuclei is due to scalar ("*J*") coupling while N*O*ESY or R*O*ESY spectra are generated when the interaction is due to dipolar relaxation. Heteronuclear spectra provide information about scalar coupling between heteronuclei (mostly commonly $^{1}H/^{13}C$ but also $^{1}H/^{15}N$ in the natural product area). In this case, the spectrum for the acquired nucleus is plotted on the horizontal axis, while information about the second nucleus (generated by incrementation of *t*1) is along the vertical axis. The cross-peaks indicate either one-bond or n-bond (n = 2 or 3) $^{1}H/^{13}C$ coupling, depending on the sequence used. Early $^{1}H/^{13}C$ correlation spectra were obtained by ^{13}C observation

("direct detection"), but, with improvements in spectrometer phase and frequency stability, these are now almost always obtained by ^{1}H observation ("indirect detection," an historical but misleading term). One common feature of heteronuclear correlation sequences is a pair of 90° pulses (^{13}C pulses for ^{1}H-detected sequences) at the beginning and end of the evolution period. By monitoring the evolution of magnetization during $t1$, the second 90° pulse acts as the equivalent of a phase-sensitive detector, allowing determination of frequency information for that nucleus, even though the receiver is tuned to detect the acquisition nucleus.

14.3.3 Absolute-Value *Versus* Phase-Sensitive Spectra

As mentioned in Sect. 14.2.4, a pulse sequence produces both real (absorption) and imaginary (dispersion) spectra. With certain pulse sequences (COSY being the most common), it is impossible to simultaneously have all peaks with the same phase since the sequence produces a mixture of absorption and dispersion peaks. In this case, an absolute-value (or magnitude-mode) spectrum is generated by squaring the real and imaginary spectra, summing them, and then taking the square root of the sum. This arbitrarily produces an apparent absorption spectrum with all peaks with the same phase. However, it does so at some cost in resolution since the dispersion components have broad "tails," which broaden the peaks.

Fortunately, most pulse sequences generate phase-sensitive (or pure-absorption) spectra, with better resolution. These can be generated in one of two ways. The first, which is usually the method of choice on Varian/Agilent spectrometers, is to acquire two sets of spectra with a phase shift of 90° between them. This is done alternately to avoid one set suffering more than the other from any degradation of resolution over time. They are then co-processed to produce the 2D spectrum. The second, usually used on Bruker spectrometers, is to acquire a single set of spectra with twice as many time increments, but having a 90° phase shift between each successive spectrum. Both approaches, which effectively mimic the approaches used for quadrature detection on Varian/Agilent and early Bruker spectrometers, yield very similar results in the same time.

One interesting exception is provided by the HMBC sequence. In its original form, it was designed for "mixed-mode" processing: absolute value along $F2$ but phase sensitive along $F1$ (*118*). This gave improvements in both resolution and sensitivity over a full absolute-value mode spectrum. Later versions of HMBC using gradients (see next section) produced straight absolute-value spectra. However, some of the recent gradient-selected sequences again allow mixed-mode processing with its associated advantages, including better ^{13}C resolution.

14.3.4 Phase Cycling *Versus* Gradient Selection

Either phase cycling or gradient selection (sometimes called gradient enhancement) or some combination of the two is used for two purposes in any multi-pulse NMR sequence. The first is coherence pathway selection and the second is artifact

suppression. The explanation of coherence pathway selection is well beyond the scope of this chapter but is discussed in various texts such as that by *Keeler* (*119*). Instead we will focus on how the two techniques are carried out and their relative advantages and disadvantages. Phase cycling consists of varying the phase of one or more of the subsequent pulses and/or the receiver, relative to the phase of the initial pulse, in consecutive scans. The phase cycle is designed so that the desired signal co-adds in the different scans while other signals are cancelled. The phase of the initial pulse, designated x, is arbitrary, but the phases of subsequent pulses can be x, y, −x, or −y (respectively corresponding to 0, 90, 180, or 270 degree phase shifts, relative to the first pulse). This is controlled by the timing circuit of the spectrometer. The receiver "phase cycling" is carried out by dividing the computer memory block in two sections and, respectively, adding the digitized signal to the first block, adding it to the second, subtracting it from the first or subtracting it from the second (corresponding to x, y, −x, and −y). The minimum possible phase cycle for coherence selection will be two scans, but incorporating artifact selection will require more scans (anywhere from 4 up to 16 or even higher).

In contrast, gradient selection uses a pair of magnetic field gradients applied along the z-axis. These are designed so that the magnetization associated with one coherence pathway is dephased by the first gradient but brought back in phase by the second for observation while other pathways are dephased by both gradients and not observed. Artifacts are eliminated in the same manner. There are two main advantages to gradient selection over phase cycling. First, it can often be carried out with as little as one scan, substantially decreasing the time needed to acquire a high sensitivity experiment such as COSY. Second, pathway selection and artifact suppression are carried out during each scan while phase cycling relies on subtraction of the data from one scan from another for artifact suppression. The latter is more susceptible to minor spectrometer instabilities. This is particularly important in ^{1}H-detected ^{1}H/^{13}C shift correlation spectra where one is detecting the 1.1% ^{1}H/^{13}C magnetization while suppressing the remaining ^{1}H magnetization. On the other hand, most gradient-selected sequences result in a $\sqrt{2}$ loss in overall sensitivity. Nevertheless, the other advantages of gradient selection are so great that most 2D experiments are now carried out with gradient selection. However, they often also incorporate some phase cycling.

14.3.5 Acquisition Times and Relaxation Delays

Two-dimensional spectra are generally carried out using much shorter acquisition times (*ca*. 0.1–0.4 s) than used for 1D spectra, both to save time and to keep the 2D data set to a reasonable size. However, this requires including a relaxation delay (*RD*) in order to allow at least partial recovery of z-magnetization before the next scan. In assessing a reasonable value for the relaxation delay, it is important to remember that, for ^{1}H-detected experiments in particular, relaxation will also be occurring during the acquisition time. Thus, the key parameter to optimize is the recycle time (*RT*), which is the sum of $AT+RD$. One can then afford to increase *AT* (and, therefore, increase *F*2 resolution) by correspondingly decreasing *RD*. It has

been shown that the optimum compromise value of *RT* for most 2D sequences (other than N*O*ESY and R*O*ESY, see below) is *ca*. $1.3T_1$. Methyl groups typically have the longest relaxation times of all ^{1}H signals in a natural product, but they are usually by far the most intense signals. Thus, one can afford to sacrifice some intensity for methyl protons and choose a value of *RT* based on average T_1 values for methylene and methine protons (*10*).

The actual *RT* values to be used depend the molecular weight of the molecule since larger molecules have shorter relaxation times. For small natural products (200–350 Da), typical ^{1}H T_1 values are *ca*. 0.7–1.2 s, corresponding to *RT*s of 0.9–1.5 s. For molecules in the 350–500 Da range, we suggest *RT* values of 0.7–1.0 s and around 0.6 s for larger molecules. Assuming $AT \sim 0.2$ s, corresponding *RD* values would be 0.2 s less. These are all significantly less than those recommended in a book, which suggests parameters for a wide range of 2D experiments (*8*), but, as we have pointed out elsewhere (*10*), the authors regard the use of such long values of *RT* as a waste of spectrometer time.

14.3.6 Number of Time Increments, Forward Linear Prediction, and Zero Filling

As noted above, the acquisition time can be increased (and *F*2 resolution improved) without increasing the total experiment time by correspondingly reducing the relaxation delay. In contrast, the total experiment time is directly proportional to the number of time increments used. Since many natural products have very crowded spectra, particularly in the aliphatic region, the authors find that one commonly needs 1,024 time increments (NI) to get satisfactory *F*1 resolution. One can use a smaller number of increments in an attempt to save time, but the risk is that the spectrum will be too poorly resolved to allow unambiguous interpretation. Thus, rather than saving time, one actually has wasted it.

Fortunately, there is a well-established method that allows one to use a significantly smaller value of NI, thus saving time, while still getting adequate resolution. This is forward linear prediction (LP) (*120*). The idea behind LP can be likened to a race where different automobiles each travel at a different, but constant, speed. If their relative positions after 256 laps are noted, one can make a very good estimate of their relative positions after 512 or 1,024 laps. In NMR LP, finite-length interferograms are extended by using information from previous data points to predict additional data points. In a time sequence of data points, the value of a particular data point, d(m), can be estimated from a linear combination (hence the name "linear prediction") of the data points that immediately precede it (*120*):

$$\mathrm{d}(\mathrm{m}) = \mathrm{d}(\mathrm{m}-1)\mathrm{a}(1) + \mathrm{d}(\mathrm{m}-2)\mathrm{a}(2) + \mathrm{d}(\mathrm{m}-3)\mathrm{a}(3) + \cdots$$

where a(1), a(2), a(3) are the LP coefficients. The number of coefficients used corresponds to the number of data points that are used to predict the value of the next data point in the series. When applying this method to phase-sensitive 2D data sets,

we have shown that one can reliably use fourfold LP, *e.g.* set NI = 256 but linearly predict it out to NI = 1024 (*10, 121*). This allows one to obtain comparable quality 2D spectra in one quarter of the time taken to obtain the full set of $t1$ interferograms or to double the *S/N* in the same time by increasing NS by a factor of four. However, fourfold linear prediction does require a reasonable number of experimental time increments, with NI =128 the suggested lower limit. For smaller values of NI, only twofold LP is recommended. Also, the authors have found that only twofold LP could be reliably carried out for absolute-value (*e.g.* COSY) 2D spectra, even for NI = 256 or larger (*121*).

The main requirement for the use of LP is that the latter parts of the experimental interferograms have sufficient *S/N* that an accurate estimation of the LP coefficients can be made. However, in over 20 years of processing well over one thousand 2D data sets with LP, we have rarely found this to be a problem. For example, we obtained an HSQC spectrum of a very dilute mixture of three polysaccharides using 16-fold linear prediction (NI = 1024 out to NI = 16384) and still obtained accurate data for very crowded spectra (*122*). For dilute solutions, due to relaxation, most of the signal intensity will occur in the first one quarter to one third of the interferogram with the signals in the later portions comparable to or even smaller than the random noise. Under these circumstances, the authors find that it is better to reduce NI (usually to ¼ of the desired value) while correspondingly increasing NS by a factor of four. In this way, *S/N* is improved (by a factor of 2) in the region of the interferogram that exceeds noise, improving the chances of successful LP of the rest of the interferogram. By contrast, if one omits LP and instead collects the full data set with the smaller value of NS, the entire interferogram may be too noisy to provide a good quality spectrum. If the former approach fails, it is probable that the sample is too dilute to obtain acceptable results in reasonable time by either method.

One additional requirement is that the number of LP coefficients should be greater than the number of signals that make up each interferogram that is being extended. The number of signals varies with the type of sequence, being as low as one or two with HSQC but generally larger. How much larger the number of coefficients should be for best quality spectra is spectrometer dependent. In our experience with Varian/Agilent spectrometers, LP works best when the number of LP coefficients is no larger than twice the expected number of signals while Bruker recommends that it should be at least two to three times larger. Too small a value may yield poor quality spectra and/or missing peaks while too large risks detecting spurious signals.

While LP is very useful for extending the number of $t1$ time increments, it is of little value for extending NP in $t2$. First, particularly for ^{1}H-detected sequences, there are typically a very large number of $F2$ signals, and thus LP would require a very large number of coefficients, which would seriously slow the calculations. Also, as noted above, one can increase NP (and *AT*) without any increase in experiment time by correspondingly reducing the relaxation delay. However, backward linear prediction can be used along $F2$. This can be used to correct any corrupted data points or to remove very broad background signals.

Finally, it should be realized that zero filling is not an alternative to LP but rather the two techniques are complementary. We recommend always using a further

equal amount of zero filling to the value of NI after LP (this is a requirement with Varian/Agilent LP software). This will further improve *F*1 data point resolution on phase-sensitive spectra by a factor of two. On the other hand, if one only used zero filling up to a factor of eight, the data point resolution would be still be four times worse than that if fourfold linear prediction were used in combination with twofold zero filling. In addition, one would have to use a more extreme apodization function to avoid artifacts due to truncation (see Sect. 14.3.8).

14.3.7 Number of Scans

The number of scans required for an acceptable spectrum depends on the sample concentration, the probe sensitivity and the type of sequence (including any essential phase-cycling requirements included in the sequence). For reasonable concentrations, gradient-selected COSY spectra can be obtained with NS = 1, but most other sequences require a larger number of scans. This is particularly true for HMBC, which is the least sensitive of all of the pulse sequences used for organic structure elucidation.

14.3.8 Apodization Functions

Due to the short acquisition and evolution times used in 2D NMR, both FIDs and interferograms have typically not decayed away to zero at the end of $t2$ or $t1$. *Fourier* transformation of a truncated FID or interferogram will result in a spectrum with distorted peaks due to "truncation wiggles." To avoid this, it is essential to use an apodization (weighting) function that goes to zero at the end of the time period. The exact shape of the apodization function is mainly determined by whether the spectrum is obtained in absolute-value or phase-sensitive mode. To minimize the broad tails characteristic of absolute-value peaks, absolute-value spectra are processed by using a resolution-enhancement function, which starts at zero for $t1$ or $t2 = 0$, peaks at the middle, and again goes to zero at t(max). The most common forms are either a sine bell or a squared sine bell (or the near-equivalent pseudo-echo function). The squared sine bell gives slightly better resolution while the sine bell gives slightly better *S*/*N*. The former is recommended for COSY spectra and the latter for other, lower sensitivity, spectra. For phase-sensitive spectra, a function that starts at a maximum at $t = 0$ and goes to zero at t(max) is recommended. Possibilities include a cosine (90° shifted sine bell) function, a *Gauss*ian function or an exponential (line broadening) function. The first gives the best resolution, the last, the best *S*/*N*, while the *Gauss*ian function is a compromise choice and is the one we generally prefer. A compromise function, which could be used for both absolute-value and phase-sensitive spectra, is a shifted sine bell function (typical shapes of this and other apodization functions are illustrated in Fig. 15). However, the authors find that it is less than ideal for either type of spectrum. In the case of an HMBC data set designed for mixed-mode processing, we recommend a sine bell along $t2$ and a *Gauss*ian

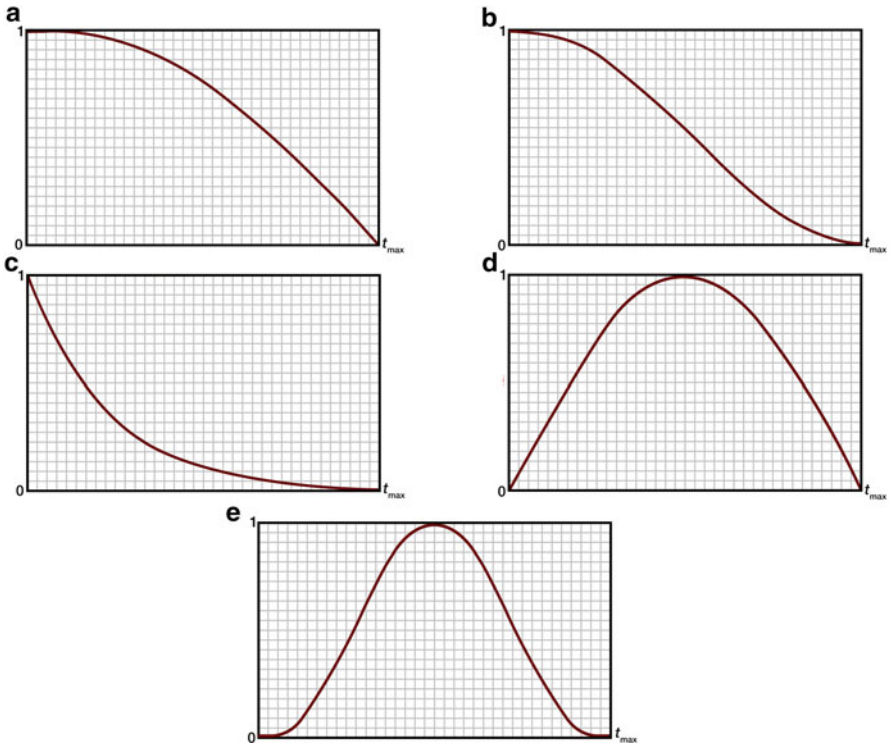

Fig. 15 The shapes of typical weighting functions used in processing 2D spectra. (**a**) cosine function 90° shifted sine bell function) (**b**) *Gauss*ian function (**c**) exponential (line broadening) function (**d**) sine bell function (**e**) squared sine bell function. Functions (**a**)–(**c**) are appropriate for phase-sensitive spectra while functions (**d**) and (**e**) are for absolute-value (magnitude-mode) spectra

along $t1$. Finally, if one is using linear prediction, it is important to remember that this effectively extends $t1$ and that the chosen apodization function should be adjusted to be zero at the extended value of $t1$.

14.3.9 Data Point Resolution in 2D NMR Spectra

In both absolute-value and phase-sensitive 2D spectra, the $F2$ data point resolution without zero filling is given by 2SW/NP, identical to the value for 1D (see Sect. 14.2.4). An equal amount of zero filling of phase-sensitive spectra will again improve digital resolution to SW/NP. However, absolute-value spectra are different. Since both the real and imaginary points from the FID are used to generate an absolute-value spectrum, zero filling does not improve the digital resolution. For that reason, it is better to use a larger number of data points in $F2$ for COSY and HMBC spectra in particular.

The situation for *F*1 data point resolution is more complex because it involves the way in which *F*1 quadrature detection is carried out. In the case of phase-sensitive spectra, the two alternative methods are closely analogous to the two methods for *F*2 quadrature detection described in Sect. 14.1.4. In the "States" method, two data sets are acquired, each with NI increments, with a 90° phase shift between them. FT yields two phase-sensitive spectra, which include both real and imaginary signals, but which can be phased to produce pure absorption-mode peaks. The difference is that one is a "cosine" spectrum where peaks of the same phase (one the true peak and the other the quadrature image peak) are mirrored about the center of SW1, the *F*1 spectral window. The second is a "sine spectrum" in which peaks are again mirrored about the middle of SW1, but now the quadrature image peak is of opposite phase to the true peak. When the two spectra are added, the quadrature image peaks cancel while the real peaks add. This co-addition of the two spectra improves the *S*/*N* by $\sqrt{2}$ but does not change the data point resolution, which is given by 2SW1/NI (since there are only NI/2 real peaks in each spectrum) or SW1/NI with an equal amount of zero filling. In the case of the TPPI method, only a single data set is collected, but NI is doubled, with every second FID phase shifted by 90°. Although the actual processing method is different, the end result is the same. Effectively, one has collected the equivalent of two data sets of NI/2 increments. Thus, the digital resolution in this case is 4SW1/NI without zero filling or 2SW1/NI with zero filling. Allowing for the fact that NI is twice as large in the TPPI method, the actual data point resolution is identical.

In the case of absolute-value spectra, the data point resolution is again 2SW1/NI or SW1/NI with one level of zero filling. However, in this case, *F*1 quadrature detection is carried out by using either phase cycling or gradient selection. This involves phase modulation of signals rather than amplitude modulation and produces signals with complex phase-twisted shapes. This is the reason that an absolute-value display is required. The need for one level of zero filling arises because carrying out quadrature detection with only a single data set results in only half of the points being used to generate the spectrum.

14.3.10 Shaped Pulses and Selective 1D Analogues of 2D NMR Spectra

Modern NMR spectrometers are equipped with wave form generators. These can be used to generate frequency-selective shaped RF pulses, including both 90° and 180° pulses (*123*). These are designed to generate uniform excitation over a defined spectral window, with ideally no excitation outside of this window. These are complex to design and difficult to implement manually. However, the software associated with spectrometer pulse sequence libraries usually makes this quite simple in practice, often using just two cursors to define the region to be excited, with the software then calculating the appropriate pulse shape.

Often in natural product research, one needs only correlation data for a limited number of protons to complete structural and/or stereochemical assignments. In these cases, using selective pulses to generate a series of 1D analogues of 2D

spectra may provide a considerable time saving. The most commonly used selective 1D sequences are 1D N*O*ESY, R*O*ESY, and TOCSY. One-dimensional TOCSY is particularly valuable since, by performing a series of measurements with increasing mixing times, one can sequentially trace out a network of coupled protons and potentially determining their coupling constants (*10*) (see Sect. 7 for an example), even when some of the protons overlap with other proton signals.

14.4 Recommended Acquisition and Processing Parameters for Commonly Used 2D Experiments and Selective 1D Experiments

The parameters listed below are designed to be appropriate for spectrometers in the 400–600 MHz range and equipped with either an indirect-detection probe or one of the newer probes with excellent sensitivity on both channels (Agilent OneNMR probe or Bruker SMART probe). If using an older direct-detection (^{13}C-optimized) probe, an increased number of scans may be necessary for dilute solutions, while smaller numbers of scans are needed if using a cryogenically cooled probe. In each case, ranges of values for two key parameters are given: the number of scans (NS) and the relaxation delay (*RD*). In the case of NS, the minimum value is recommended when one has >5 mg of sample while the maximum is for cases with *ca.* 1 mg of sample. The minimum value of *RD* is suggested for compounds of molecular weight >750 Da while the maximum is for compounds of less than 300 Da. The recommended number of steady-state (dummy) scans is defined by SS prior to data acquisition. In addition, two different sets of recommendations are provided for the number of *F*2 points (NP) and time increments (NI), the extent of linear prediction (LP) and the minimum extent of zero filling (ZF), with the latter two, respectively, defined as the total number of points after *F*1 linear prediction and after zero filling. These are labeled "low resolution" and "high resolution" and are, respectively, suitable for compounds with clearly resolved ^{1}H spectra and spectra with one or more regions with significant spectral crowding. Finally, the parameters for the phase-sensitive spectra are those that are appropriate for acquisition using the "States" method. This is the standard choice on Varian/Agilent spectrometers and one of the options on Bruker spectrometers.

14.4.1 COSY and TOCSY Experiments

14.4.1.1 Gradient-Selected COSY (Absolute-Value Mode)

*F*1 = *F*2 = –0.5 to 9.5 ppm, relative to TMS
SS = 16
NS = 1–4*
RD = 0.5–1.0 s

*F*2 apodization: sine bell squared
*F*1 apodization: sine bell squared
Low-resolution spectra: NP = 1024, ZF(F2) = 1024, NI = 256, LP = 512, ZF(F1) = 1024
High-resolution spectra: NP = 2048, ZF(F2) = 2048, NI = 512, LP = 1024, ZF(F1) = 2048

*If using the non-gradient (phase-cycled) version of COSY, NS must be a multiple of 4.

14.4.1.2 Gradient-Selected Double Quantum Filtered COSY (Phase Sensitive)

*F*1 = *F*2 = –0.5 to 9.5 ppm
SS = 16
NS = 1–8*
RD = 0.5–1.0 s
*F*2 apodization: cosine (90° shifted sine bell)
*F*1 apodization: cosine (90° shifted sine bell)
High-resolution spectra**: NP = 4096, ZF(F2) = 8192, NI = 256, LP = 1024, ZF(F1) = 2048

*If using the non-gradient DQCOSY sequence, NS must be a multiple of 4.
**Acquiring a high-resolution spectrum along *F*2 is strongly recommended since the main value of the experiment is its ability to measure coupling constants.

14.4.1.3 TOCSY or Z-TOCSY* (Phase-Sensitive)

*F*1 = *F*2 = –0.5 to 9.5 ppm
SS = 16
NS = 2–16
RD = 0.5–1.0 s
Mixing time: 80 ms**
*F*2 apodization: *Gauss*ian
*F*1 apodization: *Gauss*ian
Low-resolution spectra: NP = 1024, ZF(F2) = 2048, NI = 256, LP = 1024, ZF(F1) = 2048
High-resolution spectra: NP = 2048, ZF(F2) = 4096, NI = 256, LP = 1024, ZF(F1) = 2048

*If available, the use of Z-TOCSY is recommended since the zero-quantum filter gives undistorted cross-peak patterns.
**A shorter mixing time (25–30 ms) will give a COSY-like spectrum but with better resolution than an absolute-value COSY spectrum.

14.4.2 N*O*ESY and R*O*ESY Experiments

14.4.2.1 N*O*ESY (Phase-Sensitive)

*F*1 = *F*2 = –0.5 to 9.5 ppm
SS = 16

NS = 4–16
RD = 1.0–1.8 s
Mixing time = 0.3–0.8 s*
*F*2 apodization = *Gauss*ian
*F*1 apodization = *Gauss*ian
Low-resolution spectra: NP = 1024, ZF(F2) = 2048, NI = 256, LP = 1024, ZF(F1) = 2048
High-resolution spectra: NP = 2048, ZF(F2) = 4096, NI = 256, LP = 1024, ZF(F1) = 2048

*The choice of mixing time is critical. Small molecules need long mixing times to allow for reasonable N*O*E build-up. However, with high (>750 Da) molecules, spin-diffusion will occur with long mixing times, leading to erroneous results.

14.4.2.2 R*O*ESY *(Phase-Sensitive)

*F*1 = *F*2 = −0.5 to 9.5 ppm
SS = 16
NS = 4–16
RD = 1.0–1.8 s
Mixing time = 0.2–0.6 s
*F*2 apodization = *Gauss*ian
*F*1 apodization = *Gauss*ian
Low-resolution spectra: NP = 1024, ZF(F2) = 2048, NI = 256, LP = 1024, ZF(F1) = 2048
High-resolution spectra: NP = 2048, ZF(F2) = 4096, NI = 256, LP = 1024 ZF(F1) = 2048

*The use of R*O*ESY in place of N*O*ESY is strongly recommended for molecules with molecular weights >600 Da since N*O*ESY cross-peaks approach zero intensity for molecules much above this molecular weight, eventually become negative as molecular size increases.

14.4.3 HMQC, HSQC, HMBC, and H2BC Experiments

14.4.3.1 Gradient-Selected HMQC (Absolute-Value)

*F*2 = −0.5 to 9.5 ppm
*F*1 = −5 to 165 ppm
SS = 16
NS = 4–32
RD = 0.5–1.0 s
$^{1}J_{CH}$ = 145 Hz
*F*2 apodization = sine bell
*F*1 apodization = sine bell
Low-resolution spectra: NP = 1024, ZF(F2) = 2048, NI = 256, LP = 512, ZF(F1) = 1024
High-resolution spectra: NP = 2048, ZF(F2) = 4096, NI = 512, LP = 1024, ZF(F1) = 2048

14.4.3.2 Gradient-Selected HSQC* (With or Without ^{13}C Spectral Editing)

*F*2 = −0.5 to 9.5 ppm
*F*1 = −5 to 165 ppm
SS = 16
NS = 4–32
RD = 0.5–1.0 s
$^{1}J_{CH}$ = 145 Hz
*F*2 apodization = *Gauss*ian
*F*1 apodization = *Gauss*ian
Low-resolution spectra: NP = 1024, ZF(F2) = 2048, NI = 160, LP = 512, ZF(F1) = 1024
High-resolution spectra: NP = 2048, ZF(F2) = 4096, NI = 256, LP = 1024, ZF(F1) = 2048

*HSQC gives better resolution than HMQC and allows spectral editing. Therefore, the use of HSQC in place of HMQC is strongly recommended.

14.4.3.3 Gradient-Selected HMBC (Absolute-Value)

*F*2 = −0.5 to 9.5 ppm
*F*1 = −5 to 220 ppm*
SS = 16
NS = 16–64
RD = 0.5–1.0 s
$^{1}J_{CH}$ = 145 Hz (or 130 Hz, 165 Hz)**
$^{n}J_{CH}$ = 8 Hz
*F*2 apodization = sine bell
*F*1 apodization = sine bell
Low-resolution spectra: NP = 2048***, ZF(F2) = 4096, NI = 256, LP = 512, ZF(F1) = 1024
High-resolution spectra: NP = 4096, ZF(F2) = 8192, NI = 512, LP = 1024, ZF(F1) = 2048

*A high-frequency value of 200 ppm can be substituted if one is certain that the compound has no carbonyl groups.
**The values in parentheses are lower and upper values if a two-step *J*-filter is used.
***The use of at least a 0.2-s acquisition time is essential to avoid significant sensitivity loss, see (*12*).

14.4.3.4 Gradient-Selected HMBC (Mixed-Mode Processing)*

*F*2 = −0.5 to 9.5 ppm
*F*1 = −5 to 220 ppm**
SS = 16
NS = 16–64
RD = 0.5–1.0 s
$^{1}J_{CH}$ = 145 Hz (or 130 Hz, 165 Hz)***
$^{n}J_{CH}$ = 8 Hz

*F*2 apodization = sine bell
*F*1 apodization = *Gauss*ian
Low-resolution spectra: NP = 2048, ZF(F2) = 4096, NI = 160, LP = 512, ZF(F1) = 1024
High-resolution spectra: NP = 4096, ZF(F2) = 8192, NI = 256, LP = 1024, ZF(F1) = 2048

*This sequence gives better *F*1 resolution and better sensitivity than the absolute-value sequence. The spectra are in displayed in absolute-value mode but are processed in phase-sensitive mode along *F*1.
**A high frequency value of 200 ppm can be substituted if one is certain that the compound has no carbonyl groups.
***The values in parentheses are lower and upper values if a two-step *J*-filter is used.

14.4.3.5 Gradient-Selected H2BC (Phase-Sensitive)

*F*2 = −0.5 to 9.5 ppm
*F*1 = −5 to 220 ppm
SS = 16
NS = 16–64
RD = 0.5–1.0 s
$^{1}J_{CH}$ = 145 Hz (or 130 Hz, 165 Hz)
T(fixed time) = 0.022 s
*F*2 apodization = *Gauss*ian
*F*1 apodization = *Gauss*ian
Low-resolution spectra: NP = 1024, ZF(F2) = 2048, NI = 160, LP = 512, ZF(F1) = 1024
High-resolution spectra: NP = 2048, ZF(F2) = 4096, NI = 256, LP = 1024, ZF(F1) = 2048

14.4.4 Selective 1D Experiments

14.4.4.1 1D TOCSY*

*F*2 = −0.5 to 9.5 ppm
NP = 32,768
FN = 65,536
SS = 16
NS = 4–64**
Mix = 0.00 s and 0.08 s (or array)***
Apodization = 0.5-Hz line broadening

*If available, the use of the Z-TOCSY sequence is strongly recommended.
**If using a relatively long mixing time, a larger number of scans will be needed since the initial magnetization is spread amongst several proton multiplets.
***Acquisition of an initial spectrum with zero mixing time is recommended to ensure that one has a clean excitation of only the desired multiplet. Arraying the mixing time (*e.g.* 0.0, 0.25, 0.5, 0.75, 1.0 s) is useful since this allows one to assign sequences of coupled protons.

14.4.4.2 1D N*O*ESY or R*O*ESY*

*F*2 = −0.5 to 9.5 ppm
NP = 32,768
FN = 65,536
SS = 16
NS = 16–256**
Mix = 0.5 s
Apodization = 2-Hz line broadening

*The use of N*O*ESY is suggested for molecules of molecular weight <600 Da while R*O*ESY is strongly recommended for larger molecules.
**Both N*O*ESY and R*O*ESY measure transient N*O*E buildup and are relatively insensitive.

15 Conclusions

As indicated in the Introduction, NMR spectroscopy is a very powerful tool for natural product structure elucidation. However, in order to obtain the best results in the shortest time and to avoid making errors in structure determination, it is important to make informed choices of pulse sequences, acquisition parameters, and processing parameters. It is also important to approach unknown structural problems with an open mind and let the data point you to the correct structure rather than trying to force the data to fit a structure that you suspect. Hopefully, this contribution will provide a natural product chemist, who has a basic understanding of NMR spectroscopy, with the increased knowledge needed to apply this technique more effectively in his/her research. If so, we will have achieved our goal in writing this chapter.

Acknowledgment The authors are indebted to *Arvin Moser* of Advanced Chemistry Development, Inc. for the expert analysis of 1- and 2-dimensional NMR spectral data of three natural products in the ACD/Labs *Structure Elucidator* program.

References

1. Openshaw HT, Robinson R (1946) Constitution of Strychnine and the Biogenetic Relationship of Strychnine and Quinine. Nature 157:438
2. Woodward RB, Cava MP, Ollis WD, Hunger A, Daeniker HU, Schenker K (1954) The Total Synthesis of Strychnine. J Am Chem Soc 76:4749
3. Ernst RR, Anderson WA (1966) Application of *Fourier* Transform Spectroscopy to Magnetic Resonance. Rev Sci Instrum 37:93
4. Aue WP, Bartholdi E, Ernst RR (1976) Two-Dimensional Spectroscopy. Application to Nuclear Magnetic Resonance. J Chem Phys 64:2229

5. Ernst RR (1992) Nuclear Magnetic Resonance *Fourier* Transform Spectroscopy (*Nobel* Prize Lecture). Angew Chem Int Ed 31:805
6. Silverstein RM, Webster FX, Kiemle D (2005) Spectrometric Identification of Organic Compounds, 7th ed. John Wiley and Sons, Inc., New York
7. Lambert JB, Gronert S, Shurvell HF, Lightner DA, (2011) Organic Structural Spectroscopy, 2nd ed. Prentice Hall, Upper Saddle River, NJ, USA
8. Berger S, Braun S (2004) 200 and More NMR Experiments. A Practical Course. Wiley-VCH, Chichester, UK
9. Lambert JB and Mazzola EP (2004) Nuclear Magnetic Resonance Spectroscopy. An Introduction to Principles, Applications and Experimental Methods, Chapter 7. Pearson Education Inc., Upper Saddle River, NJ, USA
10. Reynolds WF, Enriquez RG (2002) Choosing the Best Pulse Sequences, Acquisition Parameters, Postacquisition Processing Strategies, and Probes for Natural Product Structure Elucidation by NMR Spectroscopy. J Nat Prod 65:221
11. Kwan EE, Huang SG (2008) Structural Elucidation with NMR Spectroscopy: Practical Strategies for Organic Chemists. Eur J Org Chem:2671
12. Burrow TE, Enriquez RG, Reynolds WF (2009) The Signal/Noise of an HMBC Spectrum Can Depend Dramatically Upon the Choice of Acquisition and Processing Parameters. Magn Reson Chem 47:1086
13. McLean S, Perpick-Dumont M, Reynolds WF, Jacobs H, Lachmansing SS (1987) Unambiguous Structural and Nuclear Magnetic Resonance Spectral Characterization of Two Triterpenoids of *Maprounea guianensis*. Can J Chem 65:2519
14. NMRwiki.org/wiki/index.php?title=Databases
15. Barna JCJ, Laue ED, Mayger MR, Skilling J, Worrall SJP (1987) Exponential Sampling, an Alternative Method for Sampling in Two-Dimensional NMR Experiments. J Magn Reson 73:69
16. Gray G (2011) Non-Uniform Sampling and CLEAN Processing in VnmrJ 3.2, Spinsights, Agilent Technologies, Inc., Santa Clara, CA, USA
17. Schanda P, Kupce E, Brutscher B (2005) SOFAST-HMQC Experiments for Recording Two-Dimensional Heteronuclear Correlation Spectra of Proteins Within a Few Seconds. J Biomol NMR 33:199
18. Kupce E, Freeman R (2007) Fast Multidimensional NMR by Polarization Sharing. Magn Reson Chem 45:2
19. Farias J (2007) ASAP-HMQC – Quick Multidimensional Spectra. Agilent Application Note 5990-9237EN, Agilent Technologies, Inc., Santa Clara, CA, USA
20. Pauli GF, Jaki BU, Lankin DC (2005) Quantitative ^{1}H NMR: Development and Potential of a Method for Natural Products Analysis. J Nat Prod 68:133
21. Pauli GF, Jaki BU, Lankin DC (2007) A Routine Experimental Protocol for qHNMR Illustrated With Taxol. J Nat Prod 70:589
22. www.qnmr.org
23. Jaki BU, Franzblau SG, Chadwick LR, Lankin DC, Zhang F, Wang Y, Pauli GF (2008) Purity-Activity Relationships of Natural Products: The Case of the Anti-TB Active Ursolic Acid. J Nat Prod 71:1742
24. Akoka S, Barantin L, Trierweiler M (1999) Concentration Measurement by Proton NMR Using the ERETIC Method. Anal Chem 71:2554
25. Wider G, Dreier L (2006) Measuring Protein Concentrations by NMR Spectroscopy. J Am Chem Soc 128:2571
26. Farrant RD, Hollerton JC, Lynn SM, Provera S, Sidebottom PJ, Upton RJ (2010) NMR Quantification Using an Artificial Signal. Magn Reson Chem 48:753
27. Crouch R, Russell D (2011) Easy, Precise and Accurate Quantitative NMR. Agilent Application Note 5990-7601EN, Agilent Technologies, Inc., Santa Clara, CA, USA
28. Shoolery JN (1984) Recent Developments in ^{13}C- and Proton NMR. J Nat Prod 47:226
29. Wynants C, Hallenga K, Van Binst G, Michel A, Zanin J (1984) Assignment of Amino Acids in Proteins by Correlation of α-Hydrogen and Carbonyl Carbon-13 Resonances. J Magn Reson 57:93

30. Kessler H, Griesenger C, Zarbock J, Loosli HR (1984) Assignment of Carbonyl Carbons and Sequence Analysis in Peptides by Heteronuclear Shift Correlation *via* Small Coupling Constants with Broadband Decoupling in *t*1 (COLOC). J Magn Reson 57:331

31. Reynolds WF, Enriquez RG, Escobar LI, Lozoya X (1984) Total Assignment of ^{1}H and ^{13}C Spectra of Kauradien-9(11),16-oic Acid with the Aid of Heteronuclear Correlated 2D Spectra Optimized for Geminal and Vicinal ^{13}C-^{1}H Coupling Constants: or What to Do When "INADEQUATE" is Impossible. Can J Chem 62:2421

32. Jacobs H, Ramdayal F, Reynolds WF, Mclean S (1986) Guyanin, a Novel Tetranortriterpenoid. Structure Elucidation by 2-D NMR Spectroscopy. Tetrahedron Lett 27:1453

33. Bax A, Freeman R (1981) Investigation of Complex Networks of Spin-Spin Coupling by Two-Dimensional NMR. J Magn Reson 44:542

34. Bax A, Davis DG (1985) MLEV-17-Based Two-Dimensional Homonuclear Magnetization Transfer Spectroscopy. J Magn Reson 65:355

35a. Bax A, Morris GA, (1981) An Improved Method for Heteronuclear Chemical Shift Correlation by Two-Dimensional NMR. J Magn Reson 42:501

35b. Bax A (1983) Broadband Homonuclear Decoupling in Heteronuclear Shift Correlation NMR Spectroscopy. J Magn Reson 53:517

36a. Reynolds WF Hughes DW, Perpick-Dumont M, Enriquez RG (1985) A Pulse Sequence for Establishing Carbon-Carbon Connectivities *via* Indirect ^{13}C-^{1}H Polarization Transfer Modulated by Vicinal ^{1}H-^{1}H Coupling. J Magn Reson 63:413

36b. Reynolds, WF, McLean S, Perpick-Dumont M, Enriquez RG (1989) Improved ^{13}C-^{1}H Shift Correlation Spectra for Indirectly Bonded Carbons and Hydrogens: the FLOCK Sequence. Magn Reson Chem 27:162

37. Bax A, Subramanian S (1986) Sensitivity-Enhanced Two-Dimensional Heteronuclear Shift Correlation NMR Spectroscopy. J Magn Reson 67:565

38. Bodenhausen G, Ruben DJ (1980) Natural Abundance Nitrogen-15 NMR by Enhanced Heteronuclear Spectroscopy. Chem Phys Lett 69:185

39. Bax A, Summers MF (1986) ^{1}H and ^{13}C Assignments From Sensitivity-Enhanced Detection of Heteronuclear Multiple-Bond Connectivity by 2D Multiple Quantum NMR. J Am Chem Soc 108:2093

40. Lambert JB, Mazzola EP (2004) Nuclear Magnetic Resonance Spectroscopy: An Introduction to Principles, Applications and Experimental Methods, Chapter 8. Pearson Education, Inc., Upper Saddle River, NJ, USA

41. Kock M, Kerssebaum, R, Bermel W (2003) A Broadband ADEQUATE Pulse Sequence Using Chirp Pulses. Magn Reson Chem 41:65

42. Meyer SW, Kock M (2008) NMR Studies of Phakellins and Isophakellins. J Nat Prod 71:1524

43. Cheatham SF, Kline M, Sasaki RR, Blinov KA, Elyashberg ME, Molodtsov SG (2010) Enhanced Automated Structure Elucidation by Inclusion of Two-Bond Specific Data. Magn Reson Chem 48:571

44. Martin GE, Hilton BD, Blinov KA (2011) HSQC-ADEQUATE Correlation: a New Paradigm for Establishing a Molecular Skeleton. Magn Reson Chem 49:248

45a. Zhang F, Bruschweiler R (2004) Indirect Covariance NMR Spectroscopy. J Am Chem Soc 126:13180

45b. Snyder DA, Bruschweiler R (2009) Generalized Indirect Covariance NMR Formulism for Establishment of Multidimensional Spin Correlations. J Phys Chem A 113:12898

46. Martin GE, Hadden CE (2000) Long-Range ^{1}H-^{15}N Heteronuclear Shift Correlation at Natural Abundance. J Nat Prod 63:543

47. Martin GE, Williams AJ (2005) Long-Range ^{1}H-^{15}N Heteronuclear Shift Correlation. Ann Rep NMR Spectrosc 55:1

48. Martin GE, Hilton BD, Moskau D, Freytag N, Kessler K, Colson K (2010) Long-Range ^{1}H-^{15}N Heteronuclear Shift Correlation Across Wide F1 Spectral Windows. Magn Reson Chem 48:935

49. Kline M, Cheatham S (2003) A Robust Method for Determining ^{1}H-^{15}N Long-Range Correlations: ^{15}N Optimized CIGAR-HMBC Experiments. Magn Reson Chem 41:307

50. Nicolaou KC and Snyder SA (2005) Chasing Molecules That Were Never There: Misassigned Natural Products and the Role of Chemical Synthesis in Modern Structure Elucidation. Angew Chem Int Ed 44:1012
51a. Schlegel B, Hartl A, Dahse H-M, Gollmick FA, Grafe U, Dorfelt H, Kappes B (2002) Hexacyclinol, a New Antiproliferative Metabolite of *Panus rudis* HKI 0254. J Antibiot 55:814
51b. La Clair JJ (2006) Total Synthesis of Hexacyclinol, 5-*epi*-Hexacyclinol, and Desoxocyclohexcyclinol Unveil an Antimalarial Motif. Angew Chem Int Ed 45:2769
51c. Rychnovsky SD (2006) Predicting NMR Spectra by Computational Methods: Structure Revision of Hexacyclinol. Org Lett 8:2895
51d. Porco, Jr JA, Su S, Lei X, Bardhan S, Rychnovsky SD (2006) Total Synthesis and Structure Assignment of (+)-Hexacyclinol. Angew Chem Int Ed 45:5790
52. Laszlo P (1967) Solvent Effects and Nuclear Magnetic Resonance. Prog NMR Spectrosc 3:231
53. Hansen PE (1981) Carbon-Hydrogen Spin-Spin Coupling Constants. Prog NMR Spectrosc 14:175
54. Tinto WF, Reynolds WF (unpublished results)
55. D'Armas HT, Mootoo BS, Reynolds WF (2000) An Unusual Sesquiterpene Derivative from the Caribbean Gorgonian, *Pseudopterogorgia rigida*. J Nat Prod 63:1593
56. Elyashberg ME, Blinov KA, Williams AJ, Molodtsov SG, Martin GE, Martirosian ER (2004) *Structure Elucidator*: A Versatile Expert System for Molecular Structure Elucidation from 1D and 2D NMR Data and Molecular Fragments. J Chem Inf Comput Sci 44:771
57. Blinov KA, Carlson D, Elyashberg, ME, Martin GE, Martirosian ER, Molodtsov S, Williams AJ (2003) Computer-Assisted Structure Elucidation of Natural Products with Limited 2D NMR Data: Application of the StructEluc System. Magn Reson Chem 41:359
58. Karplus M (1963) Vicinal Proton Coupling in Nuclear Magnetic Resonance. J Am Chem Soc 85:2870
59. Neuhaus D, Williamson MP (2000) The Nuclear *Overhauser* Effect in Structural and Conformational Analysis, 2nd Edition. Wiley, New York
60. Haasnoot CAG, DeLeeuw FAAM, Altona C (1980) The Relationship Between Proton-Proton NMR Coupling Constants and Substituent Electronegativities–I: An Empirical Generalization of the *Karplus* Equation. Tetrahedron 36:2783
61. Musher JI, Corey, EJ (1962) Virtual Long-Range Spin-Spin Couplings in NMR: The Linear 3-Spin System and Qualitative Implications of Higher Systems. Tetrahedron 18:791
62a. Leon I, Enriquez RG, McLean S, Reynolds WF, Yu M (1998) Isolation and Identification by 2D NMR of Two New Complex Saponins from *Michrosechium helleri*. Magn Reson Chem 36:S111
62b. Powder-George Y, Frank J, Ramsewak RS, Reynolds WF (2012) The Use of Coupled HSQC Spectra to Aid in Stereochemical Assignment of Molecules with Severe Proton Spectral Overlap. Phytochem Anal 23:274
63. Mazzola EP, Parkinson A, Kennelly EJ, Coxon B, Einbond LS, Freedberg DI (2011) Utility of Coupled-HSQC Experiments in the Intact Structural Elucidation of Three Complex Saponins from *Blighia sapida*. Carbohydr Res 346:759
64. Turner JJ, Shephard N (1959) High-Resolution Nuclear-Magnetic-Resonance Spectra of Hydrocarbon Groupings. II. Internal Rotation in Substituted Ethanes and Cyclic Ethers. Proc Roy Soc A 252:506
65. Macura S, Huang Y, Suter D, Ernst RR (1981) Two-Dimensional Chemical Exchange and Cross-Relaxation Spectroscopy of Coupled Nuclear Spins. J Magn Reson 43:259
66. Bothner-By AA, Stephens RL, Lee J-M, Warren CD, Jeanloz RW (1984) Structure Determination of a Tetrasaccharide: Transient Nuclear *Overhauser* Effects in the Rotating Frame. J Am Chem Soc 106:811
67a. Stott K, Stonehouse J, Keeler J, Hwang T-L, Shaka AJ (1995) Excitation Sculpting in High-Resolution Nuclear Magnetic Resonance Spectroscopy: Application to Selective N*O*E Experiments. J Am Chem Soc 117:4199

67b. Thrippleton MJ, Keeler J (2003) Elimination of Zero-Quantum Interference in Two Dimensional NMR Spectra. Angew Chem Int Ed 42:3938
68a. Butts CP, Jones CR, Towers EC, Flynn JL, Appleby L, Barron NJ (2011) Interproton Distance Determinations by N*O*E – Surprising Accuracy and Precision in a Rigid Organic Molecule. Org Biomol Chem. 9:177
68b. Butts CP, Jones CR, Harvey JN (2011) High Precision N*O*Es as a Probe for Low Level Conformers – A Second Conformation of Strychnine. Chem Commun 47:1193
69. Macura S, Farmer BT, Brown LR (1986) An Improved Method for the Determination of Cross-Relaxation Rates from N*O*E Data. J Magn Reson 70:493
70. Hu H, Krishnamurthy K (2006) Revisiting the Initial Rate Approximation in Kinetic N*O*E Measurements. J Magn Reson 182:173
71. Kummerlowe G, Luy B (2009) Residual Dipolar Couplings for the Configurational and Conformational Analysis of Organic Molecules. Ann Rep NMR Spectrosc 68:193
72. Gil RR (2011) Constitutional, Configurational, and Conformational Analysis of Small Organic Molecules on the Basis of NMR Residual Dipolar Couplings. Angew Chem Int Ed 50:7222
73. Kummerlowe G, Crone B, Kretschmer M, Kirsch SF, Luy B (2011) Residual Dipolar Couplings as a Powerful Tool for Constitutional Analysis: The Unexpected Formation of Tricyclic Compounds. Angew Chem Int Ed 50:2643
74. Jones CR, Butts CP, Harvey JN (2011) Accuracy in Determining Interproton Distances Using Nuclear *Overhauser* Effect Data from a Flexible Molecule. Beilstein J Org Chem 7:145
75. Dale JA, Mosher HS (1973) Nuclear Magnetic Resonance Enantiomer Reagents. Configurational Correlations *via* Nuclear Magnetic Resonance Chemical Shifts of Diastereomeric Mandelate, *O*-Methylmandelate, and α-Methoxy-α-trifluoromethylphenylacetate (MTPA) Esters. J Am Chem Soc 95:512
76. Collins DO, Reynolds WF, Reese PB (2004) New Cembranes from *Cleome spinosa*. J Nat Prod 67:179
77. Molina-Salinas GM, Rivas-Galindo VM, Said-Fernandez S, Lankin DC, Munoz MA, Joseph-Nathan P, Pauli GF, Waksman N (2011) Stereochemical Analysis of Leubethanol, an Anti-TB-Active Serrulatane from *Leucophyllum frutescens*. J Nat Prod 74:1842
78. Piozzi F, Passannanti S, Marino ML, Spiro V (1972) Structure of Grandiflorenic Acid. Can J Chem 50:109
79. Lederberg J, Sutherland GL, Buchanan BG, Feigenbaum EA, Robertson AV, Duffield AM, Djerassi C (1969) Applications of Artificial Intelligence for Chemical Inference. I. The Number of Possible Organic Compounds. Acyclic Structures Containing C, H, O and N. J Am Chem Soc 91:2973
80. Sasaki S-I, Abe H, Ouki T, Sakamoto M, Ochiai S (1968) Automated Structure Elucidation of Several Kinds of Aliphatic and Alicyclic Compounds. Anal Chem 40:2220
81. Nelson DB, Munk ME, Gash KB, Herald DL (1969) Alanylactinobicyclone. An Application of Computer Techniques to Structure Elucidation. J Org Chem 34:3800
82. Elyashberg ME, Gribov LA (1968) Formal-Logical Model for Interpreting Infrared Spectra From Characteristic Frequencies. J Appl Spectrosc 8:189
83. Christie BD, Munk ME (1987) The Application of Two-Dimensional Nuclear Magnetic Resonance Spectroscopy in Computer-Assisted Structure Elucidation. Anal Chim Acta 200:347
84. Nuzillard J-M, Massiot G (1991) Logic for Structure Determination. Tetrahedron 47:3655
85. Peng C, Yuan S, Zheng C, Hui, Y (1994) Efficient Application of 2D Correlation Information in Computer-Assisted Structure Elucidation of Complex Natural Products. J Chem Inf Comput Sci 34:805
86. Steinbeck C (1996) LUCY – A Program for Structure Elucidation from NMR Correlation Experiments. Angew Chem Int Ed 35:1984
87. Lindel T, Junker J, Koeck M (1999) 2D-NMR-Guided Constitutional Analysis of Organic Compounds Employing the Computer Program COCON. Eur J Org Chem 3:573

88. Moser A, Elyashberg ME, Williams AJ, Blinov KA, DiMartino JC (2012) Blind Trials of Computer-Assisted Structure Elucidation Software. J Cheminformatics 4:5
89. McLean S, Perpick-Dumont M, Reynolds WF, Sawyer JF, Jacobs H, Ramdayal F (1988) Guyanin, a Novel Tetranortriterpenoid: Structural Characterization by 2D NMR Spectroscopy and X-ray Crystallography. J Am Chem Soc 110:5339
90. Bamburg JR, Riggs NV, Strong FM (1968) The Structures of Toxins from Two Strains of *Fusarium tricinctum*. Tetrahedron 24:3329
91. Liler M (1971) Studies of Nuclear Magnetic Resonance Chemical Shifts Caused by Protonation. Part II. Formamide and Some *N*-Alkyl and *N,N*-Dialkyl Derivatives. J Chem Soc B:334
92. McClelland RA, Reynolds WF (1974) ^{13}C Nuclear Magnetic Resonance Spectra of *N,N*-Dimethylformamide in Aqueous Acid Solution. Evidence for Predominant *O*-Protonation at All Acidities. J Chem Soc Chem Commun:824
93. Burns D, Reynolds WF, Buchanan G, Reese PB, Enriquez RG (2000) Assignment of ^{1}H and ^{13}C Spectra and Investigation of Hindered Side-Chain Rotation in Lupeol Derivatives. Magn Reson Chem 38:488
94. Christian OE, Henry GE, Jacobs H, McLean S, Reynolds WF (2001) Prenylated Benzophenone Derivatives from *Clusia havetiodes* var. *stenocarpa*. J Nat Prod 64:23
95. Reynolds WF, McLean S, Tay L-L, Yu M, Enriquez RG, Estwick DM, Pascoe KO (1997) Comparison of ^{13}C Resolution and Sensitivity of HSQC and HMQC Sequences and Application of HSQC-Based Sequences to the Total ^{1}H and ^{13}C Spectral Assignment of Clianosterol. Magn Reson Chem 35:455
96. Kupce E, Freeman R (1995) Adiabatic Pulses for Wideband Inversion and Broadband Decoupling. J Magn Reson A 115:273
97. Wilker W, Leibfritz D, Kerssebaum R, Bermel W (1993) Gradient Selection in Inverse Heteronuclear Correlation Spectroscopy. Magn Reson Chem 31:287
98. Boyer RD, Johnson R, Krishnamurthy K (2003) Compensation of Refocusing Inefficiency with Synchronized Inversion Sweep (CRISIS) in Multiplicity-Edited HSQC. J Magn Reson 165:253
99. Hu H, Krishnamurthy K (2008) Doubly Compensated Multiplicity-Edited HSQC Experiments Utilizing Broadband Inversion Pulses. Magn Reson Chem 46:683
100. Reynolds WF, McLean S, Jacobs H, Harding WW (1999) Assignment of ^{1}H and ^{13}C Spectra for Polyprenol-12, a Molecule With Severe ^{1}H and ^{13}C Spectral Crowding, With the Aid of High-Resolution, ^{13}C-Detected, ^{13}C-^{1}H Shift Correlation Spectra. Can J Chem 77:1922
101. Schoefberger W, Schlagnitweit J, Müller N (2011) Recent Developments in Heteronuclear Multiple-Bond Correlation Experiments. Ann Rep NMR Spectrosc 72:1
102. Furrer J (2011) Recent Developments in HMBC Studies. Ann Rep NMR Spectrosc 74:293
103. Hadden CE (2005) Adiabatic Pulses in ^{1}H-^{15}N Direct and Long-Range Heteronuclear Correlations. Magn Reson Chem 43:330
104. Nyberg NT, Duus JO, Sorensen OW (2005) Heteronuclear Two-Bond Correlation: Suppressing Heteronuclear Three-Bond or Higher NMR Correlations while Enhancing Two-Bond Correlations Even for Vanishing $^{2}J_{CH}$. J Am Chem Soc 127:6154
105. Wagner R, Berger S (1998) ACCORD-HMBC: a Superior Technique for Structure Elucidation. Magn Reson Chem 36:S44
106. Hadden CE, Martin GE, Krishnamurthy VV (2000) Constant Time Inverse-Detection Gradient Accordion Rescaled Heteronuclear Multiple Bond Correlation Spectroscopy: CIGAR-HMBC. Magn Reson Chem 38:143
107. Furrer J (2010) A Robust, Sensitive and Versatile HMBC Experiment for Rapid Structure Elucidation by NMR: IMPACT-HMBC. Chem Commun 46:3396
108. Hansen DF, Kay LE (2007) Improved Magnetization Alignment Schemes for Spin-Lock Relaxation Experiments. J Biomol NMR 37:245
109. Exarchou V, Krucker M, van Beek TA, Vervoort J, Gerothanassis IP, Albert K (2005) LC-NMR Coupling Technology: Recent Advancements and Applications in Natural Products Analysis. Magn Reson Chem 43:681

110. Tang H, Xiao C, Wang Y (2009) Important Roles of the Hyphenated HPLC-DAD-MS-SPE-NMR Technique in Metabonomics. Magn Reson Chem 47:S157
111. Martin GE (2005) Small-Volume and High-Sensitivity NMR Probes. Ann Rep NMR Spectrosc 56:1
112. Brey WW, Edison AS, Nast RE, Rocca JR, Saha S, Withers RS (2006) Design, Construction, and Validation of a 1-mm Triple Resonance High-Temperature-Superconducting Probe for NMR. J Magn Reson 179:290
113. Dalisay DS, Rogers EW, Edison AS, Molinski TF (2009) Structure Elucidation at the Nanomole Scale. 1. Trisoxazole Macrolides and Thiazole-Containing Cyclic Peptides from the Nudibranch *Hexabranchus sanguineus.* J Nat Prod 72:732
114a. Schroeder FC, Gronquist M (2006) Extending the Scope of NMR Spectroscopy with Microcoil Probes. Ang Chem Int Ed 45:7122
114b. Lambert M, Wolfender J-L, Staerk D, Christensen S B, Hostettmann K, Jaroszewski JW (2007) Identification of Natural Products Using HPLC-SPE Combined with CapNMR. Anal Chem 79:727
115. Patt SL, Shoolery JN (1982) Attached Proton Test for Carbon-13 NMR. J Magn Reson 46:535
116. Doddrell, DM, Pegg DT, Bendall MR (1982) Distortionless Enhancement of NMR Signals by Polarization Transfer. J Magn Reson 48:323
117. Burger R, Bigler P (1998) DEPTQ: Distortionless Enhancement by Polarization Transfer Including the Detection of Quaternary Nuclei. J Magn Reson 135:529
118. Bax A, Marion D (1988) Improved Resolution and Sensitivity in ^{1}H-Detected Heteronuclear Multiple-Bond Correlation Spectroscopy. J Magn Reson 78:186
119. Keeler J (2010) Understanding NMR Spectroscopy, 2nd Edition. Wiley, Chichester, UK
120. Hoch JC, Stern AS (1996) NMR Data Processing. Wiley-Liss, New York
121. Reynolds WF, Yu M, Enriquez RG, Leon I (1997) Investigation of the Advantages and Limitations of Forward Linear Prediction for Processing 2D Data Sets. Magn Reson Chem 35:505
122. Reynolds WF, Enriquez RG (2003) The Advantages of Forward Linear Prediction Over Multiple Aliasing for Obtaining High-Resolution HSQC Spectra in Systems With Extreme Spectral Crowding. Magn Reson Chem 41:927
123. Freeman R (1998) Shaped Radiofrequency Pulses in High Resolution NMR. Prog NMR Spectrosc 32:59

Vibrational Circular Dichroism Absolute Configuration Determination of Natural Products

Pedro Joseph-Nathan and Bárbara Gordillo-Román

Contents

1 Introduction

Chirality is a phenomenon born with Nature, which is inherently manifested in the enormous variety of natural products produced by metabolic routes in organisms and plants. Secondary metabolites have complex stereochemistry due to the presence of several stereogenic centers (central chirality) and of certain elements of symmetry as a plane, or an alternating axis. Processes such as carbon acquisition, energy storage and information transfer are not devoid of stereochemical control because they are ultimately performed by large systems of associated molecules

P. Joseph-Nathan (✉) • B. Gordillo-Román
Departamento de Química, Centro de Investigación y de Estudios Avanzados del Instituto Politécnico Nacional, Apartado 14-740, México, DF 07000, Mexico
e-mail: pjoseph@nathan.cinvestav.mx

A.D. Kinghorn, H. Falk, J. Kobayashi (eds.), *Progress in the Chemistry of Organic Natural Products, Vol. 100*, DOI 10.1007/978-3-319-05275-5_4,

built from chiral or geometry-explicit building block precursors. Such is the case of the stereo-defined isoprene moiety from which mono-, sesqui-, di-, sester-, tri-, sesquar-, and tetraterpenes are formed in plants and in other living organisms. The generic attributes of natural products rely not only on the group constitution but also on the stereochemical descriptors as the regio, diastereomer, enantiomer, and topomer preferences, information that is necessary for completing their biosignatures (*1*).

During the formation of intricate chiral molecules, a small chiral scaffold nucleus transfers its chirality information to the complex structure, a phenomenon that is known as induced chirality. Examples are found in the geometry-defined lactones obtained from stereoselective reactions on allenes (*2*) or the four-membered ring nucleus of terpenes, cholesterol resorption inhibitors, and β-lactam antibiotics (*3*).

In order to assign the absolute configuration of natural products, non-direct or direct methods tend to be used. The non-direct methods are based on the use of previously known information, *i.e.* the relative stereochemistry of the target molecules, or of a stereo-correlated analogue, and the optical rotation ($[\alpha]_D$) of a pure enantiomer, to determine its proportion in an enantiomerically enriched mixture, among others. By the end of the last century the detection of the relative stereochemistry of natural products was carried out commonly by nuclear magnetic resonance (NMR) and/or by X-ray crystallography. Anomalous scattering X-ray crystallography is a direct, precise, and reliable method for determining absolute configurations. However, this is limited to crystalline compounds, so chiroptical spectroscopic methods such as optical rotatory dispersion (ORD), electronic circular dichroism (ECD), vibrational circular dichroism (VCD), and *Raman* optical activity (*R*OA) have been developed as methodology to establish the absolute configuration of chiral molecules in solution (*4*).

Even though an ECD spectrum contains the information on the absolute configuration of the investigated compound, ECD was initially considered a relative method because the extraction of such information depended on a semi-empirical model based on chirality rules, or on a good empirical correlation with the spectrum of an analogous compound. Nevertheless, spectroscopic chiral techniques, at wavelengths of the UV–vis radiation, are applied successfully if the model and empirical rules to predict the electronic transitions bands, or so-called *Cotton* effects (*C*Es), are accurate. *C*Es are the manifestation of the difference in refraction of linearly polarized light in ORD, or the manifestation of the difference in absorption of circularly polarized light in ECD (*5*).

Although it is true that nowadays ECD spectra can be predicted by density functional theory (DFT) calculations, these procedures do not necessarily produce confident data, since calculations must be performed both in the ground state and in the excited states of the molecule, since UV–vis absorption of light is always associated with electrons in the excited state of matter.

Chirality in natural products has been analyzed experimentally using ECD (*6*) and VCD (*7*) spectroscopy, and chirality amplification such as that observed in the molecular recognition of biomolecules has been done by induced circular dichroism (ICD) (*8*). In a number of cases VCD has been demonstrated as being superior to assess the absolute configuration of chiral natural products when compared with other techniques such as OR or ECD. A case in point is cephalochromin (**1**), a natural product containing both axial chirality and central chirality due to an axis and two stereogenic

carbons, where the ECD spectrum is dominated by its axial chirality and is not able to distinguish the (a*S*,2*S*,2′*S*) or (a*S*,2*R*,2′*R*) diastereomers, but this can be done with VCD (*9*). Moreover, with VCD it is possible to distinguish spectral elements to determine both types of chirality, demonstrating the analytical potential of the technique (*9*). Another example is (+)-(1*S*,11*S*,12*S*)-verticillol (**2**) (*10*) a fundamental diterpene in the biosynthesis of taxanes, where the application of a wrong octant rule model had led to the enantiomeric structure of that suggested by VCD and anomalous dispersion X-ray analysis of its *p*-iodobenzoate derivative. While not frequent, but still a case to be mentioned, is the success of VCD over X-ray-diffraction in the assignment of configuration of (–)-(*S*)-2-(1-hydroxyethyl)-chromen-4-one (**3**) (*11*).

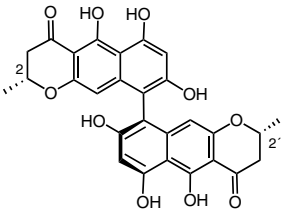

1

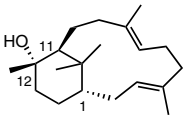

2

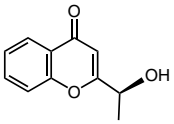

3

The use of theoretical models describing the correlation between optical activity and absolute configuration has promoted the development of methods for which the experimental results can be supported by quantum mechanical calculations giving strong support to absolute configuration assignments. The most developed *ab initio* methods for chiral spectroscopic ECD and VCD studies are those that rely on density functional theory (DFT). The simultaneous application of ECD and VCD techniques, along with optical rotation (OR) determinations, affords a robust and reliable methodology frequently used in the absolute configurations detection of natural products. By using this combined methodology, the confident absolute configuration assessments of sesquiterpenes (1*R*,2*R*,5*S*,8*R*,11*R*)-quadrone (**4**) and (1*R*,2*R*,5*S*,8*R*,11*R*)-suberosanone (**5**) (*12*), and the alkaloids (+)-(2*R*,7*S*,20*S*,21*S*)-schizozygine (**6**) (*13*) and (–)-(2*R*,7*R*,20*S*,21*S*)-isoschizozygamine (**7**) (*14*), have been reported.

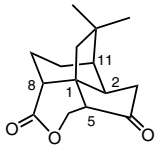

4

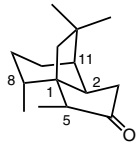

5

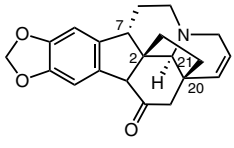

6

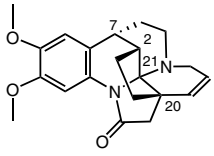

7

Conformational changes in chiral molecules greatly modify their VCD spectra, thus theoretical conformational predictions to obtain a statistical population distribution that precedes VCD calculations is a common practice, and in some cases combined methods such as IR, Raman, and VCD spectroscopy to obtain the most stable conformers of natural products may be conducted (*15*).

Vibrational circular dichroism measurements have been extended to analyze the conformation in solution of complex natural products (*16*), and to determine the secondary structure of natural chiral polymers inclusive of oligomeric nucleic acids (*17*), peptides (*18*, *19*), and carbohydrates (*20*) by targeting their chiral property. The process of recognition by means of which the secondary structure of proteins and nucleic acids is formed, rests on non-covalent interactions such as H-bonding. Monitoring H-bonding by VCD is becoming a common practice facilitated by the easy inspection of clue vibrational bands, frequently in the mid-IR region (2,000–800 cm^{-1}) of the spectra. An example is found in the VCD spectrum of the glycoprotein AGP recorded in D_2O solution that revealed through the "W" pattern observed for the bands at the amide region that AGP has a β-sheet structure mixed with an α-helix. It is not possible to extract this information from ECD due to interference of bands in the UV region of the spectrum (*21*). Helical chirality might be evidenced by the presence of a positive (–,+) bisignated band (couplet) in the carbonyl region of VCD spectra (*22*).

The wide variety of applications of VCD is revealed by the elegant work on studying supramolecular helical chirality in protein fibrils (*23*, *24*) and the analysis of the chirality of amphiphilic constituents of cell membranes, expressed at the nano supramolecular scale, where the mechanism of the chiral induction by counter-ions involves anion–cation recognition and the induction of conformationally labile chirality in cations (*25*).

Chiral recognition in host–guest complexation of organic natural products, like terpenoids and steroids in γ-cyclodextrins, has been analyzed by induced circular dichroism and fluorescence spectra (*26*). Phenomena ascribed to chirality in interfaces are also reliably broached by VCD in materials research (*27*, *28*). Local chirality at the molecular level on the pore wall surfaces of the mesoporous silicas MCM-41, chiral SBA-15, and chiral SBA-16, has served as the foundation for an understanding of chirality transfer (*29*) and has stimulated work in enantioselective chromatographic separations, wherein the interactions between enantiomeric analytes and chiral stationary phases (CSPs) revealed by VCD has provided the underlying mechanism governing efficient chiral separations (*30*). In addition, chiral surfaces and interfaces that have been shown to be able of distinguishing enantiomers play a key role as enantioselective catalysts. Thus, the conformation of polar molecules adsorbed on optically active silver nanoclusters studied by IR and VCD spectroscopy led to the interesting discovery that, whereas the IR spectra of polar molecules protected nanoclusters in D_2O and in CD_3OD are essentially identical, the VCD spectra are mirror images of one another (*31*).

Absolute configuration detection is of extreme importance in the pharmaceutical industry; here the VCD technique has become a widely used tool in the drug discovery processes. Due to the limited time to produce results, when the investigated chiral molecule is large or possesses high conformational mobility, truncations of the calculated molecules have facilitated successful analysis. The sensitivity of VCD to conformation has prompted the use of multivariate data analysis software

to understand structure–activity (SA) or structure–property (SP) relationships of potential drug leads (*32*).

After providing a broad idea of the capabilities of VCD, many of them beyond the scope of this review, the current chapter is focused on the use of VCD as an analytical tool to establish the conformation and absolute configuration of natural products. Brief introductions to the principles, instrumentation, and theoretical quantum chemistry methods for VCD spectra simulations are provided in the first sections of this chapter, followed by illustration of the VCD methodology in chiral mono-, sesqui-, di-, mero-, and triterpenoids, among other natural products, to furnish readers with information on those critical aspects that affect VCD performance, such as conformational flexibility, H-bond rapid exchange equilibrium, solvent participation, and theoretical methodology. Absolute configuration determination of diastereomers is also presented so as to show the limits of sensing chirality by the VCD technique. Chiral analysis of diastereomers is of importance in natural products, since frequently one diastereomer possessing several chiral centers is found in Nature, but only one or two of those chiral centers are of unknown absolute configuration.

2 A Brief History

VCD theory was introduced in the 1970s in order to provide a sound background for experimental investigations of optical activity in the infrared region of the electromagnetic spectrum, which at that time presented great technical difficulties (*33*, *34*). In this early work, ORD and ECD techniques using visible and ultraviolet regions (185–700 nm) were utilized commonly to determine absolute configuration and relative stereochemistry, functional group position, and conformation of natural products in solution (*6*). Characterized by bisignate ORD curves of positive (–,+) or negative (+,–) chirality, or signated ECD bands (+ or – signals), these chiroptical methods allowed stereochemical assignment of stereogenic elements as centers, axes or planes of a vast number of natural products by comparison with the ORD or ECD curves of analogous compounds of known structure and configuration. Thus, for example, the ECD of the steroidal ketones, 5α,14α- (**8**) and 5α,14β-androstan-17-one (**9**), measured at around 290 nm, displayed *Cotton* effects at the carbonyl (π–π*) absorption, which were used for reference to assign the relative *trans* configuration of the ring junction of a series of the structurally related metabolites **10**–**13**. In compounds **11** and **12**, the relative stereochemistry of carbons at ring junctions provided their absolute configuration, because the configuration at other chiral carbons was known.

Assignment of configuration by ECD measurements, based on comparison of test and reference molecules, does not always ensure a reliable comparison, because the sign and intensity of *C*Es not only depend on the correct choice of a like chromophore and its vicinity, but also depend on conformation. Therefore, the implementation of semi-empirical sector and helicity rules was necessary to provide the more reliable interpretation of experimental ECD spectra (*35*).

However, the application of ECD to differentiate enantiomers spectroscopically was not really improved until the introduction of the CD exciton chirality method, which is based on an exciton coupling between two chromophores immersed in the

molecule or introduced by chemical derivatization. Therefore, a model could be proposed wherein the location and direction of the electronic transition moments have to be correctly assigned in order to obtain unambiguous absolute configurational assessments (*36*).

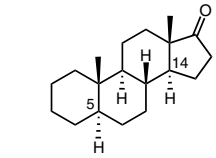

$\Delta\varepsilon$/mol^{-1}dm^{-3}cm^{-1}= +3.3 (*a* + 140)

8

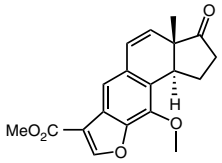

10

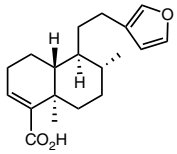

11

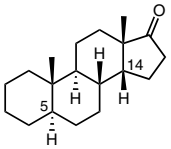

$\Delta\varepsilon$/mol^{-1}dm^{-3}cm^{-1}= +1.0 (*a* + 40)

9

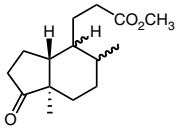

12

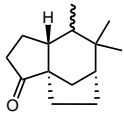

13

A full calculation of ECD spectra based on quantum mechanics is a useful alternative to permutate detailed streochemical information and on the configuration and conformation from molecular electronic sensors, especially in those situations where ECD spectra are complicated by the overlap of exciton couplets due to the presence of a considerable number of chromophores or due to high molecular flexibility. Computational *ab initio* methods for calculating ECD spectra, for example the Time Dependent Density Functional Theory (TDDFT), have been applied to assign the absolute configuration of small- and medium-sized molecules (*36*). The method is time-demanding, because of inherent difficulties in simulating electronically excited energy states.

Examples are reported in the literature that demonstrate the potential use of the ECD technique for the successful assignment of absolute configurations of organic molecules possessing natural optical activity or acquired chirality through their asymmetric syntheses. Tropane alkaloid **14**, a natural product substituted with two chromophoric mobile α,β-unsaturated esters, for which the chiral communication can be sensed by ultraviolet circular dichroic absorption, was allotted an absolute configuration as (3*R*,6*R*) by comparison of the experimental and calculated electronic *Boltzmann* weighted ECD spectra using the results of the excited states calculation of a set of simplified structures (*37*). Computational chemists demonstrating that difficulties associated with the simulation of complicated models to perform excited states calculations have proposed innovative methods suitable for application to model natural product compounds. To show the effectiveness of the method, the polyketide phomalevone (**15**) is taken as an example (*38*). Here the absolute configuration of the stereogenic centers C-10a and C-10a′ and the axial axis (2,2′) were determined as (10a*S*,10a′*S*,a*S*) by comparison of the experimental ECD spectrum with the TDDFT calculated spectra of two low-energy rotamers that produced smoothed resemblances

of signated CE bands. Besides, the assigned absolute configuration was in close correspondence to the stereochemistry of analogous compounds.

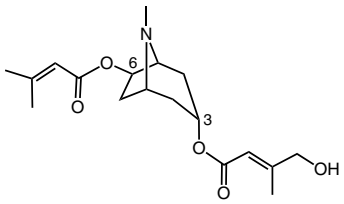

14

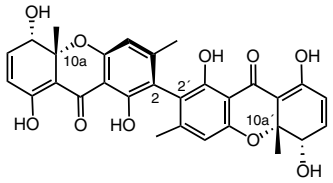

15

The development of VCD as a tool for the absolute configuration determination of natural products was accompanied by the study of those compounds lacking chromophores and/or where their analysis by ECD was complicated by the presence of overlapping absorption bands. Characterized by an energy that is one to three orders of magnitude less than electronic transitions, vibrational transitions (10^{12}–10^{14} s^{-1}) in the electronic ground state of the molecules originate vibrational optical activity (VOA) spectra, which constitute a sensitive practical measurements of local chirality. The accessible regions for VCD measurements contemplate the near-infrared (800–2,500 nm), the high-frequency zone (4,000–2,000 cm^{-1}) and the mid-infrared (2,000–800 cm^{-1}) region. VCD spectra are characterized by well-resolved bands that represent *C*Es due to chirotopic rapid atomic vibrational motions in the molecule. The differential absorption arising from the interaction of circularly polarized light (cpl) with chiral molecules is measured in terms of an absorption intensity (ΔA), which is equal to the difference absorption of the left and right cpl (1). The absorption can also be expressed in molar extinction coefficient ($\Delta\varepsilon$) units, a more appropriate molecular property to report the observed intensity of anisotropic absorption corresponding to each anharmonic vibration.

$$\Delta A = A_L - A_R \tag{1}$$

Meanwhile, IR intensities (A or ε) are determined by means of dipole strengths (D) (2), and VCD intensities are determined by rotational strengths (R) (3) (*7*, *37*). Dipole strengths are related to atomic electric dipole moments $\left(\vec{\mu}\right)$ and rotational strengths to simultaneous electric and magnetic dipole moments $\left(\vec{m}\right)$ in fundamental transitions of normal vibrational modes at electronic ground states (*39*).

$$D \propto \int \varepsilon \, dv \tag{2}$$

$$R \propto \int \Delta\varepsilon \, dv \tag{3}$$

All bands in a VCD spectrum represent chirality, and the local dissymmetry or circular dichroism effect is measured through the anisotropic factor (g), which relates the intensities of VCD bands to IR bands ($\Delta\varepsilon/\varepsilon$) and depends, largely, on the instrument sensitivity used for measurements. Nevertheless, a higher sensitivity is normally observed for ECD ($g \approx 10^{-2}$) than for VCD ($g \approx 10^{-4}$) in consideration of mass differences between electrons and nuclei (*34*). Stereogenic centers in the molecule may be expected to produce VCD bands with higher anisotropy g-factors than

non-stereogenic centers as long as the transition between electric and magnetic vector moments do not cancel each other out during vibrational motion, although substituents such as a methyl group close to an heteroatom can introduce a higher degree of asymmetry than expected because this is in a conformational anisotropic environment (*40*). The *g*-factor might be high either because circular currents are high, as is found in bending C–O–H vibrational modes with large magnetic moments (rotation), or because the linear currents are small as evident in stretching C–H vibrational modes (translation) with small electric transition moments and absorptions.

The theory on which vibrational optical activity is based assumes harmonic oscillations with force constants for individual atomic displacements that are transformed to force constants for normal vibrational modes (*34*, *39*). Therefore, a correction factor is needed to match calculated harmonic frequencies with real anharmonic vibrational frequencies, a correction known as the anharmonicity factor (an*H*) (*7*). Nevertheless, VCD theoretical models have continued in their development, thus recently the first implementation and calculation of anharmonic VCD rotational strengths for monoterpenes was reported (*41*). Since dipole moments depend not only on bond polarization but also on molecular geometry, and considering that every flexible molecule is an ensemble of conformers, dipole moment transition bands in IR and consequently in VCD, will depend on the contribution and composition of conformers. The time detection for vibrational transitions is less than picoseconds, hence conformational heterogeneous samples will display IR and VCD absorption bands due to individual conformers where the intensity is proportional to the conformational population (*4*).

The first measurements of vibrational circular dichroism in liquid samples (*42*) were performed in enantiomeric (+)-(*S*)- and (–)-(*R*)-2,2,2-trifluoro-1-phenylethanol at 2,920 cm^{-1}, and for the primary C–H stretch band at the α-carbon atom. The circular dichroism effect observed was rather low ($g = 6.5 \cdot 10^{-5}$) but enough to distinguish chirality of the enantiomers, with rotational strengths of $+2 \cdot 10^{-44}$ esu^2cm^2 for the (+)-(*S*)- and $-2 \cdot 10^{-44}$ esu^2cm^2 for the (–)-(*R*)-enantiomer, and dipole strength of $1.4 \cdot 10^{-39}$ esu^2cm^2. Even though vibrational rotatory strengths are smaller than those of electronic transitions, presently high-sensitivity chiral IR instruments can sense bands with *g*-values in the order of 10^{-3}, facilitating the assessment of absolute configuration by analysis of well-defined intensity and signated bands.

Years after the first VCD report, a formal and complete VCD theory was proposed introducing atomic polar tensors (APTs), a concept used in absorption vibrational spectroscopy, allowing the calculation of signals intensity as a change in total molecular dipole moment when all atomic nuclei of a molecule undergo a set of small displacements (*43*). The atomic axial polar tensors (AAPTs) model takes into consideration the corrected *Born-Oppenheimer* coupling effects introducing a rapid and efficient way to calculate vibrational circular dichroism spectra in a concerted manner (*44*). Thus, the first application of density functional theory (DFT) using B3LYP functional and gauge-invariant atomic orbitals (GIAOs) to calculate vibrational rotational strengths of *trans*-2,3-d_2-oxirane was reported using a powerful method based on DFT harmonic force field and AAPTs (*44*, *45*). This methodology was implemented within the Gaussian program suite and first used to predict the VCD spectra of two monoterpene natural products, (+)-(1*R*,4*R*)-camphor (**16**) and (+)-(1*S*,4*S*)-fenchone (**17**) (Fig. 1) (*46*).

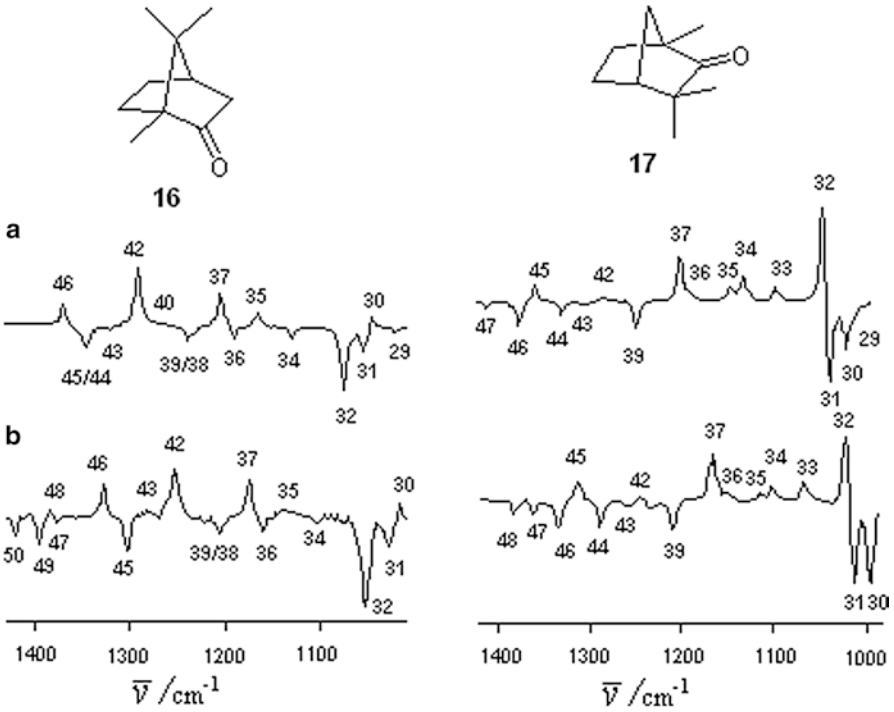

Fig. 1 C-H bending region of the VCD spectra of (+)-camphor (**16**) and (+)-fenchone (**17**) calculated (**a**) using the DFT B3PW91/6-31G(d) method and (**b**) experimental. (Adapted from (*46*))

VCD calculations provide signated rotational strengths with high accuracy for each vibrational frequency. The predicted full VCD spectrum is obtained by fitting these parameters to band shapes with *Lorentz*ian functions (*47*, *48*). Each band in a VCD spectrum has a corresponding band in the IR spectrum. However, because of the signated pattern of VCD bands, the spectrum looks simpler than an isotropic IR absorption spectrum. IR bands are prone to be broad as a result of overlap of coupled vibrational modes corresponding to rapid exchange processes such as intermolecular H-bonding or to heterogeneous conformational equilibria.

The transition dipole mechanism for vibrational coupling depends on conformation, so, therefore, efforts dedicated to define unambiguously the most stable conformation of a rigid molecule or *Boltzmann* average conformations of a flexible one are rewarded by obtaining a close-to-real calculated VCD spectrum. The absolute configurations of chiral molecules are thus defined by comparison of calculated to experimental VCD spectra using bands at equivalent frequencies. The band sign and band intensity are the parameters to observe for defining absolute configuration of dextro- or levorotatory molecules that display mirror image VCD bands, such as those observed for (+)-(*R*)-limonene (**18**) and (–)-(*S*)-limonene (**19**) in Fig. 2.

Early VCD applications were dedicated to the use of isotopic labeling to determine absolute configuration, and to kinetic studies of stereospecific reactions using hydrogen and deuterium stretching modes in the 4,000–2,000 cm^{-1} region of the spectra (*49*). Later on, with the advent of FT-VCD methods (*50*), the potential of

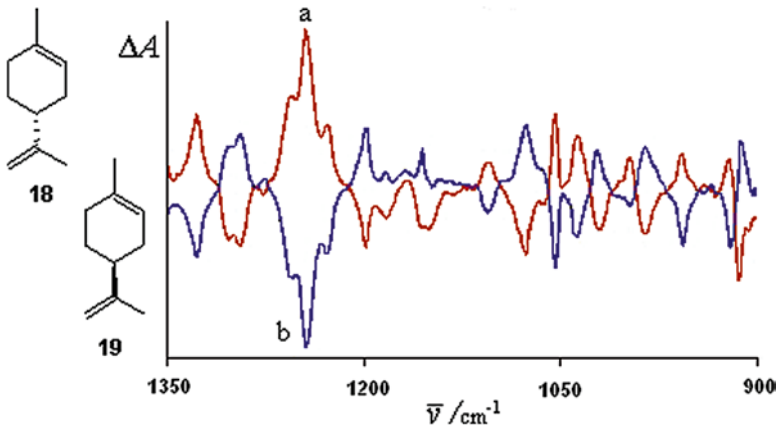

Fig. 2 VCD spectra of (+)-(*R*)-limonene (**18**) (from oranges, curve a) and (–)-(*S*)-limonene (**19**) (from lemons, curve b) in the mid-IR region

VCD was demonstrated by the real-time monitoring of the composition and % enantiomeric excess (ee) of the stereochemical processes. The experiment for the reduction reaction of (–)-(1*S*,4*S*)-camphor (**20**) to (–)-(1*S*,2*R*,4*S*)-*endo*-borneol (**21**) was simulated by periodically changing the mole fraction of camphor relative to borneol, starting from 100% camphor to reach 100% borneol (*51*). The VCD spectra registered at the start and end of the experiment are shown in Fig. 3, along with an intermediate mixture of *ca.* 1:1 of both compounds, which allows identification of the bands that correspond to borneol associated with normal stretching ($\nu_{C\text{-}O}$) of the hydroxy group in the 1,100–1,035 cm^{-1} region.

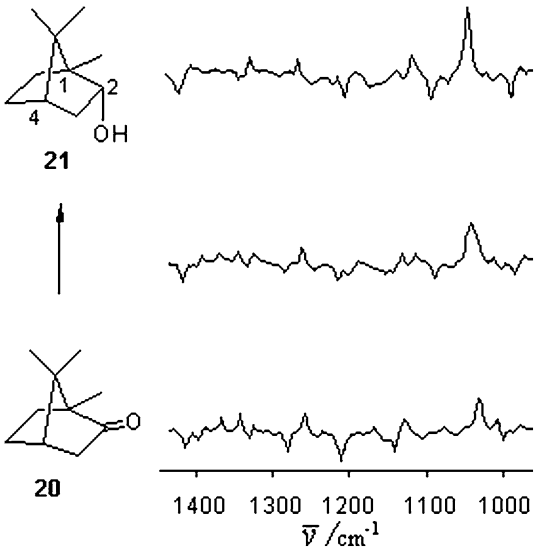

Fig. 3 Monitoring the course of the simulated chiral reaction of (–)-camphor (**20**) to (–)-borneol (**21**) by VCD spectroscopy. The central plot is the spectrum of a 1:1 mixture of both monoterpenes. (Adapted from (*51*))

For dynamic processes such as those observed in flexible molecules where two or more conformers are in equilibrium, VCD has been used to give an account of the occurrence of conformers (*15*, *16*, *52*). In this area of research VCD and ECD coupled effectively to produce an insurmountable mixed method for diagnosis of the relative mobility of fragments inside a molecule (*53*) or for intermolecular hemi-intercalative binding (*54*). The information provided by both ECD and VCD provide useful details of the molecular structure and its relationship with optical activity, since ECD focuses on chirality around chromophore sensors and VCD senses chirality in each vibronic chiral entity. Evidently, this does not imply that ECD can provide a different configurational assignment than VCD for a test molecule; on the contrary, both methods should reinforce assignment. Such is the case of tropane alkaloids **22** and **23** (Fig. 4) (*55*), for which the absolute configuration assessment by VCD is in agreement with that determined by ECD for the analogue tropane **14**. Tropanes **22** and **23** are mobile molecules, with eight conformers found populated for each molecule by searching with molecular mechanics calculations. IR and VCD spectra for the four most stable conformers of tropane **22**, calculated by *ab initio* methods are shown in Fig. 4.

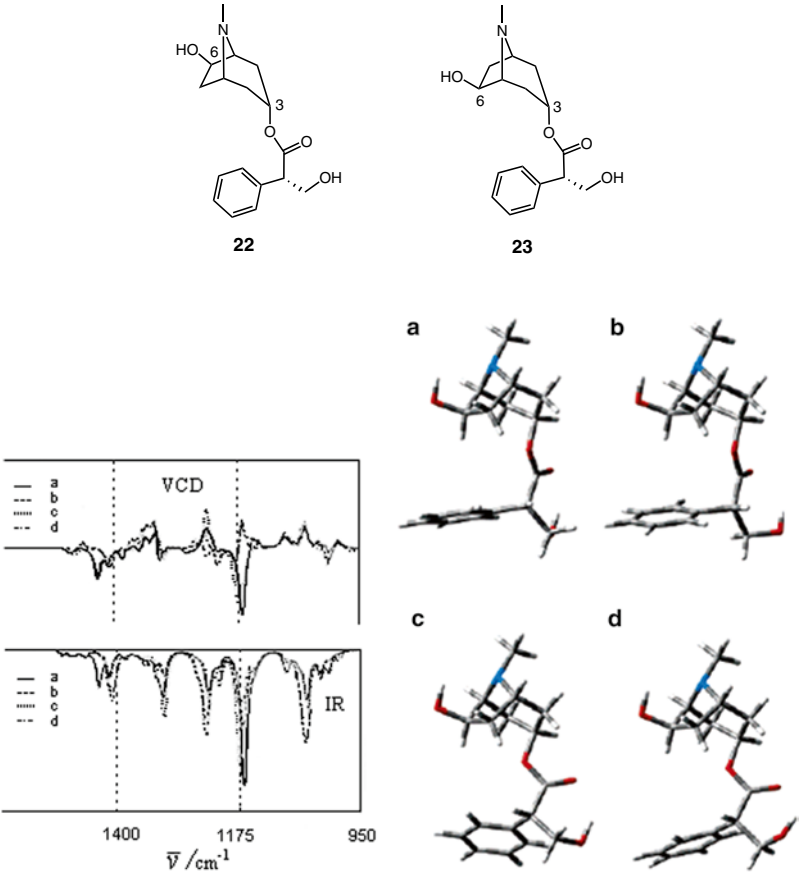

Fig. 4 Calculated IR absorption (*bottom*) and VCD spectra (*top*) of four low-energy conformers (**a**–**d**) of (3*R*,6*R*)-6*β*-hydroxyhyoscyamine (**22**) at the B3LYP/6-31G(d) level of theory. (Adapted from (*55*))

Nowadays, VCD has become the technique of choice to determine not only the absolute configuration of natural products with known relative stereochemistry, but also to determine the structure and chirality of new natural products. Such is the case of (+)-alternamin, isolated from the aerial parts of *Murraya alternans*, a dihydrofuranocoumarin for which the structure was determined as (+)-(*S*)-5,8-dimethoxymarmesin (**24**), after ruling out structures **25** and **26** that were not possible to distinguish by 2D-NMR techniques (*56*).

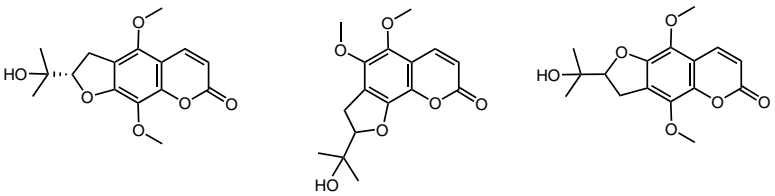

24 **25** **26**

3 Experimental Considerations

In chiroptical techniques a dissymmetric molecule is irradiated with polarized light, stimulating spectroscopic changes that can be detected in a qualitative manner (optical rotation) or as a quantitative change (differential absorption). In CD, where the differential absorption of the left and right cpl is detected, the cpl electric vector rotates in the direction of the beam propagation describing helix shapes, (*M*) and (*P*), which are not superposable mirror images. When a chiral molecule is irradiated with the cpl of UV–vis, wavelength 10^{-5}–10^{-7} cm, or IR, wavelength 10^{-2}–10^{-4} cm, interactions that are diastereomeric in character take place (Fig. 5), thereby chirality can be quantified instrumentally.

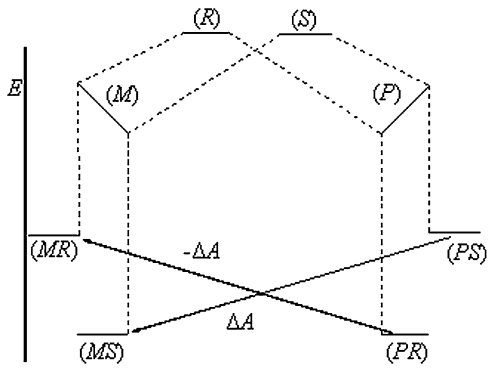

Fig. 5 Anisotropic absorption of circularly polarized light (cp) by a chiral (*R*) or (*S*) configured substrate. The symbols (*P*) and (*M*) refer to right- and left-handed helicity

The VCD spectroscopic response is thus based on transformation of the chiral information contained in vibrational modes, in a measurable energy difference associated with the rotation of cpl through a resonant IR radiation. Normal modes give rise to fundamental vibrational states and combinations to overtones. However, because of the absence of symmetry in chiral molecules, each normal mode contains components of all internal coordinates. As a result some bands are simple combinations of modes but others are quite complex combinations (*34*). In VCD spectra the bands are characterized by a frequency energy given by wavenumbers, in cm^{-1}, and by an absorption intensity (ΔA); a value that can be expressed as ($\Delta\varepsilon$), according to the *Lambert-Beer* law (4).

$$\Delta\varepsilon = \Delta A / c \bullet l \tag{4}$$

where c is the concentration in mol/dm^3 and l the pathlength in cm.

The heart of a VCD instrument is the modulator, which produces the optical phase retardation needed to furnish left and right circularly polarized light before traversing the sample (*57*). Optical activity arising from vibrations of molecules in the liquid state were first measured by alternately sending left and right circularly polarized light through the sample by means of a modulator in scanning grating setup instruments (dispersive scanning), collecting data at one wavelength a time (*39*, *58*), or in a short range of wavelengths (*59*). The instrumental sensitivity is limited by the signal-to-noise (*S/N*) ratio and by the presence of optical and electrical artifact signals (*60*). The detector own-noise signal affects the *S/N* ratio. The spectra of chiral (+)- and (–)-2,2,2-trifluoro-l-phenylethanol (neat) recorded in two dispersive scanning instruments are shown in Fig. 6; a racemate of the chiral samples is used as reference.

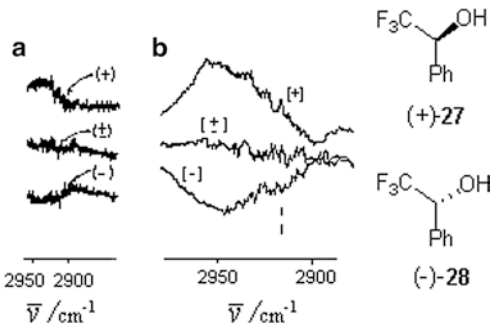

Fig. 6 VCD spectra of (+)-2,2,2-trifluoro-1-phenylethanol (**27**) and (–)-2,2,2-trifluoro-1-phenylethanol (**28**) recorded in scanning dispersive instruments: (**a**) spectral bandpass of 20 cm^{-1}, (**b**) spectral bandpass of 10 cm^{-1} in a higher sensitivity instrument. At the center of both groups of curves, a sample of a racemic mixture of **27** and **28** is taken as a reference. (Adapted from (*42*, *58*), respectively)

In experiment (**a**) a germanium modulator with piezo-electric disks oscillating at about 10 kHz and a photovoltaic InSb detector were used in the optical train of the instrument, whereas in (**b**) a polycrystalline ZnSe crystal photoelastic modulator (PEM) oscillating at about 50 kHz was used to provide phase modulation. Here the insertion of a second ZnSe modulator after the sample increased the instrumental sensitivity since artifact CD signals were diminished significantly.

Incipient registers of VCD bands with good signal-to-noise ratio in the stretching ν_{CH} region for menthol, α- and β-pinene, camphor, 3-bromocamphor, and borneol, among others, were reported using dispersive instruments (*59*). However, a great improvement in optics to detect chiral IR spectra was achieved by introducing a *Fourier* transform (FT) approach in the instrument design, allowing efficient VCD spectra determination with data collection across a wide range of IR frequencies in a simultaneous way and a reasonable time (*60*, *61*). The performance of a dispersive VCD versus a FT instrument is shown for chiral (+)- (**16**) and (–)-camphor (**20**) in Fig. 7.

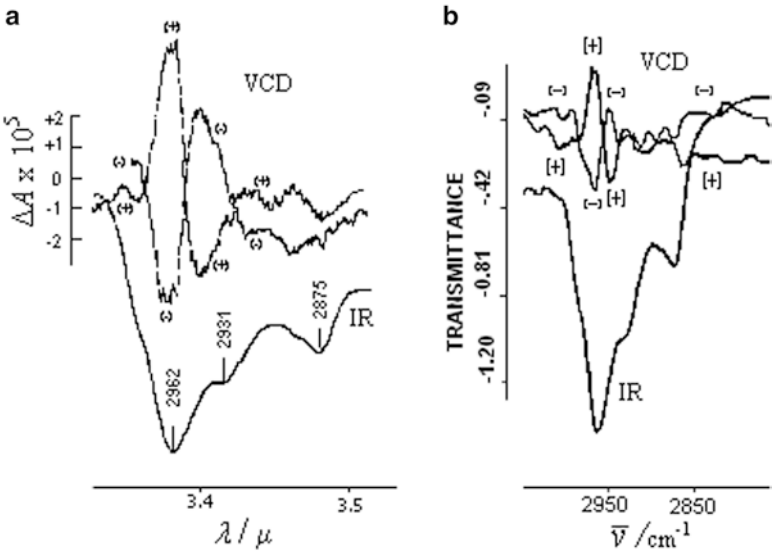

Fig. 7 VCD and IR transmission spectra of (+)-camphor (**16**) and (–)-camphor (**20**) in CCl_4: (**a**) recorded in a scanning dispersive VCD instrument and (**b**) recorded in a FT IR-VCD instrument (Adapted from (*50*, *59*))

3.1 VCD-FT Spectrophotometer

A FT-VCD spectrophotometer is in fact an instrumental version for chiral detection of IR radiation, for which a schematic optical diagram is shown in Fig. 8. A polychromatic IR radiation coming from a glower source is collimated and directed to a beam splitter, the central component of an interferometer. The two beams emerging

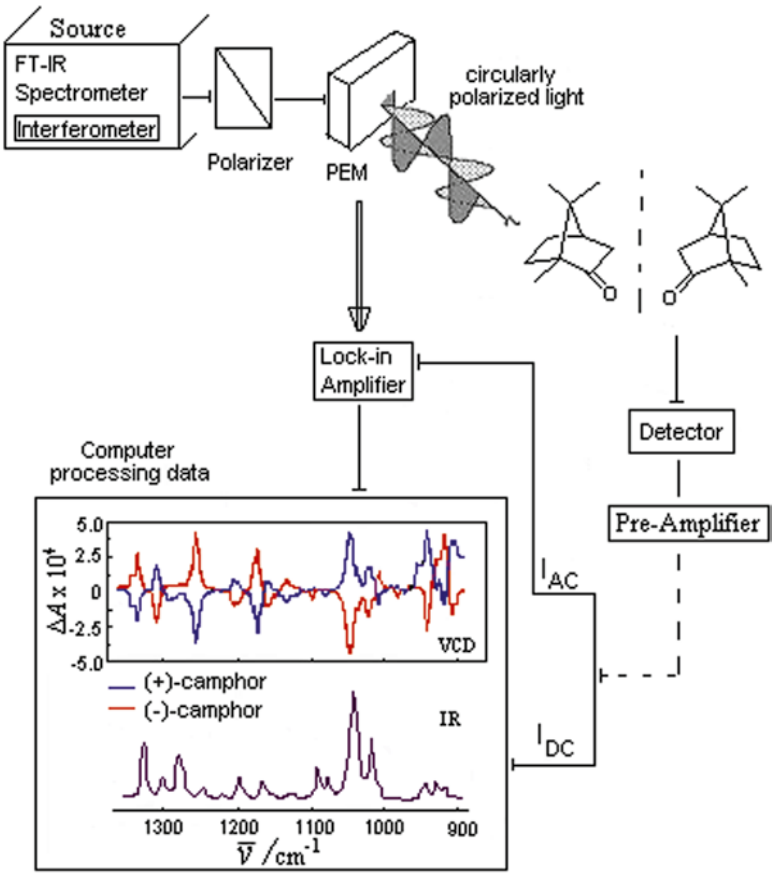

Fig. 8 Block diagram of the optical-electronic layout of a VCD spectrophotometer

from the splitter are reflected and transmitted in such a way that optical phase retardation appears between them. When the retardation is varied and the data collected, an interferogram is created. Each spectral point in the interferogram is encoded with a *Fourier* frequency.

After the interferometer, the radiation passes through an optical filter and then to a polarizer. The polarized light passes through a ZnSe PEM modulator, mechanically stressed by an adjacent piezoelectric transducer, which alternates radiation between right and left cpl chiral beams, of the same intensity, in the frequency range of tens of kHz. Polarized modulated light can then cross the sample containing a chiral molecule to produce an attenuated signal as a result of the differential absorption (A_R–A_L) in each spectral point of the interferogram encoded with VCD modulated intensity at *Fourier* frequency. The light reaching the detector is time-modulated at the PEM frequency according to the interferometer setup. A transducer in the detector converts energy to an electric signal. Phase-locked amplification of the signal provides simultaneously a DC signal (IR) and an absolute configuration signal (VCD). The lock-in amplifier demodulates the VCD spectral information.

VCD intensities are typically four to five orders of magnitude smaller than their parent IR intensities (*62*), thus the spectrophotometer requires operation with very sensitive components and time-averaging over relatively long intervals of time. The use of ZnSe photoelastic modulators and high-sensitivity detectors with low noise, as MCT (HgCdTe), provide spectral resolutions in the range 1–64 cm^{-1}, and birefringence artifacts manifested as deviations of the baseline from zero are reduced by the adaptation of a second PEM, after the sample, in an arrangement known as dual polarization modulation (DPM) that improves stabilization and adjustment to nearly zero baseline, allowing VCD measurements across a large spectral range with high quality. The comparison of VCD spectra of (–)-(*S*)-α-pinene with single modulation (SM) and DPM adaptation is shown in Fig. 9 (*63*). Artifact signals have also been reduced by using lenses to manipulate the beams after light has been circularly polarized (*64*, *65*).

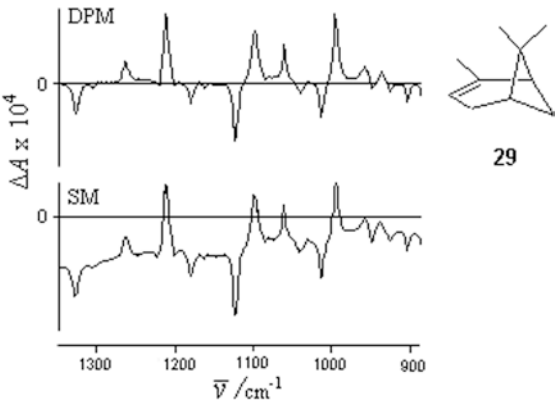

Fig. 9 Comparison of the FT-VCD spectra of (–)-(1*S*)-*α*-pinene (**29**) recorded under single modulation (SM) scanning and under dual polarization modulation (DPM). (Adapted from (*63*))

To settle the conditions for VCD measurements, the sample, solvent, concentration, and pathlength, are adjusted by recording the absorption spectrum. However, due to the low VCD sensitivity, experimental measurements typically require some 5–10 mg of sample (*16*), although in very favorable cases it has been possible to manage with as little as about 2 mg of sample. It is worth mentioning that for ECD, 1 mg of sample or less is enough (*35*). Typically, for VCD measurements 0.15 cm^3 solvent are used, while a typical ECD measurement can be performed in a 1 cm^3 solution. Using the solvent as a blank reference for VCD is acceptable. Ideal solvents for VCD measurements of natural products in the mid-IR region, are $CDCl_3$, CCl_4, and CS_2 because they do not absorb in the studied region, or alternatively CD_3CN and DMSO-d_6 for polar compounds (*66*, *67*). For those samples with very low solubility that cannot be measured in solution, film methods may eventually be adapted (*68*, *69*). Solid-state sampling methods include mulls, pellets, and a spray technique that allows for the deposition of finally divided particles to create a thin film.

Thin solid samples are superimposed with artifacts that are large contributions of linear birefringence and linear dichroism; these artifacts can be eliminated by a theoretical approach that extracts the true VCD spectrum (*70*).

The optimum decadic absorbance (*A*), or attenuation of the transmitted IR beam, is chosen according to the sensitivity of the detector (a value of *ca.* 0.4 a.u. is usual for a limited-noise detector) (*62*). Since, in practice, VCD measurements may lead to saturation of the detector signal, with the consequent reduction in sensitivity, a filter is placed before the detector. Alternatively, the use of a dual source in a four-port interferometer FT-IR, increases the *S/N* ratio by a factor of two compared to single source operation (*71*).

At the end of the experiment, collected data are stored and digitized by *in silico* software, which allows obtaining the IR and VCD spectra. Noise and reproducibility, as well as enhancing signal measurability and discrimination are carried out by rapid-scan VCD methods or by the digital signal processing (DSP) method. Both methods produce high-quality VCD spectra for solution phase rigid chiral molecules and qualitatively reasonable good spectra for biologically related molecules (*72*).

The first commercially available VCD spectrophotometer was the Chiral*IR* brought to market by Bomem/BioTools, Inc. in 1997 (7). Currently, FT VCD instruments from Thermo-Electron, JASCO, and Bruker (*73*) are also available but less widely distributed. Recently, a compact dispersive VCD instrument for the accurate analysis of peptides and proteins in the mid-infrared amide I and amide II regions was reported (*74*).

In the absolute configuration assessment of natural products, an advantage of VCD over optical rotation determinations is that possible interferences due to an achiral impurity in the sample are reduced. Moreover, if the sample is not 100% enantiomerically pure the assignment may still be carried out (*7*). The experiments are not highly time-demanding (around 5 h collection for a 0.1–0.2 *M* solution sample) in an easy-to-use instrument. Besides, it has been observed that for structurally closely related compounds, it is possible to generalize the stereochemical assignments through VCD signatures, such is the case of 3α,6β-disubstituted tropane alkaloids (*55*, *75*–*77*) where the sign of the bands of vibrational modes associated with the 1,150–950 cm^{-1} region, a region of mirror-image bands corresponding to the N–C and O–C stretching vibrations, is highly sensible to configuration (Fig. 10) (*75*), and has been of support to determine the absolute configuration of (–)-(3*R*,6*R*)-dibenzoyloxytropane (**31**) and of its antipode (+)-(3*S*,6*S*)-dibenzoyloxytropane (**32**) separated by enantioselective HPLC (*76*).

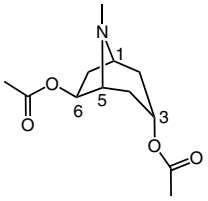

30

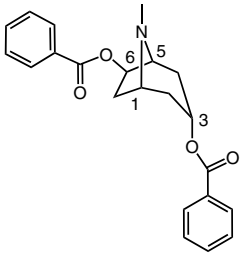

31

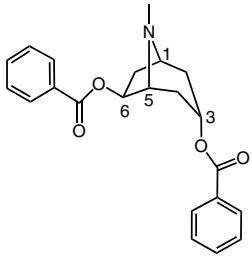

32

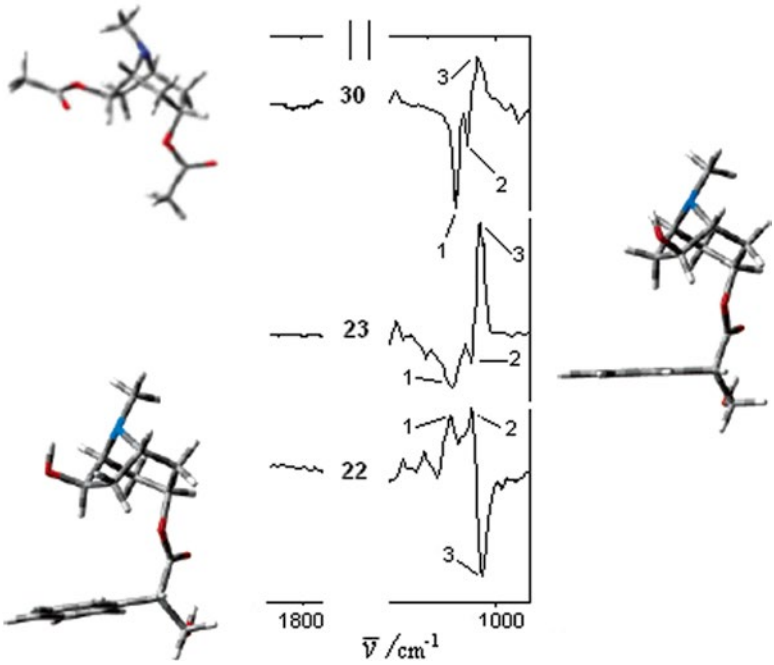

Fig. 10 Regions of the experimental VCD spectra of tropanes (1*R*,3*R*,5*S*,6*R*,2′*S*)-**22**, (1*S*,3*S*,5*R*,6*S*,2′*S*)-**23**, and (1*S*,3*S*,5*R*,6*S*)-**30**. (Adapted from (*75*))

The VCD method has been more fully exploited since a substantial progress in the theoretical prediction of VCD spectra was achieved (*39*, *44*, *62*). Spectral extension into the near-IR region as far as 10,000 cm^{-1} is commercially feasible (*7*, *78*). Considerable levels of sophistication have been made to VCD spectrophotometers, so as to use an infrared femtosecond laser source synchronized to the natural frequency of a photoelastic modulator, which has given rise to new techniques such as time-resolved vibrational spectroscopy that is employed currently in many areas of chemistry and biochemistry to unravel the fast kinetics and mechanisms of photo-induced reactions (*79*, *80*). Furthermore, innovative technology to measure chiroptical properties is provided by heterodyne-detected *Fourier*-transform spectral interferometry (*81*) in which a femtosecond IR pulse is used to characterize fully the phase and amplitude of the vibrational optical activity free-induction-decay field, providing VCD and ORD measurements altogether through the spectral interferograms. In addition, two-dimensional correlation spectroscopy (2D-COS) has been applied to VCD–VCD, IR–IR, and VCD–IR spectral analysis of L-alanine, demonstrating that 2D-COS vibrational methodology provides enhanced chemical information over traditional 1D spectra (*82*).

4 Theoretical Calculations

VCD spectroscopy is a powerful technique not only for analyzing chiral static in stereochemistry, but also for studying dynamic stereochemistry in asymmetric reactions and conformer landscapes. Moreover, VCD is endowed with all of the benefits of IR spectroscopy, being sensitive to molecular changes of intrinsic character, like bond strength, atomic mass, and extrinsic character, such as non-covalent intermolecular interactions (*i.e.* H-bonding) (*83*, *84*). *Ab initio* quantum chemical calculations based on *Hartree-Fock* (HF) (*85*) or density functional theory (DFT) (*86*) methods have proven useful in the prediction of VCD spectroscopic properties. Commercially available software packages, such as Gaussian 03 and 09 (Gaussian Inc., Wallingford, CT) include absorption and VCD dipolar and rotational strengths calculations from which basic relationships between chiroptical properties and molecular structure are properly addressed. Full VCD quantum chemical treatments do not require any *a priori* model hypothesis or approximation and are used successfully to assign absolute configuration of natural products without time-scale restrictions because of molecular size, but because of dealing with molecules having too many conformational degrees of freedom (*87*). In such a case approximated *ab initio* routines (*39*, *88*) have been written and applied satisfactorily, as, for example in VCD studies of polymeric biomolecules such as DNA or proteins, maintaining a good calculation cost-to-benefit ratio. The formalism of a model that explains vibrational transitions measured by CD differential absorption is based on energy transfer between electric and magnetic dipolar moments in the ground electronic state. A short discussion on the basic principles of vibrational theory that gave rise to the quantum mechanical model, from the perspective of experimentalists, rather than a more rigorous treatment, is presented in this section. This is intended to provide insight in order to decipher information from VCD spectra, and to be aware of how these critical aspects of molecular geometry and conformation that stimulate VCD spectroscopic changes may lead to entangling the chiral recognition of stereoisomers. The advanced treatment of VCD theory for the design of chiral computational methodology has been compiled in a very satisfactory manner in the literature (*39*, *89*–*92*).

4.1 Fundamental Parameters

4.1.1 Dipolar and Rotational Strengths in VCD Transitions

As for electronic transitions (*35*), each independent vibrational transition in the molecule is defined by an electric $(\vec{\mu})$ and a magnetic $(\vec{m})$ transition dipolar moment. However, vibrational motions, or modes, are carried out mainly by nuclei and as a consequence electronic redistributions during vibrational transitions may be considered independent of nuclei motions (*Born-Oppenheimer* approximation). Normal vibrational modes are related to fundamental transition bands in IR spectroscopy,

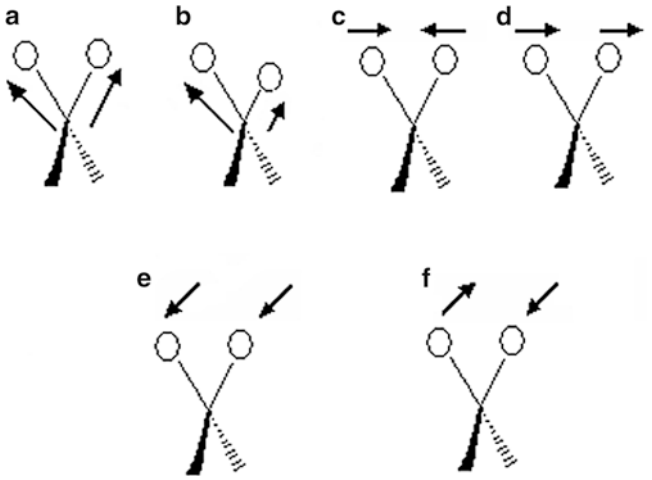

Fig. 11 Vibrational normal IR modes of a CH_2 group. Stretching: **a**, symmetric (ν_s); **b**, asymmetric (ν_a). Bending: **c**, in-plane scissoring (δ_s); **d**, in-plane rocking (ρ_s); **e**, out-of-plane wagging; and **f**, out-of-plane twisting (τ)

with an example presented in Fig. 11 for a methylene group (*93*). The number of normal vibrations for a non-linear molecule with N atoms is 3N−6. Vibrations are usually complex combinations of normal modes, and the most simple organic molecule, CH_4, a spherical top molecule, has four normal modes of vibration, one totally symmetric, $\nu_1(a_1)$, one doubly degenerate, $\nu_2(e)$, and two triply degenerate, $\nu_3(f_2)$ and ν_4 (f_2) (*94*). Note that all possible vibrational-mode degeneracies in achiral molecules vanish in chiral environments.

In each vibrational mode, atoms oscillate at the same frequency and around an equilibrium position during the transition. The amplitude of such oscillations is very small (0.01–0.1 Å). Bond electrons clouds are shifted to the most electronegative atom giving place to a dipolar moment with two transition components, the electric component due to a linear charge displacement, and the magnetic component due to electron rotations. The time-dependence of the dipolar moment is sinusoidal.

During IR irradiation the electric field of light stimulates variation of the electric dipolar moment of molecular vibrations with a permanent dipole moment $\left(\vec{\mu} \neq 0\right)$. Each vibration is characterized by a resonant frequency and by an absorption intensity. The oscillator dipolar strength (D_i) is proportional to the integrated absorption intensity of a band in the IR spectrum, and is expressed as the square of the electric dipole moment in a transition between the initial (m) and the final (n) vibronic states (5) (*39*).

$$D_i \approx \left|\vec{\mu}_{mn}\right|^2 \tag{5}$$

When a chiral molecule is irradiated with cpl, circular dichroism will occur, occurring at frequencies of allowed vibrational modes, with changes in both electric

$(\vec{\mu}_{mn})$ and magnetic $(\vec{m}_{mn})$ transition dipoles. Simultaneous charge translation and rotation occur, but vibrational electric and magnetic dipole transition moments are promoted only if the vectors are neither zero nor orthogonal, thus the absorption intensity of a VCD band will be related to the rotational strength (R_i), which measures the magnitude of such dipolar transition moments. The oscillator rotational strength (R_i) is expressed as the imaginary part of the scalar vectors product of the electric and magnetic moments (6) (*7*).

$$R_i \approx \mathrm{Im}\left(\vec{\mu}_{mn} \cdot \vec{m}_{mn}\right) \tag{6}$$

In the configurational and conformational study of chiral molecules, using VCD quantum mechanical calculations, the goal is to evaluate the sign and intensity value of R_i strengths for each fundamental, combination and overtone bands belonging to active oscillators within the molecule.

The algorithm of quantum mechanical vibrational theory considers that the electric $(\breve{\mu})$ and magnetic $(\breve{m})$ dipolar moment operators consist of electronic (E) and nuclear (N) contributions applied to electronic and vibrational-harmonic wave functions, respectively. Thus, an axial polar tensor (APT) element (P^A) (*95*), which accounts for the change in dipole moment when an atom (A) undergoes a change in rotational strength, is defined in terms of independent nuclear and electronic contributions (7).

$$P^A = \left(\frac{\partial \vec{\mu}}{\partial R_A}\right)_O = E^A + N^A \tag{7}$$

Nevertheless, considering that the electronic contribution to the magnetic transition moment vanishes under *Born-Oppenheimer* approximation, a complex separable wave function, for which the electronic part depends on nuclear velocities as well as nuclear position has to be applied in the corrected *Born-Oppenheimer* approximation giving rise to an atomic axial polar tensor (AAPT) element (M^A) (*44*, *96*) to account for the simultaneous change of electric and magnetic transition moments. The dipolar (D_i) and rotational (R_i) strengths are then defined in terms of the AP and AAP tensors as indicated in (8) and (9) (*39*).

$$D_i = \left(\frac{\hbar}{2\omega_i}\right)\left(P_i^A\right)^2 \tag{8}$$

$$R_i = \hbar^2 \mathrm{Im}\left[P_i^A - M_i^A\right] \tag{9}$$

4.1.2 Computational Calculations of Dipolar and Rotational Strengths

Theoretical principles of vibrational optical theory are confined in thorough formalisms and approximations for the prediction of electric and magnetic dipole transition moments, which, in turn, determine the dipolar and rotational strengths. In the computation of dipolar strengths, the dipole moment derivatives are solved by analytical

gradient techniques and vibrational wave functions by programmable harmonic oscillators (*91*). In the theory of vibronic coupling (*43*, *97*), the derived expressions to calculate IR absorption and VCD utilize ground electronic state linear combination atomic orbital (LCAO) wave functions. However, in magnetic field perturbation (MFP) theory, an *ab-initio* approximation of AAPTs corrected *Born-Oppenheimer* wave functions is employed to calculate rotational strengths (*44*, *90*, *96*). The magnetic dipole vibrational transition moment is considered to be a contribution of the overlap between wave function derivatives. Computation of those derivatives with respect to nuclear coordinates provides then the electronic contribution to the magnetic dipole vibrational transition moment; a moment that is, otherwise, very small because it is originated from an induced infinitesimal electronic current near the nuclei (*91*). Visualization of the flow of electron density current due to nuclear motion is possible through the transition current density (TCD) application implemented in the AVS 5.0 program (Advanced Visual Systems, Burlington, MA) (*98*).

In the formalism of *ab initio* methods to calculate magnetic dipole transition moments, through polar tensors by HF and DFT methods, a condition called origin invariance (*99*) must be fulfilled. This condition assures origin independence of vibrational transition moments, a problem solved in the DFT calculation of rotational strengths by the introduction of perturbation dependent (PD) basis functions named gauge-invariant atomic orbitals (GIAOs) (*45*) which are also known as *London* orbitals (*85*, *100*). By using analytical derivative methods (*101*) for the calculation of harmonic force field (HFF) and the corresponding coupled-perturbed *Hartree-Fock* (CPHF) or *Kohn-Sham* (CPKS) DFT equations obtained from wave function derivatives, it is possible to calculate origin invariance VCD rotational strengths. The precise form of CPHF or CPKS depends on the nature of the perturbation on chosen atomic orbital (AO) basis set functions. In addition, velocity-gauge factors, which incorporate the dependence of the electronic wave function on an electron-velocity perturbation into the AO basis functions as a gauge transformation, have also been considered in the nuclear velocity perturbation (NVP) formulism of VCD theory (*102*). In completing this concise summary on fundamentals of VCD theoretical methodology, comment may be made that the normally observed steep rise in the level of theory, for high-level electron-correlation methods is provided by coupled cluster theory (*91*, *103*) and second-order *Møller-Plesset* perturbation theory (MP2) (*89*, *104*) VCD application. Nevertheless, their use pays for the cost of consumption of CPU resources and time. Robust program packages for VCD measurements include those suites in Gaussian (*105*), CADPAC (*106*), and Dalton (*107*), among others.

4.2 Density Functional Theory

As implemented in Gaussian 03 (*105*) and other programs (*106*, *107*), DFT assignment of absolute configuration includes geometry optimization with frequency analysis, providing thermochemistry, IR and VCD spectra calculations. Numerous examples, where DFT has calculated predicted VCD spectra or has confirmed experimental chiral assignments of natural products (*7*, *16*, *52*), have been reported since a

DFT-harmonic force fields study in 1994, demonstrating that DFT at the B3LYP/6-31G(d) and B3LYP/TZ2P levels of theory, as applied to (*R*)-4-methyl-2-oxetanone (**33**) gave superior results when compared to MP2 and self-consistent-field (SCF) methodologies (*108*). DFT includes electron correlation, thereby a reliable relationship of experimental to calculated data is expected to be obtained with higher accuracy than those methods that do not include this parameter (*89*, *108*, *109*). The first application of DFT to the calculation of atomic axial tensors (AATs) using analytical derivative methods and gauge-invariant atomic orbitals (GIAOs) on *trans*-2,3-d_2-oxirane yielded vibrational rotational strengths in better agreement with experimental data rather than comparable calculations at the HF level (*45*).

Based on an efficient algorithm in which the accent is placed on integral-direct techniques, DFT methods are able to calculate VCD spectra of molecules with 40–50 non-hydrogen atoms in a routine manner and at relatively low computational costs when compared to traditional methods. However, a rather difficult task is manifested when the molecule exceeds this size and many conformations populate the low-lying conformers in the potential energy map. An example is found in (–)-stypotriol (**34**), a pentacyclic ichthyotoxin isolated from the brown alga *Stypopodium zonale*, which was studied as the triacetate derivative (**35**), a molecule with 86 atoms, with 40 of these being non-hydrogen atoms ($C_{33}H_{46}O_7$) (*110*). This meroditerpenoid derivative has 300 electrons and is one of the largest natural products for which the conformation and absolute configuration were published using VCD and the DFT method at the B3LYP/DGDZVP level of theory. The optimization of each of six conformers required between 20 and 40 calculation cycles of 2.6 h each, followed by 100 h of vibrational calculations, when using a personal computer running at 3 GHz, to account for over 1,000 h of computational time (*110*).

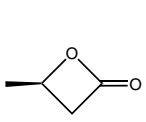

33

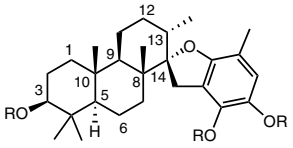

34, R = H
35, R = Ac

The reason for the VCD investigation of its triacetate derivative **35**, rather than stypotriol itself, refers to the use of a handy derivatization strategy (*111*, *112*) proposed to diminish the number of conformational arrays of a hydroxy free-rotor group in the molecule (*10*). In addition, acetyl groups are not particularly large groups that might complicate calculations because of an increase in the number of non-hydrogen atoms. Other advantages are that acetylated samples more easily dissolve in solvents with low dielectric constants, and that the broadening of VCD bands, which is linked to intermolecular H-bonding and is frequently observed in neat or solution analysis of alcohols (*112*), or carboxylic acids (*113*), under experimental concentrations used, may be avoided. Similarly, to eliminate the intermolecular H-bonding influence, carboxylic acids are best converted to their corresponding methyl esters (*114*, *115*).

In order to assure a trustworthy DFT comparison of calculated and experimental VCD spectra, simulated and observed molecules preferentially should be the same. However, in cases where the molecular size precludes obtaining the VCD spectrum in a reasonable time, calculating a molecular fragment as a model molecule, while maintaining the chiral portion intact is a strategy that often works out well. Such was the case for sargaol (**36**), a chromene with antioxidant properties that has in its structure a *tris*-isoprenyl chain linked to a 2*H*-benzopyranol through a stereogenic center, for which the absolute configuration was determined successfully by VCD methodology using DFT with the B3LYP hybrid functional and the DGDZVP basis set. These were applied to (+)-(*R*)-sargaol acetate (**37**) and to fragment models **38**–**40**, where the chain was simulated to be an ethyl group, or one and two isoprenyl units (*87*).

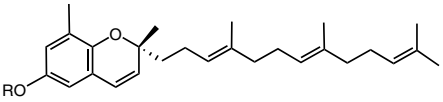

36, R = H
37, R = Ac

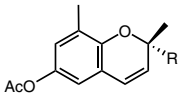

38, R = Et
39, R = $CH_2CH_2CH{=}CMe_2$
40, R = $CH_2CH_2CH{=}C(Me)CH_2CH_2CH{=}CMe_2$

Like the preceding work described for sargaol, the axial chirality of the (*S*)-curcuphenol dimers **41** and **42** was allotted through VCD analysis of the truncated model phenol atropisomer (*P*)-**43**, using the DFT B3LYP/6-31G(d) method (*116*).

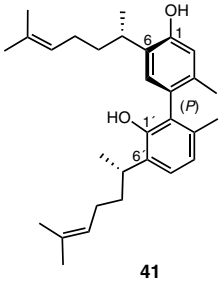

41

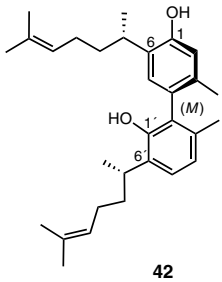

42

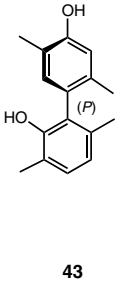

43

4.2.1 Hybrid Functionals and Basis Set

For many electron systems such as non-hydrogen atoms and molecules, the DFT modeling method would be precise if the exact exchange-correlation functionals were known. However, this part of the total-energy functional remains unknown using in the *Kohn-Sham* DFT treatment and must be approximated (*86*, *117*). The popular *Becke*-3-*Lee-Yang-Parr* (B3LYP) hybrid functional (*118*), for which an approximation comes from the exchange energy calculated from HF theory, is one the most widely used and reliable functionals (*108*, *119*, *120*) for VCD measurements, even though this functional has no foundation to describe the density transfer response, which is the fundamental property in VOA measurements (*91*). Other hybrid functionals used in VCD computational methodology are those using

the *Perdew–Wang* non-local correlation functional (PW91) derived from non-empirical generalized gradient approximations (GGA's) (*121*, *122*), as the hybrid functional B3PW91 (*46*, *90*, *120*), and the local spin density approximation (LSDA) (*108*, *123*). The power of DFT methodology to estimate the rotational strengths of the acetate derivatives of (+)-(*R*)-2-(1-hydroxyethyl)-chromen-4-one (**44**) and (+)-(*R*)-6-bromo-2-(1-hydroxyethyl)-chromen-4-one (**45**) using B3LYP and B3PW91 functionals and the TZ2P basis set allowed the comparison of functionals, which led to the result that B3LYP gives closer frequency values to experimental readings than does B3PW91 (*11*). However, the hybrid functional B3PW91 and the high level double polarized DGDZVP2 basis set improved visualization of the carbonyl stretching region of the VCD spectrum of (+)-(4*R*,9*R*,10*R*)-african-1(5)-ene-2,6-dione (**46**) as compared to the calculated VCD spectra at the B3LYP/6-31G(d) and the B3LYP/DGDZVP levels of theory (*124*). The carbonyl region of the polarized vibrational spectrum is frequently obscured by the presence of artifacts (*125*).

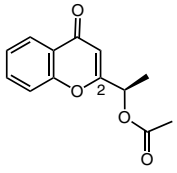

44

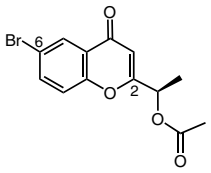

45

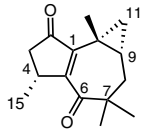

46

Functionals and basis sets with polarization functions and with or without diffuse functions are available for DFT-VCD calculations (*126*). The Gaussian basis sets double zeta valence plus polarization (DZVP) does not include *p* functions on hydrogen, and are optimized for local density functionals (*127*), thereby assuring efficiency and good level calculations. The value of the basis set in the theoretical VCD approaching methodology was analyzed for (–)-myrtenal (**47**), an oxygen-containing monoterpene of the pinane series (*128*). Since rotational strengths depend on conformation, a conformationally fixed chiral molecule such as myrtenal with only two conformers in an equilibrium highly biased towards one side was considered ideal for the study conducted (Fig. 12). Moreover, myrtenal is a molecule with only 11 non-hydrogen atoms ($C_{10}H_{14}O$) and 82 electrons, and therefore a good candidate to

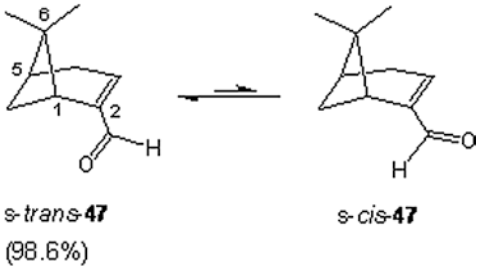

Fig. 12 Conformational equilibrium of (–)-(1*R*)-myrtenal (**47**)

ascertain the relationship between invested computer time and spectral accuracy. VCD spectra were simulated with the B3LYP functional and the polarized basis sets 6-31G(d,p), 6-31G+(d,p), 6-311G+(d,p) cited in order of increased level of theory, as well as for the DFT optimized DGDZVP and DGTZVP basis set using B3LYP and B3PW91 functionals. Comparisons between experimental and calculated VCD spectra were analyzed with the (*S*)/(*R*) neighborhood similarities in the Compare*VOA* program (*126*, *129*, *130*), which is based on a confidence level algorithm that provides the calculated optimized frequency scaling and shifting as an anharmonicity factor (an*H*) for each trial (Table 1). The band-to-band matching between experimental and calculated spectra is assessed through the similarity indexes (S_{IR}) for IR and (S_E) VCD spectra. The enantiomeric similarity index (*ESI*) leads to an unambiguous chirality assignment. It is worth mentioning here that there are other quantitative methods to accomplish absolute configuration assignments: the linear regression of theoretical-to-experimental rotational strengths (*90*), the SimIR/VCD method (*131*), in which the predetermined limits of the similarity index, S_V, allow the investigator to verify the confidence level for a comparison, and a recently introduced method that quantifies the agreement between the experimental and calculated VCD spectra through the so-called similarity of dissymmetry *g*-factor spectra (*132*).

Table 1 Confidence level data for (–)-(1*R*)-myrtenal (**47**)

B3LYP/Basis set	(an*H*)[a]	(S_{IR})[b]	(S_E)[c]	(*ESI*)[d]	*t*/h
6-31G(d,p)	0.978	84.4	83.5	79.6	4.6
6-31G+(d,p)	0.982	85.5	84.1	80.0	7.2
6-311G+(d,p)	0.984	85.2	85.2	82.1	11.5
DGDZVP	0.980	85.0	85.0	76.5	2.7
B3PW91/DGTZVP	1.007	83.3	83.3	74.5	3.4

[a]Anharmonicity Factor
[b]IR spectral similarity
[c]VCD spectral similarity for the correct enantiomer
[d]Enantiomeric similarity index

VCD spectra at the various levels of theory showed no significant differences (spectra are shown in the next section). However, the computer time invested using the DGDZVP basis set was a quarter of that using 6311G+(d,p). The reliability in the theoretical prediction of vibrational frequencies, disclosed through the closeness of an*H* values to the unit, indicates that the DGauss basis set DGTZVP is more accurate than the split valences basis sets 6-31G(d,p), 6-31G+(d,p) and 6-311G+(d,p). The S_E and *ESI* similarity parameters confirmed that (-)-myrtenal (**47**) has the absolute configuration (1*R*,5*S*). The nomenclature is in agreement with the hierarchical digraphs application to the *Cahn-Ingold-Prelog* (*CIP*) rules (*133*). Considering that the *ESI* value is high and obtained in the shortest computer time using the B3LYP/DGDZVP combination, it was concluded that this level of theory provides a superior balance between computer cost and VCD spectral accuracy. The present authors consider, however, that the predictive value of the DFT methodology applied to VCD measurements is not limited to configurational assignments; thus a careful

consideration of simulation purposes linked to structural features of each tested molecule must guide the choice of the theoretical methodology if one wishes to obtain meaningful results.

Within the circumstances that may affect the theoretical prediction of VCD spectra is the solvent effect on polar (*134*) or encaged molecules (*135*), since it has been demonstrated that chirality transfer from the chiral molecule to the achiral solvent is likely to occur (*136*, *137*). This is especially true when the solvent participates in aggregation phenomena, in many cases due to hydrogen-bonding (*138*, *139*). In such a case, a possible way of tackling the problem is to make an initial molecular dynamic search to locate solvent in the solvation shells (*140*). Another way is to calculate the VCD spectra with explicit solvation using compatible DFT models, *i.e.* polarizable continuum model (PCM) (*141*, *142*) or the continuous surface charge adapted polarizable continuum model (CSC-PCM) (*143*). For molecules with non-specific intermolecular interactions, and when *Fermi* resonances are absent, the neglect of intermolecular interactions (solvent effects) in calculations does not appear to be serious (*45*, *144*).

4.3 Conformational Optimization and Graphical VCD Methods for Absolute Configuration Assignment

In the theoretical search for configurational assignment of natural products, the spectra and conformation(s) of the molecule are predicted at the hybrid functions and basis set chosen. In our hands, the best procedure to calculate a VCD spectrum starts with the proposition of an initial molecular geometry and chirality for the studied molecule followed by a conformational rotational-circuit landscape study using a molecular mechanics force field program (*145*). For example, the Monte Carlo in Spartan 04 (Wavefunction. Irvine, CA) suite of programs may be used or Hyperchem (Hypercube Inc., Gainesville, FL), which provide the lower-lying conformers within a window of 40 kJ mol^{-1}. A single-point pre-optimization of the selected conformers using DFT at the B3LYP/6-31G(d) level is advised before optimization using Gaussian 03, Gaussian 09, or any other reliable computational software. At this point it is necessary to lessen the motifs of the conformational landscape, especially for those molecules having many insignificantly populated conformers (less than 2%), for the sake of maintaining a satisfactory balance between invested computing time and the spectral similarity of calculated-to-experimental VCD spectra, so a cut-off between 8 and 12 $kJmol^{-1}$, or above 95% population, is carried out. After the geometry minimization process, a *Boltzmann* weighted equilibrium average of conformers, using free energies at 298 K, is due for all low-energy lying conformers. Rotational strengths are then calculated for each conformer and the corresponding VCD spectrum is obtained by conversion of output data to Lorentzian bands with programs like Origin from OriginLab, PeakFit from SeaSolve Software Inc., or *View*VCD™ from BioTools Inc. (for Gaussian 09)

using band widths of 6 cm^{-1} and an anharmonicity factor (an*H*) of around 0.97 applied to the wavenumber values, in cm^{-1}. The an*H* factor compensates theoretical harmonic frequencies used to simulate real anharmonic vibrations. At the final step, *Boltzmann* weighted IR and VCD spectra are obtained.

The degree of similarity between the measured and the calculated VCD spectra can be ascertained graphically by linear regression plots of the observed rotational strengths *vs*. the calculated ones for each enantiomer. The absolute configuration is then allotted according to the slope, with a positive slope (ideally equal to unity) expected for the correct enantiomer and a negative slope for the mirror image (*7*, *14*). The absolute configuration determination of (+)-frontalin (**48**), a pheromone of the beetle *Dendroctonus frontalis*, illustrates the VCD method neatly since calculated-to-experimental rotational strengths (R_i) linear regression curves of both enantiomers indicate through the agreement of slope +1, the configuration of (+)-**48** to be (1*R*,5*S*) and the agreement of slope –1, the antipode (–)-(1*S*,5*R*)-**49** (Fig. 13) (*146*).

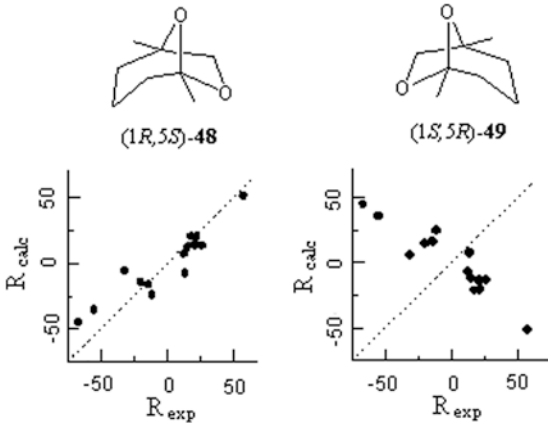

Fig. 13 Comparison of rotational strengths ($R/10^{-44}$ esu^2 cm^2) for (+)-(1*R*,5*S*)-frontalin (**48**) and its antipode (–)-(1*S*,5*R*)-**49**. (Adapted from (*146*))

Alternatively, a manual peak sequential assignment of IR and VCD measured spectra is advised preceding peak-to-peak visual comparisons of IR/IR and VCD/VCD calculated and measured spectra. The correct enantiomer or chiral diastereomer, if such is the case, gives a theoretical spectrum in agreement with the experimental spectrum. By following this method, the absolute configurations of the 3α,6β-disubstituted tropane alkaloids **22**, **23**, and **30** (Fig. 10) were assigned (*55*, *75*). Advantages in labeling IR and VCD peaks, either by sequential numbering or by frequency values, provides an accessible way to identify vibrational normal modes (*11*–*13*, *147*) and the likely identification of configurational VCD signature bands (*75*).

In the case of (–)-myrtenal (**47**) mentioned above (*128*), the sequential numbering of IR and VCD bands in the experimental spectrum (Fig. 14) allows

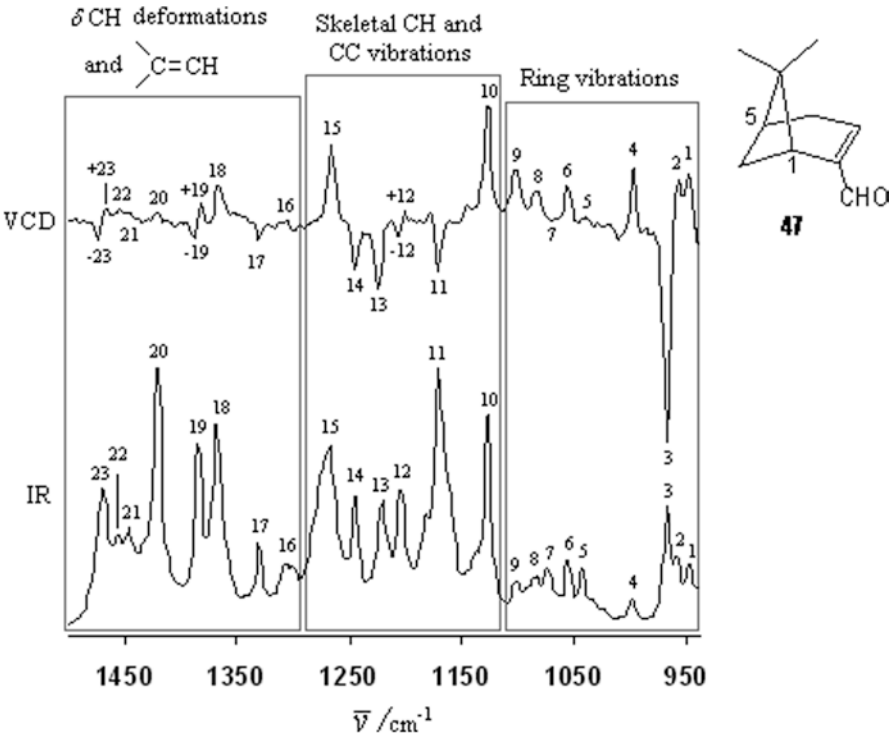

Fig. 14 Sequential band assignment of measured vibrational spectra of (–)-(1*R*)-myrtenal (**47**). Bisignated bands are labeled with (–,+) signs to indicate the presence of positive VCD couplets

identification of regions of important CH and CC vibrations from which chiral methine C-1–H and C-5–H fundamentals may be associated clearly to the cyclobutane ring vibration region (*ca.* 1,000–960 cm^{-1}) (*148*), the region of highest intensity in the VCD spectrum. VCD couplets must be allied to coupled oscillators.

The s-*trans* and s-*cis* (Fig. 12) conformers were submitted to geometry optimization using DFT calculations at the B3LYP/6-31G(d) level of theory using Spartan 04. The atom coordinates of the optimized structures were then exported to Gaussian 03 for the free energy calculation at 25 °C. The population percentage reported in Fig. 12 takes into account ΔG values calculated at the B3LYP/6-31G(d,p) level of theory. Since population of the s-*trans* conformer is higher than 98%, the s-*cis* conformer was not considered for VCD spectra calculations. VCD spectra comparison is shown in Fig. 15.

In another example, the absolute configuration of 7,9-diacetoxylongipin-2-en-1-one (**50**) was assigned by VCD using DFT at the B3LYP/DGDZVP and B3PW91/DGDZVP levels of theory (*149*). This sesquiterpene is member of a very large family of longipinene derivatives (**50**–**54**) isolated from *Stevia* (Asteraceae) species.

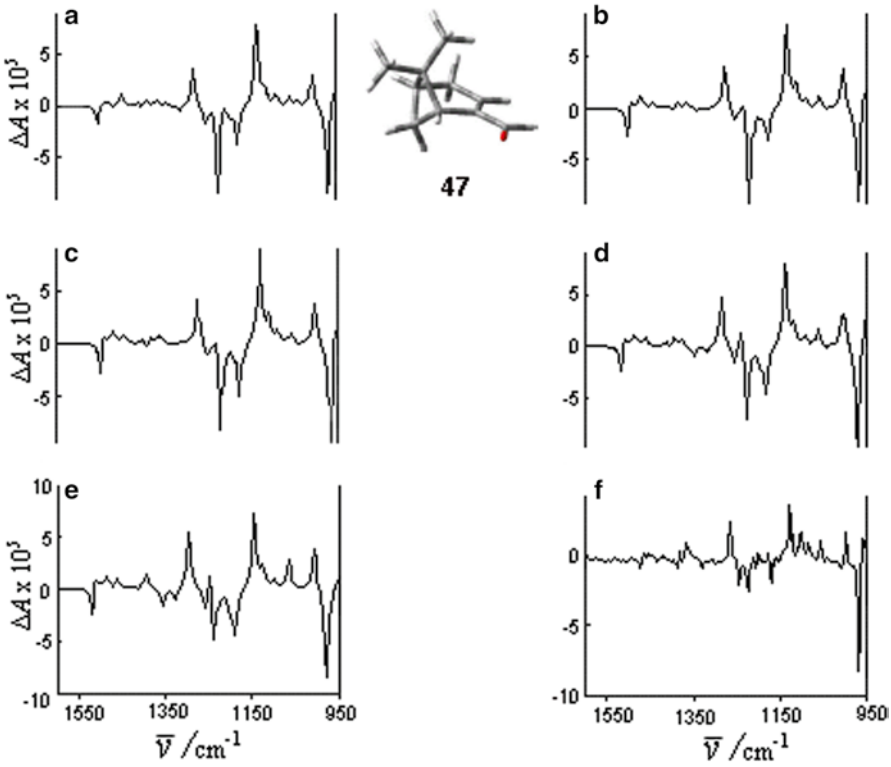

Fig. 15 VCD spectra of (–)-(1*R*)-myrtenal (**47**) calculated using DFT with the B3LYP hybrid and the following basis set: (**a**) 6-31G(d), (**b**) 6-31G+(d,p), (**c**) 6-311G+(d,p), (**d**) DGDZVP; (**e**) using the B3PW91/DGTZVP level of theory, and (**f**) experimental. (Adapted from (*128*))

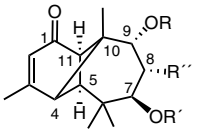

50, R = R´= Ac, R´´= H
51, R = R´= R´´= H
52, R = R´= H, R´´= OH

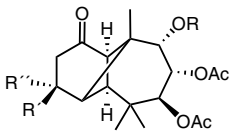

53, R = H, R´= Me, R´´= H
54, R = Ac, R´= H, R´´= Me

A search for the stable conformations using random Monte Carlo simulations gave rise to only two conformers obtained in a 9:1 ratio. The *Boltzmann* weighted conformational average IR and VCD spectra were obtained by applying an*H* factors of 0.98 and 0.97 to the B3LYP and B3PW91 vibrational frequencies. The experimental VCD spectrum displays two bisignated couplets, one at around 1,250 cm^{-1} of negative chirality (+,–), and the other at around 1,000 cm^{-1} with positive chirality

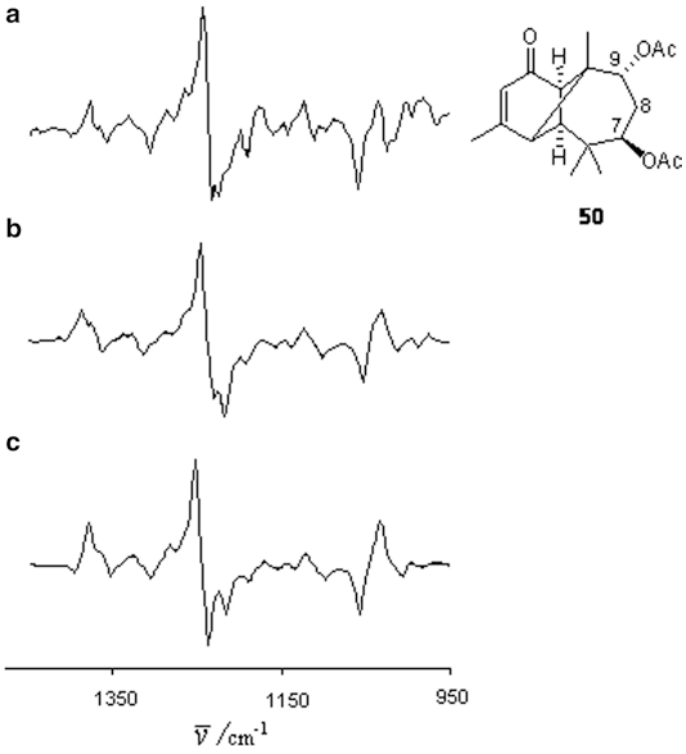

Fig. 16 VCD spectra comparison for (4*R*,5*S*,7*R*,9*R*,10*R*,11*R*)-longipinane **50**: (**a**) experimental, calculated at: (**b**) B3LYP/DGDZVP and (**c**) B3PW91/DGDZVP. (Adapted from (*149*))

(–,+) (Fig. 16), which are perfectly simulated by both, B3LYP and B3PW91, hybrid functionals in the calculated VCD spectra, and allow assignment of the absolute configuration of **50** as (4*R*,5*S*,7*R*,9*R*,10*R*,11*R*), in accordance with the assignment made by ECD (*150*).

Since the differences between the two calculated spectra are minimal, it was concluded that the B3LYP/DGDZVP method has an advantage over that using B3PW91/DGDZVP, since it allows an increase of calculations cost-to-benefit ratio. In addition, the chiroptical sensitivity of the VCD-DFT methodology was tested by means of the spectral comparison of epimeric longipinanes **55** and **56** with longipinane **50** (Fig. 17).

The couplet at *ca.* 1,250 cm^{-1} is of opposite chirality in longipinanes **55** and **56**, which are diastereomeric at the C-7 and C-9 centers. The chirality of the same couplet for longipinane **50** resembles that in **55**. However, the *C*Es of some bands in the 1,100–950 cm^{-1} region are of opposite sign, thus giving a clear indication of the change of configuration of the C-9 center. These observations allowed the conclusion to be made that theoretical VCD methodology at the B3LYP/DGDZVP level is sensitive enough to distinguish longipinane diastereomers.

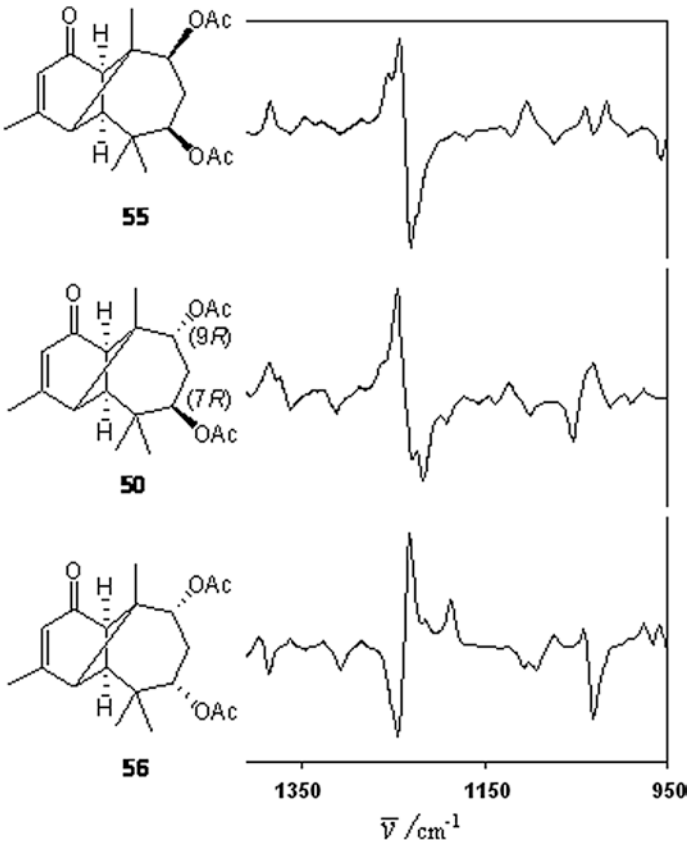

Fig. 17 Calculated VCD spectra for longipinanes (7*R*,9*S*)-**55**, (7*R*,9*R*)-**50**, and (7*S*,9*R*)-**56**. (Adapted from (*149*))

5 Studies of Natural Products and Some Chiral Structurally Related Molecules

Produced by plants and other organisms, terpenes are among the most important secondary metabolites in Nature. Terpenoids possess biological and biogenetic activity acting as building blocks of many other metabolites, vitamins, and more complex natural products; their oxidized and rearranged forms are used in industry as flavor additives for foods and fragrances. The legacy of terpene chemistry was enriched by the work of *Otto Wallach* by the end of the nineteenth century who established the structural transformations observed in monoterpenes, diterpenes, and triterpenes (*151*). More than a century has passed since this time and terpenoids are still challenging organic chemists to unravel the mysteries of Nature hidden in the chirality of their splendid but complex stereo-structures. As part of this group of

modern methods to assess the absolute configuration of terpenes in solution, ECD (*6*, *15*, *152–156*) and VCD (*7*, *16*, *52*, *90*, *155*, *157*) are two of the most widely used techniques. The most recently developed method VCD has the potential of not only to providing chiral stereogenic descriptors based on a larger number of diagnostic bands, combined with a relatively easy way of simulating a spectrum to decipher chiral information when compared with ECD (*158*). VCD relates details of three-dimensional structures such as conformation, a dynamic molecular property, with chirality, a static feature.

5.1 Fundamentals in the Interpretation of VCD Spectra

5.1.1 The Local Model

The initial local model for vibrational circular dichroism (VCD) was proposed in 1972 and is known as a degenerate coupled oscillator (DCO) mechanism (*159*), a molecular excitation produced by interaction of local transition dipoles of a pair of oscillators, which are most likely, but not necessarily, related by symmetry in a molecule (*160*). Hence DCO is a dynamic coupling or exciton coupling such as that observed between two chromophores in ECD (*15*).

Vibrational modes of organic molecules are, quite often, displayed in the absorption spectra as a group, rather than a single vibration; thus, trying to decode molecular information from IR bands is not trivial. The DCO mechanism proposes to unravel such information by applying a local mode approximation. Overtone spectra of XH stretching transitions, where X is C, N, or O easily illustrate the point (*161*). A molecule containing more than one oscillator of the same type, *i.e.* the C–H bonds of a methyl group in acetaldehyde, exhibits coupled oscillators, observed as associated couplets, of predicted energy and intensity (*162*). In the spectrum (Fig. 18), one band corresponds to the non-equivalent in-plane C–H bond and the other to out-of-plane C–H bonds in the most stable conformer, where bond strengths and thereby band frequencies may be predicted by stereoelectronic theory named a *trans* effect (*163*), which takes into account the influence of the carbonyl π and the oxygen lone pair electrons on the proximate C–H bonds (*164*).

In the VCD spectra of symmetry-related molecules an exciton coupling results in a bisignated band (couplet). The couplet intensity and sign depend on the geometric arrangement of the oscillators in the molecule (*165*). DCO has been successfully applied to the study of steroids (*166*) and other natural products (*167*).

Recently, a method was reported to calculate near-infrared (NIR) and NIR-vibrational circular dichroism (NIR-VCD) spectra for (*S*)-camphor (**20**) and (*S*)-camphorquinone (**57**) in the fundamental and up to the second CH-stretching overtone region using the local mode approximation (*168*). Relevant differences in the vibrational circular dichroism (VCD) spectra (Fig. 19) were observed and predicted by a local approach through calculations of frequencies and of dipole and rotational strengths of isolated C–H stretching modes.

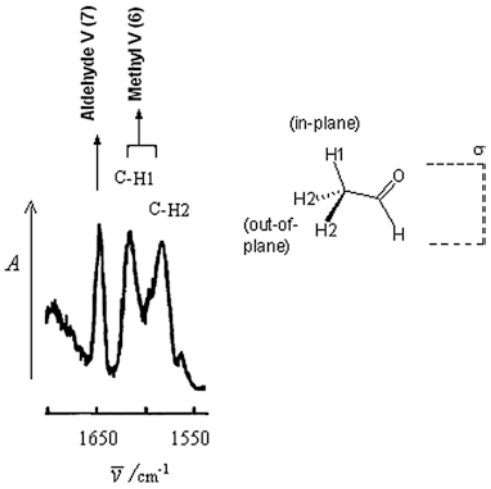

Fig. 18 Experimental overtone spectra of acetaldehyde ($\Delta\nu = 6$). (Adapted from (*162*))

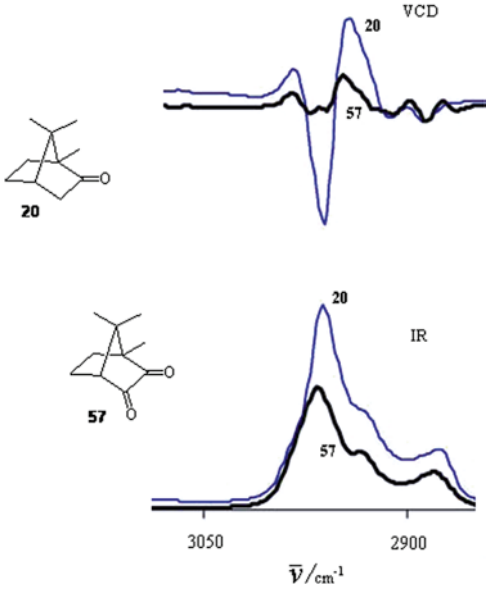

Fig. 19 Experimental IR absorption and VCD spectra of (1*S*)-camphor (**20**) and (1*S*)-camphorquinone (**57**) in the overtone C-H stretching region ($\Delta\nu = 1$). (Adapted from (*168*))

As observed, the bulk of vibrational C–H stretching modes broaden the IR band for both compounds precluding simple decode analysis of local modes; however, since several signated bands appear in the corresponding VCD spectra, single C–H oscillators were identified (*168*–*170*). The pertinence of coupled C–H oscillators of methyl *geminal* substitution, reflecting the symmetry of the lowest-energy molecular conformation (*171*), is of interest for study because *gem*-substitution is found in a considerable number of terpenes (*172*, *173*), thereby identifying its anisotropic *g*-character as an oscillator-chromophore (see definition below), and is perhaps useful for absolute configuration determination of a family of related natural products. A simple local mode procedure inherently neglects coupling between similar oscillators, but, however, a coupled oscillator model takes into account in-plane and out-of-plane C–H oscillators that in the case of chiral molecules become a "virtual chiral plane (σω)", such as that illustrated for the *gem*-dimethyl groups in α-pinene (**58**) (Fig. 20).

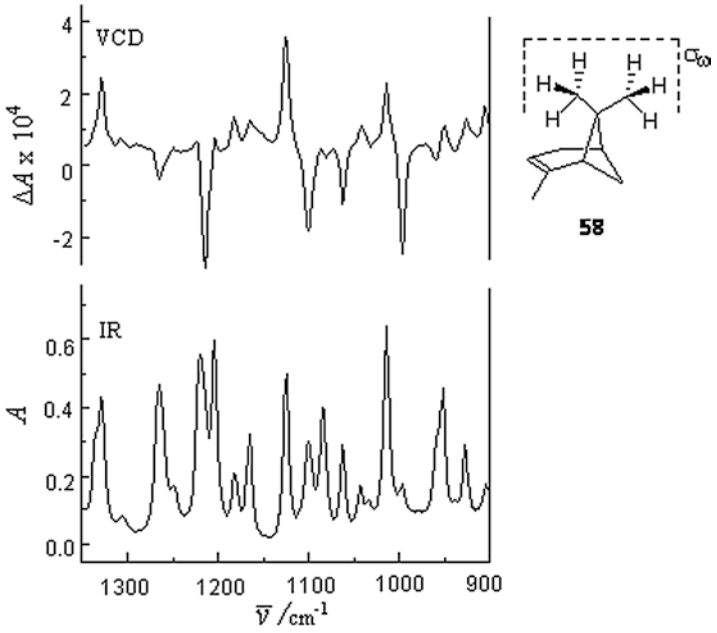

Fig. 20 IR and VCD spectra of (+)-(1*R*)-α-pinene (**58**) in the mid-IR region. (Adapted from (*51*))

In the VCD spectra of most natural products, the mid-IR region is important to analyze since it presents fingerprint bisignated bands due to C–H bending modes, as well as stretching and bending C–X modes (X = O, N). It is worth mentioning that recently a method based on exciton chirality in VCD was proposed to explain the interaction of two carbonyl chromophores giving rise to bisignated couplets of predicted chirality. This method is suitable to be used to analyze the absolute configuration of lactones and esters without having to resort to theoretical calculations (*174*).

5.1.2 Normal Versus Local Mode Assignment

Prior to the development of computational methods for the calculation of full VCD spectra by normal coordinate analysis, theoretical models using local approaches aided in establishing the mechanisms for relating molecular stereo-descriptors, like conformation and chirality, with the intensity and sign of VCD bands. Small chiral natural products such as monoterpenes were used mainly in the refinement and benchmarking of VCD theory (*46*, *175*, *176*).

Two mechanisms deserve mention: (1) The ring current mechanism applied to local vibrational motion within a ring closed by covalent or by intramolecular hydrogen bonding giving rise to monosignated VCD bands, and (2) The coupled oscillator mechanism due to the in-phase and out-of-phase coupled motion (see above) of two almost degenerate chirally oriented oscillators giving rise to bisignated VCD bands. In the first case the electronic motion does not follow perfectly nuclear motion but in the second instance it does (*177*, *178*).

Within the coupled oscillator mechanism and from the conceptual point of view, a dissymmetric chromophore oscillator is a molecular fragment for which the local symmetry is low to allow inherently electric and magnetic dipole associated transitions to occur (*179*). Coupling fragmenting of local modes such as CH_2–CH_2–C*H for the monoterpenes (–)-β-pinene (**59**), (–)-menthone (**60**), and (+)-isomenthone (**61**), among others, has helped to assign configuration using signated bands, in the fundamental C–H stretching region of VCD spectra. The comparison of the VCD spectra of menthone (**60**) with isomenthone (**61**) allowed conformational preferences to be manifested through locally defined coupled methylenes and methine modes in the above-cited fragment (Fig. 21).

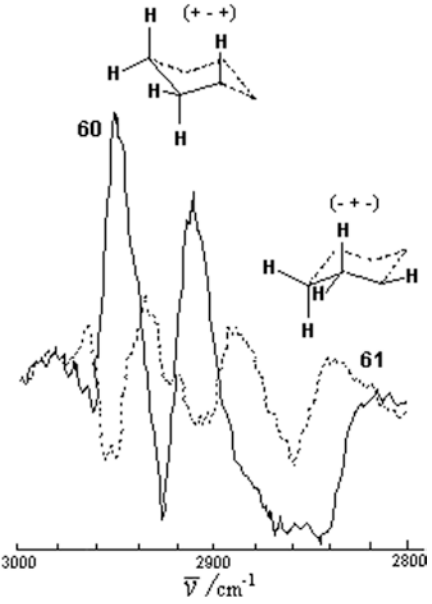

Fig. 21 VCD spectra of (–)-menthone (**60**) and (+)-isomenthone (**61**) in the 3,000–2,800 cm^{-1} region and the corresponding conformation of their six-membered rings (Adapted from (*179*))

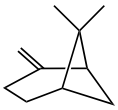

59

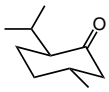

60

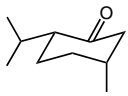

61

VCD spectra in the near-IR region for (+)-limonene (**18**), (–)-limonene (**19**), (–)-(*S*)-perillyl alcohol (**62**), (–)-(*S*)-perillaldehyde (**63**), (+)-(*R*)-*p*-menth-1-ene (**64**), and (+)-(*R*,*R*)-*p*-menth-l-en-9-ol (**65**) showed bisignated couplets ascribed to overtones associated with local CH stretching vibrations, where the ordering of signs in the couplets correlates with the known absolute configuration (*180*). However, the different behavior of a related non-natural cyclic compound prompted the authors to conclude that bisignated couplets are associated with a coupled normal mode behavior of the $CH_2CH_2C^*H$ fragment (*180*).

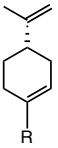

62, R = CH_2OH
63, R = CHO

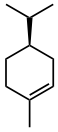

64

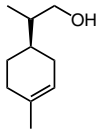

65

VCD spectra of a long list of enantiomeric monoterpenes were recorded in the 10,000–800 cm^{-1} region, including (–)-(*R*)-carvone (**66**), (+)-(*R*)-pulegone (**67**), (–)-(1*R*,2*S*,5*R*)-menthol (**68**), and (–)-(*R*)-camphorquinone (**69**) (*181*). Normal mode analysis of (+)-(*R*)-α-pinene (**58**), (–)-(*S*)-β-pinene (**59**), and (–)-(*S*)-verbenone (**70**) in the CH stretching and fingerprint region of the VCD spectra, was carried out to describe normal modes corresponding to identical molecular moieties or substructures, *i.e.* the four-membered ring with *gem*-dimethyl substitution of each monoterpene (*182*). In general, conformers of a given compound do not present substantial differences in band wavenumbers for equal normal modes, according to the analysis of potential energy distribution matrix descriptions (*183*, *184*), but differences in band intensity, magnitude and sign are often considerable (*182*, *185*–*187*). The bending δCH_3 normal mode at the four-membered ring appeared experimentally at 1,381, 1,393, and 1,386 cm^{-1} with (–), (+), (+) signs, for (+)-α-pinene, (–)-β-pinene and (–)-verbenone. Changes in the intensity and sign of vibrational modes in VCD spectra are also expected when the molecule contains a highly polar group such as the sulfonic group in (+)-(1*S*)-camphor-10-sulfonic acid (**71**) (*188*). The simulation of the IR and VCD spectra in the absence of hydration models produced important band-to-band mismatches with the corresponding experimental spectra in the 1,170–1,100 cm^{-1} region, where the νS–O stretching modes appear (*188*).

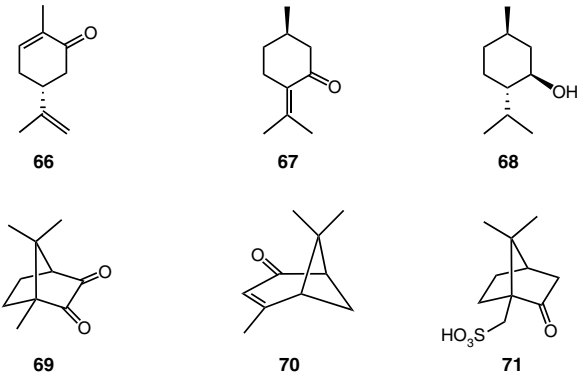

5.1.3 H-bonding and Solvent Effects. The Robust Mode Concept

Full DFT-VCD spectra in the 2,000–800 cm^{-1} region of 1-amino-2-propanol (*189*), a molecule that can be used as a model to investigate H-bonds in natural products, has allowed the assignment of normal modes corresponding to νOH stretching and δOH bending modes to bands at 1,272 and 1,412 cm^{-1}. By analogy, VCD spectra of (*R*)-2-(pyrrolidin-1-yl)-1-(1-naphthyl)ethanol (**72**) allowed assignment of a negative band at 1,425 cm^{-1} to the δOH bending mode compromised in intramolecular H-bonding with the nitrogen of its pyrrolidinyl moiety. The behavior of **72** differs from that of cinchonidine (**73**), for which the VCD spectrum gave no evidence of intramolecular H-bonding at low concentrations in chloroform (*190*). Nevertheless, a clear demonstration of induced chirality in intermolecular H-bond [chiral:achiral] complexes was provided by the observation of a negative VCD band at the carbonyl region of the (1:1) cinchonidine:trifluoroacetic-acid complex, and a positive carbonyl band for its *pseudo* enantiomeric (1:1) cinchonine:trifluoroacetic-acid complex (**74**:CF_3CO_2H) (Fig. 22) (*190*).

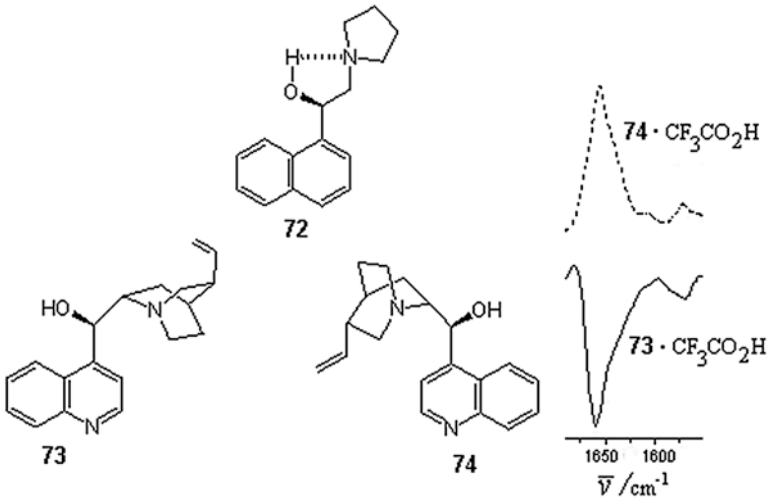

Fig. 22 Carbonyl region of the VCD spectra of H-bond complexes [cinchonidine (**73**):CF_3CO_2H] and [cinchonine (**74**):CF_3CO_2H]. (Adapted from (*190*))

Intermolecular H-bond complexes between (+)-pulegone (**67**), or its enantiomer, with chloroform as solvent, were studied through the acquisition of rotational strengths of the vibrational modes for the achiral solvent molecule and changes in rotational strength, intensity and sign of the chiral substrate (*136*). The chirality transfer process from chiral to achiral substrates (*191*, *192*), or solvents (*193*, *194*) occurring in VCD non-robust modes, defined as those having electric ($\vec{\mu}$) and magnetic ($\vec{m}$) transition dipole moment angles (ξ) close to 90°, (*136*) lead easily to unpredictable changes in frequency and band intensity and sign. In contrast, robust modes (*195*) do not change with solvent complexation, and are therefore appropriate VCD anchor signals to trace the absolute configuration of natural products. Calculations of ξ angles are necessary to tag vibrational modes as robust or non-robust modes; simulating VCD spectra in solution is not enough to account for explicit H-bond complexes formation since solvation models only provoke long-range dielectric effects to vibrational modes (*196*). To improve the reliability of the absolute configuration assignments, the robustness concept was extended using the ratio of rotational to dipole strengths, a dissymmetry factor, as a robust criterion. Thus, if the dissymmetry factor is over 10 ppm, VCD bands are robust (*197*). The analysis of robust modes in a highly flexible azetidinone molecule using the dissymmetry *g*-factor was employed successfully to distinguish conformers by robustness and to assign its absolute configuration unambiguously (*198*). The dissymmetry *g*-factor used as a robust concept is the base of the quantitative absolute configuration assignment method recently introduced (*132*).

Molecules with hydroxy groups possess at least three rotational conformers for which the bending δCCH and δCOH modes differ in frequency, intensity and sign, such as in the case of verticillol (**2**) (Fig. 23) (*10*). The observed changes are likely to be due to the formation of aggregates self-associated by means of H-bonds in solution.

Pseudo rigid backbone structures, as those of the sesquiterpenes (6*R*)-cedrol (**75**) and (6*S*)-isocedrol (**76**), allowed assignment of stretching vibrations νCO and in-plane bending δCOH to bands at 1,092 and 1,329 cm^{-1} for **75** and to bands at 1,086 and 1,308 cm^{-1} for **76** (*199*). The zone with the highest anisotropic effect (*g*-factor) in the fingerprint region of the VCD spectra for both compounds is shown in Fig. 24.

The acetonitrile solvent effect observed in the VCD spectra of tetrahydroxybicyclo[3.1.0]hexane (**77**), a carbohydrate analog forming strong intramolecular (OH···O) and (OH···N) H-bonds, was important for those conformers that change in the number of H-bonds using the implicit polarizable continuum model (IPCM). However, the *Boltzmann* average simulated VCD spectrum improved only slightly in agreement with the experimental data obtained (*200*). The spectral VCD signatures due to intramolecular H-bonding in natural products such as the cyclosporins have been used to deduce their supramolecular conformation

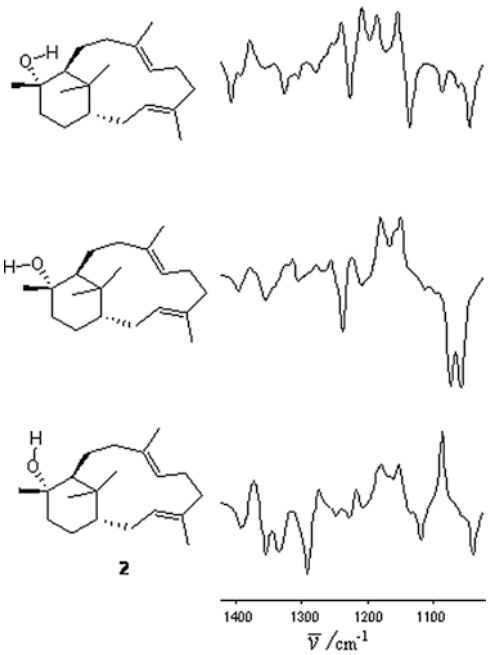

Fig. 23 Fingerprint region of the VCD spectra of hydroxy rotamers of verticillol **2**. (Adapted from (*10*))

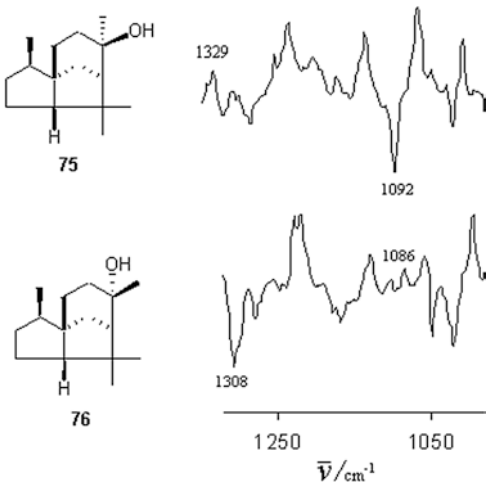

Fig. 24 Selected IR regions of the VCD spectra of (+)-(3*R*,3a*S*,6*R*,7*R*,8a*S*)-cedrol (**75**) and (–)-(3*R*,3a*S*,6*S*,7*R*,8a*S*)-isocedrol (**76**). (Adapted from (*199*))

and biological activity. An example is found in the immunosuppressive drug cyclosporin A (**78**), initially isolated from the fungus *Tolypocladium inflatum* (*201*). This compound, which contains typical peptide secondary structures (*202*), exhibited side-chain and backbone OH···O=C and NH···O=C intramolecular H-bonds, observed in the bending δNH (1,528–1,496 cm^{-1}), and stretching vibrations νC=O (1,678–1,618 cm^{-1}) and νNH (3,439–3,279 cm^{-1}) regions of its VCD spectrum.

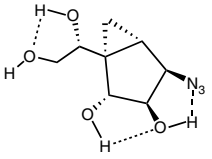

77

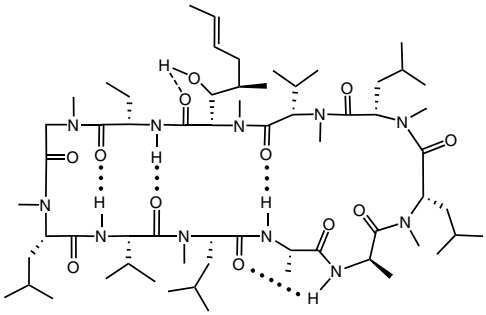

78

The timescale of IR and VCD techniques is short enough to detect H-bond structures in different arrangements with distinct conformations. Broadening of bands due to the additive superposition of individual vibrational modes is generally observed. The VCD spectra of two stereoisomers of the mutilin antibiotics, (*R*)-2-hydroxymutilin (**79**) and (*S*)-2-hydroxymutilin (**80**), indeed showed broad but mirror-image signated stretching νC=O bands at *ca.* 1,750 cm^{-1} in solutions diluted with DMSO-d_6 (Fig. 25), which were assigned to intramolecular (OH···O=C) H-bonding (*203*). As observed in Fig. 25, a simplified enantiomeric pair of five-membered ring cyclopentanone models, **81** and **82**, reproduced the fundamental H-bond carbonyl features in their VCD spectra simulated in the gas phase.

Dimethyl-L-tartrate, a dimer-like molecule presented in its lowest-energy conformation (**83**), shows the possibility of forming two intramolecular H-bonding interactions, OH···O=C, giving rise to a couplet at the carbonyl region of negative (+,–) chirality (*184*). Moreover, the observation of couplets associated with stretching νOH, νCO and bending δCOH vibrations (Fig. 26), indicates the association of degenerate coupled-oscillator (DCO) modes (*159*, *167*, *204*, *205*).

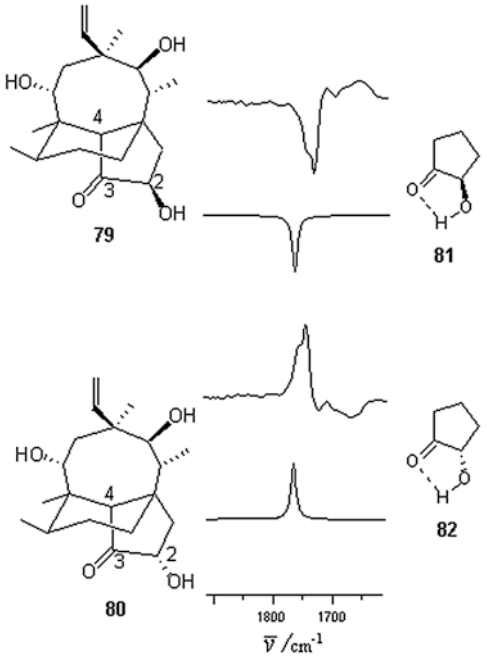

Fig. 25 Carbonyl region of the VCD spectra of (*R*)-2-hydroxymutilin (**79**), (*R*)-2-hydroxy-1-cyclopentanone (**81**), (*S*)-2-hydroxymutilin (**80**), and (*S*)-2-hydroxy-1-cyclopentanone (**82**). (Adapted from (*203*))

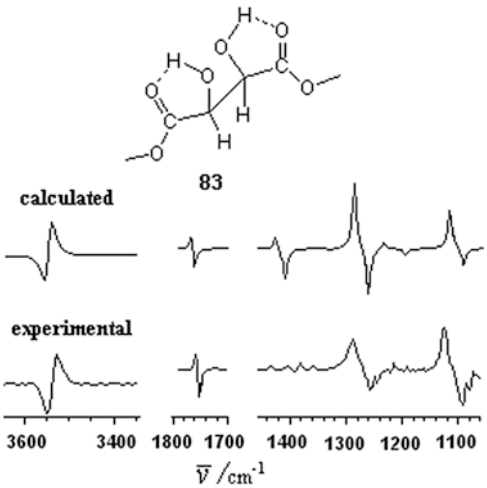

Fig. 26 VCD spectra of dimethyl L-tartrate (**83**). (Adapted from (*184*))

5.1.4 Symmetry and Conformation

Conformational interconversion barriers (*4*) for acyclic and cyclic molecules are characterized by rate constants $k = 3.9 \cdot 10^{10}\ s^{-1}$ (12 kJ/mol) and $k = 2.9 \cdot 10^{5}\ s^{-1}$ (40 kJ/mol), at 25 °C, so the VCD properties of individual chiral conformers may be detected in the IR timescale ($10^{14}\ s^{-1}$). Conformers in symmetry point groups C_n, C_s, and C_{nv} have measurable dipole moments that are small for hydrocarbons but sizeable for molecules with polar groups. From this list, chiral conformers are restricted to C_n, which includes the trivial symmetry point group C_1 to which the vast majority of natural products belong. Flexible molecules are an ensemble of conformers with measurable and no measurable dipole moments, thus a reliable theoretical search for the lowest-lying conformers of a test molecule must include the matching of IR spectra preceeding VCD simulation. The VCD spectra of high symmetry nonamethoxy cyclotriveratrylene (**84**) a C_3 symmetry molecule (*206*) and of (–)-(*S*)-perhydrotriphenylene (**85**), a D_3 symmetry chiral molecule (*207*), are shown in Figs. 27 and 28.

Rectangles are intended to highlight patterns of signals that resemble the threefold axis symmetry element that is common to **84** and **85**. Besides, C_2 symmetry is apparent in **85** from the couplet observed at around 1450 cm^{-1}. A couplet pattern is the signature of bands in the VCD spectrum of C_2 symmetry related dimethyl-L-tartrate (**83**) (Fig. 26). By analogy, the 2,2′-disubstituted-1,1′-binaphthyl derivatives **86** and **87**, which are chiral dynamic conformers of C_2 symmetry, give rise to couplet signated VCD spectra (*208*). While the unsubstituted binaphthyl (**88**) behaves

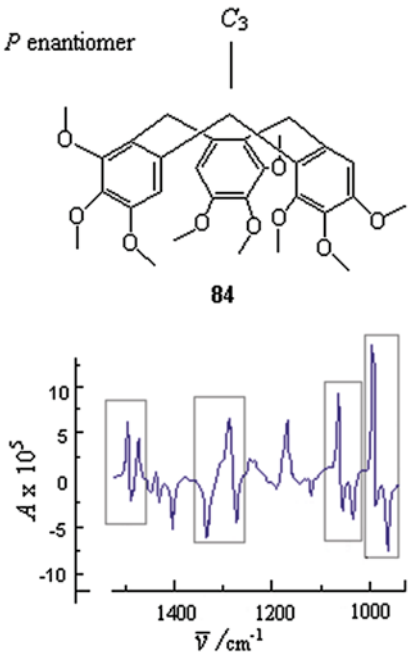

Fig. 27 Fingerprint region of the VCD spectrum of nonamethoxycyclotriveratrylene (**84**). (Adapted from (*206*))

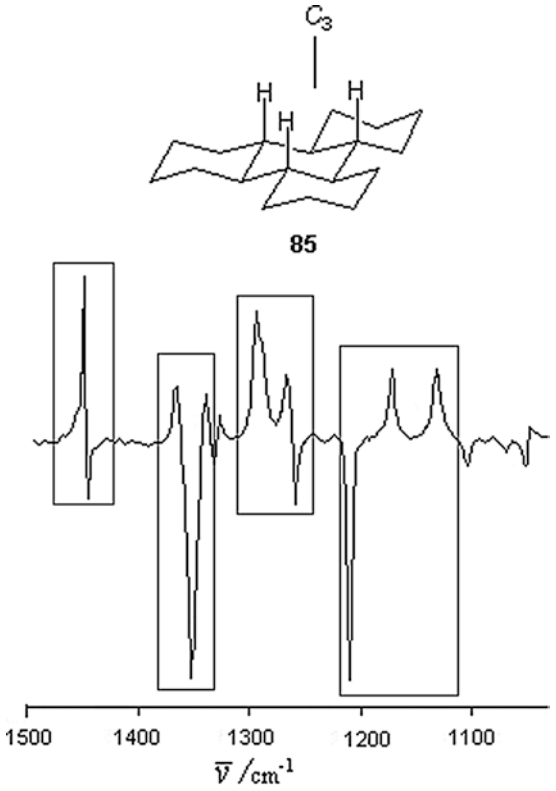

Fig. 28 Fingerprint region of the VCD spectrum of (–)-(*S*)-perhydrotriphenylene (**85**). (Adapted from (*207*))

as a chiral chromophore, VCD couplets were not present in its VCD spectrum, with monosignated biased signals appearing instead, confirming the semi-free movement nature of the binaphthyl rings in solution.

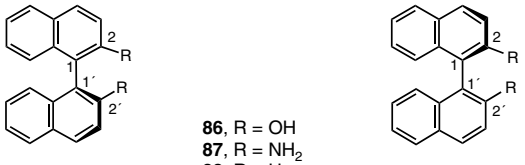

VCD spectra of the helical (+)-(*P*)- and (–)-(*M*)- enantiomers of gossypol (**89**) and (**90**), an axial chiral natural product inhibitor of human sperm maturation (*209*), also show couplet patterns due to restricted rotation about the internaphthyl bond (Fig. 29). The absorption and VCD features at the 1,450–1,100 cm^{-1} region are related to the isopropyl conformation. The VCD couplet produced by the in- and out-of-phase pair of modes, due to C_2 symmetry, at around 1,050 cm^{-1} involves ring deformation and a methyl rocking motion. The prominent positive VCD feature at around 1,200 cm^{-1} is related to the COH deformation, a vibrational mode in this case linked to intermolecular H-bond association when in solution.

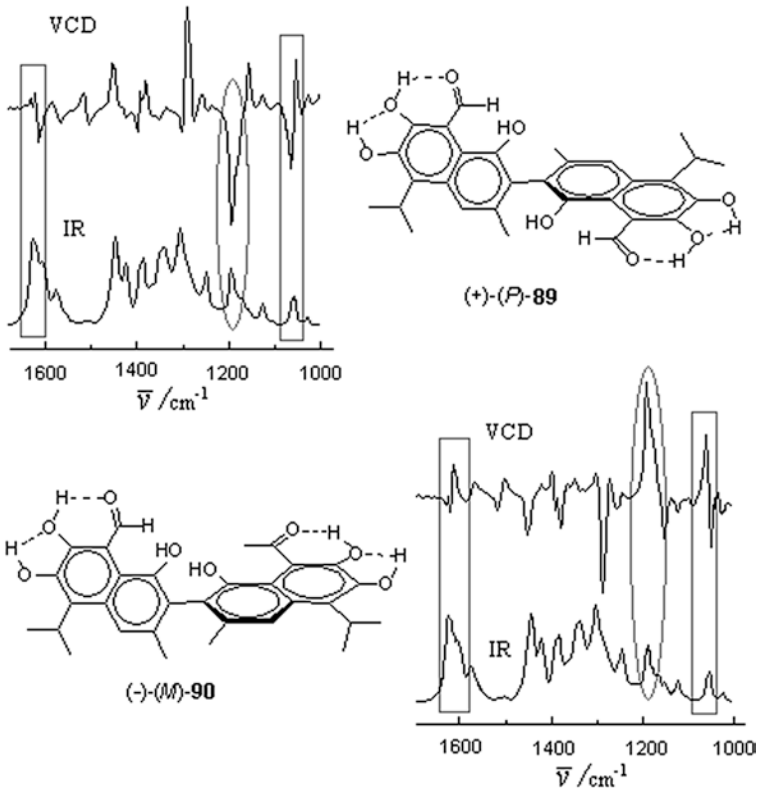

Fig. 29 Experimental VCD spectra of (+)-(*P*)- (**89**) and (–)-(*M*)-gossypol (**90**). (Adapted from (*209*))

According to ring current theory (*178*, *210*, *211*), a VCD monosignated band is the result of an enhanced magnetic transition moment in a chiral oscillator, stemmed from an adjacent self-generated electronic current in a ring of atoms or from the closeness of electron donor groups that increase the anisotropic *g*-factor of the band (*212*). In contrast, electron-withdrawing groups or chirally disposed coupled oscillators without delocalizable electron density give rise to no net intensity VCD bands. VCD spectra of chiral molecules in the C_1 point group with chiral local mirror-image νC–O oscillators, reflected by the "virtual chiral plane σ_ω" (see above), such as those in longipinenes **55** and **56** (Fig. 17) are also arranged in couplets. Similarly, a couplet signal at the stretching carbonyl region of the VCD spectrum for the steroidal 3α-hydroxy-7,12-dioxo-5β-cholanic acid (**91**) of C_1 symmetry was predicted by a degenerate coupled oscillator model (Fig. 30) (*166*).

Couplets due to conformational orientation of carbonyl groups (*165*), such as the ester groups at C-3 and C-6 of (–)-3α,6β-diacetoxytropane (**30**), were found in its VCD spectrum (Fig. 31) (*75*). In addition, the stereochemistry at the nitrogen atom (Me-*ax*. or Me-*eq*. with respect to the six-membered ring of the bicycle) is not as important as the dipolar orientation of the carbonyl esters groups to determine responses of VCD. Thus, conformers **30a** and **30b**, with mirror-image disposition of

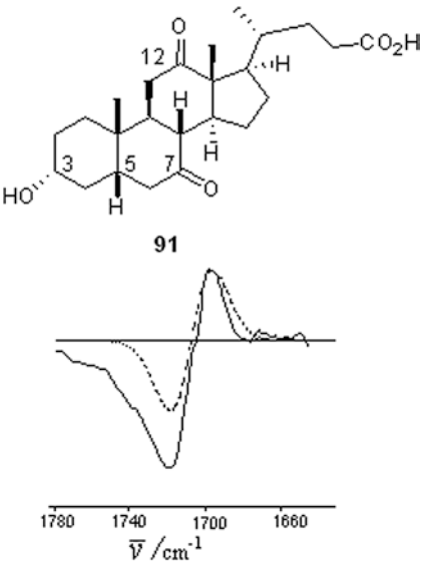

Fig. 30 Carbonyl region of the VCD spectra of 3α-hydroxy-7,12-dioxo-5β-cholanic acid (**91**). Experimental (*solid line*) and calculated (*dotted line*). Spectra were plotted using the DCO theory (Adapted from (*166*))

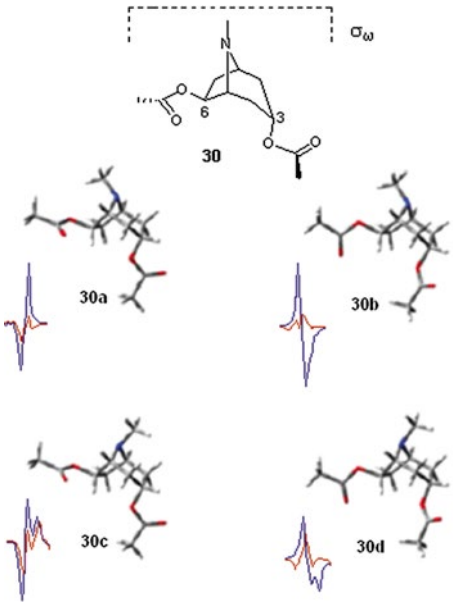

Fig. 31 Selected tropane **30** conformers and VCD signals in the 1,300–1,200 cm^{-1} region. Larger couplets correspond to conformers **a**–**d**, smaller to not shown minor conformers where the ester group at C-3 has another orientation with respect to C-6. (Adapted from (*75*))

coupled carbonyl modes at C-3 and C-6 (through the "virtual chiral plane σ_ω"), give a mirror-image νOC(=O) bisignated band, in the 1,300–1,200 cm^{-1} region, to show a couplet of positive chirality (–,+) for **30a** and a couplet of negative chirality (+,–) for **30b**. The same situation is evident for the **30c** and **30d** conformer pair. Due to steric interactions, the *N*-Me-*eq*. conformers **30c** and **30d** are more stable than the *N*-Me-*ax*. **30a** and **30b**. In contrast, in tropanes **22** and **23**, the *N*-Me group prefers an *axial* orientation due to the (C-6–OH···N) H-bonding interaction (*55*).

As mentioned in a previous section, mirror image bands corresponding to asymmetric stretching vibrations in the 1,150–950 cm^{-1} region of the VCD spectra for **22**, **23**, and **30** (Fig. 10) showed little or no variation with conformation, so therefore, their absolute configuration was assigned confidently. Vibrational modes associated with this region for **30** are shown in Fig. 32.

For paclitaxel (**92**), a cyclic diterpenoid widely used in cancer chemotherapy, the bisignated bands at 1,732 cm^{-1} and 1,715 cm^{-1} corresponding to the ν(C=O) stretching

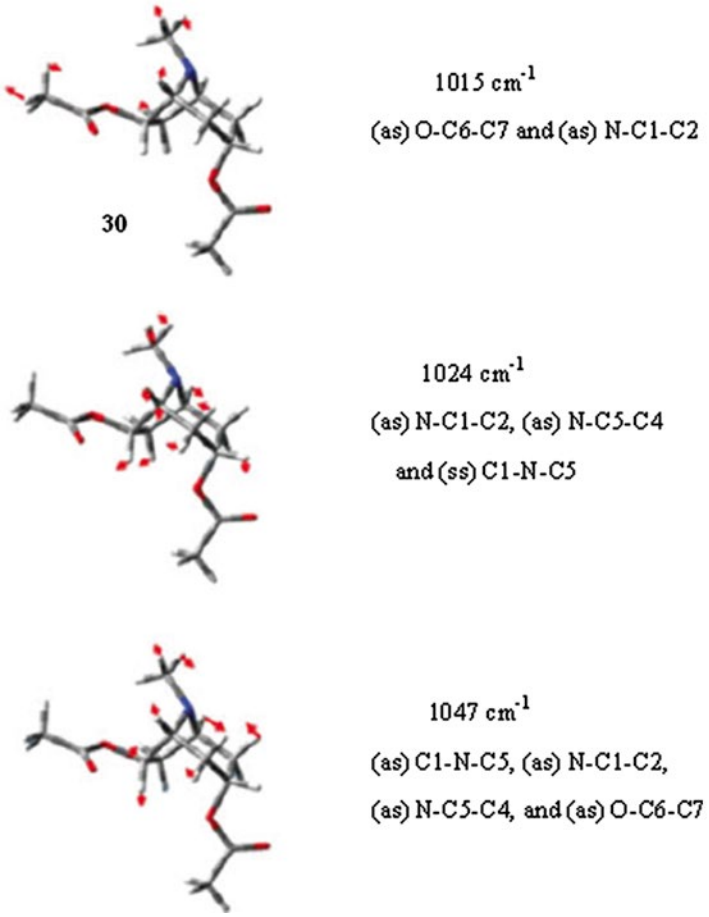

Fig. 32 Normal vibrational modes for tropane **30** calculated at the B3LYP/DGDZVP level of theory. (Adapted from (*75*))

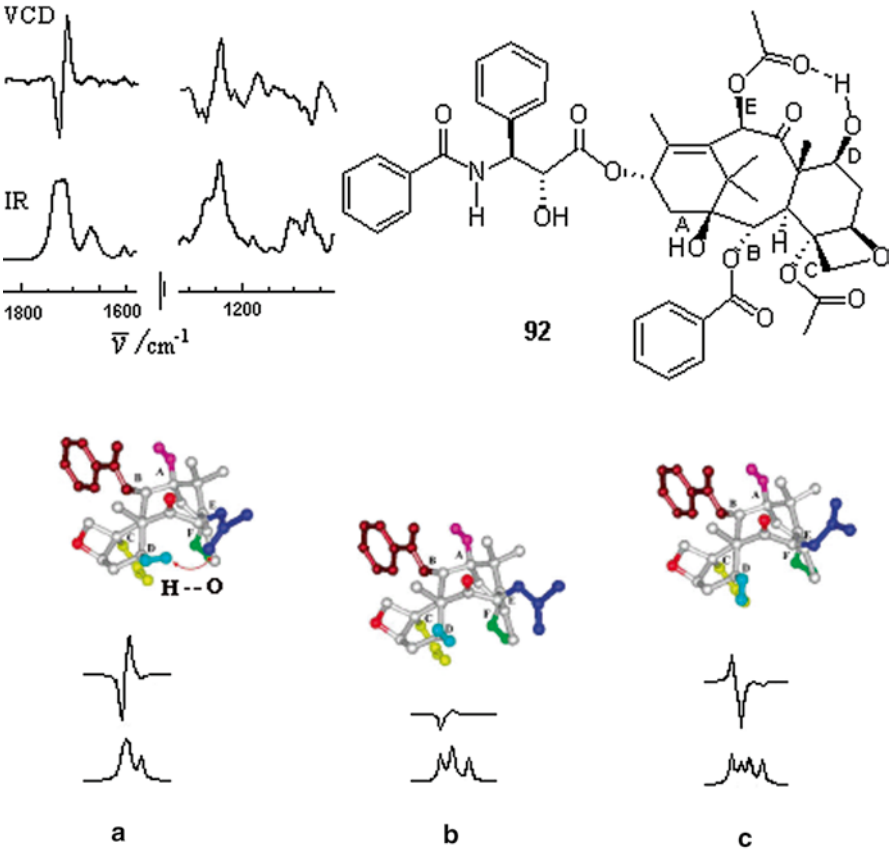

Fig. 33 IR and VCD experimental spectra for paclitaxel (**92**). Calculated baccatin III ring conformations **a**, **b**, and **c** showing carbonyl vibration IR bands and VCD couplets. (Adapted from (*213*))

mode reflect strongly the conformations of its baccatin III ring core (Fig. 33) (*213*). A couplet of positive (–,+) chirality is observed for baccatin in conformation **a**, the conformation adopted in solution, favoring intramolecular H-bonding involving the hydroxy group (D) and carbonyl of the acetoxy group (E). A couplet with no significant intensity is observed for conformation **b** and a couplet with negative chirality (+,–) is observed when the OH (D) and C=O (E) groups adopt the rotameric conformation **c**.

5.2 Assignment of Absolute Configurations of Terpenes, Aromatic Molecules, and other Natural Compounds

This section is dedicated to describing how chirality assignment of terpenes may be determined or confirmed by VCD, with the information included intended to be representative rather than exhaustive. VCD studies of sesterterpenes, sesquiterpenes, or tetraterpenes (*214*) have not been reported so far as the authors are aware. Several

authoritative reviews (*7*, *16*, *52*, *62*, *89*, *90*, *155*, *157*, *207*, *215*) may contain terpenoid VCD assignments that were inadvertently overlooked by the present authors. The reader will find among the examples included in this chapter, absolute configuration assignments of natural products for which the relationships are either enantiomeric or diastereomeric. In most of these cases, VCD has been able to distinguish diastereomers despite the closeness of their IR spectral features. Already mentioned diastereomers are: the longipinanes **50** (*149*), **55** (*149*), and **56** (*149*), which differ in the absolute configuration of one or two chiral centers of a total of six; the epimeric cedrol **75** and isocedrol **76**, differing in one chiral center of a total of five (*199*); and the epimers of 2-hydroxymutilin **79** and **80**, differing in one chiral center of a total of nine (*203*).

5.2.1 Monoterpenes

The practical ability of the VCD technique to measure and predict the absolute configuration of chiral molecules in solution has been developed largely by using monoterpenes. The value of monoterpenes as targets for chiroptical studies resides in the simplicity of their chiral structural features in possessing one or only a few stereogenic centers. Moreover, monoterpenes are found in a wide variety of natural sources. Compounds of this type already mentioned in this chapter are (+)-(1*R*,4*R*)-camphor (**16**), (–)-(1*S*,4*R*)-camphor (**20**), (+)-(1*S*)-camphorquinone (**57**), (–)-(*S*)-camphor-10-sulfonic acid (**71**), (+)-(1*S*,4*S*)-fenchone (**17**), (+)-(*R*)-limonene (**18**), (*S*)-(–)-limonene (**19**), (–)-(1*S*,2*R*,4*S*)-*endo*-borneol (**21**) (somewhat at odds the numeration of the oxygen-bearing carbon atom in **21** is given either as C-1 (*97*) or C-2; (*111*) and, as a consequence, confusion in the assignment of absolute configuration for such a center remains in the literature; here (2*R*)- is used to designate it, as observed in Fig. 3), (–)-(1*S*)-α-pinene (**29**), (+)-(1*R*)-α-pinene (**58**), (–)-(1*S*)-β-pinene (**59**), (–)-(1*R*,5*S*)-myrtenal (**47**), (–)-(2*S*,5*R*)-menthone (**60**), (+)-(2*R*,5*R*)-isomenthone (**61**), (–)-(1*S*)-perillyl alcohol (**62**) (*216*), (–)-(1)-perillaldehyde (**63**), (+)-(*R*)-*p*-menth-1-ene (**64**), (+)-(*R*,*R*)-*p*-menth-l-en-9-ol (**65**), (–)-(1*R*,2*S*,5*R*)-menthol (**68**) (*217*), (–)-(*R*)-carvone (**66**), (+)-(*R*)-pulegone (**67**), and (–)-(*S*)-verbenone (**70**). In addition, five recent applications are described in the paragraphs below.

Example 1

Cineole (**93**), a monoterpene found in many *Eucalyptus* oils, was derivatized to form a pair of enantiomerically pure 3-oxo stereoisomers (–)-**94** and (+)-**95** (Fig. 34) through chromyl acetate oxidation. The absolute configuration of the C-1 and C-4 stereogenic centers of the enantiomeric pair was established by VCD spectroscopy combined with DFT calculations at the B3LYP/DGDZVP level of theory (*218*).

Only one conformer was located in the conformational energy landscape, so visual comparison of the experimental and calculated spectra was sufficient to assign (1*S*,4*S*)-stereochemistry to the (+)-**94** enantiomer and (1*R*,4*R*) to the (+)-**95** enantiomer (Fig. 35). The ideal situation in VCD measurements is to find a molecule in which the conformational equilibrium is biased towards one conformer since VCD responses of fundamental oscillator modes will only depend on configuration; such as in the present case.

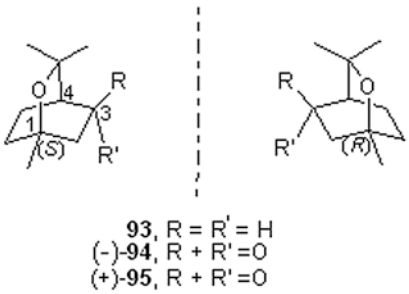

Fig. 34 Enantiomeric 3-substituted cineole derivatives

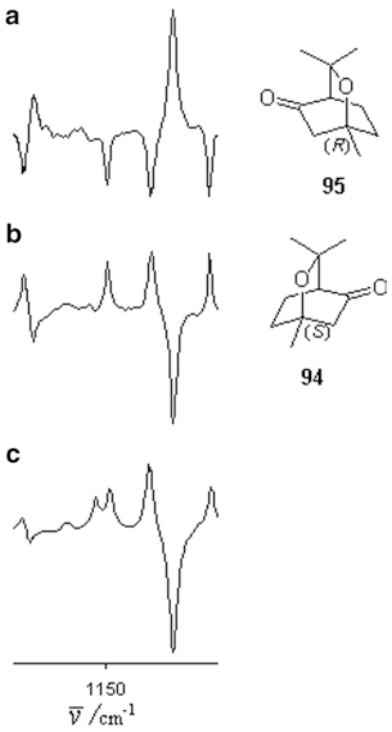

Fig. 35 Comparison of observed (**a**) (+)-**95**, (**b**) (–)-**94**, and (**c**) calculated VCD spectra for (1*S*,4*S*)-**94**. (Adapted from (*218*))

Example 2

After being isolated from the aerial parts of *Peperomia obtusifolia* and separated by chiral HPLC, the absolute configuration of six novel bornyl and fenchyl chromane ester derivatives (–)-(2*S*,1′*S*,2′*R*,4′*S*)-**96** and its enantiomer (+)-(2*R*,1′*R*,2′*S*,4′*R*)-**97**, (–)-(2*S*,1′*R*,2′*S*,4′*R*)-**98** and its enantiomer (+)-(2*R*,1′*S*,2′*R*,4′*S*)-**99**, (–)-(2*S*,1′*R*,2′*R*,4′*S*)-**100** and (+)-(2*R*,1′*R*,2′*R*,4′*S*)-**101** were determined using VCD measurements (*219*). The chiral mix of monoterpenes presented in this work represents the first tethered terpenes found in Nature. The sensitivity of VCD to specify the chirality of one center as opposed to the other three was demonstrated unambiguously by the simulation of VCD spectra using DFT theory at the B3LYP/6-31G(d) level. The VCD spectra showed fundamental modes assigned to monoterpene and chromane substructures, and the spectral signatures were proposed through the residual spectral difference method (*116*) applied to the 1,300–1,000 cm^{-1} region. The sign of couplets found at the carbonyl region was more sensitive to the configuration of the chromyl C-2 center than to the more proximate monoterpene C-2′ center.

The corresponding enantiomers (+)-**102** and (–)-**103** of fenchyl chromane diastereomers (–)-**100** and (+)-**101** were found to be mixed in a minor unresolved peak in the chiral HPLC chromatogram (*220*). The (1′*S*,2′*S*,4′*R*)-fenchyl moiety was identified in the diastereomeric (+)-**102** and (–)-**103** mixture by VCD, comparing with the average sum of the experimental VCD spectra of (–)-**100** and (+)-**101**. In the reference spectrum, no VCD peaks were observed for the chromane moiety since enantiomers cancel out by the average sum, although peaks belonging to overlapped normal modes remained. The fenchyl bands of the reference (–)-**100** and (+)-**101** average sum spectrum were of opposite signs at 1,090, 1,040, and 975 cm^{-1} to those of the analyzed mixture (+)-**102** and (–)-**103** (Fig. 36), and hence confirmed the

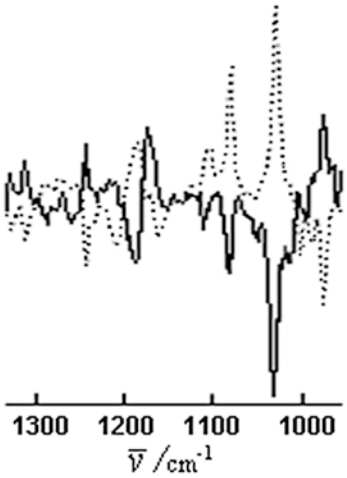

Fig. 36 Observed VCD spectra comparison of mixed fenchyl chromane diastereomers (+)-**102** and (–)-**103** (*solid line*) and reference (–)-**100** and (+)-**101** average sum spectrum (*dotted line*). (Adapted from (*220*))

enantiomeric nature of the fenchyl group between each pair of diastereomers. It is noteworthy that the absolute configuration assignment of the diastereomeric mixture (+)-**102** and (–)-**103** was carried out without further DFT calculations.

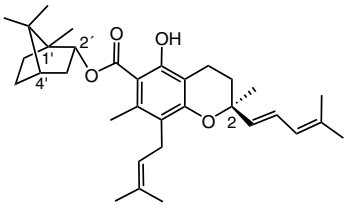

(–)-**96**

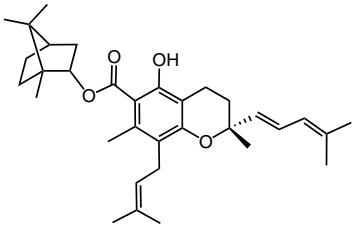

(+)-**97**

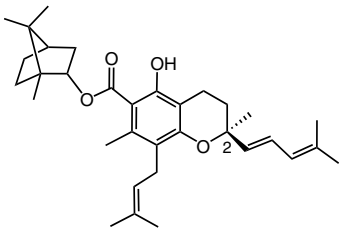

(–)-**98**

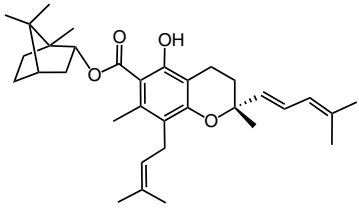

(+)-**99**

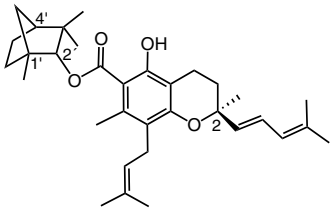

(–)-**100**

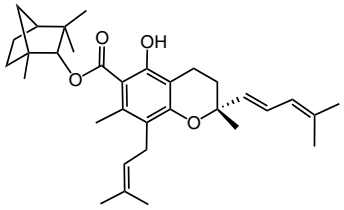

(+)-**101**

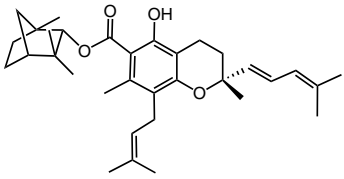

(+)-**102**

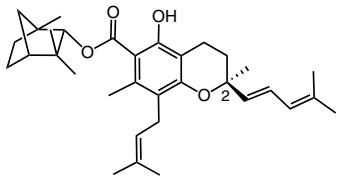

(–)-**103**

Example 3

The VCD spectrum of (–)-(*R*)-camphorquinone (**69**) was recorded in different phases. In CCl_4 solution and in suspension conditions (Nujol and Fluorolube), similar spectra were obtained, but in film conditions a clear signature for the two carbonyl groups appeared as a couplet of negative chirality (+,–) (Fig. 37) (*221*). The VCD simulation at the B3LYP/cc-pVDZ level of theory along with Natural Bond Orbital (NBO) analysis allowed the coupling between the two $\nu C=O$ stretching normal modes to be strongly delineated. Even though the vibrational analysis of the fingerprint region is complicated by the mixing of normal modes, the theoretical simulations are improved in this region due to the lower anharmonicity of the normal modes. The description of normal modes from the Potential Energy Distribution Matrix allowed vibrational assignments to be made in a confident manner.

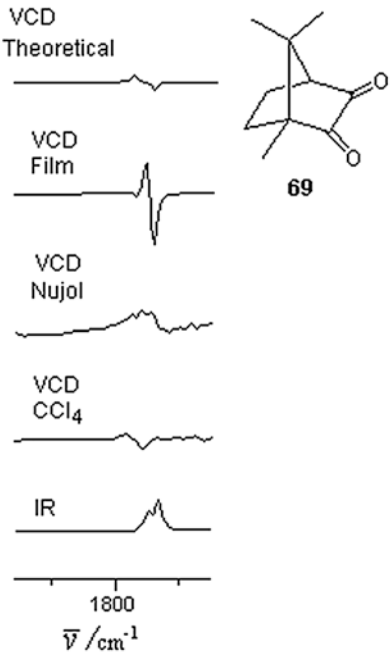

Fig. 37 Carbonyl region comparison of the IR and VCD spectra of (–)-camphorquinone (**69**). (Adapted from (*221*))

Example 4

The quantitative VCD absolute configuration assignments of (+)-(*S*)-carvone (**104**) and (+)-(1*S*,2*R*,5*S*)-menthol (**105**) based on the similarity index, S_V, and on the SimIR/VCD comparison method (*131*), was done (*222*). The conformational search, performed using the MCMM/low-mode in the Maestro 8.5 program (Schrödinger, LLC), provided six conformers for **104** and eight for **105**. The conformers of **104** were minimized with the DFT B3PW91/6-31G(d) method, the B3LYP and PBEPBE functionals were also used, but the statistical results of the IR and VCD spectra comparisons were practically the same than those obtained with the B3PW91 functional.

According to the SimIR/VCD algorithm protocol, implemented in Scitegic PipelinePilot 8.0 (Accelrys Inc.), the VCD band frequencies are optimized by taking into account a shift calculated from the IR spectrum. A $|S_V|$ value of 0.2 or greater is considered to be confident (95% or higher level) for absolute configuration assignments. Besides, a positive S_V is indicative of a matching between the weighted average simulated VCD spectrum and the experimental VCD spectrum, while a negative value indicates the simulated and the experimental VCD spectra belong to different enantiomers. A differentiation of S_V with respect to conformation in the case of carvone **104** was observed, with those conformers having the isopropylene group in *equatorial* (*eq*.) orientation being more stable than those that have the group in the *axial* (*ax*.) orientation. The calculated S_V values for the *eq*. conformers varied in the range 0.38–0.45, while for *ax*. conformers S_V these values were negative and varied between −0.15 and −0.21. The conformational weighted VCD spectrum, calculated with the *Boltzmann* distribution of the *eq*. conformers, provided the highest S_V value (0.63), confirming the (*S*) absolute configuration for (+)-carvone (**104**). In the case of menthol (**105**), to analyze the scope of the SimIR/VCD method, four diastereomers were considered (1*R*,2*R*,5*S*), (1*R*,2*S*,5*S*), (1*S*,2*R*,5*S*), and (1*S*,2*S*,5*S*), but only the correct (1*S*,2*R*,5*S*) diastereomer presented positive S_V values for its eight conformers. The S_V value for the average weighted calculated spectrum, at the PBEPBE/6-31G(d) level of theory, of (1*S*,2*R*,5*S*)-**105** was 0.71, greater than 0.55, which is the largest S_V value for a conformer, thus confirming the absolute configuration of (+)-menthol. The PBEPBE functional (*223*) is recommended for absolute configuration vibrational calculations in the fingerprint region because spectral calculations are fast and the need for frequency scaling and shifting, when calculating S_V, is removed.

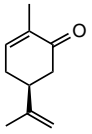

104

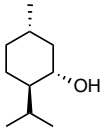

105

Example 5

(1*R*,3*R*,4*R*)- and (1*S*,3*S*,4*S*)-camphor derived *β*-diketones **106–110** were studied by the VCD exciton chirality method (*174*) for fast absolute configuration analysis and tautomerization equilibria predictions (*224*). The exciton coupling of the carbonyl groups is observed as a bisignate couplet of positive chirality (–,+) for the (1*R*,3*R*,4*R*) derivatives and of negative chirality (+,–) for the enantiomeric (1*S*,3*S*,4*S*) derivative in the 1,751–1,650 cm^{-1} region. The amplitude (*A*) of the couplet bands, defined as $\Delta\varepsilon_1$ (lower frequency) — $\Delta\varepsilon_2$ (higher frequency), was related to the position of the keto-enol equilibria, so that camphor derivatives with electron-donating groups such as **109** (*A* = 0.140) and **110** (*A* = 0.056), displayed large couplets indicating the tautomeric equilibria is shifted towards the keto form; contrarily, camphor derivatives with electron-withdrawing groups such as **108** or the parent 3-benzoylcamphor **106** (*A* = 0.030), showed small couplets assuming the tautomeric equilibria favors the enol form as in the case of (+)-(1*R*,3*R*,4*R*)-3-trifluoroacetyl camphor (**111**) for which the tautomeric equilibrium, studied by VCD (*225*), is biased towards the enolic form. The calculated anisotropy *g* ($\Delta\varepsilon/\varepsilon$) factor is greater, to some extent, for derivative **109** than for the other derivatives, particularly in the case of the VCD band at the lower frequency $\Delta\varepsilon_1$ of the couplet bands, which seem to possess the higher dissymmetry character.

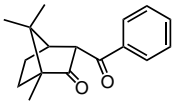

106

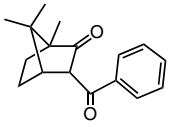

107

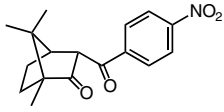

108

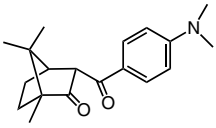

109

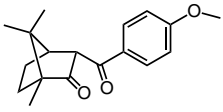

110

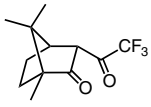

111

5.2.2 Sesquiterpenes

As the number of carbons in terpenoids increases, their structures grow in complexity. Sesquiterpenes contain acyclic and mono-, bi-, tricyclic or even polycyclic structures, a complex chiral natural architecture that supports their diverse biological functions such as possessing semiochemical activity and acting as messengers between species (pheromones) (*226*). Moreover, pheromones have attracted VCD interest to obtain their absolute configuration allowing them to be fully indentified and incorporated into insect pest management programs (*227*). Many sesquiterpenoids from marine organisms are characterized by uncommon functionalities (*228*). Molecules of this

type already in this chapter are (–)-(1*R*,2*R*,5*S*,8*R*,11*R*)-quadrone (**4**) (*12*), (–)-(1*R*,2*R*,5*S*,8*R*,11*R*)-suberosanone (**5**) (*12*), (*P*)-(*S*)-curcuphenol dimer (**41**) (*116*), (*M*)-(*S*)-curcuphenol dimer (**42**) (*116*), (4*R*,5*S*,7*R*,9*R*,10*R*,11*R*)-7,9-diacetoxylongipin-2-en-1-one (**50**) (*149*), (4*R*,5*S*,7*R*,9*S*,10*R*,11*R*)-7,9-diacetoxylongipin-2-en-1-one (**55**) (*149*), (4*R*,5*S*,7*S*,9*R*,10*R*,11*R*)-7,9-diacetoxylongipin-2-en-1-one (**56**) (*149*), (+)-(3*R*,3a*S*,6*R*,7*R*,8a*S*)-cedrol (**75**) (*199*), (–)-(3*R*,3a*S*,6*S*,7*R*,8a*S*)-isocedrol (**76**) (*199*), (+)-(*P*)-gossypol (**89**) (*209*), and (–)-(*M*)-gossypol (**90**) (*209*). Sixteen examples of the application of VCD to sesquiterpenes are presented below.

Example 1

Sesquiterpenes with conformational rigid structures such as (–)-(1*R*,2*R*,5*S*,8*R*,11*R*)-quadrone (**4**), (–)-(1*R*,2*R*,5*S*,8*R*,11*R*)-suberosanone (**5**), and (1*R*,2*R*,4*S*,8*R*,11*R*)-suberosenol A acetate (**112**), isolated from the gorgonian *Isis hippuris*, and (1*R*,2*R*,8*R*,11*R*)-suberosenone (**113**), isolated from the marine gorgonian *Subergorgia suberosa*, are compounds possessing potent cytotoxicity (*12*). In each case, only one conformer was perceived by Monte Carlo searching using MMFF94 force field methodology. The absolute configuration as assessed by VCD spectroscopy included a calculation of the VCD spectrum using the DFT B3PW91/TZ2P method on the optimized structure of quadrone (**4**). The clear correlation between experimental and calculated spectra led to a conclusive absolute configuration assignment (*12*).

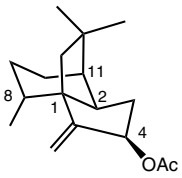

112

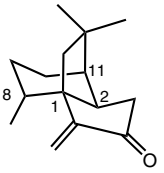

113

Example 2

Unusual carbon skeletons are also featured in terrestrial sesquiterpenes, such as those found in the picrotoxin lactones tutin (**114**), coriamyrtin (**115**), and dihydrotutin (**116**), isolated from *Coriaria ruscifolia* ssp. *ruscifolia*, which are potent transmission inhibitors of the central nervous system (*229*). The absolute configuration of **115** determined by VCD measurements confirmed the stereochemistry of analogues **114** and **116** thus supporting their electrophysiological properties. Due to its rigid core, only four conformers were found for **115** as a result of rotational freedom of the hydroxy and isopropenyl groups. *Boltzmann* average simulated VCD spectra at the B3LYP/DGDZVP level featured prominent monosignated bands at νCO and δCOH vibrations that matched neatly with the experimental VCD spectrum (*229*).

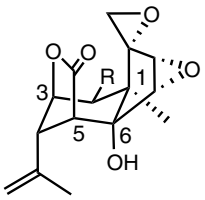

114, R = OH
115, R = H

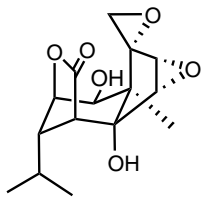

116

Example 3

Studies on secondary metabolites from plants found in the New World were initiated in Mexico when crystalline perezone (**117**) was isolated in 1852 from the roots of *Perezia adnata* var. *alamani* (*230*). Many natural products are stable; however, **117** can undergo intramolecular conversions on heating. Perezone (**117**) and dihydroperezone (**118**) are benzoquinones with a very flexible side chain, so they provided a good opportunity to evaluate the versatility of VCD to study the conformation and chirality of both sesquiterpenes (*231*). Molecular mechanics conformational mapping followed by geometry optimization of low-lying conformers at the B3LYP/DGDZVP level of theory led to 21 conformers for **117** and 34 for **118**. Extended side chain conformers were highly preferred over folded conformers in both cases. *Boltzmann* average VCD spectra of **117** and **118** were calculated and compared to their corresponding experimental spectra manually and through the Compare*VOA* program (*129*, *130*). The enantiomeric similarity index values were 77.0 for **117** and 85.4 for **118** assuring with 100% confidence their absolute configurations as (8*R*). No evidence was found for significant non-covalent π–π interaction between the quinone core and the side chain double bond as to drive preferences of **117** to folded conformations (*232*). Reference (*232*) also briefly reviews the main accomplishments in the chemistry of perezone (**117**) since its discovery in 1852.

VCD is a reliable technique to study conformational arrangements of these and other natural products (*186*, *187*, *233*, *234*), since this technique is very sensitive to molecular conformation. Furthermore, VCD has been employed to study the conformation of reactive intermediates (*235*).

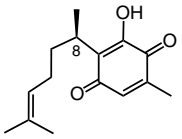

117

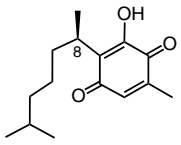

118

Example 4

Urechitol A (**119**), a trinorsesquiterpenoid, was isolated from the roots of *Pentalinon andrieuxii*, a plant that has been used since the time of the Maya civilization in Mesoamerica to remedy skin damage caused by infections of the genus *Leishmania*. The intricate structure of **119**, somewhat esthetically "offensive" as represented in the original work (*236*), was unraveled by X-ray crystallography. VCD studies of **119** and of its oxidation product urechitin (**120**) allowed their absolute configuration determination to be made (*237*). Four optimized conformers populated the potential energy diagram of **119** and three for that of **120**. The conformational average VCD spectra of **119** and **120** matched to a large degree with their corresponding observed spectra, thus allowing the absolute configuration to be assigned as (1*R*,2*S*,4*S*,5*R*,6*S*,7*S*,8*R*,10*R*) for **119** and (1*R*,4*S*,5*R*,6*S*,7*S*,8*R*,10*R*) for **120**. The observed VCD spectrum of urechitol (**119**) showed the highest dissymmetry zone around the band of CO vibrations at 1,030 cm^{-1}, with that in the VCD spectrum of the lactone derivative **120** around the band of CO vibrations at 1,260 cm^{-1} (Fig. 38).

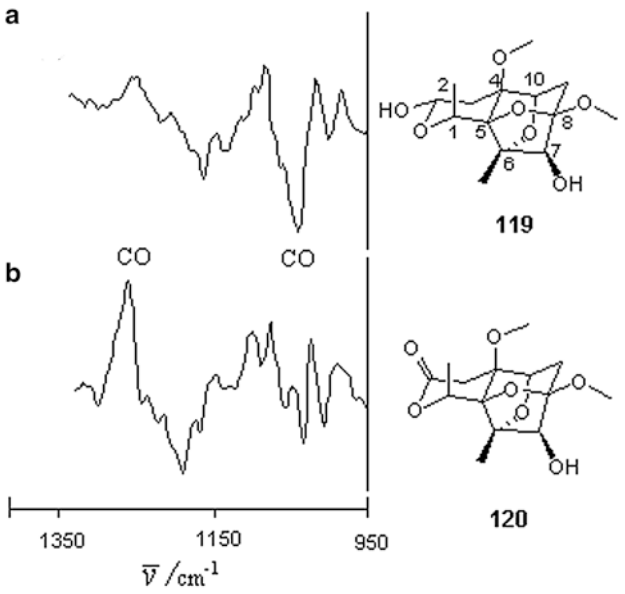

Fig. 38 Observed VCD spectra of (**a**) urechitol A (**119**), and (**b**) lactone derivative **120**. (Adapted from (*237*))

Example 5

The stereochemistry of (–)-(1*S*,4*S*,7*R*,8*R*,9*S*)-9-epipresilphiperfolan-1-ol (**121**), a triquinane sesquiterpene found as a constituent of the essential oil of *Anemia tomentosa* var. *anthriscifolia*, was determined by X-ray diffraction analysis followed by assessment of the absolute configuration by VCD spectroscopy (*238*). A significant mobility of the tricyclic skeleton in gas phase was observed giving rise to six significant conformers. The VCD simulated spectrum matched well with the observed one. Some resemblance was found between the couplets at around 1,200 cm^{-1} and 1,400 cm^{-1} (Fig. 39) and those reported for (+)-(1*R*,2*S*,5*R*,6*S*)-*endo*-bicyclo[3.3.0] octane-2,6-diol (**122**) with C_2 symmetry and derivatives that are chiral intermediates in the asymmetric synthesis of enantiomerically pure natural products (*239*). Presilphiperfolanes as **121** and analogous sesquiterpenes are obtained by catalyzed rearrangements of modhephenes, so knowing their configuration and chirality with accuracy is important to establish their biogenetic routes of formation (*240*).

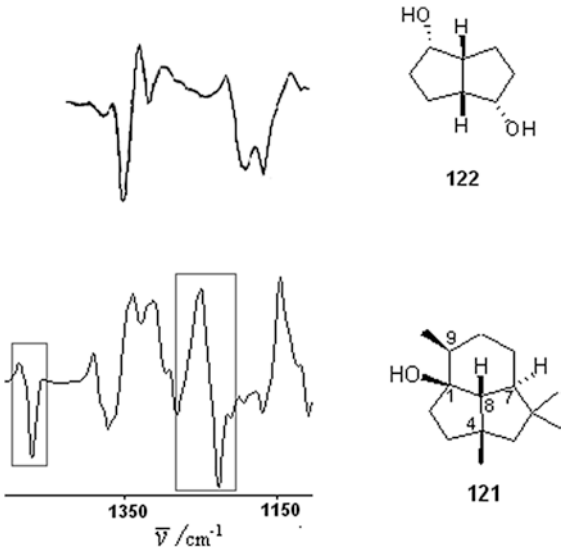

Fig. 39 Calculated VCD spectra of (–)-9-epipresilphiperfolan-1-ol (**121**) and of the structurally related bicyclo[3.3.0]octane **122**. (Adapted from (*238*, *239*))

Example 6

The VCD methodology was applied to the halogenated marine natural products majapolene B (**123**) and acetylmajapolene B (**124**) isolated from the red algal genus *Laurencia* collected in Malaysia (*241*). The conformational analysis of (7*S*,10*S*)-**123** and (7*S*,10*S*)-**124** was carried out with the MMFF94S force field in the Conflex program. Six low-lying conformers were found populated for both **123** and **124**, with two remaining for **123** and all six remaining for **124** after optimization using DFT at the B3PW91/6-31G(d,p) level of theory. Simulated VCD spectra for the two conformers of **123** were almost identical, with the exception of the main VCD signal around 1,400 cm^{-1} attributed to the δCOH bending vibration. The main difference between the VCD spectra of the six conformers of **124** was found at the carbonyl region (around 1,780 cm^{-1}). The observed and calculated VCD spectra for **123** showed excellent agreement, leading to the concluion that the absolute configuration of the naturally occurring (–)-**123** is (7*S*,10*S*). This assignment was confirmed by comparison of the VCD spectra of observed (–)-**124** and calculated (7*S*,10*S*)-**124**.

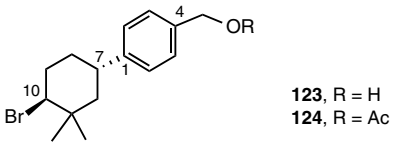

123, R = H
124, R = Ac

Example 7

The C-8 configuration of a benzoxepin sesquiterpenone (**126**) obtained in two steps from pacifenol (**125**) (Fig. 40) was determined by VCD (*242*). The vinyl bromide chamigrene intermediate obtained by reduction of **125**, rearranged to **126** when treated with *m*-chloroperbenzoic acid (*243*).

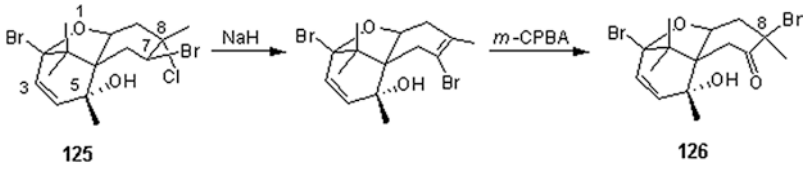

Fig. 40 Semisynthesis route to prepare sesquiterpenone **126**

The *spiro*-tether nature of the three rings, combined with the *cis*-fused stereochemistry of the union of the tetrahydrofuran and cyclohexanone rings provided **126** with a rigid structure. Geometry optimization of the global minimum conformers of the (8*R*)-**126** and (8*S*)-**127** diastereomers using DFT at the B3LYP/

DGDZVP level resulted in preference of the boat over the chair conformation of the cyclohexanone ring for **126**. In contrast, for **127**, the chair predominates. The boat conformation is stabilized by the hydrogen bonding interaction between the hydroxy group and the carbonyl group of the cyclohexanone ring showing an (OH·····O=C) H-bond distance of 2.5 Å. By comparison of the observed and calculated VCD spectra at the carbonyl region (1,728 cm^{-1}) and the CO vibrations (*ca.* 1,200 cm^{-1}), it became immediately evident that the configuration of C-8 is (*R*) (Fig. 41).

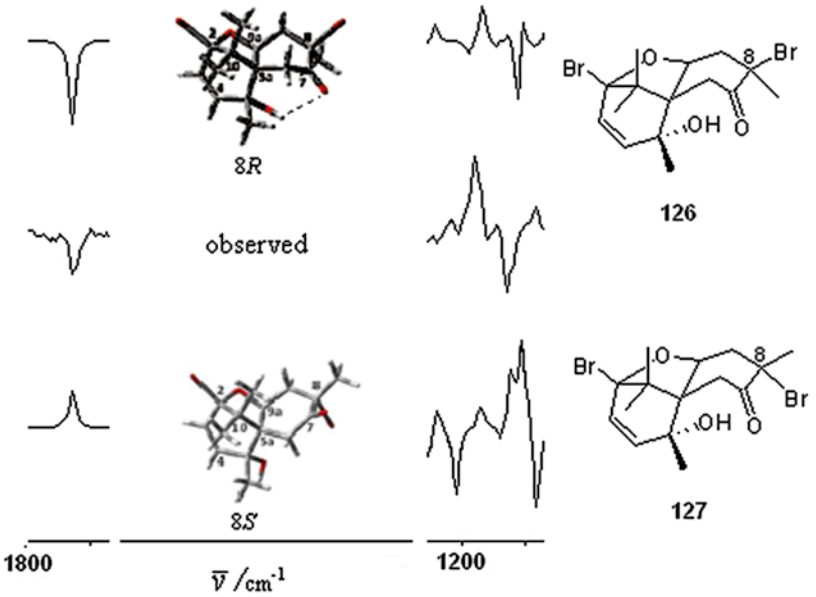

Fig. 41 Comparison of the experimental VCD spectrum (*center*) of benzoxepin sesquiterpenone with the conformer average weighted plots calculated for the (8*R*)-epimer **126** (*top*) and the (8*S*)-epimer **127** (*bottom*). (Adapted from (*242*))

Example 8

Sesquiterpenes **128**–**132** are obtained from *Mikania* species, which have medicinal value as anti-inflammatory agents, and for the treatment of respiratory tract diseases, rheumatism, and influenza. The absolute configuration of the eudesmanolide **128** isolated from the aerial parts of *Mikania campanulata* was obtained from VCD measurements (*244*). Following a Monte Carlo protocol, 40 conformers were found for this flexible molecule, although only eight remained after geometry optimization using DFT at the B3LYP/6-31G(d,p) level of theory. From comparison of the

observed VCD spectrum with the *Boltzmann* weighted theoretical one, the absolute configuration of **128** was allotted as (1*S*,4*S*,5*S*,6*S*,7*S*,10*R*), assisting with the assignments of eudesmanolides **129**–**132** isolated from the same plant extract.

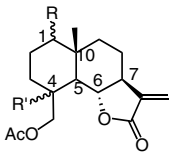

128, R = α-OH, R' = α-H
129, R = α-OH, R' = β-OH
130, R = β-OH, R' = β-OH
131, R = β-OH, R' = β-OAc
132, R = α-OAc, R' = α-OH

Example 9

The chirality of eremophilanoids **133** and **134**, sesquiterpenoids isolated from *Senecio* species, was assigned by means of VCD spectroscopy (*112*). Absolute configurations of the stereogenic centers C-4, C-5, and C-6 of the euryopsin skeleton are essential for establishing biogenetic relationships (*245*), hence the application of a strongly fundamental chiroptical method such as VCD to reassure their absolute configurations is perceived as worthwile. Sesquiterpenoids **133** and **134** have shown insect antifeedant activity. Only two significantly populated conformers resulted from a conformational search on each eremophilanoid due to the considerable rigidity of the euryopsin core. The *Boltzmann* average VCD spectrum of **133**, calculated at the B3LYP/6-31G(d,p) level, was found to be satisfactorily balanced between invested computing time and spectral similarity, assuring its configuration as (4*S*,5*R*,6*S*). Moreover, derivatization of **133** to the acetyl derivative **134** was carried out to reassure assignment with confidence since vibrational CO bands around 1,200 cm^{-1} of **133** presented no net intensity, a situation attributed to intermolecular hydrogen bonding that was confirmed by visible defined monosignated bands in the VCD spectra of **134** in this region. With the goal of supporting the biogenetic relationships among eremophilanoids isolated from different species, the absolute configuration of 1α-angeloyloxy-eremophilolide (**135**) isolated from *Psacalium paucicapitatum* was also determined by VCD. The close similarity of its calculated and observed VCD spectra confirmed the absolute configuration of **135** as (1*S*,4*S*,5*R*,8*S*,10*S*). In **135**, there are intramolecular hydrogen bonds of both hydroxy groups (*112*), thus resulting in a good comparison of the calculated and experimental plots (Fig. 42).

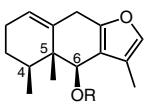

133, R = H
134, R = Ac

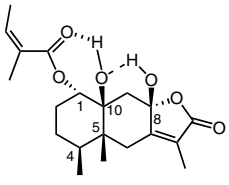

135

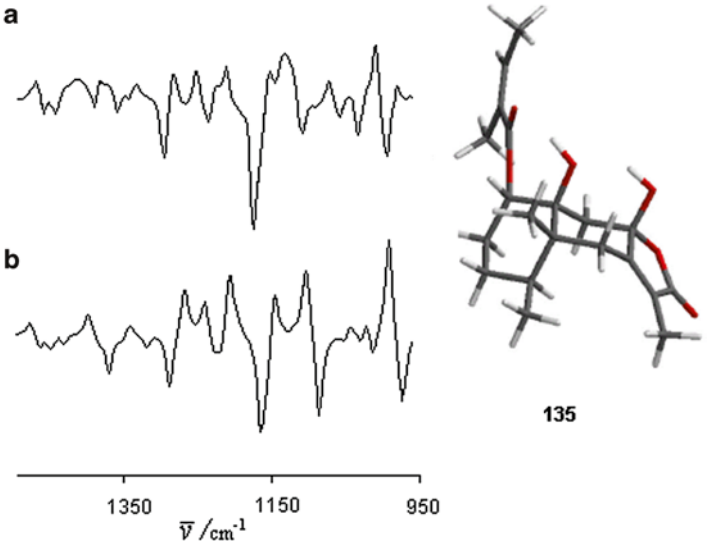

Fig. 42 Experimental (**a**) and calculated (**b**) VCD spectra of (1*S*,4*S*,5*R*,8*S*,10*S*)-1α-angeloyloxyeremophilolide (**135**). (Adapted from (*112*))

Example 10

The sesquiterpenes (+)-african-1(5)-ene-2,6-dione (**46**) and lippifoli-1(6)-en-5-one (**136**), isolated from *Lippia integrifolia* (Verbenaceae), a woody shrub with medicinal properties, were studied by VCD spectroscopy and modeled employing DFT calculations with the B3LYP and B3PW91 functionals at the DGDZVP and DGDZVP2 basis sets, respectively (*124*). Africanane **46** is related biogenetically to the lippifoliane **136**. By determining the absolute configuration of the C-4, C-9, and C-10 stereogenic centers, the relationship between these compounds was sustained and found to be in accordance with previous africanane derivative assignments. Africanane is a rigid tricyclic molecule, so only two conformers were detected in the Monte Carlo conformational search. In addition, the conformational map of lippifoliane, a less rigid molecule, was populated with four conformers. After optimization using DFT at the B3LYP/DGDZVP level of theory only one conformer remained populated for **46** and two for **136**. A general agreement between the observed and calculated VCD spectra allowed assignment of (+)-**46** as the (4*R*,9*R*,10*R*) enantiomer and lippifoliane **136** as the (4*R*,9*S*,10*R*) enantiomer. The absolute configuration of **46** is in agreement with that proposed on basis of its biogenetic relationship with **136**. Interesting features of VCD spectra for both molecules at the carbonyl region revealed that, according to ring current theory (*178*), the VCD monosignated bands come from independent enhanced magnetic transition moments in the α,β-conjugated C=O chiral induced oscillators (Fig. 43). The VCD spectrum of **46**, calculated at the B3PW91/DGDZVP2 level of theory, improved the similarity of the C=O stretching region when compared with the experimental spectrum.

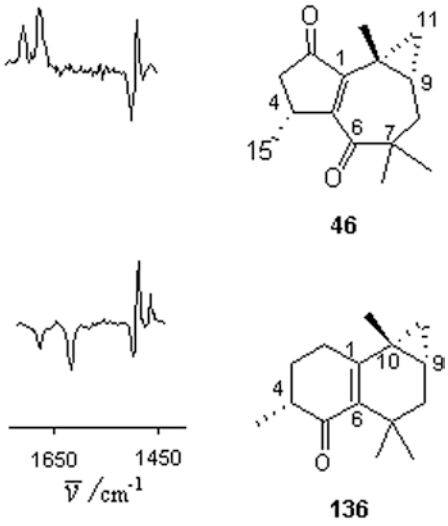

Fig. 43 Experimental VCD spectra of sesquiterpenes **46** and **136** at the α,β-conjugated carbonyl region. (Adapted from (*124*))

Example 11

The new 7*β*-angeloyloxy-8*α*-isovaleroyloxylongipin-2-en-1-one (**137**) along with the known longipinene derivatives **138** and **139** were isolated from *Stevia monardifolia* (*246*). Eighty-three conformers were found to inhabit the energy profile of **137** in the initial 40 kJ/mol. Geometry optimization of these 83 structures using DFT at the B3LYP/6-31G(d) level reorganized the conformer distribution to give 18 populated conformers in the cutoff limit of 10.3 kJ/mol. With the reoptimization of these 18 structures using the DFT B3LYP/DGDZVP method, five conformers, counting for less than 4% of the total population, were discarded with 13 structures remaining, which were used to calculate vibrational frequencies at the same level of theory. The *Boltzmann* weighted VCD spectrum showed several broad bands, apparently generated for the high degree of freedom of the angeloyloxy and isovaleroyloxy groups, complicating comparison with the experimental spectrum. To overcome this inconvenience, the absolute configuration of the acetylated product **140** was determined. In this case only three conformers were significantly populated after reoptimization using DFT B3LYP/DGDZVP calculations.

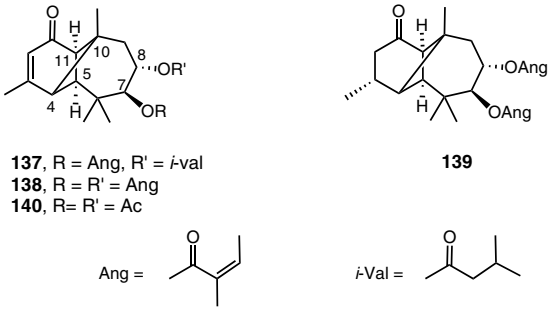

137, R = Ang, R' = *i*-val
138, R = R' = Ang
140, R= R' = Ac

139

The experimental to calculated VCD comparison of the spectra was in this case neatly observed (Fig. 44), supporting the assignment of the absolute configuration of longipinane **140**, and consequently of the new longipinane **137**, as (4*R*,5*S*,7*S*,8*S*, 10*R*,11*R*). The negative chirality (+,–) of the couplet around 1,200 cm^{-1} resembles that of longipinenes **55** and **50** (Fig. 17) wherein the stereochemistry of C-7 is also *β* (*149*).

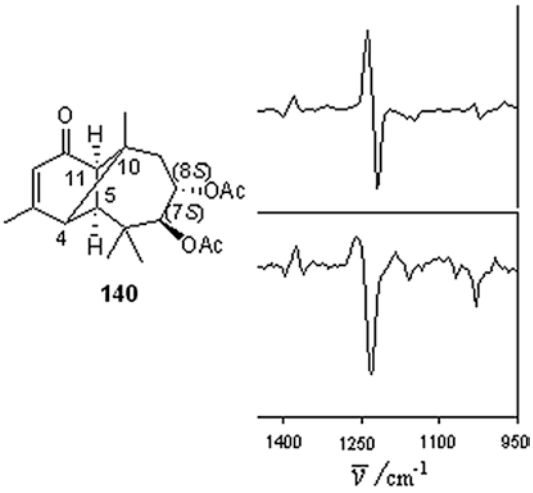

Fig. 44 Calculated (*top*) and experimental (*bottom*) VCD spectra of (4*R*,5*S*,7*S*,8*S*,10*R*,11*R*)-7,8-diacetoxylongipin-2-en-1-one (**140**). (Adapted from (*246*))

Example 12

VCD was employed to determine the absolute configuration of the sesquiterpene lactone 8-epiisolippidiol-3-*O*-*β*-D-glucopyranoside (**141**) isolated from *Crepis conyzifolia* roots (*247*). Deuterated methanol was used as the solvent to record the vibrational spectra in the 1,800–1,150 cm^{-1} region of this polar hydroxylated molecule. The stable conformations were found through a potential energy surface scan obtained by glycosidic bond rotation using semiempirical AM1 calculations. Optimization of the set of conformers with minimal energy at the HF/6-31G level of theory followed by DFT B3LYP/6-31G(d) provided six final conformers. The average IR and VCD spectra, calculated at the B3LYP/6-31G(d) level of theory, reproduced the corresponding measured spectra with good agreement of shape, relative intensities, and signs, suggesting that the solvent has no significant influence in the geometry of **141** so as to consider a theoretical model of solvation.

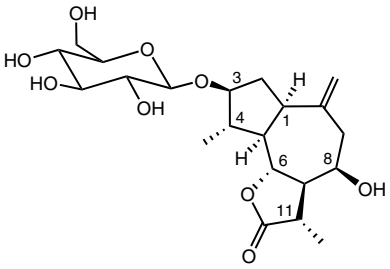

141

Example 13

The relative stereochemistry and absolute configuration of the guaianolide **142** isolated from leaves of *Hedyosmum arborescens* Swartz was evaluated by a combination of ^{1}H and ^{13}C NMR along with IR and VCD spectroscopy (*248*). From the 32 possible diastereomers, four possibilities (**142**, **143**, and their antipodes) were considered plausible candidates according to the 1D- and 2D-NMR spectra and N*O*E experiments. IR and VCD spectra simulations of these diastereomers, using DFT at the B3LYP/6-31+G(d,p) level of theory, which in both cases only showed one stable conformer due to their core rigidity, permitted a confident assignment based on close matching between the VCD spectra of (1*R*,5*R*,7*S*,8*S*,10*R*)-7,10-epoxyguaia-3,11-dien-8,12-olide (**142**) and the natural product at the fingerprint region. An analysis of vibrational normal modes at the carbonyl region led to the conclusion that **142** is associated to the solvent, $CDCl_3$, through H-bonding, although the solvent did not modify significantly the lower spectral regions used for absolute configuration assignment.

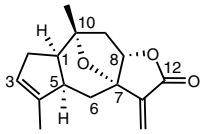

142

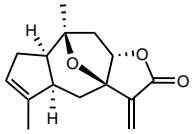

143

Example 14

Endoperoxides isolated from terrestrial and marine organisms may show antitumor and cytotoxicity activities. Acetylmajapolene A (**144**) from the red algal genus *Laurencia* was isolated abundantly as a mixture with its diastereomer endoperoxide **145** (*249*). Separation of these endoperoxides, successfully achieved by chiral HPLC, preceded elucidation of their absolute configuration using VCD measurements mainly focusing on the peroxide band at around 1,050 cm^{-1} (Fig. 45). Acetylmajapolene A (**144**) is a conformationally flexible molecule, thus MMFF94S force field calculations using the CONFLEX program provided 12 low-lying conformers for which the geometries were optimized by DFT calculations at the B3PW91/6-31G(d,p) level of theory. *Boltzmann* population-weighted VCD spectra of **144** and **145** in the 1,400–1,000 cm^{-1} region were in excellent agreement to their observed counterparts (Fig. 45), hence permitting definition of their absolute configuration as (1*R*,4*R*,7*S*,10*S*) and (1*S*,4*S*,7*S*,10*S*). Considering that assignment of endoperoxide absolute configuration normally involves a tedious chemical correlation procedure, the facile manner in which the relative stereochemistry and absolute configuration of **144** was distinguished from **145** suggests that VCD is a premium alternative method for the chiral characterization of endoperoxides.

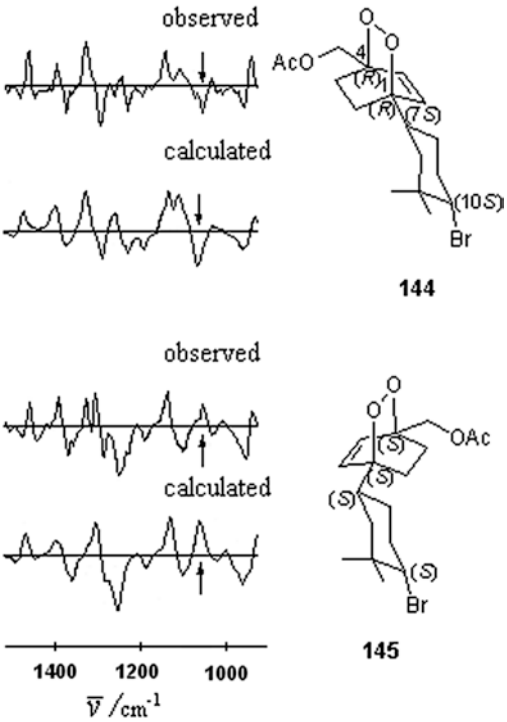

Fig. 45 Observed-to-calculated VCD spectra comparison of endoperoxides (1*R*,4*R*,7*S*,10*S*)-**144** and (1*S*,4*S*,7*S*,10*S*)-**145**. (Adapted from (*249*))

Example 15

As a pearl within the shell of an oyster, which is formed by its abnormal nacreous growth around a grain of sand, the secondary metabolite epazoyucine (–)-**146** accumulated in the aerial parts of *Stevia tomentosa* following a remarkable biochemical pathway which produced, as a gem, an unusual chiral sesquiterpene lactone containing a cyclopentane ring with two epoxy groups in a *cis* configuration and *β*-orientation (*250*). The enantiomer, (–)-**146**, was fully characterized by spectroscopic methods, establishing from NMR gCOSY, gHSQC, and gHMBC methods its relative stereochemistry, and from VCD spectroscopy its absolute configuration. The VCD spectrum of the (1*S*,3*S*,4*S*,5*R*,7*R*,8*R*,11*S*)-enantiomer, calculated at the B3LYP/DGDZVP level of theory, was obtained in a straightforward manner, since molecule **146** was found to be biased towards a single conformation. Figure 46 shows a comparison of the experimental and calculated VCD spectra where the close match between them can be appreciated visually. Nevertheless, the (–)-(1*S*,3*S*,4*S*,5*R*,7*R*,8*R*,11*S*)-**146** absolute configuration was corroborated by its quantitative assessment, which provided similarity indexes for the IR and VCD spectra comparison of S_{IR} = 87.1% and S_E = 82.5%, respectively. In addition, a crystal diffraction analysis of (–)-**146** allowed the unambiguous confirmation of its relative stereochemistry, and absolute configuration through the *Flack* (*251*) and *Hooft* parameters (*252*). As far as the authors are aware, this is the first work (*250*), together with a recent report about the XRD and VCD marriage, which gave rise to the absolute configuration determination of an enantiomeric pair of synthetic diazepinone derivatives (*253*), proving the complementary power of VCD and X-ray diffraction techniques to provide the absolute configuration of chiral molecules.

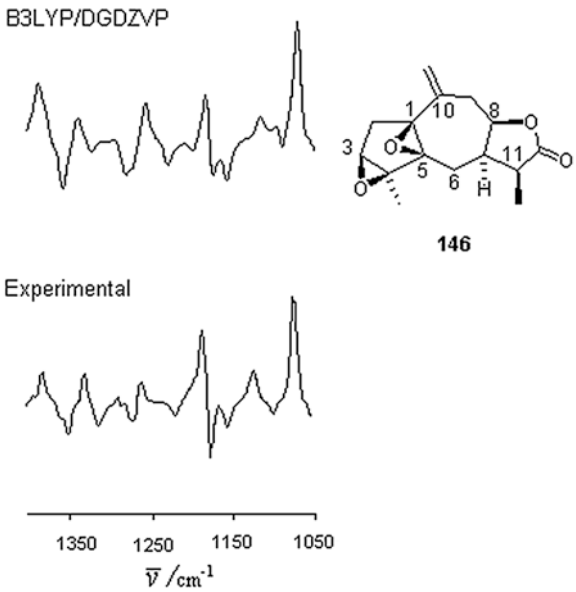

Fig. 46 Comparison of the calculated and experimental VCD spectra of (–)-(1*S*,3*S*,4*S*,5*R*,7*R*,8*R*,11*S*)-1,5:3,4-diepoxyguaia-10(14)-en-12,8-olide (**146**). (Adapted from (*250*))

Example 16

Chirality is easily observed in natural products for which the relationships are not limited to enantiomers but also to diastereomers. The components of a plant or other organism may often possess several chiral centers but only one or two of those chiral centers are of unknown absolute configuration, thus to search for reliable chiroptical techniques that can accomplish discrimination of chiral diastereomers is worthwhile. In one report (*254*), four cedranol acetates **147**–**150** of known configuration were employed as chiral trials for VCD quantitative assessments to investigate whether VCD is reliable to distinguish diastereomers **147**–**150**. Six stereogenic centers conformed to the chiral scaffold of these tricyclic sesquiterpenes, of which four of these centers (3*R*,3a*R*,7*S*,8a*S*) remain stereochemically fixed and two of them change for the diastereomers (5*R*,6*R*)-cedranol (**147**), (5*R*,6S)-neoisocedranol (**148**), (5S,6*R*)-neocedranol (**149**), and (5*S*,6*S*)-isocedranol (**150**). The simulation of the vibrational IR and VCD spectra was performed at two different levels of theory, B3LYP/DGDZVP and B3PW91/DGDZVP, on account of the fact that the B3LYP functional simulated the IR spectra of **147**–**150** with serious band frequency mismatching with the experimental spectra, leading to poor quantitative comparisons: S_{IR} values were obtained in the range of 60–70. In contrast, experimental IR and VCD spectra were simulated closely by the gradient-corrected B3PW91 correlation functional: S_{IR} values in the range of 85–95 and S_E values, for the correct enantiomer, in the range of 77–87. The reason for the different simulation performance between functionals is that cedranol acetates contain five-membered rings in their structures and these carbocycles undergo pseudorotation phenomena provoking flat conformational landscapes. Thus, to simulate vibrational properties of molecules possessing five-membered rings the B3PW91 functional is more useful than the B3LYP functional.

The number of conformers that populated the landscape of **147**–**150**, calculated at the B3PW91/DGZVP level of theory, varied in consideration to the conformational preferences of the acetyloxy group at C-5 and the methyl groups at C-3 and C-6. Hence, six conformers for **147**, two conformers each for **148** and **150**, and four conformers for **149** were taken into account for the weighted average simulated vibrational spectra of these diastereomers. The visual comparison of the experimental VCD spectra for **147**–**150** is shown in Fig. 47. It is interesting to note that the stretching C–O band of the ester group is shifted to different frequencies of the spectra depending upon the hybridization of the carbon atom, so that the C(sp^2)–O band appears as an intense signal at around 1,250 cm^{-1} and C(sp^3)–O as a non-intense band at around 1,020 cm^{-1}. Even though C–O bands usually guide visual comparison to assign configurations and/or to analyze conformations, the anisotropy factors (*g*-values) are more appropriate to disclose regions of high dissymmetry in the spectra ($g \sim 10^{-3}$), where the C–H vibrations of chiral centers appear. In the case of **147**–**150**, these regions are allied to bands absorbing at around 1,060–1,190 cm^{-1}.

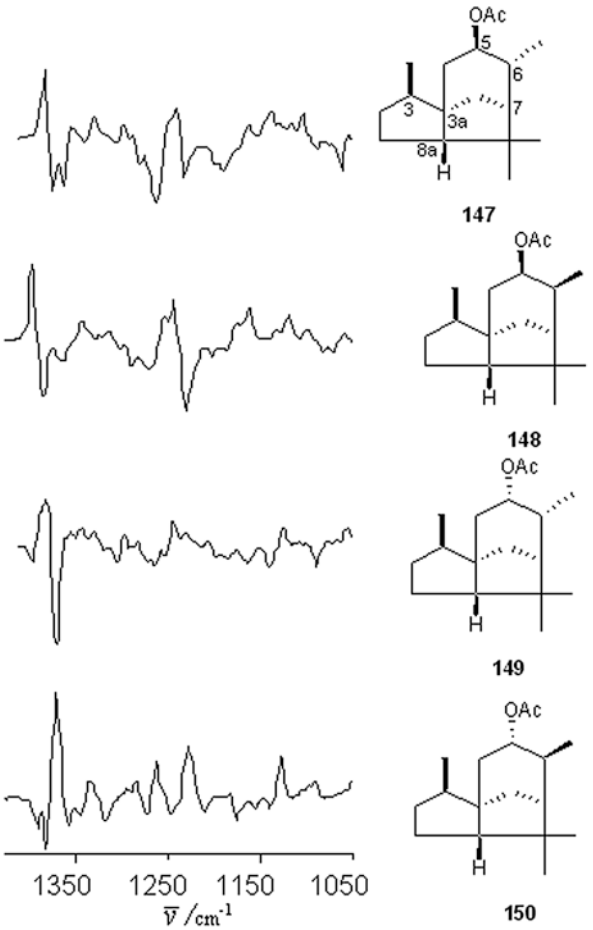

Fig. 47 Comparison of the experimental VCD spectra of (5*R*,6*R*)-cedranol **147**, (5*R*,6S)-neoisocedranol **148**, (5S,6*R*)-neocedranol **149**, and (5*S*,6*S*)-isocedranol **150**. (Adapted from (*254*))

Regarding diastereomeric discrimination, the analysis was performed by numerical comparisons of crossed experimental and calculated spectra, at the B3PW91/DGDZVP level, of **147**–**150**, using similarity indexes S_E, S_{-E} and ESI values. The results demonstrated that there was no crossed comparison superior

than the direct comparisons, for instance, the highest S_E value for a cross-comparison was 69.0 and the lowest S_E value for a direct comparison was 76.7. Therefore, it was concluded that the VCD technique is capable of distinguishing cedranol acetate diastereomers. IR crossed comparisons were by no means similar to VCD, since crossed S_{IR} values were as high as those for direct comparisons, indicating the IR technique by itself is not capable of discriminating **147**–**150**. A similar behavior was observed for the analogous tricyclic sesquiterpenes cedrol **75** and isocedrol **76** (*199*).

5.2.3 Diterpenes and Meroterpenoids

Diterpenes are biologically important natural products known for their antimicrobial and anti-inflammatory activities, among others. Vitamin precursors such as phytol and retinol are among the most distinctive diterpenoids. Meroterpenoids are mixed polyketide-terpenoids biosynthesized from terpene and polyketide precursors. Of particular relevance for the diterpenes is the configuration at C-10, since both normal and *ent* representatives are present in Nature. The already discussed diterpenoids are (+)-(1*S*,11*S*,12*S*)-verticillol (**2**) (*10*), (–)-stypotriol triacetate (**35**) (*110*), (+)-(*R*)-sargaol acetate (**37**) (*87*), (*R*)-2-hydroxymutilin (**79**) (*203*), (*S*)-2-hydroxymutilin (**80**) (*203*), and paclitaxel (**92**) (*213*), and in this section some of them are discussed in more detail.

Example 1

The absolute configuration of the endoperoxide diterpene **151**, isolated from *Calceolaria buchtieniana*, that grows in the mountainous zone of Bolivia, was ascertained using VCD methodology (*255*). As for endoperoxides **144** and **145** (Fig. 48), the peroxide band close to 1,050 cm^{-1}, along with the ester C–O peaks, are the signature bands for this molecule. The simulated *Boltzmann* averaged VCD spectrum of three conformers at the B3PW91/DGDZVP level of theory, in the fingerprint zone, matched clearly with the experimental VCD spectrum (Fig. 48) assuring the absolute configuration of **151** to be assigned unambiguously as (–)-(1*S*,5*S*,6*R*,8*S*,9*S*,10*R*,13*S*). The relative stereochemistry was independently verified by single crystal X-ray diffraction (*255*).

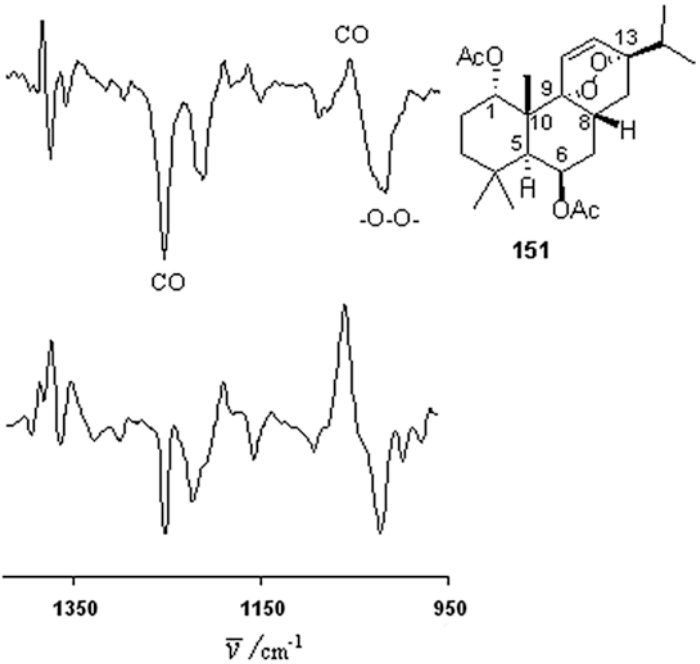

Fig. 48 Experimental (*top*) and simulated (*bottom*) VCD spectra of endoperoxide (1*S*,5*S*,6*R*,8*S*,9*S*,10*R*,13*S*)-**151**. (Adapted from (*255*))

Example 2

The stereochemistry of (+)-aframodial (**152**), a labdane diterpene isolated from the seeds of *Aframomum danielli* with both antifungal and antileukemic activity, was allotted by VCD methodology (*256*). The conformational flexibility of the side chain provided the molecule with helicity, an extra element of chirality. The eight possible chiral diastereomers were simulated with DFT at the B3LYP/6-31G(d) level of theory. VCD signal intensities and the sign for the C=C and two C=O stretch modes allowed local absolute configuration assignment for the four stereogenic centers as (1*R*,2*S*,4a*S*,8a*S*), as shown in diastereomer **153**. An induced VCD signal from the normal mode localized in the achiral dial chromophore at the side chain, was used to give rotational conformation of the two aldehyde groups, distinguishing the (*E*) diastereomerism of the double bond.

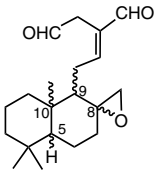

152

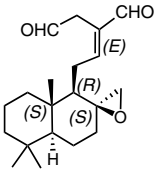

153

Example 3

Verticillane diterpenoids are fundamental key precursors in the biosynthesis of taxanes. The absolute configuration of (+)-verticillol (**2**), isolated from *Bursera suntui*, was assigned by VCD methodology (*10*). An initial conformational search performed by molecular mechanics using the Monte Carlo method was conducted on six conformers, three O–H rotamers with the six-membered ring in the chair conformation (Fig. 23) and the other three with the six-membered ring in the boat conformation. Optimization using the DFT B3LYP/6-31G(d,p) method pointed to the chair conformers as being more stable than the boat conformers. The observed and *Boltzmann* average VCD spectra, calculated at the same level of theory clearly matched, indicating that the absolute configuration of (+)-verticillol (**2**) to be (1*S*,11*S*,12*S*), in agreement with absolute configuration assignment reported for (+)-verticillol isolated from *Sciadopitys verticillata*, which was studied by anomalous dispersion X-ray analysis of its *p*-iodobenzoate derivative **154**, and the mirror image to the enantiomer suggested by application of the octant rule on norketodiepoxide **155** isolated from *Sciadopytis verticillata*.

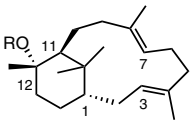

2, R = H
154, R = OC_6H_4-*p*-I

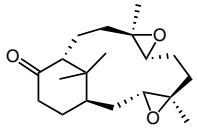

155

Example 4

Two novel rearranged neoclerodane diterpenoids, salvileucalin A (**156**) and salvileucalin B (**157**), were isolated from the aerial parts of *Salvia leucantha* (Labiatae) and their absolute configuration determined by VCD measurements (*257*). The unprecedented rearranged skeleton structure of **157** was envisaged by a two-step biogenetic pathway from **156**. Neoclerodane **156** is a selective κ-opioid receptor agonist with hallucinogenic activity. DFT-VCD calculations on **156** and **157** over the populated average conformers, three in each case, directed a clear absolute configuration assignment by comparison with measured spectra at the carbonyl region. The couplets are shown in Fig. 49. VCD at the carbonyl region is extremely sensitive to stereochemistry of chiral molecules, *e.g.* the α and β anomers of sialic acid derivatives (*258*).

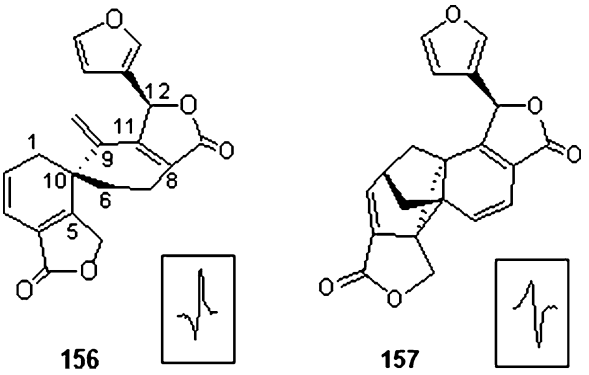

Fig. 49 Carbonyl region couplets of salvileucalin A (**156**) and salvileucalin B (**157**). (Adapted from (*257*))

Example 5

The polycyclic meroditerpenoid isoepitaondiol (**158**) is a biologically active natural product isolated from *Stypopodium flabelliforme* with potential anti-inflammatory and antitumor activities. In this work the stereochemistry of **158** was revisited to propose a new relative configuration based on NMR studies carried out on an isoepitaondiol diacetate derivative (**159**) and confirmed by X-ray crystallography. Moreover, the solid state structure of **158** revealed that the absolute configuration assignment based on the *Flack* parameter was considered non-conclusive, as evidenced by the use of *Mosher* esters. Thus, the absolute configuration assessment of **159** was determined by measurement of the VCD spectrum in combination with DFT B3LYP/DGDZVP calculations (*259*).

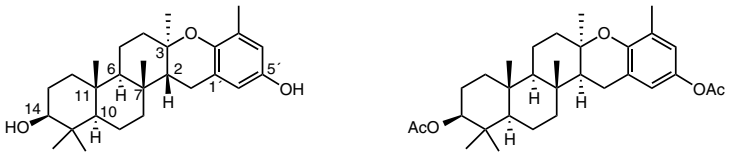

The meroditerpenoid derivative **159** is a rather large molecule ($C_{31}H_{44}O_5$) with 36 non-hydrogen atoms and 270 electrons. The X-ray structural data of **159** were used as input for a Monte Carlo guided conformational search, resulting in 13 conformers in the first 41 kJ/mol. Geometry optimization at the B3LYP/DGDZVP level of theory allowed conformers to be discarded giving rise to only two low-energy conformers in a ratio of *ca.* 3:1. All six-membered rings are chairs in both conformers but the acetyl group at C-5′ is rotated differently. VCD observed and calculated *Boltzmann* average spectra are shown in Fig. 50. The clear correlation between them supports the configuration depicted for the structures.

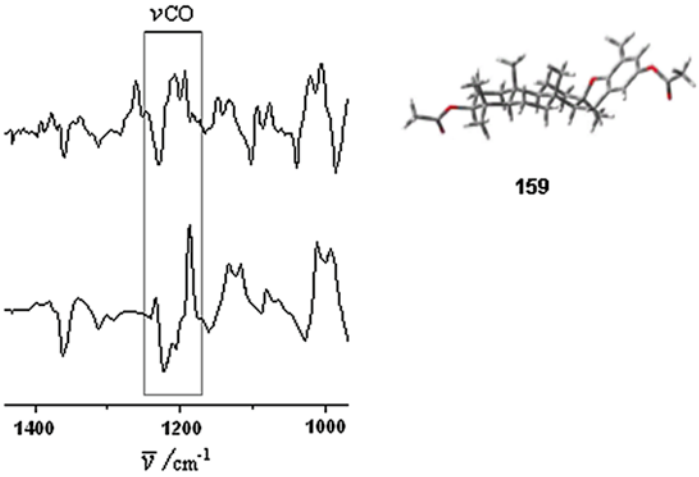

Fig. 50 Experimental (*top*) and calculated (*bottom*), at the DFT B3LYP/DGDZVP level of theory, VCD spectra of isoepitaondiol diacetate (**159**). (Adapted from (*259*))

The chiral distinction of the VCD spectrum of **159** is the bisignated bands at around 1,200 cm^{-1} allied to ester νCO stretching vibration. This vibrational mode also distinguishes the VCD spectrum of stypotriol triacetate (**35**) (*110*) (Fig. 51), a large meroditerpenoid derivative with similarities in its structure.

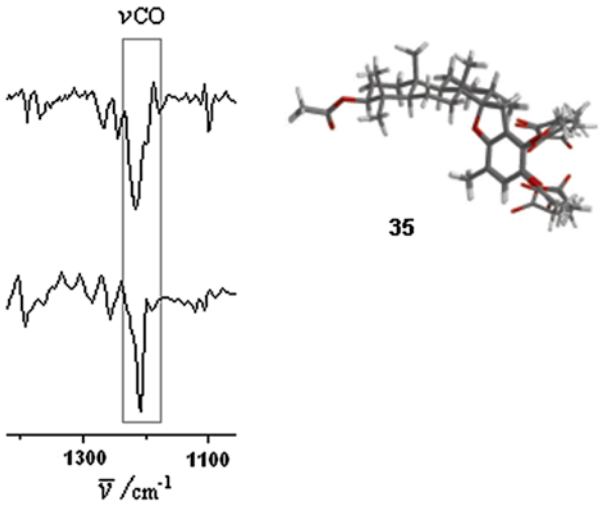

Fig. 51 Experimental (*top*) and calculated *Boltzmann* weighted (*bottom*), at the DFT B3LYP/DGDZVP level of theory, VCD spectra of stypotriol triacetate (**35**) shown with six superposed conformers. (Adapted from (*110*))

Example 6

The meroditerpenoid taondiol (*260*) is produced by marine algae in different enantiomeric forms; for instance, from the alga *Stypopodium flabelliforme* collected from Easter Island and from the alga *Taonia atomaria* (Dictyotaceae), the levorotatory form (–)-taondiol **160** was isolated, whereas from the brown alga *Stypopodium zonale* the partially racemized antipode (+)-taondiol **161** was found. Even though the structure of taondiol was reported more than 40 years ago (*261*), its absolute configuration was lacking confirmation, thus the VCD technique was applied to assign the (2*S*,3*S*,6*R*,7*R*,10*R*,11*R*,14*S*) absolute configuration for (–)-**160**, which was isolated as the diacetate derivative (–)-**162** from the alga *S. flabelliforme*, and consequently to disclose the (2*R*,3*R*,6*S*,7*S*,10*S*,11*S*,14*R*) absolute configuration for its antipode (+)-**161** (*260*). Taondiol diacetate **162** is a C-3 epimer of isoepitaondiol diacetate **159** and a C-6,C-7 diastereomer of epitaondiol diacetate **163**, another meroditerpenoid isolated from *S. flabelliforme* for which the relative stereochemistry was reassigned using 2D-NMR and N*O*E correlations (*262*), assuring its absolute configuration as (+)-(2*S*,3*S*,6*S*,7*S*,10*R*,11*R*,14*S*)-**163** by VCD (*260*).

In the conformational search of the energy low-lying conformers of **162** and **163**, it was found that only two conformers each were stable within the first 16 kJ/mol, the differences between every pair were found in the rotameric conformation of the 5′-OAc group but not in the polycyclic skeleton, which is presumably rigid in both compounds. Due to the B/C ring junction stereochemistry, the B and C rings in taondiol **162** adopt chair conformations but in epitaondiol **163**, rings B and C are in twist-boat conformations. VCD spectra calculated at the B3LYP/DGDZVP and at the B3LYP/DGDZVP2 levels of theory for **162** and **163**, matched well with their corresponding experimental spectra (Fig. 52). The VCD similarity index data S_E=82.0 for **162** and S_E=71.1 for **163** confirmed their absolute configuration assignments with 100% confidence.

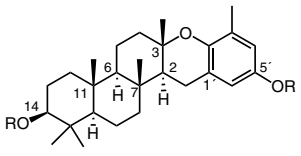

(–)-**160**, R = H
(–)-**162**, R = Ac

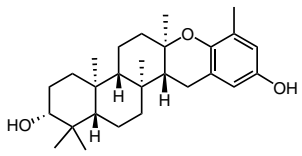

(+)-**161**

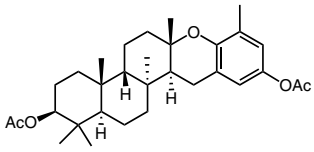

(+)-**163**

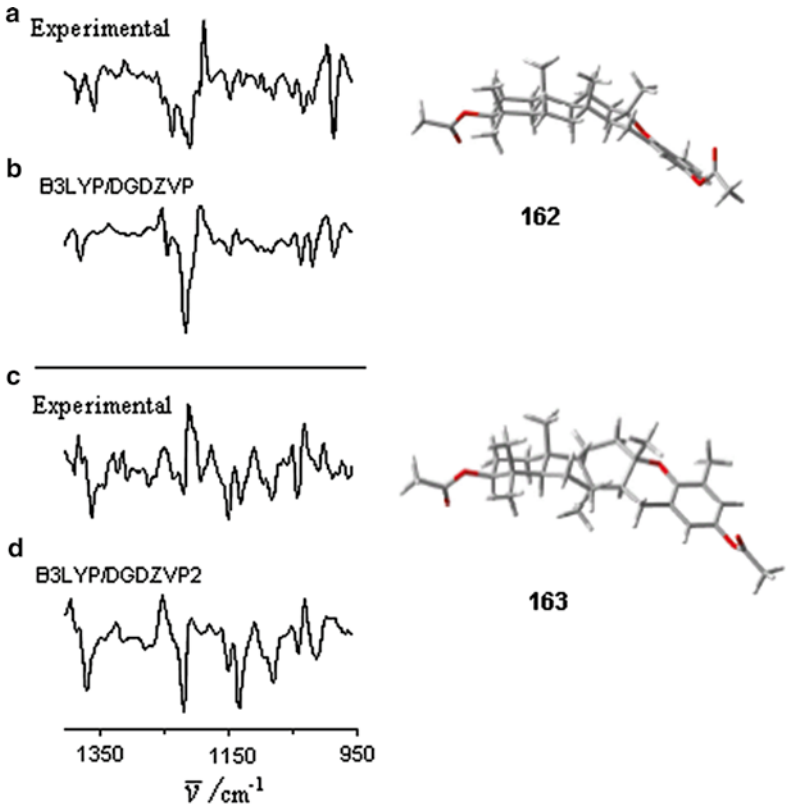

Fig. 52 Observed (**a**) and calculated (**b**), at the B3LYP/DGDZVP level, VCD spectra of (–)-(2*S*,3*S*,6*R*,7*R*,10*R*,11*R*,14*S*)-taondiol diacetate (**162**). Observed (**c**) and calculated (**d**), at the B3LYP/DGDZVP2 level, VCD spectra of (+)-(2*S*,3*S*,6*S*,7*S*,10*R*,11*R*,14*S*)-epitaondiol diacetate (**163**). (Adapted from (*260*))

Example 7

The chiral meroditerpenoid zonaquinone acetate (+)-**164** was isolated for the first time from the Jamaican brown alga *Stypopodium zonale* (*263*). The structural characterization of **164**, accomplished by 1D- and 2D-NMR spectroscopy, agreed with that reported for flabellinone (*264*) in so far as both molecules have the same skeleton. The relative stereochemistry of **164** was established from N*O*ESY correlation experiments, and its absolute configuration from VCD analysis. The enantiomer (2*R*,3*R*,6*R*,7*R*,10*R*,11*R*,14*S*)-**164** was selected for VCD calculations to enable its further confirmation by comparison with the experimental VCD spectrum of (+)-**164**.

It has been seen in the previous example that the meroditerpenoids taondiol and epitaondiol have rigid skeletons; zonaquinone **164** is also rigid so that calculations predicted it is fixed in only one conformer. The IR and VCD spectra of (2*R*,3*R*,6*R*,7*R*,10*R*,11*R*,14*S*)-**164** were calculated at the B3LYP/DGDZVP level and at the higher B3LYP/DGZVP2 and B3PW91/DGDZVP2 levels of theory, since the DGDZVP basis set complicated its comparison with the experimental VCD spectrum due to band mismatching at the shorter frequency region (1,250–950 cm^{-1}). The double polarized DGDZVP2 basis set represents a rather different situation in that the visual and quantitative matching of the VCD spectra at the whole fingerprint region (1,550–950 cm^{-1}) is good; this confirmed the (2*R*,3*R*,6*R*,7*R*,10*R*,11*R*,14*S*) absolute configuration for (+)-**164**. The correct enantiomer similarity index S_E value quantified for the comparisons of the experimental and calculated VCD spectra using the B3LYP or B3PW91 functionals and the DGDZVP2 basis set are 73.8 and 78.0, respectively, these values are indicative of the superior B3PW91 performance in vibrational calculations of **164**. A partial display of the VCD spectra showing the C–O vibrations at around 1,250 cm^{-1}, and C–H vibrations at around 1,350 and 1,050 cm^{-1}, is shown in Fig. 53. It is noticeable that zonaquinone acetate displayed *in vitro* cytotoxic activity against breast and colon cancer cell lines, comparable in potency to tamoxifen and fluorouracil (*263*).

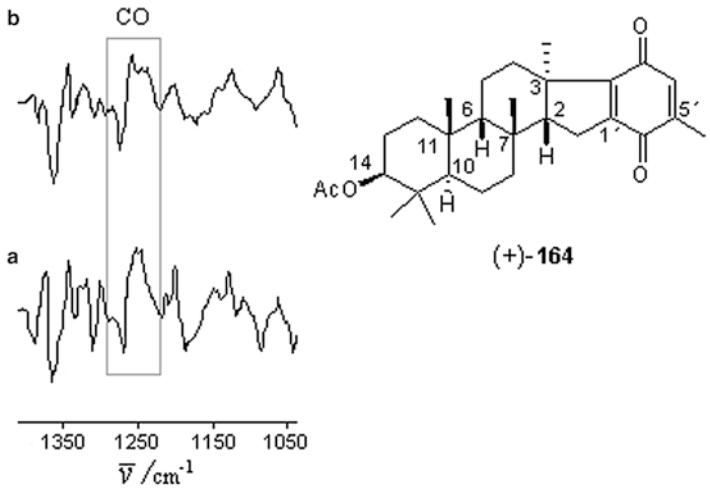

Fig. 53 Observed (**a**) and calculated (**b**), at the B3PW91/DGDZVP2 level of theory, VCD spectra of (+)-(2*R*,3*R*,6*R*,7*R*,10*R*,11*R*,14*S*)-zonaquinone acetate (**164**). (Adapted from (*263*))

Example 8

Sargaol (**36**) is a chromene meroterpenoid with antioxidant properties, for which the absolute configuration has been inconsistently reported as (*R*) or (*S*). Therefore, VCD was applied to determine unequivocally its absolute configuration through the derivative (+)-sargaol acetate (**37**) isolated from the brown alga *Stypopodium flabelliforme* (*87*). Sargaol is a conformationally very flexible molecule, thus a conformational search for models **38**–**40** and sargaol acetate using a Monte Carlo stochastic algorithm resulted in 12, 82, 596, and 2172 conformations for **38**–**40** and **37**, respectively. Since for the larger molecules **37** and **40** the number of conformers is impractical for calculations, a selection was carried out based on structural diversity, keeping only 100 conformations each.

The number of low-energy conformations taken into account in the calculations of *Boltzmann*-weighted VCD spectra were 14 for **37**, 6 for **38**, 15 for **39**, and 34 for **40**. The main differences between the conformers were found in the rotation of the OAc group and at the chain. Superimposed conformers in combination with VCD spectra for each molecule, including the experimental VCD spectrum of **37** are shown in Fig. 54. The positive chirality (–,+) of a couplet at around 1,200 cm^{-1}, corresponding to the CO vibration, could be predicted in all cases. Remarkably, there were no significant differences between VCD simulated spectra of models **38**–**40** with truncated groups for the chain and the experimental VCD spectrum of **37**. Accordingly, it was concluded that replacement of the large achiral fragment by a small fragment in meroterpenoid **37** could be used in simplifying the calculations. The absolute configuration of **37**, and consequently of sargaol (**36**), is (*R*). However, it has to be taken into account for conformationally flexible molecules that the VCD sign of some of the normal modes may be a good signature for conformation although not necessarily for absolute configuration (*264*) (Fig. 54).

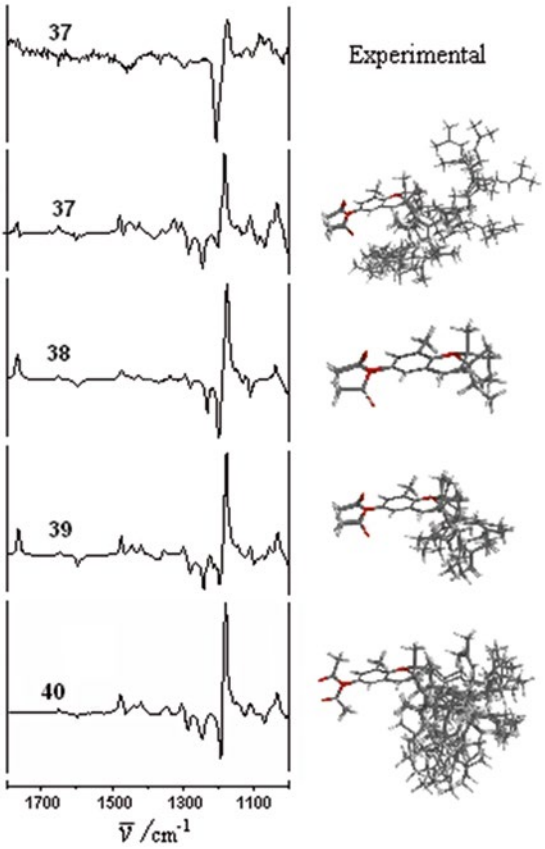

Fig. 54 VCD spectra comparison of sargaol acetate (**37**) and models **38**–**40**. Drawings show superposed conformers. (Adapted from (*87*))

Example 9

A bioassay-guided isolation of the anti-tuberculosis active principle of a methanol extract of *Leucophyllum frutescens* (Scrophulariaceae) root bark led to the diterpene serrulatane **165**, for which the partial relative stereochemistry was established by very detailed ^{1}H NMR measurements performed at 900 MHz, while the absolute configuration was determined by VCD spectroscopy (*265*). Assignment of the C-1 and C-4 configurations (1*R*,4*S*) was proposed by a non-direct method by considering the diterpene (–)-erogorgiaene. Therefore, DFT-VCD simulations were performed for the two C-11 epimers (11*S*)-**165** and (11*R*)-**166**. Due to a high conformational flexibility of the aliphatic chain, 199 conformers were found for epimer (11*S*) and 193 conformers for (11*R*) by a Monte Carlo mapping search. After optimization

using the DFT B3LYP/DGDZVP method, 10 and 13 conformers remained significantly populated for the (11*S*)- and (11*R*)-diastereomers, respectively. Comparison of their VCD spectra (Fig. 55) allowed assignment of the (*S*) configuration to C-11. This new serrulatane was given the trivial name "leubethanol". The major difference in the VCD spectra between the compounds with the (11*S*) and (11*R*) configurations is found in the sign of the bands at around 1,400 cm^{-1}, which are likely to be assigned to δCH bending vibrations, as shown in Fig. 55.

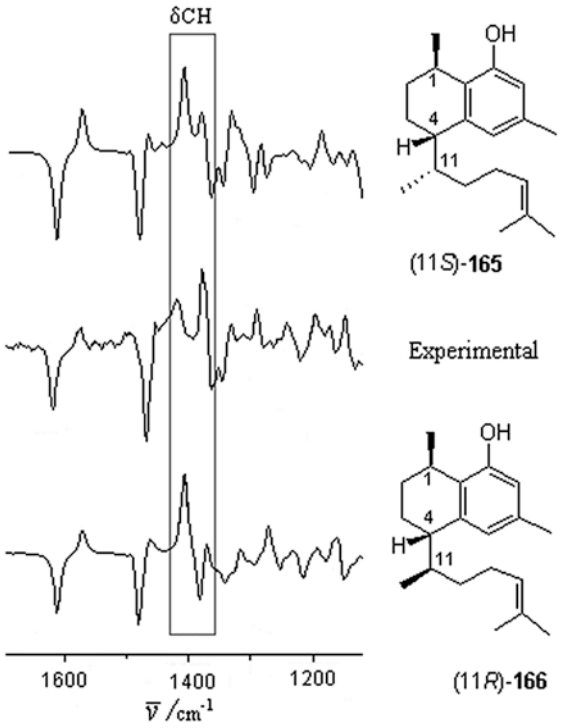

Fig. 55 Comparison of the VCD spectra of epimeric serrulatanes **165** and **166**. (Adapted from (*265*))

Example 10

On being extracted from the aerial parts of *Chromolaena pulchella*, (–)-hautriwaic acid lactone (**167**) and (+)-isoabienol (**168**) were studied by VCD. Lactone **167** belongs to the *ent*-clerodane diterpene series, which is stereo-related biogenetically to the *ent*-labdanes, but *enantio*-related to the labdane diterpenes, as represented by isoabienol (**168**). VCD was used to distinguishing the configuration of four stereogenic centers (C-5, C-8, C-9, C-10) for both diterpenes to support the proposed steps in the *ent*-clerodane and labdane biogenetic pathway (*266*). Due to the flexible side chain and the hydroxy group, the Monte Carlo conformational search resulted in 57 conformers for soabienol (**168**) and 25 for for lactone **167**. After optimization using DFT at the B3LYP/DGDZVP level of theory, nine conformers remained in the initial 8 kJmol^{-1} range for **168**, with only two for **167**. *Boltzmann*-weighted VCD spectra for both compounds, calculated at the same level of theory, were compared to the corresponding experimental VCD spectra and found to represent a good match in both cases. Moreover, a VCD spectral similarity value for the correct enantiomer (S_E=80.8%) confirmed the (5*S*,8*R*,9*S*,10*R*) absolute configuration for **167** and a (S_E=77.5%) confirmed the (5*S*,8*R*,9*R*,10*S*) absolute configuration for **168** with a 100% confidence level for both. The absolute configuration assignments support the proposed biogenetic pathway (Fig. 56).

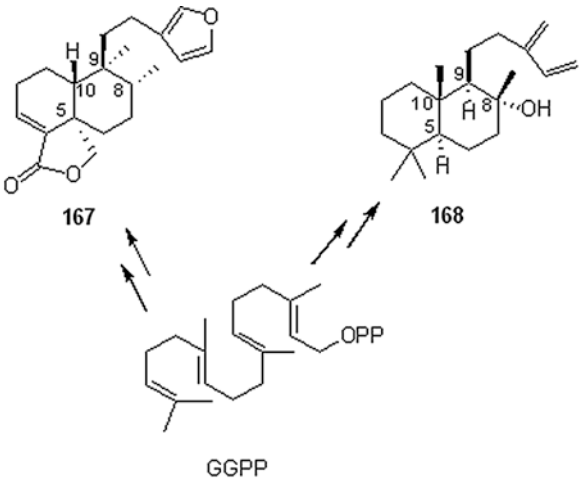

Fig. 56 Schematic representation of the biosynthetic generation of diterpenes **167** and **168**

Example 11

The stereochemistry of salvic acid (**169**), a constituent of the leaves of *Eupatorium salvia*, was investigated by VCD spectroscopy of its *O*-methyl ether methyl ester derivative **170** and the crystal diffraction analysis of its diol derivative **171** (*267*). The skeletal structure of **169** has been reported inconsistently as *normal*- or *ent-labdane*, as structures **172** and **173**, respectively. VCD combined with X-ray crystallography proved their potential to establish unambiguously the absolute configuration of (+)-**169** as an *ent*-labdane. Simulations of the conformational composition of **170** with a (13*R*) side chain absolute configuration and of its epimer **174** with a (13*S*) one, were performed at the B3LYP/DGDZVP level of theory giving rise to three and two energy low-lying conformers. Numerical VCD analyses were carried out under the Compare*VOA* algorithm (*130*) for **170** and its epimer **174**. The spectral similarity index values (S_E), for the correct enantiomer, and (S_{-E}), for the incorrect enantiomer, are fairly apart: 72.9 and 20.6 for **170** but closer to one another: 50.7 and 27.3 for **174**, with the enantiomer similarity index (*ESI*) difference for **170** almost double that for **174**: 52.3 and 23.2, leading to a 100% absolute configuration confidence assignment for (13*R*)-**170** against only a 42% confidence assignment for (13*S*)-**174**.

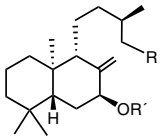

169, R = CO_2H, R´= H
170, R = CO_2Me, R´= Me
171, R = CH_2OH, R´= H

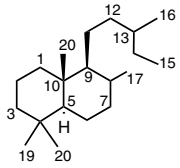

172

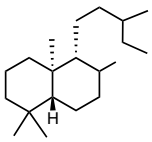

173

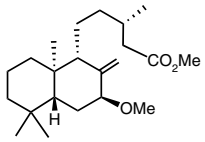

174

Example 12

The absolute configuration of rosmaridiphenol (**175**) a component of rosemary *Rosmarinus officinalis* L. (Lamiaceae), the fragrant evergreen herb with ornamental, culinary, and medicinal usage known since ancient times, was examined by spectroscopic VCD measurements of its diacetate **176** (*268*). A description of the ^{1}H NMR simulated full spin–spin assignment of **176** allowed the preferred conformation in solution to be disclosed. Moreover, the relative stereochemistry of **176** was confirmed

by its crystal X-ray diffraction study, which also provided the conformation in the solid state. The conformational landscape theoretical study of **176** was achieved using the DFT B3LYP/DGDZVP method, which constituted a global minimum conformer surrounded by four local minima conformations and together accounted for 99.3% of the *Boltzmann* distribution. The geometrical arrangement of the skeletal 6- and 7-membered rings is chair/chair and was observed commonly not only in the five calculated conformers, but also in solution and solid state conformations. The VCD comparison of the observed and calculated spectra showed two couplets, one of positive chirality (–,+) at around 1275 cm^{-1}, and the other one of negative (+,–) chirality at around 1215 cm^{-1}, allied presumably to the CO ester vibrations (Fig. 57). Visual matching of the observed and calculated VCD spectra allowed the absolute configuration determination of (+)-**176**, and consequently that of rosmaridiphenol (**176**) to be assessed as (5*S*,10*R*).

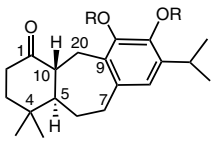

175, R = H
176, R = Ac

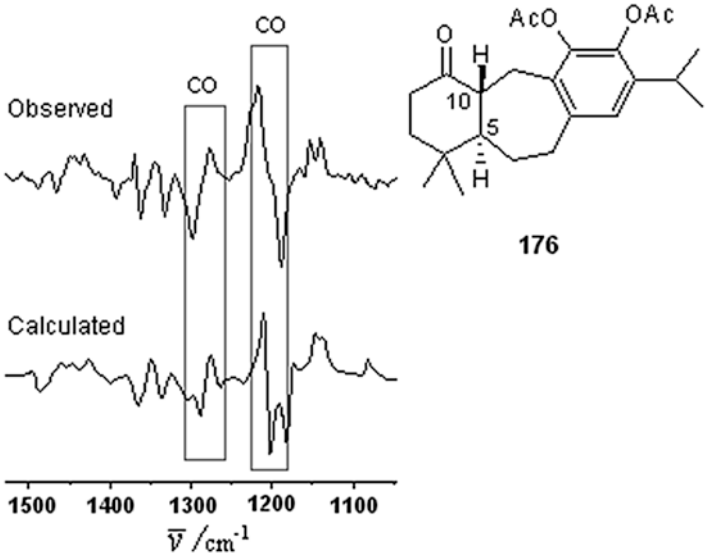

Fig. 57 Comparison of the VCD spectra of (+)-(5*S*,10*R*)-rosmaridiphenol diacetate (**176**). (Adapted from (*268*))

Example 13

The new diterpenoid (–)-(5*S*,7*R*,8*R*,9*R*,10*S*)-7,8-*seco*-7,8-oxacassa-13,15-dien-7,17-diol (**177**), along with the known (–)-(5*S*,7*R*,8*R*,9*R*,10*S*)-7,8-*seco*-7,8-oxacassa-13,15-dien-7-ol-17-aldehyde (**178**) and (–)-(5*S*,7*R*,8*R*,9*R*,10*S*)-7,8-*seco*-7,8-oxacassa-13,15-dien-7-ol (**179**) were isolated from the aerial parts of *Acacia schaffneri*, a genus known for the analgesic and antiseptic properties of some of its constituents (*269*). The stereochemistry of these *seco*-oxacassanes was established by chemical correlation and X-ray diffraction analysis. The absolute configuration of the new diterpenoid **177** was assessed by VCD spectroscopy of (–)-(5*S*,8*R*,9*R*,10*S*)-7,8-*seco*-7,8-oxacassa-13,15-dien-7-one (**180**) a derivative obtained by oxidation of lactol **179** (*269*). The rigid ring architecture of **180** rendered simulation of the VCD spectrum, at the B3PW91/DGDZVP2 level, with an average conformational equilibrium biased towards one of two conformers (99:1), the most abundant containing the s-*trans* diene fragment. The chirality signature of **180** appeared in the 1,350–1,100 cm^{-1} region of the VCD spectrum where lactone vibrations are expected. Frequency and intensity matching of simulated and observed bands were in agreement with the absolute configuration borne out by the structure drawn, and an opposite absolute configuration to that reported for known *seco*-oxacassane diterpenes.

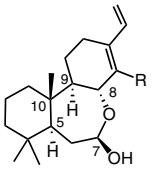

177, R = CH_2OH
178, R = CHO
179, R = CH_3

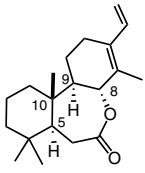

180

Example 14

The capability of Nature to biosynthesize unexpected molecules with a high degree of symmetry is exemplided from a further study of the aerial parts of the legume tree *Acacia schaffneri* (*270*). The study allowed the isolation and structural elucidation of schaffnerine (**181**) a macrocyclic dimeric diterpene with a C_2 symmetry axis. The structure of **181** was determined from its physical and spectroscopic data, in particular ^{1}H and ^{13}C NMR measurements in one- and two-dimensions and its absolute configuration and conformation followed after comparison of its VCD spectrum with that obtained after DFT calculations.

The atom coordinates that arose from a single crystal X-ray diffraction analysis of **181** generated a molecular model that was subjected to a conformational search using a Monte Carlo approach at the MMFF level affording 14 conformers in a 40 kJ/mol gap. Single point DFT calculations using the B3LYP/6-31(d) level of

theory left only four conformers, in an energy window of 20 kJ/mol, which showed variations in the C-1–C-2–C-3–C-4–C-5–C-10 and C-1′–C-2′–C-3′–C-4′–C-5′–C-10′ six-membered rings. Geometry optimization of these four conformers using the DFT B3LYP/DGDZVP level of theory and calculation of the harmonic vibrational frequencies yielded one main conformer (93.6%) and only a second conformer (6.4%) for **181**. Figure 58 provides a comparison between the theoretical and experimental VCD spectra of **181**. The X-ray measured dihedral angles and the DFT calculated values of the 12-membered heterocyclic ring of **181** are in good agreement with the values for 1,3,7,9-tetraoxacyclododecane existing in the [3333] conformation (*271*).

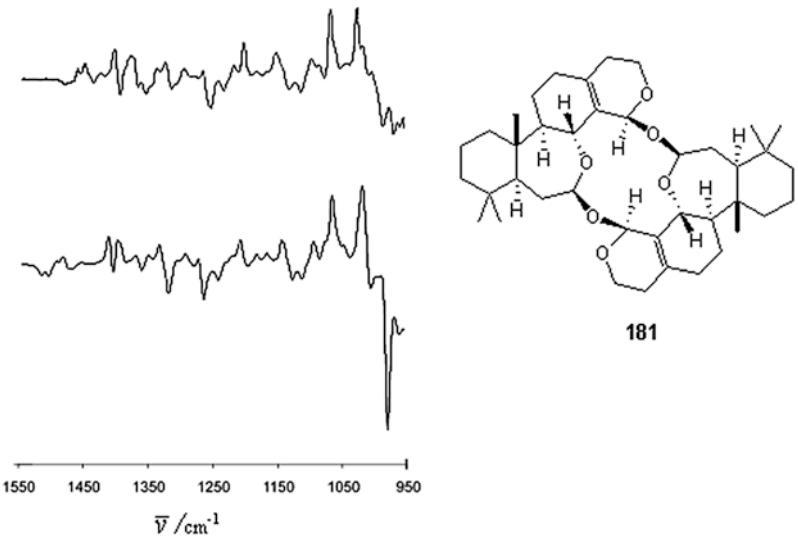

Fig. 58 Comparison of the experimental (*top*) and calculated (*bottom*) VCD spectra of (–)-schaffnerine (**181**). (Adapted from (*270*))

Example 15

The structure and relative stereochemistry of the orthoester meroterpenoid (–)-novofumigatonin (**182**), a novel *epi*-aszonalenin isolated from the pathogenic fungus *Aspergillus fumigatus*, was investigated by 2D-NMR, X-ray crystallography, and VCD-DFT methodologies to assign its absolute configuration (*272*). The X-ray structure of **182** was taken as the initial geometry for DFT calculations, the geometry optimization was carried out with OPLS-2005 force-field followed by B3LYP/6-

31-G(d,p) calculations. The DFT simulations of IR and VCD spectra were performed at the same level of theory. The bands around the carbonyl region in the experimental IR spectrum are significantly broader than in the calculated spectrum (Fig. 59), suggesting that solvent molecules are in the coordination sphere of the molecule, however calculations using implicit solvation did not improve the matching in the breadth of these bands. In any event, the good agreement between the experimental and calculated VCD spectra of the two most prominent bands at around 1,100 and 1,150 cm^{-1} corroborates the absolute configuration assignment given in structure **182** (Fig. 59).

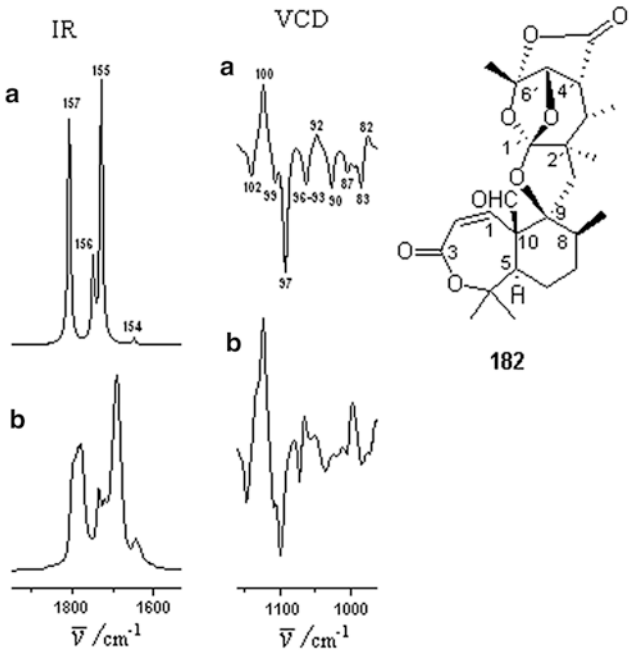

Fig. 59 Comparison of the calculated (**a**) and experimental (**b**) IR and VCD spectra of (–)-novofumigatonin (**182**). (Adapted from (272))

5.2.4 Triterpenes

Example 1

Diastereoisomers cannot easily be distinguished by dipole moment measurements since each diastereomer is an ensemble of conformers, and dipolar moments vary with conformation. Even though simulation of conformational average IR spectra based on free energy calculations is quite reliable by the DFT method (*273*), a clear distinction of diastereomers is not always easily achieved. Such is the case for the pair of sesquiterpene epimers, (6*R*)- and (6*S*)-cedrols **75** and **76** (Fig. 24), for which the configurational assignment was determined successfully using VCD. This same technique was used for diastereomers **75** and **76** as an unambiguous sensor tool of chirality for one center (C-6) in the presence of four other chiral carbons (*199*). Therefore, in order to differentiate the absolute configuration of the 20,29-epoxylupan-3-one triterpenoids, epimeric (20*R*)-**183** and (20*S*)-**184** were considered for VCD spectra calculations (*274*). These structures contain one different chiral center of a total of ten chiral centers. Therefore, in this work, the reliability of VCD as to provide chiral stressed responses leading to the differentiation of diastereomers was tested. The lupanone triterpene skeleton is a conformationally rigid structure, so only four conformers out of six, rotameric on the epoxide side chain and with chair or boat conformation in the ring A of the skeleton, were found to be populated for both **183** and **184** after a Monte Carlo search. *Boltzmann* average VCD spectra were calculated on geometry-optimized conformers, at the B3LYP/DGDZVP level of theory. The stable conformers (four for **183** and two for **184**), were compared visually and *in silico* with the observed VCD spectrum, allowing an absolute configuration assignment (*S*) to C-20.

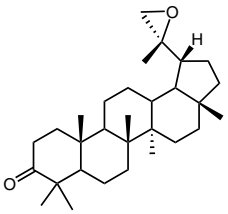

183

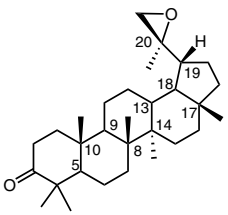

184

5.2.5 Aromatic Molecules

Several aromatic molecules, including (a*S*,2*R*,2′*R*)-cephalochromin (**1**) (*9*), (–)-(*S*)-2-(1-hydroxyethyl)-chromen-4-one (**3**) (*11*), (+)-(*S*)-5,8-dimethoxymarmesin (**24**) (*56*), (+)-(*R*)-2-(1-hydroxyethyl)-chromen-4-one (**44**) (*11*), and (+)-(*R*)-6-bromo-2-(1-hydroxyethyl)-chromen-4-one (**45**) (*11*) have been mentioned in this chapter.

Example 1

A chromone having the molecular formula $C_{20}H_{22}O_6$ was isolated from *Arracacia tolucencis*. Using ^{1}H and ^{13}C NMR spectroscopy it was not possible to identify the correct structure between **185** and **186**. However, DFT-VCD spectra simulation on a *Boltzmann*-averaged ensemble of conformers for each molecule demonstrated clearly, after comparison with the experimental data mainly at the νCO (*ca.* 1,150 cm^{-1}) and δCOH (*ca.* 1,300 cm^{-1}) vibrations, the chromone **185** to be the correct structure for the isolated molecule. X-ray crystallographic work reinforced the structural assignment (*275*).

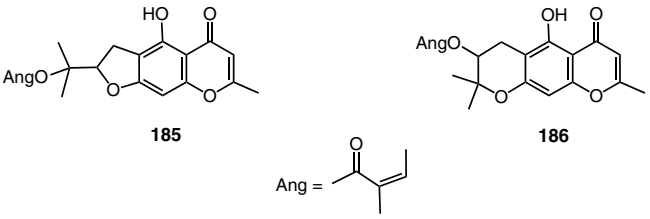

By close analogy, VCD studies of the linear and angular enantiomeric α-dihydrofuranocoumarins **24**–**26** were conducted to determine the structure and to assign the absolute configuration of coumarin **24**, a compound with antidote activity against a snake venom, isolated from *Murraya alternans* (*56*), for which the VCD spectrum shows bisignated bands that seem to be indicative of the association of CO induced coupled-oscillator (DCO) (*159*, *160*, *166*) modes (Fig 60).

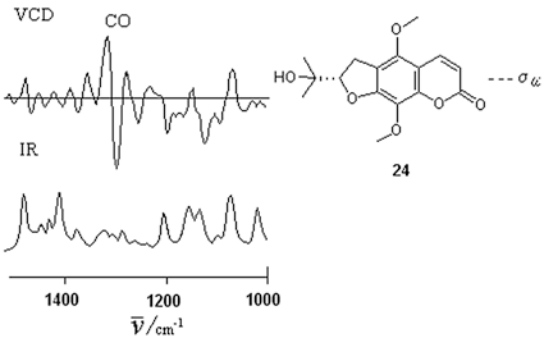

Fig. 60 IR and VCD spectra of (*S*)-5,8-dimethoxymarmesin (**24**). (Adapted from (*56*))

Example 2

Chromone esters **187** and **188** were isolated from the roots of *Prionosciadium thapsoides* (Umbelliferae) and the absolute configuration of the structurally related dihydrofurochromones **155**–**160** were established by VCD methodology applied to compound **189** followed by chemical correlation (*276*). Thus, alkaline treatment of a mixture of **187** and **188** led to (+)-5-*O*-methylvisamminol (**189**), among other products, in addition to benzofuran **190**, for which the stereochemistry was assigned by correlation to (+)-(*S*)-cimifugin (**191**). In addition, (+)-visamminol (**192**), a dihydrofurochromone isolated from *Angelica japonica* (Umbelliferae), was also assigned the (*S*) configuration based on non-direct methods.

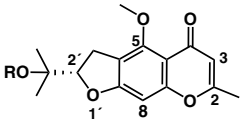

187, R = Ang
188, R = Sen
189, R = H

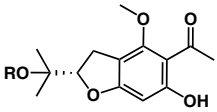

190

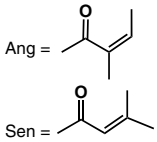

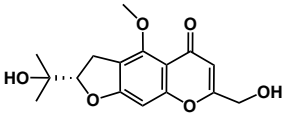

191

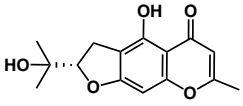

192

The observed VCD spectrum of **189** was contrasted with the calculated *Boltzmann* weighted VCD spectrum, obtained for 14 conformers, which were found by search using the Monte Carlo method, followed by geometry optimization of each conformer by DFT calculations at the B3LYP/DGDZVP level of theory. In all conformations the hydroxyisopropyl at C-2′ is in a *pseudo*-equatorial orientation. VCD bands of the average theoretical spectra were treated with *Lorentz*ian functions scaled by a factor of 0.97 and bandwidths set at 6 cm^{-1}. Comparison of VCD spectra showed good agreement assuring the absolute configuration of (+)-5-*O*-methylvisamminol (**189**) as (2′*S*) (Fig. 61), confirming as a result the absolute configurations of the dihydrochromones **187**, **188**, and **190**–**192**.

Bands at around 1,450 cm^{-1}, 1,300 cm^{-1}, and 1,100 cm^{-1}, corresponding to CH and CO vibrations, were found to be particularly distinctive (Fig. 61). The CO vibration at around 1,300 cm^{-1} may be assigned to the aromatic methyl ether (*148*), since it appears at about the same frequency as the bisignated bands of dimethoxymarmesin **24** (Fig. 60).

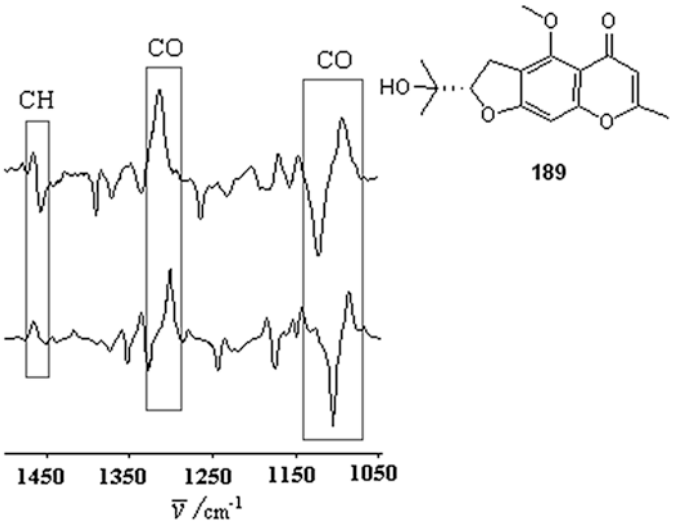

Fig. 61 Experimental (*left*) and DFT calculated at the B3LYP/DGDZP level (*right*) VCD spectra of (+)-(*S*)-5-*O*-methylvisamminol (**189**). (Adapted from (*276*))

Example 3

Three new benzofurans **193–195** were isolated from the roots of *Cyperus teneriffae*. Some species of the genus *Cyperus* are used in folk medicine, *i.e.* in traditional Chinese medicine as estrogenic and anti-inflammatory agents for the treatment of menstrual disorders, stomachache, and bowel disorders. VCD spectroscopy was used to define the absolute configuration of (+)-1-[2,3-dihydro-6-hydroxy-4,7-dimethoxy-(prop-1-en-2-yl)benzofuran-5-yl]ethanone (**193**) (*277*). Eight conformers were found populated after reoptimization, using DFT at the B3LYP/DGDZVP level, of the 20 conformers that inhabited the MM conformational energy surface initially. The conformers showed rotational freedom at the methoxy and isopropenyl groups. VCD frequencies and rotational strengths were calculated using the same functional and basis set, to find, by means of comparison with the experimental VCD spectrum, that the absolute configuration of C-2 in **193** is (*S*). The calculations are clearly indicative of intramolecular H-bonding, a molecular arrangement that favors observation VCD couplets due to mirror-image CO vibrations (Fig. 62).

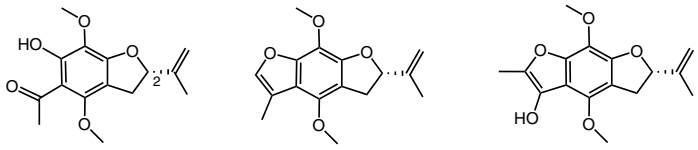

193 **194** **195**

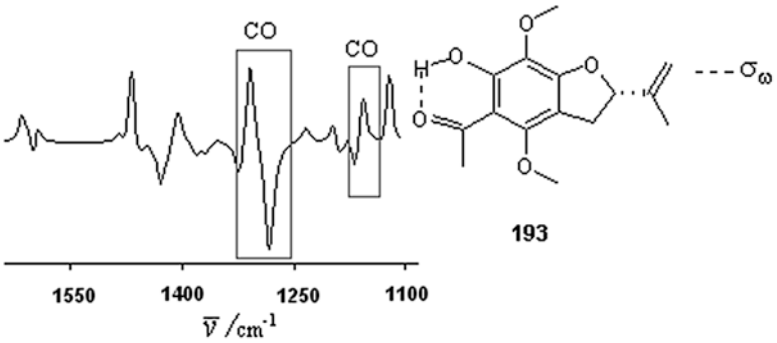

Fig. 62 DFT calculated VCD spectrum of (+)-(*S*)-benzofuran **193** at the B3LYP/DGDZVP level. (Adapted from (*277*))

Example 4

Production of secondary metabolites from the fungus *Cordyceps annullata* in culture medium led to four new 2,3-dihydrobenzofurans, annullatins **196–199**, and a new aromatic polyketide, annullatin **200** (*278*). The structure and relative stereochemistry of the annullatins were established by two-dimensional NMR spectroscopic techniques and high-resolution mass spectrometry, whereas their absolute configurations were disclosed by VCD of **197**, chemical transformations, and biosynthetic relationships. The MMFF Monte Carlo search of (*R*)-**197** led to 32 conformers within 7 kJ/mol from the most stable conformer, and these were reduced to 14 conformers upon minimization with the DFT B3LYP/6-31G(d) method. Further minimization at the B3LYP/6-311++G(d,p) level of theory guided to ten conformers obtained within the first 6 kJ/mol. IR and VCD spectra of (*R*)-**197** calculated as the *Boltzmann* weighted average of these ten conformers compared well with the observed IR and VCD spectra of the (–)-**197** enantiomer, thus allowing the assignment of the C-2 absolute configuration as (*R*). A segment of the calculated and observed VCD spectra is shown in Fig. 63. The (2*R*) absolute configuration of (+)-**196** was deduced from oxidation of (–)-**197**, and the chiral center C-9 in **198**–**200** was assigned the (*S*) absolute configuration applying the advanced *Mosher*'s method. Annullatins **196**, **197**, and **199** have cannabinoid receptor activities.

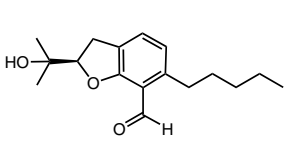

196

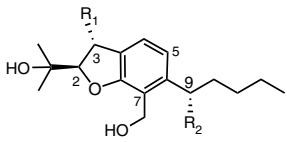

197, $R_1 = R_2 = H$
198, $R_1 = OH$, $R_2 = H$

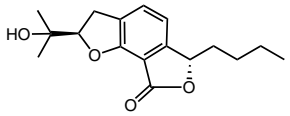

199

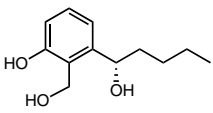

200

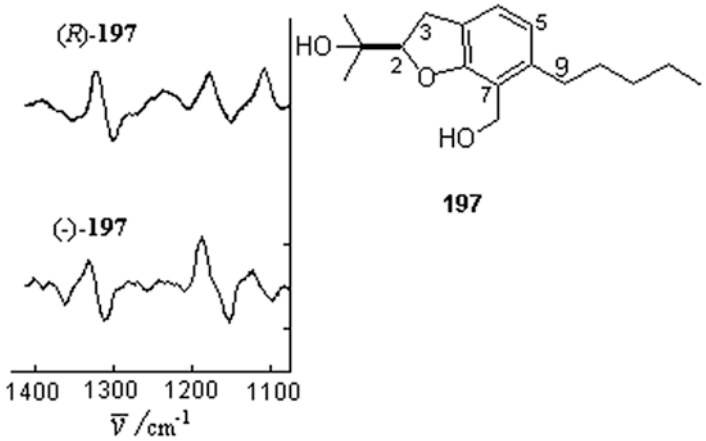

Fig. 63 Experimental (*bottom*) and calculated (*top*) VCD spectra of annullatin **197**. (Adapted from (*278*))

Example 5

Isolation and enantioselective HPLC resolution of (+)-gaudichaudianic acid (**201**) from *Piper gaudichaudianum* has been described. The absolute configuration assessment of the (+)-(*S*)-**201** and (–)-(*R*)-**202** enantiomers was achieved by means of a combination of ECD and VCD measurements using DFT calculations (*279*). This prenylated chromene is a potent trypanocidal compound when tested against the Y-strain of *Trypanosoma cruzi*. The (+)-enantiomer is more active than its antipode, but a synergistic effect makes the racemic mixture more active than any individual enantiomer. The *Boltzmann*-averaged VCD spectrum of a considered

eight low-energy lying conformers for the (*S*)-enantiomer, obtained after geometry optimization using DFT at the B3LYP/6-31G(d) level, was calculated as a H-bonding dimer with formic acid to provide gas phase calculations with a better approach to the solution environment (*280*). The comparison of the observed-to-calculated VCD spectra matched therein clearly, mainly in fundamental vibrations at the 1,350–1,100 cm^{-1} region, confirming the (2*S*) configuration assignment. Moreover, a VCD simulation with fragment model **203**, calculated also as a H-bonding dimer with formic acid, was performed and compared with the VCD simulation of (*S*)-**201**, allowing the prenylated signatures (encircled bands) to be uncovered, as shown in Fig. 64.

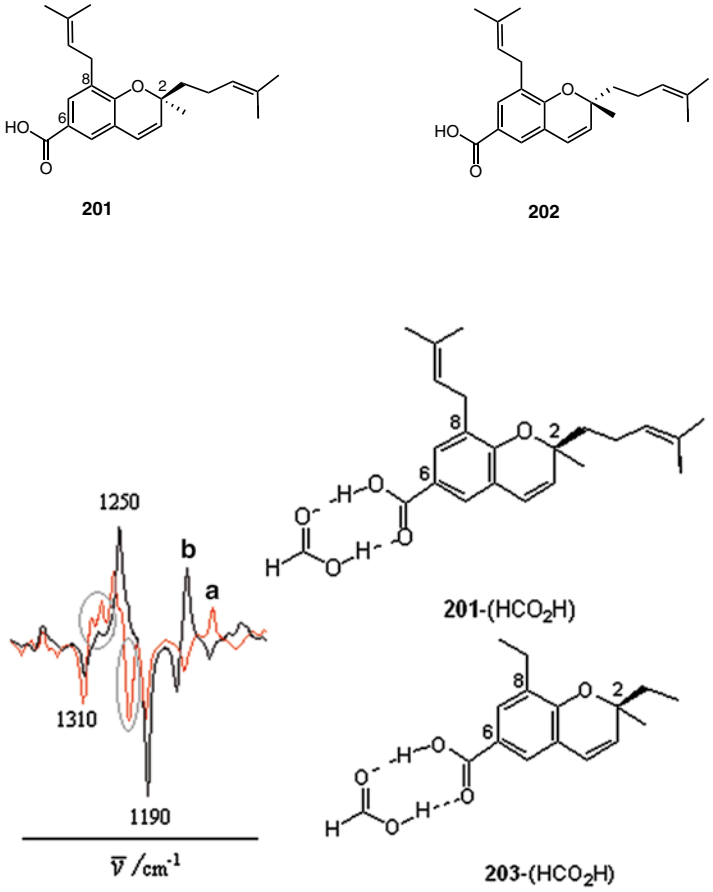

Fig. 64 DFT calculated VCD spectra of H-bonded heterodimers (**a**) (*S*)-**201**-(HCO_2H) and (**b**) (*S*)-**203**-(HCO_2H) using the B3LYP/6-31G(d) level. (Adapted from (*279*))

Example 6

Absolute configuration assurance for two chiral chromanes, peperobtusin A (**204**) and 3,4-dihydro-5-hydroxy-2,7-dimethyl-8-(3″-methyl-2′-butenyl)-2-(4′-methyl-1′,3′-pentadienyl)-2*H*-1-benzopyran-6-carboxylic acid (**205**), isolated as racemates from the leaves of *Peperomia obtusifolia* (Piperaceae), was carried out by VCD spectroscopy (*281*). Resolution was achieved by enantioselective HPLC. DFT pre-optimized calculations at the B3LYP/6-31G(d) level of theory were performed on fragment molecules (*R*)-**206** and (*R*)-**207** to efficiently share computational resources. An initial conformational search using MM+ and MMFF force fields led to 44 conformers for **206**. After adding the isoprenyl groups, 53 conformers were found as a result of a constrained search and were geometry pre-optimized. Ten conformers were chosen and four of them, representing 75% of the population, were taken to calculate the *Boltzmann*-weighted VCD spectrum of **206**. A similar procedure was applied to find the 11 conformers selected for obtaining the *Boltzmann*-weighted VCD spectrum of **207**. The *in silico* comparison of calculated and experimental spectra for both chromones was used to determine the absolute configuration of (+)-**206** and (+)-**207**, with both being (*R*). Fundamental bands in VCD spectra of independent conformers suggest that the isoprenyl group is in axial orientation, not in equatorial orientation as was assumed by the empirical ECD helicity rule for chromanes, by means of which the (*S*) configuration of (+)-**206** was assessed incorrectly (*282*).

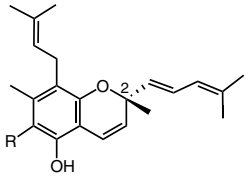

204, R = H
205, R = CO_2H

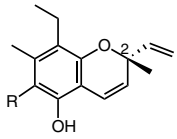

206, R = H
207, R = CO_2H

Example 7

A series of montanine-type alkaloids (**208**–**210**) was obtained by rearrangement of haemanthamine-type alkaloids induced by halogenated reactants (Fig. 65) (*283*). The relative stereochemistry was established by 2D-NMR spectroscopy. The absolute configuration of C-2, C-3, C-4a, and C-11 was allotted by VCD methodology applied to **208**. The measured VCD spectrum was compared with the conformational average calculated DFT-VCD spectrum. Initially, a full minimization of the molecule, carried out by MMFF force field, provided the global minimum conformer. This structure was used as the starting point for a conformational search performed using the Monte Carlo method to afford four conformers in the initial 40 kJ/mol. Based on energy contribution to population analysis, only two structures remained useful and were

submitted to geometry optimization using DFT at the B3LYP/6-31G(d) level, giving rise to two *O*-CH_3 rotamers with essentially identical skeleton conformation, which were re-optimized using B3LYP/DGDZVP and B3PW91/DGDZVP levels of theory before calculating their VCD spectra. Anharmonicity factors of 0.98 and 0.97 for the B3LYP/DGDZVP and for the B3PW91/DGDZVP methods, respectively, were applied to the correct frequency values. The agreement between VCD calculated and experimental spectra confirmed the absolute configuration assignment of (+)-montanine as the (2*S*,3*S*,4a*S*,11*S*)-**208** enantiomer.

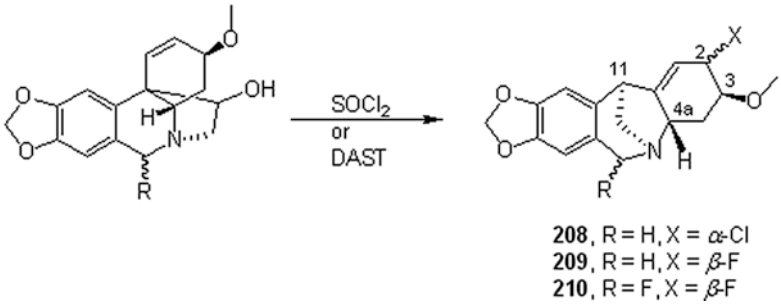

Fig. 65 Semi-synthesis route to montanine-type alkaloids

Example 8

The application of VCD spectroscopy to the structural analysis of naturally occurring glycoconjugates is scarce. Aromatic plant glycosides such as eleutheroside B1 (**211**) and salicin (**212**) have interesting biological properties (*284*). The stereochemistry at the anomeric carbon of aromatic glycosides α-phenyl glycoside (**213**), α-*p*-nitrophenyl glycoside (**214**), β-phenyl glycoside (**215**) and β-*p*-nitrophenyl glycoside (**216**) has been explored by a complementary VCD approach revealing that vibrational motion on the aglycone part provides information of structure of the sugar residue (*284*). The *axial* aromatic glycosides **213** and **214** exhibit a negative band at around 1,230 cm^{-1}, assigned to the stretching motion of the glycosidic oxygen and aromatic carbon, while equatorial **215** and **216** show flat features in this region. The same observation has been reported for the VCD spectra of disaccharides. Hence α-glycosidic-linked disaccharides give rise to a negative band around 1,145 cm^{-1}, while no bands are observed for β-glycosidic disaccharides (*285*).

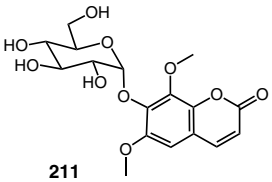

211

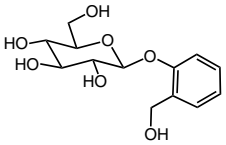

212

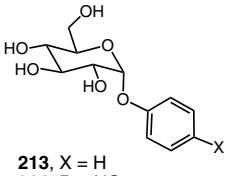

213, X = H
214, R = NO_2

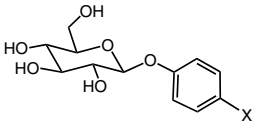

215, X = H
216, R = NO_2

Example 9

With the aim of establishing a confident chiroptical method to establish the absolute configuration of sulfur-containing cruciferous phytoalexins, the VCD methodology was applied to (+)-(*R*)-methyl *p*-toluenesulfinate (**217**), a model sulfinate of known stereochemistry, and to a synthetically prepared cruciferous phytoalexin, (–)-brassicanal C (**218**), of natural origin (*286*). Phytoalexins are antimicrobial secondary metabolites produced *de novo* after their exposure to physical, biological or chemical stress as exemplified by plants of the family Cruciferae, which include important vegetable crops inclusive of cabbage, broccoli, cauliflower, and mustard. DFT calculations were initiated with geometry optimization of 18 conformers for (*R*)-**217** and 36 for (*S*)-**218**, at the B3LYP/6–31G(d) level of theory. Some of the initial conformers converged to the same structure, thus further optimization at the DFT/B3LYP/6-311+G(2df,2p) level of theory led to three and four stable conformers for (*R*)-**217** and (*S*)-**218**, respectively. VCD spectra were calculated at the same level, and data of independent conformers were averaged to a *Boltzmann* population, obtaining the final spectra. The sulfonyl S=O stretching vibration in (*R*)-**217** appeared as a strong band around 1,125 cm^{-1} in the absorption spectrum. Signated bands at around 1,140 cm^{-1} in the VCD spectrum were assigned to S=O vibration and C-7 deformation. The observed VCD spectrum showed good agreement with the calculated one in their frequencies and relative intensities, therefore confirming the (*R*) assignment. Furthermore, even though broadening was observed in the experimental VCD spectrum of (*S*)-**218**, likely

due to intermolecular H-bonding interactions between the C-8 carbonyl of one molecule and the N-1 amino group of the other molecule, the calculated VCD features reasonably agrees with the experimental ones, thus confirming the (*S*)-configuration assignment.

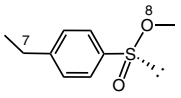

217

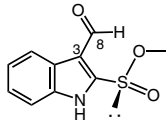

218

Example 10

The indole-related phytoalexins, (*S*)-(–)-spirobrassinin (**219**) and (+)-(*R*)-1-methoxyspirobrassinin (**220**), isolated from plants in the family Cruciferae, interestingly have opposite absolute configurations at the spiro ring junction, suggesting that *N*–OCH_3 has an effect on their biosynthesis pathways. The absolute configuration of phytoalexin (+)-(*R*)-**219** and (–)-(2*R*,3*R*)-1-methoxyspirobrassinol methyl ether (**220**) was assured by VCD measurements (*287*). Comparison of experimental VCD spectra of (–)-(*S*)-**219** and (+)-(*R*)-**220** show bands of opposite sign (Fig. 66). To determine the absolute configuration of (–)-**221** an initial conformational analysis was conducted on (2*R*,3*R*)-**221** using the MMFF94S force field, selecting the 11 lowest-energy conformers so as to achieve a cumulative *Boltzmann*-weighted population sum over 95%. Geometry optimizations, and IR and VCD spectra were calculated using DFT calculations at the B3PW91/6-31G(d,p) level. Between the observed and calculated VCD spectra, the signs of the major VCD bands showed reasonable agreement to suggest that the absolute configuration of naturally occurring (–)-**221** is indeed (2*R*,3*R*).

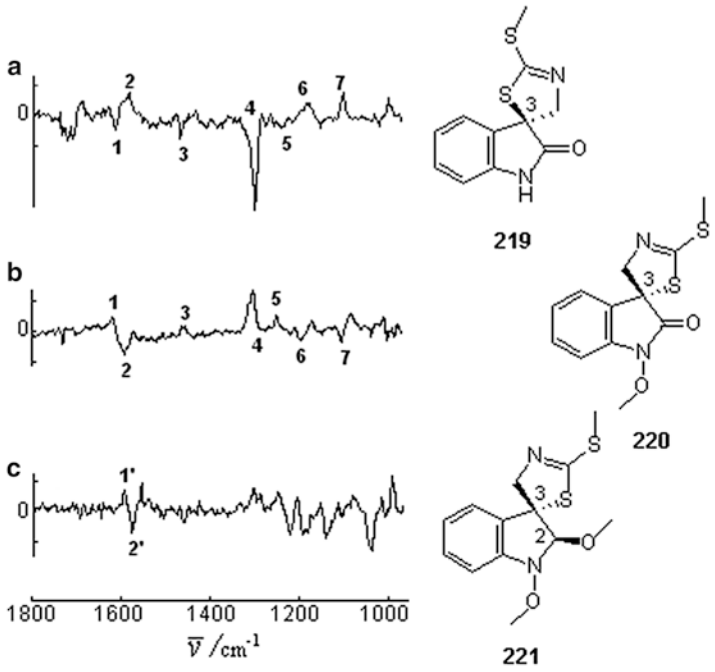

Fig. 66 Observed VCD spectra of indole-related phytoalexins: (**a**) (–)-(*S*)-spirobrassinin (**219**), (**b**) (+)-(*R*)-1-methoxyspirobrassinin (**220**) and (**c**) (–)-(2*R*,3*R*)-1-methoxyspirobrassinol methyl ether (**221**). (Adapted from (*287*))

Example 11

The stress-induced cruciferous phytoalexin metabolites (–)-(*S*)-dioxybrassinin (**222**) and (–)-(*S*)-3-cyanomethyl-3-hydroxyoxindole (**223**), first isolated from *Pseudomonas cichorii*-inoculated cabbage species (*Brassica oleracea*), were investigated for their absolute configuration by VCD spectroscopy (*288*). Conformational analysis was carried out using the MM2+ force field. Geometry optimizations using the DFT B3LYP/6-31G(d,p) method resulted in conformers differing in the orientation of the OH group and the side chain. IR and VCD of *Boltzmann* average conformer spectra, calculated at the same level of theory, showed three distinctive signated bands: one near 1,730 cm^{-1} (assigned to νC=O stretch contribution), another at 1,620 cm^{-1} (assigned to aromatic ring stretching), and the third at 1,470 cm^{-1}, for which the signs are in agreement with the observed VCD spectra, allowing one to conclude that naturally occurring (–)-**222** and (–)-**223** are both in

the (*S*) configuration. Vibrational modes of the stereogenic center C-3 were not isolated. The induced chirality observed for the carbonyl and aromatic VCD bands come from coupled vibrational chirality transfer from C-3, a useful way to determine the absolute configuration of tertiary alcohols in phytoalexin natural products that cannot otherwise be determined easily.

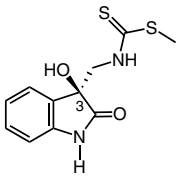

222

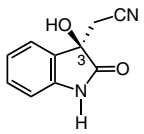

223

Example 12

The absolute configurations of the podophyllotoxin-related lignans **225**–**228**, isolated from an ethanol extract of *Bursera fagaroides* (Burseraceae), were assessed by VCD-DFT (*289*). This resinous extract showed significant cytotoxic activity in a human colon adenocarcinoma (HT-29) screening test. The stereochemistry of the lignans, (–)-deoxypodophyllotoxin (**225**), (–)-morelensin (**226**), (–)-yatein (**227**), and (–)-8′-desmethoxyyatein (**228**) was proposed according to those of the known bioactive lignans (–)-(2*R*,2′*R*,3*R*,3′*R*)-podophyllotoxin (**224**) and its acetyl derivative, and corroborated by VCD curve comparison of the DFT calculated spectra of **224** and **225** with the corresponding observed VCD spectra. Molecular modeling of (2*R*,2′*R*,3*R*,3′*R*)-**224** and (2*R*,2′*R*,3′*R*)-**225** started with a MMFF94 Monte Carlo search, from different starting geometries, to cover the conformational hypersurface, affording 20 conformations for **224** and 11 conformations for **225**. Geometry optimization using DFT at the B3LYP/DGDZVP level derived in 11 stable conformers for **224** and 9 for **225**, in arrangements where dynamics is observed in the methoxy groups, but the molecular scaffold practically remains without conformational change. VCD spectra were calculated at the same level of theory and data were treated as conformational ensembles averaged by *Boltzmann* distribution using free energies. Good agreement of observed and calculated VCD spectra, along with spectral similarity index (S_E) values of 77.2% for (–)-(2*R*,2′*R*,3*R*,3′*R*)-**224** and of 86.5% for (–)-(2*R*,2′*R*,3′*R*)-**225**, confirmed the absolute configuration assignments. The experimental VCD spectra of related lignans (–)-**226**, (–)-**227** and (–)-**228** were compared to those of podophyllotoxins (–)-**224** and (–)-**225** (Fig. 67). The fact that all five spectra displayed the same phase pattern is indicative that lignans **225**–**228**, isolated from *Bursera fagaroides*, and (–)-podophyllotoxin (**224**), belong to the same enantiomeric series. Differences in molecular flexibility between the flexible dibenzyl butyrolactone lignans (2*R*,2′*R*)-**227** and (2*R*,2′*R*)-**228**, and core-rigid (2*R*,2′*R*,3*R*,3′*R*)-**224**, (2*R*,2′*R*,3′*R*)-**225** and (2*R*,2′*R*,3′*R*)-**226**, were made evident by the broadening of most signals in the VCD spectra of the first pair. Indeed, a conformational Monte Carlo search carried out for **227** and **228** afforded 60 and 45 conformers, respectively, a larger number of conformers than for **224** or **225**.

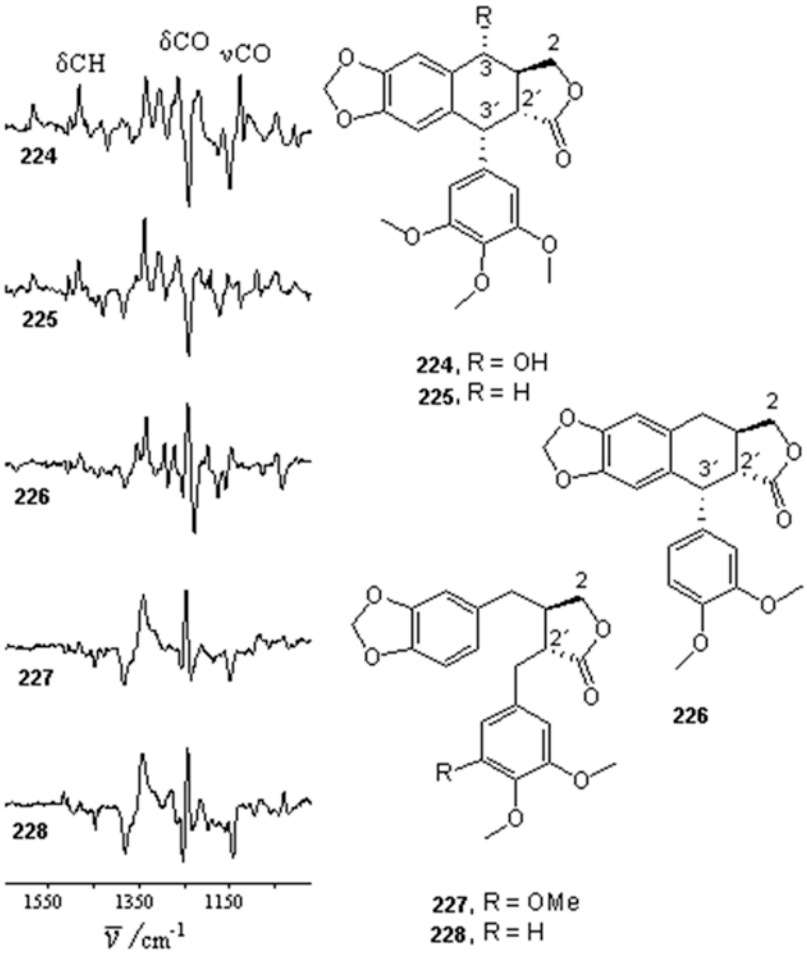

Fig. 67 Observed VCD spectra of podophyllotoxin-related lignans (–)-(2*R*,2′*R*,3*R*,3′*R*)-podophyllotoxin (**224**), (–)-(2*R*,2′*R*,3′*R*)-deoxypodophyllotoxin (**225**), (–)-(2*R*,2′*R*,3′*R*)-morelensin (**226**), (–)-(2*R*,2′*R*)-yatein (**227**) and (–)-(2*R*,2′*R*)-8′-desmethoxyyatein (**228**). (Adapted from (*289*))

Example 13

Optically active antipodes of the nyasol norlignans (+)-**229** and (–)-**230**, naturally occurring in *Asparagus africanus* and *Anemarrhena asphodeloides*, respectively, were given absolute configuration assignments by VCD spectroscopy (*290*). The conformational search of (*S*)-nyasol using MMFF force field and two DFT methods: B3LYP/6-31G(d,p) and B3LYP/AUG-cc-pVDZ, provided eight stable conformers, within 2 kJ/mol, from 26 found in the initial exploration. Having many

conformations to deal with represents a challenge in VCD studies, since the bunched arrangements generates several bands that are either broad signals or extinguish one another, increasing demands on the signal-to-noise ratio of the instrument. Furthermore, the presence of intermolecular H-bonding in molecules with hydroxy groups, such as nyasol, also aggravates the broadening and promotes frequency and intensity signal changes. For (*S*)-nyasol, the strong positive signal at 1,510 cm^{-1}, observed in the VCD spectrum in a DMSO-d_6 solution, and both the 1,650–1,590 and 1,000–800 cm^{-1} regions of a KBr pellet, were the spectral signatures used to assign the (+)-(*S*)-nyasol (**229**) absolute configuration and consequently that of (–)-(*R*)-nyasol (**230**). The hinokiresinol (+)-(*R*)-(**231**), a norlignan with an antiplasmodial effect, was correlated chemically to (+)-(*S*)-nyasol (**229**), allowing its absolute configuration to be confirmed.

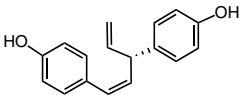

229

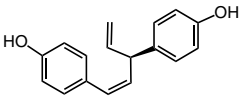

230

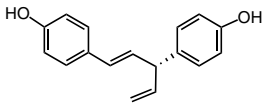

231

Example 14

Secolignans **232** and **233**, extracted from the aerial parts of the perennial herb *Peperomia blanda*, were assigned with unambiguous (+)-(2*S*,3*S*,5*S*)-**232** and (–)-(2*R*,3*S*,5*S*)-**233** absolute configurations by VCD spectroscopy (*291*). Secolignans are known constituents of certain traditional Chinese medicines used as anticancer drugs. Their chiral architecture can be described rapidly by focusing sight at the C-5 stereogenic center substituted with two different aromatic rings and a *trans*-γ-butyrolactone in **232**, but a *cis*-γ-butyrolactone in **233**. Two-dimensional NMR spectroscopy along with H-2 irradiated N*O*E enhancements, sustained the relative stereochemistry proposed for the γ-butyrolactone ring in both secolignans. The *cis* and *trans* stereochemistry was also confidently differentiated in the 1,500–1,000 cm^{-1} region of the experimental VCD spectra (Fig. 68).

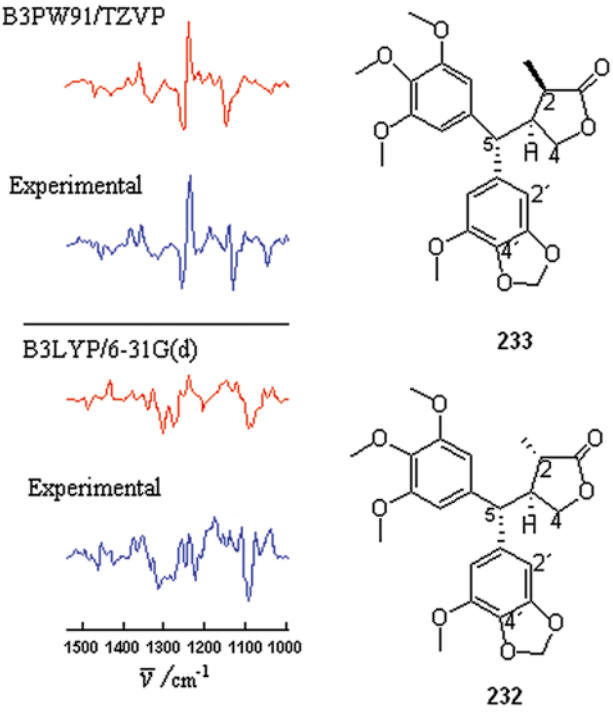

Fig. 68 Comparison of the experimental and calculated VCD spectra of (+)-(2*S*,3*S*,5*S*)-secolignan **232** (*bottom*) and (–)-(2*R*,3*S*,5*S*)-secolignan **233** (*top*). (Adapted from (*291*))

The assignment of absolute configuration for **232** and **233** was accomplished by comparison of the experimental with the calculated, *Boltzmann* average of eight conformers each, with the VCD spectra at the B3LYP/6-31G(d) and B3PW91/TZVP levels of theory, respectively (Fig. 68). Secolignan **232** was found to have the same structure and stereochemistry reported for peperomin B, isolated from *Peperomia japonica*, for which the absolute configuration was deduced from ECD as (+)-(2*S*,3*S*,5*S*). However, ECD analysis of **232** could not reproduce that of peperomin B, and, moreover ECD could not distinguish between the (5*R*)- and (5*S*)-epimers of **232**. In contrast, VCD neatly confirmed the (2*S*,3*S*,5*S*) absolute configuration for (+)-**232**, providing points of discrepancy between the signs and intensities of the bands at around 1,290 cm^{-1} in the VCD spectra of the C-5 epimers.

Example 15

Crassipins **234**–**237**, isolated from the rhizomes and roots of the fern *Elaphoglossum crassipes*, are terpenylated acylphloroglucinols with one or two chiral centers, at C-4 in **234** and **235**, and at C-4 and C-2′ in **236** and **237**, for which the absolute configurations were analyzed from ECD and VCD studies (*292*). After the structures of the crassipins were established by ^{1}H, ^{13}C, and 2D-NMR experiments, along with high-resolution mass spectrometry, the ECD spectrum of (+)-**234** was compared to the TD-DFT spectra of the (4*R*) and (4*S*) enantiomers calculated at the B3LYP/6-31G(d) level of theory on geometry-optimized structures. The pattern of the signated bands (+,–,+,+,–) in the experimental spectrum was in good agreement with the pattern observed for the (4*R*) enantiomer, thus assignment of (+)-(*R*)-**234** and (+)-(*R*)-**235** followed. Regarding the absolute configuration assignment of the C-2′ chiral center in crassipin epimers (+)-**236** and (+)-**237**, it was found that the experimental ECD spectrum of (+)-**236** was identical to that of (+)-**234**, thus the opportunity to assign the C-2′ absolute configuration by ECD was revoked by this unfortunate spectral resemblance. The predominant dissymmetric character of C-4 over C-2′ was also evident in VCD spectroscopy, since the experimental VCD spectrum of (+)-**236** matched well with the weighted average simulated VCD spectra of either (4*R*,2′*R*)- or (4*R*,2′*S*)-epimers that were calculated at the B3LYP/6-31G(d) level of theory. In addition, the experimental ECD and VCD spectra of (+)-**237** were identical to those of (+)-**236**. In sum, the absolute configuration at C-2′ could not be established either by the ECD or VCD techniques; however, the epimeric nature of **236** and **237** was indeed confirmed by NMR spectroscopy. Compound **234** showed antidepressant activity in an *in vivo* test with mice.

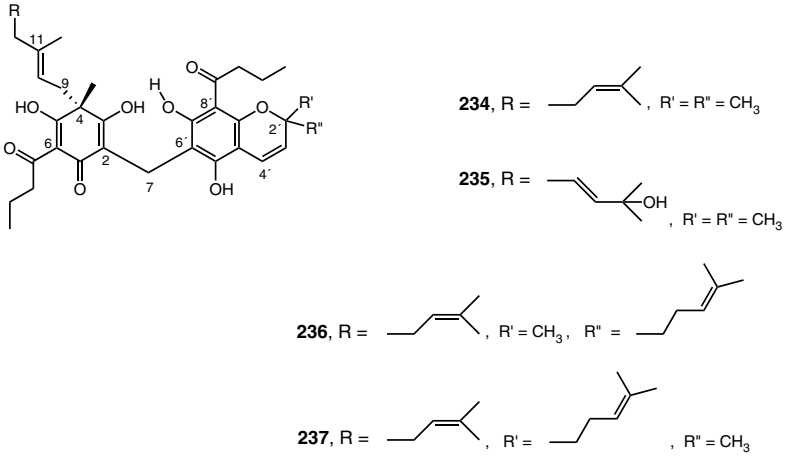

5.2.6 Other Natural Products

Alkaloids already discussed in this chapter include (+)-(2*R*,7*S*,20*S*,21*S*)-schizozygine (**6**) (*13*), (–)-(2*R*,7*R*,20*S*,21*S*)-isoschizozygamine (**7**) (*14*), (+)-(1*R*,3*R*,5*S*,6*R*,2′*S*)-6*β*-hydroxyhyoscyamine (**22**) (*55*), (–)-(1*S*,3*S*,5*R*,6*S*,2′*S*)-6*β*-hydroxyhyoscyamine (**23**) (*55*), (–)-(1*S*,3*S*,5*R*,6*S*)-3*α*,6*β*-diacetoxytropane (**30**) (*75*), cinchonidine (**73**) (*190*), and cinchonine (**74**) (*190*).

Example 1

The absolute configurations of four 3*α*,6*β*-tropanediol monoesters (**238**–**241**) isolated from a *Schizanthus* species, were determined by VCD methodology (*77*). Since tropane alkaloids appear in their host plants as complex mixtures, the 6*β*-hydroxy-3*α*-senecioyloxytropane (**238**), from *S. grahamii,* is difficult to isolate as a pure sample and was obtained as a mixture (7:3) with 6*β*-angeloyloxy-3*α*-hydroxytropane (**240**). A mixture (69:31) of 3*α*-hydroxy-6*β*-tigloyloxytropane (**239**) and 3*α*-hydroxy-6*β*-senecioyloxytropane (**240**) was also isolated from *S. pinnatus*.

Experimental VCD spectra were recorded for tropane **238** and for the mixtures mentioned above. Conformational average VCD spectra were calculated starting with an initial search of conformers distribution using the Monte Carlo random method with the MMFF94 force field, followed by optimization of the low energy conformers using the DFT B3LYP/6-31G(d) method. Two sets of topomers were found, one having the *N*-Me group in the *axial* position with respect to the six-membered ring, and the other in an *equatorial* position. As observed for analogous tropanes (*55*, *75*), hydrogen bonding between the hydroxy group at C-6 and the nitrogen atom for tropane **238** favors conformers with the *N*-Me group orientated at the *axial* position. In the absence of H-bonding interaction, the preferred topomers are those with the *N*-methyl group oriented to the *equatorial* position, such as in the case for tropanes **239** and **240**. Geometry optimization using DFT at the B3LYP/DGDZVP level of theory preceded VCD spectra calculations at the same level. Eight conformers were found for **238**, twelve for **239** and nine for **240**, accounting for 98.5%, 96.4% and 99.4%, respectively, of the conformational map considering a cutoff of 10 kJ/mol. The *Boltzmann*-averaged VCD spectrum of **238** matched reasonably well with the observed VCD spectrum. The signs of the signals in the fingerprinting region of the 3*α*,6*β*-tropanes (1,150–950 cm^{-1}) (*75*) were (+,+,–), confirming the (1*R*,3*R*,5*S*,6*R*) absolute configuration for tropane **238** (Fig. 68). Similarly, absolute configuration assignments of **239** and **240** were followed by the sign and intensity of the fingerprint bands in the calculated and observed VCD spectra of their (7:3) mixture (Fig. 69). The pattern (+,+,–) assured the (1*R*,3*R*,5*S*,6*R*) configuration for these compounds. The configuration assignment of tropane **241** was performed by spectral analogy, using the experimental VCD spectrum of the (7:3) mixture of **238** and **241**, where the pattern (+,+,–) assured its (1*R*,3*R*,5*S*,6*R*) configuration. This has been the first case where the absolute configuration of natural products is determined by VCD spectral analogy, a recurrent methodology used in ORD and ECD.

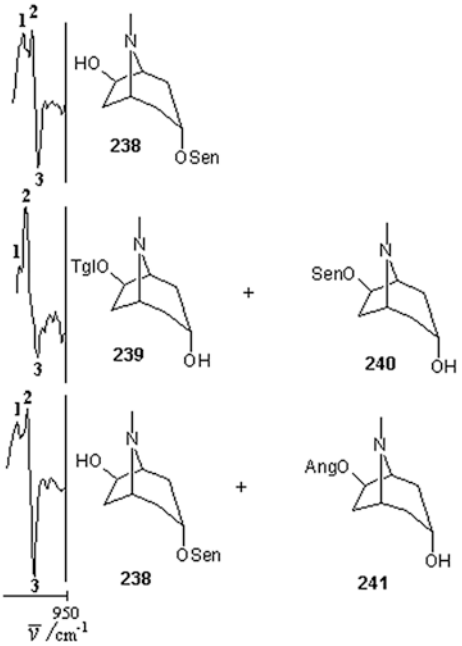

Fig. 69 Comparison of the observed VCD spectra of (1*R*,3*R*,5*S*,6*R*)-6*β*-hydroxy-3*α*-senecioyloxytropane (**238**), the (7:3) mixture of (1*R*,3*R*,5*S*,6*R*)-3*α*-hydroxy-6*β*-tigloyloxytropane (**239**) and (1*R*,3*R*,5*S*,6*R*)-3*α*-hydroxy-6*β*-senecioyloxytropane (**240**) and the (7:3) mixture of **238** and (1*R*,3*R*,5*S*,6*R*)-6*β*-angeloyloxy-3*α*-hydroxytropane (**241**). (Adapted from (*77*))

Example 2

Indoline alkaloids **242**–**248**, isolated from *Geissospermum reticulatum* leaves and bark, were structurally elucidated by 1D- and 2D-NMR spectroscopy and crystal diffraction (*293*). The structure of these aspidospermatan-type alkaloids is complex, but, however, the C-2, C-7, and C-15 relative stereochemistry is determined by their singular skeleton shape which resembles a butterfly, where the chiral centers C-7 and C-15 are the head and the tail. Epoxygeissovelline (+)-**242** is the essential component of *G. reticulatum*, therefore it was chosen to obtain its absolute configuration by VCD spectroscopy, allowing pursuit of the absolute configuration deductions for alkaloids **243**–**248** under the consideration that all aspidospermatan-type alkaloids from *G. reticulatum* share a common biosynthesis pathway (*294*). The VCD spectrum of the simulated (2*R*,7*R*,15*R*,17*S*,19*S*) enantiomer, for which the co-ordinates were obtained from the (+)-**242** crystal structure, was obtained as the weighted average of four conformers at the B3LYP/DGDZVP level of theory. Two conformers are highly populated (92.4%), and differ in the rotation of the OMe group at the indoline moiety. The C–O stretching vibrations, allied to the epoxy and methoxy groups, may be expected to show absorption in the 1,270–1,230 cm^{-1} region. Indeed there is an

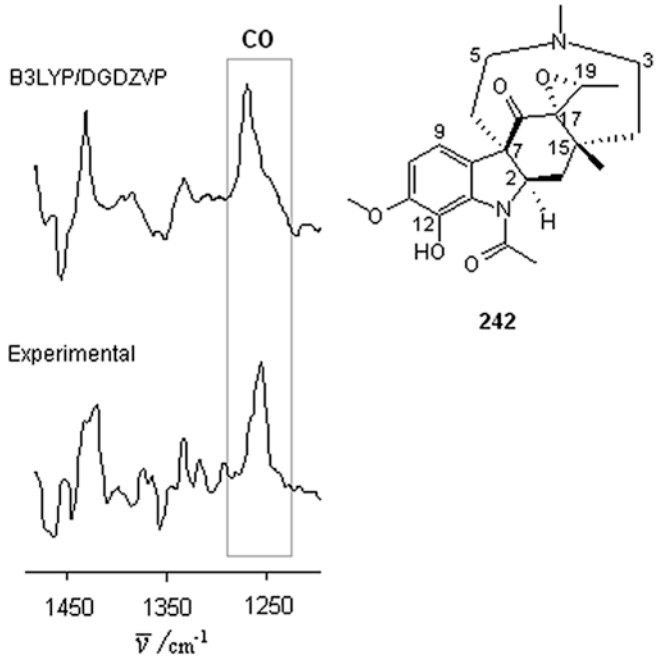

Fig. 70 Comparison of the experimental and calculated VCD spectra of (+)-(2*R*,7*R*,15*R*,17*S*,19*S*)-10-demethoxy-12-hydroxy-17,19-epoxygeissovelline (**242**). (Adapted from (*294*))

intense and broad band at the IR spectrum, which turned into a positive band in the VCD spectrum appearing near 1,250 cm^{-1}, in the experimental spectrum, and near 1,270 cm^{-1} in the calculated spectrum (Fig. 70). The (+)-**242** enantiomer was confirmed confidently to have the (2*R*,7*R*,15*R*,17*S*,19*S*) absolute configuration, the configuration that was drawn arbitrarily from the crystal structure, by its quantitative assessment using Compare*VOA* software (*130*), which provided a higher similarity index for the correct enantiomer $S_E = 71.7$ than for the antipode $S_{-E} = 22.2$.

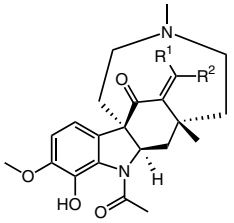

243, $R^1 = CH_3$, $R^2 = H$
244, $R^1 = H$, $R^2 = CH_3$

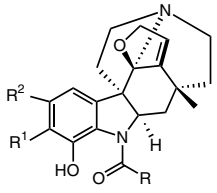

245, $R = CH_3$, $R^1 = R^2 = H$
246, $R = CH_3$, $R^1 = H$, $R^2 = OCH_3$
247, $R = CH_2\,CH_2CH_3$, $R^1 = R^2 = H$
248, $R = CH_3$, $R^1 = OCH_3$, $R^2 = H$

Example 3

Iridoid natural products are distributed widely in higher plants and are known to exhibit antifungal, antibacterial, and potential antitumor activity. (+)-Plumericin (**249**), and (+)-isoplumericin (**251**), isolated from *Plumeria rubra* (*125*), and (–)-prismatomerin (**252**), isolated from *Prismatomeris tetrandra* (*295*), were investigated structurally by VCD spectroscopy. The connectivities and relative stereochemistry of **249** and **251**, established previously by X-ray crystallography, confidently contributed to their structural analysis, but prior contradictory absolute configuration reports prompted their confirmation by VCD.

A search for the conformations of (1*R*,5*S*,8*S*,9*S*,10*S*)-**249** using the Monte Carlo MMFF94 force field identified four stable conformations, which were reoptimized using DFT at the B3LYP/6-31G(d), B3LYP/TZ2P, and B3PW91/TZ2P levels. Conformational variations at the methoxycarbonyl group and rings were found. The harmonic vibrational frequencies, and dipole and rotational strengths, calculated at the B3LYP/TZ2P and B3PW91/TZ2P levels, were treated as *Lorentz*ian bandshapes, and *Boltzmann* statistics were applied to data of the two most abundant conformers. The same treatment was applied to (1*R*,5*S*,8*S*,9*S*,10*S*)-**251**. The B3PW91/TZ2P spectra were in better agreement with the experimental one, allowing the unambiguous absolute configuration assignment of the naturally occurring (+)-**249** as (1*R*,5*S*,8*S*,9*S*,10*S*) and not as its enantiomer (1*S*,5*R*,8*R*,9*R*,10*R*)-**250** (Fig. 71). Likewise, the absolute configuration of (+)-isoplumericin **(251)** was confirmed to be (1*R*,5*S*,8*S*,9*S*,10*S*).

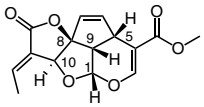

249

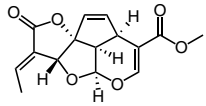

250

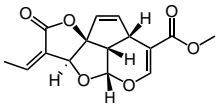

251

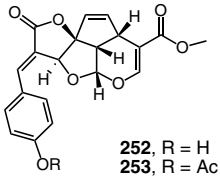

252, R = H
253, R = Ac

(–)-Prismatomerin (**252**), a new cytotoxic iridoid showing antitumor activity by interfering with mitotic spindle formation (*296*), was allotted its absolute configuration by VCD measurements of the acetate derivative (–)-**253** to minimize intermolecular aggregation likely affecting the parent compound at the concentrations used typically in the experiment. Considering the four stable conformers for (1*R*,5*S*,8*S*,9*S*,10*S*)-**249**, a conformational search for (1*R*,5*S*,8*S*,9*S*,10*S*)-**253** was carried out by replacing the methyl group at the exocyclic alkene by a phenyl acetate group in each conformer. Subsequent calculations of one-dimensional B3LYP/6-31G(d) potential energy surface scans gave rise to 12 additional conformations. These 12 conformers were reoptimized at the B3LYP/TZ2P and B3PW91/TZ2P levels and their harmonic

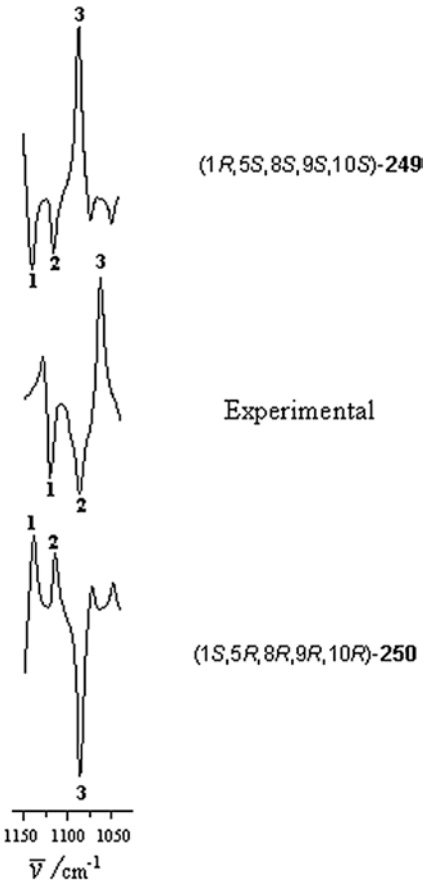

Fig. 71 Comparison of the observed VCD spectrum of (+)-plumericin (**249**) and the calculated VCD spectra of enantiomers **249** and **250.** (Adapted from (*125*))

frequencies, dipole and rotational strengths calculated at the same level of theory. The qualitative agreement of experimental and B3PW91/TZ2P VCD spectra of (1*R*, 5*S*,8*S*,9*S*,10*S*)-**253** confirmed the absolute configuration assigned to (–)-**253** and consequently to the new iridoid (–)-**252**. Remarkably, the absolute configurations of (+)-**249** and (–)-**252** are identical. However, they rotate the plane of polarized light to opposite directions confirming thereby the ambiguity existing in the assignment of absolute configuration of structurally related compounds from the sole use of empirical optical rotation measurements.

Example 4

Taking into consideration that in a VCD spectrum the rotational strengths are signated bands that are smaller than the dipole strengths, it is advisable to choose key vibrational modes to assign absolute configurations confidently. The steps can be illustrated by following absolute configuration determination of the seven-membered

lactone (+)-klaivanolide (**254**) isolated from *Uvaria klaineana* (Annonaceae), a natural product with potent *in vitro* activity against the parasite responsible for visceral leishmaniasis. IR and VCD determinations were performed using DFT at the B3PW91/TZ2P level (*297*). A clear spectroscopic manifestation of chirality was observed in the 1,300–1,200 cm^{-1} region (Fig. 72) where two absorption bands in the IR, change to positive and negative bands in VCD with decreased intensities that prove the presence of the expected *Cotton* effects. Thus, bands at 1,275 cm^{-1} and 1,232 cm^{-1}, corresponding to lactone C–O stretches, and the smaller negative peak at 1,198 cm^{-1}, due to an acetate C–O stretch, were important clues to assign configuration of the stereogenic C-7 center. A conformational search carried out using the MMFF94 force field provided 33 stable conformers. The calculated VCD spectrum was averaged between the most populated five conformers obtained by energy optimization and frequency analysis using DFT B3LYP/6-31G(d), followed by B3PW91/TZ2P level calculations. As observed in Fig. 72, the agreement in VCD spectral comparison of experimental (+)-**254** and the conformationally averaged (*S*)-**254** proved the (+)-(*S*)-**254** assignment to be correct.

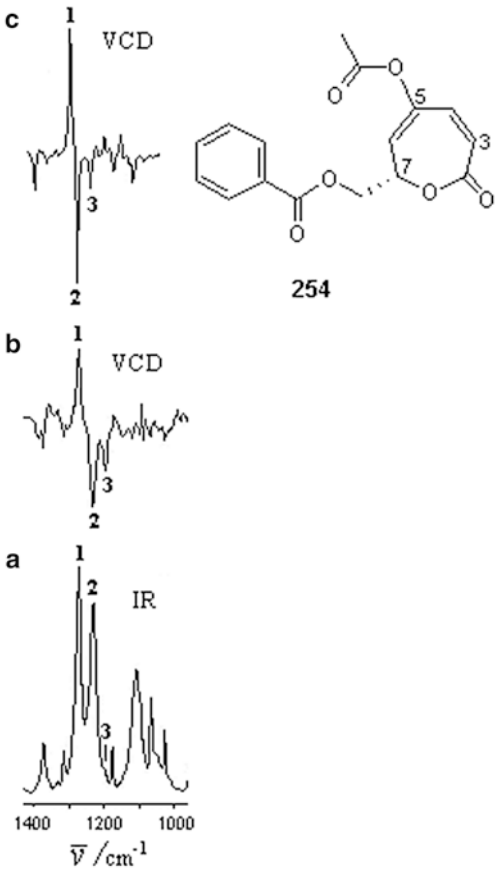

Fig. 72 Comparison of the observed (**a**) IR and (**b**) VCD spectra of (+)-**254**, and (**c**) the calculated spectrum of (*S*)-**254**. (Adapted from (*297*))

Example 5

One of the concerns in the absolute configuration determination of natural products by VCD spectroscopy is the selection of the solvent (*7*, *52*, *66*, *157*, *201*). The ideal choice contemplates a transparent solvent in the IR region of interest and the solubility of the sample; these two parameters may not always match. Examples are found in ginkgolides A (**255**), B (**256**), C (**257**), J (**258**), and M (**259**), terpene trilactones isolated from the *Ginkgo biloba* tree (*66*).

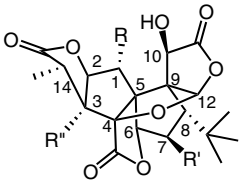

255 R = R' = H, R" = OH
256 R = R" = OH, R' = H
257 R = R' = R" = OH
258 R = H, R' = R" = OH
259 R = R' = OH, R" = H

Ginkgolide B (**256**) has potent platelet-activating-factor receptor antagonist activity. Ginkgolides are core-rigid molecules with several hydroxy groups, thus their polar nature prevents the use of solvents such as $CDCl_3$ and CCl_4, which are commonly employed in VCD. The fingerprint 1,300–850 cm^{-1} region of VCD spectra is complex and partially obscured in DMSO-d_6, a solvent in which ginkgolides are soluble, since the spectral transparency range of DMSO-d_6 is 2,100–1,100 cm^{-1}. Alternatively, CD_3CN may be chosen to record VCD spectra of ginkgolides even though the samples are not completely soluble in this solvent. The VCD spectral comparison of experimental and calculated spectra in the fingerprint region is shown in Fig. 73. *Boltzmann* weighted spectra were averaged by free energies of the two most stable conformers calculated with DFT at the B3LYP/6-31G(d) level, followed by single point calculations at the B3LYP/6-311 + G(2d,2p) level of theory. Associated with δC–O–H bending vibration, are bands at 1,170 cm^{-1} and 1,134 cm^{-1}, labeled as bands E and D in the CD_3CN trace line. The sign and intensities of bands E and D are in clear agreement with the calculated spectra, as well as the signated negative (+,–) couplet at the carbonyl region, thereby confirming the assignment of the absolute configuration shown for ginkgolide B in structure **256**. Frequency differences between the measured and the calculated VCD spectra of ginkgolide B, at the carbonyl and other wavenumbers, were conceived as the result of interactions with solvent, intermolecular ginkgolide B–ginkgolide B interactions, and the potential presence of other conformers in solution (*298*).

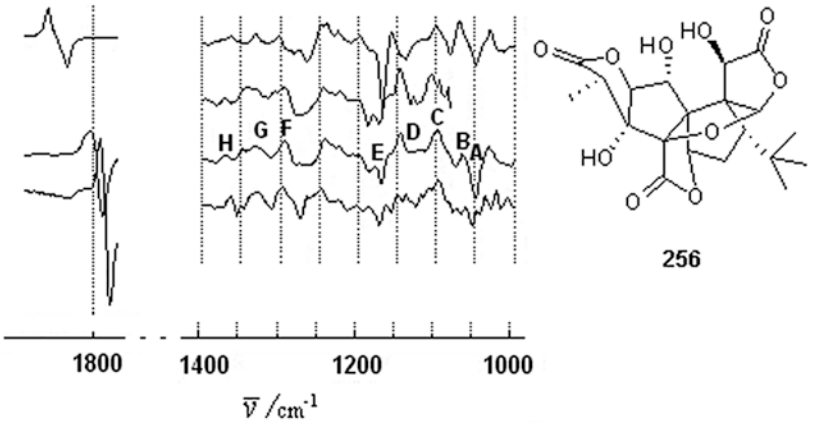

Fig. 73 VCD spectra comparison for ginkgolide B (**256**). From bottom to top the spectra correspond to: experimental in KBr, experimental in CD_3CN, experimental in DMSO-d_6 and DFT calculated at the B3LYP/6-31G(d) level. (Adapted from (*66*))

Example 6

The therapeutic effect of *Gingko biloba* extract in patients suffering dementia, which is attributed to ginkgolide terpene trilactones, has been tested by searching for intermolecular interactions between ginkgolides A (**255**) B (**256**), C (**257**) bilobalide B (**260**) as well as ginkgolide A monoether (**261**) and ginkgolide A diether (**262**) with amyloid peptide Aβ(25–35), using VCD methodology (*299*). The aggregation phenomenon in peptides, as investigated by VCD, is well documented (*300*, *301*).

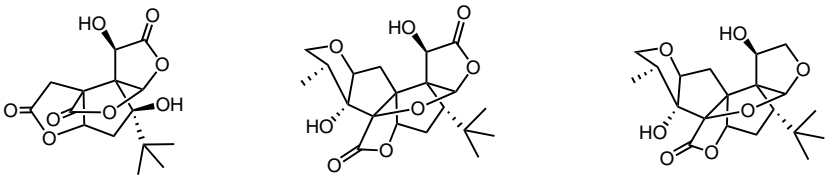

The protein fibril growing process is related to the detriment of neurons that cause *Alzheimer*'s and *Creutzfeldt-Jakob* diseases. Intermolecular recognition interactions were searched at the vibrational band frequency of the carbonyl groups in ginkgolides and bilobalide located at around 1,790 cm^{-1} and the vibrational bands of amide I in Aβ(25–35) peptide located in the 1,640–1,610 cm^{-1} region, expecting to observe changes in bands position or intensity. The study was carried out in an EtOD/D_2O solvent mixture and the predicted VCD spectra were calculated with

DFT at the B3LYP/6-31G(d) level of theory. Theoretical VCD spectra in the carbonyl region of the gingkolides were analyzed in light of normal mode compositions indicating that the band intensities and signs are sensitive to the nature of the coupling among different groups. The effect of ginkgolides in modulating peptide aggregation was found to be small, but, however, changes in VCD intensity suggest that ginkgolide A (**255**) reduces aggregation whereas bilobalide B (**260**) promotes it.

In a related vibrational study of aggregation phenomena, it was demonstrated delicately that VCD is a sensitive tool to study protein insulin fibrillation forming chiral streamer scaffolds in the solution phase (*23*). The pH dependence of the fibril stereo-structure analyzed in the enhanced normal and opposite sign VCD bands, in the amide I region, represents both a normal and a reversed sense of supramolecular chirality (Fig. 74).

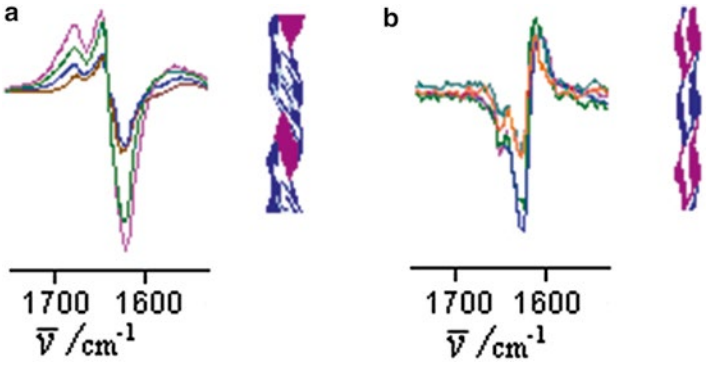

Fig. 74 The sense of chirality in insulin fibrils (**a**) normal (**b**) reversed and fragments of the VCD spectra in the amide I bands changing with pH. (Adapted from (*23*))

Example 7

The absolute configurations of hexylitaconic acids (+)-**263** and (–)-**264**, inhibitors of p53-HDM2 proteins interaction, of importance in cancer therapy, were confirmed by VCD spectroscopy (*302*). Enantiomer (+)-**263** is found in Nature as a root growth stimulator of lettuce seedlings from cultivated *Aspergillus niger*, whereas its enantiomeric form (–)-**264** is isolated as a metabolite produced by the marine endophytic fungus *Apiospora montagnei*. A racemic mixture of hexylitaconic acid was prepared by synthesis and separated by enantioselective HPLC. To avoid possible formation of complexes by intra- or intermolecular H-bonding, the methyl ester derivatization strategy on enantiomerically pure samples, to produce (+)-**265** and (–)-**266** independently, was employed to conduct VCD measurements. A conformationally restricted search for simulations was performed with the MMFF94S force

field, followed by DFT at the B3LYP/6-31++G(d,p) level of theory, on the alkyl chain-fixed (*R*)-**264**, providing 32 low-energy lying conformers, which were reduced to 14 conformers (over 95% of the population) in the *Boltzmann*-averaged statistics treatment of IR and VCD data. Considering that the major VCD bands of (–)-**264** agree reasonably with the calculated enantiomer (*R*)-**264**, in particular in the couplet found at 1,730 cm^{-1} (C=O stretch), the configuration (–)-(*R*)/(+)-(*S*) was determined confidently. This assignment was confirmed by the absolute configuration suggested by VCD measurements of the lactone derivative (+)-(*R*)-**267** obtained by a two-step synthesis from (–)-(*R*)-**264**. The stereochemistry of (–)-(*R*)-**264** is opposite to that previously reported by ECD (*303*).

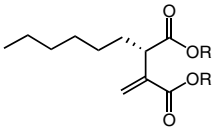

263, R = H
265, R = CH_3

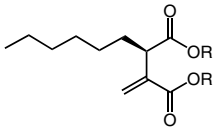

264, R = H
266, R = CH_3

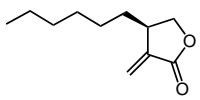

267

Example 8

The 5-substituted-2(5*H*)-furanones, sotolon (–)-(**268**) and maple furanone (+)-(**269**), responsible for the sugary sweet aroma in foodstuffs and drinks such as cane sugar, maple syrup and wine, were studied by VCD to clarify the relationship between their absolute configurations and odiferous properties (*304*). Isomeric separations were afforded by CO_2 supercritical fluid chromatography using chiral stationary phase columns; the enantiomers collected were subjected to VCD measurements. A DFT conformational search on these rigid structures resulted in one conformer for (*R*)-**268** and three low-lying conformers for (*R*)-**269**. VCD spectra of enantiomers (–)-**268** and (+)-**269** agreed with simulated VCD spectra of (*R*)-**268** and (*R*)-**269**, thus confirming the (–)-(*R*)-**268** and (+)-(*R*)-**269** absolute configuration assignments. Interestingly, this pair of closely structurally related furanones has opposite optical rotations even though both are (*R*). However, the analogous odiferous compounds (+)-(*R*)-**270** (*305*, *306*) and (+)-(*R*)-**271** (*307*), with equal structural changes to the **268** and **269** pair, display the same optical rotation and configuration. The absolute configuration assignments of **270** and **271** were also determined by VCD. The positive *Cotton* effect of the band around 1,335 cm^{-1} in the VCD spectra of (–)-**268** and (+)-**269** was attributed to C-H bending vibration at the stereogenic center (Fig. 75). Remarkably, this distinctive signal can be taken as a reliable stereochemical marker of flavorous furanones. VCD spectral differences between (–)-**268** and (+)-**269** appeared around 1,254 cm^{-1}.

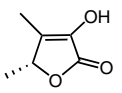

268

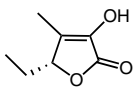

269

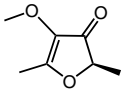

270

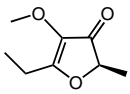

271

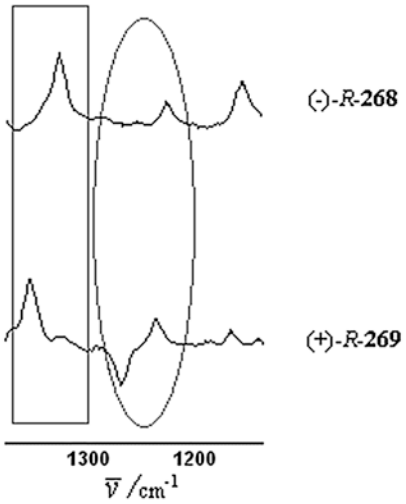

Fig. 75 Observed VCD spectra of sotolon (**268**) and maple furanone (**269**). (Adapted from (*304*))

Example 9

The reliability of predicted DFT-VCD spectra in solvation simulated environments, using Continuous Surface Charge (CSC) adapted Polarizable Continuum Model (PCM) (*143*) calculations, as implemented in the Gaussian 09 suite of programs, is pinpointed through comparison of the solvent-simulated VCD spectrum of (+)-garcinia acid dimethyl ester (**274**) with the observed VCD spectrum (*308*). The γ-lactone diester **274** is derived from (2*S*,3*S*)-2-hydroxycitric acid (**272**) present in the dried rind of the fruit of *Garcinia cambogia* (Malabar tamarind), which possesses purported antiobesity properties, among other biological activities. Compound **272** undergoes spontaneous lactonization during its isolation to produce (+)-(2*S*,3*S*)-garcinia acid (**273**), which exhibits antifungal activity.

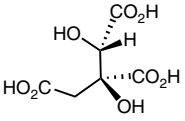

272

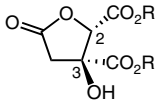

273, R = H
274, R = CH_3

To avoid possible H-bonding interaction of the carboxylic acid units in **273** with polar H_2O or DMSO solvents, VCD measurements were performed on the diester derivative **274**. Eight conformations of **274** were found to be stable, and thus subjected to geometry optimization using the DFT B3LYP/aug-cc-pVDZ method. Gas phase average populations remained without significant change respect to population calculated in CH_2Cl_2. Vibrational absorption and VCD spectra were predicted, at the same level of theory, for each conformer and for the population average sum. VCD spectra comparison of both, gas phase and solvent simulated, with the observed spectrum provided improvement in solvent PCM over that in gas-phase (Fig. 76). Worthy of note, however, is that the adapted non-continuous surface charge PCM was not as efficient in simulating solvation as this current version, thus the VCD predicted spectrum of 6,6′-dibromo-1,1′-bi-2-naphthol in the gas phase was in better agreement with the VCD observed spectrum than the solvent simulated one (*309*).

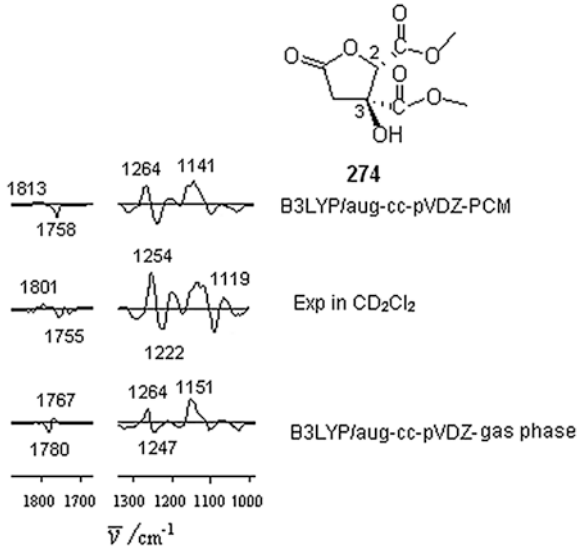

Fig. 76 VCD spectra of (+)-(2*S*,3*S*)-garcinia acid dimethyl ester (**274**). (Adapted from (*307*))

Example 10

Dimethyl esters of (+)-(2*S*,3*S*)-garcinia acid (GADE) (**274**), (+)-(2*S*,3*R*)-hibiscus acid (HADE) (**275**) and of their corresponding enantiomers **276** and **277** may be used to demonstrate the necessity of using more than one chiroptical method to assign the absolute configuration of diastereomers (*310*). Hibiscus acid, isolated from the calyxes/leaves of *Hibiscus sabdariffa* (Mathippuli-Roselle plant), is found commonly in herbal teas. The absolute configurations of GADE (**274**) (*308*) and HADE (**275**) were determined by VCD, ECD, and ORD measurements. The PCM,

implemented in the Gaussian 09 program, was conveniently applied to simulate a CH_2Cl_2 solvation environment. An exhaustive conformational analysis method, was undertaken to find the stable pseudorotational conformers of HADE (**275**), including manual search and Spartan and Conflex programs, leading to seven conformers after the optimization at the B3LYP/6-31G(d) level. Geometry optimization by DFT using the B3LYP functional and the 6-31G(d) and aug-cc-pVDZ basis sets in the gas phase preceded IR and VCD spectra calculations. Simulations using the PCM solvation were carried out by DFT B3LYP/aug-cc-pVDZ. Conformer populations dictated by free energies were employed to obtain average weighted VCD spectra. The experimental IR and VCD spectra for (+)-HADE and (+)-GADE in the fingerprint region were different enough to establish discrimination of these two diastereomers. However, comparison of the predicted VCD spectrum of (2*R*,3*R*)-**276**, enantiomer of GADE, with the VCD spectrum of its diastereomer HADE showed some resemblances. Similarly, the VCD spectrum of (2*R*,3*S*)-**277**, the enantiomer of HADE, resembled the VCD spectrum of its diastereomer GADE; these findings highlight the need to resort to IR spectra to discriminate between diastereomers. By analogy, VCD may be combined with other chiroptical techniques such as ECD or ORD to clarify ambiguities observed by comparison with only one technique (*311*, *312*), as exemplified by the VCD spectra of diastereomers in this case. The PCM simulated VCD spectrum for (2*S*,3*R*)-HADE (**275**) agreed to a larger extent with the observed spectrum than the gas phase simulated spectrum, thus confirming its absolute configuration unambiguously.

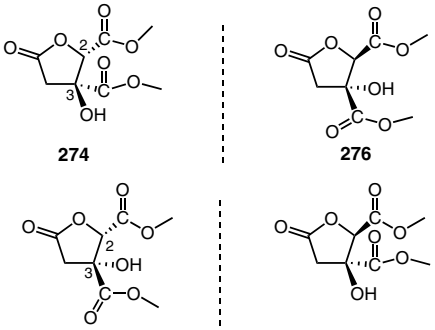

In a recent communication (*313*), it was pinpointed that aggregation phenomena that complicate the VCD analyses of garcinia acid (**273**) and hibiscus acid (**278**) may be avoided by using the corresponding disodium salts. The VCD spectra of the salts are clearly featured by a bisignate couplet (–,+) at around 1,624 cm^{-1} for the GADNa salt and a bisignate couplet (+,–) at around 1,616 cm^{-1} for HADNa salt (Fig. 77). Alternatively, the anhydride obtained from a *cis* dicarboxylic acid molecule, as **273**, is a good alternative to avoid aggregation phenomena when performing chiroptical VCD, ECD, or ORD studies of these polar molecules (*313*).

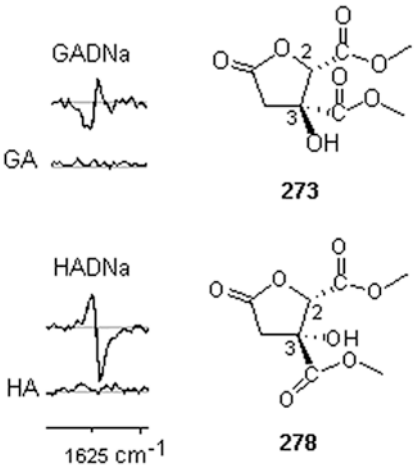

Fig. 77 Experimental VCD spectra of (+)-(2*S*,3*S*)-garcinia acid (GA) (**273**), its disodium sal GADNa, (+)-(2*R*,3*S*)-hibiscus acid (HA) (**278**), and its disodium salt HADNa, in D_2O. (Adapted from (*313*))

Example 11

Filifolinol (**279**), isolated from the cuticle of *Heliotropium filifolium*, together with filifolinyl senecionate (**280**), belongs to a series of unusual *spiro* natural products of mixed biogenesis showing the 3*H*-*spiro*-1-benzofuran-2,1′-cyclohexane structures (**281**–**284**), which exhibit antibacterial and antiviral activities. The absolute configuration of filifolinol acetate (**282**) was determined by VCD methodology using DFT at the B3LYP/DGDZVP level of theory (*314*). The atomic coordinates from its X-ray structure were used as a starting point for the conformational search using the MMFF force field. Eight conformers were found within a 40 kJ/mol window, but only two accounted significantly to the average population sum of 99.3%. Differences between them are referred only to rotameric orientations of the carbomethoxy group in an almost ideal chair conformation. The IR and VCD spectra were predicted at the same level of theory. The *in silico* comparison of the simulated and the experimental VCD data using the Compare*VOA* software (*129*, *130*), provided an anharmonicity factor of 0.983 applied to the frequency coordinate of the theoretical spectrum (Fig. 78). The visual similarity with which experimental and theoretical plots concurred and confidently allowed assignment of fillifolinol acetate (**282**) as the (2*S*,9*S*,12*R*)-enantiomer, and consequently this same absolute configuration to the whole series. The sign and intensity of the CO bands in the VCD experimental and calculated spectra matched clearly.

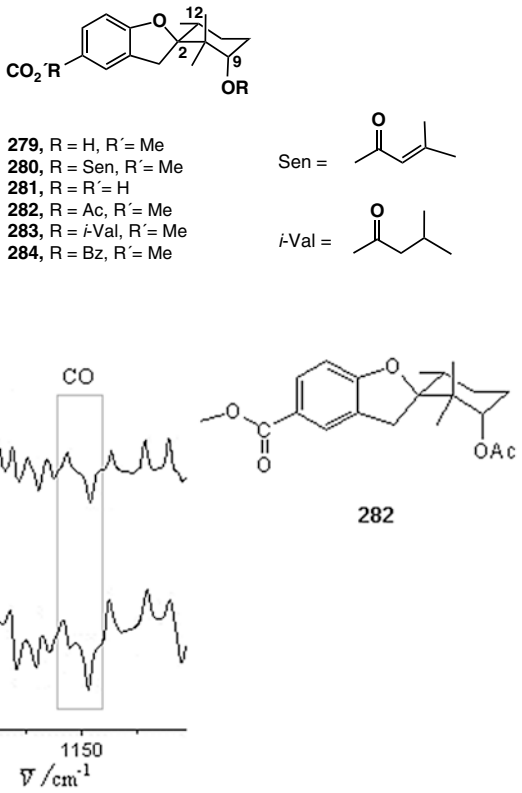

Fig. 78 Experimental (*top*) and calculated (*bottom*) VCD spectra of (2*S*,9*S*,12*R*)-fillifolinol acetate (**282**). (Adapted from (*314*))

Example 12

Chirality of the enantiomers of flavanone (**285**), the parent compound of citrus fruits flavonoids, was revisited using ECD, OR, and VCD chiroptical methods (*315*). Racemic flavanone was resolved in a HPLC system equipped with a cellulose-derived enantioselective column coupled to an ECD detector, and to a laser polarimeter detector. Inasmuch as the sensitivity of the ECD detector is higher than that of the OR detector, a 1 μg sample was enough to observe enantiomeric resolution, at 310 nm, using the enantioselective HPLC-ECD arrangement, but 10 μg were needed to observe confident enantiomeric separation peaks using the enantioselective HPLC-OR train, at 670 nm. The first eluted enantiomer was the levorotatory (negative peak) followed by the dextrorotatory (positive peak) appearing approximately after two minutes. The experimental ECD spectrum for the (–)-enantiomer was featured by three signated bands (–,–,+), which turned into a (+,+,–) trial for the (+)-enantiomer. To assign an absolute configuration, a systematic conformational search for the (*S*)-enantiomer was carried out, and the molecule was found to be conformationally fixed in one conformer (99%). A full ECD spectrum was

simulated for the (*S*)-enantiomer using TD-DFT calculations at the B3LYP/aug-cc-pVDZ and at the B3LYP/aug-cc-pVTZ levels of theory. The bands in the simulated ECD spectrum showed the pattern (–,–,+), the same as that of the (–)-enantiomer. Thus, the (–)-enantiomer was assigned with the (*S*)-configuration and the (+)-enantiomer, the (*R*)-configuration. The use of more than one chiroptical technique to assign absolute configuration is always beneficial, although the VCD technique provides a multiple chiral band test helping to reassure ECD absolute configuration predictions based on a substantially shorter number of chiral bands. Indeed, the IR and VCD spectra of the (*S*)- and (*R*)-enantiomers, calculated at the B3LYP/DGDZVP and B3PW91/DGDZVP levels of theory, visually matched with the (–)- and (+)-enantiomers, confirming that the absolute configuration assignments provided by ECD spectroscopy are correct. Figure 79 displays three segments of the VCD spectral comparisons of both enantiomers. The quantitative matching between experimental and calculated IR and VCD spectra allowed one to conclude that the B3LYP functional simulate the vibrational spectra of flavanones more accurately than the B3PW91 functional.

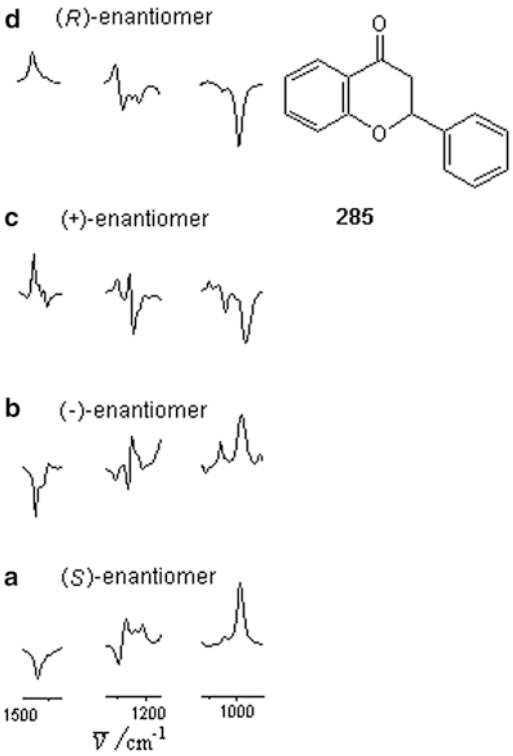

Fig. 79 Comparison of experimental (**b**) and (**c**), and calculated (**a**) and (**d**), at the B3LYP/DGDZVP level of theory, VCD spectra of flavanone (**285**). (Adapted from (*315*))

Example 13

(*S*)-Naringin, obtained from immature grapefruit, is enzymatically hydrolyzed to (*S*)-naringenin (**286**), a 5,7,4′-trihydroxyflavanone with antioxidant and potential anticancer activity. A racemic mixture of flavanone **286** was separated by enantioselective HPLC and the absolute configuration of the enantiomeric pair was confidently assigned using VCD spectroscopy (*316*). Compound **286** is a polar, conformational flexible molecule for which its vibrational analysis had to be carried out in acetonitrile-d_3, hence the observation spectral window was shortened to the 1,800–1,150 cm^{-1} region. Some calculations were performed using the polarizable continuum model (*141*, *142*) that simulates the solvent environment. A conformational search was undertaken to obtain a series of potential energy surfaces using a combined semiempirical AM1 and DFT B3PW91/TZ2P methodology. Interestingly, two shallow minima were found when the C-1′–C-2 bond is rotated, librating two close, but not identical, conformers having both the phenol ring in perpendicular orientation with respect to the chromane moiety. Thus, four conformers were found in minimal energy positions, which have as common characteristics the orientation of the phenol group to the equatorial chromane position, and the rotameric hydroxy at C5 forming an intramolecular H-bonding with the carbonyl group. The vibration movement (*316*) of the C-1′–C-2 bond is closely related to the intensity and sign of the VCD bands that correspond to vibrations at 1,600 cm^{-1}, the broad couplet (+,–) at 1,350 and 1,325 cm^{-1}, and the band at 1,250 cm^{-1}. The absolute configuration of the enantiomers of **286** was secured as (+)-(*R*) and (–)-(*S*).

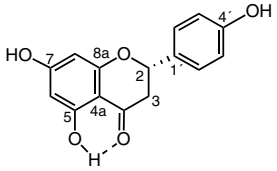

(*S*)-**286**

Example 14

The marine natural alkaloids citrinadin A (**287**) and citrinadin B (**288**), isolated from the cultured broth of fungus *Penicillium citrinum* N059 strain, are pentacyclic spiroindolinones that grow in the red alga *Actinotrichia fragilis*. Citrinadin B shows moderate cytotoxic activity against murine leukemia L1210 cells (*317*). The structure and relative stereochemistry of **287** and **288** were established by two-dimensional NMR data and the absolute configuration using the ECD and VCD techniques. In particular, VCD was applied to acquaint the absolute configuration of C-21 at the epoxide entity, therefore two chiral epoxides (*S*)-**289** and (*R*)-**290**, that model the 2,3-epoxy-3-methyl-1-oxobutyl side chain, were synthesized and the

VCD spectrum of **287** compared to the VCD spectra of models **289** and **290** at around 1,230 cm^{-1}, where these enantiomers show weak mirror-image *Cotton* effects. The negative band at 1,245 cm^{-1} for **287** matched well with the negative band observed for epoxide (*S*)-**289**, thus assuring the configuration at C-21 as (*S*). Considering the similarity between the ECD spectra of **287** and **288**, the (*S*) configuration was also assigned to **288** at C-21.

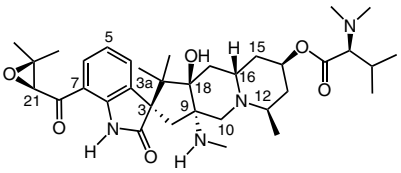

287

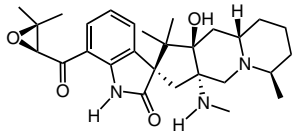

288

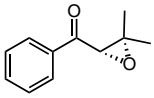

(*S*)-**289**

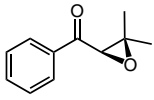

(*R*)-**290**

Example 15

Synoxazolidinone A (**291**), a marine natural product with antibacterial and antifungal properties, was isolated from the sub-Arctic ascidian *Synoicum pulmonaria* (*318*). According to a previous ECD stereochemical analysis, the C-10 and C-11 chiral centers have the (*S*,*S*) absolute configuration, and the C-6–C-7 double bond (*E*) stereochemistry. However, NMR spectroscopy suggested the double bond has a (*Z*) configuration. Therefore, a stereochemical study of the eight possible configurational isomers was planned using a combination of theoretical NMR, along with the use of ECD, ROA, and VCD methods to disclose its relative stereochemistry and absolute configuration (*318*). Molecule **291** is highly flexible, thus for every studied isomer thirty-six conformers within the first 6.5 kJ/mol were found. Conformers were minimized at the B3LYP/6-31 + G(d,p) level of theory, and those conformers from the (*Z*) isomers were further minimized with the larger 6-311++G(d,p) basis set, using empirical dispersion and considering explicit solvation. The computed ^{1}H NMR chemical shifts and selected coupling constants suggested the double bond of **291** to have (*Z*) stereochemistry, and the relative configuration of C-10 and C-11 to be (*S*,*R*). The ECD spectrum of **291** was calculated at the TD-LDA/SVP/CPCM and at the higher TD-B3LYP/6-311++G(d,p)/CPCM levels of theory. The comparison of the experimental with the calculated ECD spectra was ambiguous, giving rise to four possible matching isomers (*Z*,10*S*,11*R*), (*Z*,10*S*,11*S*), (*E*,10*R*,11*S*), and (*E*,10*R*,11*R*). In addition, the ROA technique provided a reliable stereochemical

analysis of **291** with differences in sign and intensity of the peaks allied to the double bond and the C-10 chiral center, leading to assign its configuration either as (*Z*,10*S*,11*R*) or (*Z*,10*S*,11*S*) by comparison of the experimental and calculated spectra, which were computed at the B3LYP/6-311++G(d,p)/CPCM level of theory. From these results it is clear that vibrational spectroscopy presented advantages over electronic spectroscopy in the assignment of the stereochemistry of **291**, an observation confirmed through application of the VCD technique to examine its absolute configuration. The experimental IR and VCD spectra were recorded in CD_3OD and DMSO-d_6. In the simulated spectra, deuterium exchange of acidic protons was considered when compared to CD_3OD, but no deuterium exchange was considered for DMSO-d_6. Moreover, cluster geometries with five explicit water molecules were considered when comparing with the CD_3OD solvent. In all cases, visual comparisons of the experimental and the calculated VCD spectra, at the B3LYP/6-311++G(d,p)/CPCM level of theory, in the 1,800–1,200 cm^{-1} region, suggested (*Z*,10*S*) is the correct stereochemistry for **291**. The (*R*) absolute configuration for C-11 is suggested although not unambiguously confirmed by VCD. Analogously, synoxazolidinone C (**292**), isolated from the same organism, was confirmed to have the (*Z*,10*S*,13*R*) stereochemistry when using the VCD technique, although the absolute configuration of C-11 remained elusive due to the closeness between the experimental and simulated VCD spectra found for the (*Z*,10*S*,11*R*,13*R*) and (*Z*,10*S*,11*S*,13*R*) isomers.

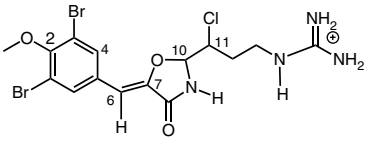

291

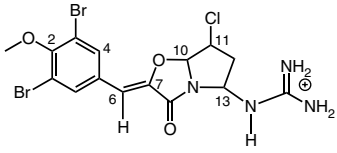

292

Example 16

A series of C_{13}-polyketides, produced by the *Chaetomium mollipilium* cultivated fungus, were intentified structurally by spectroscopic techniques (*319*). Mollipilin **293** and the spiroketal **294**, which play important roles in C_{13}-polyketide biosynthesis relationships, were selected for VCD studies to analyze the C-7 and C-11 absolute configuration in **293**, and the C-7, C-8, and C-11 absolute configuration in **294**. The agreement of the observed VCD spectrum of **293** with two calculated diastereomers (7*S*,11*R*), and (7*S*,11*S*), allowed the absolute configuration of C-7 to be assigned as (*S*), but, however, as the calculated spectra of both diastereomers were practically the same, the C-11 absolute configuration could not be assessed. Transformation of **293** to the 2,4-dinitrophenylhydrazone **295** allowed its crystal structure to be obtained, revealing the relative configuration of C-11 as (*R*). In addition, the (7*S*,8*S*,11*R*) relative configuration, suggested by NMR, for the spiroketal

294 was discarded, since the observed VCD spectrum of **294** matched well with the calculated VCD spectrum of the (7*S*,8*S*,11*S*)-diastereomer and mismatched with the VCD spectrum of the (7*S*,8*S*,11*R*)-diastereomer.

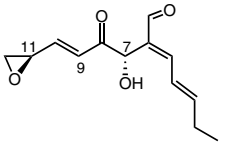

293

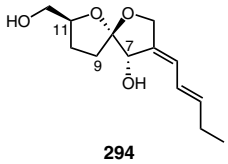

294

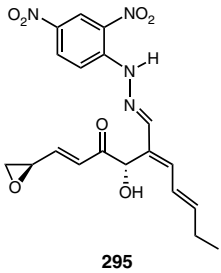

295

Example 17

Chaetocin (11*S*,15*S*,11′*S*,15′*S*)-**296**, a 3,6-epidithio diketopiperazine fungal metabolite with antibacterial function and cytotoxic activity against HeLa cells, was subjected to desulfurization to produce the disulfide derivative **297**. ECD and VCD studies of **297** were performed to analyze the relative stereochemistry at the C-11, C-15, and C-11′, C-15′ reaction center pairs at each fused heterocyclic moiety of the dimeric molecule, along with its absolute configuration (*320*). The desulfurization reaction was carried out with triphenylphosphine, an efficient reactant under which both retention and inversion of configuration have previously been reported for analog disulfide bridge molecules. Therefore, the three diastereomers (11*S*,15*S*,11′*S*,15′*S*)-**298**, (11*S*,15*S*,11′*R*,15′*R*)-**299**, and (11*R*,15*R*,11′*R*,15′*R*)-**300** were considered for the electronic and vibrational spectra simulations. According to the stereochemical outcome of the desulfurization reaction, diastereomer **298** comes from a retention pathway at both moieties, **299** from a mixed retention-inversion process, and **300** from inversion pathways. The observed ECD spectrum of **297** was compared to the calculated spectra of **298–300** which were obtained with the TD-DFT ωB97XD/6-311G (d,p) method. These comparisons invalidated diastereomer **300** as a possible reaction product, leaving **298** and **299** as potential products. Nevertheless, ECD spectra calculated at the higher ωB97XD/6-311G++(d,p) level of theory excluded not only diastereomer **300** but also diastereomer **299** as possible products of reaction, suggesting the desulfurization of chaetocin **296** proceeded with retention of configuration at both reactive disulfide bridges to give the chiral diastereomer **298**. The stereochemistry of the reaction was confirmed by the VCD technique;

since comparing the observed with the simulated spectra for diastereomers **298**–**300**, at the ωB97XD/6-311G (d,p) level of theory, showed five bands in the 1,425–1,275 cm^{-1} region, which clearly matched in sign and frequency for diastereomer **298**, while none of the other diastereomers was found to be in band featured agreement with the observed spectrum (Fig. 80).

In a complementary study (*321*), which includes quantum mechanical calculations of transition states, the universality of absolute configuration retention at the bridgehead carbon atoms of epidithiodioxopiperazines was shown.

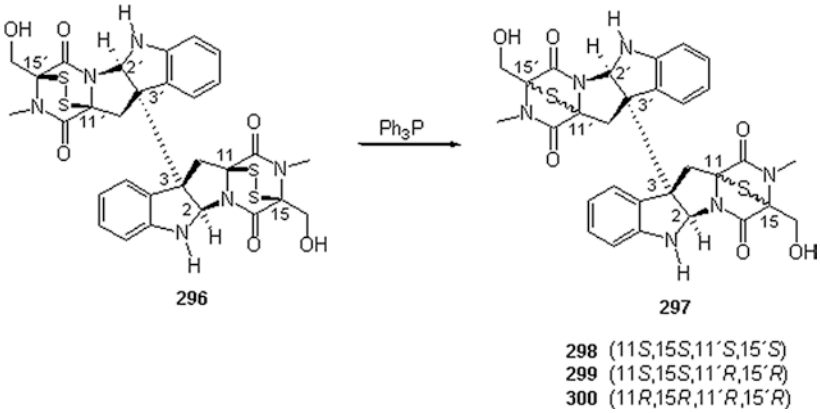

Fig. 80 Desulfurization reaction of (11*S*,15*S*,11′*S*,15′*S*)-3,6-epidithiodiketopiperazine (**296**)

6 Concluding Remarks

In the contemporary world, no pragmatic advance can be conceived without being linked to science. Nature has provided man with inspiring phenomena such as chirality, commonly observed in our daily life, the basis of which rely on dissymmetric molecules and the way they interact with each other or with an anisotropic radiation. Light in iridescent environments impacts our sense of vision to appreciate the beautiful colors of the rainbow on rainy days. Natural flavors in fruits invite our taste sensation to appreciate chirality information hidden within their molecular structures. Chirality is indeed implicated in most biological important processes, thus to find methods that accurately senses this becomes a goal to be reached in chemical research. In attaining this goal, solid steps were made initially using anomalous X-ray diffraction analysis, for which the practical use has currently been reinforced with calculations of the *Flack* (*251*) and *Hooft* (*252*) parameters, then with the ORD and ECD techniques, and more recently by the ROA, and VCD methods. The authors hope this chapter will be a useful resource for readers who wish to use VCD to investigate chirality.

Finally, of relevance it is also to mention that a revolutionary concept, which uses polarized microwaves (*322*), was introduced as a chiral technique, and is under development for the direct detection of enantiomers (*323*).

Acknowledgements We are indebted to the editors, Professors *Heinz Falk* and *Douglas Kinghorn*, for all the valuable suggestions they made for the preparation of this chapter, and thank CONACYT-Mexico for financial support through grant 152994.

References

1. Summons RE, Albrecht P, McDonald G, Moldowan JM (2008) Molecular Biosignatures. Space Sci Rev 135:133
2. Ma S (2009) Electrophilic Addition and Cyclization Reactions of Allenes. Acc Chem Res 42:1679
3. Roth HJ (2005) Four-Membered Rings. Deut Apoth Z 145:56
4. Eliel EL, Wilen, SH, Mander LN (1994) Stereochemistry of Organic Compounds. Wiley, New York, Chapters 4, 10, and 13
5. Lightner D, Gurst JE (2000) Organic Conformational Analysis and Stereochemistry from Circular Dichroism Spectroscopy. Wiley-VCH, Weinheim
6. Scopes PM (1975) Applications of the Chiroptical Techniques to the Study of Natural Products. In: Herz W, Grisebach H, Kirby GW (eds) Progress in the Chemistry of Organic Natural Products, vol 32. Springer–Verlag, New York, p 167
7. Nafie LA (2008) Vibrational Circular Dichroism: A New Tool for the Solution-State Determination of the Structure and Absolute Configuration of Chiral Natural Product Molecules. Nat Prod Commun 3:451
8. Allenmark S (2003) Induced Circular Dichroism by Chiral Molecular Interaction. Chirality 15:409
9. Polavarapu PL, Jeirath N, Kurtán T, Pescitelli G, Krohn K (2009) Determination of the Absolute Configurations at Stereogenic Centers in the Presence of Axial Chirality. Chirality 21:E202
10. Cerda-García-Rojas CM, García-Gutiérrez HA, Hernández-Hernández JD, Román-Marín LU, Joseph-Nathan P (2007) Absolute Configuration of Verticillane Diterpenoids by Vibrational Circular Dichroism. J Nat Prod 70:1167
11. Devlin FJ, Stephens PJ, Besse P (2005) Are the Absolute Configurations of 2-(1-Hydroxyethyl)-chromen-4-one and its 6-bromo Derivative Determined by X-Ray Crystallography Correct? A Vibrational Circular Dichroism Study of their Acetate Derivatives. Tetrahedron Asymm 16:1557
12. Stephens PJ, McCann DM, Devlin FJ, Smith AB, III (2006) Determination of the Absolute Configurations of Natural Products *via* Density Functional Theory Calculations of Optical Rotation, Electronic Circular Dichroism, and Vibrational Circular Dichroism: The Cytotoxic Sesquiterpene Natural Products Quadrone, Suberosenone, Suberosanone, and Suberosenol A Acetate. J Nat Prod 69:1055
13. Stephens PJ, Pan JJ, Devlin FJ, Urbanová M, Hájíček J (2007) Determination of the Absolute Configuration of Natural Products *via* Density Functional Theory Calculations of Vibrational Circular Dichroism, Electronic Circular Dichroism and Optical Rotation: the Schizozygane Alkaloid Schizozygine. J Org Chem 72:2508
14. Stephens PJ, Pan JJ, Devlin FJ, Urbanová M, Julínek O, Hájíček J (2008) Determination of the Absolute Configurations of Natural Products *via* Functional Theory Calculations of Vibrational Circular Dichroism, Electronic Circular Dichroism, and Optical Rotation: the Iso-Schizozygane Alkaloids Ioschizogaline and Isoschizogamine. Chirality 20:454

15. Avilés-Moreno JR, Partal-Ureña F, López-González JJ (2009) Conformational Landscape in Chiral Terpenes from Vibrational Spectroscopy and Quantum Chemical Calculations: *S*-(+)-Carvone. Vib Spect 51:318
16. Petrovic AG, Navarro-Vazquez A, Alonso-Gomez JL (2010) From Relative to Absolute Configuration of Complex Natural Products. Interplay between NMR, ECD, VCD, and ORD Assisted by *ab Initio* Calculations. Curr Org Chem 14:1612
17. Urbanová M (2009) Bioinspired Interactions Studied by Vibrational Circular Dichroism. Chirality 21:E215
18. Keiderling TA (2002) Protein and Peptide Secondary Structure and Conformational Determination with Vibrational Circular Dichroism. Curr Opin Chem Biol 6:682
19. Weigelt Sven, Huber T, Hofmann F, Jost M, Ritzefeld M, Luy B, Freudenberger C, Majer Z, Vass E, Greie J-C, Panella L, Kaptein B, Broxterman QB, Kessler H, Altendorf K, Hollósi M, Sewald N (2012) Synthesis and Conformational Analysis of Efrapeptins. Chem Eur J 18:478
20. Taniguchi T, Monde K (2007) Chiroptical Analysis of Glycoconjugates by Vibrational Circular Dichroism. Glycotechnology 19:147
21. Shanmugam G, Polavarapu PL (2006) Structures of Intact Glycopropteins from Vibrational Circular Dichroism. Prot: Struct Funct Bioinf 63:768
22. Petrovic AG, Polavarapu PL (2008) Quadruplex Structure of Polyriboinosinic Acid: Dependence on Alkali Metal Ion Concentration, pH and Temperature. J Phys Chem B 112:2255
23. Kurouski D, Lombardi RA, Dukor RK, Lednev IK, Nafie LA (2010) Direct Observation and pH Control Reversed Supramolecular Chirality in Insulin Fibrils by Vibrational Circular Dichroism. Chem Commun 46:7154
24. Kurouski D, Dukor RK, Lu X, Nafie LA, Lednev IK (2012) Normal and Reversed Supramolecular Chirality of Insulin Fibrils Probed by Vibrational Circular Dichroism at the Protofilament Level of Fibril Structure. Biophys J 103:522
25. Berthier D, Buffeteau T, Leger JM, Oda R, Huc I (2002) From Chiral Counterions to Twisted Membranes. J Am Chem Soc 124:13486
26. Narita M, Tashiro E, Hamada F (2002) Synthesis of a Selective Fluorescent Sensing System Based on γ-Cyclodextrin Modified with Pyrene and Tosyl on the Hetero Rims. J Incl Phenom Macro Chem 42:137
27. Bieri M, Gautier C, Buergi T (2007) Probing Chiral Interfaces by Infrared Spectroscopic Methods. Phys Chem Chem Phys 9:671
28. Gautier C, Burgi T (2009) Chiral Gold Nanoparticles. Chem Phys Chem 10:483
29. Guo Z, Du Y, Chen Y, Ng S-C, Yang Y (2010) Understanding the Mechanism of Chirality Transfer in the Formation of a Chiral MCM-41 Mesoporous Silica. J Phys Chem C 114:14353
30. Ma S, Shen S, Lee H, Eriksson M, Zeng X, Xu J, Fandrick K, Yee N, Senanayake C, Grinberg, N (2009) Mechanistic Studies on the Chiral Recognition of Polysaccharide-Based Chiral Stationary Phases using Liquid Chromatography and Vibrational Circular Dichroism. Reversal of Elution Order of N-Substituted alpha-Methyl Phenylalanine Esters. J Chromatogr A 1216:3784
31. Yao H, Nishida N, Kimura K (2010) Conformational Study of Chiral Penicillamine Ligand on Optically Active Silver Nanoclusters with IR and VCD Specroscopy. Chem Phys 368:28
32. Kuppens T, Bultinck P, Langenaeker W (2004) Determination of Absolute Configuration *via* Vibrational Circular Dichroism. Drug Discovery Today: Technologies 1:269
33. Deutsche CW, Moscowitz A (1968) Optical Activity of Vibrational Origin. I. A Model Helical Polymer. J Chem Phys 49:3257
34. Schellman JA (1973) Vibrational Optical Activity. J Chem Phys 58:2882
35. Berova N, Di Bari L, Pescitelli G (2007) Application of Electronic Circular Dichroism in Configurational and Conformational Analysis of Organic Compounds. Chem Soc Rev 36:914
36. Nakanishi K, Berova N (1994) The Exciton Chirality Method. In: Nakanishi K, Berova N, Woody RW (eds) Circular Dichroism. Principles and Applications. VCH, New York, p 361
37. Humam M, Christen P, Muñoz O, Hostettmann K, Jeannerat D (2008) Absolute Configuration of Tropane Alkaloids Bearing Two α,β-Unsaturated Ester Functions Using Electronic CD

Spectroscopy: Application to (*R,R*)-*trans*-3- Hydroxysenecioyloxy-6-Senecioyloxytropane. Chirality 20:20

38. Shim SH, Baltrusaitis J, Gloer JB, Wicklow DT (2011) Phomalevones A-C: Dimeric and Pseudodimeric Polyketide Metabolites from a Fungicolous Hawaiian Isolate of *Phoma* sp. (Cucurbitariaceae). J Nat Prod 74:395

39. Nafie LA, Freedman TB (2000) Vibrational Optical Activity Theory. In: Berova N, Nakanishi K, Woody RW (eds) Circular Dichroism. Principles and Applications, 2nd edn. Wiley-VCH, New York, p 97

40. Fang HL, Meister DM, Swofford RL (1984) Overtone Spectroscopy of Nonequivalent Methyl C-H Oscillators. Influence of Conformation on Vibrational Overtone Energies. J Phys Chem 88:410

41. Cappelli C, Bloino J, Lipparini F, Barone V (2012) Toward *ab Initio* Anharmonic Vibrational Circular Dichroism Spectra in the Condensed Phase. J Phys Chem Lett 3:1766

42. Holzwarth G, Hsu EC, Mosher HS, Faulkner TR, Moscowitz A (1974) Infrared Circular Dichroism of Carbon-Hydrogen and Carbon-Deuterium Stretching Modes Observations. J Am Chem Soc 96:251

43. Nafie LA, Freedman TB (1983) Vibrational Optical Activity Calculations Using Infrared and Raman Atomic Polar Tensors. J Chem Phys 78:7108

44. Stephens PJ (1987) Gauge Dependence of Vibrational Magnetic Dipole Transition Moments and Rotational Strengths. J Phys Chem 91:1712

45. Cheeseman JR, Frisch MJ, Devlin FJ, Stephens PJ (1996) *Ab Initio* Calculation of Atomic Axial Tensors and Vibrational Rotational Strengths Using Density Functional Theory. Chem Phys Lett 252:211

46. Devlin FJ, Stephens PJ, Cheeseman JR, Frisch MJ (1996) Prediction of Vibrational Circular Dichroism Spectra Using Density Functional Theory: Camphor and Fenchone. J Am Chem Soc 118:6327

47. Schellman JA (1975) Circular Dichroism and Optical Rotation. Chem Rev 75:323

48. Kawiecki RW, Devlin F, Stephens PJ, Amos RD, Handy NC (1988) Vibrational Circular Dichroism of Propylene Oxide. Chem Phys Lett 145:411

49. Nafie LA, Diem M (1979) Optical Activity in Vibrational Transitions: Vibrational Circular Dichroism and *Raman* Optical Activity. Acc Chem Res 12:296

50. Nafie LA, Diem M, Vidrine DW (1979) *Fourier* Transform Infrared Vibrational Circular Dichroism. J Am Chem Soc 101:496

51. Guo C, Shah RD, Dukor RK, Xiaolin C, Freedman TB, Nafie LA (2004) Determination of Enantiomeric Excess in Samples of Chiral Molecules Using *Fourier* Transform Vibrational Circular Dichroism Spectroscopy: Simulation of Real-Time Reaction Monitoring. Anal Chem 76:6956

52. Uncuta C, Ion S, Gherase D, Bartha E, Teodorescu F, Filip P (2009) Absolute Configurational Assignment in Chiral Compounds Through Vibrational Circular Dichroism (VCD) Spectroscopy. Rev Chim 60:86

53. Abbate S, Lebon F, Gangemi, R. Longhi G, Spizzichino S, Ruzziconi R (2009) Electronic and Vibrational Circular Dichroism Spectra of Chiral 4-X-[2.2]paracyclophanes with X Containing Fluorine Atoms. J Phys Chem A 113:14851

54. Nový J, Urbanová M, Volka K (2007) Electronic and Vibrational Circular Dichroism Spectroscopic Study of Non-Covalent Interactions of meso-5,10,15,20-Tetrakis(1-methylpyridinium-4-yl)porphyrin with $(dG\text{-}dC)_{10}$ and $(dA\text{-}dT)_{10}$. Vib Spect 43:71

55. Muñoz MA, Muñoz O, Joseph-Nathan P (2006) Absolute Configuration of Natural Diastereoisomers of 6β-Hydroxyhyoscyamine by Vibrational Circular Dichroism. J Nat Prod 69:1335

56. Min HM, Aye M, Taniguchi T, Miura N, Monde K, Ohzawa K, Nikai T, Niwa M, Takaya Y (2007) A Structure and an Absolute Configuration of (+)-Alternamin, a New Coumarin from *Murraya alternans* Having Antidote Activity Against Snake Venom. Tetrahedron Lett 48:6155

57. Chabay I, Hsu EC, Holzwarth G (1972) Infrared Circular Dichroism Measurement Between 2000 and 5000 cm^{-1}: Pr^{3+}-Tartrate Complexes. Chem Phys Lett 15:211
58. Nafie LA, Cheng JC, Stephens PJ (1975) Vibrational Circular Dichroism of 2,2,2-Trifluoro-l-phenylethanol. J Am Chem Soc 97:3842
59. Nafie LA, Keiderling TA, Stephens PJ (1976) Vibrational Circular Dichroism. J Am Chem Soc 98:715
60. Osborne GA, Cheng JC, Stephens PJ (1973) A Near-Infrared Circular Dichroism and Magnetic Circular Dichroism Instrument. Rev Sci Instrum 44:10
61. Lipp ED, Zimba CG, Nafie LA (1982) Vibrational Circular Dichroism in the Mid-Infrared using *Fourier* Transform Spectroscopy. Chem Phys Lett 90:1
62. Freedman TB, Cao X, Dukor RK, Nafie LA (2003) Absolute Configuration Determination of Chiral Molecules in the Solution State Using Vibrational Circular Dichroism. Chirality 15:743
63. Nafie LA. (2000) Dual Polarization Modulation: A Real-Time, Spectral-Multiplex Separation of Circular Dichroism from Linear Birefringence Spectral Intensities. Appl Spect 54:1634
64. Polavarapu PL, He J (2004) Chiral Analysis Using Mid-IR Vibrational CD Spectroscopy. Anal Chem 76:61A
65. Tsankov D, Eggimann T, Wieser H (1995) Alternative Design for Improved FT-IR/VCD Capabilities. Appl Spect 49:132
66. Andersen NH, Christensen NJ, Lassen PR, Freedman TBN, Nafie LA, Strømgaard K, Hemmingsen L (2010) Structure and Absolute Configuration of Ginkgolide B Characterized by IR- and VCD Spectroscopy. Chirality 22:217
67. Setnička V, Novy J, Bohm S, Sreenivasachary N, Urbanová M, Volka K. (2008) Molecular Structure of Guanine-Quartet Supramolecular Assemblies in a Gel-State Based on DFT Calculation of Infrared and Vibrational Circular Dichroism Spectra. Langmuir 24:7520
68. Zhang P, Polavarapu PL (2006) Vibrational Circular Dichroism of Matrix-Assisted Aminoacids Films in the Mid-Infrared Region. Appl Spect 60:378
69. Petrovic AG, Bose PK, Polavarapu PL (2004) Vibrational Circular Dichroism of Carbohydrate Films Formed from Aqueous Solutions. Carbohyd Res 339:2713
70. Merten C, Kowalik T, Hartwig A (2008) Vibrational Circular Dichroism Spectroscopy of Solid Polymer Films: Effects of Sample Orientation. Appl Spect 62:901
71. Nafie LA, Buijs H, Rilling A, Cao X, Dukor RK. (2004) Dual Source *Fourier* Transform Polarization Modulation Spectroscopy: An Improved Method for the Measurement of Circular and Linear Dichroism. Appl Spect 58:647
72. Hilario J, Drapcho D, Curbelo R, Keiderling TA (2001) Polarization Modulation *Fourier* Transform Infrared Spectroscopy with Digital Signal Processing: Comparison of Vibrational Circular Dichroism Methods. Appl Spect 55:1435
73. Urbanová M, Setnicka V, Volka K (2000) Measurements of Concentration Dependence and Enantiomeric Purity of Terpene Solutions and a Test of a New Commercial VCD Spectrometer. Chirality 12:199
74. Lakhani A, Malon P, Keiderling TA (2009) Comparison of Vibrational Circular Dichroism Instruments: Development of a New Dispersive VCD. Appl Spect 63:775
75. Muñoz MA, Muñoz O, Joseph-Nathan P (2010) Absolute Configuration Determination and Conformational Analysis of (–)-(3*S*,6*S*)-3α,6β-Diacetoxytropane Using Vibrational Circular Dichroism and DFT Techniques. Chirality 22:234
76. Muñoz MA, Martínez M, Joseph-Nathan P (2012) Absolute Configuration and Stereochemical Analysis of 3α,6β-dibenzoyloxytropane. Phytochemistry Lett 5:450
77. Reina M, Burgueño-Tapia E, Bucio MA, Joseph-Nathan P (2010) Absolute Configuration of Tropane Alkaloids from *Schizanthus* Species by Vibrational Circular Dichroism. Phytochemistry 71:810
78. Cao X, Shah RD, Dukor RK, Guo C, Freedman TB, Nafie LA (2004) Extension of *Fourier* Transform Vibrational Circular Dichroism into the Near-infrared Region: Continuous Spectral Coverage from 800 to 10,000 cm^{-1}. Appl Spect 58:1057

79. Bonmarin M, Helbing J (2009) Polarization Control of Ultrashort Mid-IR Laser Pulses for Transient Vibrational Circular Dichroism Measurements. Chirality 21:E298
80. Helbing J, Bonmarin M (2009) Time-Resolved Chiral Vibrational Spectroscopy. Chimia 63:128
81. Rhee H, June YG, Kim Z, Hwan J, Seung J, Cho M (2009) Phase Sensitive Detection of Vibrational Optical Activity Free-Induction-Decay: Vibrational CD and ORD. J Opt Soc Amer B. Opt Phys: 26:1008
82. Ma S, Freedman TB, Cao X, Nafie LA (2006) Two Dimensional Vibrational Circular Dichroism Correlation Spectroscopy: pH-Induced Spectral Changes in L-Alanine. J Mol Struct 799:226
83. Jalkanen KJ, Nieminen RM, Knapp-Mohammady M, Suhai S (2003) Vibrational Analysis of Various Isotopomers of L-Alanyl-L-Alanine in Aqueous Solution: Vibrational Absorption, Vibrational Circular Dichroism, Raman, and Raman Optical Activity. Int J Quant Chem 92:239
84. Yang G, Xu Y (2011) Vibrational Circular Dichroism Spectroscopy of Chiral Molecules. Top Curr Chem 298:189
85. Bak KL, Jørgensen P, Helgaker T, Ruud K, Jensen HJA (1994) Basis Set Convergence of Atomic Axial Tensors Obtained From Self-Consistent Field Calculations Using London Atomic Orbitals. J Chem Phys 100:6620
86. Parr RG, Yang W (1989) Density-Functional Theory of Atoms and Molecules. Oxford University Press, New York
87. Muñoz MA, Areche C, Rovirosa J, San-Martín A, Joseph-Nathan P (2010) Absolute Configuration of Sargaol Acetate Using DFT Calculations and Vibrational Circular Dichroism. Heterocycles 81:625
88. Kukushkin AK, Jalkanen KJ, (2010) Role of Quantum Chemical Calculations in Molecular Biophysics with a Historical Perspective. Theor Chem Acc 125:121
89. Stephens PJ, Devlin FJ (2000) Determination of the Structure of Chiral Molecules Using *ab Initio* Vibrational Circular Dichroism Spectroscopy. Chirality 12:172
90. Stephens PJ, Devlin FJ, Cheeseman JR (2012) VCD Spectroscopy for Organic Chemists. CRC Press/Taylor & Francis Group, New York
91. Crawford TD (2006) *Ab Initio* Calculation of Molecular Chiroptical Properties. Theor Chem Acc 115:227
92. Magyarfalvi G, Tarczay G, Vass E (2011) Vibrational Circular Dichroism. Comput Mol Sci 1:403
93. Vibrational modes animation: SHU.ac.uk
94. Herranz J, Morcillo J, Gómez A (1966) The ν_2 Infrared Band of CH_4 and CD_4. J Mol Spect 19:266
95. Freedman TB, Nafie LA. (1983) Vibrational Optical Activity Calculations Using Infrared and Raman Atomic Polar Tensors. J Chem Phys 78:27
96. Stephens PJ (1985) Theory of Vibrational Circular Dichroism. J Phys Chem 89:748
97. Bouř P, McCann J, Wieser H (1998) Measurement and Calculation of Absolute Rotational Strengths for Camphor, α-Pinene, and Borneol. J Phys Chem A 102:102
98. Nafie LA (1997) Electron Transition Current Density in Molecules. 1. Non-B*orn*-Oppenheimer Theory of Vibronic and Vibrational Transitions. J Phys Chem A 101:7826
99. Helgaker T, Jørgensen P (1991) An Electronic Hamiltonian for Origin Independent Calculations of Magnetic Properties J Chem Phys 95:2595
100. Ditchfield R (1976) Theoretical Studies of Magnetic Shielding in H_2O and $(H_2O)_2$. J Chem Phys 65:3123
101. Amos RD (1987) Molecular Property Derivatives. Adv Chem Phys 67:99
102. Nafie LA (1992) Velocity-Gauge Formalism in the Theory of Vibrational Circular Dichroism and Infrared Absorption. J Chem Phys 96:5687
103. Crawford TD, Schaefer HF (2000) An Introduction to Coupled Cluster Theory for Computational Chemists, In: Lipkowitz KB, Boyd DB (eds) Reviews in Computational Chemistry, vol 14. VCH Publishers, NewYork, Chapter 2

104. Wiberg KB, Vaccaro PH, Cheeseman JR (2003) Conformational Effects on Optical Rotation. 3-Substituted 1-Butenes. J Am Chem Soc 125:1888

105. Frisch MJ, Trucks GW, Schlegel HB, Scuseria GE, Robb MA, Cheeseman JR, Montgomery JA Jr, Vreven T, Kudin KN, Burant JC, Millam JM, Iyengar SS, Tomasi J, Barone V, Mennucci B, Cossi M, Scalmani G, Rega N, Petersson GA, Nakatsuji H, Hada M, Ehara M, Toyota K, Fukuda R, Hasegawa J, Ishida M, Nakajima T, Honda Y, Kitao O, Nakai H, Klene M, Li X, Knox JE, Hratchian HP, Cross JB, Adamo C, Jaramillo J, Gomperts R, Stratmann RE, Yazyev O, Austin AJ, Cammi R, Pomelli C, Ochterski JW, Ayala PY, Morokuma K, Voth GA, Salvador P, Dannenberg JJ, Zakrzewski VG, Dapprich S, Daniels AD, Strain MC, Farkas O, Malick DK, Rabuck AD, Raghavachari K, Foresman JB, Ortiz JV, Cui Q, Baboul AG, Clifford S, Cioslowski J, Stefanov BB, Liu G, Liashenko A, Piskorz P, Komaromi I, Martin RL, Fox DJ, Keith T, Al-Laham MA, Peng CY, Nanayakkara A, Challacombe M, Gill PMW, Johnson B, Chen W, Wong MW, Gonzalez C, Pople JA (2003) Gaussian-03. Gaussian, Inc., Wallingford, CT

106. Amos RD. CADPAC 5.0 Cambridge University, Cambridge, UK

107. Helgaker T, Rauud K. Dalton program

108. Stephens PJ, Devlin FJ, Chabalowski CF, Frisch MJ (1994) *Ab Initio* Calculation of Vibrational Absorption and Circular Dichroism Spectra Using Density Functional Force Fields. J Phys Chem 98:11623

109. Stephens PJ, Ashvar CS, Devlin FJ, Cheeseman JR, Frisch MJ (1996) *Ab Initio* Calculation of Atomic Axial Tensors and Vibrational Rotational Strengths Using Density Functional Theory. Mol Phys 89:579

110. Muñoz MA, Areche C, San-Martín A, Rovirosa J, Joseph-Nathan P (2009) VCD Determination of the Absolute Configuration of Stypotriol. Nat Prod Commun 4:1037

111. Devlin FJ, Stephens PJ, Besse P (2005) Conformational Rigidification *via* Derivatization Facilitates the Determination of Absolute Configuration Using Chiroptical Spectroscopy: A Case Study of the Chiral Alcohol *endo*-Borneol. J Org Chem 70:2980

112. Burgueño-Tapia E, Joseph-Nathan P (2008) Absolute Configuration of Eremophilanoids by Vibrational Circular Dichroism. Phytochemistry 69:2251

113. Losada M, Tan H, Xu Y (2008) Lactic Acid in Solution: Investigations of Lactic Acid Self-Aggregation and Hydrogen Bonding Interactions with Water and Methanol using Vibrational Absorption and Vibrational Circular Dichroism Spectroscopies. J Chem Phys 128:14508

114. He J, Wang F, Polavarapu PL (2005) Absolute Configurations of Chiral Herbicides Determined from Vibrational Circular Dichroism. Chirality 17:S1

115. He J, Polavarapu PL (2005) Determination of the Absolute Configuration of Chiral α-Aryloxypropanoic Acids using Vibrational Circular Dichroism Studies: 2-(2-Chlorophenoxy)propanoic Acid and 2-(3-Chlorophenoxy)propanoic Acid. Spectrochim Acta A 61A:1327

116. Cichewicz RH, Clifford LJ, Lassen PR, Cao X, Freedman TB, Nafie LA, Deschamps JD, Kenyon VA, Flanary JR, Holman TR, Crews P (2005) Stereochemical Determination and Bioactivity Assessment of (*S*)-(+)-Curcuphenol Dimers Isolated from the Marine Sponge *Didiscus aceratus* and Synthesized Through Laccase Biocatalysis. Bioorg Med Chem 13:5600

117. Eschrig H. The Fundamentals of Density Functional Theory (Revised and Extended Version) http://www.ifw-dresden.de/institutes/itf/members/helmut/dft.pdf

118. Becke AD (1993) Density-Functional Thermochemistry. III. The Role of Exact Exchange. J Chem Phys 98:5648

119. Petrovic AG, Polavarapu PL (2007) Chiroptical Spectroscopic Determination of Molecular Structures of Chiral Sulfinamides: *t*-Butanesulfinamide. J Phys Chem A 111:10938

120. Stephens PJ, Devlin FJ, Ashvar CS, Chabalowski CF, Frisch MJ (1994) Theoretical Calculation of Vibrational Circular Dichroism Spectra. Faraday Discuss 99:103

121. Perdew JP, Burke K, Wang Y (1996) Generalized Gradient Approximation for the Exchange-Correlation Hole of a Many-Electron System. Phys Rev B 54:16533

122. Engel E, Vosko SH (1993) Exact Exchange-only Potentials and the Relation as Microscopic Criteria for Generalized Gradient Approximations. Phys Rev B 47:13164
123. Becke AD (1993) A New Mixing of *Hartree-Fock* and Local Density-Functional Theories. J. Chem Phys 98:1372
124. Cerda-García-Rojas CM, Catalán CAN, Muro AC, Joseph-Nathan P (2008) Vibrational Circular Dichroism of Africanane and Lippifoliane Sesquiterpenes. J Nat Prod 71:967
125. Stephens PJ, Pan JJ, Devlin FJ, Krohn K, Kurtán T (2007) Determination of the Absolute Configurations of Natural Products *via* Density Functional Theory Calculations of Vibrational Circular Dichroism, Electronic Circular Dichroism, and Optical Rotation: The Iridoids Plumericin and Isoplumericin. J Org Chem 72:3521
126. Kuppens T, Vandyck K, van der Eycken J, Herrebout W, van der Veken B, Bultinck P (2007) A DFT Conformational Analysis and VCD Study on Methyl-tetrahydrofuran-2-carboxylate. Spectrochim Acta Part A 67:402
127. Sosa C, Andzelm J, Elkin BC, Wimmer E, Dobbs KD, Dixon DA (1992) A Local Density Functional Study of the Structure and Vibrational Frequencies of Molecular Transition-Metal Compounds. J Phys Chem 96:6630
128. Burgueño-Tapia E, Zepeda LG, Joseph-Nathan P (2010) Absolute Configuration of (–)-Myrtenal by Vibrational Circular Dichroism. Phytochemistry 71:1158
129. Debie E, Bultinck P, Nafie LA, Dukor R (2010) CompareVOA, BioTools, Inc., Jupiter, Florida, USA
130. Debie E, De Gussem E, Dukor RK, Herrebout W, Nafie LA, Bultinck P (2011) A Confidence Level Algorithm for the Determination of Absolute Configuration using Vibrational Circular Dichroism or Raman Optical Activity. Chem Phys Chem, Special Issue: *Jacobus van't Hoff* 12:1542
131. Shen J, Zhu C, Reiling S, Vaz R (2010) A Novel Computational Method for Comparing Vibrational Circular Dichroism Spectra. Spectrochim Acta Part A 76:418
132. Covington CL, Polavarapu PL (2013) Similarity in Dissymmetry Factor Spectra: A Quantitative Measure of Comparison between Experimental and Predicted Vibrational Circular Dichroism. J Phys Chem A 117:3377
133. Zepeda LG, Burgueño-Tapia E, Joseph-Nathan P (2011) Myrtenal, a Controversial Molecule for the Proper Application of the CIP Sequence Rule for Multiple Bonds. Nat Prod 6:429
134. He J, Petrovic AG, Polavarapu PL (2004) Determining the Conformer Populations of (*R*)-(+)-3-Methylcyclopentanone using Vibrational Absorption, Vibrational Circular Dichroism, and Specific Rotation. J Phys Chem B 108:20451
135. Brotin T, Cavagnat D, Dutasta JP, Buffeteau T (2006) Vibrational Circular Dichroism Study of Optically Pure Cryptophane-A. J Am Chem Soc 128:5533
136. Nicu VP, Debie E, Herrebout W, van der Veken B, Bultinck P, Baerends EJ (2010) A VCD Robust Mode Analysis of Induced Chirality: The Case of Pulegone in Chloroform. Chirality 21:E287
137. Debie E, Bultinck P, Herrebout, W, van der Veken B. (2008) Solvent Effects on IR and VCD Spectra of Natural Products: An Experimental and Theoretical VCD Study of Pulegone. Phys Chem Chem Phys 10:3498
138. Losada M, Xu Y (2007) Chirality Transfer through Hydrogen-Bonding: Experimental and *ab Initio* Analyses of Vibrational Circular Dichroism Spectra of Methyl Lactate in Water. Phys Chem Chem Phys 9:3127
139. Mazaleyrat JP, Wright K, Gaucher A, Toulemonde N, Wakselman M, Oancea S, Peggion C, Formaggio F, Setnicka V, Keiderling TA, Toniolo C (2004) Induced Axial Chirality in the Biphenyl Core of the C_α-Tetrasubstituted α-Amino Acid Residue Bip and Subsequent Propagation of Chirality in $(Bip)_n$/Val Oligopeptides J Am Chem Soc 126:12874
140. Jalkanen KJ, Degtyarenko IM, Nieminen RM, Cao X, Nafie LA, Zhu F, Barron LD (2008) Role of Hydration in Determining the Structure and Vibrational Spectra of L-Alanine and

N-Acetyl L-Alanine *N′*-Methylamide in Aqueous Solution: a Combined Theoretical and Experimental Approach. Theor Chem Acc 119:191
141. Mennucci B, Tomasi J, Cammi R, Cheeseman JR, Frisch MJ, Devlin FJ, Gabriel S, Stephens PJ (2002) Polarizable Continuum Model (PCM) Calculations of Solvent Effects on Optical Rotations of Chiral Molecules. J Phys Chem A 106:6102
142. Tomasi J, Mennucci B, Cammi R (2005) Quantum Mechanical Continuum Solvation Models. Chem Rev 105:2999
143. Scalmani G, Frisch M. J (2010) Continuous Surface Charge Polarizable Continuum Models of Solvation. I. General Formalism. J Chem Phys 132:114110
144. Kawiecki RW, Devlin FJ, Stephens PJ, Amos RD (1991) Vibrational Circular Dichroism of Propylene Oxide. J Phys Chem 95:9817
145. Kollman PA, Massova I, Reyes C, Kuhn B, Huo S, Chong L, Lee M, Lee T, Duan Y, Wang W, Donini O, Cieplak P, Srinivasan J, Case DA, Cheatham III TE (2000) Calculating Structures and Free Energies of Complex Molecules: Combining Molecular Mechanics and Continuum Models. Acc Chem Res 33:889
146. Ashvar CS, Stephens PJ, Eggimann T, Wieser H (1998) Vibrational Circular Dichroism Spectroscopy of Chiral Pheromones: Frontalin (1,5-Dimethyl-6,8-dioxabicyclo[3.2.1] octane). Tetrahedron Asymm 9:1107
147. Nafie LA (2011) Vibrational Optical Activity. Principles and Applications. Wiley, Chichester, United Kingdom
148. Bellamy LJ (1958) The Infra-Red Spectra of Complex Molecules, 2nd Ed. Wiley, New York, Chapter 2
149. Cerda-García-Rojas CM, Burgueño-Tapia E, Román-Marín LU, Hernández-Hernández JD, Agulló-Ortuño T, González-Coloma A, Joseph-Nathan P (2010) Antifeedant and Cytotoxic Activity of Longipinane Derivatives. Planta Med 76:297
150. Joseph-Nathan P, Cerda-García-Rojas CM, del Río RE, Román-Marín LU, Hernández JD (1986) Conformation and Absolute Configuration of Naturally Occurring Longipinene Derivatives. J Nat Prod 49:1053
151. Christmann M (2010) *Otto Wallach*: Founder of Terpene Chemistry and Nobel Laureate 1910. Angew Chem Int Ed 49:9580
152. Berova N (1997) *Koji Nakanishi′*s Enchanting Journey in the World of Chirality. Chirality 9:395
153. Bożena F, Olejniczak T, Latajka R, Białońska A, Ciunik Z, Lochyński S. (2005) Stereochemistry of Terpene Derivatives. Part 4: Fragant Terpenoid Derivatives with an Unsaturated *gem*-Dimethylbicyclo[3.1.0]hexane System. Tetrahedron Asymm 16:3352
154. Bringmann G, Gulder TAM, Matthias R, Gulder T (2008) The Online Assignment of the Absolute Configuration of Natural Products: HPLC-CD in Combination with Quantum Chemical CD Calculations. Chirality 20:628
155. Allenmark S (2000) Chiroptical Methods in the Stereochemical Analysis of Natural Products. Nat Prod Rep 17:145
156. Pescitelli G, Kurtán T, Flörke U, Krohn K (2009) Absolute Structural Elucidation of Natural Products. A Focus on Quantum-Mechanical Calculations of Solid-State CD Spectra. Chirality 21:E181
157. Polavarapu PL (2012) Determination of the Structures of Chiral Natural Products Using Vibrational Circular Dichroism. In: Berova N, Polavarapu PL, Nakanishi K, Woody RW (eds) Comprehensive Chiroptical Spectroscopy, Vol 2: Stereochemical Analysis of Synthetic Compounds, Natural Products, and Biomolecules. Wiley, New York, Chapter 11, p 387
158. Allenmark S, Gawronski J. (2008) Determination of Absolute Configuration. An Overview Related to this Special Issue. Chirality 20:606
159. Holzwarth G. Chabay I (1972) Optical Activity of Vibrational Transitions: A Coupled Oscillator Model J Chem Phys 57:1632
160. Bouř P, Keiderling TA (1992) Computational Evaluation of the Coupled Oscillator Model in the Vibrational Circular Dichroism of Selected Small Molecules. J Am Chem Soc 114:9100

161. Henry BR (1987) The Local Mode Model and Overtone Spectra: A Probe of Molecular Structure and Conformation. Acc Chem Res 20:429
162. Findsen LA, Fang HL, Swofford RL, Birge RR (1986) Theoretical Description of the Overtone Spectra of Acetaldehyde using the Local Mode Approach. J Chem Phys 84:16
163. McKean DC (1978) Individual CH Bond Strengths in Simple Organic Compounds: Effects on Conformation and Substitution. Chem Soc Rev 7:399
164. Bellamy LJ, Mayo DW (1976) Infrared Frequency Effects of Lone Pair Interactions with Antibonding Orbitals on Adjacent Atoms. J Phys Chem 80:1217
165. Izumi H, Futamura S, Nafie LA, Dukor RK (2003) Determination of Molecular Stereochemistry Using Vibrational Circular Dichroism Spectroscopy: Absolute Configuration and Solution Conformation of 5-Formyl-*cis,cis*-1,3,5-trimethyl-3-hydroxymethylcyclohexane-1-carboxylic Acid Lactone. Chem Record 3:112
166. Narayanan U, Keiderling TA (1983) Coupled Oscillator Interpretation of the Vibrational Circular Dichroism of Several Dicarbonyl-Containing Steroids. J Am Chem Soc 105:6406
167. Keiderling TA, Stephens PJ (1977) Vibrational Circular Dichroism of Dimethyl Tartrate. A Coupled Oscillator. J Am Chem Soc 99:8061
168. Gangemi F, Gangemi R, Longhi G, Abbate S (2009) Calculations of Overtone NIR and NIR-VCD Spectra in the Local Mode Approximation: Camphor and Camphorquinone. Vib Spect 50:257
169. Abbate S, Longhi G, Santina C (2000) Theoretical and Experimental Studies for the Interpretation of Vibrational Circular Dichroism Spectra in the CH-Stretching Overtone Region. Chirality 12:180
170. Gangemi R, Longhi G. Abbate S (2005) Calculated Absorption and Vibrational Circular Dichroism Spectra of Fundamental and Overtone Transitions for a Chiral HCCH Molecular Fragment in the Hypothesis of Couple Dipoles. Chirality 17:530
171. Ringer AL, Magers DH (2007) Conventional Strain Energy in Dimethyl-Substituted Cyclobutane and the *gem*-Dimethyl Effect. J Org Chem 72:2533
172. Rezanka P, Fahnrich J (2003) Isolation of Terpenes from Norway Spruce Needles by Distillation. Chemike Lysty 97:119
173. Terpenes: Importance, General Structure, and Biosynthesis. http://www.wiley-vch.de/books/sample/3527317864_c01.pdf
174. Taniguchi T, Monde K (2012) Exciton Chirality Method in Vibrational Circular Dichroism. J Am Chem Soc 134:3695
175. Singh RD, Keiderling TA (1981) Vibrational Circular Dichroism of Six-Membered-Ring Monoterpenes. Consistent Force Field, Fixed Partial Charge Calculations. J Am Chem Soc 103:2387
176. Devlin FJ, Stephens PJ, Cheeseman JR Frisch MJ (1997) *Ab Initio* Prediction of Vibrational Absorption and Circular Dichroism Spectra of Chiral Natural Products Using Density Functional Theory: α-Pinene. J Phys Chem A 101:9912
177. Freedman TB, Kallmerten J, Lipp ED, Young DA, Nafie LA (1988) Vibrational Circular Dichroism in the CH Stretching Region of (+)-(3*R*)-Methylcyclohexanone and Chiral Deuteriated Isotopomers. J Am Chem Soc 110:689
178. Freedman TB, Balukjian GA, Nafie LA (1985) Enhanced Vibrational Circular Dichroism *via* Vibrationally Generated Electronic Ring Currents. J Am Chem Soc 107:6213
179. Laux L, Pultz V, Abbate S, Havel HA, Overend J, Moscowitz A, Lightner DA (1982) Inherently Dissymmetric Chromophores and Vibrational Circular Dichroism. The CH_2-CH_2-C*H Fragment. J Am Chem Soc 104:4276
180. Abbate S, Longhi G, Ricard L, Bertucci C, Rosini C, Salvadori P, Moscowitz A (1989) Vibrational Circular Dichroism as a Criterion for Local-Mode versus Normal-Mode Behavior. Near-Infrared Circular Dichroism Spectra of Some Monoterpenes. J Am Chem Soc 111:836
181. Guo C, Shah RD, Dukor RK, Freedman, TB, Cao X, Nafie LA (2006) Fourier Transform Vibrational Circular Dichroism from 800 to 10,000 cm^{-1}: Near IR-VCD Spectral Standards for Terpenes and Related Molecules. Vib Spect 42:254

182. Partal-Ureña F, Avilés-Moreno, R, López-González JJ (2010) Rotational Strength Sign and Normal Modes Description: A Theoretical and Experimental Comparative Study in Bicyclic Terpenes. Chirality 22:E123
183. McCann JL, Rauk A, Wieser H (1998) A Conformational Study of (1*S*,2*R*,5*S*)-(+)-Menthol using Vibrational Circular Dichroism Spectroscopy. Can J Chem 76:274
184. Buffeteau T, Ducasse L, Brizard A, Huc I, Oda R (2004) Density Functional Theory Calculations of Vibrational Absorption and Circular Dichroism Spectra of Dimethyl-L-tartrate. J Phys Chem A 108:4080
185. Bouř P, Navrátilová H, Setnička V, Urbanová M, Volka K (2002) (3*R*,4*S*)-4-(4-Fluorophenyl)-3-hydoxymethyl-1-methylpiperidine: Conformation and Structure Monitoring by Vibrational Circular Dichroism. J Org Chem 67:161
186. Avilés-Moreno JR Partal-Ureña F, López-González JJ (2009) Conformational Preference of a Chiral Terpene. Vibrational Circular Dichroism (VCD), Infrared and Raman Study of *S*-(–)-Limonene Oxide. Phys Chem Chem Phys 11:2459
187. Partal-Ureña F, Avilés-Moreno JR, López-González JJ. (2008) Conformational Flexibility in Terpenes: Vibrational Circular Dichroism (VCD), Infrared and Raman Study of *S*-(–)-Perillaldehyde. J Phys Chem A 112:7887
188. Morita HE, Kodama TS, Takanata T (2006) Chirality of Camphor Derivatives by Density Functional Theory. Chirality 18:783
189. Shin S, Hirakawa AY, Hamada Y (2002) Vibrational Circular Dichroism Spectra of 1-Amino-2-propanol. Enantiomer 7:191
190. Bürgi T, Vargas A, Baiker A (2002) VCD Spectroscopy of Chiral Cinchona Modifiers used in Heterogeneous Enantioselective Hydrogenation: Conformation and Binding of Non-Chiral Acids. J Chem Soc Perkin Trans 2:1596
191. Sadlej J, Dobrowolski J Cz., Rode JE (2010) VCD Spectroscopy as a Novel Probe for Chirality Transfer in Molecular Interactions. Chem Soc Rev 39:1478
192. Rode JE, Jamróz MH, Dobrowolski JC, Sadlej J (2012) On Vibrational Circular Dichroism Chirality Transfer in Electron Donor-Acceptor Complexes: A Prediction for the Quinine $\cdots BF_3$ System. J Phys Chem A 116:7916
193. Debie E, Jaspers L, Bultinck P, Herrebout W, Van der Veken B (2008) Induced Solvent Chirality: a VCD Study of Camphor in $CDCl_3$. Chem Phys Lett 450:426
194. Avilés-Moreno JR, Ureña-Horno, E, Partal-Ureña F, López-González JJ (2011) IR-*Raman*-VCD Study of (*R*)-(+)-Pulegone: Influence of the Solvent. Spectrochim Acta A79:767
195. Nicu VP, Baerends EJ (2009) Robust Normal Modes in Vibrational Circular Dichroism Spectra. Phys Chem Chem Phys 11:6107
196. Nicu VP, Neugebauer J, Baerends EJ (2008) Effects of Complex Formation on Vibrational Circular Dichroism Spectra. J Phys Chem A 112:6978
197. Góbi S, Magyarfalvi G (2011) Reliability of Computed Signs and Intensities for Vibrational Circular Dichroism Spectra. Phys Chem Chem Phys 13:16130
198. De Gussem E, Bultinck P, Feledziak M, Marchand-Brynaert J, Stevens C, Herrebout W (2012) Vibrational Circular Dichroism versus Optical Rotation Dispersion and Electronic Circular Dichroism for Diastereomers: The Stereochemistry of 3-(1′-Hydroxyethyl)-1-(3′-phenylpropanoyl)-azetidin-2-one. Phys Chem Chem Phys 14:8562
199. Gordillo-Román B, Camacho-Ruiz J, Bucio MA, Joseph-Nathan P (2012) Chiral Recognition of Diastereomeric 6-Cedrols by Vibrational Circular Dichroism. Chirality 24:147
200. Yang G, Li J, Liu Y, Lowary TL, Xu Y (2010) Determination of the Absolute Configurations of Bicyclo[3.1.0]hexane Derivatives *via* Electronic Circular Dichroism, Optical Rotation Dispersion and Vibrational Circular Dichroism Spectroscopy and Density Functional Theory Calculations. Org Biomol Chem 8:3777
201. Qu ZW, Zhu H, May V (2010) Unambiguous Assignment of Vibrational Spectra of Cyclosporins A and H. J Phys Chem A 114:9768
202. Brauner JW, Flach CR, Mendelsohn R (2005) A Quantitative Reconstruction of the Amide I Contour in the IR Spectra of Globular Proteins: From Structure to Spectrum. J Am Chem Soc 127:100

203. Vogt FG, Spoors GP, Su Q, Andemichael YW, Wang H, Potter TC, Minick DJ (2006) A Spectroscopic and Computational Study of Stereochemistry in 2-Hydroxymutilin. J Mol Struct 797:5
204. Su CN, Keiderling TA (1980) Conformation of Dimethyl Tartrate in Solution. Vibrational Circular Dichroism Results. J Am Chem Soc 102:511
205. Polavarapu P L, Ewig CS, Chandramouly T (1987) Conformations of Tartaric Acid and Its Esters. J Am Chem Soc 109:7382
206. Freedman TB, Cao X, Luz Z, Zimmermann H, Poupko R, Nafie LA (2008) Isotopic Difference Spectra as an Aide in Determining Absolute Configuration Using Vibrational Optical Activity: Vibrational Circular Dichroism of ^{13}C- and ^{2}H-Labelled Nonamethoxy Cyclotriveratrylene. Chirality 20:673
207. Stephens PJ, Devlin FJ, Pan JJ (2008) The Determination of the Absolute Configurations of Chiral Molecules Using Vibrational Circular Dichroism (VCD) Spectroscopy. Chirality 20:643
208. Setnička V, Urbanová M, Bouř P, Král V, Volka K (2001) Vibrational Circular Dichroism of 1,1′-Binaphthyl Derivatives: Experimental and Theoretical Study. J Phys Chem A 105:8931
209. Freedman TB, Cao X, Oliveira RV, Cass QB Nafie LA (2003) Determination of the Absolute Configuration and Solution Conformation of Gossypol by Vibrational Circular Dichroism. Chirality 15:196
210. Nafie LA, Freedman TB (1986) Ring Current Mechanism of Vibrational Circular Dichroism. J Phys Chem 90:763
211. Freedman TB, Gao X, Shih ML, Nafie LA (1998) Electron Transition Current Density in Molecules. 2. *Ab Initio* Calculations for Electronic Transitions in Ethylene and Formaldehyde. J Phys Chem A 102:3352
212. Gigante DMP, Long F, Bodack LA, Evans JM, Kallmerten J, Nafie LA, Freedman TB (1999) Hydrogen Stretching Vibrational Circular Dichroism in Methyl Lactate and Related Molecules. J Phys Chem A 103:1523
213. Izumi H, Ogata A, Nafie LA, Dukor RK (2008) Vibrational Circular Dichroism Analysis Reveals a Conformational Change of the Baccatin III Ring of Paclitaxel: Visualization of Conformations Using a New Code for Structure-Activity Relationships. J Org Chem 73:2367
214. Sato T, Yoshida S, Hoshino H, Tanno M, Nakajima M, Hoshino T (2011) Sesquarterpenes (C_{35} Terpenes) Biosynthesized *via* the Cyclization of a Linear C_{35} Isoprenoid by a Tetraprenyl-β-curcumene Synthase and a Tetraprenyl-β-curcumene Cyclase: Identification of a New Terpene Cyclase. J Am Chem Soc 133:9734
215. He Y, Wang B, Dukor RK, Nafie LA (2011) Determination of Absolute Configuration of Chiral Molecules Using Vibrational Optical Activity: A Review. Appl. Spect 65:699
216. Partal-Ureña F, Avilés-Moreno JR, López-González JJ (2012) Characterization of H-Bonding Networks in Chiral Alcohols Using Infrared, Raman and Vibrational Circular Dichroism Spectroscopies, and Density Functional Calculations: (*S*)-(–)-Perillyl Alcohol. Tetrahedron Asymm 23:515
217. Avilés-Moreno JR, Partal-Ureña F, López-González JJ (2013) Hydrogen Bonding Network in a Chiral Alcohol: (1*R*,2*S*,5*R*)-(–)-Menthol. Conformational Preference Studied by IR-Raman-VCD Spectroscopies and Quantum Chemical Calculations. Struct Chem 24:671
218. Loandos M del H, Villecco MB, Burgueño-Tapia E, Joseph-Nathan P, Catalán CAN (2009) Preparation and Absolute Configuration of (1*R*,4*R*)-(+)-3-Oxo-, (1*S*,4*S*)-(–)-3-Oxo- and (1*R*,3*S*,4*R*)-(+)-3-Acetyloxy-5-oxo-1,8-Cineole. J Nat Prod 4:1537
219. Batista JM Jr., Batista ANL, Mota JS, Cass QB, Kato MJ, Bolzani VS, Freedman TB, López SN, Furlan M, Nafie LA (2011) Structure Elucidation and Absolute Stereochemistry of Isomeric Monoterpene Chromane Esters. J Org Chem 76:2603
220. Batista Jr JM, Batista ANL, Kato MJ, Bolzani VS, López SN, Nafie LA, Furlan M (2012) Further Monoterpene Chromane Esters from *Peperomia obtusifolia*: VCD Determination of the Absolute Configuration of a New Diastereomeric Mixture. Tetrahedron Lett 53:6051
221. Avilés-Moreno JR, Partal-Ureña F, López-González JJ (2011) Chiral Terpenes in Different Phases: *R*-(2)-Camphorquinone Studied by IR–*Raman*–VCD Spectroscopies and Theoretical Calculations. Struct Chem 22:67

222. Shen J, Li Y, Vaz R, Izumi H (2012) Revisiting Vibrational Circular Dichroism Spectra of (*S*)-(+)-Carvone and (1*S*,2*R*,5*S*)-(+)-Menthol Using SimIR/VCD Method. J Chem Theory Comput 8:2762

223. Lucotti A, Tommasini M, Fazzi D, Del Zoppo M, Chalifoux, WA, Ferguson MJ, Zerbi G, Tykwinski RR (2009) Evidence for Solution-state Nonlinearity of sp-Carbon Chains Based on IR and *Raman* Spectroscopy. J Am Chem Soc 131:4239

224. Wu T, You X (2012) Exciton Coupling Analysis and Enolization Monitoring by Vibrational Circular Dichroism Spectra of Camphor Diketones. J Phys Chem A 116:8959

225. Merten C, Jalkanen KJ, Weiss VC, Hartwig A (2010) Vibrational Circular Dichroism of 3-(Trifluoroacetyl)-Camphor and its Interaction with Chiral Amines. Chirality 22:772

226. Mori K, Tashiro T, Yoshimura T, Takita M, Tabata J, Hiradate S, Sugie, H (2008) Determination of the Absolute Configuration of the Male Aggregation Pheromone, 2-Methyl-6-(4′-methylenebicyclo[3.1.0]hexyl)hept-2-en-1-ol, of the Stink Bug *Erysarcoris lewisi* (Distant) as 2*Z*,6*R*,1′*S*,5′*S* by its Synthesis. Tetrahedron Lett 49:354

227. Figadère B, Devlin FJ, Millara JG, Stephens PJ (2008) Determination of the Absolute Configuration of the Sex Pheromone of the Obscure Mealybug by Vibrational Circular Dichroism Analysis. Chem Commun:1106

228. Capon RJ (2001) Marine Bioprospecting - Trawling for Treasure and Pleasure. Eur J Org Chem 2001:633

229. Pérez C, Becerra J, Manríquez-Navarro P, Aguayo LG, Fuentealba J, Guzmán JL Joseph-Nathan P, Jiménez V, Muñoz MA, Silva M (2011) Inhibitory Activities on Mammalian Central Nervous System Receptors and Computational Studies of Three Sesquiterpene Lactones from *Coriaria ruscifolia* subsp. *ruscifolia*. Chem Pharm Bull 59:161

230. Río de la Loza L (1852) Discurso Pronunciado por el Catedrático de Química Médica de la Escuela de Medicina (November 23, 1852). In: Noriega JM (compiler). Escritos de Leopoldo Río de la Loza, Imprenta de Ignacio Escalante: México City 1911:94

231. Burgueño-Tapia E, Joseph-Nathan P (2012) Conformational Analysis of Perezone and Dihydroperezone using Vibrational Circular Dichroism. Phytochemistry 74:190

232. Zepeda LG, Burgueño-Tapia E, Pérez-Hernández N, Cuevas G, Joseph-Nathan P (2013) NMR-Based Conformational Analysis of Perezone and Analogues. Magn Reson Chem 51:245

233. Partal-Ureña F, Avilés-Moreno JR, López-González JJ (2009) Conformational Study of (*R*)-(+)-Limonene in the Liquid Phase Using Vibrational Spectroscopy (IR, *Raman*, and VCD) and DFT Calculations. Tetrahedron Asymm 20:89

234. Mukhopadhyay P, Wipf P, Beratan DN (2009) Optical Signatures of Molecular Dissymmetry: Combining Theory with Experiments to Address Stereochemical Puzzles. Acc Chem Res 42:809

235. Mori T, Izumi H, Inoue Y (2004) Chiroptical Properties of Organic Radical Cations. The Electronic and Vibrational Circular Dichroism Spectra of α-Tocopherol Derivatives and Sterically Hindered Chiral Hydroquinone Ethers. J Phys Chem A 108:9540

236. Yam-Puc A, Escalante-Erosa F, Pech-López M, Chan-Bacab MJ, Arunachalampillai A, Wend OF, Sterner O, Peña-Rodríguez LM (2009) Trinorsesquiterpenoids from the Root Extract of *Pentalinon andrieuxii*. J Nat Prod 72:745

237. Burgueño-Tapia E, Yam-Puc JA, Peña-Rodríguez LM, Joseph-Nathan P. Absolute Configuration of Urechitol A. Unpublished results

238. Joseph-Nathan P, Leitão SG, Pinto SC, Leitão GG, Bizzo HR, Costa FLP, de Amorim MB, Martinez N, Dellacassa E, Hernández-Barragán A, Pérez-Hernández N (2010) Structure Reassignment and Absolute Configuration of 9-*epi*-Presilphiperfolan-1-ol. Tetrahedron Lett 51:1963

239. Debie E, Kuppens T, Vandyck K, Van der Eycken J, Van Der Veken B, Herrebout W, Bultinck P (2006) Vibrational Circular Dichroism DFT Study on Bicyclo[3.3.0]octane Derivatives. Tetrahedron Asymm 17:3203

240. Joseph-Nathan P, Reyes-Trejo B, Morales-Rios MS (2006) Molecular Rearrangements of (–)-Modhephene and (–)-Isocomene to a (–)-Triquinane. J Org Chem 71:4411

241. Monde K, Taniguchi T, Miura N, Vairappan CS, Suzuki M (2006) Absolute Configurations of Brominated Sesquiterpenes Determined by Vibrational Circular Dichroism. Chirality 18:335
242. Muñoz MA, Chamy C, Carrasco A, Rovirosa J, San Martin A, Joseph-Nathan P (2009) Diastereomeric Assignment in a Pacifenol Derivative using Vibrational Circular Dichroism. Chirality 21:E208
243. Darias J, San-Martin A, Rovirosa J (1990) Neighbouring Group Participation in the Biosynthesis of the Vinyl Bromide Moiety of Chamigrene Metabolites. Chem Lett 19:259
244. Krautmann M, de Riscala EC, Burgueño-Tapia E, Mora-Pérez Y, Catalán CAN, Joseph-Nathan P (2007) C-15-Functionalized Eudesmanolides from *Mikania campanulata*. J Nat Prod 70:1173
245. Burgueño-Tapia E, Hernández-Carlos B, Joseph-Nathan P (2006) DFT, Solution, and Crystal Conformation of Eremophilanolides. J Mol Struct 825:115
246. Rojas-Pérez RE, Cedillo-Portugal E, Joseph-Nathan P, Burgueño-Tapia E (2009) A New Longipinene Diester from *Stevia monardifolia* Kunth. Nat Prod Commun 4:757
247. Michalski O, Kisiel W, Michalska K, Setnicka V, Urbanova M (2007) Absolute Configuration and Conformational Analysis of Sesquiterpene Lactone Glycoside Studied by Vibrational Circular Dichroism Spectroscopy. J Mol Struct 871:67
248. Bercion S, Buffeteau T, Lespade L, Couppe de K. Martin M-A (2006) IR, VCD, ^{1}H and ^{13}C NMR Experimental and Theoretical Studies of a Natural Guaianolide: Unambiguous Determination of its Absolute Configuration. J Mol Struct 791:186
249. Monde K, Taniguchi T, Miura N, Vairappan CS, Suzuki M (2006) Absolute Configurations of Endoperoxides Determined by Vibrational Circular Dichroism (VCD). Tetrahedron Lett 47:4389
250. Valdez-Calderón A, Torres-Valencia JM, Manríquez-Torres JJ, Velázquez-Jiménez R, Román-Marín LU, Hernández-Hernández JD, Cerda-García-Rojas CM, Joseph-Nathan P (2013) An Unusual Diepoxyguaianolide from *Stevia tomentosa*. Tetrahedron Lett 54:3286
251. Flack HD, Bernardinelli G (2008) The Use of X-Ray Crystallography to Determine Absolute Configuration. Chirality 20:681
252. Hooft RWW, Straver LH, Spek AL (2008) Determination of Absolute Structure Using Bayesian Statistics on *Bijvoet* Differences. J Appl Cryst 41:96
253. Gherase D, Naubron J-V, Roussel C, Giorgi M (2012) XRD and VCD: A Marriage of Love or Convenience? Honeymoon around a Cyclic Urea Derivative. Acta Cryst C68:247
254. Gordillo-Román B, Camacho-Ruiz J, Bucio MA, Joseph-Nathan P. (2013) Vibrational Circular Dichroism Discrimination of Diastereomeric Cedranol Acetates. Chirality 25:939
255. Loayza I, Burgueño-Tapia E, Dellacassa E, Joseph-Nathan P (2013) An Endoperoxiditerpene From *Calceolaria buchtieniana* Kranzi. Unpublished results
256. Jalkanen KJ, Gale JD, Lassen PR, Hemmingsen L, Rodarte A, Degtyarenko IM, Nieminen RM, Brøgger CS, Knapp-Mohammady M, Suhai S (2008) A Configurational and Conformational Study of Aframodial and its Diastereomers *via* Experimental and Theoretical VA and VCD Spectroscopies. Theor Chem Acc 119:177
257. Aoyagi Y, Yamazaki A, Nakatsugawa C, Fukaya H Takeya K, Kawauchi S, Izumi H (2008) Salvileucalin B, A Novel Diterpenoid with an Unprecedented Rearranged Neoclerodane Skeleton from *Salvia leucantha* Cav. Org Lett 10:4429
258. Nakahashi A, Taniguchi T, Miura N, Monde K (2007) Stereochemical Studies of Sialic Acid Derivatives by Vibrational Circular Dichroism. Org Lett 9:4741
259. Areche C, San-Martín A, Rovirosa J, Muñoz MA, Hernández-Barragán A, Bucio MA, Joseph-Nathan P (2010) Stereostructure Reassignment and Absolute Configuration of Isoepitaondiol, a Meroditerpenoid from *Stypopodium flabelliforme*. J Nat Prod 73:79
260. Muñoz MA, Areche C, Rovirosa J, San Martín A, Gordillo-Román B, Joseph-Nathan P (2012) Absolute Configuration of the Meroditerpenoids Taondiol and Epitaondiol Diacetates by Vibrational Circular Dichroism. Heterocycles 85:1961
261. González AG, Darías J, Martín JD (1971) Taondiol, A New Component from *Taonia atomaria*. Tetrahedron Lett 12:2729

262. Sánchez-Ferrando F, San-Martín A (1995) Epitaondiol: The First Polycyclic Meroditerpenoid Containing Two Fused Six-Membered Rings Forced into the Twist-Boat Conformation. J Org Chem 60:1475
263. Penicooke N, Walford K, Badal S, Delgoda R, Williams LAD, Joseph-Nathan P, Gordillo-Román B, Gallimore W (2013) Antiproliferative Activity and Absolute Configuration of Zonaquinone Acetate from Jamaican Alga *Stypopodium zonale*. Phytochemistry 87:96
264. Heshmat M, Nicu VP, Baerends EJ (2012) On the Equivalence of Conformational and Enantiomeric Changes of Atomic Configuration for Vibrational Circular Dichroism Signs. J Phys Chem A 116:3454
265. Molina-Salinas GM, Rivas-Galindo VM, Said-Fernández S, Lankin DC, Muñoz MA, Joseph-Nathan P, Pauli GF, Waksman N (2011) Stereochemical Analysis of Leubethanol, an Anti-TB Active Serrulatane, from *Leucophyllum frutescens*. J Nat Prod 74:1842
266. Gómez-Hurtado MA, Torres-Valencia JM, Manríquez-Torres J, del Río RE, Motilva V, García-Mauriño S, Ávila J, Talero E, Cerda-García-Rojas CM, Joseph-Nathan P (2011) Absolute Configuration of Labdanes and *ent*-Clerodanes from *Chromolaena pulchella* by Vibrational Circular Dichroism. Phytochemistry 72:409
267. Muñoz MA, Urzúa A, Echeverría J, Bucio MA, Hernández-Barragán A, Joseph-Nathan P (2012) Determination of Absolute Configuration of Salvic Acid, an *ent*-Labdane from *Eupatorium salvia*, by Vibrational Circular Dichroism. Phytochemistry 80:109
268. Muñoz MA, Perez-Hernandez N, Pertino MW, Schmeda-Hirschmann G, Joseph-Nathan P (2012) Absolute Configuration and ^{1}H NMR Characterization of Rosmaridiphenol Diacetate. J Nat Prod 75:779
269. Manríquez-Torres JJ, Torres-Valencia JM, Gómez-Hurtado MA, Motilva V, García-Mauriño S, Ávila J, Talero E, Cerda-García-Rojas CM, Joseph-Nathan P (2011) Absolute Configuration of 7,8-*seco*-7,8-Oxacassane Diterpenoids from *Acacia schaffneri*. J Nat Prod 74:1946
270. Manríquez-Torres JJ, Torres-Valencia JM, Velázquez-Jiménez R, Valdez-Calderón A, Alvarado-Rodríguez JG, Cerda-García-Rojas CM, Joseph-Nathan P (2013) A Macrocyclic Dimeric Diterpene with a C_2 Symmetry Axis. Org Lett 15:4658
271. Borgen G, Dale J (1974) The Inherent Instability of 1,3-Dioxan and the Conformation of 1,3,7,9-Tetraoxacyclododecane. J Chem Soc Chem Commun:484
272. Rank C, Phipps RK, Harris P, Fristrup P, Larsen TO, Gotfredsen CH (2008) Novofumigatonin, a New Orthoester Meroterpenoid from *Aspergillus novofumigatus*. Org Lett 10:401
273. Izumi H, Yamagami S, Futamura S, Nafie LA, Dukor RK (2004) Direct Observation of Odd-Even Effect for Chiral Alkyl Alcohols in Solution Using Vibrational Circular Dichroism Spectroscopy. J Am Chem Soc 126:194
274. Gutiérrez-Nicolás F, Gordillo-Román B, Oberti JC, Estévez-Braun A, Ravelo AG, Joseph-Nathan P (2012) Synthesis and Anti-HIV Activity of Lupane and Olean-18-ene Derivatives. Absolute Configuration of 19,20-Epoxylupanes by VCD. J Nat Prod 75:669
275. Burgueño-Tapia E, Ordaz-Pichardo C, Buendía-Trujillo AI, Chargoy-Antonio FJ, Joseph-Nathan P (2012) Structure and Absolute Configuration of a Visamminol Derivative using IR and Vibrational Circular Dichroism. Phytochem Lett 5:804
276. Torres-Valencia JM, Chávez-Ríos OE, Cerda-García-Rojas CM, Burgueño-Tapia E, Joseph-Nathan P (2008) Dihydrofurochromones from *Prionosciadium thapsoides*. J Nat Prod 71:1956
277. Amesty A, Burgueño-Tapia E, Joseph-Nathan P, Ravelo AG, Estévez-Braun A (2011) Benzodihydrofurans from *Cyperus teneriffae*. J Nat Prod 74:1061
278. Asai T, Luo D, Obara Y, Taniguchi T, Monde K, Yamashita K, Oshima Y (2012) Dihydrobenzofurans as Cannabinoid Receptor Ligands from *Cordyceps annullata*, an Entomopathogenic Fungus Cultivated in the Presence of an HDAC Inhibitor. Tetrahedron Lett 53:2239
279. Batista JM Jr., Batista ANL, Rinaldo D, Vilegas W, Ambrósio DL, Cicarelli RMB, Bolzani VS, Kato MJ, Nafie LA, López SN, Furlan M (2011) Absolute Configuration and Selective Trypanocidal Activity of Gaudichaudianic Acid Enantiomers. J Nat Prod 74:1154

280. Freedman TB, Cao X, Phillips LM, Cheng PTW, Dalterio R, Shu Y-Z, Zhang H, Zhao N, Shukla RB, Tymiak A, Gozo SK, Nafie LA, Gougoutas JZ (2006) Determination of the Absolute Configuration and Solution Conformation of a Novel Disubstituted Pyrrolidine Acid A by Vibrational Circular Dichroism. Chirality 18:746

281. Batista JM Jr., Batista ANL, Rinaldo D, Vilegas W, Cass QB, Bolzani VS, Kato MJ, López SN, Furlan M, Nafie LA (2010) Absolute Configuration Reassignment of Two Chromanes from *Peperomia obtusifolia* (Piperaceae) Using VCD and DFT Calculations. Tetrahedron Asymm 21:2402

282. Batista JM Jr., López SN, Mota JS, Vanzolini KL, Cass QB, Rinaldo D, Vilegas W, Bolzani VS, Kato MJ, Furlan M (2009) Resolution and Absolute Configuration Assignment of a Natural Racemic Chromane from *Peperomia obtusifolia* (Piperaceae). Chirality 21:799

283. Cedrón JC, Estévez-Braun A, Ravelo AG, Gutiérrez D, Flores N, Bucio MA, Pérez-Hernández N, Joseph-Nathan P (2009) Bioactive Montanine Derivatives from Halide-induced Rearrangements of Haemanthamine-type Alkaloids. Absolute Configuration by VCD. Org Lett 11:1491

284. Taniguchi T, Tone I, Monde K (2008) Observation and Characterization of a Specific Vibrational Circular Dichroism Band in Phenyl Glycosides. Chirality 20:446

285. Monde K, Taniguchi T, Miura N, Nishimura SI (2004) Specific Band Observed in VCD Predicts the Anomeric Configuration of Carbohydrates. J Am Chem Soc 126:9496

286. Taniguchi T, Monde K, Nakanishi K, Berova N (2008) Chiral Sulfinates Studied by Optical Rotation, ECD and VCD: The Absolute Configuration of a Cruciferous Phytoalexin Brassicanal C. Org Biomol Chem 6:4399

287. Monde K, Taniguchi T, Miura N, Kutschy P, Čurillová Z, Pilátová M, Mojžiš J (2005) Chiral Cruciferous Phytoalexins: Preparation, Absolute Configuration, and Biological Activity. Bioorg Med Chem 13:5206

288. Monde K, Taniguchi T, Miura N, Nishimura S-I, Harada N, Dukor RK, Nafie LA. (2003) Preparation of Cruciferous Phytoalexin Related Metabolites, (–)-Dioxibrassinin and (–)-3-Cyanomethyl-3-hydroxyoxindole, and Determination of Their Absolute Configurations by Vibrational Circular Dichroism (VCD). Tetrahedron Lett 44:6017

289. Velázquez-Jiménez R, Torres-Valencia JM, Cerda-García-Rojas CM, Hernández-Hernández JD, Román-Marín LU, Manríquez-Torres JJ, Gómez-Hurtado MA, Valdez-Calderón A, Motilva V, García-Mauriño S, Talero E, Ávila J, Joseph-Nathan P (2011) Absolute Configuration of Podophyllotoxin Related Lignans from *Bursera fagaroides* using Vibrational Circular Dichroism. Phytochemistry 72:2237

290. Lassen PR, Skytte DM, Hemmingsen L, Nielsen SF, Freedman TB, Nafie LA, Christensen SB (2005) Structure and Absolute Configuration of Nyasol and Hinokiresinol *via* Synthesis and Vibrational Circular Dichroism Spectroscopy. J Nat Prod 68:1603

291. Felippe LG, Batista Jr. JM, Baldoqui DC, Nascimento IR, Kato MJ, He Y, Nafie LA, Furlan M. (2012) VCD to Determine Absolute Configuration of Natural Product Molecules: Secolignans from *Peperomia blanda*. Org Biomol Chem 10:4208

292. Socolsky C, Rates SMK, Stein AC, Asakawa Y, Bardón A (2012) Acylphloroglucinols from *Elaphoglossum crassipes*: Antidepressant-like Activity of Crassipin A. J Nat Prod 75:1007

293. Reina M, Ruiz-Mesia W, López-Rodríguez M, Ruiz-Mesia L, González-Coloma A, Martínez-Díaz R (2012) Indole Alkaloids from *Geissospermum reticulatum*. J Nat Prod 75:928

294. Gordillo-Román B, Reina M, Ruiz-Mesia L, Ruiz-Mesia W, Joseph-Nathan P (2013) Absolute Configuration of Indoline Alkaloids from *Geissospermum reticulatum*. Tetrahedron Lett 54:1693

295. Stephens PJ, Pan JJ, Krohn K (2007) Determination of the Absolute Configurations of Pharmacological Natural Products *via* Density Functional Theory Calculations of Vibrational Circular Dichroism: the New Cytotoxic Iridoid Prismatomerin. J Org Chem 72:7641

296. Krohn K, Gehle D, Dey SK, Nahar N, Mosihuzzaman M, Sultana N, Sohrab MH, Stephens PJ, Pan JJ, Sasse F (2007) Prismatomerin, a New Iridoid from *Prismatomeris tetrandra*. Structure Elucidation, Determination of Absolute Configuration, and Cytotoxicity. J Nat Prod 70:1339

297. Devlin FJ, Stephens PJ, Figadère B. (2009) Determination of the Absolute Configuration of the Natural Product Klaivanolide *via* Density Functional Calculations of Vibrational Circular Dichroism (VCD). Chirality 21:E48
298. Zhu WL, Puah CM, Tan X-J, Jiang HL, Chen KX, Ji RY (2000) A Density Functional Theory Calculation of the Geometry and Vibrational Spectrum of Natural Product, Ginkgolide B.J Mol Struct (Theochem) 528:193
299. He J, Petrovic AG, Dzyuba SV, Berova N, Nakanishi K, Polavarapu PL (2008) Spectroscopic Investigation of *Ginkgo biloba* Terpene Trilactones and Their Interaction with Amyloid Peptide Aβ(25-35). Spectrochim Acta Part A 69:1213
300. Shanmugam G, Polavarapu PL (2004) Structure of Aβ(25–35) Peptide in Different Environments. Biophys J 87:622
301. Ma S, Cao X, Mak M, Sadik A, Walkner C, Freedman TB, Lednev IK, Dukor RK, Nafie LA (2007) Vibrational Circular Dichroism Shows Unusual Sensitivity to Protein Fibril Formation and Development in Solution. J Am Chem Soc 129:12364
302. Nakahashi A, Miura N, Monde K, Tsukamoto S (2009) Stereochemical Studies of Hexylitaconic Acid, an Inhibitor of p53–HDM2 Interaction. Bioorg Med Chem Lett 19:3027
303. Isogai A, Sakuda S, Nakayama J, Washizu M, Shindou K, Watanabe S, Suzuki A (1987) Screening Search for Plant Growth Regulators from Microbial Metabolites. Proceedings of the Plant Growth Regulation Society of America, 14th Meeting, Honolulu, Hawaii, p 250
304. Nakahashi A, Yaguchi Y, Miura N, Emura M, and Monde K (2011) Vibrational Circular Dichroism Approach to the Determination of the Absolute Configurations of Flavorous 5-Substituted-2(5*H*)-furanones. J Nat Prod 74:707
305. Yaguchi Y, Nakahashi A, Miura N, Sugimoto D, Monde K, Emura M (2008) Stereochemical Study of Chiral Tautomeric Flavorous Furanones by Vibrational Circular Dichroism. Org Lett 10:4883
306. Emura M, Yaguchi Y, Nakanishi A, Sugimoto D, Miura N, K Monde (2009) Stereochemical Studies of Odorous 2-Substituted-3(2H)-furanones by Vibrational Circular Dichroism. J Agric Food Chem 57:9909
307. Monde K, Nakahashi A, Miura N, Yaguchi Y, Sugimoto D, Emura M (2009) Stereochemical Study of a Novel Tautomeric Furanone, Homofuraneol. Chirality 21:E110
308. Polavarapu PL, Scalmani G, Hawkins E K, Rizzo C, Jeirath N, Ibnusaud I, Habel D, Nair DS, Haleema S (2011) Importance of Solvation in Understanding the Chiroptical Spectra of Natural Products in Solution Phase: Garcinia Acid Dimethyl Ester. J Nat Prod 74:321
309. Polavarapu PL, Jeirath N, Walia S (2009) Conformational Sensitivity of Chiroptical Spectroscopic Methods: 6,6′-Dibromo-1,1′-bi-2-naphthol. J Phys Chem A 113:5423
310. Polavarapu PL, Donahue EA, Shanmugam G, Scalmani G, Hawkins EK, Rizzo C, Ibnusaud I, Thomas G, Habel D, Sebastian D (2011) A Single Chiroptical Spectroscopic Method May Not Be Able To Establish the Absolute Configurations of Diastereomers: Dimethylesters of Hibiscus and Garcinia Acids. J Phys Chem A 115:5665
311. Polavarapu PL (2008) Why it is Important to Simultaneously Use More than One Chiroptical Spectroscopic Method for Determining the Structures of Chiral Molecules? Chirality 20:664
312. Polavarapu PL (2012) Molecular Structure Determination Using Chiroptical Spectroscopy: Where We May Go Wrong? Chirality 24:909
313. Polavarapu PL, Donahue EA, Hammer KC, Raghavan V, Shanmugam G, Ibnusaud I, Nair DS, Gopinath C, Habel D (2012) Chiroptical Spectroscopy of Natural Products: Avoiding the Aggregation Effects of Chiral Carboxylic Acids. J Nat Prod 75:1441
314. Muñoz MA, Urzúa A, Echeverría J, Modak B, Joseph-Nathan P (2011) Solid State Structure and Absolute Configuration of Filifolinol Acetate. Nat Prod Commun 6:759
315. Muñoz MA, Bucio MA, Joseph-Nathan P (2013) Chiroptical Studies of Flavanone. Nat Prod Commun 8:1075
316. Abbate S, Burgi LF, Castiglioni E, Lebon F, Longhi G, Toscano E, Caccamese S (2009) Assessment of Configurational and Conformational Properties of Naringenin by Vibrational Circular Dichroism. Chirality 21:436

317. Mugishima T, Tsuda M, Kasai Y, Ishiyama H, Fukushi E, Kawabata J, Watanabe M, Akao K, Kobayashi J (2005) Absolute Stereochemistry of Citrinadins A and B from Marine-Derived Fungus. J Org Chem 70:9430
318. Hopmann KH, Šebestík J, Novotná J, Stensen W, Urbanová M, Svenson J, Svendsen JS, Bouř P, Ruud K (2012) Determining the Absolute Configuration of Two Marine Compounds Using Vibrational Chiroptical Spectroscopy. J Org Chem 77:858
319. Asai T, Morita S, Shirata N, Taniguchi T, Monde K, Sakurai H, Ozeki T, Oshima Y (2012) Structural Diversity of New C_{13}-Polyketides Produced by *Chaetomium mollipilium* Cultivated in the Presence of a NAD^+-Dependent Histone Deacetylase Inhibitor. Org Lett 14:5456
320. Cherblanc F, Lo Y-P, De Gussem E, Alcazar-Fuoli L, Bignell E, He Y, Chapman-Rothe N, Bultinck P, Herrebout WA, Brown R, Rzepa HS, Fuchter MJ (2011) On the Determination of the Stereochemistry of Semisynthetic Natural Product Analogues using Chiroptical Spectroscopy: Desulfurization of Epidithiodioxopiperazine Fungal Metabolites. Chem Eur J 17:11868
321. Cherblanc FL, Lo Y-P, Herrebout WA, Butlinck P, Rzepa HS, Fuchter MJ (2013) Mechanistic and Chiroptical Studies on the Desulfurization of Epidihiodioxopiperazines Reveal Universal Retention of Configuration at Bridgehead Carbon Atoms. J Org Chem 78:11646
322. Patterson D, Schnell M, Doyle JM (2013) Enantiomer-Specific Detection of Chiral Molecules *via* Microwave Spectroscopy. Nature 497:475
323. Nafie LA (2013) Handedness Detected by Microwaves. Nature 497:446

The Series "Progress in the Chemistry of Organic Natural Products": 75 Years of Service in the Development of Natural Product Chemistry

Rudolf Werner Soukup and Klara Soukup

1 Contents

R.W. Soukup (✉)
Institute of Chemical Technologies and Analytics, Vienna University of Technology, 1060 Vienna, Getreidemarkt 9, Austria
e-mail: rudolf.werner@kabelnet.at

K. Soukup
St. Anna Children's Cancer Research Institute, Zimmermannplatz 10, 1090 Vienna, Austria

A.D. Kinghorn, H. Falk, J. Kobayashi (eds.), *Progress in the Chemistry of Organic Natural Products, Vol. 100*, DOI 10.1007/978-3-319-05275-5_5,

1 Introduction

The monograph series "Fortschritte der Chemie Organischer Naturstoffe" (from 1945 to 2010 "Fortschritte der Chemie Organischer Naturstoffe—Progress in the Chemistry of Organic Natural Products" and from thereon "Progress in the Chemistry of Organic Natural Products") was founded by *László Zechmeister* in 1938. On the occasion of the 75th anniversary of the edition of Volume One as well as upon the publication of Volume 100, we take a retrospective look at the beginnings and development of "Progress" in order to answer the question of whether this series of contributions has been a true mirror of the rapid development of natural product chemistry from 1938 to the present.

There is no doubt that investigating the physical and material constitution of himself and his immediate environment has always been of major importance to man. The fascination of Nature and the color of blood dates back to paleolithic man. Traces of red chalk on the skull of a skeleton from a 28,000 years old burial site in Dolni Věstonice in Southern Moravia hint at the possibility that early man associated iron-containing compounds (hematite and also limonite) with vital blood (*1*). In his "Naturalis Historia", *Plinius* (approx. 23–79 AD) reports that powdered hematite is capable of staunching the flow of blood from wounds (*2*). In 1665, the Italian anatomist *Marcello Malpighi* (1628–1694) described fibrin as the major component of the blood clot (*3*). In his blood analysis from 1812, the Swedish chemist *Jöns Jacob Berzelius* (1779–1848) separated the solid and liquid parts by coagulation and examined each part separately (*4*). He found an iron oxide content of 50% in the clot (*5*). Many years later, *Hans Fischer* (1881–1945) was able to identify hemin as a porphyrin ligand complexed with an iron ion as its central atom (*6*). *Fischer* conducted his studies in Munich starting from 1912. Meanwhile, in Zurich (1913), *Richard Willstätter* (1872–1942) was able to obtain a compound he named "aetiophyllin" by introducing magnesium into hemoporphyrin (*7*). The same substance could later be obtained from chlorophyll derivatives, which proved the chemical similarity between the red pigment in blood and the green pigment in leaves.

In a nomination speech that preceded the election of *Willstätter* as a full member to the Berlin Academy of Sciences in November 1914, *Emil Fischer* (1852–1919), who had been awarded a *Nobel* Prize in 1902, underlined the significance of *Willstätter*'s discoveries in the field of physiology (*8*). *Willstätter* had several prominent students. *László Zechmeister* was one of them. It was *Willstätter* who planted the interest in investigating natural compounds in him (*9*). In the decades to come, *László Zechmeister* was to become one of the most important chemists in the field

of natural products. One of his major contributions represents the foundation of a publication organ dedicated to the progress in this special field in 1938, which still exists today: "Progress in the Chemistry of Organic Natural Products". Thus, 100 volumes of this series of monographs, which most of the time was simply called "*Zechmeister*", have now been published. Since its foundation, the publisher (Springer-Verlag) has remained the same, which is quite astonishing considering the turmoil of the twentieth century.

This retrospective comments on the professional background of the series' founder and first editor on the one hand, and on its contributions on the other, which impressively mirror the tremendous progress achieved in natural product research over the decades. They cover primarily the years of *László Zechmeister*'s editorship (between 1938 and 1969) and subsequently follow the progress of research on natural compound chemistry in Central Europe. An important focus lies on developments in Hungary and Austria, which, until only a few years before *Zechmeister* was appointed to the University of Pécs, had been joined in the Austro-Hungarian dual monarchy. Additionally, an eye is kept on the personal circumstances and changes in Zurich and Berlin, where *Zechmeister* was educated as a chemist. Later on, during World War II, the reader will follow *Zechmeister* to a new center of research in the USA. Finally—as time proceeds towards the present—this overview will reveal how excellent research is being conducted all over the globe in the field of natural products.

It goes without saying that giving a comprehensive account of all the important developments concerning research on natural products over the course of 75 years, within the frame of an anniversary edition, is simply not possible. This contribution is therefore meant to represent a recapitulatory chronology.

2 *László Zechmeister*: Editor from 1938 to 1969

2.1 Previous History: Phytochemistry in Hungary

In principle, the history of the investigation of natural products in the Austro-Hungarian Empire started when *Josef Redtenbacher* (1810–1870) was appointed to the chair of chemistry at the University of Prague in 1840. *Redtenbacher* studied under *Joseph Franz von Jacquin* (1766–1839) in Vienna and under *Justus von Liebig* (1803–1873) in Gießen. *Jacquin* was professor of botany and chemistry at the medical faculty of the Alma Mater Rudolfina—the interconnection of research on plants and substances in Austria at that time is obvious. With *Liebig, Redtenbacher* got to know the method of exact elemental analysis. The laboratory of *Redtenbacher* in Prague was the origin of the development of chemical teaching and research throughout the empire (*10*). In 1849, *Redtenbacher* received a call to establish a chair of chemistry at the philosophical faculty of the University of Vienna. *Redtenbacher* had many important students.

Concerning the development of chemistry in Hungary, *Theodor Wertheim* (1820–1864) is to be mentioned, who came to Prague in 1843 in order to be taught in organic chemistry. The work of *Wertheim* started with preliminary studies on plant alkaloids and he succeeded in also isolating an oil from garlic and identifying it as diallyl sulfide in 1845. In 1854, *Wertheim* took a position at the University of Pest, where he carried out work on quinine, narcotine, coniine, and conhydrine.

Wertheim's successor in the chair was another student of *Redtenbacher. Karl von Than* (1834–1908) who descended from the Hungarian noble family of *Ó-Becse* and went to Vienna in 1855 in order to study chemistry. Following his time in Heidelberg where he studied under *Robert Bunsen* (1811–1899), he became *Redtenbacher*'s assistant in 1859. *Than* proved to be quite successful in phytochemistry. In 1859, for example, he was able to show that the yellow crystalline substance rumicin, extracted from the roots of yellow dock (*Rumex crispus*), is chrysophanic acid. In Budapest, *Than* became the teacher of the first generation of Hungarian chemists of European standing (*11*). Of his numerous students, *Lajos Winkler* (1863–1939) should be mentioned, who became known for his method to determine oxygen dissolved in water. Furthermore, *Winkler* rendered great service to the determination of the acid number of fats and became *Than*'s successor at the University of Budapest.

In the commentary to Volume One, also *Gezá Zemplén*, who studied under *Than* and earned his doctorate in Budapest in 1904, will be mentioned.

This synopsis of important contributors to Hungarian phytochemistry should also include *Albert von Szent-Györgyi Nagyrápolt* (1893–1986), biochemist and Medicine *Nobel* laureate, who was born in Budapest and studied there shortly before World War I. In 1930—following research stays in Germany, the Netherlands, and England—he accepted a chair at the University of Szeged, where he succeeded in identifying ascorbic acid, which he had isolated from plant extracts, as vitamin C in 1932. As we will see, *Szent-Györgyi*'s visit to the California Institute of Technology in June, 1939 played quite an important role in *Zechmeister*'s biography.

2.2 A Short Biography of László Zechmeister

László Zechmeister was born in the emerging Hungarian town of Györ on May 14, 1889. He was the son of *Károly Zechmeister* (1852–1910), town mayor at the time. Between 1869 and 1906, he attended Győri Magyar Királyi Állami Főreáliskolában school, which today is called Révai Miklós Gimnázium. After serving a year in the military (*12*), *Zechmeister* began to study at the Swiss Federal Institute of Technology (Eidgenössische Technische Hochschule) (ETH) in Zurich in the autumn of 1907.

The situation in Zurich at that time must have been tremendously productive. After all, *Zechmeister*'s teacher at the ETH, *Richard Willstätter* (1872–1942), was awarded a *Nobel* Prize in 1915—based mainly on work he had performed between 1905 and 1912. *Alfred Werner* (1866–1919), who taught at the University of Zurich at that time, earned a *Nobel* Prize in 1913. *Paul Karrer* (1889–1971), *Nobel* laureate of 1937, obtained his doctorate in Zurich in 1911 and was *Werner*'s assistant. And finally, in 1912, *Leopold Ružička* (1887–1976)—*Nobel* laureate of 1939—accompanied his

dissertation adviser *Hermann Staudinger* (1881–1965, *Nobel* Prize in 1953) to ETH Zurich, when *Staudinger* became professor there and started the investigation of high-molecular substances such as rubber and cellulose.

When *Richard Willstätter* moved from Zurich to Berlin-Dahlem as director of the Kaiser Wilhelm Institute in 1912, he invited *Zechmeister* to join him as his assistant. Following these events, *Zechmeister* earned his doctorate in Zurich in 1913. As of 1913, *Zechmeister* published contributions on the hydrolysis of cellulose together with his teacher *Willstätter* (*13*). In 1914, *Willstätter*'s and *Zechmeister*'s paper "Synthesis of Pelargonidin" ("Synthese des Pelargonidins") was printed in the minutes of proceedings at the Royal Prussian Academy of Sciences in Berlin (*14*).

At the outbreak of World War I, *Zechmeister* was drafted into the Hungarian Army. After having been captured at the Russian front, he was kept imprisoned in Siberia from 1915 until 1917. During these 2 years of imprisonment, he taught himself English by means of a Russian-English dictionary (*15*). After the war, *Zechmeister* took over the research laboratory at "Chinoin A.-G."—a factory of chemical-pharmaceutical products in Budapest-Ujpest. He rejoined *Willstätter*, who had taken over *Adolf von Baeyer*'s chair in Munich. The results of their investigation of the anthocyanin cyanidin were submitted at a session of the Bavarian Academy of Sciences in 1920 (*16*).

Along with *Georg Hevesy* (1885–1966), *Zechmeister* performed experiments with radioactive metal ions and organic ligands at the Veterinary School of Budapest in 1919/1920. *Hevesy* and *Zechmeister* extended earlier investigations of exchange processes. They mixed radioactive tetravalent lead acetate with inactive bivalent lead acetate and measured how the activity of the former gradually diminished to half of the original value, proving that the active isotopes exchange with the inactive ones. They also proved that an exchange process between atoms of the same molecules can only be experienced if the molecules are present in their dissociated state (*17*). This contribution extended the isotope indicator method to the organic world (*18*).

From 1921 to 1943, *Zechmeister* was a scientific assistant of *Niels Bjerrum* (1879–1958) and instructor at the Danish Royal Veterinary and Agricultural Academy, Copenhagen. With *Bjerrum* he published a contribution on the dehydration of methanol with the help of magnesium (*19*).

In 1923, *Zechmeister* became full professor of chemistry at the faculty of medicine of the University of Pécs. Regarding his own early studies, *Zechmeister* published on various plant and animal pigments, sugar derivatives and sterols in papers from Pécs. Together with *Pál Szécsi*, for example, he published a paper on the occurrence of fumaric acid and inositol in 1921 (*20*), and, in 1926, he worked together with *Vera* (*Verával*) *Vrabély* on ajkait—an organic mineral found in Hungary (*21*). In 1927, a contribution on the paprika pigment was published together with his long-term assistant *László (von) Cholnoky* (1899–1967) as co-author (*22*). Publications followed on constitutional assignments of carotene in 1928 (*23*), on the phytosterol of the stinging nettle in 1929 (*24*), on conversions of capsanthin (*25*), and on the pigment of orange peel with *Pállal Tuzson* in 1936 (*26*). In 1934, *Zechmeister*'s monography "Carotenoids. A Biochemical Report on Plant and Animal Polyene Pigments" ("Carotinoide. Ein biochemischer Bericht über pflanzliche und tierische Polyenfarbstoffe") was published by Julius Springer-Verlag in Berlin.

In 1940, on board of the last ship that left Italy heading towards the USA, *Zechmeister* immigrated to the United States. Following an invitation by *Linus Pauling* (1901–1994) to work at the Gates and Crellin Laboratories, *László Zechmeister* arrived at the California Institute of Technology by mid-March 1940 (*27*). We can get to know the background of *Pauling*'s invitation from a letter by *Pauling* to *Warren Weaver* at the Rockefeller Foundation dated July 14, 1939 (*28*):

> *At present we are considering very seriously the possibility of giving appointment to Zechmeister. Szent-Györgyi, during his visit here last month, spoke very highly of Zechmeister, and even remarked, perhaps jocularly, that it would be fine if an institute for him and Zechmeister could be built on the northwest corner of the campus.*

Zechmeister was very much worried about the political situation in Hungary. In a letter written on June 13, 1939 (*28*), he told *Pauling* that he and his wife *"are inclined to leave if conditions were offered which would enable me to carry on with my work possibly on a larger scale than in this country."*

At the end of the second week of March, 1940, *Zechmeister* arrived in Pasadena and immediately was appointed professor of organic chemistry at the California Institute of Technology (*29*). In Pasadena, *Zechmeister* worked first on the isomerism of carotenoids. His two first assistants at CalTech were *Arthur LeRosen*, who died much too early in 1952, and *Andor Polgár*, whom he had brought along from Hungary. In 1941, *Walter A. Schroeder* and *William McNeely* were appointed assistants to *Zechmeister* (*30*). In 1949, *Zechmeister* was awarded a *Guggenheim* fellowship in order to lecture at European universities, and, in 1959, he became professor emeritus. In his 1956/1957 lecture "Selected Chapters of Organic Chemistry" he considered the following topics: chromatography, fats, steroids, sex hormones, alkaloids, chlorophyll, carotenoids, anthocyanins, flavones, pterins, bile pigments; structure and physiological action; the chemistry of chemotherapeutics and insecticides; detoxification processes, nitrogen metabolism, carbohydrate metabolism, nucleic acids, and the history of organic chemistry (*31*). In addition to numerous articles, which *Zechmeister* published together with *Pauling, Le Rosen, Schroeder*, *Polgar*, *Fritz Went*, and others in Pasadena, he dedicated himself to the editorship of the book series "Fortschritte in der Chemie organischer Naturstoffe" until 1970—many years after his retirement (Fig. 1).

In contrast to his teacher *Willstätter*, *Zechmeister* highly valued the significance of chromatography as a chemist's tool. As of 1937, he studied the possibilities of this separation method extensively. "30 Years of Chromatography" was the title of *Zechmeister*'s contribution published together with his assistant and later successor on his chair in Hungary, *László Cholnoky*, in "Monatshefte der Chemie" (now: "Chemistry Monthly"), in 1936 (*34*). One year later the monograph "Die chromatographische Adsorptionsmethode: Grundlagen, Methodik, Anwendungen"—published by Springer-Verlag in Vienna (*35*) appeared. The English translation of this book "Principles and Practice of Chromatography" by *Alfred Louis Bacharach* (1891–1966) and *Frank Arnold Robinson* (1907–1988), which was printed for the first time in 1941 (*36*), played an important role in the development of chromatographic methods in the U.S. (*11*). The fact that

Fig. 1 Members of the CalTech chemistry faculty in 1950. From *left* to *right*: *Verner Schomaker, Stuart Bates, László Zechmeister, Dan Campbell* (author of a contribution to Vol. 9), *Joseph Koepfli, Ernest Swift, Carl G. Niemann* (see Vol. 7), *Don Yost, Howard J. Lucas, J. Holmes Sturdivant, Stanley M. Swingle, Robert Corey* (see Vols. 8, 11, 26), and *Zechmeister's* former assistant *Walter A. Schroeder* (see Vols. 11, 17, 23). Courtesy *Ava Helen* and *Linus Pauling* Papers, Oregon State University Special Collections (*32*)

Zechmeister had always been interested in the historical development of this method is documented by his contribution on "Mikhail Tswett—the Inventor of Chromatography", published in the journal *Isis* in 1946 (*37*). It was only in 1951 that he took the liberty of writing and editing a contribution in his own series (Vol. 8) together with *Margarete Rohdewald* (1900–1994) from Bonn. This contribution was oriented especially to the use of chromatography for the separation of enzymes (Z60).

Zechmeister did not only follow the development of methods but he also focused on their possible applications. This becomes evident when looking at one of his favorite fields of research: carotenoids. In particular, the separation of (*Z*)- and (*E*)-isomers by the use of column chromatography is wedded to the name of *Zechmeister*. In 1958, he published his own contribution in Volume 15 of the Series: "Some *in vitro* Conversions of Naturally Occurring Carotenoids" (Z109).

In 1935, *Zechmeister* was awarded the *Pasteur* Médaille in 1937, the major prize of the Hungarian Academy, in 1938 an honorary membership of the Austrian Chemical Society ("Gesellschaft Österreichischer Chemiker") (*38*), in 1949 the Médaille *Claude Bernard*, in 1960 the *Semmelweis* Medal, and in 1962 the Labline Award of the American Chemical Society. In 1971, the University of Pécs Medical School conferred an honorary M.D. degree on him.

Zechmeister was married twice. His first wife died in Budapest in 1941. In 1947, he married *Elizabeth Sulzer,* a young lady born in Zurich (*39*). Sometimes *Zechmeister* referred to his second wife as his associate in editing the series "Progress in the Chemistry of Organic Natural Products", because of her assistance in both editing and translating submitted material. He died on February 28, 1972 in Pasadena, California.

Volume 55 of the Series opens with a dedication by the editors following *Zechmeister* on the occasion of the 100th anniversary of his birth on May 14, 1899: *"Those who knew him remember him for his contributions to science, for his stimulus he provided for his contemporaries and his students and, in his capacity as editor, for his meticulous attention to detail".*

3 Volumes One to Three: Edited in Pécs

3.1 Editorial Board

Besides *Zechmeister*, *Adolf Butenandt* from Berlin, *Fritz Kögl* from Utrecht, and *Ernst Späth* from Vienna, are listed as members of the editorial board of the first three volumes, published between 1938 and 1939 (Fig. 2). *Walter Norman Haworth* from Birmingham was responsible only for Volumes One and Two.

At the time of publication of the first volume, *Adolf Butenandt* (1903–1995) was director of the Kaiser Wilhelm Institute of Biochemistry in Berlin-Dahlem and had just been appointed honorary professor of biochemistry at the university. He was regarded as *the* great steroid chemist and—together with *Leopold Ružička*—was awarded the *Nobel* Prize in chemistry in 1939 for the identification of the sex hormones estrogen, progesterone, and androsterone.

Fritz Kögl (1897–1959) studied under *Heinrich Otto Wieland* at the TH Munich. From 1921 to 1926 he was a coworker of *Hans Fischer* in Munich. As of 1931 he became full professor of organic chemistry and biochemistry at the University of Utrecht. In 1931, *Kögl* isolated muscarine and in 1936, he and his doctoral student *Benno Tönnis* succeeded in isolating biotin in its pure form. From 1933 on, *Kögl* and his assistants *Arie Jan Haagen-Smit* (1900–1977) and *Hanni Erxleben* (1903–2002) studied extensively plant growth hormones of the auxin group.

Sir Walter Norman Haworth (1883–1950), *Nobel* laureate of 1937, had been awarded this honor together with *Paul Karrer* (a chemist from Switzerland whom we will get to know in Volume 5 of the Series) for his investigations on carbohydrates and vitamin C. In 1925, he was appointed Mason Professor of Chemistry at the University of Birmingham.

Ernst Späth (1886–1946), son of a Moravian farrier, started his studies of natural sciences in Vienna in 1906. He earned his doctorate under *Rudolf Wegscheider* at the I Chemical Institute at the University of Vienna in 1910. In 1924, he followed *Wilhelm Schlenk* as professor at the II Chemical Institute in Vienna. His first independent studies brought him to the field of isoquinoline alkaloids, of which he characterized

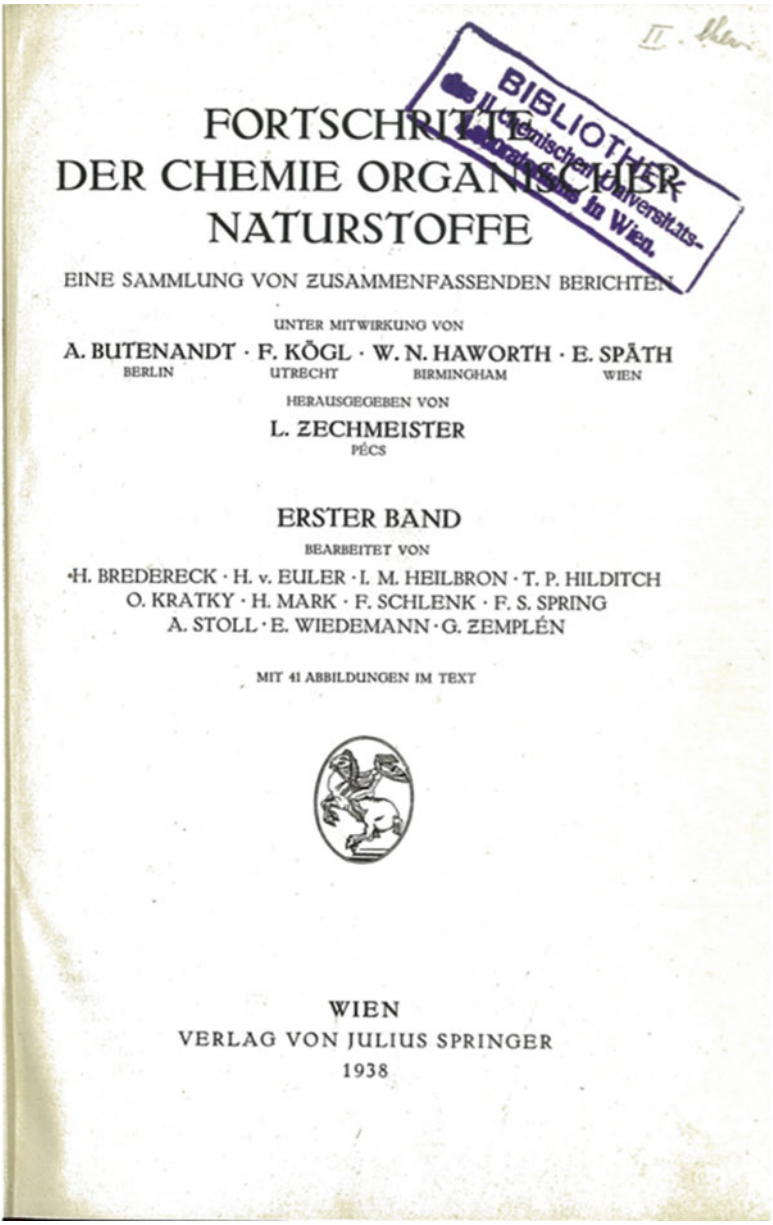

Fig. 2 Title page of volume 1 displaying the starting editorial board

the main alkaloid in greater celandine (*Chelidonium majus*)—chelidonine—among others. Many of *Späth*'s later investigations were dedicated to the alkaloids of cactuses, golden chain (*Laburnum anagyroides*), tobacco, and opium. His work on cytisine earned him the *Ignaz Lieben* Prize in 1920 (*39*).

3.2 Volume One: Overture

The first volume of the Series represented a sublime start. *Zechmeister* succeeded in winning the creme de la creme of the research elite in the area of natural products at the time to contribute. The series of contributions commenced with a text by *László Zechmeister*'s colleague, *Géza Zemplén* (1883–1956), who served as the chair of organic chemistry of the Technical University Budapest, entitled "New Directions in Glycoside Synthesis" (*Z1*). The educational background and development of *Zemplén* were quite similar to those of *Zechmeister*. He was born in Trencsén (originally a Hungarian town, today Trenčín in Western Slovakia), attended grammar school in Fiume (Rijeka) and studied at the Eötvös Józef-Kollegium in Budapest. In 1905, he became assistant at the chair of silvicultural chemistry of the Academy of Mining and Forestry in Schemnitz (today Banská Štiavnica). In 1907, he was sent to Berlin where he studied under *Emil Fischer* and conducted research in the field of carbohydrate chemistry. *Zemplén* habilitated at the University of Budapest on "Chemistry of Carbohydrates, Proteins, and Enzymes" and became chair of technical chemistry at the Royal Joseph University of Technology in Budapest (*40*). Considering the research topics that *Zemplén* and his students were working on, one soon gets to realize that *Emil Fischer* played quite an important role in the development of organic chemistry in Hungary (*41*). In 1923, *Zemplén* (together with *Alfons Kunz*) developed the *Zemplén* saponification of ac(et)ylated sugars (*42*), which is still used today. The Hungarian Academy of Science elected him as a full member in 1927 and his work on the decomposition of reduced disaccharides earned him the Great Prize of the Academy in 1928. Today, *Géza Zemplén* is regarded as the founder of scientific organic chemistry in Hungary (*43*).

In his contribution (*Z1*), following an overview of various methods of alkyl glycoside syntheses, *Zemplén* described a synthesis using mercury salts, that was developed by himself, *Zoltan Bruckner* (1902–1958), and *Árpád Gerecs* (1903–1982) in 1930/1931. He reported on similar experiments in which iron trichloride and alcohol containing chloroform were used. Finally, he referred to a phenol glycoside synthesis using zinc chloride, performed by *Burckhardt Helferich* (1887–1982).

For the second contribution "The Component Glycerides of Vegetable Fats" (*Z2*), *Zechmeister* was able to engage a specialist on fatty acids: *Thomas Percy Hilditch* (1886–1965), who held the Campbell Brown Chair of Industrial Chemistry of the University of Liverpool. *Hilditch* was born in London. Following a career at the Universities of London, Jena, and Geneva he was hired as research chemist at the soap and chemical factory of Joseph Crosfield and Sons in Warrington in 1911. There he was concerned with the process of fat hydrogenation and with the constitution of some of the less common commercial fats, such as palmitoleic acid. In 1926, he became professor of industrial chemistry at the University of Liverpool. His student and colleague *Frank Denby Gunstone* (*1923) said about him, "*Between 1926 and 1951 no one did more than he to discern the patterns which run through the related areas of component acids and component glycerides*" (*44*).

Hilditch began his contribution with a historical survey drawing our attention back to 1860, when *Marcelin Berthelot* (1827–1907) pointed out the possibility of the existence of mixed triglycerides in natural fats. At that time, with chromatography and other modern analytical methods not developed yet, such investigations were very time-consuming. In 1902, *Richard Fritzweiler* succeeded in isolating 6% oleodistearin from cocoa butter by fractional crystallization. When it came to triglycerides, this method failed—except for laurel oil and nutmeg butter. *Hilditch* subsequently reported on his own successes, which concerned solving the problem of glyceride structure by means of chemical methods: when fat is oxidized with powdered potassium permanganate in acetone solution, all glycerides containing one or more unsaturated acyl radicals are ultimately converted into the corresponding azelaic glycerides, while the completely saturated glycerides remain intact. The main part of *Hilditch*'s contribution included results of his investigation of the composition of various natural fats regarding their content of saturated and unsaturated fatty acids. Finally, the author gave a detailed description of certain fats regarding their content of C_{14}, C_{16}, C_{18}, and C_{20} saturated acids.

Acknowledging the successes in the field of sterol chemistry (a subgroup of the steroids) in the 1930s, a review by *I. M. Heilbron* and *F. S. Spring* from Manchester followed *Hilditch*'s overture: "Recent Advances in the Chemistry of the Sterols" (*Z3*). From 1933 to 1938, *Isidor* (*Ian*) *Morris Heilbron* (1886–1959) was Sir Samuel Hall Professor of Chemistry at the University of Manchester. In 1938, he became Longstaff Medallist of the Chemical Society and moved to Imperial College in London. *Heilbron* grew up in the city of Glasgow. After studying at the Glasgow Royal College of Technology, he received a PhD at the University of Leipzig in 1909 and a DSc at the University of Glasgow in 1918. In Liverpool, *Heilbron*'s research interests turned to the chemistry of natural products. His research on the relationship between sterols and vitamin D, the field of vitamin A and polyene synthesis earned him international renown (*45*). The most prominent contribution by *Heilbron*'s longterm co-worker *Frank Stuart Spring* (1907–1997) was the development of mechanisms for the introduction of an oxygen atom at position 11 of the steroid nucleus, and the development of possibilities for the synthesis of cortisone from ergosterol as a more convenient starting point than the bile acids that had been used previously (*46*). In their review on steroid chemistry, *Heilbron* and *Spring* referred to different studies—including some that had been conducted before the turn of the century. For example, they mentioned a paper by the Austrian chemists *Wilhelm Suida* (1853–1922) and *Julius Mauthner* (1852–1917) from 1896, which described the synthesis of 3,6-diketo-Δ^4-cholestene (*47*). Numerous new syntheses and methods had been developed since—among other examples by *Diels* and *Abderhalden* in 1903 (*48*), by *Windaus* and *Linsert* in 1928 (*49*), by *Butenandt* and *Schramm* in 1936 (*50*), and by *Rosenheim* and *Starling* in 1937 (*51*). Already at that time, the two authors realized that a study by *Hans Herloff Inhoffen* (1906–1992) on the aromatization of the A-ring by removal of hydrogen bromine from the dibromine of androstanedione (*52*) would influence the direction of future investigations on the sex hormones.

Hans von Euler-Chelpin (1873–1964), *Nobel* laureate of 1929, wrote a contribution on cozymase together with his assistant at the Biochemical Institute of the University of Stockholm, *Fritz Schlenk* (1909–1998) (*Z4*). *Hans von Euler-Chelpin*'s interest in chemistry was awakened when he engaged in studying the nature of colors in the course of his art studies. He finished his chemistry studies, which he started in Munich in 1893, as early as 1895 by earning a doctorate in Berlin. He then became an assistant of *Walter Nernst* in Göttingen and worked together with *Svante Arrhenius* in Stockholm. In 1899 he became adjunct professor and in 1906 full professor at the University of Stockholm. Finally, in 1929, he was appointed director of the Institute of Vitamins and Biochemistry at the University of Stockholm. *Euler'*s assistant in Stockholm—*Fritz Schlenk*—was born in Munich and studied at the University of Berlin. His doctorate advisor was his father, the famous organic chemist *Wilhelm Schlenk* (1879–1943). In 1934, *Fritz Schlenk* went first to work under *Hans von Euler-Chelpin* in Stockholm and then immigrated to the USA in 1940 (*53*). From 1940 to 1943, he was a professor of biochemistry at the University of Texas. Afterwards, he became professor at Iowa State University and from 1954 to 1974 he worked as a research associate in the biomedical division at Argonne National Laboratory. From 1965 to his retirement in 1985, *Schlenk* was a faculty member of the University of Illinois at Chicago (*54*).

Schlenk and *Euler* reported on methods and results of determining the constitution of cozymase. They stated explicitly that it was not yet sure whether the pentose of the nicotinamide nucleotide is D-ribose. At that time it had also not been determined which kind of phosphoric acid molecule was bound to the nicotinamide in a way that resembles a betaine bond. *Schlenk* and *Euler* hypothesized that cozymase constituted a phosphate-transferring coenzyme.

The following section was dedicated especially to nucleic acids occurring in the cell nucleus. The author engaged for that purpose was *Helmut Bredereck* (1904–1982), who at that time was adjacent professor at the University of Leipzig. *Brederick* studied in Frankfurt/Main and Greifswald and worked as assistant at the University of Leipzig, where he habilitated in 1933. In 1941, he became full professor of organic chemistry and biochemistry at the University of Jena. As of 1947, he became professor of organic chemistry at the TH Stuttgart.

In a preliminary statement to his contribution of 1938, *Bredereck* points to the fact that the knowledge of nucleic acids had become a lot better understood within recent years (*Z5*). He mentioned that by that time, vitamin B_2, lactoflavin, and a number of cofermented products had been found to be nucleic acid derivatives. Even the constitution of some nucleosides and nucleotides could be determined. The role of cozymase and some other specific co-fermented products as hydrogen carriers could be deduced and *Brederick* stated that hydrogen transfer is linked to phosphate transfer in both fermentation and glycolysis.

The penultimate contribution to Volume One represents an extensive overview of the state of research on chlorophyll (*Z6*). It was written by *Zechmeister*'s former colleague at ETH Zurich, *Arthur Stoll* (1887–1971) and *Stoll'*s co-worker at the scientific laboratory of the Sandoz Company in Basel, *Erwin Wiedemann*. At the beginning of their text, *Stoll* and *Wiedemann* described the unsatisfying situation of

investigations on chlorophyll, prior to *Richard Willstätter*'s studies. Following this, they gave some of the results of *Willstätter* and his assistants that had been obtained before 1913; subsequently they mentioned *Hans Fischer*'s findings concerning the constitution of hemin and finally they commented on successes achieved between 1932 and 1938. Regarding methodology, it is interesting that *Stoll* and *Wiedemann* mentioned a comment by *Alfred Winterstein*, who worked in the laboratory of *Richard Kuhn* in Heidelberg, and his assistant *Gertrud Stein* (1905–?) (*55*), in which they stated that it was only possible to obtain pure chlorophyll components by chromatographic adsorption—a method described by *Michail Tswett* (*Mikhail Semyonovich Tsvet* 1872–1919). *Stoll* started his studies at ETH Zurich and soon became a student of *Willstätter*. In 1916, he was appointed as a professor at the University of Munich. From 1917, *Stoll* was active at Sandoz in Basel. *Stoll*'s co-author *Wiedemann* studied at the TH Munich and had been working as a scientific assistant at Sandoz since 1930.

The final contribution of Volume One was written by the Austrian chemists *Otto Kratky* and *Hermann Mark* (*Z7*). Today, *Otto Kratky* (1902–1995) is known as the discoverer of small angle X-ray scattering and the inventor of the small angle X-ray camera. He was born in Vienna and studied chemistry at the Technical University of Vienna. In 1938, he habilitated in physical chemistry at the University of Vienna. In 1940, he became head of the Department of Physical Chemistry and Electrochemistry at the Kaiser Wilhelm Institute in Berlin-Dahlem and in 1943 he became full professor and director of the Physical-Chemical Institute at the Deutsche Technische Hochschule in Prague. From 1946 to 1972, *Kratky* was full professor of theoretical and physical chemistry at the University of Graz and as of 1972 he served as chairman at the Institute of X-Ray Diffraction Research at the Austrian Academy of Sciences and the Research Center Graz. It is quite amazing to note that his son, *Christoph Kratky* (Karl Franzens University Graz, Institute of Molecular Biosciences) contributes to this very volume 100 with "Structure Elucidation of Natural Compounds by X-ray Crystallography".

Hermann Mark (1895–1992) is regarded as one of the founders of polymer science. *Mark* was also born in Vienna. During a leave of absence in order to recover from a war injury, *Mark* started to study chemistry at the University of Vienna. In 1921, his graduation year, he went to the University of Berlin to become an assistant of *Wilhelm Schlenk.* The following year, *Fritz Haber* invited *Mark* to work at the newly established Institute of Fibrous Materials. At the KWI in Berlin, *Mark* investigated the molecular structure of natural textile fibers, such as cellulose, silk, and wool by X-ray diffractometry and was able to show that these materials consist of long-chain molecules. In 1926, he was offered a position as deputy research director of the research laboratory of the I.G. Farbenindustrie A.G. and in 1933, *Mark* went to Vienna where he became professor of physical chemistry at the University of Vienna. In his 6 years in Vienna he continued his studies in the field of macromolecules. Following the annexation of Austria to Germany in March 1938, *Mark* and his family fled to England *via* Switzerland and France, from where *Mark* went to Canada and finally to the United States. He began working at the Polytechnic Institute of New York in Brooklyn in 1940—first as associate professor, and

two years later as full professor. Apart from this primary employment, he also worked as a consultant for DuPont. In 1944, he established the Institute of Polymer Research at the Polytechnic Institute in Brooklyn. *Mark* died 1992 in Austin, Texas.

In their contribution of 1939, entitled "Anwendung physikalischer Methoden zur Erforschung von Naturstoffen: Form und Größe dispergierter Moleküle. Röntgenographie" ("Applying Physical Methods for the Investigation of Natural Products: Shape and Size of Dispersed Molecules. Roentgenography"), *Kratky* and *Mark* described initially the osmotic method for determining the molecular weight of large molecules. They also acknowledged the method of ultracentrifugation—developed by *Theodor Svedberg* (1884–1971)—as an important auxiliary tool. Furthermore, the authors discussed the determination of diffusion coefficients of filamentous molecules and gave substantial credit to roentgenographic investigations. In a preliminary statement, they mentioned that in 1935, *John Desmond Bernal* (1901–1971) and *Dorothy Crawfoot* (1910–1994) succeeded in correcting false theories on the sterol structure following spectroscopic measurements. Finally, *Kratky* and *Mark* turned to the X-ray investigation of proteins and describe results that were obtained regarding keratin and some particular viruses.

3.3 Volume Two: A Respectable Prolongation

Volume Two started with an overview of lignin research (*Z8*). The first author was *Karl Freudenberg* from the University of Heidelberg. In 1939, when Volume Two was published, *Karl Freudenberg* (1886–1983) was regarded as *the* specialist in cellulose and starch chemistry. He had studied under *Emil Fischer* at the University of Berlin and following positions in Munich, Freiburg, and Karlsruhe, was appointed full professor at the University of Heidelberg in 1926. In 1928, *Freudenberg* published the structure of cellulose (*56*). His studies from the early 1930s were crowned by the publication "Stereochemie" ("Stereochemistry") in 1932 (*57*), which soon rose to being a standard reference. In 1938, he organized the "Vierjahresplan—Forschungsinstitut für Holz und Polysaccharide" ("Four-Year-Plan—Research Institute of Wood and Polysaccharides") (*58*).

The second contribution was dedicated to lichen substances. It was written by the Japanese chemist *Yasuhiko Asahina* (1880–1975) of the Institute of Pharmacy at the University of Tokyo (*Z9*). *Asahina* was one of very few pioneers in the identification of chemical compounds produced by lichens. *Asahina* was born in Tokyo as a son of a postal administration officer. In 1902, he entered the Institute of Pharmacy at the Tokyo Imperial University. He graduated in 1905. In 1909, *Asahina* visited Zurich to study phytochemistry under *Richard Willstätter*. He also was a colleague of *Zechmeister* and in 1910, he published a paper on "Untersuchungen über Chlorophyll" ("Investigations of Chlorophyll") together with *Willstätter* in the *Annalen der Chemie* (*59*). In 1912, he moved to Berlin to spend some months in *Emil Fischer*'s laboratory. After returning to Tokyo, *Asahina* was named associate professor at Tokyo Imperial University. For the following ten years, he devoted

himself to research on some alkaloids and the chemistry of camphor. In 1925, *Asahina* published a paper on gyrophoric acid (*60*), which occurs in various lichens. Between 1935 and 1939, he analyzed the following lichen acids using microchemical methods: lecanoric, anzic, olivetoric, usnic, evernic, divaricatic, barbatinic, diffractic, perlatolinic, imbricaric, squamatic, sekikaic, ramalinolic, boninic, collatolic, lobaric, physodic, thamnolic, salazinic, stictinic, norstictinic, psoromic, protocetraric, and fumarprotocetraric acid (*61*).

What followed next was a contribution on flavins (*Z10*) by *Hermann Rudy* (1904–1966) from the chemical laboratory at the University of Erlangen—a student of *Heinrich Wieland* and former co-worker of *Richard Kuhn*. The research of *Kuhn* and *Rudy* from 1934 to 1936 helped show that lumiflavin (**1**) plays an enzymatic role in the hydrogenation of lactic acid, pyruvic acid, and succinic acid. In addition, by combining a flavin mononucleotide with a protein moiety of *Warburg*'s yellow enzyme, *Kuhn* and *Rudy* performed the very first partial synthesis of a fully functional enzyme. This was the first suggestion of a reversible relationship between vitamins and enzymes (*62*). Together with *Otto Majer*, *Rudy* produced azaflavins in 1938 by replacing the benzene ring by a pyridine ring (*63*). In 1955, *Rudy* became an associate professor in Heidelberg.

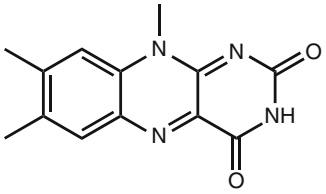

1 (lumiflavin)

The next contribution was entitled "Chemistry of the Iodine Compounds of the Thyroid" and was written by *Charles Robert Harington* (1897–1972) (*Z11*), professor of chemical pathology at the University of London and director of the Graham Research Laboratories at University College Hospital Medical School. Thyroxine had been isolated by *Edward Celvin Kendall* (1886–1972) in 1914 but not in sufficient quantities for accurate chemical investigations. With some collaborators, *Harington* devised an improved method of thyroxine isolation. He determined its structure, synthesized it, and resolved it into its enantiomers (*64*).

Edmund Langley Hirst (1898–1975), who was still working at the University of Bristol at that time (*65*), was invited by *Zechmeister* to write on "The Structure and Synthesis of Vitamin C" (*Z12*). Together with *Norman Haworth*, *Hirst* had synthesized vitamin C for the first time in 1934.

We are already familiar with the author of the next contribution on "Neuere Richtungen der Oligosaccharid-Synthese" ("New Directions in Oligosaccharide Synthesis") (*Z13*): *Géza Zemplén*.

Zechmeister himself, the editor of this Series, wrote a contribution entitled "Chitin und seine Spaltprodukte" ("Chitin and its Cleavage Products") (*Z14*), together with his assistant *Géza Tóth* (1907–1990), who had earned his doctorate in Pécs in 1929.

The contribution "La Spectrochimie de Fluorescence dans l'Ėtude des Produits Biologiques" ("The Spectrochemistry of Fluorescence in the Investigation of Biological Products") (*Z15*), was by *Charles Dhéré* (1876–1955) of Fribourg in Switzerland, who was professor of physiological chemistry at Fribourg University. *Dhéré* had worked on the very sensitive infrared fluorescence technique in addition to electrodialysis, chromatography, and absorption spectroscopy for the detection of minimal amounts of substance since 1937.

Ernst Späth (1886–1946) and *Friedrich Kuffner* (1905–1989) were accorded the honor of writing the final contribution of Volume Two on "Tobacco Alkaloids" (*Z16*). This necessitates a short comment on the Austrian school of phytochemistry. Exploring plant ingredients had been the main topic of chemical research conducted at Austrian universities since the mid-nineteenth century. After *Redtenbacher* stepped down, *Friedrich Rochleder* (1819–1874) took over the chair of chemistry at the Charles University of Prague in 1849. During that period, the University of Prague was at the front line in research on plant compounds. *Rochleder*, for example, developed a procedure for the extraction of pure alizarin from madder root. Among *Rochleder*'s assistants was *Heinrich Hlasiwetz* (1825–1875), who took over the chair of chemistry at the University of Innsbruck in 1851. *Hlasiwetz* also studied the chemistry of natural products extensively, and was especially fond of the field of phytochemistry. He investigated resins, tannins, phloroglucinol, and plant alkaloids. In 1856, the hemlock alkaloid conhydrine was discovered by *Theodor Wertheim*, who was professor at the University of Pest in Hungary at that time. The identification of nicotinic acid as an oxidation product of nicotine by *Hugo Weidel* (1849–1899), a student of *Hlasiwetz*, in 1873, and *Weidel*'s finding of the formula of berberonic acid in 1879, marked further milestones in Austrian alkaloid chemistry. In 1883, *Simon Zeisel* (1854–1933), a student of *Adolf Lieben* (1836–1914) at the II Chemical Institute, tried to elucidate the structure of colchicine, which is the main alkaloid in meadow saffron. *Zeisel* proposed a test reaction for colchicine and related compounds that is still used even today: the *Zeisel* reaction, which is the formation of a green iron tropolone complex following the hydrolysis of colchicine to colchiceine and the addition of an iron(III) salt (*66*). The first complete determination of the constitution of the opium alkaloid papaverine by *Guido Goldschmiedt* (1850–1915) in 1887 evoked a considerable response within the international scientific community (*67*).

After World War I, *Ernst Späth* and his students successfully investigated tobacco and companion alkaloids. The synthesis of nicotine by *Späth* and *Ludwig Hermann Bretschneider* (1905–1985) in 1928 (*68*) caused a minor sensation. This work proved a formula, which had been proposed by *Adolf Pinner* (1842–1909) in Berlin in 1893 (*69*). *Späth* and *Friederike Kesztler* succeeded in identifying anabasine in certain mother liquors (*70*). In 1937, they synthesized this substance using a known procedure for nicotine synthesis. Some companion alkaloids can be understood as derivatives of dipyridyl. Dipyridyl had already been synthesized from *m*-diaminobenzene by *Zdenko Hans Skraup* (1850–1910) in 1882, performing a classical *Skraup* reaction (*71*). In 1933, *Adolf Wenusch* (1894–1949), the later director of the laboratory at the Austrian Tabakregie (*72*), had discovered an alkaloid in

tobacco smoke, which was called myosmine (*73*). In 1936, *Ernst Späth* and *Luigi Mamoli* (1949) finally synthesized myosmine (*74*).

Friedrich Kuffner was *Späth*'s assistant from 1936 to 1941. From 1948 on, he headed a department at the II Chemical Institute in Vienna. For quite some time scientists were groping in the dark when it came to the formula of the tobacco companion alkaloid nicotelline. In 1954, *Kuffner* and *Ernst Kaiser* reported that during the oxidation of nicotelline, apart from the well-known nicotine acid, also pyridine-2,4-dicarboxylic acid is formed (*75*).

3.4 Volume Three: Swan Song of an Ending Era

The first contribution to Volume Three (published also in 1939) was written by *Otto Diels* (1876–1954), who was awarded a *Nobel* Prize in 1950. It is entitled "Bedeutung der Dien-Synthese für Bildung, Aufbau und Erforschung der Naturstoffe" ("Significance of Diene Synthesis for Investigations on Natural Products") (*Z17*). *Diels* was a student of *Emil Fischer* (1852–1919) and professor at the University of Kiel from 1916 on. In his introduction, *Diels* mentioned that there are only very few synthesis methods that have significance within the whole field of modern organic chemistry. In 1928, *Otto Diels* and *Kurt Alder* (1902–1958) added the synthesis of dienes to the well-known reactions of *Friedel-Crafts* and *Barbier-Grignard. Diels* emphasized that Nature itself uses this method in order to form thousands of isoprenoids from isoprene—a simple diene. This knowledge thereafter enabled chemists to synthesize a tremendous number of compounds. *Diels* pointed to several examples in the field of terpenes, camphor, and some derivatives of pyrrole.

In the early 1940s, *Walter Siedel* (1906–1968) of the TH Munich was concerned with the intensive investigation of pyrroles. *Siedel*, who—together with *Hans Fischer* (1881–1945)—was engaged in the exploration of the bilirubin structure in 1933, was the author of a contribution about "Gallenfarbstoffe" ("Bile Pigments") (*Z19*).

A contribution by *Franz Gottwald Fischer* (1902–1960) of the University of Würzburg entitled "Biochemische Hydrierungen" ("Biochemical Hydrogenations") (*Z18*) preceded *Siedel*'s paper. *Franz Gottwald Fischer* also was a co-worker of *Hans Fischer*. In 1928, he succeeded in elucidating the structure of phytol. *F. G. Fischer*'s structural formula of this diterpene alcohol was a prerequisite for the synthesis of vitamin E. In his contribution of 1945, *F. G. Fischer* discussed the hydrogenation of C=C double bonds by yeast, bacteria, and within the animal body.

The topic studied, which at that time was quite unusual, rather than the results of *Rudolph John Anderson* (1879–1961), make his contribution on the chemistry of lipoids of the tubercle bacillus worth mentioning (*Z20*). *Anderson*, who was born in Sweden, worked in the laboratory of *Emil Fischer* in Berlin in 1909 and again in 1914 (*76*). In 1927, he became a professor at Yale University in New Haven, Connecticut. In his contribution, *Anderson* repeatedly quoted studies on the same subject by *Erwin Chargaff* (1905–2002) from Vienna.

Volume Three, which was published in the same year as Volume Two, concluded with an contribution by *Linus Pauling* (1901–1994), *Zechmeister*'s future mentor in the U.S. Interestingly, this text is not about protein structures but about the theory of the chemical bond: "Recent Work on the Configuration and Electron Structure of Molecules with Some Applications to Natural Products" (*Z21*). *Pauling*'s argument for such a theoretical approach to the chemistry of natural products was the following: structural information about simple substances may be used to develop a structural theory applicable to more complex substances. At first *Pauling* referenced X-ray-diffraction, which was already described by *Kratky* and *Mark* in Volume One. This method enables the determination of bond lengths in molecules, he reported. From 1929 on, interatomic distances could also be deduced successfully from the rotational fine structure of molecular spectra, *e.g.* by *Raman* spectroscopy. *Pauling* stressed the possibility of a correlation of interatomic distances and bond angles with chemical structure. This correlation is based largely on the electron theory of valence, originally suggested by *Gilbert N. Lewis* in 1916. *Pauling* discussed some conclusions of his own theory on resonance concerning molecules where an unambiguous assignment of a simple valence-bond structure cannot be made. *Pauling*'s examples were: the porphin nucleus, uric acid, anthocyanidins, β-carotene, and an extended polypetide chain.

4 Volumes 4–27: Edited in Pasadena

Volume Four was published in Vienna in 1945—shortly after the war, when printing paper was scarce. The title pages of Volume Four included the following names listed as members of the editorial board: *A. Butenandt*, *U. Westphal* (Berlin) and *L. Zechmeister* (Pasadena).

Ulrich Westphal was an assistant of *Butenandt.* He became known for his investigations on the biosynthesis of sex hormones at the Kaiser Wilhelm Institute in Berlin (*77*). He habilitated in 1941, and became professor in Tübingen seven years later. From 1949, *Westphal* worked at the *Field Research Laboratory* in Kentucky (*78*).

Interestingly, as of Volume Five (1958), *Zechmeister* was listed as the sole editor until 1969.

4.1 Volume Four: European Research Results during World War II

Volume Four comprises contributions exclusively from Europe—it seems to be a volume referring to important developments during the time of war: *Rudolf Tschesche* from Berlin reported on "The Chemistry of Plant Cardiac Glycosides, Toad Venoms, Saponins and Sterol Alkaloids" (*Z22*), *Theodor Wieland* and *Irmentraut Löw* from Heidelberg presented a contribution entitled "On the Biochemistry of the Vitamin B Group" (*Z23*), *Robert Purrmann* from Munich

wrote about pterins (a group of insect pigments) (*Z24*), *Gerhard Schramm* from Berlin-Dahlem gave a status report on "The Biochemistry of Viruses" (*045*), *Karl Bernhard* and *Harold Lincke* from Zurich summarized new findings in the area of biological oxidations (*Z26*), and finally, *H. J. Trurnit*, from the Physiological Institute of the University of Heidelberg, provided a chapter entitled "On Monomolecular Films at Water Interfaces and Laminated Films" (*Z27*).

Rudolf Tschesche (1905–1981) had studied the chemistry of toad venoms and cardiac glycosides since the mid-1930s. Born in Liegnitz, *Tschesche* became a student of *Karl Heinrich Slotta* in Breslau. In 1933, he habilitated in Göttingen but due to disagreements with the National Socialism regime, he was denied a university lectureship. During the war he served as director of the department for chemotherapy at Schering AG in Berlin. In 1947, he became an associate professor at the University of Hamburg and in 1960 he followed *Burckhardt Helferich* as professor at the University of Bonn.

Theodor Wieland (1913–1995), who worked as lecturer in Heidelberg from 1942 and as associate professor in Mainz from 1946, was the son of *Nobel* laureate *Heinrich Wieland* (1877–1957). Ever since going to work with *Richard Kuhn* (1910–1976) in Heidelberg, where he went after having earned his doctorate under his father, he studied pantothenic acid in particular. His co-author, *Irmentraut Löw*, was a long-time assistant of *Richard Kuhn*.

Gerhard Schramm (1910–1969) studied under *Adolf Windaus* and *Heinrich Wieland* and is regarded as one of the pioneers in virus research. *Schramm* was a coworker of *Adolf Butenandt* in the course of a joint virus research project that started in 1937. *Schramm*, who previously worked on the enzymatic modification of steroid hormones and cholesterol, followed *Butenandt* from Danzig to Berlin and visited *Theodor Svedberg* in Uppsala to get acquainted with advanced techniques of analytical ultracentrifugation (*79*).

Another student of *Heinrich Wieland*, *Robert Purrmann* (1914–1992), succeeded in proving the structure of pterins by synthesizing leucopterin in 1940 (*80*). *Wieland* termed the basic structure, from which pterins are derived, "pteridine" (**2**). In 1948, *Purrmann* founded the ESPE factory for pharmaceutical products in Seefeld, Bavaria. Today, *Purrmann*'s company forms a subsidiary of 3M.

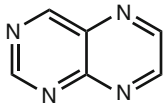

2 (pteridine)

Karl Bernhard (1905–1993) was born in Winterthur. After his university education in Zurich he was promoted in Geneva in 1932. In 1938, he habilitated in Zurich. The next year, *Bernhard* was appointed professor and director of the Physiological-Chemical Institute in Basel. Moreover, he was director of the Swiss "Vitamininstitut". His major fields of interest were lipid metabolism and carotenoids. *Bernhard* was a member of the "Deutsche Akademie der Naturforscher Leopoldina".

Hans Joachim Trurnit (1907–1980) belonged to the broader network of scientists involved in *Butenandt*'s virus research project at the Pathological Institute of the Charité in Berlin (*79*). Born in Essen, *Trurnit* studied in Hamburg, Kiel, and Heidelberg. From 1943 to 1945, he was director of a laboratory run by the "Reichsministerium für Wirtschaftsaufbau" at the castle of Babenhausen. He became well known for his technique of producing monomolecular protein films (on glass) and the interferometric measurement of the layer thickness of such films. Soon after the war, *Trurnit* was granted U.S. citizenship and subsequently worked at the Medical Division of the Army Chemical Center in Maryland. He died in Palo Alto, California.

4.2 Volume Five: Both Americas Are Gaining Ground

When Volume Five (edited in 1948) is considered, the situation is quite different. No less than eight out of its eleven contributions were written by authors from the U.S. (of which six came from universities or research institutes in California). Additionally, one contribution each was submitted from Buenos Aires, Zurich, and Liverpool.

An important focus of the subjects covered was on wood research—with, in particular, cellulose and lignin being addressed. As *Friedrich Emil Brauns* mentions in a preliminary statement to his contribution, significant successes in lignin research had been achieved within the preceding years (*Z37*). *Brauns*, born in 1890, received his PhD in Berlin in 1915, was awarded a Fulbright lectureship at Osaka University Nishinomiya (Japan) and worked at the Institute of Paper Chemistry in Appleton, Wisconsin. In 1956, he became professor of chemistry at the Science Research Institute in Oregon (*81*).

Two contributions of Volume Five were about carotenoids (*Z28*, *Z29*), and the others were on azulenes (*Z30*), fats (*Z31*), enzymatically synthesized polysaccharides (*Z32*), cellulose (*Z33*), toad venoms (*Z35*), fish proteins (*Z36*), and genetics (*Z37*). With *Paul Karrer* (1880–1971), *Nobel* laureate of 1937, probably the outstanding authority in the field of carotenoids could be won over. *Karrer* provided a relatively short report on the state of research concerning carotenoid epoxides (*Z29*).

Researchers from California who contributed to Volume Five were: *Denis L. Fox*, two experts on polysaccharides, *Michael Doudoroff* and *William Zev Hassid* as well as *Arie Jan Haagen-Smit*, *George Wells Beadle*, and *Robert S. Rasmussen. Denis Llewellyn Fox* (1901–1983), who was born in Udimore, Sussex, England, and who had worked at the Division of Marine Biology of the Scripps Institution of Oceanography, University of California, San Diego, La Jolla since 1931 (*82*), was a world authority in animal pigments (*83*). As we know from a letter by *Linus Pauling* dated November 10, 1944, *Zechmeister* was informed about *Fox*'s research projects (*84*). Furthermore, in 1952, *Zechmeister* published a paper about the marine "blood worm" together with *Fox et al.* (*85*).

Michael Doudoroff (1911–1975) was born in St. Petersburg. The family left Russia shortly before the October revolution for Tokyo and finally moved to Palo

Alto in 1930. *Doudoroff* provided the first substantial evidence that an enzyme may function as a glucosyl carrier. His investigations of glucose oxidation resulted in the discovery of a major pathway of glucose degradation in bacteria, the *Entner-Doudoroff* pathway (*86*).

William Zev Hassid (1899–1974) was originally from Jaffa, Palestine, but spent most of his childhood in a village in the Russian Ukraine (*87*). In 1920, he immigrated to the United States. He was appointed professor of plant nutrition in 1947, and professor of biochemistry at the University of California, Berkeley in 1950 (*88*).

At the time when he was writing his essay on "Azulenes", *Arie Jan Haagen-Smit* (1900–1977) was employed at the California Institute of Technology, Pasadena. *George Wells Beadle* (1903–1989), future *Nobel* laureate and working at CalTech as well, contributed to Volume Five with a contribution summarizing "Some Recent Developments in Chemical Genetics" (*Z37*).

Regarding methodology, the contribution by *Robert S. Rasmussen* of the Shell Development Company in Emeryville, California, entitled "Infrared Spectroscopy in Structure Determination and its Application to Penicillin" (*Z38*), is especially noteworthy.

A contribution on toad venoms by *Venancio Deulofeu* was the first submitted for publication in "Fortschritte" from South America (*Z35*). *Venancio Deulofeu* (1902–1984) studied at the Facultad de Ciencias Exactas, Físicas y Naturales de la Universidad de Buenos Aires. *Zemplén*'s work on the degradation of acetylated aldononitriles inspired *Deulofeu* to start investigations in the field of carbohydrates, which was virgin territory at that time in Latin America (*89*). From 1939 on, *Deulofeu* was titular professor in Buenos Aires. In the introduction of his paper, *Deulofeu* reminded us that *H. Wieland* and *R. Alles* had been the first to isolate bufotoxin in 1922.

In his contribution "Recent Advances in the Study of Component Acids and Component Glycerides of Natural Fats" (*Z31*) *Thomas P. Hilditch* reported on relevant research results obtained since the publication of his first contribution in Volume One.

Eugen Pacsu from Budapest also summarized then current research results in his contribution on "Recent Developments in the Structural Problem of Cellulose" (*Z33*). *Eugene (Jenö) Pacsu* (1891–1972) studied under *Zemplén* at the University of Budapest, worked for the U.S. Public Health Service at Bethesda, Maryland, beginning in 1929 and became professor at Princeton University in 1947.

Finally, *Ernest Geiger* from the Department of Pharmacology, University of Southern California Medical School in Los Angeles commented on the "Biochemistry of Fish Proteins" (*Z36*). *Ernest Geiger* (1896–1959) received his medical degree in his native country of Hungary from the University of Pécs. His academic career led him from being an assistant instructor in pharmacology at the University of Graz to Pécs. For 3 years he served as Research Director of Gideon Richter Ltd. in London, after which he came to the United States and became a naturalized citizen. Subsequently, he became Director of Research at the *Van Camp* Laboratories and held this position for 19 years. During this period he studied and qualified for the degree of Doctor of Philosophy at the University of Southern California, which he finally received in 1947 (*90*). Following this he served as professor in biochemistry

and nutrition in Los Angeles. *Ernest Geiger* was particularly interested in the digestion, absorption, and metabolism of proteins as well as in the measurement of the thyroid cell height.

4.3 *Volume Six: A New Sign of Life from the Viennese School of Phytochemistry*

The first contribution of Volume Six, published in 1950, was by *Harry James Deuel Jr.* (1897–1956) and *Samuel M. Greenberg* from the Department of Biochemistry and Nutrition, University of Southern California, Los Angeles, and on fat chemistry (*Z39*). *Deuel*'s studies demonstrated the high nutritive value of vegetable fats, proving that there are no particular requirements for saturated fatty acids. *Zechmeister* and *Deuel* were closely connected—not only due to their intense and more than 10-year long scientific collaboration in the field of research on vitamin A—but also by a personal friendship (*91*).

Volume Six also included a text by *Edgar Lederer* (1908–1988). Until 1930, *Lederer* had been a co-worker of *Ernst Späth* at the II Chemical Institute in Vienna. In 1933, he emigrated from Heidelberg to Paris. After the war, he first was Maître de Recherche and later Directeur at the Centre National de la Recherche Scientifique. His contribution to Volume Six was entitled "Odeurs et Parfums des Animaux" ("Odors and Smells of Animals") (*Z40*).

The fledgling lecturer *Otto Hoffmann-Ostenhof* (1914–1992) from the I Viennese Chemical Institute was also a contributor in this same volume. His paper was entitled "Vorkommen und biochemisches Verhalten der Chinone" ("Occurrence and Biochemical Behaviour of Quinones") (*Z41*). *Hoffmann-Ostenhof* had studied in Vienna and Innsbruck before he went to work with *Paul Karrer* in Zurich, where he investigated the syntheses of different tocopherols. After World War II, he became an assistant in Vienna and was appointed titular professor in 1959.

Like Volume Five, Volume Six also included a contribution from Argentina. In the introduction of his chapter on cactus alkaloids, *Ladislao Reti* (1901–1973), of the Compañía Nacional para la Industria Quimica "Atanor", referred to certain indigenous tribes who had been using peyote for many centuries (*Z42*). The first time this substance was mentioned in writing dates back to the Franciscan monk *Bernardino de Sahagún* in 1560. The author, *Ladislao Reti*, was an organic chemist who was born in Fiume (Rijeka, Croatia) and received a degree in chemical engineering from the Technische Hochschule in Vienna. Reti moved to Argentina, where he founded Atanor Chemical Industries in São Paulo. Later in life, *Reti*'s interest turned more and more to the history of science (*92*, *93*).

The penultimate paper of Volume Six was written by *James Frederick Bonner* (1910–1996) from Pasadena and was given the title "Plant Proteins" (*Z43*). *Bonner* found out that certain proteins of the cell nucleus, called histones, are responsible for turning genes off (*94*). Volume Six concluded with an addendum to his previous contribution on fluorescence spectroscopy by *Charles Dhére* (*Z44*).

4.4 *Volume Seven: Contributions from Great Britain, Switzerland, and the U.S.*

To this day, the conclusion of the fourth contribution of Volume Seven entitled "Penicillin and its Place in Science" (*Z48*) is still worth reading. This chapter, written by *Arthur Herbert Cook* (1911–1988), from a brewing industry laboratory at Nutfield, Surrey, England was published in 1950 and gave a remarkable impression of the rapid developments in this field since 1940. In *Cook*'s own words it read, *"Stupendous as has been the impact of the penicillins on medicine, it has as well an importance as a milestone along so many of the roads in science. Perhaps for the first time it has focussed attention on the natural phenomena of antibiosis, it is leading to new concepts and techniques in elucidating the metabolism of bacteria; it has most effectively opened up many hitherto neglected fields of heterocyclic organic chemistry, and it has been the means of bringing into existence an industry which even ten years ago was completely unknown."*

The other contributions of Volume Seven focused on the constitution of triterpenes (*Z45*) and aglycones (*Z46*), on thyroxines (*Z47*), Senna (*Z49*), and the chemistry of antibodies (*Z50*). The contribution on triterpenes was written by *Oskar Jeger* (1917–2002) from ETH Zurich, who was a student of *Ružička*. Also *Hans Heusser* (1917–1982), the author of the paper on aglycones, studied under *Ružička*. He was promoted in Zurich as a result of work performed on this same class of compounds in 1945.

In their contribution on "Sennosides A and B, the Active Principles of Senna" (*Z49*), *Arthur Stoll* (see Volume One), at that time President of the Chemische Fabrik Basel (formerly Sandoz), and his co-worker *B. Becker*, pointed out that the earliest mention of this plant dates back to the nineth century, when Senna first appeared among medications used by certain Arabs. In 1936, *W. Straub* and *H. Gebhardt* demonstrated that the active principles of Senna must be anthranol glycosides (*95*). A few years later, *Stoll* and *Becker* succeeded in the isolation of sennosides A and B in their pure crystalline forms. They proposed the structure **3**.

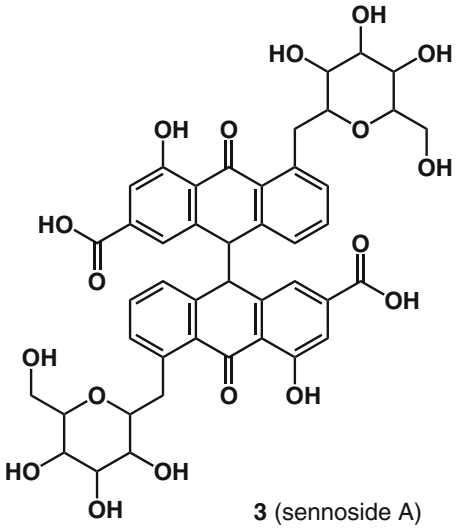

3 (sennoside A)

Now to the remaining contributions to Volume Seven submitted from the USA. A contribution on thyroxine (*Z47*) was written by *Zechmeister*'s colleague in Pasadena, *Carl G. Niemann* (1908–1964). *Niemann* came to CalTech in 1937, and started to study the structure of proteins together with *Pauling*. *Niemann* and *Pauling* came to the conclusion that polypeptides are held together primarily by hydrogen bonds. In the following years, *Niemann* focused on the investigation of reactions induced by digestive enzymes such as chymotrypsin (*96*).

The report on "Some Recent Developments in the Chemistry of Antibodies" (*Z50*) was submitted by *John Warren Williams* (1898–1988) from Madison, Wisconsin. *Williams* was convinced that closer insights into the physical behavior of polymers would be useful in understanding proteins. Already during the time of World War II, he had used ultracentrifugation and electrophoresis to measure size and purity of fractionated proteins and succeeded in subfractionating an antibody-containing γ-globulin. He was well known to *Zechmeister* because he was a visiting professor in Pasadena in 1946/1947 and 1953/1954 (*97*).

4.5 Volume Eight: Traditional Centers of Research on the Chemistry of Natural Products Back on Stage

In his contribution in Volume Eight, *Arthur B. Lamb* (1880–1952) from Harvard University stated, *"One cannot but stand in awe at the energy and virtuosity of the organic chemists, who with infinite patience … have deciphered the arrangements of the atoms in molecules as complex as those discussed in this Volume, namely the nucleotides, the alkaloids of the lupins and of ipecacuanha, the Flechtenstoffe [lichen compounds], and the essential constituents of the aroma of the violet"* (*98*). About the first chapter of Volume 8 *Lamb* said, *"One cannot but be astonished at the remarkable cellulosic fine-structure of the cell walls of plants, and the power of the techniques that have been used in their study"* (*98*). The contribution mentioned was entitled "Fine Structure of Cellulose" and was written by *Albert Frey-Wyssling* and *Kurt Mühlethaler* (*Z51*). *Albert Frey-Wyssling* (1900–1988) was professor of general botany at ETH Zurich. *Kurt Mühlethaler* (1919–2002), a molecular biologist at ETH, became known as one of the scientists who developed the technique of freeze-etching, which enables excellent imaging of the ultrastructure of cellular objects in an electron microscope's high vacuum. According to *Zechmeister*, the opening contribution of Volume Eight was *"a wonderful work, which would give great pleasure to our readers"* (*99*).

Concerning the second contribution from the Chemistry Department at Birmingham University written by *M. Stacey* and *C. R. Ricketts* "Bacterial Dextrans" (*Z52*), *Lamb* mentioned how he was impressed by the many possibilities opening up due to recently acquired knowledge on dextran in the context of blood transfusion. *Maurice Starcey* (1907–1994) obtained BSc, PhD, and DSc degrees at Birmingham

University under *Norman Haworth* and *Edmunt Hirst*. In 1946, he was promoted to Mason Professor. His main interest in the chemistry of polysaccharides covered the bacterial polyglucose dextran, which he helped to develop as a blood plasma substitute (*100*).

Luis Federico Leloir (1906–1977), the author of the text "Sugar Phosphates" (*Z53*) was originally from Paris, but immigrated to Argentina when he was a child. He was awarded the *Nobel* Prize in Chemistry in 1970 for the discovery of sugar nucleotides as an Argentinian biochemist. *Leloir* took over the chair of physiology at the University of Buenos Aires in 1941, but also worked at the Instituto de Investigaciones Biochimicas in Buenos Aires.

The next contribution was written by *George Wallace Kenner* (1922–1978), former postdoctoral associate of *Vladimir Prelog* at ETH Zurich in the late 1940s and later a professor at the University Chemical Laboratory in Cambridge (*101*). The title was "The Chemistry of Nucleotides" (*Z54*). *Hans Schinz* (1899–1990), a student of *Ružička* at ETH, published the following essay, entitled "Die Veilchenriechstoffe" ("The Odorous Substances of Violets") (*Z55*). The essential point of this contribution was the synthesis of α-irone, which was performed simultaneously by *Schinz, Ružička, et al.* as well as by *Y. R. Naves* and co-workers in 1946/1947.

In Volume Eight, *Yasuhiko Asahina*, the lichen specialist, received another chance to write on the "New Developments in the Field of Lichen Substances" (*Z56*). One could believe that around 1950 there were no other experts on lichens—but this is actually incorrect considering the expertise of *Georg Koller* (1894–1985). *Koller* habilitated under *Späth* at the II Chemical Institute in Vienna in 1930. *Koller* elucidated the structures of umbilicaric acid (*102*), pinastric acid (*103*), diploschistic acid (*104*), and other compounds. In 1934, he received a big surprise while studying a substance extracted from *Evernia furfuracea*: in a derivative of *para*-orsellinic acid he was able to detect organically bound chlorine for the first time (*105*). In fact, *Koller*'s achievement was acknowledged in Volume 68 of the Series, dedicated to "Naturally Occurring Organohalogen Compounds" (*Z346*) under reference *1662*. The reason why *Koller* was not given an opportunity to write a contribution for the Series was not a scientific one, since *Koller* had been an exposed member of the NSDAP. He was removed from his university position in 1945 and, as a result, was unable to find another position (*106*).

Nevertheless, two members of the II Chemical Institute of the University of Vienna contributed to Volume 8: *Friedrich Galinovsky* (1908–1957) and *Matthias Pailer* (1910–2011). *Galinovsky* wrote the contribution on "Lupinen-Alkaloide und verwandte Verbindungen" ("Lupine Alkaloids and Related Compounds") (*Z57*), in which he pointed out the tricyclic structure of cytisine, discovered by *Späth* and himself around 1936. *Pailer* was responsible for the paper on ipecac alkaloids. *Pailer*—like *Galinovsky*—was a student of *Späth. Pailer* habilitated in organic chemistry in Vienna in 1949, took over the chair of food chemistry in 1969, and was appointed full professor of pharmaceutical chemistry in 1971. One of his most important achievements was the elucidation of the molecular constitution of emetine (**4**) (*107*). *Pailer* described in detail structural determinations in his contribution (*Z58*).

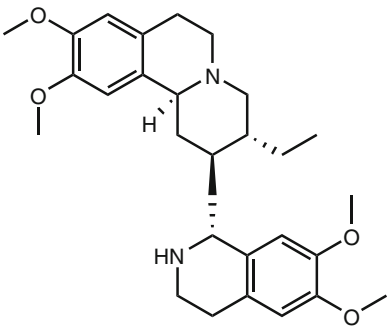

4 (emetine)

From a methodological point of view, the contribution written by *Robert Brainard Corey* (1897–1971) from Pasadena (*Z59*) is important. *Corey* revealed the then latest results of X-ray diffraction studies on crystalline amino acids. At the end of his contribution, *Corey* provided a perspective on the possible structures of peptides. Helices were not mentioned in this context yet, but this would be changing soon.

Finally, we owe the last contribution to Volume Eight to the editor of this Series, *László Zechmeister*, and *Margarethe Rohdewald* from Bonn. The authors addressed "Some Aspects of Enzyme Chromatography" (*Z60*). *Margarethe Rohdewald* (1900–1994) was a former PhD student of *Richard Kuhn*. Before the war, she had been *Richard Willstätter*'s closest co-worker for many years (*108*). It was *Arthur Stoll* who established the contact between *Margarethe Rohdewald* and *Zechmeister*, as he emphasized in a letter to *Zechmeister* that he would be glad if this most loyal disciple of *Willstätter* could be supported in utilizing her enormous experience for scientific purposes (*109*). In 1949, *Margarethe Rohdewald* became a research fellow at the Gates and Crellin Laboratories under *Zechmeister* (*110*).

4.6 Volume Nine: Papers from All Over Europe and California

In Volume Nine published in 1952, a contribution by *Hans Herloff Inhoffen* (1906–1992) and *Harm Siemer* from TH Braunschweig, entitled "Synthetic Chemistry of Carotenoids" (*Z61*), is particularly worth mentioning. *Inhoffen* was deputy head of the main scientific laboratory at Schering AG in Berlin from 1936 to 1945. During his time in Berlin, *Inhoffen*, who worked with *Walter Hohlweg* (1902–1992), a former assistant of *Eugen Steinach* (1861–1944) from Vienna, gained outstanding success regarding the development of orally active estrogen and gestagen preparations. These results constituted important steps towards the development of the "pill" (*111*). *Inhoffen* habilitated in 1943, became a lecturer in Marburg, and in 1946 professor of organic chemistry at TH Braunschweig. In 1950, *Inhoffen et al.* reported on a total synthesis of β-carotene (*112*), and, on the basis of this, an industrial process was developed subsequently (*113*).

Regarding the other papers of Volume Nine, *James G. Baxter* (Distillation Products Industries, Rochester, N.Y.) was responsible for a contribution on vitamin A synthesis (*Z62*). During World War II, *Baxter* undertook great efforts in separating and determining vitamin A from fish liver oils.

Paul Meunier (1908–1954), professor at the Faculté des Sciences de Lyon, reported on antivitamins (*Z63*), *Arthur Stoll* (Basel), already mentioned several times, on ergot alkaloids *(Z64)*, *Masao Tomita* (University of Tokyo) on alkaloids of the Menispermaceae (*Z65*), *Francis Medcalf Dean* (*1925), lecturer at the University of Liverpool, on coumarins (*Z66*), *Herman Moritz Kalckar* (1908–1991) from the University of Copenhagen, the founder of bioenergetics and former postdoctoral research fellow at the California Institute of Technology in 1939, on "The Enzymes of Nucleoside Metabolism" (*Z68*), and *W. S. McNutt* (School of Medicine, Nashville, Tennessee) on "Nucleosides and Nucleotides as Growth Substances for Microorganisms" (*Z69*). *Walter Scott McNutt* (*1918) earned his PhD degree at the University of Wisconsin. From 1951 to 1953 he was a research fellow at CalTech. In 1959, he became professor of pharmacology at the School of Medicine at Tufts University.

Henry Borsook (1897–1984) was working as professor of biochemistry at the division of biology at CalTech (*114*) when writing his essay on the "Biosynthesis of Proteins and Peptides, Including Isotopic Tracer Studies" *(Z67)*. A further colleague of *Zechmeister* at CalTech, *Dan Hampton Campbell* (1908–1974), together with his assistant *Norman Bulman* provided the final contribution on "Some Current Concepts of the Chemical Nature of Antigens and Antibodies" (*Z70*). *Dan Hampton Campbell* was *the* great pioneer in immunochemistry of his time.

4.7 Volumes 10–27: Still Bearing Zechmeister's Signature

Counting all the contributions of Volumes 1–27 that were submitted by colleagues at *Zechmeister*'s home university—ETH Zurich—there are as many as eight. And no less than 24 contributions were written by scientists associated with the California Institute of Technology (*33*)—so *Zechmeister*'s signature is therefore undoubtedly recognizable.

4.7.1 Volume 10

In his review of Volume Ten in an issue of the *Journal of the American Chemical Society* of 1954 (*115*), *Carl Djerassi* (*1923)—one of the leading experts in the field of steroid chemistry at the time—wrote about a paper by *George Rosenkranz* (*1916) and *Franz Sondheimer* (1926–1981) entitled "Synthesis of Cortisone" (*Z74*): *"[it] covers a subject of great current interest as shown by the fact that five other extensive reviews covering the same ground appeared during 1953 and that approximately 150 of the references apply to articles published since 1951.*

There is little question that the present chapter is the most complete one." Rosenkranz was born in Budapest. He studied under *Leopold Ružička* (1887–1976) in Zurich, and emigrated initially to Cuba and later to Mexico in 1945, where he started working for Syntex. Syntex was involved in the production of cortisone from plant precursor molecules. *Rosenkranz*'s research team was subsequently reinforced with the young chemist *Carl Djerassi* in 1949. In 1951, *Djerassi*'s research group produced norethisterone, a 19-*nor*-analogue of a compound that had been synthesized by *Inhoffen* some years earlier (*116*).

In the contribution that follows, *Kurt Alder* (1902–1958) and *Marianne Schumacher* (Institute of Chemistry, University of Cologne) discussed the progress that had been achieved in diene synthesis since *Otto Diel*'s contribution to the Series in 1939 (*Z71*).

Furthermore, *Hermann Mark*—who, following his emigration, was employed at the Polytechnic Institute of Brooklyn—gave an overview on the "Physical Chemistry of Rubbers" (*Z72*). As *Carl Djerassi* noted in his review of Volume 10: *"the inclusion of this chapter in the present volume [is] somewhat surprising since the other chapters deal with strictly organic chemical subjects"* (*115*).

Jean Asselineau and *Edgar Lederer* (Paris) devoted their contribution to the "Chimie des Lipides Bactériens" ("Chemistry of Bacterial Lipids") (*Z73*). *Asselineau* and *Lederer* established that mycolic acids represent major and specific components of the cell envelope of mycobacteria, including *Mycobacterium tuberculosis* (*117*).

Asima Chatterjee, affiliated with the University College of Science and Technology in Calcutta, reported on *Rauwolfia* alkaloids (*Z75*). *Asima Chatterjee* (1917–2006) was the first woman to be conferred a doctorate of science by an Indian university, in 1944. In 1948/1949, she undertook a postdoctoral fellowship at CalTech, where she worked with *Prof. Zechmeister*, and spent the following year at *Paul Karrer*'s institute. In 1962, *Chatterjee (née Mookerjee)* was bestowed with the prestigious Khaira Professorship of Chemistry at the University of Calcutta.

Louis Feinstein and *Martin Jacobson* (Beltsville, Maryland) gave an insight into the topic "Insecticides Occurring in Higher Plants" (*Z76*). *Martin Jacobson* received his PhD degree in chemistry at the City University of New York. From 1964 to 1972, *Jacobson* worked as a Project Leader at the U.S. Department of Agriculture's Entomological Research Division, Beltsville, Maryland. Later on, he became head of the Biologically Active Natural Products Laboratory (*118*). *Louis Feinstein* was born in 1912. He earned his PhD at the University of Georgetown and became head of the Seed Quality Laboratory, USDA, Beltsville, in 1967.

4.7.2 Volume 11

Volume 11 was published in 1954. In its first contribution, *Stanley Peat* (1902–1969) from the University College of North Wales, stressed how enzymological studies had played an important role in elucidating the constitution of starch (*Z77*).

Karl Freudenberg (University of Heidelberg, see Volume Two) reported again on new results in lignin research (*Z78*). Lignin chemistry had long been struggling with the question of if this natural product represented nothing other than a structure-less pile of different substances or if it actually follows a strict organizational order. *Freudenberg* pointed out that a principle of organization was emerging in which dehydration reactions of coniferyl alcohol were to play a major role.

Hans Herloff Inhoffen (see Volume Nine) and *Klaus Brückner* dedicated the third contribution of Volume 11 to recent progress in the field of vitamin D chemistry (*Z79*). After *Windaus* had stipulated the basic constitution of vitamin D_2 in 1936, many questions concerning the fine structure remained unanswered. At the time this contribution was written, total synthesis was still beyond the then current chemical capabilities. It was not until 1959 that *Inhoffen et al.* reported on the partial syntheses of vitamins D_2 and D_3 (*119*).

In his contribution on "Natürlich vorkommende Chromone" (Naturally Occurring Chromones) (*Z80*), *Hans Eduard Schmid* (1917–1976) mentioned that by 1953, 11 plant compounds had been identified as chromones. *Schmid* himself determined the relatively simple structure of eugenitin and its derivative eugenone (**5**). In the early 1940s, *Späth* and his students succeeded in elucidating the properties of peucenin and visnagin. This was well known to *Schmid*, who earned his doctorate under *Späth* in Vienna and who returned to his home country of Switzerland in 1942.

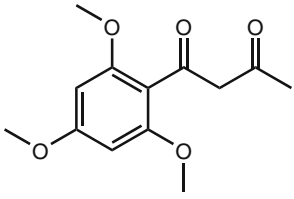

5 (eugenone)

It was only in Volume 11—published in 1954, the year that he was awarded the *Nobel* Prize in Chemistry—that *Pauling*, together with *Robert B. Corey* from Pasadena, reported on groundbreaking views on the helical configuration of polypetide chains (*Z81*). In this contribution, we learn about α- and γ-helices as well as parallel- and antiparallel-chain pleated sheet structures. *Corey*'s biographer, *Richard Edward Marsh*, referring to the papers published by *Pauling* and *Corey* in the early 1950s, stated, *"The age of molecular biology had arrived"* (*120*).

The next contribution to Volume 11 was by *Walter A. Schroeder* (1917–2001), on "Column Chromatography in the Study of the Structure of Peptides and Proteins" (*Z82*). In July 1941, *"Walt" Schroeder* was recommended by *Linus Pauling* in connection with being appointed assistant to *Zechmeister* (*121*). Indeed, *Walter Schroeder* became subsequently a member of the CalTech Chemistry Faculty at Pasadena (see Fig. 1).

Volume 11 was concluded by a paper by *Max Rudolf Lemberg* (Sydney) about "Porphyrins in Nature" (*Z83*), and a contribution by *Adrien Albert* (Canberra)

entitled "The Pteridines" (*Z84*). The great biochemist *Max Rudolf Lemberg* (1886–1975) was originally from Breslau (today known as Wrocław). *Lemberg* found a patron at the University of Heidelberg—in *Karl Freudenberg*—and later immigrated to Sydney in 1935. *Adrien Albert* (1907–1988) was born in Sydney and was a research fellow at the Wellcome Research Institute, London, before being appointed foundation professor of medical chemistry at the Australian National University in 1949.

4.7.3 Volume 12

In Volume 12 (published in 1955), *George Wells Beadle* (1903–1989), who at that time was working at CalTech, Pasadena, like *Zechmeister*, and who was to be awarded a *Nobel* Prize three years later, described a sensational discovery in his contribution "Gene Structure and Gene Action" (*Z93*), *"In 1953, Watson and Crick proposed a structure of DNA that may well represent one of the most significant advances in biology in recent years."* A reviewer of Volume 12 was enthusiastic: *"This is the most exciting chapter, since it moves the frontiers of science so close to the very key problems of life, gene function and reproduction"* (*122*).

The same volume contained an overview of the performance capability of paper chromatography in the study of peptide and protein structures, by *Edward Owen Paul Thompson*, and *Adrienne R. Thompson* (*Z90*), of the Wool Textile Research Laboratories at the Commonwealth Scientific and Industrial Research Organisation, Melbourne, Australia. In 1952, the two-time *Nobel* laureate *Frederick Sanger* (1918–2013) and the Australian biochemist *Edward Owen Paul Thompson* (1925–2012) determined the sequence of the glycyl chain of insulin using two-dimensional paper chromatography (*123*).

Arie Jan Haagen-Smit, whom we know already from Volume Five, began his essay on "Sesquiterpenes and Diterpenes" with the comment that two dozen years after *Wallach* started categorizing the terpenes (in 1890), the structures of most of the more than one hundred monoterpenes then isolated were well established (*Z85*). In the 1950s, when chromatographic procedures became regular experimental tools for the terpene chemist, a rapid expansion of knowledge took place, especially in sesqui- and higher terpene chemistry.

Ewart Ray Herbert Jones (1911–2002) and *Thomas G. Halsall* from Manchester, when reporting on then recent research results in "Tetracyclic Triterpenes", pointed to the fact that the discovery of a close structural relationship between triterpenes and steroids was of outstanding importance (*Z86*).

Rudolf Tschesche, whom we have also met before, discussed questions concerning the biogenesis of steroids in his contribution on new developments in the field of steroid biosynthesis and related natural products (*Z87*). Tracer technology enabled *Tschesche* to gain deep insights, which would not have been possible by other means.

Other contributions of Volume 12 were dedicated to the following subjects: fungal carotenoids, discussed by *Francis Theodore Haxo* (1921–2010) from the

Scripps Institution of Oceanography in La Jolla, California (*Z88*); pyrrolizidine alkaloids *(Z89)*, described by *Frank Louis Warren* (1925–1967) of the University of Natal, Pietermaritzburg, South Africa; and a final paper on iodine-containing amino acids and iodoproteins (*Z91*) by *Jean Roche* (1901–1992) and *Raymond Michel*, Collège de France, Paris.

In his contribution on snake venoms, *Karl Heinrich Slotta* (1895–1987), São Paulo, Brazil, reported that in 1938, he and his brother-in-law, *Heinz Ludwig Fraenkel-Conrat* (1910–1999), succeeded in obtaining a snake venom component—namely, crotoxin—in its crystalline form for the first time (*Z92*). Crotoxin shows strong enzymatic activity, which led to the hypothesis that the toxic effect might be identical to the enzymatic one. In the meantime, components of several more snake venoms had been isolated or even crystallized, respectively, such as hemolysin. *Slotta* immigrated to Brazil during the Nazi regime in Germany. *Fraenkel-Conrat,* who had Jewish ancestors, emigrated from Breslau in Germany to Edinburgh in Scotland in 1936, and later to New York and finally to Berkeley.

4.7.4 Volume 13

Recent years had seen a consolidation and critical appreciation of infrared (IR) spectroscopy—which was the starting point of *Andrew Reginald Howard (A. R. H.) Cole'*s contribution entitled "Infrared Spectra of Natural Products" (*Z94*). As of the early 1940s, IR spectroscopy was used routinely. A firm basis for its application in structure determinations was established by authors such as *Robert Bowling Barnes*, *Robert Cummins Gore,* and *Van Zandt Williams* at the Stanford Research Laboratories of the American Cyanamid Company, Connecticut, *Harrison McAllister Randall* at the University of Michigan, as well as *Harold Warris Thompson* at Oxford University. *Cole*'s contribution contains the following topics: IR methods, instruments and sampling techniques, applications, compound comparison, and structural analysis. *Cole* (*1924), when writing the above-mentioned paper, was a senior lecturer at the University of Western Australia. He actively contributed to many advances in the field of IR spectroscopy, both in terms of instrumental development and in the use of this technology to answer structural questions.

In his summary on "Natural Tropolones and Some Related Troponoids" (*Z97*), *Tetsuo Nozoe* (1902–1996) of Tohoku University Sendai, Japan, mentioned that *Michael J. S. Dewar* (1918–1997) proposed a seven-membered enolone structure for stipitatic acid and the alkaloid colchicine and that he named the parental structure "tropolone". As early as 1941, *Nozoe* himself expressed his conjecture that hinokitiol (today called 4-isopropyltropolone) might contain a seven-membered ring (*124*). *Nozoe* mentioned subsequently a study by the Austrian chemist *Simon Zeisel* (1854–1913), who succeeded in determining the molecular formula of the meadow saffron alkaloid, colchicine, in 1883 (*66*, *125*).

Furthermore, *Otto Theodor Schmidt* (1894–1972, Heidelberg), a former student of *Willstätter*, gave an overview entitled "Gallotannine und Ellagengerbstoffe" ("Gallotannins and Ellagitannins") (*Z95*).

Christoph Tamm reported on "Neuere Ergebnisse auf dem Gebiet der glykosidischen Herzgifte: Grundlagen und Aglykone" ("Recent Results in the Field of Cardiac Glycosides: Principles and Aglycones"). In continuation of this contribution, *Tamm* submitted a contribution partially entitled "Zucker und Glykoside" ("Sugars and Glycosides") to Volume 14 (*Z102*). For biographical data on *Christoph Tamm*, see Sect. 5.1.

James Robert Price (1912–1999, Melbourne) introduced his readership to "Alkaloids Related to Anthranilic Acid" (*Z98*), *Asima Chatterjee* and *Satyesh C. Pakrashi* (Calcutta) together with *G. Werner* (São Paulo) summed up "Recent Developments in the Chemistry and Pharmacology of *Rauwolfia* Alkaloids" (*Z99*), and last but not least new information was provided on "Synthese von Peptiden" ("Synthesis of Peptides") (*Z100*), thanks to *Wolfgang Grassmann* (1898–1978) and *Erich Wünsch*, from the Max Planck Institute of Protein and Leather Research in Regensburg. In this contribution the authors pointed out that already by 1904, *Theodor Curtius* (1857–1928)—a student of *Bunsen*—was able to synthesize polypeptides (*126*). Nevertheless, it was not before 1949 that rapid developments came about in this research area.

4.7.5 Volume 14

With 377 pages, Volume 14 was much shorter than its predecessor. From the first essay by *Ferdinand Bohlmann* (1921–1991) and *Heinz-Jürgen Mannhardt* the reader got to know that in the years before publication of Volume 14 (1957), it was discovered that acetylene compounds are quite widespread within the plant kingdom (*Z101*). This contribution was submitted from the Organic Chemical Institute of the Technische Hochschule in Braunschweig. According to the authors, most polyynes owe their discovery to distinct UV absorption patterns whereas another important tool in their structure elucidation was IR spectroscopy. And finally—"naturally", quoting the authors—also chemical methods (such as ozonation) were still applied frequently.

Christoph Tamm's contribution "Neuere Ergebnisse auf dem Gebiet der glykosidischen Herzgifte: Zucker und Glykoside" ("Recent Results on Cardiac Poisons: Sugars and Glycosides") was provided as a supplement to his paper in Volume 13.

Hans Brockmann (1903–1988), of Göttingen, who had become known due to his reagents for the detection of vitamins D_2 and D_3 as well as for his total synthesis of actinomycin, described "Photodynamisch wirksame Pflanzenfarbstoffe" ("Photodynamically Active Plant Dyes") (*Z103*). *Brockmann* earned his PhD in Halle, habilitated under *Adolf Windaus* in Göttingen, and was director of the Institute of Organic Chemistry in Göttingen from 1945 to 1972.

Born in Sydney, *Arthur John Birch* (1915–1995)—known worldwide for the *Birch* reaction named after him—held a position at the University of Manchester at the time when his contribution on "Biosynthetic Relations of Some Natural Phenolic and Enolic Compounds" (*Z104*) was published.

In their essay on "The Aminochromes", *Harry Sobotka* (1899–1965), *Norman Barsel*, and *Jacob David Chanley* from New York, reported that aminochromes are formed as intermediates during the oxidation of tyrosine, dihydroxyphenylalanine, epinephrine, and their congeners, and to the pigment melamine (*Z105*). The first author (*Sobotka*) was born in Vienna, where he also began his chemistry studies, and earned his doctorate under *Willstätter* in Munich in 1922 as a result of a thesis on enzyme chemistry. From 1928 to 1965, *Sobotka* was director of the Department of Chemistry at Mount Sinai Hospital in New York (*127*). *Chanley* became associate professor at the City University of New York in 1967.

"Visual Pigments" was the title of a contribution submitted from Liverpool by *Richard Alan Morton* (1899–1972) and his co-worker *G. A. J. Pitt* (*Z106*). A turning point in the investigation of visual purple was reached in 1944, when *Morton* and his co-workers discovered that retinene is identical to vitamin A_1 aldehyde.

Volume 14 closed with a quite short viewpoint on "The Carbon Cycle in Nature" (*Z107*) by *Harrison Scott Brown* (1917–1986), a geochemist working in Pasadena at that time, who was famous not only for his studies regarding meteorites and the earth's origin but also for his role in isolating plutonium.

4.7.6 Volume 15

This volume contained only four contributions. *Hans Heinrich Schlubach* (1899–1975) from the "Chemisches Staatsinstitut der Universität Hamburg" shared his findings concerning the carbohydrate metabolism of grasses (*Z108*). Already at that time, scientists were aware of problems arising—given large increases in population numbers and the threat of lack of food associated with it—even though the global population was less than half the size it is today.

Zechmeister himself contributed to Volume 15 by writing a survey on "Some *in vitro* Conversions of Naturally Occurring Carotenoids" (*Z109*). *Jonathan L. Hartwell* and *Anthony W. Schrecker* (Bethesda) reported on "The Chemistry of *Podophyllum*" (*Z110*), and finally *Dorothy Crowfoot Hodgkin* (Oxford) presented results concerning the "X-ray Analysis and the Structure of Vitamin B_{12}" (*Z111*). The *Nobel* laureate of 1964, *Dorothy C. Hodgkin* (1910–1994) concluded her paper in almost prophetic words: *"There is nothing about the B_{12} crystal structures that now suggests that they represent the limit of molecular size that can be explored by X-ray analysis. Indeed already promising stages have been reached in the study of larger molecules."*

4.7.7 Volume 16

Volume 16, which was published in 1958 like Volume 15, was opened by a contribution on "Catechine, andere Hydroxy-flavane und Hydroxy-flavene" ("Catechins, Other Hydroxy Flavans and Hydroxy Flavenes") by *Karl Freudenberg* (for biographical data see Volume Two) and *Klaus Weinges* from Heidelberg (*Z112*). Catechins are phenolic plant metabolites and represent a group of flavanols like **6**.

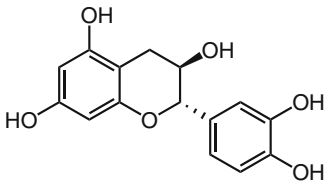

6

Two chemists from the University of New Brunswick in Fredericton, Canada, *Karel Wiesner* (1919–1986) and *Zdenek Valenta* (*1927), presented a contribution on aconite-*Garrya* alkaloids (*Z113*). *Karel Wiesner* was born in Prague. He studied under *Vladimir Prelog* at ETH Zurich and became professor at the University of New Brunswick in 1948. *Zdenek Valenta* has a similar *curriculum vitae*, as he was born in the former Czechoslovakia as well. *Valenta* attended ETH from 1946 to 1950. He commenced his studies under *Wiesner* and became full professor in 1963.

A further contribution to Volume 16 is one on the "Structural Chemistry of Actinomycetes Antibiotics", written by *Eugen Earle van Tamelen* (1925–2009) from Wisconsin (*Z114*). *van Tamelen* was the first to identify squalene oxide as a precursor in cholesterol biosynthesis.

The next paper was on the topic "Protein Synthesis in Plants" (*Z115*). It was submitted by *James Frederick Bonner* (Pasadena), whom we already know from Volume Six.

The last contribution of this volume gives the reader detailed information on quantum theoretical considerations concerning the explanation of organic compound colors. The author who wrote on "The Electron Gas Theory of the Color of Natural and Artificial Dyes: Problems and Principles" (*Z116*) was *Hans Werner Kuhn* (1919–2012), a physical chemist from Bern. *Kuhn* had been professor and director of the Institute of Physical Chemistry at the Philipps University of Marburg since 1953. He studied at ETH Zurich and worked as a postdoctoral fellow with *Linus Pauling* in Pasadena between 1946 and 1947 as well as with *Niels Bohr* in Copenhagen for several months in 1950.

4.7.8 Volume 17

Volume 17 opened with a contribution on "Flavones and Isoflavones" by *Krishnasami Venkataraman* from the National Chemical Laboratory, Poona (Pune), in India (*Z117*). *Venkataraman* (1901–1981) was one of the two scientists who gave their name to the well-known *Baker-Venkataraman* rearrangement to obtain substituted flavones (*128*). *Venkataraman* reminded us that the first flavone to be extracted from poplar buds was chrysin, which was isolated by *Jules Piccard* (1840–1933) in 1864. The structures of fisetin and quercetin were elucidated between 1884 and 1891 by the Viennese chemist *Josef Herzig* (1853–1924) (*129*). In 1898, *Stanislaus von Kostanecki* (1860–1910), who made flavones his life work, succeeded in performing

the first synthesis of a flavone (*130*). It was *Kostanecki* who gave the names flavone and flavonol to the parental ring system and its 3-hydroxy derivative, respectively.

Hans Herloff Inhoffen and *Klaus Irmscher* dedicated their contribution to Volume 17 to the elaboration of progress made in the field of vitamin D research (*Z118*). They mentioned that due to the application of three-dimensional electron density measurements, *Dorothy Crowfoot Hodgkin* and her co-workers succeeded in gaining deeper insight into the fine structure of vitamin D_2. *Inhoffen* and *Irmscher* described novel degradation products of these vitamins, and some partial syntheses as well as *Inhoffen*'s famous total synthesis of vitamin D_3 dating from 1958.

*Friedhelm Korte (*1923), Hans Barkemeyer,* and *Ingeborg Korte* of the Chemical Institute at Bonn University addressed plant bitter principles (*Z119*). They described substances that were isolated from several plant families, including those of Asclepiadaceae, Coriariaceae, Gentianaceae, Menispermaceae, and Urticaceae.

Karl Bernauer of the University of Zurich presented a paper on "Alkaloide aus Calebassencurare und südamerikanischen Strychnosarten" ("Alkaloids from Calebas Curare and South American *Strychnos* Species"), which was also the topic of his professorial dissertation (*Z120*). He commenced by reminding the reader of the work of the German pharmacologist *Rudolf Boehm* (1840–1933), who in 1897 classified the paralyzing arrow poisons of South American Indians as calebas, pot, and tubocurare. Calebas curare was packed into hollow gourds (calebas). Research on curare began with *H. Wieland* around 1937 and in the early 1950s, and a team working with *Paul Karrer* was finally able to separate calebas curare and succeeded in isolating several novel alkaloids of the same kind with the help of paper chromatography. By the time this contribution was written, 42 calebas curare alkaloids had already been identified.

Bruce B. Stowe (1928–2003), working at the Biological Laboratories at Harvard University, Cambridge, Massachusetts, summarized recent findings concerning the "Occurrence and Metabolism of Simple Indoles in Plants" (*Z121*). The application of new techniques not only helped to detect many naturally occurring indoles, but, more importantly, the hormonal nature of some of these compounds in plants and animals could be determined. To give an example, tryptamine, *i.e.* 2-(1*H*-indol-3-yl) ethane-1-amine (**7**), isolated from *Acacia floribunda*, was recognized as having an adrenergic effect in mammals.

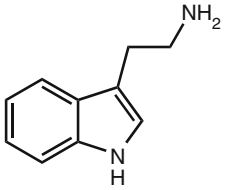

7 (tryptamine)

Albert Eugen Dimond (1914–1972) from the Connecticut Agricultural Experimental Station in New Haven, who did pioneering work in the chemotherapy of plant diseases (*131*), wrote on "Some Biochemical Aspects of Disease in Plants" (*Z122*).

Walter A. Schroeder from Pasadena wrote a contribution on "The Chemical Structure of the Normal Human Hemoglobins" (*Z123*). He reminded the reader of an earlier point: *"The conspicuous red color of the blood has no doubt been a source of wonder, interest, and curiosity even since it was first observed by man." Schroeder* focused on the linkage between heme and globin, the sequence of amino acids in the vicinity of the linkage and their determination by *Hans Tuppy* (*1924) and *Sven Paléus* in 1955, and made reference to preliminary X-ray studies conducted by *Max Perutz et al.* in 1955. Finally, the author expressed his hope, *"One can, then, hope to determine the amino acid sequence and the complete structure of hemoglobin"*. In the end, he was to be proved correct.

Decomposition processes of living matter were the central aspect of the text following: "Paleobiochemistry and Organic Geochemistry" (*Z124*), by *Philip Hauge Abelson* (1913–2004) from the Geophysical Laboratory of the Carnegie Institute, Washington, DC. The author, who was a key contributor to the Manhattan Project during World War II, stated that in spite of the enormous potential degradation activity of bacteria, most of the organic matter deposited in an anerobic environment is not destroyed nor altered substantially.

Volume 17 closed with some important applications of the electron gas theory of dye colors presented by *Hans Kuhn* in Volume 16. Examples are phthalocyanins, benzoporphyrones, cyanins, and polyacetylenes (*Z125*).

4.7.9 Volume 18

Volume 18 (published in 1960) started with a contribution by *Hans Brockmann* (1903–1988) from Göttingen University about research conducted by himself and his co-workers concerning the elucidation of the peptide and chromophore groups of actinomycins (*Z126*). Actinomycins are orange-red, very toxic antibiotics produced by various *Streptomyces* species. In 1940, actinomycin A was isolated by the later *Nobel* laureate *Selman Abraham Waksman* (1888–1973) together with *H. Boyd Woodruff* (*132*).

The Austrian chemist *Matthias Pailer*, whom we know from Volume Eight, reported particularly on his results concerning aristolochic acid in his contribution on "Natürlich vorkommende Nitroverbindungen" ("Naturally Occurring Nitro Compounds") (*Z127*). *Julius Pohl* (1861–1942), a pharmacologist born in Prague, was the first to isolate the compound that he would name aristolochin (aristolochic acid) from *Aristolochia clematitis* and he determined its chemical formula in 1891 (*133*).

Nguyen Van Thoai and *Jean Roche* (1901–1992), members of the College de France, Paris, were the authors of a paper entitled "Dérivés Guanidiques Biologiques" ("Biological Guanidine Derivatives") (*Z128*). In this contribution, *Van Thoai* and *Roche* addressed questions of nomenclature, compound biogenesis, and analytical methods as well as the preparation of guanidine derivatives.

The next contribution was authored by *Anders Kjaer* (*1918) from the Royal Veterinary and Agricultural University, Copenhagen. It was concerned with the chemical structure and the biological properties of "Naturally Derived Isothiocyanates (Mustard Oil) and Their Parent Glucosides" (*Z129*). *Kjaer* became professor of the Danmarks Teknishe Højskole Byning in 1968.

Kjaer's paper was followed by a contribution by *Otto Völker* from the Zoological Institute of the University of Gießen, entitled "Die Farbstoffe im Gefieder der Vögel" ("Pigments in Bird Plumage") (*Z130*), which describes carotenoids, yellow and red pigments in the plumage of parrots, as well as colorful pyrrole derivatives.

After some historical remarks, the editor of the Series, *László Zechmeister*, presented a comprehensive overview on "*cis-trans* Isomeric Carotenoid Pigments" including their UV spectra, preparation, and configurational assignments in certain stereoisomeric sets (*Z131*).

In 1930, *Teijiro Yabuta* (1888–1977) and *T. Hayashi*, from the University of Tokyo, were the first to obtain crystalline material from the fungus *Gibberella fujikuroi*, for which they coined the name "gibberellin" (*134*). In their paper, "The Gibberellins" (*Z132*), *P. W. Brian, J. F. Grove,* and *J. MacMillan* reported on the chemistry of these substances and on plant growth in connection with this group of phytohormones. *Percy Wragg Brian* (1910–2003)*, John Frederick Grove* (1921–2003), and *Jake MacMillan* (1926–2014) were working at the Imperial Chemical Industries, Ltd., Akers Research Laboratories, Welwyn, Herfordshire, England (*135*). In his autobiography "Reflections of a Bio-organic Chemist" (*136*), *MacMillan* described the years of research on gibberellins at the Akers Laboratories in detail.

The theory and practice of the use of ultracentrifugation for analytical purposes was presented in the contribution "Selected Subjects in Sedimentation Analysis, with Some Applications to Biochemistry", by *John Warren Williams* (1898–1988), of the Department of Chemistry at the University of Wisconsin (*Z133*). Professor *Williams* worked with *Theodor Svedberg* and had access to two very rare *Svedberg* ultracentrifuges (*96*, *137*).

The ultimate contribution of Volume 18 confronted the reader with the topic "Structure and Immunological Specificity of Polysaccharides" (*Z134*). The author was *Michael Heidelberger* (1888–1991), a researcher at that time at the College of Physicians and Surgeons at Columbia University, New York. *Heidelberger* is considered a co-founder of modern immunology (*138*). To him is owed basic research on immunochemical analytical methods such as enzyme-linked immunosorbent assays (ELISA). *Zechmeister* got to know *Heidelberger* in Zurich in 1911/1912, which we know from a signature by *Zechmeister* on a menu for *Heidelberger*'s farewell dinner (*139*). Around that time, *Heidelberger* was working in *Willstätter*'s laboratory for several months. In the early 1920s, *Heidelberger*—by then at the Rockefeller Institute, New York, and strongly influenced by the Austrian *Karl Landsteiner* (1868–1943)—turned to immunological working techniques (*140*). With *Oswald Avery* (1877–1955), *Heidelberger* discovered that polysaccharides are powerful antigens of the highly pathogenic *Pneumococcus* (*138*).

4.7.10 Volume 19

In his contribution "Medium-ring Terpenes", *František Šorm* (1913–1980), member of the Institute of Organic Chemistry and Biochemistry at the Czechoslovak Academy of Sciences, Prague, referred to terpenes containing nine-membered carbon rings like caryophyllene, ten-membered rings like germacrone, and finally eleven-membered rings like humulene or zerumbole (*Z135*). Since 1936, when the

structure of azulene was defined by *Alexander St. Pfau* and *Placidius A. Plattner* (*141*) as a bicyclic ring structure with a condensed unsaturated five- and a seven-membered ring (**8**), great interest had arisen on these exceptional compounds. Taking account of this fact, *Tetsuo Nozoe* (1902–1996) and *Shô Itô* from Tohoku University, Sendai wrote a contribution on "Recent Advances in the Chemistry of Azulenes and Natural Hydroazulenes" (*Z136*). For biographical notes on *Nozoe*, see Volume 13.

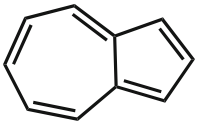

8 (azulene)

The next contribution in Volume 19 dealt with insecticides that have the advantage of low mammalian toxicity. It was entitled "Chemistry of the Natural Pyrethrins" (*Z137*). The authors were *Leslie Crombie* (1923–1999), from King's College, University of London, and *Michael Elliott* (1924–2007), who was working at the Rothamsted Experimental Station in Harpenden, Hertfordshire. They mentioned that the basic form of the pyrethrin structure was not appreciated until investigations were carried out by *Hermann Staudinger* and *Leopold Ružička* between 1910 and 1916, which were published in 1924 (*142*).

"Conformational Analyses of Steroids and Related Natural Products" was a contribution concerning the application of conformational principles in the field of steroids and triterpenoids. Spectroscopic correlations were discussed by *Sir Derek Harold Richard Barton* and *G. A. Morrison*, who were members of the Imperial College of Science and Technology at the University of London (*Z138*). In 1969, *Barton* (1918–1998) shared the *Nobel* Prize in Chemistry with *Odd Hassel* for contributions to the development of the concept of conformation and its application in chemistry.

Yet again the editor of "Progress" was able to convince *Eugen Earle van Tamelen* to contribute a chapter—this time on the "Biogenetic-type Syntheses of Natural Products". *van Tamelen* stated that biogenetic-type syntheses are often neater, shorter, and even more efficient than normal routes, in which no attention is paid to natural processes (*Z139*). Indeed, *van Tamelen* was a pioneer of what today is called "biomimetic synthesis".

In addition, *Hans Heinrich Schlubach*, the author of the next contribution, is already known to us. In Volume 19, *Schlubach* dedicated his text to the topic "Kohlenhydratstoffwechsel in Roggen und Weizen" ("Carbohydrate Metabolism in Rye and Wheat") (*Z140*).

Jean Émile Courtois (1907–1989) and *Andréa Lino* from the Laboratoire de Chimie Biologique, Faculté de Pharmacie de Paris, chose the following title for their contribution: "Les Phosphatases de Végétaux Supérieurs: Répartition et Action" ("The Phosphatases of Higher Plants: Distribution and Action") (*Z141*) *Courtois* was the long-time secretary general of the "Société Française de Chimie Biologique".

He was not only very active in his scientific life—he will be remembered for his work on sugars and enzymology—but also showed tremendous courage by hiding members of the resistance during World War II (*143*).

4.7.11 Volume 20

John Howard Birkinshaw and *C. E. Stickings* of the London School of Hygiene and Tropical Medicine, opened Volume 20 with a summary description of "Nitrogen-containing Metabolites of Fungi". The nitrogen-containing fungal metabolites are classified as acyclic nitrogen-containing compounds like amides or nitro-compounds, and heterocyclic compounds like pyrrole, indole, ergot or pyridine derivatives (*Z142*).

In his report "Forschungen am Lignin" ("Research on Lignin"), *Karl Freudenberg* gave an update of his contribution published in Volume 11. This time he described mainly the detection of intermediate products in lignin formation (*Z143*).

Othmar Schindler from the research institute of Dr. A. Wander A.G. in Bern presented an overview of the state of research concerning the ubiquinones (**9**), which were termed "coenzymes Q" by American scientists: "Die Ubichinone (Coenzyme Q)" ("The Ubiquinones (Coenzymes Q)") (*Z144*). Today, there is no more doubt about their identity—they are components of the electron transport chain and participate in ATP production.

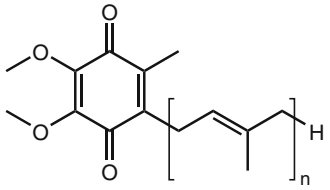

9 (ubiquinones)

Walter Baptist Mors, *Mauro Taveira Magalhães* and *Otto Richard Gottlieb* from the Ministério da Agricultura, Instituto de Químico Agricola, Rio de Janeiro, began their contribution on "Natural Occurring Aromatic Derivatives of Monocyclic α-Pyrones" (*Z145*) by stating that alkaline degradation was the key method in the structural elucidation of monocyclic α-pyrones. They mentioned that *Giacomo Ciamician* (1857–1922) and *Paul Silber* (1851–1930) identified acetopiperone and piperonylic acid among products of alkali treatment of paracotoin in 1893. *Ciamician* and *Silber* proposed a structure including a lactone ring (**10**). *Mors, Magalhães,* and *Gottlieb* took into account that α-pyrones had attracted considerable attention in recent years. *Walter Baptist Mors* (1920–2008), a native of São Paulo, founded the Centro de Pesquisas de Produtos Naturais at the University of Brasilia in 1962, promoting a multidisciplinary vision of plant research (*144*). *Otto Richard Gottlieb* (1920–2011) was born in Brno, emigrated to Brazil in 1939 and

joined the Instituto de Química Agrícola in Rio de Janeiro in 1955, where he pursued his major interest in phytochemistry. In 1964, he was appointed full professor at the Universidade de Brasilia, and, in 1967, he moved to the Universidade de São Paulo (*145*). *Mauro Taveira Magalháes* was a long-time co-worker of *Gottlieb*.

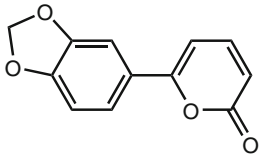

10 (paracotoin)

Jeffrey Barry Harborne (1928–2002), then from the John Innes Institute, Hertford, Hertfordshire, England, discussed in "Anthocyanins and their Sugar Components" the isolation, identification, natural occurrence, and biosynthesis of anthocyanins (*Z146*).

"Aminozucker, Synthesen und Vorkommen in Naturstoffen" ("Amino Sugars, Syntheses and Distribution in Natural Products") is the title of a contribution by *Gerhard Baschang* (*Z147*), who was affiliated with two institutions: the Max Planck Institute, Heidelberg, and the Rockefeller Institute, New York. This particular type of monosaccharides, in which one or more of the hydroxy groups is(are) replaced by amino groups, was discovered by *Georg Ledderhose* (1855–1925) in 1876, when he obtained crystals from boiling the claws and shell of a lobster in hydrochloric acid (*146*). *Baschang* described the syntheses of amino sugars in great detail.

Karel Wiesner, who has already been mentioned as the co-author of an contribution published in Volume 17, was responsible for the next paper on the "Structure and Stereochemistry of the *Lycopodium* Alkaloids" (*Z148*), inclusive of the structures of lycopodine, acrifoline, annofoline, fawcettiine, clavolonine, selagine, and lycodine.

"Newer Developments in the Field of *Veratrum* Alkaloids" were discussed by *C. R. Narayanan*, from the National Chemical Laboratory in Poona, India. *Narayanan* focused on the jerveratrum and cerveratrum alkaloids, including germine, zygadenine, and protoverine (*Z149*).

Volume 20 again includes a methodological paper—"Equilibrium Sedimentation of Macromolecules and Viruses in a Density Gradient" by *Jerome Vinograd* (1913–1976) and *John E. Hearst* (*1935), of California Institute of Technology, Pasadena (*Z150*). *Vinograd's* initial major contribution was the development of density gradient ultracentrifugation in 1957 (*147*). He became well known for his work on the properties of circular DNA in 1965.

Another contribution that is also still worth reading today is the essay "Current Theories on the Origin of Life" by *Norman Harold Horowitz* (1915–2005) and *Stanley Lloyd Miller* (1930–2007) (*Z151*). The authors discussed what the conditions of previous atmospheres of the earth might have looked like in order for life to

develop on our planet. *Miller* had already performed his famous experiment as a student at the California University in Berkeley in 1953. At the time of publication of Volume 18 (1962), *Miller* had just been appointed professor at the Department of Chemistry of the University of California in San Diego.

4.7.12 Volume 21

Volume 21 was published in Austria in 1963. Topics covered in this volume were: rubber, antifungal antibiotics, anthracyclinones, anthracyclines, folic acid, and natural rotenoids. Initially, *James Bonner* presented a rather short overview on "The Biosynthesis of Rubber" (*Z152*). He pointed out the biosynthesis pathway of carbon atoms in common plant metabolites such as carbohydrates during the conversion to polyisoprene. Nevertheless, questions remained. As *Bonner* stated, it was not known how many polymerization enzymes are actually involved. Also, the mechanisms of chain growth quenching were unknown. *James Frederick Bonner* (1910–1996) was a professor of biology at CalTech, Pasadena.

In the introduction of their contribution "The Polyene Antifungal Antibiotics", *William Oroshnik* from the Central Research Laboratory Shulton at Clifton, New Jersey, and *Alexander D. Mebane* (1923–2004) from the Ortho Research Foundation, Raritan, New Jersey, mentioned that the analysis of some very characteristic multipeaked ultraviolet absorption spectra of antifungal antibiotics produced by Actinomycetes led to the identification of straight-chain conjugated polyenes, comprising tetraenes, hexaenes, and heptaenes (*Z153*).

Hans Muxfeldt (1927–1974) and *R. Bangert*, from the University of Wisconsin, turned to a completely different class of antibiotics. Their contribution was entitled "Die Chemie der Tetracycline" ("The Chemistry of Tetracyclines") (*Z154*). Thanks to a collaboration with *Robert B. Woodward*, the structure of terramycin (**11**)—isolated in the laboratories of "Chas. Pfizer and Co." in 1950–was resolved (*148*).

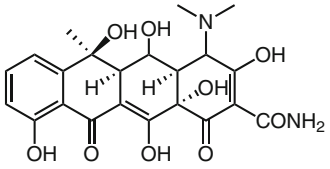

11 (terramycin)

Orange-red pigments were also isolated from *Streptomyces* species, collectively proposed to be named "anthracyclinones" in 1963. Their glycosides are called anthracyclines. These substances are of high antibiotic efficacy but due to their substantial toxicity they had not been used medicinally up to that date. *Hans Brockmann*, who contributed to Volume 18, rendered great service through the isolation and elucidation of the structures of numerous anthracyclinones. In this volume,

he reported on "Anthracyclinone und Anthracycline" ("Anthracyclinones and Anthracyclines") (*Z155*). The parent compound of all anthracyclinones is given by *Brockmann* as structure **12**.

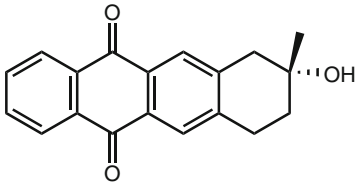

12 (anthracyclinone parent compound)

Since eight years of intense research had passed since *Adrien Albert* gave a summary on the biochemistry of folic acid in Volume 11, *Lothar Jaenicke (*1923)* and *Carl Kutzbach* from the University of Cologne now wrote about progress made in the meantime. Essential parts of their text on "Folsäure und Folat-Enzyme" ("Folic Acid and Folate Enzymes") comprised the biogenesis of folic acid, the analysis and separation of folate compounds as well as folate-catalyzed enzymatic reactions (*Z156*).

Some plants in the family Leguminosae, especially *Derris* species, contain rotenone—an important insecticide and fish poison. Therefore, indigenous populations in some parts of the world used to fish by throwing preparations of crushed plant material into ponds or streams. *Leslie Crombie*, then at King's College of the University of London, whom we already know from Volume 19, reported on the "Chemistry of the Natural Rotenoids" (*Z157*). Rotenone was isolated for the first time by *Emmanuel Geoffroy* (1862–1894) shortly before his death. The stereochemistry was assigned by *George Büchi* (1921–1998) and *L. Crombie* and their collaborators (*149*).

4.7.13 Volume 22

As early as 1913, *Giacomo Ciamician* (1857–1922) enthusiastically propagated the developmental possibilities of organic photochemistry (*150*, *151*). In Volume 22, *Kurt Schaffner* (*1931) from ETH Zurich gave an overview of selected chapters of photochemical conversions in his contribution on "Photochemische Umwandlungen ausgewählter Naturstoffe" ("Photochemical Conversions of Selected Natural Products") (*Z158*).

"Stilbene im Pflanzenreich" ("Stilbenes in the Plant Kingdom") were the topic of an essay by *Gerhard Billek* (1924–2004) from the Institute of Organic Chemistry at the University of Vienna (*Z159*). In 1962, *Billek* habilitated in the field of organic experimental chemistry with special regard to radiochemical methods at the University of Vienna. In his introduction, *Billek* pointed out that *G. L. Hornemann* had isolated rhaponticin, a glucoside of rhapontigenin, from rhubarb by 1822 (*152*). In 1939, *Holger Erdtman* then determined the constitution of pinosylvin (**13**) (*153*),

a stilbene derivative extracted from the heartwood of pine trees, and emphasized that this stilbene causes inhibition of sulfite digestion in this kind of wood. Resveratrol, which differs from pinosylvin only by an additional hydroxy group, was described by *Michio Takaoka* in 1939 (*154*). Resveratrol has repeatedly appeared in press headlines due to frequent and manifold claims of its positive effects on human well-being—such as in November, 2010 (*155*).

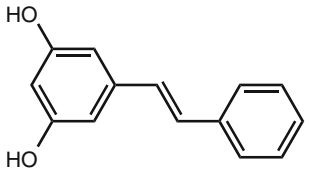

13 (pinosylvin)

Since big steps forward were taken regarding the stereochemistry of triterpenes over the decades earlier, *Thomas G. Halsall* and *Robin T. Aplin*, from the Dyson Perrins Laboratory of the University of Oxford, were invited to write a contribution entitled "A Pattern of Development in the Chemistry of Pentacyclic Triterpenes". They focused on platanic acid, triterpenes of ferns, C-28-nor-triterpenes, ceanothic acid, and related compounds. A table of known pentacyclic triterpene structures (elucidated until 1964) listed 167 such compounds (*Z160*).

Griseofulvin (**14**), an antifungal antibiotic, was first isolated from the mycelium of *Penicillium griseofulvum* in 1939 by *Harold Raistrick* (1890–1971) (*156*). *John Frederick Grove* (1921–2003) from the London School of Hygiene and Tropical Medicine mentioned this fact in the introduction of his contribution "Griseofulvin and Some Analogues" (*Z161*).

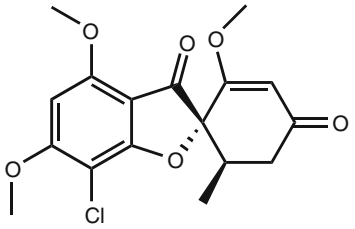

14 (griseofulvin)

In the next contribution, *Paul J. Scheuer* (1915–2003) from Honolulu, explained "The Chemistry of Toxins Isolated from Some Marine Organisms" and described toxins isolated from chordates, echinoderms, mollusks, annelids, coelenterates, and protozoans (*Z162*). *Scheuer* was born in Heilbronn, Germany. After he was denied university admission during *Hitler*'s rise to power, *Scheuer* became a tannery apprentice. In 1938, he immigrated to New York. Students and colleagues called *Paul Scheuer*, professor at the University of Hawaii, the "father of marine natural product chemistry" (*157*).

The last contribution of Volume 22 was entitled "Siderochrome. Natürliche Eisen(III)-trihydroxamat-Komplexe" ("Siderochromes. Natural Iron(III)-trihydroxamate-Complexes") (*Z163*). The authors were all from ETH Zurich: *Walter Keller-Schierlein* (*1922), the *Nobel* laureate of 1975, *Vladimir Prelog* (1906–1998), and *Hans Zähner* (1929–2008). Some compounds of this group of iron complexes, which were isolated from microorganisms and showed antibiotic activity, were termed "sideromycins". In this paper, the elucidation of their structure is described. *Prelog*, who was born in Sarajevo, was awarded a *Nobel* Prize in particular for his services rendered to the investigation and description of chiral molecules.

4.7.14 Volume 23

Volume 23 opened with a report by *Stanley Peat* and *James R. Turvey* on "Polysaccharides of Marine Algae" (*Z164*). *Stanley Peat* (1902–1969), who was appointed to the chair of chemistry at the University College of North Wales at Bangor in 1948 (*158*), and his co-author commented on skeletal polysaccharides of the algal cell wall, food reserve polysaccharides, polysaccharides containing sulfate esters like fucoidin, and galactan sulfates of red algae.

Hans Heinrich Schlubach, well known to us as a previous author in this book series, informed the reader on the topic "Kohlenhydratstoffwechsel in Gerste, Hafer und Rispenhirse" ("Carbohydrate Metabolism in Barley, Oat and Common Millet") (*Z165*).

Fritz Schlenk, working in 1965 at the Argonne National Laboratory, Lemont, Illinois and already known to us from Volume One, now reported on "The Chemistry of Biological Sulfonium Compounds" (*Z166*). *Schlenk* gave an account of some chemical features, *in vitro* synthesis, and the metabolism of sulfonium compounds. A well-known example for this group of compounds is *S*-methylmethionine (**15**), which has sometimes been referred to as "vitamin U".

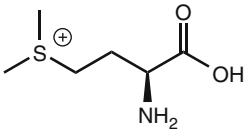

15 (*S*-methylmethionine)

Since the complete hemoglobin amino acid sequence was known within three years after the last paper on hemoglobin was published (1959) and the *Nobel* Prize awarded to *Max Perutz* on this topic, certain new aspects—especially chain abnormalities—were discussed by *Walter A. Schroeder* and *Richard T. Jones* in their contribution "Some Aspects of the Chemistry and Function of Human and Animal Hemoglobins" (*Z167*).

A contribution "Kollagen" ("Collagen"), written by a group working with *Wolfgang Grassmann* (1898–1978) at the *Max Planck* Institute for Protein and Leather Research in Munich, contained many new insights concerning collagen.

The amount of work required—according to the authors—was tremendous, as this molecule, which forms skin, tendons, cartilage, bones, and teeth, proved to be far more complicated than expected. It was possible to connect certain characteristics of collagen (*e.g.* its cross-striation pattern) to already known facts about its primary structure at the time the contribution was written in 1965 (*Z168*).

The final contribution to Volume 23 represented a synopsis of the then brand new technique of NMR spectroscopy, entitled "Some Applications of Nuclear Magnetic Resonance Spectroscopy in Natural Product Chemistry" (*Z169*), written by *Lloyd Miles Jackman*, who was professor of organic chemistry at the University of Melbourne from 1962 to 1967 (*159*).

4.7.15 Volume 24

In Volume 24 (1966), mass spectrometry was presented for the first time as a new method of structural analysis: "Mass Spectroscopy of Selected Natural Products" (*Z170*). During the 1940s, the 1950s, and even the beginning of the 1960s, the organic chemist had become increasingly used to being able to take advantage of more and more complex instrumentation for physical measurements, in lieu of laborious, time-consuming, and often ambiguous chemical transformations. As the author *Klaus Biemann* from the Department of Chemistry at the Institute of Technology in Cambridge, Massachusetts, stressed, mass spectrometry had become the most recent addition to this field. *Biemann,* who has been called the "father of organic mass spectrometry", was born in Innsbruck in 1926 (*160*). He studied in Innsbruck before going to the USA. On various occasions, *Biemann* pointed out that *Josef Mattauch* and his student *Richard F. K. Herzog* from the Physics Department at the University of Vienna had developed in 1936 a double-focusing mass spectrograph with high resolving power (*161*). As can be inferred from recent newspaper reports, *Biemann*, who has now retired, is still active in cosmochemistry. In September 2010, he commented on a controversy regarding the evaluation of data obtained during the Viking 1 mission to Mars in 1976. In this regard, *Biemann* spoke in the same manner as the above-mentioned *Norman Harold Horowitz* (see Volume 20) who had been in charge of the experiments on the possible existence of life on Mars and who—as soon as the data had arrived—had declared that earth was the only planet in this area of the galaxy to generate life.

We owe the second contribution in Volume 24 to *Rudolf Tschesche* from Bonn. The title of his contribution was "Pflanzliche Steroide mit 21 Kohlenstoffatomen" ("Plant Steroids with 21 Carbon Atoms") (*Z171*). The first C_{21}-steroid was diginin, isolated by *Walter Karrer* (*162*), brother of *Paul Karrer,* in 1936.

In 1966, the Austrian chemist *Otto Hoffmann-Ostenhof* (1914–1992) was accorded the honor of writing another contribution for the Series. His co-author of "Cyclite: Biosynthese, Stoffwechsel und Vorkommen" ("Cyclites: Biosynthesis, Metabolism, and Occurrence") was *Helmut Kindl*. Some of the more abundant cyclites (*e.g.* L-quercite or D-pinite) had already been known in the nineteenth

century. *Hoffmann-Ostenhof* and *Kindl* reported mainly on the biosynthesis, degradation, and occurrence of cyclites using the example of myo-inositol (*Z172*). As of 1971, *Otto Hoffmann-Ostenhof* was appointed to the chair of biochemistry at the University of Vienna (*163*). Also in 1971, *Helmut Kindl* (*1936) became professor of biochemistry at the University of Marburg (*164*).

Holger Erdtman (1902–1989) from the Royal Institute of Technology in Stockholm and *Torbjörn Norin* (*1933) from the Swedish Forest Products Research Laboratory in Stockholm discussed the constituents of the Cupressales, *i.e.* cyclitols and simple phenols, lignans, flavonoids, leaf waxes, tropolones, and terpenes, in their report on "The Chemistry of the Order Cupressales" (*Z173*). *Erdtman* studied at Stockholm University and was a Ramsay fellow with Professor *Sir Robert Robinson* in England from 1929 to 1931. He completed his practical thesis work in the laboratories of *Friedrich Fichter* in Basel and *Ernst Späth* in Vienna (*165*).

The next contribution entitled "Quinone Methides in Nature" was written by *Alan B. Turner* from the Department of Chemistry of the University of Aberdeen. Quinone methides occur as products of fungal metabolism and as plant pigments. Stable quinone methides comprise citrinin, pulvilloric acid, ascochitine, purpurogenone, fuscin, celastrol, and perinaphthenone (*Z174*).

"The Pyrrolizidine Alkaloids II" by *Frank Louis Warren (Z175)* represented a follow-up of a contribution included in Volume 12. Volume 24 concluded with "Some Aspects of Virus Chemistry", a contribution by *H. Fraenkel-Conrat* from the Virus Laboratory at the University of California in Berkeley (*Z176*). *Heinz Ludwig Fraenkel-Conrat* (1902–1999), who was mentioned in connection with his participation in Volume 12, left Germany in 1936 and joined the Virus Laboratory at Berkeley in 1952. He was the first scientist to dissemble and rebuild a virus out of its constituents. His most important discovery was that the nucleic core of each virus contains information that controls viral reproduction (*166*). His father was *Ludwig Fraenkel* (1870–1951), the discoverer of the steroid hormone progesterone.

4.7.16 Volume 25

"Biogenetische Beziehungen der natürlichen Acetylenverbindung" ("Biogenetic Relations of the Natural Acetylene Compounds") was the title of the first essay of Volume 25. This topic was covered by *Ferdinand Bohlmann* (1921–1991) from the Technical University (TU) Berlin (*Z177*). Around 1955, about 50 natural acetylene compounds were known. Only ten years later, this number rose to approximately 440. *Bohlmann* earned his doctorate under *Hans Brockmann* in Göttingen in 1946, then moved to Braunschweig where he worked under *Hans Herloff Inhoffen,* and in 1959 became the successor of *Friedrich Weygand* at the TU Berlin.

Following this essay, *Philip R. Ashurst*, a graduate of the Imperial College London then working at the Brewing Industry Research Foundation, Nutfield,

Surrey, England described "The Chemistry of the Hop Resin". Some functions of hops in brewing as well as substances present in the hop resin were covered (*Z178*). Today, *Ashurst* is still working as a consulting chemist (*167*).

Jesús Romo Armería (1922–1977) and his co-worker *Alfonso Romo de Vivar* (*1928) from the Instituto de Quimica, Universidad National Autonoma de Mexico specialized in "The Pseudoguaianolides" (*Z179*). The term "pseudoguaianolides" applies to sesquiterpene lactones with an abnormal guaiane skeleton resulting from migration of the C-4 methyl group to C-5 in the guaianolide system (**16**, **17**) during biosynthesis. *Armería*'s most prominent achievement was the development of a cost-efficient method to synthesize estradiol and progesterone using precursors extracted from *Dioscorea.* In 1953, *Zechmeister* visited the Instituto de Química in Tacuba, Mexico, where *Jesús Romo* and *Romo de Vivar* worked (*168*).

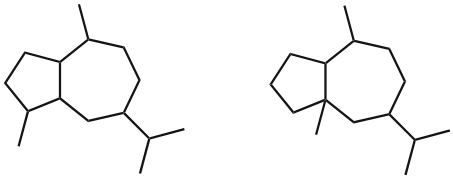

16 (guaiane) **17** (pseudoguaiane)

J.K. Sutherland from the Imperial College of Science and Technology, London, summarized all that was known about "The Nonadrides", a small group of fungal metabolites characterized by the presence of a nine-membered ring and two five-ring anhydride groups (*Z180*). Glauconic acid (**18**), a member of the nonadride group, was isolated by *Nadine Wijkman* in 1931 (*169*).

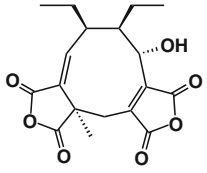

18 (glauconic acid)

A series of contributions dealing with topics of chemical classification was continued by *Loránd Farkas* (1914–1986), who was a student of *Zemplén*, and *László Pallos* from the Technical University of Budapest, with their summary on "Natürlich vorkommende Auronglykoside" ("Naturally Occurring Aurone Glycosides") (*Z181*). Leptosin (**19**)—isolated from blossoms of *Coreopsis grandiflora* Nutt. in 1943—is given as an example[1].

[1] It should be mentioned that the name "leptosin" has been assigned later on for a second time to the different compound, methyl syringate 4-*O*-*β*-D-gentiobiose, from *Leptospermum* sp.

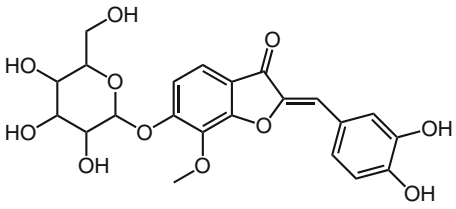

19 (leptosin)

Next in line were *Raphael Mechoulam* (*1930) from the Laboratory of Natural Products, The Hebrew University, Jerusalem and *Yehiel Gaoni* from the Weizmann Institute of Science in Rehovot with their contribution on "Recent Advances in the Chemistry of Hashish" (*Z182*). *Mechoulam* and *Gaoni* were the first to isolate tetrahydrocannabinol in 1964 (*170*).

Theodor Wieland (1913–1995), son of *Nobel* laureate *Heinrich Wieland*, wrote on the "Toxic Peptides of *Amanita phalloides*" (*Z183*). *Heinrich Wieland* had already begun investigating substances from the death cap mushroom (*Amanita phalloides*) as early as the 1920s. *Theodor Wieland* became full professor at the Institute of Organic Chemistry in Frankfurt/Main in 1951.

In "Die Prolamine" ("The Prolamines"), *Ernst Waldschmidt-Leitz* and *Hans Kling* from the Institute of Experimental Biology in Heiligenberg collected recent information on these specific storage proteins that occur mainly in grain seeds (*Z184*).

George A. Morrison from the Department of Organic Chemistry at the University of Leeds, who also published a contribution in Volume 19, wrote on "Conformational Analysis of Some Alkaloids" (*Z185*). *Morrison* confined himself to describing certain problems using only few specific examples, such as yohimbine, tazettine, and lyconine.

4.7.17 Volume 26

The first third of Volume 26 was dedicated to a thorough discussion of specific topics of protein research. It commenced with a text on "X-Ray Diffraction Studies of Crystalline Amino Acids, Peptides and Proteins" by *Robert Brainard Corey* and *Richard Edward Marsh* from Pasadena, California, where the authors pointed out—in contrast to previous findings—they could then present data obtained directly from crystallized proteins (*Z186*).

Eberhard Schröder and *Klaus Lübke* from the Schering Main Laboratory in Berlin continued with a description of the "Synthese von Peptiden und Peptidwirkstoffen" ("Synthesis of Peptides and Peptide Agents") (*Z187*). Examples given included hypophyseal peptide hormones (such as the adrenocorticotropic hormone, the melanocyte-stimulating hormone, oxytocin and vasopressin), intestinal peptide hormones (like gastrin or secretin) as well as tissue hormones (*e.g.* angiotensin, the kinins, eledoisin, and physalaemin).

Finally, recent findings in the field of "Insulin, Structure, Synthesis and Biosynthesis of the Hormone" were presented by *Anthony C. Trakatellis* and *Gerald P. Schwartz* from the Department of Biochemistry, Mount Sinai School of Medicine, New York (*Z188*). *Antonios Trakatellis* was born in Thessaloniki in 1931. He lectured at several Greek and American universities and was rector of Aristotle University of Thessaloniki from 1988 to 1994. *Trakatellis* has published a large number of papers and books concerning insulin, nucleic acids, and vitamin B_6 deficiency. In 2004, he was elected as one of 14 vice presidents of the European Parliament (*171*).

W. Keller-Schierlein and *H. Gerlach* from the Laboratory of Organic Chemistry at ETH Zurich were responsible for a contribution on "Makrotetrolide" ("Macrotetrolides") (*Z189*). *Walter Keller-Schierlein* (*1922) habilitated on microbial metabolic products at ETH in 1963 and *Hans Gerlach* wrote his dissertation under *Vladimir Prelog* and *Albert Eschenmoser* in 1962 entitled "Über die Konstitution und Konfiguration der Makrotetrolide Nonactin, Monactin, Dinactin und Trinactin" ("On the Constitution and Configuration of the Macrotetrolides Nonactin, Monactin, Dinactin and Trinactin"). Macrotetrolides are a family of macrocyclic compounds active as antibiotics containing four tetrahydrofuranylcarboxylic acid residues linked together.

During the 1960s, *David L. Dreyer* (*1930) isolated a number of new citrus bitter principles at the Fruit and Vegetable Chemistry Laboratory, Pasadena, California (*172*). "Limonoid Bitter Principles" was the title of his contribution in Volume 26 of the Series (*Z190*), in which he discussed the structure of approximately 70 limonoids.

In "Proaporphin-Alkaloide" ("Proaporphine Alkaloids") by *Karl Bernauer* and *Werner Hofheinz* (Hoffman-LaRoche, Basel), the constitution of cyclohexadienone, cyclohexenone, cyclohexenol, and cyclohexanol proaporphines was given (*Z191*). Pronuciferine, stephanine, and linearisine were some examples. The next contribution "Chemie der Chlorine und Porphyrine" ("Chemistry of Chlorines and Porphyrins") by *Hans Herloff Inhoffen, Johann Walter Buchler,* and *P. Jäger* (TH Braunschweig) contained information on a new porphyrin synthesis (*Z192*). Today, *Buchler* is still working on the coordination chemistry of metal porphyrins as professor emeritus at the University of Technology Darmstadt (*173*).

Volume 26 was concluded by an overview on "Methoden und Ergebnisse der Sequenzanalyse von Ribonucleinsäuren" ("Methods and Results of the Sequence Analysis of Ribonucleic Acids") by *Dieter Dütting*, *Max Planck* Institute of Virus Research, Tübingen (*Z193*). *Dütting* reported on the successful deciphering of the amino acid codon triplet in mRNA.

4.7.18 Volume 27

The essay by *A. Frey-Wyssling* from ETH Zurich on "The Ultrastructure and Biogenesis of Native Cellulose" (*Z194*) was a presentation of progress achieved in cellulose research at the time of writing. The discussion was based on an article published in Volume Eight of this Series. *Albert Frey-Wyssling* (1900–1988) was appointed to the chair of general botany and plant physiology at ETH Zurich in 1938, due to his groundbreaking studies in the field of the fine structure of cell walls.

In the three decades from 1940 to 1970, gradually it became evident that ethylene is a compound generally present among living things. The metabolism and physiological activity of ethylene, used nowadays as a commercial ripening agent for different kinds of fruits, were discussed in *Mary Spencer*'s contribution "Ethylene in Nature" (*Z195*). She was professor of plant science and biochemistry at the University of Alberta, Edmonton, Canada, and an international authority on ethylene, its production, and effect on the environment (*174*).

"Spectroscopic Methods for Elucidating the Structures of Carotenoids" was the subject of a paper by *B. C. L. Weedon*, which summarized the techniques of visible, UV, IR, and NMR spectroscopy, and mass spectrometry as well as optical rotatory dispersion (*Z196*). Using NMR spectroscopy, *Basil Charles Leicester Weedon* (1923–2003), who was appointed to the chair of organic chemistry at Queen Mary College, London in 1960, was the first to determine the structures of carotenoid pigments, including astaxanthin, rubixanthin, and canthaxanthin (*175*).

Georgine M. Sanders, Jan Pot, and *Egbert Havinga*, from the University of Leiden, collected new information about the so-called "overirradiation products" in their contribution "Some Recent Results in the Chemistry and Stereochemistry of Vitamin D and Its Isomers" (*Z197*). *Egbert Havinga* (1909–1988), a student of *Fritz Kögl*, accepted an offer from the University of Leiden to become full professor of organic chemistry in 1946 (*176*).

The investigation of flavonoid tannin chemistry had already begun in 1920 with the elucidation of the catechin structure by *Karl Freudenberg.* Acid-catalyzed tannin formation as well as plant polyphenol formation by enzymatic dehydration were described in detail in the contribution "Konstitution, Entstehung und Bedeutung der Flavenoid-Gerbstoffe" ("Constitution, Formation and Significance of Flavonoid Tannins") by *Klaus Weinges, Wolfgang Bähr* (*1942), *Werner Ebert* (*1934)*, Klaus Göritz,* and *Hans-Dieter Marx* (*Z198*), all from the Organic Chemistry Institute of Heidelberg University.

There is no doubt about the pharmacological significance of the discovery in 1869 of muscarine in fly agaric (*Amanita muscaria*), as described by *Oswald Schmiedeberg* and *Richard Koppe* (*177*). However, muscarine is not the only agent responsible for the numerous symptoms of fly agaric poisoning, such as ataxia, excitation, and hallucinations. In his contribution "Chemie der Wirkstoffe aus dem Fliegenpilz (*Amanita muscaria*)" ("Chemistry of the Active Substance in Fly Agaric" (*Amanita muscaria*)) *(Z199)*, *Conrad Hans Eugster* (1921–2012) from the University of Zurich argued in favor of ibotenic acid (**20**) and muscimol (**21**) as being the main active constituents of fly agaric.

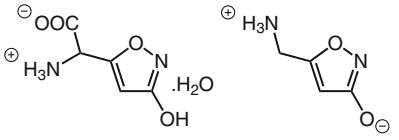

20 (ibotenic acid) **21** (muscimol)

In his contribution "The Chemistry of Some Toxins Isolated from Marine Organisms", *P.J. Scheuer* (Honolulu) focused on pahutoxin, ciguatoxin, holothurins, asterosaponins, saxitoxin, aplycin, palytoxin, and prymnesin (*Z200*). For biographical notes on *Paul J. Scheuer*, see Volume 22.

The final essay of Volume 27, "The Chemistry of Lysozyme" was written by two scientists from CalTech. *Michael A. Raftery* (1936–2007) became professor of chemical biology in 1967. *Frederick Willis Dahlquist* was a research fellow in 1968/1969, and is still publishing in the field of biochemistry. Their paper dealt with studies of structure, substrate specificity, and catalytic mechanisms of the hen egg-white enzyme lysozyme, which was identified as a basic protein containing 129 amino acid residues (*Z201*).

5 Since 1970: Not "Edited by" but "Founded by" *L. Zechmeister*

5.1 The Editorial Board Since 1970

At the beginning of Volume 28, which was published in 1970, the editor gives a personal statement for the first time, *"After the publication of Volume 27, I have asked the Springer-Verlag to relieve me from my duties, because of my advanced age, although this was not an easy decision after 32 years of editorial work. I shall sorely miss the scientific contact with a number of contributing authors and with those readers who have written to me concerning one and the other of the almost 200 review articles published in this series"*.

The then re-established editorial board consisted of *Werner Herz* from Tallahassee, *Hans Griesebach* from Freiburg, and *Alastair Ian Scott* from New Haven. *Werner Herz* (*1921) was born in Stuttgart, Germany. He was educated at the University of Colorado. In 1959, he became Robert O. Lawton Distinguished Professor at Florida State University in Tallahassee. He was also senior editor of *The Journal of Organic Chemistry*.

Hans Griesebach (1926–1990) was born in Breslau as the son of *August Griesebach*—an art historian—and the Jewish writer and gallery owner *Hanna Griesebach* (née *Blumenthal*). He survived the war in Potsdam, studied in Heidelberg and later started working as an assistant in Heidelberg and Tübingen. *Griesebach* habilitated in Freiburg in 1960, was appointed to the chair of biochemistry at the University of Freiburg in 1964 and was entrusted with the editorship of the "Progress" series five years later. His research focus lay on the biosyntheses of phenylpropanoid compounds and antibiotics as well as on induction mechanisms of plant antigens.

Alastair Ian Scott (1928–2007) was born in Scotland, studied at the universities of Glasgow and London and at Yale University, and worked with *Nobel* Prize laureate *Sir Derek Barton* at Imperial College, London. In 1971, he resigned from his position as co-editor. *Zechmeister* was annoyed by *Scott*'s resignation. According to *Zechmeister*, *Scott* had "*not accepted co-editorship in the first place"* (*178*).

One year later, *Gordon William Kirby* from Loughborough took *Scott*'s place. This team of three was destined to define the direction of the Series for many years. As of 1967, *Kirby* (*1934) had been professor at the University of Technology, Loughborough, Leicestershire, in England, before he went to the University of Glasgow, where he was Regius Professor of Chemistry from 1972 to 1997.

In Volume 28, the new editors also addressed the reader directly, *"The present volume of 'Fortschritte' is the first which does not carry the familiar line 'Edited by L. Zechmeister'. Zechmeister's devotion to the success of this series and his exacting editorial standards have made this line a by-word for all scientists interested in the chemistry of natural products."*

Christoph Tamm (*1923) also served as editor from 1984 to 1999. He earned his doctoral degree in Basel in 1948, then became a postdoctoral researcher in the USA and habilitated under *Tadeusz Reichstein* in 1955. *Tamm* was appointed professor at the Institute of Organic Chemistry at the University of Basel in 1966.

Concerning further historical facts about the editorial board, there was no further change in 1971. For the publication of Volumes 57 and 58, *Wolfgang Steglich* was asked to join the board in addition to *Herz, Kirby*, and *Tamm. Wolfgang Steglich* (*1933) studied chemistry at the Technical University of Berlin and later at the Technical University of Munich, where he received his PhD in 1959. He became professor at the Technical University of Munich in 1969. In 1975, he went to Bonn. He succeeded *Rolf Huisgen* as head of the Organic Chemistry Department at the University of Munich in 1991. *Steglich* formed part of the editorial team until the publication of Volume 74.

Beginning with Volume 59 and ending with Volume 74, the editorial board consisted of *W. Herz, G. W. Kirby, R. E. Moore, W. Steglich*, and *Ch. Tamm. Richard E. Moore* was born in San Francisco on July 30, 1933, where he later also attended university. After earning his PhD at the University of California in Berkeley in 1962, he moved to Hawaii where he joined the faculty of the Department of Chemistry at the University of Hawaii until his retirement in 2003. Professor *Moore* was a leading authority in the field of marine natural product chemistry and drug discovery. He died in Honolulu in December 2007.

In 1998, *Heinz Falk* was appointed to the editorial board. *Falk* (*1939), who was born in St. Pölten in Lower Austria and today is professor emeritus at the Johannes Kepler University in Linz, has been serving as co-editor of the series since Volume 75. *Falk*'s main areas of research include a group of organic natural dyes derived from the phenanthroperylenedione chromophore found in natural pigments like hypericin, stentorin, fringelite, gymnochrome, and blepharismin. He was heavily involved in the research of open chain tetrapyrroles (bile pigments) as well as closed ones like hemin-analogous corrphycene derivatives thought to be possible blood substitutes and suppressors of heme oxygenase. Furthermore, members of his working group were focused on the natural sun blocker urocanic acid.

W. Herz, H. Falk, G. W. Kirby, and *R. E. Moore* edited Volumes 79–83. The editorial board for Volumes 84–88 consisted of *W. Herz, H. Falk,* and *G. W. Kirby.* Since Volume 89, the editors have been *A. Douglas Kinghorn, H. Falk,* and *Jun-ichi Kobayashi.*

Since 2004, *A. Douglas Kinghorn* has been Professor and Jack L. Beal chair of natural products chemistry and pharmacognosy at The College of Pharmacy of Ohio State University. *Kinghorn* earned his bachelor's degree in pharmaceutical sciences from the University of Bradford, a master's degree in forensic science from the University of Strathclyde, and PhD and DSc degrees from the School of Pharmacy at the University of London. At the University of Illinois at Chicago, he became professor and was assistant head of the Department of Medicinal Chemistry and Pharmacognosy. *Kinghorn* is an internationally renowned scholar in the area of natural products and molecular biodiversity in drug discovery. His research focuses on the isolation, characterization, and biological evaluation of natural products of higher plant origin. He has been senior editor of the *Journal of Natural Products* since 1994 (*179*).

Jun-ichi Kobayashi was born in Hirosaki, Japan, in 1949. He completed his BS degree in 1973, and his MS degree in 1975 at Hokkaido University, working on studies of nucleic acid synthesis. After receiving his PhD from Hokkaido University in 1979, he initiated his research program on marine natural products and worked at the University of Illinois with Professor *Kenneth L. Rinehart*. In 1989, he was appointed full professor at Hokkaido University, Graduate School of Pharmaceutical Sciences, where he still continues his research career. *Kobayashi*'s main research interests focus on the search for bioactive natural products from marine organisms, terrestrial plants and marine/terrestrial microorganisms and their application to the basic research of life sciences as well as the development of new drugs (*180*).

As of Volume 89, an advisory board was established in order to ensure broader potential coverage of the book series. *Werner Herz*, who had to resign from his function for reasons of health, is listed as Honorary Editor from this volume on. The advisory board consists of *Verena Dirsch, Simon Gibbons, Nicolas H. Oberlies*, and *Yang Ye.*

Verena Dirsch studied pharmacy at the University of Munich, Germany where she received her PhD in 1993 in the group of *Hildebert Wagner*, who also appears as an author in Volume 31 of the Series. As a fellow of the German Research Council (DFG), she joined the group of *Koji Nakanishi* as a postdoctoral at Columbia University for one year. From 1995 to 2004, she held several positions in the group of *Angelika Vollmar*, first at the Institute of Pharmacology, Toxicology and Pharmacy of the Faculty of Veterinary Medicine and later at the Department of Pharmacy, both at the University of Munich. Since 2004, she has been a full professor at the University of Vienna and since 2006 head of the Department of Pharmacognosy. Her main research fields include the molecular mechanisms of natural products affecting vascular smooth muscle cell growth or nitric oxide production in endothelial cells as well as the identification of new anti-inflammatory compounds using various signaling pathways for cell-based screenings in collaboration with phytochemical groups.

Simon Gibbons is currently professor of medicinal phytochemistry and head of the Department of Pharmaceutical and Biological Chemistry at The School of Pharmacy, University College London. *Gibbons* received BSc and PhD degrees in chemistry and phytochemistry, respectively. In October 1997, he was appointed

assistant professor of pharmaceutical chemistry at the Faculty of Pharmacy at Kuwait University and in 1999 moved to the University of London to lecture in pharmacognosy. In 2007, he was appointed as a full professor. His research focuses on the isolation and structure elucidation of bioactive natural products from plants, particularly antibacterials and bacterial-resistance modifying agents.

Nicholas H. Oberlies received his BS in chemistry from Miami University (Oxford, Ohio) in 1992 and his PhD from Purdue University (West Lafayette, Indiana) in 1997, where he studied under *Jerry L. McLaughlin*. He then spent a year as a postdoctoral chemist at American Cyanamid (Princeton, New Jersey). In 1998, he joined the Natural Products Laboratory at Research Triangle Institute (RTI) in North Carolina. In 2009, he relocated his research group to the Department of Chemistry and Biochemistry at the University of North Carolina at Greensboro. *Oberlies* is currently leading a multidisciplinary effort to identify, isolate, and characterize new drug entities from natural sources, such as plants, fungi, and bacteria. His laboratory also examines herbal drugs, especially for the development of reference standards.

Born in 1965, *Yang Ye* earned his PhD from the Shanghai Institute of Materia Medica, Chinese Academy of Sciences in 1992. He was an Alexander von Humboldt fellow and underwent postdoctoral study at the Institute of Organic Chemistry, University of Munich. He now is full professor and deputy director of the Shanghai Institute of Materia Medica, Chinese Academy of Sciences. *Ye* mainly studies secondary metabolites from traditional herbal medicinal plants. His goal is to disclose the chemical essence of traditional Chinese medicine, as well as to find potential pharmaceutical lead structures.

5.2 Volumes 28–38: New Centers of Research, New Fields of Research

Following the change of editors, the list of countries from where contributions were submitted became even wider. From now on we can find contributions from Brazil, India, Korea, South Africa, Australia, Italy, the Netherlands, the former GDR, New Zealand, and many more countries.

5.2.1 Volume 28

Volume 28, published in 1970, surprised the reader by containing the first contribution submitted by a researcher from behind the Iron Curtain, *i.e.* the Institute of Plant Biochemistry, Halle/Saale, GDR. *Dieter Gross* presented work on "Naturstoffe mit Pyridinstruktur und ihre Biosynthese" ("Natural Compounds with Pyridine Structure and Their Biosynthesis") (*Z204*). The Institute of Plant Biochemistry (IBP) was a non-university research institute, which—as an academic institute—formed part of the research community of the German Academy of Sciences, Berlin—the later Academy of Sciences of the GDR.

The opening paper of Volume 28 was entitled "Structural and Biogenetic Relationships of Isoflavonoids" by *Edmond Wong* from the Applied Biochemistry Division, Department of Scientific and Industrial Research, Palmerston North, New Zealand (*Z202*). It not only took note of complex isoflavones, but also covered isoflavanones, rotenoids, pterocarpans, isoflavans, 3-aryl-4-hydroxycoumarins, and coumestans.

This paper was followed by "Recent Advances in the Chemistry of Cyanogenic Glycosides" written by *Reynir Eyjólfsson* from The Royal Danish School of Pharmacy, Copenhagen (*Z203*). Cyanogenic glycosides are widespread plant toxins consisting of a glycoside containing an additional nitrile group.

In his contribution "Peptide Alkaloids" (*Z205*), *Edgar W. Warnhoff* from the University of Western Ontario in Canada described the structure and properties of natural compounds like pandamine, zizyphine, ceanothine-B, scutianine, integerrine, lunarine, homaline, adouétine-X, and several more.

In "Insektensexuallockstoffe" ("Insect Pheromones" (*Z206*), *Karl Eiter*—private lecturer from the Bayer, Leverkusen, Cologne-Stammheim—classified these special pheromones as olefinic, aliphatic, terpene-like, or heterocyclic. At this point, also the contribution "Insect Pheromones" of Volume 37 should be mentioned.

A main discussion point in the paper "Arthropod Molting Hormones" by *Hiroshi Hikino* and *Yasuko Hikino*, Tohoku University, Sendai (*Z207*), was the structure determination and chemistry of substances like ecdysone, ponasterone, inokosterone, and cyasterone.

What followed next was a report on the "Total Synthesis of Prostaglandins" by *John E. Pike*, The Upjohn Company, Kalamazoo, Michigan (*Z208*). *Robert Bennett Morin* (*1931) and *Bill G. Jackson* from the University of Wisconsin described the "Chemistry of Cephalosporin Antibiotics" (*Z209*). Cephalosporins are a class of β-lactam antibiotics originally derived from the fungal genus *Acremonium*.

"Oligosaccharide der Frauenmilch" ("Oligosaccharides in Breast Milk") by *Herbert Wiegandt* (*1937) and *Heinz Egge*, Institute of Physiological Chemistry at the University of Marburg (*Z210*), dealt with the isolation, analysis and description of these very special sugars. Before *Wiegandt* was called to the Philipps University of Marburg in 1965, he had worked on gangliosides—a group of glycolipids found in nerve tissue—together with *Richard Kuhn* in Heidelberg.

The last contribution of Volume 28 was entitled "Glucagon: Chemistry and Action" by *William W. Bromer* (*1928), The Lilly Research Laboratories, Indianapolis, Indiana (*Z211*). Glucagon is a peptide hormone and its main function is increasing blood sugar levels.

5.2.2 Volume 29

In Volume 29, published in 1971, *Dieter Gross*, who has been mentioned earlier, received another opportunity to report his findings concerning "Struktur und Biosynthese natürlicher Piperidinverbindungen" ("Structure and Biosynthesis of Natural Piperidine Compounds") (*Z212*).

Volume 29 contained another contribution submitted from the same institute. *Siegfried Huneck* (1928–2011), recently (2010) published a book on his

expeditions to Mongolia in the 1970s and 1980s (*181*, *182*). *Hunek* presented the third contribution on "Chemie und Biochemie der Flechtensäuren" ("Chemistry and Biochemistry of Lichen Acids") *(Z214)*. He started by providing a description of progress achieved in this field of research. Around 1900, the structure of lecanoric acid was the only one known of the many substances contained in lichens. By 1954, 74 lichen compounds had been described, and, between 1954 and 1970, 65 more of these compounds were isolated—mainly owing to the development of thin-layer chromatography. According to the author, mass spectrometry and NMR spectroscopy were used extensively in the structure elucidation of these compounds.

Especially worth noting is the contribution by *David Lavie* and *Erwin Glotter*, both from the Department of Chemistry, The Weizmann Institute of Science, Rehovot, Israel, which carried the title "The Cucurbitanes, a Group of Tetracyclic Triterpenes" (*Z216*). *David Lavie* (1916–2003) was one of the first scientists employed at the Weizmann Institute. He received his MSc degree from the Hebrew University of Jerusalem in 1939. After completing his PhD he performed postdoctoral studies at Harvard University. This work, performed in the group of *Moris Capchun*, dealt with structural investigations of alkaloids. Upon returning to the Sieff Research Institute, he initiated pioneering research in the field of natural compounds for medicinal purposes. He developed methods for the isolation and identification of natural compounds from plants and insects and studied their biological activity. He isolated thebaine from the poppy *Papaver bracteatum*, which grows wild throughout Asia Minor. Thebaine is used as a starting material for the preparation of the anti-addiction drug naloxone and the analgesic opioid codeine. *Lavie* studied certain biogenetic pathways and factors controlling the process of germination and also isolated compounds from apricot tree bark, which attract certain insects (*183*). *Lavie*'s co-author *Erwin Glotter*, born in Bacău, Romania, received his Ph.D. at the Weizmann Institute in 1965 and was professor of chemistry at the Hebrew University of Jerusalem from 1992 until 1996. Cucurbitanes are a class of triterpenoid substances that can be isolated from plants of the family Cucurbitaceae. They are of concern on account of their high toxicity, which was described as *Elisha*'s Miracle in The Bible: "*Elisha and the young prophets following him went to Gilgal, near Jericho. They were hard-pressed for a meal, and one of the young prophets went to gather some herbs in the field. He came back with some wild gourds, and no one knew that they were poisonous. When they ate of the pottage, they cried, "Oh, Man of God, there's death in the pot!*"" (Kings II/4, 38–40).

Further contributions in Volume 29 were "The Chemistry of Glutarimide Antibiotics" by *Francis Johnson* from The Dow Chemical Company, Eastern Research Laboratory, Wayland, Massachusetts (*Z213*), "Biogenetic-type Synthesis of Terpenoid Systems" by *David Goldsmith*, Department of Chemistry, Emory University, Atlanta, Georgia (*Z215*), and "The Biosynthesis of the Diterpenes" by *James R. Hanson*, University of Sussex (*Z217*).

Eugene Premuzic was the author of the last contribution of Volume 29, entitled "Chemistry of Natural Products Derived from Marine Sources" (*Z218*). *Eugene Premuzic* moved to California in 1971 to become a senior scientist with the International Biotechnological Centre at the Wild Life Research Institute in Colton. Later on, he lectured at Fordham University and became a professor at Southampton College.

5.2.3 Volume 30

For Volume 30, published in 1973, *Milton J. Cormier*, *John E. Wampler*, and *Kazuo Hori* from the Department of Biochemistry at the University of Georgia in Athens, Georgia, wrote a contribution on "Bioluminiscence: Chemical Aspects". In detail, the authors discussed emissions of visible radiation by enzyme-catalyzed reactions including *Renilla* (sea pansy), fire fly, cypridine, bacterial, *Latia*, and earthworm bioluminiscence (*Z219*). Comments on a general mechanism were given as well. The first author of this paper, *Milton J. Cornier*, was born in 1926 in a rural town in Northern Louisiana. He recieved a BS degree from the University of Louisiana at Lafayette and a MS degree from the University of Texas in Austin. He finished his PhD at the Oak Ridge National Laboratory in Tennessee. *Cornier* later became research professor of biochemistry at the University of Georgia.

Lothar Jaenicke (*1923) and *Dieter G. Müller* (Institute of Biochemistry at the University of Cologne) summarized their studies on sirenin, ectocarpene, and dictyopterene in "Gametenlockstoffe bei niederen Pflanzen und Tieren" ("Gamete Pheromones in Lower Plants and Animals") (*Z220*).

Judith Polonsky, working together with *Edgar Lederer* at the Centre National de la Recherche Scientifique, Gif-sur-Yvette gave a comprehensive synopsis of a new area of terpenoid chemistry in her paper on "Quassinoid Bitter Principles" (*Z221*). The first structure determination of a bitter substance constituent yielded from the plant family Simaroubaceae was performed by *Zdenek S. Valenta* (*1927) *et al.* in 1961 (*184*).

In their contribution on "Die Ergochrome" ("The Ergochromes"), *Burchard Franck* (*1926) and *Hubert Flasch* from the University of Münster were concerned with pigments contained in the permanent mycelium of *Claviceps purpurea*, a filamentous fungus growing on rye ears—the so-called "ergot" *(Z222)*. The first pigments of this kind had been isolated as early as 1877 by *G. Dragendorff* and *V. Podwyssotski* (*185*). Nevertheless, their structures could not be elucidated for another 100 years.

"The Chemistry of Biflavonoid Compounds" was a contribution written by *Harry D. Locksley* from the University of Salford (*Z223*). As the author stated, the interest in flavonoids can be traced back to the times of *Robert Boyle*. Nevertheless, the first biflavonoid, a biflavone, was only isolated in 1929 by *S. Furukawa*, who extracted the autumnal leaves of the maidenhair tree, *Ginkgo biloba* (*186*).

In the next essay, "Chemie der Makrolid-Antibiotica" ("Chemistry of Macrolide Antibiotics"), *Walter Keller-Schierlein* stressed that the structures of many members of this class of molecules, which have a high medical impact, and can be determined through the use of NMR spectroscopy (*Z224*). *Walter Keller-Schierlein* (*1922) was titular professor at ETH Zurich from 1968 to 1987.

The last contribution to Volume 30 was submitted by *Rudolf Tschesche* and *Günter Wulff* from the University of Bonn. *Tschesche* and *Wulff* dealt with "Chemie und Biologie der Saponine" ("Chemistry and Biology of Saponins") (*Z225*). Their contribution discussed mainly the structure elucidation and a correlation between the structure and properties of these natural substances, which are characterized by their distinctive foaming potential in aqueous solution. In 1979, *Tschesche'*s student

Günter Wulff was appointed as a full professor at the Heinrich Heine University, Düsseldorf. His research interests have included the synthesis of polymers with enzyme-analogous properties through imprinting using template molecules.

5.2.4 Volume 31

Volume 31 consisted of ten contributions. The first—"Recent Developments in the Chemistry of Penicillins"—originated from the pen of *Donald N. McGregor*, Research Division, Bristol Laboratory, Syracuse, New York. Developments in penicillin chemistry during the period from 1965 through 1972 were reported, especially reactions at the β-lactam ring and at the thiazolidine ring (*Z226*).

"The Antibiotic Complex of the Verrucarins and Roridins" was the title of the next contribution, written by *Christoph Tamm* in Basel (*Z227*). Verrucarins and roridins are secondary metabolites of the soil fungi *Myrothecium verrucaria* and *M. roridum*, which occur parasitically on leaves of tomatoes, violets, kidney beans, and other common plants. The first total synthesis of a member of the trichothecane family, namely, roridin C, was reported by *Ernest W. Colvin et al.* in 1971 (*187*).

Sterigmatocystin (**22**) was the first of the very dangerous mycotoxins to be isolated and it was also the first to be elucidated structurally by *Y. Hatsuda* and *S. Kuyama* in 1954 (*188*). This and more information was included in the contribution "Aflatoxins and Sterigmatocystins" by *John C. Roberts* from the University of Nottingham (*Z228*).

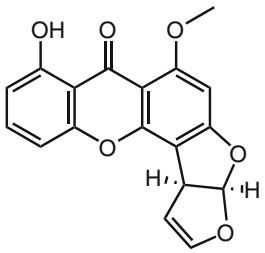

22 (sterigmatocystin)

In his contribution on "Flavonoid-Glykoside" ("Flavonoid Glycosides") (*Z229*), *Hildebert Wagner* (*1929) from the Institute of "Pharmazeutische Arzneimittellehre" at the University of Munich, expressed his gratitude for suggested improvements to Professor *Loránd Farkas* in Budapest, a former co-worker of *Gezá Zemplén,* who had worked earlier on the structure determination and synthesis of flavonoid glycosides in the late 1960s.

The next essay, "Biogenetic-Type Synthesis of Polyketide Metabolites", had three authors: *Thomas H. Harris*, *Constance M. Harris*, and *Keith B. Hindley* (*Z230*). All three were researchers at the Department of Chemistry, Vanderbilt University, in Nashville, Tennessee. After *Johann Georg Geuther* (1833–1889) had observed the formation of a "dehydroacetic acid" by self-condensation of ethyl acetoacetate in 1866 (*189*), the chemist and alpinist *John Norman Collie*

(1859–1942) in 1907 proposed that in this reaction, polymers of ketenes, hence "polyketides", play a key role as intermediates (*190*). In 1953, *Arthur John Birch* (1915–1995) restated *Collie's* early ideas (*191*). In their contribution, *Harris*, *Harris*, and *Hindley* described important preparative routes for linear β-polyketones and β-polyketo acids.

James A. Marshall from Northwestern University, Evanston, Illinois, *Stephen F. Brady* from Merck Sharp and Dohme Research Laboratories, Rahway, New Jersey, and *Niels H. Andersen* from the University of Washington in Seattle gave an account of acoranes, alaskanes, and spirovetivanes in their contribution on "The Chemistry of Spiro[4.5]decane Sesquiterpenes" (*Z231*).

The following description of the extremely poisonous croton oil was dedicated to his *"distinguished teacher in natural product chemistry"*, *Adolf Butenandt*, on the occasion of his 70th birthday, by *Erich Hecker*—one of the authors and the then director of the Biochemical Institute of the German Cancer Research Center, Heidelberg. The co-author of the paper "Phorbolesters—the Irritants and Cocarcinogens of *Croton tiglium* L." was *Hecker*'s colleague *Rainer Schmidt* (*Z232*). The study focused on the biologically active esters of the tetracyclic diterpene phorbol (**23**).

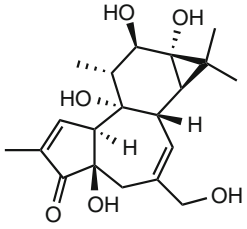

23 (phorbol)

E. Winterfeldt's report on the "Stereoselektive Totalsynthese von Indolalkaloides" ("Stereoselective Total Synthesis of Indole Alkaloids") began on page 469 (*Z233*). *Ekkehard Winterfeldt* (*1932), professor at the Technical University, Hannover, gave an insight into the syntheses of corynantheidine, strychnine, velbanamine, and tabersonine.

"Structure, Chemistry, and Biosynthesis of the Melanins" was the title of *George A. Swan*'s contribution from the University of Durham, Newcastle upon Tyne. It is now well recognized that animal melanins can be classified into two major groups: the brown-to-black insoluble eumelanins and the yellow-to-reddish-brown pheomelanins that are soluble in alkali. Studies carried out by *Swan*'s group at Newcastle led to the conclusion that eumelanin is a highly heterogeneous polymer consisting of different oxidative states of 5,6-dihydroxyindole and 5,6-dihydroxyindole-2-carboxylic acid units (*Z234*). In this contribution, the reader was confronted with the enzymatic nature of melanogenesis, in which allomelanins, eumelanins, adenochrome-melanins, dopamine-melanins, and pheomelanis were described.

Volume 31 concluded with a contribution by *Gerhard N. Schrauzer*: "Mechanisms of Corrin Dependent Enzymatic Reactions" (*Z235*). The author, then a researcher at the University of California at San Diego, La Jolla, California, who received his

PhD from the University of Munich in 1956, described some of the more important properties and reactions of corrins and of vitamin B_{12} model compounds. The mechanism of a corrin-dependent enzymatic reaction is discussed. The literature covered went up to October 1972.

5.2.5 Volume 32

Wolfgang K. Seifert, Senior Research Associate at the Chevron Oil Field Research Company in Richmond, California reminded the reader that it was *Alfred Treibs* (1899–1983) who discovered the occurrence of porphyrins in petroleum in 1936 (and was the founder of the area of geological biomarkers), in his contribution on "Carboxylic Acids in Petroleum and Sediments". This discovery signaled the biological origin of petroleum and represented the birth of modern organic geochemistry (*Z236*). *Seifert*'s contribution summarized the progress in elucidating the structures of naphthenic acids isolated from petroleum and gave a biogeochemical interpretation of the results.

In 1888, *Theodor Curtius* (1857–1928) and *Franz Goebel* were the first to prepare 2,5-dioxopiperazine. They named it "Glycinanhydrid" (*192*). *Emil Fischer* synthesized some members of the family of 2,5-dioxopiperazines in the early 1900s. *Peter G. Sammes* from the Department of Chemistry at the Imperial College of Science and Technology in London mentioned this historical information in the introduction of his contribution on "Naturally Occurring 2,5-Dioxopiperazines and Related Compounds" (*Z237*).

By the 1970s, NMR investigations already formed part of the standard repertoire of methods for structural analysis. "Structural Investigation of Natural Products by Newer Methods of NMR Spectroscopy" was the title of a paper written by *Robert J. Highet* and *Edward A. Sokoloski* from the National Heart, Lung and Blood Institute, NIH, Behesda, Maryland. In their contribution, *Highet* and *Sokoloski* emphasized that straightforward NMR techniques are the natural product chemist's first tools in the examination of natural materials. They described solvent effects on NMR signals, *in situ* reactions, lanthanide-induced shifts, computer-aided interpretation of spectra, the nuclear *Overhauser* effect, *Fourier* transformation techniques, and ^{13}C NMR spectroscopy (*Z238*). *Robert J. Highet* (1925–2002) was an organic chemist who specialized in nuclear magnetic resonance studies of natural products. *Highet* was well-known for his skills in interpreting the complex signals using at that time a Varian A-60 NMR instrument for a wide variety of natural products (*193*).

Other spectroscopic techniques were developed further, especially for the identification of optical isomers. In the same volume, *Patricia M. Scopes* from the Department of Chemistry at Westfield College in London wrote a contribution on the "Applications of the Chiroptical Techniques to the Study of Natural Products" (*Z239*).

The penultimate contribution of Volume 32 was that by *Hans Carel van Hummel*, working at the Katholicke Universiteit, Nijmegen: "Chemistry and Biochemistry of Plant Galactolipids" (*Z240*). At the turn of the twentieth century it was *Ernst Winterstein* of the agricultural chemical laboratory at the Polytechnikum Zurich who isolated lipid fractions from various plant materials. Following acid hydrolysis

of this fraction, *Winterstein* obtained a variety of sugars, including galactose. The contribution under discussion summarized the knowledge on synthesis and degradational chemistry of galactolipids as of 1975. The function of galactolipids in the photosynthesis of algae and higher plants was discussed.

The final contribution of Volume 32 dealt with "Recent Advances in Polynucleotide Synthesis". *Hans Kössel* (1934–1995) and *Hartmut Seliger*, both from the University of Freiburg/Breisgau, presented a compilation of contributions to this field of research between 1970 and 1974, in order to enhance the understanding of gene function (*Z241*).

5.2.6 Volume 33

Volume 33 (1976) started with a contribution submitted from the Laboratorio per la Chimica di Molecole di Interesse Biologica del C.N.R. in Arco Felice, Naples, entitled "Natural Products from Porifera", which reviewed about 100 unusual compounds present in sponges, such as bromo- compounds, specialized terpenes, and sterols. All of the authors were members of the group of *Guido Cimino,* the noted Italian researcher in the field of marine natural products, namely, *Luigi Minale, Salvatore de Stefano, Guido Sodano*, and—of course—*Guido Cimino* himself (*Z242*).

The following contribution was a quite comprehensive study entitled "Biogenetic-type Rearrangements of Terpenes" by *Robert Mercer Coates* (*1938), of the University of Illinois. Up to 1970, more than 200 different carbon skeletons of naturally occurring terpenes had been identified (*Z243*). Today, the research group of Emeritus Prof. *Coates* at Urbana-Champaign is engaged in the synthesis and investigation of novel carbocyclic structures, isotope labeling for the elucidation of stereochemistry, and inhibitors of key enzymes in the isoprenoid biosynthesis pathway (*194*).

The next contribution of Volume 33 on the "Chemistry of Ansamycin Antibiotics" was the work of *Kenneth L. Rinehart* (1929–2005) and *Lois S. Shield*, who were both researchers at the Roger Adams Laboratory of the University of Illinois. Ansamycins constitute a class of antibiotics charaterized by an aliphatic bridge linking non-adjacent positions of an aromatic nucleus (*Z244*).

The contribution "The Chemistry of Tryptophan in Peptides and Proteins", written by *Angelo Fontana* and *Claudio Toniola* (Instituto di Chimica Organica dell'Università Padova), covered the chemistry of the tryptophan amino acid residue (*Z245*). A section dealing with techniques used in assessing structural characteristics of tryptophan (UV spectroscopy, circular dichroism, NMR- and X-Ray studies) was included.

The renowned flavin expert, *Peter Hemmerich* (1929–1981), who at the time was lecturing at the University of Konstanz, provided an essay on "The Present Status of Flavin and Flavocoenzyme Chemistry". As the author stated, the "heroic period" of enzymology ended with *Hugo Theorell*'s description of the first enzyme to be split reversibly to yield coenzyme and apoprotein in 1934. The structure of this particular coenzyme was later shown to be rivoflavin-5′-phosphate. The two aims of *Hemmerich*'s contribution were the interpretation of the flavoprotein manifold and the closure of the gap between chemistry and enzymology (*Z246*).

5.2.7 Volume 34

Volume 34 was published in 1977. *Curt R. Enzell, Inger Wahlberg,* and *Arne J. Aasen*, from the Swedish Tobacco Company in Stockholm, were responsible for its first contribution on "Isoprenoids and Alkaloids of Tobacco". The authors emphasized that the processing of tobacco leaves after harvest is of vital importance to the final product. The substituents are subjected to various reactions. This was shown by quite different gas chromatograms of volatile fractions derived from mature freeze-dried tobacco on the one hand and from tobacco aged for 24 months on the other (*Z247*).

In the contribution by *Albert Reginald Pinder*, professor at Clemson University in South Carolina, entitled "The Chemistry of the Eremophilane and Related Sesquiterpenes" (*Z248*), the reader was introduced to sesquiterpenes related to eremophilane (**24**), which do not conform structurally to the isoprene rule first proposed in 1887 by *Otto Wallach* (1847–1931). The first members of this group of compounds were discovered in 1932 by *Alan Edwin Bradfield* (1897–1953), *Arthur Ramon Penfold* (1890–1980), and *John Lionell Simonsen* (1884–1957). *Bradfield* and *Simonsen* were members of the University College of North Wales, Bangor (*195*), whereas *Penfold* was the director of the Technological Museum in Sydney (*196*).

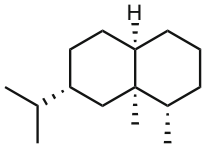

24 (eremophilane)

The next contribution was provided by *Dieter Gross*, an author we know already, and is entitled "Phytoalexine und verwandte Pflanzenstoffe" ("Phytoalexins and Related Phytochemical Substances"). It commented on endogenous plant-derived substances exhibiting fungitoxic activity (*Z249*).

Karl H. Overton (1925–2009) and *Douglas J. Picken* from the Department of Chemistry at the University of Glasgow opened their contribution entitled "Studies in Secondary Metabolism with Plant Tissue Cultures" with the statement that the first successful experiments of culturing plant cells *in vitro* were conducted in 1939 (*Z250*). *Overton* and *Picken* gave a brief outline of the basic techniques and then focused on the biosyntheses of polyisoprenoids, polyketides, aromatic plant constituents, and alkaloids. *Karl Overton* was born in Vienna as *Karl Oberweger* and came to the UK as one of thousands of Jewish child refugees in 1939—just before war broke out. He entered London University in 1944, where he graduated first in pharmacy and subsequently in chemistry. In 1973, he was appointed to a personal chair of organic chemistry at Glasgow University (*197*).

Carbazole was discovered and identified in coal tar by *Carl Graebe* (1841–1927) and *Carl Glaser* (1841–1935) in 1872, but was completely unknown as a plant product until the discovery of ulein and olivacine (**25**) by *J. Schmutz* and co-workers

in 1957 (*198*). In "Carbazole Alkaloids", by *D. P. Chakraborty* from the Bose Institute, Calcutta, methods of structure elucidation and the synthesis of numerous compounds of this group were discussed in great detail (*Z251*).

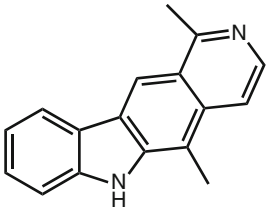

25 (olivacine)

In the penultimate contribution of Volume 34, *Jürgen Jacob* from the Biochemical Institute of Environmental Carcinogens at Ahrensburg/Holstein wrote on "Bürzeldrüsenlipide" ("Uropygial Gland Lipids"). Thanks to the combination of gas chromatography and mass spectrometry (GC-MS), the structure determination of isomeric fatty acids and alcohol composites occurring in the uropygial glands of birds became possible (*Z252*).

Wolfgang Voelter (*1936) from the Eberhard-Karls-Universität, Tübingen, who became known mainly due to his elucidation of the structures of mistletoe constituents, dedicated his contribution on "Hypothalamus-Rezeptorhormone" ("Hypothalamus Receptor") to the structure determination, synthesis and derivatives of thyrotropin-releasing hormone (TRH) as well as luteinizing (LH) and follicle-stimulating hormones (FSH), which are regulated by the gonadotropin-releasing hormone (GRH) (*Z253*). It was *Andrzej (Andrew) Wiktor Schally* (*1926) in 1966, who was the first to isolate a hormone belonging to this group.

5.2.8 Volume 35

In his contribution entitled "Neolignans", *Otto R. Gottlieb* from the University of São Paulo stated that neolignans represent a rapidly expanding domain of natural product chemistry with no delimitations yet in sight (*Z254*). For *Gottlieb*'s biography, see Volume 20.

Karl Herrmann, then holding the chair of food chemistry at the TU Hannover, gave an overview on esters of acids such as coumaric acid, caffeic acid, ferulic acid, salicylic acid, resorcylic acid, gallic acid and syringic acid in his contribution "Hydroxyzimtsäuren und Hydroxybenzoesäuren enthaltende Naturstoffe in Pflanzen" ("Hydroxycinnamic and Hydroxybenzoic Acids-Containing Natural Plant Products") (*Z255*).

The third contribution to Volume 35 was written by *Gerald Pattenden* and uncovered "Natural 4-Ylidenebutenolides and 4-Ylidenetetronic Acids" (*Z256*). It reflected, in particular, on the distribution of 4-ylidenebutenoids and 4-ylidenetetronic acids (**26**). *Gerald Pattenden* was the *Sir Jesse Boot* Professor of Organic Chemistry at the University of Nottingham.

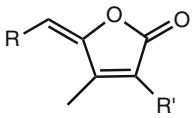

26 (4-ylidenetetronic acids)

Robert D. H. Murray from the Department of Chemistry of the University of Glasgow dedicated his treatment of "Naturally Occurring Plant Coumarins" to the nomenclature, isolation, identification, synthesis and biosynthesis of about 520 coumarins (*Z257*). In 1820, *Heinrich August Vogel* was the first to isolate the parent oxygen heterocycle, coumarin (**27**), from *Coumarouna odorata* (*199*). Coumarin is the compound responsible for the specific smell of fresh hay and dried woodruff.

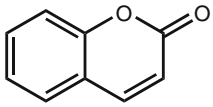

27 (coumarin)

The author of the last contribution of this volume is *Günther Ohloff*, of Firmenich Research Laboratories, Geneva. He discussed "Recent Developments in the Fields of Naturally Occurring Aroma Components" (*Z258*). A short biographical information on *G. Ohloff* can be found in the description of Volume 36 (below).

5.2.9 Volume 36

In "The Use of Carbon-13 Nuclear Magnetic Resonance Spectroscopy in Natural Products Chemistry", *Felix Werner Wehrli* (Varian AG, NMR Applications Laboratory, Zug, Switzerland) and *Toshiaki Nishida* (Swedish Tobacco Company Research Department, Stockholm) referred to a contribution of *Highet* and *Sokoloski* in Volume 32 and considered more recent literature published between 1974 and 1977 (*Z259*). Today, *Wehrli* is professor of radiology at the Medical Center of the University of Pennsylvania in Philadelphia.

The pyranone derivative maltol (**28**), which is characterized by its caramel-like smell, was discovered in 1894 by *J. Brand* at the Chemical Laboratory of the Scientific Station for Brewery in Munich as one of the characteristic key compounds in malt (*200*). Maltol is an example of an organic compound that contains a heteroatom, and is distributed widely among aroma compounds. In their contribution "The Role of Heteroatomic Substances in the Aroma Compounds of Foodstuffs", *Günther Ohloff* (1924–2005) and *Ivon Flament* restricted themselves to the description of aroma compounds resulting from thermal degradation of higher molecular weight precursors. Thus, the 310 volatile compounds identified in cocoa by 1975 comprised 60 nitrogen-containing derivatives belonging to six different heterocyclic systems (*Z260*). *Ohloff* and *Flament* were working at the Firmenich SA, Research Laboratories, Geneva, where *Ohloff* had taken over the process research

group leadership in 1962. He was then one of the leading scientists in the field of the systematic investigation of the structure and activity of odorant substances. His opus "*Riechstoffe und Geruchssinn. Die molekulare Welt der Düfte*" (published in 1990; the English edition "*Scent and Fragrances: The Fascination of Odors and Their Chemical Perspectives*" was published in 1994) is considered the standard reference in odorant chemistry. His co-author *Ivon Flament* became known through her books on coffee flavor chemistry (*201*).

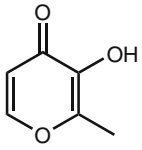

28 (maltol)

Cembranes, a new group of diterpenes, were described for the first time in 1962. *Alfred J. Weinheimer* and *James A. Matson* from the Department of Medicinal Chemistry and Pharmacognosy at the University of Houston as well as *Clifford W. J. Chang* from the Faculty of Chemistry at the University of West Florida (UWF), Pensacola, were the authors of "Naturally Occurring Cembranes" (*Z261*). *Chang* served at the UWF Chemistry Department from 1968 to 2003. In particular, he conducted research on marine natural products.

5.2.10 Volume 37

"Insect Pheromones: A Critical Review of Recent Advances in Their Chemistry, Biology, and Application" was the first contribution of Volume 37, which was published in 1979 (*Z262*). The three authors involved worked at three different institutions. *John M. Brand* was a member of the Biochemistry Department at the University of Fort Hare in Alice, South Africa, *J. Chr. Young* was employed at the Chemistry and Biology Research Institute of the Canadian Department of Agriculture in Ottawa, and *Robert M. Silverstein* was a faculty member at the Department of Chemistry, College of Environmental Science and Forestry, State University of New York, Syracuse. At the time of writing this contribution, about 10,000 scientific papers had been published on insect chemistry. One area of insect chemistry covers molecules that serve as messenger substances, the so-called "pheromones", the first of which was detected by *Adolf Butenandt* in 1959 (*202*). In order to isolate bombykol, the silk moth (*Bombyx mori*) pheromone, *Butenandt* used about 500,000 insects.

"The Structural Polymers of the Primary Cell Walls of Dicots" by *Michael McNeil, Alan G. Darvill*, and *Peter Albersheim* from the Department of Chemistry, University of Colorado, Boulder, was the second contribution of Volume 37 (*Z263*). Today, *Peter Albersheim* (*1934), who earned his PhD at CalTech in 1959, is an internationally renowned scientist in the structure and interaction of molecules involved in growth control, reproduction and disease resistance in plants.

Peter Albersheim and *Alan Darvill* co-founded the Complex Carbohydrate Research Center at the University of Georgia, Athens, in 1985 (*203*).

"Dehydroamino Acids, α-Hydroxy-α-amino Acids, and α-Mercapto-α-amino Acids", written by *Ulrich Schmidt*, *Johannes Häusler*, *Elisabeth Öhler*, and *Hans Poisel* from the Institute of Organic Chemistry at the University of Vienna, was the final contribution of Volume 37 (*Z264*). *Ulrich Schmidt* (1924–2004) was one of the leading peptide chemists of his time. He was born in Woldenburg in the district of Friedeberg (Neumark)—which is today Dobiegniew in Poland—in 1924. Following State Labor Service, and serving in the Wehrmacht army and then war imprisonment, he started his chemistry studies in Greifswald in 1946. He came to Freiburg *via* Halle, and was promoted from lecturer to extracurricular professor in 1964. At that time, his main research field was the chemistry of sulfur and phosphorus compounds. From the mid-1970s, *Schmidt* turned to the field of amino acids, and, in 1967, he became full professor at the University of Vienna. In 1977, he accepted the Chair of Organic Chemistry, Biochemistry, and Isotope Research at the University of Stuttgart. *Schmidt'*s development of new synthesis methods for complex cyclopeptides has been recognized internationally. In their contribution, *Schmidt* and his Austrian co-authors focused the attention of the reader to the fact that in the 1970s, numerous α,β-dehydroamino acids had been identified as constituents of fungal metabolites. It was recognized that some of these, such as ostreogrycin, griseoviridin, telomycin, and thiostreptone, are active against *Gram*-positive bacteria.

5.2.11 Volume 38

Volume 38 was comprised of only two contributions. The shorter one was written by *Richard W. Franck* (*1936), professor at Fordham University, Bronx, New York, on "The Mitomycin Antibiotics" (*Z265*). Mitomycins were obtained for the first time in 1956 from *Streptomyces caespitosus* by *Toju Hata* and co-workers (*204*) from Kitasato University, Tokyo.

The other, much longer contribution, "The Biogenesis and Chemistry of Sesquiterpene Lactones", was submitted by *Nikolaus H. Fischer (*1936), Errol Joseph Olivier,* and *H. D. Fischer* from Louisiana State University, Baton Rouge. The major goal of this contribution was to present all known naturally occurring sesquiterpene lactones and their distribution in the plant kingdom. At the end of 1977, no less than 980 compounds of this kind were known (*Z266*). A list of hitherto unidentified sesquiterpene lactones at the end of the contribution proved to be a useful guide for chemists facing related structural problems (*205*).

5.3 Volumes 39–88: A New Design

Starting from Volume 39, the Series was delivered in a characteristic light green cover, which made it quite easy to spot in any science library.

5.3.1 Volume 39

The first contribution of Volume 39 (which appeared in 1980) was entitled "Carbohydrate Derivatives in the Asymmetric Synthesis of Natural Products" (*Z267*). The very first enantioselective synthesis was described by *Willy Marckwald* (1864–1942) in 1904 (*206*). The 1970s saw an intensified effort to develop such syntheses. The authors of this contribution on asymmetric synthesis were *Bertram Fraser-Reid* (*1934) and *Roy Clayton Anderson* (1926–2001), from the Guelph-Waterloo Centre for Graduate Work in Chemistry at the University of Waterloo, Ontario.

Howard Jones, then director of medical chemistry at the USV Pharmaceutical Corporation in Tuckahoe, New York and *Gary H. Rasmusson*, at that time senior research fellow in synthesis chemical research at the Merck Sharp and Dohme Therapeutic Research Laboratories, Rahway, New Jersey were the authors of "Recent Advances in the Biology and Chemistry of Vitamin D" (*Z268*). It was *Theobald Adrian Palm* (1848–1928) who in 1890 determined that sunlight is the critical factor determining the geographical distribution of the disease rickets (rachitis) (*207*). In 1919, *Edward Mellanby* (1884–1955) reported the presence of an antirachitic factor in cod liver oil. Subsequently, in 1932, *Adolf Windaus* (1879–1959) and *Frederic Anderton Askew* isolated independently pure crystalline vitamin D (*208*). Six years later, synthesis work on vitamin D culminated in the photochemical synthesis of vitamin D_3, simultaneously by *Basil Lythgoe* in England and *Hans Herloff Inhoffen* in Germany. The decade from 1970 to 1980 saw a startling advance in understanding the biochemical mechanisms of action of vitamin D. In their contribution, *Jones* and *Rasmusson* focused primarily on biochemical aspects, *e.g.* photolytic and thermal conversions of vitamin D isomers.

The contribution "Stereochemistry of Naturally Occurring Carotenoids", by *Synnøve Liaaen-Jensen* (*1932), of the Organic Chemistry Laboratories at the Norwegian Institute of Technology at the University of Trondheim was related to the work of *Zechmeister* in 1960 concerning geometrical diastereomerism (*Z269*). From 1971 to 1980, 150 new carotenoids were described, whereas the number of references almost tripled.

The concluding contribution of Volume 39 was an account of "Chemistry and Biochemistry of γ-Glutamyl Derivatives from Plants Including Mushrooms (Basidiomycetes)" by *Takanori Kasai* from the Department of Agricultural Chemistry at Hokkaido University in Sapporo and *Peder Olesen Larsen* from the Royal Veterinary and Agricultural University, Copenhagen (*Z270*).

5.3.2 Volume 40

Volume 40 brought about an encounter with an old acquaintance: *Edgar Lederer*, who in the interim had become professor emeritus at the Université Paris Sud. Together with *Pierre Lefrancier* from the Institut Choay, Montrouge, *Lederer* provided the contribution "Chemistry of Synthetic Immunomodulant Muramyl Peptides" (*Z271*).

What followed was a contribution by *Sukh Dev* (*1923) entitled "The Chemistry of Longifolene and Its Derivatives" (*Z272*). Professor *Dev's* research interests covered a broad range of topics in the field of natural product chemistry—from non-benzenoid hydrocarbons, organic reactions, reagents and techniques, and drug development from Ayurvedic leads, to technology development (*209*).

Werner Heller's and *Christoph Tamm's* next paper discussed "Homoisoflavanones and Biogenetically Related Compounds" (*Z273*). Since 1986, *Werner Heller* has been head of a research group focusing on secondary metabolites at the Institute of Biochemical Plant Pathology of the Helmholtz Zentrum Munich.

Raymond G. Cooke's and *J. Michael Edwards*' text on "Naturally Occurring Phenalenones and Related Compounds" (*Z274*) was the penultimate contribution of Volume 40. *Michael Edwards* held a faculty position at the School of Pharmacy of the University of Connecticut. During sabbaticals at the Universities of Surrey, Cape Town and Western Australia he studied the occurrence and biosynthesis of unusual phenalenone pigments in the plant family Haemodoraceae (*210*). Nowadays, the substance phenalenone is considered to be a useful reference compound for the determination of quantum yields of singlet oxygen sensitization (*211*).

Exciting reading is guaranteed for *Charles W. Jefford's* and *Peter A. Cadby's* contribution entitled "Molecular Mechanisms of Enzyme-Catalysed Dioxygenation" (*Z275*). The subtitle read "An Interdisciplinary Review". In this paper, arguments of the MO-theory were used to understand fundamental chemical processes. From a thermodynamic point of view, it might seem strange that there should be a need for enzymes to catalyze reactions where oxygen is introduced into an organic substrate. As a matter of fact, most organic molecules are stable kinetically to uncatalyzed oxygenation. The reason lies in the spin restriction in the reaction of a ground-state organic molecule (normally in the singlet state) with ground-state molecular oxygen (in the triplet state). The authors, who worked at the University of Geneva, examined the prerequisites for oxygen activation by metal proteins.

5.3.3 Volume 41

In Volume 41, *E. Haslam* set out to explain "The Metabolism of Gallic Acid and Hexahydroxydiphenic Acid in Higher Plants" (*Z276*). *Edwin Haslam* (1932–2013) was formerly Professor, Department of Chemistry, University of Sheffield. Based on earlier proposals, he advocated a comprehensive definition of plant polyphenols, which included specific structural characteristics common to all phenolics exhibiting tanning properties, referred to as the *White-Bate-Smith-Swain-Haslam* (WBSSH) definition (*212*).

The contribution on "Streptonigrin"by *Steven J. Gould* and *Steven M. Weinreb* covered the chemistry of an important cytotoxic antibiotic obtained from *Streptomyces flocculus* (*Z277*). *Steven J. Gould* was then a professor at Oregon State University, Corvallis. In 1981, his co-author *Steven M. Weinreb* (*1941) succeeded in performing the total synthesis of streptonigrin (*213*), a compound showing pronounced anticancer activity. *Weinreb* became known for the *Weinreb* ketone synthesis, which enables mono-addition of an organometallic reagent to an amide.

David J. Robins from the Department of Chemistry, University of Glasgow published a contribution entitled "The Pyrrolizidine Alkaloids" (*Z278*). *Robins* was appointed lecturer at the University of Glasgow in 1974, promoted to professor of bioorganic chemistry in 1990, and elected Fellow of the Royal Society of Edinburgh in 1994.

The final contribution of Volume 41 is perhaps the most interesting. It informed the reader of the "Alkaloids of Neotropical Poison Frogs (*Dendrobatidae*)", and was written by *John William Daly* (1933–2008), from the Laboratory of Bioorganic Chemistry at the National Institute of Arthritis, Diabetes, and Digestive and Kidney Diseases, National Institutes of Health, Bethesda, Maryland (*Z279*). *Daly* was considered the world authority in amphibian alkaloids (*214*). As a matter of fact, indigenous peoples of the rain forest of Western Colombia used secretions of certain brightly colored frogs to poison blow darts in pre-colonial times. A thorough investigation of the active principles of such poison dart frogs was not initiated until 1961. The structures of members of the first dendrobatid alkaloid class were published in 1968. *Daly* reported on the structures, synthesis, and biological activity of the batrachotoxins, pumiliotoxins, histrionicotoxins, and gephyrotoxins.

5.3.4 Volume 42

The first contribution of Volume 42 (1982) comprised almost 300 pages. *Yoshinori Asakawa* (*1941), head of the Institute of Pharmacognosy at Tokushima Bunri University, Tokushima, Japan, reviewed "Chemical Constituents of Hepaticae" (*Z280*). This contribution represented a summary of research on all known terpenoids and aromatic compounds occurring in liverworts until 1982. As early as 1905, some non-polar constituents found in these lower plants had been found to be sesquiterpenoids, but the chemical constituents were not further investigated until 1965. From 1978 to 1981, no less than 121 papers on the chemistry of Hepaticae were published. *Asakawa* focused on biologically active compounds and chemosystematics.

The second paper of Volume 42, "Cross Reactions of Plant Polysaccharides in Antipneumococcal and Other Antisera" (*Z281*), by *Michael Heidelberger,* New York University Medical Center, School of Medicine, New York, provided an update of the author's earlier contribution to Volume 18 of this book series.

5.3.5 Volume 43

The first contribution of Volume 43, "Naturally Occurring Isoflavonoids (1855–1981)", by *John L. Ingham*, from the Department of Botany at the Plant Science Laboratory of the University of Reading, was concerned mainly with the structures, sources, and biological properties of natural products containing a 1,2-diphenylpropane unit (*Z282*). Their discovery dates back to 1855, when *Heinrich Hlasiwetz* (1825–1875) reported the extraction of formononetin (the aglycone of ononin) from roots of the thorny restharrow *Onosis spinosa* (*215*). Ononin is regarded as the very first isoflavonoid to

have been discovered. Although *Hlasiwetz* demonstrated elegantly the glucosidic nature of this substance, its structure elucidation was a task only accomplished in 1933 by *Fritz Wessely* (1897–1967) in Vienna (*216*). *Gezá Zemplén* synthesized ononin successfully in 1944 (*217*). *Ingham* listed the structures, molecular weights, formulas, trivial names, and sources of 644 isoflavonoids that had been described by December, 1981.

Volume 43 concluded with a contribution by *Ari Koskinen* (*1956) and *Mauri Lounasmaa* (*1933) from the Laboratory of Organic Chemistry at the Technical University of Helsinki, entitled "The Sarpagine-Ajmaline Group of Indole Alkaloids" (*Z283*). The first indole alkaloid, strychnine, was isolated by *Pierre Joseph Pelletier* (1788–1842) and *Joseph Bienaimé Caventou* (1795–1877) in 1818 from plants of the genus *Strychnos. Robert B. Woodward* (1917–1979) succeeded in performing the first synthesis of strychnine in 1954 (*218*). Ajmaline was isolated for the first time by *Salimuzzaman Siddiqui* (1897–1994) in 1931 from the roots of *Rauwolfia serpentina*. It was named after *Hakim Ajmal Khan* (1863–1927), an Indian physician. The total synthesis of ajmaline was performed by *Satoru Masamune* (1928–2003) and co-workers at the Massachusetts Institute of Technology (MIT) in 1967 (*219*).

5.3.6 Volume 44

"Pro-Inflammatory, Tumour-Promoting and Anti-Tumour Diterpenes of the Plant Families Euphorbiaceae and Thymelaeaceae" was the title of the first contribution of Volume 44, published in 1983. In their historical introduction, *Fred J. Evans* (1943–2007) and *S. E. Taylor* from the Department of Pharmacognosy, School of Pharmacy at the University of London, reminded the reader that the isolation and first structure elucidation of the tumor-promoting phorbol-12,13-diesters occurred from the seed oil of *Croton tiglium* by *Erich Hecker* in 1968 (*Z284*). These pure diterpene esters have been instrumental in gaining a better understanding the carcinogenesis and inflammatory processes.

The next contribution by *Albert Mondon* (1911–1991) and *Bernd Epe* (*1950) from the Institute of Organic Chemistry at Kiel University dealt with "Bitter Principles of Cneoraceae" (*Z285*). The Cneoraceae is a Mediterranean relict shrub family rich in polyphenols.

Mondon and *Epe* were followed by a contribution on "Chemical and Biological Aspects of Marine Monoterpenes" (*Z286*). The authors of the latter, *Steve Naylor, F. Joe Hanke,* and *Phillip Crews* from the Thimann Laboratories and Center of Coastal Marine Studies at the University of California, Santa Cruz, dedicated their work to Professor *Paul Scheuer* (1915–2003) from the University of Hawaii, who, as mentioned earlier, was a distinguished pioneer in the field of marine natural products chemistry. Marine monoterpenes remained unobserved until 1955, when *Teruhisa Katayama* reported seven monoterpenes as constituents of the green alga *Ulva pertusa*. Within a decade (1973–1983), over a hundred monoterpenes of this sort were published. The contribution of 1983 considered important chemical and biological aspects of this specific terpenoid class.

The last contribution to Volume 44 was by *John Grant Buchanan* (1926–2012) from the Department of Chemistry at Heriot-Watt University, Edinburgh, entitled "The C-Nucleoside Antibiotics" (*Z287*). Since 1960, a number of nucleosides in which a carbohydrate unit is linked to a heterocyclic base had been discovered in microorganisms. Some of these exhibit antibiotic properties. *Buchanan's* contribution mentioned showdomycin, formycin, pyrazofurin, oxazinomycin, and esomycin.

5.3.7 Volume 45

When it came to Volume 45 (1984), the reader was confronted initially with the chemistry of limonoids. Research on limonoid chemistry of the Mahogany family (Meliaceae) began in 1960 with the isolation of gedunin from the West African timber tree *Entandrophragma angolense.* As shown quite recently, the tetranortriterpenoid gedunin manifests potential anticancer activity (*220*). In his contribution of 1984, *David A. H. Taylor* from the Department of Pure and Applied Chemistry at the University of Natal in South Africa listed 280 compounds. Several of these occur in esterified form in different species (*Z288*).

"Recent Progress in the Chemistry of Lichen Substrates" by *John Alan Elix* (*1941), and *Andrew A. Whitton* from the University of Canberra, and *Melvyn V. Sargent* from the University of Western Australia, represented another contribution to lichen chemistry. The authors pointed out that thin-layer chromatography (TLC) and high-performance liquid chromatography (HPLC) have proven rapid and efficient methods for the detection and purification of lichen substances. More sophisticated techniques of ^{13}C- and ^{1}H-NMR spectroscopy facilitated structural studies tremendously. The development of lichen metabolite chemistry was discussed in detail (*Z289*).

Paralytic shellfish may contain toxins responsible for acute and often fatal poisoning caused by their consumption. Saxitoxin was the first toxin of this sort to be obtained in its pure form in 1957 by *Edward J. Schantz* (1908–2005) and co-workers (*221*). In his essay on "Paralytic Shellfish Poisons", *Yuzuru Shimizu* from the Department of Pharmacognosy and Environment Health Science at the University of Rhode Island in Kingston stressed that shellfish toxins are of particular importance as pharmacological tools because of their unique effect on sodium channels involved in membrane excitation (*Z290*).

5.3.8 Volume 46

The presence of saponins in ginseng was reported as early as 1854 by *Samuel S. Garrigues* (1828–1889) (*222*). Since the beginning of the twentieth century, a number of Japanese, European, and Korean chemists have been engaged in the isolation and structure elucidation of ginseng saponins, including *Yasuhiko Asahina* (1880–1975), *Munio Kotake* (1894–1976), and *Theodor Wagner-Jauregg* (1903–1992), the son of *Nobel* laureate *Julius Wagner von Jauregg*. However, even the basic skeleton of the major sapogenin was not characterized until 1960.

In Volume 46, *Osamu Tanaka* (1926–2002) and *Ryoji Kasai*, from the Institute of Pharmaceutical Sciences at Hiroshima University School of Medicine summarized all of the relevant structural information at the time of publication in their contribution entitled "Saponins of Ginseng and Related Plants" (*Z291*).

Another contribution, "Diterpenoids of *Rabdosia* Species" (*Z292*), was co-authored by *Eiichi Fujita* (1922–2011) and *Manabu Node* (*1945) from the Institute for Chemical Research of the University of Kyoto. In Japan, the leaves of *Rabdosia japonica* and *R. trichocarpa* have been used in traditional medicine for gastrointestinal disorders for centuries. Also in China, some *Rabdosia* species growing in mountainous regions have folkloric use as antitumor and antiphlogistic remedies. In 1964, research on the structure of *enmei,* one of the major *Rabdosia* constituents, came to a successful conclusion. By 1984, no less than 108 different diterpenoid constituents from from *Rabdosia* species had been isolated and characterized.

Volume 46 was concluded by an overview of "The Quinazoline Alkaloids" by *Siegfried Johne* (*Z293*). *Johne* was then a member of the Institute of Plant Biochemistry at the GDR Academy of Sciences in Halle/Saale. The first known quinazoline alkaloid was vasicine (peganine), isolated from *Adhatoda vasica* by *David Hooper* (1858–1947) in 1888 (*223*). For centuries, this plant was used in Indian indigenous medicine. Research on the antimalarial activity of the alkaloid febrifugine isolated in 1946 through 1948 and structurally characterized in 1950 (*224*), provided a stimulus for the synthesis and biological screening of a large number of quinazoline derivatives.

5.3.9 Volume 47

In 1985, Volume 47 of the Series was published. In the introduction of their paper on "Naturally Occurring β-Lactams", *Robert Southgate* and *S. Elson* from the Beecham Pharmaceuticals Research Division in Betchworth, Surrey, U.K. pointed out that from the discovery of penicillin in 1928 until 1970, β-lactam research was concerned mainly with the penicillin and cephalosporin compound groups (*Z294*). Since then, research in this field had expanded widely—with several highlights described such as the discovery of various new natural β-lactam structures including the cephamycins (1971), norcardicins (1976), carbapenems (1977), and monobactams (1981).

In "New Techniques for the Mass Spectrometry of Natural Products", *Ian Howe* and *Michael Jarman* emphasized that mass spectrometry had provided a unique combination of selectivity and sensitivity (*Z295*), but could be even more powerful when used in combination with spectroscopic (NMR, UV, IR) and chromatographic methods (HPLC, GC, TLC). At that time, *Howe* and *Jarman* were members of the Drug Metabolism Team of the Cancer Research Campaign Laboratory at the Cancer Research Institute in Sutton, Surrey, United Kingdom.

"Chemical Syntheses of the Trichothecenes" by *Patrick G. McDougal,* representing the Department of Chemistry, Georgia Institute of Technology, Atlanta and *Norman R. Schmuff*, from the Laboratory of Chemistry at the National Heart and Lung Institute, NIH, Bethesda, Maryland (*Z296*) offered a recapitulation of progress

achieved within a specialized branch of mycotoxin research. Trichothecenes represent a group of closely related sesquiterpenoids produced by various species of imperfect fungi. The first compounds of this class were discovered during an extensive search for new antibiotics at the laboratories of the Imperial Chemical Industries in 1946 (*225*). From 1976 to 1982, *Schmuff* and *McDougal* were both members of the research group of *Barry Trost* at Stanford University.

As the title suggests, *Judith Polonsky's* contribution "Quassinoid Bitter Principles II" (*Z297*) was an extension of her chapter on the same subject published in Volume 30. Interest in these terpenoids had increased enormously by then—due in part to the finding in the early 1970s that some of these compounds display antileukemic activity.

5.3.10 Volume 48

As the authors of the first contribution of Volume 48, *Pieter S. Steyn* (*1940) and *Robert Vleggaar* (*1945), from the Council for Scientific and Industrial Research in Pretoria, South Africa, reported on "Tremorgenic Mycotoxins" (*Z298*). Tremorgenic mycotoxins induce neurological symptoms ranging from mental confusion to tremors, seizures, and death (*226*). This contribution was devoted solely to the chemistry and some biological properties of tremorgens produced by certain species of *Aspergillus, Claviceps*, and *Penicillium*.

The second contribution of Volume 48 was written by *R. E. Moore* and concerned with the elucidation of the "Structure of Palytoxin" (*Z299*). The marine organism producing palytoxin, *Palythoa toxica*, had an ancient tradition of use as an arrow poison by certain indigenous people in Hawaii. *Richard Elliott Moore* (1933–2007) and his group from the University of Hawaii performed the detailed structure elucidation of this complex neurotoxic compound.

Concluding Volume 48, *Phillip Crews* and *Steve Naylor* wrote a contribution entitled "Sesterterpenes: an Emerging Group of Metabolites from Marine and Terrestrial Organisms" (*Z300*). Sesterterpenes are a relatively large group of C_{25} isoprenoid compounds found in plants, marine organisms, and vertebrates. Today, *Phillip Crews* is Distinguished Professor at the University of California, Santa Cruz. *Steve Naylor's* home university is the University of Cambridge. When writing this very contribution, both authors were working at the Tiemann Laboratories and Centre for Costal Marine Studies, University of California, Santa Cruz.

5.3.11 Volume 49

Isocoumarins (**29**) are compounds isomeric with coumarins. Some of these—*e.g.* hydrangenol, phylloducin, and chebulic acid—are found in plants (*227*): hydrangenol and phylloducin in *Hydrangea macrophylla*, chebulic acid in *Terminalia chebula*. *Robert A. Hill* summarized recent findings concerning this compound class in "Naturally Occurring Isocoumarins" (*Z301*). Today, *Bob Hill* is head of teaching at the Chemistry Department of the University of Glasgow.

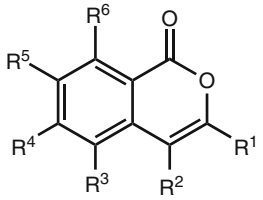

29 (isocoumarins)

In their contribution on "Anthraquinones in the Rubiaceae" (*Z302*) *Rommert Wijnsma* and *Robert Verpoorte* (Centre for Bio-Pharmaceutical Sciences, Gorleus Laboratories, Leiden University) listed the anthraquinone content of ten *Morinda* species that had been investigated at the time the chapter was written. About 90% of these compounds occur as derivatives of 9,10-anthracenedione (= 9,10-anthraquinone (**30**) with several hydroxy and other functional groups, such as methyl, hydroxymethyl, and carboxyl residues. Between 1971 and 1978, about 50 new anthraquinones were isolated from Rubiaceae species.

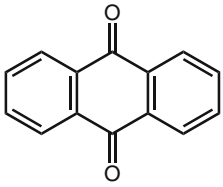

30 (9,10-anthracenedione)

Hans Christoph Krebs from the Chemical Institute at the University of Veterinary Medicine in Hannover reported on "Recent Development in the Fields of Marine Natural Products with Emphasis on Biologically Active Compounds" (*Z303*). For quite some time, the diversity of microbes in the marine environment and their capacity to produce interesting compounds were not fully realized by the scientific community (*228*). In his contribution, *Krebs* considered recent developments concerning substances derived from marine invertebrates, *e.g.* steroids from Porifera, terpenes from *Octocorallia*, and saponins from starfish.

5.3.12 Volume 50

In the first 26 pages of Volume 50, *Lothar Jaenicke* and *Franz-Josef Marner* from the University of Cologne informed the reader on "The Irones and Their Precursors" (*Z304*). Irones are pleasant-smelling terpenoids of orris oil—extracted from the rhizomes of certain sword-lily or iris species in which they accumulate during storage—which have proven to be important for the perfume industry (*229*). They were identified as ionone homologues, cyclogeranyl acetonides easily accessible from the abundant natural citral, as described by *Ferdinand Tiemann* and *Paul Kruger* in 1895 (*230*). *Lothar Jaenicke* contributed to this Series in Volumes 21 and 30.

Mauri Lounasmaa's and *Pekka Somersalo's* essay on "The Condylocarpine Group of Indole Alkaloids" started on page 27 (*Z305*). Twenty-four alkaloids with

a precondylcarpine-type pentacyclic skeleton were considered by the authors, who were then affiliated with the Laboratory for Organic and Bioorganic Chemistry at the Technical University in Helsinki.

Urs Séquin (*1943), a student of *Christoph Tamm* at Basel University, habilitated in 1976. He is the author of the contribution "The Antibiotics of the Pluramycin Group (4*H*-Anthra[1,2-*b*]pyran Antibiotics)" (*Z306*). The first pluramycin antibiotics were isolated in 1956 and found to exhibit both antimicrobial and potential anticancer activity (*231*).

The next contribution was written by *Roland Maurice Wenger* (Sandoz Ltd., Basel): "Cyclosporine and Analogues—Isolation and Synthesis—Mechanism of Action and Structural Requirements for Pharmacological Activity" (*Z307*). In 1983, an immunosuppressive drug of the cyclosporine family was launched onto the market under the name Sandimmun®. This compound, which opened up new opportunities of selective immune modulation, was isolated from fungal cultures and characterized as a cyclic undecapeptide containing a novel skeleton as well as several *N*-methylated amino acids (*232*).

Volume 50 concluded with a contribution by *Hiroyuki Inouye* and *Shinichi Uesato* from Kyoto University, Japan, entitled "Biosynthesis of Iridoids and Secoiridoids" (*Z308*). Iridoids are secondary plant metabolites forming part of the terpenoid class. Today, more than 2,500 different iridoids are known.

5.3.13 Volume 51

A special volume of around 300 pages was dedicated to an introduction to the plethora of macromycete substances by the pioneer and doyen of fungal pigments, *Wolfgang Steglich* (*Z309*). In particular, their biogenesis was described in great detail, involving the shikimate-chorismate pathway, the acetate-malonate pathway, as well as the mevalonate pathway. One example of such a compound is prasinone (**31**)—an octaketide. From 1975 until 1991, *Wolfgang Steglich* (*1933) was head of the Institute of Organic Chemistry and Biochemistry at the University of Bonn, as the successor to *Rudolf Tschesche*. From 1991 on, *Steglich* taught and worked at the University of Munich. The co-author of this contribution of 1987 was *Melvyn Gill*, who today is working at the University of Melbourne.

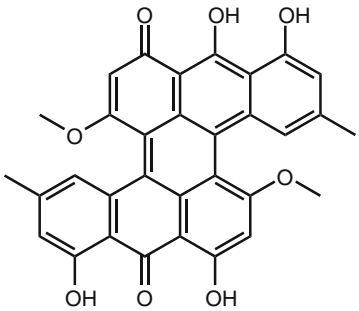

31 (prasinone)

5.3.14 Volume 52

The perylene quinones, especially the dihydroxy substituted perylene quinones (**32**), which are produced by phytopathogenic fungi, are still an important study subject today—mostly due to their photodynamic activity that can be used experimentally for the topical therapy of certain cancer types. *Lucio Merlini* (*1934), the first of three authors contributing to the chapter on "Naturally Occurring Perylenequinones" (*Z310*), had previously worked at the University of Milan. His co-authors were *Gianluca Nasini* from the Chemical Institute, Politecnico di Milano and *Ulrich Weiss* from the Laboratory of Chemical Physics at the National Institutes of Health, Bethesda, Maryland.

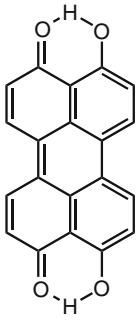

32 (dihydroxy-perylenequinone skeleton)

In his contribution "The Pigments of the Flexirubin Type. A Novel Class of Natural Products" (*Z311*), the co-discoverer of flexirubin-type pigments, *Hans Achenbach* (*1931), from the Chemical Laboratory of the University of Freiburg, described comprehensively the state of research on this group of pigments isolated from *Flexibacter* and *Cytophaga* species. These red compounds are interesting as they are phenolic esters of polyene carboxylic acids—see also the structure of flexirubin (**33**)—and thus analogous to carotenoids.

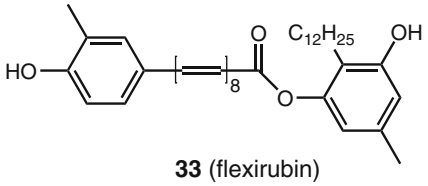

33 (flexirubin)

In "Structure, Stability, and Color Variation of Natural Anthocyanins" (*Z312*), *Toshio Goto* (1929–1990), an anthocyanin expert who worked at the Laboratory of Organic Chemistry at Nagoya University, described how flowers can be colorful even though anthocyanins do not feature any chromophore structural variants as such. Essentially, color formation does not only result from protonation or

deprotonation, as *Willstätter* hypothesized, but also occurs through complexation involving cations as well as through self-association. An example underlining the complexity of these compounds is the blue flower pigment of *Commelia communis*—commelinin—which represents a magnesium chelate complex with two anthocyanin and two flavocommelin ligands.

In 1977 (in Volume 34), *D. P. Chakraborty* already provided a contribution on carbazole alkaloids. His contribution of 1987, "Carbazole Alkaloids" (*Z313*), gave an updated overview of progress and discoveries that had been accomplished in this active field of research over a ten-year period. During this time, numerous new alkaloids of this type were isolated from different plant sources and characterized structurally. Many proved to be of interest regarding their possible pharmacological applications.

5.3.15 Volume 53

The interdisciplinary field of chemical ecology, the basis of which is formed by chemistry and its tremendous range of different secondary metabolite structures, was discussed by *Luca Fabiana Alves* in a paper entitled "Chemical Ecology and the Social Behavior of Animals" (*Z314*). Future problems or challenges were addressed, such as the relationship between pheromones and steroid hormones or the possible existence of human pheromones. Today, *Luca Fabiana Alves* is at the Laboratory of Comparative Neurophysiology and Neuroanatomy, Department of Physiology, School of Medicine of Ribeirão Preto at the University of São Paulo.

In the second contribution of Volume 53, *Taro Nomura* (*1935), Toho University, Chiba, Japan introduced the reader to "Phenolic Compounds of the Mulberry Tree and Related Plants" (*Z315*). The mulberry tree and related species are producers of many diverse compounds, mainly phenolic derivatives and isoprenoid flavonoids, such as mulberranol (**34**), which exhibits hypotensive activity. Mulberry bark is also used in traditional oriental medicine.

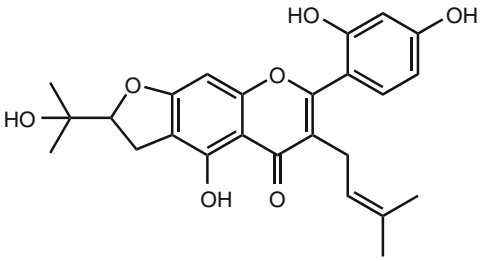

34 (mulberranol)

Andrzej Chimiak (*1932) and *Maria J. Milewska*, from the Technical University of Gdańsk, Poland (*Z316*), uncovered the chemistry of siderophores, a class of modified amino acids, which had probably been discovered by *Wilhelm von Miller*

(1848–1899) und *J. Plöchl* as early as 1893 (*233*). Interest in this group of compounds arose again due to their presence in organic natural products capable of coordinating metal ions. A known member of this group is the cyclic hexapeptide ferrichrome, which forms iron(III) complexes.

5.3.16 Volume 54

The entire volume 54—comprising about 300 pages—was dedicated to the constituents of ferns, and was concerned with styrenes, chromenes, xanthones, flavonoids, terpenes, steroids, and lipids. The volume was written by *Takao Murakami* and *Nobutoshi Tanaka* and was entitled "Occurrence, Structure, and Taxonomic Implications of Fern Constituents" (*Z317*). *Murakami* and *Tanaka* were both working at the Faculty of Pharmaceutical Sciences and Technology, Science University of Tokyo, when the contribution was written.

5.3.17 Volume 55

In the first contribution to Volume 55, *Michael T. Davies-Coleman* and *Douglas E. A. Rivett*, Department of Chemistry, Rhodes University Grahamstown, South Africa, discussed "Naturally Occurring 6-Substituted 5,6-Dihydro-α-pyrones" (*Z318*). The 6-substituted 5,6-dihydro-α-pyrones (**35**), which occur in many plants and fungi, are of significance due to their various biological activities—such as bacteriostasis and phytopathogenicity. Possible applications as plant growth inhibitors, fungistatic drugs, antifeedants or even muscle relaxants were discussed. *Michael Davies-Coleman* was professor of organic chemistry at Rhodes University until 2012, when he moved to the University of Western Cape. For biographical data on *Douglas Rivett*, see the description in Volume 75.

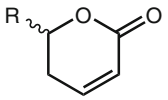

35 (6-substituted 5,6-dihydro-α-pyrones)

The next section of Volume 55 was dedicated to the principles of anthracyclinone biosynthesis, compounds found mainly in *Streptomyces* species and already mentioned in Volume 21 (*Z319*). An example of such a glycoside—of which many are known as antibiotics or active antitumor compounds—is daunorubicin (**36**). The author of this contribution, *Karsten Krohn* (*1944), studied in Kiel, habilitated in Hamburg and was professor at TU Braunschweig at the time when his contribution to the Series was published. Today, *Krohn* holds the chair of organic chemistry at the University of Paderborn.

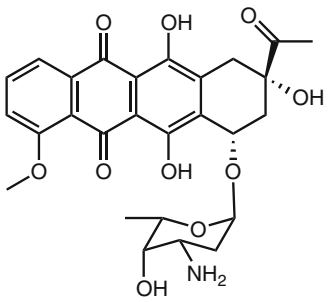

36 (daunorubicin)

Under certain conditions, cell suspension cultures of *Catharanthus roseus*, a medicinal herb, accumulate antileukemic, antihypertensive, or sedative indole alkaloids. Such an ecological production of active constituents is of high interest to the pharmaceutical industry and provided the basis for the contribution on "Indole Alkaloid Production in Cell Suspension Cultures" by *M. Lounasmaa* and *J. Galambos* (*Z320*). We already know one of the authors—*Mauri Lounasmaa* (*1933) from the Laboratory of Organic and Bioorganic Chemistry, Technical University of Helsinki—from an earlier description of a group of indole alkaloids that appeared in Volume 43.

The final essay of Volume 55 showed that the subject of renewable resources is not a modern phenomenon, especially in relation to its technical aspects. The contribution of *Catherine E. James, Leslie Hough*, and *Riaz A. Khan*, entitled "Sucrose and its Derivatives" (*Z321*), has not lost its topicality even today. In 1976, *Leslie Hough* together with the Indian chemist *Shashikant Phadnis* discovered the artificial sweetener, sucralose. *James* and *Hough* were working at Queen Elizabeth College, London, and *Khan* at Tate and Lyle Research and Technology, Whiteknights, Reading.

5.3.18 Volume 56

Volume 56 commenced with the announcement that former co-editor *Hans Griesebach* had died in March, 1990.

Its first contribution was provided by *Jean Asselineau* (*1921), professor of biochemistry at the University of Toulouse. It was entitled "Bacterial Lipids Containing Amino Acids or Peptides Linked by Amide Bonds" (*Z322*) and discussed the acylated amino acids that form part of several bacterial metabolites and are considered responsible for the solubility of peptides and proteins due to their lipid side chains.

Jacques Kagan (*1933) from the University of Illinois at Chicago wrote the next contribution: "Naturally Occurring Di- and Trithiophenes" (*Z323*). Members of this class of compounds (**37**) can be found in the plant family Asteraceae, and represent an interesting research field due to their structural characteristics on the one hand and their various biological activities (nematocide, insecticide, piscicide) on the other.

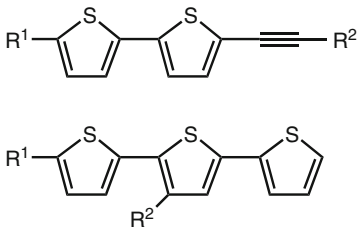

37 (di- and trithiophenes)

5.3.19 Volume 57

Pierre Metzger, Claude Largeau, and *Eliette Casadevall* from the Laboratoire de Chimie Bioorganique et Organique Physique, Paris wrote on the topic "Lipids and Macromolecular Lipids of the Hydrocarbon-rich Microalga *Botryococcus braunii*. Chemical Structure and Biosynthesis. Geochemical and Biotechnological Importance" (*Z324*). This dealt with various hydrocarbons, such as C_n botryococcicenes (**38**) and C_n cyclobotryococcicenes (**39**) of the stated organisms. These compounds serve, for example, as biomarkers in geomicrobiological oil prospection, since *Botryococcus* species have existed since Proterozoic times.

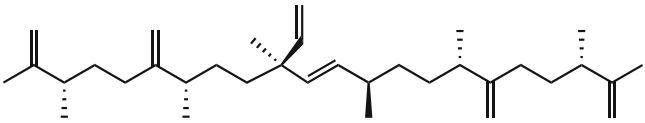

38 (C_{34} botryococcicene)

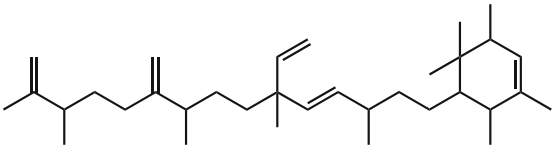

39 (C_{34} cyclobotryococcicene)

The contribution "Carbazole Alkaloids III" by *D. P. Chakraborty* (*Z325*) represented an update of the corresponding compound class published in Volume 52. *Chakraborty's* co-author of this contribution, *Shyamali Roy*, is still working at the Institute of Natural Products, Calcutta.

The group of bryostatins, which are based on the bryopyran skeleton (**40**), exhibit promising antineoplastic and cytostatic activities, with some compounds shown to inhibit tumor promotion. Futhermore, bryostatins are characterized by immunological, hematopoietic, and microbiological activities. Many of these compounds are derived from *Bugula neritina* L., a marine bryozoan species. *George R. Pettit,* from Arizona State University, acknowledged the importance of this compound class in his contribution "The Bryostatins" (*Z326*), the last contribution of Volume 57.

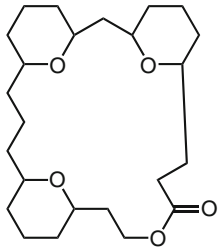

40 (bryopyran skeleton)

5.3.20 Volume 58

John A. Robinson, who moved from Southampton to Zurich as full professor of organic chemistry in 1989, was the author of the opening contribution of Volume 58—"Chemical and Biochemical Aspects of Polyether-Ionophore Antibiotic Biosynthesis" (*Z327*). The polyketide antibiotics, such as *e.g.* monensin A (**41**), formed the basis of a whole new area of chemistry—namely, the area of crown ethers, cryptands or podands—which today are of paramount importance in catalysis and synthesis.

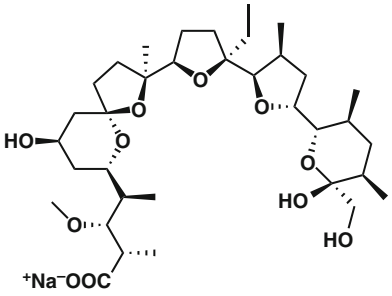

41 (monensin A)

In a comprehensive treatment entitled "Naturally Occurring Plant Coumarins" (*Z328*), *Robert D. H. Murray* from the University of Glasgow described many newly identified natural products in the coumarin class, and thus documented progress made since his corresponding contribution that appeared in Volume 35.

5.3.21 Volume 59

The introductory contribution of Volume 59 was presented by *Shin-ichi Hatanaka* from the Biological Institute, College of General Education, University of Tokyo: "Amino Acids from Mushrooms" (*Z329*). In regard to their abundance, quite a large number of essential amino acid derivatives are of major interest for mushroom taxonomic and phylogenetic studies.

Inger Wahlberg, who contributed to Volume 34, and *Ann-Marie Eklund*, were the authors of "Cembranoids, Pseudopteranoids, and Cubitanoids of Natural Occurrence" (*Z330*). These compound groups include the cembrane diterpenoids (**42**), which are produced by plants (*e.g.* tobacco), insects, and marine invertebrates. Some of these compounds are important in terms of their biological effects.

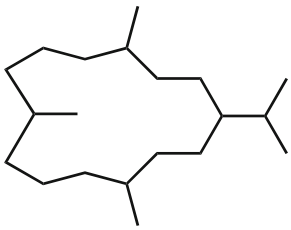

42 (cembrane skeleton)

5.3.22 Volume 60

The first contribution of Volume 60 was by *Inger Wahlberg* and *Ann-Marie Eklund*, who reported on "Cyclized Cembranoids of Natural Occurrence" (*Z331*). They described around 200 compounds derived from the cembrane skeleton (see Vol. 59) by cyclization. An example given was the basmane skeleton (**43**), typified by certain substances occurring in tobacco plants. Furthermore, cyclic cembranoids can be found in insects and marine invertebrates.

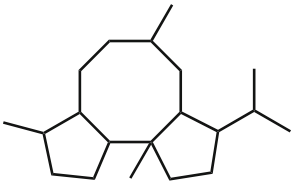

43 (basmane skeleton)

Maurice Petitou's and *Constant A. A. van Boeckel's* contribution "Chemical Synthesis of Heparin Fragments and Analogues" (*Z332*) was the second and last contribution to Volume 60. The field covered by *Petitou* and *Boeckel* is of major importance in regard to natural and synthetic coagulants. The discovery that one distinct pentasaccharide domain of some heparin chains (**44**) activates the serine protease inhibitor antithrombin III, which inhibits thrombin in the coagulation cascade (*234*), was a real breakthrough in heparin research in the early 1980s.

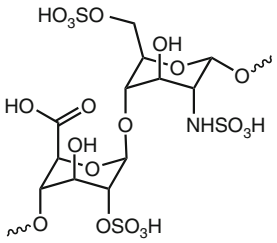

44 (heparin fragment)

5.3.23 Volume 61

Volume 61 was dedicated entirely to the taxane diterpenoids. On the one hand, the marked toxicity of *Taxus* (yew tree) substances has been known since ancient times, as seen in Caesar’s *De Bello Gallico*, *“Catuvolcus, … poisoned himself under the curse and malediction of Ambiorix …, with the juice of yew tree berries, which grow abundantly in Gaul and Germania” (De Bello Gallico VI, 31).* On the other hand, taxane diterpenoids are significant antitumor agents—and their investigation may have gained steam by the publication of this particular progress report. Today, Taxol® (paclitaxel) (**45**) is used in the treatment of breast, ovarian, lung, head, and neck cancers as well as in percutaneous transluminal coronary angioplasty for the coating of stents against restenosis. *David G. I. Kingston, Anthony A. Molinero,* and *John M. Rimoldi* from the Department of Chemistry, Virginia Polytechnic Institute and State University, Blacksburg reported mainly on developments concerning total synthesis (*Z333*). Total synthesis was an urgent research objective as a consequence of the scarce availability of paclitaxel from natural sources, although today paclitaxel may be obtained by plant tissue culture.

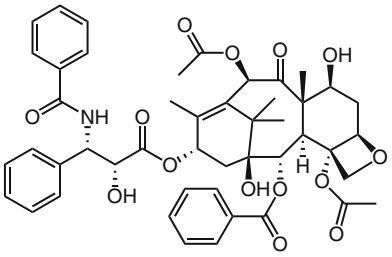

45 (paclitaxel)

5.3.24 Volume 62

The labdane diterpenoid, forskolin (**46**), is isolated from powdered roots of *Coleus forskohlii*. *Sujata V. Bhat* from the Indian Institute of Technology, Bombay, summarized findings on forskolin and other labdane diterpenoids in the first contribution of Volume 62 "Forskolin and Congeners" (*Z334*). Six years after its publication, it was reported that certain labdane diterpenoids show activity at the dopamine D_2 receptor (*235*).

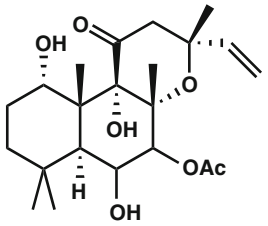

46 (forskolin)

The next contribution of Volume 62 was entitled "Steroidal Oligoglycosides and Polyhydroxysteroids from Echinoderms" (*Z335*). This referred to saponins and their saccharide and steroid aglycone "building block" units, which can be found in almost all echinoderm species. Some of these exhibit cytotoxic, antifungal, and antineoplastic characteristics. *Luigi Minale* (1936–1997)*, Raffaele Riccio,* and *Franco Zollo* (*1949) from the University of Naples contributed to this chapter.

5.3.25 Volume 63

Withania somnifera (Indian ginseng)—known from Sanskrit medicine—produces several biologically active withanolides (**47**), which are modified steroids. Compounds of this kind are also present in solanaceous plants. The first chapter in Volume 63, "Withasteroids, a Growing Group of Naturally Occurring Steroidal Lactones"—was written by *Anil B. Ray* and *Mohini Gupta* (*Z336*) from the Department of Medicinal Chemistry, Institute of Medical Sciences, Banaras Hindu University, Varanasi, India.

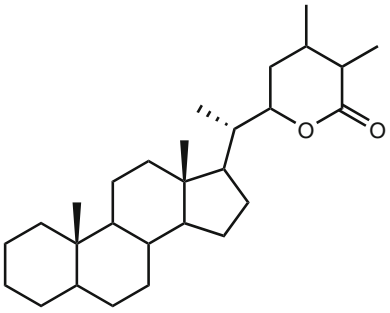

47 (withanolide skeleton)

The clerodane diterpenes, of which some are characterized by a *neo*-clerodane skeleton (**48**), occur widely in the plant family Labiatae and are mainly important in regard to chemotaxonomy. *Lydia Rodríguez-Hahn, Baldomero Esquivel*, and *Jorge Cárdenas* from the Universidad Nacional Autónoma de México jointly wrote the contribution "Clerodane Diterpenes in Labiatae" (*Z337*).

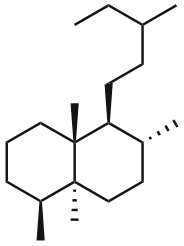

48 (*neo*-clerodane skeleton)

Lydia Rodríguez-Hahn (1932–1998) was born in Madrid. She and her family left Spain during the Civil War in 1936. After spending 9 years in the Soviet Union, she emigrated further to Mexico. *Rodríguez-Hahn* studied at the University of Chile in Santiago and at Imperial College in London. In 1962, she was appointed titular professor at the National University of Mexico. Her major scientific contributions include structure determinations of natural products of higher plants and their use as systemic biochemical markers (*236*).

5.3.26 Volume 64

A contribution on the "Chemistry and Sources of Mono- and Bicyclic Sesquiterpenes from *Ferula* Species" (*Z338*) was co-authored by *Jaime Bermejo Barrera* and *Antonio G. González* (1917–2002), from the Institute of Natural Products and Agrobiology of the Canary Islands of CSIC, University of La Laguna, Tenerife. The *Ferula* genus includes about 170 species of flowering plants of the Apiaceae family.

The biogenesis and chemistry of important skin and hair pigments, originating from the amino acid, tyrosine, is depicted in much detail by a well-known investigator of melanin biogenesis, *Giuseppe Prota* (1938–2003), then from the University of Naples, in his contribution entitled "The Chemistry of Melanins and Melanogenesis" (*Z339*).

To *H. J. M. Gijsen, Joannes B. P. A. Wijnberg*, and *Aede de Groot*, Wageningen University, The Netherlands, we owe a comprehensive overview of a large compound group based on the aromadendrane skeleton (**49**), which is found widely in Nature. Their contribution was entitled "Structure, Occurrence, Biosynthesis, Biological Activity, and Chemistry of Aromadendrane Sesquiterpenoids" (*Z340*), and concluded Volume 64.

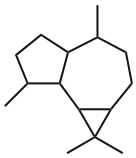

49 (aromadendrane skeleton)

5.3.27 Volume 65

Yoshinori Asakawa (*1941) became associate professor in 1976 and full professor in 1981 at the Faculty of Pharmaceutical Sciences of Tokushima Bunri University. In Volume 65, he provided the reader with a detailed presentation of the "Chemical Constituents of the Bryophytes" (*Z341*), in which he described a large number of compounds present in liverworts, mosses, and hornworts, occupying almost 600 pages and focusing mainly on their chemosystematic significance.

5.3.28 Volume 66

Volume 66 opened with a contribution by *Takuo Okuda* (*1927), *Takashi Yoshida*, and *Tsutomu Hatano* from the Faculty of Pharmaceutical Sciences, Okayama concerning "Hydrolyzable Tannins and Related Polyphenols" (*Z342*). Tannins and other polyphenols are of special interest due to their antioxidant, antitumor, and antiviral activities. In addition, the distribution of the hydrolysable tannins is also interesting from a taxonomic point of view.

The pufferfish toxin, tetrodotoxin—belonging to a natural compound class of substances containing a guanidine fragment—has won great notoriety. The first recorded cases of tetrodotoxin poisoning were found in the log of Captain *James Cook* from 7 September 1774, on which date he recorded his crew eating pufferfish and feeding the remains to pigs kept on board (*237*). In 1963/1964, *Robert B. Woodward* as well as the research teams of *Kyosuke Tsuda* (1907–1999) and *Toshio Goto* (see Volume 52) were finally able to elucidate the tetrodotoxin structure (**50**).

The author of "Some Aspects of Guanidine Secondary Metabolism" (*Z343*), *Roberto Gomes de Souza Berlinck,* was working at the Instituto de Química de São Carlos, Universidade de São Paulo, when he wrote this contribution.

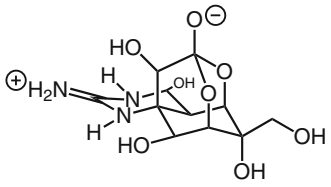

50 (tetrodotoxin)

5.3.29 Volume 67

A. A. Leslie Gunatilaka is still working at the Center for Natural Products Research and Commercialization at the University of Arizona today. This researcher, who did his postdoctoral studies under *Sir Derek Barton* in the 1970s and later under *Carl Djerassi*, published a contribution on "Triterpenoid Quinonemethides and Related Compounds (Celastroloids)" to Volume 67 (*Z344*). The quinonemethides represent a relatively small compound class and are restricted to the plant family Celastraceae, from where their name "celastroloids" originates. Initially, celastroloids were of interest as naturally occurring insecticides—with an example being celastrol (**51**). Later on, celastrol has become of interest as a potential drug lead for the treatment of *Alzheimer*'s disease (*238*).

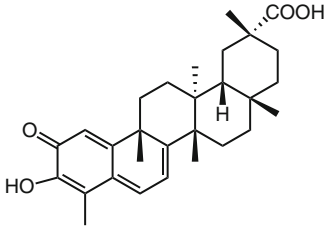

51 (celastrol)

Staphyltrichum coccosporum, a soil-dwelling fungus, is an important producer of spirostaphylotrichin A (**52**)—the substance from which spirostaphylotrichins are derived. Its biogenesis and derivative production are discussed in a contribution by *Paula Walser-Volken* and *Christoph Tamm* (Basel) entitled "The Spirostaphylotrichins and Related Microbial Metabolites" (*Z345*).

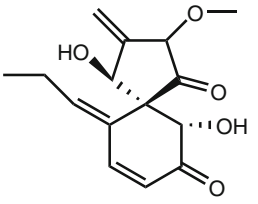

52 (spirostaphylotrichin A)

5.3.30 Volume 68

Volume 68, published in 1996, is dedicated to organohalogen compounds (*Z346*). *Gordon W. Gribble* contributed a monograph on this topic: "Naturally Occurring Organohalogen Compounds—A Comprehensive Survey". *Gordon W. Gribble* (*1941) is a native of San Francisco. He completed his undergraduate education at

the University of California at Berkeley in 1963 and earned a PhD in organic chemistry at the University of Oregon in 1967. He joined the faculty of Dartmouth College, Hanover, in New Hampshire in 1968, where he has been full professor of chemistry since 1980.

Since the Vietnam War and even more so since the chemical spill of Seveso in July of 1976, chlorinated organic compounds have repeatedly made the headlines. Professor *Gribble* treated the "dioxin" problem with its own entry (p. 273 f.), *"Dioxin—no chemical is more feared by the general public, and no chemical has been more scrutinized by policy regulators and environmental scientists. It is now recognized that dioxins and furans form during most if not all combusting processes such as waste incineration, coal burning, automobile exhaust, tobacco smoke, power plants and others. These chlorinated compounds are the product of natural combustion processes (e.g., forest fires) and have been on earth for eons. …"* These realizations were the product of investigations that had begun in the course of the 1970s. Prof. *Gribble* added, *"More surprising are the observations of the biogenetic formation. Natural enzymes like horseradish peroxidase or lactoperoxidase oxidize chlorophenols to PCDDs and PCDFs in the ppm range."*

5.3.31 Volume 69

The first contribution of Volume 69 was entitled "Non-Macrocyclic Trichothecenes, Part 2" (*Z347*). Part 1 on this topic was not published in the same Series but in "*Natural Products Reports*" (*239*). *John Frederick Grove* (1921–2003), then of the School of Molecular Science, University of Sussex, was the author of both parts. The featured compounds were based on the sesquiterpenoid trichothecane skeleton (**53**) and included more than 100 naturally occurring representatives produced by *Fusarium* species.

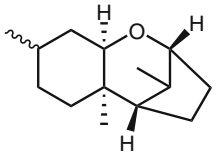

53 (trichothecane skeleton)

Cardiac steroidal glycosides, which occur mostly in plants, but can also be found in animals, are still used for the treatment of heart disease. Around 370 compounds of this kind are described in a contribution published in Volume 69 (*Z348*), written by *Desh Deepak, Soman Srivastava, Naveen K. Khare,* and *Anakshi Khare*, from the Department of Chemistry, University of Lucknow in India.

Shikimic acid (**54**), which is formed from D-erythrose-4-phosphate and phosphenolpyruvate, is a biosynthetic precursor of many natural aromatic compounds.

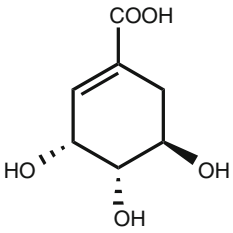

54 (shikimic acid)

The third contribution of Volume 69 (*Z349*) covered mainly the enzymatic systems involved in the shikimate pathway of biosynthesis. *Edwin Haslam*, known to the reader from Volume 41, was the author of "Aspects of the Enzymology of the Shikimate Pathway".

5.3.32 Volume 70

The Indian Ocean sea hare *Dolabella auricularia* has been known for its poisonous effects since ancient times. The substances it contains, peptidic dolastatins—see dolastatin 11 as an example (**55**)—show manifold physiological activities, especially their cytostatic and antineoplastic effects. Dolastatins extracted from the marine shell-less mollusk *Dolabella auricularia* were first isolated by *George R. Pettit* and associates (*240*, *241*), and were described in the contribution by *Pettit* entitled "The Dolastatins" (*Z350*).

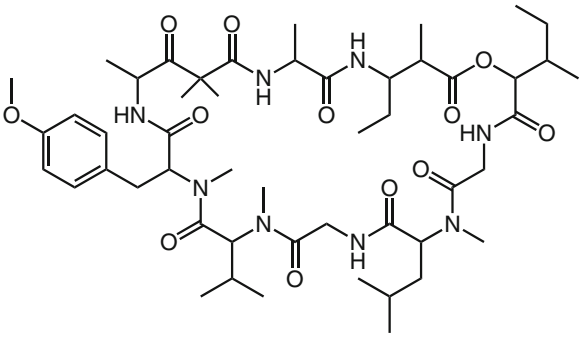

55 (dolastatin 11)

As acetogenins (**56**) from the plant family Annonaceae display multiple biological or pharmacological activities, they have attracted the attention of several researchers. Such activities range from cytotoxic, antitumor, antiparasitic, pesticidal, and antimicrobial to immunosuppressive effects. Structurally, acetogenins are characterized by a long-chain fatty acid residue, one to three tetrahydrofuran rings and a terminal lactone. Their biogenesis, distribution, and synthesis were presented

by *André Cavé* (1934–2011)*, Bruno Figadère, Alain Laurens,* and *Diego Cortes*, of the Pharmacognosy Laboratory, Université Paris XI (*Z351*).

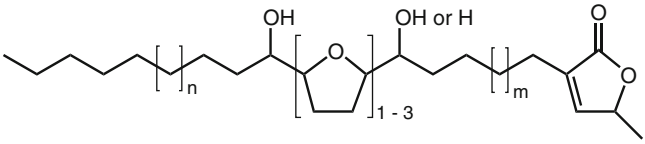

56 (Annonaceae acetogenins)

5.3.33 Volume 71

In Volume 71, *Gerd Gäde* from the Zoology Department at the University of Cape Town, Rondebosch, South Africa wrote on the topic "The Explosion of Structural Information on Insect Neuropeptides" (*Z352*). The explosion of information referred to in this title only became possible due to the availabilty of cDNA methods in addition to classical methods, such as MS or Edman sequencing. *Gerd Gäde* received his academic education in biology and chemistry at the Universities of Münster and Kiel. In 1989, he was appointed chair of zoology at the Zoology Department of the University of Cape Town.

For centuries, preparations of *Thapsia garganica* roots were used in Arabic and European medicine for the treatment of lung diseases and catarrh, and also as pain medication for rheumatoid symptoms. An example of a sesquiterpene lactone constituent of this species is thapsigargin (**57**), which has become used as means of modulating Ca^{2+} homeostasis in cardiac cells in the laboratory.

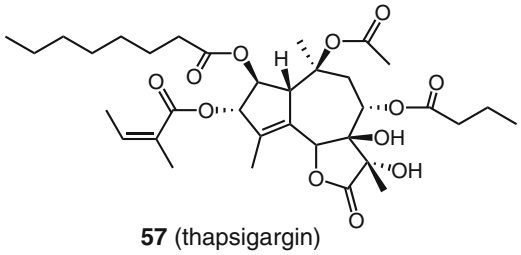

57 (thapsigargin)

Thapsigargin has been investigated by Danish pharmaceutical scientist *Søren Brøgger Christensen* (*1947) and his co-workers. *Christensen* was the first author of "Sesquiterpenoids from *Thapsia* Species and Medicinal Chemistry of the Thapsigargins" (*Z353*). His co-authors were *Annette Andersen* and *Ulla W. Smith*.

"Pregnane Glycosides" are plant compounds that consist of a pregnane aglycone, which is glycosylated at one or more hydroxylated positions, where oligomeric sugars up to hexasaccharides may be present. Up to the time of writing of the contribution by *Desh Deepak, Sanjay Srivastav*, and *Anakshi Khare* (*Z354*), almost 100 such substances had been discovered. *Desh Deepak* and *Anakshi Khare* provided an earlier contribution to Volume 69.

5.3.34 Volume 72

In Volume 72, *Robert D. H. Murray* delivered a sequel to his contributions to Volumes 35 and 58 in "Naturally Occurring Plant Coumarins" which contained the description of 434 "newcomers" of this type (*Z355*).

This was followed by an offering from *H. Ziffer, R. J. Highet*, and *D. L. Klayman* entitled "Artemisinin: An Endoperoxidic Antimalarial from *Artemisia annua* L." (*Z356*). In Chinese medicine, decoctions of the quinhao plant (*Artemisia annua* L.) have been used for millenia for the treatment of fever. This antifebrile property is mediated through the constituent, artemisinin (**58**), which proved to be a highly effective substance against *Plasmodium* species. These are protozoal parasites, many of which act as pathogens. A structural feature of artemisinin is its endocyclic peroxide group, which is rather unusual for a natural product. One of the authors was *Daniel L. Klayman* (1929–1992), an authority on antimalarial drugs. *Klayman* was head of the organic chemistry section at the Walter Reed Army Institute of Research in Washington. His co-authors were the NMR spectroscopy specialist *Robert J. Highet* (1918–1994), and an expert in circular dichroism at the NIDDK (National Institute of Diabetes and Digestive and Kidney Diseases, NIH, Bethesda, Maryland), and *Herman Ziffer* (1930–2009).

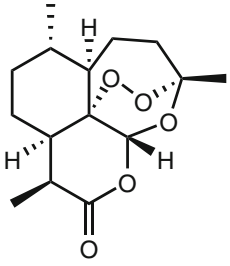

58 (artemisinin)

Ernesto Fattorusso (1937–2012) and *Alfonso Mangoni* from the Department of the Chemistry of Natural Substances, Naples, reported on glycolipids, which are able to act like perfect haptens (*Z357*). In the presence of a strong immunogen they induce an immune response resulting in an antiserum highly specific for the hapten saccharide structure, and therefore represent a valuable vehicle enabling localization of glycolipids in cell structures. For this approach, mostly glycolipids from mollusks and echinoderms are used. Also, several members of this class of compounds have been found to have antitumor and antiviral properties. The structural formula **59** shows a representative glycoglycerolipid.

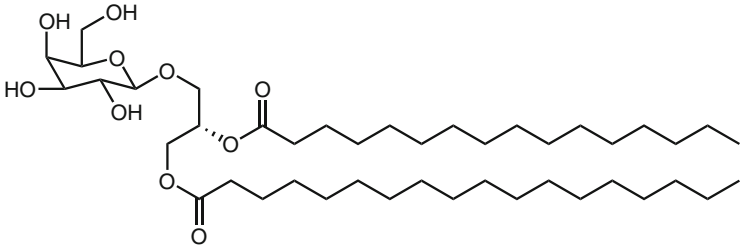

59 (representative glycoglycerolipid)

5.3.35 Volume 73

Besides saponin components such as glycyrrhizic acid (**60**), licorice is rich in phenolic compounds of flavonoids and coumarins, which share many biological activities, such as antibacterial, anti-inflammatory, antileishmanial, and cytotoxic properties. Volume 73 addresses primarily the distribution, structural variation and other characteristics of these phenolic constituents. It was written by *Taro Nomura* and *Toshio Fukai* from the School of Pharmaceutical Sciences, Toho University, Chiba, Japan and entitled "Phenolic Constituents of Licorice (*Glycyrrhiza* Species)" (*Z358*).

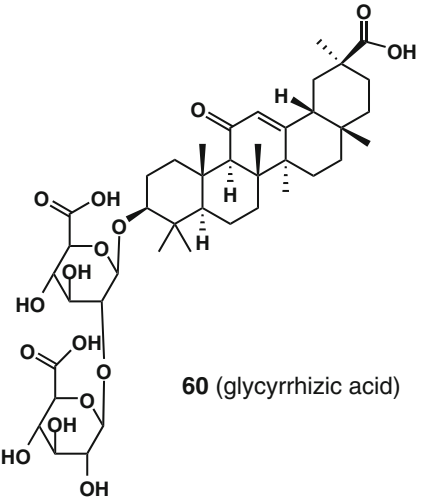

60 (glycyrrhizic acid)

5.3.36 Volume 74

An overview of "Triterpenoid Saponins" by *Shashi B. Mahato* and *Saraswati Garai* from the Indian Institute of Chemical Biology, Calcutta, (*Z359*) focused mainly on the quite diverse biological activities of the members of this compound class. The contribution included an extensive chart of all triterpenoid saponins isolated and structurally determined up to the time of writing.

6-Deoxyamino sugars are widespread components of highly biologically active natural products, as exemplified by heparin and a number of antibiotics like daunomycin, erythromycin, and azithromycin. These sugars also occur in the enediyne antibiotics dynemicin, calicheamycin, and kedarcidin. Therefore, such hexoses are of considerable interest in terms of approaches to their total or partial synthesis. The authors of a contribution entitled the "Synthesis of 6-Deoxyamino Sugars" were *Leena A. Otsomaa* and *Ari M. P. Koskinen* (*Z360*) from the Department of Chemistry, University of Oulu, Finland.

5.3.37 Volume 75

In Volume 75, a contribution was presented by *Dimitris C. Gournelis* and *Gregory G. Laskaris* from the Department of Pharmacy of the Aristotelian University of Thessaloniki, Greece and *Robert Verpoorte* (*1946) from Leiden University, The Netherlands, on "Cyclopeptide Alkaloids" (*Z361*). The cyclopeptide alkaloid class is characterized by an *ansa* structure over a benzene ring, which is composed of a hyroxystyryl group and a hydroxy amino acid. To this system, one to two amino acids may be linked by amide bonds. Such cyclopeptide alkaloids (**61**)—of which around 160 were known at the time this contribution was written—have sedative, antibacterial, and antifungal properties.

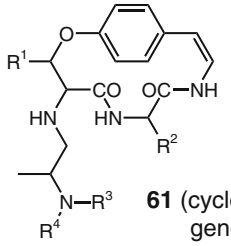

61 (cyclopeptide alkaloids general structure)

The second contribution to Volume 75—co-authored by *Lynne A. Collett, Michael T. Davies-Coleman*, and *Douglas Eric Arthur Rivett*, from the Department of Chemistry, Rhodes University, Grahamstown, South Africa—dealt with progress made in the field of 6-substituted 5,6-dihydro-α-pyrones since the previous contribution on this topic was published in Volume 55 (*Z362*). *Douglas Eric Arthur Rivett* (1921–2010) established a reputation for high quality natural product chemistry research at Rhodes University and has been the only South African scientist ever to publish chemistry research papers continually over seven decades (*242*).

5.3.38 Volume 76

Within the last 20 years, perhaps no discovery caused more head shaking and astonishment than the finding that—of all things—the small nitric oxide molecule (NO) plays a key role as a messenger molecule in signal transduction. Consistent with this discovery, the *Nobel* Prize in Medicine of 1998 was awarded to U.S. pharmacologists, *Robert Francis Furchgott* (1916–2009), *Louis J. Ignarro* (*1941), and *Ferid Murad* (*1936). The editors of "Progress" dedicated a complete volume to this spectacular discovery: *David R. Adams* (Department of Chemistry, Heriot-Watt University, Edinburgh), *Maryna Brochwicz-Lewinski* (Department of Radiology, The Royal Infirmary, Edinburgh), and *Anthony R. Butler* (School of Chemistry, University of St. Andrews) gave in 1999 the title "Nitric Oxide: Physiological Roles, Biosynthesis, and Medical Uses" to Volume 76 (*Z363*). The main topics covered were: "Discovery of NO in the Vasculature", "Platelet Aggregation", "*S*-Nitrosothiols as NO-Donor Drugs", "NO and the Immune System", "NO and the

Nervous System" and "NO Activity in the Mammalian Eye". Nitric oxide biogenesis takes place in the organism by oxidation of ω-*N*-hydroxy-L-arginine, which thereby is degraded to L-citrulline.

5.3.39 Volume 77

The first contribution of Volume 77 by *William Alfred Ayer* (1932–2005) and *Latchezar S. Trifonov* from the Department of Chemistry, University of Alberta, Canada (*Z364*), discussed the problem of wood discoloration in conifers and broadleaf trees caused by fungi. This process leads to either a blue coloration (mostly due to *Ophiostoma piliferum* infestation) or degradation of the wood, for which a number of organisms such as *Anisomyces odoratus* or *Armillaria ostoyae* can be held responsible. Mostly phenolic secondary metabolites of these organisms cause such effects. This contribution described possibilities to tackle these problems and also described the chemistry behind the processes. *William Ayer* was an early practitioner of the rapidly developing field of chemical ecology (*243*).

Wood constituents were also the topic of the next contribution on "Condensed Tannins" (*Z365*). The tannins treated in this essay were a widespread group of phenolic products, known for their positive health-related properties. Examples are proanthocyanidins, present in tea, fruit juices and red wine. The first author of this paper was *Daneel Ferreira*, then from the University of the Orange Free State, South Africa. *Daneel Ferreira* graduated from the University of Pretoria, South Africa in 1964. In 1977, he worked under the supervision of a *Nobel* laureate, the late *Sir Derek Barton*—author of a contribution published in Volume 19 of this Series—at Imperial College, London. In 2000, *Ferreira* was appointed chair of the Department of Pharmacognosy at the University of Mississippi. *Ferreira'*s coauthors were *Edward V. Brandt, Johan Coetzee*, and *Elfranco Malan.*

Włodzimierz M. Daniewski from the Institute of Organic Chemistry, Polish Academy of Sciences, Warsaw, Poland and *Giovanni Vidari,* Universitá di Pavia, Italy, were responsible for "Constituents of *Lactarius* (Mushrooms)" (*Z366*). Their contribution focused on the large number of sesquiterpenes occurring in fungi in this genus. These substances are of potential importance because of their antifeedant activity against "storage pests" such as *Tribolium confusum*, *Trogoderma granarium,* and *Sitophylus granarius*, as well as against mammals, insects, and fish. Distinct members of this group of substances show antibacterial, antifungal, cytotoxic, algicidal, and even mutagenic activities.

5.3.40 Volume 78

In the 1970s, a quite potent plant growth factor was isolated from rapeseed pollen (*Brassica napus*) (*244*), namely, brassinolide (**62**) (*245*). At the time of publication of "Brassinosteroids" by *Gunter Adam, Jürgen Schmidt*, and *Bernd Schneider* from the Institute of Plant Biochemistry, Halle, Germany (*Z367*), around 40 members of this steroid family had been characterized from more than 50 *Brassica* subspecies.

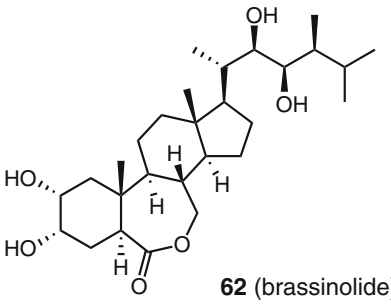

62 (brassinolide)

Anand Akhila and *Kumkum Rani* from the Central Institute of Medicinal and Aromatic Plants in Lucknow, India, wrote a contribution entitled "Chemistry of the Neem Tree (*Azadirachta indica* A. Juss.)" (*Z368*). This tree, native to India, has received a lot of attention due to several substances it produces, which can be used, for example, in agriculture, medicine, veterinary medicine, pest control, and population control. Its extracts were found to have amebicidial, antiallergic, antidiabetic, antieczemic, antigingivitis, antimalarial, antimicrobial, antiscabic, antitubercular, cardiotonic, diuretic, immunomodulatory, insecticidal, nematicidal, piscicidal, as well as spermicidal properties. These activities are ascribed partly to the limonoid (**63**) constituents, inclusive of several *seco*-meliacins present. Biogenetically, the limonoids are formed from protolimonoids. An example of a *seco*-meliacin from the neem tree is nimbin.

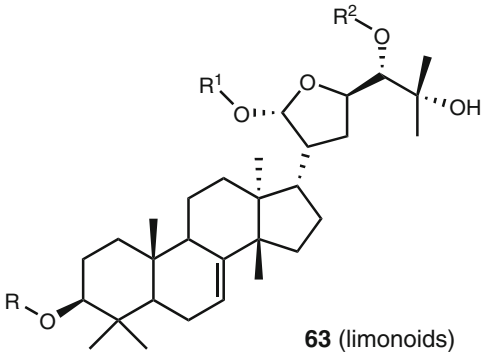

63 (limonoids)

5.3.41 Volume 79

Henrik Franzyk, a researcher at the Department of Organic Chemistry, Technical University of Denmark in Lyngby, expanded on "Synthetic Aspects of Iridoid Chemistry" in Volume 79 (*Z369*). Since iridoid glycosides with carbocyclic and secoiridoid skeletons (**64**, **65**) are of major interest regarding taxonomy and ecology, their synthesis was discussed in considerable detail.

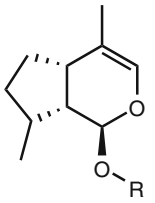

64 (carbocyclic skeleton)

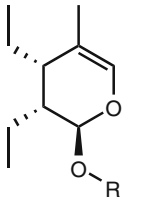

65 (secoiridoid skeleton)

Jean-Claude Braekman (*1942) at the time of writing the next contribution was the director of the Department of Organic Chemistry of the Faculty of Sciences at the Free University of Brussels. He focused his research on the study of bioactive secondary metabolites derived from insects, marine invertebrates and African plants, in particular on their isolation, structure determination, synthesis and biosynthesis, and the structure-activity relationships inherent of these molecules (*246*). "The Defensive Chemistry of Ants" (*Z370*), a contribution he wrote together with *Sabine Leclercq, Désiré Daloze*, and *Jacques M. Pasteels* for Volume 79, was focused on non-protein poisons derived mainly from piperidine, pyridine, pyrrolidine, pyrroline, and indolizine alkaloids. The first to isolate an organic acid (formic acid) from ants by distillation was the English natural scientist *John Ray* (1627–1705) in 1671.

5.3.42 Volume 80

In the first contribution of Volume 80, *Clifford W. J. Chang* (1938–2007), then professor at the Department of Chemistry, University of West Florida, Pensacola, reported on "Naturally Occurring Isocyano/Isothiocyanato and Related Compounds" (*Z371*). The compounds described are produced mainly by marine organisms such as cyanobacteria.

The authors of the second contribution of Volume 80 were *Otmar Hofer* (1942–2009) and *Harald Greger* from the University of Vienna. *Otmar Hofer's* interest in the structure elucidation of plant components dated back to 1980 when he started a close collaboration with *Prof. Dr. Harald Greger* from the Institute of Botany of the University of Vienna that would last for almost 30 years. The aim of this collaboration was the isolation and spectroscopic characterization of natural products from tropical plants (*e.g.* Rutaceae, Meliaceae, Zingiberaceae) as well as the elucidation of their structure and investigation of their bioactivity (*247*). *Glycosmis* species, which are described in this contribution from 2001, contain noteworthy enamide thioethers and their derivatives (*e.g.* krabin (**66**), isolated from *Glycosmis mauritiana*). Both the distribution and taxonomic significance as well as the interesting chemistry and biogenesis of these substances were pointed out. This group also includes sulfoxides, sulfones and thiocarbonic acid derivatives, which are of major interest mainly due to their antifungal and insecticidal properties. *Hofer* and *Greger* entitled their contribution "Sulfur-Containing Amides from *Glycosmis* Species" (*Z372*).

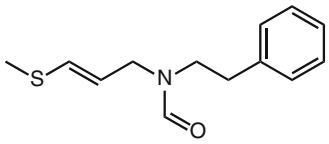

66 (krabin)

5.3.43 Volume 81

"New Results on the Chemistry of Lichen Substances" was the title of a contribution by *Siegfried Huneck* (1928–2011). *Huneck*, from the Martin Luther Universität, Halle-Wittenberg, Germany, was a leading expert in the field of lichen chemistry in the second half of the twentieth century. His contribution (*Z373*) represented an overview of lichen substances. Lichen natural products are important for the production of cosmetics and perfumes as well as dying agents. Lichens themselves are of high significance as biomonitors. Many of the compounds synthesized by lichens can be used for chemotaxonomic studies and show antiviral, antibacterial and cytotoxic activities, among others. Structurally, they are represented mainly by aromatics and terpenoids.

5.3.44 Volume 82

Most naturally occurring biaryls result from oxidative coupling of phenols. Biaryls are widespread and except for their common aryl-aryl bond structurally quite diverse. They provide great insight into the phenomenon of atropisomerism—a special case of axial chirality. Many biaryls are of biological interest. Close to 300 pages were dedicated to this natural product class—represented in a contribution by *Gerhard Bringmann* (*1951), *Christian Günther, Michael Ochse, Olaf Schupp,* and *Stefan Tasler* from the University of Würzburg in Germany entitled "Biaryls in Nature: A Multi-Faceted Class of Stereochemically, Biosynthetically, and Pharmacologically Intriguing Secondary Metabolites" (*Z374*).

5.3.45 Volume 83

Robert D. H. Murray's contribution "The Naturally Occurring Coumarins" (*Z375*), which occupied the whole of Volume 83, was a 670-page overview of all naturally occurring coumarins then known. Excluded, however, were 3,4-benzocoumarins as well as ellagic acid derivatives. The compounds, listed in tabular form, included 1785 monomeric coumarins, 77 biscoumarins, four triscoumarins, as well as 17 structurally incompletely resolved compounds.

5.3.46 Volume 84

A concise summary of the classification, biogenesis and structure of cyclic tetrapyrrole derivatives, inclusive of the porphyrins, chlorins, bacteriochlorins, isobacteriochlorins, higher saturated hydroporphyrins, and corrins was provided in an contribution published by two researchers from the Institute of Organic Chemistry at the University of Bremen in Germany: "Naturally Occurring Cyclic Tetrapyrroles" (*Z376*). The first author—*Franz-Peter Montforts* (*1948)—became known for his research on hydroporphinoids, like bonellin, in the course of the 1990s. His co-author was *Martina Glasenapp-Breiling*. The extraordinary importance of the compounds described ranged from those involved in photosynthesis to vitamin B_{12}.

The topic of paclitaxel (Taxol®)—originally known as "taxol" and used widely today as an antitumor agent—has been discussed several times in the "Progress" series. One of the long-time editors of the Series, *Werner Herz*, was involved in the success story of this plant-derived diterpenoid (*248*), which was first discovered in the bark of western yew (*Taxus brevifolia*). In 1960, *Werner Herz* was asked to collaborate by *Jonathan L. Hartwell* (1906–1991) and *Monroe E. Wall* (1916–2002), two of the pioneers in this field of research, since *Herz* knew how phytochemicals could be extracted with solvents efficiently. In 2002, the "Bioorganic and Natural Products Chemistry" research group of *David G. I. Kingston* at the Virginia Polytechnic Institute and State University, wrote a contribution entitled "The Chemistry of Taxol and Related Taxoids". In this treatment, they focused specifically on the "Synthesis of Taxol and Taxol Side Chain Analogs from Baccatin III" (*Z377*). *Kingston's* co-authors were *Prakash G. Jagtap, Haiqing Yuan*, and *Lakshman Samala.* The tetracyclic diterpene moiety of Taxol®, 10-deacetylbaccatin III, which has been used as a "building block" in partial synthesis, is readily available from the leaves of *Taxus baccata* (European Yew) as a renewable resource.

5.3.47 Volume 85

The first contribution to Volume 85 was made by *Karsten Krohn* and was given the title "Natural Products Derived from Naphthalenoid Precursors by Oxidative Dimerization" (*Z378*). Spirobisnaphthalene analogues synthesized by fungi (*e.g.* preussomerin E (**67**) by *Preussia isomera*) have been investigated with great interest owing to their antifungal, antibacterial, and cytotoxic properties. *Krohn* explained their biological activity, biogenesis and synthesis. For the biographical data of *Karsten Krohn*, see the synopsis of Volume 55.

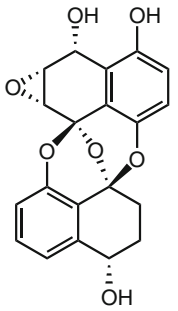

67 (preussomerin E)

Today, peptide glycosylation is regarded as a major contributor to the pathogenicity of certain pathogens, such as *Neisseria*, *Mycobacteria*, and *Streptococcus* strains. Furthermore, such glycosylated proteins are key elements in the formation of S-layers by prokaryotes—structures of technical interest. *Paul Messner* and *Christina Schäffer* from the research group of *Uwe B. Sleytr* (*1942) at the Department of Nanobiotechnology of the University of Natural Resources and Life Sciences, Vienna, wrote a contribution entitled "Prokaryotic Glycoproteins" (*Z379*). This research group established a good reputation in the field of S-layer glycoproteins.

The final contribution of Volume 85 represented an update on the state of research on carbazole alkaloids and was provided by *D. P. Chakraborty* (Institute of Natural Products, Calcutta) (*Z380*).

5.3.48 Volume 86

Vertebrates, plants, fungi, and bacteria produce a myriad of monopyrrolic compounds and tetramic acids of diverse biological importance. Examples of this class of compounds include the tetrapyrrole precursor, porphobilinogen, and batrachotoxin (**68**) of the Colombian Kokoe poison dart frog *Phyllobates aurotaenia,* as well as the tetramic acid derivative α-lipomycin (**69**) produced by *Streptomyces aureofaciens. Albert Gossauer* from the Department of Chemistry, University of Fribourg in Switzerland was responsible for a contribution entitled "Monopyrrolic Natural Compounds Including Tetramic Acid Derivatives" (*Z381*).

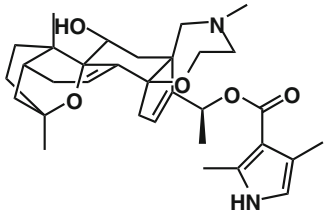

68 (batrachotoxin)

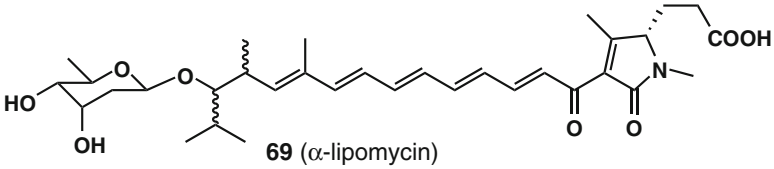

69 (α-lipomycin)

5.3.49 Volume 87

In Volume 87, *Timon Flessner, Rolf Jautelat, Ulrich Scholz,* and *Ekkehard Winterfeldt* (*1932), from the University of Hannover, reported on "Cephalostatin Analogues—Synthesis and Biological Activity" (*Z382*). The marine worm, *Cephalodiscus gilchristi*, produces a number of bis-steroids (*e.g.* cephalostatin 1 (**70**)), which possess extraordinarily potent antitumor activity. As mentioned in the title, primarily aspects of the synthesis and biological activity were described in detail.

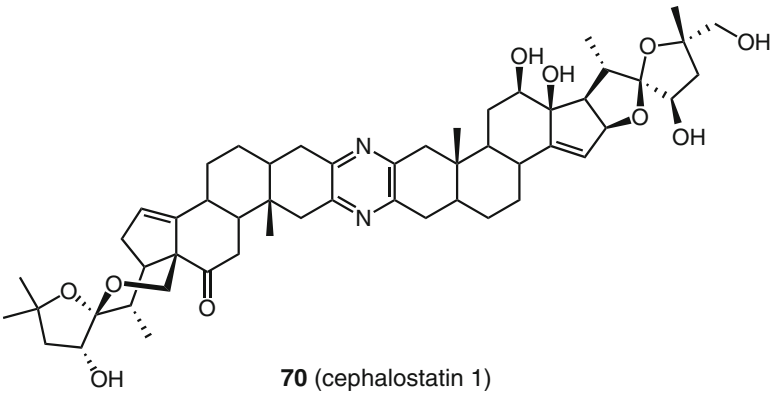

70 (cephalostatin 1)

There is almost no other bacterial genus that attracts so much public interest as does *Pseudomonas*. Species such as *Pseudomonas aeruginosa*, are the reason for some hospital infections; *Pseudomonas solanacearum* is held responsible for potato crop failures; *Pseudomonas syringae* helps prolong the Alpine ski season; *Pseudomonas putida* plays a major role in waste water treatment, and *Pseudomonas chlororaphis* is used for plastic waste degradation. The siderophores, produced by these *Gram*-negative bacteria, are presented in the next contribution. Such compounds are relevant in terms of their many different applications, but also in regard to their role in iron metabolism. The author of "Siderophores of the Pseudomonadaceae *sensu stricto* (Fluorescent and Non-Fluorescent *Pseudomonas* spp.)" (*Z383*), *Herbert Budzikiewicz* (*1933), was born in Vienna and earned his doctorate in organic chemistry in this same city in 1959. In the 1960s, *Budzikiewicz*, together with *Carl Djerassi*, was responsible for building up the mass spectrometric facility at Stanford University. In 1970, *Budzikiewicz* was appointed full professor at the University of Cologne.

5.3.50 Volume 88

Eberhard Reimann (*1936), who represented the Department of Pharmacy, University of Munich, wrote on the "Synthesis Pathways to *Erythrina* Alkaloids and *Erythrina* Type Compounds" (*Z384*). Some of these alkaloids formed by

approximately 50 *Erythrina* species have been found to exhibit a neuromuscular blocking property similar to curare. The basic skeleton of all these erythrina alkaloids is illustrated by the structure of erythraline (**71**). The biogenesis, synthesis and pharmacology of this substance class were described comprehensively.

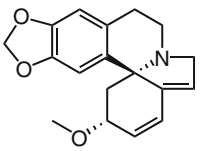

71 (erythraline)

By early in the first decade of the twenty-first century, 217 trichothecenes based on the sesquiterpenoid trichothecene skeleton were known. Their non-macrocyclic members were presented in Volume 69 (when only 100 structures were known). In "The Trichothecenes and Their Biosynthesis", representing a posthumous contribution by *John Frederick Grove* (*Z385*), who passed away in 2003, the biogenesis of this compound group was described.

In addition to the progress made in the field of melanin chemistry and biogenesis, as also discussed in Volume 64, the focus of the final contribution in Volume 88 lay also on a consideration of vitiligo—an idiopathic skin pigmentation disorder. "Melanin, Melanogenesis, and Vitiligo" (*Z386*) was written by *Shyamali Roy* from the Institute of Natural Products, Calcutta, India.

5.4 Volumes 89–100: Another Change of Appearance

Undoubtedly, the color design and cover picture both send a clear signal: this book Series has its finger on the pulse of the time, it is of high scientific impact, and is designed attractively. Volume 89 was published in 2008.

5.4.1 Volume 89

Chlorophyll degradation during leaf senescence leads to colorless non-fluorescent and red fluorescent open-chain tetrapyrroles, analogous to bile pigments. These were presented by *Bernhard Kräutler,* a pioneer in this particular research field, in "Chlorophyll Catabolites" (*Z387*), which unraveled the mystery of the green pigment "disappearing" from leaves. The structures—such as *Hv*-NCC-1 (**72**), a metabolite of chlorophyll a and b—as well as the biochemistry of this compound class were explained.

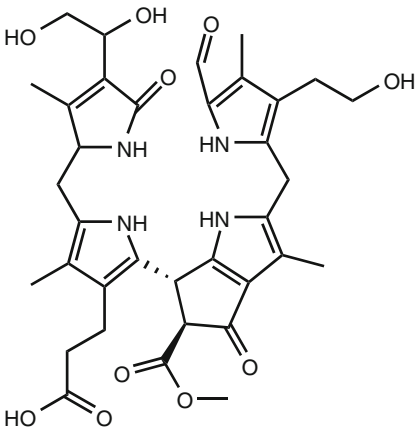

72 (*Hv*-NCC-1)

Bernhard Kräutler, born in Dornbirn, Austria, in 1946, has contributed remarkable papers in three fields of research: vitamin B_{12} chemistry, fullerenes, and chlorophyll catabolites. He performed his doctoral work at ETH Zurich in the laboratory of *Albert Eschenmoser*, where he graduated in 1976. Subsequently, *Kräutler* continued with postdoctoral studies at the University of Texas and at Columbia University, and then followed a call to the faculty of the University of Innsbruck in 1991.

Saponins are a group of naturally occurring plant glycosides, characterized by their foam-forming properties in aqueous solution. Steroidal glycosides are naturally occurring sugar conjugates of C_{27} steroidal compounds. In their contribution "Steroidal Saponins" (*Z388*), *Niranjan P. Sahu, Sukdeb Banerjee, Nirup B. Mondal,* and *Debayan Mandal* from the Indian Institute of Chemical Biology, Calcutta, revisited a topic presented earlier in Volume 74 by several colleagues from the same institute.

5.4.2 Volume 90

Volume 90 (2009) of the "Progress" series was entitled "The Epothilones: An Outstanding Family of Anti-Tumor Agents" and guest-edited by *Johann H. Mulzer. Johann Hermann Mulzer* (*1944) studied in Munich and is full professor at the Institute of Organic Chemistry at the University of Vienna. In Volume 90, *Mulzer* emphasized that epothilones received unusual attention over the past 10 years (*Z389*). They are novel antitumor drugs, which act *via* microtubule stabilization—very much like the plant diterpenoid, paclitaxel (Taxol®). Initially, the epothilones such as **73** were isolated from the myxobacterium *Sorangium cellulosum*, but these compounds can also be produced synthetically. The first anticancer drug of this kind was brought to the market as "ixabepilone" (*249*).

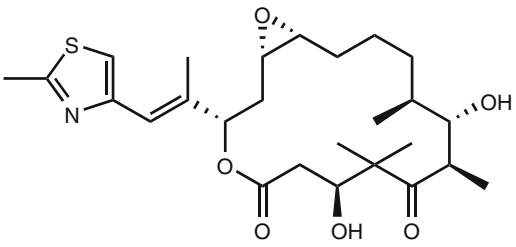

73 (epothilone A)

The authors of this volume were *Gerhard Höfle* (*Helmholtz* Center for Insect Research, Braunschweig), *Rolf Müller* (Institute of Pharmaceutical Biotechnology, Saarland University, Saarbrücken), *Kathrin Prantz* (Institute of Organic Chemstry, University of Vienna), and *Karl-Heinz Altmann* (Institute of Pharmaceutical Sciences, ETH Zurich). *Höfle* contributed to "General Aspects" (*Z390*), *Müller* informed the reader of the "Biosynthesis and Heterologous Production of Epothilones" (*Z391*), *Mulzer,* together with his co-worker *Prantz*, wrote a contribution entitled "Total Synthesis of Epothilones A–F" (*Z392*), and *K. H. Altmann* contributed three chapters: "Semisynthetic Derivatives of Epothilones" (*Z393*), "Preclinical Pharmacology and Structure–Activity Studies of Epothilones" (*Z394*), and "Clinical Studies with Epothilones" (*Z395*).

5.4.3 Volume 91

Volume 91, "Naturally Occurring Organohalogen Compounds—A Comprehensive Update" was written by *Gordon Gribble* and published in 2010 (*Z396*). This represented a comprehensive update of a subject also covered earlier in Volume 68. Since 1996, an additional 2,500 organochlorine, organobromine, and other organohalogen compounds were discovered. These natural organohalogens are biosynthesized by bacteria, fungi, lichens, higher plants, marine organisms of all types, insects, and other animals including humans. In some instances, natural organohalogens are precisely the same chemicals that man synthesizes for industrial use, and some of the quantities of these natural chemicals by far exceed the quantities emitted by man.

5.4.4 Volume 92

Different siderophore types (peptide, diamino or triamino skeleton-containing siderophores based on citrate and pyochelin derivatives) occurring in microorganisms, which are very important in Nature's iron metabolism, were described by *Herbert Budzikiewicz* in "Microbial Siderophores" (*Z397*). This followed his contribution to Volume 87, where he discussed siderophores from the Pseudomonadaceae.

In another contribution, *Rogelio Pereda-Miranda, Daniel Rosas-Ramírez*, and *Jhon Castañeda-Gómez* from the Department of Pharmacy, Faculty of Chemistry, National Autonomous University of Mexico, presented a discussion of "Resin Glycosides from the Morning Glory Family" (*Z398*). These compounds are prominent secondary metabolites of the plant family Convolvulaceae and can act as drastic purgatives.

5.4.5 Volume 93

Oxidative coupling of phenylpropanoate units leads to the formation of lignans or dimeric phenylpropanoids, which are connected *via* a β-C-atom. Coumarinolignans, flavonolignans, and stilbenolignans are unusual compounds and were presented for the first time together by *Sajeli A. Begum, Mahendra Sahai* (Banaras Hindu University, Varanasi) and *Anil B. Ray* in their contribution "Non-conventional Lignans: Coumarinolignans, Flavonolignans, and Stilbenolignans" (*Z399*).

Edda Gössinger from the Institute of Organic Chemistry at the University of Vienna wrote a contribution on "Picrotoxanes" (*Z400*). Picrotoxanes form a group of complex sesquiterpenes of mostly tetra- or pentacyclic structures, of which over 100 members are known today, with some containing nitrogen. An example is picrotoxinin (**74**), a potent plant toxin present in the seeds of *Menispermum cocculus* (Indian berry) along with the less toxic picrotin, the hydrated derivative of **74**. Picrotoxin, which is a mixture of picrotoxinin and picrotin, was first isolated by *Pierre F. G. Boullay* in 1812 (*250*).

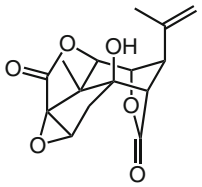

74 (picrotoxinin)

Through metabolic engineering of suitable organisms such as *Streptomyces*, the production of very active drugs belonging to the polyketide group can be performed biotechnologically with very high efficacy. The reader became informed of this process from a contribution by *Marta Luzhetska, Johannes Härle,* and *Andreas Bechthold* from the Institute of Pharmaceutical Sciences, Albert-Ludwigs-University, Freiburg entitled "Combinatorial and Synthetic Biosynthesis in Actinomycetes" (*Z401*).

5.4.6 Volume 94

Following the isolation in 1982 of the first member of a new compound class, namely, rocaglamide (**75**) from *Aglaia elliptifolia*, more than 100 rocaglamide derivatives have been extracted from around 30 *Aglaia* species. Some of these compounds show insecticidal, anti-inflammatory, cytostatic, and antineoplastic effects (*Z402*).

Such properties explain the current broad interest in this group of compounds. *Sherif Saeed Ebada* (*1978), *Neil Lajkiewicz, John A. Porco Jr., Min Li-Weber,* and *Peter Proksch* (*1953) wrote a collaborative contribution on the rocaglamides. These authors represented either the University of Düsseldorf or Boston University.

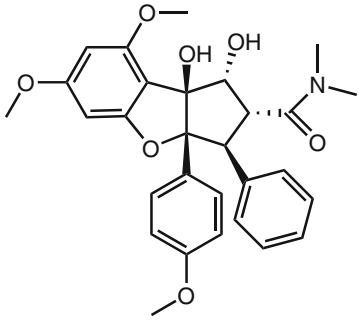

75 (rocaglamide)

Murty A. R. C. Bulusu, Karl Baumann, and *Anton Stütz* from the Novartis Institutes for BioMedical Research, Vienna, wrote on the "Chemistry of the Immunomodulatory Macrolide Ascomycin and Related Analogues" (*Z403*). With the synthesis of terbinafine (Lamisil®), *Anton Stütz* (*1947) succeeded in developing a completely new drug for the treatment of fungal infections in 1980. Together with *Karl Baumann* and other co-workers, *Stütz* also discovered the first non-cortisone-containing therapy for neurodermatitis (atopic eczema), based on the application of ascomycin (**76**). The natural product ascomycin is a calcineurin inhibitor, produced by *Streptomyces hygroscopicus* var. *ascomyceticus*. The chemistry of ascomycin derivatives is quite complex due to stereochemical relationships and isomer equilibria, but much progress had been made by the authors of this contribution.

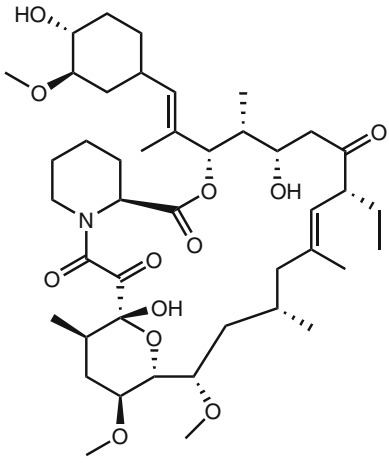

76 (ascomycin)

Rosana I. Misico, Viviana E. Nicotra, Juan Carlos Oberti, Gloria Barboza, Roberto R. Gil, and *Gerardo Burton* from the Universities of Buenos Aires and Córdoba, Argentina, reported on the withanolides in their contribution entitled "Withanolides and Related Steroids" (*Z404*), in the final contribution of Volume 94. This group of steroids was described earlier in Volume 63. This contribution represented a comprehensive update of the chemistry, physiological properties (insecticidal, phytotoxic, antiparasitic, antimicrobial, anti-inflammatory, CNS activity, and cancer-related activities). Also covered were chemotaxonomic studies (Physaleae, Hyoscyameae, Lyceieae, Solanaceae, and Datureae) of this plant compound class, which includes about 12 other basic skeletons in addition to the original skeleton (see Volume 63). This group of steroids now comprises approximately 650 members. Volume 94 was published in 2011.

5.4.7 Volume 95

Yoshinori Asakawa, Agnieszka Ludwiczuk, and *Fumihiro Nagashima* contributed a lengthy and thorough treatise for Volume 95, entitled "Chemical Constituents of Bryophytes: Bio- and Chemical Diversity, Biological Activity, and Chemosystematics" (*Z405*). For over 40 years, Professor *Asakawa* and his group at Tokushima Bunri University in Japan have focused their research on the chemical constituents of bryophytes and found that these lower plants contain large numbers of specialized secondary metabolites, such as terpenoids, acetogenins, and aromatic compounds representative of many new skeletons, which exhibit interesting biological activities. *Asakawa* covered the literature on bryophytes in two earlier volumes of "Progress in the Chemistry of Organic Natural Products", namely, in Volumes 42 (1982) and 65 (1995).

5.4.8 Volume 96

Besides the broad range of different transformations that can be achieved by metal catalysis, the use of substoichiometric amounts of small-organic molecule catalysts has proved to possess enormous potential in the syntheses of biologically active molecules. The author of "Asymmetric Organocatalysis in Natural Product Syntheses" (*Z406*), *Mario Waser* (*1977), studied at Johannes Kepler University, Linz. He finished his PhD in 2005 in the group of *Heinz Falk*. Following a postdoctoral fellowship at the Max Planck Institute for Coal Research in Mülheim, he spent two years as a research and development chemist for DSM-Fine Chemicals in Linz. Since 2009, he has been assistant professor at his *alma mater*. His contribution occupied the whole of Volume 96 and provided an illustrative overview of successful and widely used applications of organocatalysis in the field of natural product synthesis.

5.4.9 Volume 97

It is estimated that well over 1,000 mycotoxins have been isolated and characterized so far. In Volume 97 entitled "Recent Progress in the Chemistry of Mycotoxins", a summary of the most important mycotoxin classes and their chemistry is discussed (*Z407*). The biological activity of mycotoxins ranges from antibacterial to strongly mutagenic (*e.g.* aflatoxins, patulin), carcinogenic (*e.g.* aflatoxins), teratogenic, neurotoxic (*e.g.* ochratoxins), nephrotoxic (*e.g.* fumonisins, citrinin), hepatotoxic, and immunotoxic (*e.g.* ochratoxins, diketopiperazines) properties. The authors of this volume were *Stefan Bräse* (*1967), *Franziska Gläser, Carsten Kramer, Stephanie Lindner, Anna Linsenmeier, Kye Masters, Anne Meister, Bettina M. Ruff,* and *Sabilla Zhong* (*1987), and are from the Karlsruhe Institute of Technology. *Stefan Bräse* has been professor at this institution since 2003.

5.4.10 Volume 98

David A. Lightner, professor emeritus at the University of Nevada, Reno, has been recognized for distinguished contributions to relating chiroptical properties to stereochemistry and for clarifying the molecular mechanisms of phototherapy for neonatal jaundice. His extensive treatment entitled "Bilirubin: *Jekyll* and *Hyde* Pigment of Life" (*Z408*) represents a historically structured and very detailed discussion of progress made in the structure elucidation of one of the most important mammalian metabolites, bilirubin (**77**).

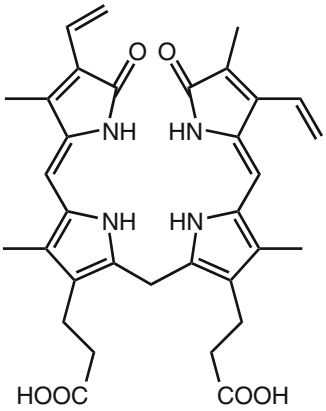

77 (bilirubin)

Like the red color of blood and the green color of leaves, the yellow color of bile has been observed for millenia. In 1824, *Leopold Gmelin* (1788–1853) and *Friedrich Tiedemann* (1781–1861) discovered a test reaction for bilirubin (*251*). Efforts to determine the structure of this air-sensitive natural product began with the

experimental work of *Oskar Piloty* (1866–1915) and *William Küster* (1863–1929). The structure and total synthesis of bilirubin were reported by *Hans Fischer* (1881–1945) and *Hans Plieninger* (1914–1984) in 1942 (*252*). Yet knowing the constitutional structure is not the same as knowing its conformational or stereostructure, the proof of which had to wait some 34 years for the application of modern spectroscopic methods.

5.4.11 Volume 99

In its first part, volume 99 confronts us with "The Pharmacognosy of Black Cohosh: Phytochemical and Biological Profile of a Major Botanical Dietary Supplement". This review was written by *Guido F. Pauli* and members of his group at the College of Pharmacy at the University of Illinois, Chicago, namely, *Feng Qiu*, *James B. McAlpine*, *Elizabeth C. Krause*, and *Shao-Nong Chen* (*Z409*). Preparations from *Actaea racemosa* roots or rhizomes contain almost 50 cycloartane triterpenes, over 70 alkaloids, and 11 phenolic acids. The chemistry of the relevant secondary metabolome was discussed in detail.

Indigo and Tyrian purple are two of the most ancient dyes known. Indigo has been known since 2500 BC and Tyrian purple was probably first used by the ancient Phoenicians as early as 1570 BC. The aim of the contribution "The Evolution of Indigoids: A Colorful History" was to describe the fascinating story of indigoids and their evolution as important compounds from textile science to medicinal chemistry (*Z410*). Indirubin, the second major metabolite of the Indigo dye, was discovered to be the active component of *Danggui Longhui Wan*, a formula that has been used in Traditional Chinese Medicine for four millennia to treat symptoms of leukemia. The authors from the Department of Pharmacognosy and Natural Products Chemistry, School of Pharmacy, University of Athens and the Beckman Molecular Medicine Research Institute, City of Hope Comprehensive Cancer Center, Duarte, California—*Nicolas Gaboriaud-Kolar*, *Sangkil Nam*, and *Alexios-Leandros Skaltsounis*—stressed that this discovery has propelled indirubin and its marine relative, 6-bromoindirubin, as major scaffolds in medicinal chemistry for the study of biological processes and the development of active drug candidates.

In the third part of Volume 99, *Masami Ishibashi*—Professor of Natural Products Chemistry at Chiba University, Japan—reported on various screening studies performed in order to identify novel bioactive compounds targeting distinct cancer-related signaling pathways. In their approach, which primarily focused on TRAIL, Wnt, and Hedgehog signaling, *Ishibashi* and his co-workers investigated bioactive metabolites isolated from various actinomycete strains, including aromatic heterocyclic natural products, such as izumiphenazines and izuminosides as well as new pyranonaphthoquinones, such as (+)-deacetylgriseusin A. The latter could be shown to be very effective in inducing TRAIL-resistance overcoming activity resulting in a significant reduction of cell viability. As another prominent example, they found a known indole alkaloid, teleocidin A-2, to act as a strong enhancer of promotor activity of the TRAIL receptor death-receptor 5 (DR5), which represents an important mediator of apoptosis.

The final contribution published in Volume 99 was written by *Markus Nett* from the Leibniz Institute for Natural Product Research and Infection Biology (Hans-Knöll-Institute) in Jena and was entitled "Genome Mining—Concept and Strategies for Natural Product Discovery". In his contribution, *Nett* gave a comprehensive overview of how recent genome sequencing projects have provided a much deeper understanding of metabolic pathways involved in small molecule production, specifically in microorganisms and plants. Novel bioinformatical tools can be utilized in the context of genetic approaches for the discovery of new natural products. *Nett's* research is focused on investigating the potential of bacteria and plant pathogens—especially from the microbial genome perspective—for the identification of new biosynthesis pathways and natural products for drug discovery and development.

6 Concluding Remarks

In his review of Volume 10 from 1954, *Carl Djerassi* mentions an interesting point about the series "Progress in the Chemistry of Organic Natural Products" (*115*), *"The "Fortschritte" series is at the present time the most useful collection of review articles in the field of natural products … This series consists largely of critical and exhaustive discussions in certain restricted areas. … The international character is demonstrated by the fact that of the six contributing groups, two come from the U.S.A. and one each from Germany, France, Mexico and India." Djerassi*'s judgement is valid for far more than this particular volume of the series. The register of authors of all volumes bears resemblance to a "Who's Who" of the professional circles of their time. It is therefore not really surprising to find out that the list of contributing authors, who were awarded a *Nobel* Prize, is quite long: *Alder*, *Barton*, *Beadle, Crowfoot-Hodgkin*, *Diels, Euler-Chelpin*, *Karrer*, *Leloir*, *Pauling*, and *Prelog,* with *Haworth* and *Butenandt* serving as members of the editorial board.

Whereas the first volumes had been more European-centered, as of 1948, more and more authors from the U.S. contributed to the Series. *Zechmeister* was undoubtedly able to win over many of his colleagues—first those from Zurich or Pécs, and later on some from Pasadena—to submit a contribution to "his" series. Between 1948 and 1970, no less than 20 researchers from Pasadena had been convinced to present their findings in the "Progress" series. With *Zechmeister'*s retirement as editor in 1970, the situation changed radically. From 1970 on, researchers from all parts of the world contributed to this series. The high percentage of contributions by emigrants, who mostly were forced to leave their native countries for political reasons and who only got the chance to unfold their potential in their new home countries, is quite remarkable. The list of those emigrants is almost endless: *Zechmeister* himself, *Dounderoff, Hassid, Lederer, Sondheimer, Rosenkranz, Scheuer, Biemann, Fraenkel-Conrat, Overton,….*

Strikingly, *Zechmeister* always focused his attention on methodology. Volume One, in which *Kratky* and *Mark* describe the application of physical methods for the investigation of natural products, can be considered emblematic. Since *Zechmeister* was a pioneer of chromatography himself, his editorship included in-depth

descriptions of various separation techniques: paper and column chromatography, later on thin-layer, high-performance liquid, and gas chromatography.

These techniques enabled chemists to deal with ever-decreasing amounts of materials. Therefore, in addition to previously investigated plant samples, also natural products from microbial sources could be studied. Additionally, in the 1960s and 1970s, increasing attention was paid to marine sources and to insects.

The results of investigating further sources were that new and even unprecedented chemical structures were elucidated, which had not been encountered earlier from traditional terrestrial plant and animal sources.

Carl Djerassi, who is considered one of the most important natural product chemists—not only due to his excellent successes in the field of steroid chemistry, but also due to his abiding influence on the development of important investigation methods (*e.g.* mass spectrometry and optical rotatory dispersion) (*253*)—described the dramatic developments in the history of structure elucidation in the twentieth century in two historical reflections (*254*, *255*). Until the middle of the century, the chemical structure of a natural product was accomplished almost exclusively by degradative chemistry: alkaline, thermal and oxidative degradation, acid and base hydrolysis, zinc-dust distillation, isolation of degradation products and identification by melting or boiling point. Therefore, great chemical skills, experience and chemical intuition were essential. The development and application of so far unknown spectroscopic and spectrometric methods changed the situation significantly. From the beginning, "Progress in the Chemistry of Organic Natural Products" gave much space to the application of new findings in regard to X-ray diffraction, mass spectrometry, nuclear magnetic resonance spectroscopy, IR-, UV-, vis-, and fluorescence spectroscopy, as well as optical rotatory dispersion and circular dichroism.

A mere quantitative measure of the development may be seen in the numbers of characterized compounds, *e.g.* the halogenated organic natural products (*Z376, Z426*, *256*) (Table 1).

Table 1 Halogenated organic natural products identified between 1935 and 1999

1935	1
1954	12
1968	30
1973	200
1991	1,500
1999	2,900

Upon superficial observation of the plot shown in Fig. 3, one could assume that a rapid development started only in 1970. However, this is not quite true—at least in relation to content. The reader comes to realize quite dramatically how science progressed between 1955 and 1968 when comparing the contribution on genetics by *George Wells Beadle* in Volume 12 to the one by *Dieter Dütting* in Volume 26. What a difference! Yet there were only 13 years of rapid development in between these contributions.

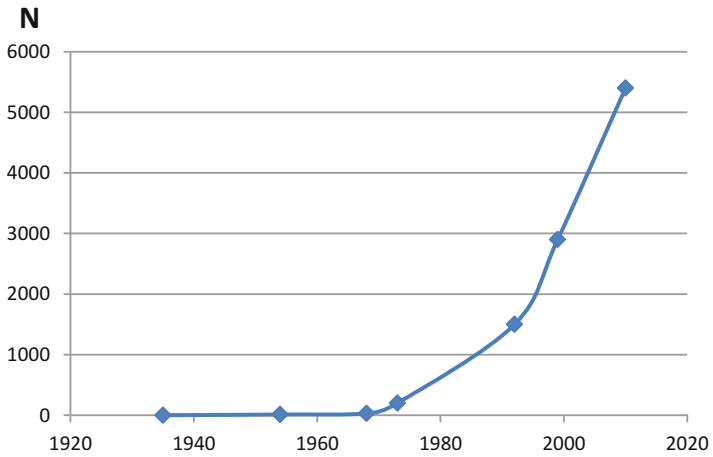

Fig. 3 Number of characterized organic natural halogen compounds

The chapters that have contributed to this book Series have had their finger on the pulse of the time. However, they did not only mirror the state of research, they also stimulated progress. This becomes clear when reading the comments of recent authors on the contributions of previous authors.

Acknowledgements The authors gratefully acknowledge the altruistic and active support of *Prof. Dr. Heinz Falk*. Thanks are also given to *Frau Mag. Michaela Wirth* –who wrote her diploma thesis on the scientific work of *László Zechmeister* at the TU Vienna in the spring of 2012—especially for valuable literature suggestions.

Literature

Biographical Encyclopedias

American Men and Women of Science (1976–1996) 13th–19th ed., RR Bowler Comp, New York, London

Gierlich E, Wilming E (2012) Ostdeutsche Biographie: http://www.ostdeutsche-biographie.de/

Historisches Lexikon der Schweiz. Online-Lexikon: http://www.hls-dhs-dss.ch/textes/d/D44456.php (accessed May 6, 2012)

Kürschners Deutscher Gelehrten-Kalender (1925–2009)

National Centre of Biography at the Australian National University. Australian Dictionary of Biography: http://adb.anu.edu.au/ (accessed on April 27, 2012)

Neumüller OA (1979–1992) Römpps Chemie-Lexikon, 8th and 19th ed. Franckh'sche Verlagshandlung Stuttgart

Poggendorff JC (1938, 1992, 1999) Poggendorff's biographisch-literarisches Handwörterbuch zur Geschichte der exacten Wissenschaften. Volumes 6, 7b, 8

Österreichisches Biographisches Lexikon 1815–1950 (1947–2012) Österreichische Akademie der Wissenschaften. Wien
Pötsch WR (1989) Lexikon bedeutenden Chemiker. Harri Deutsch, Thun
Schweizer Lexikon. (1993) Verlag Schweizer Lexikon, Luzern
Who's Who in America (1924–1987) Marquis & Corp., Chicago
Who's Who in Science in Europe (1967–1989) 1st–6th ed

References

1. Soukup RW (2007) Chemie in Österreich. Bergbau, Alchemie und frühe Chemie, Böhlau, Wien, p 10
2. Plinius (1765) Naturgeschichte. Übersetzt von Johann Daniel Denso. Anton Ferdinand Rösens Buchhandlung, Rostock and Greifswald, Band II; p 723
3. Belloni L (2008) Malpighi, Marcello. Complete Dictionary of Scientific Biography. Encyclopedia.com: http://www.encyclopedia.com/topic/Marcello_Malpighi.aspx (accessed on June 20, 2014)
4. Coley NG (2001) Early Blood Chemistry in Britain and France. Clin Chem 47:2166
5. Berzelius JJ (1812) General Views of the Composition of Animal Fluids. Med Chir Trans 3:198
6. Lieben F (1935) Geschichte der Physiologischen Chemie, p 290. Deuticke, Leipzig und Wien
7. Willstätter R, Stoll A (1913) Untersuchungen über Chlorophyll. Methoden und Ergebnisse. Springer, Berlin, p 392ff: http://www.biodiversitylibrary.org/item/16759#page/406/mode/1up (accessed on March 22, 2013)
8. Greiner A (1986) Chemiker über Chemiker. Wahlvorschläge zur Aufnahme in die Berliner Akademie 1822 – 1925, p 180 f. Akademie, Berlin
9. Ettre LS (1972) In Memoriam *László Ze*chmeister 1889 – 1972. Chromatographia 5:317; Móra L (1997) Emlékezés Zechmeister Lászlóra. Természet Világa 128:377 — http://www.kfki.hu/chemonet/hun/olvaso/histchem/legenda/zchm.html (accessed on April 27, 2012)
10. Rosner R (2004) Chemie in Österreich 1740-1914. Lehre-Forschung-Industrie. Böhlau, Wien, p 88
11. Soukup W (2004) *Karl von Than*. In: Soukup RW (ed.) Die wissenschaftliche Welt von gestern. Böhlau, Wien, p 43
12. Zechmeister L (1913) Lebenslauf. In: Zechmeister L, Zur Kenntnis der Cellulose und des Lignins. Dissertation, ETH Zürich, p 74: http://e-collection.library.ethz.ch/eserv/eth:20083/eth-20083-01.pdf (accessed on May 3 2012)
13. Willstätter R, Zechmeister L (1913) Zur Kenntnis der Hydrolyse von Cellulose I. Ber dtsch chem Ges 46:2401
14. Willstätter R, Zechmeister L (1914) Synthese des Pelargonidins. Sitzungsberichte der Königlich Preussischen Akademie der Wissenschaften 1914, II:886
15. Ettre LS, Zlatkis A (1979) 75 Years of Chromatography – a Historical Dialogue. J Chromatogr Lib 17: 492; Staff (1972) *Laszlo Zechmeister* 1890-1972. Engineering and Science 35:26 — http://calteches.library.caltech.edu/2910/1/1890.pdf (accessed May 3, 2012)
16. Willstätter R, Zechmeister L, Kindler W (1924) Synthesen des Pelargonidins und Cyanidins. Ber dtsch chem Ges 57:1938
17. Hevesy GV, Zechmeister L (1920) Über den Verlauf des Umwandlungsvorganges isomerer Ionen. Zeitschrift für Elektrochemie und angewandte physikalische Chemie 26:151
18. Palló G (2009) Isotope Research before Isotopy: *George Hevesy*'s Early Radioactivity Research in the Hungarian Context. Dynamis, Universidad de Granada: http://scielo.isciii.es/scielo.php?pid=S0211-95362009000100008&script=sci_arttext (accessed on April 28 2012)
19. Bjerrum N, Zechmeister L (1923) Beurteilung und Entwässerung des Methylalkohols mit Hilfe von Magnesium. Ber dtsch chem Ges 56:894

20. Zechmeister L, Szécsi P (1921) Notiz über ein Vorkommen von Fumarsäure und von Inosit. Ber dtsch chem Ges 54:172
21. Zechmeister L, Vrabély V (1926) Notiz über Ajkait (ein organisches Mineral aus Ungarn). Ber dtsch chem Ges 59:1426
22. Zechmeister L, Cholnoky L (1927) Untersuchungen über den Paprika-Farbstoff. II. Liebigs Ann 455:70
23. Zechmeister L, Cholnoky L (1928) Beitrag zum Konstitutions-Problem des Carotins. Ber dtsch chem Ges 61:1534
24. Zechmeister L, Tuzson P (1928) Über das Phytosterin der Brennessel. Ztschr physiol Chem 183:74
25. Zechmeister L, Cholnoky L (1930) Untersuchungen über den Paprika-Farbstoff. IV. Einige Umwandlungen des Capsanthins. Liebigs Ann 478:95
26. Zechmeister, Tuzson P (1936) Über das Polyen-Pigment der Orange (I. Mitteil.). Ber dtsch chem Ges 69:1878
27. Paradowski R (2011) Pauling Chronology – The War Years (1940 – 1945), p 14. Oregon State University, Part 1: http://osulibrary.orst.edu/specialcollections/coll/pauling/chronology/page28.html (accessed on April 28, 2012)
28. Pauling L (1939) Letter to Dr. Warren Weaver, July 14, 1939. Linus Pauling Day by Day. Special Collections, OSU Libraries, Oregon State University: http://osulibrary.oregonstate.edu/specialcollections/coll/pauling/calendar/1939/07/14-xl.html (accessed on April 29, 2012)
29. California Institute of Technology (1947) Catalogue Number for 1946-1947. Bulletin of the California Institute of Technology, Pasadena 56:41: http://caltechcampuspubs.library.caltech.edu/28/1/1947-1948.pdf (accessed on April 27, 2012)
30. Pauling L (1941) Letter to Mr. *Edward C. Barrett*. Special Collections, OSU Libraries, Oregon State University. Linus Pauling Biographical: Academia: Box #1.029 file 29.1: http://osulibrary.oregonstate.edu/specialcollections/coll/pauling/calendar/1941/07/31.html (accessed on May 3, 2012)
31. California Institute of Technology (1956) Catalog 1956-1957. Bull California Institute of Technology 56:251 — http://caltechcampuspubs.library.caltech.edu/91/1/1956-1957.pdf (accessed on May 3, 2012)
32. Oregon State University Libraries (2010) Special Collections, It’s in the Blood! A Documentary History of *Linus Pauling*, Hemoglobin and Sickle Cell Anemia, ID = 1950i.24: http://osulibrary.oregonstate.edu/specialcollections/coll/pauling/blood/pictures/1950i.24-large.html (accessed on March 26, 2013)
33. Wirth M (2012) *László Zechmeister* - From Pioneering Work in Chromatography to the Foundation of the Series “Progress in the Chemistry of Organic Natural Products”. Diplomarbeit, TU Wien. Wirth M (2013) *László Zechmeister*: His Life and Pioneering Work in Chromatography. Springer, Berlin
34. Zechmeister L, Cholnoky L (1936) Dreißig Jahre Chromatographie. Monatsh Chem 68:68
35. Zechmeister L, Cholnoky L (1937) Die chromatographische Adsorptionsmethode: Grundlagen, Methodik, Anwendungen, Springer, Wien
36. Zechmeister L, Cholnoky L, Bacharach AL, Robinson FA (1941) Principles and Practics of Chromatography, Chapman and Hall, London
37. Zechmeister L (1946) *Mikhail Ts*wett — the Inventor of Chromatography. Isis 36:250
38. Markl P (1997) Chemie in Österreich. Wurzeln und Entwicklung. 100 Jahre Gesellschaft Österreichischer Chemiker 1897 – 1997, p 58. GÖCH, Wien; see also: http://www.goech.at/HallOfFame/ehrenmit.shtml (accessed May 3, 2012)
39. Soukup RW (2004) *Ernst Späth*. In: Soukup RW (ed) Die wissenschaftliche Welt von gestern. Böhlau, Wien, p 209
40. Móra L (2002) *Gezá Zemplén* (1883 – 1956), der Begründer der wissenschaftlichen Chemie Ungarns. Humboldt Nachrichten 22:13 — http://www.humboldt.hu/HN22/HN22MZ3.pdf (accessed on March 22, 2012)
41. Lichtenthaler FW (2002) *Emil Fischer* und die Entwicklung der organischen Chemie in Ungarn I – III. Humboldt Nachrichten 22:3 — http://www.humboldt.hu/HN22/tart.htm (accessed on April 25, 2012)

42. Zemplén G, Kunz A (1923) Über die Natriumverbindungen der Glucose und die Verseifung acylierter Zucker. Ber dtsch chem Ges 56:1705
43. Morá L (2004) *Zemplén Gezá*. Neumann Kht, Budapest: http://mek.oszk.hu/04800/04854/04854.htm (accessed April 30, 2012)
44. Gunstone FD (1965) T. P. Hilditch, C.B.E., D.Sc., F.R.I.C., F.R.S. J Am Oil Chem Soc 42:a474
45. Marasco C (2008) 1945 *Ian Morris Heilbron* (1886–1959). Chem Eng News 86:14
46. Mitchell V, Spring J (2008) *Frank Stuart Spring* (1907 – 1997). Biogr Mem Fell Roy Soc 54:375
47. Soukup RW (2011) *Wilhelm Suida*. Österreichisches Biographisches Lexikon vol 14. ÖAW, Wien, p 40; Suida W (1918) Julius Mauthner. Nekrolog. Ber dtsch chem Ges 51:1025
48. Diels O, Abderhalden E (1903) Über den Abbau des Cholesterins. Ber dtsch chem Ges 36:3179
49. Windaus A, Linsert O (1928) Über die Ultraviolett-Bestrahlung des Dehydro-ergosterins. Liebig's Ann 465:148
50. Butenandt A, Schramm G (1936) Über die Bromierung des Δ^5-Cholestenon-dibromids. Ber dtsch chem Ges 69:2289
51. Rosenheim O, Starling WW (1937) The Action of Selenium Dioxide on Sterols and Bile Acids. Part III. Cholesterol. J Chem Soc London 1937:377
52. Inhoffen HH (1940) Übergang von Sterinen in aromatische Verbindungen. Angew Chem 53:471
53. Barnett JA (2005) Glucose Catabolism in Yeast and Mussel: Semenza G, Turner AJ (eds.) A History of Biochemistry. Selected Topics in the History of Biochemistry: Personal Recollections. IX. Comprehensive Biochemistry 44:11
54. Manier J (1998) *Fritz Schlenk*, Researcher and Teacher. Chicago Tribune 1998, July 8: http://articles.chicagotribune.com/1998-07-08/news/9807080234_1_researcher-and-teacher-enzyme-basic-research (accessed March 26, 2013)
55. Rürup R, Schüring M (2008) Schicksale und Karrieren: Gedenkbuch für die von den Nationalsozialisten aus der Kaiser Wilhelm-Gesellschaft vertriebenen Forscherinnen und Forscher. p 325, Wallstein, Göttingen
56. Freudenberg K (1928) Nachtrag zu der Mitteilung über Lignin und Cellulose. Ann Chem 461:130
57. Freudenberg K (1932) Stereochemie. F. Deuticke, Leipzig & Wien
58. Kipnis A (2002) *Freundenberg, Karl Johann*, Chemiker. Baden-Württembergische Biogr 3:87
59. Willstätter R, Asahina Y (1910) Untersuchungen über Chlorophyll IX. Oxydation der Chlorophyllderivate. Liebigs Ann 373:227
60. Asahina Y, Kutani N (1925) Über die Gyrophorsäure. J Pharm Soc Japan 519:1
61. Shibata S (2000) *Yasuhiko Asahina* (1880–1975) and his Studies on Lichenology and Chemistry of Lichen Metabolites. The Bryologist 103:710
62. Nobelprizes.org (2011) *Richard Kuhn* and the Chemical Institute. Double Bonds and Biological Mechanisms: http://nobelprize.org/nobel_prizes/medicine/articles/states/richard-kuhn.html (accessed on July 25, 2011)
63. Rudy H, Majer O (1938) 9-Propyl-8-aza-flavin. Ber dtsch chem Ges 71:1243
64. Himsworth H, Pitt-Rivers R (1972) *Charles Robert Harington*. 1897-1972: Biogr Mem Fell Roy Soc 18:266
65. Stacey M, Percival E (1976), *Edmund Largely Hirst*. Biogr Mem Fell Roy Soc 22:137
66. Zeisel S (1888) Über Colchicin. Monatsh Chem 9:1
67. Soukup RW (2006) A Century of Alkaloid Research: The Austrian Contribution to Organic Chemistry, Ignaz Lieben Workshop, Vienna, 2006
68. Späth E, Bretschneider H (1928) Eine neue Synthese des Nikotins und einige Bemerkungen zu den Arbeiten *Nagais* über Ephedrine. Ber dtsch chem Ges 61:327
69. Pinner A (1893) Über Nicotin. Die Constitution des Alkaloids. Ber dtsch chem Ges 26:292
70. Späth E, Kesztler F (1937) Über das Vorkommen von *d*,*l*-nor-Nicotin, *d*,*l*-Anatabin und *l*-Anabasin im Tabak. Ber dtsch chem Ges 70:704

71. Skraup ZH, Vortmann G (1882) Über Derivate des Dipyridyls. Monatsh Chem 3:570
72. Bentley HR (1984) Thirty Years in Tobacco Science - A Personal Reflection. Coresta 84 Technology Group Vienna Congress. Invited Papers and Statements, p 86: http://tobaccodocuments.org/rjr/504202652-2666.html (accessed on April 2, 2012)
73. Späth E, Wenusch A (1936) Die Konstitution des Myosmins (V. Mitteil. über Tabakbasen) Ber Dtsch Chem Ges 69:393
74. Späth E, Mamoli L (1936) Synthese des Myosmins (VI. Mitteil. über Tabakbasen) und Bemerkungen zu einer Notiz von Miss *T. M. Reynolds* und *R. Robinson*. Ber Dtsch Chem Ges 69:757
75. Kuffner F, Kaiser E (1954) Über das Nicotellin und die Synthese eines neuen Terpyridyls. Monatsh Chem 85:896
76. Vickery HB (1962) *Rudolph John Anderson* (1979 – 1961). A Biographical Memoir. National Academy of Sciences Biographical Memoirs 36: 19: http://books.nap.edu/html/biomems/randerson.pdf (accessed on July 5, 2011)
77. Westphal U (1942) Über die reduktive Umwandlung des Desoxy-corticosterons zu Pregnandiol im Organismus des Kaninchens. Hoppe-Seyler's Z physiol Chem 273:13
78. Hermann A, Wankmüller A (1980) Physik, Physiologische Chemie und Pharmazie an der Universität Tübingen. Mohr, Tübingen, p 72
79. Rheinberger HJ (2010) An Epistemology of the Concrete. Twentieth-Century Histories of Life. Duke University Press, Durham, NC, USA, p 133
80. Rüchardt C (2007) Die Farbe der Schmetterlingsflügel und anderer Insekten. Die Entdeckung der Pterine in der *Wieland*-Schule. In: 550 Jahre Albert Ludwigs Universität Freiburg. Sonderdrucke aus der Albert Ludwigs Universität 4:211
81. Oregon State Board of Higher Education (1959) Oregon State College Catalog 1959 – 1960. Oregon State Bulletin 76:19
82. Fox DL (1977) My Yesteryears and Later Days in La Jolla, California: http://scilib.ucsd.edu/sio/biogr/Fox_Yesteryears.pdf (accessed on March 17, 2012)
83. Weisel GF (1993) After the War. In: KK Kuhns, B Shor, Scripps Stories. Days to Remember. Scripps Institution of Oceanography, San Diego, La Jolla: p 14: http://escholarship.org/uc/item/5581g26h (accessed on March 26, 2013)
84. Pauling L (1944) Letter to *Denis L. Fox*, November 10, 1944: http://osulibrary.oregonstate.edu/specialcollections/coll/pauling/calendar/1944/11/10.html (accessed on March 17 2012)
85. Fox DL, Koe BK, Petracek FJ, Zechmeister L (1952) Some Fluorescent Substances Contained in the Marine "Blood Worm" (*Thoracophelia mucronata*). Arch Biochem Biophys 40:135
86. Barker HA (1993) *Michael Doudoroff* 1911 – 1975. A Biographical Memoir, National Academy of Science, Washington: http://www.nap.edu/openbook.php?record_id=2201&page=119 (accessed on March 26, 2013)
87. Barker HA, Koshland DE, Jr (2011) *William Zev Hassid*, Biochemistry: Berkeley. 1899 – 1974: http://texts.cdlib.org/view?docId=hb1199n68c&doc.view=frames&chunk.id=div00050&toc.depth=1&toc.id= (accessed on March 8, 2012)
88. Ballou C, Barker HA (1979) *Willam Zev Hassid* (1899 – 1974) National Academy of Sciences. Biographical Memoirs 50:196 — http://books.nap.edu/html/biomems/whassid.pdf (accessed on March 26, 2013)
89. Tipson RSt, Horton D, Deulofeu V (1988) *Venancio Deulofeu*, 1902-1984. Adv Carbohydr Chem Biochem 46:11
90. Cowgill GR (1962) In: Scrimsham NS, Contributions of Biochemistry to Understanding and Solving the World Problem of Protein Malnutrition in Children, Am J Clin Nutr 11:593; http://ajcn.nutrition.org/content/11/6/593.abstract (accessed on April 1, 2013)
91. Mehl JW (1958) *Harry James Deuel, Jr* 1897 – 1956. J. Nutr. 65:1; http://jn.nutrition.org/content/65/1/1.full.pdf+html (accessed on March 17, 2012)
92. Dibner B (1974) Éloge *Ladislao Reti*. Isis 65:376
93. Dibner B (1974) *Ladislao Reti* (1901 – 1973). Technology and Culture 15:440
94. Freeman K, Bonner JF (1996) Studied Gene Regulation. The New York Times, Sept. 19, 1996

95. Straub W, Gebhardt H (1936) The Active Ingredients of Senna Leaves. Naunyn-Schmiedebergs Arch exp Path 181:399
96. Roberts JD (1969) *Carl Niemann* 1908 – 1964. Biographical Memoir, p 290, National Academy of Sciences, Washington DC: http://books.nap.edu/html/biomems/cniemann.pdf (accessed May 3, 2012)
97. Baldwin RL, Ferry JD (1994) *John Warren Williams* (1898 – 1988), National Academy of Sciences. Biographical Memoirs 65:373
98. Lamb AB (1952) Progress in the Chemistry of Organic Natural Products. Volume 8. J Am Chem Soc 74:2698
99. Zechmeister L (1950) Letter to *A. Frey-Wyssling*, July 3, 1950. ETH-Bibliothek, Archive und Nachlässe. Eidgenössische Technische Hochschule Zürich. Zechmeister-Stoll. Hs 443-1321
100. Jones AS (1994) Obituary: Professor *Maurice Stacey*. The Independent, Oct 15, 1994
101. Todd L (1979) *George Wallace Kenner*. 1922 - 1978. Biogr Mem Fell Roy Soc 25:390; http://links.jstor.org/sici?sici=0080-4606%28197911%2925%3C390%3AGWK1N1%3E2.0.CO%3B2-M (accessed on March 5, 2012)
102. Koller G, Pfeiffer G (1933) Über Enzyme der Flechten und über die Konstitution der Umbilikarsäure. Monatsh Chem 62:359
103. Koller G, Pfeiffer G (1933) Über die Konstitution der Pinastrinsäure, Monatsh Chem 62:160
104. Koller G, Hamburg H (1934) Über die Konstitution der Diploschistessäure. Monatsh Chem 65:367
105. Koller G, Pöpl K (1934) Über ein chlorhaltigen Flechtenstoff, Monatsh Chem 64:106, 126
106. Soukup RW (2004) *Georg Koller*. In: Soukup RW (ed) Die wissenschaftliche Welt von gestern. Böhlau, Wien, p 275
107. Fleischhacker W (2011) Nachruf auf Prof. Dr. *Matthias Pailer*. Sci Pharm 79:387
108. Altman J (2009) Naturwissenschaftler vor und nach *Hitlers* Aufstieg zur Macht, Aus dem Hebräischen von Inka Arroyo Antezana, p 5: http://www-sop.inria.fr/members/Eitan.Altman/PAPERS/weisseR1.pdf (accessed on January 31 2012)
109. Stoll A (1948) Letter to *L. Zechmeister*, June 1, 1948. ETH-Bibliothek, Archive und Nachlässe. Eidgenössische Technische Hochschule Zürich. Zechmeister-Stoll. Hs1426b-1032, p 401
110. California Institute of Technology (1949) Bulletin of the California Institute of Technology, Pasadena 58:45 http://caltechcampuspubs.library.caltech.edu/31/1/1949-1950.pdf (accessed on May 23 2012)
111. Wiechert R (2010) Zur Geschichte kontrazeptiver Steroide in der Schering AG. In: Soukup RW, Noe C (ed) Pioniere der Sexualhormonforschung, p 112. Book of Abstracts, Gumpoldskirchen, Austria
112. Inhoffen HH, Pommer H, Bohlmann F (1950). Synthesis of Carotenoids. XIV. Total Synthesis of β-Carotene. Ann Chem 569:237
113. Working Group on the Evaluation of Cancer Preventive Agents (1997) Carotenoids. IARC Handbook of Cancer Prevention vol 2, Lyon, p 26
114. Terrall M (1978) *Henry Borsook* (1897- 1984) interviewed April 5, 1978. Archives, California Institute of Technology, Pasadena, California: http://oralhistories.library.caltech.edu/24/0/OH_Borsook_H.pdf (accessed on January 5, 2012)
115. Djerassi C (1954) Fortschritte der Chemie Organischer Naturstoffe. Volume X. J Am Chem Soc 76:6415
116. Djerassi C (2001) This Man's Pill. Haymon-Verlag, Innsbruck, p 42
117. Complete Dictionary of Scientific Biography (2008) *Lederer, Edgar*. Encyclopedia.com: http://www.encyclopedia.com/doc/1G2-2830905849.html (accessed on December 27, 2011)
118. National Research Council (2002) Neem: A Tree for Solving Global Problems, Reprint of 1992, p 125. Book for Business, New York: http://www.nap.edu/openbook.php?record_id=1924&page=125 (accessed on March 27, 2013)
119. Inhoffen HH, Irmscher K, Hirschfeld H, Stache U, Kreutzer A (1958) Studien in der Vitamin D-Reihe XXVI. Partialsynthesen der Vitamie D_2 und D_3. Chem Ber 91:2309

120. Marsh RE (2011) *Robert Brainard Corey*. The National Academies Press: http://www.nap.edu/readingroom.php?book=biomems&page=rcorey.html2 (accessed on July 5, 2011)
121. Pauling L (1941) Letter to *Edward C. Barrett*, July 31, 1941. *Linus Pauling* Day by Day. Special Collections, OSU Libraries, Oregon State University: http://osulibrary.oregonstate.edu/specialcollections/coll/pauling/calendar/1941/07/index.html (accessed on April 29, 2012)
122. Witkop B (1956) Progress in the Chemistry of Organic Natural Products. Vol XII. Science 123:898
123. Sanger F, Thompson, EOP (1953) The Amino-Acid Sequence in the Glycyl Chain of Insulin. Biochem J 53:353, 366
124. Masanori K (2008) *Nozoe, Tetsuo*. Complete Dictionary of Scientific Biography. Retrieved July 24, 2011 from Encyclopedia.com: http://www.encyclopedia.com/doc/1G2-2830905956.html (accessed on July 10, 2011)
125. Fleischmann U, Fleischmann SK (1969) Dreißig Jahre Colchicinforschung. Ber nat med Ver Innsbruck 57:147
126. Curtius T (1904) Verkettung von Aminosäuren I. Abh. J Prakt Chem 70:57
127. Appleton HD (1966) In Memoriam *Harry H. Sobotka*. Clin Chem 12:115: http://www.clinchem.org/content/12/3/115.full.pdf+html (accessed on May 6, 2012)
128. Ingle PK, Sivaram S, Kumar R (2008) *Venkataraman, Krishnasami*. Complete Dictionary of Scientific Biography. Encyclopedia.com: http://www.encyclopedia.com/doc/1G2-2830906170.html (accessed on November 14, 2011)
129. Soukup RW (2004) *Josef Herzig* 1853 – 1924. Der Namensgeber der *Herzig-Meyer*-Reaktion und große Naturstoffforscher – ein Jugendfreund *Sigmund Freuds*. In: Soukup RW (ed) Die wissenschaftliche Welt von gestern, p 105. Böhlau, Wien
130. Tambor J (1912) *Stanislaus von Kostanecki* (1860 – 1910). Ber dtsch chem Ges 45:1683
131. Horsefall JG (1991) *Albert Eugen Dimond*, 1914 – 1972: One of the Bright Lights of Plant Physiology, Ann Rev Phytopathol 29:29 — http://www.annualreviews.org/doi/pdf/10.1146/annurev.py.29.090191.000333 (accessed on December 21, 2011)
132. Waksman SA, Woodruff HB (1941) *Actinomyces antibioticus*, a New Soil Organism Antagonistic to Pathogenic and Non-pathogenic Bacteria. J Bacteriol 42:231
133. Pohl J (1891) Über das Aristolochin, einen giftigen Bestandtheil der Aristolochia-Arten. Naunyn-Schmiedeberg's Archiv Pharmacol 29:282
134. Soni NK (2010) Fundaments of Botany vol 2. Tata McGraw-Hill, West Patel Nagar, New Delhi, p 210
135. Garrett SD (1981) *Percy Wragg Brian*. Biogr Mem Fell Roy Soc 27:103
136. MacMillan J (1996) Reflection of a Bio-organic Chemist. Annu Rev Plant Physiol Plant Mol Biol 47:1 — http://www.annualreviews.org/doi/pdf/10.1146/annurev.arplant.47.1.1 (accessed on December 29, 2011)
137. Van Holde KE (2008) Learning How to be a Scientist. J Biol Chem 283:4461
138. Eisen HN (2001) *Michael Heidelberger* (1888 – 1991). National Academy of Sciences Biographical Memoirs 80:222
139. U.S. National Library of Medicine (2006) Profiles in Science. The *Michael Heidelberger* Papers: http://profiles.nlm.nih.gov/ps/retrieve/ResourceMetadata/DHBBLH (accessed on April 24, 2012)
140. Stacey M (1994) *Michael Heidelberger*. 29 April 1888 - 25 June 1991. Biogr Mem Fell Roy Soc 39:179
141. Pfau A, Plattner PA (1939) Zur Kenntnis der flüchtigen Pflanzenstoffe VI. Helv Chim Acta 22:202
142. Staudinger H, Ruzicka L (1924) Insektentötende Stoffe I. Über Isolierung und Konstitution des wirksamen Teiles des dalmatinischen Insektenpulvers. Helv Chim Acta 7:177
143. Percheron F (1990) *Jean-Emile Courtois* (1907-1989). Rev d'Hist Pharm 286:331
144. Leitão, SG (2008) In memoriam - *Walter Baptist Mors* - 1920 – 2008. Rev Bras Farmacogn 18: editorial: http://dx.doi.org/10.1590/S0102-695X2008000400001 (accessed on April 5, 2012)
145. Bolzani V, Cragg GM (2004) Professor *Otto Richard Gottlieb* – A Tribute. ARKIVOC 6: 1: http://www.arkat-usa.org/get-file/19712/ (accessed on April 5, 2012)

146. Ledderhose G (1976) Über salzsaures Glycosamin. Ber dtsch chem Ges 9:1200
147. Sinsheimer RL (2007) Jerome Vinograd. National Academy of Sciences. Biographical Memoirs 89:357 — http://www.nap.edu/openbook.php?record_id=12042&page=357 (accessed on April 2, 2012)
148. Hochstein FA, Stephens CR, Conover LH, Regna PP, Pasternack R., Gordon PN, Pilgrim F.J., Brunings KJ, Woodward RB (1953) The Structure of Terramycin. J Amer Chem Soc 75:5455
149. Büchi G, Kaltenbronn JS, Crombie L, Godin PJ, Whiting DA (1960) The Stereochemistry of Rotenone, Proc Chem Soc (London) 1960:274
150. Ciamician G (1913) La Fotochimica dell' Avvenire, Zanichelli, Bologna
151. Nasini R (1926) *Giacomo Luigi Ciamician*. J Chem Soc 1926:996
152. Hornemann GL (1822) Ueber die Verwechslung der Wurzeln der Rhabarber mit denen der Rhapontik, nebst einem Auszuge aus meinen Analysen mehrerer Rhabarbersorten und der Rhapontikwurzel. Berliner Jahrbuch für die Pharmacie 8:252
153. Erdtman H (1939) Zur Kenntnis der Extraktivstoffe des Kiefernkernholzes, Naturwissenschaften 27:130
154. Takaoka M (1939) Resveratrol, a New Phenolic Compound, from *Veratrum grandiflorum*. Nippon Kagaku Kaishi 60:1090
155. Karberg S (2010) Geschäft mit dem Leben. Zeit online 9. 11. 2010: http://www.zeit.de/zeit-wissen/2010/06/Resveratrol (accessed on February 10, 2012)
156. Birkinshaw JH (1972) *Harold Raistrick* 1890 – 1971. Biogr Mem Fell Roy Soc 18:488
157. Bernardo R (2003) *Paul Scheuer* (1915 – 2003). Honolulu Starbulletin.com 15. 1. 2003: http://archives.starbulletin.com/2003/01/15/news/story12.html (accessed on February 10, 2012)
158. Hirst EL, Turvey JR (1970) *Stanley Peat*, 1902–1969. Biogr Mem Fell Roy Soc 16:441
159. Rasmussen C, Tropea R (2001) Faculty of Science of the University of Melbourne. Biographica entry. Australian Science and Technology Heritage Centre: http://www.austehc.unimelb.edu.au/umfs/biogs/UMFS065b.htm (accessed on April 6, 2012)
160. Chung DDL (2006) The Road to Scientific Success. World Scientific Publ Comp, Singapore, p 143
161. Borman S (1998) A Brief History of Mass Spectrometry Instrumentation, Scripps Center for Metabolomics and Mass Spectrometry: http://massepc.scripps.edu/mshistory/perspectives/sborman.php (accessed May 7, 2012)
162. Karrer W (1936) Untersuchungen über herzwirksame Glykoside. Festschrift für *E. C. Barrell*. Basel, p 238 (Chem Zentralbl 1936: 2727)
163. Karlson P (1984) *Otto Hoffmann-Ostenhof* zum 70. Geburtstag. Naturwissenschaften 71:491
164. Feußner I, Löffelhardt W (2006) Brücke zwischen den Disziplinen. Zum 70. Geburtstag des Biochemikers *Helmut Kindl*, UniLeute & UniBund, Universität Marburg 21:73
165. Norin T (1990) *Holger Erdtman* (1902 – 1989) Phytochemistry 28, 1713: http://www.kth.se/en/che/divisions/orgkem/2.12715/holger-erdtman-1902-1989-1.33364 (accessed on March 27, 2013)
166. Scalise K (1999) UC Berkeley Biochemist *Heinz Fraenkel-Conrat*, Pioneer in Viral Research, Has Died at the Age of 88. University of California, Berkeley. News Release 4:99 — http://berkeley.edu/news/media/releases/99legacy/4-29-1999a.html (accessed on May 26, 2012)
167. Ashurst PR (2012) Dr Philip R Ashurst: http://www.expertsearch.co.uk/cgi-bin/find_expert?1104 (accessed on May 26, 2012)
168. Olivares FL (2007) Jesús Romo Amería: Pionero de la Investigación Química en Mexico, Tesis, Centro de Investigación y de Estudios Avanzados del Instituto Politécnico Nacional. México, p 147
169. Wijkman N (1931) Über einige neue, durch Schimmelpilze gebildete Substanzen. Ann Chem 485:61
170. Gaoni Y, Mechoulam R (1964) Isolation, Structure, and Partial Synthesis of an Active Constituent of Hashish. J Am Chem Soc 86:1646
171. Tregaskis S (2012) Out of Darkness, Pittmed Winter 2012/13, University of Pittsburgh School of Medicine 14/4:15 — http://pittmed.health.pitt.edu/Winter_2012/Winter_2012.pdf (accessed on March 28 2013)

172. Teranishi R, Wick EL, Hornstein I (1999) Flavor Chemistry: Thirty Years of Progress. Kluwer Academic, New York, p 92
173. Wannowius KJ (2003) Research Group Prof. Dr. *J. W. Buchler*. Technische Universität Darmstadt. Fachbereich Chemie: http://www1.tu-darmstadt.de/fb/ch/Fachgebiete/AC/bioac/index.tud (accessed on May 26, 2012)
174. Clogg C (2001) Three U of A staff appointed to the Order of Canada. University of Alberta News Archive: http://www.archives.expressnews.ualberta.ca/article/2001/08/885.html (accessed on April 6, 2012)
175. Pattenden G (2005) *Basil Charles Leicester Weedon*. 18 July, 1923 - 10 October, 2003. Biogr Mem Fell Roy Soc 51:425
176. Cornelisse J, Jacobs HJC (1988) Obituary. *Egbert Havinga* (1909-1988): http://umchemistry.cox.miami.edu/MurthyGroup/pundits/obituary-havinga.pdf (accessed on February 20, 2012)
177. Schmiedeberg O, Koppe R (1869) Das Muscarin: Das giftige Alkaloid des Fliegenpilzes (*Agaricus muscarius* L.), Verlag F. C. W. Vogel, Leipzig
178. Herz W (1971) Letter to *L. Zechmeister*, on May 10 1971. The Caltech Archives, California Institute of Technology Pasadena. The Papers of *László Zechmeister*, Box 1, File 1,25
179. Webmaster, The Ohio State University (2012) College of Pharmacy appoints internationally renowned expert as *Jack L. Beal* Chair in Natural Products Chemistry: http://www.pharmacy.ohio-state.edu/news/Kinghorn.cfm (accessed on February 27, 2012)
180. Kobayashi J, Ishibashi I (1993) Bioactive Metabolites of Symbiotic Marine Microorganisms. Chem Rev 93:1753
181. Huneck S (2010): 10.000 Kilometer unterwegs im Herzen Asiens. Expeditionsberichte aus der Mongolei. Weissdorn-Verlag, Jena
182. Stordeur R, Sipman HJM, Elix JA (2011) In Memory of *Siegfried Huneck*. 9 September 1928 – 9 October 2011. Herzogia 24:185
183. Milstein D (2003) Obituary of Prof. *David Lavie*, Department of Organic Chemistry, Weizmann Institute of Science: http://www.weizmann.ac.il/Organic_Chemistry/lavie-obit.shtml (accessed on August 28, 2011)
184. Valenta Z, Papadopoulos S, Podesva C (1961) Quassin and Neoquassin. Tetrahedron 15:100
185. Dragendorff G, Podwyssotzki V (1877) Über die wirksamen und einige andere Bestandtheile des Mutterkorns. Arch Expt Path Pharm 6:153
186. Furukawa S (1932) Constituents of *Ginkgo biloba* L. Leaves. Sci Papers Inst Phys Chem Res Tokyo 19:27
187. Colvin EW, Raphael RA, Roberts JS (1971) Total Synthesis of (+)-Trichodermin. J Chem Soc Chem Commun 1971:858
188. Hatsuda Y, Kuyama S (1954) Studies on the Metabolic Products of *Aspergillus versicolor*. Part 1. Cultivation of *Aspergillus versicolor*, Isolation and Purification of Metabolic Products. J Agric Chem Soc Jpn 28:989
189. Geuther A (1866) Über Essigsäure. Jena'sche Z 2:387
190. Collie JN (1907) Derivatives of the Multiple Keten Group. J Chem Soc 91:1806
191. Frandsen R (2010) History of Polyketide Research: http://www.rasmusfrandsen.dk/polyketide_synthases.htm (accessed on February 26, 2012)
192. Curtius T, Goebel F (1888) Über Glycinanhydrid und seine. Verbindungen. J Prakt Chem 37:173
193. National Institutes of Health (2002) NHLBI Chemist *Highet* Dies. NIH Record-10/01/2002-Obituaries: http://nihrecord.od.nih.gov/newsletters/10_01_2002/obits.htm (accessed on August 28, 2011)
194. Department of Chemistry at the University of Illinois at Urbana-Champaign (2011) *Robert M. Coates*, Professor Emeritus: http://chemistry.illinois.edu/faculty/Robert_Coates.html (accessed on September 21, 2011)
195. Watson HB, Watson HE, Bennett GM (1953) Obituary Notices: *Alan Edwin Bradfield*, 1897–1953. J Chem Soc 1953:4189
196. McKern HHG (1988) *Penfold, Arthur de Ramon* (1890–1980), Australian Dictionary of Biography, National Centre of Biography, Australian National University: http://adb.anu.edu.au/biography/penfold-arthur-de-ramon-8013/text13965 (accessed on September 24, 2011)

197. Overton A, Froebel K (2009) *Karl Overton*, The Scotsman: http://news.scotsman.com/obituaries/Karl-Overton.5540887.jp (accessed on September 24 2011)
198. Schmutz J, Hunziker F, Hirt R (1957) Ulein, das Hauptalkaloid von *Aspidosperma ulei Mgf.* *Aspidosperma*-Alkaloide, 1. Mitteilung, Helv Chim Acta 40:1189
199. Vogel A (1820) Darstellung von Benzoesäure aus der Tonka-Bohne und aus den Melioten- oder Steinklee-Blumen. Gilbert's Ann Phys 64:161
200. Brand J (1894) Ueber Maltol. Ber dtsch chem Ges 27:806
201. Flament I (2002) Coffee Flavor Chemistry, John Wiley & Sons, New York
202. Butenandt A, Beckmann R, Hecker E (1961) "Über den Sexuallockstoff des Seidenspinners. 1. Der biologische Test und die Isolierung des reinen Sexuallockstoffes Bombykol". Hoppe-Seylers Z Physiol Chem 324:71
203. Dendy LB (2005) UGA Blue Key Chapter to Honor two Georgia Law Alumni - *Stuckey* and *Carr* - as well as *Albersheim* and *Bryan*: http://www.law.uga.edu/news/archives/050927bluekey.html (accessed on September 17, 2011)
204. Hata T, Sano Y, Sugawana R, Matsumae A, Kanamori K, Shima T, Hoshi T (1956) Mitomycin, a New Antibiotic from *Streptomyces* I. J Antibiotics Ser A9:141
205. Acheson RM (1980) Reviews. New Phytol 86:243
206. Marckwald W (1904) Über asymmetrische Synthesen, Ber dtsch chem Ges 37:349
207. Ekpe J (2009) The Chemistry of Light: the Life and Work of *Theobald Adrian Palm* (1848–1928). J Med Biol 17:155
208. Wolf G (2004) The Discovery of Vitamin D: The Contribution of *Adolf Windaus*. J Nutr 134: 1299: http://jn.nutrition.org/content/134/6/1299.full.pdf+html (accessed on April 6, 2012)
209. Singh V, Srikrishna A (2003) Professor *Sukh Dev* – A Tribute. ARKIVOC 3: 1: http://www.arkat-usa.org/get-file/19562/ (accessed on August 5, 2011)
210. Cragg GM, Beutler JA, Jones WP (2009) The American Society of Pharmacognosy. 50 Years of Progress in Natural Products Research 1959 – 2009. Omnipress, Madison, Wisconsin, p 58
211. Schmid R, Tanielian Ch, Tunsbach R, Wolff Ch (1999) Universal Reference Compound for the Determination of Quantum Yields of Singlet Oxygen O_2 ($^1\Delta_g$) Sensitization, J Photochem Photobiol A 79:11
212. Quideau S (2009) Why Bother with Polyphenols? http://www.groupepolyphenols.com/index.php?option=com_content&view=article&id=53&Itemid=59&b528026c36a38313c3bc0e90a25fbe0c=7012a845601d61b99d4b8fbc24b709de (accessed on January 2, 2012)
213. Weinreb SW, Basha FZ, Hibino S, Khatri NA, Kim D, Pye WE, Wu TT (1982) Total Syntheses of Antitumor Antibiotic Streptonigrin. J Am Chem Soc 104:537
214. Garraffo HM (2009) *John William Daly* (1933 – 2008). Cell Mol Neurobiol 29:439
215. Hlasiwetz H (1855) Über die Wurzel der *Onodis spinosa*. Sitzungsber math naturw Klass kaiserl Akad Wiss 15:142
216. Wessely F, Lechner F (1933) Über das Ononin II. Monatsh Chem 63:201
217. Zemplén G, Farkas L, Bien A (1944) Synthese des Ononins. Chem. Ber 77:452
218. Woodward RB, Cava MP, Ollis WD, Hunger A, Daeniker HU, Schenker K (1954) The Total Synthesis of Strychnine. J Am Chem Soc 76:4749
219. Masamune S, Ang S, Egli C, Nakatsuka N, Sarkar S, Yasunari Y (1967) The Synthesis of Ajmaline. J Am Chem Soc 89:2506
220. Brandt GLE, Schmidt MD, Prisinzano TE, Blagg BSJ (2008) Gedunin, a Novel Hsp90 Inhibitor: Semisynthesis of Derivatives and Preliminary Structure – Activity Relationship. J Med Chem 51:6495
221. Schantz EJ, Mold JD, Stanger DW, Shavel J, Bowden FJB, Lynch JM, Wyler RS, Riegel BR, Sommer H (1957) Paralytic Shellfish Poison VI. J. Am Chem Soc 59:5230
222. Garrigues SS (1854) Chemical Investigations on Radix Ginseng Americana, Oleum Chenopodii Anthelmintici and Oleum Menthae Viridis. Universität Göttingen
223. Hooper D (1888) Isolation of Quinazoline Alkaloids: Vasicine and Vasicinone. Pharm J 18:841

224. Gross D (1971) Struktur und Biosynthese Natürlicher Piperidinverbindungen. Prog Org Chem Prod 29:17

225. Kover RX (1999) Radical Fragmentation Towards the Synthesis of FS-2. Dissertation, Yale University. New Haven, p 8: http://www.jandr.org/rxk_files/chapter1.PDF (accessed on March 24, 2012)

226. Valdes JJ, Cameron JE, Cole RJ (1985) Aflatrem: A Tremorgenic Mycotoxin with Acute Neurotoxic Effects. Environ Health Perspect 62:459

227. Qadeer G (2008) Synthesis, Characterization and Biological Activities of Isocoumarins, Triazoles, Thiodiazoles and Indolinones. Dissertation, Department of Chemistry, Quaid-i-Azam University, Islamabad, Pakistan, p 2: http://prr.hec.gov.pk/Thesis/641S.pdf (accessed on April 4, 2012)

228. Imhoff JF, Labes A, Wiese J (2011) Bio-mining the Microbial Treasures of the Ocean: New Natural Products. Biotechnology Advances 29:468

229. Jaenicke L, Marner FJ (1990) The Irons and Their Origin. Pure Appl Chem 62:1365

230. Tiemann F, Kruger P (1895) Zum Nachweis von Ionon und Iron. Ber Dt Chem Ges 28:1754

231. Hansen MR, Hurley MH (1996) Pluramycins. Old Drugs Having Modern Friends in Structural Biology. Acc Chem Res 29:249

232. Wenger RM (1985) Synthese von Cyclosporin und Analoga: Zusammenhang zwischen Struktur und Immunsuppressiver Aktivität. Angew Chem 97:88

233. Miller W, Plöchl J (1893) Über Amidoxylsäuren. Ber dtsch chem Ges 26:1545

234. Petitou M, van Boeckel CAA (2004) Ein synthetisches Antithrombin III bindendes Pentasaccharid ist jetzt ein Wirkstoff! Was kommt danach? Angew Chem 116:3180

235. Hoberg E (1999) Phytochemical and Analytical Investigations of *Vitex agnus-castus* L., Dissertation, ETH Zürich

236. Fischer NH (1999) Prof. Dr. *Lydia Rodríguez-Hahn* (1932 – 1998). Rev Soc Quím México 43:79

237. Clark RF, Williams SR, Nordt SP, Manoguerra AS (1999) A Review of Selected Seafood Poisonings. Undersea Hyperb Med 26:175

238. Allison AC, Cacabelos R, Lombardi VR, Alvarez XA, Vigo C (2001) Celastrol, a Potent Antioxidant and Anti-inflammatory Drug, as a Possible Treatment for *Alzheimer*'s Disease. Prog Neuropsychopharmacol Biol Psychiat. Oct 25:1341

239. Grove JF (1988) Non-Macrocyclic Trichothecenes, Part 1. Nat Prod Rep 5:187

240. Pettit GR, Kamano Y, Herald CL, Tuinman AA, Boettner FE, Kizu H, Schmidt JM, Baczynskyj L, Tomer KB, Bontems RJ (1987) The Isolation and Structure of a Remarkable Marine Animal Antineoplastic Constituent: Dolastatin-10. J Am Chem Soc 109:6883

241. Vaishampayan U, Glode M, Du W, Kraft A, Hudes G, Wright J, Hussain M (2000) Phase II Study of Dolastatin-10 in Patients with Hormone-refractory Metastatic Prostate Adenocarcinoma. Clin Cancer Res 6:4205

242. Morris J (2010) *Douglas Eric Arthur Rivett* (27 June, 1921 – 25 January, 2010) The South African Chemical Institute. Promoting Chemistry, Chemists, the Chemical Industry and Chemical Education in South Africa: http://www.saci.co.za/obituaries.html (accessed on January 2, 2012)

243. Kopecky KR (2005) *William Alfred Ayer* (1932 – 2005): http://www.rsc.ca/documents/AyerWilliamAElectedin197919322005.pdf (accessed on January 2, 2012)

244. Mitchell JW, Mandava N, Worley JF, Plimmer JR, Smith MV (1970) Brassins - a New Family of Plant Hormones from Rape Pollen. Nature 225:1065

245. Grove MD, Spencer GF, Rohwedder WK, Mandava N, Worley JF, Warthen JD, Steffens GL, Flippen-Anderson JL (1979) Brassinolide, a Plant Growth-promoting Steroid Isolated from *Brassica napus* Pollen. Nature 281:216

246. Bolton B, Alpert G, Ward PS, Naskrecki P (2007) Jean-Claude Braekman. *Bolton*'s Catalogue of the Ants of the World. Harvard University Press: http://gap.entclub.org/taxonomists/Braekman/index.html (accessed on January 3, 2012)

247. Weissensteiner W, Widhalm M (2009) Die Fakultät für Chemie trauert um *Otmar Hofer*. Archiv der online-Zeitung der Universität Wien: http://www.dieuniversitaet-online.at/perso-

nalia/beitrag/news/in-memoriam-otmar-hofer-1942-2009/308/neste/1.html (accessed on January 2, 2012)
248. Stephenson F (2002) A Tale of Taxol. Florida State University Office of Research: http://www.rinr.fsu.edu/fall2002/taxol.html (accessed on March 30, 2012)
249. Hirrle B (2009) Neu zugelassenes Chemotherapeutikum durchbricht Resistenzen. Onkologie 4:36
250. Boullay PFG (1812) Analyse chimique de la Coque du Levant, *Menispermum cocculus*. Bull Pharm 4:1
251. Gmelin L, Tiedemann F (1826) Die Verdauung nach Versuchen, Vol 1, p 80. Karl Groos, Heidelberg, Leipzig
252. Fischer H, Plieninger, H (1942) Synthese des Biliverdins (Uteroverdin) und Bilirubins, der Biliverdine XIIIa und IIIa sowie der Vinylneoxanthosäure. Z physiol Chem 274:231
253. Garfield E. (1982) A Tribute to *Carl Djerassi*: Reflections on a Remarkable Scientific Entrepreneur. Essays of an Information Scientist 5:721; Current Contents 42:5 — http://www.garfield.library.upenn.edu/essays/v5p721y1981-82.pdf (accessed on April 16, 2012)
254. Djerassi C (1995) Natural Product Structure Elucidation: 1950 – 2000, in: Fleischhacker W, Schönfeld T (1995) Pioneering Ideas for the Physical and Chemical Sciences. *Josef Loschmidt*'s Contributions and Modern Developments in Structural Organic Chemistry, Atomistics, and Statistical Mechanics, p 16. Plenum Press, New York and London
255. Djerassi C (1975) Natural Products Chemistry 1950 - 1980: A Personal View. Pure Appl Chem 41:113
256. Gribble GW (1992) Naturally Occurring Halogen Compounds - A Survey. J Nat Prod 55:1353

References to the Volumes of the Series

Z1. Zemplén G (1938) New Directions in Glycoside Synthesis. Prog Chem Org Nat Prod 1:1
Z2. Hilditch TP (1938) The Component Glycerides of Vegetable Fats. Prog Chem Org Nat Prod 1:24
Z3. Heilbron IM, Spring FS (1938) Recent Advances in the Chemistry of the Sterols. Prog Chem Org Nat Prod 1:53
Z4. Schlenk F, von Euler-Chelpin H (1938) Cozymase. Prog Chem Org Nat Prod 1:99
Z5. Bredereck H (1938) Nucleinsäuren. Prog Chem Org Nat Prod 1:121
Z6. Stoll A, Wiedemann E (1938) Chlorophyll. Prog Chem Org Nat Prod 1:159
Z7. Kratky O, Mark H (1938) Anwendung physikalischer Methoden zur Erforschung von Naturstoffen: Form und Größe dispergierter Moleküle. Röntgenographie. Prog Chem Org Nat Prod 1:255
Z8. Freudenberg K (1939) Lignin. Prog Chem Org Nat Prod 2:1
Z9. Asahina Y (1939) Flechtenstoffe. Prog Chem Org Nat Prod 2:27
Z10. Rudy H (1939) Flavins. Prog Chem Org Nat Prod 2:61
Z11. Harington CR (1939) Chemistry of the Iodine Compounds of the Thyroid. Prog Chem Org Nat Prod 2:103
Z12. Hirst EL (1939) The Structure and Synthesis of Vitamin C. Prog Chem Org Nat Prod 2:132
Z13. Zemplén G (1939) Neuere Richtungen der Oligosaccharid-Synthese. Prog Chem Org Nat Prod 2:160
Z14. Zechmeister L, Tóth G (1939) Chitin und seine Spaltprodukte. Prog Chem Org Nat Prod 2:212
Z15. Dhéré C (1939) La Spectrochimie de Fluorescence dans l’Etude des Produits Biologiques. Prog Chem Org Nat Prod 2:301
Z16. Späth E, Kuffner F (1939) Tobacco Alkaloids. Prog Chem Org Nat Prod 2:248
Z17. Diels O (1939) Bedeutung der Dien-Synthese für Bildung, Aufbau und Erforschung der Naturstoffe. Prog Chem Org Nat Prod 3:1
Z18. Fischer FG (1939) Biochemische Hydrierungen. Prog Chem Org Nat Prod 3:30
Z19. Siedel W (1939) Gallenfarbstoffe. Prog Chem Org Nat Prod 3:81
Z20. Anderson RJ (1939) The Chemistry of the Lipoids of the Tubercle Bacillus and Certain Other Microorganisms. Prog Chem Org Nat Prod 3:145
Z21. Pauling L (1939) Recent Work on the Configuration and Eletronic Structure of Molecules with Some Applications to Natural Products. Prog Chem Org Nat Prod 3:203
Z22. Tschesche R (1945) The Chemistry of Plant Cardiac Glycosides, Toad Venoms, Saponins and Sterol Alkaloids. Prog Chem Org Nat Prod 4:1
Z23. Wieland T, Löw I (1945) On the Biochemistry of the Vitamin B Group. Prog Chem Org Nat Prod 4:28
Z24. Purrmann R (1945) Pterine. Prog Chem Org Nat Prod 4:64
Z25. Schramm G (1945) The Biochemistry of Viruses. Prog Chem Org Nat Prod 4:87
Z26. Bernhard K, Lincke H (1945) Biologische Oxidationen. Prog Chem Org Nat Prod 4:188
Z27. Trurnit HJ (1945) On Monomolecular Films at Water Interfaces and Laminated Films. Prog Chem Org Nat Prod 4:347
Z28. Karrer P (1948) Carotinoidepoxide und -furanoide Oxyde von Carotinoidfarbstoffen. Prog Chem Org Nat Prod 5:1
Z29. Fox DL (1948) Some Biochemical Aspects of Marine Carotenoids. Prog Chem Org Nat Prod 5:20
Z30. Haagen-Smit AJ (1948) Azulenes. Prog Chem Org Nat Prod 5:40
Z31. Hilditch TP (1948) Recent Advances in the Study of Component Acids and Component Glycerides of Natural Fats. Prog Chem Org Nat Prod 5:72
Z32. Hassid WZ, Doudoroff M (1948) Enzymatically Synthesized Polysaccharides and Disaccharides. Prog Chem Org Nat Prod 5:101

Z33. Pacsu E (1948) Recent Developments in the Structural Problem of Cellulose. Prog Chem Org Nat Prod 5:128
Z34. Brauns FE (1948) Lignin. Prog Chem Org Nat Prod 5:175
Z35. Deulofeu V (1948) The Chemistry of the Constituents of Toad Venoms. Prog Chem Org Nat Prod 5:241
Z36. Geiger E (1948) Biochemistry of Fish Proteins. Prog Chem Org Nat Prod 5:267
Z37. Beadle GW (1948) Some Recent Developments in Chemical Genetics. Prog Chem Org Nat Prod 5:300
Z38. Rasmussen RS (1948) Infrared Spectroscopy in Structure Determination and its Application to Penicillin. Prog Chem Org Nat Prod 5:131
Z39. Deuel J, Greenberg SM (1950) Some Biochemical and Nutritional Aspects in Fat Chemistry. Prog Chem Org Nat Prod 6:1
Z40. Lederer E (1950) Odeurs et Parfums des Animaux. Prog Chem Org Nat Prod 6:87
Z41. Hoffmann-Ostenhof O (1950) Vorkommen und biochemisches Verhalten der Chinone. Prog Chem Org Nat Prod 6:154
Z42. Reti L (1950) Cactus Alkaloids and Some Related Compounds. Prog Chem Org Nat Prod 6:242
Z43. Bonner JF (1950) Plant Proteins. Prog Chem Org Nat Prod 6:290
Z44. Dhére C (1950) Progrès Récents en Spectrochimie de Fluorescence des Produits Biologiques. Prog Chem Org Nat Prod 6:311
Z45. Jeger O (1950) Über die Konstitution der Triterpene. Prog Chem Org Nat Prod 7:1
Z46. Heusser H (1950) Konstitution, Konfiguration und Synthese Digitaloider Aglykone und Glycoside. Prog Chem Org Nat Prod 7:87
Z47. Niemann CG (1950) Thyroxine and Related Compounds. Prog Chem Org Nat Prod 7:167
Z48. Cook AH (1950) Penicillin and its Place in Science. Prog Chem Org Nat Prod 7:193
Z49. Stoll A, Becker B (1950) Sennosides A and B, the Active Principles of Senna. Prog Chem Org Nat Prod 7:248
Z50. Williams JW (1950) Some Recent Developments in the Chemistry of Antibodies. Prog Chem Org Nat Prod 7:270
Z51. Frey-Wyssling A, Mühlethaler K (1951) Fine Structure of Cellulose. Prog Chem Org Nat Prod 8:1
Z52. Stacey M, Ricketts CR (1951) Bacterial Dextrans. Prog Chem Org Nat Prod 8:28
Z53. Leloir F (1951) Sugar Phosphates. Prog Chem Org Nat Prod 8:47
Z54. Kenner GW (1951) The Chemistry of Nucleotides. Prog Chem Org Nat Prod 8:96
Z55. Schinz H (1951) Die Veilchenriechstoffe. Prog Chem Org Nat Prod 8:146
Z56. Asahina Y (1951) New Developments in the Field of Lichen Substances. Prog Chem Org Nat Prod 8:207
Z57. Galinovsky F (1951) Lupinen-Alkaloide und Verwandte Verbindungen. Prog Chem Org Nat Prod 8:245
Z58. Pailer M (1951) Brechwurzel-Alkaloide. Prog Chem Org Nat Prod 8:278
Z59. Corey B (1951) X-Ray Diffraction Studies on Cristalline Amino Acids and Peptides. Prog Chem Org Nat Prod 8:310
Z60. Zechmeister L, Rohdewald M (1951) Some Aspects of Enzyme Chromatography. Prog Chem Org Nat Prod 8:341
Z61. Inhoffen HH, Siemer H (1952) Synthetic Chemistry of Carotenoids. Prog Chem Org Nat Prod 9:1
Z62. Baxter JG (1952) Synthesis and Properties of Vitamin A and Related Compounds. Prog Chem Org Nat Prod 9:41
Z63. Meunier P (1952) Les Antivitamines. Prog Chem Org Nat Prod 9:88
Z64. Stoll A (1952) Recent Investigations on Ergot Alkaloids. Prog Chem Org Nat Prod 9:114
Z65. Tomita M (1952) Alkaloide der Menispermaceae-Pflanzen. Prog Chem Org Nat Prod 9:175
Z66. Dean FM (1952) Naturally Occurring Coumarins. Prog Chem Org Nat Prod 9:225
Z67. Borsook H (1952) Biosynthesis of Proteins and Peptides, including Isotopic Tracer Studies. Prog Chem Org Nat Prod 9:292

Z68. Kalckar HM (1952). The Enzymes of Nucleoside Metabolism. Prog Chem Org Nat Prod 9:363
Z69. McNutt WS (1952) Nucleosides and Nucleotides as Growth Substances for Microorganisms. Prog Chem Org Nat Prod 9:401
Z70. Campbell DH, Bulman N (1952) Some Current Concepts of the Chemical Nature of Antigens and Antibodies. Prog Chem Org Nat Prod 9:443
Z71. Alder K, Schumacher, M (1953) Anwendungen der Dien-Synthese für die Erforschung von Naturstoffen. Prog Chem Org Nat Prod 10:1
Z72. Mark H (1953) Physical Chemistry of Rubbers. Prog Chem Org Nat Prod 10:119
Z73. Asselineau J, Lederer E (1953) Chimie des Lipides Bactériens. Prog Chem Org Nat Prod 10:170
Z74. Rosenkranz G, Sondheimer F (1953) Synthesis of Cortisone. Prog Chem Org Nat Prod 10:274
Z75. Chatterjee A (1953) *Rauwolfia* Alkaloids. Prog Chem Org Nat Prod 10:390
Z76. Feinstein L, Jacobson M (1953) Insecticides Occurring in Higher Plants. Prog Chem Org Nat Prod 10:423
Z77. Peat S (1954) Starch: Its Constitution, Enzymatic Synthesis, and Degradation. Prog Chem Org Nat Prod 11:1
Z78. Freudenberg K (1954) Neuere Ergebnisse auf dem Gebiete des Lignins und der Verholzung. Prog Chem Org Nat Prod 11:43
Z79. Inhoffen HH, Brückner K (1954) Probleme und neuere Ergebnisse in der Vitamin D-Chemie. Prog Chem Org Nat Prod 11:83
Z80. Schmid HE (1954) Natürlich vorkommende Chromone. Prog Chem Org Nat Prod 11:124
Z81. Pauling L, Corey RB (1954) The Configuration of Polypeptide Chains in Proteins. Prog Chem Org Nat Prod 11:180
Z82. Schroeder WA (1954) Column Chromatography in the Study of the Structure of Peptides and Proteins. Prog Chem Org Nat Prod 11:240
Z83. Lemberg MR (1954) Porphyrins in Nature. Prog Chem Org Nat Prod 11:299
Z84. Albert A (1954) The Pteridines. Prog Chem Org Nat Prod 11:350
Z85. Haagen-Smit AJ (1955) Sesquiterpenes and Diterpenes. Prog Chem Org Nat Prod 12:1
Z86. Jones ERH, Halsall TG (1955) Tetracyclic Triterpenes. Prog Chem Org Nat Prod 12:44
Z87. Tschesche R (1955) Neuere Vorstellungen auf dem Gebiete der Biosynthese der Steroide und Verwandter Naturstoffe. Prog Chem Org Nat Prod 12:131
Z88. Haxo FT (1955) Some Biochemical Aspects of Fungal Carotenoids. Prog Chem Org Nat Prod 12:169
Z89. Warren FL (1955) The Pyrrolizidine Alkaloids. Prog Chem Org Nat Prod 12:198
Z90. Thompson EOP, Thompson AR (1955) Paper Chromatography in the Study of the Structure of Peptides and Proteins. Prog Chem Org Nat Prod 12:270
Z91. Roche J, Michel R (1955) Acides Aminés Iodés et Iodoprotéines. Prog Chem Org Nat Prod 12:349
Z92. Slotta KH (1955) Chemistry and Biochemistry of Snake Venoms. Prog Chem Org Nat Prod 12:406
Z93. Beadle GW (1955) Gene Structure and Gene Action. Prog Chem Org Nat Prod 12:466
Z94. Cole ARH (1956) Infrared Spectra of Natural Products. Prog Chem Org Nat Prod 13:1
Z95. Schmidt OT (1956) Gallotannine und Ellagengerbstoffe. Prog Chem Org Nat Prod 13:70
Z96. Tamm C (1956) Neuere Ergebnisse auf dem Gebiet der glykosidischen Herzgifte: Grundlagen und Aglykone. Prog Chem Org Nat Prod 13:137
Z97. Nozoe T (1956) Natural Tropolones and Some Related Troponoids. Prog Chem Org Nat Prod 13:232
Z98. Price JR (1956) Alkaloids Related to Anthranilic Acid. Prog Chem Org Nat Prod 13:302
Z99. Chatterjee A, Pakrashi SC, Werner G (1956) Recent Developments in the Chemistry and Pharmacology of *Rauwolfia* Alkaloids. Prog Chem Org Nat Prod 13:346
Z100. Grassmann W, Wünsch E (1956) Synthese von Petiden. Prog Chem Org Nat Prod 13:444

Z101. Bohlmann F, Mannhardt HJ (1957) Acetylenverbindungen im Pflanzenreich. Prog Chem Org Nat Prod 14:1
Z102. Tamm C (1957) Neuere Ergebnisse auf dem Gebiet der Glykosidischen Herzgifte: Zucker und Glykoside. Prog Chem Org Nat Prod 14:71
Z103. Brockmann H (1957) Photodynamisch wirksame Pflanzenfarbstoffe. Prog Chem Org Nat Prod 14:141
Z104. Birch AJ (1957) Biosynthetic Relations of Some Natural Phenolic and Enolic Compounds. Prog Chem Org Nat Prod 14:186
Z105. Sobotka H, Barsel N, Chanley JD (1957) The Aminochromes. Prog Chem Org Nat Prod 14:217
Z106. Morton RA, Pitt GAJ (1957) Visual Pigments. Prog Chem Org Nat Prod 14:244
Z107. Brown H (1957) The Carbon Cycle in Nature. Prog Chem Org Nat Prod 14:317
Z108. Schlubach HH (1958) Der Kohlenhydratstoffwechsel der Gräser. Prog Chem Org Nat Prod 15:1
Z109. Zechmeister L (1958) Some *in vitro* Conversations of Naturally Occurring Carotenoids. Prog Chem Org Nat Prod 15:31
Z110. Hartwell JL, Schrecker AW (1958) The Chemistry of *Podophyllum*. Prog Chem Org Nat Prod 15:83
Z111. Crowfoot Hodgkin D (1958) X-ray Analysis and the Structure of Vitamin B_{12}. Prog Chem Org Nat Prod 15:167
Z112. Freudenberg K, Weinges K *(1959)* Catechine, andere Hydroxy-flavane und Hydroxy-flavene. Prog Chem Org Nat Prod 16:1
Z113. Wiesner K, Valenta Z (1959) Recent Progress in the Chemistry of the Aconite-Garraya Alkaloids. Prog Chem Org Nat Prod 16:26
Z114. van Tamelen EE (1959) Structural Chemistry of Actinomycetes Antibiotics. Prog Chem Org Nat Prod 16:90
Z115. Bonner JF (1959) Protein Synthesis in Plants. Chem Org Nat Prod 16:139
Z116. Kuhn HW (1959) The Electron Gas Theory of the Color of Natural and Artificial Dyes: Problems and Principles. Prog Chem Org Nat Prod 16:169
Z117. Venkataraman K (1959) Flavones and Isoflavones. Prog Chem Org Nat Prod 17:1
Z118. Inhoffen HH, Irmscher K (1959) Fortschritte der Chemie der Vitamine D und ihrer Abkömmlinge. Prog Chem Org Nat Prod 17:70
Z119. Korte F, Barkemeyer H, Korte I (1959) Neuere Ergebnisse der Chemie pflanzlicher Bitterstoffe. Prog Chem Org Nat Prod 17:124
Z120. Bernauer K (1959) Alkaloide aus Calebassencurare und südamerikanischen Strychnosarten. Prog Chem Org Nat Prod 17:183
Z121. Stowe BB (1959) Occurrence and Metabolism of Simple Indoles in Plants. Prog Chem Org Nat Prod 17:248
Z122. Dimond AE (1959) Some Biochemical Aspects of Disease in Plants. Prog Chem Org Nat Prod 17:298
Z123. Schroeder WA (1959) The Chemical Structure of the Normal Human Hemoglobins. Prog Chem Org Nat Prod 17:322
Z124. Abelson PH (1959) Paleobiochemistry and Organic Geochemistry. Prog Org Nat Prod 17:379
Z125. Kuhn H (1959) The Electron Gas Theory of Colour of Natural and Artificial Dyes: Applications and Extensions. Prog Chem Org Nat Prod 17:404
Z126. Brockmann H (1960) Die Actinomycine. Prog Chem Org Nat Prod 18:1
Z127. Pailer M (1960) Natürlich vorkommende Nitroverbindungen. Prog Chem Org Nat Prod 18:55
Z128. Van Thoai N, Roche J (1960) Dérivés Guanidiques Biologiques. Prog Chem Org Nat Prod 18:83
Z129. Kjaer A (1960) Naturally Derived Isothiocyanates (Mustard Oil) and Their Parent Glucosides. Prog Chem Org Nat Prod 18:122

Z130. Völker O (1960) Die Farbstoffe im Gefieder der Vögel. Prog Chem Org Nat Prod 18:177
Z131. Zechmeister L (1960) *cis-trans* Isomeric Carotenoid Pigments. Prog Chem Org Nat Prod 18:223
Z132. Brian PW, Grove JF, MacMillan J (1960) The Gibberellins. Prog Chem Org Nat Prod 18:350
Z133. Williams JW (1960) Selected Subjects in Sedimentation Analysis, with Some Applications to Biochemistry. Prog Chem Org Nat Prod 18:434
Z134. Heidelberger M (1960) Structure and Immunological Specificity of Polysaccharides. Prog Chem Org Nat Prod 18:503
Z135. Šorm F (1961) Medium-ring Terpenes. Prog Chem Org Nat Prod 19:1
Z136. Nozoe T, Itô S (1961) Recent Advances in the Chemistry of Azulenes and Natural Hydroazulenes. Prog Chem Org Nat Prod 19:32
Z137. Crombie L, Elliott M (1961) Chemistry of the Natural Pyrethrins. Prog Chem Org Nat Prod 19:120
Z138. Barton DHR, Morrison GA (1961) Conformational Analyses of Steroids and Related Natural Products. Prog Chem Org Nat Prod 19:165
Z139. van Tamelen EE (1961) Biogenetic-type Syntheses of Natural Products. Prog Chem Org Nat Prod 19:242
Z140. Schlubach HH (1961) Kohlenhydratstoffwechsel in Roggen und Weizen. Prog Chem Org Nat Prod 19:291
Z141. Courtois JE, Lino A (1961) Les Phosphatases de Végétaux Supérieurs: Répartition et Action. Prog Chem Org Nat Prod 19:316
Z142. Birkinshaw JH, Stickings CE (1962) Nitrogen-containing Metabolites of Fungi. Prog Chem Org Nat Prod 20:1
Z143. Freudenberg K (1962) Forschungen am Lignin. Prog Chem Org Nat Prod 20:41
Z174. Schindler O (1962) Die Ubichinone (Coenzyme Q). Prog Chem Org Nat Prod 20:73
Z145. Mors WB, Magalháes MT Gottlieb OR (1962) Natural Occurring Aromatic Derivatives of Monocyclic α-Pyrones. Prog Chem Org Nat Prod 20:131
Z146. Harborne JB (1962) Anthocyanins and their Sugar Components. Prog Chem Org Nat Prod 20:165
Z147. Baschang G (1962) Aminozucker, Synthesen und Vorkommen in Naturstoffen. Prog Chem Org Nat Prod 20:200
Z148. Wiesner K (1962) Structure and Stereochemistry of the *Lycopodium* Alkaloids. Prog Chem Org Nat Prod 20:271
Z149. Narayanan CR (1962) Newer Developments in the Field of *Veratrum* Alkaloids. Prog Chem Org Nat Prod 20:298
Z150. Vinograd J, Hearst JE (1962) Equilibrium Sedimentation of Macromolecules and Viruses in a Density Gradient. Prog Chem Org Nat Prod 20:372
Z151. Horowitz NH, Miller SL (1962) Current Theories on the Origin of Life. Prog Chem Org Nat Prod 20:423
Z152. Bonner J (1963) The Biosynthesis of Rubber. Prog Chem Org Nat Prod 21:1
Z153. Oroshnik W, Mebane AD (1963) The Polyene Antifungal Antibiotics. Prog Chem Org Nat Prod 21:17
Z154. Muxfeldt H, Bangert R (1963) Die Chemie der Tetracycline. Prog Chem Org Nat Prod 21:80
Z155. Brockmann H (1963) Anthracyclinone und Anthracycline. Prog Chem Org Nat Prod 21:121
Z156. Jaenicke L, Kutzbach C (1963) Folsäure und Folat-Enzyme. Prog Chem Org Nat Prod 21:183
Z157. Crombie L (1963) Chemistry of the Natural Rotenoids. Prog Chem Org Nat Prod 21:275
Z158. Schaffner K (1964) Photochemische Umwandlungen ausgewählter Naturstoffe. Prog Chem Org Nat Prod 22:1
Z159. Billek G (1964) Stilbene im Pflanzenreich. Chem Org Nat Prod 22:115
Z160. Halsall TG, Aplin RT (1964) A Pattern of Development in the Chemistry of Pentacyclic Triterpenes. Prog Chem Org Nat Prod 22:153

Z161. Grove JF (1964) Griseofulvin and Some Analogues. Prog Chem Org Nat Prod 22:203
Z162. Scheuer PJ (1964) The Chemistry of Toxins Isolated from Some Marine Organisms. Prog Chem Org Nat Prod 22:265
Z163. Keller-Schierlein W, Prelog V, Zähner H (1964) Siderochrome. Natürliche Eisen(III)-trihydroxamat-Komplexe. Prog Chem Org Nat Prod 22:279
Z164. Peat S, Turvey JR (1965) Polysaccharides of Marine Algae. Prog Chem Org Nat Prod 23:1
Z165. Schlubach HH (1965) Kohlenhydratstoffwechsel in Gerste, Hafer und Rispenhirse. Prog Chem Org Nat Prod 23:46
Z166. Schlenk F (1965) The Chemistry of Biological Sulfonium Compounds. Prog Chem Org Nat Prod 23:61
Z167. Schroeder WA, Jones RT (1965) Some Aspects of the Chemistry and Function of Human and Animal Hemoglobins. Prog Chem Org Nat Prod 23:113
Z168. Grassmann W, Engel J, Hannig K, Hörmann H, Kühn K, Nordwig A (1965) Kollagen. Prog Chem Org Nat Prod 23:195
Z169. Jackman LM (1965) Some Applications of Nuclear Magnetic Resonance Spectroscopy in Natural Product Chemistry. Prog Chem Org Nat Prod 23:315
Z170. Biemann K (1966) Mass Spectroscopy of Selected Natural Products. Prog Chem Org Nat Prod 24:1
Z171. Tschesche R (1966) Pflanzliche Steroide mit 21 Kohlenstoffatomen. Prog Chem Org Nat Prod 24:99
Z172. Hoffmann-Ostenhof O, Kindl, H (1966) Cyclite: Biosynthese, Stoffwechsel und Vorkommen Prog Chem Org Nat Prod 24:149
Z173. Erdtman H, Norin T (1966) The Chemistry of the Order Cupressales. Prog Chem Org Nat Prod 24:206
Z174. Turner AB (1966) Quinone Methides in Nature. Prog Chem Org Nat Prod 24:288
Z175. Warren FL (1966) The Pyrrolizidine Alkaloids II. Prog Chem Org Nat Prod 24:329
Z176. Fraenkel-Conrat H (1966) Some Aspects of Virus Chemistry. Prog Chem Org Nat Prod 24:407
Z177. Bohlmann F (1967) Biogenetische Beziehungen der natürlichen Acetylenverbindung. Prog Chem Org Nat Prod 25:1
Z178. Ashurst PR (1967) The Chemistry of the Hop Resin. Prog Chem Org Nat Prod 25:63
Z179. Romo J, Romo de Vivar AR (1967) The Pseudoguaianolides. Prog Chem Org Nat Prod 25:90
Z180. Sutherland JK (1967) The Nonadrides. Prog Chem Org Nat Prod 25:131
Z181. Farkas L, Pallos L (1967) Natürlich Vorkommende Auronglykoside. Prog Chem Org Nat Prod 25:150
Z182. Mechoulam R, Gaoni Y (1967) Recent Advances in the Chemistry of Hashish. Prog Chem Org Nat Prod 25:175
Z183. Wieland T (1967) Toxic Peptides of *Amanita phalloides*. Prog Chem Org Nat Prod 25:214
Z184. Waldschmidt-Leitz E, Kling H (1967) Die Prolamine. Prog Chem Org Nat Prod 25:251
Z185. Morrison GA (1967) Conformational Analysis of Some Alkaloids. Prog Chem Org Nat Prod 25:269
Z186. Corey RB, Marsh RE (1968) X-Ray Diffraction Studies of Crystalline Amino Acids, Peptides and Proteins. Prog Chem Org Nat Prod 26:1
Z187. Schröder E, Lübke K (1968) Synthese von Peptiden und Peptidwirkstoffen. Prog Chem Org Nat Prod 26:48
Z188. Trakatellis AC, Schwartz GP (1968) Insulin, Structure, Synthesis and Biosynthesis of the Hormone. Prog Chem Org Nat Prod 26:120
Z189. Keller-Schierlein W, Gerlach H (1968) Makrotetrolide. Prog Chem Org Nat Prod 26:161
Z190. Dreyer LD. (1968) Limonoid Bitter Principles. Prog Chem Org Nat Prod 26:190
Z191. Bernauer K, Hofheinz W (1968) Proaporphin-Alkaloide. Prog Chem Org Nat Prod 26:245
Z192. Inhoffen HH, Buchler JW, Jäger P (1968) Chemie der Chlorine und Porphyrine. Prog Chem Org Nat Prod 26:284

Z193. Dütting D (1968) Methoden und Ergebnisse der Sequenzanalyse von Ribonucleinsäuren. Prog Chem Org Nat Prod 26:356
Z194. Frey-Wyssling A (1969) The Ultrastructure and Biogenesis of Native Cellulose. Prog Chem Org Nat Prod 27:1
Z195. Spencer M (1969) Ethylene in Nature. Prog Chem Org Nat Prod 27:31
Z196. Weedon BCL (1969) Spectroscopic Methods for Elucidating the Structures of Carotenoids. Prog Chem Org Nat Prod 27:81
Z197. Sanders GM, Pot J, Havinga, E (1969) Some Recent Results in the Chemistry and Stereochemistry of Vitamin D and Its Isomers. Prog Chem Org Nat Prod 27:131
Z198. Weinges K, Bähr W, Ebert W, Göritz K, Marx HD (1969) Konstitution, Entstehung und Bedeutung der Flavenoid-Gerbstoffe. Prog Chem Org Nat Prod 27:158
Z199. Eugster CH (1969) Chemie der Wirkstoffe aus dem Fliegenpilz (*Amanita muscaria*). Prog Chem Org Nat Prod 27:261
Z200. Scheuer PJ (1969) The Chemistry of Some Toxins Isolated from Marine Organisms. Chem Org Nat Prod 27:322
Z201. Raftery MA, Dahlquist FW (1969) The Chemistry of Lysozyme. Org Nat Prod 27:340
Z202. Wong E (1970) Structural and Biogenetic Relationships of Isoflavonoids. Prog Chem Org Nat Prod 28:1
Z203. Eyjólfsson R (1970) Recent Advances in the Chemistry of Cyanogenic Glycosides. Prog Chem Org Nat Prod 28:74
Z204. Gross D (1970) Naturstoffe mit Pyridinstruktur und ihre Biosynthese. Prog Chem Org Nat Prod 28:109
Z205. Warnhoff EW (1970) Peptide Alkaloids. Prog Chem Org Nat Prod 28:162
Z206. Eiter K (1970) Insektensexuallockstoffe. Prog Chem Org Nat Prod 28:204
Z207. Hikino H, Hikino Y (1970) Arthropod Molting Hormones. Prog Chem Org Nat Prod 28:256
Z208. Pike JE (1970) Total Synthesis of Prostaglandins. Prog Chem Org Nat Prod 28:313
Z209. Morin RB, Jackson BG (1970) Chemistry of Cephalosporin Antibiotics. Prog Chem Org Nat Prod 28:343
Z210. Wiegandt H, Egge H (1970) Oligosaccharide der Frauenmilch. Prog Chem Org Nat Prod 28:404
Z211. Bromer W (1970) Glucagon: Chemistry and Action. Prog Chem Org Nat Prod 28:429
Z212. Gross D (1971) Struktur und Biosynthese natürlicher Piperidinverbindungen. Prog Chem Org Nat Prod 29:1
Z213. Johnson F (1971) The Chemistry of Glutarimide Antibiotics. Prog Chem Org Nat Prod 29:140
Z214. Huneck S (1971) Chemie und Biosynthese der Flechtenstoffe. Prog Chem Org Nat Prod 29: 209
Z215. Goldsmith D (1971) Biogenetic-type Synthesis of Terpenoid Systems. Prog Chem Org Nat Prod 29:363
Z216. Lavie D, Glotter E (1971) The Cucurbitanes, a Group of Tetracyclic Triterpenes. Prog Chem Org Nat Prod 29:307
Z217. Hanson RJ (1971) The Biosynthesis of the Diterpenes. Prog Chem Org Nat Prod 29:395
Z218. Premuzic W (1971) Chemistry of Natural Products Derived from Marine Sources. Prog Chem Org Nat Prod 29:417
Z219. Cormier MJ, Wampler JE, Hori K (1973) Bioluminiscence: Chemical Aspects. Prog Chem Org Nat Prod 30:1
Z220. Jaenicke L, Müller DG (1973) Gametenlockstoffe bei niederen Pflanzen und Tieren. Prog Chem Org Nat Prod 30:61
Z221. Polonsky J (1973) Quassinoid Bitter Principles. Prog Chem Org Nat Prod 30:101
Z222. Franck B, Flasch H (1973) Die Ergochrome. Prog Chem Org Nat Prod 30:151
Z223. Locksley HD (1973) The Chemistry of Biflavonoid Compounds. Prog Chem Org Nat Prod 30:207
Z224. Keller-Schierlein W (1973) Chemie der Makrolid-Antibiotica. Prog Chem Org Nat Prod 30:313

Z225. Tschesche R, Wulff G (1973) Chemie und Biologie der Saponine. Prog Chem Org Nat Prod 30:461
Z226. McGregor DN (1974) Recent Developments in the Chemistry of Penicillins. Prog Chem Org Nat Prod 31:1
Z227. Tamm C (1974) The Antibiotic Complex of the Verrucarins and Roridins. Prog Chem Org Nat Prod 31:63
Z228. Roberts JC (1974) Aflatoxins and Sterigmatocystins. Prog Chem Org Nat Prod 31:119
Z229. Wagner H (1974) Flavonoid-Glykoside. Prog Chem Org Nat Prod 31:153
Z230. Harris TH, Harris CM, Hindley KB (1974) Biogenetic-Type Synthesis of Polyketide Metabolites. Prog Chem Org Nat Prod 31:217
Z231. Marshall JA, Brady SF Andersen NH (1974) The Chemistry of Spiro[4.5]decane Sesquiterpenes. Prog Chem Org Nat Prod 31:283
Z232. Hecker E, Schmidt R (1974) Phorbolesters – the Irritants and Cocarcinogens of *Croton tiglium* L. Prog Chem Org Nat Prod 31:377
Z233. Winterfeldt E (1974) Stereoselektive Totalsynthese von Indolalkaloides. Prog Chem Org Nat Prod 31:469
Z234. Swan GA (1974) Structure, Chemistry, and Biosynthesis of the Melanins. Prog Chem Org Nat Prod 31:521
Z235. Schrauzer GN (1974) Mechanisms of Corrin Dependent Enzymatic Reactions. Prog Chem Org Nat Prod 31:583
Z236. Seifert WK (1975) Carboxylic Acids in Petroleum and Sediments. Prog Chem Org Nat Prod 32:1
Z237. Sammes PG (1975) Naturally Occurring 2,5-Dioxopiperazines and Related Compounds. Prog Chem Org Nat Prod 32:51
Z238. Highet RJ, Sokoloski EA (1975) Structural Investigation of Natural Products by Newer Methods of NMR Spectroscopy. Prog Chem Org Nat Prod 32:119
Z239. Scopes PM (1975) Applications of the Chiroptical Techniques to the Study of Natural Products. Prog Chem Org Nat Prod 32:167
Z240. van Hummel HC (1975) Chemistry and Biochemistry of Plant Galactolipids. Prog Chem Org Nat Prod 32:267
Z241. Kössel H, Seliger H (1975) Recent Advances in Polynucleotide Synthesis. Prog Chem Org Nat Prod 32:297
Z242. Minale L, Cimino G, de Stefano S, Sodano G (1976) Natural Products from Porifera. Prog Chem Org Nat Prod 33:1
Z243. Coates RM (1976) Biogenetic-type Rearrangements of Terpenes. Prog Chem Org Nat Prod 33:73
Z244. Rinehart KL Jr, Shield LS (1976) Chemistry of Ansamycin Antibiotics. Prog Chem Org Nat Prod 33:231
Z245. Fontana A, Toniola C (1976) The Chemistry of Tryptophan in Peptides and Proteins. Prog Chem Org Nat Prod 33:309
Z246. Hemmerich P (1976) The Present Status of Flavin and Flavocoenzyme Chemistry. Prog Chem Org Nat Prod 33:451
Z247. Enzell CR, Wahlberg I, Aasen AJ (1977) Isoprenoids and Alkaloids of Tobacco. Prog Chem Org Nat Prod 34:1
Z248. Pinder AR (1977) The Chemistry of the Eremophilane and Related Sesquiterpenes. Prog Chem Org Nat Prod 34:81
Z249. Gross D (1977) Phytoalexine und verwandte Pflanzenstoffe. Prog Chem Org Nat Prod 34:187
Z250. Overton KH, Picken DJ (1977) Studies in Secondary Metabolism with Plant Tissue Cultures. Prog Chem Org Nat Prod 34:249
Z251. Chakraborty DP(1977) Carbazole Alkaloids. Prog Chem Org Nat Prod 34:300
Z252. Jacob J (1977) Bürzeldrüsenlipide. Prog Chem Org Nat Prod 34:373
Z253. Voelter W (1977) Hypothalamus-Rezeptorhormone. Prog Chem Org Nat Prod 34:349
Z254. Gottlieb OR (1978) Neolignans. Prog Chem Org Nat Prod 35:1

Z255. Herrmann K (1978) Hydroxyzimtsäuren und Hydroxybenzoesäuren enthaltende Naturstoffe in Pflanzen. Prog Chem Org Nat Prod 35:73
Z256. Pattenden G (1978) Natural 4-Ylidenebutenolides and 4-Ylidenetetronic Acids. Prog Chem Org Nat Prod 35:133
Z257. Murray RDH (1978) Naturally Occurring Plant Coumarins. Prog Chem Org Nat Prod 35:199
Z258. Ohloff G (1978) Recent Developments in the Fields of Naturally Occurring Aroma Components. Prog Chem Org Nat Prod 35:431
Z259. Wehrli FW, Nishida T (1979) The Use of Carbon-13 Nuclear Magnetic Resonance Spectroscopy in Natural Products Chemistry. Prog Chem Org Nat Prod 36:1
Z260. Ohloff G, Flament I (1979) The Role of Heteroatomic Substances in the Aroma Compounds of Foodstuffs. Prog Chem Org Nat Prod 36:231
Z261. Weinheimer AJ, Chang CWJ, Matson JA (1979) Naturally Occurring Cembranes. Prog Chem Org Nat Prod 36:285
Z262. Brand JM, Young JC, Silverstein RM (1979) Insect Pheromones: A Critical Review of Recent Advances in Their Chemistry, Biology, and Application. Prog Chem Org Nat Prod 37:1
Z263. McNeil M, Darvill AG, Albersheim P (1979) The Structural Polymers of the Primary Cell Walls of Dicots. Prog Chem Org Nat Prod 37:191
Z264. Schmidt U, Häusler J, Öhler E, Poisel H (1979) Dehydroamino Acids, α-Hydroxy-α-amino Acids and α-Mercapto-α-amino Acids. Prog Chem Org Nat Prod 37:251
Z265. Franck RW (1980) The Mitomycin Antibiotics. Prog Chem Org Nat Prod 38:1
Z266. Fischer NH, Olivier EJ, Fischer HD (1980) The Biogenesis and Chemistry of Sesquiterpene Lactones. Prog Chem Org Nat Prod 38:47
Z267. Fraser-Reid B, Anderson RC (1980) Carbohydrate Derivatives in the Asymmetric Synthesis of Natural Products. Prog Chem Org Nat Prod 39:1
Z268. Jones H, Rasmusson GH (1980) Recent Advances in the Biology and Chemistry of Vitamin D. Prog Chem Org Nat Prod 39:63
Z269. Liaaen-Jensen S (1980) Stereochemistry of Naturally Occurring Carotenoids. Prog Chem Org Nat Prod 39:123
Z270. Kasai T, Larsen PO (1980) Chemistry and Biochemistry of γ-Glutamyl Derivatives from Plants Including Mushrooms (Basidiomycetes). Prog Chem Org Nat Prod 39:173
Z271. Lefrancier P, Lederer E (1981) Chemistry of Synthetic Immunomodulant Muramyl Peptides. Prog Chem Org Nat Prod 40:1
Z272. Dev S (1981) The Chemistry of Longifolene and Its Derivatives. Prog Chem Org Nat Prod 40:49
Z273. Heller W, Tamm C (1981) Homoisoflavanones and Biogenetically Related Compounds. Prog Chem Org Nat Prod 40:105
Z274. Cooke RG, Edwards JM (1981) Naturally Occurring Phenalenones and Related Compounds. Prog Chem Org Nat Prod 40:153
Z275. Jefford CW, Cadby PA (1981) Molecular Mechanisms of Enzyme-Catalysed Dioxygenation. Prog Chem Org Nat Prod 40:191
Z276. Haslam E (1982) The Metabolism of Gallic Acid and Hexahydroxydiphenic Acid in Higher Plants. Prog Chem Org Nat Prod 41:1
Z277. Gould J, Weinreb SM (1982) Streptonigrin. Prog Chem Org Nat Prod 41:77
Z278. Robins DJ (1982) The Pyrrolizidine Alkaloids. Prog Chem Org Nat Prod 41:115
Z279. Daly JW (1982) Alkaloids of Neotropical Poison Frogs (Dendrobatidae). Prog Chem Org Nat Prod 41:205
Z280. Askawa Y (1982) Chemical Constituents of Hepaticae. Prog Chem Org Nat Prod 42:1
Z281. Heidelberger M (1982) Cross-Reactions of Plant Polysaccharides in Antipneumococcal and Other Antisera, an Update. Prog Chem Org Nat Prod 42:287
Z282. Ingham JL (1983) Naturally Occurring Isoflavonoids (1855 – 1981). Prog Chem Org Nat Prod 43:1

Z283. Koskinen A, Lounasmaa M (1983) The Sarpagine-Ajmaline Group of Indole Alkaloids. Prog Chem Org Nat Prod 43:267
Z284. Evans FJ, Taylor SE (1983) Pro-Inflammatory, Tumour-Promoting and Anti-Tumour Diterpenes of the Plant Families Euphorbiaceae and Thymelaeaceae. Prog Chem Org Nat Prod 44:1
Z285. Mondon A, Epe B (1983) Bitter Principles of Cneoraceae. Prog Chem Org Nat Prod 44:101
Z286. Naylor S, Hanke FJ, Crews P (1983) Chemical and Biological Aspects of Marine Monoterpenes. Prog Chem Org Nat Prod 44:189
Z287. Buchanan JG (1983) The C-Nucleoside Antibiotics. Prog Chem Org Nat Prod 44:243
Z288. Taylor DAH (1984) The Chemistry of the Limonoids from Meliaceae. Prog Chem Org Nat Prod 45:1
Z289. Elix JA, Whitton AA (1984) Recent Progress in the Chemistry of Lichen Substrates. Prog Chem Org Nat Prod 45:103
Z290. Shimizu Y (1984) Paralytic Shellfish Poisons. Prog Chem Org Nat Prod 45:235
Z291. Tanaka O, Kasai R (1984) Saponins of Ginseng and Related Plants. Prog Chem Org Nat Prod 46:1
Z292. Fujita E. Node M (1984) Diterpenoids of *Rabdosia* Species. Prog Chem Org Nat Prod 46:77
Z293. Johne S (1984) The Quinazoline Alkaloids. Prog Chem Org Nat Prod 46:159
Z294. Southgate R, Elson S (1985) Naturally Occurring β-Lactams. Prog Chem Org Nat Prod 47:1
Z295. Howe I, Jarman M (1985) New Techniques for the Mass Spectrometry of Natural Products. Prog Chem Org Nat Prod 47:107
Z296. McDougal PG, Schmuff NR (1985) Chemical Syntheses of the Trichothecenes. Prog Chem Org Nat Prod 47:153
Z297. Polonsky J (1985) Quassinoid Bitter Principles II. Prog Chem Org Nat Prod 47:221
Z298. Steyn PS, Vleggaar R (1985) Tremorgenic Mycotoxins. Prog Chem Org Nat Prod 48:1
Z299. Moore RE (1985) Structure of Palytoxin. Prog Chem Org Nat Prod 48:81
Z300. Crews P, Naylor S (1985) Sesterterpenes: An Emerging Group of Metabolites from Marine and Terrestrial Organisms. Prog Chem Org Nat Prod 48:203
Z301. Hill RA (1986) Naturally Occurring Isocoumarins. Prog Chem Org Nat Prod 49:1
Z302. Wijnsma R, Verpoorte R (1986) Anthraquinones in the Rubiaceae. Prog Chem Org Nat Prod 49:79
Z303. Krebs HC (1986) Recent Development in the Fields of Marine Natural Products with Emphasis on Biologically Active Compounds. Prog Chem Org Nat Prod 49:151
Z304. Jaenicke L, Marner FJ (1986) The Irones and Their Precursors. Prog Chem Org Nat Prod 50:1
Z305. Lounasmaa M, Somersalo P (1986) The Condylocarpine Group of Indole Alkaloids. Prog Chem Org Nat Prod 50:27
Z306. Séquin U (1986) The Antibiotics of the Pluramycin Group (4*H*-Anthra[1,2-*b*]pyran Antibiotics). Prog Chem Org Nat Prod 50:57
Z307. Wenger RM (1986) Cyclosporine and Analogues – Isolation and Synthesis – Mechanism of Action and Structural Requirements for Pharmacological Activity. Prog Chem Org Nat Prod 50:124
Z308. Inouye H, Uesato S (1986) Biosynthesis of Iridoids and Secoiridoids. Prog Chem Org Nat Prod 50:169
Z309. Gill M, Steglich W (1987) Pigments of Fungi (Macromycetes). Prog Chem Org Nat Prod 51:1
Z310. Weiss U, Merlini L, Nasini G (1987) Naturally Occurring Perylenequinones. Prog Chem Org Nat Prod 52:1
Z311. Achenbach H (1987) The Pigments of the Flexirubin-Type. A Novel Class of Natural Products. Prog Chem Org Nat Prod 52:73
Z312. Goto T (1987) Structure, Stability, and Color Variation of Natural Anthocyanins. Prog Chem Org Nat Prod 52:113
Z313. Bhattacharyya P, Chakraborty DP (1987) Carbazole Alkaloids. Prog Chem Org Nat Prod 52:159

Z314. Alves LF (1988) Chemical Ecology and the Social Behavior of Animals. Prog Chem Org Nat Prod 53:1
Z315. Nomura T (1988) Phenolic Compounds of the Mulberry Tree and Related Plants. Prog Chem Org Nat Prod 53:87
Z316. Chimiak A, Milewska MJ (1988) *N*-Hydroxylamino Acids and Their Derivatives. Prog Chem Org Nat Prod 53:203
Z317. Murakami T, Tanaka N (1988) Occurrence, Structure, and Taxonomic Implications of Fern Constituents. Prog Chem Org Nat Prod 54:1
Z318. Davies-Coleman MT, Rivett DEA (1989) Naturally Occurring 6-Substituted 5,6-Dihydro-α-pyrones. Prog Chem Org Nat Prod 55:1
Z319. Krohn K (1989) Building Blocks for the Total Synthesis of Anthracyclinones. Prog Chem Org Nat Prod 55:37
Z320. Lounasmaa M, Galambos J (1989) Indole Alkaloid Production in Cell Suspension Cultures. Prog Chem Org Nat Prod 55:89
Z321. James CE, Hough L, Khan R (1989) Sucrose and its Derivatives. Prog Chem Org Nat Prod 55:117
Z322. Asselineau J (1991) Bacterial Lipids Containing Amino Acids or Peptides Linked by Amide Bonds. Prog Chem Org Nat Prod 56:1
Z323. Kagan J (1991) Naturally Occurring Di- and Trithiophenes. Prog Chem Org Nat Prod 56:88
Z324. Metzger P, Largeau C, Casadevall E (1991) Lipids and Macromolecular Lipids of the Hydrocarbon-rich Microalga *Botryococcus braunii*. Chemical Structure and Biosynthesis. Geochemical and Biotechnological Importance. Prog Chem Org Nat Prod 57:1
Z325. Chakraborty DP, Roy S (1991) Carbazole Alkaloids III. Prog Chem Org Nat Prod 57:71
Z326. Pettit GR (1991) The Bryostatins. Prog Chem Org Nat Prod 57:153
Z327. Robinson JA (1991) Chemical and Biochemical Aspects of Polyether-Ionophore Antibiotic Biosynthesis. Prog Chem Org Nat Prod 58:1
Z328. Murray RDH (1991) Naturally Occurring Plant Coumarins. Prog Chem Org Nat Prod 58:83
Z329. Hatanaka S-I (1992) Amino Acids from Mushrooms. Prog Chem Org Nat Prod 59:1
Z330. Wahlberg I, Eklund A-M (1992) Cembranoids, Pseudopteranoids, and Cubitanoids of Natural Occurrence. Prog Chem Org Nat Prod 59:141
Z331. Wahlberg I, Eklund A-M (1992) Cyclized Cembranoids of Natural Occurrence. Prog Chem Org Nat Prod 60:1
Z332. Petitou M, van Boeckel CAA (1992) Chemical Synthesis of Heparin Fragments and Analogues. Prog Chem Org Nat Prod 60:143
Z333. Kingston DGI, Molinero AA, Rimoldi JM (1993) The Taxane Diterpenoids. Prog Chem Org Nat Prod 61:1
Z334. Bhat SV (1993) Forskolin and Congeners. Prog Chem Org Nat Prod 62:1
Z335. Minale L, Riccio R, Zollo F (1993) Steroidal Oligoglycosides and Polyhydroxysteroids from Echinoderms. Prog Chem Org Nat Prod 62:75
Z336. Ray AB, Gupta M (1994) Withasteroids, a Growing Group of Naturally Occurring Steroidal Lactones. Prog Chem Org Nat Prod 63:1
Z337. Rodriguez-Hahn L, Esquivel B, Cárdenas J (1994) Clerodane Diterpenes in Labiatae. Prog Chem Org Nat Prod 63:107
Z338. González AG, Bermejo Barrera J (1995) Chemistry and Sources of Mono- and Bicyclic Sesquiterpenes from *Ferula* Species. Prog Chem Org Nat Prod 64:1
Z339. Prota G (1995) The Chemistry of Melanins and Melanogenesis. Prog Chem Org Nat Prod 64:93
Z340. Gijsen HJM, Wijnberg BPA, deGroot A (1995) Structure, Occurrence, Biosynthesis, Biological Activity, and Chemistry of Aromadendrane Sesquiterpenoids. Prog Chem Org Nat Prod 64:149
Z341. Asakawa Y (1995) Chemical Constituents of the Bryophytes. Prog Chem Org Nat Prod 65:1
Z342. Okuda T, Yoshida T, Hatano T (1995) Hydrolyzable Tannins and Related Polyphenols. Prog Chem Org Nat Prod 66:1

Z343. Gomes de Souza Berlinck R (1995) Some Aspects of Guanidine Secondary Metabolism. Prog Chem Org Nat Prod 66:119
Z344. Gunatilaka AAL (1996) Triterpenoid Quinonemethides and Related Compounds (Celastroloids). Prog Chem Org Nat Prod 67:1
Z345. Walser-Volken P, Tamm Ch (1996) The Spirostaphylotrichins and Related Microbial Metabolites. Prog Chem Org Nat Prod 67:125
Z346. Gribble GW (1996) Naturally Occurring Organohalogen Compounds – A Comprehensive Survey. Prog Chem Org Nat Prod 68:1
Z347. Grove JF (1996) Non-Macrocyclic Trichothecenes, Part 2. Prog Chem Org Nat Prod 69:1
Z348. Deepak D, Srivastava S, Khare NK, Khare A (1996) Cardiac Glycosides. Prog Chem Org Nat Prod 69:71
Z349. Haslam E (1996) Aspects of the Enzymology of the Shikimate Pathway. Prog Chem Org Nat Prod 69:157
Z350. Pettit GR (1997) The Dolastatins. Prog Chem Org Nat Prod 70:1
Z351. Cavé A, Figadère B, Laurens A, Cortes D (1997) Acetogenins from Annonaceae. Prog Chem Org Nat Prod 70:81
Z352. Gäde G (1997) The Explosion of Structural Information on Insect Neuropeptides. Prog Chem Org Nat Prod 71:1
Z353. Christensen SB, Andersen A, Smitt UW (1997) Sesquiterpenoids from *Thapsia* Species and Medicinal Chemistry of the Thapsigargins. Prog Chem Org Nat Prod 71:129
Z354. Deepak D, Srivastav S, Khare A (1997) Pregnane Glycosides. Prog Chem Org Nat Prod 71:169
Z355. Murray RDH (1997) Naturally Occurring Plant Coumarins. Prog Chem Org Nat Prod 72:1
Z356. Ziffer H, Highet RJ, Klayman DL (1997) Artemisinin: An Endoperoxidic Antimalarial from *Artemisia annua* L. Prog Chem Org Nat Prod 72:121
Z357. Fattorusso E, Mangoni A (1997) Marine Glycolipids. Prog Chem Org Nat Prod 72:215
Z358. Nomura T, Fukai T (1998) Phenolic Constituents of Licorice (*Glycyrrhiza* Species). Prog Chem Org Nat Prod 73:1
Z359. Mahato SB, Garai S (1998) Triterpenoid Saponins. Prog Chem Org Nat Prod 74:1
Z360. Otsomaa LA, Koskinen AMP (1998) Synthesis of 6-Deoxyamino Sugars. Prog Chem Org Nat Prod 74:197
Z361. Gournelis DC, Laskaris GG, Verpoorte R. (1998) Cyclopeptide Alkaloids. Prog Chem Org Nat Prod 75:1
Z362. Collett LA, Davies-Coleman MT, Rivett DEA (1998) Naturally Occurring 6-Substituted 5,6-Dihydro-α-pyrones. Prog Chem Org Nat Prod 75:181
Z363. Adams DR, Brochwicz-Lewinski, Butler AR (1999) Nitric Oxide: Physiological Roles, Biosynthesis and Medical Uses. Prog Chem Org Nat Prod 76:1
Z364. Ayer WA, Trifonov LS (1999) Secondary Metabolites and the Control of Some Blue Stain and Decay Fungi. Prog Chem Org Nat Prod 77:1
Z365. Ferreira D, Brandt EV, Coetzee J, Malan E (1999) Condensed Tannins. Prog Chem Org Nat Prod 77:21
Z366. Daniewski WM, Vidari G (1999) Constituents of *Lactarius* (Mushrooms). Prog Chem Org Nat Prod 77:69
Z367. Adam G, Schmidt J, Schneider B (1999) Brassinosteroids. Prog Chem Org Nat Prod 78:1
Z368. Akhila A, Rani K (1999) Chemistry of the Neem Tree (*Azadirachta indica* A. Juss.). Prog Chem Org Nat Prod 78:47
Z369. Franzyk H (2000) Synthetic Aspects of Iridoid Chemistry. Prog Chem Org Nat Prod 79:1
Z370. Leclercq S, Braekman JC, Daloze D, Pasteels JM (2000) The Defensive Chemistry of Ants. Prog Chem Org Nat Prod 79:115
Z371. Chang CWJ (2000) Naturally Occurring Isocyano/Isothiocyanato and Related Compounds. Prog Chem Org Nat Prod 80:1
Z372. Hofer O, Greger H (2000) Sulfur-Containing Amides from *Glycosmis* Species (Rutaceae). Prog Chem Org Nat Prod 80:187

Z373. Huneck S (2001) New Results on the Chemistry of Lichen Substances. Prog Chem Org Nat Prod 81:1
Z374. Bringmann G, Günther C, Ochse M, Schupp O, Tasler S (2001) Biaryls in Nature: A Multi-Facetted Class of Stereochemically, Biosynthetically, and Pharmacologically Intriguing Secondary Metabolites. Prog Chem Org Nat Prod 82:1
Z375. Murray RDH (2002) The Naturally Occurring Coumarins. Prog Chem Org Nat Prod 83:1
Z376. Montforts F-P, Glasenapp-Breiling M (2002) Naturally Occurring Cyclic Tetrapyrroles. Prog Chem Org Nat Prod 84:1
Z377. Kingston DGI, Jagtap PG, Yuan H, Samala L (2002) The Chemistry of Taxol and Related Taxoids. Prog Chem Org Nat Prod 84:53
Z378. Krohn K (2003) Natural Products Derived from Naphthalenoid Precursors by Oxidative Dimerization. Prog Chem Org Nat Prod 85:1
Z379. Messner P, Schäffer C (2003) Prokaryotik Glycoproteins, Prog Chem Org Nat Prod 85:51
Z380. Chakraborty DP, Roy S (2003) Carbazole Alkaloids IV. Prog Chem Org Nat Prod 85:125
Z381. Gossauer A (2003) Monopyrrolic Natural Compounds Including Tetramic Acid Derivatives. Prog Chem Org Nat Prod 86:1
Z382. Flessner T, Jautelat R, Scholz U, Winterfeldt E (2004) Cephalostatin Analogues – Synthesis and Biological Activity. Prog Chem Org Nat Prod 87:1
Z383. Budzikiewicz H (2004) Siderophores of the Pseudomonadaceae *sensu stricto* (Fluorescent and Non-Fluorescent *Pseudomonas* spp.). Prog Chem Org Nat Prod 87:81
Z384. Reimann E (2007) Synthesis Pathways to *Erythrina* Alkaloids and *Erythrina* Type Compounds. Prog Chem Org Nat Prod 88:1
Z385. Grove JF (2007) The Trichothecenes and Their Biosynthesis. Prog Chem Org Nat Prod 88:63
Z386. Roy S (2007) Melanin, Melanogenesis, and Vitiligo. Prog Chem Org Nat Prod 88:131
Z387. Kräutler B (2008) Chlorophyll Catabolites. Prog Chem Org Nat Prod 89:1
Z388. Sahu NP, Banerjee S, Mondal NB, Mandal D (2008) Steroidal Saponins. Prog Chem Org Nat Prod 89:45
Z389. Mulzer J (2009) Preface. Prog Chem Org Nat Prod 90:1
Z390. Höfle G (2009) General Aspects. Prog Chem Org Nat Prod 90:5
Z391. Müller R (2009) Biosynthesis and Heterologous Production of Epothilones. Prog Chem Org Nat Prod 90:29
Z392. Mulzer J, Prantz K (2009) Total Synthesis of Epothilones A–F. Prog Chem Org Nat Prod 90:55
Z393. Altmann K-H (2009) Semisynthetic Derivatives of Epothilones. Prog Chem Org Nat Prod 90:135
Z394. Altmann K-H (2009) Preclinical Pharmacology and Structure–Activity Studies of Epothilones. Prog Chem Org Nat Prod 90:157
Z395. Altmann K-H (2009) Clinical Studies with Epothilones. Prog Chem Org Nat Prod 90:221
Z396. Gribble GW (2010) Naturally Occurring Organohalogen Compounds – A Comprehensive Update. Prog Chem Org Nat Prod 91:1
Z397. Budzikiewicz H (2010) Microbial Siderophores. Prog Chem Org Nat Prod 92:1
Z398. Pereda-Miranda R, Rosas-Ramírez D, Castañeda-Gómez J (2010) Resin Glycosides from the Morning Glory Family. Prog Chem Org Nat Prod 92:77
Z399. Begum SA, Sahai M, Ray AB (2010) Non-conventional Lignans: Coumarinolignans, Flavonolignans, and Stilbenolignans. Prog Chem Org Nat Prod 93:1
Z400. Gössinger E (2010) Picrotoxanes. Prog Chem Org Nat Prod 93:71
Z401. Luzhetska M, Härle J, Bechthold A (2010) Combinatorial and Synthetic Biosynthesis in Actinomycetes. Prog Chem Org Nat Prod 93:211
Z402. Ebada SS, Lajkiewicz N, Porco Jr JA, Li-Weber M, Proksch P (2011) Chemistry and Biology of Rocaglamides (= Flavaglines) and Related Derivatives from *Aglaia* Species (Meliaceae). Prog Chem Org Nat Prod 94:1
Z403. Bulusu MARC, Baumann K, Stuetz A (2011) Chemistry of the Immunomodulatory Macrolide Ascomycin and Related Analogues. Prog Chem Org Nat Prod 94:59

Z404. Misico RI, Nicotra VE, Oberti JC, Barboza G, Gil RR, Burton G (2011) Withanolides and Related Steroids. Prog Chem Org Nat Prod 94:127
Z405. Asakawa Y, Ludwiczuk A, Nagashima F (2012) Chemical Constituents of Bryophytes: Bio- and Chemical Diversity, Biological Activity, and Chemosystematics. Prog Chem Org Nat Prod 95:1
Z406. Waser M (2012) Asymmetric Organocatalysis in Natural Product Syntheses. Prog Chem Org Nat Prod 96:1
Z407. Bräse S, Gläser F, Kramer C, Lindner S, Linsenmeier A, Masters K, Meister A, Ruff BM, Zhong S (2012) Recent Progress in the Chemistry of Mycotoxins. Prog Chem Org Nat Prod 97:1
Z408. Lightner DA (2013) Bilirubin: *Jekyll* and *Hyde* Pigment of Life. Prog Chem Org Nat Prod 98:1
Z409. Qiu F, McAlpine JB, Krause EC, Chen S-H, Pauli GF (2014) The Pharmacognosy of Black Cohosh. Prog Chem Org Nat Prod 99:1
Z410. Gaboriaud-Kolar N, Nam S, Skaltsounis A-L (2014) A Colorful History: The Evolution of Indigoids. Prog Chem Org Nat Prod 99:69
Z411. Ishibashi M (2014) Bioactive Natural Products from Actinomycetes Having Effects on Cancer-related Signaling Pathways. Prog Chem Org Nat Prod 99:147
Z412. Nett M (2014) Genome Mining – Concept and Strategies for Natural Product Discovery. Prog Chem Org Nat Prod 99:199